

NASA/SP-2009-566-ADD2



Human Exploration of Mars Design Reference Architecture 5.0 Addendum #2

*Bret G. Drake and Kevin D. Watts, editors
NASA Johnson Space Center, Houston, Texas*

March 2014

NASA STI Program ... in Profile

Since its founding, NASA has been dedicated to the advancement of aeronautics and space science. The NASA scientific and technical information (STI) program plays a key part in helping NASA maintain this important role.

The NASA STI program operates under the auspices of the Agency Chief Information Officer. It collects, organizes, provides for archiving, and disseminates NASA's STI. The NASA STI program provides access to the NASA Aeronautics and Space Database and its public interface, the NASA Technical Report Server, thus providing one of the largest collections of aeronautical and space science STI in the world. Results are published in both non-NASA channels and by NASA in the NASA STI Report Series, which includes the following report types:

- **TECHNICAL PUBLICATION.** Reports of completed research or a major significant phase of research that present the results of NASA Programs and include extensive data or theoretical analysis. Includes compilations of significant scientific and technical data and information deemed to be of continuing reference value. NASA counterpart of peer-reviewed formal professional papers but has less stringent limitations on manuscript length and extent of graphic presentations.
- **TECHNICAL MEMORANDUM.** Scientific and technical findings that are preliminary or of specialized interest, e.g., quick release reports, working papers, and bibliographies that contain minimal annotation. Does not contain extensive analysis.
- **CONTRACTOR REPORT.** Scientific and technical findings by NASA-sponsored contractors and grantees.

- **CONFERENCE PUBLICATION.** Collected papers from scientific and technical conferences, symposia, seminars, or other meetings sponsored or co-sponsored by NASA.
- **SPECIAL PUBLICATION.** Scientific, technical, or historical information from NASA programs, projects, and missions, often concerned with subjects having substantial public interest.
- **TECHNICAL TRANSLATION.** English-language translations of foreign scientific and technical material pertinent to NASA's mission.

Specialized services also include creating custom thesauri, building customized databases, and organizing and publishing research results.

For more information about the NASA STI program, see the following:

- Access the NASA STI program home page at <http://www.sti.nasa.gov>
- E-mail your question via the Internet to help@sti.nasa.gov
- Fax your question to the NASA STI Help Desk at 443-757-5803
- Phone the NASA STI Help Desk at 443-757-5802
- Write to:
NASA STI Help Desk
NASA Center for AeroSpace Information
7115 Standard Drive
Hanover, MD 21076-1320

NASA/SP-2009-566-ADD2



Human Exploration of Mars Design Reference Architecture 5.0 Addendum #2

*Bret G. Drake and Kevin D. Watts, editors
NASA Johnson Space Center, Houston, Texas*

March 2014

“We are all . . . children of this universe. Not just Earth, or Mars, or this System, but the whole grand fireworks. And if we are interested in Mars at all, it is only because we wonder over our past and worry terribly about our possible future.”

— Ray Bradbury, 'Mars and the Mind of Man,' 1973

Available from:

NASA Center for AeroSpace Information
7115 Standard Drive
Hanover, MD 21076-1320

National Technical Information Service
5301 Shawnee Road
Alexandria, VA 22312

Available in electric form at <http://ston.jsc.nasa.gov/collections/TRS/>

FOREWORD



This report serves as the second Addendum to NASA-SP-2009-566, “Human Exploration of Mars Design Reference Architecture 5.0.” The data and descriptions contained within this Addendum capture some of the key assessments and studies produced since publication of the original document, predominately covering those conducted from 2009 through 2012. The assessments and studies described herein are for the most part independent stand-alone contributions. Effort has not been made to assimilate the findings to provide an updated integrated strategy. That is a recognized future effort. This report should not be viewed as constituting a formal plan for the human exploration of Mars. Specific contributions to this document were provided by Leslie Alexander, John Baker, Brent Barbee, Kendall Brown, Tim Collins, Cassie Conley, Steve Creech, Bret Drake, Alicia Dwyer-Cianciolo, Kandyce Goodliff, Rob Grover, Jeff Gutkowski, Mike Hembree, Steve Hoffman, Rickey Jedrey, Larry Kos, Craig Kundrot, Damon Landau, Kathy Laurini, Roger Lepsch, Stan Love, Lee Mason, Todd May, Dan Mazanek, Michelle Munk, Steve Oleson, Don Palac, James Pope, Michelle Rucker, Margret Race, Randy Rust, Jonette Stecklein, Walter Stephens, Larry Toups, and Scott Vangen. Special thanks go to Kevin Watts for his patience and dedication to the technical editing of this Addendum.

Bret G. Drake

This page intentionally left blank

TABLE OF CONTENTS



1.	Summary of Assessments Conducted since DRA 5	1
1.1.	Lunar Capability Concept Review (2008).....	1
1.2.	Review of U.S. Human Spaceflight Plans Committee (2009).....	3
1.2.1.	Mars Relevant Scenarios	3
1.2.2.	Assessments Conducted at the Request of the Committee	5
1.3.	International Participation	15
1.4.	HEFT and HAT (2010 to present).....	16
1.5.	Bibliography.....	16
2.	Earth-Mars Trajectories	17
2.1.	Trip Time Sensitivities	17
2.1.1.	Key Barriers to Exploring Mars	17
2.1.2.	Mars Design Reference Architecture 5.0.....	17
2.1.3.	Round-Trip Mars Mission Design	18
2.1.4.	Exploration Strategies for the Moons of Mars and the Surface	22
2.1.5.	Transportation Technologies Considered	24
2.1.6.	Crew Trip time Sensitivity Results.....	27
2.1.7.	Additional Mission Design Considerations	29
2.1.8.	Total Architecture Mass Comparisons	30
2.1.9.	Conclusion: Summary of Key Challenges.....	31
2.2.	Earth Departure Scenarios	34
2.2.1.	Introduction	34
2.2.2.	Interplanetary Trajectories.....	34
2.2.3.	Departure from Earth-Moon L2	35
2.2.4.	Departure from High-lunar Orbit	37
2.2.5.	Departures from High-Earth Orbit	38
2.2.6.	Departure from Low-Earth Orbit.....	39
2.2.7.	Comparison of Departure Options.....	40
2.2.8.	Earth Departure Scenario Conclusions	41
2.3.	Mars Conceptual Flight Profile	42
2.3.1.	Conceptual Flight Profile Overview.....	42
2.3.1.	DRA 5 Investigation and CFP Ground Rules, Constraints, and Assumptions	43
2.3.1.	Mission Timeline	45
2.3.2.	First End-to-End Impulsive CFP Iteration.....	54
2.3.3.	Second End-to-End Impulsive CFP Iteration	58
2.3.4.	Possible Trade Studies.....	64
2.3.5.	Forward Work	65
2.4.	Bibliography.....	66
3.	Advanced In-space Transportation.....	67
3.1.	Nuclear Cryogenic Propulsion System.....	67
3.1.1.	Overall NCPS Project.....	67
3.1.2.	Task 2 - NCPS Mars Architecture: Trajectory & Sizing	77
3.2.	Nuclear Electric Propulsion.....	95
3.2.1.	Nuclear Electric Propulsion Study Executive Summary	95
3.2.1.	Study Background and Assumptions.....	97
3.2.2.	Baseline NEP Design	111
3.2.3.	NEP Subsystem Breakdown.....	127
3.3.	A Combined Solar Electric and Storable Chemical Propulsion	152

3.3.1.	Introduction	152
3.3.1.	Design.....	153
3.3.2.	Trajectory Analysis	155
3.3.3.	Baseline Vehicle.....	156
3.3.4.	Parametric Assessments of Power and Propulsion	159
3.3.5.	Propulsion Trades.....	162
3.3.6.	Power System Trades	163
3.3.7.	Results	163
3.3.8.	Conclusion.....	164
3.3.9.	Acknowledgments	164
3.4.	Bibliography.....	165
4	Mars Entry, Descent, and Landing	169
4.1	Section Summary	169
4.2	Descent and Ascent Trajectories	174
4.2.1	Initial Ascent Orbit Selection Trades	174
4.2.2	Ascent Trajectory Trade Space.....	175
4.3	Lander Trades and Sensitivities.....	175
4.3.1	Initial Ascent Sizing Trade Space	176
4.3.2	Initial Descent Sizing Trade Space.....	184
4.3.3	ENVISION Ascent Vehicle Sizing.....	187
4.3.4	ENVISION Descent Stage Sizing	189
4.3.5	ENVISION Results	189
4.4	TeamX Sizing and EDL Concept Assessments.....	190
4.4.1	Study Overview	190
4.4.2	Vehicle Configurations and Design Drivers.....	190
4.4.3	Primary Risk Drivers	198
4.4.4	Summary and Conclusions	198
4.5	Aerodynamic Entry and Descent.....	199
4.5.1	Rationale for Additional Entry and Descent Work.....	199
4.5.2	The EDL-SA Study	199
4.5.3	Human Architecture Team Efforts	200
4.5.4	Future Work	200
4.6	Configurations and Analyses.....	201
4.6.1	Purpose and Approach.....	201
4.6.2	Assumptions	203
4.6.3	Configuration Brainstorming.....	207
4.6.4	Configuration Down Selection	215
4.6.5	Sizing and Analysis	222
4.6.6	Summary Comparison of Analysis Results	230
4.6.7	Comparison to TeamX Mass Estimates.....	231
4.6.8	Launch Vehicle Integration	232
4.6.9	Uncertainties and Suggested Future Work	234
4.7	Propulsion and Propellants	237
4.7.1	Engine Performance and Sizing	237
4.7.2	Cryogenic Fluid Management & Interfaces with ISRU	238
4.8	Descent Module Design	243
4.8.1	Physical Design Description.....	243
4.8.2	Configuration Summary	244
4.8.3	Subsystem Data	245
4.8.4	Performance.....	248
4.9	Mars Ascent Vehicle	252
4.9.1	MAV Ground Rules and Assumptions	252
4.9.2	Approach	253
4.9.3	Habitable MAV Crew Cabin	254
4.9.4	Taxi MAV Crew Cabin	264

4.9.5	MAV Propulsion Stages	269
4.9.6	Discussion	274
4.9.7	MAV Mass Reduction Opportunities	279
4.10	Transition Event	281
4.10.1	Transition Conditions	281
4.10.2	Evaluation Process.....	282
4.10.3	Figures of Merit.....	282
4.10.4	High Level Assessments: Preliminary Options and Rankings	283
4.10.5	Initial Most Viable Options	304
4.10.6	Transition Modeling and Simulation	306
4.10.7	Recommended Future Work.....	316
4.11	Mars Lander Architecture Modeling Approach	316
4.11.1	Introduction	316
4.11.2	Process Formulation	317
4.11.3	Process Execution.....	324
4.11.4	Functional Architecture Execution	326
4.11.5	Summary	328
4.12	Summary of Mars Lander Technology Needs.....	329
4.12.1	EDL Systems.....	329
4.12.2	Propulsion and CFM Systems	329
4.12.3	Power Systems	330
4.12.4	Avionics, C&DH and C&T	330
4.12.5	Thermal, Life Support and Human Factors	331
4.13	Recommended Forward Work	333
4.13.1	Forward Work in Aerodynamic Entry and Descent	333
4.13.2	Forward Work in Descent Module Configurations	333
4.13.3	Forward Work in Descent Module Design	336
4.13.4	Forward Work Mars Ascent Vehicle	336
4.13.5	Forward Work Transition Event.....	337
4.13.6	Forward Work Mars Lander Architecture Modeling Approach	337
4.14	Appendix A: Master Equipment Lists	338
4.15	Appendix B: Vehicle Baseball Cards	343
4.16	Bibliography.....	345
5.	Space Launch System	347
5.1.	Introduction	347
5.2.	Architecture Overview and Accomplishments	348
5.3.	One Rocket, Many Missions	354
5.4.	Management Approach, Plans, and Progress	354
5.5.	Conclusions.....	357
5.6.	Bibliography.....	358
6.	Mars Launch Campaign Ground System Architecture Considerations	359
6.1.	Introduction	359
6.2.	Mars Launch Campaign Sensitivity Analysis	361
6.2.1.	Sensitivity to Launch Campaign Duration	362
6.2.1.	Sensitivity to Processing Workforce	362
6.2.2.	Sensitivity to Launch Infrastructure	362
6.2.3.	Sensitivity to First-Stage Booster and Payload Type	364
6.3.	Other Potential Risks & Considerations.....	364
6.4.	Key Decision Points	365
6.5.	Launch Campaign Ground System Architecture Summary	365
6.6.	Bibliography.....	365

7.	Deep Space Habitat.....	367
7.1.	Introduction	367
7.2.	Mass Trades	367
7.3.	Commonality between Transit and Surface Habitat Designs	370
7.4.	Future Studies.....	371
7.5.	Bibliography.....	371
8.	Surface Strategy	373
8.1.	Summary of DRA 5 Surface Strategies	373
8.2.	Support to the Review of United States Human Space Flight Plans Committee.....	376
8.3.	Capability Driven Framework.....	378
8.4.	Functional Breakdown.....	380
8.5.	Surface Strategy Assessment Utilizing Functional Breakdown	381
8.6.	Summary	385
8.7.	Bibliography.....	385
9.	Mars Surface Systems.....	387
9.1.	Surface Power Systems	387
9.1.1.	Introduction	387
9.1.2.	Project Context	387
9.1.3.	Derived Requirements	388
9.1.4.	Design Summary	389
9.1.5.	Lunar and Mars Architecture Studies	391
9.1.6.	Conclusion.....	398
9.1.7.	Acknowledgments	398
9.2.	Extravehicular Activity and Mobility.....	399
9.2.1.	EVA System Assumptions and Questions/Forward Work	401
9.2.2.	EVA Operations Concept for Mars Surface	404
9.2.3.	Advanced EVA Suit Baseball Cards	405
9.3.	Logistics, Maintenance, and Repair	406
9.3.1.	Logistics	406
9.3.2.	Supportability	407
9.4.	Bibliography.....	416
10.	Technology Needs.....	417
10.1.	Introduction	417
10.2.	HAT Technology Development	417
10.3.	Architectural Elements and Destinations	417
10.4.	Technology Selection Method.....	419
10.5.	Technologies	420
10.6.	Discussion	422
10.7.	Summary	425
10.8.	Bibliography.....	427
11.	Analogs.....	429
11.1.	Introduction	429
11.2.	Analogue History, Context and Rationale.....	429
11.3.	Definitions	430
11.4.	Analog Projects and Teams	431
11.4.1.	Autonomous Mission Operations (AMO)	431
11.4.2.	Desert Research and Technology Studies (D-RATS).....	432
11.4.3.	Haughton-Mars Project (HMP)	433
11.4.4.	In-Situ Resource Utilization (ISRU)	436
11.4.5.	International Space Station Test-bed for Analog Research (ISTAR)	438
11.4.6.	NASA Extreme Environment Mission Operations (NEEMO)	438

11.4.7.	Pavilion Lake Research Project (PLRP).....	440
11.4.8.	Analog Project/Mission Locations	442
11.4.9.	Other Relevant Analog Projects and Missions	442
11.5.	ANALOG CAMPAIGNS (by year and location).....	446
11.6.	Historic Analogue Campaigns.....	453
11.7.	Summary	457
11.8.	Bibliography.....	457
12.	Human Research.....	459
12.1.	Standards for the Human System	459
12.1.1.	Crew Health.....	459
12.1.2.	Human Factors, Habitability, and Environmental Health.....	459
12.2.	Additional Assumptions Made to Assess the Human Health and Performance Risks	460
12.2.1.	HRP Mars DRM Additional Assumptions	460
12.3.	Challenges Associated with DRA 5.0	462
12.3.1.	HRP Health and Performance Risks.....	462
12.3.2.	Introduction to HRP Research Ratings.....	463
12.3.3.	HRP Research Ratings for DRA 5.0.....	464
12.4.	Preliminary Assessment of Challenges for a Mars Orbital Mission with no Landing.....	465
12.4.1.	Patterns of Change in Risk Posture	465
12.5.	Identification of Trade Space Factors.....	468
12.6.	HRP use of Analogs for Risk Reduction	469
12.7.	Medical Care	471
12.8.	Artificial Gravity	472
12.8.1.	Background	472
12.8.2.	Design Questions.....	473
12.8.3.	Physiological Questions	473
12.8.4.	Example: Engineering Considerations for Whole Vehicle Centrifugation.....	475
12.9.	An Integrated Human Countermeasure Suite for Mars Exploration Missions	479
12.10.	Food Considerations.....	479
12.11.	Bibliography.....	480
13.	Special Studies and Strategic Assessments.....	481
13.1.	Orbital Missions	481
13.1.1.	Phobos/Deimos Destination Assessment.....	481
13.1.2.	Mission Design for the Exploration of Phobos and Deimos.....	504
13.2.	Mars Program Planning Group Summary	533
13.2.1.	Mars Program Planning Group Charter	533
13.2.2.	Human Exploration beyond LEO: A Capability Driven Framework	533
13.2.3.	Humans to Mars Risk Assessments.....	537
13.2.4.	Human Support Risks.....	537
13.2.5.	Key Challenges for Orbital and Surface Missions.....	538
13.2.6.	Humans to Mars Roadmap Observations	540
13.2.7.	Precursor Investigations/Measurements necessary for Humans to Mars.....	545
13.2.8.	Human and Robotic Mission Collaboration Opportunities	548
13.3.	Risk Assessments	552
13.3.1.	Methodology	553
13.3.2.	Risk Analysis.....	553
13.3.3.	Future Risk Analysis Work	556
13.4.	Planetary Protection Requirements for Human and Robotic Missions to Mars	557
13.4.1.	Overview	557
13.4.2.	Background	557
13.4.3.	COSPAR Planetary Protection Policy for Robotic and Human Missions	558
13.4.4.	Applying Planetary Protection Considerations to Future Human Design Reference Architectures	559
13.4.5.	Protecting Astronauts and Designing Human Rated Systems	560

13.4.6.	Planetary Protection Conclusions:.....	563
13.5.	Bibliography.....	563
14.	Acronyms, Abbreviations, & Glossary of Terms.....	567
14.1.	Acronyms	567
14.2.	Nomenclature	570

LIST OF FIGURES



Figure 1-1 LCCR era Ares-V launch vehicle capabilities for Mars missions.....	4
Figure 1-2 LCCR era Orion crew vehicle capabilities for Mars missions.....	5
Figure 1-3 Mars ascent stage minimum size for various stage concepts.....	7
Figure 1-4 Surface manifest for differing landed payload capabilities.....	9
Figure 1-5 Influence of number of crew and payload size on key launch vehicle characteristics.....	10
Figure 2-1 Representative mission profiles for the major mission classes for human Mars missions.....	20
Figure 2-2 Example round-trip ΔV as a function of total mission duration.....	22
Figure 2-3 Variation in mission co-planar ΔV across a 15-year cycle.....	23
Figure 2-4 Sensitivity of the estimated crew vehicle mass as a function of round-trip mission duration for the short-stay, 60 days at Mars, opposition-class missions.....	28
Figure 2-5 Sensitivity of the estimated crew vehicle mass as a function of useful time at Mars for the long-stay conjunction-class missions.....	29
Figure 2-6 Nuclear thermal propulsion crew vehicle mass as a function of one-way transit time to and from Mars for the conjunction-class long-stay missions.....	30
Figure 2-7 Example Mars orbit capture strategies for both high-thrust and low-thrust propulsion technologies.....	31
Figure 2-8 Estimated total architecture mass for nuclear thermal propulsion technology concept. Total mass includes both the cargo and crew vehicles for both surface missions and orbital missions to Phobos and Deimos.....	31
Figure 2-9 Departure characteristics of Earth-Mars transfers vary among launch opportunities.....	35
Figure 2-10 The Earth escape asymptote has moderate variation over a 2-month span.....	36
Figure 2-11 Earth-Moon L2 remains in line with the Moon beyond the Moon’s orbit. For short-duration transfers, it behaves similar to a high circular orbit.....	36
Figure 2-12 Three-burn escape sequence from L2.....	37
Figure 2-13 Departures from L2 span approximately 3 days and have an opportunity to retry TMI.....	37
Figure 2-14 Departure characteristics from high-lunar orbit are similar to L-2.....	38
Figure 2-15 Lunar gravity assists and maneuvers near apogee shape HEO for efficient departures.....	38
Figure 2-16 Departure opportunities from HEO occur for short durations near perigee passages.....	39
Figure 2-17 Performance for single impulse departures from LEO depends on launch declination.....	40
Figure 2-18 Three-burn sequence enables out of plane departures. Plane change is most efficient at low apogee speed with long period orbits.....	40
Figure 2-19 Flight phases and knobs for Earth portion of CFP.....	43
Figure 2-20: Flight phases and knobs for Mars portion of CFP.....	44
Figure 2-21: Equatorial view of the first CFP iteration cargo vehicle’s trans-Mars injection.....	55
Figure 2-22: Polar view of the first CFP iteration cargo vehicle’s trans-Mars injection.....	55
Figure 2-23: Heliocentric view of cargo vehicle transfer trajectory.....	56
Figure 2-24: Equatorial view of the first CFP iteration crew vehicle’s trans-Mars injection.....	56
Figure 2-25: Polar view of the first CFP iteration crew vehicle’s trans-Mars injection.....	57
Figure 2-26: Mars orbit insertion.....	57
Figure 2-27: First CFP iteration trans-Earth injection.....	58
Figure 2-28: First CFP iteration Orion entry interface and MTV disposal.....	58
Figure 2-29 Mars pork chop plot.....	60
Figure 2-30: Second CFP iteration cargo vehicle’s trans-Mars injection.....	60
Figure 2-31: Second CFP iteration cargo vehicle’s transfer in heliocentric space.....	61
Figure 2-32: Second CFP iteration aerocapture and Mars parking orbit alignment.....	61
Figure 2-33: Equatorial view of the second CFP iteration crew vehicle’s trans-Mars injection.....	62
Figure 2-34: Polar view of the second CFP iteration crew vehicle’s trans-Mars injection.....	62
Figure 2-35: Second CFP iteration crew vehicle trans-Earth injection.....	63
Figure 2-36: Second CFP iteration Orion entry interface and MTV disposal flyby.....	64
Figure 3-1 Schematic of an NCPS engine.....	68
Figure 3-2 Material specimen under test in flowing hydrogen in NTREES.....	70

Figure 3-3 NTREES primary chamber configuration.....	71
Figure 3-4 CFEET	71
Figure 3-5 NCPS fuel element design.	72
Figure 3-6 Images of the Rover/NERVA Phoebus Reactor fuel	72
Figure 3-7 CFEET sample configuration.....	73
Figure 3-8 NTP test topology	74
Figure 3-9 SAFE bore hole concept for full scale NTP testing	75
Figure 3-10 JSC robotic instrumentation.....	75
Figure 3-11 Nuclear safety review and launch approval process	76
Figure 3-12 Configuration concept for NCPS stack to Mars	78
Figure 3-13 TMI ΔV s across 15-year cycle	80
Figure 3-14 MOI ΔV s across this 15-year cycle.....	80
Figure 3-15 TEI ΔV s across the 15-year cycle	81
Figure 3-16 2033 opportunity outbound porkchop plot.....	82
Figure 3-17 2033 opportunity outbound plot with fixed departure dates	82
Figure 3-18 2035 opportunity outbound porkchop plot.....	83
Figure 3-19 2037 opportunity outbound porkchop plot.....	84
Figure 3-20 2039 opportunity outbound porkchop plot.....	84
Figure 3-21 2041 opportunity outbound porkchop plot.....	85
Figure 3-22 2043 opportunity outbound porkchop plot.....	85
Figure 3-23 2046 opportunity outbound porkchop plot.....	86
Figure 3-24 SLS with extended, large 10-m diameter shroud.	91
Figure 3-25 Piloted Mars NEP	97
Figure 3-26 Alphas for a 400-day Mars stay time	101
Figure 3-27 Alphas for a 450-day Mars stay time	101
Figure 3-28 Alphas for a 500-day Mars stay time	102
Figure 3-29 Final design point for Case 1	102
Figure 3-30 Trajectory for Case 1 conjunction.....	103
Figure 3-31 Performance curves for a 60-day stay at Mars, 2033 opposition	104
Figure 3-32 Performance curves for a 45-day stay at Mars, 2033 opposition	105
Figure 3-33 Trajectory for Case 2 – opposition.....	106
Figure 3-34 Piloted Mars NEP concept of operations graphic.	109
Figure 3-35 Mars NEP block diagram.....	112
Figure 3-36 Hab/EP element stowed inside the SLS Payload Shroud.....	117
Figure 3-37 Isometric views of the Hab/EP element stowed within the SLS Payload Shroud.....	118
Figure 3-38 Various views of the Hab/EP element in its stowed configuration	118
Figure 3-39 The power element stowed within the extended SLS Payload Shroud	119
Figure 3-40 The power element stowed within the extended SLS Payload Shroud	119
Figure 3-41 Various views of the power element in its stowed configuration.....	120
Figure 3-42 Fully deployed Piloted Mars NEP Vehicle	121
Figure 3-43 Piloted Mars NEP Vehicle radiator types and locations	121
Figure 3-44 Reactor shield cone	122
Figure 3-45 Isometric view of the fully deployed Piloted Mars NEP Vehicle	122
Figure 3-46 Reactor end of the Piloted Mars NEP Vehicle	123
Figure 3-47 Transparent view of the Piloted Mars NEP Vehicle	123
Figure 3-48 Transparent view of the Piloted Mars NEP Vehicle bus.....	124
Figure 3-49 Overall dimensions of the fully deployed power element.....	124
Figure 3-50 Additional dimensions of the fully deployed power element.....	125
Figure 3-51 Dimensions of the fully deployed Hab/EP element	125
Figure 3-52 Basic dimensions of the fully deployed Piloted Mars NEP Vehicle	126
Figure 3-53 Major external components of the full Piloted Mars NEP Vehicle	126
Figure 3-54 Major internal bus components of the full Piloted Mars NEP Vehicle	127
Figure 3-55 Mars Transit Habitat	127
Figure 3-56 Communications system schematic	129
Figure 3-57 X-band link budget	130
Figure 3-58 S-band link budget	131

Figure 3-59	Power system schematic	137
Figure 3-60	Major external components of the full Piloted Mars NEP Vehicle	139
Figure 3-61	Hab segment propulsion layout.....	140
Figure 3-62	Power segment propulsion layout	142
Figure 3-63	A) The habitat and electric propulsion module and B) the power element	143
Figure 3-64	NEP Mars Spacecraft Thermal Components	146
Figure 3-65	Example cold plates with integral heat pipes.....	148
Figure 3-66	Example of a spacecraft heat pipe system.....	148
Figure 3-67	Radiator energy balance.....	149
Figure 3-68	Electric strip heater	149
Figure 3-69	Illustration of MLI	150
Figure 3-70	MLI blankets	150
Figure 3-71	Size of the piloted combined SEP-chemical vehicle (left).....	154
Figure 3-72	Baseline trajectory.	155
Figure 3-73	Trajectory trades after the SEP to E-M L2 arrival	156
Figure 3-74	SEP-Chem stage docked with deep-space habitat. Major external components shown.....	157
Figure 3-75	SEP-Chem module configured for launch within an SLS.....	157
Figure 3-76	Electric thruster plume cone in relation to solar arrays.....	158
Figure 3-77	Internal bus components, including chemical thrusters and propellant system.....	159
Figure 4-1	Ascent ΔV results for varying initial thrust-to-weight ratio (Earth), final orbit, and number of phases.....	175
Figure 4-2	Trajectory plots for SPTO Mars ascent for initial thrust-to-weight=0.7 Earth G.....	176
Figure 4-3	Thrust levels required for various MAV T/W ₀ (i.e. its associated gross liftoff weight, or GLOW).	181
Figure 4-4	MAV masses at Earth for HMO, TPTO with various T/W ₀ & ISRU options.....	182
Figure 4-5	Results for MPS and payload mass trades.	183
Figure 4-6	Results for MPS and payload mass trades.	186
Figure 4-7	Thrust levels required for various descent vehicle T/W ₀	187
Figure 4-8	TeamX study overview – inputs and outputs.....	190
Figure 4-9	TeamX mid L/D architecture.	191
Figure 4-10	Mid L/D architecture aeroshell with lander inside.....	192
Figure 4-11	Mid L/S architecture descent stage with payload area and MAV.....	192
Figure 4-12	Mid L/D architecture transition event sequence.....	193
Figure 4-13	Mid L/D architecture launch configuration.....	194
Figure 4-14	TeamX HIAD architecture.....	195
Figure 4-15	HIAD architecture HID with lander.....	195
Figure 4-16	HIAD architecture lander with payload area and MAV.....	196
Figure 4-17	HIAD architecture transition configuration.....	197
Figure 4-18	HIAD architecture launch configuration.....	198
Figure 4-19	EDL-SA Technology combinations form 8 unique entry, descent and landing architectures.....	200
Figure 4-20	Notional horizontal (top row) and vertical (bottom row) lander configurations.....	202
Figure 4-21	Engine configuration assumptions.....	204
Figure 4-22	Assumed rover configuration.....	205
Figure 4-23	Assumed FSPS.....	206
Figure 4-24	MAV configuration with four nested LCH ₄ /LOX propellant tanks.....	207
Figure 4-25	Horizontal configuration H1 (cage and platform).....	208
Figure 4-26	Horizontal configuration H2 (truss-bays)	209
Figure 4-27	Horizontal configuration H3 (partial-circle platform).....	210
Figure 4-28	Horizontal configuration H4 (compact horizontal).....	211
Figure 4-29	Vertical configuration V1 (stacked cargo bays).....	212
Figure 4-30	Vertical configuration V2 (stacked with flat-bed)	213
Figure 4-31	Vertical configuration V3 (compact vertical)	214
Figure 4-32	Vertical configuration V4 (ring-symmetric vertical)	215
Figure 4-33	Summary of horizontal lander rankings (all FOMs equally important)	217
Figure 4-34	Overall horizontal lander rankings with weighted FOMs.....	219
Figure 4-35	Summary of vertical lander rankings (all FOMs equally important).....	220

Figure 4-36 Overall vertical lander rankings with weighted FOMs.221

Figure 4-37 Modified V1 configuration222

Figure 4-38 Final horizontal (H3) lander configuration (as-analyzed CAD model).....224

Figure 4-39 Horizontal (H3) lander shroud arrangement and finite-element analysis model.....225

Figure 4-40 Final vertical (V1) lander configuration (as-analyzed CAD model).....228

Figure 4-41 Vertical (V1) lander finite-element analysis model.229

Figure 4-42 Baseline vertical lander integration (HIAD on top).....232

Figure 4-43 Alternate vertical lander integration (HIAD on bottom).....232

Figure 4-44 Alternate vertical lander integration (inverted orientation).....233

Figure 4-45 Integration options of vertical lander with rigid aeroshell.234

Figure 4-46 Integration of horizontal lander with HIAD.....234

Figure 4-47 LOX/LCH₄ engine for Mars Ascent Vehicle and lander descent stage.....238

Figure 4-48 Vertical and horizontal descent stage configurations.....239

Figure 4-49 Two stage ascent vehicle.....239

Figure 4-50 Sink temperatures and LEO & Mars orbits.....240

Figure 4-51 Mars seasonal and diurnal cycle data (A. Dwyer).....242

Figure 4-52 HIAD plus SRP plus Vertical Lander: (left) sensed acceleration and (right) throttle setting versus time on the terminal descent engines.250

Figure 4-53 Rigid aeroshell plus SRP plus Horizontal Lander: (left) sensed acceleration and (right) throttle setting versus time on the terminal descent engines.....251

Figure 4-54 4-crew habitable MAV cabin dimensions.....254

Figure 4-55 6-crew habitable MAV height.....255

Figure 4-56 6-crew habitable MAV cabin dimensions.....256

Figure 4-57 Altair-derived integrated power subsystem.....258

Figure 4-58 Habitable MAV thermal subsystem schematic.....258

Figure 4-59 Habitable MAV ECLS subsystem schematic.....260

Figure 4-60 MAV tank arrangement comparison.....262

Figure 4-61 4-Crew Taxi MAV cabin dimensions.....264

Figure 4-62 Taxi MAV electrical power subsystem.....266

Figure 4-63 Taxi MAV thermal subsystem.....267

Figure 4-64 MAV staging.....270

Figure 4-65 Two stage MAV MECO mass vs. staging time.....270

Figure 4-66 MAV engine gimbal clearance.....271

Figure 4-67 MAV engine spacing.....271

Figure 4-68 MAV propellant tank placement (top view).....272

Figure 4-69 MAV second stage configuration.....272

Figure 4-70 6-crew habitable MAV.....274

Figure 4-71 Taxi MAV habitability (top view).....275

Figure 4-72 External equipment placement (fore).....275

Figure 4-73 External equipment placement (aft).....276

Figure 4-74 Internal cabin configuration.....276

Figure 4-75 6 EVA suited crew in MAV (outfitted for 1 week).....277

Figure 4-76 MAV conceptual crew landing protection.....278

Figure 4-77 Crew MAV habitability.....279

Figure 4-78 Transition conditions from EDL-SA architecture studies.....282

Figure 4-79 Transition event assessment process.....282

Figure 4-80 Forward exit clam shell option.....283

Figure 4-81 Side exit clamshell option.....285

Figure 4-82 Rear exit with separation thrusters on aeroshell.....285

Figure 4-83 Forward exit with separation thruster on lander.....286

Figure 4-84 Forward with drag flaps on aeroshell.....287

Figure 4-85 Forward exit option.....288

Figure 4-86 Forward exit with separation thruster on aeroshell.....288

Figure 4-87 Forward exit with parachute on aeroshell.....289

Figure 4-88 Forward exit with SIAD on aeroshell.....290

Figure 4-89 Rear exit using lander descent engines.....291

Figure 4-90 Rear exit with SIAD on lander.....291

Figure 4-91 Front exit with trailing IAD attached to aeroshell.....292

Figure 4-92 Rear exit with trailing IAD attached to lander – ellipse sled version.....293

Figure 4-93 Rear exit with trailing IAD attached to lander.....294

Figure 4-94 Side exit with SIAD on lander.....295

Figure 4-95 Front exit with canted descent thrusters and subsonic heatshield jettison.....296

Figure 4-96 Front exit with supersonic heatshield jettison from HIAD/lander combination.....297

Figure 4-97 Front exit with supersonic heatshield jettison after lander separation from HIAD.....297

Figure 4-98 Front exit with separation thruster on lander.....298

Figure 4-99 Rear exit with separation thrusters on lander.....299

Figure 4-100 Rear exit with parachute attached to lander.....300

Figure 4-101 Rear exit with SIAD attached to lander.....300

Figure 4-102 Rear exit with IAD attached to lander.....301

Figure 4-103 Rear exit with separation thrusters on HIAD.....302

Figure 4-104 No exit carrying inflated HIAD to surface.....303

Figure 4-105 No exit carrying deflated HIAD to surface.....304

Figure 4-106 Options assessed as most viable for the mid L/D architecture transition event.....305

Figure 4-107 Options, per category, assessed as most viable for the HIAD architecture transition event.....305

Figure 4-108 Separation distance vs. transition start time.....308

Figure 4-109 Altitude vs. transition start time.....309

Figure 4-110 Angle of attack vs. transition start time.....309

Figure 4-111 Flight path angle vs. transition start time.....310

Figure 4-112 Mach number vs. transition start time.....310

Figure 4-113 Velocity vs. transition start time.....311

Figure 4-114 Sensed acceleration (Earth G’s) vs. transition start time.....311

Figure 4-115 Separation distances vs. transition start time.....312

Figure 4-116 Propellant mass vs. transition start time.....313

Figure 4-117 Altitude vs. transition start time.....313

Figure 4-118 Velocity vs. transition start time.....314

Figure 4-119 Mach number vs. transition start time.....314

Figure 4-120 Angle of attack vs. transition start time.....315

Figure 4-121 Flight path angle vs. transition start time.....315

Figure 4-122 Sensed acceleration (Earth G’s) vs. transition start time.....316

Figure 4-123 Integrated architecture modeling scope.....317

Figure 4-124 System architecture design layer development approach.....318

Figure 4-125 Exploration campaign model diagram.....319

Figure 4-126 Exploration design reference mission model diagram.....319

Figure 4-127 Exploration mission phases model diagram.....320

Figure 4-128 Exploration mission activity model diagram.....321

Figure 4-129 Operational to functional architecture cross reference matrix structure.....322

Figure 4-130 Requirements process data mapping needs.....324

Figure 4-131 Example capabilities mapping to functional & operational model.....327

Figure 4-132 Architecture context diagram.....328

Figure 4-133 Entry system mass for horizontal lander and Mid L/D aero entry system.....338

Figure 4-134 Lander mass at powered descent initiation for the horizontal lander configuration.....339

Figure 4-135 Lander mass at touchdown for horizontal lander configuration.....339

Figure 4-136 Mars Ascent Vehicle mass at ascent initiation for horizontal configuration.....340

Figure 4-137 Mars Ascent Vehicle mass at docking after return from Mars surface.....340

Figure 4-138 Entry system mass for vertical lander configuration and HIAD aero entry system.....341

Figure 4-139 Lander mass at powered descent initiation for the vertical lander configuration.....341

Figure 4-140 Lander mass at touchdown for vertical lander configuration.....342

Figure 4-141 Mars Ascent Vehicle mass at ascent initiation for the vertical lander configuration.....342

Figure 4-142 Mars Ascent Vehicle docked mass after return from Mars surface.....342

Figure 5-1 Advancing human space exploration – Saturn V, Space Shuttle, and Space Launch System..... 348

Figure 5-2 Careful planning and deliberations are helping the SLS Program meet its commitments..... 349

Figure 5-3 SLS scale relative to other U.S. systems..... 350

Figure 5-4 Flexible, modular evolution through planned block upgrades. 350

Figure 5-5 RS-25 core stage engines in inventory. 351

Figure 5-6 J-2X upper stage engine testing. 351

Figure 5-7 A 5-segment booster development test. 352

Figure 5-8 Booster qualification motor casting. 353

Figure 5-9 SLS avionics software testing. 353

Figure 5-10 Over 900 SLS wind-tunnel tests have been conducted. 353

Figure 5-11 SLS on the launch pad (artist’s concept). 354

Figure 5-12 Pursuing opportunities for affordability. 356

Figure 5-13 The SLS rocket will launch in 2017 (artist’s concept). 357

Figure 6-1 Ground system capability summary – maximum throughput. 361

Figure 6-2 Effect of launch campaign duration on launch throughput. 362

Figure 6-3 Effect of workforce on launch throughput. 363

Figure 6-4 Effect of launch infrastructure on launch throughput. 363

Figure 6-5 Effect of (a) booster and (b) payload type on launch throughput. 364

Figure 7-1 Notional Mars Transit Habitat 1000 days, 6 crew (to scale) 367

Figure 7-2 Baseline strategy - HAT MTH summary for 6 crew, 1000 days 369

Figure 7-3 Aggressive mass reduction strategy – HAT MTH summary for 6 crew, 1000 days 369

Figure 8-1 Notional image of large rovers 374

Figure 8-2 Notional image of commuter 375

Figure 8-3 Notional image of telecommuter 376

Figure 8-4 Example of alternative surface system manifests for differing transportation system options 377

Figure 8-5 The Capability Driven Framework helps to achieve an ever-expanding human presence beyond low-Earth orbit with increased flexibility, greater cost-effectiveness, and sustainability 379

Figure 8-6 Range of Mars surface exploration options in the Capability Driven Framework environment. 379

Figure 8-7 Functional breakdown to achieve the top-level objective of explore Mars 383

Figure 8-8 Evaluation matrix based on the tradable mission options and the functional breakdown of those capabilities needed to achieve surface mission objectives 383

Figure 8-9 Hardware systems and mass estimates previously described in some detail as part of DRA 5.0 that were used to provide the functions identified. 384

Figure 8-10 Mass estimates resulting from analysis of each cell in the evaluation matrix. 384

Figure 9-1 FSP concept layout 390

Figure 9-2 FSP concept schematic 391

Figure 9-3 FSP System for LAT2 Option 6 392

Figure 9-4 Mars FSP concept 393

Figure 9-5 Lander-Integrated FSP System for LSS Scenario 5 393

Figure 9-6 Scenario 5 Shielding Options 394

Figure 9-7 Mobile Fission Power System Concept 396

Figure 9-8 Deep space suit (Block 3) - baseball card 405

Figure 9-9 Exploration maintainability analysis tool structure 414

Figure 10-1 HAT cost analysis approach 418

Figure 10-2 Notional HAT architectural elements 419

Figure 10-3 HAT technology development assessment: data capture process 421

Figure 10-4 Correlation between technologies identified as critically important by HAT and high priority technologies identified by the NRC. 424

Figure 11-1 Analogue activity composition and continuum. 431

Figure 11-2 Desert RATS testing at the BPLF. 433

Figure 11-3 BPLF test site. 434

Figure 11-4 HMP traverse tests. 435

Figure 11-5 HMPRS. 436

Figure 11-6 ISRU field testing at the PISCES Test Site. 437

Figure 11-7 Rover testing to support ISRU demonstrations at the PISCES Test Site 437

Figure 11-8 International Space Station as an analogue test facility. 438

Figure 11-9 NASA Extreme Environment Mission Operations analogue testing. 439

Figure 11-10 The Aquarius testing facility. 440

Figure 11-11 Single-person submersibles as analog traverse vehicles supporting the Pavilion Lake Research Project.....	441
Figure 11-12 Pavilion Lake Research Project traverse analogue planning.....	441
Figure 11-13 Analogue mission and testing locations.....	442
Figure 11-14 Inflatable habitat analogues as tested at McMurdo Station, Antarctica.....	443
Figure 11-15 NASA, NSF, ILC Dover inflatable habitat testing.....	444
Figure 11-16 Testing at McMurdo Station in January 2008.....	445
Figure 11-17 Mars 500 day test conducted at the Russian IBMP in Moscow.....	446
Figure 11-18 Analogue testing history.....	447
Figure 11-19 Apollo LRV.....	448
Figure 11-20 D-RATS unpressurized rover tests.....	448
Figure 11-21 D-RATS pressurized rover tests.....	449
Figure 11-22 Summary of time delay experiments.....	450
Figure 12-1 Comprehensive systems engineering model incorporating the human.....	468
Figure 12-2 HRP use of Earth analogs.....	471
Figure 12-3 A simple action-reaction approach can initiate or stop the spinning. The angular momentum remains zero at all times, and multiple spin/de-spin cycles can be performed with no propellant.....	476
Figure 12-4 A rotating mass, shown in the center of this ‘vehicle’, can slew the rotational plane of the assembly and, thus, the thrust vector. It is spun only during a portion of each rotation of the assembly. Other locations of the mass in the vehicle are feasible.....	477
Figure 13-1 Composite Image of Deimos and Phobos (Credits: NASA/JPL-Caltech/University of Arizona).....	482
Figure 13-2 Notional concept for short-stay Mars vicinity operations.....	485
Figure 13-3 Notional concept for long-stay Mars vicinity operations.....	486
Figure 13-4 Notional reference landing and sampling sites on Phobos and Deimos.....	487
Figure 13-5 Goals for human presence in the Mars system.....	489
Figure 13-6 Preliminary DMC development approach.....	491
Figure 13-7 High-level concept of operations.....	491
Figure 13-8 In-system telerobotics approach.....	492
Figure 13-9 Short-stay class mission.....	494
Figure 13-10 Long-stay class mission.....	494
Figure 13-11 Total architecture mass as a function of total mission duration for high thrust propulsion concepts.....	496
Figure 13-12 Total architecture mass as a function of total mission duration for low thrust propulsion concepts.....	497
Figure 13-13 Robotically visited NEAs at approximate scale with Mars moons.....	500
Figure 13-14 Precursor platforms.....	503
Figure 13-15 Characteristics of Phobos and Deimos.....	504
Figure 13-16 Nominal areocentric inertial orbits of Phobos and Deimos.....	505
Figure 13-17 Time histories of Phobos and Deimos orbital elements.....	507
Figure 13-18 Angle between Phobos and Deimos orbit planes.....	508
Figure 13-19 Evolution of the synodic period between Phobos and Deimos.....	508
Figure 13-20 Pork Chop Contour plots for rendezvous trajectories between Phobos and Deimos using trajectory.....	510
Figure 13-21 Example optimal two-impulse rendezvous trajectories between Phobos and Deimos, three-dimensional view.....	510
Figure 13-22 Example optimal two-impulse rendezvous trajectories between Phobos and Deimos, Mars equatorial plane.....	511
Figure 13-23 Comparison of optimal rendezvous Δv and flight time between Phobos and Deimos for the precise Lambert.....	511
Figure 13-24 Phasing rates relative to Deimos as a function of altitude offset from Phobos' orbit.....	512
Figure 13-25 Phasing rates relative to Deimos as a function of altitude offset from Phobos' orbit.....	512
Figure 13-26 Example terminal rendezvous trajectory for Phobos.....	513
Figure 13-27 Example Phobos terminal rendezvous trajectory shown with unequal plot scaling, along with a detailed view of the end of the trajectory.....	514
Figure 13-28 Example terminal rendezvous trajectory for Deimos.....	515

Figure 13-29 Example Deimos terminal rendezvous trajectory shown with unequal plot scaling, along with a detailed view of the end of the trajectory.	515
Figure 13-30 Sphere of Influence and Hill Sphere radii of Phobos and Deimos.	517
Figure 13-31 Example Deimos-captured orbit (retrograde) propagated for 20 days.	517
Figure 13-32 Example Phobos-captured orbit attempt propagated for 2.4 hours.	518
Figure 13-33 Trajectory scan results for total ΔV at Mars, stay time at Mars, mission duration, and differences between asymptotic declinations for Mars arrival and departure.	522
Figure 13-34 ΔV at Mars between arrival (capture) and departure as a function of arrival and departure declinations.	523
Figure 13-35 Example optimal two-impulse transfer trajectories between highly elliptical Mars orbits of different orientations.	525
Figure 13-36 Rates at which the Ω and ω of a 250 x 33813 km altitude Mars orbit will change as a function of orbit inclination due to non-spherical Mars gravity effects (J2).	526
Figure 13-37 Relative cost of orbit reorientation techniques.	527
Figure 13-38 Example transfer to and from Phobos.	527
Figure 13-39 Typical mission profile for a Mars orbital mission.	536
Figure 13-40 Typical mission profile for a Mars surface mission.	536
Figure 13-41 Key challenges and risks for future human exploration of Mars.	540
Figure 13-42 An example development schedule flow and timing.	542
Figure 13-43 Integrated roadmap for the human exploration of Mars.	544
Figure 13-44 Preliminary Mars Science Laboratory radiation observations.	546
Figure 13-45 Key technologies for EDL, ISRU, and Mars ascent.	551
Figure 13-46 Example SLS secondary payload accommodation.	552
Figure 13-47 Planetary protection principles.	559

LIST OF TABLES



Table 1-1 Typical Mars Surface Payload Sizes	6
Table 1-2 Manifest Results for Combinations of Crew and Lander Capacity.	7
Table 1-3 Potential Venues for Testing Future Mars Systems and Technologies.	12
Table 1-4 Testing Venue Relevance to Reducing Future Human Mars mission Risk.	14
Table 2-1 Tenets of Mars Design Reference Architecture 5.0 as they Relate to an Orbital Only Mission.....	19
Table 2-2 Low-thrust Trajectory Search Space	21
Table 2-3 Payload and Propulsion System Design Characteristic Assumptions.	25
Table 2-4 Key Challenges for the Various Mars Exploration Options.	33
Table 2-5 Departure Scenario Considerations for Human Missions to Mars.	42
Table 2-6 Mass Property Discrepancies.	44
Table 2-7 Conjunction Class Mission Assumptions	46
Table 2-8 Opposition Class Mission Assumptions	49
Table 2-9: Cargo Vehicle Mass History Timeline	52
Table 2-10: Crew Vehicle Mass History Timeline	53
Table 2-11: Cargo Vehicle Trans-Mars Injection Sequence	56
Table 2-12: Crew Vehicle Trans-Mars Injection Sequence	57
Table 2-13: Crew Vehicle Mars Orbit Insertion	57
Table 2-14: Crew Vehicle Trans-Earth Injection Sequence	58
Table 2-15: Varied Assumptions in Second CFP Iteration	59
Table 2-16: Second CFP Cargo Vehicle Trans-Mars Injection Breakdown	61
Table 2-17: Second Iteration Crew Vehicle Trans-Mars Injection Maneuvers	63
Table 2-18: Second CFP Iteration Crew Vehicle Trans-Earth Injection Maneuver Magnitudes.....	63
Table 2-19: First and Second CFP Iterations Δv Comparison	64
Table 3-1 NCPS Piloted Trajectory Summary for 15-year Cycle using 4 SLS Launches.	87
Table 3-2 NCPS Cargo Aerocapture Trajectory Summary for 15-year Cycle.....	87
Table 3-3 Input Parameters for 2037 Piloted Stack Sizing Analyses	88
Table 3-4 Summary of Sizing for the 2037 Opportunity.	89
Table 3-5 Sizing Results Across 15-year Cycle.	90
Table 3-6 SLS 178.35.00 Family for Various Launch Options	92
Table 3-7 NCPS “Baseball Card” for 2037 Mission Opportunity	94
Table 3-8 NEP Study Assumptions and Requirements	98
Table 3-9 Liens Listing.....	99
Table 3-10 ΔV Summary for Case 1	107
Table 3-11 ΔV Summary for Case 2	107
Table 3-12 Mars NEP Mission Events Case 1 Conjunction	110
Table 3-13 Deep Space Habitat HAT variations	111
Table 3-14 Mars NEP MEL WBS Format--Conjunction	113
Table 3-15 Conjunction Stack Architecture	113
Table 3-16 Mars NEP Conjunction System Summary, Hab/EP Summary.....	114
Table 3-17 Mars NEP Conjunction System Summary, Hab/EP Summary.....	115
Table 3-18 Definition of the Power Modes—Mars NEP.....	115
Table 3-19 PEL/TWH Mars NEP Conjunction, Launch 1 – Hab/EP Element.....	116
Table 3-20 PEL/TWH Mars NEP Conjunction, Launch 2 – Power Element	116
Table 3-21 Mars NEP MTH Mass Breakdown.....	128
Table 3-22 Mars NEP Habitat System, Case 1 Conjunction, Hab/EP Element.....	128
Table 3-23 Mars NEP Communications Case 1 Conjunction MEL, Power Element	132
Table 3-24 Mars NEP C&DH Case 1 Conjunction MEL, Hab/EP Element	133
Table 3-25 Mars NEP C&DH Case 1 Conjunction MEL, Power Element.....	134
Table 3-26 Mars NEP GN&C Case 1 Conjunction MEL, Hab/EP Element	135
Table 3-27 Mars NEP GN&C Case 1 Conjunction MEL, Power Element.....	135
Table 3-28 Mars NEP Electrical Power System Case 1 Conjunction MEL, Hab/EP Element.....	137

Table 3-29 Mars NEP Electrical Power System Case 1 Conjunction MEL, Power Element	138
Table 3-30 Mars NEP Propulsion System (Chem Hardware) Case 1 Conjunction MEL, Hab/EP Element	140
Table 3-31 Mars NEP Propulsion System (EP Hardware) Case 1 Conjunction MEL, Hab/EP Element	141
Table 3-32 Mars NEP Propulsion (Chem Hardware) System Case 1 Conjunction MEL, Power Element	141
Table 3-33 Mars NEP Propulsion (EP Hardware) System Case 1 Conjunction MEL, Power Element	142
Table 3-34 Mars NEP Structures and Mechanisms System Case 1 Conjunction MEL, Hab/EP Element	144
Table 3-35 Mars NEP Structures and Mechanisms System Case 1 Conjunction MEL, Power Element.....	144
Table 3-36 Cold Plate & Heat Pipe Specifications.....	147
Table 3-37 Mars NEP Thermal System Case 1 Conjunction MEL, Hab/EP Element.....	151
Table 3-38 Mars NEP Thermal System Case 1 Conjunction MEL, Power Element.....	151
Table 3-39 Concept Vehicles for Mars Landing.....	153
Table 3-40 Mass Distribution of Baseline SEP-Chem Piloted Vehicle including the DSH.	160
Table 3-41 Summary of Mission and Technology Options. Key Differences between the Options are Shown in Red.	161
Table 3-42 ΔV Summary for Each Variant	161
Table 3-43 Mass Summary for Each Variant.	162
Table 4-1 Trajectory State at Insertion Plus Additional Parameters.....	177
Table 4-2 Comparison for MAV to Mars Orbit Destination and Staging.....	178
Table 4-3 Comparison for MAV Initial Thrust-to-Weight Levels.....	178
Table 4-4 Comparison for MAV Propulsion System Choices.....	179
Table 4-5 Comparison for MAV Payload (crew + samples) Sizes.....	180
Table 4-6 Comparison for MAV LOX/LCH ₄ Propulsion Options.	180
Table 4-7 LOX/CH ₄ MAV Masses for Various Mars Orbits, Staging and ISRU Options.	182
Table 4-8 MAV Options Recommended for use in Detailed Sizing Analyses	183
Table 4-9 Comparison for Descent Propulsion System Choices, 20.8 t Payload.	185
Table 4-10 Comparison for LOX/LCH ₄ MPS (pump-fed) Descent vs. Payload.....	186
Table 4-11 ENVISION Model Definition for Ascent Vehicle First Stage	188
Table 4-12 ENVISION Model Definition for Ascent Vehicle Second Stage.....	188
Table 4-13 ENVISION Model Definition for Descent Stage.	189
Table 4-14 Mid L/D Architecture Wet Entry Mass.	192
Table 4-15 Mid L/D Architecture Lander Mass.	193
Table 4-16 HIAD Architecture Wet Entry Mass.	196
Table 4-17 HIAD Architecture Lander Mass	197
Table 4-18 General Configuration and Analysis Assumptions.....	203
Table 4-19 Descent Module Propellant Volume and Engine Assumptions.....	204
Table 4-20 Cargo Element Assumptions.	205
Table 4-21 Mars Ascent Vehicle Assumptions.	206
Table 4-22 System-level Figures of Merit for Evaluating Lander Configurations.	217
Table 4-23 Horizontal Lander Basic Mass Summary.....	226
Table 4-24 Horizontal Lander, 1st Lateral Mode Frequency Results.	227
Table 4-25 Vertical Lander Basic Mass Summary.....	229
Table 4-26 Vertical Lander, 1st Lateral Mode Frequency Results	230
Table 4-27 Comparison of H3, V1 and TeamX Structural Mass Estimates	231
Table 4-28 Sink Temperatures for LEO, Transit, & Mars Orbit.	240
Table 4-29 Descent Vehicle CRYOSIM Results.....	241
Table 4-30 Ascent Vehicle CRYOSIM Results.....	241
Table 4-31 Ascent Vehicle CRYOSIM Results.....	242
Table 4-32 Ascent Vehicle CRYOSIM Results.....	243
Table 4-33 MDM Configuration Basic Mass Summary (no growth/margin allocation).	245
Table 4-34 HIAD plus SRP plus Vertical Lander: Mass Results.	249
Table 4-35 HIAD plus SRP plus Vertical Lander: Engine Assumptions.	249
Table 4-36 HIAD plus SRP plus Vertical Lander: Conditions at Terminal Descent Initiation.	249
Table 4-37 Rigid Aeroshell plus SRP plus Horizontal Lander: Mass Results.....	250
Table 4-38 Rigid Aeroshell plus SRP plus Horizontal Lander: Engine Assumptions.....	251
Table 4-39 Rigid Aeroshell plus SRP plus Horizontal Lander: Conditions at Terminal Descent Initiation.....	251
Table 4-40 Habitable MAV Crew Cabin Mass Comparison.	263

Table 4-41 4-Crew Taxi MAV Mass Summary	269
Table 4-42 6-Crew Habitable MAV Propellant Load.....	273
Table 4-43 4-Crew Taxi vs. Habitable Variant Volume Comparison.....	277
Table 4-44 Flight Conditions at the Start of Transition.....	306
Table 4-45 Thrust and Mass Properties at the Start of Transition.	307
Table 4-46 Ground Rules, Assumptions, and Constraints.	307
Table 4-47 Model Framework Data Types.....	323
Table 4-48 Framework Data Architecture.	325
Table 4-49 Summary of Mars Lander technology Needs.	332
Table 5-1 Selected SLS Life-Cycle Milestones.....	356
Table 7-1 Deep Space Habitat Sizing Assumptions.	368
Table 7-2: Comparison of Gross Masses between HAT Assumptions and Aggressive Mass Reduction Assumptions.....	370
Table 8-1 Manifest Results for Combinations of Crew and Lander Capacity	377
Table 9-1 FSP-Derived Requirements.....	389
Table 9-2 FSP Mass Summary	391
Table 9-3 Scenario 5 Power Transmission Analysis	395
Table 9-4 Mobile Fission Power System Mass Summary	396
Table 9-5 Crew Requirements	406
Table 9-6 Gas and Liquid Assumptions	406
Table 9-7 Logistics Required for a 900-day Mars Mission	407
Table 9-8 Supportability Strategy Elements	410
Table 10-1 Technologies That Enable Human Space Exploration	422
Table 10-2 NRC’s “Top 16” Technologies, with HAT Human Exploration Focused Critical Technologies Shown in Bold.....	424
Table 10-3 Technologies Mapped to Elements and Destinations.....	426
Table 12-1 HRP Research Ratings for Mars Surface Missions (DRA 5.0)	466
Table 12-2 Research Ratings for Mars Orbital Missions.....	467
Table 13-1 Characteristics Deimos and Phobos.	482
Table 13-2 Implementation Implications of Science Objectives.	488
Table 13-3 Implementation Implications of Exploration Objectives.....	490
Table 13-4 High and Medium MPD Cislunar Synergies Priorities.	499
Table 13-5. SKGs Related to an Orbital Mission	501
Table 13-6 SKGs Related to a Mission to Phobos or Deimos.	502
Table 13-7 Minimum, Mean, and Maximum Values for Phobos' Classical Keplerian Orbital Elements during the Interval between 2030 and 2040.	506
Table 13-8 Minimum, Mean, and Maximum Values for Deimos' Classical Keplerian Orbital Elements during the Interval between 2030 and 2040.	506
Table 13-9 Example Terminal Rendezvous Sequence for Phobos.	513
Table 13-10 Example Terminal Rendezvous Sequence for Deimos.....	514
Table 13-11 Example Maneuver Sequence in which Deimos is Visited First, then Phobos.	520
Table 13-12 Example Maneuver Sequence in which Phobos is Visited First, then Deimos.	521
Table 13-13 Total Δv (m/s) / Total Flight Time (hours) Required to Transfer between 250 x 33813 km Altitude Mars Orbits with $\Delta i = 5^\circ$ as a Function of $\Delta\Omega$ and $\Delta\omega$, using Minimum Δv Two-impulse Transfers.	524
Table 13-14 Total Δv (m/s) / Total Flight Time (hours) Required to Transfer between 250 x 33813 km Altitude Mars Orbits with $\Delta i = 20^\circ$ as a Function of $\Delta\Omega$ and $\Delta\omega$, using Minimum Δv Two-impulse Transfers.	524
Table 13-15 Total Δv (m/s) / Total Flight Time (hours) Required to Transfer between 250 x 33813 km Altitude Mars Orbits with $\Delta i = 45^\circ$ as a Function of $\Delta\Omega$ and $\Delta\omega$, using Minimum Δv Two-impulse Transfers.	525
Table 13-16 Total Δv (m/s) / Total Flight Time (hours) Required to Transfer between 250 x 33813 km Altitude Mars Orbits with $\Delta i = 70^\circ$ as a Function of $\Delta\Omega$ and $\Delta\omega$, using Minimum Δv Two-impulse Transfers.	525

Table 13-17 Mars Arrival and Departure Vectors for Short-Duration (opposition class) Missions 2020–2050.....	528
Table 13-18 DSV Transfers for 250 km x 1 sol Parking Orbits with Equal Weighting on DSV and SEV ΔV	529
Table 13-19 Exploration Vehicle Transfers for 250 km x 1 sol Parking Orbits with Equal Weighting on DSV and SEV ΔV	530
Table 13-20 Deep Space Vehicle Transfers for 250 km x 1 sol Parking Orbits with Full Weighting on DSV ΔV	530
Table 13-21 Space Exploration Vehicle Transfers for 250 km x 1 sol Parking Orbits with Full Weighting on DSV ΔV	531
Table 13-22 Deep Space Vehicle Transfers for 250 km x 3 sol Parking Orbits with Full Weighting on DSV ΔV	531
Table 13-23 Space Exploration Vehicle Transfers for 250 km x 3 sol Parking Orbits with Full Weighting on DSV ΔV	532
Table 13-24 Human Support Challenges.....	539
Table 13-25 Example Risk Mitigation Venues for Top Exploration Risks.....	540
Table 13-26 Schedule Development Subject Matter Experts.....	543

1. SUMMARY OF ASSESSMENTS CONDUCTED SINCE DRA 5

1.1. Lunar Capability Concept Review (2008)

Primary Contributors:

Bret G. Drake, National Aeronautics and Space Administration, Johnson Space Center

During formulation of the Mars Design Reference Architecture (DRA) 5.0,¹ several human exploration related activities were being conducted in parallel. The initial framing of the Global Exploration Strategy² included dialog and workshops with 17 international space agencies and science organizations focused on goals and objectives of future exploration endeavors. During that same time period, NASA chartered the Lunar Architecture Team to play a key role in the continual development and implementation of the strategies outlined in the Vision for Space Exploration,³ NASA Authorization Act of 2005,⁴ and later the NASA Authorization Act of 2008.⁵ The Architecture Team was a comprehensive Agency effort that included contributions from more than 200 NASA personnel representing nine NASA Centers with emphasis to:

- Develop a baseline architecture for robotic and human lunar missions that can be traced directly to specific objectives;
- Formulate a concept of operations for planned lunar missions;
- Develop individual requirements for incorporation into NASA’s Exploration Architecture Requirements Document; and
- Assess functional needs and analyze required technologies.

Throughout all of these studies and activities, Mars was consistently used as the long-term destination to frame the discussions and future planning. NASA was continuing the definition of the key elements of the Constellation Program (CxP), namely the Ares-I/Ares-V launch vehicles, Orion crew exploration vehicle, and supporting ground operations infrastructure. The framework for the Constellation Program was to establish core capabilities that could be utilized for numerous future destinations including human missions to the Moon and Mars. Although the original framing focused on the Moon, with Mars as the ultimate destination, it was recognized that the decision to terminate the Space Shuttle Program to free funding for exploration endeavors would leave a deficiency in the ability of the United States to deliver crew and cargo to the International Space Station (ISS).¹ Thus, early emphasis was placed on establishing initial capabilities to support the operations of the ISS, with missions to the Moon as the logical next step.

As the formulation of the ISS support elements proceeded through their initial programmatic design phases (Systems Requirements Review and Systems Definition Review), Agency management determined that a key checkpoint was necessary to provide further definition of the future lunar program elements, including demonstration of direct applicability of the Initial Capability elements supporting ISS operation (Ares-I, Orion, and ground operations) in that formulation. This synchronization between the initial capability (ISS focused) and lunar capability needs was accomplished through the Lunar Capability Concept Review (LCCR), which was conducted in June 2008 in parallel with the Initial Capability Systems Definition Review.

The purpose of the LCCR was to define a point of departure transportation architecture for the CxP lunar capability including the ability to deliver and return crew to the surface of the moon for short duration (i.e., human lunar return) and evolve to the establishment of a lunar outpost. Although the LCCR focused on the conceptual designs and key driving requirements for Ares V launch vehicle and Altair crew and cargo lunar landers, the review showed how the transportation architecture, including extravehicular activity (EVA) and ground operations could support a range of mission campaigns and possible surface architecture solutions. Although specific concepts for neither the lunar surface systems, nor human missions to Mars, were explicitly included in the LCCR success criteria, the lunar

¹ This period was commonly referred to as the “gap”, or the time between Shuttle decommissioning and when the Ares-I and Orion systems would be available to support ISS operations.

surface and Mars mission concepts were used to help formulate the key driving requirements for the initial capability systems. The ability of the LCCR transportation elements to meet key Mars needs was included via an extensibility figure of merit. Since the LCCR focused predominately on the transportation capability necessary for human lunar return, namely the Ares-V launch vehicle and Orion crew vehicle, assessments were conducted on those elements to determine their applicability to Mars missions.

As described in Mars DRA 5.0, the reference architecture requires launch and aggregation of mission elements in low-Earth orbit (LEO) for checkout prior to departure for Mars. In the initial framing of DRA 5.0, both the Nuclear Thermal Propulsion (NTP) and chemical propulsion architectures would utilize a reference launch vehicle that could provide approximately 120 t to LEO. This notional launch vehicle capability not only would include adequate mass performance, but also would include a large payload shroud necessary to encapsulate the anticipated size of the Mars payloads. In addition, assessments were conducted on some elements, namely the NTP system, to determine whether the number of launches could be reduced by trying to find an appropriate match between mass and volume performance of the launch system. Follow-on studies showed that a good balance could be found when the appropriate launch vehicle mass and volume capabilities could be “matched” with the specifics of the in-space transportation system [Borowski, 2009]⁶. Specifically, the number of required launches could be reduced from nine to seven with a launch vehicle performance of 140 t and corresponding payload shroud of 10 m by 30 m in diameter and length respectively. This mass/volume matching is especially important with the NTP transportation concept since the hydrogen propellant requires more volume than the other transportation concepts assessed.

During LCCR, an assessment was made to determine how well the emerging Ares-V lunar launch vehicle could be utilized for future Mars missions. As the lunar systems trade space evolved, assessments were made to determine the specific performance of the leading Ares-V launch vehicle concepts, namely the 51.00.48 and 51.00.47 configurations. As shown in Figure 1-1, these launch systems could deliver approximately 154 t and 162 t to a reference circular orbit with an altitude of 222 km. Although slightly lower than the reference 407 km altitude orbit used in formulation of DRA 5, it was determined that these reference configurations could provide ample launch vehicle performance in terms of both launch mass and volume for the envisioned future human missions to Mars. This included options for pure payload delivery to LEO (131 t and 137 t) as well as options where the launch vehicle shroud could be used as a dual-purpose system comprising the aerobrake at Mars. In this dual use shroud mode, it was estimated that between 84 and 90 t would be available for the Mars lander, which is far greater than the Mars DRA 5 estimated lander wet mass of 67 t². The Lunar Capability Concept Review concluded that the Ares-V launch vehicle concepts would provide adequate performance in terms of both mass and volume. This is an important finding, especially in light of the degraded performance associated with the current [circa 2012] Space Launch System, which would provide less performance in terms of both mass and volume, to a sub-orbital staging point. Reduction in launch vehicle payload mass, volume, and delivery point (negative perigee staging) would place greater demands on the in-space transportation elements and result in additional launches necessary to conduct both the cargo and crew Mars missions. The current status of the Space Launch System is discussed in more detail later in this Addendum.

Assessments were also conducted regarding the Orion crew exploration vehicle to assess the applicability of the vehicle in supporting Mars mission needs. Emerging from DRA 5.0, the following key capabilities would be required from the Orion system:

- Delivery of 6 crew to LEO
- Return of crew (direct entry) at the end of the Mars mission
- Active crew duration of 21 days
- Dormant duration of 900 days after mission initiation
- Entry speed at Earth return less than 12 km/s

The Lunar Capability Concept Review concluded that the Orion block upgrade strategy (Block 3 composing the upgrades necessary for Mars missions) remained a viable strategy and an enabling element of future human Mars missions. Crew delivery to LEO would be encompassed by LCCR Orion concept. As depicted in Figure 1-2, assessments also determined that the Earth return entry speeds would be within “Orion family” at 12 km/s and the

² Since the aeroshell mass is considered part of the launch vehicle in this dual shroud mode, the wet mass does not include the aeroassist system but only the descent stage mass.

Orion lunar skip entry techniques directly applicable to Mars Earth return as well as Mars aerocapture. The LCCR process provided guidance on further follow-on assessments including the need for refinements to service module (tailor for the overall less demanding Mars mission requirements for delta-v and crew consumables), assessment of dormant timeline, and incorporation of lightweight thermal system approaches to increase entry speed capabilities and reduce mass.

1.2. Review of U.S. Human Spaceflight Plans Committee (2009)

Primary Contributors:

Bret G. Drake, National Aeronautics and Space Administration, Johnson Space Center

In May 2009, the White House announced the formation of an independent committee that was charged to review the U.S. human spaceflight plans.⁷ Specifically, the committee was charged with “assess[ing] a number of architecture options, taking into account such objectives as: 1) expediting a new U.S. capability to support use of the International Space Station; 2) supporting missions to the Moon and other destinations beyond low Earth orbit; 3) stimulating commercial space flight capabilities; and 4) fitting within the current budget profile for NASA exploration activities.” The committee formed four separate subgroups organized to address different aspects of the overall committee’s charter. At the request of the exploration sub-committee, NASA provided mission and system architecture assessments for consideration by the overall committee. NASA support was initiated June 30, 2009, and was completed by the end of July 2009. Findings of the Committee were released in October 2009.⁸ This section provides a summary of the NASA Mars-related assessments conducted at the request of the Committee.

1.2.1. Mars Relevant Scenarios

The beyond LEO subgroup outlined five architectures constructed to assess different potential exploration scenarios, including: A) Lunar Base, B) Lunar Global, C) Moon to Mars, D) Mars First, and E) Flexible Path.

Scenario C - Moon to Mars: Moon to Mars, or more completely Moon on the way to Mars, is a fundamentally different idea than proposed in the beyond LEO’s subgroup Lunar Global scenario. In this scenario, the primary objective would be Mars exploration. All systems would be designed for Mars, and a development and test plan would be created to reduce risk and gain confidence and experience with the Mars exploration system. When beneficial to use the Moon as a true test bed for these Mars exploration systems, flights to the Moon would be conducted. The Moon would not be a conceptual test bed for Mars, but an actual test bed for Mars. Since all recent Mars design reference missions call for extended sorties, this would be surface exploration mode on the Moon as well. From an international perspective, the United States would be a clear leader in this program. Commercial participation would be enhancing, probably be limited to activities such as launch to LEO. The human exploration of the Moon and Mars would be complementary to the ongoing robotic exploration, and synergies would be exploited, but would not fundamentally drive the program.

Scenario D – Mars First: Mars First is, as the name implies, a plan to exclusively pursue human exploration of Mars as fast as possible, without using the Moon as a first destination for any purpose. Exploration would be done in extended sorties, but technology now would become an enabler, as systems such as nuclear rockets and/or Mars atmospheric aero breaking and aero capture become essential much more so than in other scenarios. Again, the United States would be the clear leader of the program within the international community, and commercial participation would be enhancing, probably limited to launch to LEO. The human exploration would be complementary to the robotic exploration of Mars.

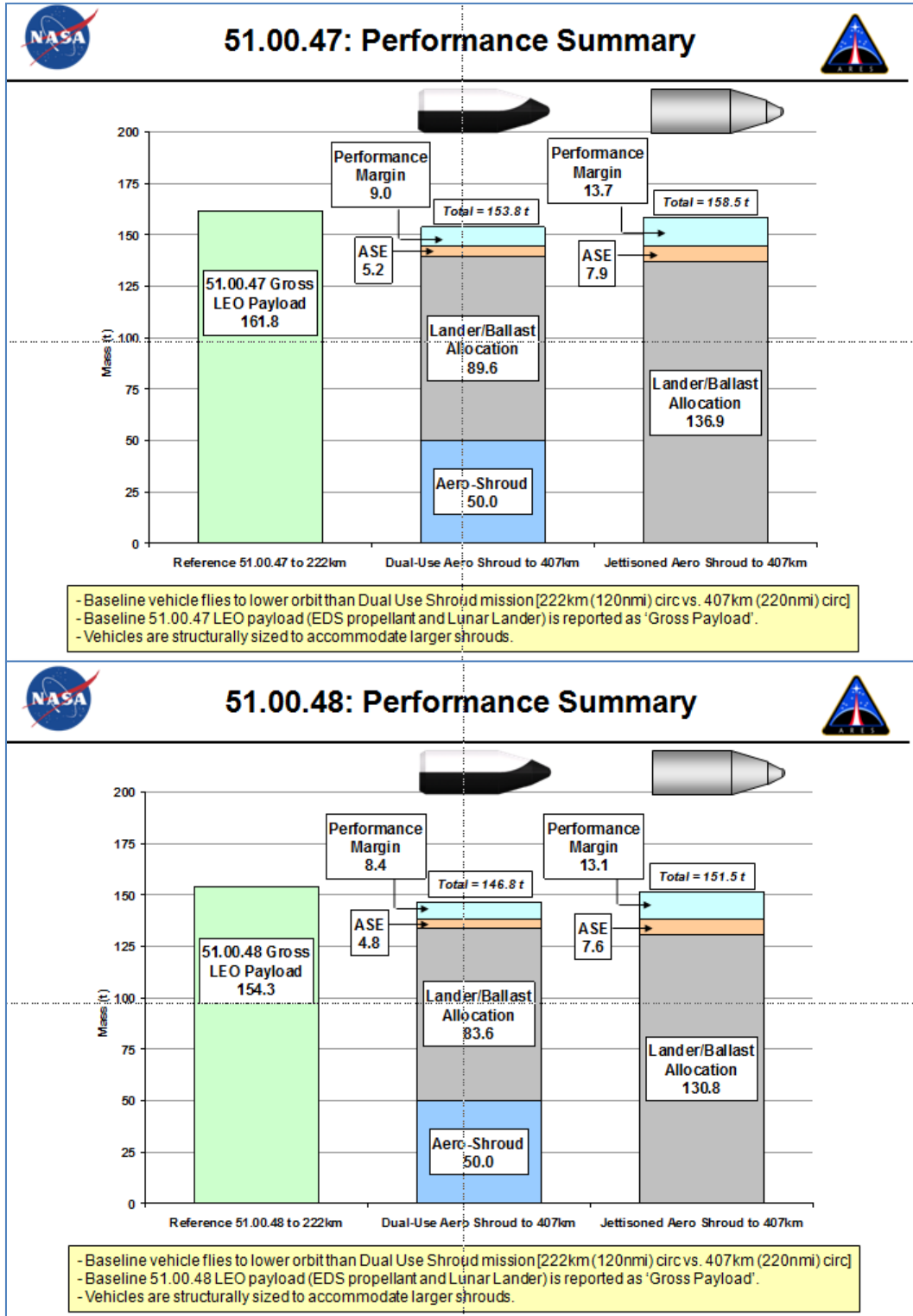


Figure 1-1 LCCR era Ares-V launch vehicle capabilities for Mars missions.

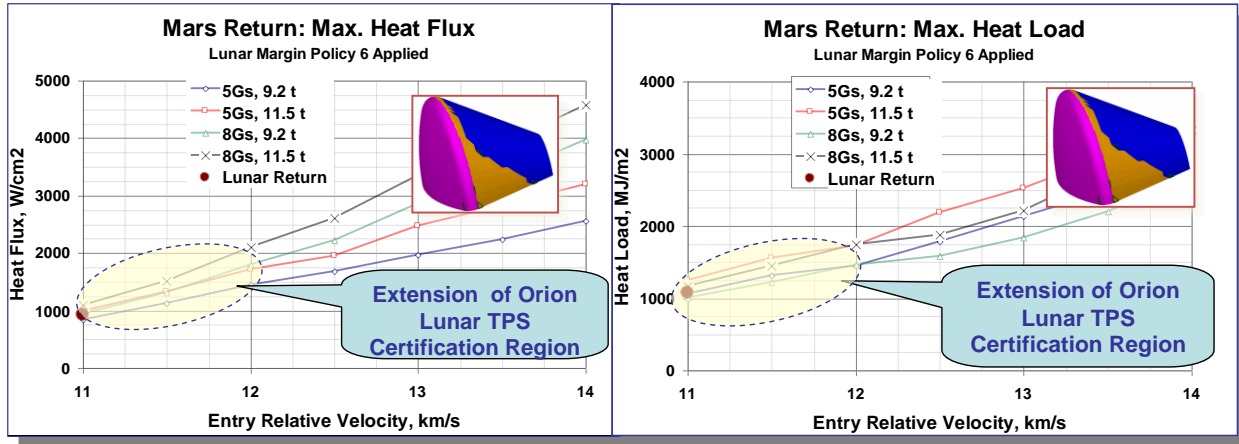


Figure 1-2 LCCR era Orion crew vehicle capabilities for Mars missions.

1.2.2. Assessments Conducted at the Request of the Committee

Due to the time constraints under which the Committee was operating, complete end-to-end architecture analyses were not possible. Instead, emphasis was placed on those aspects of the mission architecture that would provide the best insight into the Committee’s deliberations, namely launch vehicle requirements and relationship of the longer-term Mars needs with more near-term activities such as operational and systems testing.

1.2.2.1. Payload to the Surface of Mars

The beyond LEO subgroup requested data to provide better insight into the relationship between the payload landed on the surface of Mars and how that translated into the overall lander size and resulting architecture. During formulation of DRA 5.0, emphasis was placed on trying to find a good match between the lander size, as measured by the total mass of payload the lander could deliver to the surface, number of landers within the architectural framework necessary to satisfy the goals and objectives, and complexity of the operations required to establish surface operations. This analysis resulted in a strategy whereby two landers, each capable of landing approximately 40 t of useful payload on the surface, would be utilized to support a crew of six for 500 days on the surface of Mars. The Committee’s beyond LEO subgroup was interested to know what other strategies were available to potentially reduce the size of the landers and how that strategy affected the resulting architecture.

The surface strategy portion of this assessment involved assembling manifests for all of the combinations of two different crew sizes (four and six crew members) with three different lander sizes (delivered payload capacities of 10, 20, 30, and 40 tons). Due to time constraints, it was not possible to put significant effort into assessing the ability of these crews to accomplishing specific scientific or mission objectives; no relevant baseline existed against which such a comparison could be made. Rather this became an exercise in distributing surface systems identified in DRA 5 (appropriately scaled for the crew size) among as many landers as necessary to deliver the mission payload. Table 1-1 provides an example of the size of typical payload elements, quantity required, and whether the payload can be further subdivided; i.e., could potentially be split up and manifested on different landers, if required. As the payload elements are manifested onto more landers, due to reduced lander performance, additional surface operations are required to assemble the elements together to meet the functional needs of the mission. This table demonstrates that many of the payload elements could be accommodated on the range of landers considered from 20 to 40 t payload capabilities, but the 10 t landed capacity would require further subdivision of the habitat function among multiple landers, thus increasing the operational complexity.

The other major element required to be landed on the surface of Mars is the ascent vehicle, which would be used by the crew to depart Mars surface. Understanding the minimal size of the ascent stage is important since it represents one of the largest elements that must be landed on Mars intact. That is, assembly of an ascent stage on the surface of Mars comprised of smaller, multiple indivisible units, was not deemed practical. Top-level sensitivity analyses were conducted on different ascent stage strategies including sensitivity to crew module mass; stage dry (inert) mass, and

propulsion system performance (pressure fed and various pump fed concepts). To reduce the total mass landed on the surface of Mars, for these analyses it was assumed that all of the ascent oxidizer (oxygen in this case) would be produced via In-Situ Resource Utilization (ISRU) by extracting the oxygen from the atmosphere of Mars per the concepts outlined in DRA 5.0. For this strategy, the fuel (methane in this case) was assumed to be brought from Earth in the ascent stage. Thus, these options represent the near-minimum mass required to be landed on the surface (stage inert mass, crew module, and ascent fuel), but not the oxidizer. Results for the sensitivity analysis on differing assumed stage performance, pressure and pump fed, are provide in Figure 1-3. Examination of this figure shows that the minimum stage size representing the most aggressive assumptions is 15 t when the fuel is taken from Earth. Also, only the most aggressive cases where all propellant is delivered separately from the ascent stage accompanied with aggressive mass properties (total inert mass plus crew module mass of 5 t) are able to come close to the 10 t landed limit. From this analysis it was determined that a 10 t landed delivery capability would be insufficient and a more reasonable lower limit would be on the order to 20 t to allow for other manifested items, systems growth and margin. Figure 1-3 also shows the total wet mass prior to ascent from the surface of Mars, as represented by the height of each representative bar (inert mass + fuel + oxidizer). As can be seen from this figure, typical wet ascent stages would be on the order of 40-60 t. This demonstrates further how the incorporation of ISRU into the overall architecture can drastically reduce the lander delivery requirement to the surface of Mars, where the produced oxygen, represents nearly 60% of the wet ascent stage mass.

Results from these assessments indicated that the ascent vehicle and the habitat were the systems determined the largest individual elements that the lander needed to deliver to accomplish a surface mission. Further subdividing either of these systems was not considered a viable approach. Due to the transit time required to get to Mars, on the order of 180 days or more, it is anticipated that upon arrival the crew would be deconditioned to the gravity environment of the surface. Current assessments from the Human Research Program indicate that sufficient time, on the order of 7-14 days, should be provided for the crew to acclimate to the surface gravity of Mars³. During this period, critical time-dependent activities required by the crew should be minimized to the greatest extent possible. Thus, significant surface assembly operations, such as construction or major outfitting of the surface habitat or assembly of the ascent stage, would need to be conducted robotically: 1) by the crew upon arrival, or 2) from Earth with much longer communication delays. The remaining item on the manifest of surface payload could be reasonably distributed on the landers carrying these two large systems or placed on additional landers. The results of this manifesting exercise are summarized in Table 1-2.

Table 1-1 Typical Mars Surface Payload Sizes

Payload	6 Crew 40 t Lander		4 Crew 20 t Lander		Can Payload be Subdivided?
	Qty.	Unit Mass (kg)	Qty.	Unit Mass (kg)	
Crew Consumables	1	7940	1	5220	Yes
Science	1	1200	1	960	Yes
Robotic Rovers	2	200	2	200	No
Drill	1	250	1	250	No
Unpressurized Rover	1	200	1	200	No
Pressurized Rover	2	7500	2	7500	No
LOX Transfer Cart	0		2	400	No
Habitat	1	24560	1	19870	No
Stationary Power System	2	7800	2	7800	No
ISRU Plant	1	1230	2	1230	No

³ The time required for the crew to acclimate to the surface environment of Mars is highly dependent on crew selection, countermeasures instituted and followed by the crew during transit to Mars, the health and medical equipment provided in the transit habitat, and the degree of difficulty and timeline associated with crew critical tasks. The HRP continues to gain vital data from each ISS crew rotation, each of which simulates the 180-day transit to Mars. Through this research program, it is anticipated that the acclimation time may not be as long as outlined in DRA 5, but a final determination has not been made as of this writing.

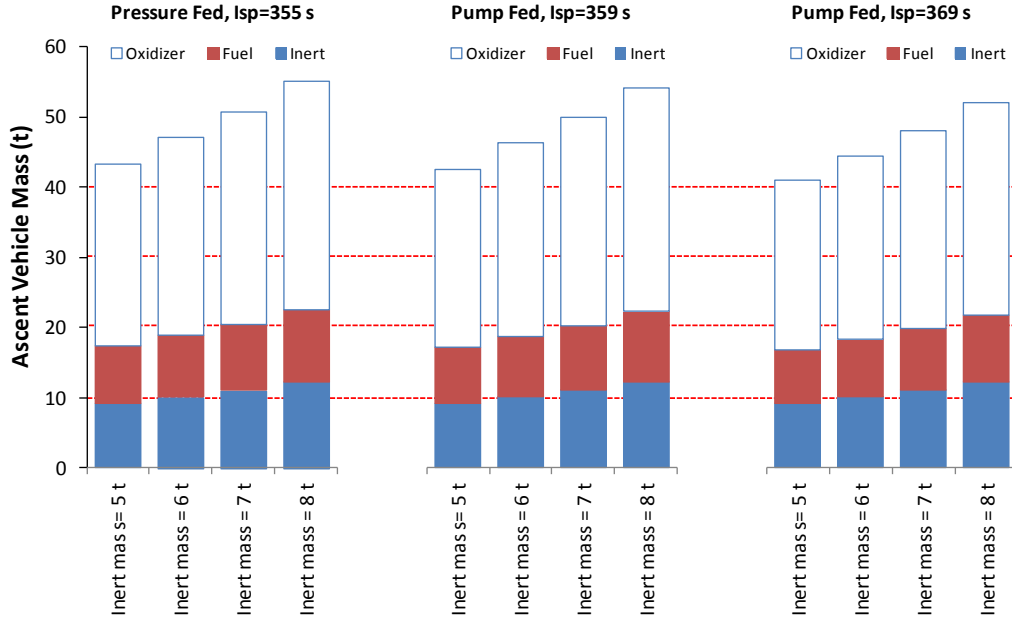


Figure 1-3 Mars ascent stage minimum size for various stage concepts.

Table 1-2 Manifest Results for Combinations of Crew and Lander Capacity

Number of Crew	Lander Payload Mass Capacity (t)	Total Delivered Surface Payload Mass (t)	Number of Landers Required	Wet Lander Mass (t)
6	40	88.4	2	111.1
6	30	89	3	84.5
6	20	(too small)	N/A	N/A
6	10	(too small)	N/A	N/A
4	40	80.2	2	106.8
4	30	80.2	3	84.7
4	20	82.2	4	68.9
4	10	(too small)	N/A	N/A

Several surface strategy-related observations can be made from these results. For the 6 crew, 40 t lander case, the total landed payload mass exceeded the stated capacity of the lander by approximately 10 percent. Normally, this would have caused the estimates for the payload to be reexamined or the lander and other entry systems to be resized. However, an initial examination of the payload mass estimates indicated at least one of the payload compliments (i.e., the ascent stage, ISRU, and power plant combination) was unlikely to be reduced in mass and insufficient time was available during this assessment to resize the Entry, Descent, and Landing (EDL) elements. Thus, the results were acknowledged to be undersized in this one case. For the six-person crew cases, the 20 t capacity lander was found to be too small to land the ascent stage even with no other payload on board, defining a lower bound on the landing system and other associated elements in the transportation system.

In the four-person crew cases, the surface system payloads could be redistributed among two 40 t landers or three 30 t landers without change to surface operations. However, for a 20 t lander case the previously assumed strategy of landing an ascent stage, ISRU plant and power plant as a single package could no longer be accomplished. The

ISRU plant and power plant were placed on a separate lander. This required the introduction of temporary storage tanks and propellant transfer vehicles to offload propellants from the “ISRU lander,” move these commodities to the ascent stage and then load the propellants into the ascent stage as shown in Figure 1-4. These additional systems are the cause of the increased total delivered surface payload mass seen in Table 1-2. Thus, subdividing the number of elements across multiple additional landers increases the complexity of surface operations required to complete the mission. One last observation from the results of this table is that the difference in total delivered surface payload mass and initial mass in low-Earth orbit (IMLEO) requirement for a crew of four and a crew of six is relatively small – on the order of five percent or less, even after the ascent vehicles, surface habitats, and crew consumables were resized for these different crew sizes. This observation is consistent with other comparisons of crew size discussed in this addendum. Namely, that the mass associated with a Mars mission does not scale linearly with the size of the crew, and that once a basic capability to transport and support a crew, changes in the size of the crew have a relatively small impact on the overall mass of the mission.

Total mission mass as measured by the initial mass in LEO was determined to provide further insight into how manifesting the necessary surface elements onto additional landers affects the resulting launch campaign and launch vehicle size. Figure 1-5 provides the launch vehicle results for both the Nuclear Thermal Propulsion (NTP) and chemical propulsion cases. These launch vehicle results are provided for both the NTP and chemical architectures for combinations of four or six crew with lander capacities of 20 t or 40 t of useful payload to the surface of Mars.

Figure 1-5a presents the results of the required size of the launch vehicle in terms of useful payload delivered to LEO. In this analysis, LEO is defined as a circular 400 km orbit at Earth at the necessary inclination required for the necessary Earth departure maneuver. As can be seen from this figure, both the NTP and chemical architectures require launch vehicle performance of approximately 120 t – 140 t to LEO. The NTP architecture tends to require more launch vehicle performance only if it can achieve a good match of payload shroud volume. This “matching” of launch vehicle mass and volume for the NTP architecture allows closure of the strategy with fewer overall launches as shown in Figure 1-5b. As can be seen, the NTP architecture requires fewer overall launches than the chemical architecture, due to the higher performance of the NTP propulsion technology. Figure 1-5c provides the volume needs for the two propulsion concepts. Due to the low packaging efficiency of the liquid hydrogen associated with the NTP concept, the NTP architecture requires much larger launch vehicle shrouds. Whereas chemical propulsion packages better requiring smaller launch vehicle shrouds, it required more launches and higher overall mass than the NTP concept.

Figure 1-5d provides a summary of the total architecture mass associated with the crew and lander delivery options. Two general trends appear. 1) Architecture mass increases as less-efficient propulsion concepts are considered. This is evident in the upward trend in mass from NTP to chemical in Figure 1-5d. 2) The architecture mass also increases as the surface payloads are manifested on smaller landers. This affect is predominately due to the fact that additional “un-used” inert mass, in the form of the landers themselves, must be introduced into the overall architecture to land the payloads in additional packages on the surface. That is, an inherent architectural efficiency can be gained by using fewer larger landers.

1.2.2.1. Testing Venues to Reduce the Risk for Human Missions to Mars

As was described previously, the beyond LEO subgroup outlined five scenarios to help drive different implementation and technology strategies for future exploration endeavors. Scenarios C and D, “Moon to Mars” and “Mars First,” respectively, represented two different paths for Mars exploration with primary focus on different strategies associated with the testing and validation concepts that might be necessary prior to execution of the actual human mission to Mars. The Committee was also interested in the role of the Moon as a testing venue prior to future Mars exploration.

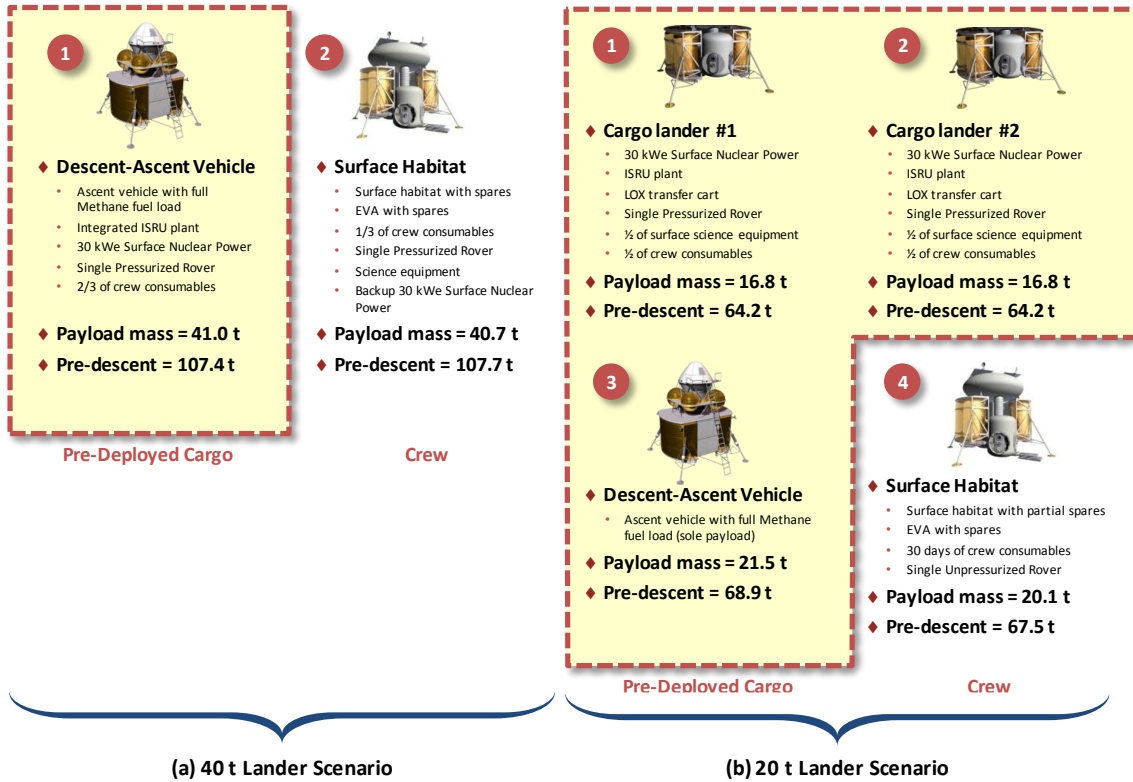


Figure 1-4 Surface manifest for differing landed payload capabilities.

At the request of the Committee, NASA conducted several workshops specifically focusing on the test and validation strategies necessary for a balanced risk posture for future Mars missions. Specifically, these workshops assessed verification and validation strategies that would ensure the safety and effectiveness of Mars exploration systems, including, but not limited to: use of ground test facilities; use of analog test sites on the Earth; atmospheric flight testing; testing of human performance on ISS; lunar surface tests and robotic tests. In this context, emphasis was placed on deciding what could be done on the Moon for testing of Mars-bound systems and elements, thereby minimizing the specialization of the equipment for the Moon.

Key focus for these workshops included:

- What must be tested?
- Why must it be tested?
- How much must be tested?
- How relevant are various testing venues in the testing strategy?
- What are the risks if the testing activity is not conducted on the Moon?

Testing encompassed all aspects of future Mars missions including testing technologies at various levels of maturity, systems and capabilities, as well as operational testing. Table 1-3 provides a list of the example testing venues considered. These venues range from Earth-based laboratories, to robotic missions, as well as operational tests with humans in deep space.

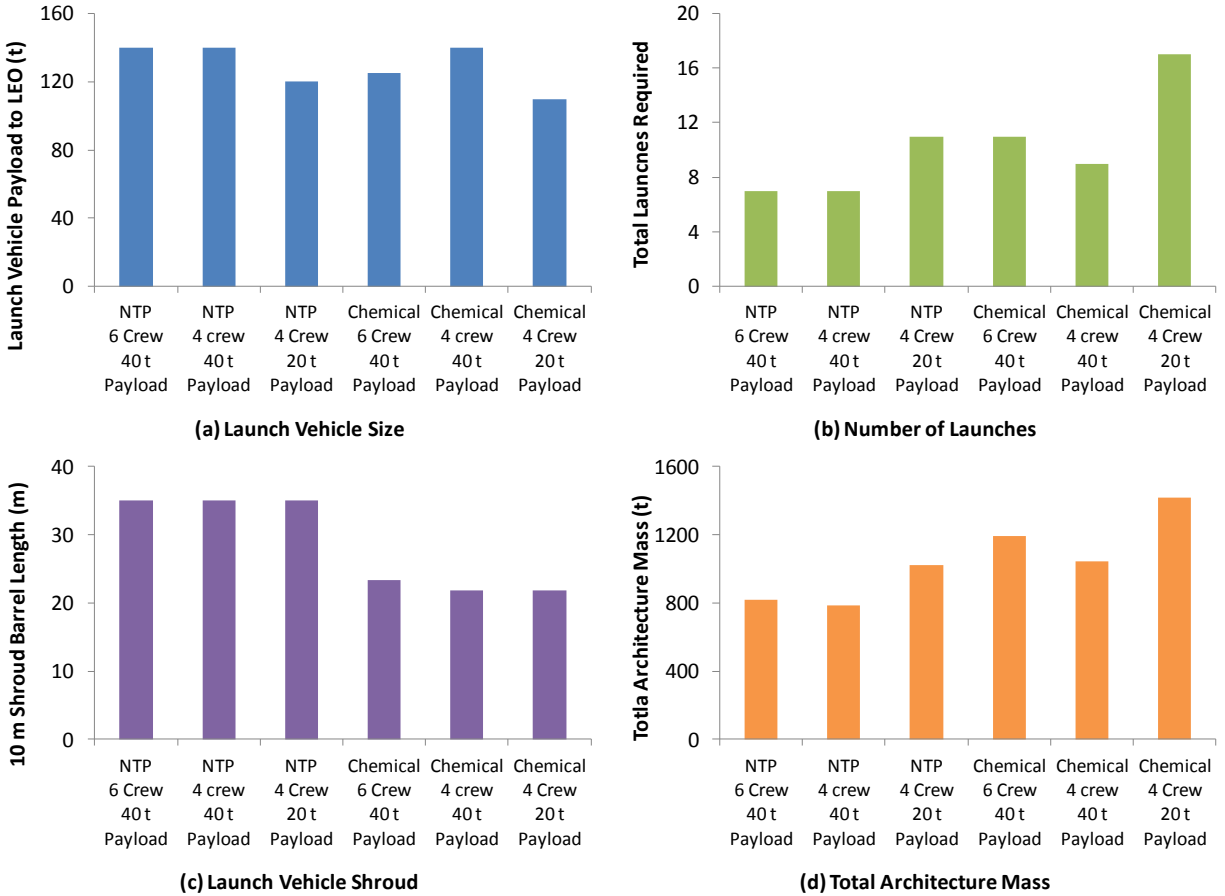


Figure 1-5 Influence of number of crew and payload size on key launch vehicle characteristics.

Through this assessment process, subject matter experts from across the Agency were solicited to provide their expertise into the relevancy of each of the potential testing venues in mitigating key risks for their system, subsystem, or technology. The resulting relevancy of the various testing venues is provided in Table 1-3.

For these assessments, the following criteria were used to measure relevancy:

- Preferred Testing Location: Denotes a preferred testing venue. Expected data return considered to be very relevant. Testing venue adequately represents flight-like conditions, environments, or constraints.
- Most Relevant: Testing venue provides flight-like conditions, environments, or constraints. Although this venue can serve as a good testing location, the expected difficulty or costs are expected to be higher than a preferred location.
- Somewhat Relevant: Testing venue can serve only as a moderately good location. Environmental conditions are expected to be not flight-like or of sufficient to derive adequate testing or operational performance data.
- Less Relevant: Venue is not considered to be an adequate location for testing that specific subsystem or system.

Key overall findings from this workshop activity in many respects mirrored the findings from previous similar assessments.⁹ Testing of large and subscale integrated systems with humans is an absolute necessity in terms of preparing for human Mars missions. That is, tests of Mars prototype systems should be conducted in environmentally similar “flight-like” conditions. In addition, due to the fact that the elements of a typical Mars mission must be launched separately and assembled in orbit prior to use, testing in space is required to evaluate the performance of large integrated systems in deep-space conditions. Human exploration of Mars should begin first with test missions that are short in duration and conducted relatively close to Earth. These near-term human

missions in near-Earth space are an essential element of revitalizing exploration experience and technical competence needed for future deep-space missions. Robust robotic missions are a vital element of risk reduction strategies for future human exploration of Mars, including gathering necessary environmental data as well as demonstrating sub-scale human relevant mission technologies. Demonstration of applicable advanced technologies and operational concepts is needed to reduce risk of future technology choices and system designs.

From this assessment, some interesting findings are present regarding the role of various testing venues in reducing future Mars mission risk.

Ground-Based Testing: Ground-based testing including laboratory and Earth analogs are necessary and cost-effective elements of a robust test program. These testing venues provide the ability to repeat testing procedures, isolate key performance and environmental factors, and allow for the easy testing of key technological and operational options and strategies. Ground testing is relatively benign in terms of both risk and cost. Since the test “subject”, be that hardware itself or with humans in the loop, doesn’t leave Earth, it is relatively easy to access, change, and repeat the test protocols. Ground-based test facilities and vacuum chambers can be used to economically and repeatedly test various operational concepts, technologies, components, and systems in a variety of simulated environments. This strategy lends itself to a “build a little; test a little” concept that can provide greater insight to “go/no go” technical decisions. In addition, analog field tests including simulated environments and terrain, such as high-altitude testing of surface models and landing conditions, can be conducted easily and repeatedly. Ground-based testing allows both individual component and system-level testing to be conducted for certification of advanced technologies and systems before use, thus reducing the risk to future human missions. From an operational perspective, test repeatability of hardware performance, maintenance procedures, and operational concepts is necessary prior to commitment to long-duration Mars missions. Although ground facilities serve a vital role in the testing protocols, it was also recognized that limitations of ground facilities would inhibit the size of integrated vehicles that could be tested. This is an important finding since the size of the integrated Mars vehicles is expected to be quite large. Thus, it was recognized that space-based testing would be required for those large-scale integrated Mars systems that cannot be tested on Earth. Examination of Table 1-3 shows that both ground-based and analog testing venues are very relevant to just about each testing area.

Table 1-3 Potential Venues for Testing Future Mars Systems and Technologies

Testing Venue	Description
Ground Based	Basic laboratory testing of subsystems and systems in a relevant simulated environment or facility. Includes computer simulation testing. Low to mid-TRL (1-6) technology testing. Physical testing of integrated components in a relevant simulated environment. Includes testing of integrated systems and vehicles to validate the integrated performance of the “whole” . Low to mid-TRL (1-6) technology testing.
Earth Analog	Tests conducted in remote locations on the Earth that provide similar environments expected on planetary surfaces. Low to mid-TRL (1-6) technology testing.
LEO / ISS	Includes testing conducted at the ISS in LEO. Zero-g testing of gravity sensitive systems. Mid to high-TRL (6-9) technology testing. Includes testing conducted in LEO, but not at ISS as well as testing conducted in Near-Earth space beyond LEO such as Earth orbit and entry from near-Earth space. Mid to high-TRL (6-9) technology testing.
Lunar Surface	Mission conducted to the surface of the moon of adequate duration to obtain critical system performance and operational data necessary for performance validation. The required number of missions and required duration are system dependent consistent with the level of risk mitigation required for that specific system.
Mars Robotic	Small robotic missions are considered similar to today’s mission capability with constrained surface delivery capabilities and resources. Mid to high-TRL (6-9) technology testing. Larger robotic missions considered to be of sufficient scale to adequately demonstrate and validate human scale system performance. Missions which pre-deploy cargo for future human missions are included in this class. Mid to high-TRL (6-9) technology testing.

Testing in LEO and near-Earth: For this assessment, LEO and near-Earth can include the ISS, a separate facility either in Earth orbit or near the Moon, and destinations beyond LEO but not at Mars. As can be seen in Table 1-4, it was determined that these destinations play an important role in the demonstration and testing of gravity-sensitive phenomena such as crew physiology, gas/liquid separation, and large-scale structure deployments. Since missions in this venue are by definition “near-Earth”, they provide the capability to conduct critical applied research and technology demonstrations leading to safe and effective long-duration human space flight at a close and safe distance from Earth. This is important when humans are in the test loop and especially when systems and capabilities are less mature. Conducting missions close to Earth allows for quick and safe return of the crew should something go wrong with the operational test. These missions in LEO and near-Earth can be used to simulate flight environments for the transit (zero-g) mission phases. In fact, each ISS crew rotation mission is essentially testing a flight to Mars from an operational and human physiology perspective. Flight tests in LEO or near-Earth space can also provide the opportunity to test larger integrated systems than what could be tested in Earth-based facilities, thus providing critical performance data of both hardware and operational concepts of the larger integrated systems. Existing platforms, such as the ISS, can provide an ideal venue for long-duration system testing, including crew interaction with hardware, software, and operational procedures. Extending the testing venue beyond LEO allows for long-term exposure of systems to the deep-space environment, including radiation and zero-g. Lastly, tests in LEO and in near-Earth space can be utilized for extended testing that provides better understanding of long-duration system performance in flight like conditions.

Testing on the Moon: Lunar surface missions may prove useful as long-term “dry run” dress rehearsals, and “what if” scenarios, for future human Mars missions, especially for surface-related operational concepts and systems. Missions to the surface of the Moon can also provide the opportunity to test Mars-prototype systems, thus gaining operational experience on full-scale systems prior to system deployment on a Mars mission. This could include systems such as habitats, life support, power, mobility, and science systems as well as a plethora of operations tests and protocols. One key point brought up by workshop participants is that test missions conducted in flight-like conditions provide the ability to test unknown-unknowns. That is, Earth-based testing is a vital component, but those tests are only as good as the tests that are designed and conducted. Not all combinations of testing parameters can be adequately anticipated to simulate actual nominal and contingency flight conditions. In flight, unique

combinations of system performance in unique environments cannot always be predicted ahead of time in the testing procedures. The cost as well as the associated risks of test failure increase as testing extends beyond the surface of the Earth. In addition, when humans are introduced into the testing protocol, the costs associated with the test increase. Thus, it is important to tie the test objectives with other exploration-related goals, such as scientific investigations and exploration of non-terrestrial bodies – e.g., global exploration of the Moon. Conducting missions in near-Earth space, including the surface of the Moon, provides an opportunity to “run out the systems and procedures” as part of the lunar exploration phase, which could serve as a precursor simulator to the eventual Mars mission. As the testing venue is extended beyond LEO to cis-lunar distances and beyond, deep-space conditions as well as high-speed Earth entry or Mars arrival can be simulated and demonstrated.

Testing at Mars via Robotic Missions: Mars robotic missions are key to providing environmental data of Mars (dust composition, thermal, radiation, terrain, hazards, etc.), which is necessary for proper human systems development. In addition, Mars robotic missions can be a vital tool for demonstration of subscale systems needed for future human missions including integrated aeroassist technologies system performance (aerodynamics, aero thermodynamics, thermal protection, guidance and navigation, supersonic decelerators, precision landing, and hazard avoidance), ISRU, and ascent flight techniques.

Table 1-4 Testing Venue Relevance to Reducing Future Human Mars Mission Risk

Area	Earth Lab	Earth Analog	ISS / LEO	Lunar Surface	Mars Robotic
Human Health and Performance					
Long duration zero-g countermeasures	⊙	○	●	○	○
Long duration hypo-g countermeasures	⊙	○	○	●	○
Radiation protection	●	○	○	⊙	●
Medical care	●	⊙	⊙	⊙	○
Remote isolation / human factors	⊙	●	⊙	⊙	○
Extra Vehicular Activity					
Light weight mobility suit	●	⊙	○	●	○
Long duration / maintenance / reliability	●	⊙	○	●	○
Habitation					
Closed loop life support	●	⊙	●	●	○
Radiation protection	●	○	⊙	●	○
Long duration / maintenance / reliability	●	⊙	⊙	●	○
Mobility					
Long distance and operations	⊙	●	○	●	⊙
Long duration / maintenance / reliability	⊙	●	○	●	⊙
Power					
Emplacement	⊙	●	○	⊙	○
Long duration / maintenance / reliability	●	○	○	⊙	○
In-Situ Resource Utilization					
Cryogenic fluid storage	●	○	○	○	●
Quality (Propellant and ECLSS)	●	○	○	○	●
Long duration / maintenance / reliability	●	○	○	○	●
Aerocapture / Entry					
Flight profile / trajectory	●	○	●	○	●
Thermal protection system	●	○	●	○	●
Structures	●	○	●	○	●
Lander					
Hazard avoidance and precision landing	●	●	○	●	●
Long duration / maintenance / reliability	●	●	○	⊙	●
Communications					
	●	○	○	⊙	⊙
Autonomous Operations					
	⊙	●	○	⊙	●
Cryogenic Fluid Management					
	●	○	⊙	⊙	⊙
Advanced Chemical Propulsion (LO2/CH4)					
	●	○	○	⊙	○
Nuclear Thermal Propulsion					
	●	○	○	○	○

Preferred ● Most Relevant ● Somewhat Relevant ⊙ Less Relevant ○

1.3. International Participation

Primary Contributors:

Kathy Laurini, National Aeronautics and Space Administration, Johnson Space Center

Since 2007, NASA has been a major participant in the International Space Exploration Coordination Group (ISECG). Through this participation, we have had the opportunity to discuss human space exploration goals, objectives, and possible mission architectures with a large number of international space agencies. Although the main focus has been on collaborative approaches to defining architectures for exploration of intermediate destinations, such as the Moon and near-Earth asteroids, agencies have shared Mars mission conceptual architectures to understand the big drivers to the current state of the art in technologies and capabilities.

In 2010, senior managers of ISECG participating agencies decided to embark on a multilateral human spaceflight road mapping effort. The goal was to collaboratively define space exploration mission scenarios that meet common goals and objective, and can inform near-term decisions within individual space agencies regarding investments in exploration preparatory activities, such as technology development and robotic precursor missions. Work on the international roadmap identified that all participating agencies shared the long-term goal of sustainable human exploration of Mars, including missions to the Mars surface. Agencies also discussed and agreed on the high-priority technology needs that would contribute to future Mars exploration missions.

The status of ISECG's exploration road mapping work is reflected in the Global Exploration Roadmap (GER),¹⁰ initially released in Sept 2011 and updated in August 2013, available at www.globalspaceexploration.org or on the NASA website. The international focus remains on advancing toward eventual human exploration of Mars in a way that delivers benefits to multiple stakeholder groups as each intermediate destination is explored. As an international roadmap to Mars, the updated Global Exploration Roadmap follows a path which allows multiple agencies to be in the position to contribute critical capabilities to a future Mars mission.

The agencies participating in GER development have agreed that it is important that any future Mars exploration conceptual architecture be consistent with common guiding principles. The agencies have defined the following principles to inform the roadmap and near-term mission scenarios.

- Mars is the most interesting destination for human missions we can imagine today. It is not the ultimate destination for human space exploration.
- Human exploration of Mars should be part of a sustainable and international human exploration effort, not a one-time mission to say we have been there.
- There is much work to be done before risks associated with a human mission can be reduced to an acceptable level and the required technologies are matured to enable a sustainable approach.
- Future Mars missions have been the driving long-term goal for the capabilities and exploration objectives associated with intermediate destinations (Moon, deep space/asteroids).
- Human missions to Mars must make a meaningful contribution to advancing scientific priorities.

Through the ISECG, agencies have shared conceptual Mars human exploration architectures. This was done in March 2010 within the ISECG Exploration Roadmap Working Group (ERWG) to identify key technology and capability needs as well as any operational drivers to near-term mission scenarios.

NASA presented a summary of Mars DRA5. Other agencies shared similar concept studies. Although mission approaches varied, it was noted that agencies had reached very similar conclusions related to needed technologies and functional capabilities. It was agreed that a common reference architecture for human missions to Mars was not needed at this time as the availability of key enhancing technologies as well as the implications of future robotic mission discoveries would likely have a major influence on specific architectural approaches. So would the number of partners involved.

1.4. HEFT and HAT (2010 to present)

In February 2010, the President sent to Congress his proposal for a new vision for NASA via his budget for Fiscal Year 2011. The proposed 2011 budget reflected a shift in strategy away from that outlined in the Vision for Space Exploration as reflected in the implementation associated with the Constellation Program. This budget proposal, for all practical purposes, cancelled elements of the Constellation Program, namely the Orion crew vehicle and Ares-I/V launch vehicles. The new strategy also outlined a course whereby the next human destination would focus on missions to a Near-Earth Asteroid (NEA) by 2025, leading to humans to Mars orbit by the mid-2030s.¹¹

With this announcement, NASA was handed a new challenge for future human exploration. In response, the Agency conducted a series of internal assessments of future human exploration endeavors. These assessments included the Human Exploration Framework Team (HEFT)¹² and the Human Spaceflight Architecture Team (HAT).¹³ Although the Agency had performed some limited assessments of the role of human exploration of NEAs in the past, never before was it presented as “the” next challenge for human exploration beyond LEO. Consequently, the primary focus of both the HEFT and early HAT activities centered on the implementation options associated with these new NEA missions. In all cases, Mars continued to remain the “horizon destination” that was used to guide technology, operations testing, and capability development efforts.

1.5. Bibliography

-
- ¹ Drake, Bret G., Editor, “Human Exploration of Mars, Design Reference Architecture 5.0,” National Aeronautics and Space Administration, NASA-SP-2009-566, July 2009.
 - ² ISECG, “The Global Exploration Strategy, The Framework for Coordination”, International Space Exploration Coordination Group, <http://www.globalspaceexploration.org/>, April 2007.
 - ³ NASA, “The Vision for Space Exploration,” National Aeronautics and Space Administration, NP-2004-01-334-HQ (Rev), February, 2004
 - ⁴ Public Law 109-155, “National Aeronautics and Space Administration Authorization Act of 2005”, 109th Congress, December 30, 2005.
 - ⁵ Public Law 110-422, “National Aeronautics and Space Administration Authorization Act of 2008”, 110th Congress, October 15, 2008.
 - ⁶ Borowski, Stanley K., et al, “7-Launch” NTR Space Transportation System for NASA’s Mars Design Reference Architecture (DRA) 5.0, 45th AIAA/ASME/SAE/ASEE Joint Propulsion Conference & Exhibit, AIAA-2009-5308, August 2009.
 - ⁷ White House, “U.S. Announces Review of Human Space Flight Plans, Independent Blue-Ribbon Panel will Delineate Options,” Office of Science and Technology Policy Press Release, May 7, 2009.
 - ⁸ Augustine, Norman R., “Seeking a Human Spaceflight Program Worthy of a Great Nation,” Review of U.S. Human Spaceflight Plans Committee, October 2009.
 - ⁹ Drake, Bret G., “Reducing the Risk of Human Missions to Mars Through Testing”, National Aeronautics and Space Administration, JSC-63726, February 2007.
 - ¹⁰ ISECG, “The Global Exploration Roadmap”, International Space Exploration Coordination Group, <http://www.globalspaceexploration.org/>, April 2011.
 - ¹¹ Office of the President of the United States (2010), “National Space Policy of the United States of America,” June 28, 2010.
 - ¹² Muirhead, Brian, et al, “Human Exploration Framework Team: Strategy and Status,” IEEEAC paper#1759, March 2011.
 - ¹³ Culbert, Chris, “Human Spaceflight Architecture Team (HAT) Overview”, Presentation to the Global Exploration Workshop, November 2011, http://www.nasa.gov/pdf/603232main_Culbert-HAT%20Overview%20for%20GER%20Workshop.pdf, site accessed October 12, 2012.

2. EARTH-MARS TRAJECTORIES

2.1. Trip Time Sensitivities¹

Primary Contributors:

Bret G. Drake, National Aeronautics and Space Administration, Johnson Space Center
John D. Baker, Jet Propulsion Laboratory, California Institute of Technology, USA
Stephen J. Hoffman, Ph.D., Science Applications International Corporation, USA
Damon Landau, Ph.D., Jet Propulsion Laboratory, California Institute of Technology, USA
Stephen A. Voels, Ph.D., Science Applications International Corporation, USA

Recent discussions within the exploration community have focused on the prospect of the strategy of conducting a mission to orbit Mars as a validation test prior to the surface mission.² Emerging from these discussions is the current National Space Policy that specifically states: “By the mid-2030s, send humans to orbit Mars and return them safely to Earth.”³ These strategies and conclusions are drawn in part from the historical precedence of Apollo missions where multiple preparatory missions were conducted prior to the first human landing on the Moon. Apollo 8 performed the first human lunar fly-by and Apollo 10 performed the first human orbital mission. Both Apollo 8 and 10 were conducted consistent within the same capabilities and operational profile of the subsequent Apollo 11 landing mission, but that same “orbital testing at the destination before surface landing” philosophy may not hold true for much longer and demanding missions to Mars. Careful examination of the necessary capabilities and knowledge required for both orbital and surface missions, focusing on the similarities between the two, must be conducted to fully understand the potential synergism.

2.1.1. Key Barriers to Exploring Mars

One prime consideration in trajectory choice for potential human exploration of Mars would be the exposure of the mission crew to the hazards of deep space. This includes the effects of bone loss and muscle atrophy due to the zero-g transits as well as exposure of the crew to the radiation environment of deep space, predominately solar proton events and galactic cosmic radiation. To minimize these effects, it is desired to minimize the trip time to the greatest extent possible.

Unfortunately, reducing the round-trip mission duration increases the propulsive energy (ΔV) that would be required by the transportation systems. To reduce the overall mission mass and required number of launches, advanced propulsion technologies would be desired.

These two needs – (1) reducing the mission duration and (2) minimizing the propulsion technologies needed – and mission mass are mutually exclusive. The mission designer is thus faced with the issue of trying to find the right balance between these key drivers. There are other important considerations regarding the operations conducted once at the destination.⁴ But the issues associated with transporting the crew to Mars and back remain predominant, and thus understanding strategies to minimize crew exposure to deep space through proper mission design and proper application of transportation technology is the prime focus of this section.

2.1.2. Mars Design Reference Architecture 5.0

Mars Design Reference Architecture (DRA) 5.0⁵ is the latest in a series of NASA Mars reference missions. It provides a vision of one potential approach describing how various exploration systems could be used to implement the first landing on Mars. The strategy and example implementation concepts associated with DRA 5.0 should not be viewed as constituting a formal plan for the human exploration of Mars, but rather provide a common framework for future planning of systems concepts, technology development, and operational testing as well as potential Mars robotic missions, research that is conducted on the International Space Station, and future potential missions to Near-Earth asteroids or the Moon.

NASA’s DRA 5.0 was conducted as an agency-wide effort with representatives from the major mission directorates as well as other key offices. The primary focus of development of this reference architecture was to confirm our Mars mission knowledge base utilizing previous studies combined with necessary assessments on the key drivers for potential human exploration of Mars. Emphasis was placed on obtaining a balance among key figures of merit, namely risk, cost, performance, scientific return, and schedule. The study process required the formulation of a broad trade tree and performing conceptual design and systems-of-systems studies to strike a proper balance between the key figures of merit. As data were generated, specific decision packages were brought to agency leadership for concurrence. The key tenets of the resulting balanced approach from the development of Mars DRA 5.0 are summarized in Table 2-1.

When reviewing the body of work and decisions related to NASA’s Mars DRA 5.0, a subtle but very important, question must be addressed: “How valid are the key tenets and decisions of DRA 5.0 when applied to the strategy associated with the 2010 National Space Policy of potential humans to Mars orbit first?” Further examination of Table 2-1 shows that since orbital missions are conducted entirely in deep space, strategies for minimizing crew risk from exposure to deep space radiation and zero-g transits should be investigated. Key areas of focus for Mars orbital missions include reducing overall mission duration (crew exposure risk) and propulsion type (increased emphasis on advanced propulsion to reduce total mass for short trip times).

2.1.3. Round-Trip Mars Mission Design

Round-trip missions between Earth and Mars are, in effect, a double rendezvous problem. The outbound trajectory from Earth must be established while considering the position of Mars at the end of this trajectory arc. Upon arrival at Mars, the Earth would be in a relatively unfavorable alignment (phase angle) for an energy-efficient return. This unfavorable alignment results in two distinct classes of potential round-trip Mars missions: opposition-class missions, which are also commonly referred to as short-stay missions, and conjunction-class missions, referred to as long-stay missions. Practical considerations, such as total propulsive requirements, mission duration, surface objectives, and human health must be considered in the mission design process when choosing between these mission classes. Earth departure dates for Mars occur on the order of every 26 months. But, the mission characteristics such as mission duration, trip times, and propulsive requirements for a specific opportunity vary over a 15-year cycle due to the eccentricity of Mars’ orbit, typically referred to as the “synodic cycle”.

2.1.3.1. Short-Stay Missions

Short-stay missions get this name because of the short-stay-times (typically 30 to 60 days) at Mars. Round-trip mission times typically range from 560 to 850 days. This is also referred to as an opposition-class mission. A typical trajectory profile for a typical short-stay mission is shown in Figure 2-1a. This class of mission has high propulsive requirements. Short-stay missions usually have one short transit leg, either outbound or inbound, and one long transit leg, the latter requiring close passage by the sun (0.7 AU or less) when available. After arrival at Mars, rather than waiting for a near optimum return alignment, a crew would initiate the return after a brief stay. Distinguishing characteristics of the short-stay mission class are: (1) short-stay at Mars, (2) total mission duration on the order of 560-850 days, (3) perihelion passage inside the orbit of Venus on the transit to or from Mars, (4) large total energy (propulsive ΔV) requirements, and (5) large variation in ΔV from opportunity to opportunity.

2.1.3.2. Long-Stay Missions

The second Mars mission class is typified by long-duration stay-times (as much as 550 days) at Mars and long round-trip times, approximately 900 to 1,100 days (see Figure 2-1b). These missions represent the global minimum-energy solutions for a given launch opportunity. Unlike the short-stay mission approach, instead of departing Mars on a non-optimal return trajectory, time would be spent at Mars waiting for more optimal alignment between the planets for lower energy return. Distinguishing characteristics of the long-stay mission class include the following: (1) long-stays at Mars, (2) long total mission durations, (3) bounding of both transfer arcs by the orbits of Earth and Mars (closest perihelion passage of 1 AU), and (4) relatively little energy change between opportunities, and (5) relatively short transits to and from Mars (less than 200 days).

Table 2-1 Tenets of Mars Design Reference Architecture 5.0 as they Relate to an Orbital-only Mission

Key Tenet / Decision	Mars DRA 5.0 Rationale (Surface Mission)	Orbital Mission Issue?
Pre-deploy cargo	Agency decision. Pre-deploying cargo could reduce mission mass as well as some risk areas while at the same time enabling unique mission concepts. Pre-deployed mission must occur at least one opportunity before the crew, as early as 2028.	Address, but minimal impact expected
First human mission by 2030	Steering Group ground rule to enable the first human mission in the early 2030's. This was only used for study guidance and does not represent a policy position.	National Space Policy states human mission to Mars orbit and return by mid-2030s
Utilize Long-Stay (Conjunction-class) missions	Agency decision. Long-stay missions provided the best balance of performance, missions return, cost and risk. These missions also not only represent lowest total mass approach, but demonstrate lower variability across mission opportunities.	Yes. Major issue
Minimize crew exposure to the deep-space environment	Long-stay missions enable transits to and from Mars (~180 days), which are within our current ISS experience base, while maximizing time at Mars. It is believed that the 3/8-g at Mars would help ameliorate the effects of zero-g transits, but at this time, it is uncertain if it would be sufficient.	Yes. Major issue
In-Situ Resource Utilization (ISRU)	Agency decision. Utilizing propellants (oxygen) generated from the atmosphere of Mars provided significant architecture leverage. Not only does the use of ISRU reduce total mission mass, but it significantly reduces the mass and volume of the Mars lander. Unlike lunar missions, abort to orbit during the entry phase were not seen as feasible due to the aerodynamic entry physics at Mars, thus landing without ascent propellants was viewed as a viable strategy.	Not Applicable
Heavy Lift Launch	Even with the incorporation of many advanced technologies across the architecture, multiple heavy-lift launches are required. The number of launches is dependent on the in-space propulsion technology. DRA 5 results indicated that surface Mars missions require 7-11 launches, 110-140 t per launch to low Earth orbit (LEO), with launch vehicle shrouds 10 m diameter with 30 m barrel length.	Yes. Major issue coupled with mission duration and transportation propulsion choice
40 t Payload to Mars Surface	Providing the capability to land 40 t of useful cargo to the surface of Mars was found to be a good balance between lander size and number of required landers.	Not Applicable
Advanced Propulsion	Advances in space propulsion are required, most specifically the ability to store cryogenic propellants for long durations. Incorporation of advanced propulsion technologies, such as Nuclear Thermal Propulsion or aerocapture in conjunction with chemical propulsion could reduce the total mission mass and resulting number of launches. The degree of advancement in propulsion technologies is highly dependent on the mission type and the speed of the transits to and from Mars.	Yes. Key strategy for reducing trip time
System Reliability	Due to the orbital mechanics, human missions to Mars are long in duration, with no just-in-time logistics capability and no quick aborts. System reliability, maintainability, and support are essential for these missions.	Orbital missions would remain long and similar order of magnitude with DRA 5.0

2.1.3.3. Round-Trip Trajectory Generation

To resolve the issues related to understanding the relationships between mission duration and propulsive energy required, generation of an extensive Earth-Mars round-trip trajectory database was required. The Mars trajectory generation followed a “broad search” philosophy of calculating every trajectory spanning a four-dimensional grid of Earth launch, Mars arrival, Mars departure, and Earth arrival dates. To save computation time, the trajectories are modeled as conic arcs (Lambert fits) between the planets (i.e., the patched conic model) with impulsive ΔV maneuvers. The potential launch years range from 2020 to 2070 with 10-day search intervals on all encounter dates. The trajectory ΔV at arrival or departure are computed by the change in energy required to enter or escape a 10-day period orbit at an altitude of 400 km at Earth or 250 km at Mars with a 1-day orbit period. In addition to propulsive capture at the planets, trajectories with a maximum allowable atmospheric entry speed are calculated. The maximum speed at Mars is 6, 7 or 8 km/s, and the maximum entry at Earth is 11.5, 12, 12.5, or 13 km/s. Deep-space

maneuvers are also included in the search, where the position and time of the maneuver is varied

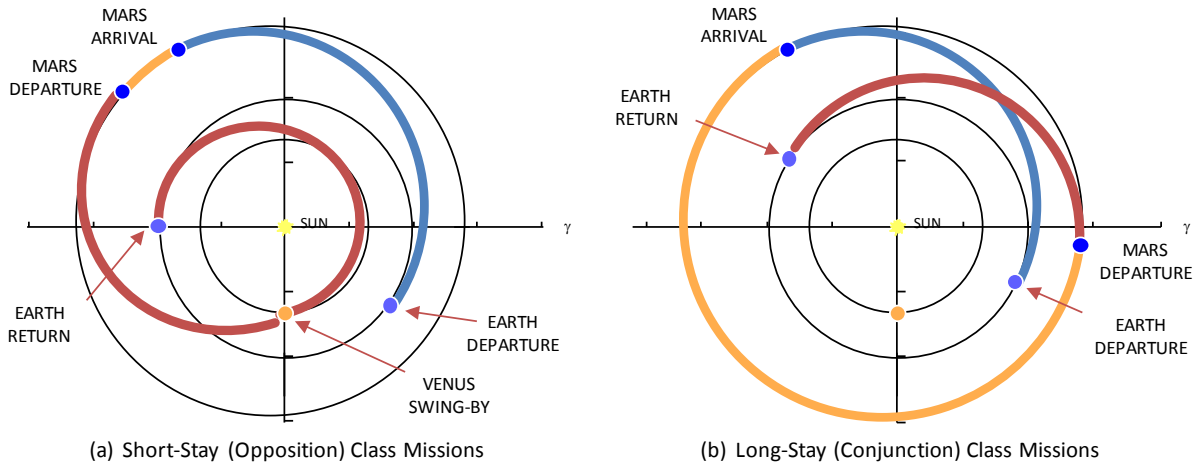


Figure 2-1 Representative mission profiles for the major mission classes for human Mars missions.

using the Nelder-Mead Simplex algorithm to minimize total ΔV on the Earth-to-Mars and Mars-to-Earth legs. That is, for each combination of departure and arrival dates in the grid, a maneuver position and time that minimizes the sum of departure, deep-space maneuver, and arrival ΔV was found. Opposition-class trajectories typically include deep-space maneuvers whereas conjunction-class typically does not.

A major driver for the ΔV of conjunction-class trajectories is the maximum allowable interplanetary transit times. To determine the sensitivity to this parameter, the maximum time is varied from 60 to 360 days in 20-day increments and each minimum ΔV trajectory is saved. The different launch opportunities are distinguished by saving the locally minimum ΔV trajectory for each launch year. (If a given launch year does not contain a local minimum, then no trajectory is saved.) The potential stay time at Mars varies from 400 to 900 days and the total round-trip time varies from 800 to 1,100 days to find a minimum ΔV solution for each launch opportunity and maximum transit time combination.

The short-stay opposition-class ΔV is driven by a combination of potential Mars stay time and total mission duration; each combination of stay time from 20 to 100 days in 20-day increments and mission duration from 160 to 920 days in 40-day increments is saved to the database. The interplanetary transit time is allowed to vary from 60 to 760 days to minimize ΔV . Opposition-class trajectories could also benefit from a gravity assist from Venus; thus, three additional trajectory options with a Venus flyby on the Earth-Mars leg, Mars-Earth leg, or on both legs were performed.

A variety of low-thrust trajectories are also computed to examine the mission characteristics of solar electric or nuclear electric propulsion. Because the calculation of low-thrust trajectories is inherently more computationally intensive than impulsive transfers, a broad grid search was not employed. Instead, the minimum ΔV results from the impulsive mission were used as “seed trajectories” to optimize low-thrust transfers for several different mission design parameters given in Table 2-2. The trajectories were optimized using the Mission Analysis Low Thrust Optimization (MALTO) tool,⁶ and the resulting raw data are scaled to match the vehicle masses for a given Mars architecture.

Table 2-2 Low-thrust Trajectory Search Space

Parameter	Value
Propulsion type	Solar or nuclear electric
Launch opportunities	2028–2046 (15-year cycle)
Mission design	Flight time from 360–1,080 days in 40-day increments with 60-day minimum stay, or stay time from 370–580 days in 30-day increments with 1,096 day maximum round trip
Initial guess	Min. ΔV conjunction-class or opposition-class from impulsive trajectory search
Earth departure	Lunar-assisted escape or impulsive maneuver
Mars arrival	Spiral to Deimos
Mars departure	Spiral from Deimos only
Earth arrival	Spiral to Earth-Moon L_2 or 13 km/s max entry speed
Specific Impulse	1800, 3000, or 4000 s
Power system design	Minimum possible power for a fixed return mass, or optimized for maximum net mass with fixed Earth escape mass (30 kg/kW for SEP or 20 kg/kW for NEP)

2.1.3.4. Co-Planar Trajectory Results and Trends

The trajectory generation process described in the previous section provided a rich and consistent set of potential trajectories for each combination of round-trip mission duration, time at Mars, and Earth departure date. From this database, a further refined set of optimum short-stay trajectories could be found by selection of the optimum mission strategy, which are characterized by employing Venus swing-by maneuvers either outbound to Mars, inbound from Mars, both outbound and inbound, or not at all. As described earlier, the Venus swing-by strategy does not apply to long-stay conjunction missions. Once these further considerations have been applied, the resulting subset of trajectories represents more optimum solutions that could be used to further understand mission mass behavior for different propulsion technologies.

An example trajectory solution set of Pareto front trajectories for the Earth departure year of 2033 is provided in Figure 2-2. This figure demonstrates the behavior of total potential round-trip mission ΔV (co-planar missions from Earth orbit to Mars orbit and return with direct entry at Earth) for both long-stay and short-stay missions. The right-most of the curves shows the variation in long-stay mission ΔV as the transit time to and from Mars is reduced. Since the long-stay conjunction-class missions are characterized by adjusting the time spent at Mars to ensure optimum phasing between the planets, and thus lower total ΔV , these missions would remain long even if the transit times were reduced. Although the time spent getting to and from Mars could be reduced quite a bit for the long-stay conjunction missions (typically on the order of 180 days), the total mission duration would remain roughly 900 days.

The left-side curves of Figure 2-2 shows the variation in ΔV for the short-stay opposition-class missions with various combinations of both stay time at Mars and total mission duration. As can be seen from this figure, the optimum trajectory solution varies as total mission duration would be shortened, as depicted by whether a Venus swing-by was utilized. Some interesting characteristics of the potential short-stay missions could be determined from further examination of this figure, including the following:

- There is a marked increase in total ΔV as the trip time is reduced
- The sensitivity to stay time is greater as the round-trip time is reduced. That is, more ΔV is required as both the trip time is shortened and stay time is increased.
- Although the total ΔV decreases with longer mission durations, the total ΔV remains higher than the long-stay mission class. This is due to the fact that unlike the conjunction (long-stay) missions, the time at Mars is forced to be less than an optimum for short-stay missions.

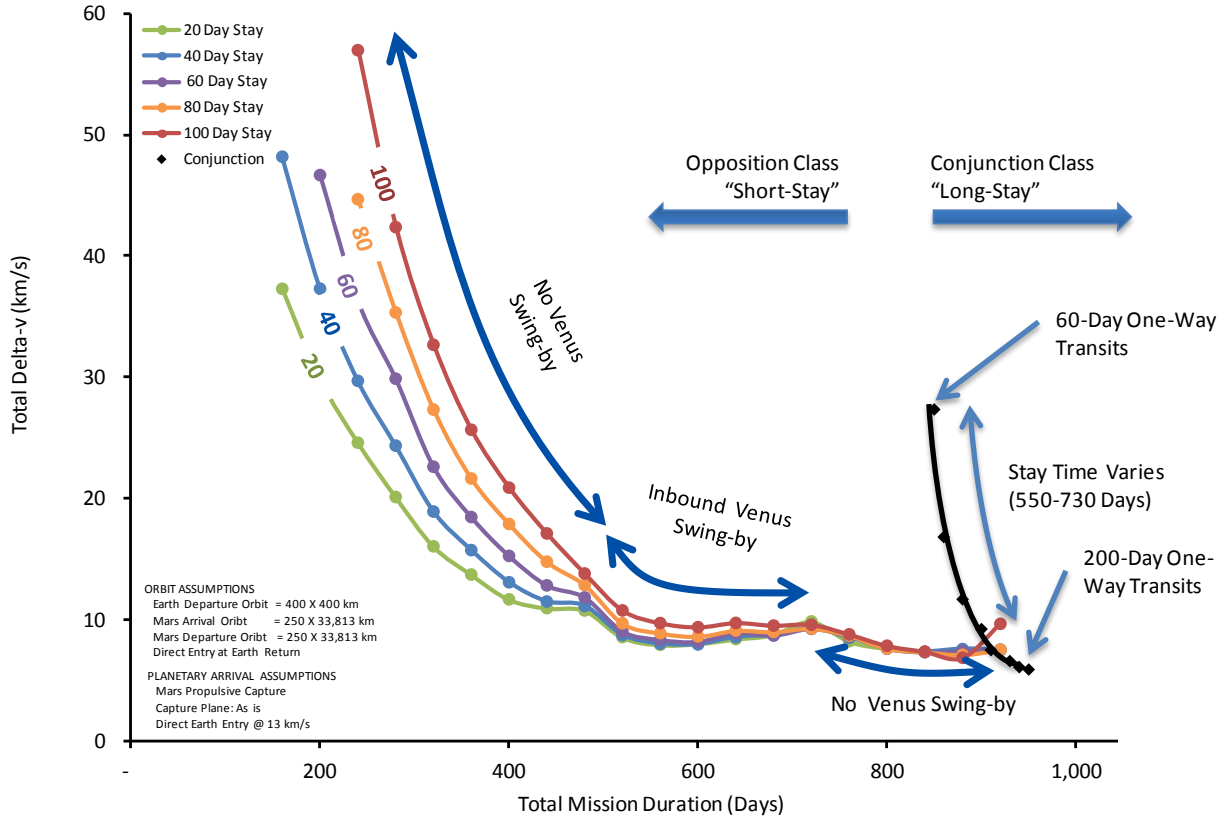


Figure 2-2 Example round-trip ΔV as a function of total mission duration.

Because of the difference in orbits of the Earth and Mars (predominately distance, eccentricity, and inclination), the magnitude of ΔV for the trajectories would vary for each Earth departure date. Mission opportunities occur approximately every 2.1 years in a cycle that repeats every 15 years. The potential trajectories from one 15-year cycle to the next do not match exactly, but are very similar and sufficient for initial planning purposes. Figure 2-3 demonstrates the variability of ΔV for both the short-stay (60 days at Mars, chosen for illustrative purpose) as well as the long-stay (transit times varying from 60-200 days one way) for Earth departure opportunities 2028 to 2045, which is a little more than one 15 cycle. When comparing the variability of ΔV for both the short-stay and long-stay missions, Figure 2-3 demonstrates that the long-stay missions show far less variability in magnitude of total ΔV (for the same trip time constraints) across a 15-year period as compared to the short-stay opposition-class missions. This variability from one opportunity to the next is an important consideration that would be discussed in further detail later.

2.1.4. Exploration Strategies for the Moons of Mars and the Surface

Human exploration of Mars has been a long-standing goal of human spaceflight and the subject of a great number of proposed approaches for accomplishing this goal. Two classes of Mars exploration missions are being carried as leading strategies for potential exploration of Mars: missions where a crew remains in orbit focused on understanding the two Martian moons or teleoperating robotic devices on the surface of Mars, and missions where a crew lands on Mars for direct exploration of the surface.

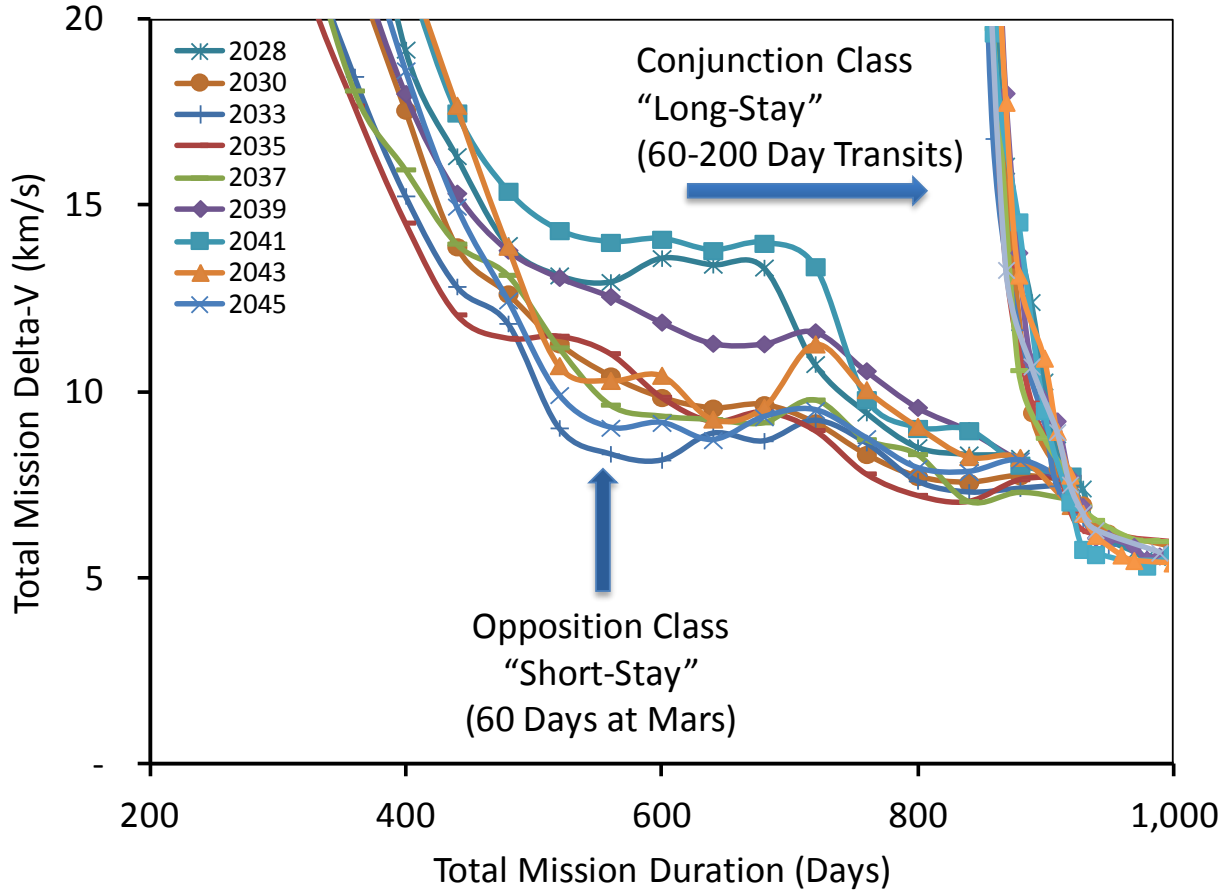


Figure 2-3 Variation in mission co-planar ΔV across a 15-year cycle.

2.1.4.1. Mars Orbital Missions

Because there are two distinct trajectory types for a round-trip mission to Mars, there are also two distinct approaches for potentially conducting exploration missions while in Mars orbit. In both cases, the crew spends the entire mission in the deep-space environment and, likely, in a zero-gravity condition. Thus, in one respect there is an incentive to construct these missions to reduce crew exposure by flying the trajectories as fast as possible (i.e., short-stay class trajectories) within the capabilities of the propulsion technologies and number of heavy lift launches. On the other hand, using the longer-duration trajectories (i.e., the long-stay class) would reduce the number of launches (for a fixed payload mass) but at the expense of increasing a crew’s exposure to the deep-space zero-gravity and radiation environment. To reduce zero-gravity effects, the suggestion has been made to fly in an artificial-gravity (i.e., spinning) mode if possible (although there is as yet no conclusive evidence that artificial-gravity completely mitigates zero-gravity effects or does not introduce other deleterious effects on a crew). These factors are still being discussed and evaluated and, as a consequence, two different approaches to Mars continue to be studied.

The first approach for potential Mars orbital exploration uses the short-stay class of trajectories to minimize the total duration of the mission and thus a crew’s exposure to the deep-space and zero-gravity environment. The short-stay trajectory class limits the time spent in orbit around Mars.⁴ The concept calls for a large interplanetary spacecraft to transport a crew to and from Mars. The spacecraft would be placed into a high Mars orbit (assumed to be a one-sol elliptical parking orbit for high-thrust propulsion concepts or a high circular orbit essentially at the altitude of

⁴ Since the requirements for short-stay missions have not been finalized, analysis associated with this class of missions assumes stay times of 60 days. Further assessments are required to confirm the stay time.

Deimos for low-thrust technologies). Upon arrival, a crew vehicle would rendezvous with cargo placed in this parking orbit on a previous transfer opportunity. Half of the crew would use a Space Exploration Vehicle (SEV) and one of three chemical orbit transfer stages (OTS) to transfer from this parking orbit to the vicinity of Deimos and spend the next 2 weeks exploring this moon. After returning from this Deimos mission, the other two crew members would use a second SEV and OTS to transfer from the parking orbit to the vicinity of Phobos and spend the next 2 weeks exploring the other Martian moon. A third OTS would be available to rescue either crew should they become stranded at either Phobos or Deimos. Crew time not used to explore Phobos or Deimos would be available to potentially retrieve samples from a separate robotic sample return mission or perhaps teleoperate robotic systems on the surface of Mars when a communication path is available. At the end of the 60-day stay, all SEV and OTS assets would be jettisoned, and the large interplanetary spacecraft would depart from its parking orbit for the return trip to Earth.

The second approach for potential Mars orbital exploration uses the long-stay class of trajectories to maximize the amount of time available for exploring the Martian moons and any teleoperation of robots on the Martian surface. An interplanetary spacecraft used to transport a crew to and from Mars would be captured into a temporary parking orbit and then transferred into orbit in the vicinity of Deimos, allowing the crew to spend an extended period of time (as necessary) exploring this moon, using one of two SEVs (the second SEV would be available for rescuing the first). The interplanetary vehicle would then transfer to a parking orbit in the vicinity of Phobos, where the crew would spend an extended period of time (as necessary) exploring this moon. The long-stay class of orbits would allow a crew to spend approximately 500 days exploring these two moons or teleoperating robots on the surface of Mars when a communication path is available.

2.1.4.2. Mars Surface Missions

For the surface long-stay mission class, the NASA Design Reference Architecture 5.0 (Drake, 2009) was utilized as the basis for the analysis in this paper. For this mission, a crew would be sent to Mars on a long-stay class trajectory. On arrival, the crew would place their large interplanetary vehicle into a high-Mars parking orbit to rendezvous with one of two cargo vehicles sent to Mars on the prior orbit transfer opportunity. The second cargo vehicle would have already landed at the intended surface exploration location, where automated systems would have set up a power plant and a propellant manufacturing plant. When all necessary systems have been verified operational and landing conditions determined to be satisfactory, the crew would initiate the landing sequence. Due to the seasonal atmospheric conditions on Mars, winds could generate dust storms that could be local, regional or even global in scale. The existence of a dust storm at the landing location could inhibit the crew from performing the landing. Once the crew landed at this site, they would spend approximately 500 days exploring the vicinity in a series of long traverses (several 100 km) extending from this fixed central base – an approach dubbed the “commuter” strategy. At the completion of this surface mission, the crew would ascend from their surface base, using propellants manufactured there, and return to the waiting interplanetary vehicle. At the appropriate time the crew would depart from Mars for a 6-month transfer back to Earth.

For the short-stay surface missions, the crew would be sent to Mars on high-energy transfers with an assumed time available at Mars of 60 days. On arrival, the crew places their large interplanetary vehicle into a high-Mars parking orbit to rendezvous with a pre-deployed lander sent to Mars on the prior orbit transfer opportunity.⁵ Once the crew lands, they would have less than 60 days for actual exploration since time must be reserved for operations required upon arrival in Mars orbit and prior to departure. But perhaps more important, unless advanced human health strategies are provided, such as artificial-gravity by spinning the crew vehicle while in transit to Mars, the crew would be deconditioned. Acclimation to the surface gravity of Mars may take 1 to 2 weeks. The time available on the surface would be very time-constrained and, in many respects, similar to the Apollo surface missions. At the completion of this surface mission, the crew ascends from the surface and returns to the waiting interplanetary vehicle.

2.1.5. Transportation Technologies Considered

The efficient and cost-effective delivery of both cargo and humans to and from Mars is critical for human

⁵ At this point it is not clear whether all of the surface exploration systems could be accommodated in a single lander. But for the purposes of this analysis, one large lander was assumed.

exploration missions. Given the total mass involved in many exploration architectures, this area is of prime importance and thus has been the focus of many studies and technology development efforts. Historically, propulsion technologies include high- and low-thrust propulsion systems involving chemical, nuclear, and solar forms of energy exchange. Examples of the high-thrust systems are the well-known and highly developed chemical propulsion systems and the less well-developed systems based on nuclear thermal propulsion. Low-thrust concepts include nuclear electric and solar electric propulsion.

To understand the interrelationship between the mission class and mission duration, examination of the various propulsion concepts is warranted. The first step in constructing an appropriate physical architecture is to decompose each operational concept into functional elements of the architecture. Due to the sheer magnitude of number of simulations run, parametric mass sizing was utilized in a fashion similar to previous studies.^{7,8} Although the parametric results have been validated with results from more detailed assessments, the results contained herein should be used for comparative purposes only. That is, understanding the relative trends of one approach versus another is appropriate. The assumed physical characteristics for the payloads as well as transportation systems used to model the expected masses for the various mission architectures is provided in Table 2-3.

2.1.5.1. Chemical Propulsion (High-Thrust Class)

Chemical transportation systems for in-space propulsion have been utilized for decades. These systems are well understood, and have substantial heritage and existing test facilities. But, for human exploration missions beyond low Earth orbit, improvements in performance must be made, specifically changing from lower-performing, storable propellants, to higher-performing cryogenic propellants such as liquid hydrogen and oxygen. Utilizing these higher-performing propellants raises other challenges, including the capability to store and acquire these cryogenics for long durations in space.

The all-chemical propulsion option is a high-thrust ballistic architecture utilizing near-zero boil-off cryogenic liquid oxygen and liquid hydrogen engines for each propulsive stage. For this analysis, each stage is ideally sized for each of the major maneuvers, and each stage is expended at the conclusion of the maneuver.

Table 2-3 Payload and Propulsion System Design Characteristic Assumptions

Payload System	Characteristic
Orion MPCV Inert Mass	14 t
Orion MPCV Propellant Capacity	8.6 t kg
Orion MPCV Specific Impulse	327.5 sec
Deep Space Habitat Mass	34 – 53 t
Space Exploration Vehicle Mass	6.5 t
SEV Stage Mass Fraction	15%
SEV Propulsion Stage Isp	355 sec
Mars Lander – short-stay missions	113 t
Mars Lander – long-stay missions	89 t (ea)
Propulsion System	Characteristic
Cryogenic Propulsion Stage	
Mass Fraction	23%
Specific Impulse	465 sec
Nuclear Thermal Propulsion	
Core Stage Mass	21 t
Drop Tank Fraction	26%
Specific Impulse	900 sec
Electric Propulsion	
SEP Specific Mass	30 kg/kW
NEP Specific Mass	20 kg/kW
Specific Impulse	1800 - 6000 sec
Propellant Tank Fraction	5%

2.1.5.2. Nuclear Thermal Propulsion (High-Thrust Class)

Nuclear thermal rocket propulsion systems were demonstrated in the late 1960s as part of the Nuclear Engine for Rocket Vehicle Application program. Advanced nuclear thermal propulsion concepts promise higher specific impulse than chemical systems (twice the efficiency), potentially providing the capability of reducing total mission mass and trip-time. Nuclear thermal propulsion uses liquid hydrogen as the propellant, and thus retains the technical challenges of long-term cryogenic storage.

The potential option of all-Nuclear Thermal Propulsion (NTP) is a high-thrust ballistic architecture similar in construct to the all-chemical option. The only major difference is the use of a single, higher performing, NTP core stage with expendable drop tanks.

2.1.5.3. Solar Electric Propulsion (Low-Thrust Class)

Low-thrust electric propulsion concepts utilize solar or nuclear power to accelerate propellant to higher exit velocities than those from a chemical reaction. Such systems have the advantage of high efficiency (specific impulse) at the expense of high thrust. This characteristic of low thrust means that the vehicle must spend significant amounts of time, usually measured in months, accelerating out of and into the gravity field of each planet.

The Solar Electric Propulsion (SEP) option would be characterized by the incorporation of a high-power solar electric stage for a majority of the propulsive maneuvers. In this mission architecture, the SEP system is sized for the heliocentric portion of the mission (high Earth orbit to high Mars orbit and back, with direct entry at Earth). A second SEP tug was used in the architectural analysis to deliver the mission payloads, including the deep-space habitat and space exploration vehicle to a high-energy staging point. The crew is then transported from Earth to the staging point separately in a high-thrust chemical stage. A small kick stage is used to accelerate the entire stack to just above escape velocity, and then the SEP vehicle is used for the remainder of the trip to Mars and back.⁹

2.1.5.4. Nuclear Electric Propulsion (Low Thrust Class)

The Nuclear Electric Propulsion (NEP) option would be very similar to the SEP architecture. The only major change would be the use of a nuclear power source instead of utilizing solar panels for power generation. This would allow the NEP vehicle to thrust continuously, even when in the shadow of each planet during the spiral phases, and the thrust does not drop off with solar distance.

2.1.5.5. Orion

The Orion Multi-Purpose Crew Vehicle (MPCV) was assumed to be the primary vehicle used for transportation of the crew from the surface of the Earth to Earth orbit. Orion's design legacy from the Constellation Program has shown to be a good fit with the mission needs of human exploration of near-Earth asteroids (such as four crew with a growth path to six, a minimum of 21 days active operation, rendezvous and docking, contingency extravehicular activity (EVA) capability, high-speed direct entry, etc.). When combined with a chemical propulsion stage, the Orion could be used to transport crew to high-Earth orbit (HEO), GEO, and lunar vicinity (L1, L2, or lunar orbit) in a single SLS launch. In addition to providing transportation function to low Earth orbit (LEO), Orion also would be used by the mission crew for return from the hyperbolic return trajectory for a direct entry and landing on the Earth.¹⁰

2.1.5.6. Deep Space Habitat

The Orion system is a very capable vehicle for transporting crews in near-Earth space for mission durations of 21 days or less. But missions to and from Mars would be much longer in duration. These longer-duration missions would require additional crew support systems including life support, food, accommodations, exercise, etc., all of which are dependent on the total duration of the mission. The estimated mass of the appropriate Deep Space Habitat for mission durations ranging from 360 – 1,200 days is provided in Table 2-3.

2.1.5.7. Space Exploration Vehicle

There are still many unknowns with respect to how exploration of the moons of Mars would be conducted. Since it is unclear what that exploration strategy would be like, some equipment and capabilities would need to be taken with the crew to perform the necessary exploration. For modeling purposes, it was assumed that for Mars moon missions an independent vehicle would be used. The Space Exploration Vehicle concept envisions a small livable volume for a crew of two for up to 2 weeks in duration.¹¹ The SEV would provide limited translational ΔV , on the order of 200-300 m/s, and thus an additional propulsive stage is needed to transport the SEV and crew from the high-Mars parking orbit down to the orbit of the moon to be explored.

2.1.5.8. Mars Surface Lander

Delivery of large payloads to the surface of Mars remains a key challenge for potential human missions to the surface. With current technology approaches, the most mass that could be delivered to the surface is believed to be similar to what will be demonstrated on the Mars Science Laboratory, or 1 metric ton (t). Human missions would require much more than that, on the order of 20 to 40 t, thus new approaches and technologies are required.¹² An advanced inflatable aeroshell approach was utilized for this analysis. Data from previous studies were used to perform top-level assessments of the amount of required payload needed to support a potential crew of four for the short-stay missions, and support a potential crew of six for the long-stay missions. These assessments indicated that a single lander of 114 t would be needed for the short-stay missions and two 89 t landers were required for the long-stay missions. It should be noted that these assessments are very preliminary and further detailed and comprehensive analyses are required before firm conclusions can be drawn. But for the purpose of these analyses, the above landers were used.

2.1.6. Crew Trip Time Sensitivity Results

Examination of ΔV alone does not provide enough insight to make concrete decisions in terms of the overall mission design. Other considerations, such as the effects of deep-space travel on a crew; vehicle size and number of launches; and mission scientific return must be included in the decision-making process. These propulsive maneuvers must be translated into estimated vehicle mass, as described by the various propulsion technologies, to be more meaningful to the mission designer.

The sensitivity of total mass required to transport an exploration crew from low Earth orbit to high Mars orbit and return to Earth via direct entry, for the short-stay class missions, are provided in Figure 2-4. Several key points about the short-stay opposition-class mission could be seen from examination of this figure:

- The chemical propulsion architecture results in high overall mission mass as well as high sensitivity in mass.
- Solar electric propulsion cannot significantly reduce trip time.
- Both nuclear transportation technologies, nuclear thermal and nuclear electric, indicate reasonable mass for round-trip times approaching 600 days, with a slight advantage of nuclear thermal in some opportunities.
- Both electric propulsion concepts, solar and nuclear, demonstrate less sensitivity and variability across mission opportunities predominately due to the higher propulsion efficiency (specific impulse).

When comparing all four propulsion technologies, it becomes clear that there is a general limiting “wall” in terms of trip time and mission mass. That is, round-trip mission duration could be reduced, but there is a reasonable limit for each propulsion type. This limit is due to the combination of both the efficiency of the propulsion concept (specific impulse) as well as thrust provided. Based on these analyses, the practical limits for each propulsion concept appear to be around 560 days for nuclear thermal propulsion and 600 days for nuclear electric. Neither all-chemical nor solar electric propulsion were competitive for the short-stay missions, and, thus, may only be applicable to long-stay conjunction-class missions.

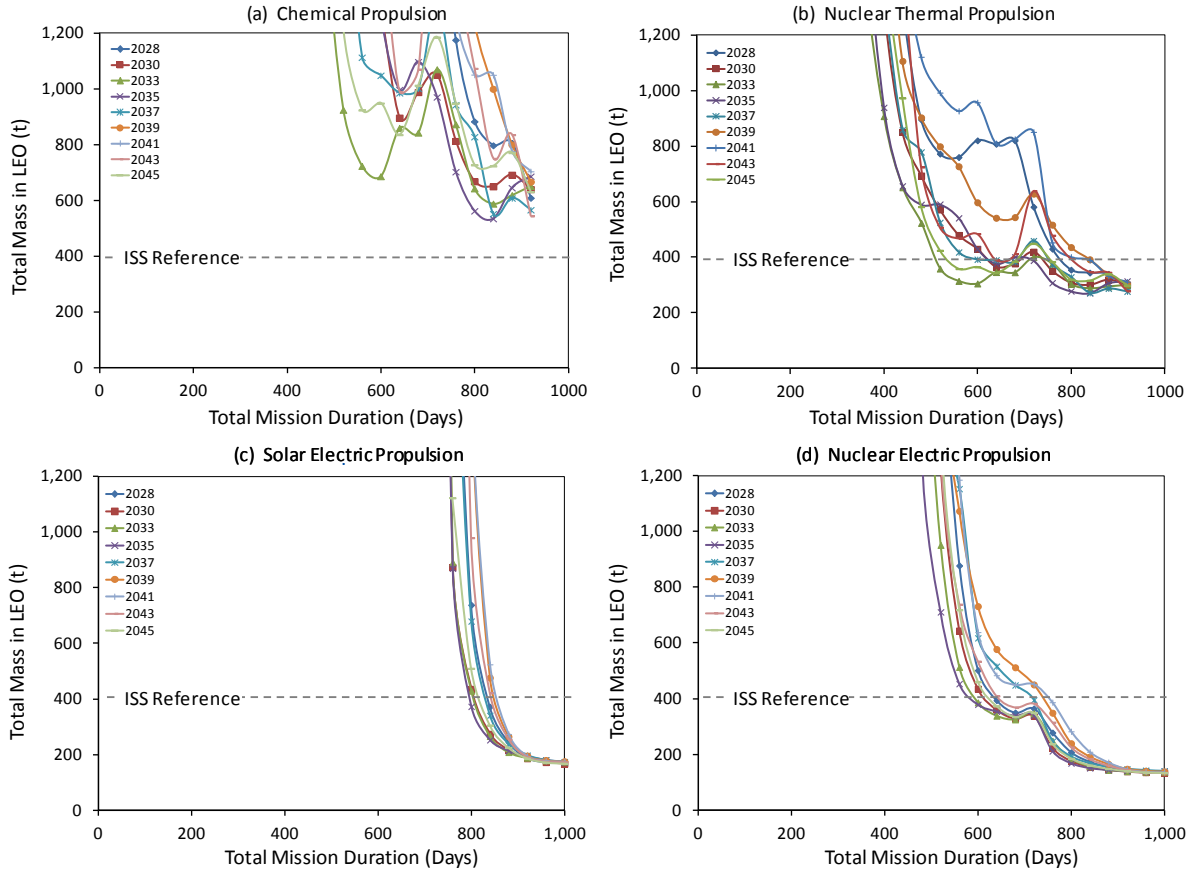


Figure 2-4 Sensitivity of the estimated crew vehicle mass as a function of round-trip mission duration for the short-stay, 60 days at Mars, opposition-class missions.

As trip time is increased for the short-stay opposition-class missions, it may become advantageous to switch to the long-stay mission class. That is, as the mission duration is increased to 800 days or more, all necessary capabilities and human support strategies would need to be solved, so why artificially limit the stay at Mars flying non-optimal trajectories rather than increasing time at Mars for a small, overall increase in mission time?

Figure 2-5 shows the sensitivity of total mission mass for various times at Mars for the long-stay conjunction-class missions. Examination of this figure shows that for the long-stay conjunction-class missions, all four propulsion concepts analyzed provide competitive mass results with the higher performing technologies, nuclear thermal and nuclear electric, showing a distinct advantage both in terms of crew vehicle mass and mass sensitivity across opportunities. But before a final decision could be made, further assessments are required to delineate between the transportation technologies. These assessments should include other figures of merit including launch packaging, technology development required, and mission and technical risk, to name a few.

In addition, since the conjunction-class missions are long in duration, there is often a desire to reduce the transit times to and from Mars as much as possible to minimize human health risks. Figure 2-6 shows the variation of crew vehicle mass as a function of one-way transit time to and from Mars utilizing advanced propulsion technologies, namely nuclear thermal propulsion for this specific case. For this strategy, as transit times are reduced, the time spent in the vicinity of Mars is increased to reduce the total ΔV . As could be seen from this figure, the one-way transits could be reduced, but as with the short-stay opposition-class missions, physics dictates that there is a practical limit. Although this strategy may be used to get the crew to Mars faster, it does not shorten the total mission duration since time at Mars increases as the transit times are reduced, resulting in round-trip missions that remain about 1,000 days.

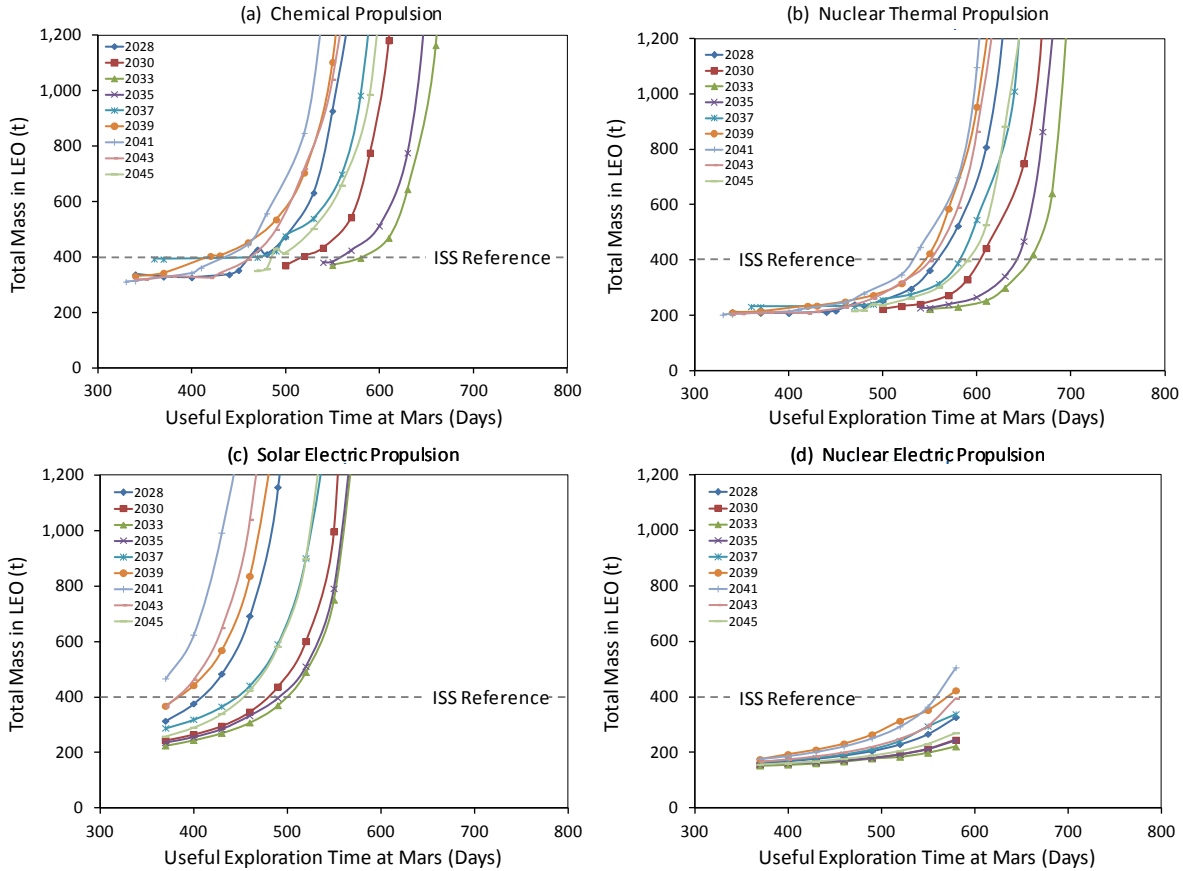


Figure 2-5 Sensitivity of the estimated crew vehicle mass as a function of useful time at Mars for the long-stay conjunction-class missions.

2.1.7. Additional Mission Design Considerations

In addition to the total energy required to get a crew from Earth to Mars and back, it is important to understand the exploration strategy at Mars and what is to be accomplished. Depending on the objectives, additional operational maneuvers must be conducted in the vicinity of Mars. In addition, the time available to accomplish the necessary maneuvers would be highly dependent on the mission class chosen and the propulsion technology. Short-stay missions, by their very nature, are more constraining upon arrival at Mars. Likewise, low-thrust electric propulsion vehicles require additional time to capture into and depart from Mars orbit.

Heliocentric transfers between the Earth and Mars result in varying arrival and departure declinations at Mars. These differences in declination could increase the required ΔV , depending on the propulsion type. For low-thrust propulsion concepts such as solar or nuclear electric propulsion, this misalignment could be accounted for as part of the spiral capture maneuver (Figure 2-7).¹³

But for high-thrust ballistic trajectories, this misalignment must be managed either during the Mars orbit insertion maneuver or during the time in Mars orbit. For long-stay Mars missions, the strategy usually favored is to use time and the irregular gravity field of Mars, due to non-spherical planet shape, to modify the orbit from the natural arrival condition to the necessary geometry for departure⁶. But for short-stay missions, there is not sufficient time to use this gravity shaping strategy; thus, upon arrival at Mars, a plane change must be performed to alter the arrival declination to match that for departure. Depending on the arrival conditions and required Mars parking orbit, this additional plane change could add additional ΔV to the mission architecture.

⁶ Although theoretically possible, further assessments are required to confirm this strategy.

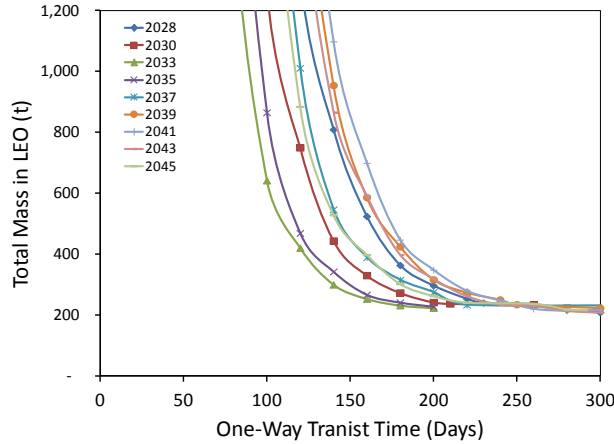


Figure 2-6 Nuclear thermal propulsion crew vehicle mass as a function of one-way transit time to and from Mars for the conjunction-class long-stay missions.

In addition, exploration of Phobos and Deimos add yet another level of complexity to orbital operations at Mars. The orbits of both Phobos and Deimos are essentially in the equatorial plane of Mars (1.1 and 2.5 degrees, respectively) with essentially circular orbits (semi-major axes of 9,378 km and 23,459 km, respectively).¹⁴ The difference in orbital inclination of the moons with the parking orbit of the crew vehicle combined with the orbital altitude difference again adds additional ΔV to the mission architecture. These orbital considerations combined could add 1.5 to 3.5 km/s of total ΔV to the exploration systems.

Missions to the surface of Mars represent a different architectural challenge. Although Mars has an atmosphere, it is not very dense, approximately equivalent to the Earth at 30 km. Even so, the atmosphere could be used for some deceleration of landing vehicles. Based on current mission strategies, the total delta-v to get from high-Mars orbit, to the surface of Mars and return requires on the order of 6.3 km/s for the landing vehicles

2.1.8. Total Architecture Mass Comparisons

Analysis of various strategies for human exploration of both the moons of Mars, as well as the surface, continues. Although no final conclusions could be drawn, some interesting trends could be seen. A summary of the nuclear thermal propulsion total architecture mass is provided in Figure 2-8. Analysis of the other transportation concepts (SEP, NEP, and chemical propulsion) is currently in progress, thus results could not be provided by the publication date of this article. Initial emphasis was placed on the nuclear thermal propulsion architecture since it represents a good example of the behavior of advanced transportation technologies. Included in Figure 2-8 are results for the short- and long-stay missions for orbital exploration of both moons as well as surface landed missions. Total architecture mass includes the total mass of both the round-trip crew vehicle as well as the total mass required to deploy any necessary cargo one opportunity prior to the crew mission. Since significant variation could occur in the ΔV across the 15-year cycle, both the best- and worst-case results are provided, representing the easiest and hardest opportunities. For the short-stay missions in this analysis, emphasis was placed on reducing the round-trip mission duration to the greatest extent practical, which for the nuclear thermal propulsion occurred at approximately 560 days round trip with 60 days at Mars (see Figure 2-4b). The total mass for the NTP architecture is provided in Figure 2-8.

- The high energy needs (ΔV) of the short-stay missions, both surface and missions to the moons of Mars, results in both large magnitude and wide variation in total architecture mass. This large variation in mass for the short-stay missions makes it difficult to design a single exploration vehicle for all mission opportunities. In fact, for the short-stay missions it may be necessary to skip some, perhaps half or more, of the mission opportunities to achieve reasonable mass.
- Long-stay missions demonstrate less variation in total architecture mass for both the orbital and surface missions.

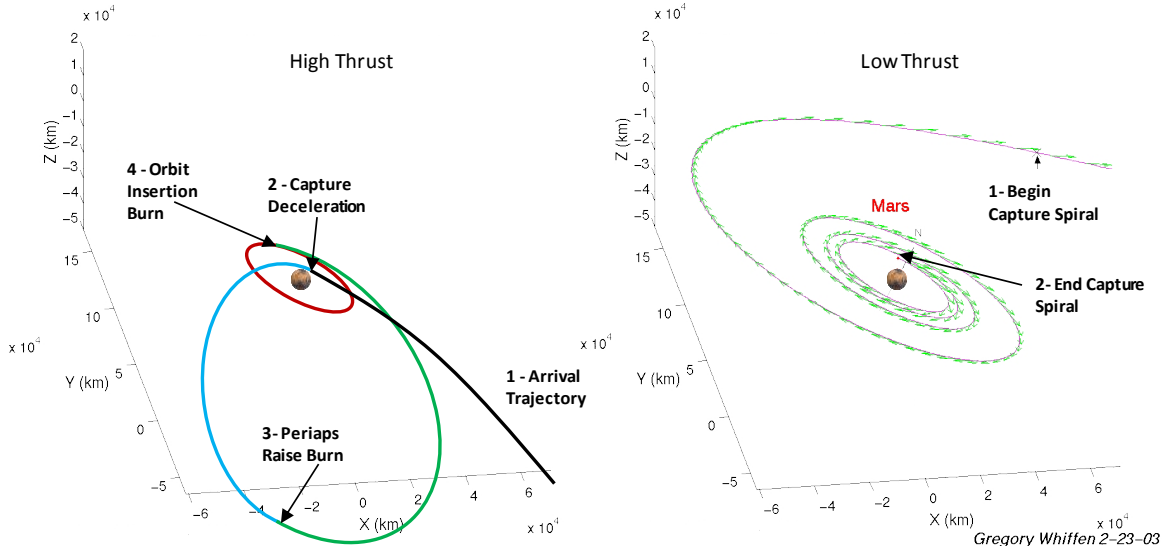


Figure 2-7 Example Mars orbit capture strategies for both high-thrust and low-thrust propulsion technologies.

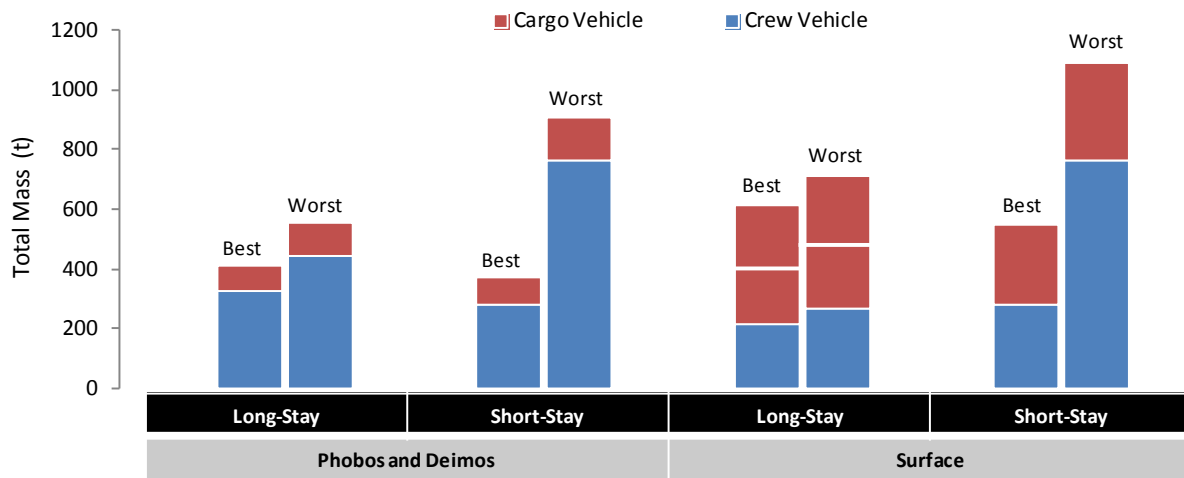


Figure 2-8 Estimated total architecture mass for nuclear thermal propulsion technology concept. Total mass includes both the cargo and crew vehicles for both surface missions and orbital missions to Phobos and Deimos.

- Pre-deployment of exploration cargo for the orbital missions provided marginal benefit in terms of total mission mass. That is, the size of the crew vehicle dominates the total architecture mass. There may be other reasons to pre-deploy cargo that may make that strategy a good choice; e.g., risk reduction or complexity of the larger integrated vehicle stack that would result if the cargo were taken with the crew.
- Long-stay surface missions seem to provide the best “balance” between the relative size of the crew vehicle and the corresponding two cargo vehicles needed for the architecture. This could potentially allow for the design on a single transportation element to handle both the crew and cargo transportation functions across all opportunities in the 15-year cycle.

2.1.9. Conclusion: Summary of Key Challenges

NASA has recently embarked on a different path for the future exploration of the inner solar system by human crews. At the current stage in its development, this different path – a capability-driven framework – is being framed in terms of a series of design reference missions, each of which is focused on a specific destination but in the

aggregate describe a building block approach to expanding human presence in the solar system. Within this framework, human exploration of Mars and the moons of Mars remain the “horizon destinations” that are being used to help inform near-term investment and development strategies. Table 2-4 provides a summary of the key challenges associated with both orbital and surface exploration of the martian system. This table indicates that a substantial number of key technological advances would be necessary to make the implementation of this mission a reasonable endeavor. Improvements in a wide range of technologies would be required for human Mars missions. But even with these technological improvements, the mission parameters shown indicates that challenges remain.

2.1.9.1. Key Orbital Mission Challenges

Since Mars orbital missions are by their very nature conducted entirely in the deep-space environment, the challenges associated with maintaining the health and performance of the crew, both during and after the mission, remains the primary driver. Of particular concern are the effects of radiation and zero-gravity on the human body. With our current state of knowledge it is not clear whether the current mitigation strategies would suffice. Thus, for orbital missions, there is a strong desire to reduce the overall mission duration by employing short-stay opposition-class missions. Since these missions are higher energy in terms of ΔV , there is a subsequent need for advanced propulsion technologies coupled with a greater number of launches. Even with the incorporation of advanced propulsion, analysis indicates that there is a limit to how short the round trip mission could be. That practical limit appears to be at around 560-850 days, and the limit is highly dependent on the propulsion technology. The short-stay missions also result in higher entry speeds at return to Earth as well as close perihelion passage, thus introducing additional technical and environmental challenges. But if the human health support challenges could be overcome to allow very long missions (around 1000 days) in deep space, then it may make sense to fly long-stay conjunction-class missions. This strategy would ease the need for advanced propulsion.

Exploring the moons of Mars introduce additional mission complexities as well. Both moons orbit in the equatorial plane of Mars, which, unfortunately, is not co-planar with the trajectory arrival and departure planes. Significant orbital maneuvers are therefore required to move the exploration assets from the Mars parking orbits to match the orbits of the moons.

2.1.9.2. Key Surface Mission Challenges

The strategy adopted in NASA’s Mars Design Reference Architecture 5.0 was, in essence, to make the surface of Mars the second safest place in the solar system. This was achieved by adjusting the time spent at Mars, using the long-stay conjunction-class missions, to allow the crew to be transported to and from Mars on fast transits. With this strategy, the transit legs are essentially identical to the mission increments that are currently flown on the International Space Station, namely 180 days. These transit times are well within our current knowledge base of human performance from a zero-g deconditioning perspective. The response of the crew to 500 days on the surface of Mars at 3/8-g gravity is unknown but thought to be beneficial compared to zero-g. It is also unclear what the radiation environment is on the surface of Mars. The Mars Science Laboratory, scheduled to land in August of this year, should provide valuable data on the radiation environment experienced on the surface, thus helping significantly reduce the modeling uncertainties. If it is desired to fly short-stay missions instead of the long-stay missions, then the same human health concerns associated with the orbital missions previously discussed remain. In addition, if enhanced techniques such as artificial-gravity during the transits are not applied, then the crew would require several days, perhaps up several weeks, to acclimate to the gravity environment upon arrival at the Mars surface. This inserts additional schedule pressure as well as lander design features not present with the long-stay missions. Operational planning for short-stay missions must also consider the potential presence of dust storms at the landing location that could preclude landing.

The ability to land large payloads on the order of 40 t or more of useful cargo remains a primary challenge for human missions to the surface of Mars. The challenge of entry, descent, and landing would require new approaches and technologies, since the current robotic mission strategy would be capable of landing only 1-2 t of payload. Further assessments are required to determine the feasibility, size, and number of the landers required for such surface missions.

Table 2-4 Key Challenges for the Various Mars Exploration Options

Typical Mission	Mars Moons Short-stay	Mars Moons Long-stay	Mars Surface Short-stay	Mars Surface Long-stay
In-Space ΔV (km/s)	8.3 – 14.1	6.6 – 8.0	8.3 – 14.1	6.0 – 7.1
Orbital Transfer ΔV (km/s)	1.3 – 2.6 (ea)	2.4	-	-
Descent / Ascent ΔV (km/s)	-	-	6.3	6.3
Total Mission Duration (days)	560	900	560	900
Outbound Time (days)	200	180	200	180
Time at Mars (days)	60	540	60	540
Return Time (days)	300	180	300	180
Crew Mission Mode	Artificial-g (?)	Artificial-g (?)	Artificial-g (?)	0-3/8-g
Pre-Deployed Cargo (t)	25 – 59	13	113	190
Abort to Earth Duration	Long	Long	Long	Long
Closest Perihelion Passage (AU)	0.5 – 0.7	1.0	0.5 – 0.7	1.0
Earth Entry Speed (km/s)	13.6	12.2	13.6	12.2
Number of SLS Launches for Mission	4 – 9	4 – 5	5 – 10	6 – 7
Initial Mass to LEO (t)	400 – 900	400 – 550	500 – 1,000	600 – 700
Typical Systems Required				
Orion MPCV	✓✓	✓	✓✓	✓
Heavy Lift Launch	✓	✓	✓✓	✓
Advanced In-Space Propulsion	✓✓	✓	✓✓	✓
Destination Exploration Systems	SEVs + Stages	SEVs	1 Lander (?)	2 Landers
Deep Space Habitat	✓✓	✓✓	✓✓	✓?
Planetary Lander	-	-	✓(✓?)	✓✓
Key Technologies				
Cryogenic Propulsion	✓	✓	✓	✓
Radiation Protection	✓✓	✓✓	✓✓	✓(?)
Advanced Propulsion (NTP, NEP)	✓✓	✓	✓✓	✓
Near-Zero Boil-off Cryogenic Storage	✓	✓	✓	✓
High-Speed Earth Entry	✓✓	✓	✓✓	✓
Life Support System Enhancements	✓	✓	✓	✓
Zero-g Countermeasures	✓✓	✓✓	✓✓	?
In-Situ Resource Utilization	-	-	-	✓
Entry, Descent, and Landing	-	-	✓	✓
Nuclear Surface Power	-	-	-	✓

2.1.9.3. Concluding Remarks

Human exploration of Mars, of either the surface itself or the Martian moons, remains a significant challenge for human exploration. It would require advances in numerous technologies and improved operational approaches. Reducing the exposure of the mission crew to the hazards of deep space, namely radiation and zero-g, is of prime concern. Unfortunately, reducing the round-trip mission duration increases the propulsive energy (ΔV) required by the transportation systems and, in many cases, the number of launches as well. The analyses in this paper have shown that mission durations could be reduced, but practical limits remain. In fact, without major advances in anticipated technologies or dramatic alterations in the mission architecture and resulting risk posture, mission durations may be not be much shorter than 600 days. Thus, for Mars orbital missions the challenges associated with health of the crew and their performance cannot be obviated via propulsion technology alone. Further research is required to determine the best strategies and mitigation approaches for protecting humans for these long-duration missions. In fact, focus should also be placed on determining whether there is a difference between 600 and 900 days in free space, since those times continue to be the distinguishing characteristic between short-stay (opposition-class) and long-stay (conjunction-class) missions, respectively. If future human performance research shows there to be little difference between these mission durations, then the choice is obvious and long-stay conjunction-class missions would be the preferred option. But if human performance continues to be a limiting factor, as is expected, then emphasis on propulsion technologies must remain for orbital missions.

The need to fly short opposition-class trajectories for surface missions is not so clear. It is anticipated, though yet to be confirmed, that the surface environment of Mars, both in terms of radiation protection and zero-g deconditioning,

may provide sufficient human health mitigation for long-stay missions and thus the strategies outlined in Mars Design Reference Architecture 5.0 would suffice.

2.2. Earth Departure Scenarios¹⁵

Primary Contributors:

Damon Landau, Ph.D., Jet Propulsion Laboratory, California Institute of Technology, USA

A human mission to Mars would likely involve several vehicle elements that are staged near Earth, and the choice of staging location can significantly affect the efficiency and robustness of a Mars exploration campaign. The key figures of merit are overall ΔV , departure windows, backup opportunities, and contingency options. These characteristics are detailed and compared for Earth-Moon L2, high-lunar orbit, high-Earth orbit, and low-Earth orbit. Earth-Moon L2 and high-lunar orbit are found to be operationally and energetically similar, and require additional ΔV to enter and depart before leaving for Mars. High-Earth orbit enables trans-Mars injection backup opportunities by reorienting the orbit at apogee. This type of orbit can shift between many inclinations, periods, and perigees with lunar gravity assists. Direct departure from low-Earth orbit requires the fewest number of critical maneuvers, but does not benefit from potential efficiencies from solar electric propulsion or reuse of deep space vehicles.

2.2.1. Introduction

Several alternative staging locations have been proposed for the human exploration of deep space [Drake, 2009]. Depending on the exploration architecture and development path, a deep space vehicle could station in low-Earth orbit (LEO), high-Earth orbit (HEO), high-lunar orbit, or Earth-Moon L1/L2. (We exclude Earth-Sun Lagrange points from the present analysis because the associated transfer times are typically over a month, whereas the other locations can be reached within a week.) Prior to Earth departure, the crew must first rendezvous with the deep space vehicle at its staging node, and then fly a departure sequence onto the interplanetary trajectory. The choice of staging node therefore strongly affects the vehicle designs, crew contingency options, and mission backup opportunities. A systematic comparison of these alternative strategies for Earth departure informs decisions for which technologies and architectures provide the best opportunities to land people on Mars.

2.2.2. Interplanetary Trajectories

Each Earth departure sequence must ultimately result in a transfer that intercepts Mars, regardless of the choice of staging node. The interplanetary trajectory therefore drives the design of the departure strategies, where a variety of interplanetary transfers provides a range of Earth departure characteristics. Because the orbit of Mars is relatively inclined and elliptical compared to Earth, the energy and declination of trans-Mars injection (TMI) varies from opportunity to opportunity. The 2033 and 2035 launch opportunities span a range of departure characteristics that stress different design options.

In Figure 2-9a, the 2033 launch opportunity has a large declination of -55 deg from the equator (and -36 deg from the Moon's orbit) and strains out-of-plane launch requirements. The launch energy ($C3$ in km^2/s^2) is lower in 2033 than for the 2035 launch (Figure 2-9b), which has a launch direction that happens to be mostly in the equatorial plane as well as in the Moon's orbital plane. The large declination associated with the 2033 opportunity cannot be reached from inclinations less than 55 deg, so departures that launch from Cape Canaveral to 28.5 deg inclination alter the orbital plane either propulsively or via lunar gravity assist prior to departure. Thus the 2035 opportunity, which has a higher $C3$, could require less ΔV than the 2033 launch due to the orbital geometry considerations. Launch inclinations of both 28.5 degrees and 51.6 degrees (similar to Space Station orbit) will be considered for the 2033 opportunity. For consistency with the Mars Design Reference Architecture, the Earth-to-Mars transfer time is constrained to 180 days. The Earth departure date is varied from -28 to 28 days from the optimal to examine launch period effects and backup opportunities.

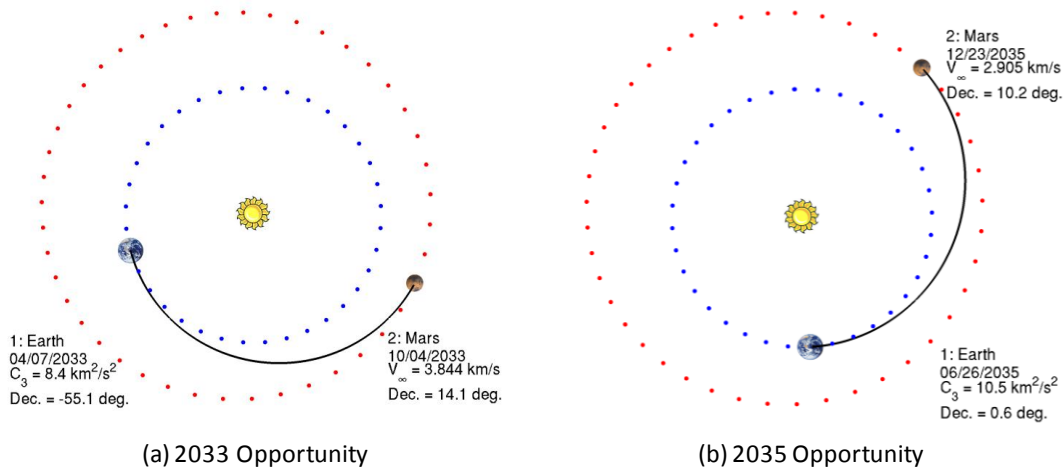


Figure 2-9 Departure characteristics of Earth-Mars transfers vary among launch opportunities.

2.2.3. Departure from Earth-Moon L2

The Earth-Moon L2 point lies just outside the orbit of the Moon and has the distinction of being farther than humans have yet to travel. Its location remains relatively fixed along the Earth-Moon line and thus makes one revolution around Earth every month, as seen in Figure 2-11. From Figure 2-10, the escape direction to Mars points in the same general direction during the course of a month, thus there are only a few days each month when the Moon (and L2 along with it) is in the proper direction for a transfer to Mars.

Earth-Moon L2 is a dynamically unstable environment, and vehicles may enter and depart the vicinity with negligible ΔV . Vehicles near L2 must therefore be actively controlled to remain in orbit, though the station keeping ΔV is minimal. A vehicle can also enter orbit around L2 with almost no ΔV if the transfer time from LEO is sufficiently long (typically 3 to 4 months).¹⁶ The transfer ΔV is essentially the energy required to escape from LEO, which is around 3100 m/s. (All ΔV values are assumed impulsive and deterministic and do not include contingency for gravity loss or execution errors.) These trajectories are ideal to deliver massive vehicle components that are not sensitive to longer flight times. The crew, on the other hand, is sensitive to trip time and requires a shorter duration transfer to L2. A 7–8 day transfer from LEO to L2 is available by performing a powered flyby of the moon with ~175 m/s ΔV then inserting into L2 with an additional ~175 m/s. This ~350 m/s rendezvous ΔV is in addition to the 3150 m/s required to escape LEO. (An alternative short-duration transfer without the lunar flyby requires around 700 m/s to rendezvous at L2 in about 5 to 6 days.) The post-rendezvous departure sequence is essentially the short-duration transfer in reverse, with around 350 m/s to depart L2 and fly by the Moon to target a low perigee for TMI, as depicted in Figure 2-12.

Trans-Mars injection ΔV is typically several hundred meters per second, depending on the interplanetary C3. Departure from L2 is relatively insensitive to the escape declination because the outbound lunar flyby can change the inclination from near the plane of the Moon into the departure plane. However, the orbital motion of the Moon limits the low ΔV escape opportunity to about 3 days, as shown in Figure 2-13. The TMI maneuver should be performed near perigee to keep the ΔV minimized, providing a single nearly instantaneous opportunity to depart on the orbit following lunar flyby. If some contingency prevents the TMI attempt, a second attempt is initiated by reorienting the orbit into a new departure plane at the following apogee, then performing TMI at the following perigee (one orbit period following the first attempt). From Figure 2-13, the backup opportunity requires about 100 m/s additional ΔV . Alternatively, if a contingency occurs while in orbit near L2, then the crew must still follow the same departure sequence down to a low perigee that intercepts the atmosphere to return to Earth. The crew contingency return from L2 thus requires about 350 m/s and 8 days to return. The post-lunar orbit is constrained to direct (prograde) motion to reduce atmospheric entry speed in case of a contingency.

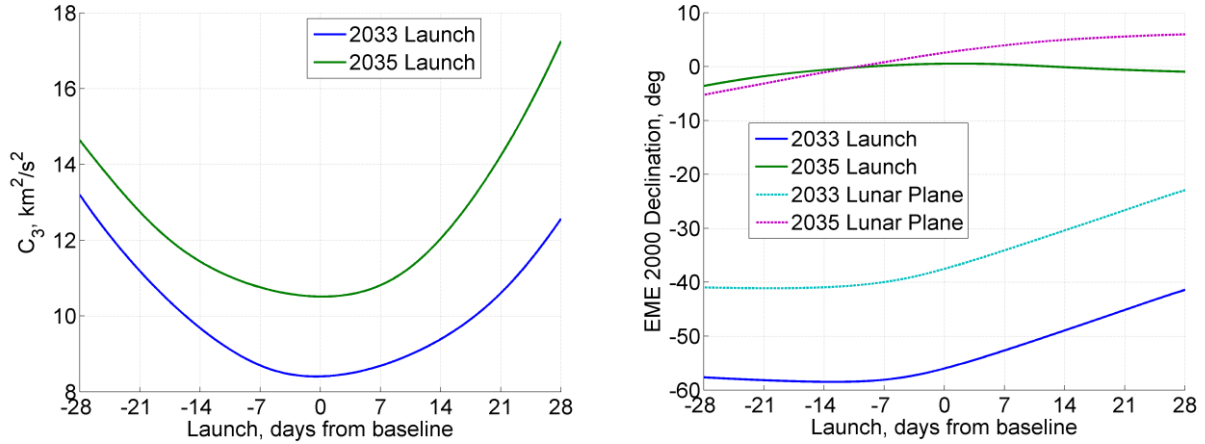


Figure 2-10 The Earth escape asymptote has moderate variation over a 2-month span.

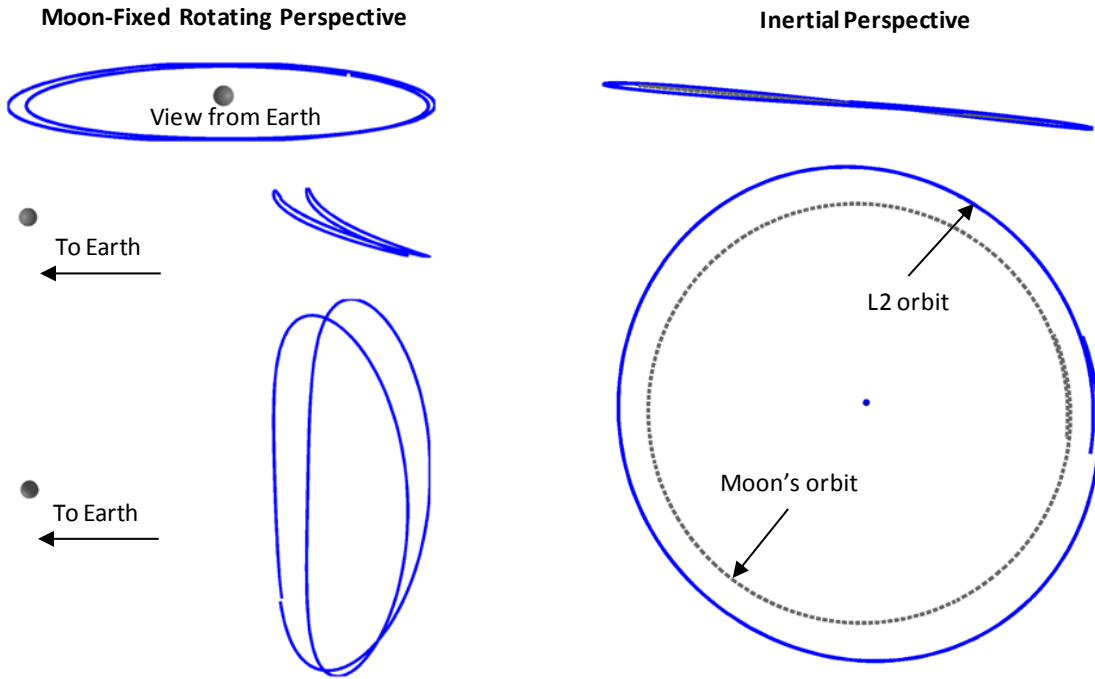


Figure 2-11 Earth-Moon L2 remains in line with the Moon beyond the Moon's orbit. For short-duration transfers, it behaves similar to a high circular orbit.

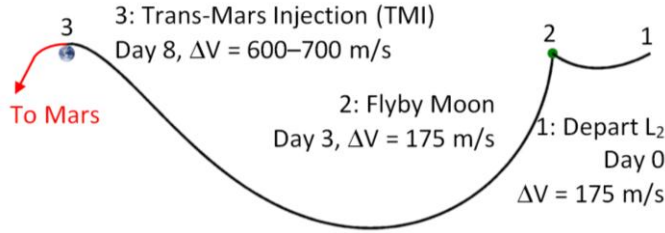


Figure 2-12 Three-burn escape sequence from L_2 .

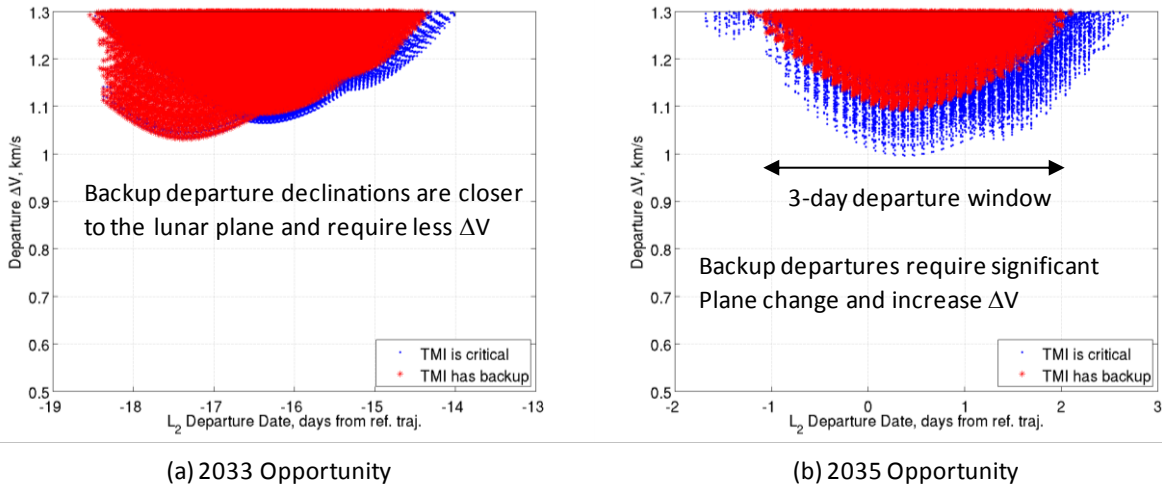


Figure 2-13 Departures from L_2 span approximately 3 days and have an opportunity to retry TMI.

2.2.4. Departure from High-lunar Orbit

The concept of operations for the high-lunar orbit staging node is very similar to the L_2 node. As with the L_2 sequence, the crew departs LEO on a lunar intercept trajectory and performs a maneuver at closest approach to the Moon. This maneuver would increase orbital energy to reach L_2 ; however, the lunar orbit maneuver is simply reversed to capture the vehicle into orbit around the Moon. No other rendezvous maneuvers are required. The high-lunar orbit is characterized by a low perilune at around 100 km with an approximately 2-day period, resulting in significant orbital eccentricity. There is also significant freedom in choice of lunar inclination and argument of periapsis that place the vehicle in a dynamically stable orbit with a long uncontrolled lifetime compared to L_2 .¹⁷ An alternative stable orbit is the “Distant Retrograde Orbit,” which can remain stable for over 100 years, but requires significantly more ΔV to enter (and depart, hence the stability), making it less favorable than the elliptic orbit for Earth departure applications. Transfer to high-lunar orbit takes around 4 days with ~ 3100 m/s to depart LEO and ~ 200 m/s for orbit insertion. Also similar to L_2 , the departure window from the staging node is only a couple days while the Moon is in a favorable direction for Mars departures. The critical events for the departure sequence are lunar orbit escape at perilune followed by TMI at a low perigee. Both maneuvers have one backup opportunity on the subsequent periapsis passage, requiring approximately 100 m/s of additional contingency ΔV . The crew can return to Earth in four days with a 200 m/s escape maneuver, should a contingency occur while in lunar orbit.

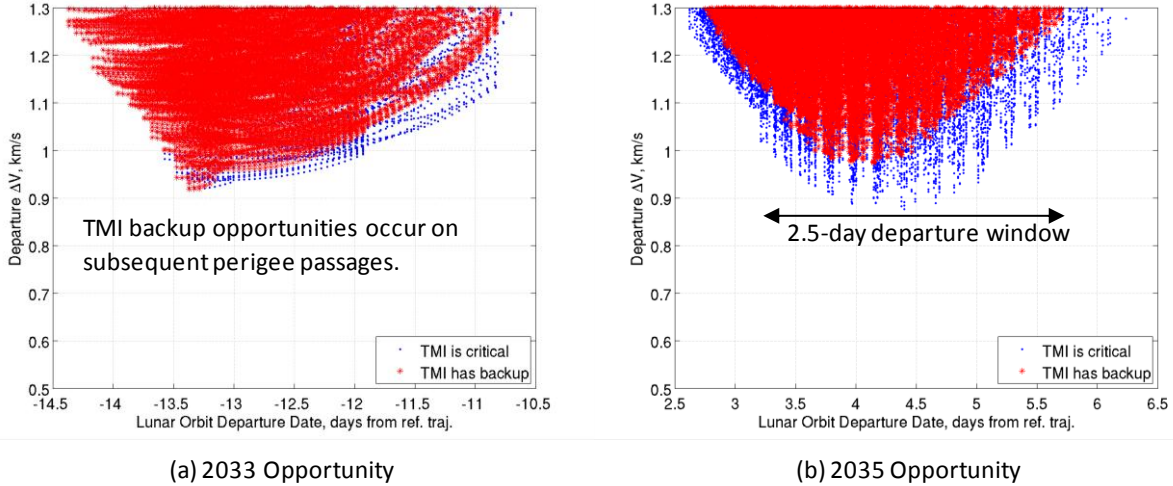


Figure 2-14 Departure characteristics from high-lunar orbit are similar to L-2.

2.2.5. Departures from High-Earth Orbit

High-Earth orbit is characterized by a low perigee at a few hundred kilometers altitude and an apogee that crosses lunar orbit, resulting in an eccentric 10- to 14-day period orbit. This orbit spends at most 1% of the time passing through the van Allen belts. Should this belt passage prove to be unacceptable, the perigee can be raised above the belts for approximately 300 m/s or via lunar gravity assist for negligible ΔV . In contrast to the L2 and high-lunar orbit staging nodes, the inclination of the staging orbit is constrained by the inclination of the launch orbit. Ideally, HEO would have a 28.5 degree inclination for launches from Florida, or 51.6 degrees for transfers from Space Station orbit. (Though transfers from the Space Station itself add an extra constraint on HEO to match the node of the station’s orbit.) However, Earth-Mars transfers with large declinations (e.g., 2033) are expensive to reach when the inclination is less than the (absolute magnitude of) declination. An efficient method to overcome this limitation is to rotate the orbit along the line of apsides (the “apo-twist” maneuver⁴) into a plane that shares the departure asymptote. An example sequence is depicted in Figure 2-15. High departure declinations may be achieved propulsively from HEO, whereas these declinations are more easily achieved via the Moon’s gravity for the L2 and high-lunar orbit locations.

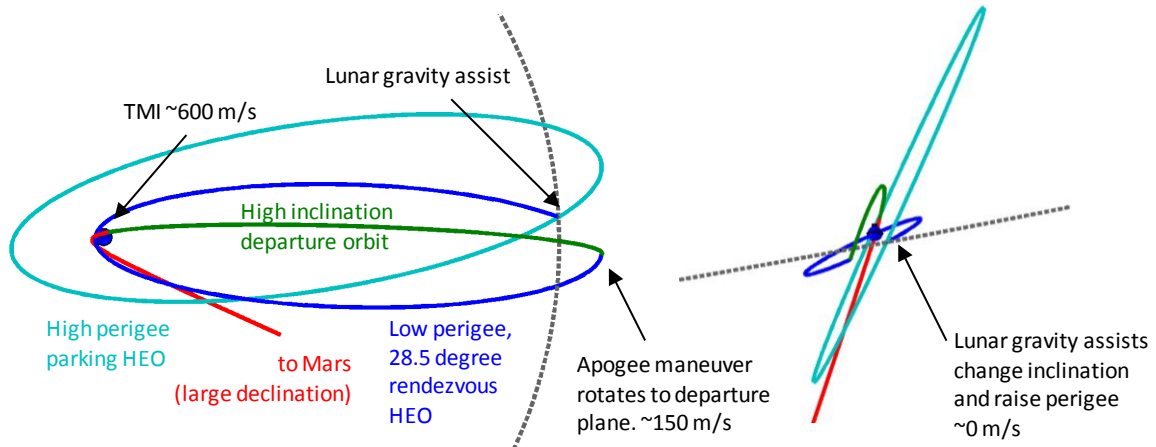


Figure 2-15 Lunar gravity assists and maneuvers near apogee shape HEO for efficient departures.

The departure sequence begins by departing LEO (which is chosen to share the plane of HEO at LEO departure) and to rendezvous with HEO within about 1 day for less than 25 m/s ΔV . If a reorientation to a higher inclination is required, then the rendezvous should be completed before apogee (5 to 7 days after LEO departure) where the orbit plane is changed to provide an efficient TMI ΔV on the following perigee. If the TMI does not occur, then there are one or two backup opportunities on the following one or two perigees (similar to the TMI backup procedure for L2 and high-lunar orbit departures), as shown in Figure 2-16. Alternatively, the crew could return to Earth for less than 25 m/s in 5 to 7 days in a contingency situation.

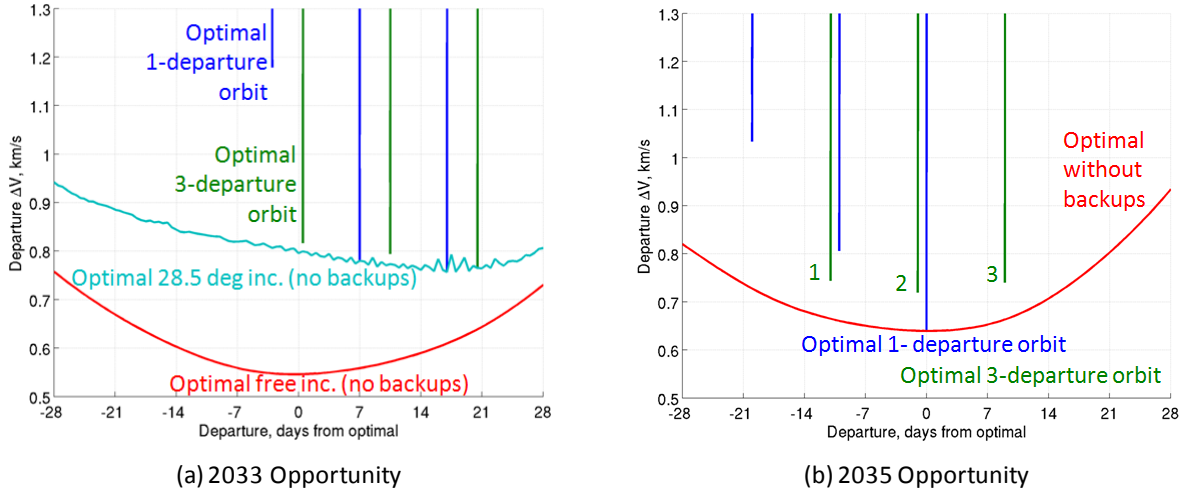


Figure 2-16 Departure opportunities from HEO occur for short durations near perigee passages.

2.2.6. Departure from Low-Earth Orbit

Assembly of the deep space vehicle could also occur in LEO. With LEO departures, there is no intermediate staging node at a high energy with respect to Earth (as with the other options), so low-thrust transfers with high-efficiency electric propulsion could not be used to lower propellant mass at this location. This location is also not as useful for exploration campaigns that would reuse interplanetary vehicles by “parking” them in a high energy staging location. On the other hand, the lack of an intermediate destination in the departure sequence makes the escape sequence less complex. As with HEO staging, the ΔV depends on the departure declination, where large declinations benefit from an intermediate HEO to reorient the orbit. This results in a 3-burn sequence where the vehicle would depart LEO into an elliptical HEO, reorient the high-Earth orbit into the departure plane, then perform TMI for escape. Departure windows from LEO typically exist from one to several days, depending on the difference between launch inclination and departure declination. The duration of the departure window is mainly driven by the precession of LEO due to Earth’s oblateness. The direction of the escape asymptote toward Mars typically changes by about half a degree per day, while the node (angular momentum) of LEO regresses by 7 degrees per day for 28.5 deg inclination and about 5 degrees per day for 51.6 deg inclination. Thus, the duration that LEO is near the plane of the departure asymptote is typically less than a day. An exception occurs when the departure declination is nearly equal to the orbital inclination and departures with relatively little plane change are available for several days. The departure characteristics for large declination (2033) and low declination (2035) are detailed in Figure 2-17 for single impulse escape from LEO and in Figure 2-18 for escape with an intermediate HEO. Crew contingency return from LEO would require 100 m/s ΔV to de-circularize the orbit and takes less than 1 day to return to Earth.

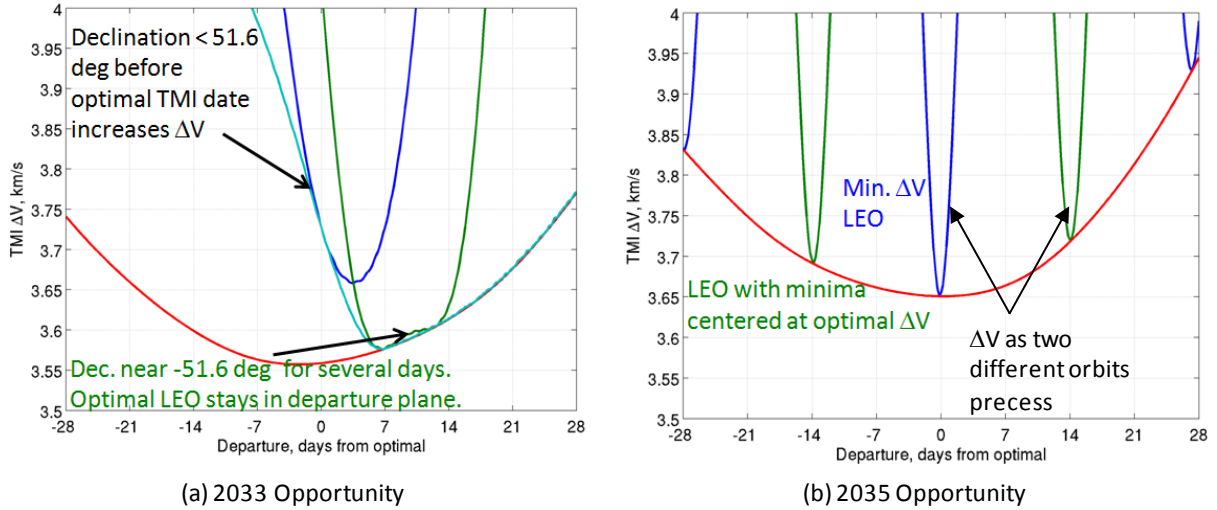


Figure 2-17 Performance for single impulse departures from LEO depends on launch declination.

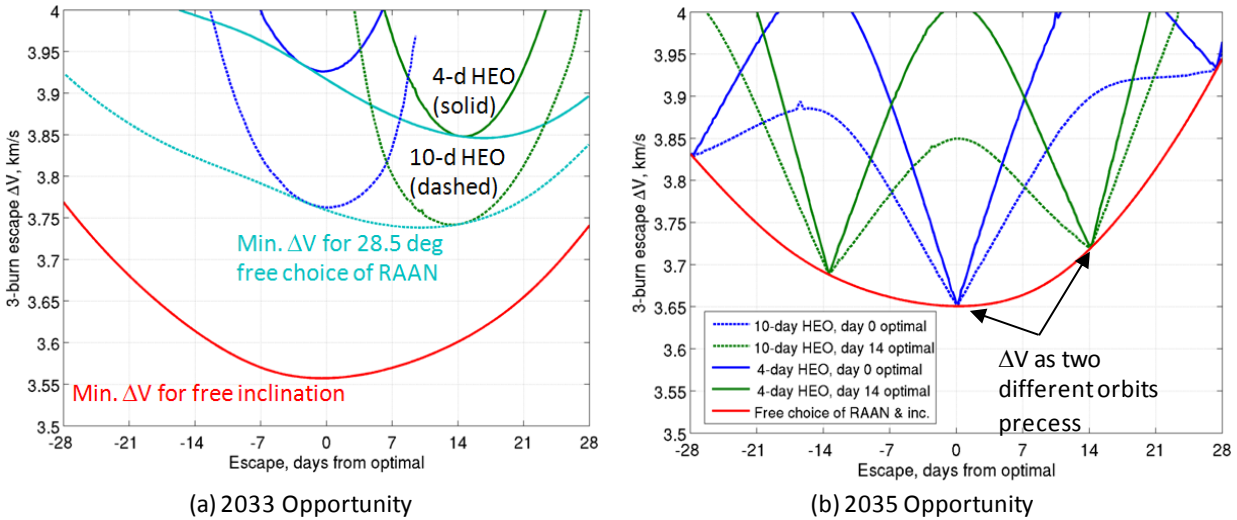


Figure 2-18 Three-burn sequence enables out of plane departures. Plane change is most efficient at low apogee speed with long period orbits.

2.2.7. Comparison of Departure Options

The overall figures of merit for the considered staging options are compiled in Table 2-5. The ΔV for the crew to arrive at the rendezvous location is largest for the L2 staging node. This ΔV is larger because L2 is essentially in a high circular orbit with respect to Earth (as shown in Figure 2-11) and requires circularization maneuvers at the Moon and at L2. The ΔV to reach high-lunar orbit is also relatively high due to the orbit capture maneuver at the Moon. The ΔV to reach high-Earth orbit is lower essentially because it is at a lower energy with respect to Earth than either L2 or high-lunar orbit, and no additional rendezvous maneuvers required after escaping LEO. It is noteworthy that long transfers to the Moon can take advantage of solar perturbations to lower the energy with respect to the Moon, and lower the ΔV to insert in L2 or high-lunar orbit by about 300 m/s. However, this efficiency is only available for time-insensitive cargo transfer out to these points. The ΔV to depart to Mars from L2 and high-lunar orbit is generally higher than HEO and LEO because the vehicle must first energetically “backtrack” down to a low perigee to efficiently escape Earth. Conversely, both HEO and LEO require additional ΔV for departures to

large declinations when the launch inclination is constrained to 28.5 degrees. High-lunar orbit and L2 are relatively insensitive to departure declination because there is a free choice of inclination following the maneuver at the Moon (and L2 and the Moon are always accessible from 28.5 degree inclination). Departures from HEO or LEO still typically require less ΔV to reach Mars, even during opportunities with large departure declinations.

However, comparisons based solely on ΔV can be misleading because vehicle masses and specific impulse of the propulsion systems also affect the efficiency of a mission. From a mission mass perspective, high-energy staging points are only beneficial when combined with some efficiency to offset the increase in ΔV , such as solar electric propulsion or vehicle reuse. Programmatic reasons to stage at a high-energy node are also likely to come into play, such as to maintain assets in cis-lunar space.

The robustness of a mission is another key driver when comparing staging options. Since minimum ΔV isn't the only criteria, a range of ΔV is provided in Table 2-5 to provide backup escape opportunities and some flexibility in mission timing. For launch timing, L2 and high-lunar orbit are accessible from LEO at any time, though the precession of the selected orbit limit LEO departure opportunities to about once a week. Once in orbit around L2 or the Moon, there is a short but continuous window of a few days to depart to the intermediate orbit before TMI. Once on this pre-TMI orbit, there are generally only two opportunities spaced over a week apart to inject onto the interplanetary trajectory. Arrival onto and departure from HEO is limited to discrete opportunities at perigee passages. Launch window concerns (e.g., Florida weather) can be mitigated by launching a few days early to a preselected LEO that will precess into the HEO plane at the time of its perigee passage. There is also some freedom in the choice of HEO plane to allow up to three TMI opportunities (spaced an orbit period apart) for relatively little ΔV once in HEO. While a direct launch and departure from LEO is operationally less complex, orbital precession complicates departure should a delay occur. If the launch declination is significantly less than the LEO inclination, then departure opportunities come about once every 28 days (180 degrees of nodal precession). A single TMI backup is available for about 50 m/s, but two backup opportunities could require up to 300 m/s of additional ΔV . If the departure declination is near the LEO inclination, then LEO remains near the departure plane for 5–10 days, providing a shorter but continuous departure window from LEO.

The number of critical maneuvers and contingency options also affect the risk of a mission. The number of critical maneuvers to escape is greatest for L2 and least for LEO. The “criticality” of these maneuvers is mitigated somewhat by the available backup opportunities. In terms of contingency options, L2 is farthest from Earth and therefore requires the most time and ΔV to return. Return from HEO requires the least ΔV because it is relatively easy to lower perigee to atmospheric interface at apogee, but the return must wait until next perigee passage. LEO is the closest staging node to Earth and can provide emergency return in a few hours, but requires around 100 m/s to target the atmosphere.

2.2.8. Earth Departure Scenario Conclusions

When considering the overall magnitude, number, and timing of escape maneuvers, L2 and high-lunar orbit are very similar both energetically and operationally. High-Earth orbit requires less ΔV and few maneuvers, but the maneuver timing is driven by perigee passages. High-Earth orbit provides additional versatility with a wide range of inclinations, periods, and perigees that are achievable via lunar gravity assists. Backup opportunities for trans-Mars injection are available for any of the departure options with an intermediate high-Earth orbit. Low-Earth orbit is distinct from other options because it has no intermediate staging node, and requires fewer maneuvers to depart. Indirect departures with large declinations to Mars are available via a reorientation maneuver at apogee on an intermediate HEO. Departures from LEO generally require the lowest ΔV , but could require more mass if efficiencies such as solar electric propulsion and deep-space-vehicle reuse are available with the other staging locations.

Acknowledgments

The author thanks John Baker and Bret Drake for their support of this research. This research was carried out at the Jet Propulsion Laboratory, California Institute of Technology, under a contract with the National Aeronautics and Space Administration.

Table 2-5 Departure Scenario Considerations for Human Missions to Mars

Aggregation Location	L ₂ Halo	Lunar Orbit	10-d HEO	Low Earth Orbit
Crew to rend. location (from LEO)	3450 m/s, 8 d	3300 m/s, 4 d	3100 m/s, 1 d	0 m/s, 0 d
Departure 2033 (51.6 deg LEO)	1050-1200 m/s	900-1200 m/s	600-650 m/s	3600 m/s
Departure 2033 (28.5 deg LEO)	1050-1200 m/s	900-1200 m/s	750-850 m/s	3750-3800 m/s
Departure 2035 (28.5 deg LEO)	1000-1300 m/s	900-1300 m/s	650-750 m/s	3650-3950 m/s
Total DV through TMI	4450-4750 m/s	4200-4600 m/s	3650-3950 m/s	3600-3950 m/s
Trans-Mars Departure Window Length	3-4 days	2.5-3.5 days	20 days	For Dec=Inc (e.g. 2033) 5-10 days, 75-100 opp.
# TMI Opportunities	1-2 Opportunities	1-2 Opportunities	1-3 Opportunities	For Dec<Inc. (e.g. 2035) 0-56 days, 1-2 opp.
Crew Critical Maneuvers	Depart LEO Lunar Flyby Out/In L2 Halo Arr./Dep. TMI	Depart LEO Lunar orbit arrival Lunar orbit departure TMI	Depart LEO HEO arrival TMI	LEO arrival TMI
Crew Contingency Return	350 m/s, 8 d	200 m/s, 4 d	<25 m/s, 4 d	100 m/s, 0 d

2.3. Mars Conceptual Flight Profile

Primary Contributors:

Jeffrey P. Gutkowski, National Aeronautics and Space Administration, Johnson Space Center
Richard M. Jedrey, National Aeronautics and Space Administration, Johnson Space Center

2.3.1. Conceptual Flight Profile Overview

The purpose of this task was to go above and beyond the trajectory analysis performed in DRA 5 in terms of creating a more realistic reference trajectory. This trajectory product would integrate together multiple flight phases of this conjunction-class Mars mission. This would help determine how much more expensive (in terms of delta velocity (Δv) or propellant usage) actually orchestrating a Mars mission would be while trying to seamlessly connect the independent cargo and crew trajectories for a successful Mars mission.

2.3.1.1. Conceptual Flight Profile Definition and Uses

A Conceptual Flight Profile (CFP) is an end-to-end trajectory encompassing multiple flight phases. This CFP is a stand-alone Mars mission with specific assumptions (epoch, mass, Mars parking orbit, etc.). For this CFP, a list of Ground Rules, Constraints, and Assumptions (GRC&As) were created, and are outlined in Section 2.3.1. Developing a CFP is like putting together a puzzle of multiple flight phases (puzzle pieces) to form a smooth, continuous mission. A CFP provides a check of how flyable baselines and mission requirements are across multiple flight phases. It also identifies disconnects between disciplines and owners of specific flight phases. This is especially helpful in terms of this multi-center Mars Addendum #2 team. The final CFP product also supplies disciplines with a common trajectory reference so they can perform additional detailed analyses. During the development of a CFP, the main drivers of the Δv cost and other mission factors can be identified. These can be turned into separate trade studies that can be performed during or after the final CFP product. Certain mission factors may become known during the CFP integration process that may not otherwise be noticed in separate independent analyses.

2.3.1.2. CFP Methodology

This Mars CFP consists of many flight phases. One way to connect each flight phase together is to utilize various mission design knobs. These knobs could be as simple as allowing the time of flight of the cargo vehicle to vary to help it connect with the crew vehicle’s optimal Mars parking orbit 2 years later. The main vehicles involved in the CFP are the cargo Descent/Ascent Vehicle (DAV), the cargo Surface Habitat vehicle (SHAB), the crewed Mars Transfer Vehicle (MTV), and Orion. The DAV and SHAB are separate vehicles, but were only considered in one independent trajectory. Orion is mainly only used as a crew transfer vehicle in Earth orbit to the MTV and in Mars orbit from the MTV to the SHAB. See Table 2-7 and Table 2-8 for a list of the flight phases and mission design knobs available to help create an end-to-end mission.

Earth	
FlightPhase	Knobs
Launch campaign	
LEORendezvous	LEO launch time
DAV outbound	
SHAB outbound	DAV/SHAB/MTV loiter time
MTV outbound	3-burn sequence targeting
	DAV/SHAB/MTV time of flight

Figure 2-19 Flight phases and knobs for Earth portion of CFP.

The flight phases boxed in red are the main interplanetary trajectory elements called the backbone flight phases. These backbone flight phases are modeled in the optimal trajectory tool Copernicus and are the first essential flight phases that need to be connected continuously, end-to-end. Table 2-7 and Table 2-8 do not necessarily capture all of the independent variables used by Copernicus to optimize the flight phases, but only highlight how the different phases of the mission can be altered to affect the entire end-to-end mission. Once the backbone flight phases are sufficiently connected and optimized to form a flyable mission, the other remaining flight phases can be added to the backbone.

All these other flight phases can use the knobs to help iterate and connect with the backbone flight phases. The goal of the backbone flight phases is to find not just individual optimal solutions (i.e., lowest Δv cost) for each flight phase, but to find the overall optimal solution for the mission. This refers to finding what sub-optimal trajectory solutions connect together to form the cheapest overall mission while satisfying all the GRC&As defined.

At the time of this DRA 5 Addendum #2 writing, only the backbone portion of the CFP has been completed. In addition, this end-to-end trajectory assumes all impulsive maneuvers. The mass and engine property assumptions discussed in the following sections would be used for the next step in CFP development, which would convert the impulsive maneuvers to finite. A more detailed discussion about forward work is contained in Section 2.3.5.

2.3.1. DRA 5 Investigation and CFP Ground Rules, Constraints, and Assumptions

One of the first tasks when creating a CFP is to investigate what previous assumptions had been made. The references for this information were the DRA 5 Overview and DRA 5 Addendum #1 documents. Some of the information collected included mass properties, Δv values, V-infinity target values, parking orbits, flight times, etc. This was to provide a good initial guess for the start of the CFP creation process. For example, mass and engine properties are important for calculating correct finite burn solutions for each of the maneuvers. However, during this information collection stage, multiple mass property assumptions outlined in the reference documents mentioned above had some discrepancies between them or did not agree.

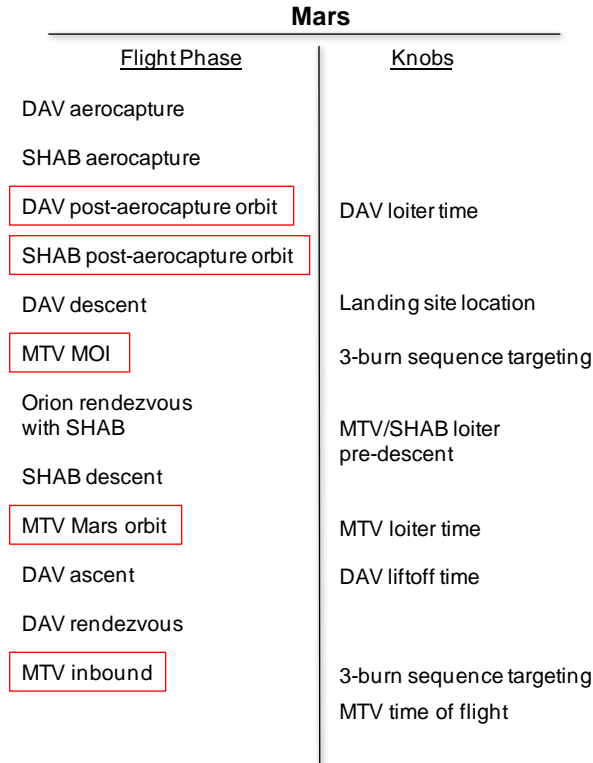


Figure 2-20: Flight phases and knobs for Mars portion of CFP.

2.3.1.1. Discrepancies found within DRA 5 documentation

Several discrepancies in mission and vehicle parameters were found in different sections within DRA 5. Mass properties were among some of the parameters that were inconsistently referenced within DRA 5. Table 2-6 shows which mass properties were inconsistent and what values are being used for trajectory design.

Table 2-6 Mass Property Discrepancies

Mass Property	Value #1	Value #2	Value #3	Value Used for CFP
Total Cargo Lander	115 m-t (DRA 5 p54)	103 m-t (DRA 5 Table 4-1)	--	115 m-t
Cargo Descent Pinpoint Landing Prop Used	3.03 m-t listed but unaccounted for (DRA 5 Add. #1 Table 5-21)	--	--	3.03 m-t accounted for
Initial Assembled Cargo Vehicles	246.2 m-t (DRA 5 Table 4-1)	258.2 m-t (Sum of assumed values)	--	258.2 m-t
Initial Assembled Crew Vehicle	356.4 m-t (DRA 5 Table 4-1)	356.6 m-t (Sum of elements in DRA 5 Table 4-1)	370 m-t (Sum of assumed values)	370 m-t
Orion CM, SM, & Crew	10.6 m-t (DRA 5 Table 4-1)	14 m-t (DRA 5 p31)	24 m-t (Current Wet Orion Design)	
Aeroshell Mass (prior to aerocapture)	42.9 m-t (DRA 5 Table 5-1)	37.1 m-t (DRA 5 Add. #1 Table 5-21)	--	42.9 m-t

Clearly, there are many mass discrepancies with the current information available. As the CFP matures, a more accurate estimate of propellant usage will be obtained, and this will allow for a more accurate mass timeline. Also, propellant reserved for orbit maintenance and Trajectory Correction Maneuvers (TCMs) has not yet been accounted for. In general, larger masses were assumed for the CFP and Mass Timeline to be conservative when determining the necessary propellant loading.

A very significant mass discrepancy is in Orion's mass. DRA 5 discusses an estimate for the Crew Module (CM) to be around 10 t and 4 t to account for a Service Module (SM). Value #1 in Table 2-6 accounts for Orion on the assembled MTV and it is assumed to not account for the SM mass estimate, plus an additional 0.6 t for crew. However, the current Orion vehicle design (CM + SM) is significantly higher than 14 t and is closer to 24 t when fully loaded with propellant. The final propellant load will be dependent on the maneuvers allocated to the Orion as the mission design matures. Most notable would be any pre-Earth arrival slowdown maneuvers necessary to meet entry speed limits for the Orion capsule.

2.3.1. Mission Timeline

In an effort to compile key GRC&As, a mission timeline was put together to encompass all major events from the first campaign launch to crew reaching Entry Interface (EI) for both a conjunction mission and an opposition class mission. The CFP focused on a conjunction class mission as that was the preferred mission discussed in DRA 5. Table 2-7 captures the current mission timeline derived from DRA 5 for the CFP, a conjunction class mission. Although neither analyzed as part of the CFP development, nor baselined as part of DRA 5, Table 2-8 contains the current working timeline for an opposition class mission. All of the assumed values contained in these mission timelines were the best initial guesses found in DRA 5 and Addendum #1 at the time the CFP was started.

Table 2-7 Conjunction Class Mission Assumptions

Flight Phase	Assumptions	Value	Units
<u>General Mission</u>			
	Trajectory tools used	STK/Copernicus	
	Maneuvers	Finite	
	Type	Conjunction	
	Propulsive element	NTR	
	Model SLS launches	No	
	Mass properties	See other sheet	
	Engine properties	See other sheet	
<u>Cargo LEO Assembly</u>			
	Year	2035	
	Gravity Model	GGM02C 8x8	
	Number of SLS launches	5	
	Time between launches	30	days
	SLS insertion orbit inclination	28.5	deg
	Minimum periapsis altitude in LEO	185	km
	SLS launch of PE1 into orbit of	-87 x 241	km
	SKS performs perigee raise of PE1		
	SLS launch of PE2 into orbit of	-87 x 241	km
	SKS performs perigee raise of PE2		
	SLS launch of 2 LH2 tanks into orbit of	-87 x 241	km
	SKS performs perigee raise of LH2 tanks		
	Rendezvous of PE1 and LH2 tank	RCS	
	Rendezvous of PE2 and LH2 tank	RCS	
	SLS launch of DAV into orbit of	-87 x 241	km
	SKS performs perigee raise of DAV		
	SLS launch of SHAB into orbit of	-87 x 241	km
	SKS performs perigee raise of SHAB		
	Rendezvous of PE1 and DAV	RCS	
	Rendezvous of PE2 and SHAB	RCS	
<u>Cargo Earth Departure</u>			
	Orbit altitude prior to departure	407 x 407	km
	DAV loiter time before TMI	4	months
	DAV performs trans-Mars injection (TMI)	2-burn	
	Time between Cargo TMIs	30	days
	SHAB performs TMI	2-burn	
<u>Cargo Outbound</u>			
	Gravity model	Earth/Sun/Mars	
	Duration	202	days
	TCM1 time after TMI	1	day
	TCM2 time after TMI	50	days
	TCM3 time before aerocapture	50	days
	TCM4 time before aerocapture	1	day
	DAV detaches from PE1 time before aerocapture	12	hrs
	SHAB detaches from PE2 time before aerocapture	12	hrs
<u>Cargo Mars Arrival</u>			
	Gravity model	GMM2B	
	Atmospheric model	Mars GRAM 2005	
	Mars Capture	Aerocapture	
	Maximum Mars arrival V _{inf}	5.45	km/s
	Minimum periapsis altitude for Aerocapture	50	km
	SHAB Minimum periapsis altitude	185	km
	SHAB Mars parking orbit altitude	250 x 33,793	km
	DAV intermediate orbit		km
<u>Cargo Mars Descent</u>			
	DAV time in intermediate orbit	2	revs
	DAV performs de-orbit maneuver	main engines	
	Landing site		

Conjunction Class Mission Assumptions – Continued

Flight Phase	Assumptions	Value	Units
<u>MTV LEO Assembly</u>			
	Year	2037	
	Time since DAV/SHAB TMI	2	years
	Time since Mars ascent prop complete	30	days
	Number of SLS launches	5	
	Time between launches	30	days
	SLS insertion orbit inclination	28.5	deg
	Minimum periapsis altitude in LEO	185	km
	SLS launch of PE3 into orbit of	-87 x 241	km
	SKS performs perigee raise of PE3		
	SLS launch of LH2 tank into orbit of	-87 x 241	km
	SKS performs perigee raise of LH2 tank		
	Rendezvous of PE3 and LH2 tank	RCS	
	SLS launch of LH2 drop tank and truss into orbit of	-87 x 241	km
	SKS performs perigee raise of LH2 drop tank/truss		
	Rendezvous of PE3 stack and LH2 drop tank/truss	RCS	
	SLS launch of into orbit of payload	-87 x 241	km
	SKS performs perigee raise of payload		
	Rendezvous of PE3 stack and payload	RCS	
	MTV to departure orbit	407 x 407	km
<u>Crew Launch and Departure</u>			
	SLS launch of Crew into orbit of	-87 x 241	km
	SKS performs perigee raise of Delivery Orion		
	Rendezvous of Delivery Orion with MTV	OME/Aux	
	Jettison of Delivery Orion	spring	
	MTV performs TMI	2-burn	
	Maximum TMI Vinf	4.426	km/s
<u>Crew Outbound</u>			
	Gravity Model	Earth/Sun/Mars	
	Duration range	220	days
	LH2 drop tank jettison post TMI	1	day
	TCM1 time after TMI	1	day
	TCM2 time after TMI	50	days
	TCM3 time before aerocapture	50	days
	TCM4 time before aerocapture	1	day
<u>Crew Mars Arrival</u>			
	Gravity model	GMM2B	
	Mars Capture	Propulsive	
	MTV performs MOI	NTR	
	Maximum MOI Vinf	4.176	km/s
	MTV initial orbit altitude	250 x 33,793	km
<u>Crew Mars Rendezvous</u>			
	Rendezvous of Orion with SHAB	OME/Aux	
	Undock of Orion from SHAB	spring	
	Rendezvous of Orion with MTV	OME/Aux	

Conjunction Class Mission Assumptions – Concluded

Flight Phase	Assumptions	Value	Units
<u>Crew Mars Descent</u>			
	Atmospheric model SHAB performs de-orbit maneuver	Mars GRAM 2005 main engines	
<u>Mars Surface Stay</u>			
	Surface Stay Duration MTV remains in orbit Minimum periapsis altitude	539 185	days km
<u>Crew Mars Ascent</u>			
	DAV performs ascent	main engines	
<u>Mars Departure</u>			
	Rendezvous of DAV with MTV Jettison DM and contingency consumables MTV performs TEI Maximum TEI Vinf	RCS spring NTR 4.004	 km/s
<u>Inbound</u>			
	Gravity Model Duration range TCM5 time after TEI TCM6 time after TEI TCM7 time before EI TCM8 time before EI	Earth/Sun/Mars 220 1 50 50 1	 days day days days day
<u>Earth Arrival and EDL</u>			
	Maximum Earth return Vinf Earth entry EI inertial velocity limit Orion separation from MTV Orion performs maneuver to target EI Landing site MTV performs Earth flyby to heliocentric space Minimum altitude for MTV flyby	6.813 Direct 12 36 OME Pacific (San Diego) 185	km/s km/s hrs km

Table 2-8 Opposition Class Mission Assumptions

Flight Phase	Assumptions	Value	Units
<u>General Mission</u>			
	Trajectory tools used	STK/Copernicus	
	Maneuvers	Finite	
	Type	Conjunction	
	Propulsive element	NTR	
	Model SLS launches	No	
	Mass properties	See other sheet	
	Engine properties	See other sheet	
<u>Cargo LEO Assembly</u>			
	Year	2031	
	Gravity Model	GGM02C 8x8	
	Number of SLS launches	5	
	Time between launches	30	days
	SLS insertion orbit inclination	28.5	deg
	Minimum periapsis altitude in LEO	185	km
	SLS launch of PE1 into orbit of	-87 x 241	km
	SKS performs perigee raise of PE1		
	SLS launch of PE2 into orbit of	-87 x 241	km
	SKS performs perigee raise of PE2		
	SLS launch of 2 LH2 tanks into orbit of	-87 x 241	km
	SKS performs perigee raise of LH2 tanks		
	Rendezvous of PE1 and LH2 tank	RCS	
	Rendezvous of PE2 and LH2 tank	RCS	
	SLS launch of DAV into orbit of	-87 x 241	km
	SKS performs perigee raise of DAV		
	SLS launch of SHAB into orbit of	-87 x 241	km
	SKS performs perigee raise of SHAB		
	Rendezvous of PE1 and DAV	RCS	
	Rendezvous of PE2 and SHAB	RCS	
<u>Cargo Earth Departure</u>			
	Orbit altitude prior to departure	407 x 407	km
	DAV loiter time before TMI	4	months
	DAV performs trans-Mars injection (TMI)	2-burn	
	Time between Cargo TMIs	30	days
	SHAB performs TMI	2-burn	
<u>Cargo Outbound</u>			
	Gravity model	Earth/Sun/Mars	
	Duration	202	days
	TCM1 time after TMI	1	day
	TCM2 time after TMI	50	days
	TCM3 time before aerocapture	50	days
	TCM4 time before aerocapture	1	day
	DAV detaches from PE1 time before aerocapture	12	hrs
	SHAB detaches from PE2 time before aerocapture	12	hrs
<u>Cargo Mars Arrival</u>			
	Gravity model	GMM2B	
	Atmospheric model	Mars GRAM 2005	
	Mars Capture	Aerocapture	
	Maximum Mars arrival V _{inf}	5.45	km/s
	Minimum periapsis altitude for Aerocapture	50	km
	SHAB Minimum periapsis altitude	185	km
	SHAB Mars parking orbit altitude	250 x 33,793	km
	DAV intermediate orbit		km
<u>Cargo Mars Descent</u>			
	DAV time in intermediate orbit	2	revs
	DAV performs de-orbit maneuver	main engines	
	Landing site		

Opposition Class Mission Assumptions – Continued

Flight Phase	Assumptions	Value	Units
<u>MTV LEO Assembly</u>			
	Year	2033	
	Time since DAV/SHAB TMI	2	years
	Time since Mars ascent prop complete	30	days
	Number of SLS launches	5	
	Time between launches	30	days
	SLS insertion orbit inclination	28.5	deg
	Minimum periapsis altitude in LEO	185	km
	SLS launch of PE3 into orbit of	-87 x 241	km
	SKS performs perigee raise of PE3		
	SLS launch of LH2 tank into orbit of	-87 x 241	km
	SKS performs perigee raise of LH2 tank		
	Rendezvous of PE3 and LH2 tank	RCS	
	SLS launch of LH2 drop tank and truss into orbit of	-87 x 241	km
	SKS performs perigee raise of LH2 drop tank/truss		
	Rendezvous of PE3 stack and LH2 drop tank/truss	RCS	
	SLS launch of into orbit of payload	-87 x 241	km
	SKS performs perigee raise of payload		
	Rendezvous of PE3 stack and payload	RCS	
	MTV to departure orbit	407 x 407	km
<u>Crew Launch and Departure</u>			
	SLS launch of Crew into orbit of	-87 x 241	km
	SKS performs perigee raise of Delivery Orion		
	Rendezvous of Delivery Orion with MTV	OME/Aux	
	Jettison of Delivery Orion	spring	
	MTV performs TMI	2-burn	
	Maximum TMI Vinf	4.426	km/s
<u>Crew Outbound</u>			
	Gravity Model	Earth/Sun/Mars	
	Duration range	174	days
	LH2 drop tank jettison post TMI	1	day
	TCM1 time after TMI	1	day
	TCM2 time after TMI	50	days
	TCM3 time before aerocapture	50	days
	TCM4 time before aerocapture	1	day
<u>Crew Mars Arrival</u>			
	Gravity model	GMM2B	
	Mars Capture	Propulsive	
	MTV performs MOI	NTR	
	Maximum MOI Vinf	4.176	km/s
	MTV initial orbit altitude	250 x 33,793	km
<u>Crew Mars Rendezvous</u>			
	Rendezvous of Orion with SHAB	OME/Aux	
	Undock of Orion from SHAB	spring	
	Rendezvous of Orion with MTV	OME/Aux	

Opposition Class Mission Assumptions – Concluded

Flight Phase	Assumptions	Value	Units
Crew Mars Descent			
	Atmospheric model SHAB performs de-orbit maneuver	Mars GRAM 2005 main engines	
Mars Surface Stay			
	Surface Stay Duration MTV remains in orbit Minimum periapsis altitude	60 185	days km
Crew Mars Ascent			
	DAV performs ascent	main engines	
Mars Departure			
	Rendezvous of DAV with MTV Jettison DM and contingency consumables MTV performs TEI Maximum TEI Vinf	RCS spring NTR 4.004	km/s
Inbound			
	Gravity Model Venus Swing-by Minimum periapsis altitude at Venus Minimum Perihelion altitude Duration range TCM5 time after TEI TCM6 time after TEI TCM7 time before EI TCM8 time before EI MTV performs a breaking maneuver	Earth/Sun/Mars 300 0.62 400 1 50 50 1 NTR	km AU days day days days day
Earth Arrival and EDL			
	Maximum Earth return Vinf Earth entry EI inertial velocity limit Orion separation from MTV Orion performs maneuver to target EI Landing site MTV performs Earth flyby to heliocentric space Minimum altitude for MTV flyby	6.813 Direct 13 36 OME Pacific (San Diego) 185	km/s km/s hrs km

2.3.1.1. Mass History Timeline

For propellant requirements and finite maneuvers to be modeled, the vehicle mass throughout the mission needs to be modeled. Table 2-9 describes the progression of the cargo vehicles’ mass, and Table 2-10 describes the progression of the crew vehicle’s mass throughout the mission. Since the DAV and SHAB are assumed to have the same mass and aerocapture vehicle to capture into Mars’ orbit, only one trajectory was constructed for both of the cargo vehicles. A conjunction class mission was the only mission class examined. These numbers were based on the assumptions and maneuvers taken from DRA 5 and Addendum #1.

The total surface delivery capability is for each cargo vehicle since the current mass history timeline assumes the same mass properties for the DAV and SHAB. Due to mass inconsistencies and no information regarding orbit maintenance or trajectory correction maneuvers, there are incomplete areas within Table 2-9 and Table 2-10.

Table 2-9: Cargo Vehicle Mass History Timeline

Component / Event	Mass (m-t)	Mass (kg)	Notes/Reference (reference to the main DRAS document unless otherwise noted)
Initial Assembled	258.20	258,200.00	Table 4-1 for all elements unless otherwise stated
Core Stage Dry Mass	33.70	33,700.00	
LH2 Propellant Load	59.40	59,400.00	
RCS Propellant Load	3.60	3,600.00	
Total Stage Mass	96.60	96,600.00	
In-Line Tank Dry Mass	10.80	10,800.00	
LH2 Propellant Load	34.10	34,100.00	
RCS Propellant Load	1.70	1,700.00	
Total In-Line Mass	46.60	46,600.00	
Payload: Total Cargo Lander	115.00	115,000.00	p54 lists a reference 40 t useful payload on Mars with a Mars arrival mass of 115 t, but Table 4-1 lists 103 t
Ares V: Earth Departure Stage?	252.50	252,500.00	(Mass of EDS + Altair, Ref. DRA 5.0 Add. P172) - (Mass of Altair, Ref. DRA 5.0 Add. p181)
Pre-TMI			
Orbit Maintenance Prop			
Post-TMI	167.20	167,200.00	
Propellant Used	(91.00)	(91,000.00)	Ref. p25
TCM Propellant			
PE 1 and 2 Released	(52.20)	(52,200.00)	1 day prior to aerocapture; Equals dry mass + propellant remaining
Pre-MOI (Aerocapture Maneuver)	115.00	115,000.00	(Payload)
Post-MOI (Aerocapture Maneuver)	110.31	110,308.00	Circularization dv average of 19 m/s with maximum of 66 m/s assuming arrival mass of 115 t? Ref. p54
Propellant Used	(4.69)	(4,692.00)	Ref. Table 5-21 in DRA 5.0 Add.
Surface Delivery Capability	47.82	47,821.00	Ref. Table 5-21 DRA 5.0 Add. for all components and events here
Deorbit Propellant Used	(0.46)	(458.00)	
RCS Propellant Used	(1.22)	(1,218.00)	
RCS Dry Mass	(0.99)	(994.00)	Presumably used in calculation of Landed Mass in Table 5-21 from DRA 5.0 Add, but not sure of function
Terminal Descent Prop Used	(13.89)	(13,887.00)	
Pinpoint Landing Prop Used	(3.03)	(3,030.00)	Or is this included in terminal descent prop since it's excluded in the calculation of landed mass in Table 5-21 of DRA 5.0 Add.
Total Propellant Usage	(19.59)	(19,587.00)	
Aeroshell Structure			
TPS			
Structural Mass Changes	(42.90)	(42,900.00)	
Total Payloads Delivered	58.83	58,830.00	Ref. Table 5-1; Combination of payloads from both cargo vehicles
Habitat Lander System Mass	40.40	40,400.00	Ref. Table 5-1
DAV Lander System Mass	18.43	18,430.00	Ref. Table 5-1

Table 2-10: Crew Vehicle Mass History Timeline

Component	Mass (m-t)	Mass (kg)	Notes/Reference (reference to the main DRAS document unless otherwise noted)
Initial Assembled	370.00	370,000.00	Table 4-1. Actual adding up of numbers gives a higher mass though
Core Stage Dry Mass	41.70	41,700.00	
LH2 Propellant Load	59.70	59,700.00	
RCS Propellant Load	4.90	4,900.00	
Total Core Stage Mass	106.30	106,300.00	
In-Line Tank Dry Mass	21.50	21,500.00	
LH2 Propellant Load	69.90	69,900.00	
RCS Propellant Load	Left Blank in	#VALUE!	
Total In-Line Mass	91.40	91,400.00	
Saddle Truss Mass	8.90	8,900.00	
Drop Tank Mass Dry Mass	14.00	14,000.00	
LH2 Propellant Load	73.10	73,100.00	
Total Assembly Mass	96.00	96,000.00	
Short Saddle Truss	4.70	4,700.00	
Contingency Food	9.80	9,800.00	
2nd Docking Module	1.80	1,800.00	
Fwd RCS Propellant Load	3.20	3,200.00	
Transit Habitat	32.80	32,800.00	
Orion CM, SM, and Crew	24.00	24,000.00	Seems small; Orion is around 24,000 kg (includes 8602 kg of prop)
Total Payload Mass	76.30	76,300.00	
Pre-TMI			
Orbit Maintenance Prop			
Post-TMI	224.91	224,911.80	
Propellant Used	(131.09)	(131,088.20)	Currently assumes initial mass is total vehicle mass excluding orbit maintenance; 57.8 min burn time (p26)
Drop Tank Released	(14.00)	(14,000.00)	1 day after TMI completes
Drop Tank + Propellant Remaining	(145.09)	(145,088.20)	
TCM Propellant			
Post-MOI	185.97	185,974.40	
Food	(2.65)	(2,650.00)	Table 4-4. Any unconsumed food for outbound trip to be dropped
MOI Maneuver	(36.29)	(36,287.40)	Ref. p26 for 16 min burn time which equals a dv of 1663 m/s
Crew Transfer	--	--	MTV becomes unmanned, SHAB becomes manned, mass updates specified by light green highlighting
New MTV Mass	185.37	185,374.40	
New SHAB Mass	60.07	60,068.00	See Table 5-1 + orion dock + orion undock - aeroshell structure - post-a/c orbit insert prop
Orion undocks from MTV	(24.00)	(24,000.00)	
Orion docks with SHAB	24.00	24,000.00	
Orion undocks from SHAB	(23.40)	(23,400.00)	Orion mass without crew (estimated as 600 kg according to Table 4-1)
Orion docks with MTV	23.40	23,400.00	
Crew Arrival on Surface	25.88	25,881.00	MTV mass assumed unchanged during crew descent. Mass changes taken from cargo vehicle descent. Final number seems too low?
Deorbit Propellant Used	(0.46)	(458.00)	
RCS Propellant Used	(1.22)	(1,218.00)	
RCS Dry Mass	(0.99)	(994.00)	
Terminal Descent Prop Used	(13.89)	(13,887.00)	
Pinpoint Landing Prop Used	(3.03)	(3,030.00)	As was with cargo vehicle
Total Propellant Usage	(19.59)	(19,587.00)	
TPS	(14.60)	(14,600.00)	
Surface Stay	--	--	Mass deltas on surface irrelevant to trajectory construction
New MTV Mass			
Orbit Maintenance Prop Used			
Crew Mars Ascent to MTV	197.74	197,736.40	Adds in ascent stage dry mass
Ascent Vehicle	(46.44)	(46,442.00)	Ref. Table 3-27 DRA 5.0 Add.
Ascent Stage 1	(27.90)	(27,902.00)	
Ascent Stage 2	(18.54)	(18,540.00)	
Stage 1 Dry Mass	7.20	7,202.00	
Stage 2 Dry Mass	5.16	5,160.00	
Pre-Mars Departure	177.43	177,434.40	
Ascent Vehicle	(12.36)	(12,362.00)	
Food Drop	(7.94)	(7,940.00)	Contingency food dropped
Post-TEI	153.17	153,167.20	
TEI Propellant Used	(24.27)	(24,267.20)	Determined using 10.7 min TEI burn and rocket equation Ref. p26. Creates a dv of only 295 m/s
TCM Propellant Used			
Earth Arrival	--	--	
New MTV Mass	129.17	129,167.20	Final mass seems reasonable and total propellant consumed within budget
Orion Separates	(24.00)	(24,000.00)	

2.3.2. First End-to-End Impulsive CFP Iteration

An effort was made to construct a continuous, end-to-end trajectory for both the cargo and crew vehicles using the GRC&As pulled together from DRA 5. These trajectories were designed using software built in-house at NASA's Johnson Space Center (JSC), Copernicus. Figures depicting key phases of the mission are also provided in this section with discussion on the important features.

DRA 5 outlines that the cargo vehicles will be sent 2 years (one opportunity) prior to the crew vehicle. Trajectories for both the cargo and crew vehicles will be discussed. Since the DAV and SHAB are assumed to have the same mass and aerocapture vehicle to capture into Mars' orbit, only one trajectory was constructed for both of the cargo vehicles.

Copernicus, the software used in constructing this CFP, has a built-in optimizer to find a solution with a low Δv for the given design space. The next few lines detail what key parameters were free for the optimizer to vary for both the cargo and crew trajectories in both CFP iterations. A reference epoch was chosen based on previous work done and/or using external resources. The reference epochs chosen for the first CFP iteration were based on a previous mission opportunity scan. However, since this previous scan did not incorporate the same specific departure and arrival conditions being used in the CFP, the internal optimizer within Copernicus was given flexibility on the date of departure of +/- 30 days of the reference epoch. An initial guess utilized a three-burn Trans-Mars Injection (TMI) sequence. However, Copernicus was given the option to eliminate one of the maneuvers for a more optimal solution. The trip duration was allowed to float between 180 and 220 days. The arrival orbit state was also optimized except for the necessary constraints and assumptions detailed in Section 2.3.1. However, the cargo and crew must have similar orbits when the crew arrives such that the crew can rendezvous with the SHAB that has been loitering in Mars orbit for 2 years.

The separately optimized cargo and crew trajectory do not share the same orbit upon the crew's arrival. An investigation on the geometry between the individual optimal trajectories and differences between the orbits upon crew arrival was conducted. The optimal cargo trajectory was propagated forward to the day of the crew's arrival, and the optimal crew's trajectory was propagated backward to the optimal cargo vehicle's arrival. For the desired fidelity of this CFP, the effect of orbit maintenance on the movement of the orbital plane was ignored. Since one of the trajectories inserts into a prograde orbit and the other into a retrograde, and the resulting plane change necessary to match the cargo and crew vehicles' orbits was about 90° from visual inspection, it was clear that just by altering the time of flight or departure/arrival epochs for either vehicle would not offset the undesirable impact to the current maneuver magnitudes since the rate of precession for an elliptical one-sol orbit was too small. Therefore, an extra maneuver was added to the crew's insertion sequence such that they arrived in the same orbit as the loitering SHAB. This maneuver is discussed further in Section 2.3.2.1.

Once the crew vehicle has completed the insertion sequence, the crew undocks from the MTV, docks with the SHAB, and descends to the surface. During the crew stay, the MTV maintains the orbital dimensions, but the orbit plane itself will still move. As with the cargo vehicle's loiter period, the effect of orbit maintenance on the movement of the orbital plane was not monitored. Thus, the MTV's orbit was propagated for the crew stay outlined in DRA 5 of 539 days. A visual inspection of the post-crew-stay orbit of the MTV indicated that a plane change would be required to depart Mars and return to Earth. Here, up to two maneuvers were used to return to Earth. The first maneuver occurred near apoapse of the Mars Parking Orbit (MPO) to conduct the plane change and any reshaping of the orbit to achieve an optimal powered flyby to return to Earth. The return trip was again allowed to float between 180 and 220 days.

The Trans-Earth Injection (TEI) sequence targeted an Entry Interface (EI) state for Orion. The EI geodetic altitude was fixed to 121.92 km, and the centric flight path angle to -5.86° . The longitude was allowed to float between 210° and 110° West to target an area in the Pacific Ocean. The detic latitude was allowed to float between 50° South and 30° North. The centric azimuth was allowed to be anywhere between 0° and 180° . The velocity at EI was given an upper bound of 12 km/s.

2.3.2.1. Cargo Vehicle Trajectory

The CFP assumes the cargo vehicle is already assembled in a 407 x 407 km Earth Parking Orbit (EPO). A minimum of a two-burn sequence was used for TMI to reduce any anticipated gravity losses. A third maneuver was utilized to reduce any necessary plane change from taking place during the maneuvers near perigee. Figure 2-21 shows the TMI sequence utilized for the cargo vehicles.

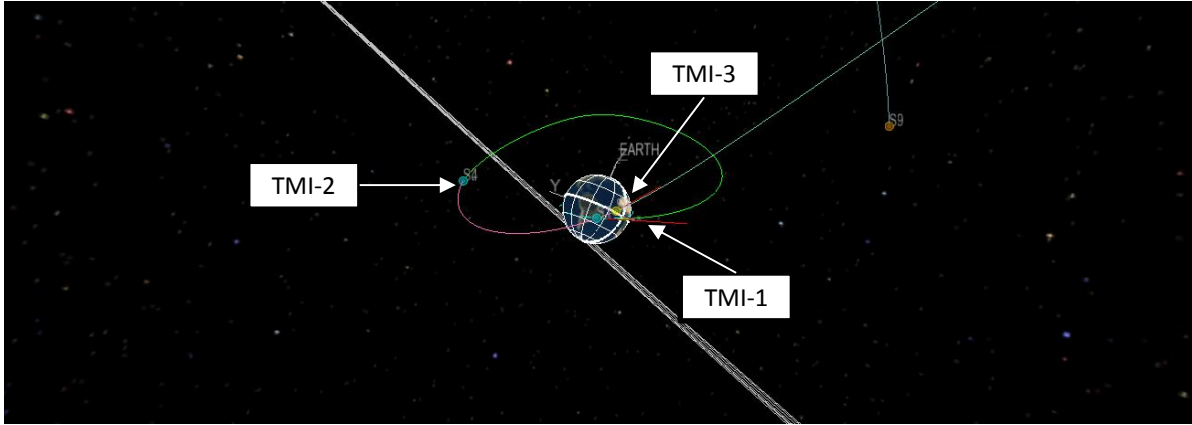


Figure 2-21: Equatorial view of the first CFP iteration cargo vehicle's trans-Mars injection.

Figure 2-21 depicts a near-equatorial view of the TMI sequence. As can be seen, this trajectory takes advantage of third body perturbations that bend the trajectory, thereby minimizing the amount of additional Δv needed by TMI-2. Figure 2-22 shows a near-polar view of the orbit.

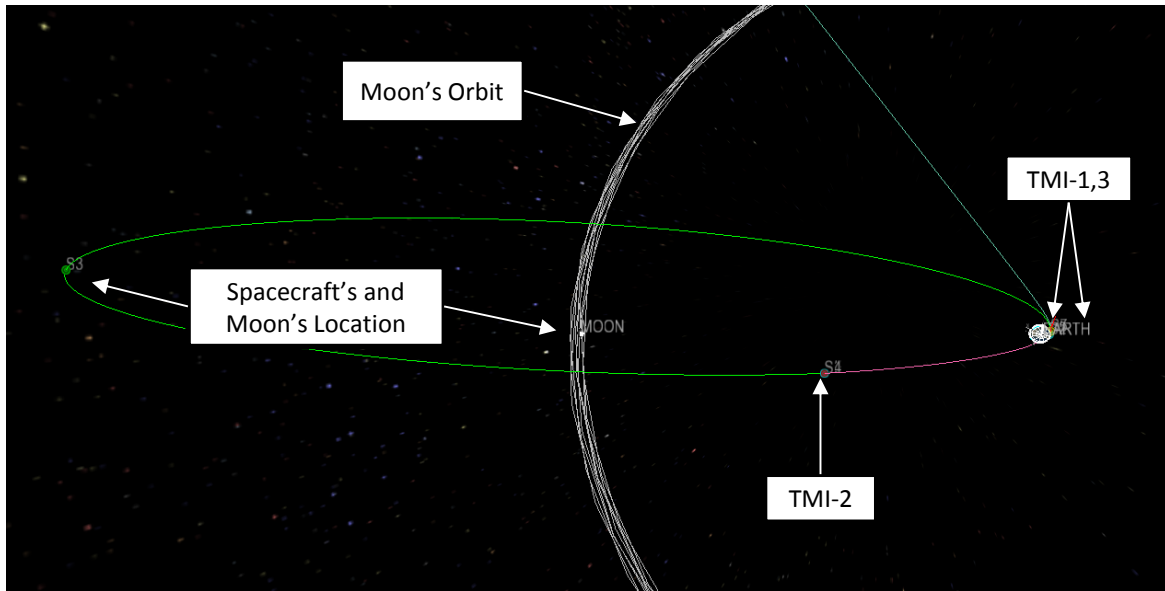


Figure 2-22: Polar view of the first CFP iteration cargo vehicle's trans-Mars injection.

The near-polar view shown in Figure 2-22 shows how highly elliptical the TMI sequence is and the location of the Moon and spacecraft as the TMI sequence is executed. The Δv 's associated with these maneuvers are shown in Table 2-11.

Table 2-11: Cargo Vehicle Trans-Mars Injection Sequence

<u>Maneuver</u>	<u>Magnitude (km/s)</u>
TMI-1	3.13
TMI-2	0.03
TMI-3	1.98

The transfer trajectory in heliocentric space can be seen in Figure 2-23.

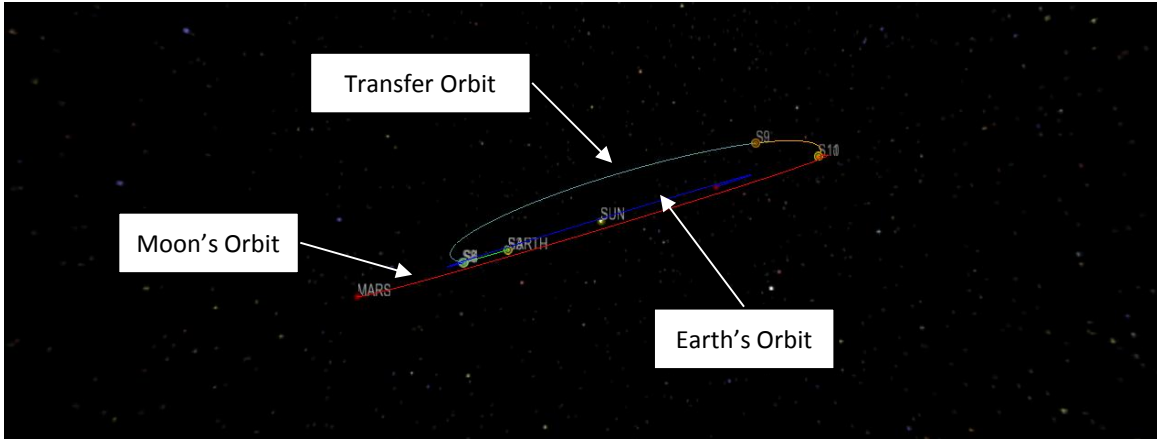


Figure 2-23: Heliocentric view of cargo vehicle transfer trajectory.

This trajectory targeted an aerocapture state with an altitude of 126.06 km, an optimized right ascension and declination, an entry speed of 7.36 km/s, an optimized azimuth, and a flight path angle fixed at -12.77° .

2.3.2.2. Crew Vehicle Trajectory

The crew vehicle is assembled in an Earth orbit of the same size and inclination as the cargo vehicle. Another 3-burn sequence was allowed for use in the optimizer. Figure 2-24 and Figure 2-25 depict the TMI sequence used by the crew vehicle.

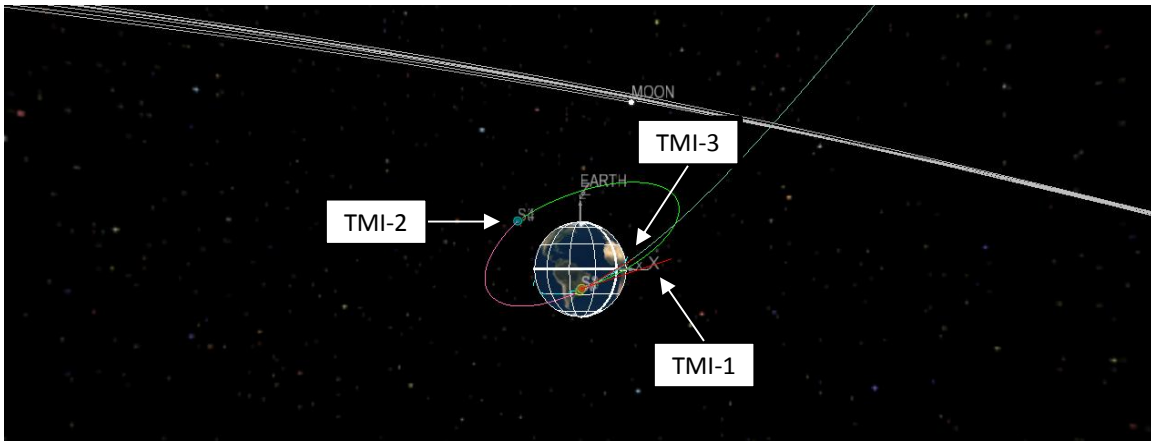


Figure 2-24: Equatorial view of the first CFP iteration crew vehicle's trans-Mars injection.

As in contrast to the cargo vehicle's trajectory, there is less of a plane change required in this sequence. Figure 2-25 shows a near-polar view of the crew TMI sequence.

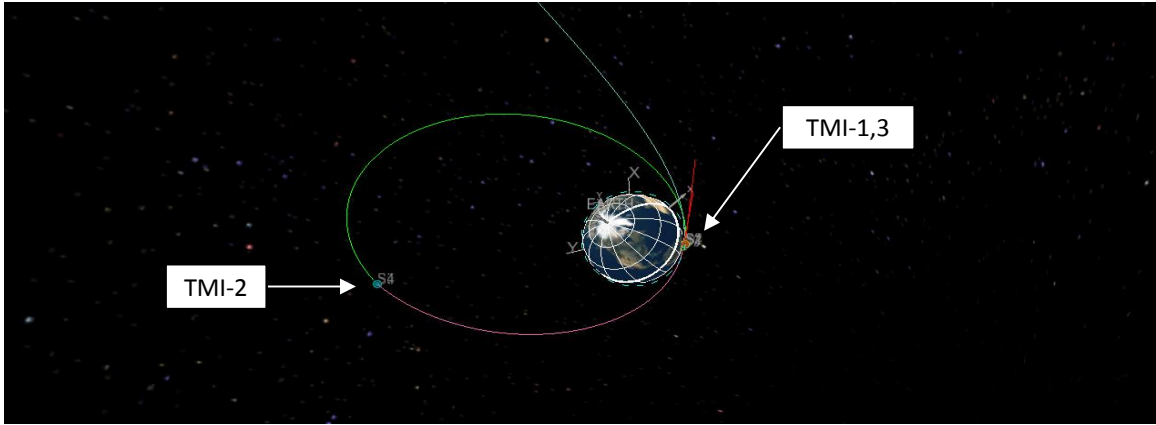


Figure 2-25: Polar view of the first CFP iteration crew vehicle’s trans-Mars injection.

Since less of a plane change is required in comparison to the cargo vehicle’s trajectory, a less elliptical TMI sequence is necessary. This departure sequence was also optimized to include an injection sequence at Mars such that the crew vehicle would insert into the same orbit as the loitering SHAB. Table 2-12 provides a breakdown of the crewed TMI sequence maneuver magnitudes, and Figure 2-26 shows the Mars Orbit Insertion (MOI) sequence used.

Table 2-12: Crew Vehicle Trans-Mars Injection Sequence

Maneuver	Magnitude (km/s)
TMI-1	2.398
TMI-2	0.274
TMI-3	1.611

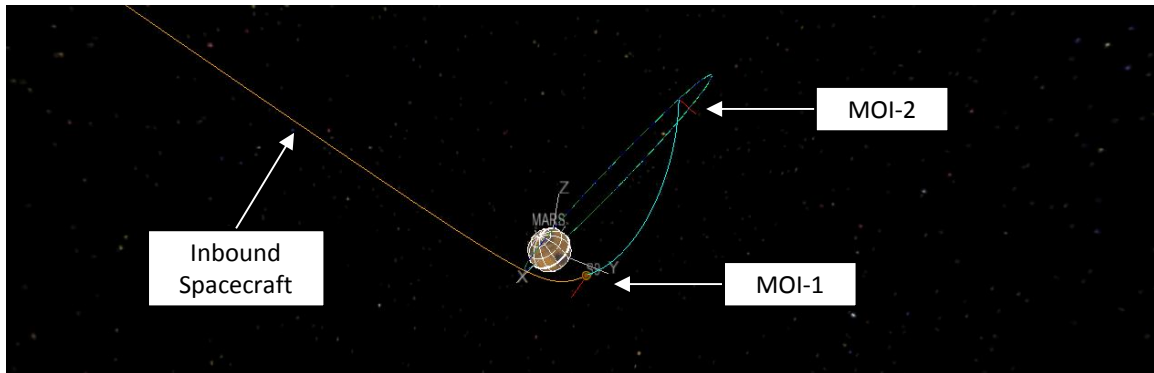


Figure 2-26: Mars orbit insertion.

This trajectory utilizes Mars’ gravity to alter the velocity of the spacecraft and assist MOI-1 with capturing the spacecraft into orbit and intersecting the target orbit where MOI-2 induces the plane change and corrects the periapee. The magnitude, location, and angles of both insertion maneuvers were optimized. A summary of these maneuvers and their magnitudes are given in Table 2-13.

Table 2-13: Crew Vehicle Mars Orbit Insertion

Maneuver	Magnitude (km/s)
MOI-1	1.376
MOI-2	0.667

This orbit was then propagated for 539 days according to the crew stay duration outlined in DRA 5. After the crew stay, another two-burn sequence was used to divide the plane change and velocity change required to return to Earth.

As described in Section 2.3.1, this trajectory targeted an EI condition for Orion with the MTV performing its own disposal maneuver up to 2 days prior to EI. Figure 2-27 shows the Trans-Earth Injection (TEI) sequence, and Figure 2-28 shows Orion EI and the MTV disposal.

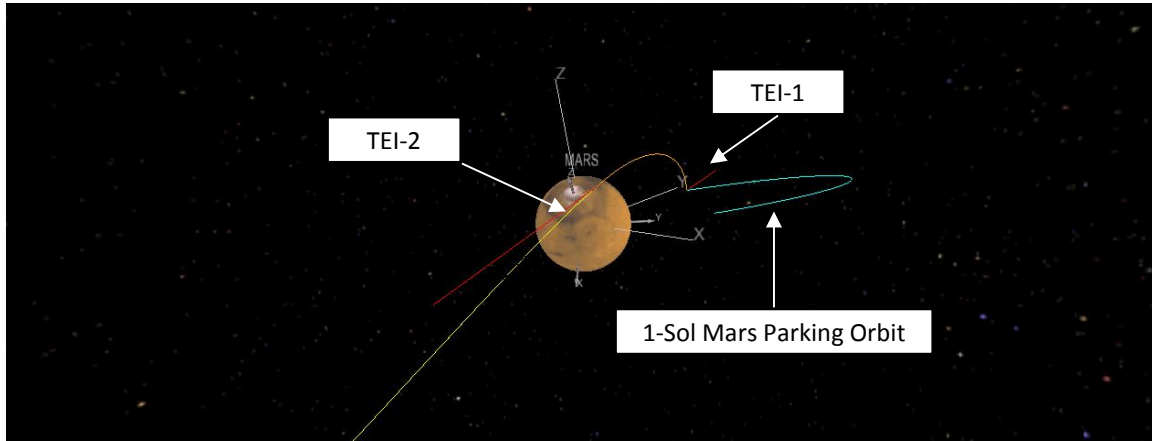


Figure 2-27: First CFP iteration trans-Earth injection.

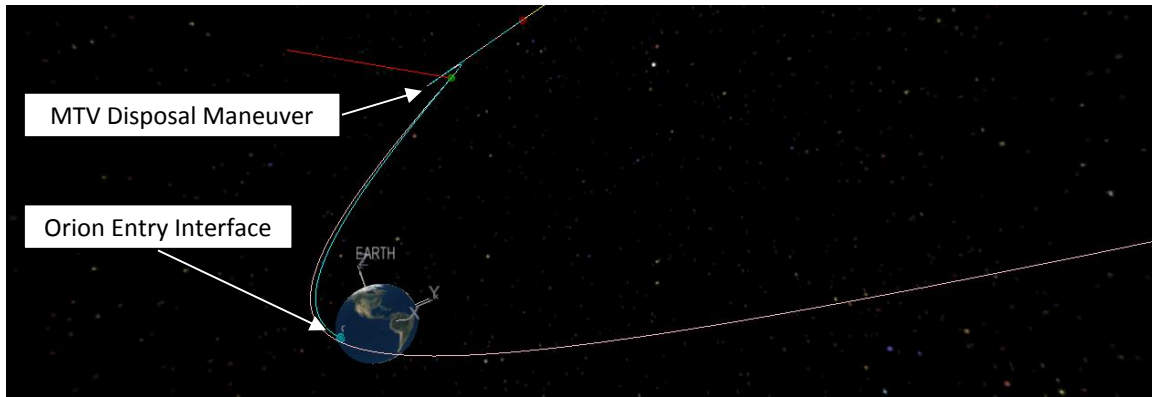


Figure 2-28: First CFP iteration Orion entry interface and MTV disposal.

The TEI maneuvers and their magnitudes are given in Table 2-14.

Table 2-14: Crew Vehicle Trans-Earth Injection Sequence

Maneuver	Magnitude (km/s)
TEI-1	1.301
TEI-2	2.577

The location of the MTV disposal maneuver was optimally located 2 days prior to EI (2 days is the upper bound). The maneuver magnitude was only 5 m/s. The EI state is 121.92 km detic altitude, 154° West longitude, 4° detic latitude, 11.68 km/s entry speed, 117.82° centric azimuth, and -5.86° centric flight path angle.

The total Δv for this mission is 15.41 km/s.

2.3.3. Second End-to-End Impulsive CFP Iteration

After analyzing the results from the first CFP iteration, it was decided that a lower total mission Δv was desired. Therefore, an additional iteration at creating the CFP was attempted. This time, some of the original DRA 5 assumptions were altered and more combinations of trajectories were tried to minimize the impact of having the

MTV insert into the same orbit as the loitering SHAB. Table 2-15 lists which assumptions were varied to construct a CFP with a lower total Δv .

Table 2-15: Varied Assumptions in Second CFP Iteration

Parameter	Original Value	New Value
Cargo Vehicles Minimum Trip Time	180 days	No Lower Limit
Allowable Aerocapture Entry Speeds	7.36 km/s only	6-8 km/s
Crew Mars Stay Duration	539 days only	509 days (Copernicus optimal value)

Another difference in the optimization between the first and second CFP iterations is that the longitude of the ascending node of the Earth Parking Orbit (EPO) was allowed to be an independent variable for further assistance in minimizing the mission Δv . The rest of this section highlights key aspects of the second CFP iteration and differences between the first and second CFP iterations.

One major aspect of this iteration is the methodology used in picking which trajectories to utilize to minimize the total mission Δv . In the first iteration, separately optimized crew and cargo vehicle trajectories were constructed, and the only work put into minimizing the impact of having the MTV insert into the same orbit as the loitering SHAB was to try altering the SHAB aerocapture state such that it would be in the MTV’s optimal orbit upon the MTV’s arrival, or by adding an additional maneuver during the MTV MOI sequence. In the second iteration, two separately optimized crew and cargo trajectories were constructed, giving a total of four trajectories altogether. Then, eight different combinations of having the crew and cargo trajectories target the necessary Mars Parking Orbit (MPO) such that they would match could be examined to find which results in the most favorable geometry. Also, the trajectory targeting the post-loiter orbit would only target the orbital plane of the post-loiter orbit. A separate strategy was used to rotate the line of apsides. This is discussed further in Section 2.3.3.1. Ultimately, the post-aerocapture maneuver in the cargo trajectory was utilized to ensure the SHAB was in-plane with the MTV’s optimal Mars Orbit Insertion (MOI). Other parameters that were varied will be discussed in further detail in the following sections. Unless otherwise specified, all figures in this section are from the final decided upon CFP.

2.3.3.1. Cargo Vehicle Trajectory

An initial attempt to determine ways to reduce the Δv for the mission was to search for departure and arrival epochs using an external resource. One resource examined was a “pork chop” plot. These are contour plots that have the Earth departure/arrival epoch on the x-axis and the Mars departure/arrival epoch on the y-axis. An example of a “pork chop” plot is shown in Figure 2-29.

Following the x-axis from where the desired departure date of June 2035 takes place and locating the desired Mars entry speed shows a trip time of approximately a quarter-year is required, not 180 days.

Examining the first iteration’s cargo vehicle trajectory in Figure 2-21 shows a large portion of the trajectory is out-of-plane with the ecliptic. Given the “pork chop” plot above, and the out-of-plane trajectory shown in Figure 2-21, it is hypothesized that the out-of-plane motion was the only way to achieve a flight time of at least 180 days. Therefore, for this iteration of the CFP, the transit time for the cargo vehicle was allowed to be much lower. Also, a second cargo trajectory was designed that allowed the entry speed to vary between 6 and 8 km/s. Both cargo trajectories shared the same initial guess for optimization and all of the independent variables were left unchanged so both versions of the cargo trajectory could converge to solutions with different departure and arrival dates.

With this in mind, the software built in-house at JSC, SOLSYSTR, that was used to generate these “pork chop” plots was used to get a more accurate Earth departure and Mars arrival date. Eventually, the cargo trajectory that was chosen for the CFP was the trajectory utilizing the original entry speed of 7.36 km/s. This higher entry speed leads to a higher Trans-Mars Injection (TMI) injection Δv than the other cargo trajectory with an entry speed of 6 km/s, but led to a more favorable geometry for aligning with the optimal MTV trajectory. Figure 2-30 shows the TMI sequence for the second CFP iteration’s cargo vehicle trajectory.

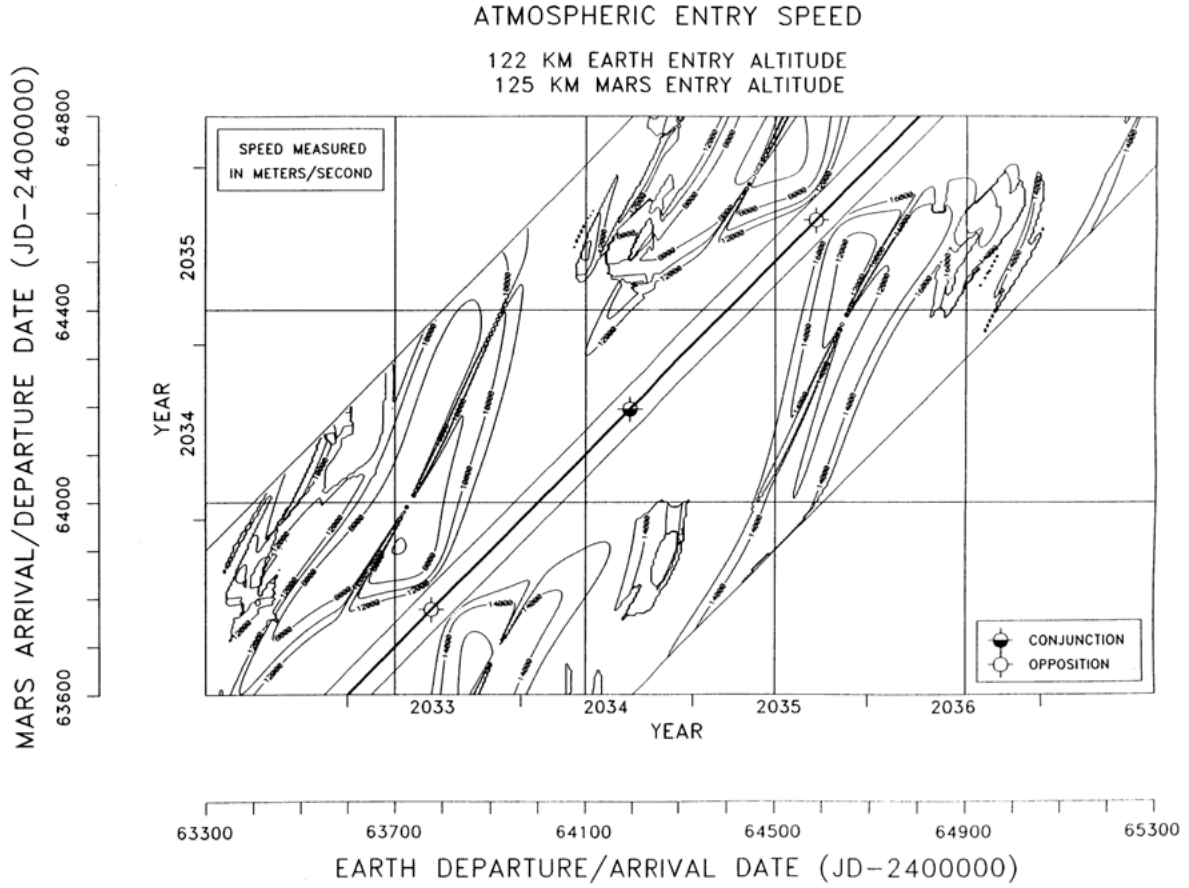


Figure 2-29 Mars pork chop plot.

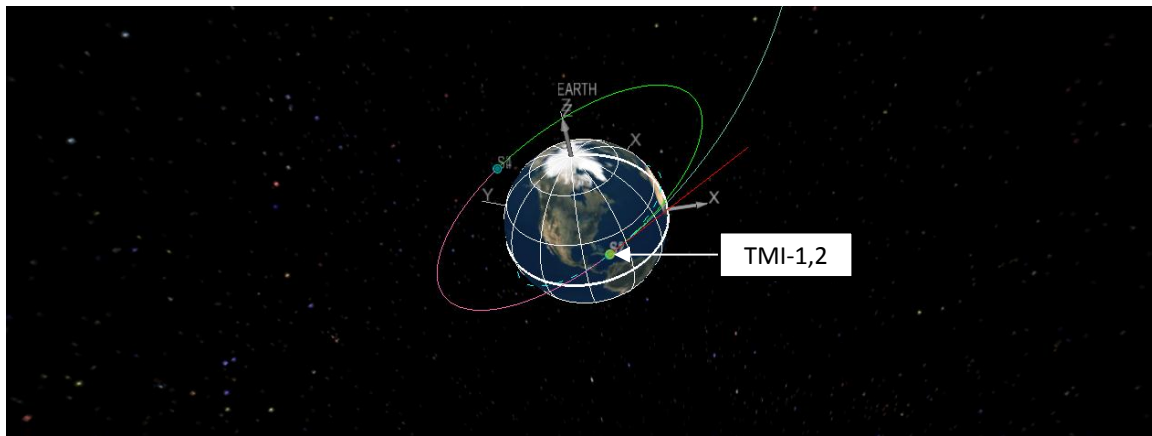


Figure 2-30: Second CFP iteration cargo vehicle’s trans-Mars injection.

This TMI sequence requires little to no plane change. The optimizer chose to eliminate the intermediate maneuver since there was such a small plane change requirement. This immediately creates a Δv reduction between the first and second CFP’s TMI sequence. The Δv requirement is reduced by 1.24 km/s. Table 2-16 gives a breakdown of the TMI sequence.

Table 2-16: Second CFP Cargo Vehicle Trans-Mars Injection Breakdown

Maneuver	Magnitude (km/s)
TMI-1	1.98
TMI-2	1.92

The resulting trajectory is now much more in the ecliptic, as shown by Figure 2-31.

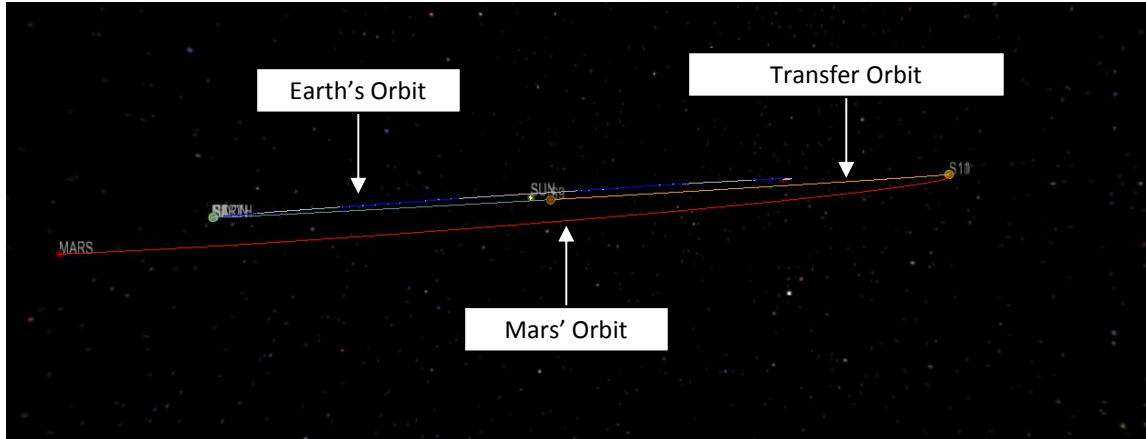


Figure 2-31: Second CFP iteration cargo vehicle's transfer in heliocentric space.

This trajectory captured into Mars orbit via aerocapture, and as it was stated above, targeted an orbit such that it would match the MTV's optimal insertion orbit. The aerocapture and post-aerocapture maneuver were optimized to insert into the proper orbital plane. This maneuver and the strategy utilized to rotate the line of apsides are shown in Figure 2-32.

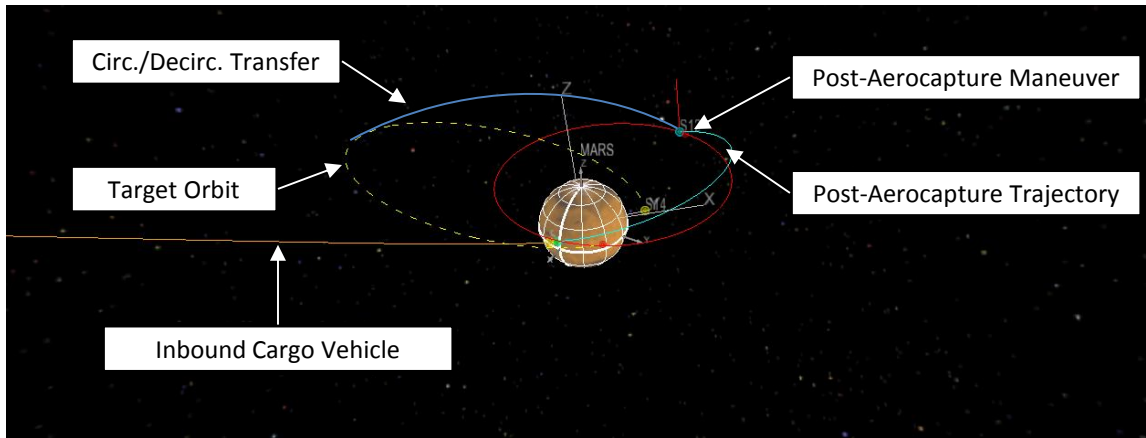


Figure 2-32: Second CFP iteration aerocapture and Mars parking orbit alignment.

For the given aerocapture state, it was assumed that the post-aerocapture state adjusted the apoapse to the one-sol orbit apoapse, and all of the other parameters were inherited from the aerocapture state. The post-aerocapture maneuver then adjusted the periapse of the orbit to make it one-sol and changed the plane such that the orbit was in-plane with the target orbit.

Several methods were considered to rotate the line of apsides. The first method would be to reverse the radial component of the velocity vector where the orbit and target orbit intersect. Thus, the magnitude of this maneuver will increase as the necessary angle of rotation increases since the velocity magnitude will increase at the point of intersection. The second method considered was to simply circularize and decircularize the orbit. The magnitude of this maneuver was assumed fixed as only two maneuvers taking place at the original apoapse and apoapse of the

target orbit. The third maneuver considered was Baker’s Equation. This method is similar to reversing the radial velocity component in that the necessary Δv associated with the method increases as the necessary apsidal rotation increases. A final method considered, which was only applied to the MTV, was to initially insert into a circular orbit with its radius equal to the apoapse of a one-sol orbit. This method would increase the capture Δv but decrease any necessary plane change required. Then, another maneuver would lower the periapse to a one-sol orbit at the necessary point.

All combinations of having the cargo and crew trajectories insert into the possible target orbits were considered. For each case, the addition of the most optimal apsidal rotation maneuver was added, along with the TMI Δv , and the Δv associated with the other vehicle’s optimal trajectory. The lowest total Δv was then used and the resulting geometry after the crew surface stay was visually inspected to ensure it was favorable for the return portion.

For this CFP, the cargo trajectory insert into the target orbit using the circularize – decircularize method since the apsidal rotation magnitude made the other methods less favorable.

2.3.3.2. Crew Vehicle Trajectory

The cargo vehicle inserts into an orbit such that it will match the optimal crew vehicle trajectory. This section outlines the key aspects of the crew vehicle trajectory. Similarly, to the cargo vehicle trajectory, SOLSYSTR, was utilized to find an initial guess for the Earth departure and Mars arrival epochs. This, combined with allowing the Earth Parking Orbit (EPO) longitude of the ascending node to be an independent variable, greatly aided the optimizer in finding a solution more optimal than the first CFP iteration. Figure 2-33 and Figure 2-34 show the Trans-Mars Injection (TMI) sequence for the crew trajectory.

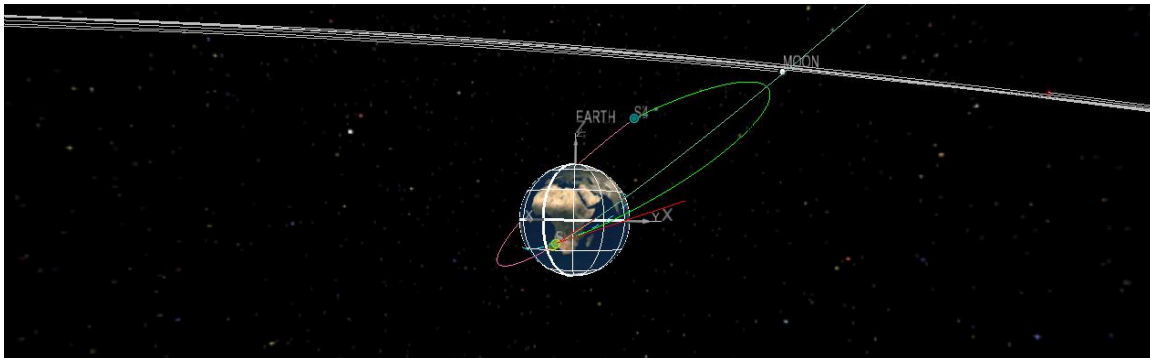


Figure 2-33: Equatorial view of the second CFP iteration crew vehicle’s trans-Mars injection.

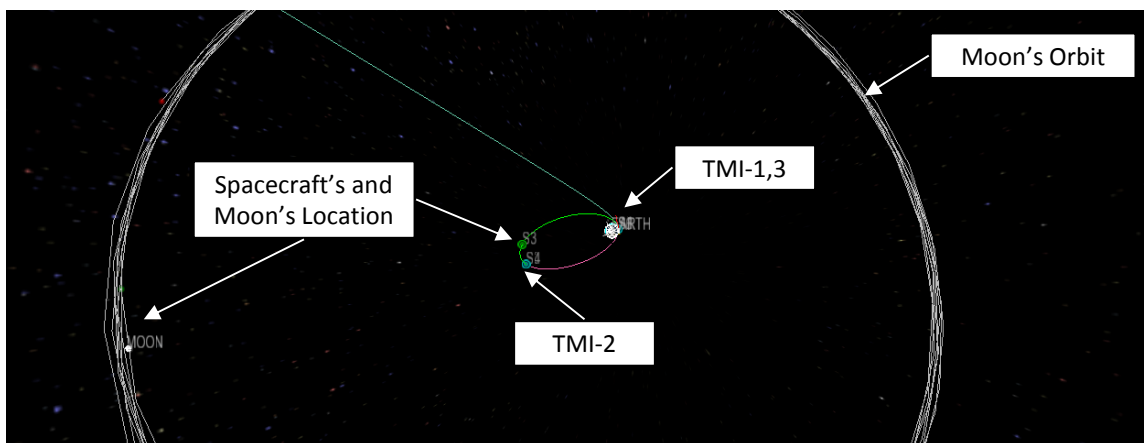


Figure 2-34: Polar view of the second CFP iteration crew vehicle’s trans-Mars injection.

This three-burn TMI sequence utilizes the Moon’s gravity and the second maneuver to induce a small plane change. Attempts were made to alter the departure and arrival epochs as well as trip time, but no lower Δv could be found for TMI and Mars Orbit Insertion (MOI). A summary of the maneuvers for this TMI sequence are given in Table 2-17.

Table 2-17: Second Iteration Crew Vehicle Trans-Mars Injection Maneuvers

Maneuver	Magnitude (km/s)
TMI-1	2.796
TMI-2	0.165
TMI-3	1.229

The MOI maneuver was just a single impulsive maneuver with almost no plane change. The beta angle associated with the maneuver was less than 1° . This trajectory inserts the vehicle into an orbit with a 14.71° inclination.

The MTV orbit was then propagated for 539 days according to the surface stay directed in DRA 5. Then, this epoch and a transit time of 180 to 220 days was used as parameters to determine the optimal Mars departure and Earth arrival epochs using a Lambert solution. The resulting crew stay was reduced from 539 days to 509. Then, the return portion was designed using the same method as the first CFP iteration except additional loiter time was allowed for in the optimizer. Figure 2-35 depicts the Trans-Earth Injection sequence.

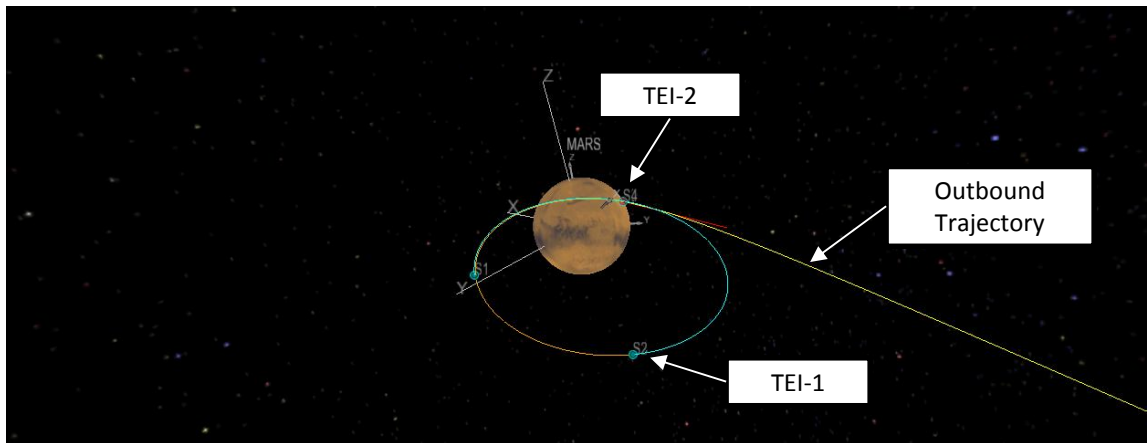


Figure 2-35: Second CFP iteration crew vehicle trans-Earth injection.

Two maneuvers are utilized in the TEI sequence, the first to induce a small plane change. However, the first maneuver is only 4 m/s in magnitude. Table 2-18 gives a summary of the maneuvers and their magnitudes for TEI.

Table 2-18: Second CFP Iteration Crew Vehicle Trans-Earth Injection Maneuver Magnitudes

Maneuver	Magnitude (km/s)
TEI-1	0.004
TEI-2	1.876

Figure 2-36 depicts Orion EI and the MTV disposal flyby.

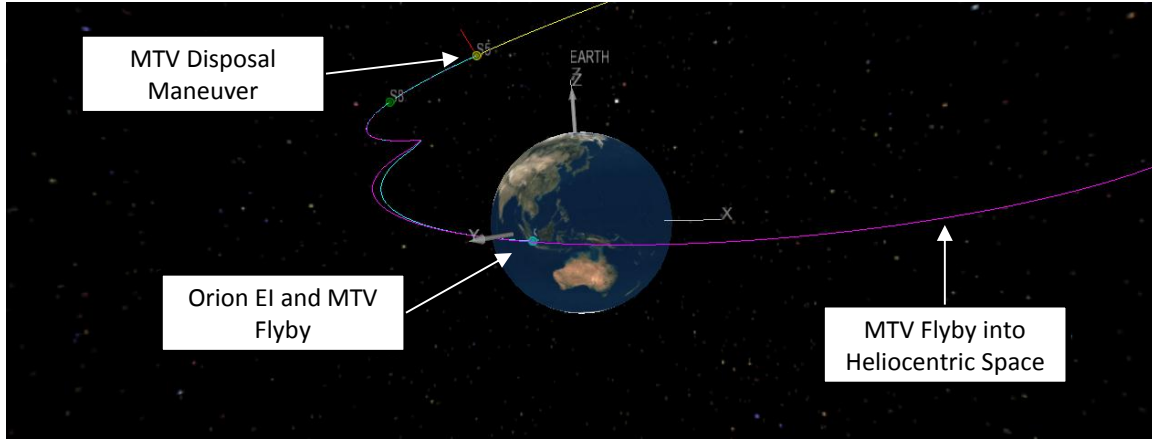


Figure 2-36: Second CFP iteration Orion entry interface and MTV disposal flyby.

The disposal maneuver was only 1 m/s and performed by the MTV 2 days prior to Orion EI.

A comparison between the assumptions made in the development of DRA 5 as well as the first and second CFP iteration Δv magnitudes is given in Table 2-19.

Table 2-19: First and Second CFP Iterations Δv Comparison

Maneuver(s)	DRA 5 Assumption (km/s)	First CFP Magnitude (km/s)	Second CFP Magnitude (km/s)
Cargo TMI	3.95	5.14	3.90
Post-AC Maneuver	0.15	0.05	0.14
Crew MTV TMI	4.25	4.28	4.20
Crew MTV MOI	1.80	2.05	0.90
Crew Apsidal Rotation	--	--	1.23
Crew TEI	1.59	3.88	1.88
MTV Disposal	--	0.005	0.001
Total	11.75	15.41	12.25

The methods utilized in the second CFP iteration reduced the total mission Δv by 3.16 km/s.

2.3.4. Possible Trade Studies

By working through two CFP iterations, some insight has been gained into what may be some potential trade studies to aid in further optimization of the total mission Δv . Some of the areas of primary interest are utilizing different Earth departure strategies, further optimization of the apsidal rotation methods, or other methods to reduce the performance loss in having the crew and cargo Mars Parking Orbit (MPO) match at the crew’s arrival at Mars.

Both of these CFPs focused on departing from a circular Earth Parking Orbit (EPO). Both the cargo and crew trajectories utilized either a two- or three-burn Trans-Mars Injection (TMI). Further reduction in the TMI Δv may be accomplished by including a lunar flyby or perhaps by departing from the Earth-Moon L2. A lunar flyby would only involve careful timing of the departure epoch. However, to thoroughly examine departing from L2, further work would be required to determine the impacts of building the spacecraft at this point.

Only a generic application of the apsidal rotation strategies could be utilized to examine the several combinations of trajectories used in the second CFP iteration. None of the methods utilized a high-order gravity model or considered the plane change necessary before applying the apsidal rotation maneuver(s). With a current trajectory designed, more time can be used to further optimize the apsidal rotation technique by possibly utilizing the post-aerocapture maneuver or adding additional maneuvers.

Other methods may also be used in further optimization of the total mission Δv . Some strategies that may be considered involve the effect that different opportunities may play on the total mission Δv (i.e., delaying the mission one more opportunity or 2 years), using maneuvers during the long loiter periods to tweak the orbits instead of using apsidal rotation, or possibly sending the SHAB with the MTV instead of worrying about lining up their MPOs upon the MTV's arrival 2 years later.

2.3.5. Forward Work

The CFP currently is a work-in-progress where the main trajectory (backbone) flight phases have been completed and stitched together end-to-end with impulsive maneuvers. Many other flight phases can be added to this impulsive CFP solution, but have not been included at this point. See Figure 2-19 and Figure 2-20 for a list of the backbone and other flight phases. This section will discuss those missing flight phases and the plan forward.

2.3.5.1. Flight phases missing in current CFP

For the Earth portion of the CFP, the launch campaigns for both cargo (DAV and SHAB) and the crew (MTV) vehicles were not modeled. This was because the pre-Mars departure Earth parking orbit is circular. The launches and rendezvous assembly of these vehicles can start to occur when needed to be ready for the departure epoch dictated by the outbound backbone flight phases. The number of launches might be updated since DRA 5 assumed an Ares-V launch vehicle whereas the current heavy lift launch vehicle is the Space Launch System (SLS). The multiple assembly rendezvous were not assessed in detail in DRA 5, but this is one area that can induce higher Δv costs once an actual rendezvous analysis is performed. This is mainly because of the complexity of the rendezvous plan and the number of rendezvous.

The aerocapture of both the DAV and SHAB are not modeled; although, in CFP Iteration #2, the aerocapture of the SHAB was loosely modeled. This was to provide an approximate post-aerocapture state to aid in connecting the SHAB trajectory with the MTV's orbit after propagation for 2 years. A representative pre-aerocapture state was targeted while creating the DAV and SHAB outbound flight phases so that these missing flight phases could be easily generated and connected with the rest of the CFP.

The DAV descent flight phase was not modeled either because selection of a landing site for the CFP has not been performed. However, the DAV descent can be connected to the CFP by allowing the DAV to loiter after aerocapture to help it find a desired de-orbit and landing condition.

Once the MTV inserts into Mars orbit, the crew transfers via Orion to the SHAB prior to its descent to the DAV landing site. This rendezvous is not modeled, but can be integrated with the CFP with aid from loitering in the MTV prior to rendezvous initiation. One other Mars parking orbit flight phase that needs to occur, but which was omitted from DRA 5, is that Orion needs to perform an automated rendezvous and docking back to the MTV after it transfers the crew to the SHAB. This Orion is needed for the Earth EDL at the end of the mission.

The final flight phases that are missing from the CFP are the DAV ascent and rendezvous at the end of the Mars surface stay. The crew in the DAV can wait on the surface site until it is in plane and has the optimal phase angle for the ascent and rendezvous with the MTV. Prior analysis has been performed on this rendezvous for DRA 5 and looks as if it is applicable for the CFP, as well.

2.3.5.2. CFP plan forward

The next steps for CFP development will involve determining whether the other missing flight phases should be added to this impulsive maneuver CFP or whether that process should wait until the backbone flight phases have a finite burn solution. If the next major step is to convert all the maneuvers to finite burns, then the mass and engine properties will need to be reviewed one final time to ensure consistency. Creating a finite burn solution of the CFP will provide a representative calculation on how much more Δv needs to be taken into account compared to assuming only impulsive maneuvers. Converting just one maneuver to a finite burn creates a discontinuity in the end-to-end CFP, which then, in the process of re-integrating that flight phase, creates discontinuities in the other flight phases. Therefore, the CFP has to be connected together starting from the beginning of the mission (i.e., the first flight phase of the CFP).

The other flight phases can be designed and completed in parallel to speed up the CFP development time. For example, the Earth assembly rendezvous can be created while another team develops the aerocapture trajectories. This is because the main backbone flight phase segments are already continuously connected and can be used as pre- and post-reference states for the other flight phase development.

The original CFP task included creating a CFP for an opposition class Mars mission as well. Some of the same lessons learned and possibly same flight phases in the conjunction class CFP could be reused. Also, additional opposition and conjunction class CFPs could be created that model other Mars mission opportunities.

2.4. Bibliography

- ¹ Drake, Bret G., et al, “Alternative Strategies for Exploring Mars and the Moons of Mars,” GLEX-2012.08.2.2x12575, Global Space Exploration Conference, Washington, D.C., May 2012.
- ² Augustine, N.R., “Seeking a Human Spaceflight Program Worthy of a Great Nation,” Final report of the Review of U.S. Human Spaceflight Plans Committee, October 2009.
- ³ Office of the President of the United States of America, “National Space Policy of the United States of America”, June 28, 2010.
- ⁴ Hoffman, Stephen J., Drake, Bret G., Baker, John D., Voels, Stephen A., “Mars as a Destination in a Capability-Driven Framework”, ASCE Earth and Space 2012 Conference, Pasadena, CA, 16-18 April, 2012.
- ⁵ Drake, Bret G., editor, “Human Exploration of Mars Design Reference Architecture 5.0,” NASA-SP-2009-566, July 2009.
- ⁶ Sims, J. A., Finlayson, P. A., Rinderle, E. A., Vavrina, M. A., and Kowalkowski, T. D., "Implementation of a Low-Thrust Trajectory Optimization Algorithm for Preliminary Design," AIAA/AAS Astrodynamics Specialist Conference, Paper No. AIAA-2006-6746, Keystone, Colorado, August 21-24, 2006.
- ⁷ Drake, Bret. G., “Strategic Considerations of Human Exploration of Near-Earth Asteroids,” 2012 IEEE Aerospace Conference, IEEEAC paper #1069, March 2012.
- ⁸ Landau, D., Chase, J., Randolph, T., Timmerman, P., and Oh, D., "Electric Propulsion System Selection Process for Interplanetary Missions," Journal of Spacecraft and Rockets, Vol. 48, No. 3, May-June 2011, pp. 467-476.
- ⁹ Landau, D. and Strange, N., “Human Exploration of Near-Earth Asteroids via Solar Electric Propulsion,” in Proceedings of the 21st AAS/AIAA Space Flight Mechanics Meeting, New Orleans, LA, 13-17 February 2011. Paper AAS 11-102.
- ¹⁰ NASA, “Orion, America’s Next Generation Spacecraft”, NP-2010-10-025-JSC, 2010.
- ¹¹ NASA, “Space Exploration Vehicle Concept”, NF-2010-06-499-HQ, http://www.nasa.gov/pdf/464826main_SEV_Concept_FactSheet.pdf
- ¹² Munk, M. M. and Cianciolo, A. D., “Entry, Descent, and Landing for Human Mars Missions,” GLEX-2012.08.2.6x12677, Washington, D.C., May 2012.
- ¹³ Condon, Gerald L., “Earth-Mars Artificial-G NEP Architecture Sun-Earth L2 Architecture, 3-Week Parametric Trade Study,” Presentation to the JSC Exploration Office, March 3, 2003.
- ¹⁴ Barbee, Brent W., “Preliminary Analysis of Trajectories Within the Martian System for Human Exploration of Phobos and Deimos,” Internal NASA Presentation, February 3, 2012.
- ¹⁵ Landau, D., “Comparison of Earth Departure Strategies for Human Missions to Mars,” Paper AIAA 2012-5143, AIAA SPACE Conference, Pasadena, CA, September 11–13, 2012
- ¹⁶ Farquhar, R., Dunham, D., Guo, Y., and McAdams, J., “Utilization of Libration Points for Human Exploration in the Sun–Earth–Moon System and Beyond,” Acta Astronautica, Vol. 55, No. 3–9, August–November 2004, pp. 687–700.
- ¹⁷ Russell, R. P., Lara, M., “Long-Life Lunar Repeat Ground Track Orbits,” Journal of Guidance, Control, and Dynamics, Vol. 30, No. 4, 2007, pp. 982-993.

3. ADVANCED IN-SPACE TRANSPORTATION

3.1. Nuclear Cryogenic Propulsion System

Primary Contributors:

Mike Houts, National Aeronautics and Space Administration, Marshall Space Flight Center
Larry Kos, National Aeronautics and Space Administration, Marshall Space Flight Center

3.1.1. Overall Nuclear Cryogenic Propulsion Stage Project

Development efforts in the United States have demonstrated the viability and performance potential of NTP systems. For example, Project Rover (1955 – 1973) completed 22 high-power rocket reactor tests. Peak performances included operating at an average hydrogen exhaust temperature of 2550 K and a peak fuel power density of 5200 MW/m³ (Pewee test), operating at a thrust of 930 kN (Phoebus-2A test), and operating for 62.7 minutes on a single burn (NRX-A6 test).¹ Results from Project Rover indicated that an NTP system with a high thrust-to-weight ratio and a specific impulse greater than 900 s would be feasible. Excellent results have also been obtained by Russia. Ternary carbide fuels developed in Russia may have the potential for providing even higher specific impulses.

Many factors would affect the development of a 21st-century nuclear thermal rocket (NTR). Test facilities built in the United States during Project Rover are no longer available. However, advances in analytical techniques, the ability to utilize or adapt existing facilities and infrastructure, and the ability to develop a limited number of new test facilities may enable an affordable, viable development, qualification, and acceptance testing strategy for the NCPS. Although fuels developed under Project Rover had good performance, advances in materials and manufacturing techniques may enable even higher performance fuels. Potential examples include cermet fuels and advanced carbide fuels. Precision manufacturing will also enable NTP performance enhancements.

NTP will only be utilized if it is affordable. Testing programs must be optimized to obtain all required data while minimizing cost through a combination of non-nuclear and nuclear testing. Strategies must be developed for affordably completing required nuclear testing. A schematic of an NCPS engine is shown in Figure 3-1.

NASA's Nuclear Cryogenic Propulsion Stage (NCPS) project was initiated in October 2011, with the goal of assessing the affordability and viability of an NCPS. Key elements of the project include: 1) Pre-conceptual design of the NCPS and architecture integration; 2) Development of a High Power (~1 MW input) Nuclear Thermal Rocket Element Environmental Simulator (NTREES); 3) NCPS Fuel Design and Testing; 4) NCPS Fuels Testing in NTREES; 5) Affordable NCPS Development and Qualification Strategy, and 6) Second Generation NCPS Concepts. The NCPS project involves a large (~50 person) NASA/Department of Energy (DOE) team supplemented with a small amount of procurement funding for hardware and experiments. In addition to evaluating fundamental technologies, the team will be assessing many aspects of the integrated NCPS, and its ability to significantly enhance or enable NASA architectures of interest.

The NCPS is an in-space propulsion system/stage using fission as the energy source to heat propellant (hydrogen) and expand it through a nozzle to create thrust. The increase in engine performance available from even a first generation NCPS would enable more ambitious exploration missions, both robotic and human. It is the intent of the NCPS project to develop a pre-conceptual design of a first generation stage with one or more nuclear thermal rocket(s) capable of interfacing with soon-to-be-available launch vehicles and possible payloads and missions. The design must utilize technologies that are readily available with minimal risk to development. The design must take into account the development viability/feasibility, affordability, and potential reusability. A strategic method of development must be considered, assessing both commonality and scalability for miniaturization or growth. Other strategic considerations are the testing approach (a combination of terrestrial and space testing to validate the engine) and the need for sustained funding.

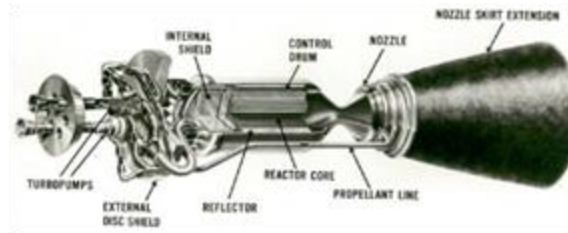


Figure 3-1 Schematic of an NCPS engine.

3.1.1.1. Pre-Conceptual Design of the NCPS and Architecture Integration

The NCPS must show relevance to the U.S. space exploration goals and must provide a development path toward a feasible, affordable, and sustainable Nuclear Cryogenic Propulsion Stage. United States' National Space Policy (June 28, 2010, pg. 11) specifies that NASA shall: By 2025, begin crewed missions beyond the Moon, including sending humans to an asteroid. By the mid-2030s, send humans to orbit Mars and return them safely to Earth. The NCPS design will focus on ensuring maximum benefit to human Mars mission, although the NCPS could have numerous other applications as well. Detailed studies are ongoing, building on work performed in previous programs².

NCPS mission analysis and definition will stay synchronized with the NASA Human Architecture Team (HAT) for application toward future human missions and the currently developing Space Launch System (SLS). One potential SLS configuration would help maximize the benefit from the NCPS by balancing mass and volume constraints.

The sensitivity of NCPS performance to specific impulse, engine thrust-to-weight ratio, and other parameters is being assessed as one initial step in stage design. The design of the NCPS will favor proven and tested technologies and the design will also identify critical technologies that will be required for development. A historical perspective for a common, scalable fuel element will help provide flexibility in design. During the Rover program, a common fuel element / tie tube design was developed and used in the 50 klbf Kiwi-B4E (1964), 75 klbf Phoebus-1B (1967), 250 klbf Phoebus-2A (June 1968), and 25 klbf Pewee engine (Nov-Dec 1968).

To help ensure affordability, the NCPS must take maximum advantage of technologies, components, and subsystems that are developed elsewhere in the architecture, as well as provide input and requirements to those technologies to obtain the capabilities needed for effective integration of the NCPS. The NCPS must also stay coordinated with the SLS and upper Cryogenic Propulsion Stage (CPS) projects to take advantage of common elements and to leverage technologies and configurations to reduce cost.

The NCPS project will also evaluate Bi-modal Nuclear Thermal Electric Propulsion (BNTEP). The design of such a system would likely be more complex than the design of either a pure NEP system or a pure NTP system, but there could be potential performance advantages. In addition, from an overall vehicle and mission standpoint, the use of BNTEP could potentially reduce complexity. For applications requiring small amounts of electricity, a simpler system could be used to provide that power, especially for missions that will have limited access to solar energy. Both propulsion-only and “bimodal” (propulsion and power) systems will be assessed under the NCPS Project.

To support the NCPS design effort, available analytical tools will be enhanced and refined. The DOE has developed sophisticated computer modeling tools for nuclear system design. Since the initial fuel elements under consideration are very similar to those previously developed under the Rover/NERVA and other programs, the NCPS will be able to take advantage of these available models. In addition, NASA rocket system simulation tools will be applicable. The computational modeling tools from DOE and NASA will allow needed trade studies and mission analysis. Initial efforts will focus on benchmarking of the nuclear models with test data and/or between similar models. After confidence in the nuclear models has been established, an iterative design process will begin convergence of NASA and DOE models for best design solutions.

One engine system model under consideration is the closed expander cycle, which derives fluid-pumping power from excess heat generated within the engine and passes the entire propellant flow through the nozzle. The cycle is currently of interest due to its high Isp performance. However, several other candidate cycles have been considered in the past and will be evaluated. Also, hydrogen is the most desirable propellant based on its thermodynamic properties; similarly for high Isp performance. However, hydrogen is also very challenging to store for long-duration missions without significant boil-off losses and will require cryogenic fluid management technology refinement. Liquid hydrogen also has a very low density, and high-volume tanks are advantageous for many missions. Other potential propellants will be evaluated in the engine balance studies. In-situ propellant usage is also a consideration.

The safety of all rocket engines (including nuclear engines) is paramount. Although a nuclear engine is essentially non-radioactive prior to operation at significant power, the engine must be designed to avoid inadvertent start. This is particularly true for times when individuals could be in close proximity to the reactor, such as during launch processing. Safety of the nuclear engine will be ensured via design and by drawing on more than 7 decades of reactor operating experience.

Crew health and safety may benefit from the use of an NCPS. The NCPS may enable shorter mission times (reducing crew exposure to microgravity, cosmic rays, solar flares, and other hazards) or increased payload mass (allowing for increased shielding, supplies, or equipment).

3.1.1.2. Nuclear Thermal Rocket Element Environmental Simulator (NTREES)

A high-temperature, high-power density fissile fuel form is a key technology for an NCPS. In addition, affordable development and qualification of the fuel form is important to overall NCPS affordability. Fuel life and performance is largely limited by mass loss in a hot gas/cyclic environment. Hence a major milestone of the NCPS project is the completion of the 1-MW Nuclear Thermal Rocket Element Environmental Simulator (NTREES) test chamber. The purpose of the NTREES facility (including an arc heater and a compact hydrogen test chamber) is to perform realistic non-nuclear testing of NTR fuel elements and fuel materials. Although the NTREES facility cannot mimic the effects of the neutron and gamma environment of an operating NTR, it can simulate the thermal hydraulic environment within an NTR fuel element to provide critical information on material performance and compatibility.

Initial upgrades to NTREES have been completed. The hydrogen system has been upgraded to enable computer control through the use of pneumatically operated variable position valves (as opposed to manual hydrogen flow control). The upgrade also allows hydrogen flow rate to be increased to 200+ gm/sec. The operational complexity of NTREES has been reduced by consolidating controls and reworking the purge system so as to permit simplified purging operations.

Prior to initiating the second stage of modifications, NTREES was used to test a “fuel element like” test article. The purpose of the test was to evaluate the behavior of the fuel and to demonstrate the test capabilities of NTREES. The test element consisted of a 12-inch-long, 5/8-inch-diameter specimen having seven hydrogen flow holes. The materials comprising the test element consisted of pure tungsten with 40 volume % hafnium nitride particles encased in 0.030 inch niobium can.

The total duration of the tests was about 4.5 hours at maximum induction heater power (about 30 kW). The tests were performed in flowing hydrogen at a flow rate equivalent to what would be expected in a NERVA-type engine operating at full power (about 0.7 gm/sec). Ten power cycles equivalent to about 2.5 Mars missions were performed on the fuel element. Because no suitable insulation was available for the test element so as to prevent high heat losses from radiation and convection processes, the nominal operating temperature of the test element was approximately 1300 K. Nevertheless, in one brief test sequence in which there was no hydrogen flowing, the temperature in the test element approached 2100 K. A picture of the specimen under test is presented in Figure 3-2.



Figure 3-2 Material specimen under test in flowing hydrogen in NTREES.

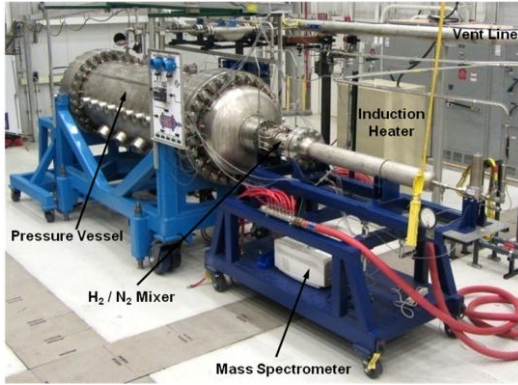
In the second stage of modifications to NTREES, the capabilities of the facility will be increased significantly. In particular, the current 50 kW induction power supply will be replaced with a 1.2 MW unit, which will allow more prototypical fuel element temperatures to be reached. To support this power upgrade, the water cooling system will also be upgraded to be capable of removing 100% of the heat generated during testing. Also required will be the upgrade of the nitrogen system and the complete redesign of the hydrogen nitrogen mixer assembly. In particular, the nitrogen system will be upgraded to increase the nitrogen flow rate from its current 1.2 lb/sec to at least 4.5 lb/sec. The mixer upgrade will incorporate a number of design features that will minimize thermal stresses in the unit and allow for the increased flow rate of nitrogen and water required by the increased operational power level. The new setup will require that the NTREES vessel be raised onto a platform along with most of its associated gas and vent lines. The induction heater and water systems will then be located underneath the platform. The new design will also allow for additional upgrades that could take the power level of NTREES to 5 MW. Once fully operational, the 1-MW NTREES test chamber will be capable of testing fuel elements and fuel materials in flowing hydrogen at pressures up to 1000 psi, at temperatures up to and beyond 3000 K, and at near-prototypic reactor channel power densities. NTREES will be capable of testing potential fuel elements with a variety of propellants, including hydrogen with additives to inhibit corrosion of certain potential NTR fuel forms; however, the focus of Fiscal Year (FY) 2012 activities will be on pure hydrogen propellants.

The NTREES facility is licensed to test fuels containing depleted uranium. The facility includes a pyrometer suite to measure fuel temperature profiles and a mass spectrometer to help assess fuel performance and evaluate potential material loss from the fuel element during testing. Additional diagnostic upgrades planned for NTREES include the addition of a gamma ray spectrometer located near the vent filter to detect uranium fuel particles exiting the fuel element in the propellant exhaust stream and to provide additional information of any material loss occurring during testing. Using propellant fed from gas storage trailers located external to the facility, NTREES is configured to allow continuous, uninterrupted testing of fuel elements for any desired length of time. A picture of the most recent operational NTREES primary chamber configuration is shown in Figure 3-3a.

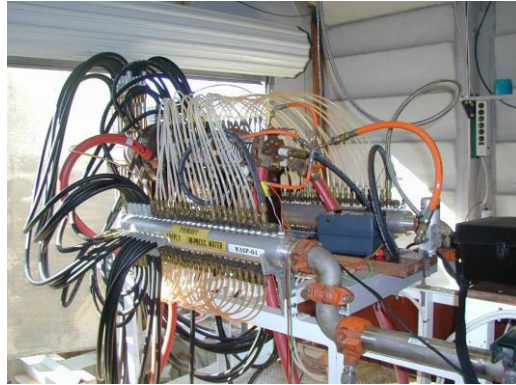
Additional test facilities includes an operational arc heater (Figure 3-3b) that is capable of flowing hot hydrogen over a material or fuel sample at a hydrogen gas temperature of up to 3160 K for approximately 30 minutes, and which will be used for the preliminary vetting of material samples.

Also available will be a compact test chamber capable of testing small fuel samples at high temperatures in a hydrogen environment. This small fuel sample test facility is called the Compact Fuel Element Environmental Test facility (CFEET) (Figure 3-4).

This project will also develop a detailed understanding of the energy deposition and heat transfer processes in NTREES, along with effects on material mechanics and fluid/material interaction, to better improve future test conditions and obtain as much information as possible to accurately extrapolate non-nuclear test data to real reactor conditions.



(a) Nuclear Thermal Rocket Environmental Element Simulator



(b) Arc Heater

Figure 3-3 NTREES primary chamber configuration.



Figure 3-4 Compact Fuel Element Environmental Test facility.

3.1.1.3. NCPS Fuel Design / Fabrication

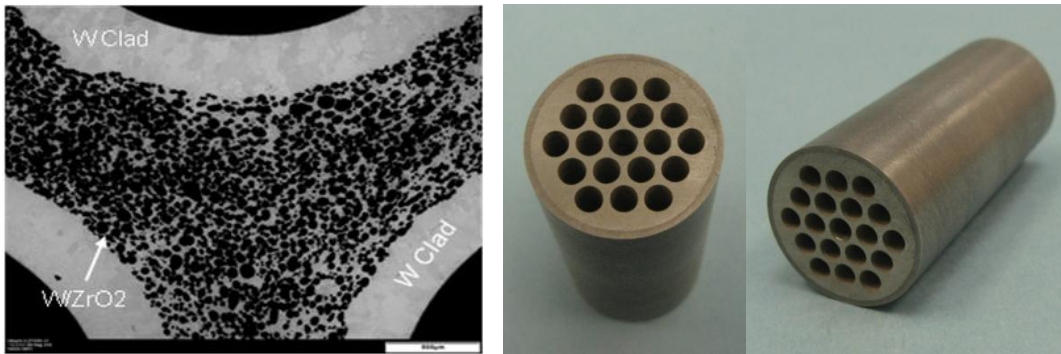
Early fuel materials development is necessary to validate requirements and minimize technical, cost, and schedule risks for future exploration programs. The development of a stable fuel material is a critical path, long lead activity that will require a considerable fraction of program resources. The objective of the NCPS Fuel Design and Fabrication task is to demonstrate materials and process technologies for manufacturing robust, full-scale CERMET and graphite fuel elements. The elements will be based on the starting materials, compositions, microstructures, and fuel forms that were demonstrated on previous programs. The development will be a phased approach to recapture key technologies and produce quality fuels. Samples will then be tested in flowing hot hydrogen to understand processing and performance relationships. As part of this demonstration task, a final full-scale element test will be performed to validate robust designs. These demonstrations are necessary to enable a future fuel material down-select and potential follow-on non-nuclear and nuclear ground test projects. A major focus of the NCPS project is the use of a highly integrated NASA/DOE fuels development team. The goal is to enhance and utilize existing infrastructure and capabilities to minimize cost.

Current research at Marshall Space Flight Center (MSFC) and Idaho National Laboratory (INL) is focused on developing fabrication processes for prototypical W/UO₂ CERMET fuel elements. CERMETS are typically formed by densification of powders using Powder Metallurgy (PM) processes. Tungsten-based CERMETS with surrogate ceramic particles have been fabricated to near theoretical density using Hot Isostatic Press (HIP) and Pulsed Electric Current (PEC) techniques. During HIP, the CERMET powders are consolidated in sacrificial containers at 2000°C and pressures up to 30 ksi. The PEC process consists of high-speed consolidation of powders using DC current and graphite dies. For both HIP and PEC processing, the powder size and shape, powder loading, and processing parameters significantly affect the quality and repeatability of the final part. Figure 3-5 shows a typical

microstructure and image of a net shape consolidated CERMET part. The part is a 19-hole configuration that had uniform shrinkage during consolidation and good tolerance on the flow channel geometry.

The nature of this initial task is rapid materials and process screening as a precursor to the detailed development that will be required to fully optimize and qualify a CERMET fuel. CERMET materials and processes were demonstrated at subscale level on previous efforts, but there are significant technical and programmatic challenges for key technologies. Some of the materials and process approaches being developed to maximize performance are the size of the fuel particles and resultant shape in the consolidated part, CVD tungsten coating of spherical UO₂ particles prior to consolidation, complete surface cladding of the elements with tungsten, and additions of small amounts of fuel particle and matrix stabilization materials such as Gd₂O₃.

Significant work is also being done at Oak Ridge National Laboratory (ORNL) to recapture Rover/NERVA graphite composite fuel materials. Various graphite-based fuels consisting of UO₂, UC₂, or (U, Zr)C particles in a graphite matrix were tested in the Rover/NERVA program. The materials were successfully demonstrated in full-scale nuclear test engines. However, the fuel materials and fabrication technologies are not currently available. The NCPS task is focused on developing the graphite composite extrusion and ZrC coating capabilities. The composite fuel matrix is a carbide-based ceramic fuel composition consisting of uranium carbide, zirconium carbide, and graphite materials. Subscale matrix samples are being fabricated and tested to demonstrate microstructure and properties. In parallel, coating trials are being performed on short elements for hot hydrogen testing at MSFC. The goal is to validate recapture of the graphite composite fuel materials using full-scale testing of a Rover/NERVA fuel element. Figure 3-6 shows images of Phoebus reactor fuels from the 1960s.



(a) Micrograph of a W/60 vol% ZrO₂ CERMET with integral W claddings

(b) Consolidated W/40 vol% HfN CERMET sample.

Figure 3-5 NCPS fuel element design.



Figure 3-6 Images of the Rover/NERVA Phoebus Reactor fuel.

3.1.1.4. NCPS Fuels Testing in NTREES

Testing in NTREES will range from fuel sample testing using the CFEET to the testing of near-prototypic fuel elements. A primary goal of the testing is to demonstrate adequate fuel performance and to increase confidence in fuel system designs (e.g., materials, coatings, geometries) prior to potential nuclear testing. CERMET and graphite composite samples will be thermal cycle tested in a static and flowing environment. Several iterations of testing will be performed to evaluate fuel mass loss impacts from density, microstructure, fuel particle size and shape, chemistry, claddings, particle coatings, and stabilizers. Initial subscale testing will be performed in the CFEET system. The CFEET test samples will be approximately 0.5 in. diameter x 3 in. length for solid slug and prototypic 7-hole channel configurations. Testing of solid slugs will be performed to baseline performance prior to introducing geometric variables.

The 7-hole channel configuration was chosen for CFEET (Figure 3-7) screening to rapidly evaluate thermal cyclic effects on prototypic geometries from surface vaporization, diffusion/migration, and cracking. Testing has shown that fuel mass loss is significantly impacted by thermal cycling and geometry. The prototypical geometry will be much more susceptible to cracking induced migration and volatilization of the exposed fuel particles. The fuel materials and forms such as coated particles, claddings, and stabilizers being evaluated on this effort have all been demonstrated to control fuel migration and loss. The initial screening is not to determine or characterize specific modes of fuel loss or mechanisms. The intent is to verify performance improvements of the materials and processes prior to expensive full-scale fabrication and testing. Post-test analysis will include weight percent fuel loss, microscopy (SEM, EBSD, and EDS), and dimensional tolerance and cracking.

Subsequent testing of full-scale fuel elements will be performed in NTREES. The test samples will be based on the Rover/NERVA and ANL 200MW designs. The goal is to benchmark performance in NTREES for comparison to future materials and process improvements, alternate fabrication processes, and other fuel materials of interest. The iterative materials and process development, CFEET screening, and NTREES testing will continue through FY 2012-2014 NCPS effort with numerous subscale and full-scale element testing milestones.

This element will focus on ensuring the overall affordability of the NCPS by accounting for all programmatic and engineering considerations, including environmental and security.

The current strategy is to start with a small prototype NTP engine, then increase size, safety factors, and redundancy for use with human missions; focus on non-nuclear testing in the beginning; utilize as many engine components, subsystems, and test facilities currently funded by other projects or is heritage; and utilize lessons learned from other recent NASA flight development programs. Fig. 8 shows the overall strategy.

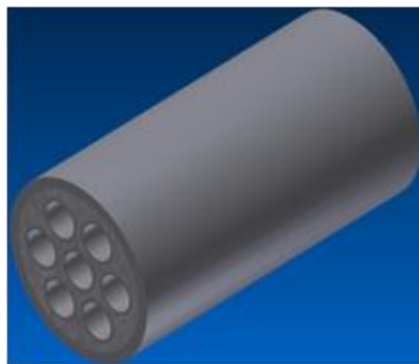


Figure 3-7 CFEET sample configuration.

3.1.1.5. Affordable NCPS Development and Qualification Strategy

Lessons learned have been acquired from the J-2X rocket engine program, ARES 1-X Test Flight Program, and X-43A Flight Demo Program. The major factors from the lessons learned include the following: follow NASA standards unless deviation has concurrence from the chief engineer and safety officer; start with low safety factors and evolve; upfront involvement from Safety Mission Assurance (including Risk Management) and Systems Engineering Integration; test development engines to the extremes and test two certification engines for flight with double the burn duration and double the number of start-ups.

It has also been determined that the design, development, test, and evaluation (DDT&E) approach and requirements for NTP will take advantage of those used for liquid rocket engines (LREs) and solid rocket motors (SRMs). LREs are hot fired many times to assure the design and manufacturing workmanship. SRMs have a very limited full-scale motor firing and rely on subscale tests and manufacturing process checks. NTP engines can't be started up for acceptance testing like the LRE, which is another reason why there is similarity with the SRM.

Human rating the NTP for future human missions will require the following design characteristics: Fault avoidance by designing out the failure modes, design with sufficient margin to be robust, design redundancy capability in the system to be tolerant of failures, and detection capability to detect, warn, and provide other systems to activate or respond to avoid loss of crew scenarios.

The NTP test topology is shown in Figure 3-12. Past NTP development programs had in-depth testing planned involving a ground test complex with a special reactor to test fuel elements, a nuclear furnace for material characterization and critical assemblies to test reactor physics. To save time and money, the current plans are to avoid having a nuclear furnace and fuel element reactor. Focus on non-nuclear testing of the fuel elements, followed by irradiation specimen testing using existing facilities, and use an existing reactor for sub-element testing. Final fuel element testing will take place at the full-scale ground test facility.

The Rover/NERVA engine tests in the past released the unfiltered exhaust into the open air. Current environmental standards do not allow radioactive particulates to be released into the air. The current NTP full-scale facility design must have an exhaust filter to contain any radioactive particulates released. Also, past NTP ground test facilities for Rover/NERVA are currently not useable. An above-ground exhaust scrubber system is being investigated, but is expected to be costly.

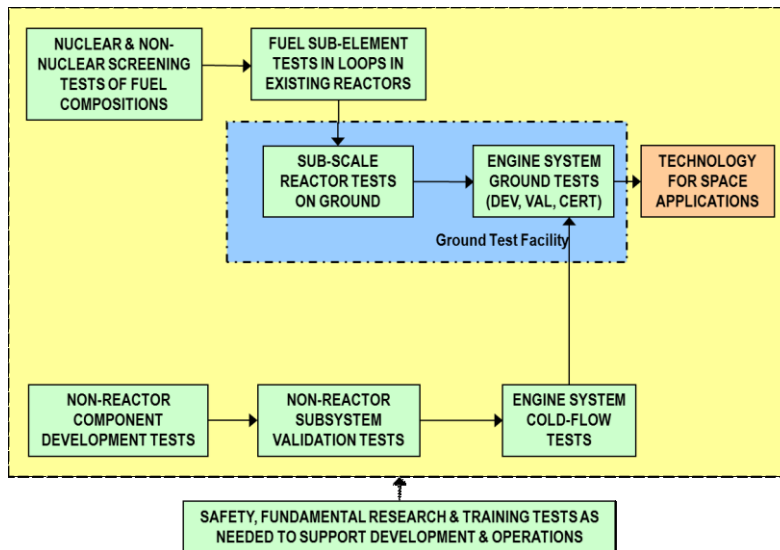


Figure 3-8 NTP test topology.

Another ground test concept being investigated involves using bore holes at the Nevada Test Site (or a different appropriate site) to filter the engine exhaust. The bore holes are about 1200 ft deep and 8 ft in diameter. The soil is made of alluvium. Current soil analysis indicates permeability will allow the hydrogen exhaust gas to rise up through the soil while trapping any radioactive particulates that could potentially be released underground. Back pressures in the bore hole up to 35 psi could take place with a full-scale NTP engine and affect the coupling of the engine to the bore hole. More investigations are under way. The Subsurface Active Filtering of Exhaust (SAFE)³ concept is shown in Figure 3-9.

In addition to ground testing a full-scale NTP engine, a flight demonstration is being investigated to help qualify the engine system and possibly used by a potential customer for a science mission. A very low thrust (~8 klbf) engine is being considered to allow for longer burn times and restarts, given volume limitations of the payload shroud. Another flight demonstration option could be to use a full-size (25 klbf) engine operating at either rated or slightly de-rated conditions to gain experience with the actual engine system that could potentially be used to support human Mars missions. A flight demo would also allow operation of a high area ratio nozzle, which is truncated for ground testing. Advanced instrumentation and robotics is being investigated to use on the NTP flight demo for inspection of the major engine components. Figure 3-10 shows similar instrumentation already used on the space shuttle.

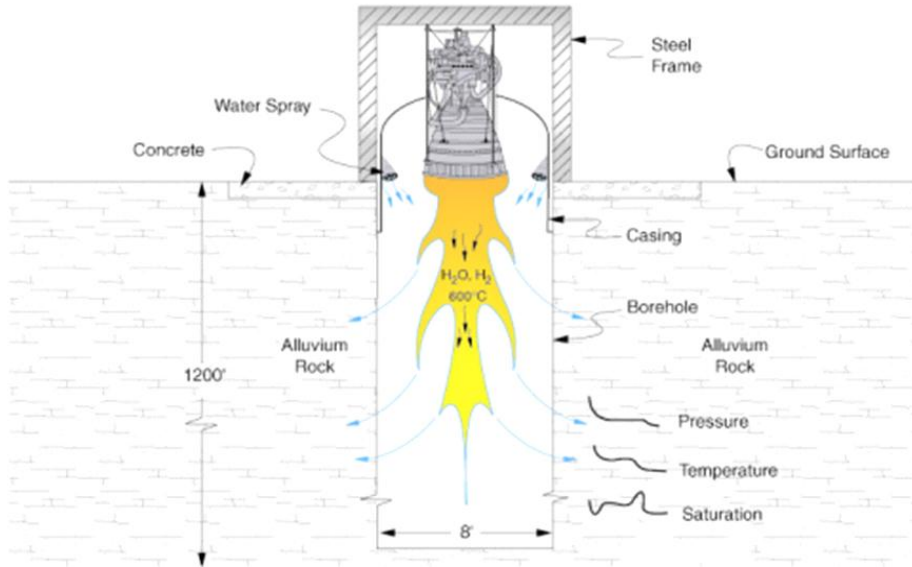


Figure 3-9 SAFE bore hole concept for full-scale NTP testing.

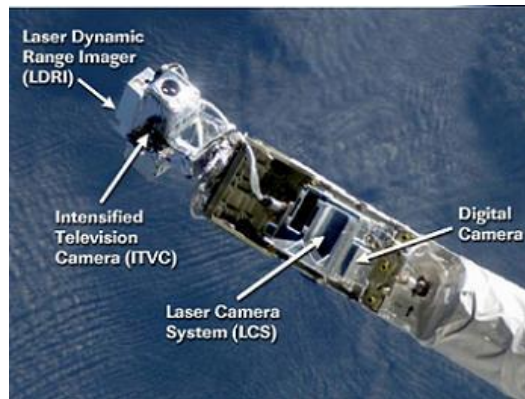


Figure 3-10 JSC robotic instrumentation.

A flight demonstration would also demonstrate the capability of the launch facilities to launch fission systems. Although the United States has had tremendous success in launching nuclear systems, launch processing for fission systems may be different than launch processing for radioisotope systems. A nuclear safety review and launch approval process is required and shown in Figure 3-11. The launch approval process could take up to 5 years to complete and needs to be accounted for in the overall development plan. Both strategies for ground testing and flight demonstration appear to show promise.

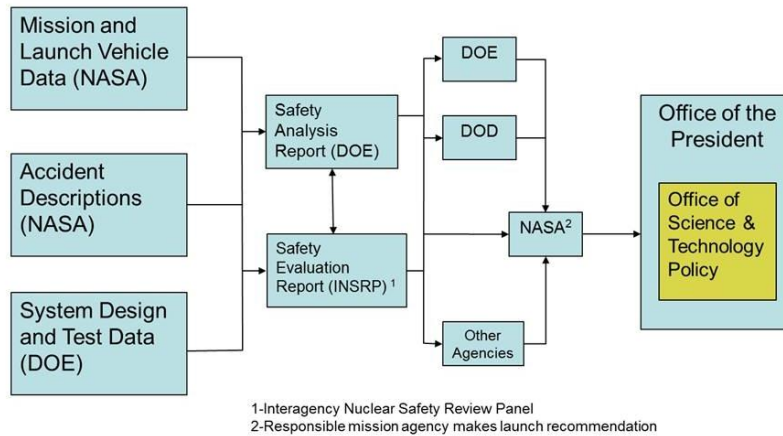


Figure 3-11 Nuclear safety review and launch approval process.

3.1.1.6. Second Generation NCPS Concepts

The “affordability” of the NCPS is also indirectly related to the ultimate performance potential of space fission propulsion systems. The future potential for extremely high performance space fission propulsion systems further increases the benefit from NCPS development.

To help assess the eventual performance potential of space fission propulsion systems, a small fraction of the NCPS project is dedicated to second generation systems. In the relatively near term, modern materials and fabrication techniques may enable an NCPS capable of providing an Isp in excess of 1000 s with a high thrust-to-weight ratio. Radically different design approaches could yield even higher performance. The work being performed under this task will devise new concepts and reevaluate existing concepts taking into account recent advancement in materials and technologies. Concepts with high performance potential and moderate technology risk (such as ternary carbide encapsulated UC2) will receive particular attention. Novel approaches for capitalizing on the unique attributes of fission systems will also be investigated. Such approaches include the direct use of volatiles available in space for NTP propellant. This task will also include system concepts for very high performance BNTEP.

Numerous concepts could potentially extend the capability of the baseline NTP. These concepts extend the NERVA/Rover design using new fuels and fuel compositions, geometries that promise to increase propellant core temperature efficiency and reduce mass, or involve a completely different method for reaching criticality, such as liquid and gas core systems. The vast number of potential concepts means that only a few can be investigated with the resources available on the NCPS project. A three-step process is envisioned to select which concepts will receive further attention. First, a catalog of existing concepts will be created. This catalog will be in Wiki format so that all team members of the NCPS can contribute. The wiki articles will discuss the fundamental physics of each NTP concept, as well as their current TRLs, expected performance, and development needs.

Second, a trajectory parametric will be developed. This parametric will quantify achievable payload ratios for a given specific power and specific impulse. These parametrics will be limited to positive payload ratios and the specific power and impulse combinations that are achievable by nuclear thermal and electric propulsion systems. These parametric curves will be specific to a given mission. Thus, one set of payload fraction contours would be developed for a 2-year round-trip mission to Mars, and another for a mission to a particular NEO. Several of these contours will be developed for each mission considered to be of high interest to NASA.

Finally, a selection process will identify the best candidate technologies and missions that are achievable with advanced nuclear propulsion. Candidate technologies and missions will continue to be refined as experience is gained from first generation systems. Trajectory parametrics and technology capabilities will be superimposed on one another. Such a combined graph will clearly show which propulsion technologies are suited with which missions. By factoring in which missions are of highest interest with the research on development difficulty for various propulsion concepts, a small set of cases can be selected. These cases will be investigated further, with detailed modeling of the mission and the propulsion technology. The strength of this process is that if NASA’s mission interests change, then these data can be used to find more suitable technology candidates.

3.1.1.7. Conclusion

The potential capability of NTP is game changing for space exploration. A first generation NCPS based on NTP could provide high thrust at a specific impulse above 900 s, roughly double that of state-of-the-art chemical engines. Near-term NCPS systems would provide a foundation for the development of significantly more advanced, higher-performance systems.

President John F. Kennedy made his historic special address to Congress on the importance of Space on May 25, 1961, “First, I believe that this nation should commit itself to achieving the goal, before this decade is out, of landing a man on the Moon and returning him safely to the Earth...” This was accomplished. President Kennedy also made a second request, “Secondly ... accelerate development of the Rover nuclear rocket. This gives promise of someday providing a means for even more exciting and ambitious exploration of space, perhaps beyond the Moon, perhaps to the very end of the solar system itself.” The investment in the Rover nuclear rocket program provided the foundation of technology that gives us assurance for greater performing rockets that are capable of taking us further into space. Combined with current technologies, the vision to go beyond the Moon and to the very end of the solar system can be realized with nuclear thermal propulsion (NTP).

3.1.2. Task 2 - NCPS Mars Architecture: Trajectory & Sizing

NCPS trajectory and sizing tasks were performed to determine what benefit an NCPS can provide to a Human Mars Mission (HMM) architecture. Quantifiable measures of an architecture can be characterized by: the amount of mass required in LEO to accomplish a mission using NTP, the number of SLS launch vehicles (LVs) a mission requires, and the associated interplanetary trip times (that would specifically match the mass and number SLS LVs) among the possible benefits of NTP. These results will be used to further refine the NTP architecture, NTP stacks (crew and cargo), and NTP element designs (core stage, in-line tank, drop tank) and data for eventual incorporation into the definition of DRA 6.0.

Since the NCPS technology will certainly affect the mission design, a customized set of long-stay trajectories were run for this study to show the duration of the associated interplanetary trip times NCPS would require for a minimal number of SLS launches.

3.1.2.1. Trajectory and Sizing Ground Rules and Assumptions

A number of trajectory ground rules and assumptions (GR&A) were adopted for this work. A majority of these come directly from either the Human Architecture Team (HAT) or derived, lower-level GR&A not out of synch with the HAT GR&A. The short list of GR&A for the long-stay mission is as follows:

Trip times are to be as short as possible to take advantage of NTP technology

- Stay times are optimized for minimal ΔV (minimal stack mass)
- Ameliorate/minimize Earth departure declination when greater than ~36 degrees
- Earth departure (parking) orbit: 400 km circular, up to 36° inclination
- Mars arrival/parking/departure orbit: 250 km x 33,800 km altitude (1 Sol)
- Earth return entry speed limited to ≤ 13 km/s (at 125 km reference atmosphere altitude)

A number of stack and element (including propellant) sizing GR&A were also adopted for this work, and again, a majority of these come directly from either the HAT or the derived, lower-level GR&A not out of synch with HAT.

GR&A for the long-stay mission include:

- The stack mass for each opportunity should fit within the lift capability and volume capacity of four 178.35.0x SLS launches -- 100.6 metric tons (mt) to -50 x 220 nautical miles (nmi) altitude initial orbit
- SLS cylindrical dynamic packaging volume envelope for NCPS is: 9.1 m x 25.2 m
- Size stack mass for all following opportunities: 2033, 2035, 2037, 2039, 2041, 2043 and 2046
- HAT payload mass, Deep Space Hab: 52 mt (with 922-day round-trip mission including contingency consumables & canister)
- HAT payload mass, MPCV: 14.5 mt (including a dry Service Module for its life support functions)
- NCPS payload, short trust mass: 6.9 mt
- NCPS tank fractions: From as low as 25% (for the drop tank element) up to 31% (for the core stage element) of usable (ΔV) propellant
- NCPS thrust: Three engines @ 25,000 lbf each = 75,000 lbf (333,600 N) total
- NCPS engine T/W: 3.5 (does not include the 2.4 mt external shielding for engine)
- NCPS Isp: 900 seconds (incl. Isp margin)

3.1.2.2. Configuration Description

The stack shown in Figure 3-12 has been the typical configuration for an NTP piloted stack for the last few DRMs/DRAs. This stack requires an SLS launch for each element – the core stage, the in-line tank, the drop tank, and the payload – thus typically four launches. The two tank-only elements (the in-line tank and drop tank) are designed to utilize both the full lift capability of the SLS LV as well as the full volume capacity of the shroud. For these designs, the LV runs out of performance and volume at almost the same time, nearly optimally utilizing the LV. Depending on future sizing analyses, the stack may need to include an additional half-length drop tank element for faster trajectories with larger ΔV s, or for greater/heavier payload manifesting, or for heavier burn-out masses for transportation elements, among the possibilities for accommodating growth and/or margin.

Nuclear Thermal Propulsion -- Mars Piloted Stack



Figure 3-12 Configuration concept for NCPS stack to Mars.

The primary element is the core stage with the three nuclear thermal engines (NTEs). These engines are currently baselined to be 25,000 lbf thrust each for a total of 75,000 lbf for the stack for all four of the major maneuvers: trans-Mars injection, Mars orbit insertion, and trans-Earth injection (TMI-1, TMI-2, MOI, & TEI). All three engines also have an external shadow shield to provide protection for the crew during the approximate 80 to 102 minutes of burn time required for the various mission options (e.g., different opportunities and mission types). The configuration at the subsystem level is not finalized, as it is almost certain that the solar arrays and cryogenic fluid management (CFM) radiators will be mounted at the forward end and deployed from stowage volumes at that end of the element. Numerous other subsystem trades are also continuing in FY13 & FY14. As the core stage gets put up on a single SLS, it is a spacecraft in itself for 2 days or so, until docking to the element delivered first in the assembly sequence.

The core stage is also the primary element for performing trajectory correction maneuvers (TCMs) or sometimes

referred to as midcourse corrections (MCCs) en route to Mars and on the return. Thus, a significant portion of the stack RCS propellant required for the ~900-day mission is launched with the core stage. Since the stack attitude cannot be fully controlled from only the core stage, some use of RCS on the other elements (and payload portion if necessary) has also been assumed in the current sizing analyses.

The in-line tank element is used to hold as much liquid hydrogen (LH₂) propellant as can fit on a single SLS launch, from both a lift and a volume capacity, for use during the TMI-1 and TMI-2 maneuvers. Due to the overall stack length – likely near 100 meters, when the payload is included – this element comprises an integral part of the structural stiffness and strength for the stack during the entire in-space portion of the piloted mission. As this piece generally is manifested to go up first, it is a self-sufficient spacecraft for 2 months or so (depending on SLS launch frequency or launch ‘centers’). Ideally, the in-line tank could be empty after TMI-1 and TMI-2 for all flight cases; therefore, for example, the active CFM system is no longer needed and the power system on this element could be utilized as a back-up power system after TMI (the last ~900 days of the mission).

The drop tank element is also intended to essentially maximize the use of a single SLS launch, both mass-wise and volume-wise (same as the in-line tank), also for use during the TMI-1 and TMI-2 maneuvers. This tank is to be jettisoned soon after TMI-2 is complete and before TCM-1 is done. This can save having to carry (usually more than) 20 mt dry mass for the remainder of the mission (e.g., through MOI and TEI). The spine of the stack is left intact, as all subsequent in-space structural loads are carried through the saddle truss in which the drop tank fits. This piece goes up last, just before the payload, and has been assumed to use only passive CFM, to minimize complexity and maximize the amount of mass that can be dropped after TMI-2. Subsystems necessary to be retained are attached to the saddle truss (e.g., back-up power distribution, RCS) and remain throughout the mission.

3.1.2.3. NCPS NTP Long-Stay Trajectory Results for the 15-year Cycle

To understand the constraints on the sizing analyses from the trajectory, a series of trajectory sweeps were run to facilitate automating the sizing analyses. In other words, the trajectory was the independent parameter – trip times and the associated TMI, MOI, and TEI ΔV s – such that the vehicle would be able to fit within four 178.35.0x SLS launches for all opportunities.

Each series of trajectories represents a sweep over a range of both outbound and return leg durations to determine major maneuver delta velocities (ΔV s) as a function of trip time. Each opportunity is somewhat different from the others, as can be seen in Figure 3-13. This set of piloted trajectories was run for the 2033, 2035, 2037, 2039, 2041, 2043, and 2046 opportunities. The first of these three plots shows the TMI ΔV s using outbound trip time as the independent variable while running the trajectories.

Optimal outbound trip-times for the TMI ΔV range from 198 to 260 days across the 15-year cycle, with many of these curves unique in one way or another. The easiest opportunity, by far, is the 2035 opportunity. Usually, in a given 15-year cycle, two opportunities are easier than the rest, but with the declination problem in 2033, 2035 is all that is left as easier to do. The 2037 opportunity is a little unusual, as the TMI ΔV does not go below 4000 m/s, even at long trip times. Since the piloted outbound trajectory legs are all-propulsive, there is, per se, no constraint on departure and approach V-infinities other than how they manifest in necessary propellant.

The second of these plots, Figure 3-14, shows the MOI ΔV as a function of outbound trip time. The optimal outbound trip-times for the MOI ΔV range from 200 days to greater than 270 days across the 15-year cycle. Again, somewhat unusual behavior is seen for this set of curves as well. Due to declination constraints, the 2033 trip time cannot go much below 180 days. Again, it is seen that 2035 is the only relatively easy opportunity when considering MOI ΔV and as-short-as-possible outbound flight times. The 2037 MOI ΔV s become reasonable, but only for longer outbound trip times.

The third and last of these major maneuver plots, Figure 3-15, shows the TEI ΔV as a function of return trip time. Again, the optimal outbound trip-times for the MOI ΔV range from 200 days to greater than 270 days across the 15-year cycle. While all of these curves look similar, or at least more similar to each other than the TMI or MOI sets of curves, there is still only one opportunity (2046) that gives low ΔV s for returning to Earth with reasonably short trip times, and one (2033) that allows fast return trips with modest ΔV investment.

Although all trajectories were run as round-trip missions, the outbound and return legs are essentially independent of each other for this trajectory analysis, as the stay time at Mars was completely free such that both outbound and return legs could be customized and/or constrained independently. This is what allows both outbound and return trip time trades to be made in an optimal fashion. This, of course, is at the expense of the very small mass sensitivity that the piloted stack has, while parked in Mars orbit, to the surface stay duration.

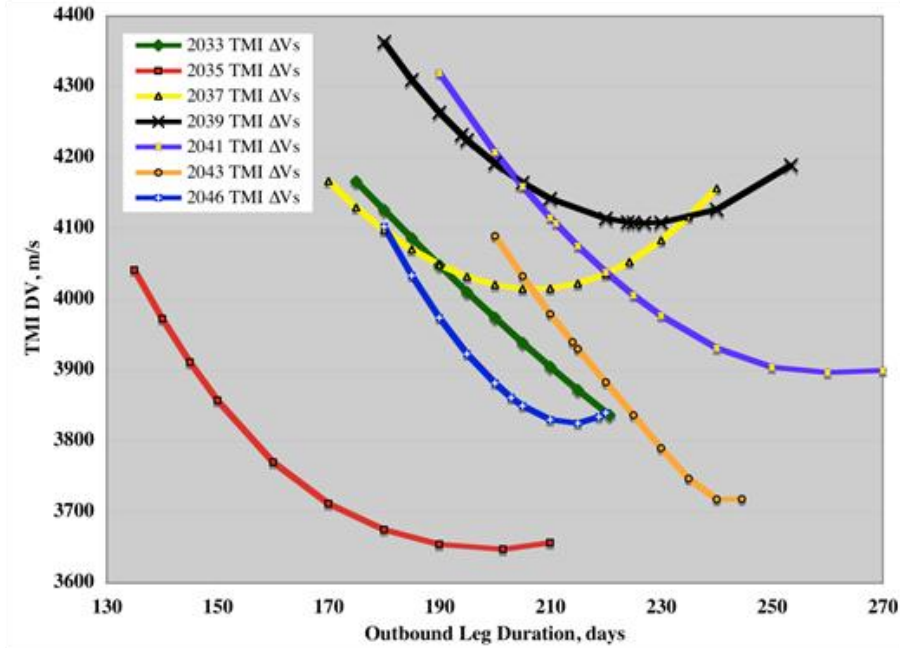


Figure 3-13 TMI ΔVs across 15-year cycle.

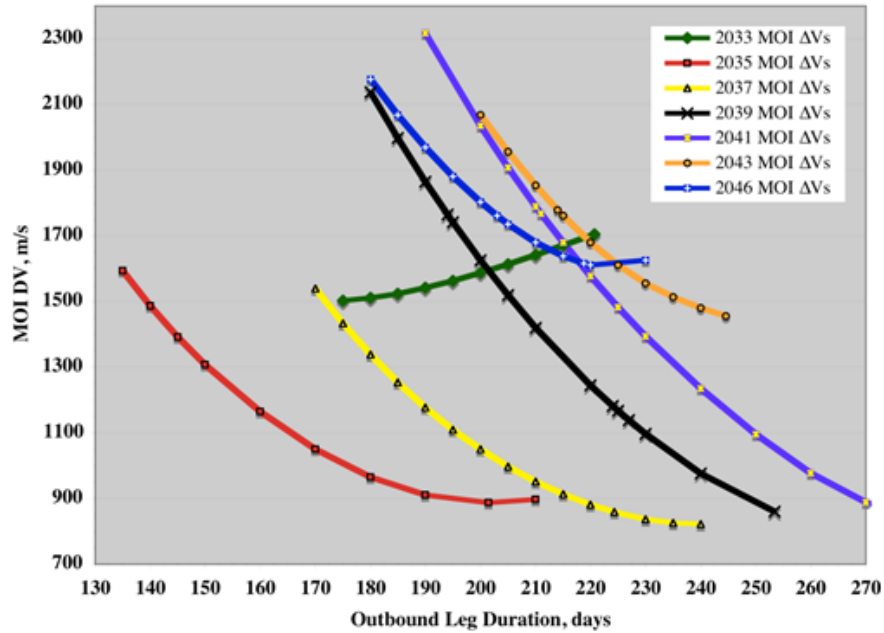


Figure 3-14 MOI ΔVs across this 15-year cycle.

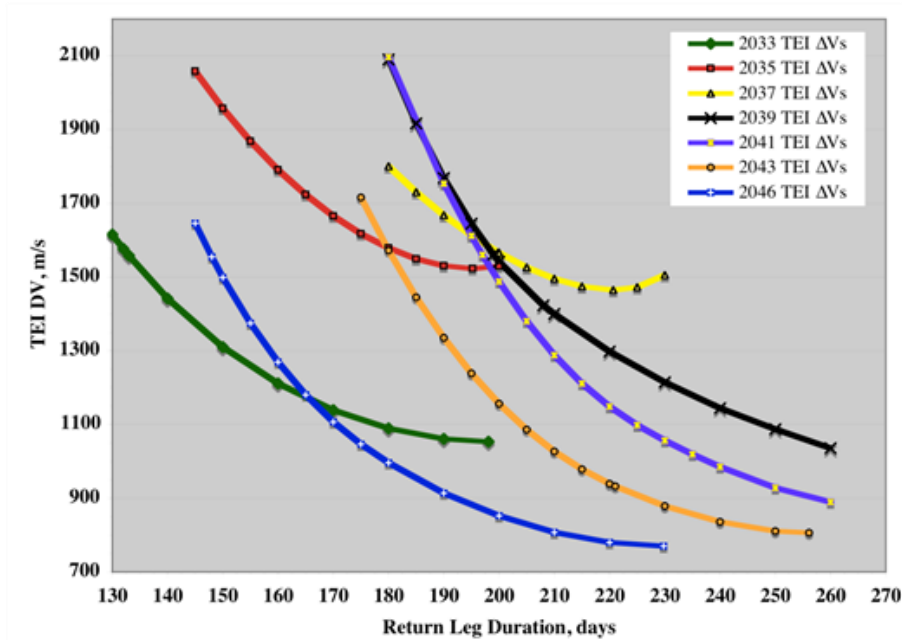


Figure 3-15 TEI ΔVs across the 15-year cycle.

3.1.2.4. Trajectory Porkchop Plots

The first of seven porkchop plots is shown below in Figure 3-16. The 2033 opportunity is definitely a challenging one due to its having very high declinations at departure dates with the lowest TMI ΔVs, and much higher TMI ΔVs at the departure dates with the lower departure declinations.

Porkchop plots are very intuitive to read. Imagine a custom-carved wooden salad bowl, as shown, and a marble in it settling at the lowest/optimal point. Departure date is on the x-axis and arrival date is on the y-axis, so the difference between them for any coordinate is the outbound trip time. The black contours are the primary data, which are C_3 values (proportional to energy necessary for departure and equal to V_{∞}^2), shown on porkchop plots. The red contours show the necessary outbound declination for an in-plane trajectory (from Earth parking/assembly orbit). Declinations greater than 28.5 degrees in absolute value require some method, SLS azimuth targeting or other plane change method, to attain those V-infinities. The contour shown in blue is an example of an arrival V-infinity contour at a typical value of 4.0 km/s. The last line, in green, is comprised of the specific data points for the NCPS trajectories. All of these points making up the green lines are also points on the TMI ΔV and MOI ΔV curves/plots.

As a matter of interest, the ‘steep’ sloped parts of the contours, with many of the red lines bunched up together, represent a ‘cliff’ of transfers of less than 180 degrees (less than a true 180° Hohmann transfer) transitioning to those greater than 180 deg. Note that in 2033, at the spot with the lowest C_3 value ($\sim 10 \text{ km}^2/\text{s}^2$, and also the lowest TMI ΔV), Figure 3-17 has a declination of approximately 55 degrees (that could be taken care of by a 55° LEO inclination), which is too high for SLS to attain without a large, adverse decrement in performance to LEO. From this plot it is evident departures from LEO in late May of 2033 are desirable for piloted in-plane outbound trajectories.

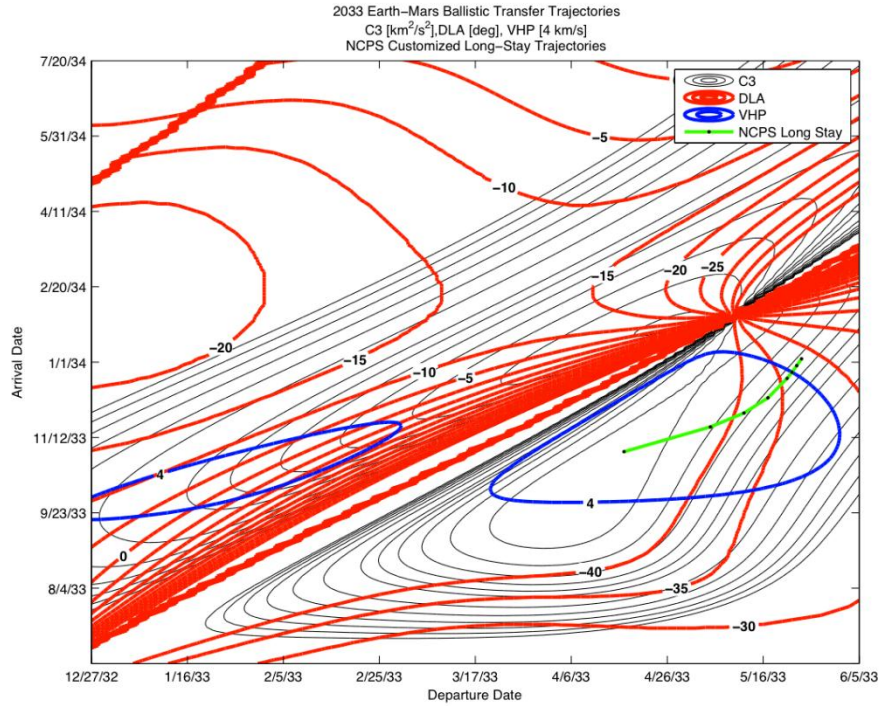


Figure 3-16 2033 opportunity outbound porkchop plot.

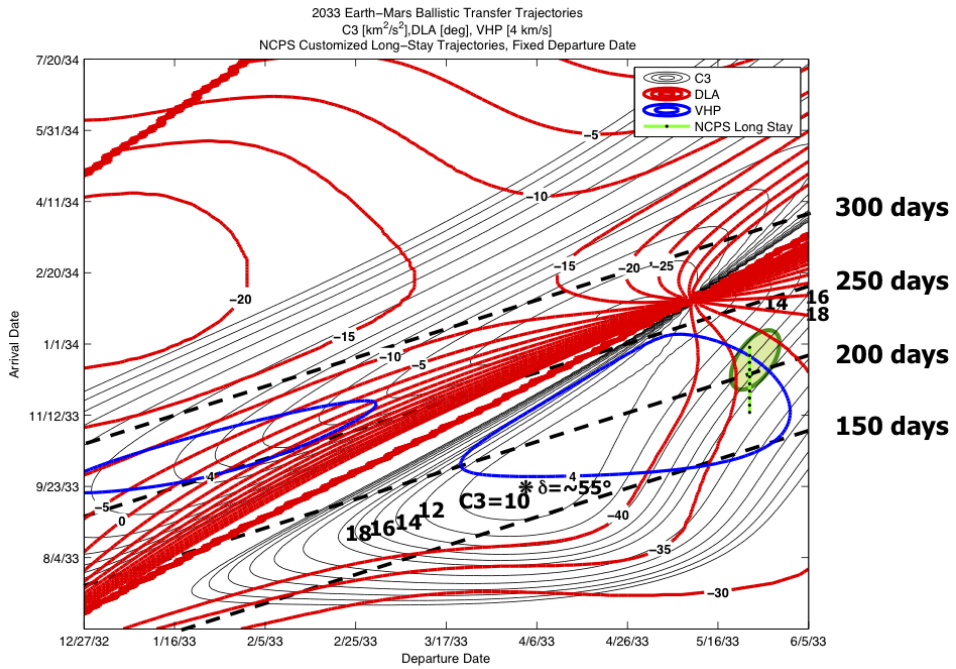


Figure 3-17 2033 opportunity outbound plot with fixed departure dates.

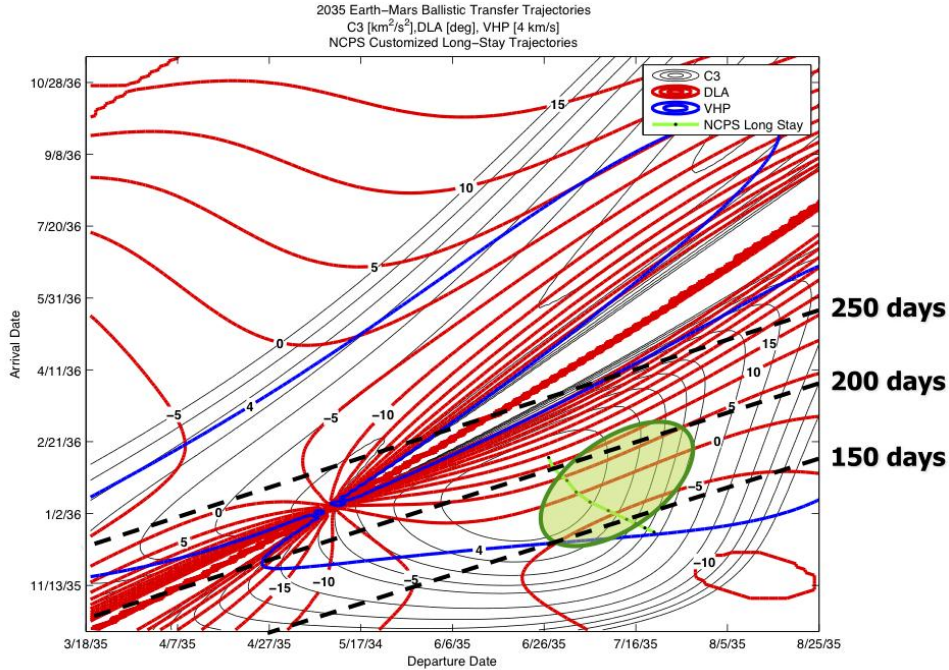


Figure 3-18 2035 opportunity outbound porkchop plot.

The 2035 opportunity shown in Figure 3-18 illustrates the wide range of fast trips available in this one particular very-favorable opportunity for piloted mission utilization. C_3 values can be near optimum for even reasonable trip times and declinations are not a problem at all, while arrival V-infinity is also not a problem. C_3 values can be increased to decrease outbound trip time in a very flexible manner. Note all plots have the viable and most desirable portions highlighted with semi-transparent green ovals; generally, the customized NCPS trajectories fall within them.

The 2037 opportunity shown in Figure 3-19 demonstrates how quickly the opportunities get difficult in this 15-year cycle. Minimal C_3 values with manageable declinations do not go below values of 18 to 19 km^2/s^2 . Attaining both manageable C_3 values and declinations result in outbound trip times of 200 to 210 days. The values for 2039 shown in Figure 3-20 are 21 to 24 km^2/s^2 and 220 to 230 days, but also with the declination as high as 40 degrees, this still as an unresolved issue. Huge TMI ΔV s can get this down to 36 degrees.

As shown in Figure 3-21 typical C_3 values for 2041 are 18 to 21 km^2/s^2 with associated trip times limited to 220 to 235 days, due mainly to the high arrival V-infinity at Mars.

For 2043, Figure 3-22, these values are in the more manageable ranges of 15 to 17 km^2/s^2 and 210 to 225 days, although arrival V-infinity at Mars is still somewhat high. Declinations appear manageable in 2041 and are not a problem in 2043.

The 2046 opportunity shown in Figure 3-23 is getting back to the easier opportunities to go to Mars using reasonable piloted trajectories. Departure C_3 values and outbound trip times are again coming down and becoming manageable, while the declination is not a problem at all. However, the arrival V-infinity at Mars can be high, which does limit how much the outbound durations can be decreased.

While the 2048 opportunity is not included here in this dataset, a few quick looks have already shown it to be nearly as good as the 15-year minimal/optimal opportunity, which may be in 2050 (no quick looks have yet been done for 2050 opportunity), before the opportunities start becoming more difficult again in 2052 and later in the next ~15-year cycle (2048 through approximately 2063).

Mars Design Reference Architecture 5.0 – Addendum #2

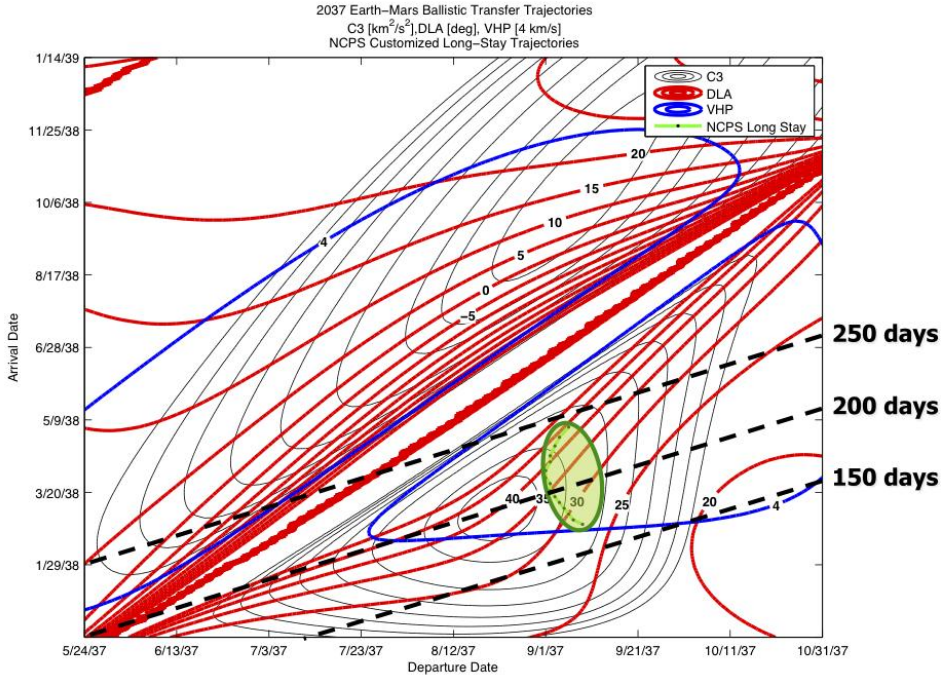


Figure 3-19 2037 opportunity outbound porkchop plot.

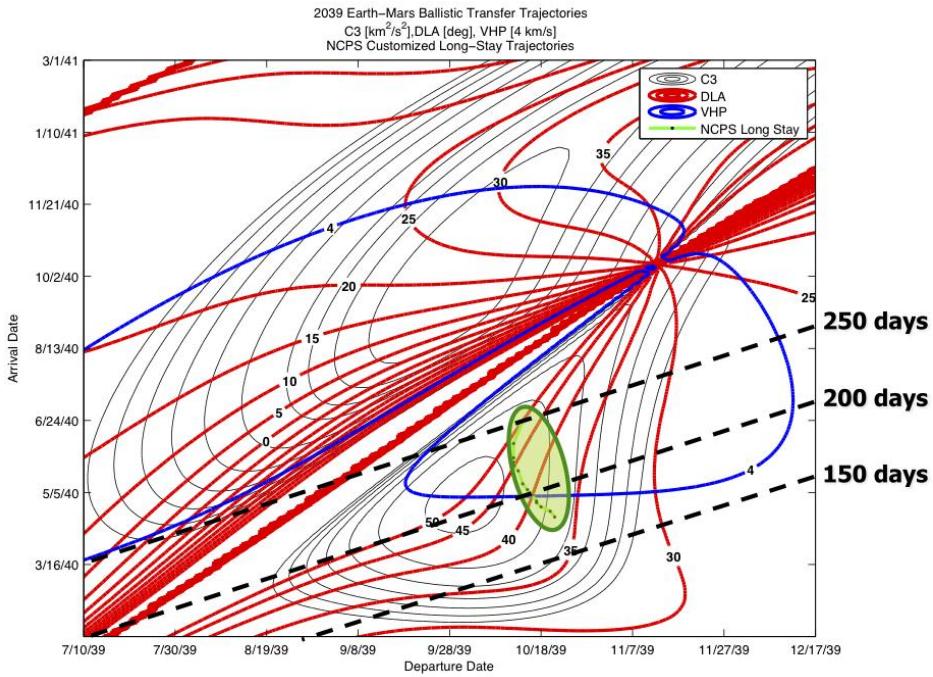


Figure 3-20 2039 opportunity outbound porkchop plot.

Mars Design Reference Architecture 5.0 – Addendum #2

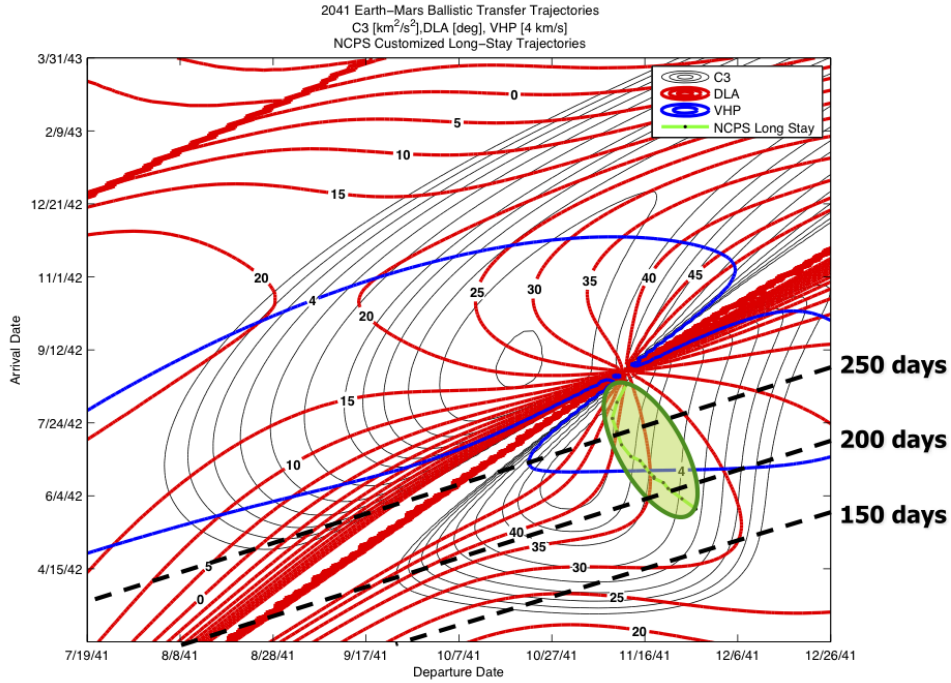


Figure 3-21 2041 opportunity outbound porkchop plot.

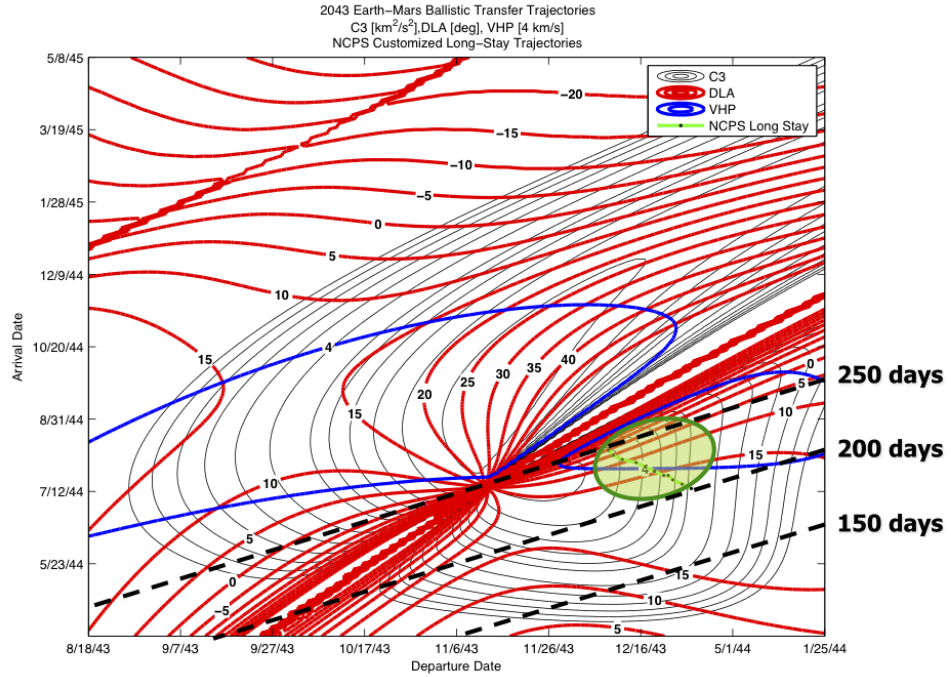


Figure 3-22 2043 opportunity outbound porkchop plot.

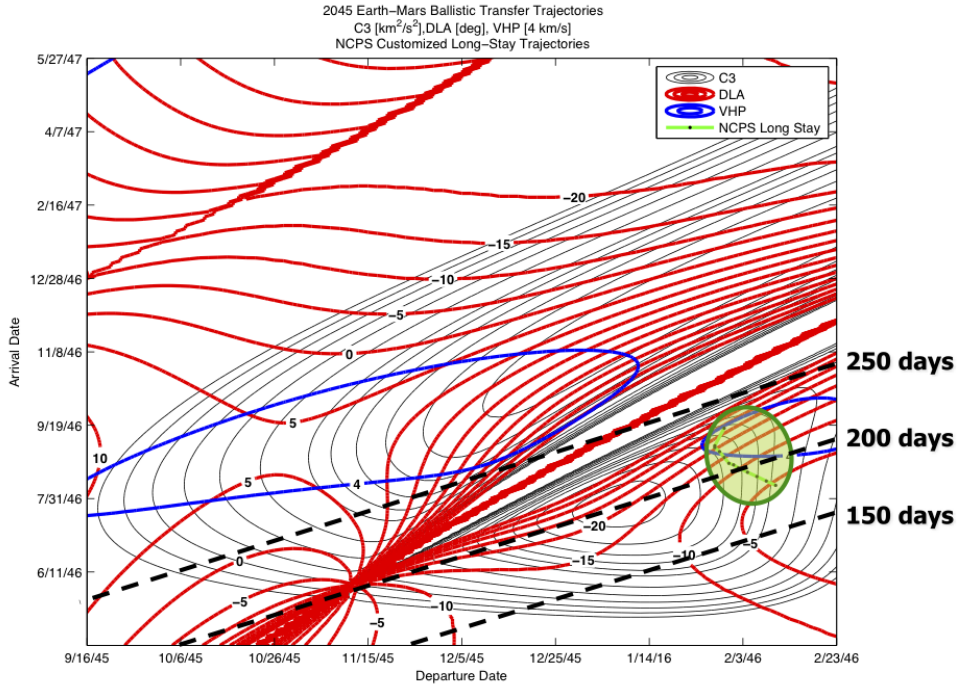


Figure 3-23 2046 opportunity outbound porkchop plot.

3.1.2.5. Trajectory Summary

The suite of primary NCPS all-propulsive piloted trajectories is summarized in Table 3-1 for the 2033 - 2046 set of piloted round-trip missions/opportunities. This set is a result of the large number of trajectories run as well as the vehicle and propellant sizing associated with them. The set that allowed the NCPS stack to fit on four SLS launches across the 15-year cycle verifies this result. Much more detailed data are available on this trajectory analysis work, and will be documented in a subsequent publication. This set of trajectories currently represents the best set for the piloted long-stay NCPS Mars missions.

A cargo trajectory summary is also shown in Table 3-2, as that small, additional task was done in anticipation of performing cargo “fall-out” sizing analyses in FY13. This fall-out sizing involves using the elements defined by the piloted missions for prepositioning cargo elements one opportunity earlier.

Table 3-1 NCPS Piloted Trajectory Summary for 15-year cycle using 4 SLS Launches

Opportunity	2033	3025	2037	2039	2041	2043	2046
Departure Date (d-mmm-yy)	23-May-33 !	12-Jul-35	2-Sep-37	12-Oct-39	15-Nov-41	18-Dec-43	2-Feb-46
Round-Trip Duration, days	913	922	921	915	911	907	908
Outbound Time	208	158	202	224	225	225	200
Stay Time, days	507	569	499	459	448	472	503
Return Time, days	198	195	220	232	238	210	205
Earth Dep. V_{∞} , km/s	4.08	3.69	4.35	4.60*	4.32	3.87	3.97
Dep. C_3 , km^2/s^2	16.62	13.60	18.95	21.14	18.66	14.95	15.78
Mars Arrival V_{∞}	3.96	3.22	2.91	3.2	3.72	3.95	4.22
Mars Dep. V_{∞}	2.96	3.78	3.69	3.23	2.85	2.91	2.51
Earth Arrival V_{∞}	3.04	3.91	4.41	5.35	6.16	6.813	5.58
TMI ΔV , m/s	3917	3788	4016	4109 *	4006	3834	3862
MOI ΔV , m/s	1630	1191	1029	1181	1480	1613	1806
TEI ΔV , m/s	1053	1524	1475	1200	998	1031	827
TMI+MOI+TEI ΔV	6600	6503	6520	6490	6484	6478	6496
Post-TMI ΔV , m/s	2683	2715	2504	2381	2478	2644	2633

* Declination >36° ! Isp = 912 sec

One should note that all TEI ΔV s are quoted as being associated with the outbound departure date from Earth; e.g., the 2033 TEI ΔV actually occurs in 2035 (i.e., 715 days after TMI).

Table 3-2 NCPS Cargo Aerocapture Trajectory Summary for 15-year Cycle

Opportunity	Dep. Date (d-mmm-yyyy)	TMI ΔV (m/s, ideal)	Trip time (days)	Departure V_{∞} (km/s)	Arrival V_{∞} (km/s)
2031	23-Feb-2031	3550	321	2.87	5.45
2033	28-Apr-2033	3529	274	2.79	4.38
2035	23-Jun-2035	3637	195	3.19	2.70
2037	6-Sep-2037	3841	396	3.85	3.35
2039	27-Sep-2039	3724	361	3.49	2.70
2041	20-Oct-2041	3620	316	3.13	2.49
2043	14-Nov-2043	3585	305	3.00	2.79
2046	12-Jan-2046	3565	323	2.93	4.63

The cargo stack is flown as an aerocapture mission (i.e., no MOI propulsive capture ΔV), since the payload requires a shroud for launch from Earth, an aeroshell for aerocapture at Mars, and an aeroentry shield to get from Mars orbit to the surface for both the descent/ascent vehicle and for the surface habitat. It is still possible, at this time, that a single piece of hardware can perform all three functions, thus making aerocapture the choice for cargo flights.

3.1.2.6. NCPS NTP Piloted Stack Sizing for 2037 Opportunity, Inputs

As mentioned in section 3.1.2, the piloted stack sizing is dependent on many factors. These factors include the lift capability and shroud volume capacity of the SLS launch vehicle (LV), the ΔV s resulting from the selected opportunity and the selected trajectories, the masses of the payload items, mass of crew capsule and service module, NCPS MPS and RCS propulsion characteristics, and transportation burn-out masses. Table 3-3 summarizes the most pertinent inputs for the 2037 baseline/reference case sizing analyses.

Table 3-3 Input Parameters for 2037 Piloted Stack Sizing Analyses

Item/Parameter	Value	Units	Qualifier or other characteristic
SLS LV lift capability:	100.6	mt	SLS 178.35.0x Initial orbit: -50 x 220 nmi
SLS LV delivery capability:	95.1	mt	Assembly orbit: 220 nmi circ. (less RCS & RPOD propellant)
SLS LV volume capacity:	9.1 x 25.2	m	Cylindrical dynamic envelope
2037 TMI-1 ΔV :	1901.3	m/s	Burn 1 st half of TMI propellant
2037 TMI-2 ΔV :	2441.1	m/s	Burn 2 nd half of prop, Incl. gravity losses & FPR
2037 MOI ΔV :	1049.5	m/s	Incl. gravity losses & FPR
2037 TEI ΔV :	1504.8	m/s	Incl. gravity losses & FPR
Outbound trip time:	202	days	
Return trip time:	220	days	
Stay time:	499	days	
NCPS Isp:	900	sec	Nominal/baseline Isp
NCPS Total Thrust:	75,000	lbf	Three engines x 25,000 lbf each
NCPS element burn-out mass fractions:	31.3% + engines, 29.8%, 25.2%	% of ΔV propellant	Core Stage, In-line tank, Drop tank & truss, respectively
NCPS engines + shields:	17.0	mt	3 engines + 3 shields
NCPS trusses:	15.6	mt	1 saddle truss, 1 payload truss
Crew consumables:	6 * 2.2 = 13.2	kg/day	Both nominal & contingency cons. for crew of 6 (incl. in DSH mass)
Payload: Deep Space Hab	51.8	mt	Range: 51.6 - 51.9 mt Depending on opportunity & stay
Payload: MPCV	14.5	mt	Crew module plus necessary parts of Service Module
Payload: 6 Crew	0.79	mt	Crew only
Return samples:	0.25	mt	Rocks/etc.
Total RCS ΔV Budget:	191	m/s	>>7 burns
NCPS RCS Isp:	300 - 328	sec	Intermittent to steady state

3.1.2.7. NCPS NTP Piloted Stack Sizing for 2037 Opportunity, Output

The primary, enveloping opportunity to drive the sizing analyses was selected to be the 2037 opportunity. Part of the reason for this is that 2037 is a very difficult opportunity, and most resulting mission options in the other opportunities in this 15-year cycle can likely be enveloped by this one in 2037, one way or another. A number of sizing outputs/values are listed in Table 3-4, including stack masses at various points throughout the mission.

To fit this mission in 2037 into four SLS launches, the major ‘dials’ to tune were the outbound and return trip times. The 2037 legs were lengthened from the typical 180 to 190 day trip-times until the stack closed on four LVs, ending up with 202 days for the trip out to Mars (longer than 6 months) and 220 days back to Earth (a little longer than 7 months). The return leg begins in August of the 2039 calendar year, when is when Mars is nearer its aphelion, thus making the return trip time longer than preferred.

Table 3-4 Summary of Sizing for the 2037 Opportunity

Parameter	Value	Units	Comment
Total for 4 SLS launches:	381.95	mt	4 separate pieces on launch pad
Circularization & RPOD RCS propellant:	5.46, 5.18, 5.46, 4.37	mt, mt, mt, mt	Core Stage, In-line Tank, Drop Tank & Truss, & Payload
Stack initial mass in low Earth orbit (IMLEO):	361.5	mt	Assembled @ TMI-14 days (no crew yet)
Stack mass @ TMI-:	359.95	mt	Just before TMI-1 ΔV
Stack T/W ₀ at TMI:	0.095	g's	Earth g's
Stack mass @ tank drop:	200.3	mt	Prior to TCM-1 ΔV
Stack mass @ MOI-:	196.3	mt	Just prior to the MOI ΔV
Stack mass @ TEI-:	162.4	mt	Just prior to the TEI ΔV
Stack mass @ disposal:	133.3	mt	Just prior to separation
Core Stage masses:	$m_{bo} = 33.45$ $m_{DV_{prop}} = 48.92$	mt mt	33.45 mt includes engines and external shielding
In-line tank masses:	$m_{bo} = 22.35$ $m_{DV_{prop}} = 71.3$	mt mt	Goes up first in some scenarios
Drop tank masses:	$m_{bo} = 26.55$ $m_{DV_{prop}} = 66.41$	mt mt	26.55 mt includes saddle truss
Total RCS ΔV prop: (incl. Circ/RPOD in LEO)	16.2, 5.79, 6.08	mt, mt mt	Core Stage, In-line Tank, Drop Tank & Truss
Total MPS ΔV prop:	186.6	mt	Core + In-line & Drop Tanks
Total engine burn time:	82.3	minutes	= 30.7 + 30.7 + 9.7 + 11.2

Note that miscellaneous items such LH₂ boil-off, propellant for NCPS start-up and shutdown, and orbit maintenance, station-keeping, and disposal RCS, and ACS propellant are not summarized here but are still accounted for in the FY12 detailed NCPS mission model.

3.1.2.8. Sizing for the 15-year Cycle

The sizing analysis was done for each opportunity to find out what it would take to fit each piloted mission within four SLS launches. The primary knobs to turn, as mentioned before, were the outbound and return trip durations. Note that the IMLEO is always about the same. This is one indication all missions fit on four SLS 178.35.0x launches.

Note that these ΔV s are larger than the ideal ΔV s shown in the trajectory summary previously in Table 3-1. The sizing analyses summarized below includes additional ΔV for gravity losses and other types of margin (i.e., FPR).

Table 3-5 Sizing Results Across 15-year Cycle

Opportunity	IMLEO mass (mt)	Outbound trip time (days)	Return trip time (days)	TMI ΔV (m/s, w/ margin)	MOI ΔV (m/s, w/ margin)	TEI ΔV (m/s, w/ margin)
2033	361.4	208	198	4243	1662	1074
2035	358.9	158	195	4110	1215	1555
2037	361.5	202	220	4342	1050	1505
2039	361.3	224	232	4436	1205	1224
2041	361.4	225	238	4332	1510	1018
2043	361.0	225	210	4157	1645	1052
2046	361.2	200	205	4188	1842	844

There are numerous ways to reduce trip time and to continue to fit on four SLS launches. These include, but are not limited to:

- Increasing NCPS Isp.
- Decreasing payload mass, whether this is lighter payloads or items that are reused at Mars and do not need to be manifested again on subsequent missions, once the first mission or two takes them out. This could be, for example, rovers (robotic or crewed, pressurized or unpressurized), surface power units, or science equipment, etc.
- Decreasing MPCV mass, most likely in the Service Module, which does not carry any propellant in these NCPS missions/architectures (no significant translational DV is necessary, at this time, on this “payload” element).
- Decreasing NCPS element masses, most likely the element burn-out masses. However, this could also occur by having higher NCPS engine T/W, which could manifest as higher thrust engines at same mass or lighter engines at the same thrust.
- Increasing SLS launch mass lift capability and volume capacity to accommodate a few additional tons of LH₂ MPS propellant.
- Have SLS deliver the same (or larger) payload masses into higher initial LEOs. For example, instead of a -50 x 220 nmi initial orbit, an initial orbit of 130 x 220 nmi decreases required RCS to get to the assembly orbit, thus leaving more of the SLS delivery capability for useful payload.

Trip times for the difficult opportunities (2037 through 2043) do get to be nearly 8 months, but these trip durations can easily be reduced with additional propellant on an additional launch. Trip times can also be shortened by reducing dry mass and replacing it with additional usable propellant.

3.1.2.9. SLS 178.35.00 Launch Vehicle Series

The SLS LV used for this NCPS sizing analyses comes from the 178.35.00 series (Figure 3-24). For FY12, the NCPS project was limited to a 1.5-stage LV. This was due to the only available second stage as being much too long, resulting in limiting utilization of the lift capability to approximately 70% (of ~123 mt net mass) before the volume capacity ran out. Note that all shrouds used in all NCPS sizing analyses are 10 meters in (outside) diameter.

The first SLS vehicle flight drops its payload off directly into the -50 x 220 nmi orbit, which after circularization at the its first apogee (220 nmi), becomes the 220 nmi circular assembly orbit. For the FY12 analyses, all subsequent elements flew into a -50 x 200 nmi orbit to circularize there to allow for some amount of phasing prior to rendezvousing in the assembly orbit with the elements previously launched (and assembled) in that orbit.

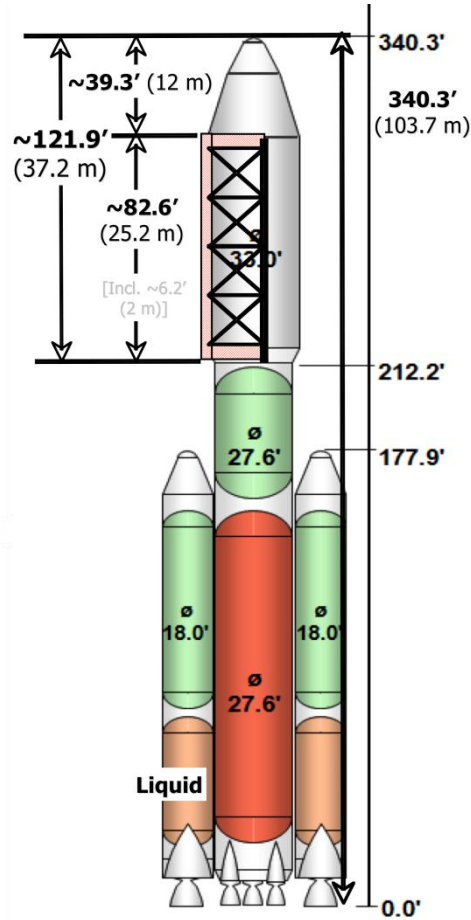


Figure 3-24 SLS with extended, large 10-m diameter shroud.

Note that this SLS launch vehicle clears the VAB door height limit (of about 390 ft) by approximately 50 ft. Therefore, an appropriate SLS second stage fitting within this envelope will increase lift capability without impacting volume capability in subsequent sizing analyses (to be performed in FY13). This subsequent SLS vehicle (188.77.xx) will likely better optimize the full utilization of both performance and volume for NCPS elements than the 178.35.xx LV.

The shroud was stretched from a cylindrical section length of approximately 17.3 meters on the baseline reference shroud to 25.2 meters for the custom NCPS shroud. Payload capability did drop a small amount when accounting for a longer, heavier shroud.

The 178.35.xx series of launch vehicles were designed with NCPS in mind, and this is apparent by the result from the greater lift capability launch vehicle (the 178.30.xx family at ≥ 130 mt gross lift capability). This other, larger lift LV requires an additional launch to get all the NCPS LH2 up. While the small volume available is 100% utilized, the capability lift (mass) only approximately 70% is utilized (for all three NCPS elements), thus an additional launch/shroud is needed to put the necessary volume of propellant into LEO.

With the NCPS core stage on the 178.35.xx family of LVs, with its three very dense engines and their three associated external radiation shields (also very dense) fill up only approximately 90% of the volume of that flight, and still uses the full mass lift capability. Both the NCPS in-line tank launch and the NCPS drop tank launch utilize 97% to 99% the SLS lift capability while fully utilizing the volume capacity – a much better payload/LV match than with the 178.30.xx family.

There is some flexibility regarding which of the first two elements goes up first (core stage or in-line tank); however, at this early stage, the decision is not critical. A driving reason to manifest one or the other first may arise later. However, a single convention was/is needed for analyses; therefore, at this time, the launch sequence adopted is:

- SLS #1: In-line Tank (could be 2nd),
- SLS #2: Core Stage (could be 1st),
- SLS #3: Drop Tank and Saddle Truss (could be two of these in a five-launch scenario),
- SLS #4: Payload (DSH w/ supplies, MPCV, short truss w/ contingency supplies).

Table 3-6 SLS 178.35.00 Family for Various Launch Options

Parameter	178.35.01	178.35.00	178.35.08	178.30.xx
Delivery orbit (nmi):	-50 x 220	-50 x 200	-50 x 200	-50 x 220
Gross payload capability (mt):	117.6	118.3	119.5	136.7
Net payload cap. (-10%, mt):	105.8	106.5	107.5	123.0
Less HAT 5% margin (mt):	100.6	101.16	102.2	116.9
Barrel section length (m):	25.2	25.2	25.2	17.2
NCPS mass/volume utilization (%):	87-97%	88-98%	89-99%	68-71%
# SLSs, NCPS piloted stack:	4	4	4	5
Volume comparison (mt): (Amt. LH2 fitting in barrel section)	105.2	105.2	105.2	71.9
LEO ΔVs to 220 nmi circ (m/s)	170.4	179.9	179.9	170.4

3.1.2.10. Mars Sizing Conclusions

The current sizing for the Human Mars Mission piloted stack can fit within four SLS launches for all opportunities during the 15-year cycle currently under investigation. Custom long-stay sizing models have been developed for the NCPS Project to allow assessment of the stack for a number of independent parameters: NCPS Isp and thrust level (in part for determining gravity losses), outbound and return leg trip times, launch vehicle lift capability and volume capacity, NCPS element burn-out masses (e.g., NCPS engine T/W), NCPS element propellant capacities, boil-off, and numerous RCS maneuvers throughout the mission. A summary of the mass estimates for the reference configuration is provided in Table 3-7.

Almost all RCS (translational) maneuvers are made with the set of thrusters on the core stage due to the convention assumed that the stack maneuvers to the necessary direction for the ΔV (e.g., TCM-1), performs the TCM RCS ΔV, then rotates back to previous attitude. At this early stage of the design, trying to utilize unknown pairs of thrusters up and down the stack to perform a ΔV in an unknown direction required for an RCS maneuver, is precluded by this simplifying assumption. Thus, the RCS propellant load on the core is much greater than either the in-line tank or the drop tank truss. Also unknown is the degree to which RCS impingement occurs up and down the stack from RCS on the in-line tank and drop tank truss, and using the core for all translational RCS maneuvers circumvents this problem as well (for now).

Element lengths range from 22 meters (drop tank) to 24.5-m (core stage w/ 7-m length engines). All elements fit within the 25.2-m cylindrical length of this shroud specifically lengthened for NCPS payloads. As mentioned in the previous section, it is apparent the current design is quite successful at running out of packaging volume at nearly the same time it runs out of lift capability, thus nearly fully utilizing the SLS launch vehicle in both respects.

Element propellant mass fractions (PMFs or λs) range from as high as 0.76 for the in-line tank, to 0.72 for the drop tank when the saddle truss is included in the calculation, and 0.6 for the core stage carrying the extremely dense NCPS engines and external shields. The three propellant tank masses are less than half of the mass that comprises

each element, thus the tank-only PMFs are all likely to be around 0.9 (these will be explicitly computed in the next round of analyses).

Cargo missions, were not focused on closely in FY12, as they are considered “fall-out” missions (fall-out analyses means using the piloted stack elements as-is, or unchanged in constructing the two cargo flights). In other words, they are ground-ruled in that they are assumed to not drive the designs of the NCPS elements. Although, previous analyses iterations prove this to be a very reasonable mode for analyses, cargo missions were briefly looked at to verify how they were shaping up.

The quick look for cargo missions show each payload/stack requires 2.5 SLS launches, with a total of five launches needed to send both payloads to Mars to support the long-stay mission. Along with the four launches necessary for the piloted flight/stack, nine 178.35.xx SLS LVs are needed every 2.1 years for each human Mars mission opportunity/flight.

3.1.2.11. Overall NCPS Mars Trajectory and Sizing Conclusions

The next step in the development of the trajectory and sizing analysis to further the long-stay NCPS design reference mission beyond DRA 5.0 has been completed. Many tools and pre-emplaced capabilities have been developed over the course of FY12 to allow progression up through the development of DRA 6.0.

The trajectory analyses documented here allowed the sizing analysis to be done with the trajectory accounted for in the iterative sizing analyses/process (via customized curve fits for the current 15-year cycle). Both the trajectory work and the sizing analyses processes will continue to be improved during the next round of DRA development.

The sizing analyses performed during FY12 and documented here has also provided for the next step in NCPS design reference mission development. Data generated in FY12 will be used to provide the necessary inputs to a more detailed pre-conceptual design activity. Digging down a level or two below the system level will provide additional confidence of the feasibility of a human Mars mission utilizing nuclear thermal propulsion as the main propulsion system.

3.1.2.12. Future Analyses for NCPS Missions

The next round of analyses, to be conducted in FY13, will include tasks such as resizing and re-manifesting the entire NCPS Mars mission on a 2.5-stage SLS launch vehicle (soon to be available to the NCPS Project), burrowing down at least one level into the NCPS elements (core stage, in-line tank(s) and drop tank(s)), providing an additional level of fidelity into the design of the NCPS mission.

This additional level of fidelity will allow engine subsystem trade studies to be performed (e.g., thrust level, number of engines, engine thrust-to-weight, engine cycle, engine startup and shutdown), trip time sensitivity evaluations, margins evaluations, NCPS element trades (at system levels – e.g., engine-out assessments, LH₂ tank boil-off and leakage, alternate element configurations, etc.), NCPS engine component assessments (e.g., fuel element trades, turbo-pump arrangement and number of them), and as always NCPS Isp trades and sensitivities.

Many tasks, such as the IMLEO stack masses and the associated trip times for each opportunity on four SLS flights (and/or other number of SLSSs), will be updated. Payload masses (DSH, MPCV, etc.) will also likely be updated, requiring transportation design and analysis tasks to follow suit. Cargo missions will again be assessed as fall-out missions, and be included in the full DRA 6.0 description.

Table 3-7 NCPS “Baseball Card” for 2037 Mission Opportunity

Description/Parameter	Value	Units
2037 Core stage (C)		
Burn-out Mass	33.45	mt
Three 25,000 lbf NTP Engines	9.72	mt
Three External Radiation Shields	7.31	mt
Tank burn-out mass (with everything else)	16.41	mt
Propellant Mass	48.92	mt
RCS Prop Load	16.19	mt
Stage wet mass total (on pad)	100.53	mt
Engine Isp	900	sec
Stage Length (engines, RCS, I/F)	~24.5	m
Effective LH ₂ PMF / λ	0.594	n.d.
2037 In-line Tank (I)		
Burn-out Mass (w/ everything)	22.35	mt
Propellant Mass	71.30	mt
RCS Prop Load	5.80	mt
Stage wet mass total (on pad)	100.43	mt
Engine Isp	900	sec
Stage Length (including RCS & I/F)	~23.2	m
Effective LH ₂ PMF / λ	0.761	n.d.
2037 Saddle Truss & LH₂ Drop Tank (D)		
Burn-out Mass	26.55	mt
Saddle Truss (with everything)	8.71	mt
Drop Tank burn-out mass (with everything)	17.84	mt
Propellant Mass	66.41	mt
RCS Prop Load	6.08	mt
Boil-off	0.5	mt
Stage wet mass total (on pad)	100.52	mt
Engine Isp	900	sec
Stage Length (including RCS & I/F)	~22.0	m
Effective LH ₂ PMF / λ	0.714	n.d.
Payload Mass Total (on pad)		
Deep Space Hab (stocked)	51.85	mt
MPCV (CM+SM, no propellant)	14.49	mt
Payload RCS / Truss / Canister	14.15	mt
Mars stack interim total		
Start-up / Shut-down (stack total, 4 burns)	3.96	mt
Crew	0.79	mt
Less mass expended prior to TMI (RCS, etc.)	-22.83	mt
Total Stack Mass, (just prior to TMI-1)	359.95	mt

3.2. *Nuclear Electric Propulsion*

Primary Contributors:

Steve Oleson, National Aeronautics and Space Administration, Glenn Research Center

3.2.1. Nuclear Electric Propulsion Study Executive Summary

The COMPASS team was approached by HAT to assess a Nuclear Electric Propulsion option to provide crew transportation to/from Mars using the DRA 5.0 requirements and assumptions. These designs resulted in a multi-Mega Watt NEP crew vehicle that supports the human exploration of Mars. The scope of the conceptual design work focused on two bookend crew vehicle mission concepts:

- Opposition class mission with 60 days at Mars – 2033 easiest opportunity
- Conjunction class – 2037 harder opportunity across the synodic cycle

The objective of the conceptual designs is to drive out a higher fidelity concepts, taking into consideration other aspects such as a more detailed operational concept including configurations and launch packaging as well as to drive out key technologies and sensitivities such as power level and alpha.

The main figure of merits included: number of SLS launches, Mars Stay time, transit time, and complexity. The products of the conceptual design study included a Design Reference Mission (DRM) overview, a CONOPS, two spacecraft concepts (Conjunction and Opposition), a MEL, a PEL, and risks. Due to time constraints, the COMPASS team started with conjunction vehicle then modified it for opposition.

3.2.1.1. NEP Concept for Conjunction Class Missions

The final conjunction NEP concept consisted of a 2.5 MW, 5000s Isp NEP Vehicle to deliver six crew to and from a circular 1 SOL orbit. The piloted NEP vehicle only required two SLS launches (one with a 25-m cylindrical shroud for the simple large reactor radiator array packaging) to LEO to place the two NEP elements. Limiting the NEP vehicle to only two SLS launches would only allow a 400-day stay at Mars (as opposed to the All-Chemical or NTR options), 980-day total piloted mission duration (includes 400-day stay). (Additional reactor power and SLS launches could be added to increase the stay time but initial results showed this as a diminishing return.)

A top-level CONOPS had the two parts of the NEP vehicle (one the habitat and electric propulsion system and the other the reactor power system, xenon propellant on both) launch to an orbit of 400 km using a built in bipropellant kick system based on MPCV. This system is reused for rendezvous phasing, docking, RCS, and re-boost (if needed). Once docked, the reactor boom is deployed as well as the radiator panels and the reactor is started (small solar arrays provide power up to this point). The powered NEP system (still unmanned) spirals in a gravity gradient attitude out to almost escape (options for use of Earth-Moon libration points should be explored further) where the crewed (of six crewmembers) MPCV is launched by another SLS to rendezvous with the NEP vehicle. From here, the crewed NEP spirals to Mars, parks in the 1 SOL circular Mars orbit, and waits for the crew to venture to/from the surface. Once they return, the NEP spirals out of Mars orbit and propels the crew for a hyperbolic flyby of the Earth where the MPCV provides the hyperbolic capture. Options exist to return the unmanned NEP vehicle to a libration point for reuse. Due to the orbit well spirals, the ΔV of the NEP system is quite large (~24 km/s), which necessitated an Isp higher than planned Hall thrusters (5000s) to reduce the propellant sufficiently to fit on two SLS launches. The power system consists of a 2.5 MW Nuclear Reactor with Brayton Power Conversion system. A Large Reactor radiator ‘box’ provides a large area and simple deployment using an expendable boom and flip-out radiators. The propulsion system consists of ten, 280 kW xenon Annular Ion thrusters using Direct Drive (1630VAC to 2200 direct voltage current [Vdc]) units, which are all gimbaled. Again, this system was chosen due to its high Isp (5000 sec) and predicted high efficiency. This configuration allows for an engine out. Each thruster is gimbaled to track center of mass. The > 60t of xenon are stored in two large 3-m-diameter COPV Xenon tanks (one on each SLS launch to allow the low volume (but relatively low mass) reactor radiators and habitat to be launched separately). The other major subsystems are summarized as follows:

- Guidance, Navigation & Control
 - Each Element inserts itself into orbit using STS OMS engines and maneuvers to mate at 400 km
 - Star trackers, IMUs, Monopropellant RCS
- Command and Data Handling
 - Shielded system to control NEP module – housekeeping relayed by Habitat
- Thermal and Mechanical
 - MMOD shielding for tank, radiator loops redundant

3.2.1.2. NEP Concept for Opposition Class Missions

Due to time constraints, the 2.5 MW reactor designed for the opposition case was repurposed in three launches to provide the required 5 kW of power to complete this more difficult mission. Two 2.5 MW systems were joined to each end of the electric propulsion / habitat launch. Thus, three SLS launches are required.

The 5 MW NEP vehicle delivers the crew of six to a 1 SOL circular orbit similar to the conjunction class except that the crew only ventures to Mars for 45 days. The total piloted mission time (from crew rendezvous near Earth escape to Earth return flyby) is 700-day total piloted mission duration (includes the 45-day stay). It was found that total of three launches was just short of that needed; therefore, additional Xenon tanker launches (fuels empty top and tops off bottom tank on Hab/EP launch), perhaps using ATV derived systems, could be used.

3.2.1.3. Lessons Learned

Several valuable lessons were learned during the conceptual design process. It is hoped these lessons will help guide future Piloted Mars designs. The first was that using simple radiator packaging and an SLS cylindrical shroud height of 25 m the reactor power level is limited to approximately 2.5 MW. Thus, if more power needs to be placed on an SLS, an exotic radiator stowage approach would be needed to increase power level. Study time did not allow for such exotic designs to be developed. Given this 2.5 MW per SLS launch power limit, it was found that the chosen Conjunction and Opposition missions are challenging for a 500-day crew surface stay. However, allowing for slightly more trip time while reducing stay time (400-day conjunction and 45-day opposition) reduces NEP power requirements significantly (by ~30% to 50%.) It should be noted that various propulsion options exist – this design effort however did NOT seek to find the best (again due to time constraints). The two SLS launch target drove Isp, and efficiency requirements drove the design away from Hall thrusters. Perhaps with additional xenon tanker flights, a lower Isp and Hall thrusters could be used. The device most similar to the Hall thruster (which is considered the most mature) is the annular ion thruster (electrostatic, high current cathodes, xenon propellant). Other systems such as MPDs, PIT, and VASIMR thrusters should be assessed separately since each greatly changes the vehicle layout. Finally, IF the requirements of crew radiation protection (mass) and artificial gravity are imposed, the design found would be markedly different.

3.2.1.4. Next Steps

A quick list of next steps for each mission option is provided below.

Conjunction Class Missions

- Evaluate how to get MPCV to near escape and rendezvous with Spiraling NEP Vehicle
- Determine what launcher/stages are needed
- Reiterate with more detailed design of deep space habitat
- Adjust design to allow radiation protection and artificial gravity (NOT in the requirements for the design shown here.)
- Trade other propulsion systems
- Recognize that annular ion shown here is due to similarity with large Hall systems
- Determine other options that may provide similar performance (MPD, PIT, other)
- Investigate more exotic radiator packaging schemes to get the power element onto a 17 m cylindrical shroud

- Change the NEP elements design as SLS design changes (shroud size, launch mass, insertion capability)
- Provide more volume for easier radiator stowage approaches
- Provide more mass to allow more propellant and longer stay times
- Insert SLS into 400 km to remove the integrated high thrust system

Opposition Class Missions

- Perform a complete COMPASS run; only a day was spent using elements from the conjunction class to create a first cut MEL – no cad integration performed
- Develop approach to get the additional xenon to the vehicle
- Address how Expendable Launch Vehicles (ELVs) can be used in conjunction with SLS
- Note that increased SLS performance might require only three SLS launches
- Come up with an exotic way to package 5 MW of radiator to allow a single launched power element
- Recognize that increased SLS performance will still be required to reduce number of launches

3.2.1. Study Background and Assumptions

3.2.1.1. Assumptions and Approach

The assumptions and requirements, including those that were known prior to starting the COMPASS design study session, are shown in Table 3-8. This table gathers the assumptions and requirements and calls out trades that were considered during the course of the design study, as well as off-the-shelf materials that were used wherever possible.

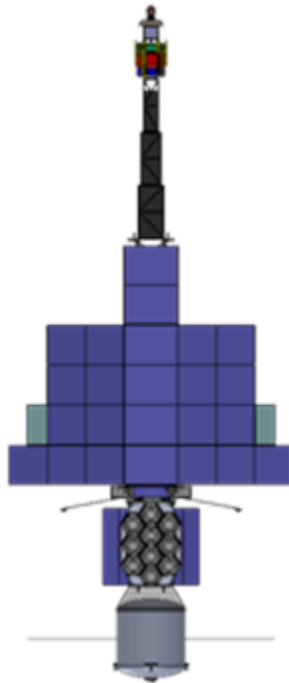


Figure 3-25 Piloted Mars NEP.

Table 3-8 NEP Study Assumptions and Requirements

	Assumptions and study requirements	Critical trades
Top-level	2.5 MW (TBR) NEP module to deliver a crew hab from LEO to Deimos Orbit and back (6 crew Orion joins at C3=0), Orion returned to Ventry max of 13 km/s	Option to reuse nuclear power module for subsequent trips
System	Off-the-shelf equipment where possible, TRL 6 cutoff 2024, 2033 launch, Single Fault Tolerant, 10% launch margin, 30% power growth - EXCEPT for NEP thrusters (assume 5% growth), 5% propellant margins, 50% data storage, 95% NEP duty cycle, Mass Growth per AIAA S-120-2006 (add growth to make system level 30%)	
Mission, Operations, and GN&C	Integrated NEP system , gimbaled EP, 200m/s secondary Biprop, >24 km/s primary mission (NEP), Nuclear power module is passive docking element. 407 km LEO assembly orbit. Dock with Habitat/EP module, spiral to HEO (~lunar orbit), rendezvous with Orion, thrust to Mars, spiral down to Diemos orbit, crew departs for surface operations (400 d), crew returns to NEP, spiral to esc, helio transfer to earth, 13 km/s Ventry for Orion, NEP vehicle avoids earth	Reactor power level, lsp, starting orbit
Launch vehicle	Heavy lift to -97x407 km, 28.5°, 9 m x 25m cylindrical Shroud volume, Element insertion by integrated biprop system (reused for orbit maneuvers during mission) Launch Loads: Axial 5+/- 1 g, Lateral .4 +/- 1.6g	
Propulsion	Primary: 10, 300 KW annular ion, 5000 sec, two 3.6m xenon tanks, xenon propellant ~(90,000 kg TBR) Secondary: OMS engines (insertion and orbit maneuvers), Bi-prop, 100 lbf thrusters RSC	Primary: Number/power level of thrusters, Hall w krypton propellant, VaSIMR, MPD, PIT Secondary: Mono-prop
Power	Single 2500 kW(TBR) nuclear power system,4 brayton power conversion systems Direct Drive Units (DDUs) to interface between nuclear system (2000 VAC TBR) and Ion thrusters (2000 Vdc TBR). 18000 kW to habitat, (with 1500 W housekeeping), Batteries for launch, eclipse	Power conversion temp (1200K vs 1500 K), Rankin vs Brayton, Direct drive vs PPU's, Bus Voltage, 'box truss' or 'folded booms' radiator design
C&DH and Communications	Main Computers to operate Modules – interface with habitat housekeep), 100 GB data storage, Mars: multi-Mb/s real-time downlink, Mars: multi-MB/s, Gimbaled HGA for GEO-NEO ops, four medium gain antennas helical for earth ops, X-band	
Thermal and environment	Body mounted propulsion/housekeeping radiators (main loads 50,000W/wh) Tank heaters, heat pipe radiators, Earth and 1 AU thermal environment Proton belt Radiation level , orbital debris micrometeroid environment	Deployed radiators, can NEP propellant (xenon) be used to shield crew?
Mechanisms	Radiator Deployment, Thruster gimbals +/- 12 °,	Radiator deployment
Structures	Primary: ~5 m thrust tube , Al-Li, Secondary: 4% of Stage components	

Table 3-9 lists the assumptions of liens for the Mars NEP spacecraft. These data spell out which functions are controlled by or performed by which element of the complete spacecraft. These data are used by the subsystem engineers in designing their systems.

Table 3-9 Liens Listing

Subsystem area	Liens on Habitat Vehicle/Propulsion Module	Liens on Power Module
Mission, operations, and GN&C	Habitat Vehicle is the primary docking component GN&C for the cruise and coast phases (has LEO GN&C for rendezvous and dock)	Power module provides all power, Power module is passive docking element (has LEO GN&C for rendezvous and dock)
Propulsion	Primary and RCS for Cruise/Pointing. Portion of the primary propellant	Some primary propellant. Has RSC also.
Power	Solar power for pre-rendezvous AND contingency operations	Provide up to 2.5 MW to primary propulsion and 18kW to Hab vehicle during all docked operations (continuous)
Communications	Primary Deep Space Communications (Also LEO communications)	NEP vehicle relays housekeeping for Habitat vehicle (when attached), (Also LEO communications)
C&DH	Primary Control of integrated vehicle	Hab vehicle top-level commands for PM operations, Power Module integrates stage telemetry into main data stream
Thermal and Environment	Possible Contamination from thrusters (back sputter flux) Thruster EMI including magnetic field from thrusters, EP thrust vector defines habitat thermal attitudes, heat soak back from large solar arrays	Waste heat from habitat viewing the Power module
Mechanisms	Propulsion module supports habitat during launch	
ECLSS		Power Module has large volumes available for consumables, batteries, misc. Equipment

3.2.1.2. Mission Description

3.2.1.2.1. Mission Analysis Assumptions – Case 1

The following were the assumptions made for the mission analysis for case 1:

- Conjunction class mission, 2037 opportunity
- Each element must insert itself into a 407 km circular orbit
 - SLS delivers each element to a -92.6 km x 407 km orbit
 - Leads to an orbit insertion delta-v of 148 m/s
- Chemical Isp = 315 s
- The Hab/EP element performs AR&D with the power element in LEO
- Power available to the EP thrusters is 95% of the total power (5% for housekeeping)
- The crew meets up with the vehicle at Earth escape
- Mass of the MPCV = 24 Mt
- The vehicle spirals down to/up from a circular orbit essentially at the altitude of Deimos at Mars arrival/departure

3.2.1.2.2. Mission Analysis Details—Case 1

Choosing a power and Isp:

To choose an operating power level and an Isp for the EP thrusters, the design team generated a series of alpha capability curves using the Mission Analysis Low Thrust Optimization (MALTO) program for various Mars stay times. These curves can be seen in Figure 3-26 through Figure 3-28 . It was initially estimated that the final inert mass delivered back to Earth would be roughly 140 Mt. This consists of an estimated 77 Mt for the Hab/EP element, a fixed 24 Mt for the MPCV, and an estimated 39 Mt for the power element, knowing that the mass of the power element would change depending on the chosen power level. Looking at the figure for the 500-day Mars stay time, assuming an operating Isp of 3000 s, a final alpha of 50 kg/kWe would be required to complete the mission. Assuming the 140 Mt of final inert mass, this would lead to a required operating power of 2800 kWe (140000 kg / 50 kg/kWe). The corresponding starting alpha for an Isp of

3000 s is 112 kg/kWe, leading to an Earth departure mass of 314,841 kg. This is the required amount of mass at Earth departure to complete a mission with a 500-day stay at Mars. Since it was desired to complete the mission with no more than two SLS launches, the corresponding mass in LEO was required to be calculated. The 314,841 kg includes the mass of the MPCV at the time of Earth departure. Subtracting out the 24 Mt for the MPCV leaves 290,841 kg for the combined mass of the Hab/EP element and the power element at the time of Earth departure. The delta-v to spiral out from LEO to escape was estimated using the Satellite N-body Analysis Program (SNAP) to be approximately 7640 m/s. Applying the rocket equation using the 7640 m/s of delta-v and the 290,841 kg of mass at Earth departure leads to a mass in LEO of 377,096 kg. It was then necessary to calculate how much mass could be delivered to LEO using two SLS launches and compare this mass to the 377,096 kg of mass required to complete the mission with a 500-day stay time. It was assumed that the SLS launch vehicle could inject a mass of 113.775 Mt into a -92.6 km x 407 km orbit. After applying the necessary 148 m/s of delta-v to circularize to a 407 km orbit, this left 108.445 Mt for each element in LEO, leading to a maximum mass in LEO of 216,890 kg using two SLS launches. This is much less than the 377,096 kg required to complete a 500-day stay mission with an Isp of 3000 s and power level of 2800 kWe. Repeating this analysis, assuming an Isp of 4000 s for a 500-day stay, leads to an operating power of 3186 kWe and a mass in LEO of 270,828 kg, also over the 216,890 kg limit for two SLS launches. Similarly, an Isp of 5000 s required a power level of 3500 kWe and an IMLEO of 216,547 kg. This mass is below the limit for two SLS launches; however, it was decided that the required power level of 3500 kWe was too high. It was concluded that a 500-day stay time was not achievable for this mission given the above assumptions. In summary, this process was repeated until a suitable power level and Isp were found that met the requirements. In the end, it was decided that 400 days would be the nominal stay time at Mars, with an operating power of 2500 kWe and an Isp of 5000 s. Since it was assumed that 5% of the total power would be used for housekeeping, this led to 2375 kWe of power available to the EP thrusters. After the power level and Isp were chosen, a few additional trajectories were generated with interplanetary trip times less than 1000 days to attempt to allow for the time it would take the crew to meet up with the vehicle at Earth escape and still stay under the required 1000 days of total trip time for the crew. The final design point, which can be seen in Figure 3-29, was a heliocentric trip time of 980 days, which would allow 20 days for the crew to meet up at Earth escape and still remain under the 1000 days of total trip time.

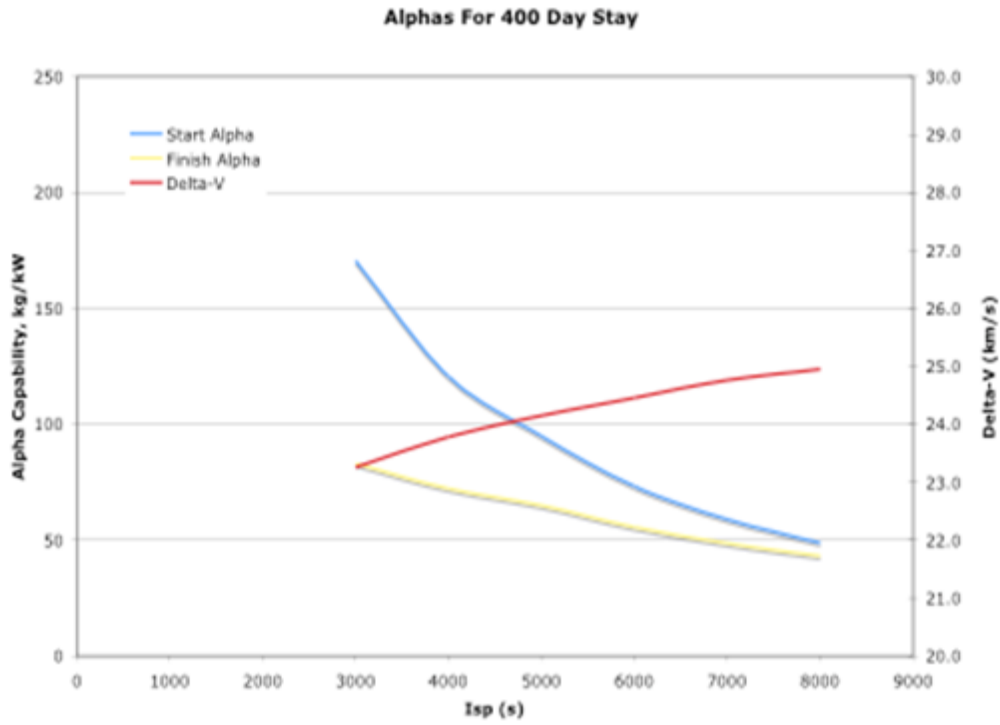


Figure 3-26 Alphas for a 400-day Mars stay time.

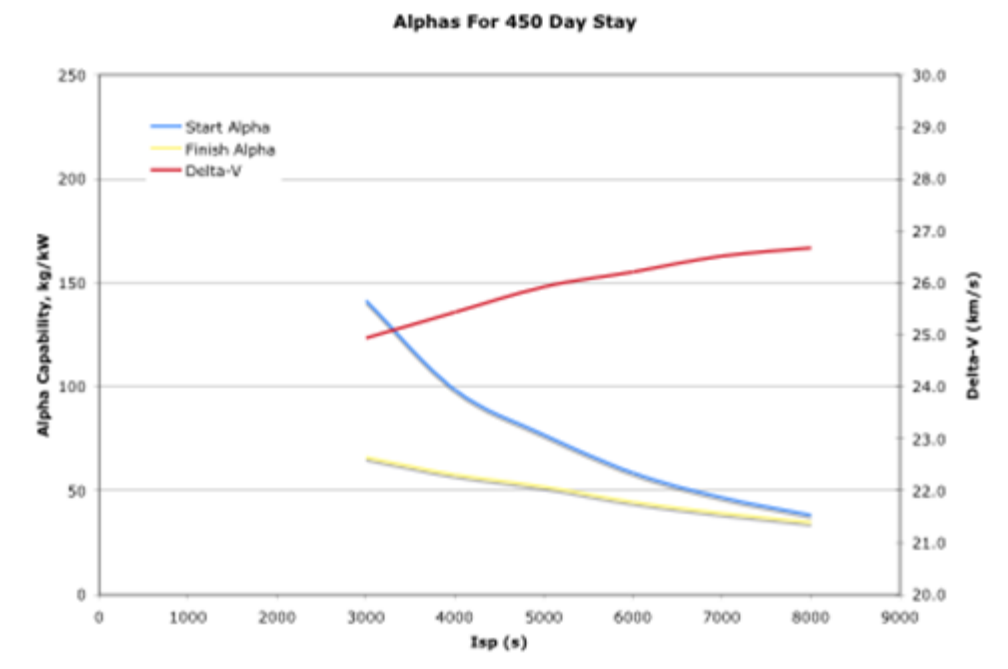


Figure 3-27 Alphas for a 450-day Mars stay time.

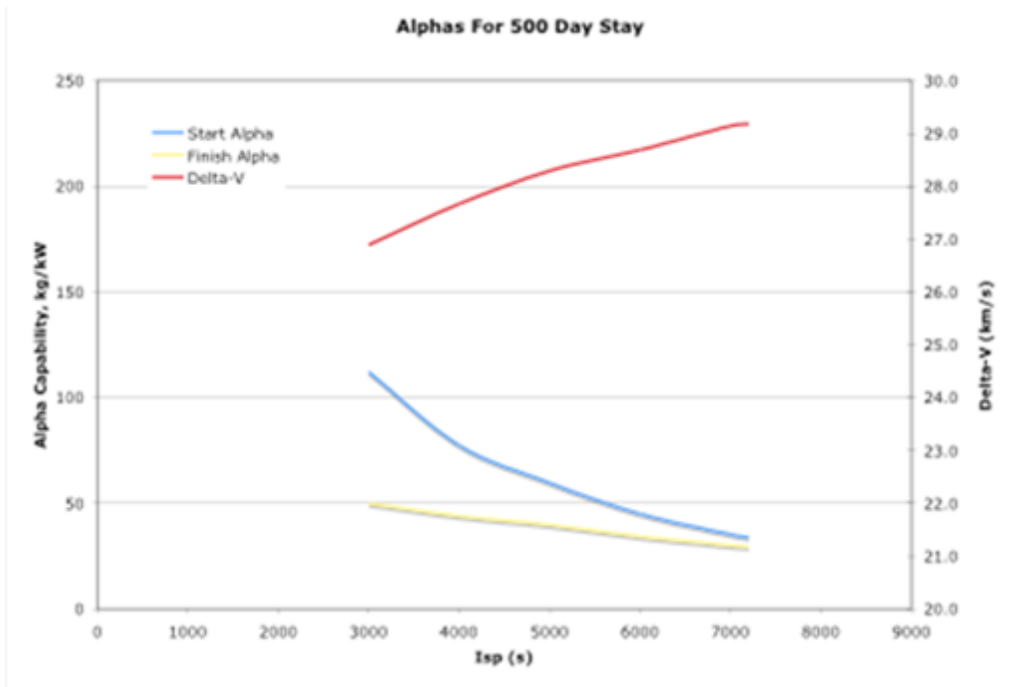


Figure 3-28 Alphas for a 500-day Mars stay time.

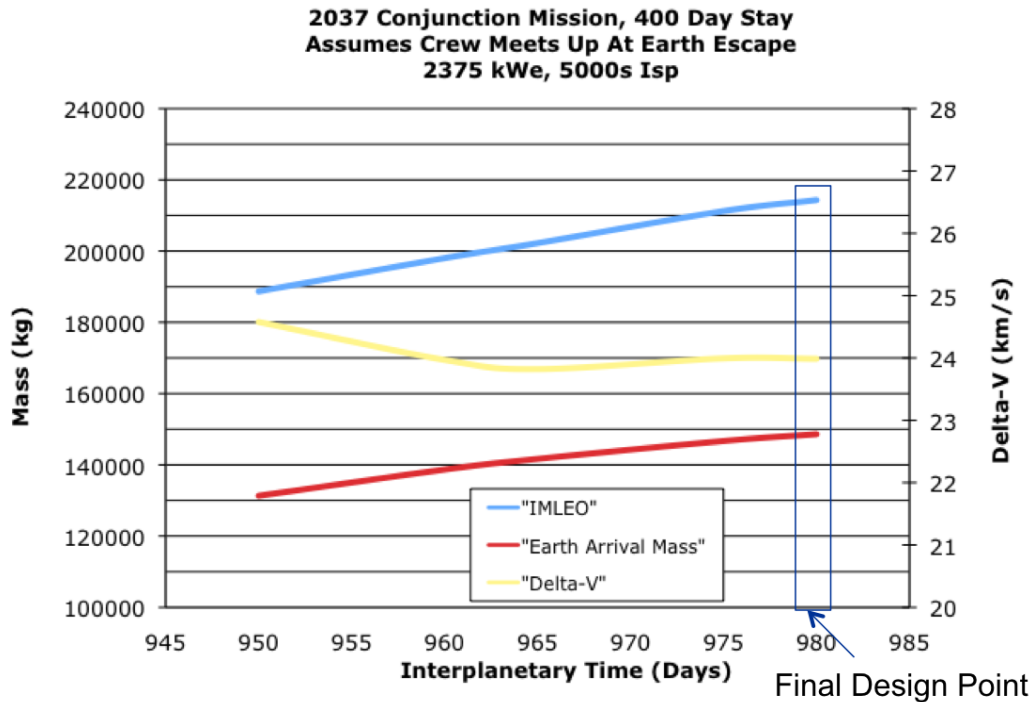


Figure 3-29 Final design point for Case 1.

3.2.1.2.3. Mission Analysis Event Timeline—Baseline Case 1

Figure 3-30 is the trajectory for Case 1 with mission event dates labeled at the appropriate places along the trajectory

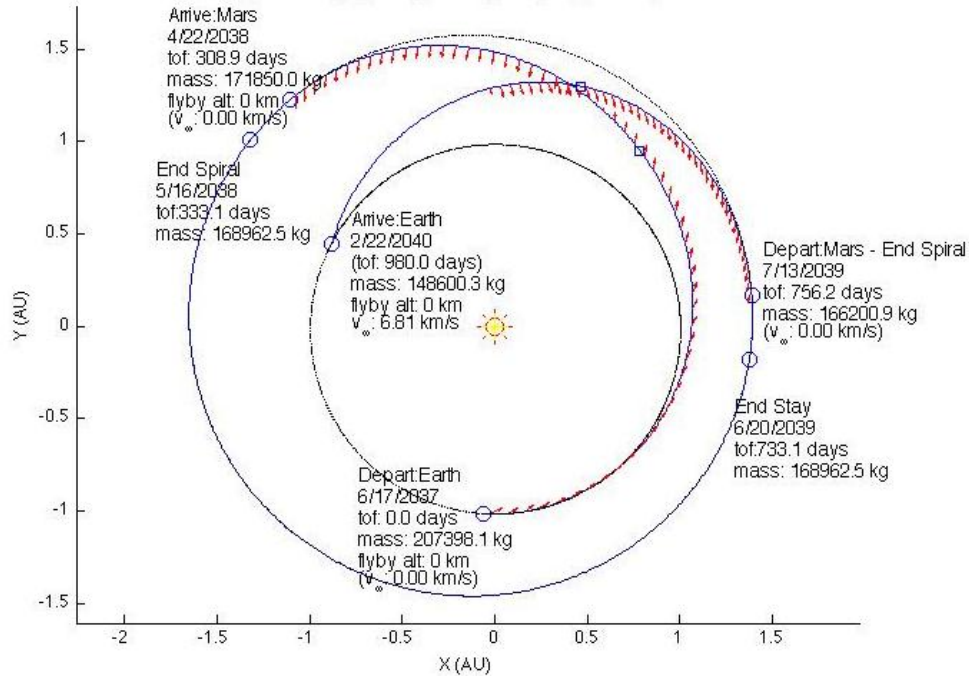


Figure 3-30 Trajectory for Case 1 conjunction.

3.2.1.2.4. Mission Analysis Assumptions – Case 2

The following were the assumptions made for the mission analysis for case 2:

- Opposition class mission, 2033 opportunity
- Each element must insert itself into a 407 km circular orbit
 - SLS delivers each element to a -92.6 km x 407 km orbit
 - Leads to an orbit insertion delta-v of 148 m/s
- Chemical Isp = 315 s
- The Hab/EP element performs AR&D with the power element in LEO
- Power available to the EP thrusters is 5.0 MWe
- EP thruster efficiency = 70%
- EP Isp of 5000s
- The crew meets up with the vehicle at Earth escape
- Mass of the MPCV = 24 Mt
- The vehicle spirals down to/up from a circular orbit essentially at the altitude of Deimos at Mars arrival/departure

3.2.1.2.5. Mission Analysis Details—Case 2

The goal was to meet a 60-day stay time at Mars using no more than three SLS launches while limiting the crew time to 600 days,; however, it was found that this was not possible. Figure 3-31 shows curves for the IMLEO mass as well as the Earth arrival mass for heliocentric trip times of 600 days and above. The curves were generated using MALTO along with the rocket equation. MALTO was used to find the required initial mass departing Earth to deliver the maximum final mass delivered back to Earth after a 60-day stay at Mars. The mass of the MPCV was then subtracted from the required Earth departure mass and the rocket equation was used to estimate the required mass in LEO assuming a delta-v of 7640 m/s to go from LEO to Earth escape. While the figure shows results for various Isp’s, the desire was to use the same Isp as for Case 1, 5000 s. The final inert mass that the design ended up at was 207 Mt and the capability of three SLS launches to LEO, assuming each element is responsible for circularizing to a 407 km circular orbit, is 324 Mt. For the design to close, the IMLEO mass must be lower than the 324 Mt limit to stay under three SLS launches while the Earth arrival mass must be at or above the 207 Mt inert

mass from the team design. Figure 3-31 shows that this is not possible, even for Isps higher than 5000 s and also allowing for longer heliocentric trip times than 600 days.

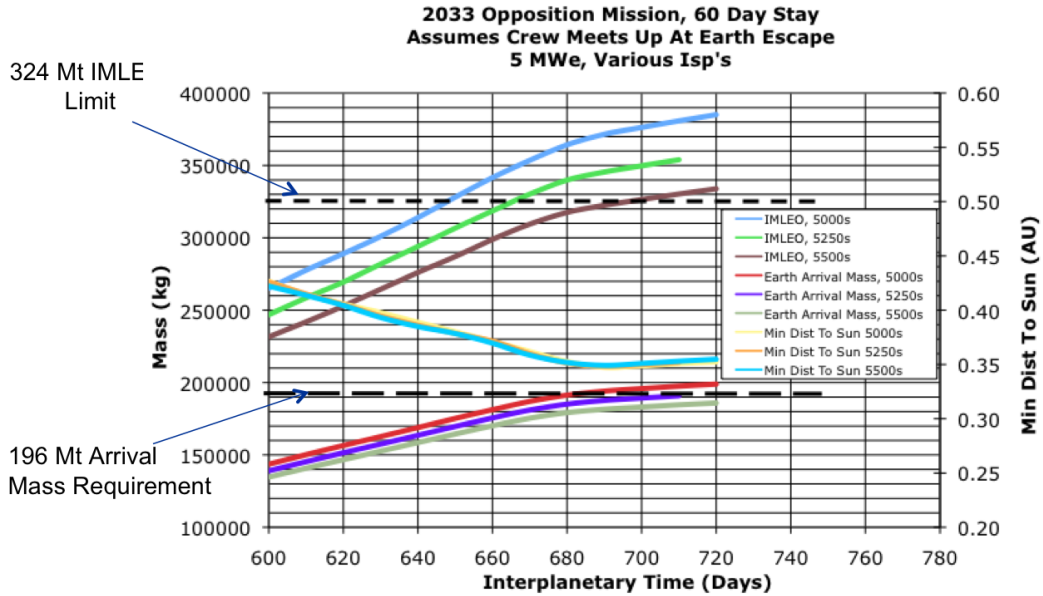


Figure 3-31 Performance curves for a 60-day stay at Mars, 2033 opposition.

Additional analysis was carried out for shorter stay times; however, there was a desire to have a stay time at Mars no less than 45 days. Figure 3-32 shows the results for a 45-day stay at Mars. While the performance for a 45-day stay is slightly better than a 60-day stay, it's still not possible to deliver the 207 Mt of inert mass back to Earth while staying under the 324 Mt IMLEO requirement. Since it was desired to have a stay time at Mars of no less than 45 days, and also due to the short duration of time spent on the opposition class mission (~1 day), the decision was made to assume that tanker flights of xenon could be launched to “top off” the propellant tanks before departing from LEO. The final design point was assumed to be a 700-day heliocentric trip time, requiring approximately 66 Mt of xenon to be launched and transferred to the vehicle propellant tanks before departing from LEO.

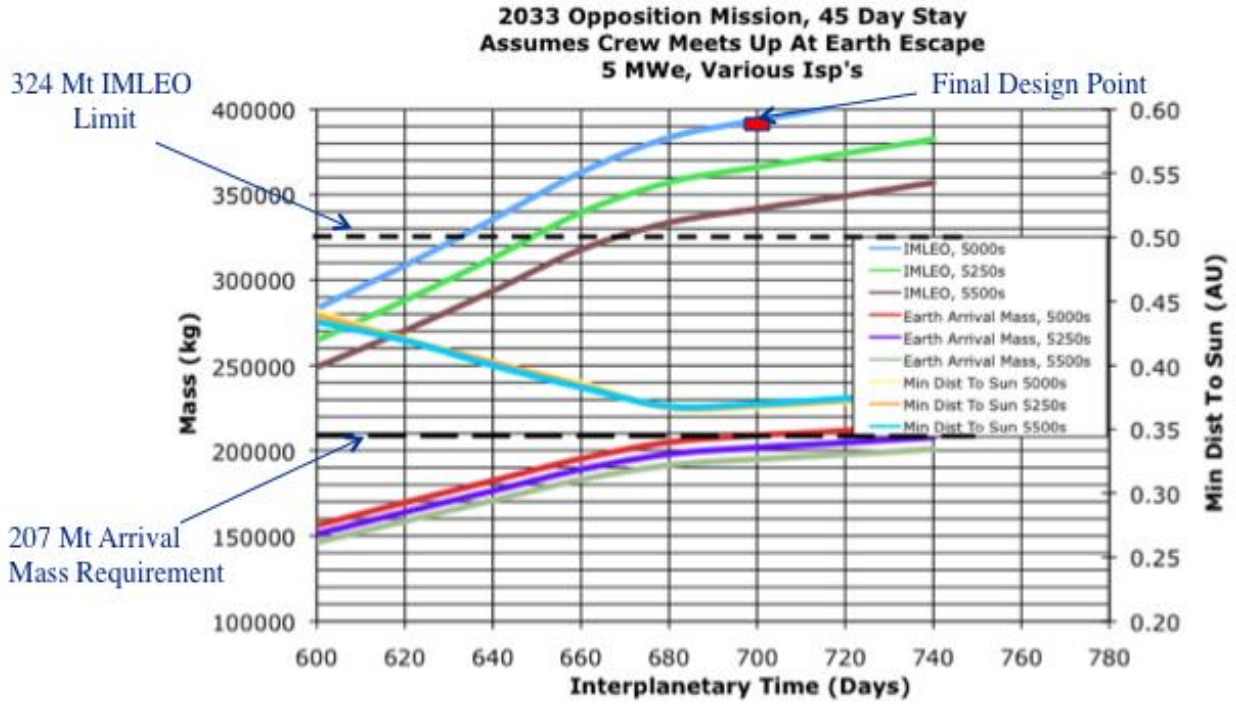


Figure 3-32 Performance curves for a 45 day stay at Mars, 2033 opposition.

3.2.1.2.6. Mission Analysis Event Timeline – Case 2

Figure 3-33 is the trajectory for Case 2 with mission event dates labeled at the appropriate places along the trajectory.

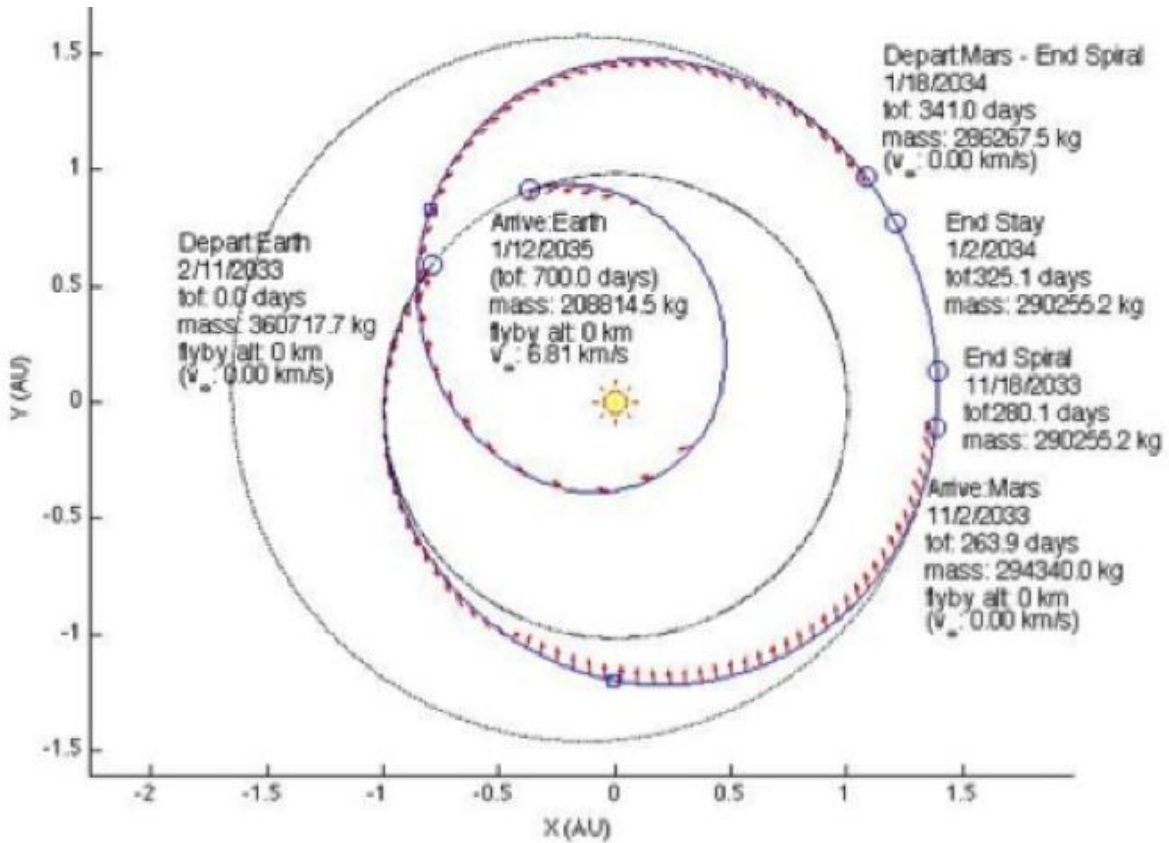


Figure 3-33 Trajectory for Case 2 – opposition.

3.2.1.2.7. Case 1, Mission ΔV Details

3.2.2.2.7.1 Mission ΔV Summary for Case 1, Conjunction

The delta-v summary for the conjunction case, case 1, can be seen in Table 3-10. In an attempt to ensure that each element had the same wet mass at launch, some of the delta-v's were divided between the two elements after they docked with each other. For the EP delta-v's, the Hab/EP element always performs the delta-v. Since that is where the EP thrusters are located, it's just a matter of where the propellant is pulled from. For instance, phase 5 is the spiral out from LEO to Earth escape. The Hab/EP element performs this delta-v since that is where the EP thrusters are located, but 20,798 kg of propellant was used from the power element whereas 10,243 kg of propellant was used from the Hab/EP element. This propellant split is only representative for this study and, again, it was done so that each element had the same wet mass at launch. The actual split would likely be different for CG management or some other consideration.

Table 3-10 ΔV Summary for Case 1

Mission DeltaV Summary								
Phase #	Phase Name	Propellant Utilization	Pre-Burn Mass (kg)	Main DV (m/s)	ACS DV (m/s)	Main Prop (kg)	ACS Prop (kg)	Post Burn Mass (kg)
1	Orbit Boost, Hab/EP	Hab/EP	113303	0	148	0	5300	108003
2	Stationkeeping, Hab/EP	Hab/EP	108003	0	20	0	697	107306
3	Orbit Boost, Power Element	Power	113307	0	148	0	5301	108006
4	AR&D	Hab/EP	107306	0	5	0	174	107132
5	Spiral Out To Escape	Power	215139	4985	0	20798	0	194341
5	Spiral Out To Escape	Hab/EP	194341	2655	0	10243	0	184098
6	Dock With MPCV	Hab/EP	184098	0	0	0	0	184098
7	Outbound Heliocentric Leg	Power	207918	6015	0	24005	0	183913
7	Outbound Heliocentric Leg	Hab/EP	183913	3204	0	11632	0	172281
8	Spiral In To Deimos	Power	172281	542	0	1895	0	170387
8	Spiral In To Deimos	Hab/EP	170387	289	0	1001	0	169386
9	Stationkeeping	Power	169386	0	23	0	1278	168108
9	Stationkeeping	Hab/EP	168108	0	7	0	359	167749
10	Spiral Out from Deimos	Power	167749	527	0	1794	0	165955
10	Spiral Out from Deimos	Hab/EP	165955	281	0	948	0	165008
11	Inbound Heliocentric Leg	Power	165008	3582	0	11623	0	153385
11	Inbound Heliocentric Leg	Hab/EP	153385	1907	0	5852	0	147532
	Total			23987	351	89789	13109	

3.2.2.2.7.2 Mission ΔV Summary for Case 2, Opposition

The delta-v summary for the opposition class mission, case 2, can be seen in Table 3-11. Similarly to case 1, an attempt was made to ensure that each element had the same wet mass on the launch pad; therefore, some of the delta-v's were divided between the three elements after they had docked with each other.

Table 3-11 ΔV Summary for Case 2

Phase #	Phase Name	Propellant Utilization	Pre-Burn Mass (kg)	Main DV (m/s)	ACS DV (m/s)	Main Prop (kg)	ACS Prop (kg)	Post Burn Mass (kg)
1	Orbit Boost, Hab/EP	Hab/EP	113030	0	148	0	5288	107742
2	Stationkeeping, Hab/EP	Hab/EP	107742	0	20	0	695	107047
3	Orbit Boost, Power Element1	P1	112681	0	148	0	5271	107410
4	AR&D With Power Element1	Hab/EP	107047	0	5	0	173	106874
5	Orbit Boost, Power Element2	P2	113373	0	148	0	5304	108070
6	AR&D With Power Element2	Hab/EP	214284	0	5	0	347	213937
7	Spiral Out To Escape, Power1	P1	393537	2106	0	16543	0	376994
7	Spiral Out To Escape, Power2	P2	376994	2106	0	15848	0	361146
7	Spiral Out To Escape, Hab	Hab/EP	361146	602	0	4404	0	356742
7	Spiral Out To Escape, Tanker		356742	2827	0	19985	0	336757
8	Dock With MPCV	P2	0	0	0	0	0	0
9	Outbound Heliocentric Leg, Power2	P1	360577	2749	0	19656	0	340921
9	Outbound Heliocentric Leg, Power1	Hab/EP	340921	2749	0	18584	0	322337
9	Outbound Heliocentric Leg, Hab	P2	322337	785	0	5121	0	317216
9	Outbound Heliocentric Leg, Tanker	P2	317216	3690	0	22994	0	294222
10	Spiral In To Deimos, Power2	Hab/EP	294222	189	0	1131	0	293091
10	Spiral In To Deimos, Power2	P1	293091	189	0	1126	0	291965
10	Spiral In To Deimos, Hab	P2	291965	54	0	321	0	291644
10	Spiral In To Deimos, Tanker	Hab/EP	291644	253	0	1504	0	290140
11	Stationkeeping, Power1	P1	290140	0	12	0	1097	289043
11	Stationkeeping, Power2	P2	289043	0	12	0	1093	287950
11	Stationkeeping, Hab	Hab/EP	287950	0	7	0	615	287336
12	Spiral Out from Deimos, Power1	P1	287336	187	0	1093	0	286243
12	Spiral Out from Deimos, Power2	P2	286243	187	0	1089	0	285154
12	Spiral Out from Deimos, Hab	Hab/EP	285154	53	0	310	0	284844
12	Spiral Out from Deimos, Tanker	Hab/EP	284844	251	0	1454	0	283390
13	Inbound Heliocentric Leg, Power1	Hab/EP	283390	4264	0	23601	0	259789
13	Inbound Heliocentric Leg, Power2	Hab/EP	259789	4264	0	21635	0	238154
13	Inbound Heliocentric Leg, Hab	Hab/EP	238154	1218	0	5844	0	232310
13	Inbound Heliocentric Leg, Tanker	Hab/EP	232310	5724	0	25594	0	206716
	Total			18724	504	129709	19882	

3.2.1.2.8. Concept of Operations (CONOPS)

As shown in

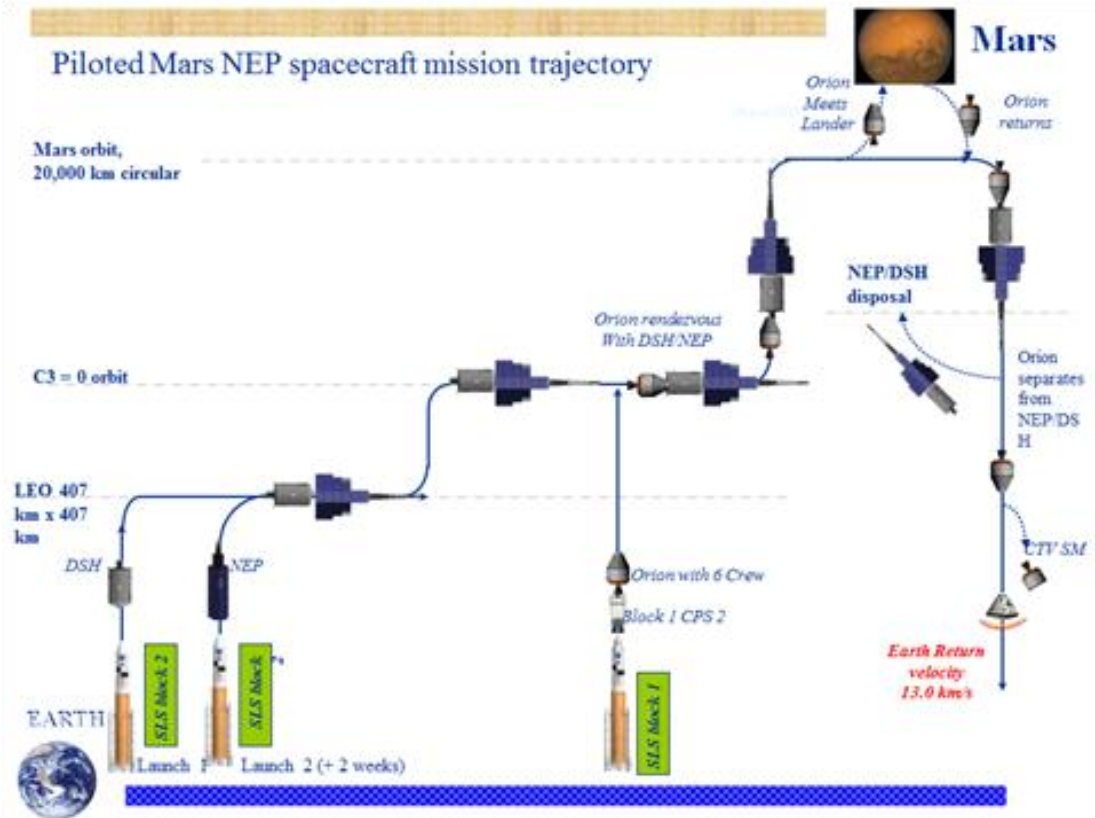


Figure 3-34, the CONOPS of the piloted Mars NEP is described as follows:

1. Launch DSH and NEP modules to LEO (407 km, 28.5°)
The launch vehicle is two units of SLS Block 2. The first launch is for DSH/Electric propulsion (EP) module. The second launch occurs in 14 days for NEP module. It is assumed that each module inserts itself into orbit. OMS fires for orbit insertion. Assembly NEP module and DSH/EP module will complete within 28 days.
2. NEP spirals DSH to High Earth Orbit (HEO) staging point (c3 = 0 orbit)
It takes 354 days.
3. Launch Orion (with stretch SM) with six crews from Earth to HEO staging point
Orion is launched 8 days before NEP/DSH reach c3 = 0 orbit. It can take 6 days. The launch vehicle is one unit of SLS Block 1. At insertion stage, the Cryogenic Propulsion Stage (CPS) performs perigee kick and circularization maneuvers.
4. Orion rendezvous with DSH/NEP (2 days)
It is assumed that Orion is fully fueled. Crew will direct rendezvous with NEP/DSH. This step takes 2 days. If the rendezvous cannot be accomplished within 11 days, the mission will be aborted.
5. NEP performs heliocentric transfer and arrivals at Mars
It takes 293 days.
6. NEP spiral to High Mars Orbit (HMO, 20,000 km circular → essentially Deimos orbit altitude)
It takes 21 days.
7. NEP remains in HMO during destination exploration (surface or Moons)
It lasts 400 days.
8. NEP spiral out of Mars orbit
It takes 21 days.
9. NEP performs heliocentric transfer back to Earth

It takes 215 days.

10. Orion separates from NEP/DSH (7 days, TBR), NEP/DSH performs maneuvers to storage orbit for follow-on mission, and Orion returns Earth.
11. Crews direct Earth entry in Orion at an entry speed of 13 km/s.

During NEP activation and checkout, commands are sent from ground to 1) deploy communication antennas; 2) deploy radiator; 3) start the reactor; and 4) check the power output, leaks from fluid lines and others. Before NEP performs spiral to HEO ($c3 = 0$ orbit), the EP system is started and is in continuous propulsion. Commanding is sent from the ground.

During NEP perform the rest of spiral Earth departure and spiral Mars departure, EP is in continuous operation and RCS will operate during this phase too.

During NEP performs heliocentric transfer to Mars and back to Earth, it is necessary to start and shut down the EP system during thrusting and coasting phases. Nuclear power (NP) system is in continuous operation. When EP is shut down, the extra power goes to shunt. NP power output can be adjusted if it is needed.

During NEP/DSH stay in HMO and wait for Orion, EP is shut down, communicate with both ground and Orion.

Table 3-12 lists the mission events and times for the Mars NEP baseline trajectory (Case 1, Conjunction).

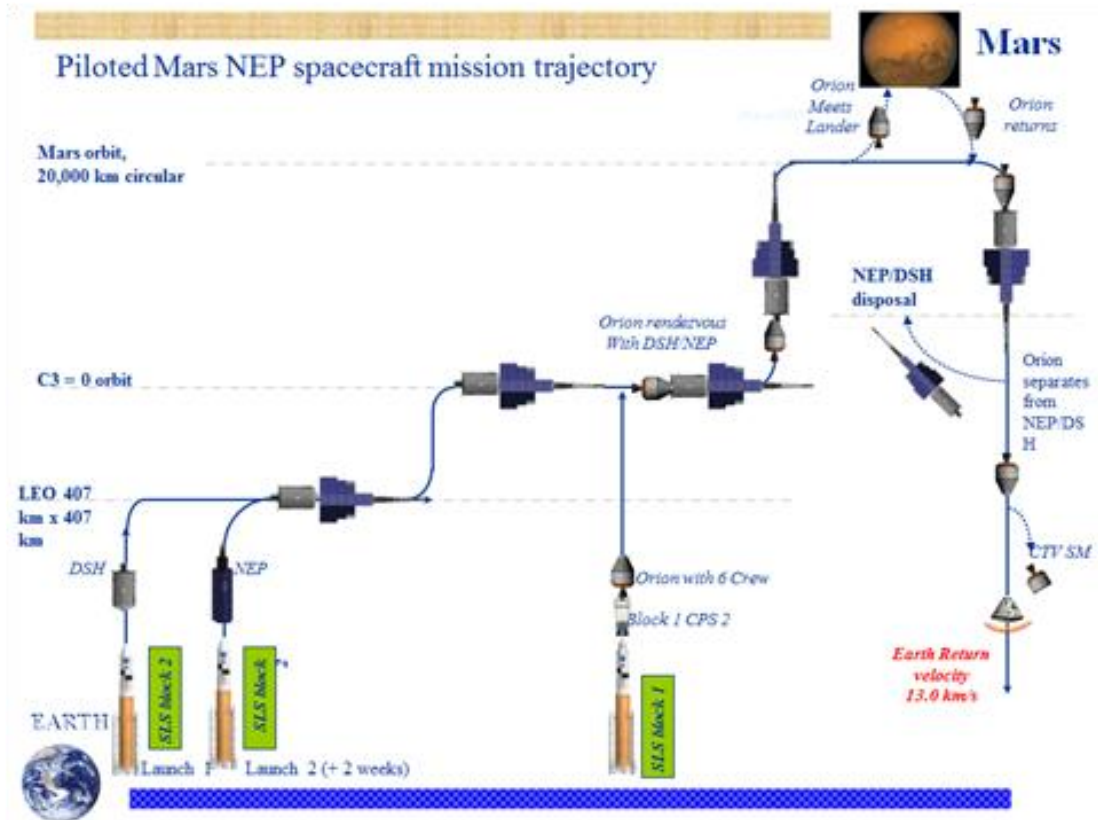


Figure 3-34 Piloted Mars NEP concept of operations graphic.

Table 3-12 Mars NEP Mission Events Case 1 Conjunction

Event	Time	Notes
Launch DSH and NEP Modules	T=0 and T+14	DSH/Electric propulsion (EP) module: launch 1, NEP module, launch 2
Assembly NEP module and DSH/EP module	T+14d to T+42	(28d) Each module inserts itself into orbit
NEP spirals DSH to High Earth Orbit (HEO)	T+42 to T+396	(354d) staging point (c3 = 0 orbit)
Launch Orion (with stretch SM)	T+(TBD)	6 crew, insertion stage: Cryogenic Propulsion Stage (CPS) (performs perigee kick and circularization maneuvers), Orion fully fueled
Orion rendezvous with DSH/NEP	T+396 to T+404	(8d) 11 days for aborting mission
NEP performs heliocentric transfer and arrivals at Mars	T+404 to T+697	(293d)
NEP spiral to High Mars Orbit	T+697 to T+718	(21d)HMO, 20,000 km circular essentially Deimos orbit altitude (21 days)
NEP remains in HMO	T+718 to T+1118	(400d) Mars surface operations (400d)
NEP spiral out of Mars orbit	T+1118 to T+1139	(21d)
NEP performs heliocentric transfer	T+1139 to T+1354	(215d)
Orion separates from NEP/DSH	T+(TBD)	NEP/DSH maneuvers to storage orbit for follow-on mission, Orion returns Earth
Orion Direct Earth Entry	T=1354	Entry speed is 13 km/s

3.2.1.3. Launch Vehicle and Payload Details

3.2.1.3.1. Launch Vehicle Trade Space

The SLS vehicles were identified to place the elements of the Piloted Mars NEP mission into LEO. Specifically, the DSH and NEP elements would be boosted by an SLS Block 2 vehicle and the Orion with crew would utilize an SLS Block 1 with CPS. The following assumptions were made regarding the SLS for this study:

1. SLS mass and payload volume estimates are continuing to evolve
2. SLS gross payload delivery for this study is 123 t to LEO
3. LEO is -92.6 km x 407 km
4. Net payload delivery capability:
 - a) Gross Payload Delivery – 123 t
 - b) Customer Reserve (5%) – 6.15 t
 - c) Spacecraft adapter (2.5%) – 2.92 t
 - d) Net Payload to LEO – 113.93 t
5. SLS delivery point is a negative perigee condition, thus an appropriate kick stage must be included in the payload for perigee raise and all other orbital maneuvers required in Earth orbit.
6. Upper Stage Details:
 - a) SLS Upper Stage
 - b) Number of J-2X engines – 2
 - c) Vacuum thrust – 285,000 lbm
 - d) Vacuum Specific Impulse – 435 seconds
 - e) Burnout mass – 33.038 t (72836 lbm)
 - f) Useable Propellant – 210.65 t (464401 lbm)
7. Payload Shroud Details:
 - a) Fairing configuration: Ogive nose, overall length 31.09 m (1224 inches), hammerhead
 - b) Outer Diameter- 10.06 m (396 inches)
 - c) Dynamic envelope diameter- ~9.14 m (~360 inches)
 - d) Dynamic envelope length is dependent on payload geometry and how far it can extend up into the ogive
 - e) Barrel Section Length, HAB/EP Element- 17.21 m (677.70 inches)
 - f) Barrel Section Length, Power Element = 25.0 m (984.25 inches)

g) Mass- 15.68 t (34571 lbm)

Collect the table or a listing of the launch vehicles considered for this design study. If only one launch vehicle was considered, and chosen, document that as well.

3.2.1.3.2. Deep Space Habitat Payload

Deep Space Habitat:

1. Initial core habitat (constant based on #crew and duration)
2. Initial accommodations (constant based on #crew and duration)
3. Accommodations rate (varies with #crew and duration)
4. Mass estimates based on parametric sizing performed by the HAT DSH team:
5. For this design activity assume a crew of 6 roundtrip to Mars.

Table 3-13 Deep Space Habitat HAT Variations

# Crew	4	4	6	6
Mission Duration (days)	600	1,000	600	1,000
Core Mass (kg)	24,741	28,313	29,830	34,842
Initial Accommodations (kg)	4,110	4,128	4,819	4,846
Accommodation Rate (kg/crew/day)	2.218	2.226	2.193	2.200
Total Mass (t)	34.2	41.3	42.5	52.9

3.2.1.3.3. Orion Payload

1. Orion Payload Assumptions:
 - a) Mass estimates based on current Waypoint mission analysis: “Orion Capabilities for Waypoint Missions, Jim Geffre & Wayne Jermstad, 11 January 2012, Revision: NC”
 - i. Orion_CM (kg) 10,101
 - ii. Orion_SM (kg) 5,121
 - iii. Total Inert Mass (kg) 15,222
 - iv. Orion Max Prop Load (kg) 8,598
 - v. Orion Isp (sec)³ 26
 - vi. Orion Max Delta-v (m/s) 1,432
 - vii. Max Wet Mass (kg) 23,820

3.2.2. Baseline NEP Design

3.2.2.1. System-Level Summary

The system block diagram that captures the theory behind the Mars NEP design is shown in Figure 3-35

3.2.2.1. Top-Level Design Details

3.2.2.1.1. Master Equipment List (MEL)

The MEL lists these two major elements in terms of the major subsystems within them. The Piloted Mars NEP spacecraft is listed as work breakdown structure (WBS) element 06. The Hab/EP element itself is listed in the MEL as WBS element 06.1. The power element is listed as WBS element 06.2. Table 3-14 shows the MEL listing of the Hab/EP element and power element as the elements that make up the Piloted Mars NEP spacecraft, performed by the COMPASS Team and documented in this study.

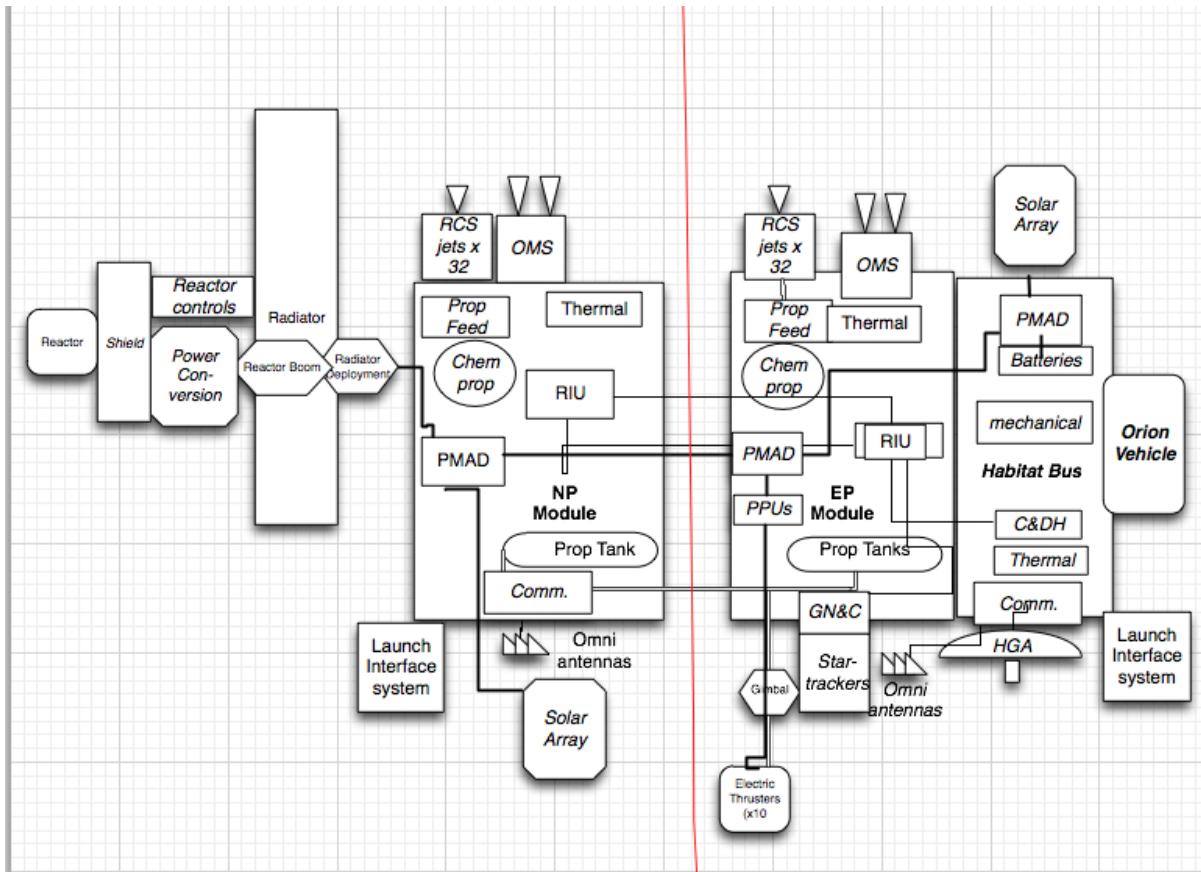


Figure 3-35 Mars NEP block diagram.

Table 3-14 Mars NEP MEL WBS Format—Conjunction

WBS	Description	QTY	Unit Mass	Basic Mass	Growth	Growth	Total Mass
Number	Case 1 Piloted Mars NEP Spacecraft CD-2012-73		(kg)	(kg)	(%)	(kg)	(kg)
06	Piloted Mars NEP Spacecraft			211907.69	3.1%	6590.54	218498.23
06.1	Hab/EP Element			108360.60	2.3%	2517.89	110878.49
06.1.1	Habitat			52888.00	0.0%	0.00	52888.00
06.1.2	Attitude Determination and Control			91.84	3.0%	2.76	94.60
06.1.3	Command & Data Handling			46.80	21.4%	10.00	56.80
06.1.4	Communications and Tracking			0.00	0	0.00	0.00
06.1.5	Electrical Power Subsystem			41.00	14.8%	6.05	47.05
06.1.6	Thermal Control (Non-Propellant)			1740.34	18.0%	313.26	2053.61
06.1.7	Propulsion (Chemical Hardware)			961.47	3.5%	33.30	994.77
06.1.8	Propellant (Chemical)			7622.26	0.0%	0.00	7622.26
06.1.9	Propulsion (EP Hardware)			7963.73	14.3%	1139.04	9102.77
06.1.10	Propellant (EP)			31374.70	0.0%	0.00	31374.70
06.1.11	Structures and Mechanisms			5630.46	18.0%	1013.48	6643.94
06.2	Power Element			103547.09	3.9%	4072.66	107619.75
06.2.1	Other (N/A)			0.00	0	0.00	0.00
06.2.2	Attitude Determination and Control			28.38	3.1%	0.87	29.25
06.2.3	Command & Data Handling			121.00	19.2%	23.26	144.26
06.2.4	Communications and Tracking			55.10	0.0%	0.00	55.10
06.2.5	Electrical Power Subsystem			25956.95	12.9%	3358.77	29315.72
06.2.6	Thermal Control (Non-Propellant)			515.46	18.0%	92.78	608.25
06.2.7	Propulsion (Chemical Hardware)			995.55	2.8%	28.30	1023.85
06.2.8	Propellant (Chemical)			7679.52	0.0%	0.00	7679.52
06.2.9	Propulsion (EP Hardware)			1708.60	0.1%	1.54	1710.15
06.2.10	Propellant (EP)			63335.77	0.0%	0.00	63335.77
06.2.11	Structures and Mechanisms			3150.75	18.0%	567.14	3717.89

3.2.2.1.2. Mars NEP Architecture Details

Table 3-15 gathers the top-level architecture details of the Mars NEP. The Hab/EP and the NEP power element launched on SLS Block II and had to fit within the performance minus the performance reserve.

Table 3-15 Conjunction Stack Architecture

Architecture details Launch 1 Hab Module (ELV performance)		Architecture details Launch 2 NEP (Power) Module (ELV performance)	
Launch vehicle	SLS Block II	Launch vehicle	SLS Block II
V _∞	n/a	V _∞	n/a
Energy, C ₃	n/a	Energy, C ₃	n/a
ELV performance (pre-margin).....	123000 kg	ELV performance (pre-margin).....	123000 kg
ELV Margin (%).....	6%	ELV Margin (%).....	6%
ELV performance (post-margin)	116112 kg	ELV performance (post-margin)	116112 kg
ELV custom adaptor, C22 (stays with ELV)	2706 kg	ELV custom adaptor, C22 (stays with ELV)	2706 kg
ELV performance (post-adaptor)	113406 kg	ELV performance (post-adaptor)	113406 kg
ELV spacecraft total wet mass	113303	ELV spacecraft total wet mass	113307
Available ELV margin	103 kg	Available ELV margin	99 kg
Available ELV margin (%).....	0%	Available ELV margin (%).....	0%

3.2.2.1.3. Spacecraft Total Mass Summary

The MEL shown in Table 3.3 captures the bottoms-up estimation of CBE and growth percentage of the Mars NEP Hab/EP element and the power element that the subsystem designers calculated for each line subsystem. To meet the total required mass growth of 30%, an allocation is necessary for growth on basic dry mass at the system level in addition to the growth calculated on each individual subsystem. This additional system-level mass is counted as part of the inert mass to be flown along the required trajectory. Therefore, the additional system-level growth mass impacts the total propellant required for the mission design.

The system-level summary for the baseline case, which includes the additional system-level growth, is shown in Table 3-16. With 4% growth on the basic dry mass of the Hab/EP element and 13% growth on the basic dry mass of the power element, the total mass with the 30% growth is 113303 kg for the Hab/EP element and 113307 kg for the power element. The inert mass and dry mass of the Mars NEP are also shown. After summarizing the bottoms-up masses from Table 3-16, an additional system-level growth was applied and shown in Table 3-17. To reach the 30% total MGA on basic dry mass required for this study, an additional system-level margin growth mass of 2425 kg on the Hab/EP element (additional 15%) and 5687 kg on the power element (additional 17%) was carried.

Table 3-16 Mars NEP Conjunction System Summary, Hab/EP Summary

COMPASS study: Mars Piloted NEP CD-2012-73				Study Date	3/26/2012
GLIDE container: Mars_NEP: Mars_NEP_1					
Spacecraft Master Equipment List Rack-up (Mass) - CD-2012-73					
WBS	Main Subsystems	Basic Mass (kg)	Growth (kg)	Total Mass (kg)	Aggregate Growth (%)
06	Piloted Mars NEP Spacecraft	211907.7	6590.5	218498	
06.1	Hab/EP Element	108360.6	2517.9	110878	2%
06.1.1	Habitat	52888.0	0.0	52888	0%
06.1.2	Attitude Determination and Control	91.8	2.8	95	3%
06.1.3	Command and Data Handling	46.8	10.0	57	21%
06.1.4	Communications and Tracking	0.0	0.0	0	TBD
06.1.5	Electrical Power Subsystem	41.0	6.1	47	15%
06.1.6	Thermal Control (Non-Propellant)	1740.3	313.3	2054	18%
06.1.7	Propulsion (Chemical Hardware)	961.5	33.3	995	3%
06.1.8	Propellant (Chemical)	7622.3		7622	0%
06.1.9	Propulsion EP Hardware)	7963.7	1139.0	9103	14%
06.1.10	Propellant (EP)	31374.7		31375	0%
06.1.11	Structures and Mechanisms	5630.5	1013.5	6644	18%
	Hab/EP consumables (for reference)	13200		13200	
	Estimated Spacecraft Dry Mass(no prop,consum)	56164	2518	58682	4%
	Estimated Spacecraft Wet Mass	108361	2518	110878	
System Level Growth Calculations_Hab/EP				Total Growth	
	Dry Mass Desired System Level Growth	16476	4943	21418	30%
	Additional Growth (carried at system level)		2425		15%
	Total Wet Mass with Growth	108361	4943	113303	

Table 3-17 Mars NEP Conjunction System Summary, Hab/EP Summary

06.2	Power Element	103547.1	4072.7	107620	4%
06.2.1	Other	0.0	0.0	0	TBD
06.2.2	Attitude Determination and Control	28.4	0.9	29	3%
06.2.3	Command and Data Handling	121.0	23.3	144	19%
06.2.4	Communications and Tracking	55.1	0.0	55	0%
06.2.5	Electrical Power Subsystem	25957.0	3358.8	29316	13%
06.2.6	Thermal Control (Non-Propellant)	515.5	92.8	608	18%
06.2.7	Propulsion (Chemical Hardware)	995.5	28.3	1024	3%
06.2.8	Propellant (Chemical)	7679.5		7680	0%
06.2.9	Propulsion EP Hardware)	1708.6	1.5	1710	0%
06.2.10	Propellant (EP)	63335.8		63336	0%
06.2.11	Structures and Mechanisms	3150.8	567.1	3718	18%
	Launch 2 Pwr Element consumables (for reference)	0.0		0	
	Estimated Spacecraft Dry Mass	32532	4073	36604	13%
	Estimated Spacecraft Wet Mass	103547	4073	107620	
System Level Growth Calculations _ Launch 2 Pwr Element					Total Growth
	Dry Mass Desired System Level Growth	32532	9760	42291	30%
	Additional Growth (carried at system level)		5687		17%
	Total Wet Mass with Growth	103547	9760	113307	

3.2.2.1.4. Power Equipment List (PEL)

To model the power systems in this Mars NEP design study, 10 modes of operation were defined for the mission. These modes were defined based on the mission profile and they identify which items and subsystems of the Mars NEP are operating, and which items are dormant and require no power, at any time throughout the mission. The definitions of these modes are shown in Table 3-18

Table 3-18 Definition of the Power Modes—Mars NEP

Mode	Title	Description
Power mode 1	Pre-Launch	On the launch pad, 5 mins
Power mode 2	Launch	SLS launch for both DSH and NEP, 15 mins
Power mode 3	NEP activation and checkout	42 days
Power mode 4	Orion rendezvous with NEP/DSH	2 days
Power mode 5	LEO spiral departure	354 days
Power mode 6	Interplanetary thrusting	It includes both inbound and outbound, 314 days
Power mode 7	Interplanetary coast	It included both inbound and outbound, 154 days
Power mode 8	Mars spiral departure	21 days
Power mode 9	Sciences mission on Mars	400 days
Power mode 10	Post mission	14 days

Table 3-19 shows the assumptions about the power requirements in all the modes of operation. The power requirements from the bottoms-up analysis on the Mars NEP listed in Table 3-20 are used by the power system designers (described in Section 4.5) to size the power system components. The waste heat is also listed under each power mode and used to design the thermal system. The highest waste heat load is 50,124 W occurring during Power mode 5

Table 3-19 PEL/TWH Mars NEP Conjunction, Launch 1 – Hab/EP Element

4/19/2012 6:00 PM	Power Mode 1	Power Mode 2	Power Mode 3	Power Mode 4	Power Mode 5	Power Mode 6	Power Mode 7	Power Mode 8	Power Mode 9	Power Mode 10
Power Mode Title	(W)	(W)	(W)	(W)	(W)	(W)	(W)	(W)	(W)	(W)
System operating Duty Cycle	5 minutes	15 minutes	42 days	2 days	354 Days	314 Days	154 Days	21 Days	400 days	14 days
Launch 1 Hab/EP Element	619	1,120	5,945	15,897	2,505,672	2,515,672	15,897	2,515,672	5,632	5,105
Habitat	0	0	5000	15,000	5000	15,000	15,000	15,000	5000	5000
Attitude Determination and Control	0	110.36	110.36	62.36	62.36	62.36	62.36	62.36	62.36	0
Command & Data Handling	46	37	37	37	37	37	37	37	37	37
Communications and Tracking	0	0	0	0	0	0	0	0	0	0
Electrical Power Subsystem	0	0	0	0	0	0	0	0	0	0
Thermal Control (Non-Propellant)	68.00	68.00	68.00	68.00	68.00	68.00	68.00	68.00	68.00	68.00
Propulsion (Chemical Hardware)	30	430	30	30	30	30	30	30	30	0
Propellant (Chemical)	0	0	0	0	0	0	0	0	0	0
Propulsion (EP Hardware)	475	475	700	700	2,500,475	2,500,475	700	2,500,475	435	0
Propellant (Aux)	0	0	0	0	0	0	0	0	0	0
Structures and Mechanisms	0	0	0	0	0	0	0	0	0	0

Table 3-20 PEL/TWH Mars NEP Conjunction, Launch 2 – Power Element

4/19/2012 6:00 PM	Power Mode 1	Power Mode 2	Power Mode 3	Power Mode 4	Power Mode 5	Power Mode 6	Power Mode 7	Power Mode 8	Power Mode 9	Power Mode 10
Power Mode Title	(W)	(W)	(W)	(W)	(W)	(W)	(W)	(W)	(W)	(W)
System operating Duty Cycle	5 minutes	15 minutes	42 days	2 days	354 Days	314 Days	154 Days	21 Days	400 days	14 days
Launch 2 Power Element	1188.00	341.00	1181.00	581.00	523.00	83.00	83.00	83.00	83.00	49.00
Attitude Determination and Control	15	58	58	58	0	0	0	0	0	0
Command & Data Handling	63	53	53	53	53	53	53	53	53	49
Communications and Tracking	1080	0	1040	440	440	0	0	0	0	0
Electrical Power Subsystem	0	0	0	0	0	0	0	0	0	0
Thermal Control (Non-Propellant)	0.00	0.00	0.00	0.00	0.00	0.00	0.00	0.00	0.00	0.00
Propulsion (Chemical Hardware)	30	230	30	30	30	30	30	30	30	0
Propellant (Chemical)	0	0	0	0	0	0	0	0	0	0
Propulsion (EP Hardware)	0	0	0	0	0	0	0	0	0	0
Propellant (Aux)	0	0	0	0	0	0	0	0	0	0
Structures and Mechanisms	0	0	0	0	0	0	0	0	0	0
Total with EP	1,807	1,461	7,126	16,478	2,506,195	2,515,755	15,980	2,515,755	5,715	5154
+30% except EP	2,349	1,899	9,264	21,421	2,507,911	2,520,339	20,774	2,520,339	7,430	6,700
Waste heat*	727	1,461	1,086	1,038	50,124	50,315	980	50,315	715	154

3.2.2.2. Concept Drawing and Description

The piloted Mars NEP vehicle was split into two different elements to be launched on two different launches. The first launch, shown in Figure 3-36 thru Figure 3-38, was the Hab/EP element. This element fit within the given SLS Payload Shroud envelope of 9.14 meters in diameter with a barrel section length of 17.21 meters. For the power element launch, shown in Figure 3-39 thru Figure 3-41, the barrel section length for the SLS Payload Shroud needed to be increased from 17.21 meters to 25.0 meters to accommodate the required radiator area.

Deployable components on the Hab/EP element that are stowed at launch include the Hab solar arrays, EP bus radiators, and the panel containing the 10 EP thrusters. The EP thruster panel is deployed so that the panel is 9.5 degrees from the vehicle centerline, which in conjunction with the individual thruster gimbals allows thrusting through the vehicle's center of gravity (CG) during all phases of the mission. Deployable components on the power element that are stowed at launch include the radiators and the reactor boom. The reactor boom is a telescoping boom that ensures the reactor is at the required distance from the electronics contained on within the bus.

The remaining Figures in this section show multiple views of the stowed elements and the fully deployed and mated vehicle, and include overall dimensions and locations of the various radiators and other subsystem components. Details on all the subsystems contained on the vehicle can be found in the later sections of this documentation.

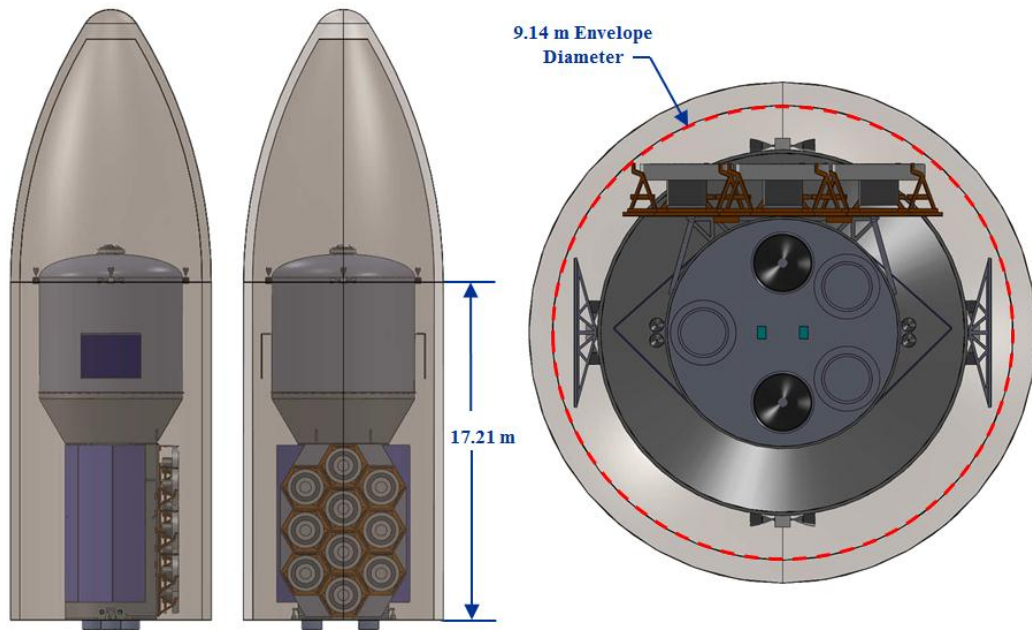


Figure 3-36 Hab/EP Element stowed inside the SLS Payload Shroud.

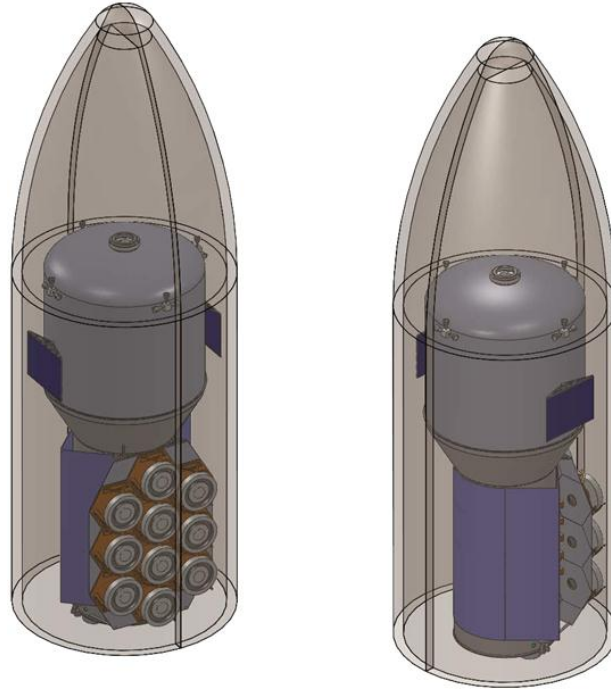


Figure 3-37 Isometric views of the Hab/EP element stowed within the SLS Payload Shroud.

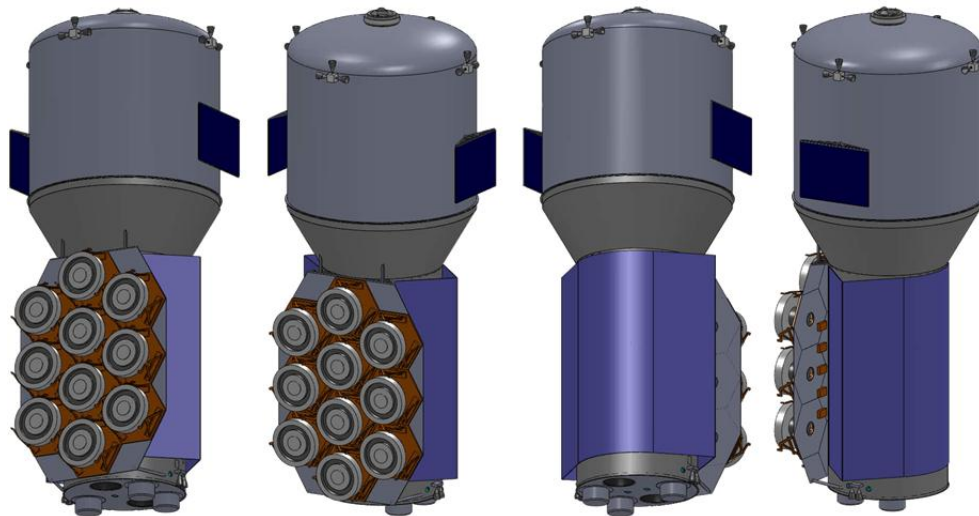


Figure 3-38 Various views of the Hab/EP element in its stowed configuration.

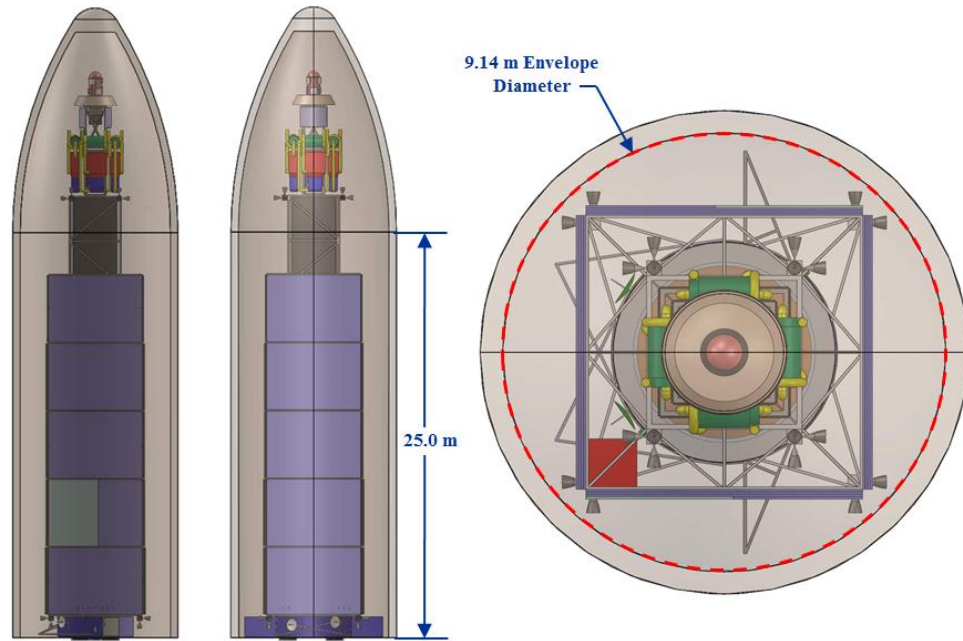


Figure 3-39 The power element stowed within the extended SLS Payload Shroud.

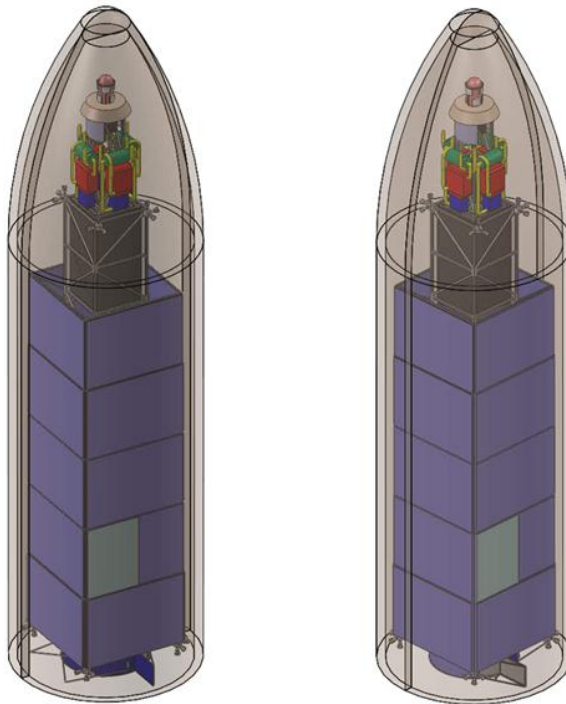


Figure 3-40 The power element stowed within the extended SLS Payload Shroud.

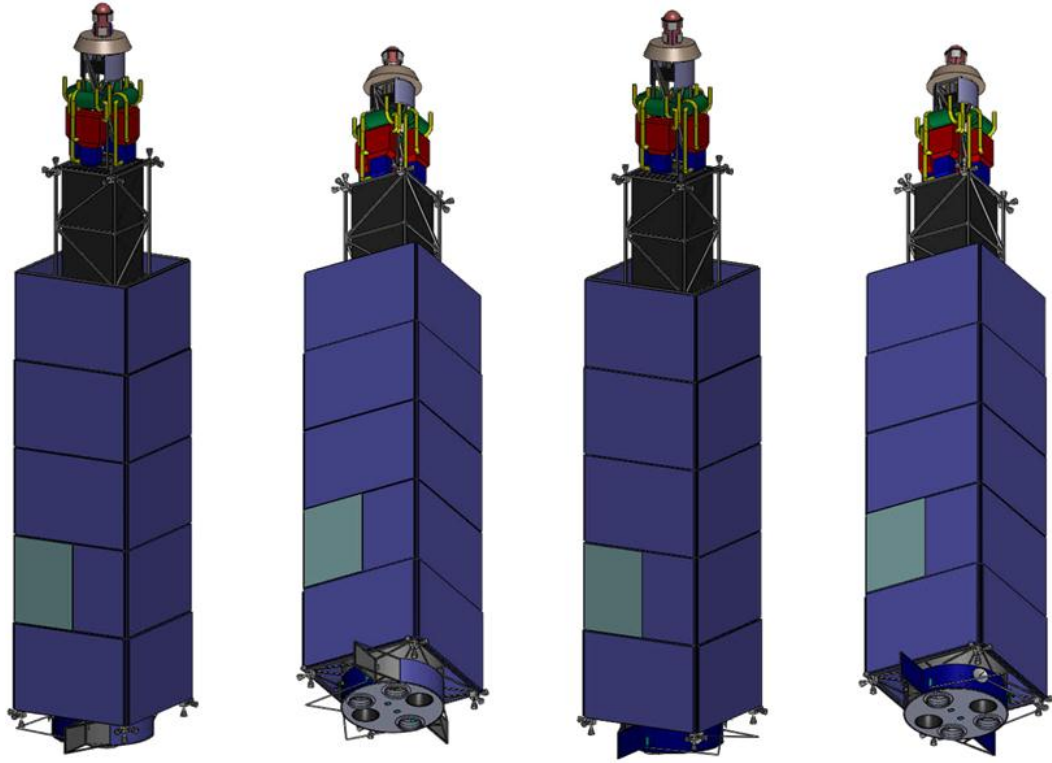


Figure 3-41 Various views of the power element in its stowed configuration.

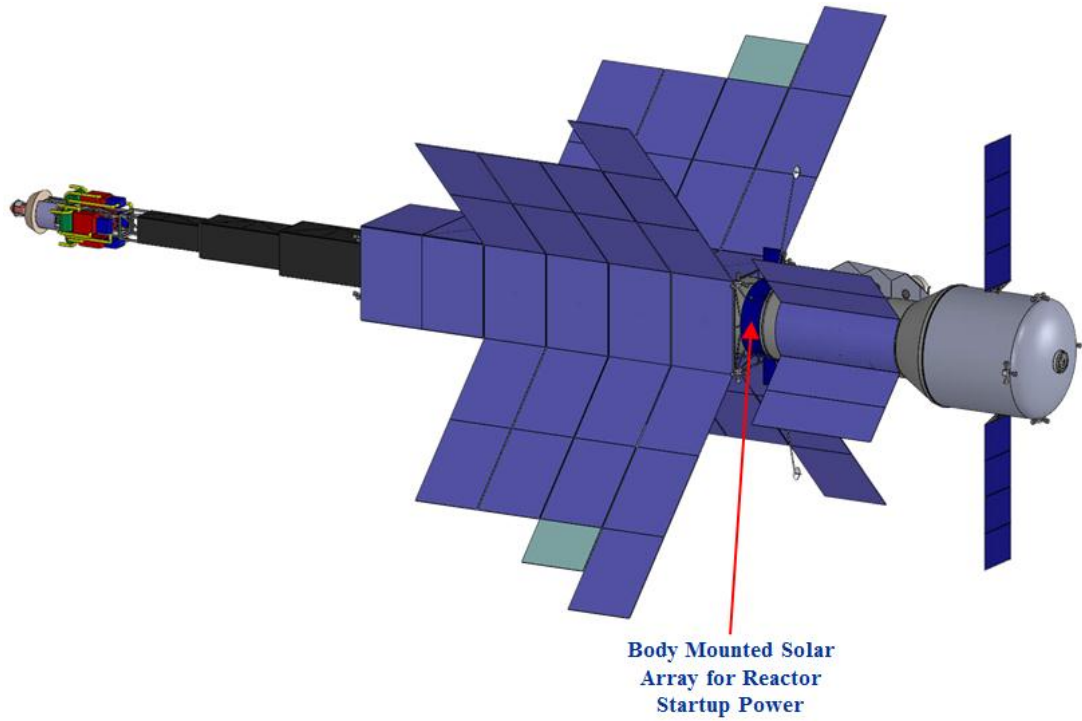


Figure 3-42 Fully deployed Piloted Mars NEP Vehicle.

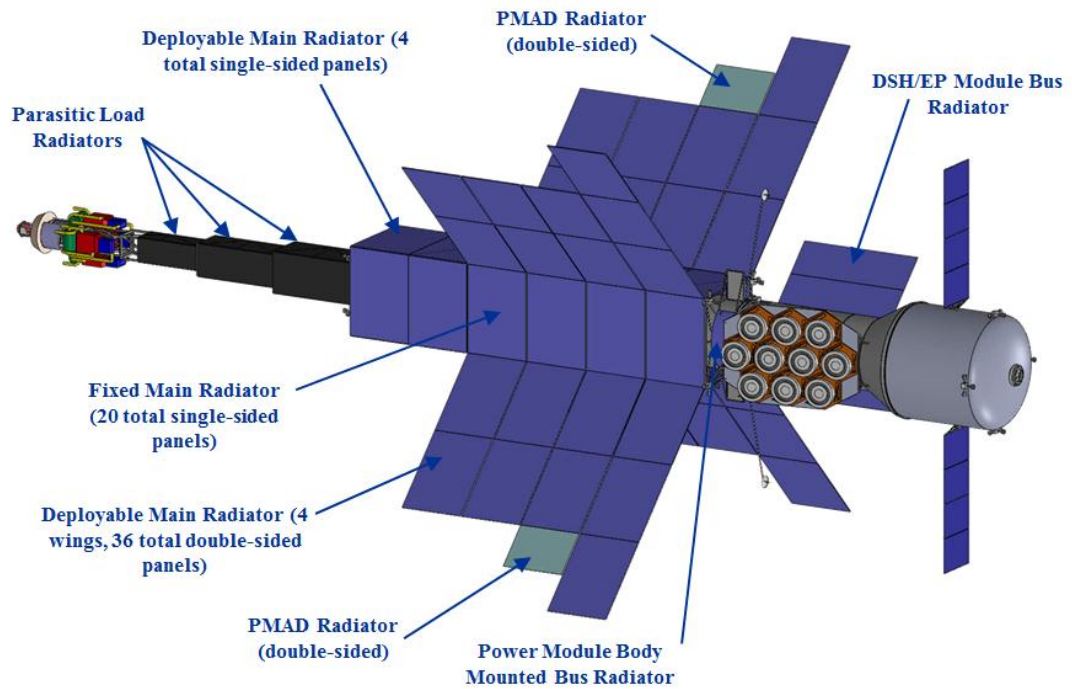


Figure 3-43 Piloted Mars NEP Vehicle radiator types and locations.

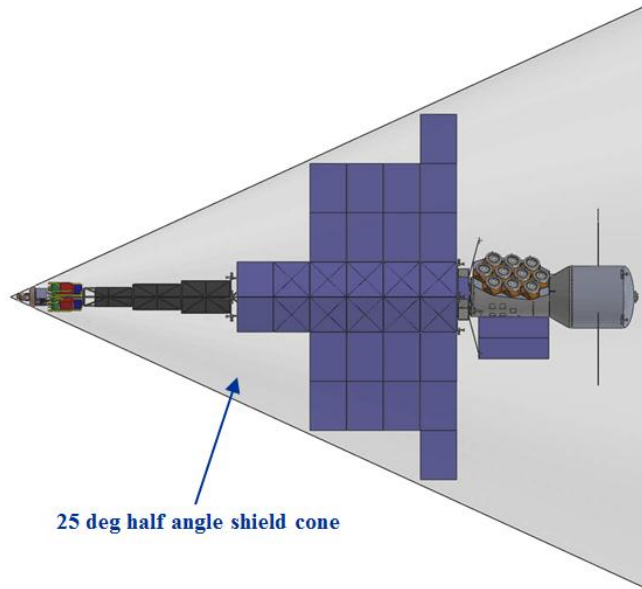


Figure 3-44 Reactor shield cone.

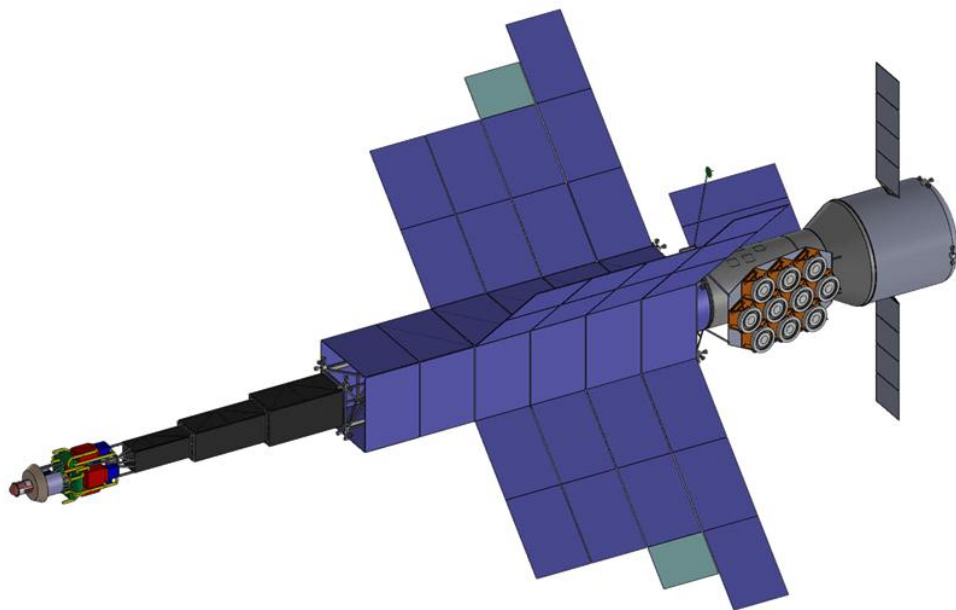


Figure 3-45 Isometric view of the fully deployed Piloted Mars NEP Vehicle.

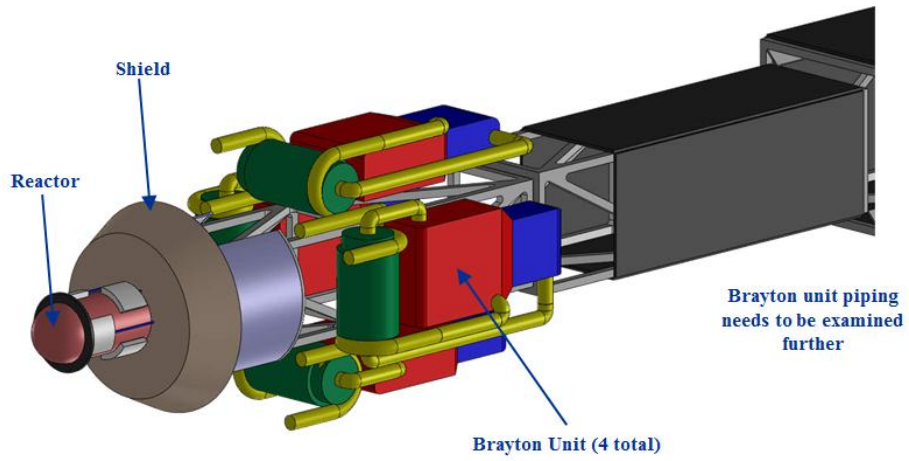


Figure 3-46 Reactor end of the Piloted Mars NEP Vehicle.

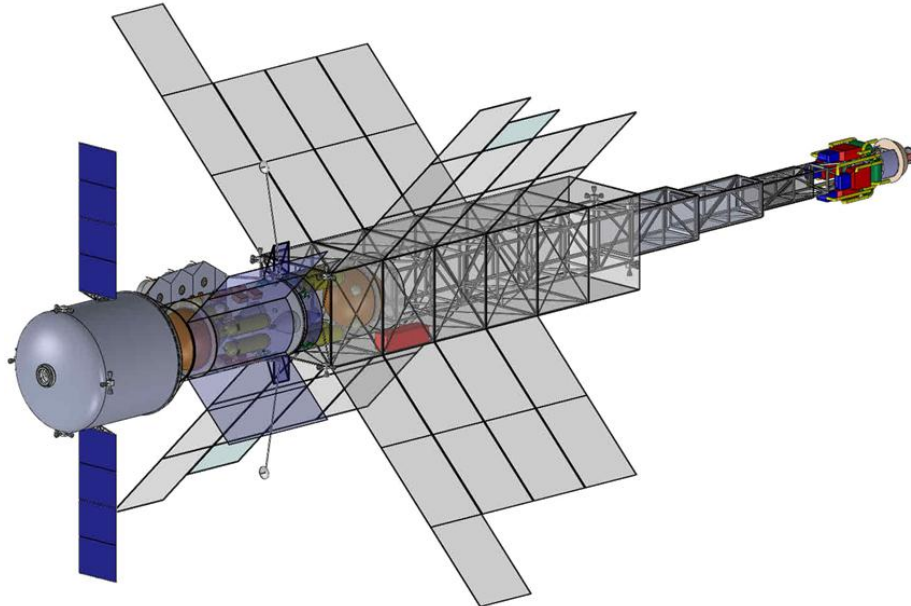


Figure 3-47 Transparent view of the Piloted Mars NEP Vehicle.

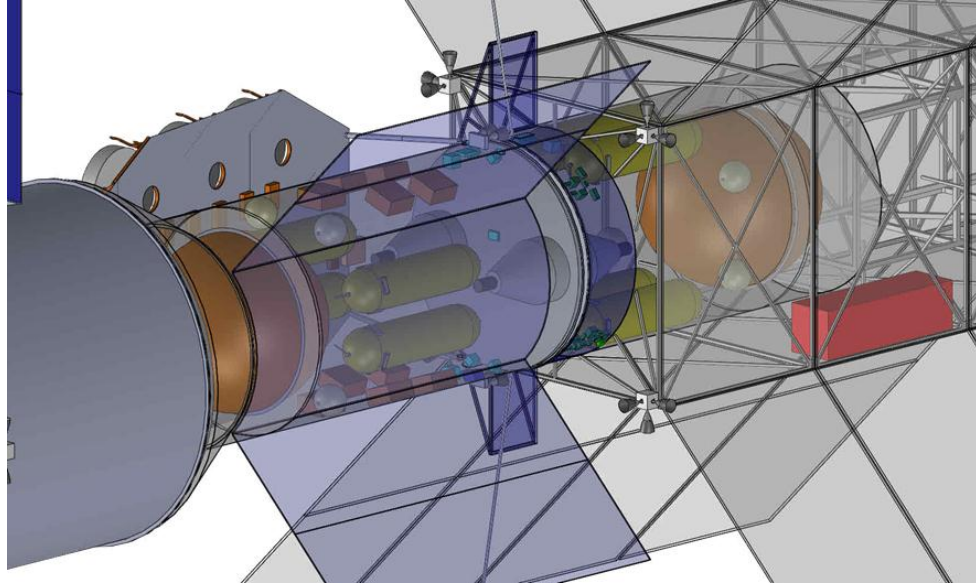


Figure 3-48 Transparent view of the Piloted Mars NEP Vehicle bus.

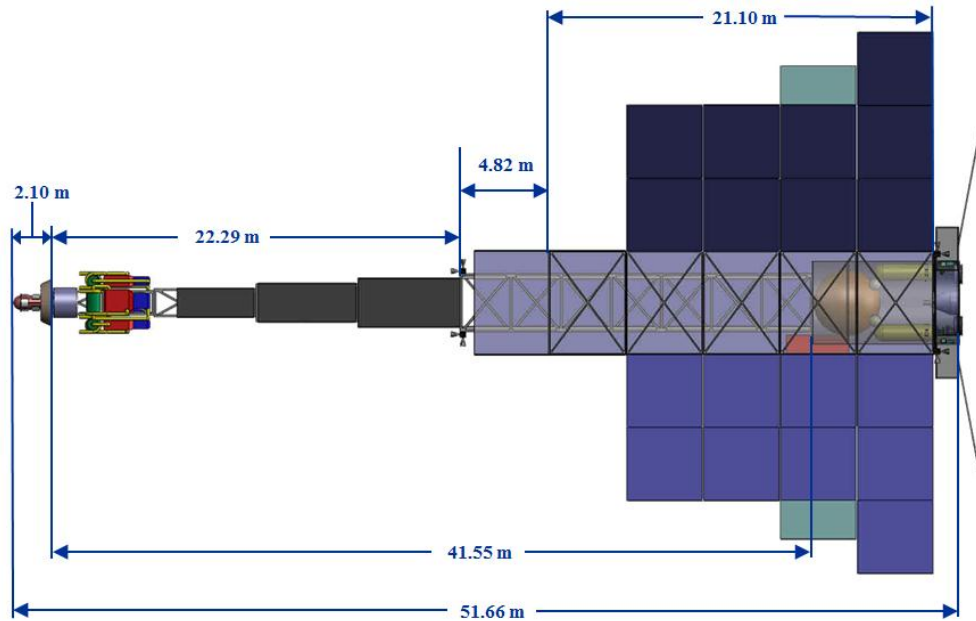


Figure 3-49 Overall dimensions of the fully deployed power element.

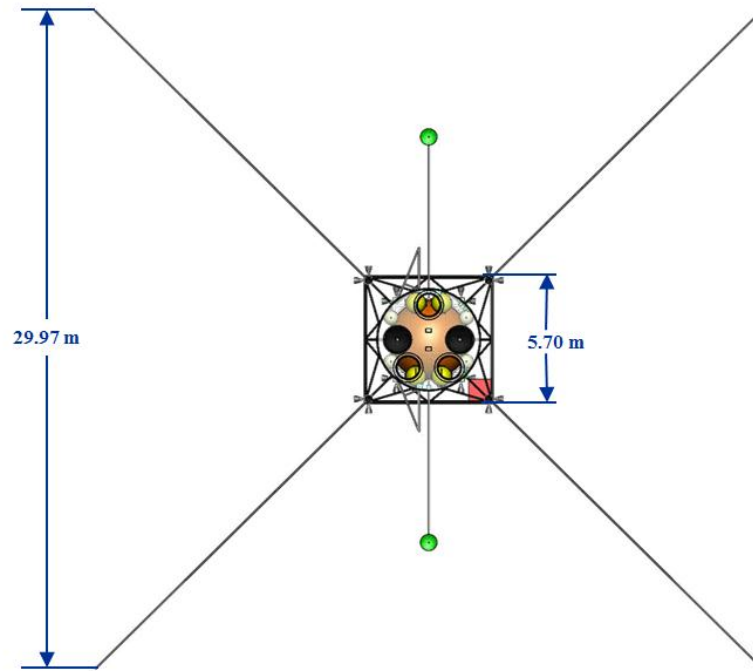


Figure 3-50 Additional dimensions of the fully deployed power element.

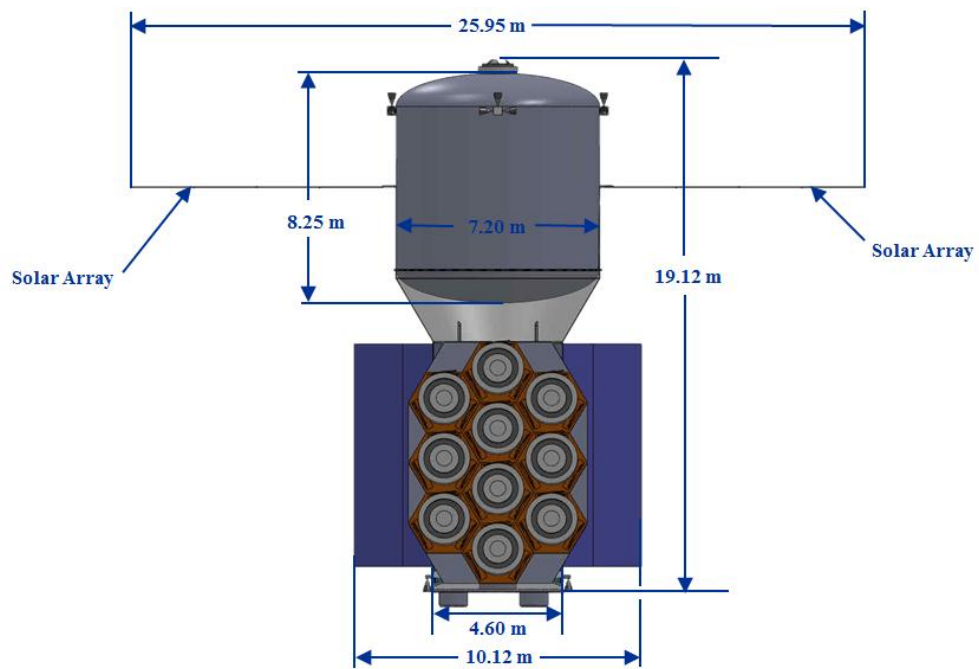


Figure 3-51 Dimensions of the fully deployed Hab/EP element.

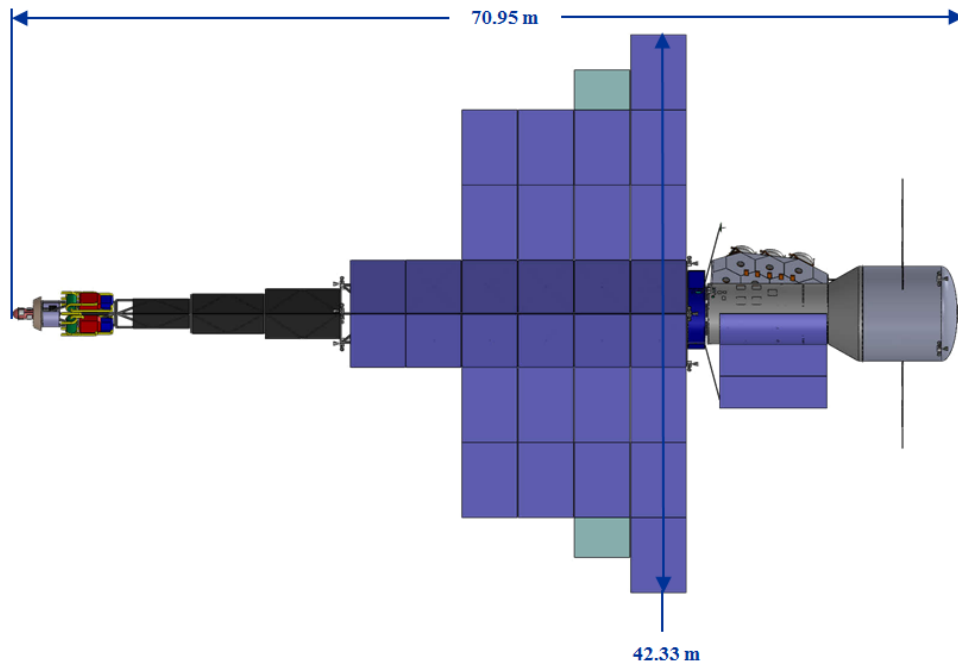


Figure 3-52 Basic dimensions of the fully deployed Piloted Mars NEP Vehicle.

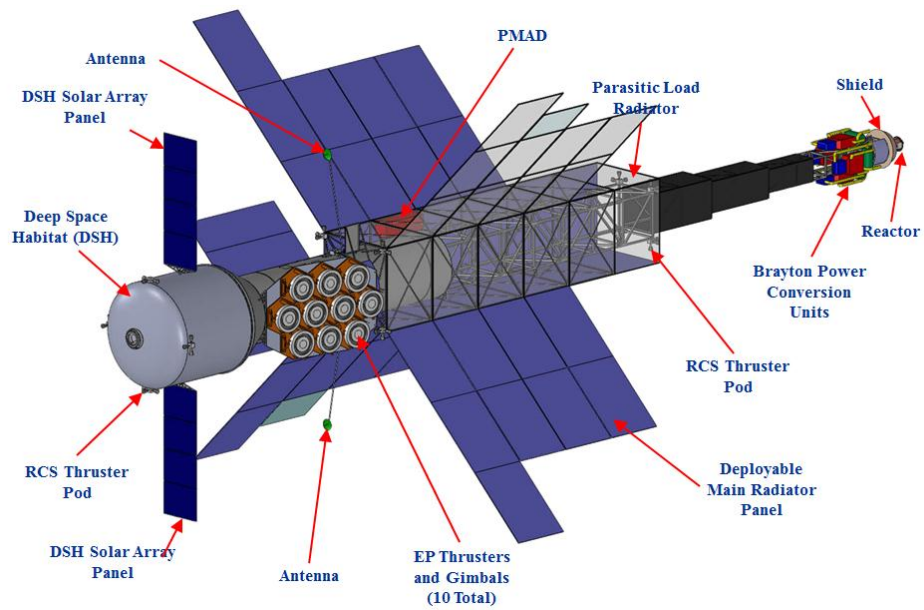


Figure 3-53 Major external components of the full Piloted Mars NEP Vehicle.

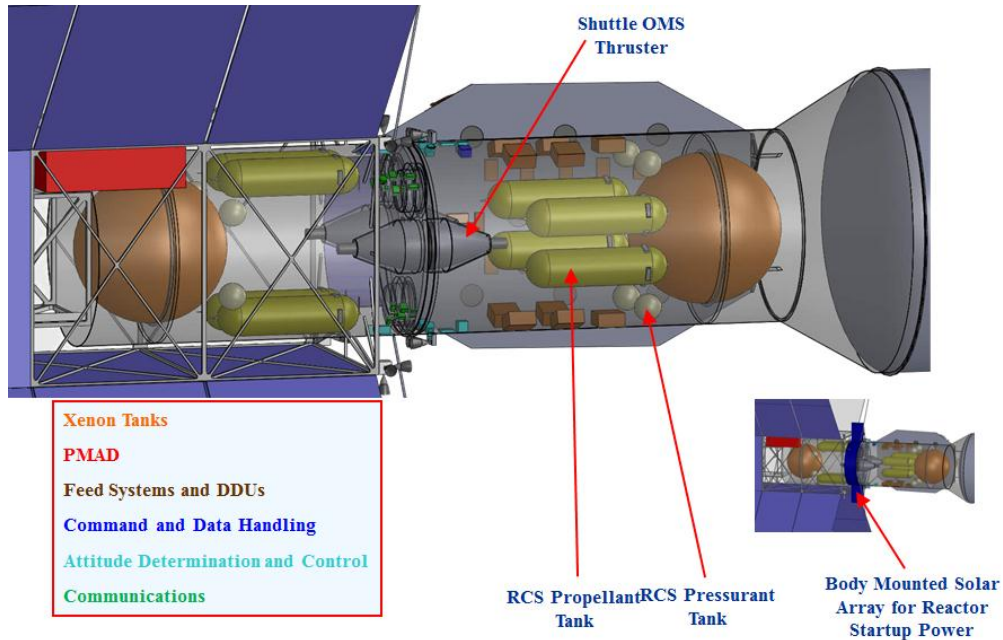


Figure 3-54 Major internal bus components of the full Piloted Mars NEP Vehicle.

3.2.3. NEP Subsystem Breakdown

3.2.3.1. Habitat Elements

The Mars Transit Habitat provides habitation for crew member for long-duration transits to Mars or Mars moons. The Mars NEP study sized the MTH for a crew of 6 on a 1000-day Mars mission. The habitat has connection adapters to dock with the SEV, MPCV, MSH, and the propulsion unit(s). An internal bulkhead 2 m from the aft dome with airlock services act as a contingent airlock. For this study, the MTH was treated as a fixed mass for sizing purposes. The MTH fixed mass is allocated into Core Hab Mass (includes ECLSS) and Outfitted mass, which represents the items specifically needed for the crew during transit and a 1000-day Mars mission stay duration.



Figure 3-55 Mars Transit Habitat.

Table 3-21 Mars NEP MTH Mass Breakdown

Category	Mass, kg	
Structure	6,332	Core Hab Mass 34,842
Protection	431	
Propulsion	0	
Power	2,212	
Control	0	
Avionics	453	
Environ./Active Therm	15,549	
ECLSS	10,715	
Air Subsystem	1,416	
Water Subsystem	6,130	
Food (storage)	2,144	
Human Accommodations	90	
Other	935	
EVA systems	253	
Thermal Control System	1,324	
Crew Accommodations	3,257	
Growth	7,810	
DRY MASS SUBTOTAL	32,787	
Cargo - Radiation Protection (waterwall)	2,055	Outfitted Mass 18,045
Non-cargo	15,876	
Galley & Food System	8,857	
Clothing	236	
Miscellaneous Provisions	1,980	
EVA	0	
Recreational Equipment	150	
Crew Health Care	250	
Waste Collection and Personal Hygiene	1,459	
Housekeeping Supplies	476	
Operational Supplies	273	
Maintenance Equip. & Spares	2,021	
Photography Supplies	120	
Sleep Accommodations	54	
INERT MASS SUBTOTAL	50,718	
Contingency ECLSS Consumables+Tanks	1,688	
Nominal ECLSS Consumable Fluids	481	
TOTAL WET MASS	52,887	Total 52,887

3.2.3.1.1. Habitat Design and MEL

Table 3-22 Mars NEP Habitat System, Case 1 Conjunction, Hab/EP Element

WBS	Description	QTY	Unit Mass	Basic Mass	Growth	Growth	Total Mass
Number	Case 1 Piloted Mars NEP Spacecraft CD-2012-73		(kg)	(kg)	(%)	(kg)	(kg)
06	Piloted Mars NEP Spacecraft			211907.69	3.1%	6590.54	218498.23
06.1	Hab/EP Element			108360.60	2.3%	2517.89	110878.49
06.1.1	Habitat			52888.00	0.0%	0.00	52888.00
06.1.1.a	Crew Accommodations			18046.00	0.0%	0.00	18046.00
06.1.1.a.a	Initial Accommodations	1	4846.00	4846.00	0.0%	0.00	4846.00
06.1.1.a.b	Consumables	1	13200.0	13200.00	0.0%	0.00	13200.00
06.1.1.b	Core Habitat			34842.00	0.0%	0.00	34842.00
06.1.1.b.a	Core Habitat	1	34842.0	34842.00	0.0%	0.00	34842.00
06.1.1.b.b	Solar Array (mass in core hab)	0	0.0	0.00	0.0%	0.00	0.00

3.2.3.2. Communications

The main communications function will be provided by the Habitat Module communication system. However, the backup communication system is at X-band and will utilize X-band 34 meter DSN sites, will be double sting redundant with two-way communication at 10 kbps minimum. A secondary backup communication system will be at S-band and use S-band 34 meter DSN sites, bill be double string redundant with two-way communication at 10 bps minimum. S-band safing mode will use omni-antennas. Both dual X-band and S-band antennas will be gimbaled.

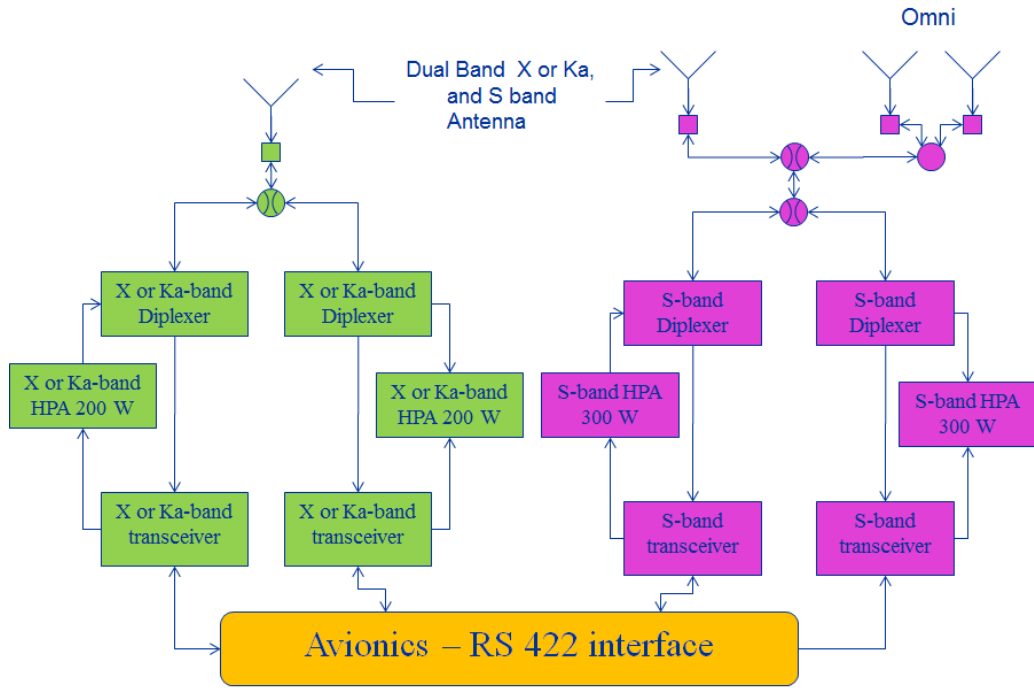


Figure 3-56 Communications system schematic.

Mars Design Reference Architecture 5.0 – Addendum #2



Figure 3-57 X-band link budget.

Mars Design Reference Architecture 5.0 – Addendum #2



Figure 3-58 S-band link budget.

3.2.3.2.1. Communications Design and MEL

Table 3-23 Mars NEP Communications Case 1 Conjunction MEL, Power Element

WBS	Description	QTY	Unit Mass	Basic Mass	Growth	Growth	Total Mass
Number	Case 1 Piloted Mars NEP Spacecraft CD-2012-73		(kg)	(kg)	(%)	(kg)	(kg)
06	Piloted Mars NEP Spacecraft			211907.69	3.1%	6590.54	218498.23
06.1	Hab/EP Element			108360.60	2.3%	2517.89	110878.49
06.2	Power Element			103547.09	3.9%	4072.66	107619.75
06.2.1	Other (N/A)			0.00	0	0.00	0.00
06.2.2	Attitude Determination and Control			28.38	3.1%	0.87	29.25
06.2.3	Command & Data Handling			121.00	19.2%	23.26	144.26
06.2.4	Communications and Tracking			55.10	0.0%	0.00	55.10
06.2.4.a	X band Communications System			26.70	0.0%	0.00	26.70
06.2.4.a.a	X Band Transceiver (200 W)	2	2.80	5.60	0.0%	0.00	5.60
06.2.4.a.b	X Band Coax Switch	1	0.40	0.40	0.0%	0.00	0.40
06.2.4.a.c	X Band Coax Cables	1	3.00	3.00	0.0%	0.00	3.00
06.2.4.a.d	X-Band Diplexer	2	1.00	2.00	0.0%	0.00	2.00
06.2.4.a.e	X-band HPA	2	3.10	6.20	0.0%	0.00	6.20
06.2.4.a.f	X-band Switch Box	0	0.00	0.00	0.0%	0.00	0.00
06.2.4.a.g	X Band Antenna, 0.75m	1	2.00	2.00	0.0%	0.00	2.00
06.2.4.a.h	Gimbal for X Band Antenna	1	6.00	6.00	0.0%	0.00	6.00
06.2.4.a.i	Feed	1	1.50	1.50	0.0%	0.00	1.50
06.2.4.b	S Band Communications System			28.40	0.0%	0.00	28.40
06.2.4.b.a	S Band Tranceiver (20 W)	2	2.80	5.60	0.0%	0.00	5.60
06.2.4.b.b	S Band Diplexer	2	0.70	1.40	0.0%	0.00	1.40
06.2.4.b.c	S Band HPA	2	3.10	6.20	0.0%	0.00	6.20
06.2.4.b.d	MGA S Band Antenna	1	2.00	2.00	0.0%	0.00	2.00
06.2.4.b.e	S Band Switches	3	0.40	1.20	0.0%	0.00	1.20
06.2.4.b.f	S Band Switch Box	1	1.00	1.00	0.0%	0.00	1.00
06.2.4.b.g	Gimbal for S Band Antenna	1	6.00	6.00	0.0%	0.00	6.00
06.2.4.b.h	S Band Cables	1	3.00	3.00	0.0%	0.00	3.00
06.2.4.b.i	Feed	1	1.00	1.00	0.0%	0.00	1.00
06.2.4.b.j	S Band Omni Antennas	2	0.50	1.00	0.0%	0.00	1.00

3.2.3.3. Command and Data Handling (C&DH)

3.2.3.3.1. C&DH Design and MEL

The C&DH system consists of PowerPC-class processor boards configured to provide for single fault tolerance. Each processor board includes an embedded PowerPC-class main processor capable of supporting C&DH functions, a 5-plus GB solid-state memory card, as well as communications and payload interface cards. The primary processor is capable of autonomous failover to a redundant cold spare unit if a fault is detected.

Flight computers will use a real-time operating system such as VxWorks or Green Hills Integrity. To support all mission phases, the number of source lines of code (SLOC) has been estimated. However, this estimate and implied development cost should be tempered with the understanding that recent developments in autocode technologies that generate known good instruction loads will become a design standard.

The following list is comprised of the main avionics components and their quantities, as input to the MEL shown in Table 3-24:

- Main computers (one main computer and one redundant cold spare)
- Data acquisition units contain redundant paths
- Solid-state memory
- Instrumentation (Lander)
 - Maximum of 48 sensors, mass of 6 ounces each, power requirement of 50 mW each

- Sensor estimate based on a preliminary assumption of number of channels for input and output

Note: As shown in the MEL, there are two 48-channel analog-to-digital and digital-to-analog serial digital interface (SDI) cards and one 48-channel serial data output (SDO) card in the lander, giving 144 channels of input/output, not including any serial bus input/output, all used to estimate worst-case mass and power.

- Lander cabling (per Monte Carlo simulation):
- Instrumentation nominal approximately xx m (one-half the length of the vehicle) per sensor run
- C&DH estimate: approximately 100 m total, 20-24 American Wire Gauge (AWG) Tefzel (not for high currents)

Table 3-24 Mars NEP C&DH Case 1 Conjunction MEL, Hab/EP Element

WBS	Description	QTY	Unit Mass	Basic Mass	Growth	Growth	Total Mass
Number	Case 1 Piloted Mars NEP Spacecraft CD-2012-73		(kg)	(kg)	(%)	(kg)	(kg)
06	Piloted Mars NEP Spacecraft			211907.69	3.1%	6590.54	218498.23
06.1	Hab/EP Element			108360.60	2.3%	2517.89	110878.49
06.1.1	Habitat			52888.00	0.0%	0.00	52888.00
06.1.2	Attitude Determination and Control			91.84	3.0%	2.76	94.60
06.1.3	Command & Data Handling			46.80	21.4%	10.00	56.80
06.1.3.a	C&DH Hardware			28.30	21.0%	5.95	34.25
06.1.3.a.a	FPGA IP CPU rad hard LEON3 - Main	4	2.00	8.00	30.0%	2.40	10.40
06.1.3.a.b	Watchdog switcher	1	1.00	1.00	30.0%	0.30	1.30
06.1.3.a.c	Mass Memory Module	1	2.00	2.00	0.0%	0.00	2.00
06.1.3.a.d	Command and Control Harness (data)	1	10.00	10.00	15.0%	1.50	11.50
06.1.3.a.e	cPCI enclosure with power supply	1	4.00	4.00	20.0%	0.80	4.80
06.1.3.a.f	Ultra-Oscillator /Atomic Clock Module	1	0.30	0.30	15.0%	0.05	0.35
06.1.3.a.i	SLOCS -- Main	900000	0.00	0.00	0.0%	0.00	0.00
06.1.3.a.l	FPGA IP CPU rad hard LEON3 - RIU	2	1.50	3.00	30.0%	0.90	3.90
06.1.3.a.m	SLOCS - RIU	100000	0.00	0.00	0.0%	0.00	0.00
06.1.3.b	Instrumentation & Wiring			18.50	21.9%	4.05	22.55
06.1.3.b.a	Sensor Card	2	1.40	2.80	30.0%	0.84	3.64
06.1.3.b.b	Data Cabling	1	10.00	10.00	15.0%	1.50	11.50
06.1.3.b.c	Driver Card	2	1.35	2.70	30.0%	0.81	3.51
06.1.3.b.d	Pressure and Temperature Sensors	60	0.05	3.00	30.0%	0.90	3.90

Table 3-25 Mars NEP C&DH Case 1 Conjunction MEL, Power Element

WBS	Description	QTY	Unit Mass	Basic Mass	Growth	Growth	Total Mass
Number	Case 1 Piloted Mars NEP Spacecraft CD-2012-73		(kg)	(kg)	(%)	(kg)	(kg)
06	Piloted Mars NEP Spacecraft			211907.69	3.1%	6590.54	218498.23
06.1	Hab/EP Element			108360.60	2.3%	2517.89	110878.49
06.2	Power Element			103547.09	3.9%	4072.66	107619.75
06.2.1	Other (N/A)			0.00	0	0.00	0.00
06.2.2	Attitude Determination and Control			28.38	3.1%	0.87	29.25
06.2.3	Command & Data Handling			121.00	19.2%	23.26	144.26
06.2.3.a	C&DH Hardware			31.30	20.0%	6.25	37.55
06.2.3.a.a	FPGA IP CPU rad hard LEON3 - Main	4	2.00	8.00	30.0%	2.40	10.40
06.2.3.a.b	Watchdog switcher	1	1.00	1.00	30.0%	0.30	1.30
06.2.3.a.c	Mass Memory Module	1	2.00	2.00	0.0%	0.00	2.00
06.2.3.a.d	Command and Control Harness (data)	1	10.00	10.00	15.0%	1.50	11.50
06.2.3.a.e	cPCI enclosure with power supply	1	10.00	10.00	20.0%	2.00	12.00
06.2.3.a.f	Ultra-Oscillator /Atomic Clock Module	1	0.30	0.30	15.0%	0.05	0.35
06.2.3.a.m	SLOCS	900000	0.00	0.00	0.0%	0.00	0.00
06.2.3.b	Instrumentation & Wiring			89.70	19.0%	17.01	106.71
06.2.3.b.a	Sensor Card	4	1.40	5.60	30.0%	1.68	7.28
06.2.3.b.b	Data Cabling	1	66.00	66.00	15.0%	9.90	75.90
06.2.3.b.c	Driver Card	6	1.35	8.10	30.0%	2.43	10.53
06.2.3.b.d	Pressure and Temperature Sensors	100	0.10	10.00	30.0%	3.00	13.00

3.2.3.4. Guidance, Navigation and Control (GN&C)

3.2.3.4.1. GN&C Design and MEL

The following assumptions were made during the design of the GN&C subsystem:

- Hab/EP element performs the AR&D with the Power element
 - Power element is passive in LEO during AR&D
- MPCV is the active element when docking with the Hab/EP elements at Gateway
- Updated navigation states and commanded thrust direction are obtained from the ground at ~1 week intervals
- The designs of both the Hab/EP and Power elements were based heavily on Orion hardware and are as follows:
- Hab/EP Element
 - Eight Sun sensors for coarse attitude determination
 - Two Orion IMUs
 - Three single axis rate gyros to measure vehicle body rates
 - Three single axis accelerometers to measure vehicle body accelerations
 - Four Orion Star Trackers
 - Two data processing units each with 2 optical heads
 - Two Orion vision navigation sensors
 - Generate range, bearing and attitude measurements during AR&D via directed returns from target retro-reflectors
- Power Element
 - Two Orion IMUs
 - Four Orion Star trackers
 - Two GPS receivers
 - Used for navigation updates before docking with the Hab/EP element as well as aiding in yaw attitude determination
 - Two Retro-reflectors
 - Used by the vision navigation sensors on the Hab/EP element during AR&D

The mass breakdown for each element can be seen in Table 3-26 and Table 3-27

Table 3-26 Mars NEP GN&C Case 1 Conjunction MEL, Hab/EP Element

WBS	Description	QTY	Unit Mass	Basic Mass	Growth	Growth	Total Mass
Number	Case 1 Piloted Mars NEP Spacecraft CD-2012-73		(kg)	(kg)	(%)	(kg)	(kg)
06	Piloted Mars NEP Spacecraft			211907.69	3.1%	6590.54	218498.23
06.1	Hab/EP Element			108360.60	2.3%	2517.89	110878.49
06.1.1	Habitat			52888.00	0.0%	0.00	52888.00
06.1.2	Attitude Determination and Control			91.84	3.0%	2.76	94.60
06.1.2.a	Guidance, Navigation, & Control			91.84	3.0%	2.76	94.60
06.1.2.a.a	Inertial Measurement Units	2	9.64	19.28	3.0%	0.58	19.86
06.1.2.a.b	Sun Sensors	8	0.06	0.48	3.0%	0.01	0.49
06.1.2.a.c	Star Tracker Optical Head	4	0.98	3.92	3.0%	0.12	4.04
06.1.2.a.d	Star Tracker Electronics Unit	2	9.80	19.60	3.0%	0.59	20.19
06.1.2.a.e	Vision Navigation Sensor	2	24.28	48.56	3.0%	1.46	50.02

Table 3-27 Mars NEP GN&C Case 1 Conjunction MEL, Power Element

WBS	Description	QTY	Unit Mass	Basic Mass	Growth	Growth	Total Mass
Number	Case 1 Piloted Mars NEP Spacecraft CD-2012-73		(kg)	(kg)	(%)	(kg)	(kg)
06	Piloted Mars NEP Spacecraft			211907.69	3.1%	6590.54	218498.23
06.1	Hab/EP Element			108360.60	2.3%	2517.89	110878.49
06.2	Power Element			103547.09	3.9%	4072.66	107619.75
06.2.1	Other (N/A)			0.00	0	0.00	0.00
06.2.2	Attitude Determination and Control			28.38	3.1%	0.87	29.25
06.2.2.a	Guidance, Navigation, & Control			28.38	3.1%	0.87	29.25
06.2.2.a.a	Inertial Measurement Units	2	9.64	19.28	3.0%	0.58	19.86
06.2.2.a.b	Lidar Reflectors	2	0.05	0.10	20.0%	0.02	0.12
06.2.2.a.c	GPS Receiver	2	1.00	2.00	3.0%	0.06	2.06
06.2.2.a.d	Misc#3	0	0.00	0.00	0.0%	0.00	0.00
06.2.2.a.e	Horizon Sensor	2	3.50	7.00	3.0%	0.21	7.21

Estimates of the location of the CG were made for various points throughout the mission to get an estimate on the required gimbal angle of the thrusters to thrust through the CG. With the origin defined as the interface point between the power element and Hab/EP element, the estimates of the CG location were as follows:

- In LEO, after docking the two elements
 - CG is located approximately 1.3 m toward the reactor side
 - Requires a gimbal angle of ~17 degrees to be able to thrust through the CG when spiraling out of LEO
 - The thrusters are permanently canted 9 degrees in this direction
 - This requires the thrusters to be gimballed 8 degrees to thrust through the CG
- After docking with MPCV at escape
 - CG is located approximately 0.43 m toward the Hab/EP element
 - This requires a net gimbal angle of 6 degrees in the opposite direction compared to the direction during the spiral out
 - Requires a total thruster gimbal angle of 15 degrees since the 9 degree pre-cant needs to be overcome
 - This assumes the propellant is pulled appropriately from each element to maintain the 1.3 m offset during the spiral out
 - 12 Mt of propellant from the Hab/EP element

- 18 Mt of propellant from the power element
- End of mission, Earth Arrival
 - CG is located approximately 0.7 m towards the Hab/EP element
 - Requires a net gimbal angle of ~ 10 degrees
 - Requires a total thruster gimbal angle of 19 degrees since the 9 degree pre-cant needs to be overcome

It is recommended as future work to get a better estimate of the CG location throughout the mission. Estimates made during the study were based on rough estimates of vehicle dimensions and location(s) of the large mass items. The full layout of the vehicle, including dimensions, is one of the last things to be done during a study. More accurate estimates of the CG location will give better estimates of moment arms and hence vehicle control authority.

3.2.3.5. Electrical Power System

The electrical power system delivers 2.5 MWe to the spacecraft. The 2.5 Mwe electrical power system consists of three distinct building blocks that include the liquid metal-cooled, fast-spectrum reactor, a dynamic Brayton power conversion combined with an AC power management and distribution system and finally a heat rejection system combining a liquid NaK pumped loop fluid system combined with a lightweight sodium heat pipe radiator panels. To allow for easy deployment combinations of 5 m X 5 m deployable radiator panels are arranged behind the angle subtended by the 25-degree reactor radiation shadow shield cone. Figure 3-44 shows a sketch of the deployed reactor power system.

3.2.3.5.1. Power Design and MEL

The power system consists of a lithium-cooled, fueled fast reactor with a lithium exit temperature of 1500 K. The reactor utilizes highly enriched U235 with uranium nitride as the fuel form combined with refractory fuel clads and housing to achieve these high temperatures. The lithium is pumped via an electromagnetic pump to a lithium-to-Helium-Xenon liquid to gas heat exchanger that removes the heat generated by the reactor and places it into the hot section of our Brayton power conversion loop. The Brayton power conversion loop has a 1450 K turbine inlet temperature with the rotating turbo-alternator and compressor spinning at 24 krpm. There are four separate Brayton loops with three of the four required for full power. Heat is rejected from the Brayton system via a He-Xe gas to NaK heat exchanger. This NaK is pumped to stainless steel sodium heat pipes that are connected to two-sided carbon radiator panels. Total area for the radiator is 2200 m² with an average radiator temperature of 500 K rejecting into a 4 K sink environment. Note the design has added 10% additional area to the radiator to ensure full power operation due to either the loss of surface area due to micrometeoroid impacts or heat pipe failures.

2727 kWe of 3 phase AC is generated by the Brayton alternators. This AC power is used for a combination of both the spacecraft loads and the reactor power system itself. The Power Management and Distribution System (PMAD) is responsible for both providing power to the loads and running the various power system loads. The PMAD consists of the following:

1. A power electronics and control system, which provides power to reactor and power conversion subsystem and transforms the 1480 Vac bus to DC
2. An auxiliary power system which includes the startup power batteries and solar array
3. A parasitic load radiator to dump excess power the power system generates that can't be used by the loads
4. PMAD radiator that rejects the heat generated in the AC to DC power conversion along with the heat generated by the control functions
5. Power and data cabling that move both power and control signals to and from their appropriate connections.

Figure 3-59 shows the power system schematic for the 2.5 Mwe system with Table 3-28 and Table 3-29 showing the estimated masses for all of the major components in the electrical power system. Note that in addition to the carried redundancy in both the radiator and power conversion systems, additional mass margin is also carried for each subcomponent.

Mars Design Reference Architecture 5.0 – Addendum #2

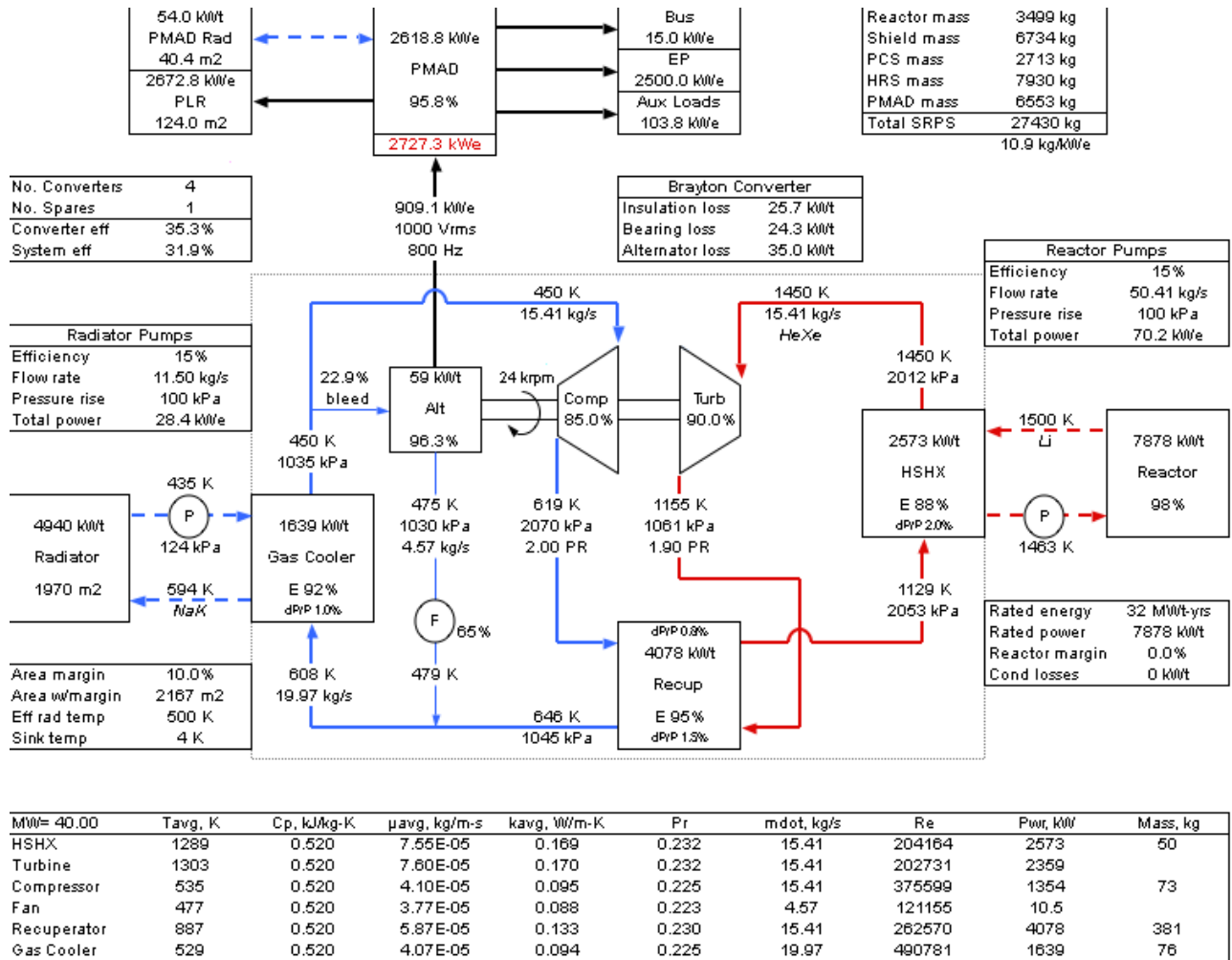


Figure 3-59 Power system schematic.

Table 3-28 Mars NEP Electrical Power System Case 1 Conjunction MEL, Hab/EP Element

WBS	Description	QTY	Unit Mass	Basic Mass	Growth	Growth	Total Mass
Number	Case 1 Piloted Mars NEP Spacecraft CD-2012-73		(kg)	(kg)	(%)	(kg)	(kg)
06	Piloted Mars NEP Spacecraft			211907.69	3.1%	6590.54	218498.23
06.1	Hab/EP Element			108360.60	2.3%	2517.89	110878.49
06.1.1	Habitat			52888.00	0.0%	0.00	52888.00
06.1.2	Attitude Determination and Control			91.84	3.0%	2.76	94.60
06.1.3	Command & Data Handling			46.80	21.4%	10.00	56.80
06.1.4	Communications and Tracking			0.00	0	0.00	0.00
06.1.5	Electrical Power Subsystem			41.00	14.8%	6.05	47.05
06.1.5.d	Power Cable and Harness Subsystem (C and HS)			40.00	15.0%	6.00	46.00
06.1.5.d.a	Spacecraft Bus Harness	10	1.00	10.00	15.0%	1.50	11.50
06.1.5.d.b	connector	10	3.00	30.00	15.0%	4.50	34.50

Table 3-29 Mars NEP Electrical Power System Case 1 Conjunction MEL, Power Element

WBS	Description	QTY	Unit Mass	Basic Mass	Growth	Growth	Total Mass
Number	Case 1 Piloted Mars NEP Spacecraft CD-2012-73		(kg)	(kg)	(%)	(kg)	(kg)
06	Piloted Mars NEP Spacecraft			211907.69	3.1%	6590.54	218498.23
06.1	Hab/EP Element			108360.60	2.3%	2517.89	110878.49
06.2	Power Element			103547.09	3.9%	4072.66	107619.75
06.2.1	Other (N/A)			0.00	0	0.00	0.00
06.2.2	Attitude Determination and Control			28.38	3.1%	0.87	29.25
06.2.3	Command & Data Handling			121.00	19.2%	23.26	144.26
06.2.4	Communications and Tracking			55.10	0.0%	0.00	55.10
06.2.5	Electrical Power Subsystem			25956.95	12.9%	3358.77	29315.72
06.2.5.a	Power Conversion			2713.41	12.0%	325.61	3039.02
06.2.5.a.a	Turboalternator	4	72.73	290.91	12.0%	34.91	325.82
06.2.5.a.b	Recuperator	4	381.18	1524.74	12.0%	182.97	1707.70
06.2.5.a.c	Gas Cooler	4	75.91	303.63	12.0%	36.44	340.06
06.2.5.a.d	Ducting & Structure	4	148.53	594.13	12.0%	71.30	665.43
06.2.5.b	Power Management & Distribution			6080.32	14.8%	899.34	6979.66
06.2.5.b.a	Power Electronics & Control	1	2688.95	2688.95	15.0%	403.34	3092.30
06.2.5.b.b	Auxiliary Power	1	221.67	221.67	12.0%	26.60	248.27
06.2.5.b.c	PMAD Radiator	1	201.82	201.82	12.0%	24.22	226.04
06.2.5.b.d	Parasitic Load Radiator	1	1239.88	1239.88	15.0%	185.98	1425.86
06.2.5.b.e	Power & Data Cabling	1	1728.00	1728.00	15.0%	259.20	1987.20
06.2.5.c	Reactor and Radiation Shield			10233.12	12.7%	1302.21	11535.33
06.2.5.c.a	Core & Reflectors	1	1944.52	1944.52	15.0%	291.68	2236.19
06.2.5.c.b	Instrumentation & Control	1	529.87	529.87	15.0%	79.48	609.35
06.2.5.c.c	Primary Heat Transport	1	825.22	825.22	12.0%	99.03	924.24
06.2.5.c.d	Heat Source Heat Exchanger	4	49.92	199.68	12.0%	23.96	223.64
06.2.5.c.e	Gamma Shield	1	1204.66	1204.66	12.0%	144.56	1349.22
06.2.5.c.f	Neutron Shield	1	4650.85	4650.85	12.0%	558.10	5208.95
06.2.5.c.g	Structure	1	878.33	878.33	12.0%	105.40	983.73
06.2.5.d	Heat Rejection			6930.10	12.0%	831.61	7761.72
06.2.5.d.a	Main Radiator	2	2307.73	4615.47	12.0%	553.86	5169.32
06.2.5.d.b	Secondary Heat Transport	4	578.66	2314.64	12.0%	277.76	2592.39

3.2.3.6. Propulsion System

The propulsion system consists of three individual systems, a high-thrust chemical system for orbital insertion, a dedicated RCS, and a Next Generation Electric Propulsion Thruster-based electric propulsion system. Both vehicle segments utilize two shuttle OMS (AJ-10 derivative) engines to perform LEO insertion, but these engines are rendered inoperable once the two segments are docked. These engines consume MMH and NTO (MON-3) as propellants, as do the RCS thrusters. In an effort to reduce complexity and mass, both chemical propulsion systems utilize the same propellants and tanks. The chemical feed system is designed so that once the segments are docked, propellants can be shared between the two segments, and even potentially refueled.

3.2.3.6.1. Propulsion System Design and MEL

The RCS system is composed of forty R-4D thrusters. Sixteen thrusters are located on the habitat segment, and are arranged in four pods of four thrusters at one end of the vehicle, and two pods with two thrusters each at the other end giving redundancy in the axial direction. The power segment has 24 thrusters located in a classic eight pods of three thrusters type of configuration. Both systems have a nominal single fault tolerant feed system comprised of

commercial off-the-shelf (COTS) components, line and tank heaters, and a nominal instrumentation suite.

The chemical propellants are stored in identical COTS tanks on both vehicle segments. There are a total of four chemical propellant tanks per segment: two for fuel and two for oxidizer. The tanks are ATK model 80-431, which are made from 6Al-4V titanium alloy, have a diameter of 90.4 cm (35.6 in), a length of 340.1 cm (133.9 in), an internal propellant management device, and a mean operating pressure of 2.8M PA (300 psig). These tanks are pressurized with nitrogen gas stored in 16 Arde D4790 COPV pressurant tanks. There are four of these tanks per vehicle segment, and they are 63.5 cm (25.0 in) in diameter with a mean operating pressure of 31.0 MPa (4500 psig).

The electric thruster system consists of a total of 10 gimbaled 280kW thrusters in a 9+1 configuration. The gimbaled thrusters are mounted on a plate that is at a 9.5-deg incline relative to the vehicle centerline. This is to aid in accommodating CG shift during the mission as xenon is consumed and to reduce the required gimbal travel. Each thruster string is zero fault tolerant, and there is no cross strapping between thruster strings. The thrusters receive power from individual direct drive units (DDUs) that take 3-phase 1630Vac power from the electrical generation system and convert it to 220Vdc via what is essentially a fully controlled full bridge rectifier circuit. All of the DDU and xenon feed systems are controlled by a dedicated digital control interface unit, where the gimbals are controlled directly by the S/C computer. A system schematic showing these relationships is shown in Figure 3-60.

Xenon for the thrusters is stored in two 4-meter-diameter COPV tanks. There is a single xenon tank and high pressure feed system on each segment. Xenon can thus be utilized from either tank to assist in S/C CG control, while only low-pressure xenon is passed between the modules. Each thruster has its own low-pressure feed system, and all the xenon flow control modules (both high and low pressure) have internal redundancy. A diagram of the Hab segment showing the placement of propulsion system components is shown Figure 3-61, and the master equipment list for this segment (both chemical and electrical propulsion systems) is shown in Table 3-30 and Table 3-31. Figure 3-61 and Figure 3-62 shows the propulsion system layout for the power module, and Table 3-34 and Table 3-35 show the master equipment lists for the propulsion systems on this segment.

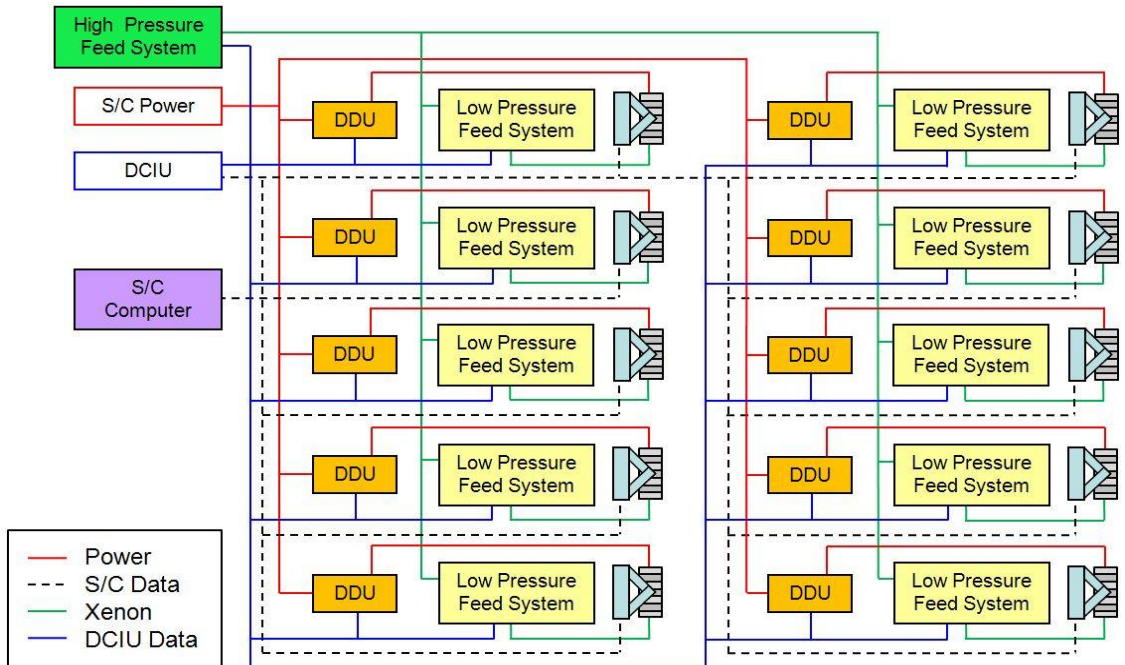


Figure 3-60 Major external components of the full Piloted Mars NEP Vehicle.

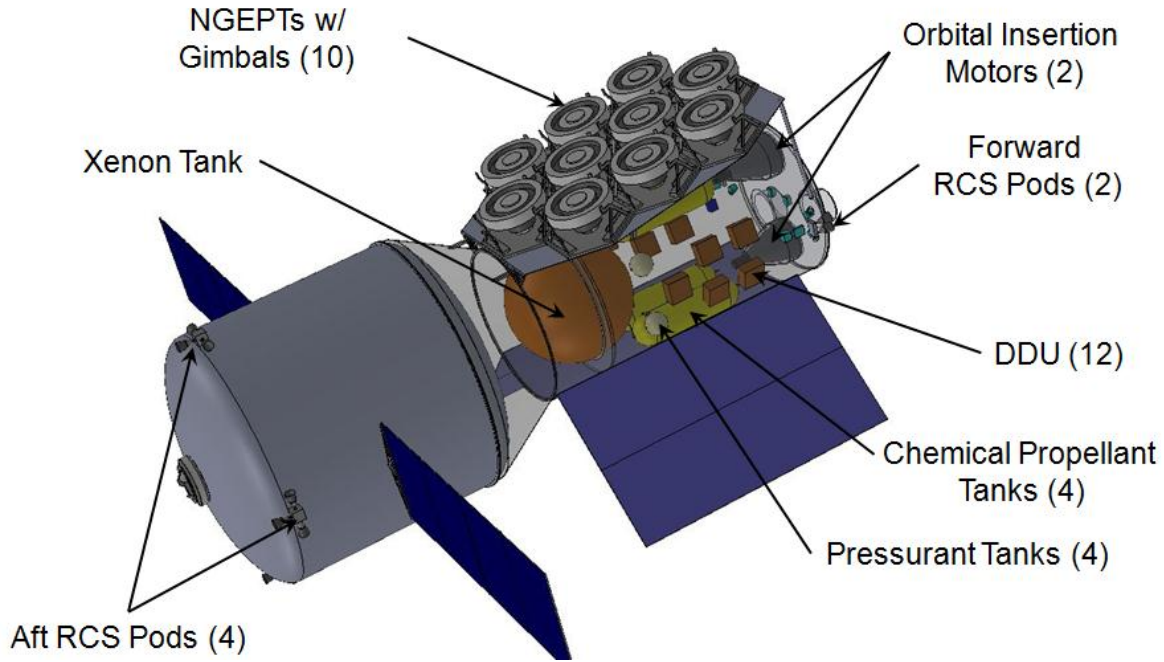


Figure 3-61 Hab segment propulsion layout.

Table 3-30 Mars NEP Propulsion System (Chem Hardware) Case 1 Conjunction MEL, Hab/EP Element

WBS	Description	QTY	Unit Mass	Basic Mass	Growth	Growth	Total Mass
Number	Case 1 Piloted Mars NEP Spacecraft CD-2012-73		(kg)	(kg)	(%)	(kg)	(kg)
06	Piloted Mars NEP Spacecraft			211907.69	3.1%	6590.54	218498.23
06.1	Hab/EP Element			108360.60	2.3%	2517.89	110878.49
06.1.1	Habitat			52888.00	0.0%	0.00	52888.00
06.1.2	Attitude Determination and Control			91.84	3.0%	2.76	94.60
06.1.3	Command & Data Handling			46.80	21.4%	10.00	56.80
06.1.4	Communications and Tracking			0.00	0	0.00	0.00
06.1.5	Electrical Power Subsystem			41.00	14.8%	6.05	47.05
06.1.6	Thermal Control (Non-Propellant)			1740.34	18.0%	313.26	2053.61
06.1.7	Propulsion (Chemical Hardware)			961.47	3.5%	33.30	994.77
06.1.7.a	Primary Chemical System Hardware			314.16	2.9%	9.16	323.32
06.1.7.a.a	<i>Main Engine Hardware</i>			236.00	2.0%	4.72	240.72
06.1.7.a.a.a	Shuttle OMS Engine	2	118.00	236.00	2.0%	4.72	240.72
06.1.7.a.b	<i>Reaction Control System Hardware</i>			78.16	5.7%	4.44	82.60
06.1.7.a.b.a	RCS Engines	16	3.76	60.16	2.0%	1.20	61.36
06.1.7.a.b.b	RCS Thruster Subassembly	6	3.00	18.00	18.0%	3.24	21.24
06.1.7.b	Propellant Management (Chemical)			647.31	3.7%	24.14	671.45
06.1.7.b.a	<i>Main Engine Propellant Management</i>			431.21	3.2%	14.00	445.21
06.1.7.b.a.a	Fuel Tanks	2	94.37	188.75	2.0%	3.77	192.52
06.1.7.b.a.b	Fuel Lines	0	0.00	0.00	0.0%	0.00	0.00
06.1.7.b.a.c	Oxidizer Tanks	2	94.37	188.75	2.0%	3.77	192.52
06.1.7.b.a.f	Feed System - regulators, valves, etc	1	53.72	53.72	12.0%	6.45	60.16
06.1.7.b.b	<i>RCS Propellant Management</i>			216.09	4.7%	10.14	226.24
06.1.7.b.b.e	Pressurization System - tanks, panels, lines	1	39.21	39.21	12.0%	4.71	43.92
06.1.7.b.b.f	Feed System - regulators, valves, etc	1	19.00	19.00	12.0%	2.28	21.28
06.1.7.b.b.g	ARDE 4790	4	39.47	157.88	2.0%	3.16	161.04

Table 3-31 Mars NEP Propulsion System (EP Hardware) Case 1 Conjunction MEL, Hab/EP Element

WBS	Description	QTY	Unit Mass	Basic Mass	Growth	Growth	Total Mass
Number	Case 1 Piloted Mars NEP Spacecraft CD-2012-73		(kg)	(kg)	(%)	(kg)	(kg)
06	Piloted Mars NEP Spacecraft			211907.69	3.1%	6590.54	218498.23
06.1	Hab/EP Element			108360.60	2.3%	2517.89	110878.49
06.1.1	Habitat			52888.00	0.0%	0.00	52888.00
06.1.2	Attitude Determination and Control			91.84	3.0%	2.76	94.60
06.1.3	Command & Data Handling			46.80	21.4%	10.00	56.80
06.1.4	Communications and Tracking			0.00	0	0.00	0.00
06.1.5	Electrical Power Subsystem			41.00	14.8%	6.05	47.05
06.1.6	Thermal Control (Non-Propellant)			1740.34	18.0%	313.26	2053.61
06.1.7	Propulsion (Chemical Hardware)			961.47	3.5%	33.30	994.77
06.1.8	Propellant (Chemical)			7622.26	0.0%	0.00	7622.26
06.1.9	Propulsion (EP Hardware)			7963.73	14.3%	1139.04	9102.77
06.1.9.a	Primary EP System Hardware			3912.00	18.0%	704.16	4616.16
06.1.9.a.a	EP System Hardware			3912.00	18.0%	704.16	4616.16
06.1.9.a.a.a	Primary EP Thrusters	10	350.00	3500.00	18.0%	630.00	4130.00
06.1.9.a.a.b	Main Engine Gimbal	10	40.00	400.00	18.0%	72.00	472.00
06.1.9.a.a.c	EPS Control (DCIU)	1	12.00	12.00	18.0%	2.16	14.16
06.1.9.a.b	Reaction Control System Hardware			0.00	0	0.00	0.00
06.1.9.a.b.a	RCS Engines	0	0.00	0.00	0.0%	0.00	0.00
06.1.9.a.b.b	RCS Thruster Subassembly	0	0.00	0.00	0.0%	0.00	0.00
06.1.9.b	Power Processing Unit (PPU)			2056.00	18.0%	370.08	2426.08
06.1.9.b.a	PPU Mass	10	180.60	1806.00	18.0%	325.08	2131.08
06.1.9.b.b	Cabling (PPU to thrusters)	10	25.00	250.00	18.0%	45.00	295.00
06.1.9.c	Propellant Management (EP)			1995.73	3.2%	64.80	2060.53
06.1.9.c.a	EP Propellant Tank system			1995.73	3.2%	64.80	2060.53
06.1.9.c.a.a	Xe Propellant Tanks	1	1635.73	1635.73	0.0%	0.00	1635.73
06.1.9.c.a.b	Feed System	1	60.00	60.00	18.0%	10.80	70.80
06.1.9.c.a.c	Low Pressure Feed System	10	30.00	300.00	18.0%	54.00	354.00

Table 3-32 Mars NEP Propulsion (Chem Hardware) System Case 1 Conjunction MEL, Power Element

WBS	Description	QTY	Unit Mass	Basic Mass	Growth	Growth	Total Mass
Number	Case 1 Piloted Mars NEP Spacecraft CD-2012-73		(kg)	(kg)	(%)	(kg)	(kg)
06	Piloted Mars NEP Spacecraft			211907.69	3.1%	6590.54	218498.23
06.1	Hab/EP Element			108360.60	2.3%	2517.89	110878.49
06.2	Power Element			103547.09	3.3%	4072.66	107619.75
06.2.1	Other (N/A)			0.00	0	0.00	0.00
06.2.2	Attitude Determination and Control			28.38	3.1%	0.87	29.25
06.2.3	Command & Data Handling			121.00	19.2%	23.26	144.26
06.2.4	Communications and Tracking			55.10	0.0%	0.00	55.10
06.2.5	Electrical Power Subsystem			25956.95	12.9%	3358.77	29315.72
06.2.6	Thermal Control (Non-Propellant)			515.46	18.0%	92.78	608.25
06.2.7	Propulsion (Chemical Hardware)			995.55	2.8%	28.30	1023.85
06.2.7.a	Primary Chemical System Hardware			350.24	3.1%	10.84	361.08
06.2.7.a.a	Main Engine Hardware			236.00	2.0%	4.72	240.72
06.2.7.a.a.a	Main Engine	2	118.00	236.00	2.0%	4.72	240.72
06.2.7.a.b	Reaction Control System Hardware			114.24	5.4%	6.12	120.36
06.2.7.a.b.a	RCS Engines	24	3.76	90.24	2.0%	1.80	92.04
06.2.7.a.b.b	RCS Thruster Subassembly	8	3.00	24.00	18.0%	4.32	28.32
06.2.7.b	Propellant Management (Chemical)			645.31	2.7%	17.45	662.76
06.2.7.b.a	Main Engine Propellant Management			431.21	1.8%	7.55	438.76
06.2.7.b.a.a	Fuel Tanks	2	94.37	188.75	2.0%	3.77	192.52
06.2.7.b.a.c	Oxidizer Tanks	2	94.37	188.75	2.0%	3.77	192.52
06.2.7.b.a.f	Feed System - regulators, valves, etc	1	53.72	53.72	0.0%	0.00	53.72
06.2.7.b.b	RCS Propellant Management			214.09	4.6%	9.90	224.00
06.2.7.b.b.e	Pressurization System - panels, lines	1	39.21	39.21	12.0%	4.71	43.92
06.2.7.b.b.f	Feed System - regulators, valves, etc	1	17.00	17.00	12.0%	2.04	19.04
06.2.7.b.b.g	Pressurant Tank	4	39.47	157.88	2.0%	3.16	161.04

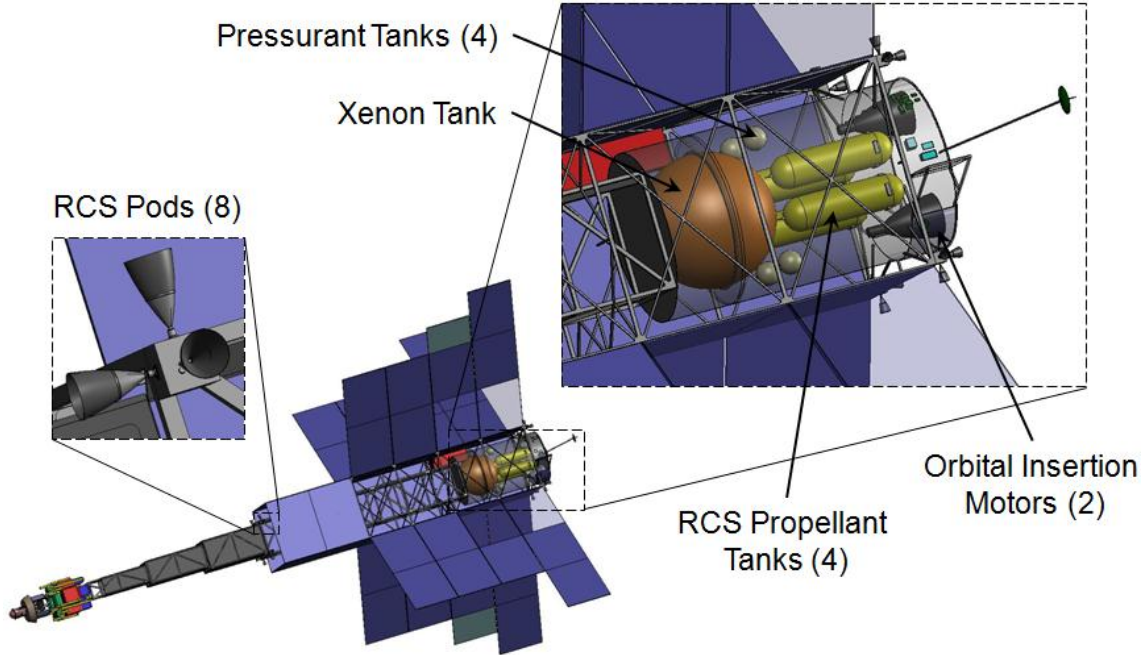


Figure 3-62 Power segment propulsion layout.

Table 3-33 Mars NEP Propulsion (EP Hardware) System Case 1 Conjunction MEL, Power Element

WBS	Description	QTY	Unit Mass	Basic Mass	Growth	Growth	Total Mass
Number	Case 1 Piloted Mars NEP Spacecraft CD-2012-73		(kg)	(kg)	(%)	(kg)	(kg)
06	Piloted Mars NEP Spacecraft			211907.69	3.1%	6590.54	218498.23
06.1	Hab/EP Element			108360.60	2.3%	2517.89	110878.49
06.2	Power Element			103547.09	3.9%	4072.66	107619.75
06.2.1	Other (N/A)			0.00	0	0.00	0.00
06.2.2	Attitude Determination and Control			28.38	3.1%	0.87	29.25
06.2.3	Command & Data Handling			121.00	19.2%	23.26	144.26
06.2.4	Communications and Tracking			55.10	0.0%	0.00	55.10
06.2.5	Electrical Power Subsystem			25956.95	12.9%	3358.77	29315.72
06.2.6	Thermal Control (Non-Propellant)			515.46	18.0%	92.78	608.25
06.2.7	Propulsion (Chemical Hardware)			995.55	2.8%	28.30	1023.85
06.2.8	Propellant (Chemical)			7679.52	0.0%	0.00	7679.52
06.2.9	Propulsion (EP Hardware)			1708.60	0.1%	1.54	1710.15
06.2.9.a	Primary EP System Hardware			60.00	0.0%	0.00	60.00
06.2.9.a.a	<i>EP System Hardware</i>			60.00	0.0%	0.00	60.00
06.2.9.a.a.d	High Pressure Feed System	1	60.00	60.00	0.0%	0.00	60.00
06.2.9.a.b	<i>Reaction Control System Hardware</i>			0.00	0	0.00	0.00
06.2.9.b	Power Processing Unit (PPU)			0.00	0	0.00	0.00
06.2.9.c	Propellant Management (EP)			1648.60	0.1%	1.54	1650.15
06.2.9.c.a	<i>EP Propellant Tank system</i>			1648.60	0.1%	1.54	1650.15
06.2.9.c.a.a	Xe Propellant Tanks	1	1635.73	1635.73	0.0%	0.00	1635.73
06.2.9.c.a.b	Feed System	1	12.87	12.87	12.0%	1.54	14.42

3.2.3.7. Structures and Mechanisms

3.2.3.7.1. Structures and Mechanisms Design and MEL

The system consists of two main components. There is a power element and a habitat and electric propulsion element. The components are illustrated in Figure 3-63. The system structures must contain the necessary hardware for instrumentation, avionics, communications, propulsion, and power. The structural components must be able to withstand applied loads from the launch vehicle and operational loads. Launch loads are on the order of 5.5 g. In addition, the structural components must provide minimum deflections, sufficient stiffness, and vibration damping. The goal of the design is to minimize weight of the components that comprise the structure of the spacecraft bus, and must also fit within the physical confines of the launch vehicle.

The mechanisms are required to function for single events or continuously throughout the mission, depending on the types of mechanisms. The separation mechanisms must release the spacecraft upon completion of the launch vehicle's part of the trajectory in a single short-duration event.

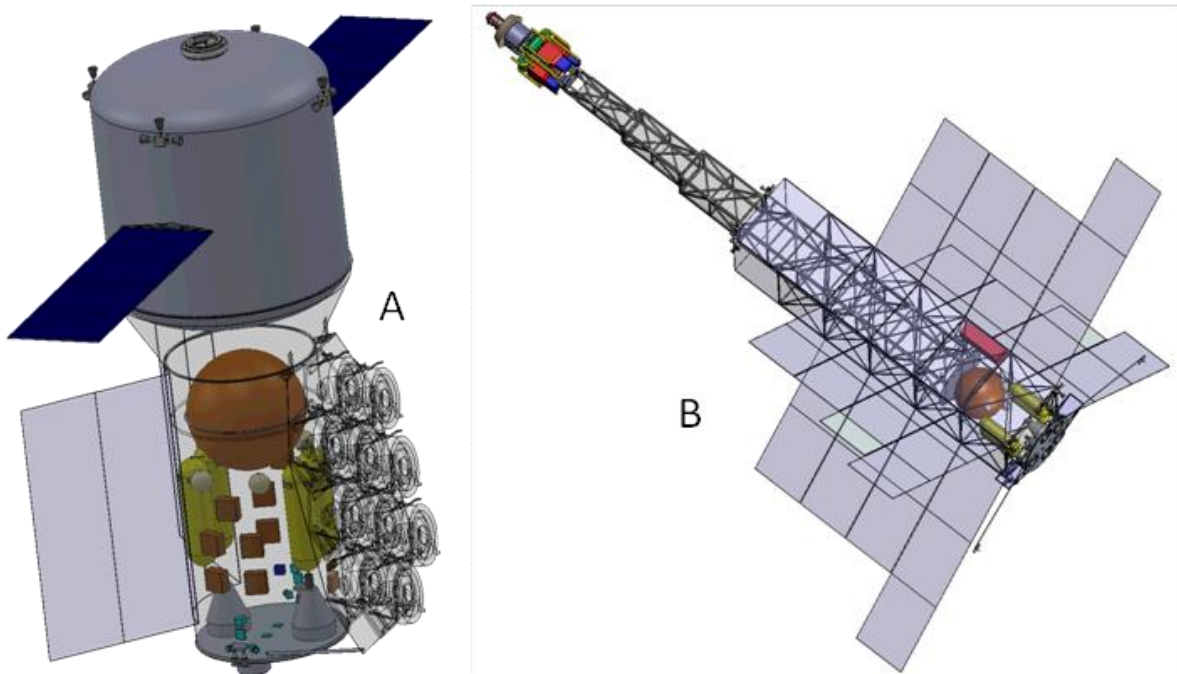


Figure 3-63 A) The habitat and electric propulsion module and B) the power element.

Mars Design Reference Architecture 5.0 – Addendum #2

Table 3-34 Mars NEP Structures and Mechanisms System Case 1 Conjunction MEL, Hab/EP Element

WBS	Description	QTY	Unit Mass	Basic Mass	Growth	Growth	Total Mass
Number	Case 1 Piloted Mars NEP Spacecraft CD-2012-73		(kg)	(kg)	(%)	(kg)	(kg)
06	Piloted Mars NEP Spacecraft			211907.69	3.1%	6590.54	218498.23
06.1	Hab/EP Element			108360.60	2.3%	2517.89	110878.49
06.1.1	Habitat			52888.00	0.0%	0.00	52888.00
06.1.2	Attitude Determination and Control			91.84	3.0%	2.76	94.60
06.1.3	Command & Data Handling			46.80	21.4%	10.00	56.80
06.1.4	Communications and Tracking			0.00	0	0.00	0.00
06.1.5	Electrical Power Subsystem			41.00	14.8%	6.05	47.05
06.1.6	Thermal Control (Non-Propellant)			1740.34	18.0%	313.26	2053.61
06.1.7	Propulsion (Chemical Hardware)			961.47	3.5%	33.30	994.77
06.1.8	Propellant (Chemical)			7622.26	0.0%	0.00	7622.26
06.1.9	Propulsion (EP Hardware)			7963.73	14.3%	1139.04	9102.77
06.1.10	Propellant (EP)			31374.70	0.0%	0.00	31374.70
06.1.11	Structures and Mechanisms			5630.46	18.0%	1013.48	6643.94
06.1.11.a	Structures			5221.44	18.0%	939.86	6161.30
06.1.11.a.a	<i>Primary Structures</i>			2617.40	18.0%	651.13	4268.53
06.1.11.a.a.a	main bus, element	1	3617.40	3617.40	18.0%	651.13	4268.53
06.1.11.a.b	<i>Secondary Structures</i>			1604.04	18.0%	288.73	1892.77
06.1.11.a.b.a	Deck, Tank Mount	1	80.74	80.74	18.0%	14.53	95.27
06.1.11.a.b.b	Tank Support	0	0.00	0.00	0.0%	0.00	0.00
06.1.11.a.b.c	propulsion hardware mount truss	1	12.65	12.65	18.0%	2.28	14.93
06.1.11.a.b.d	propulsion hardware mount panel	1	1279.19	1279.19	18.0%	230.25	1509.44
06.1.11.a.b.e	docking guide pin	3	77.15	231.46	18.0%	41.66	273.13
06.1.11.b	Mechanisms			409.01	18.0%	73.62	482.63
06.1.11.b.a	<i>Power System Mechanisms</i>			0.00	0	0.00	0.00
06.1.11.b.b	<i>Science Payload</i>			0.00	0	0.00	0.00
06.1.11.b.c	<i>Communications Mechanisms</i>			0.00	0	0.00	0.00
06.1.11.b.d	<i>Thermal Mechanisms</i>			0.00	0	0.00	0.00
06.1.11.b.e	<i>Adaptors and Separation</i>			0.00	0	0.00	0.00
06.1.11.b.f	<i>Installations</i>			409.01	18.00%	73.62	482.63
06.1.11.b.f.a	Adaptors Installation	0	0.00	0.00	0.00%	0.00	0.00
06.1.11.b.f.b	ECLSS Installation	0	0.00	0.00	0.00%	0.00	0.00
06.1.11.b.f.c	GN&C Installation	1	3.67	3.67	18.00%	0.66	4.33
06.1.11.b.f.d	Command and Data Handling Installation	1	1.85	1.85	18.00%	0.33	2.19
06.1.11.b.f.e	Communications and Tracking Installation	0	0.00	0.00	0.00%	0.00	0.00
06.1.11.b.f.f	Electrical Power Installation	1	1.64	1.64	18.00%	0.30	1.94
06.1.11.b.f.g	Thermal Control Installation	1	45.89	45.89	18.00%	8.26	54.15
06.1.11.b.f.h	EP Propulsion Installation	1	317.50	317.50	18.00%	57.15	374.65
06.1.11.b.f.i	Chemical Propulsion Installation	1	38.46	38.46	18.00%	6.92	45.38

Table 3-35 Mars NEP Structures and Mechanisms System Case 1 Conjunction MEL, Power Element

WBS	Description	QTY	Unit Mass	Basic Mass	Growth	Growth	Total Mass
Number	Case 1 Piloted Mars NEP Spacecraft CD-2012-73		(kg)	(kg)	(%)	(kg)	(kg)
06	Piloted Mars NEP Spacecraft			211907.69	3.1%	6590.54	218498.23
06.1	Hab/EP Element			108360.60	2.3%	2517.89	110878.49
06.2	Power Element			103547.09	3.9%	4072.66	107619.75
06.2.1	Other (N/A)			0.00	0	0.00	0.00
06.2.2	Attitude Determination and Control			28.38	3.1%	0.87	29.25
06.2.3	Command & Data Handling			121.00	19.2%	23.26	144.26
06.2.4	Communications and Tracking			55.10	0.0%	0.00	55.10
06.2.5	Electrical Power Subsystem			25956.95	12.9%	3358.77	29315.72
06.2.6	Thermal Control (Non-Propellant)			515.46	18.0%	92.78	608.25
06.2.7	Propulsion (Chemical Hardware)			995.55	2.8%	28.30	1023.85
06.2.8	Propellant (Chemical)			7679.52	0.0%	0.00	7679.52
06.2.9	Propulsion (EP Hardware)			1708.60	0.1%	1.54	1710.15
06.2.10	Propellant (EP)			63335.77	0.0%	0.00	63335.77
06.2.11	Structures and Mechanisms			3150.75	18.0%	567.14	3717.89
06.2.11.a	Structures			2912.44	18.0%	524.24	3436.68
06.2.11.a.a	<i>Primary Structures</i>			2176.17	18.0%	391.71	2567.88
06.2.11.a.a.a	Main Body	1	804.86	804.86	18.0%	144.87	949.73
06.2.11.a.a.b	Box, deployable	1	1068.26	1068.26	18.0%	192.29	1260.55
06.2.11.a.a.c	Radiator Support	1	303.05	303.05	18.0%	54.55	357.60
06.2.11.a.b	<i>Secondary Structures</i>			736.27	18.0%	132.53	868.80
06.2.11.a.b.a	Deck, Tank Mount	1	80.74	80.74	18.0%	14.53	95.27
06.2.11.a.b.b	Tank Support	1	110.28	110.28	18.0%	19.85	130.13
06.2.11.a.b.c	Propulsion Hardware Mount	1	53.77	53.77	18.0%	9.68	63.45
06.2.11.a.b.d	docking guide rail	3	77.15	231.46	18.0%	41.66	273.13
06.2.11.a.b.e	Deck, aft/docking	1	260.03	260.03	18.0%	46.80	306.83
06.2.11.b	Mechanisms			238.31	18.0%	42.90	281.21
06.2.11.b.a	<i>Power System Mechanisms</i>			103.41	18.00%	18.61	122.02
06.2.11.b.a.a	deployment mechanism, deployable boom	1	103.4	103.41	18.0%	18.61	122.02
06.2.11.b.f	<i>Installations</i>			134.90	18.00%	24.28	159.18
06.2.11.b.f.c	GN&C Installation	1	1.14	1.14	18.00%	0.20	1.34
06.2.11.b.f.d	Command and Data Handling Installation	1	3.88	3.88	18.00%	0.70	4.58
06.2.11.b.f.e	Communications and Tracking Installation	1	2.20	2.20	18.00%	0.40	2.60
06.2.11.b.f.f	Electrical Power Installation	0	0.00	0.00	0.00%	0.00	0.00
06.2.11.b.f.g	Thermal Control Installation	1	20.60	20.60	18.00%	3.71	24.31
06.2.11.b.f.h	EP Propulsion Installation	1	67.28	67.28	18.00%	12.11	79.39
06.2.11.b.f.i	Chemical Propulsion Installation	1	39.80	39.80	18.00%	7.16	46.96

The main bus of the power element and the bus of the habitat support consist of a thrust tube design, which is assumed to provide the optimum architecture for housing the power modules, thrusters, and various instruments. The thrust tube is easily adapted to the launch vehicle. The bus wall material of the power element and the frustums of the Habitat Module is assumed to be T 300 3k/934 plain weave fabric carbon fiber reinforced polymer matrix composite. The flanges are assumed to be of the Al Li alloy, 2090.

The analysis performed in this study assumed a maximum axial load from launch of 5.5 g with a mass of 80 metric tons on top of the NEP Stage. A safety factor of 1.4 on the ultimate strength and 1.0 on the yield strength for metallic materials is assumed as per the NASA standard, NASA STD 5001 (1996), for a prototype design. A safety factor of 2.0 is assumed for the composite materials as per the NASA standard for composites with discontinuities in prototype hardware.

A deployable 2090 aluminum space frame is used to support the nuclear reactor and Brayton power conversion unit. Mass of the complete boxed space frame is carried under the power generation section of this report and the MEL.

The secondary structures consist of a composite sandwich structure decks for supporting the main tank and propulsion hardware. Additional supports consist of Al tubular members for supporting more propulsion hardware and radiators. Internal hardware for the power element and the habitat/propulsion element is illustrated Figure 3-64.

Mechanisms are utilized to separate the spacecraft from the launch vehicle and to deploy the space frame boom of the nuclear reactor and Brayton power conversion unit. Pyrotechnic fasteners and springs are assumed for the separation mechanism.

Internal hardware includes components for communications and tracking; control and data handling; guidance, navigation, and control; electrical power; and propulsion. External hardware includes thermal radiators of the electric propulsion element and the main components of the propulsion hardware and thrusters. The external hardware of the power element includes thermal radiators on the space frame structure and other radiators mounted to the extendable boom of the power conversion unit.

Preliminary structural analysis utilized a launch load of 5.5 g and dimensions of the proposed spacecraft bus. The thrust tube structure of the electric propulsion element supports the payload of 63 metric tons with the maximum launch acceleration. The resulting static stress within the thrust tube is 30 MPa providing a margin of 12.6 with the allowable stress of 407 MPa.

The thrust tube of the NEP bus of the power element bears a load of 9 MPa and a 5.5 g launch acceleration. The specified material is T 300 3k/934 with an allowable stress of 314 MPa provides a positive margin of 34 for the static loading condition under the launch load.

The space frame bears the load of the nuclear reactor and Brayton power conversion unit upon launch while in a stowed position. Assuming an even distribution of the load, the resulting stress is 110 MPa. The resulting margin is 2.7.

Installation mass was estimated as being 4% of the installed hardware mass. The 4% magnitude for an initial estimate compares well with values reported by Heineman (1994) for various manned systems.

Risks for the structures includes the potential impact with a foreign object during flight or insufficient stiffness in the bus, which may affect the performance of the spacecraft and its instrumentation. Insufficient damping in the structure may cause issues with long-term fatigue.

Finite element analysis should be used to provide a high fidelity model of the structure. The results of the analysis would determine stresses, displacements, and also modal frequencies for vibrations.

3.2.3.8. Thermal Control

The thermal control subsystem is to maintain the desired temperature of the internal components of the spacecraft and propulsion system throughout the mission. This section describes the thermal control for the main spacecraft and propulsion system. It does not include the thermal control for the nuclear reactor and its associated components or for the habitat module. Those are included under the power subsystem described in Section 3.2.3.5.

The thermal system modeling provides power and mass estimates for the various aspects of the vehicle thermal control system based on a number of inputs related to the vehicle geometry, flight environment and component size. The thermal system consists of the following elements

- Micrometeoroid and Orbital Debris (MMOD) Shielding
- Multi-Layer Insulation (MLI)
- Thermal Paint
- Radiator
- Thermal Control Components (Sensors, switches, data acquisition)
- Engine PPU Cooling using a Pumped Loop Cooling System
- Electric Heaters

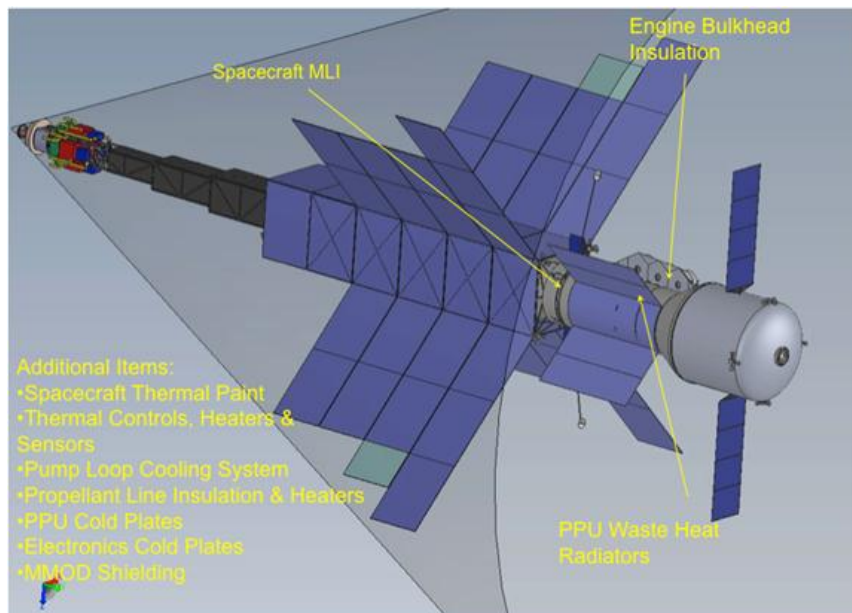


Figure 3-64 NEP Mars Spacecraft Thermal Components

The thermal requirements for the mission were to provide a means of cooling and heating of the spacecraft equipment and propulsion system to remain within their maximum and minimum temperature requirements during Earth orbit, transit and orbit insertion at Mars. The propulsion system utilized electric propulsion thrusters. The PPUs for the thrusters provided the main heat load to the thermal system.

The spacecraft utilized a nuclear reactor power system. The reactor unit has its own integrated radiator system and therefore did not require any cooling from the spacecraft thermal control system. The thermal control system was used to maintain the temperature of the internal electronics and payload as well as the PPUs for the thrusters. The maximum heat load to be rejected by the thermal system was 50 kW. The desired operating temperature for the PPUs and electronics was 320 K and a minimum of 250 K for the spacecraft structure. The spacecraft was required to maintain these temperature requirements at the various stages of the mission, Earth orbit, and transit to Mars. Electric heaters mounted near critical components within the vehicle supplied internal heat. All outer surfaces were covered with either multi-layer insulation (MLI) or thermal control paint depending on their temperature requirements.

Since this was a manned mission, MMOD shielding was used to protect the propellant tanks during transit to minimize the mission risk.

The assumptions utilized in the analysis and sizing of the thermal system were based on the operational environment, including LEO and transit to the Kuiper belt. The following assumptions were used to size the thermal system.

- The near-Earth parking orbit provided the worst-case hot operating condition. Therefore the radiator system was sized for this environment.
- The Kuiper belt environment at ~30 AU provided the worst-case cold operating conditions. This operating location was used to size the MLI insulation and heater.
- Radiator designed to see deep space with minimal view factors to the spacecraft and reactor radiators.
- The maximum angle of the radiator to the sun was 30°.
- The radiator temperature was 300 K.
- View factor of the radiator to the spacecraft was 0.25.
- A redundant radiator was not used in the design.
- MLI was used to insulate the spacecraft to minimize heat transfer to and from the surroundings.
- Electric heaters and the waste heat from the electronics were used to maintain the desired internal temperature of the spacecraft.

Since excess power is available from the reactor, louvers were not utilized with the radiator. Variable conductance heat pipes were utilized to regulate the heat transfer to the radiator.

3.2.3.8.1. Thermal Design and MEL

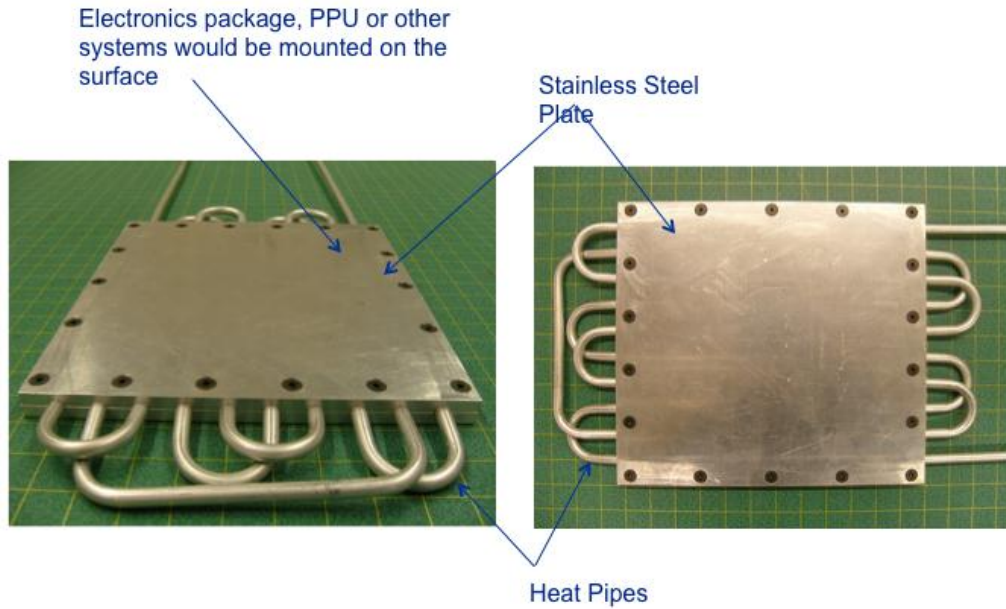
The thermal system is used to remove excess heat from the electronics and other components of the system as well as provide heating to thermally sensitive components throughout the mission.

Excess heat is collected from a series of stainless steel cold plates located throughout the interior of the spacecraft. Electronics and other temperature-sensitive components are mounted to the cold plates to regulate their temperature. Heat is extracted from the cold plate by heat pipes, which are integral to the plate’s design. An example of this integrated design is shown in Figure 3-65. Multiple redundant heat-pipe lines are used between each cold plate and the radiator. Each cold plate has four heat pipes connecting it to the radiator. The details on the cold plates are given in Figure 3-66.

Table 3-36 Cold Plate & Heat Pipe Specifications

Variable	Value
Cooling Plate & Heat-Pipe Material	Stainless Steel
Cooling Plate & Heat-Pipe Material Density	7,978 kg/m ³
Number of Cooling Plates	5 electronics, 2 engine PPU
Cooling Plate Length	0.1 m electronics, 0.15 m PPU
Cooling Plate Width	0.1 m electronics, 0.15 m PPU
Cooling Plate Thickness	5 mm
Heat Pipe Type/Working Fluid	Variable Conductance, Water

The heat pipes utilized are variable conductance heat pipes. This type of heat pipe can adjust the boiling point of the internal working fluid by varying the internal pressure within the heat pipe. This allows the heat pipe to be effectively turned off under conditions when excess heat generated is needed to warm the spacecraft interior instead of being rejected to deep space. Water is utilized as the working fluid within the heat pipe due to the selected operating temperature of 300 K.



AstroBotic technology Web site, <http://astrobotic.net>, March 2011.

Figure 3-65 Example cold plates with integral heat pipes.

The heat pipes transfer heat from the cold plates to the radiator, which radiates the excess heat to space. A typical radiator, heat pipe, cold plate arrangement is shown in Figure 3-66. This figure shows the heat pipe runs from the cold plates to the backside of the radiator. The radiator rejects heat by radiation heat transfer between with its surrounding. Items that are hotter than the radiator will provide an energy input to the radiator and must be accounted for in its sizing. The radiator is sized based on an energy balance between the incoming radiation from these “hot” sources and the view to deep space. This energy balance is illustrated in Figure 3-67.

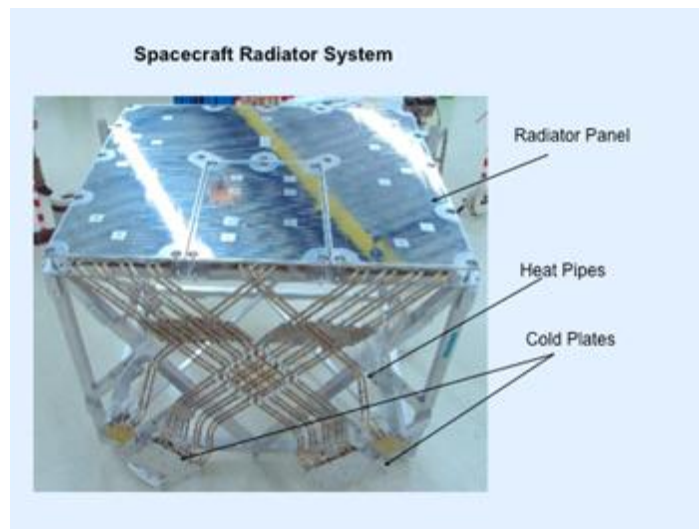


Figure 3-66 Example of a spacecraft heat pipe system.

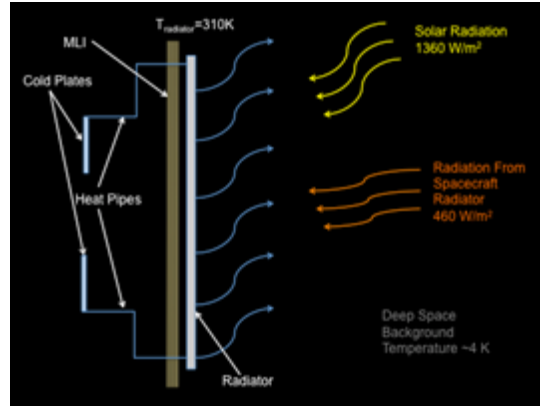


Figure 3-67 Radiator energy balance.

Using the energy balance, a radiator area of 4.68 m^2 was needed to reject the 1500 W of excess heat at the 1 AU worst-case warm operating environment. From the required area, a series of scaling equations were used to determine the mass of the radiator. The radiator is broken into the following components: panel, coating, tubing, header, adhesive, stringer and attachment.

To provide heat to the internal components, electric heaters are mounted to the cold plates and other critical devices or components to maintain their desired temperature throughout the mission. Strip heaters of various shapes are used to conform to the device being heated. An example of this type of heater is shown in Figure 3-68. The strip heaters are operated through the spacecraft control system. Thermocouples are used to read the temperature of the various components throughout the spacecraft. The output of the thermocouples goes to a data acquisition system that reads and monitors the thermocouple temperatures. If the temperature on a device is too low, the control system turns on a nearby heater through control switches and regulates the current to the heater to raise the temperature of the device to the desired level. Once at the correct level, the control system will turn the heater off.

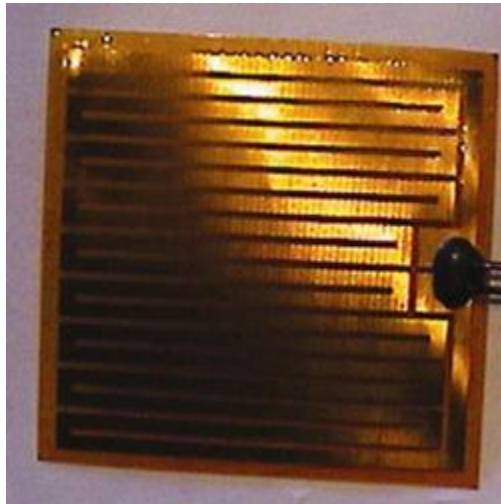


Figure 3-68 Electric strip heater.

MLI insulation was used to insulate the spacecraft and minimize heat loss for deep space operation. MLI is constructed of a number of layers of metalized material with a nonconductive spacer between the layers. The metalized material has a low absorptivity that resists radiative heat transfer between the layers. The general layout of MLI is illustrated in Figure 3-69 and Figure 3-70.

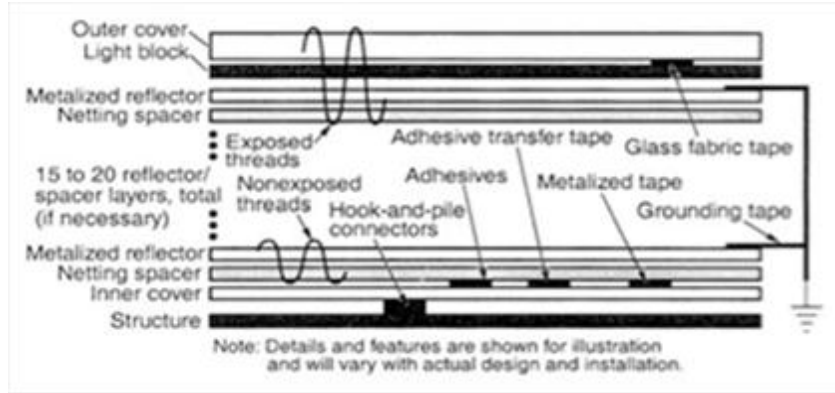


Figure 3-69 Illustration of MLI.

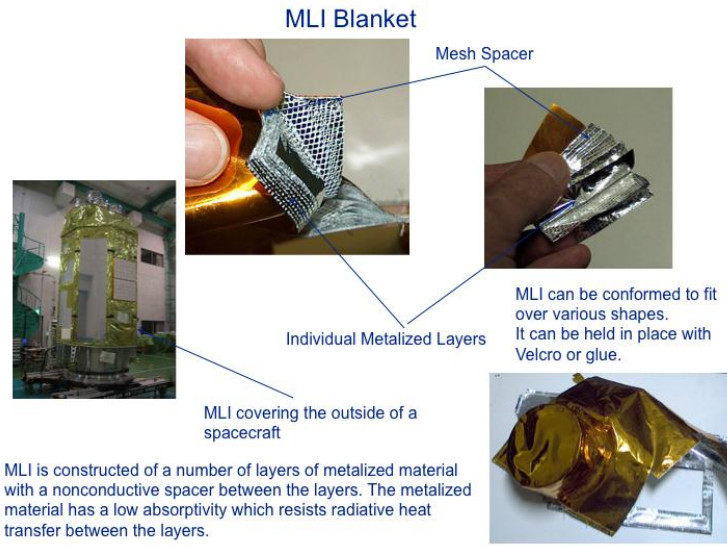


Figure 3-70 MLI blankets.

Table 3-37 Mars NEP Thermal System Case 1 Conjunction MEL, Hab/EP Element

WBS	Description	QTY	Unit Mass	Basic Mass	Growth	Growth	Total Mass
Number	Case 1 Piloted Mars NEP Spacecraft CD-2012-73		(kg)	(kg)	(%)	(kg)	(kg)
06	Piloted Mars NEP Spacecraft			211907.69	3.1%	6590.54	218498.23
06.1	Hab/EP Element			108360.60	2.3%	2517.89	110878.49
06.1.1	Habitat			52888.00	0.0%	0.00	52888.00
06.1.2	Attitude Determination and Control			91.84	3.0%	2.76	94.60
06.1.3	Command & Data Handling			46.80	21.4%	10.00	56.80
06.1.4	Communications and Tracking			0.00	0	0.00	0.00
06.1.5	Electrical Power Subsystem			41.00	14.8%	6.05	47.05
06.1.6	Thermal Control (Non-Propellant)			1740.34	18.0%	313.26	2053.61
06.1.6.a	Active Thermal Control			127.00	18.0%	22.86	149.86
06.1.6.a.a	Heaters	0	0.00	0.00	18.0%	0.00	0.00
06.1.6.a.b	Thermal Control/Heaters Circuit	35	0.20	7.00	18.0%	1.26	8.26
06.1.6.a.c	Data Acquisition	35	1.00	35.00	18.0%	6.30	41.30
06.1.6.a.d	Thermocouples	175	0.10	17.50	18.0%	3.15	20.65
06.1.6.a.e	Coolant Pumps	10	6.75	67.50	18.0%	12.15	79.65
06.1.6.b	Passive Thermal Control			1606.34	18.0%	289.14	1895.49
06.1.6.b.a	Heat Sinks	10	3.43	34.35	18.0%	6.18	40.53
06.1.6.b.b	Coolant Lines	1	110.00	110.00	18.0%	19.80	129.80
06.1.6.b.c	Radiator	1	600.14	600.14	18.0%	108.03	708.17
06.1.6.b.d	MLI	1	274.33	274.33	18.0%	49.38	323.71
06.1.6.b.e	Temperature sensors	0	0.00	0.00	18.0%	0.00	0.00
06.1.6.b.f	Spacecraft MMOD	1	391.49	391.49	18.0%	70.47	461.96
06.1.6.b.g	Thermal Coatings/Paint	1	6.80	6.80	18.0%	1.22	8.03
06.1.6.b.h	Spacecraft Engine MLI	1	55.95	55.95	18.0%	10.07	66.02
06.1.6.b.i	Coolant	1	62.53	62.53	18.0%	11.25	73.78
06.1.6.b.j	Cold Plates	0	0.00	0.00	18.0%	0.00	0.00
06.1.6.b.k	Raidator MMOD	1	70.75	70.75	18.0%	12.74	83.49
06.1.6.c	Semi-Passive Thermal Control (cruise deck and internal)			7.00	18.0%	1.26	8.26
06.1.6.c.a	Louvers	0	0.00	0.00	18.0%	0.00	0.00
06.1.6.c.b	Thermal Switches	35	0.20	7.00	18.0%	1.26	8.26

Table 3-38 Mars NEP Thermal System Case 1 Conjunction MEL, Power Element

WBS	Description	QTY	Unit Mass	Basic Mass	Growth	Growth	Total Mass
Number	Case 1 Piloted Mars NEP Spacecraft CD-2012-73		(kg)	(kg)	(%)	(kg)	(kg)
06	Piloted Mars NEP Spacecraft			211907.69	3.1%	6590.54	218498.23
06.1	Hab/EP Element			108360.60	2.3%	2517.89	110878.49
06.2	Power Element			103547.09	3.9%	4072.66	107619.75
06.2.1	Other (N/A)			0.00	0	0.00	0.00
06.2.2	Attitude Determination and Control			28.38	3.1%	0.87	29.25
06.2.3	Command & Data Handling			121.00	19.2%	23.26	144.26
06.2.4	Communications and Tracking			55.10	0.0%	0.00	55.10
06.2.5	Electrical Power Subsystem			25956.95	12.9%	3358.77	29315.72
06.2.6	Thermal Control (Non-Propellant)			515.46	18.0%	92.78	608.25
06.2.6.a	Active Thermal Control			18.00	18.0%	3.24	21.24
06.2.6.a.c	Data Acquisition	18	1.00	18.00	18.0%	3.24	21.24
06.2.6.b	Passive Thermal Control			497.46	18.0%	89.54	587.01
06.2.6.b.a	MMOD	1	226.78	226.78	18.0%	40.82	267.61
06.2.6.b.b	Heat Pipes	16	3.14	50.25	18.0%	9.05	59.30
06.2.6.b.c	Radiators	1	40.51	40.51	18.0%	7.29	47.81
06.2.6.b.d	Insulation	1	143.78	143.78	18.0%	25.88	169.66
06.2.6.b.e	Temperature sensors	91	0.10	9.10	18.0%	1.64	10.74
06.2.6.b.f	Cold Plates	8	1.60	12.76	18.0%	2.30	15.06
06.2.6.b.g	Thermal Coatings/Paint	1	14.26	14.26	18.0%	2.57	16.83

3.3. A Combined Solar Electric and Storable Chemical Propulsion

Primary Contributors:

Carolyn R. Mercer, National Aeronautics and Space Administration, Glenn Research Center

Steven R. Oleson, National Aeronautics and Space Administration, Glenn Research Center

Bret G. Drake, National Aeronautics and Space Administration, Johnson Space Center


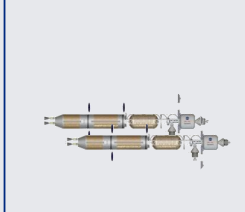
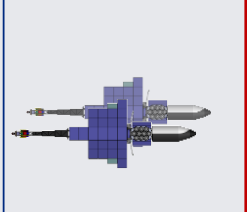
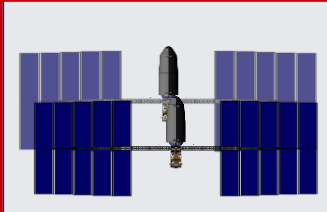


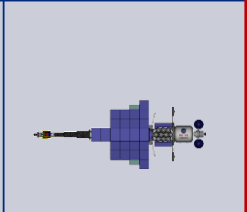
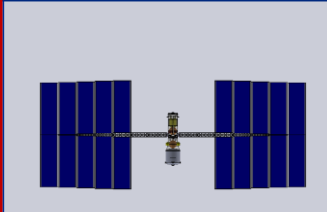
3.3.1. Introduction

NASA’S goal for human spaceflight is to expand permanent human presence beyond low-Earth orbit (LEO). To achieve this goal, NASA is identifying potential missions and technologies needed to conduct those missions safely and cost effectively. Mission options include piloted destinations to LEO and the International Space Station (ISS); high-Earth orbit and geosynchronous orbit; cislunar space, lunar orbit, and the surface of the Moon; near-Earth objects; and the moons of Mars, Mars orbit, and the surface of Mars. The Mars Design Reference Architecture (DRA) 5.0 explores a piloted mission to Mars in the 2030 timeframe, focusing on architecture and technology choices.⁴ Table 1 shows propulsion options that have been considered to transport crew and cargo to Mars, including all-chemical propulsion, nuclear thermal propulsion (NTP), and nuclear electric propulsion (NEP). This paper describes a transportation architecture using solar electric propulsion (SEP) coupled with small chemical thrusters to transport six crew and needed cargo for a long-stay Mars mission using solar arrays constrained to provide no more than 1 MW of power. This relatively low mass and robust transportation system can deliver the crew to an elliptical 1-sol orbit similar to chemical or NTP systems, and can substantially reduce the number of launches needed for such a mission when compared to an all-chemical system. This concept is dubbed “SEP-Chem” and its size is shown in Figure 3-71 relative to the ISS. Its essential feature is the use of SEP to efficiently traverse the long, deep-space portions of the mission and thereby reduce the amount of needed propellant relative to an all-chemical stage, and the use of a small Orion-derived chemical system to provide final capture at and initial departure from Mars, thereby preventing the long spirals needed by an all-SEP stage. The transit trip times will be longer than needed with all-chemical propulsion or NTP, but will allow for a 300-day surface stay with a total trip time of 1050 days, which is only 65 days longer than the targeted 1000 days. It should be noted that this comparison shows that the nominal trip times for the three types of architectures are similar only for the particular mission studied, namely a conjunction class mission with a 2037 launch date. Also, the chemical, NTP, and NEP systems shown in Table 3-39 are included solely to show that the trip times and number of launches needed by the SEP-Chem system are reasonable.

The design trades used to determine this SEP-Chem concept are described in Section II, including an analysis of an all-SEP system, several SEP-Chem variants, a comparison with an all-chemical system, and an analysis of several propulsion and power variants. Per DRA 5.0, the assumed mission includes the transportation of six crew in a habitation element to and from Mars, and also the delivery of two 100-t cargo vehicles to Mars, each captured using an aeroshell. The difference from the chemical or NTP versions of DRA 5.0 is that the SEP-Chem crew vehicle will spiral from LEO to the Earth-Moon (E-M) L2 point unpowered, and the crew will rendezvous with it there. SEP-Chem accomplishes the crew portion of this architecture with three heavy lift launch vehicles: two for the SEP-Chem and habitat vehicles which mate in LEO, and one for the crew to the L2 point. All three launches use NASA’s planned Space Launch System (SLS). A separate delivery of about 18 t of crew consumables to the habitat in LEO is needed, using a resupply system like the European Automated Transfer Vehicle.

In addition to payload requirements and launch vehicle assumptions, design constraints included a round-trip piloted mission duration of less than 1000 days to minimize crew exposure to the deep-space environment and a maximum solar array power delivery of 1 MW to permit the use of existing design concepts. Additional design constraints and considerations are given in Section II, as well as a description of the vehicles and trajectories studied, and the key system-level impacts for several propulsion and power technologies. Finally, the conclusions reached regarding relevant SEP technologies for piloted missions to Mars are compared to technologies needed for other exploration destinations such as asteroids and cislunar space. A roadmap for building the stepping-stones needed to reach Mars is also presented. Although these results are not definitive because the full breadth of design space was not explored nor were the design impacts of contingency operations, we believe that they are representative and provide insight into the relative benefits of power and propulsion technologies for solar electric vehicles of this class. This work can help guide technology development investments to enable future missions to Mars.

Table 3-39 Concept Vehicles for Mars Landing

Cargo Missions				
Crew Mission				
2037 Conjunction Class “long stay” mission	Chemical Propulsion	Nuclear Thermal	Nuclear Electric	Solar /Chem
Electric Propulsion Power level	n/a	n/a	2.5MW crew/ 1MW cargo	800kW Solar
Total Mass (t)	~1,250	~890	~770	~780
# Heavy Lift (SLS) Launches	~12	9 (7)	~7	~7
SLS Delivery to LEO (t)	105 & 130	105 (130)	105 & 130	105 & 130
SLS Shroud Dia. /Barrel Length	10 / 22	10 / 25	10 / 25	10 / 15
Trip Duration (days to Mars, On Mars, back home)	180 / 500 / 200 880 days total trip	174 / 539 / 201 914 days total trip	309 / 400 / 224 980 days total trip	439 / 300 / 326 1065 days total trip
Comments	Requires propellant depot	Number of launches reduced to 7 with 130mt SLS		1-2 ATV launches required to provide consumables to L2

3.3.1. Design

Consistent with DRA 5.0, the design reference mission for this study is a conjunction-class (long-stay) trajectory for six crew in the mid-2030 timeframe, with pre-deployed cargo. The baseline architecture used in DRA 5.0 included a nuclear thermal rocket with an outbound transit time for the crew of about 180 days in 2037, a surface stay of about 500 days, and a return trip of about 200 days, yielding a total piloted-trip time of about 900 days. The date of 2037 was chosen because it represents a challenging opportunity across the 15-year synodic cycle⁷. We therefore set an objective to keep the total crew time to 1000 days or less, including a Mars surface stay of 365 days or more. We further set a goal of requiring only two heavy-lift SLS launches, and solar arrays sized to provide no more than 1 MW of electrical power. In addition to the SEP stage, the system elements include a 24-t multipurpose crew vehicle (MPCV) and a 53-t deep-space habitat (DSH). All design trades reported in this paper begin with the SEP spacecraft spiraling from LEO to E-M L2 for rendezvous with a pre-positioned MPCV in a high energy condition—E-M L2 was chosen for this study, though a near-Earth escape would suffice as well. The figures of merit, trajectory trades, and guiding design principles are described in Section II.A; trajectory analyses are described in Section II.B; and the baseline vehicle and its variants are described in Section II.C.

⁷ For Mars, opportunities to depart from Earth occur every 26 months and the total energy required essentially repeats over this 15-year cycle. This repetition of energy is referred to as the synodic cycle.

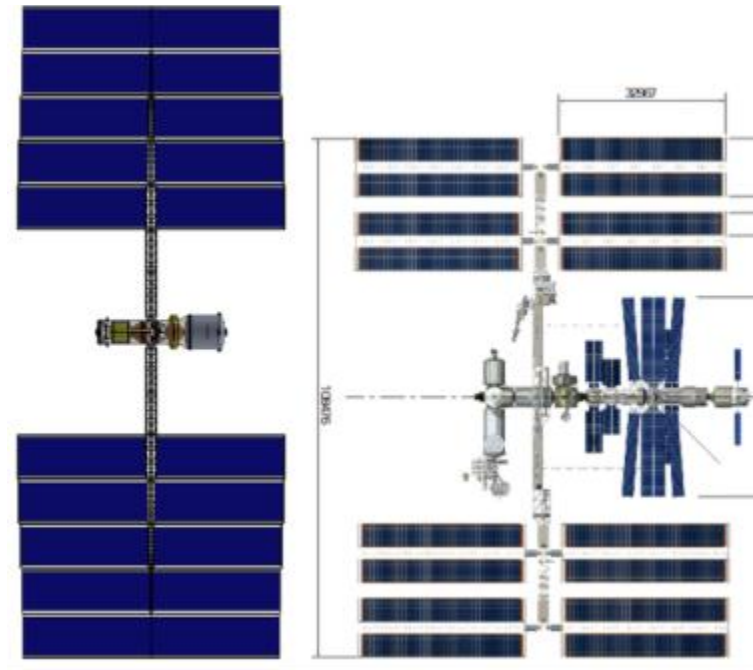


Figure 3-71 Size of the piloted combined SEP-chemical vehicle (left).

3.3.1.1. Design Approach

To conduct the parametric assessment of propulsion and power technologies, the Collaborative Modeling for Parametric Assessment of Space Systems (COMPASS)⁵ team at the NASA Glenn Research Center started with a clean sheet design using the following figures of merit:

- Total crew time of 1000 days or less (final design is 65 days over)
- Mars stay time of 365 days or more (final design is 300 days)
- Mass and volume
- Initial spacecraft in mass in LEO sufficiently low to require only two SLS launches for the unpiloted crew vehicle
- SLS net launch capability of 113.8 t delivery to LEO (–92.5 km by 407 km), with an 8.5- by 25-m shroud (final design also required ~18 t of crew consumables on ELV to LEO)
- No more than 1 MW of electric power to the electric propulsion system at beginning of life

Then the following mission trades were conducted:

- All-SEP – SEP provides all change in velocity (ΔV) from L2 to Mars and back
- All-Chemical – Chemical propulsion provides all ΔV from L2 to Mars and back
- SEP-Chem – SEP provides interplanetary ΔV s; chemical propulsion provides gravity well ΔV s
- Interplanetary transit with and without an Earth gravity assist flyby
- SEP technology variants
- Specific impulse (Isp): 2000 to 3000 s
- Power to thrusters: 600 to 900 kW
- Bus voltage: 300 to 500 V
- Thruster type: Hall effect and nested Hall effect
- Power processor: Direct drive unit (DDU) and conventional power processing unit (PPU)
- Chemical technology variants
- Storable and cryogenic systems

The spacecraft was designed to be single-fault tolerant in the design of the subsystems, where possible. Exceptions to this include the electric power system, propellant tanks, and radiators that have zero fault tolerance, although they

are designed to accommodate some performance degradation. Note that because contingency operations are not included in this analysis, conclusions about the relative merits of parameterized power and propulsion technologies must be treated as preliminary. Mass growth calculations were conducted according to AIAA S-120-2006, “Standard Mass Properties Control for Space Systems.” The percent growth factors specified in this standard were applied to each subsystem before an additional growth was carried at the system level to ensure an overall growth of at least 30% on the dry mass of the entire system. Growth in the propellant mass was carried in the propellant calculation. A 30% growth factor on the bottoms-up power requirements for the bus subsystems was used, with a 5% margin for the electric thruster power requirements.

The Spacecraft N-body Analysis Program⁶ was used to conduct trajectory analyses. The Mission Analysis Low-Thrust Optimization interplanetary low-thrust trajectory optimization tool⁷ was used to determine the propellant mass needed to perform the heliocentric phase of the mission. Detailed descriptions of the mission design and trades can be found in Burke 2013⁸.

3.3.2. Trajectory Analysis

For all variants employing SEP, the SEP spacecraft carrying the DSH spirals from 400 km to E-M L2 for rendezvous with the MPCV. The baseline SEP-Chem configuration then maneuvers to Mars with thrust from the SEP, and switches to chemical thrusters for insertion into a 24-h Mars elliptical orbit. Upon return, the chemical stage is used for Mars departure and SEP is used for transit back to Earth. Note that this baseline mission includes an additional 18 t of cargo delivery to LEO consisting of crew consumables for the DSH.

Three key trajectories were studied in addition to the baseline. All assume the unpiloted spiral of the DSH and SEP-Chem stage to the E-M L2 point. From there, the other three options assumed an Earth flyby, all-chemical propulsion to Mars (SEP discarded at E-M L2) and all electric propulsion (no chemical). The baseline trajectory is shown in Figure 3-72, and a summary of all trajectory variants is shown in Figure 3-73. In each case, the portions powered by SEP and by chemical propulsion are shown.

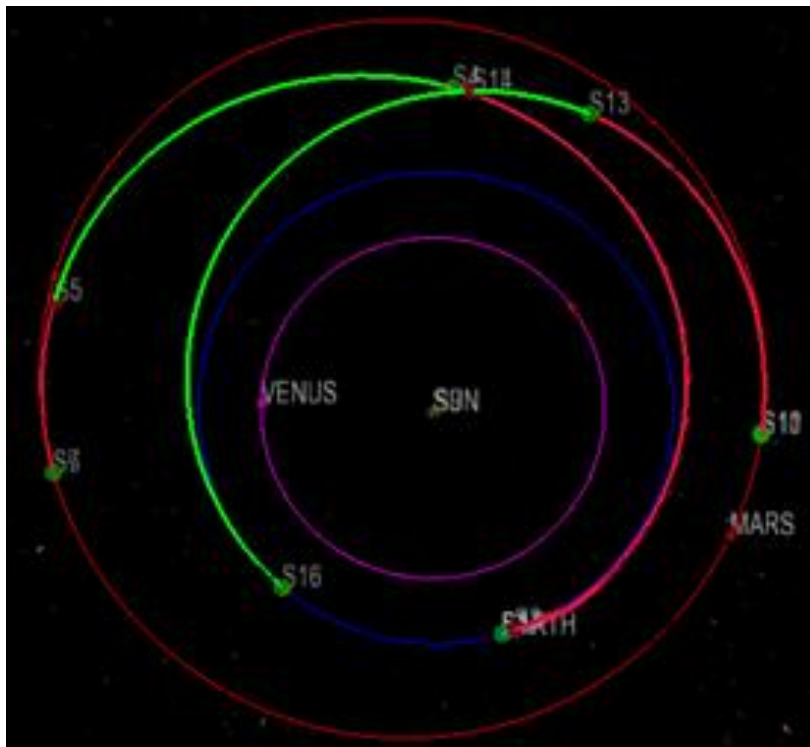


Figure 3-72 Baseline trajectory.

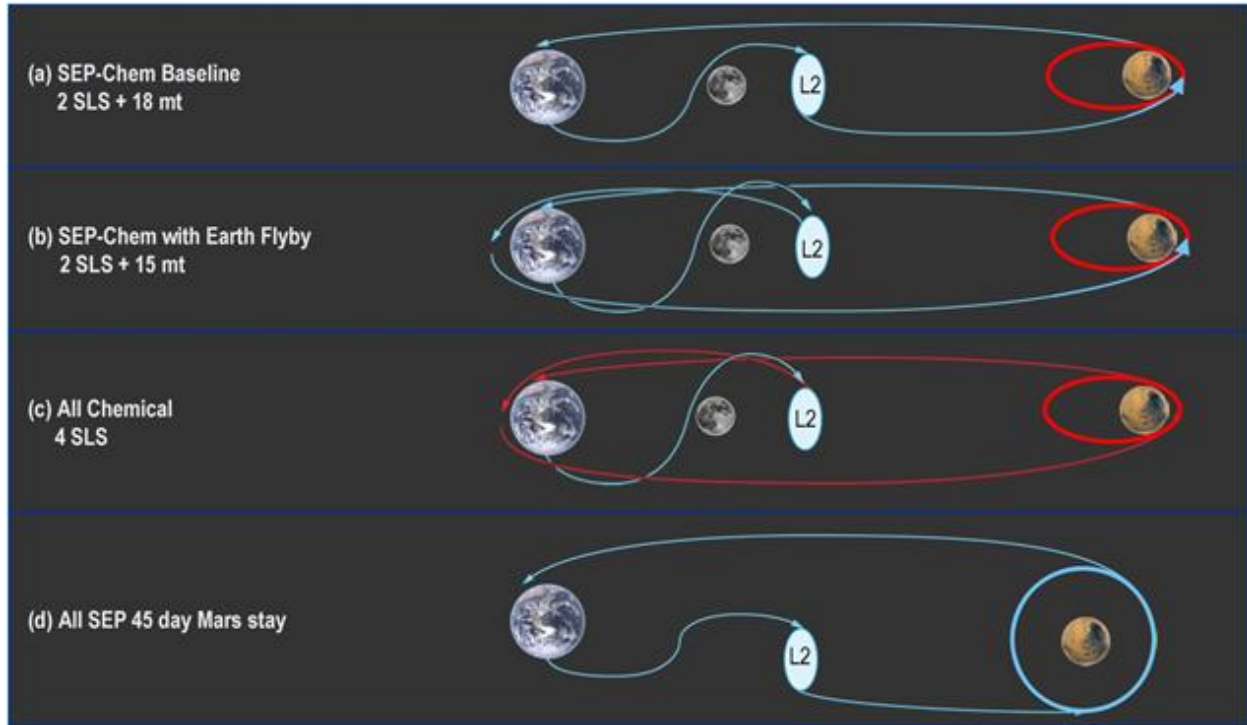


Figure 3-73 Trajectory trades after the SEP to E-M L2 arrival.

3.3.3. Baseline Vehicle

Following the design approach of using the simplest, most mature technology that can meet design objectives, we selected as the best design an SEP system combined with a relatively small storable bipropellant chemical system to realize the benefits of both propulsion types: the chemical stage provides the high thrust needed to prevent long spirals from arrival to Mars orbit and back out to departure. The external components of the SEP-Chem stage consist of primary and commissioning solar arrays, electric and chemical thrusters, and radiators; these are shown with the SEP-Chem stage mated to a deep-space habitat in Figure 3-74 and configured for launch within an SLS in Figure 3-75.

The SEP system uses a suite of eight nested Hall thrusters, each using nominally 125 kW of power at 2400 s of Isp, and two planar solar arrays providing nominally 400 kW each at end-of-life at 1 AU. Booms extend the solar arrays away from the thrusters to provide a 45° “keep away” zone from the exhaust plumes as shown in Figure 3-76. This design eliminates the need for power and propellant transport to boom-mounted thrusters. Power from the arrays is delivered to the thrusters using a direct-drive configuration⁹ rather than a conventional power processing unit, with both the arrays and thrusters operating at nominally 500 V. Two spherical tanks each store 55 t of xenon propellant for the electric thrusters.

The eight nested Hall thrusters were configured so that six were used for primary propulsion and two were carried as spares. The chemical thrusters also provide redundancy. The Isp was set to 2400 s to match the thrusters to the 500-Vdc solar array output, and as a conservative trade between trip time and propellant mass. To a certain extent, the Isp can be increased to reduce the propellant mass for variants that would otherwise exceed the mass allocation. This option is limited for direct-drive architectures with solar arrays, however, as the thrusters must match the array voltage. For a fixed power level, a higher Isp will reduce interplanetary coast times and require longer Earth-spiral mission times. The Earth spiral is uncrewed so a longer trip time for this portion does not impact crew exposure concerns. Reduced coast times for the piloted heliocentric transfer phase might be undesirable once abort scenarios are assessed.

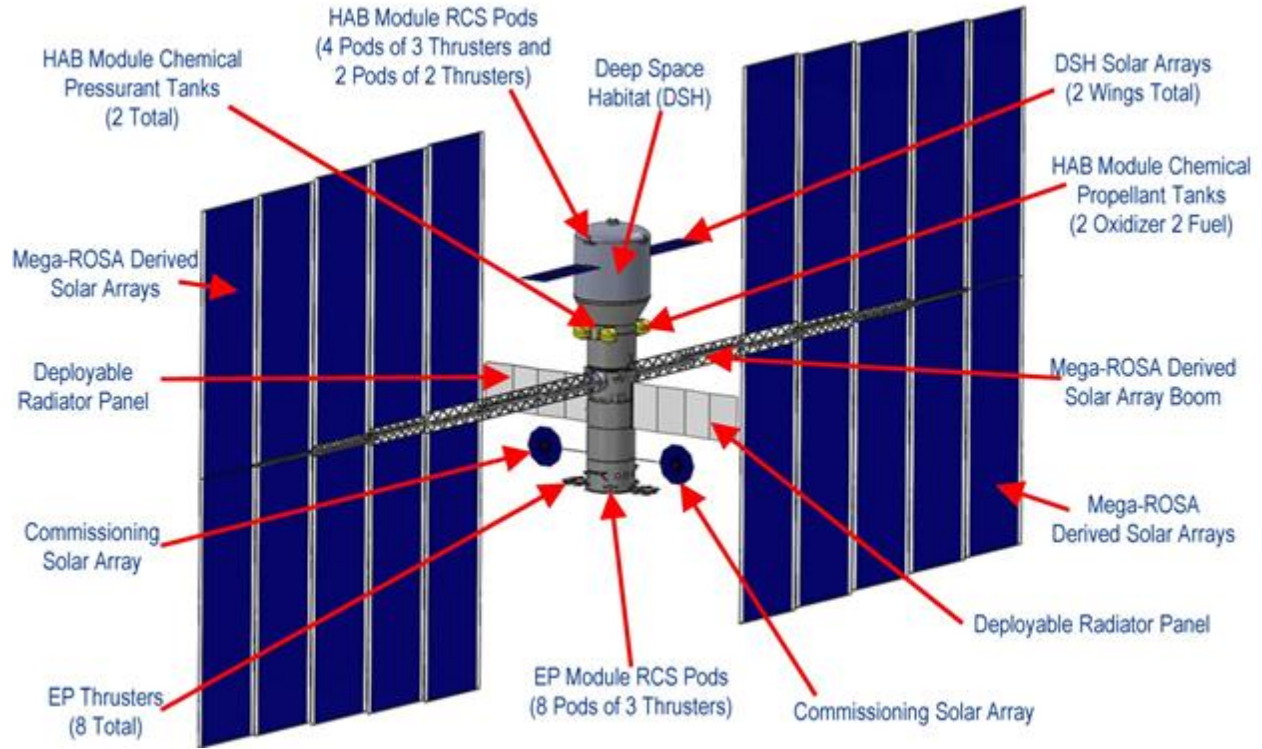


Figure 3-74 SEP-Chem stage docked with deep-space habitat. Major external components shown.

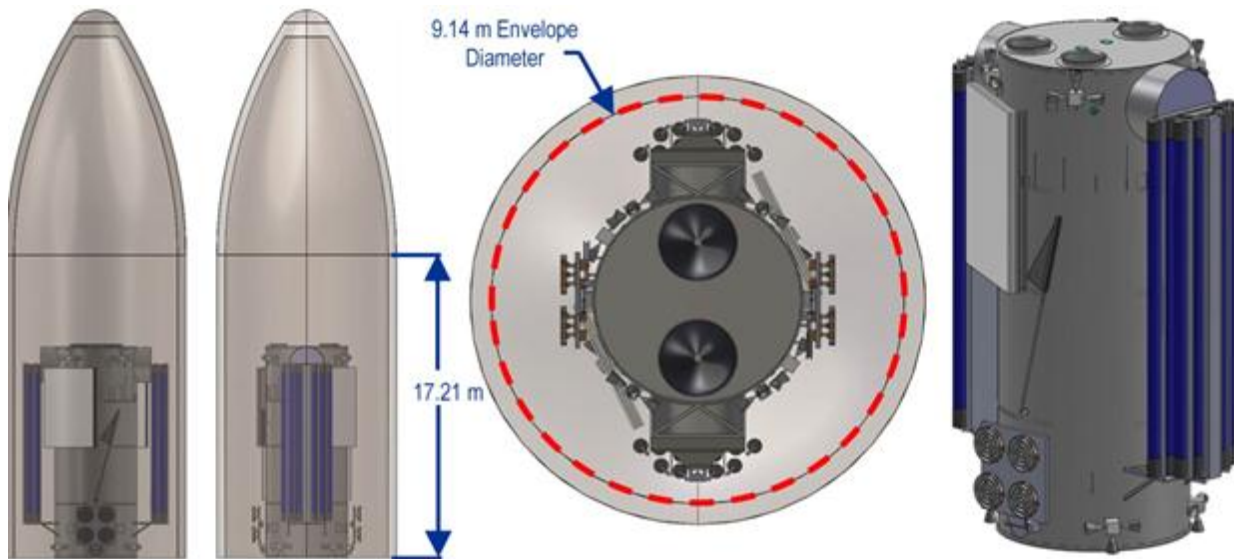


Figure 3-75 SEP-Chem module configured for launch within an SLS.

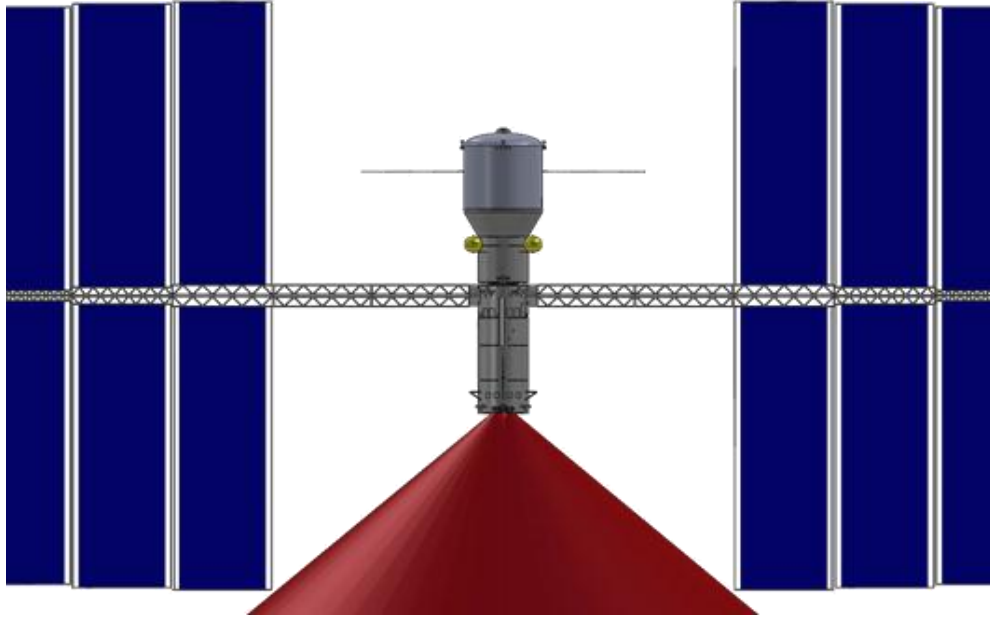


Figure 3-76 Electric thruster plume cone in relation to solar arrays.

The thrusters were grouped in fours and mounted on either side of the bottom deck. The outer four thrusters were gimballed to augment the attitude control provided by reaction control system thrusters; the remaining four were statically mounted. Eight direct-drive units (one for each thruster) were mounted on the inside of the bottom deck. Two bipropellant chemical rockets derived from Orion were mounted in the center of the bottom deck, with the propellant tanks mounted directly above. The electric thrusters, chemical thrusters, and propellant system configurations are shown in Figure 3-77.

Xenon was chosen as the propellant because its low ionization energy enables high thruster efficiency, and it is more easily stored than other heavy noble gases. Two 3.9-m-diameter spherical composite overwrap pressure vessel tanks stored the xenon as a supercritical gas at 1200 psia. Note that because of packaging constraints, one of the xenon tanks is launched with the DSH.

Inverted metamorphic multijunction solar cells with a beginning-of-life efficiency at 1 AU of 33% were chosen as the baseline. Exposure to the Van Allen belt and scattered ions from the Hall thruster plumes is expected to degrade the solar arrays; we used 6-mil coverglasses and assumed an 18.8% EOL degradation from these sources when sizing the arrays. No damage was assumed to occur in heliocentric space. As the solar array voltage degrades, the current is adjusted, altering the thruster mass flow rate to maintain a fixed Isp. Arrays were sized such that each of the two wings have an area of 2383 m² to provide 1 MW at BOL and 800 kW at EOL. Two 12-m² solar arrays provide commissioning power at 120 V before deployment of the main arrays. Avionics assume 100 kRad survivability.

Two 120-V batteries were used with one serving as a spare. Array regulation units were used on each of the two primary solar arrays to prevent the arrays from exceeding 600 V open circuit when exiting eclipse. “No-roll” steering was chosen to eliminate the considerable mass of control moment gyroscopes and as a result, we accepted secondary-axis Sun pointing errors and the attendant power loss. Since only one revolute axis is available for tracking, the arrays are revolved to minimize the Sun off-pointing angle while under thrust. Array tracking is controlled with ISS-derived solar alpha rotary joint gimbals, with mass reduced by removing the ISS in-flight servicing requirement. The assumed launch date was favorable for the use of no-roll steering because the maximum angle between the arrays and Sun occurs early in the spiral trajectory, when the beginning-of-life power is still available. This beta angle may occur later in the trajectory for different launch dates, requiring either oversized arrays or longer trip times because of the reduced power. Four RCS thruster pods provide roll, pitch, and yaw control, augmented by four gimballed Hall thrusters.

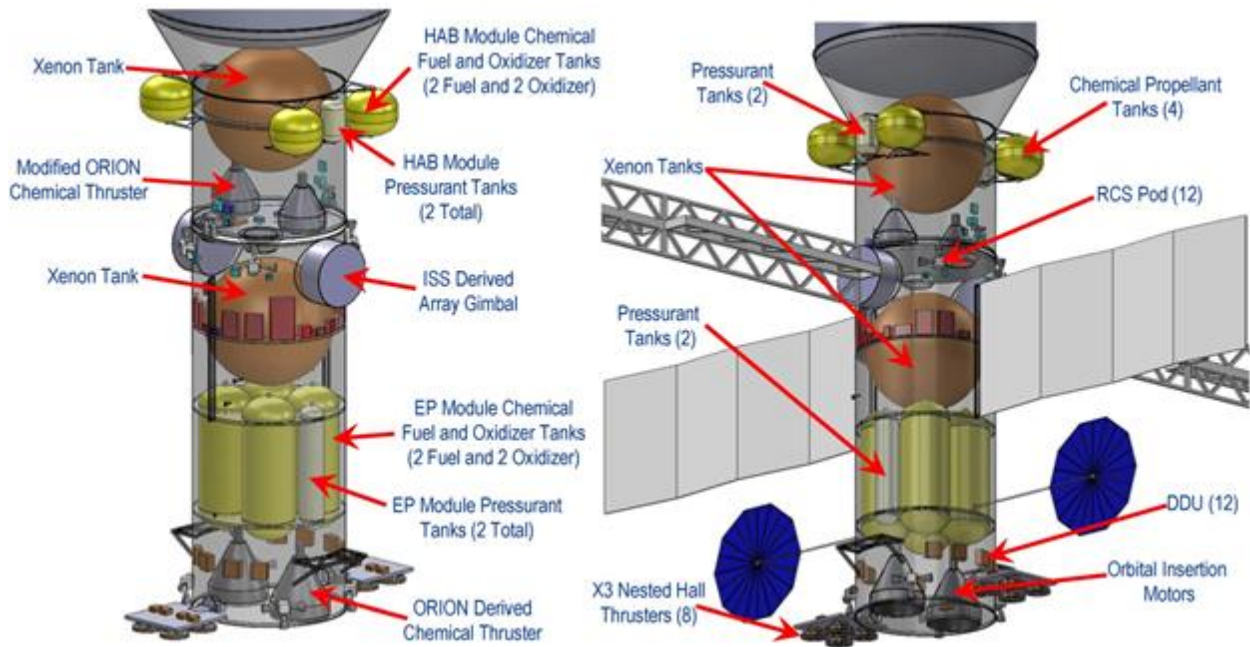


Figure 3-77 Internal bus components, including chemical thrusters and propellant system.

Radiators located directly below the solar array gimbals are pointed perpendicular to the arrays to point away from the sun to provide the best view for thermal rejection. All components of the thermal system were sized for the worst-case environmental conditions (LEO), with no redundancy. MMOD shielding was used to protect critical systems such as the propellant tanks and exposed heat pipes. Shielding by the aluminum structure is expected to be sufficient to protect electronics from radiation. The composite thrust tube design was sized to carry the mass of the DSH and space exploration vehicle during launch. All communications are assumed to be performed by the DSH, including relaying housekeeping commands and data for the SEP module. The mass of the major system elements are shown in Table 3-40. The mass of the DSH was provided by the Human Space Flight Architecture Team.¹⁰

Two cargo vehicles that precede the piloted SEP-Chem stage by one opportunity were each assumed to deliver 103-t aeroshells, one carrying a Mars lander and the other carrying the Mars landed habitat. The trajectories of both cargo missions use an all-SEP system, with the chemical propulsion system replaced by an additional tank of Xe propellant. Without the chemical stage to reduce the ΔV to that needed for Mars capture, the SEP cargo vehicle flies by Mars, and the cargo uses its aeroshell for aerocapture to deliver itself into Mars orbit.

3.3.4. Parametric Assessments of Power and Propulsion

Four propulsion variants were studied to determine their effect on the SEP-Chem vehicle mass and cost relative to the baseline: smaller nested Hall thrusters at a lower Isp, smaller single-channel Hall thrusters, nested Hall thrusters using a dual Isp and a conventional power processing unit, and cryogenic chemical propellant storage. Power variants were studied only to determine feasibility. Two bus voltages (500 V and 300 V), two solar array structures (roll out and fold out), and two types of array configurations (planar and concentrators) were considered, but detailed mass analyses were not done for these variants. The effect of each propulsion variant on trip time is provided in Table 3-41, Table 3-42 shows the ΔV for each portion of the trip for each variant, and the dry, wet, and inert masses for each are shown in Table 3-43. A description of each variant is provided in the following two sections.

Table 3-40 Mass Distribution of Baseline SEP-Chem Piloted Vehicle including the DSH

Main Subsystems	Basic Mass (kg)	Growth (kg)	Predicted Mass (kg)	Aggregate Growth (%)
SEP Mars Piloted Vehicle	234058	4256	238313	
SEP Piloted SLS Launch 1 - HAB Module	126660	848	127508	1%
Habitat and systems	53680	0	53680	0%
Attitude Determination and Control	92	3	95	3%
Command and Data Handling	47	10	57	21%
Communications and Tracking	0	0	0	TBD
Electrical Power Subsystem	46	23	69	50%
Thermal Control (Non-Propellant)	398	72	470	18%
Propulsion (Chemical Hardware)	1179	155	1334	13%
Propellant (Chemical)	9644		9644	0%
Propulsion (EP Hardware)	1509	127	1636	8%
Propellant (EP)	57359		57359	0%
Structures and Mechanisms	2706	458	3164	17%
Element 1 consumables (if used)	13992		13992	
Estimated Spacecraft Dry Mass (no prop,consum)	45665	848	46513	2%
Estimated Spacecraft Wet Mass	126660	848	127508	
L Growth Calculations SEP Piloted SLS Launch 1 - HAB Module				Total Growth
Dry Mass Desired System Level Growth	5977	1793	7771	30%
Additional Growth (carried at system level)		946		16%
Total Wet Mass with Growth	126660	1793	128454	
SEP Piloted SLS Launch 2 - SEP Module	107397	3408	110805	3%
Science	0	0	0	TBD
Attitude Determination and Control	45	1	47	3%
Command and Data Handling	121	23	144	19%
Communications and Tracking	55	15	70	28%
Electrical Power Subsystem	6915	1110	8025	16%
Thermal Control (Non-Propellant)	2506	451	2957	18%
Propulsion (Chemical Hardware)	2310	375	2685	16%
Propellant (Chemical)	34269		34269	0%
Propulsion EP Hardware)	3680	437	4117	12%
Propellant (EP)	51870		51870	0%
Structures and Mechanisms	5626	994	6620	18%
Element 2 consumables (if used)	0		0	
Estimated Spacecraft Dry Mass	21258	3408	24666	16%
Estimated Spacecraft Wet Mass	107397	3408	110805	
L Growth Calculations SEP Piloted SLS Launch 2 - SEP Module				Total Growth
Dry Mass Desired System Level Growth	21258	6377	27636	30%
Additional Growth (carried at system level)		2969		14%
Total Wet Mass with Growth	107397	6377	113775	

Table 3-41 Summary of Mission and Technology Options; Key Differences Between Options are Shown in Red

		SEP-Tug	SEP-Chem		SEP-Chem					All SEP	SEP Cargo
		all Chem	Earth Flyby		Baseline	LOX LCH ₄		PPU	all SEP	SEP Cargo	
		1.1	2.1	5.1	3.1	3.2	3.3	3.4	3.5	4.1	6.1
Transport	LEO to L2	SEP	SEP		SEP					SEP	SEP Cargo
	Earth / Moon depart flyby	Chem	Chem/SEP		None - SEP from L2					None - SEP from L2	None - SEP from L2
	Interplanet propulsion	None - coast	SEP		SEP					SEP	SEP
	Mars gravity well propulsion	Chemical	Chemical	SEP	Chemical					SEP	None - cargo aerocapture
	Mars parking orbit	Elliptic 1 sol	Elliptic 1 sol	Circular 1 sol	Elliptic 1 sol					Circular 1 sol	None - SEP flies by Mars
	Launch requirements	~4 SLS	2 SLS + 3 ATV		2 SLS + 2 ATV					2 SLS + 2 ATV	2 SLS (1 SEP + 1 aeroshell cargo)
	Outbound / Inbound transit time		344 / 315 days		439 / 326 days	416 / 321 days	470 / 330 days	439 / 326 days	405 / 337 days		
	Mars stay time	~500 days	367 days		300 days	300 days	270 days	300 days	300 days	45 days	N/A
	Total trip time		1026 days		1066 days	1037 days	1070 days	1066 days	1041 days		
	Power system	800 kW EOL / 1 AU, 500 V				800 kW EOL/1 AU, 500 V					800 kW, 500 V
Propulsion	Electric thruster type (Direct drive unless noted)	Nested Hall 8 @ 125 kW			Nested Hall 8 @ 125 kW	Nested Hall 12 @ 75 kW	Nested Hall 8 @ 125 kW	Hall 20 @ 50 kW	Nested Hall (PPU) 12 @ 75 kW		PPU
	Electric thruster Isp	2400 s			2400 s	2000 s		2400 s	3000 / 2140 s	2400 s	2870 s
	Xenon mass				109 mt						74 mt
	Chemical propulsion	Orion-derivative storable chemical propulsion (327 s Isp)			327 s Orion-derived		349 s LOX/LCH ₄	327 s Orion-derived		N/A	N/A
	Notes	SEP tug to L2 only	ATV tankers bring up 15 mt of biprops and crew consumables		ATV tankers bring up 18 mt of biprops and crew consumables - adds 3 months to stay time					Chemical tanks replaced with an additional Xe tank on SEP	Chemical tanks replaced with an additional Xe tank on SEP

Table 3-42 ΔV Summary for Each Variant

		SEP-Chem	SEP-Chem				
		Earth Flyby	Baseline			LOX LCH ₄	PPU
		2.1	3.1	3.2	3.3	3.4	3.5
ΔV (m/s)	Earth/E-M L2 Departure ΔV	3309 (SEP) / 68 (chem)	4204 (SEP)	3614 (SEP)	4063 (SEP)	4204 (SEP)	2064 (SEP)
	Moon Flyby ΔV	233					
	Mars Arrival ΔV	283 (SEP) / 794 (Chem)	391 (SEP) / 345 (Chem)	614 (SEP) / 309 (Chem)	383 (SEP) / 323 (Chem)	391 (SEP) / 345 (Chem)	647 (SEP) / 332 (Chem)
	Mars Departure ΔV	226 (Chem) / 2026 (SEP)	226 (Chem) / 2203 (SEP)	226 (Chem) / 2068 (SEP)	226 (Chem) / 2166 (SEP)	226 (Chem) / 2203 (SEP)	226 (Chem) / 2256 (SEP)
	Total trip ΔV		~1400 m/s SEP ~700 m/s Chem				

Table 3-43 Mass Summary for Each Variant

	SEP-Chem					SEP Cargo
	Baseline		LOX LCH ₄		PPU	SEP Cargo
	3.1	3.2	3.3	3.4	3.5	6.1
	SEP			SEP Cargo		
SEP Piloted SLS Launch 1 - HAB Module Totals						
SEP Piloted SLS Launch 1 - HAB Module Wet Mass	128	161	131	128	125	111
SEP Piloted SLS Launch 1 - HAB Module Dry Mass	47	48	50	47	48	105
SEP Piloted SLS Launch 1 - HAB Module Inert Mass	65	68	68	65	66	106
SEP Piloted SLS Launch 2 - SEP Module Totals						
SEP Piloted SLS Launch 2 - SEP Module Wet Mass	114	114	114	114	114	114
SEP Piloted SLS Launch 2 - SEP Module Dry Mass	28	30	30	28	33	32
SEP Piloted SLS Launch 2 - SEP Module Inert Mass	33	36	36	33	39	36
Combined Vehicle totals						
Total Vehicle Wet Mass (mt)	242	275	245	242	239	225
Total Vehicle Dry Mass (mt)	75	79	81	75	81	137
Total Vehicle Inert Mass (mt)	98	103	104	98	104	142

3.3.5. Propulsion Trades

At megawatt vehicle power levels, individual Hall thruster power levels of 50 to 100 kW provide a balance between integrated system complexity, fault tolerance, and mass and cost.¹¹ One variant was run using twenty 50-kW Hall thrusters at 2400 s and while this system is feasible, packaging this many individual thrusters was challenging. Nested Hall thrusters reduce integration and complexity and provide more continuous thrusting.

Because of the reduction in thruster footprint and specific mass, 125-kW nested-channel Hall thrusters traded well compared to single-channel monolithic Hall thrusters.¹² The nested Hall thruster performance used for this study was based on the measured performance of the AFRL/UofM X2 nested Hall thruster, predicted performance of the AFRL/UofM X3-80 nested-Hall thruster, and high-power single-channel Hall thruster data from the NASA 300M and 457Mv2 thrusters. The single-channel 50-kW Hall thruster data used for this study was based on measured NASA 457Mv2 thruster performance.¹³ Magnetic shielding is required to meet the thruster lifetime requirements for this mission.¹⁴

Hall thrusters are designed for a given current density of the channel. As the operating voltage is increased, at fixed current density, the thruster power level increases. The X3-80 nested Hall thruster operates at nominally 250 A when all channels are operating, and it can be operated at 175 kW at 700 V (3000 s Isp), 125 kW at 500 V (2400 s Isp), or at 75 kW at 3000 V (2000 s Isp). Similarly, the NASA 457Mv2 single-channel Hall thruster is nominally a 100-A device and can be operated at 70 kW at 700 V (3000 s Isp), 50 kW at 500 V (2400 s Isp), or at 30 kW at 300 V (2000 s Isp). For direct drive power processing, thruster Isp for the mission is fixed based upon the fixed solar array voltage. When using a power processing unit, variable Isp operation allows greater mission flexibility to optimize the electric propulsion system performance for different mission segments (e.g., 3000 s Earth spiral, 2000 s interplanetary) at the expense of mass and efficiency. Alternate propellants (e.g., Krypton) and thruster technologies (e.g., magnetoplasmadynamic) were considered but not selected because of storability/efficiency and maturity considerations, respectively.

One variant was run with a conventional PPU using twelve 75-kW nested Hall thrusters. This required a dual set point for the Isp: 3000 s during the unpiloted spiral to L2, and either 2140 or 3000 s for the piloted LEO to L2 spiral. The increased Isp increased this spiral trip time from 480 to 630 days. The use of PPUs instead of DDU's increases the system mass primarily because isolation transformers must be added to regulate the voltage generated by the solar arrays to match that needed by the thrusters, and bigger radiators are needed to reject the additional heat generated by the less efficient PPUs (~95% efficient PPU vs. 99% efficient DDU). PPU mass was assumed to be 100 kg each, although they may be as low as 88 kg. Note that while the DDU's reduce system mass, they potentially increase operational risk because of their inability to operate over wide voltage swings.

For the chemical thruster, Orion-derived storable systems provide better performance for the low impulsive ΔV (~600 m/s) SEP-Chem mission requirements when compared to cryogenic systems such as liquid oxygen

(LO_x)/liquid methane (LCH₄) due to lighter/denser storage systems. Table 3 shows that the use of LO_x/LCH₄ reduces the Mars stay time by 30 days, even as the total piloted trip time is slightly increased.

3.3.6. Power System Trades

The roll-out Mega-ROSA¹⁵ solar array design was used for all mass and packaging studies, and was found to notionally provide the required stowed dimensions to fit within the SLS fairing and to provide the needed strength and stiffness for deployed operation. The Mega-ROSA design chosen for the baseline used 10 winglets per wing. Each winglet's dimension is 8.7 m wide by 27.3 m long for a total wing area of 2383 m². The fold-out MegaFlex¹⁶ design was not included in the detailed studies because of time constraints, but it was determined that the circular MegaFlex arrays could be configured with two 30-m-diameter winglets on each side of the spacecraft to provide the needed power and allow for testing in existing ground-test facilities. Deployment booms would be needed to keep the circular arrays outside the cone of the electric thruster plume. In addition to the primary solar arrays, commissioning solar arrays were used for startup power and were derived from an Orion-based UltraFlex design. NASA relies on vendor-provided data to add realism to these concept designs and does not endorse any particular approach.

A 300-V bus voltage coupled with a high-power Hall thruster using a PPU has a larger inert mass than a 500-V system coupled directly to a 2400-s Hall thruster, but provides equivalent performance and more flexibility because it permits the Isp to be varied depending on mission phase or abort needs. The higher mass did not exceed mission requirements, so either a 300- or 500-V system could be considered.

Inverted metamorphic multijunction solar cells were baselined for these very large solar arrays because it is assumed that at launch time these will be the state of the art in space solar cells and therefore the most economical. Higher efficiency cells would of course be beneficial, but are not required. Using terrestrial cells with much lower efficiencies but lower unit costs per cell would not be prudent because of the need to oversize the arrays to accommodate both the lower power and the large expected radiation losses.

A 2X concentrator array based on “pop-up” flexible reflectors was designed to reduce the total area of photovoltaic cells. The areal size of the array must increase slightly (~10%) to account for the higher operating temperature of the concentrator cells while collecting sufficient solar flux. The concentrators lower the mass of the power system by about 6%, and they can potentially lower the cost of arrays by replacing high-cost solar cells with lower cost reflective elements. It is difficult to assess this cost savings because the concentrators will add complexity that will have some associated costs. The pointing requirements needed to maintain full illumination were sufficiently lax to maintain the ability for no-roll steering, so no other changes to the baseline configuration were required.

3.3.7. Results

Through this analysis it has been determined that power limited (<1 MW) SEP systems can perform piloted Mars missions especially when a relatively small storable bipropellant system is integrated. The addition of a small chemical stage into the architecture not only reduces the time to capture into Mars orbit, thus providing more useful exploration time, this strategy can place the SEP crew vehicle into an elliptical orbit at Mars, which can significantly reduce the propulsive burden on the Mars lander and ascent vehicles. This SEP-Chem system can deliver the crew vehicle to an elliptical 1-sol orbit similar to chemical or NTP systems, without requiring staging. With 800 kW at EOL, the SEP-Chem can provide 300-day Mars surface stay times for nominally 1050-day missions. The transit trip times (outbound ~400 days, inbound ~300 days) are longer than all-chemical or nuclear thermal rocket systems, but not substantially so. Although the trip duration is a little longer, and the surface stay a little shorter for the SEP concept, the total deep-space crew exposure may be acceptable as additional research on human performance are conducted on the ISS and other intermediate missions beyond LEO prior to the first human Mars mission. The SEP-Chem vehicle requires an unpowered transit of >400 days to spiral from LEO to E-M L2 to meet the crew, but this will not affect the total deep-space hazard exposure experienced by the crew.

Given the SLS delivery capabilities assumed for this analysis, it was found that the SLS payloads are about 6 t short for the current SEP-Chem concept, and some consumables or storable propellant (~18 t) will need to be delivered using vehicles similar to the Automated Transfer Vehicle (ATV). However, the planned SLS shroud (17 m cylindrical height) is larger than needed for the SEP-Chem concept payloads: if the shroud is shortened to 10 to 12

m, the increased payload capability could accommodate the additional mass and remove the requirement for an additional ATV-like launch. Either way, the number of SLS launches is substantially fewer than needed for all-chemical, or even NTP, systems.

Finally, SEP-Chem may have better reliability and abort capabilities because it has two propulsion systems and ample power.

The technologies able to most significantly reduce mass are a flexible blanket solar array, high-voltage power bus, nested Hall thrusters with dual Isp, and large xenon tanks. Each of these requires technology development to bring to flight readiness. A 300-V ‘Mega’ solar array coupled with a high-power Hall thruster using a PPU, although heavier inertly, provides equivalent performance and more flexibility (due to variable Isp depending on mission phase or abort needs) than a 500-V solar array coupled with a direct-drive 2400-s Hall thruster.

There are limits to the results of these studies. If a different mission is selected, or if additional abort constraints are included, or if a different suite of technologies is considered, the results will change. For instance, these results are applicable for an architecture where a single habitat is used to transport the crew from near-Earth locations, to Mars orbit, and back. Power levels can be reduced if a new architecture is envisioned whereby additional mission assets, such as orbiting habitats or return stages, are pre-deployed ahead of the crew and a smaller habitat is used for the outbound leg. However, we believe that these results are reasonable and provide insight into the relative benefits of key power and propulsion technologies for solar electric vehicles of this class of mission.

Solar electric propulsion technologies currently being developed by NASA’s Game Changing Technology Development program are laying the foundation needed for SEP vehicles of this class. In particular, the MegaFlex and Mega-ROSA solar array concepts have a credible chance of scaling up to the nominally 1-MW BOL sizes needed for this mission, with ample room for stowage within the SLS launch vehicle. 20-kW-class wings are being built and tested at the time of this writing, and a nominally 50-kW-sized flight demonstration coupled with analysis and ground deployment tests of very large wings would do much to reduce the technical risk for much larger systems. A previous study¹⁷ showed the capabilities of a 300-kW SEP system to transport crew to a near-Earth asteroid requiring 150 kW per wing. A progression of 30-kW, then 150-kW, then 500-kW wings is a reasonable technical progression. Similarly, 125-kW nested Hall thrusters for Mars are a reasonable extension of current laboratory work on 100-kW-class nested Hall thrusters.¹⁸ Although there are technical risks associated with vehicles this large, the system builds upon technologies that are currently at a high state of development and is well within the realm of feasibility and practicality.

3.3.8. Conclusion

Vehicle concepts were assessed to determine the applicability of using SEP technology for piloted Mars missions as well as to understand the key technology needs. These analyses have shown that power-limited SEP vehicle concepts are viable for human exploration of Mars, especially when high-thrust chemical systems are included as part of the vehicle architecture. The addition of chemical systems can be used to increase the exploration time at Mars as well as place the SEP vehicle into a more favorable elliptical parking orbit. Power required for this vehicle concept was limited to less than 1 MW of total power, adding further to the viability of the concept. These SEP concepts require fewer heavy lift launches compared to other transportation technologies being considered. They also package well into the launch vehicle shrouds and can serve as the transportation vehicle for both crew and unpiloted cargo delivery to Mars. Although reference concepts and implementations have been provided in this paper, many design trades on specific technology implementations and mission modes remain.

3.3.9. Acknowledgments

The authors gratefully acknowledge the efforts of the COMPASS team at the NASA Glenn Research Center: Melissa McGuire, Micheal Martini, David Grantier, Laura Burke, James Fittje, Dan Herman, John Gyekenyesi, Anthony Colozza, Kristen Bury, James Fincannon, Glenn Williams, Joe Warner, Tom Packard, Jon Drexler, and Anita Tenteris. This work was supported by the SEP Project in the Game Changing Technology Development Program within NASA’s Space Technology Mission Directorate.

3.4. Bibliography

- ¹ Koenig D. R. (1986) Experience Gained from the Space Nuclear Rocket Program (Rover), LA-10062-H, Los Alamos National Laboratory, Los Alamos, NM
- ² Borowski S. K., D. R. McCurdy and T. W. Packard (2012) “Nuclear Thermal Propulsion (NTP): A Proven Growth Technology for Human NEO / Mars Exploration Missions,” 2012 IEEE Aerospace Conference, Big Sky, MT, March 3-10, 2012
- ³ Bhattacharyya S., “A Rationale Strategy for NTR Development”, AIAA Joint Propulsion Conference, AIAA-2011-5945, San Diego, CA
- ⁴ NASA, “Human Exploration of Mars Design Reference Architecture 5.0”, NASA-SP-2009-566, July 2009.
- ⁵ Collaborative Modeling for Parametric Assessment of Space Systems
<http://www.grc.nasa.gov/WWW/compass/> [cited 19 Aug 2013].
- ⁶ Rapid Calculation of Spacecraft Trajectories Using Efficient Taylor Series Integration,” NASA Tech Briefs, Jan. 1, 2011 <http://www.techbriefs.com/component/content/article/9031> [cited 19 Aug 2013].
- ⁷ The In-Space Propulsion Technology Project Low-Thrust Trajectory Tool Suite: MALTO
http://ntrs.nasa.gov/archive/nasa/casi.ntrs.nasa.gov/20080047350_2008047178.pdf [cited 19 Aug 2013].
- ⁸ Burke, L.M, Martini, M.C., and Oleson, S.R. “A High Power Solar Electric Propulsion–Chemical Mission for Human Exploration of Mars,” to be published as a NASA Technical Report in 2013.
- ⁹ Hoffman, D. et al., “Concept Design of High Power Solar Electric Propulsion Vehicles for Human Exploration,” Presented at the 62nd International Astronautical Congress, Cape Town, South Africa, Oct 3-7, 2011, IAC-11-D2.3.5.
- ¹⁰ NASA, “HAT Cycle C: Mars Transit Habitat and Mars Surface Habitat Modeling”, Internal document, August 18, 2011.
- ¹¹ Hofer, R.R, and Randolph, T.M., “Mass and Cost Model for Selecting Thruster Size in Electric Propulsion Systems,” Journal of Propulsion and Power, Vol. 29, No. 1, 2013.
- ¹² Brown, D.L., Beal, B.E., and Haas, J.M., “Air Force Research Laboratory High Power Electric Propulsion Technology Development,” 2010 IEEE Aerospace Conference, Big Sky, MT, March 6-13, 2010.
- ¹³ Soulas, G.C, Haag, T.W., Herman, D.A., Huang, W., Kamhawi, H., and Shastry, R., “Performance Test Results of the NASA-457M v2 Hall Thruster,” 48th AIAA/ASME/SAE/ASEE Joint Propulsion Conference, Atlanta, GA, July 30 – August 1, 2012.
- ¹⁴ Mikelides, I.G., Katz, I., Hofer, R.R., and Goebel, D.M., “Magnetic Shielding of Walls from the Unmagnetized Ion Beam in a Hall Thruster,” Applied Physics Letters Vol. 102 January 2013
- ¹⁵ White, S. et al., “Mega-ROSA Solar Array – Highly Modular Game-Changing Solar Array Technology for NASA SEP and DoD Ultra-High Power Missions,” Presented at the 31st Annual Space Power Workshop, Manhattan Beach, CA, April 22-25, 2013.
- ¹⁶ Eskenazi, M., Murphy, D., McEachen, M., and Spink, J. “MegaFlex – Near Term High Power for Solar Electric Propulsion,” Presented at the 31st Annual Space Power Workshop, Manhattan Beach, CA, April 22-25, 2013.
- ¹⁷ Brophy, J.R., Gershman, R., Strange, N., Landau, D., Merricll, R., and Kerslake, T., “300-kW Solar Electric Propulsion System Configuration for Human Exploration of Near-Earth Asteroids,” AIAA/ASME/SAE/ASEE Joint Propulsion Conference, San Diego, CA, July 31 – August 3, 2011.
- ¹⁸ Florenz, R., Gallimore, A.D., and Peterson, P.Y., “Developmental Status of a 100-kW Class Laboratory Nested Channel Hall Thruster,” 32nd International Electric Propulsion Conference, Wiesbaden, Germany, September 11 – 15, 2011.

Selected additional references pertaining to Nuclear Electric Propulsion

System

AIAA S-120-2006, AIAA Standard Mass Properties Control for Space Systems.

ANSI/AIAA R-020A-1999, Recommended Practice for Mass Properties Control for Satellites, Missiles, and Launch Vehicles.

Larson, W.J. and Wertz, J.R. (eds.), (1999) Space Mission Analysis and Design, Third Edition, Space Technology Library, Microcosm Press.

Mission

- Anderson, David J., Pencil, Eric J., Liou, Larry C., Dankanich, John W., Munk, Michelle M., and Hahne, David, (2010), “The NASA In-Space Propulsion Technology Project’s Current Products and Future Directions,” AIAA–2010–6648, 46th AIAA/ASME/SAE/ASEE Joint Propulsion Conference & Exhibit, July 25–28, 2010, Nashville, TN.
- “COMPASS Final Report: Mars Earth Return Vehicle (MERV),” CD–2009–31, February–March 2009.
- Desai, P.N., Braun, R.D., Engelund, W.C., Cheatwood, F.M., Kangas J.A., (1998), “Mars Ascent Vehicle Flight Analysis,” 7th AIAA/ASME Joint Thermophysics and Heat Transfer Conference June 15–18, 1998, Albuquerque, NM, AIAA 98-2850.
- Dillman, Robert and Corliss, James, (2008), “Overview of the Mars Sample Return Earth Entry Vehicle,” Sixth International Planetary Probe Workshop, June 26, 2008.
- Dux Ian J., Huwaldt, Joseph A., McKamey, R. Steve, Dankanich, John W., (2010) Mars Ascent Vehicle Gross Liftoff Mass Sensitivities for Robotic Mars Sample Return, NASA Deep Space Missions, NASA TM 2010.
- ESA Aurora Program, http://www.esa.int/esaMI/Aurora/SEMCWB1A6BD_0.html
- Holmberg, Neil A.; Robert P. Faust, H. Milton Holt (1980), “Viking ‘75 Spacecraft Design and Test Summary Volume III–Engineering Test Summary,” NASA Reference Publication 1027, Nov. 1980.
- Johnston, M.D., Esposito, P.B., Alwar, V., Demcak, S.W., Graat, E.J., and Mase, R.A. (1998), “Mars Global Surveyor Aerobraking at Mars,” AAS 98-112 <http://Mars.jpl.nasa.gov/mgs/sci/aerobrake/SFMech.html>
- Matousek, S., Adler, M., Lee, W., Miller, S.L., Weinstein, S., (1998), “A Few Good Rocks: The Mars Sample Return Mission Architecture,” AIAA/AAS Astrodynamics Specialist Conference, August 10–12, 1998, Boston, MA, AIAA–98–4282.
- Palaszewski, B. and Frisbee, R., (1988), “Advanced Propulsion for the Mars Rover Sample Return Mission,” AIAA–88–2900, AIAA/ ASME/SAE/ASEE 24th Joint Propulsion Conference, July 11–13, 1988, Boston, MA
- Preliminary Planning for an International Mars Sample Return Mission, Report of the International Mars Architecture for the Return of Samples (iMARS) Working Group, June 1, 2008.
- Rose, J., (1989), “Conceptual Design of the Mars Rover Sample Return System,” 27th Aerospace Sciences Meeting, Jan. 9–12, 1989, Reno, NV, AIAA–89–0418.
- Spencer, D.A., Tolson, R., (2007), “Aerobraking Cost and Design Considerations,” Journal of Spacecraft and Rockets, Vol. 44, No. 6, Nov/Dec. 2007
- Stephenson, David, (2002), “Mars Ascent Vehicle—Concept Development,” 38th Joint Propulsion Conference and Exhibit, July 7–10, 2002, Indianapolis, IN, AIAA 2002-4318.
- Whitehead, John C., (1997), “Mars Ascent Propulsion Options for Small Sample Return Vehicles.” 33rd AIAA/ASME/SAE/ASEE Joint Propulsion Conference and Exhibit, July 6–9, 1997, Seattle, WA, AIAA 97-2950.
- Williams, R., Gao, Y., Kluever, C.A., Cupples, M., and Belcher, J., (2005), “Interplanetary Sample Return Missions Using Radioisotope Electric Propulsion,” 41st AIAA/ASME/SAE/ASEE Joint Propulsion Conference & Exhibit, July 10–13, 2005, Tucson, AZ, AIAA–2005–4273.
- Zubrin, Robert, (1996), “A comparison of approaches for the Mars Sample Return Mission,” AIAA 34th Aerospace Sciences Meeting and Exhibit, Reno, NV, Jan. 15–18, 1996, A9618450, AIAA Paper 96-0489.

GN&C

- L. Norris, Y.C. Tao, R. Hall, J. Chuang, M. Whorton, “Analysis of Ares I Ascent Navigation Options”, AIAA 2008-6290.

Structures

- D. Persons, L. Mosher, T. Hartka, (2000), “The NEAR and MESSENGER Spacecraft: Two Approaches to Structure and Propulsion Design,” AIAA–00–1406, A00-24531.
- Zibdeh, Hazim S., and Heller, Robert A., (1989), “Rocket motor Service Life Calculations Based on the First-Passage Method,” Virginia Polytechnic Institute and State University, Blacksburg, VA, Journal of Spacecraft and Rockets, 0022-4650, Vol. 26, No. 4 pp. 279–284.

Thermal

Aerodynamic Heating Wikipedia entry. http://en.wikipedia.org/wiki/Aerodynamic_heating

Alexander, M. (ed.) (2001), “Mars Transportation Environment Definition Document,” NASA/TM—2001-210935.

Bejan, A. and Kraus, A.D., (2003), Heat Transfer Handbook, John Wiley & Sons.

Chapman, A.J., (1974), Heat Transfer, Third Edition, Macmillan Publishing Company.

Gilmore, David G. (ed.), (2002), Spacecraft Thermal Control Handbook: Volume 1 Fundamental Technologies, AIAA.

Hyder, A.J., Wiley, R.L., Halpert, G., Flood, D.J. and Sabripour, S., (2000), Spacecraft Power Technologies, Imperial College Press.

Incopera, F.P. and DeWitt, D.P., (1990), Fundamentals of Heat and Mass Transfer, John Wiley and Sons.

Larson, W.J. and Wertz, J.R. (eds.), (1999), Space Mission Analysis and Design, Third Edition, Space Technology Library, Microcosm Press.

Olds, J. and Walberg, G., (1993), “Multidisciplinary Design of Rocket-Based Combined Cycle SSTO Launch Vehicle using Taguchi Methods,” AIAA 93-1096, AIAA/AHS/ASEE Aerospace Design Conference, February 16-19, 1993, Irvine, CA.

Penuela, David, Simon, Mathew, Bemis, Eammon, Hough, Steven, Zaleski, Kristina, Jefferies, Sharon and Winski, Rick, “Investigation of Possible Heliocentric Orbiter Applications for Crewed Mars Missions,” NIA/Georgia Institute of Technology, Project 1004. http://www.nianet.org/rascal/forum2006/presentations/1004_nia_paper.pdf

RP-07-100_05-019-I; Volume I: Ice Mitigation Approaches for Space Shuttle External Tank Final Report.

Sutton, Kenneth and Graves, Randolph A. Jr., (1971), “A General Stagnation Point Convective-Heating Equation for Arbitrary Gas Mixtures,” NASA TR R-376.

This page intentionally left blank

4 MARS ENTRY, DESCENT, AND LANDING

Primary Contributors:

Cindy Albertson, National Aeronautics and Space Administration, Langley Research Center
Leslie Alexander, National Aeronautics and Space Administration, Marshall Space Flight Center
Kendall Brown, National Aeronautics and Space Administration, Marshall Space Flight Center
Tim Collins, National Aeronautics and Space Administration, Langley Research Center
Alicia Dwyer Cianciolo, National Aeronautics and Space Administration, Langley Research Center
Rob Grover, Jet Propulsion Laboratory
Larry Kos, National Aeronautics and Space Administration, Marshall Space Flight Center
Roger Lepsch, National Aeronautics and Space Administration, Langley Research Center
Michelle Munk, National Aeronautics and Space Administration, Langley Research Center
Philip Nerren, National Aeronautics and Space Administration, Marshall Space Flight Center
Tara Polsgrove, National Aeronautics and Space Administration, Marshall Space Flight Center
Michelle Rucker, National Aeronautics and Space Administration, Lyndon B. Johnson Space Flight Center
Ron Sostaric, National Aeronautics and Space Administration, Lyndon B. Johnson Space Flight Center

4.1 Section Summary

To enable delivery of payloads to the Martian surface of the size and mass suitable to support human-scale missions, viable approaches to the critical EDL phases of flight must be devised and investigated. Prior to the Human Architecture Team (HAT) studies described here, a significant amount of analysis on EDL approaches was performed during the EDL Systems Analysis (EDL-SA) study.³ From the results and recommendations of that study, a number of areas for further work were identified. These included: detailed lander concept definition, lander/aero-assist system integration and packaging, and transition from aerodynamic to powered flight during descent. Two particular aero-assist architectures highlighted for further investigation were the mid-Lift to Drag (L/D) rigid aeroshell and the Hypersonic Inflatable Aerodynamic Decelerator (HIAD).

The definition of detailed lander point designs was undertaken during the HAT Cycle D study phase to provide greater insight into potential integration and packaging issues between the lander and its entry aero-assist system and/or the launch vehicle. Design aspects of the landers were also influenced by the ability to carry specific payloads and by surface operations. The point designs allowed determination of mass properties necessary to assess the suitability of certain aero-assist/lander combinations with regard to aerodynamic stability and control during entry. The mass estimates produced also provided verification data for higher-level, parametric sizing models.

Prior to defining detailed lander concepts, a series of high-level sizing investigations was performed in HAT Cycle C, bounding the size and mass of the Mars lander. These included trade studies and sensitivities on the number of crew, Mars rendezvous orbit, payload delivery capacity, sample return payload capacity, number of lander stages, extent of in situ resource utilization (ISRU) for propellant, propulsion types, and propulsion performance parameters. The investigations initially made use of first-order sizing techniques to examine a wide trade space. This was followed by the use of a more detailed parametric modeling tool (ENVISION) to focus on a narrower trade space and also to set a design point-of-departure for further detailed study.

The Mars lander concepts assessed in the studies were each defined to consist of a Mars Ascent Vehicle (MAV) and a Mars Descent Module (MDM). The MAV design, along with its requirements, has a large influence on the overall lander mass and size. The high-level sizing investigations examined a number of important sizing factors for the MAV, the most important ones being: the number of vehicle phases/stages (one or two), the parking/rendezvous orbit (low or high), and the choice of propulsion system and propellants – Nitrogen Tetroxide/Monomethyl Hydrazine (NTO/MMH), liquid oxygen/liquid methane (LOX/LCH₄), or liquid oxygen/liquid hydrogen (LOX/LH₂).

With certain propellant choices, there is an opportunity to utilize ISRU on the Martian surface to supply MAV ascent propellant. It was found (or reconfirmed) that a propellant choice that enables ISRU combined with a high Mars parking orbit assumption allows a significantly more mass-efficient overall transportation architecture.

Assuming a high rather than low orbit means that more propellant can be supplied by ISRU, reducing the total propellant mass brought from Earth. The disadvantage of a high parking orbit is that keeping the crew in the ascent vehicle for a longer ascent will drive the ascent vehicle's mass. Among the propellant choices investigated, the LOX/LCH₄ combination is seen as most attractive. Both propellants are producible on Mars with atmospheric ISRU (using seed H₂ brought from Earth) rather than requiring resources mined from below the Martian surface. Results show that most of the benefits of ISRU can be obtained with only LOX being generated. Also, in comparison with LH₂, LCH₄ is an easier-to-store cryogen, and reduces tank volume requirements for the lander due to its higher density.

Ascent performance results showed a mass advantage for a two-stage MAV approach compared with a single-stage approach, due to staging efficiency. This advantage would be achieved at some expense of ascent reliability due to the staging event, with a corresponding increase in probability of loss of crew, which will need to be assessed in a future effort. A summary of the trajectory assessment work that supported the MAV performance analysis is shown in Section 4.2. A more detailed summary of the high-level MAV sizing work and trade study results is found in Section 4.3.1.

With initial sizing data on the MAV in hand, trades and sensitivities were conducted on the descent module, the primary ones being the payload capacity and propulsion type. The payload delivery capacity was varied in a trade study to envelope the anticipated range of payload masses (10 – 40 t), consisting of the MAV and surface systems. The propulsion options examined included LOX/LH₂ and LOX/LCH₄ types. Only small differences in MDM mass were noted between the propulsion options, indicating that a LOX/LCH₄ propulsion system would be a logical choice to allow potential commonality in engines with the MAV. A more detailed summary of the MDM sizing work and trade study results can be found in Section 4.3.2.

After the conclusion of the high-level sizing studies, and guided by the results from those, a narrower trade space was defined for the more detailed parametric sizing studies. The MAV was sized for only the two-stage scenarios, both for low and high Mars parking orbits. The propulsion type selected was LOX/LCH₄. The propulsion options sized were 1) bringing all ascent propellant from Earth (no ISRU), 2) bringing just fuel from Earth (LOX-only ISRU), and 3) bringing no ascent propellant (full ISRU). The crew options were four and six crew. The first stage of the MAV is powered by four pump-fed engines each with a maximum thrust of 97.9 kN (22,000 lbf) and Isp of 355 s. A single engine of the same type and performance powers the second stage. To develop commonality between the MAV and the MDM, the MDM was assumed to use four of the same LOX/LCH₄ engines used on the MAV, providing a total descent maximum thrust of 391 kN (88,000 lbf). For the sizing work, a descent delta-v of 800 m/s (approximately the same as in the high-level sizing studies) was assumed, being representative of that achievable with use of an entry aero-assist system designed for deceleration to supersonic speeds.

Building on lander vehicle sizing experience gained during Constellation's Altair Project, the parametric sizing analysis of the MAV and MDM was performed with the ENVISION vehicle sizing tool. Among many others, the ENVISION tool takes as inputs required delta-v, crew size, use duration and expected accelerations, and outputs vehicle and propellant masses. Because of the similarities in expected use for the Altair lunar lander and the HAT Mars lander, the ENVISION tool as configured for Altair served as a good first pass at sizing descent and ascent vehicles for Mars. ENVISION was used to size vehicles for a sweep of landed payloads from 20 t to 60 t. For a landed payload of 40 t, the ENVISION-derived descent vehicle mass is 5-6 t more massive than the Design Reference Architecture 5.0² (DRA 5.0) Mars lander. Limitations on the sizing included the assumption of fixed descent thrust across all lander sizes resulting in unrealistically low descent initial thrust-to-weight (T/W_0) for the more massive landers. This simplification was removed in follow-on work described in Section 4.8.4. A more detailed summary of the ENVISION sizing work is found in Section 4.3.3 and Section 4.3.4.

To provide an independent lander sizing assessment for both the mid L/D and HIAD architectures, a study was commissioned utilizing Jet Propulsion Laboratory's (JPL's) Advanced Projects Design Team, called TeamX. TeamX was provided the architectural framework of the mid L/D and HIAD architectures, and was asked to design and size vehicles capable of executing the architectures, focusing primarily on the powered descent landers. TeamX was also asked to design the sequence of events required to execute the challenging supersonic transition from aero-assisted flight to powered descent. The resulting vehicle designs had wet entry masses of 98.5 t for the mid L/D system and 85.7 t for the HIAD system. The TeamX mid L/D wet entry mass agrees well with the DRA 5.0 wet entry mass. In the course of the study, TeamX also generated a high-level architectural risk assessment containing

13 unrated risks. Among the risks identified by TeamX: vehicle mass for human missions is more than an order of magnitude greater than our current experience base, precision landing drives system risk, and the use of aerocapture drives arrival risk. A more detailed summary of the TeamX study can be found in Section 4.4.

Following the ENVISION and TeamX assessments, a bottoms-up effort was conducted to obtain Mars lander configurations and structural mass estimates having greater fidelity than is possible with spreadsheet or parametric analysis. This process began with a brainstorming activity intended to produce a variety of representative and feasible lander configurations. The brainstorming activity focused on the placement of propellant tanks, cargo, engines, and a MAV within the available shroud diameter and launch volume. The results of the earlier ENVISION analysis were used to provide the propellant mass and tank volume assumptions for the descent modules. Notional structural arrangements (including landing gear placement) were also considered. The purpose of the brainstorming activity was to generate feasible concepts for further consideration. Eight lander configurations (four horizontal and four vertical) were generated and ranked by the Mars lander team as a whole using the analytical hierarchy process (AHP). Two lander configurations (one horizontal and one vertical) were down selected for detailed modeling and analysis. A more detailed description of the brainstorming activity and configuration down-selection process and results can be found in Sections 4.6.3 and 4.6.4, respectively.

After down selection, computer aided design (CAD) models used during the brainstorming phase were refined and converted into finite-element analysis models. Strength, buckling, and normal modes (frequency) analyses were conducted for the two down-selected configurations. The results of the analyses were used to refine the CAD representations and to generate Master Equipment Lists (MELs). The masses of some components not included in the detailed analyses (such as porch and ladder structure) were estimated based on previous experience. The mass estimates for each lander were compared to preliminary TeamX estimates for similar (but different) configurations. Mass moments of inertia and center of gravity locations were also determined for each lander configuration and will be used in future trajectory and entry analyses. A more detailed summary of the structures sizing and mass properties analyses can be found in Section 4.6.5. Finally, for the lander configurations investigated, preliminary options for launch vehicle integration were considered, including possible implications for the aeroassist system and transition/entry events. Details of these options can be found in Section 4.6.7.

The propulsion system definition for the point-design lander configurations was validated through first-order parametric analysis. The propellant and propulsion system definition began with the MAV, and the descent stage propulsion system was evaluated based upon commonality concepts. The parametric analysis identified that the use of in-situ produced propellant allows for significantly more capability on the Mars surface for a given Mars arrival mass, with in-situ oxygen produced via atmospheric processing as being a good balance for overall system performance and packaging. With oxygen selected as the oxidizer, numerous hydrocarbon fuels could be considered; however, with methane having similar thermodynamic characteristics and with good specific impulse, it was chosen for this conceptual design activity. While hydrogen can provide significantly greater specific impulse, the fuel tank volume and additional cryogenic fluid management required makes its use problematic. The thrust level and propellant volume needed to reach a High Mars Orbit (HMO) rendezvous with the Mars Transfer Vehicle indicate that turbopump-fed engines are required. A single 100 kN engine is needed for the second stage, and a thrust of 300kN is needed for the first stage. To provide for engine-out at liftoff, a fourth engine was assumed with the engines operating at 75% power level. From previous EDL analysis with HIADs and rigid aeroshells the powered descent thrust to landing 40t of cargo was shown to be in the range of 800 kN to 1,600 kN. A total thrust level of 1,200 kN was chosen to begin the MDM configuration studies while integrated EDL trajectory analysis was ongoing. To achieve 1,200 kN of total thrust, 12 engine thrust chamber assemblies (TCAs) were assumed to maintain commonality with the MAV main engine. However, to increase reliability, it was assumed that two TCAs would be configured with a new single turbopump to create a 200 kN engine system. This configuration represents a derivative development program that will be less expensive than two different engines for ascent and descent. This configuration also assists in packaging and allows the vehicle to be closer to the surface for unloading cargo and crew access to the habitat. Additional engine details can be found in Section 4.7.1.

The mission operational timeline requires that the MDM and MAV propellants be stored for extended time in space and on the Mars surface; as such, the solar radiation in space and the radiation and atmospheric environment on the surface will have a net heat transfer to the tanks. The cryogenic fluid management (CFM) system is configured to maintain the cryogenic propellants without propellant loss with the use of a cryo-cooler system that circulates cold helium to a vapor-cooled-shield system (VCS) that is attached to the tank external wall to intercept the radiative and

conductive heat transfer, with multi-layer insulation on top of the VCS to reduce the heat gain. Within the tanks, a thermodynamic vent system is also used to account for the residual heat gain and to ensure the propellants are not thermally stratified. Depending upon the radiation environment and the attitude of the vehicle, the cryocooler system can have a large power demand, which can be a significant consideration in the sizing of the Power and Thermal systems. The ISRU processing equipment is located in the MDM and gaseous oxygen is fed to the MAV oxidizer tanks. The cryocooler system is configured so that the VCS condenses the oxygen at the tank. A more detailed summary of the CFM subsystem and associated analyses can be found in Section 4.7.2.

To generate a full mass build-up of the point-design vertical and horizontal MDM configurations, a MEL was defined with mass originating from several sources: historical heritage hardware, previous spacecraft studies, and calculations from CAD models. The Altair lunar lander was a large source of data for component definition and mass. The structural definition was derived and calculated directly from CAD models for the two Mars lander configurations. The vertical MDM dry mass totaled nearly 13 t and the horizontal MDM dry mass totaled to 15.5 t, the primary mass difference coming from the structures subsystem. These dry masses included a 30% addition to account for a combination of mass growth allowance and margin. A more complete description of MDM physical design, including subsystem hardware and masses can be found in Section 4.8.1 and Section 4.8.3.

To determine the payload capability of the point-design vertical and horizontal lander configurations, descent trajectory analyses were conducted and a parametric sizing model was utilized. The sizing model, developed during the EDL-SA study, accounted for all systems required at Mars atmospheric interface and was adjusted to match the mass and engine performance characteristics of the point-design landers. Different engine throttle strategies were also examined to understand the impact this choice would have on payload performance. Payload is defined to include the MAV and surface cargo elements and has a target value of 40 t. The vertical and horizontal landers assume use of a HIAD and a mid-L/D rigid aeroshell as their respective aero-assist systems for deceleration to supersonic conditions, where rocket-powered decent is initiated. The descent modules employ six LOX/LCH₄ engines of 200 kN (45 klbf) maximum thrust each and a vacuum Isp of 360 s. Depending on the throttle strategy employed, the resulting payload capability ranged from 49 to 58 t for the vertical lander-HIAD combination and from 37 to 52 t for the horizontal lander-aeroshell combination, with the most payload being achieved with a potentially higher-risk 100% throttle setting strategy. The entry mass of those same systems ranged from 101 to 112 t and from 109 to 126 t, respectively, which were higher than DRA 5.0 and JPL TeamX estimates. In general, payload results indicate that the propellant mass quantities from the ENVISION analysis may have been overly conservative (particularly for the vertical lander plus HIAD) due to different engine Isp assumptions, and reducing propellant mass would allow a better match of the payload capability to the 40-t target value, as well as reduce the overall Mars orbit arrival mass. A more detailed summary of the descent performance and payload capability analysis is found in Section 4.8.4.

As part of the point-design lander definitions, detailed assessments of the MAV were conducted. The crew cabin is a particularly important design aspect of the MAV. In sizing the crew cabin, two pieces of information are critical: 1) which suits (extravehicular activity [EVA] or intravehicular activity [IVA]) will the crew wear? And, 2) will the crew need to don/doff suits inside the MAV? Both suits require considerable “elbow room” for don/doff and, once off, require significant stowage volume—all of which increases MAV mass. Once the suits come off, additional crew provisions (such as waste/hygiene) are required, which further increases the MAV’s mass. Whether the suits come off during ascent is largely a function of ascent duration—hence the interest in a Low Mars Orbit (LMO) trip that takes less than a day, versus an HMO rendezvous duration of 43 hours, including contingencies.

The MAV study team leveraged earlier work supporting crewed Lunar expeditions to develop a conceptual MAV. First, a 4-crew baseline MAV concept was patterned after the Constellation Program’s 4-crew Altair Ascent Module. Because Altair was outfitted for a week-long mission, this baseline design easily enveloped the 43 hour HMO ascent timeline, plus a few days of shirt-sleeve crewed system check-outs prior to lift-off from the Martian surface. With surface resupply, this “habitable” MAV could be used to either supplement or back up the Mars Surface Habitat (SHAB), potentially allowing the SHAB to shrink in size and/or mass, which would in turn allow the Lander to shrink in size/mass. The first design variant was achieved by expanding the cabin diameter and outfitting for six crew members. These two variants—one for 4 crew, the other for 6 crew—together are referred to as the “Habitable” MAVs. Although the avionics, life support, habitability, EVA, and cabin structure were relatively well characterized, extrapolating the single LOX/LH₂ Lunar propulsion stage to a two-stage LOX/Methane Mars vehicle was difficult without detailed design analysis; for the purpose of this exercise, broad assumptions were made

for the first propulsion stage, thermal, and power subsystems, with further design refinement left as forward work. For the purpose of exploring alternative architecture options, the MAV Study Team also considered 4- and 6-crew “Taxi” MAVs, drawn from work previously performed on the Lunar Orbit Rendezvous (LOR) study. Intended as a brief (12 hour or less) “taxi” ride to Lunar Orbit, the LOX-Methane LOR Ascent Module had virtually no habitability provisions and represented the lower mass boundary for a pressurized ascent vehicle. Although a similar Mars “taxi” ascent vehicle would force the deep space habitat (DSH) to rendezvous in a lower Mars orbit, the study team wanted to explore whether the lower cabin mass could offset the DSH fuel penalty. As with the Habitable concept extrapolation, many subsystems were relatively well characterized but broad assumptions had to be made for the Taxi concept’s first propulsion stage, thermal, and power subsystems, with further design refinement left as forward work. The detailed descriptions and mass build-ups of the MAV options assessed are found in Section 4.9.

Following the recommendations of the EDL-SA study, HAT Cycle C work focused on the mid-L/D rigid aeroshell and the HIAD for hypersonic deceleration, both transitioning to supersonic retropropulsion (SRP), a system that also performs the subsonic terminal descent. Both architectures still appear feasible following Cycles C and D. Further refinement of the aeroentry and descent portions of DRA 5 requires the configuration work described in Sections 4.6 and 4.7, to enable 6-degree-of-freedom simulations, stability analyses, and more detailed definition of the systems required and the risk associated with transitioning from the hypersonic to the supersonic vehicle configurations. In preparation for this, a preliminary assessment of transition options was conducted, and is described in Section 4.10.

The transition from aero-assisted supersonic flight to supersonic-powered descent is called the transition event. It involves both a separation of elements and a reconfiguration of the vehicle, and has been identified as a particular challenge area for landing humans on Mars. The EDL-SA study put forth effort to identify promising techniques for executing the transition event for both the mid L/D and HIAD architectures. Building upon that work, this report contains a summary of a figure of merit (FOM)-based assessment carried out on 15 options for the mid L/D transition event and 11 options for the HIAD transition event. A team provided a high-level assessment based on projected mass, mechanical complexity, propulsion challenge, and recontact risks, among other FOMs. The assessment found a clamshell style opening of the aeroshell followed by transition to powered flight to be the most promising option for the mid L/D architecture. Among the most promising for the HIAD architecture was a forward exit of the lander through the HIAD followed by transition to powered descent. A summary of the transition option assessment work is shown in Section 4.10.4. A high-fidelity simulation tool was exercised using the top-rated options for mid L/D and HIAD architectures. Initial results from the high-fidelity tool assessment are shown in Section 4.10.6.

At the initiation of the EDL study effort, it was envisioned that an extensive model-based systems engineering (MBSE) process would be employed for the purpose of interrogating inter-related mission architectures and to maximize reuse (and insure interoperability) between interrelated missions over the course of a long-range space program. The scope of these interrelated and diverse missions include human, robotic, long and short duration, as well as destinations. The process accounts for four fundamental viewpoints; 1) data architecture, 2) operational architecture, 3) functional architecture, and 4) physical architecture. An output of the physical architecture assessment was a MEL/Power Equipment List (PEL) hierarchical list of a human and cargo lander in the 40-60 metric ton range. The MEL and PEL is the hierarchical equipment listing that follows the functional architecture decomposition. The mass properties are captured as attributes of the equipment items in the model. As a result, the MEL and PEL are simply a report from a relational database. The MEL items are cross-referenced to both the functional and operational models. This resulted in traceability matrices for showing the mass variations throughout the stage sequences of the mission as well producing power profiles throughout the missions. Although resource restrictions prevented this MBSE process from being fully implemented at this study phase, the entire process (as envisioned) is described in Section 4.11.

Lastly, technology development is critical to provide core capabilities for the Mars Lander. Enabling technologies are highlighted throughout the Mars Lander design to achieve the necessary performance capability to the destination; provide infrastructure or support systems; and for crew systems and biomedical concerns. Risk to a surface mission to Mars will be minimized by selective technology development and maturation to a technology readiness level (TRL) of 6 or higher prior to insertion at a flight system Preliminary Design Review.

Complementary investments that will maximize payload mass fraction are needed to meet mission performance requirements. This includes advanced entry descent and landing concepts; aero-entry thermal protection systems

(TPS); and propulsion technology for effective controlled entry into the Mars environment. Cryogenic propellant systems may offer necessary performance benefits, making CFM a potentially enabling technology for controlling propellant boil-off. To support a DRA 5.0-type mission architecture, additional assumptions going forward include infrastructure systems for surface fission power and in situ resource utilization to leverage the indigenous environment. Technologies for guidance navigation and control, Lander power and energy storage, and thermal control are noted among the mission architecture and vehicle support systems. To ensure the safety and viability of the crew, space suit development and risk mitigation for long-term exposure to microgravity and radiation environments must be considered. Reliable Environmental Control and Life Support (ECLS) systems include, but are not limited to, technologies, such as high-pressure oxygen, environmental monitoring, and carbon dioxide (CO₂) and waste removal. A more detailed summary of technology needs can be found in Section 4.12.

4.2 Descent and Ascent Trajectories

The primary objective of this work was to develop delta-V budgets to be used for sizing tools. Secondary objectives include trade studies and sensitivities to gain insight and to make an informed selection of propulsion system design. For the ascent, a set of trajectories and trades was run. For the descent, due to limited input, coupling with the entire EDL phase, and schedule constraints, the decision was made to anchor delta-V assumptions to the EDL-SA work and postpone descent trajectory updates to the following cycle (Cycle D).

4.2.1 Initial Ascent Orbit Selection Trades

4.2.1.1 Trajectory Trades Ground Rules and Assumptions

- LMO = 500 x 500 km circular altitude
- HMO = 250 x 33,800 km altitude (~24.6 hr orbit period)
- Two Phase to Orbit (TPTO), (an interim step toward full two stage to orbit trajectory)
- Single Phase to Orbit (SPTO), (an interim step toward full single stage to orbit trajectory)
- All cases injected initially into a 100x250 km LMO, then:
 - All cases use a 3-burn scenario to get to the final parking orbit (LMO or HMO)
 - T/W₀ trade -- 0.6 to 1.4 g's (Earth g's)
 - Specific impulse (Isp) trade done as a 1-D trade space

4.2.1.2 Tools and Methodology

- Simulation to Optimize Rocket Trajectories (SORT) is a 3-degree-of-freedom simulation with built-in optimization capability and was used for generating the ascent trajectories
- Ascent trajectories were flown using 8 segments, allowing the optimizer to solve for the maximum mass to orbit by varying thrust angle at each transition point
- For the SPTO solutions, constant thrust was used.
- For the initial TPTO solutions, the optimizer was additionally allowed to choose the thrust level during each segment
 - Generally, the solution was a maximum thrust phase followed by a minimum thrust phase. In some cases, an mid-level throttle was chosen by the optimizer in between the maximum thrust and minimum thrust phase (i.e., a ramp down)
 - No mass changes (other than fuel depletion) were implemented (e.g., dropping a stage was not considered)
 - Note: Eventually, the optimizer will be replaced by guidance. This optimization is an initial analysis useful for developing the guidance strategy.
- LMO 3-burn sequence (100 x 250 km -> 250 x 500 km -> 500 km circ)
- HMO 3-burn sequence (100 x 250 km -> 250 x 250 km -> 250 x 33,793 km)
- The 3-burn scenario was devised to facilitate flexibility in selecting the post-ascent parking orbit line of apsides. This is especially crucial for the elliptical HMO case – one wants that highly energetic orbit to be pointed in the right direction (i.e., the out-going asymptote to return to Earth).

4.2.2 Ascent Trajectory Trade Space

- TPTO & SPTO
- LMO – 500 km // HMO – 250 x 33,793 km
 - Both use 3-burn scenarios to get to final parking orbit
 - The last 2 burns are impulsive and done in the sizing analyses
- TPTO stage ΔV split is determined by trajectory
- LOX/LCH₄ cases only shown in Figure 4-1.

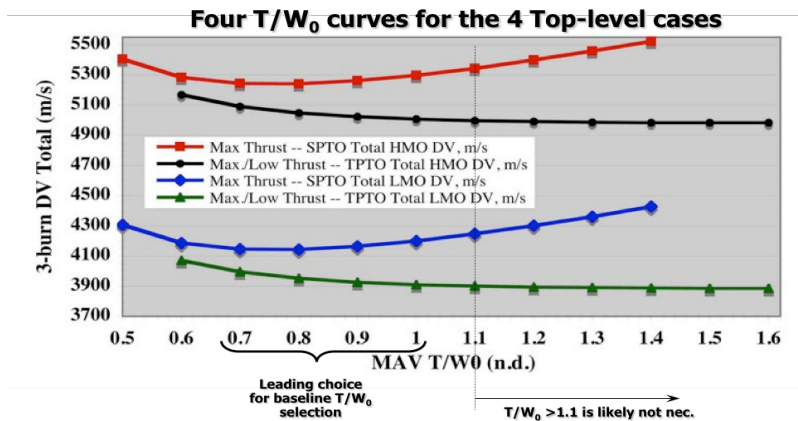


Figure 4-1 Ascent ΔV results for varying initial thrust-to-weight ratio (Earth), final orbit, and number of phases.

A key feature of this integrated performance analysis effort was to understand the sensitivity of the ascent trajectory (all facets of it) to the driving variable initial-thrust-to-weight (T/W_0 , in Earth Gs) as shown in Figure 4-1. This plot is especially useful for illustrating these physics. Note that there is an upper limit to the usefulness of thrust. Once a certain T/W_0 is reached, more thrust does not reduce gravity losses further due to the flight path necessary (as determined by Mother Nature) to get to orbit. There are also other reasons for selecting not too large of a thrust level, namely propulsion subsystem mass, and acceleration levels the crew experiences during the Mars-to-Orbit (MTO) ascent.

4.2.2.1 Sample Nominal Trajectory

An example nominal trajectory is included for the SPTO, $T/W_0=0.7$ case. The thrust is constant at 7716.2 lbs and the post-powered ascent orbit is 100 x 250 km. The mass was assumed to be 5000 kg; however, the exact mass is not important as the ascent performance depends on the thrust-to-mass ratio and is independent of the absolute mass. The plots shown in Figure 4-2 are a subset of those generated for each individual trajectory case. Table 4-1 includes additional information regarding the insertion conditions along with some additional relevant parameters for this sample nominal trajectory case.

4.3 Lander Trades and Sensitivities

The size of the Mars ascent and descent vehicles were traded across a range of propulsion system options – for Cycle C, this first order sizing was done mainly as a function of specific impulse (I_{sp}), e.g., propulsion system. Using the 2007 DRA 5.0 elements masses as an anchoring point, the size of the vehicles were traded across a range of stage burn-out masses as well – with the intention of bounding the Mars ascent and descent vehicle sizes for the next round of higher fidelity analyses.

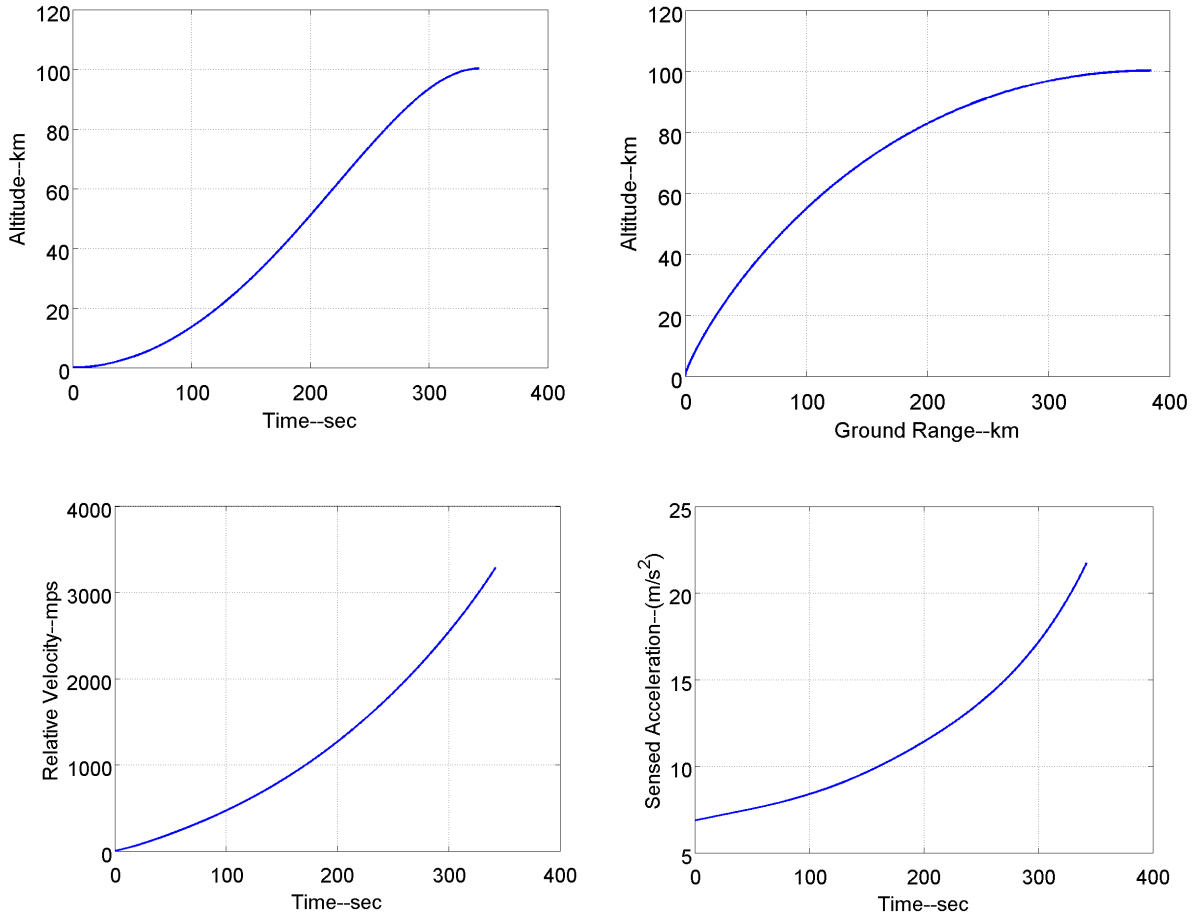


Figure 4-2 Trajectory plots for SPTO Mars ascent for initial thrust-to-weight=0.7 Earth G.

The sizing tool used in this HAT Mars Cycle C analyses was an updated/augmented version of the tool that was used for the ~3-week Summer 2009 Augustine Report¹ analyses/activity. With a timeframe of months, instead of weeks, both a larger trade space of independent variables and slightly higher fidelity sizing analyses was performed.

Also, as seen in the immediately preceding section (Section 4.2), a large body of trajectory analyses was performed (which was not done in 2009) to fully inform this initial sizing and the subsequent higher fidelity sizing (shown in Section 4.3.3 and Section 4.3.4).

4.3.1 Initial Ascent Sizing Trade Space

Many factors drive the size of a Mars ascent system, with the target burn-out/parking orbit, the number of stages comprising the vehicle, as well as the propellant choice being the major factors. These three factors, especially the choice of propulsion system for the MAV, are also significant drivers in determining the size of the overall Mars architecture mass – which, in the case of DRA 5.0, consists to two cargo stacks followed by a piloted stack on the subsequent opportunity. It should be noted that some propulsion system/propellant options allow for the possibility of ISRU, whereas others do not.

Table 4-1 Trajectory State at Insertion Plus Additional Parameters

Insertion Condition	Value
Altitude (km)	100.26
Radius magnitude (m)	34,974,589
Latitude (deg)	0.0004
Longitude (deg)	6.487
Velocity (m/s)	3287.88
Inertial Flight Path (deg)	0.1003
Inertial Azimuth (deg)	89.997
Total burn length (sec)	342.1
RAAN (deg)	0.433
Inclination (deg)	0.003
Mass (kg)	1578.94
DV (m/s)	3956.387
Apoapsis (km)	250.0
Periapsis (km)	100.0
Additional Data	
Initial Mass (kg)	5000
Launch Site Latitude (deg)	0.0
Launch Site Longitude (deg)	0.0
Thrust (lbf)	7716.2
Max G (Earth G)	2.217
T/W Initial (Earth G)	0.7

The factors/independent variables used while performing the sizing analyses (the first three of which were integral in the trajectory analyses discussed above):

- LMO vs. HMO
- TPTP vs. SPTO
- MAV lift-off Thrust-to-Weight: 0.6 to 1.4 Earth g's
- Main Propulsion System (MPS) options:
- LOX / LH₂: Isp = 440 sec
- LOX / LCH₄: Isp = 355 sec
- NTO / MMH: Isp = 323 sec
- Number of Crew: Four vs. six (81.4 kg each)
- Amount of Mars samples: 100 kg vs. 250 kg vs. 400 kg

Note that if the entire trade space were run, 648 cases (2*2*9*3*2*3) would have been necessary. However, only specific portions of the trade space were run due to the pointed intent of this analyses to determine and understand MAV sensitivities to these variables.

Table 4-2 Comparison for MAV to Mars Orbit Destination and Staging

MAV: 4 crew + 250 kg T/W ₀ = 0.9 LOX/LCH ₄	TPTO To LMO	TPTO To HMO	SPTO To LMO	SPTO To HMO
Isp (sec)	355	355	355	355
Ascent DV (m/s) (70% or 78% on 1 st stage)	3777 (70%)	3777 (78%)	4016	4016
In-orbit DV (m/s)	149	1247	149	1247
4 Crew + samples (kg)	576	576	576	576
2nd stage DV prop (kg)	2218	4106	n/a	n/a
1st stage DV prop (kg)	13,790	18,861	23,233	36,029
MAV mass @ ETO (kg)	12,703	14,212	13,837	16,358
2nd stage Thrust (lb _f)	14,200	18,200	n/a	n/a
1st stage Thrust (lb _f)	51,600	65,600	66,100	91,800
MAV @ Mars LO (kg)	25,981	33,034	33,300	46,224

The MAV trade-space, at the top level, consists of two options for two independent variables – the first two shown in the itemized list above. Table 4-2 shows the results for this set of cases.

The table above was set to show the MAV size increasing from left to right – to provide an initial feel for the effect of the two top-level independent parameters. The SPTO cases end up being heavier than the TPTO options due, in part, to the efficiency of staging for the two-stage MAV.

The reference (baseline) set of cases in this trade space was considered to be the TPTO, LOX/LCH₄ cases to HMO, with T/W₀ as the independent variable for this baseline set of cases. Most comparisons that follow will be compared to this set of cases. Note that in Figure 4-1 of Section 4.2, of the four MAV permutations (2 variables, 2 options each), notably specific for the LOX/LCH₄ propulsion option, provide the basic comparison and basic product of the trajectory work that will also be the basic comparison and basic product of the sizing work.

Table 4-3 Comparison for MAV Initial Thrust-to-Weight Levels

TPTO to HMO 4 crew + 250 kg LOX/LCH ₄	T/W ₀							
	0.7	0.8	0.9	1.0	1.1	1.2	1.3	1.4
Isp (sec)	355	355	355	355	355	355	355	355
Ascent DV (m/s) (63% or 78% on 1 st stage)	3845 (78%)	3802 (78%)	3777 (78%)	3761 (78%)	3751 (78%)	3744 (63%)	3741 (63%)	3738 (63%)
In-orbit DV (m/s)	1247	1247	1247	1247	1247	1247	1247	1247
4 Crew + samples (kg)	576	576	576	576	576	576	576	576
2 nd stage DV m _{pr} (kg)	4146	4121	4106	4097	4091	5684	5679	5677
1 st stage DV m _{pr} (kg)	19,426	19,066	18,861	18,733	18,650	15,264	15,238	15,223
MAV @ ETO (kg)	14,338	14,258	14,212	14,184	14,165	13,753	13,747	13,743
2 nd stage Thrust (lb _f)	14,200	16,200	18,200	20,200	22,200	28,400	30,700	33,100
1 st stage Thrust (lb _f)	52,000	58,700	65,600	72,600	79,600	82,100	88,800	95,600
MAV @ Mars LO (kg)	33,638	33,253	33,034	32,897	32,808	31,014	30,983	30,965

Table 4-3 shows the sizing results of a MAV T/W_0 sweep. The sizing shows the diminishing improvement (i.e., decrease) in MAV mass (and the corresponding MAV thrust level) when using higher T/W_0 . As observed in the previous section, the MPS subsystem mass will be proportional to thrust level, so there is a point in the T/W_0 where larger thrust does not help; thus, an optimal thrust-to-weight. The optimal thrust-to-weight for the SPTO cases in Figure 4-1 is apparent, but is no less a factor in the TPTO cases.

Similar tables to Table 4-3 above have also been documented for the other four main top-level branches of the MAV trade space: TPTO to LMO, SPTO to LMO, and SPTO to HMO.

4.3.1.1 Propellant/MPS Options: LOX/LH₂, LOX/LCH₄, NTO/MMH

The comparison for the three propulsion system options is shown in Table 4-4. Specific impulses selected for each option represent achievable values per the propulsion community (nozzle area ratio, chamber pressure, oxidizer to fuel (O:F) mixture ratio, etc.). All three of these cases were run with the same crew mass, sample mass, stage 1 and stage 2 burn-out masses, T/W_0 ratio (same for both 1st and 2nd stages), and same Mars parking orbit to provide an indication of MAV sensitivity to only Isp. Note that the storable propulsion option requires all propellant (incl. 17.7 metric tons of NTO oxidizer) to be present at Earth lift-off at the beginning of the mission. The two ISRU options, LCH₄ and LH₂, require 17.5 t and 13.6 t of ISRU-produced LOX at Mars.

Table 4-4 Comparison for MAV Propulsion System Choices

TPTO to HMO 4 crew + 250 kg $T/W_0 = 0.9$	NTO / MMH	LOX / LCH ₄	LOX / LH ₂
Isp (sec)	323	355	440
Ascent DV (m/s) (78%, 1 st stage; 22%, 2 nd)	3777	3777	3777
In-orbit DV (m/s)	1247	1247	1247
4 Crew + samples (kg)	576	576	576
2nd stage DV prop (kg)	4663	4106	3111
1st stage DV prop (kg)	22,603	18,860	12,904
MAV mass @ ETO (kg)	37,332	14,212*	11,989*
2nd stage Thrust (lb _f)	19,300	18,200	16,200
1st stage Thrust (lb _f)	74,100	65,600	51,800
MAV @ Mars LO (kg)	37,332	33,033	26,082

The results for the three main propulsion options show a stark difference between the non-ISRU storable propulsion option and the two ISRU options. It is clear from this propellant trade the extent ISRU facilitates Mars exploration – as the two ISRU options are two-and-half to three times smaller than the non-ISRU option on the launch pad at Earth. It should be noted that there is only an 18% difference in the Earth on-pad mass for the two ISRU, and cryogenic, options. The easier-to-handle methane cryogen will likely be found to be sufficiently more tractable to employ in practice, as many previous studies have also theorized.

4.3.1.2 Payload Options: Four Crew or Six Crew and Sample Return Mass

The sensitivity of the MAV to the ‘payload’ mass was also evaluated. The payload consists of the crew along with all return samples (soil, rocks, and other types of samples). The range of sample masses used was 100 kg as a minimal sample return mass, 250 kg for a nominal mass return, and 400 kg as a value for an upper limit of samples that could be lifted through the huge Mars ascent ΔV . Due to the large ascent ΔV and the great amount of propellant required for any MAV, the payload mass is a secondary driver. The MAV cabin size and its associated structure mass for a larger crew size may have a larger effect on the MAV mass than the mass of the actual number of crew.

Table 4-5 Comparison for MAV Payload (crew + samples) Sizes

TPTO to HMO T/W ₀ = 0.9 LOX/LCH ₄	4 crew + 100 kg samples	4 crew + 250 kg samples	6 crew + 400 kg samples
Isp (sec)	355	355	355
Ascent DV (m/s) (78%, 1 st stage; 22%, 2 nd)	3777	3777	3777
In-orbit DV (m/s)	1247	1247	1247
4 Crew + samples (kg)	426	576	888
2nd stage DV prop (kg)	3984	4106	4362
1st stage DV prop (kg)	18,499	18,861	19,617
MAV mass @ ETO (kg)	14,113	14,212	14,418
2nd stage Thrust (lb _f)	17,600	18,200	19,300
1st stage Thrust (lb _f)	64,300	65,600	68,200

4.3.1.3 LOX/LCH₄ Propulsion Options

The following table shows the sensitivity of a LOX/LCH₄ MAV to the performance variable Isp, also showing this as a secondary effect when compared to target orbit, staging and MPS option.

Table 4-6 Comparison for MAV LOX/LCH₄ Propulsion Options

TPTO to HMO 4 crew + 250 kg T/W ₀ = 0.9	LOX / LCH ₄ Pressure-fed Engines	LOX / LCH ₄ Pump-fed Engines	LOX / LCH ₄ Advanced Engines
Isp (sec)	340	355	369
Ascent DV (m/s) (78%, 1 st stage; 22%, 2 nd)	3777	3777	3777
In-orbit DV (m/s)	1247	1247	1247
4 Crew + samples (kg)	576	576	576
2nd stage DV prop (kg)	4350	4106	3902
1st stage DV prop (kg)	20,463	18,861	17,560
MAV mass @ ETO (kg)	14,594	14,212	13,901
2nd stage Thrust (lb _f)	18,700	18,200	17,800
1st stage Thrust (lb _f)	69,300	65,600	62,600
MAV @ Mars LO (kg)	34,880	33,034	31,528

Results for low-Isp pressure-fed engines, compared to the high-Isp high-tech engines (e.g., high area ratio nozzle, high chamber pressure, etc.) show a difference of 16% in MAV required propellant mass for the difference of nearly 30 seconds of Isp. This difference in propellant will likely be a little larger once MPS subsystem sizing is performed for the heavier pressure-fed tanks, but will be partly ameliorated by the pump-fed MPS need for turbo-pumps in the nominal case as well as heavier nozzles and combustion chambers for the high-tech option.

4.3.1.4 Resulting Engine Thrust Levels

The required engine thrust, as dictated by the trajectory analysis and the assumption on stage T/W_0 , provide results to begin sizing the MPS subsystem. The results for the two top-level independent parameters are shown in Figure 4-3.

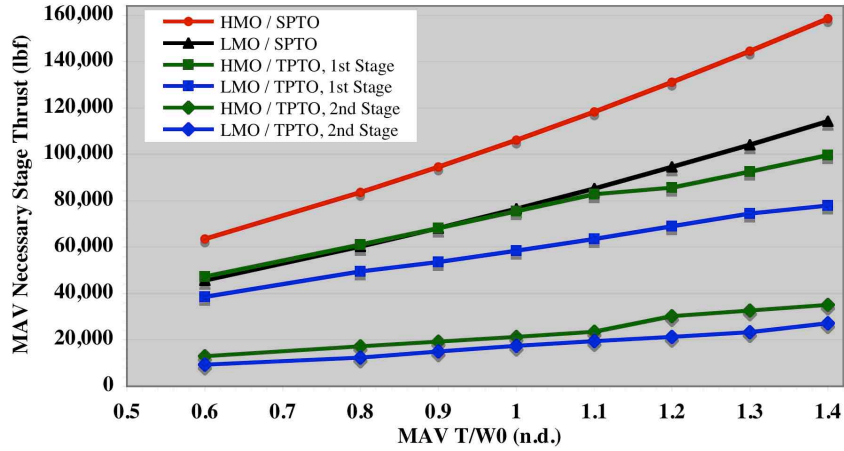


Figure 4-3 Thrust levels required for various MAV T/W_0 (i.e. its associated gross liftoff weight, or GLOW).

The first stage for a TPTO MAV will typically require three to four of the second stage engines due to interest in producing a single size engine for the MAV and for engine-out (reliability analyses will be done in future studies). The SPTO MAV may have other driving considerations for determination of its thrust level, for example possible synergy with the Mars in-space engine for Mars orbit insertion (MOI) and trans-Earth injection (TEI). For the plotted points at $T/W_0 = 0.9$, the MAV thrust level requirements are shown in Table 4-6 above.

4.3.1.5 MAV ISRU Options Using Methane

Depending on the selected option for LOX/LCH₄ ISRU, the MAV mass can vary greatly as it is sitting on the launch pad at Earth on its Space Launch System (SLS) launch vehicle. The three options available are: 1) Full ISRU – producing both LOX and methane at Mars; 2) LOX-only ISRU – i.e., just the oxidizer; and 3) No ISRU at all.

LOX-only ISRU requires access to only the Mars CO₂ atmosphere to produce oxygen, while bringing the methane from Earth and storing it in its tank(s) until needed for ascent at the end of the crewed mission (typically ~1500 days after cargo launch at Earth). Full-ISRU requires seed LH₂ to be brought from Earth for the process (e.g., Sabatier) that produces both LCH₄ and LOX. No ISRU means launching the entire MAV fully wet from the pad at Earth to Mars’ surface.

The MAV masses on the launch pad at Earth for the non-ISRU LOX/LCH₄ option range from 31 metric tonnes (t) to 34 t (shown in the plot above and the table below) for the TPTO staging option to HMO, and vary from 28 t to 50 t for the top-level 2x2 trade space. As in the propulsion system trade previously (Table 4-4), there is a factor of two to three reduction in the required MAV mass on the launch pad at Earth. Once the large reductions for the LOX-ISRU have been captured, there is only another incremental improvement for the more difficult full-ISRU option.

The following cases in Table 4-8 were selected for use in subsequent higher fidelity sizing analyses, notably to include MPS subsystem sizing mass estimating relationships (MERs). This next step in the sizing analysis will provide a better “optimally” sized vehicle, in addition to the previous extra steps of including trajectory and a larger independent variable trade space (compared to the 2009 effort).

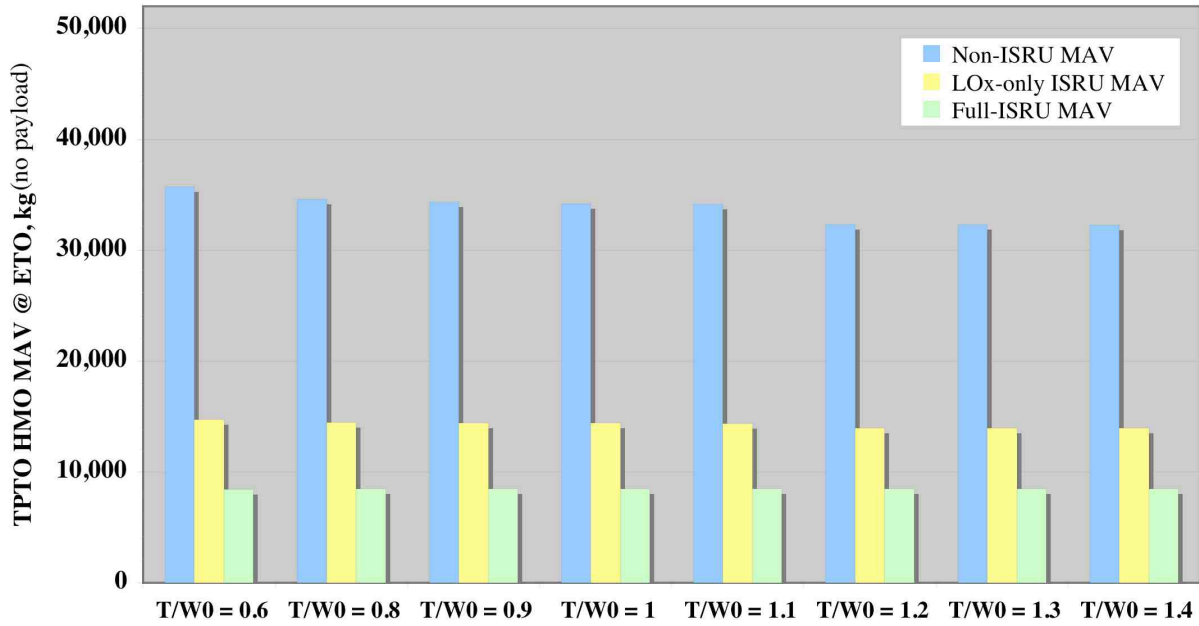


Figure 4-4 MAV masses at Earth for HMO, TPTO with various T/W₀ & ISRU options.

Table 4-7 LOX/CH₄ MAV Masses for Various Mars Orbits, Staging and ISRU Options

MAV mass on pad @ Earth 4 crew + 250 kg T/W ₀ = 0.7 - 1.4 LOX/LCH ₄	TPTO to LMO	TPTO to HMO	SPTO to LMO	SPTO to HMO
No ISRU (t)	~28	31.0 - 33.6	~36	~50
LOx-only ISRU (t)	~13	13.7 - 14.3	~14	~17
Full ISRU (t)	~9	8.5 - 8.7	~9	~9

4.3.1.6 Cases Considered for Subsequent Detailed Sizing

Table 4-8 MAV Options Recommended for use in Detailed Sizing Analyses

MAV: 4 crew + 250 kg LOX/LCH ₄	TPTO to LMO T/W ₀ = 1.0	TPTO to HMO T/W ₀ = 0.7	SPTO to LMO T/W ₀ = 0.9	SPTO to HMO T/W ₀ = 0.7
Isp (sec)	355	355	355	355
Ascent DV (m/s) (66% or 78% on 1 st stage)	3761 (66%)	3845 (78%)	4016	4036
In-orbit DV (m/s)	149	1247	149	1247
4 Crew + samples (kg)	576	576	576	576
2nd stage DV prop (kg)	2474	4146	n/a	n/a
1st stage DV prop (kg)	13,049	19,426	23,233	35,771
MAV mass @ ETO (kg)	12,595	14,338	13,837	16,310
2nd stage Thrust (lb _f)	16,400	14,200	n/a	n/a
1st stage Thrust (lb _f)	56,300	52,000	66,100	71,000
MAV @ Mars LO (kg)	25,496	33,639	33,300	45,966

To iterate in the higher fidelity analysis, ΔV vs. T/W_0 curve-fits were generated to allow some degree of optimization between the two vehicle sizing factors. A linear fit, for $\Delta V(T/W_0)$, below across the range of interest ($T/W_0 = \sim 0.7 - \sim 1.0$) was considered sufficient at this time to achieve some better understanding of MAV candidate options.

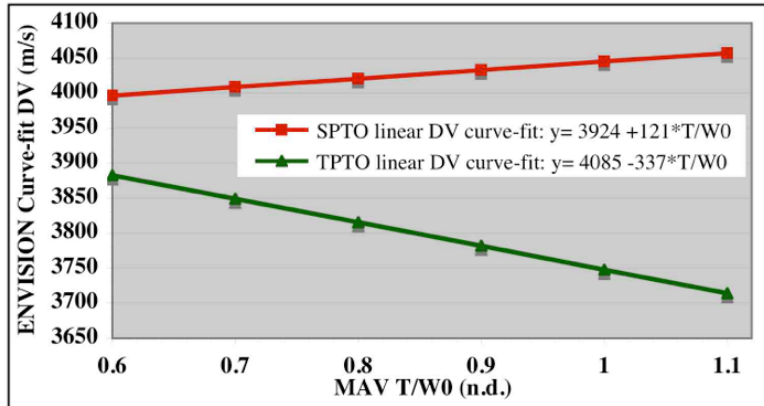


Figure 4-5 Results for MPS and payload mass trades.

The behavior of the simple linear fits above still follows well the behavior seen in Figure 4-1 from the SORT finite-burn, numerically integrated trajectory analyses. Note that these linear fits are constrained for use in to only the first rev/target orbit of 100x250 km altitude at Mars. The in-orbit ΔV s (and are called out in each table where applicable) are considered impulsive maneuvers added to this curve-fit ΔV to get the entire MAV ascent ΔV .

4.3.1.7 Mars Ascent Trajectory and Sizing Conclusions

There are a number of pros and cons for both the TPTO and SPTO options, and some facets not yet clearly going one way or the other. Single-stage (phase) to orbit will have a lower probability of loss of crew (pLOC) result due to not having an extra event where staging occurs – always a critical event during any multistage ascent scenario. However, the two-stage (phase) to orbit option likely allows for a lighter mass MAV, lower thrust level in part due to a smaller MAV, and lower maximum accelerations (especially when throttling capability is limited as it often is). At this time, it is unknown which option will have a better overall pLOC, better program risk outlook, and which one will package better in whatever launch vehicle shroud becomes available.

The LMO MAVs are smaller and require lower thrust levels than the HMO MAVs, but with the great advantage of ISRU, much of the mass is not brought from Earth, thus allowing much smaller architectures (notably the propellant necessary for an additional 1200 m/s on both the MOI and TEI burns) for the HMO architecture option. Secondary concerns are the thermal environment and the solar array shadowing constraints, both of which are less onerous in the HMO orbit.

The baseline MAV – TPTO, using LOX/LCH₄ propulsion, flying into a HMO parking orbit was baselined for a reason. As the data in this section show, from a sizing and architecture point of view, this option allows for the most architecturally optimal MAV.

4.3.2 Initial Descent Sizing Trade Space

A number of factors also drive the size of a Mars descent system, with the initial parking orbit and the descent propulsion system choice being the major factors.

The factors/independent variables used while performing the sizing analyses (the first three of which were integral in the trajectory analyses):

- MAV descent vehicle Thrust-to-Weight: ~0.6 - 0.7 Earth g's
- MPS options:
 - LOX / LH₂: Isp = 440 sec
 - LOX / LCH₄: Isp = 355 sec (pump-fed)
 - LOX / LCH₄: Isp = 340 sec (pressure-fed)
- Mars descent vehicle payload range: 10 - 40 t
- *Descent ΔV: 798 m/s (Rigid aeroshell) vs. 601 m/s (HIAD)*
- *LMO vs. HMO*
- *Number of Crew: Four vs. six*
- *Rigid aeroshell vs. HIAD*

Note that changing the number of crew will be considered in the next analysis phase in the higher fidelity sizing analyses. The initial parking orbit will also be investigated later once the EDL transitions are characterized more fully. Same for the rigid aeroshell vs. HIAD trade – this will also be done when the transition characterization is complete. The descent ΔV for the HIAD vs. rigid aeroshell trade will also likely be updated from the current values of 601 m/s and 798 m/s respectively.

4.3.2.1 Propellant/MPS Options: LOX/LH₂ vs. LOX/LCH₄

The options for descent propulsion investigated included only the cryogenic options, since the descent ΔV is small compared to the ascent ΔV and occurs much earlier in the mission than the piloted ascent event. Therefore, the descent event cannot be the driver for the choice of Mars ascent/descent MPS. Thus, the large storable MAV finding indicates storable descent is also not a viable option. However, it is still advantageous to trade descent vehicle characteristics for pump-fed vs. pressure-fed methane, so that option is also included.

Table 4-9 Comparison for Descent Propulsion System Choices, 20.8 t Payload

Mars Descent MPS Trade	LOX / CH ₄ Pump-fed	LOX / LH ₂	LOX / CH ₄ Pressure-fed
Isp (sec)	355	440	340
Descent DV (m/s)	798	798	798
Descent stage DV prop (kg)	7984	6296	8381
Terminal Descent m0 (kg)	38,986	37,298	39,383
Descent Thrust, T/W ₀ = 0.6 (lb _f)	51,600	49,400	52,100
Req. Throttle, T/W ₀ =0.6 (%)	37.8%	39.5%	37.4%
Descent Thrust, T/W ₀ = 0.7 (lb _f)	60,200	57,600	60,800
Req. Throttle, T/W ₀ =0.7 (%)	32.4%	33.9%	32.1%

The small difference in the descent propellant load (highest to lowest) is only a couple of tons (out of typically ~70 t for the entire descent vehicle), indicating that the LOX/LCH₄ option is sufficient keep the descent stack manageable in mass (and size). Again, it is apparent the ascent event will be a much larger driver for selecting the Mars ascent/descent MPS.

4.3.2.2 Payload Sensitivity: LOX/LCH₄ w/ 10 t, 20.8 t, 30 t, 40 t of payload

The payload sensitivity trade was run using the baseline MPS assumption as for ascent, namely the pump-fed LOX/LCH₄ option. For a very large range of descent payloads, a factor of four between the smallest and largest, results in factor of ~2.5 between the smallest prop load required and the largest. Similar results are seen in the total thrust required for descent – at the assumed T/W₀ levels of 0.6 and 0.7 – but is quite likely this can be taken care by selecting the appropriate number of engines already sized by the MAV needs. With no engine-out requirement the descent (T/W₀ = 0.6 - 0.7) needs two engines for a 10 t payload, and four engines for the 40 t payload. Depending on the eventual lander configuration, these engine counts could increase to four for a 10 t payload, and six engines for 40 t. If the required T/W₀ doubles due to propulsive needs during and after the transition from aeroassist flight to propulsive controlled flight, the engine counts could go as high as six MAV engines for the 10 t payload to ten MAV engines for the 40 t payload.

A summary of the four main descent cases (pump-fed LOX/LCH₄) is shown in the table below. Note that the throttling requirements do not change appreciably, since the descent propellant expended is a somewhat small percentage of the descent stack.

The result from both of these individual trades is shown as a complete 3x4 trade-space in the bar chart below. At this time, the baseline payload that can be accommodated is targeted at 20.8 t – i.e. the red bars shown.

4.3.2.3 Resulting Engine Sizes

The required total thrust is plotted below. Again, the entire 3x4 trade space is shown. For example, with the red line below, in the 40 t initial mass range, three engines at 89 kN (20,000 lbf) are required. A symmetrical arrangement would indicate four could be necessary (in likely the pitch and roll directions), and with one extra engine in each locale, a total of six 89 kN (20,000 lbf) would be needed. Of course, there are many permutations to selecting and arranging multiple engines (for both vertical and horizontal landers), so the previous example is just that – one possibility.

Table 4-10 Comparison for LOX/LCH₄ MPS (pump-fed) Descent vs. Payload

Mars Descent LOX / LCH ₄ , Pump-fed	Payload Mass			
	10 t	20.8 t	30 t	40 t
Isp (sec)	355	355	355	355
Descent DV (m/s)	798	798	798	798
Descent stage DV prop (kg)	5207	7984	10,358	12,934
Terminal Descent m0 (kg)	25,426	38,986	50,577	63,153
Descent Thrust, T/W ₀ = 0.6 (lb _f)	33,700	51,600	67,000	83,600
Req. Throttle, T/W ₀ =0.6 (%)	37.7%	37.8%	37.7%	37.6%
Descent Thrust, T/W ₀ = 0.7 (lb _f)	39,300	60,200	78,100	97,500
Req. Throttle, T/W ₀ =0.7 (%)	32.3%	32.4%	32.3%	32.3%

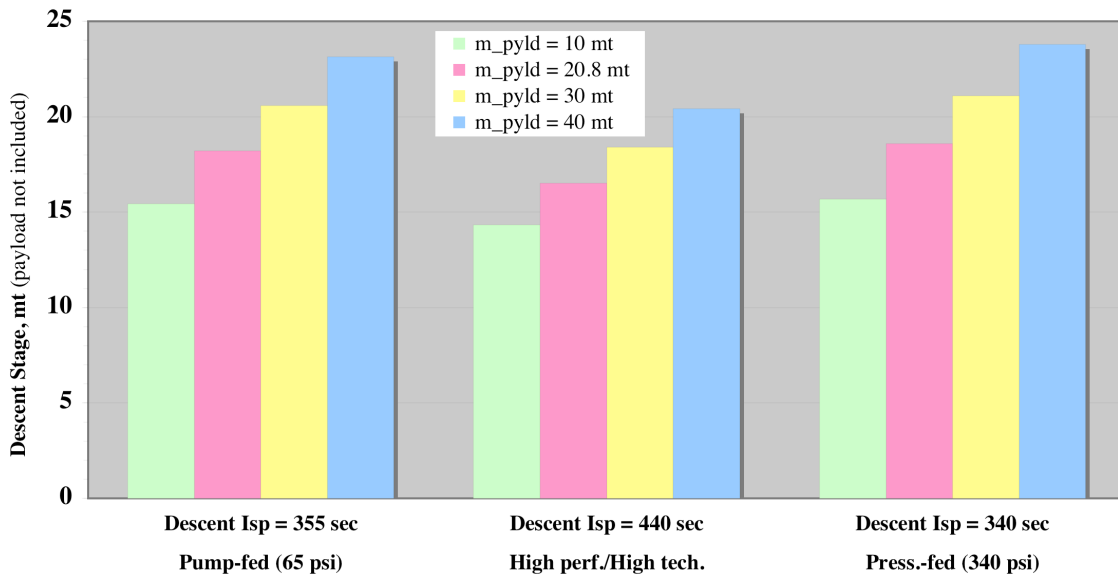


Figure 4-6 Results for MPS and payload mass trades.

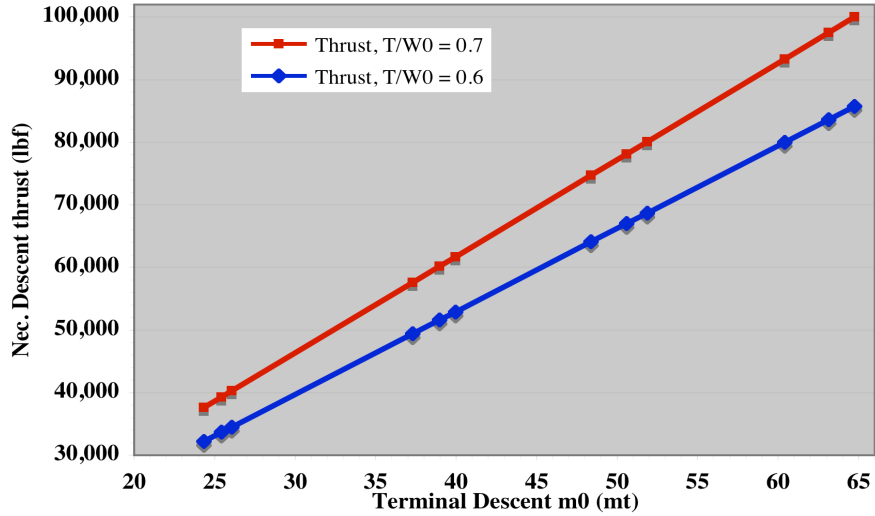


Figure 4-7 Thrust levels required for various descent vehicle T/W_0 .

4.3.2.4 Mars Descent Conclusion

Initial characterization of the descent propulsion requirements are shown here, but with much analytical work to follow in the near-term, these initial results are pending. This descent sizing will be rerun once more is known about the transition from aeroassist flight to propulsive controlled flight, as well as payload and packaging requirements.

Throttling does not appear to be a concern for Mars descent at T/W_0 levels of 0.6 - 0.7 (i.e. <1.0), and will also be revisited once the complicated transition is more fully understood.

It is clear, though, that the driver for Mars ascent/descent propulsion system choice is the ascent event and not the descent event; thus, most emphasis has been, and will continue to be, put on assessing Mars ascent.

4.3.3 ENVISION Ascent Vehicle Sizing

ENVISION is a parametric sizing tool used to size the MAV and MDV based on the trajectory optimization work described above. The version of the ENVISION tool used in this initial Mars vehicle sizing was evolved from a version of the tool used for parametric sizing work for the Constellation Program’s lunar lander Altair. The tool provides vehicle system and subsystem mass sizing based on delta-v, vehicle configuration, and operational parameters. Although functioning in a different planetary environment, the lander Altair, and the Mars lander with MAV have the same basic vehicle elements and thus evolving the Altair version of ENVISION provides a reasonable initial sizing of vehicle elements for initial ascent and descent scenarios. It should be noted that this initial ENVISION parametric sizing work was done without a specific vehicle layout, which can lead to large uncertainty in the sizing of vehicle structural mass, vehicle landing gear size, and propulsion tank mass, among other vehicle elements.

The ascent vehicle was sized for only the TPTO scenarios, both for LMO and HMO. The propulsion options sized were 1) bringing all ascent propellant from Earth (full ISRU), and 2) bringing just fuel (LCH_4) from Earth (LOX-only ISRU). The crew options were four and six crew. Table 4-11 shows the sizing input assumptions for the ascent vehicle first stage sizing. The input assumptions for the ascent vehicle second stage ENVISION sizing are shown in Table 4-12.

Table 4-11 ENVISION Model Definition for Ascent Vehicle First Stage

ENVISION Model Definition – Ascent 1st Stage							
Parameter	Value	Parameter	Value	Parameter	Value	Parameter	Value
General		MPS Engine	Pump-fed	MSP Fuel Tank Storage Pressure	70 psi	Axial Acceleration (nx)	5.0 g
Number of Crew	0	Number of MPS Engines	4	Number of MPS Oxidizer Tanks	2	Lateral Acceleration (ny)	2.0 g
Crew Time in Vehicle	0 days	MPS Mixture Ratio	3.3	MPS Oxidizer Tank Storage Pressure	70 psi	Lateral Acceleration (nz)	2.0 g
Cabin Pressure	0 psi	MPS Engine Thrust	22000 lbf	Number of RCS Fuel Tanks	1	Stage Diameter	6.8 m
Total Pressurized Volume	0 m ³	MSP Delivered Isp	355 s	RCS Fuel Tank Storage Pressure	200 psi	Stage Length	1.7 m
Total Crew Mass	0 kg	RCS Fuel	None	Number of RCS Oxidizer Tanks	1	Thermal	
Return Sample Mass	0 kg	RCS Oxidizer	None	RCS Oxidizer Tank Storage Pressure	200 psi	Fluid Loop Heat Rejection	Fluid Evap only
Propulsion		Number of RCS Engines	0	Power		Radiator	None
MPS Total Delta-V	2999 m/s	RCS Mixture Ratio	0	Vehicle Peak Power	4000 W		
RCS Total Delta-V	0 m/s	RCS Engine Thrust per Engine	0 lbf	Primary Voltage	28 V		
MPS Fuel	CH ₄	RCS Delivered Isp	0 s	Structures			
MPS Oxidizer	O ₂	Number of MPS Fuel Tanks	2	Crew Cabin Material	Unknown		

Table 4-12 ENVISION Model Definition for Ascent Vehicle Second Stage

ENVISION Model Definition – Ascent 2 nd Stage							
Parameter	Value	Parameter	Value	Parameter	Value	Parameter	Value
General		MSP Delivered Isp	355 s	Atmosphere	Mixed	Fuel Cell	PEM Fuel Cell
Number of Crew	4	RCS Fuel	CH ₄	Oxygen Storage	High Pressure	Reactant Storage State	High Press Gas
Crew Time in Vehicle	2 days	RCS Oxidizer	O ₂	Nitrogen Storage	High Pressure	Number of Fuel Cell Oxygen Tanks	1
Cabin Pressure	10.2 psi	Number of RCS Engines	20	Number of ECLSS Oxygen Tanks	1	Number of Fuel Cell Hydrogen Tanks	1
Total Pressurized Volume	7 m ³	RCS Mixture Ratio	3.0	Number of ECLSS Nitrogen Tanks	1	Structures	
Total Crew Mass	324 kg	RCS Engine Thrust per Engine	100 lbf	Allowable Number of Full Cabin Repress	1	Crew Cabin Material	Unknown
Return Sample Mass	250 kg	RCS Delivered Isp	347 s	Regenerative CO2 Technology	CAMRAS	Stage Structure Material	Al
Propulsion		Number of MPS Fuel Tanks	2	Non-regenerative CO2 Removal Technology	None	Axial Acceleration (nx)	5.0 g
MPS Total Delta-V	2073 m/s	MSP Fuel Tank Storage Pressure	70 psi	Cabin Heat Exchanger Technology Selection	Condens.	Lateral Acceleration (ny)	2.0 g
RCS Total Delta-V	100 m/s	Number of MPS Oxidizer Tanks	2	Fixed-size RCO2 Removal Technology Unit	TRUE	Lateral Acceleration (nz)	2.0 g
MPS Fuel	CH ₄	MPS Oxidizer Tank Storage Pressure	70 psi	Atmosphere Composition Monitoring Technology	O ₂ /CO ₂ Sensors	Stage Diameter	6.8 m
MPS Oxidizer	O ₂	Number of RCS Fuel Tanks	1	Trace Contaminant Control Technology	ATCO	Stage Length	1.7 m
MPS Engine	Pump-fed	RCS Fuel Tank Storage Pressure	200 psi	Cabin Ventilation Selection	Cabin Fan	Thermal	
Number of MPS Engines	1	Number of RCS Oxidizer Tanks	1	Power		Fluid Loop Heat Rejection	Fluid Evap only
MPS Mixture Ratio	3.3	RCS Oxidizer Tank Storage Pressure	200 psi	Vehicle Peak Power	4000 W	Radiator	None
MPS Engine Thrust	22000 lbf	ECLS		Primary Voltage	28 V		

The first stage of the ascent vehicle is powered by four pump-fed LOX/LCH₄ engines, each with a maximum thrust of 97.9 kN (22,000 lbf) and Isp of 355 s. A single engine of the same type and performance powers the second stage. The second stage houses the crew and has additional assumptions for Environmental Closed Loop Life Support (ECLS), power and mission timeline that are not included in the first stage assumptions.

4.3.4 ENVISION Descent Stage Sizing

ENVISION was also used to provide an initial sizing of the descent stage with critical use of performing powered descent. To develop commonality between the ascent vehicle and lander descent stage, for the ENVISION sizing the descent stage was assumed to use four of the same LOX/LCH₄ engines used on the ascent vehicle, providing a total descent maximum thrust of 391 kN (88,000 lbf). For the sizing work, a total descent delta-v of 800 m/s was assumed. The ENVISION input assumptions for the descent vehicle sizing are shown in Table 4-13.

Table 4-13 ENVISION Model Definition for Descent Stage

ENVISION Model Definition – Descent Stage							
Parameter	Value	Parameter	Value	Parameter	Value	Parameter	Value
General		MPS Engine	Pump-fed	MSP Fuel Tank Storage Pressure	70 psi	Number of Batteries for Sizing	3
Number of Crew	0	Number of MPS Engines	4	Number of MPS Oxidizer Tanks	2	Rechargeable	True
Crew Time in Vehicle	0 days	MPS Mixture Ratio	3	MPS Oxidizer Tank Storage Pressure	70 psi	Structures	
Cabin Pressure	0 psi	MPS Engine Thrust	22000 lbf	Number of RCS Fuel Tanks	1	Crew Cabin Material	Aluminum
Total Pressurized Volume	0 m ³	MSP Delivered Isp	355 s	RCS Fuel Tank Storage Pressure	200 psi	Axial Acceleration (nx)	5.0 g
Total Crew Mass	0 kg	RCS Fuel	CH ₄	Number of RCS Oxidizer Tanks	1	Lateral Acceleration (ny)	2.0 g
Return Sample Mass	0 kg	RCS Oxidizer	O ₂	RCS Oxidizer Tank Storage Pressure	200 psi	Lateral Acceleration (nz)	2.0 g
Propulsion		Number of RCS Engines	16	Power		Stage Diameter	6.8 m
MPS Total Delta-V	800 m/s	RCS Mixture Ratio	3	Vehicle Peak Power	58710 W	Stage Length	1.7 m
RCS Total Delta-V	50 m/s	RCS Engine Thrust per Engine	100 lbf	Primary Voltage	28 V	Thermal	
MPS Fuel	CH ₄	RCS Delivered Isp	347 s	Battery #1 Technology	Li-ion	Fluid Loop Heat Rejection	Radiators
MPS Oxidizer	O ₂	Number of MPS Fuel Tanks	2	Total Number of Batteries	3	Radiator	ULTRA

4.3.5 ENVISION Results

The results from parametric sizing from ENVISION compare well with vehicle sizing from DRA 5.0, and was used to seed more detailed sizing efforts summarized in Section 4.6 and Section 4.8. For an equivalent landed payload mass of 40 t, crew of 6 and return to HMO, ENVISION produced a wet lander mass of 72.6 t. The wet lander mass reported by DRA 5.0 is 66.9 t. Thus the ENVISION work resulted in a wet lander approximately 6 t heavier than the DRA 5.0 lander.

It should be noted that the ENVISION sizing summarized in this section made the simplifying assumption that the maximum lander descent thrust remained fixed at 3.9 MN across all lander masses analyzed. This results in a declining T/W₀ as the mass of the lander increases. For the more massive landers sized by ENVISION, the resulting T/W₀ is unrealistically small. In practice, this would result in a long-duration, less-efficient burn and likely result in a descent profile that is not compatible with the Mach and altitude conditions of the supersonic transition event discussed in more detail in Section 4.10. It also results in excessive propellant mass required. Because the descent stage propellant mass from ENVISION was used to seed more detailed descent stage design work, as can be seen in Section 4.8, when a more appropriate T/W₀ is used, there is excess descent stage propellant and/or excess landed payload capability when assuming the ENVISION propellant quantity. As stated in later sections, continued refinement of powered descent throttle strategy and descent stage design is forward work.

4.4 TeamX Sizing and EDL Concept Assessments

An intensive, 4-day study was undertaken at NASA’s JPL by the Advanced Projects Design Team, called TeamX, to provide an independent design and sizing assessment for the two HAT Mars Lander architectures. TeamX is comprised of spacecraft systems and subsystems experts who work in a highly collaborative environment to provide rapid mission and spacecraft design. The remainder of this section provides an overview of the TeamX study that was conducted at JPL February 21-23, 2012.

4.4.1 Study Overview

The two HAT Mars Lander architectures assessed by TeamX were the mid L/D architecture and the HIAD architecture, shown as architectures #1 and #2 in Figure 4-8. TeamX was not asked to re-architect as part of the study, but rather to provide an independent sizing of spacecraft elements within the architectures, and for each architecture propose a transition method for transitioning from supersonic flight to powered descent. As shown in Figure 4-8, TeamX was provided various inputs for the study, including a hypersonic/supersonic trajectory for each architecture, MAV mass and dimensions, landed payload mass and volume, and launch fairing dimensions. TeamX then used these inputs to size the aeroassist vehicles (mid L/D aeroshell and HIAD), the landers (descent module and cargo) and the method of transition from supersonic flight to powered descent. In a final report, TeamX provided configurations, MELs and PELs for all the elements in the architectures, and sequence of events for the transitions. The remaining sections below are a summary of the study outcomes.

4.4.2 Vehicle Configurations and Design Drivers

The following sections provide entry sequence and vehicle configuration details for the mid L/D and HIAD architectures.

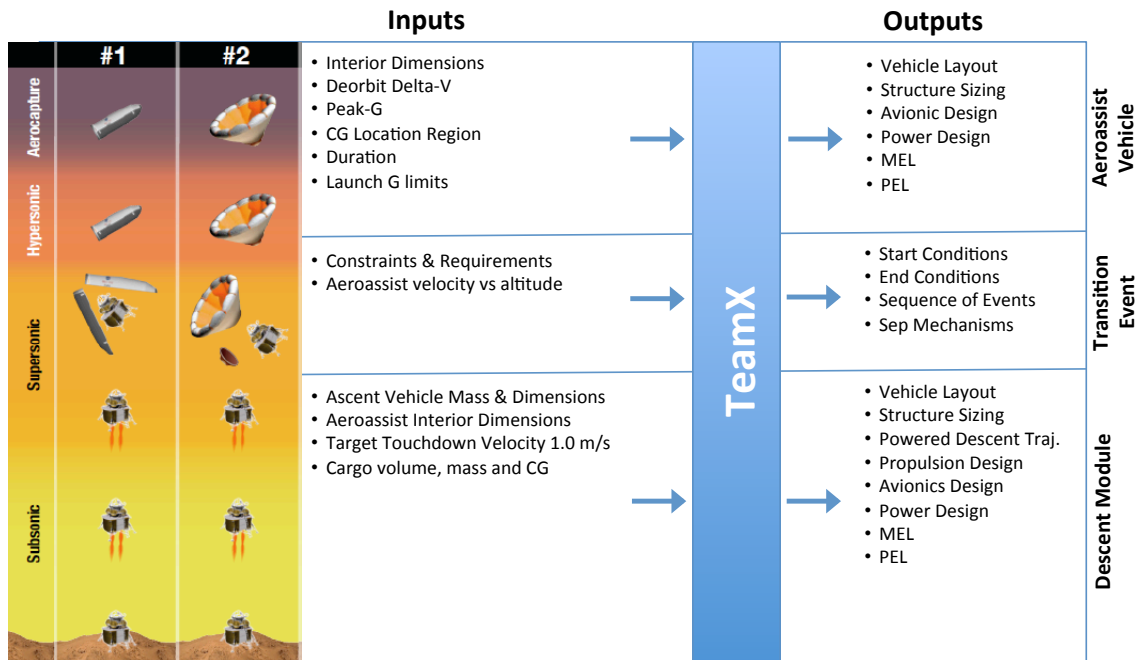


Figure 4-8 TeamX study overview – inputs and outputs.

4.4.2.1 Mid L/D Architecture

The sequence of events for the mid L/D architecture, as designed by TeamX, is shown in Figure 4-9. The entry begins at entry interface at 129 km altitude. The mid L/D vehicle flies through the hypersonic regime and decelerates until supersonic. At Mach 3.0, the vehicle pitches to 0° angle of attack in preparation for the transition to powered descent. At Mach 2.97, the transition sequence begins with the opening of the aeroshell in clamshell fashion, initiated by a series of pyro firings, allowing the lander to separate from the aeroshell. Once free of the aeroshell, the lander initiates powered descent at Mach 2.89 at an altitude of 7.3 km, having been in free-fall for a total of 10 seconds. Under powered descent, the lander decelerates further and touches down at 2.48 m/s. A more detailed illustration of the transition event is provided by Figure 4-12.

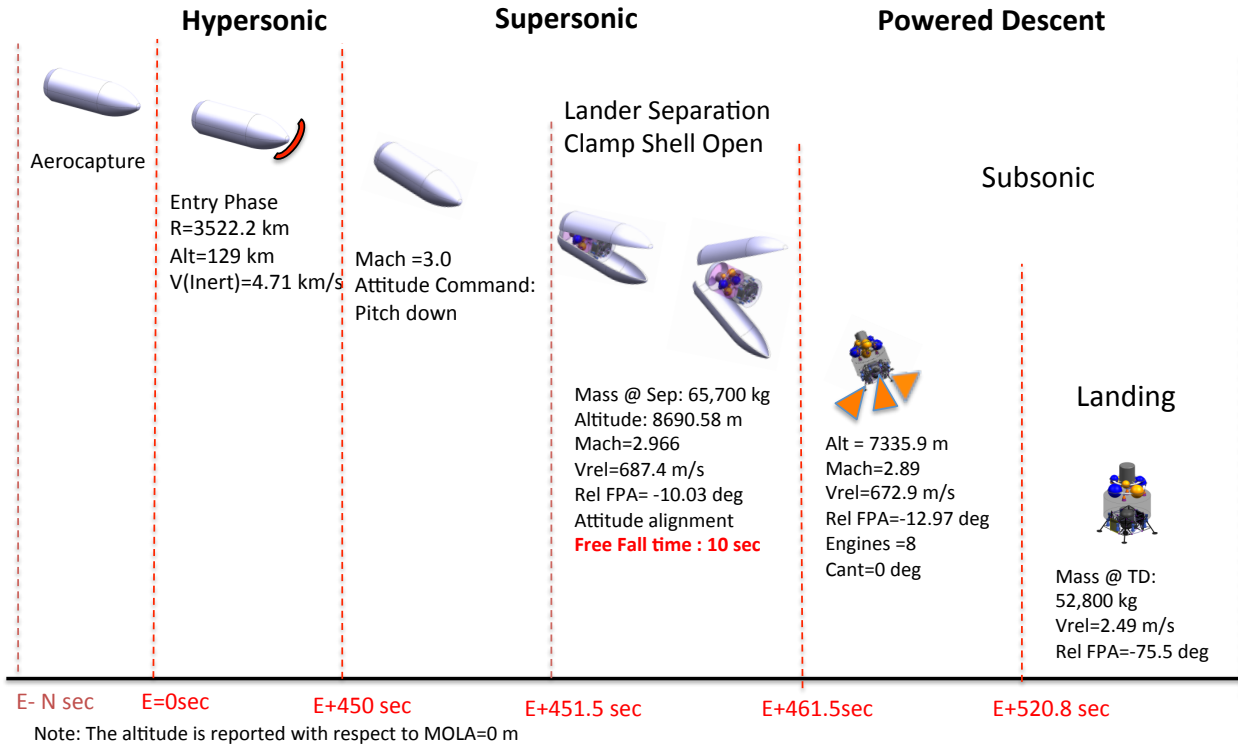


Figure 4-9 TeamX mid L/D architecture.

As shown in Figure 4-10, the lander is package inside two halves of a mid L/D aeroshell. The aeroshell has dimension 30 m x 10 m. The clamshell-style packaging was a result of designing for a workable and robust transition method from supersonic flight to powered descent. The aeroshell has a dual use as an aeroshell for atmospheric entry at Mars, but also as the launch vehicle payload fairing during ascent from Earth. This is beneficial for system mass efficiency, but also presents some unique challenges for, among others, protection of the entry TPS during Earth ascent. In addition to the two aeroshell halves, there is a fairing base ring at the rear of the vehicle as shown in Figure 4-10.

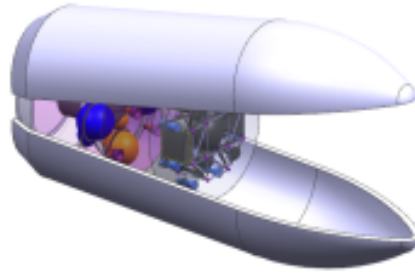


Figure 4-10 Mid L/D architecture aeroshell with lander inside.

The entry mass for the mid L/D architecture is the combined mass of the mid L/D aeroshell and the wet mass of the lander, including 40 t of payload. Table 4-14 shows the total wet entry mass for the architecture, which is 98.5 t, as sized by the TeamX study.

Table 4-14 Mid L/D Architecture Wet Entry Mass

Component	Mass (t)	Study Input/Output
Wet Lander Mass (including payload)	73.0	Output
Aeroshell Mass	25.5	Output
Wet Entry Mass	98.5	Output

The mid L/D architecture lander configuration is shown in Figure 4-11. The ascent vehicle design, shown atop the lander, was provided to TeamX and represents an early first order HAT Mars Lander MAV design. For obvious reasons, the MAV is mounted atop the lander to allow an unobstructed launch for crew return to orbit. The gray cylindrical volume shown below the MAV represents the payload volume where cargo in addition to the MAV is housed. The TeamX study did not include detailed packaging design of likely payload manifests for human Mars missions, but rather included a generic payload packing area, indicated in gray. The descent stage main body is

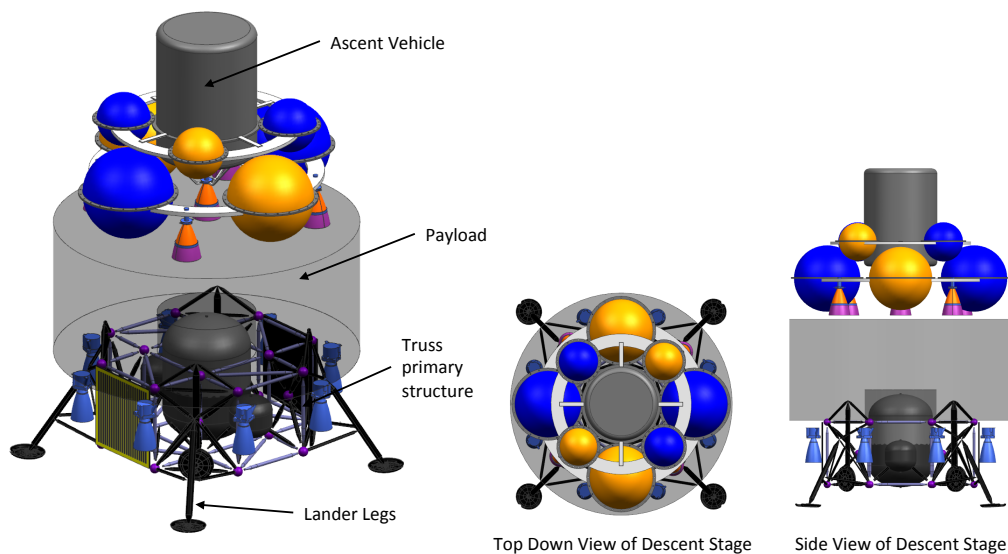


Figure 4-11 Mid L/S architecture descent stage with payload area and MAV.

cylindrical with propulsion tanks inside. Lander legs are mounted on the outside of the main body, and shown in the deployed configuration in Figure 4-11. At launch, they are folded up against the spacecraft, as can be seen in Figure 4-13. Radiator panels are also mounted on the side of the spacecraft. Mounted around the perimeter of the descent stage are eight 100 kN LOX/LCH₄ descent engines providing a total of 800 kN of descent thrust.

Table 4-15 Mid L/D Architecture Lander Mass

Component	Mass (t)	Study Input/Output
Cargo	20.2	Input
Mars Ascent Vehicle	19.8	Input
Dry Descent Stage	17.1	Output
Propellant	15.9	Output
Total Lander Wet Mass	73.0	Output
Total Landed Mass	57.0	Output

The mid L/D total lander wet mass, including MAV and cargo is 73.0 t, as shown in Table 4-15. The total landed mass of the lander, assuming all descent propellant is consumed, is 57.0 t, delivering a total of 40 t of landed payload.

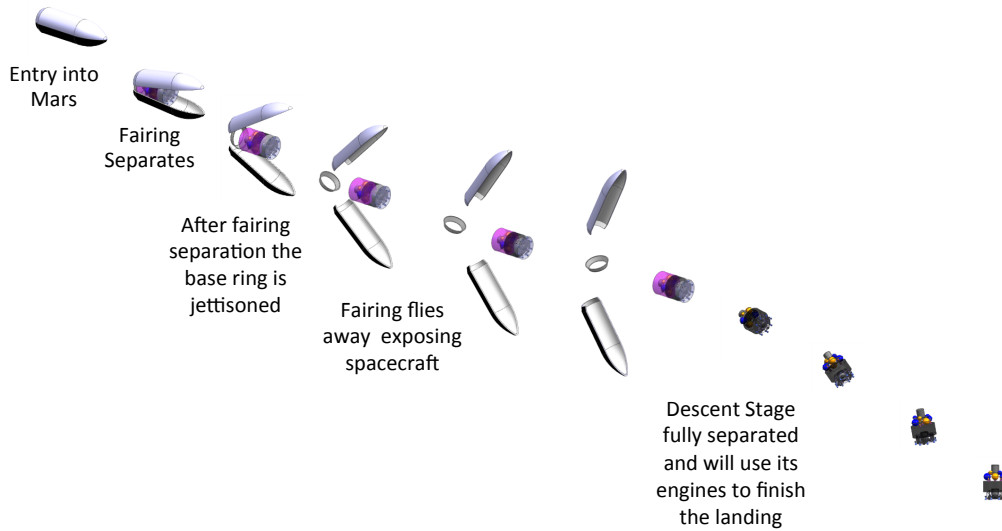


Figure 4-12 Mid L/D architecture transition event sequence.

Figure 4-12 illustrates in more detail the transition event sequence design to transition the mid L/D entry vehicle from supersonic flight through lander separation to lander-powered descent. After considering a number of options for the transition event, TeamX settled on the clamshell method for its mechanical simplicity, potential for rapid execution, and similarity to launch vehicle payload fairing jettison techniques. This method of transition was also the top choice of NASA’s EDL-SA study executed in 2010.³ The TeamX study provides independent confirmation that the clamshell transition option should be considered as among the top candidates for the mid L/D architecture.

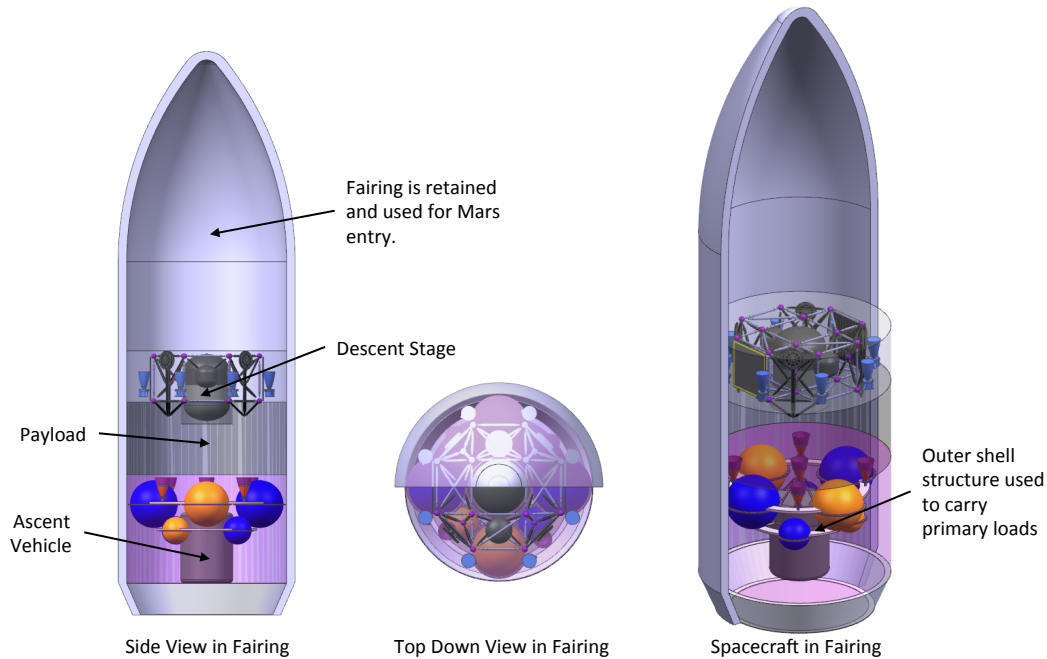


Figure 4-13 Mid L/D architecture launch configuration.

In addition to the entry architecture, lander design is also driven by launch requirements. Figure 4-13 shows the TeamX launch configuration design for the mid L/D architecture. Because the launch vehicle payload fairing serves as mid L/D aeroshell at entry, the lander is stowed inside the fairing in the same configuration as seen at entry. The lander is mounted toward the rear of the fairing in a top-down position, which provides the correct orientation for the lander transition event during the entry and landing sequence. To keep launch loads from driving lander and MAV structural design, the lander is mounted and attached to the inside of the fairing such that the primary launch loads are carried through the outer shell structure of the fairing.

4.4.2.2 HIAD Architecture

The sequence of events for the HIAD architecture landing, as designed by TeamX, is shown in Figure 4-14. The entry begins at entry interface at 129 km altitude. The HIAD vehicle flies through the hypersonic regime and decelerates until supersonic. As with the mid L/D architecture, at Mach 3.0 the vehicle pitches to 0° angle of attack in preparation for the transition to powered descent. At Mach 2.02, the transition sequence begins with the separation of the lander from the HIAD as it slides forward through the HIAD. The rigid heatshield remains attached to the lander. The separation is initiated by pyro firings. Once free of the HIAD, at Mach 2.01 and at an altitude of 6.8 km, the lander initiates powered descent using canted descent engines, having been in free-fall for a total of 6 seconds. At an altitude of 1.2 km, the heatshield is jettisoned and the two remaining descent engines fire as well. Under powered descent, the lander decelerates further and touches down at 2.47 m/s. A more detailed illustration of the transition event is shown in Figure 4-17.

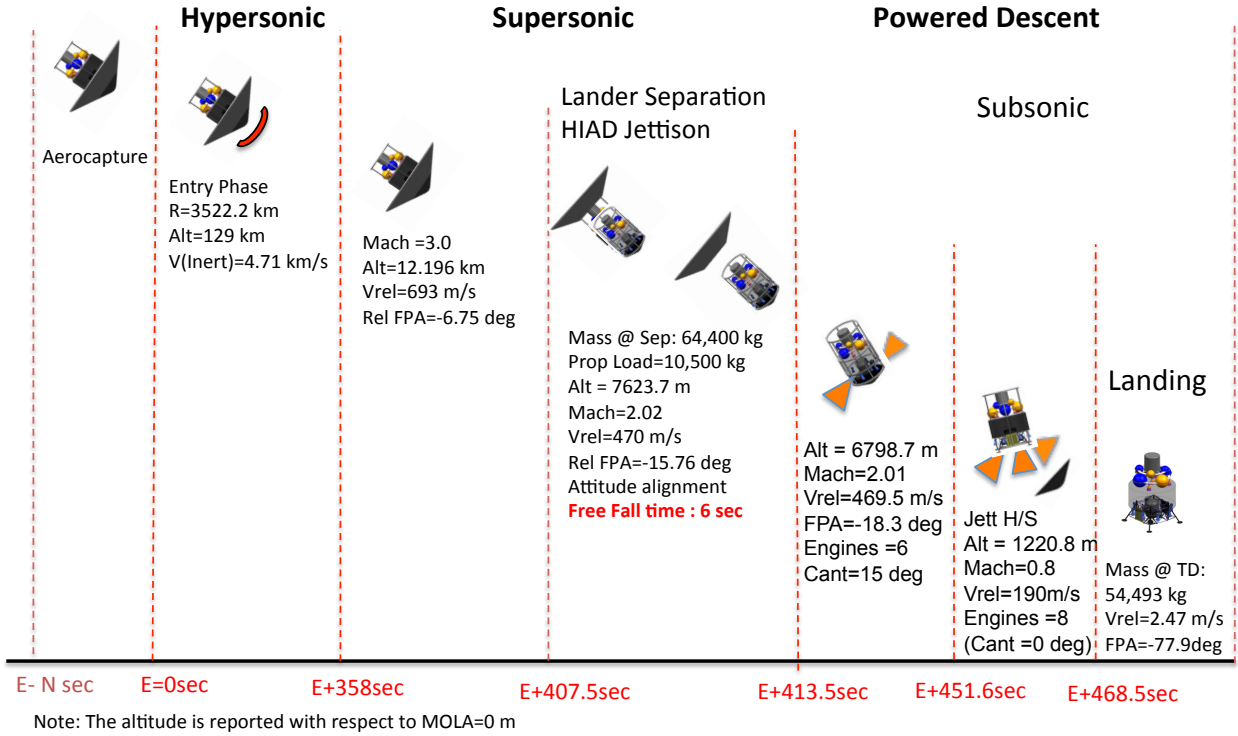


Figure 4-14 TeamX HIAD architecture.

The entry configuration for the HIAD architecture is shown in Figure 4-15. The lander is mounted to a 23 m HIAD, which is deployed and inflated prior to entry. The HIAD consists of a 9 m rigid heatshield at the center of the HIAD and flexible, inflated structure extending beyond the heatshield out to the perimeter of the HIAD. The lander structure is hard-mounted to the rigid heatshield. The heatshield and HIAD fabric are both protected by TPS. In contrast to the mid L/D architecture, the launch fairing does not play a role in the HAID entry architecture.

The entry mass for the HIAD architecture is the combined mass of the HIAD structure and the wet mass of the lander, including 40 t of payload. Table 4-16 shows the total wet entry mass for the architecture, which is 85.7 t.

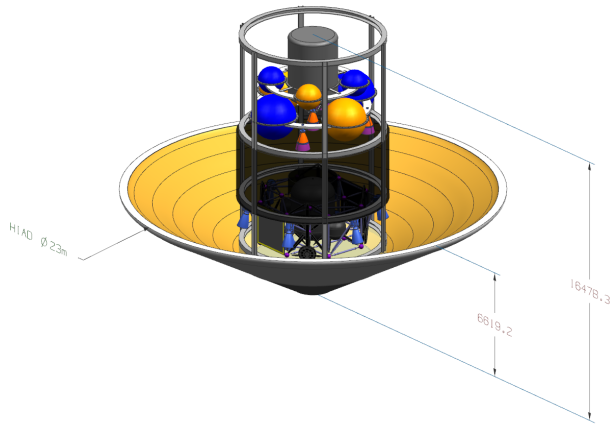


Figure 4-15 HIAD architecture HID with lander.

Table 4-16 HIAD Architecture Wet Entry Mass

Component	Mass (t)	Study Input/Output
Wet Lander Mass (including payload)	74.2	Output
HIAD Mass	11.5	Output
Wet Entry Mass	85.7	Output

The lander configuration for the HIAD architecture is shown in Figure 4-16. As with the mid L/D architecture, the ascent vehicle design, shown atop the lander, was provided to TeamX and represents an early first order HAT Mars Lander MAV design. Also, as with the mid L/D architecture lander, the dark gray cylindrical volume shown below the MAV represents the payload volume where cargo in addition to the MAV is housed. The TeamX study did not include detailed packaging design of likely payload manifests for human Mars missions, but rather included a generic payload packing area, indicated in dark gray. The HIAD architecture version of the lander is housed in a launch/transition cylindrical support structure that serves to support the lander during entry and provides rail guidance as the lander slides through the HIAD during lander separation. The cage structure remains with the lander through powered descent to the surface. Once on the surface, this cage structure needs to be at least partially removed or deployed to provide an unobstructed path for the MAV to depart the top of the lander upon crew return to orbit. The descent stage main body is cylindrical with propulsion tanks inside. Lander legs are mounted on the outside of the main body, and shown in the deployed configuration in Figure 4-16. At launch, they are folded up against the spacecraft, as can be seen in Figure 4-18. Radiator panels are also mounted on the side of the spacecraft. Mounted around the perimeter of the descent stage are eight 100 kN LOX/LCH₄ descent engines providing a total of 800 kN of descent thrust. Six of the descent engines are canted outward by 15° to provide plume clearance around the heatshield during the initial stages of powered descent. The remaining two engines are not canted and fire only after heatshield deployment.

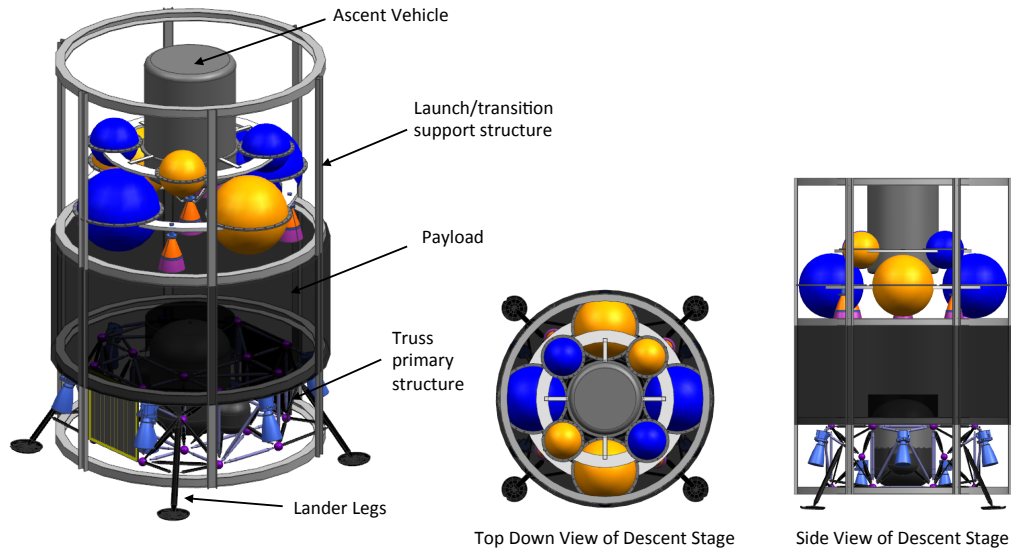


Figure 4-16 HIAD architecture lander with payload area and MAV.

The HIAD architecture total lander wet mass, including MAV and cargo is 74.2 t, as shown in Table 4-17. The total landed mass of the lander, assuming all descent propellant is consumed, is 60.0 t, delivering a total of 40 t of landed payload.

Table 4-17 HIAD Architecture Lander Mass

Component	Mass (t)	Study Input/Output
Cargo	20.2	Input
Mars Ascent Vehicle	19.8	Input
Dry Descent Stage	20.0	Output
Propellant	14.0	Output
Total Lander Wet Mass	74.2	Output
Total Landed Mass	60.0	Output

A more detailed representation of the HIAD architecture transition event is shown in Figure 4-17. The transition event sequence design begins during supersonic flight, transitions the lander configuration for landing, and ends at the initiation of powered descent. After considering a number of options for the transition event, TeamX settled on the forward exit method for its mechanical simplicity, potential for rapid execution and leveraging of large difference in ballistic coefficients between separation elements. This method of separation was also identified as a preferred option by NASA’s EDL-SA study, providing independent confirmation that the forward separation method should be considered among the most desirable for the HIAD architecture.

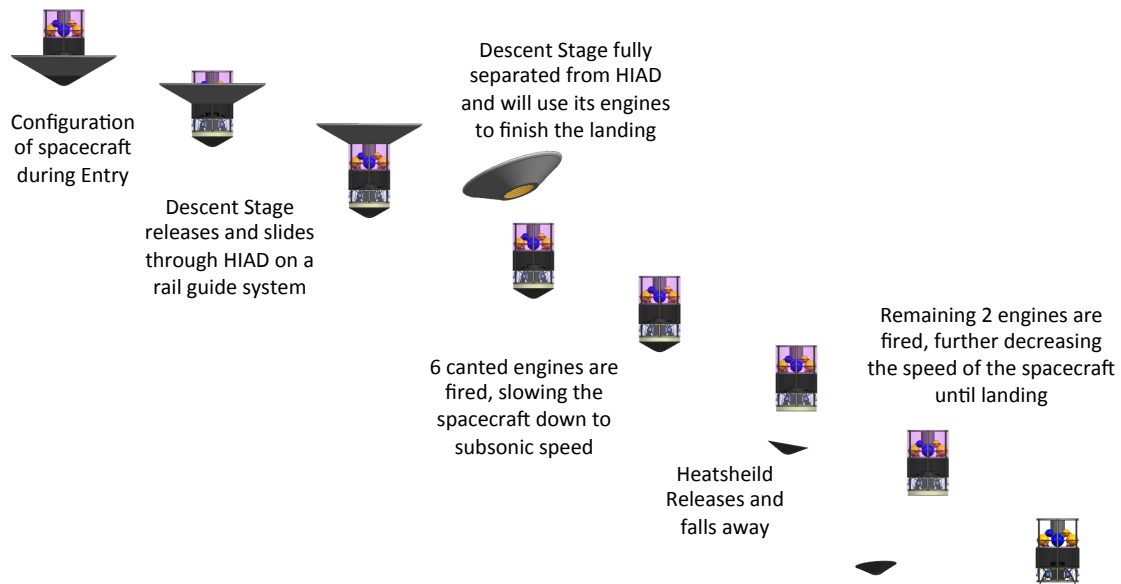


Figure 4-17 HIAD architecture transition configuration.

Figure 4-18 illustrates the launch configuration for the HIAD architecture. Like the mid L/D configuration, the lander is packaged in the launch fairing top down. This is to prevent launch loads from being carried through the HIAD heatshield. Instead the launch loads are carried through the launch/transition support structure that surrounds the lander. Unlike the mid L/D architecture, the launch vehicle payload fairing is used only during launch. The HIAD/lander vehicle travels to Mars without the launch vehicle payload fairing.

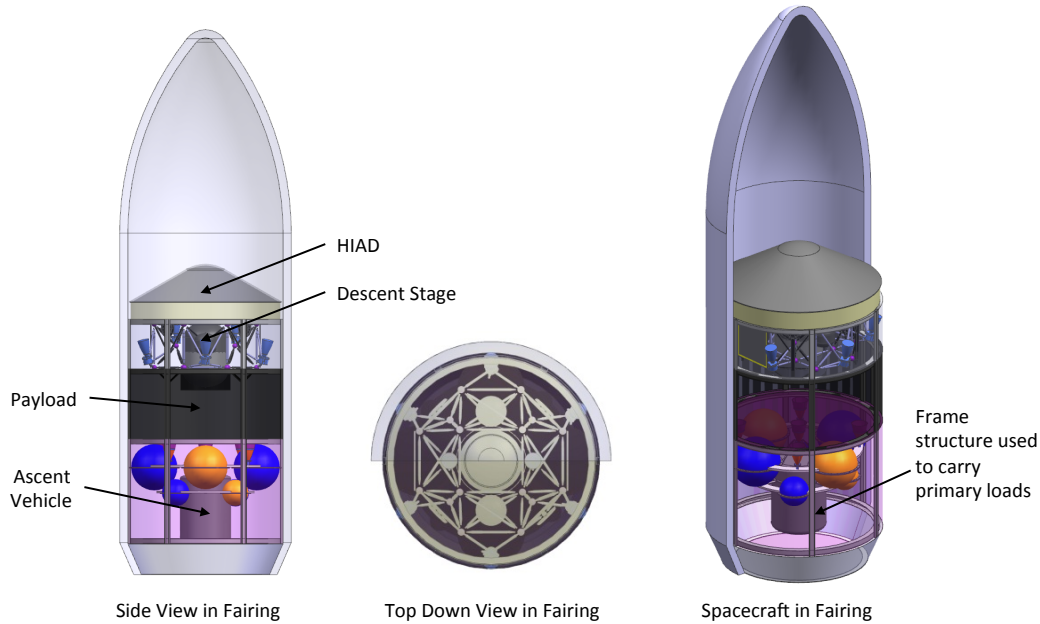


Figure 4-18 HIAD architecture launch configuration.

4.4.3 Primary Risk Drivers

During the TeamX study, the design team identified and documented architecture risks. In all, 13 risks were identified but none were rated due to the early nature of the architectures. Of the risks identified, the primary risk drivers were:

- Vehicle mass is an order of magnitude larger than anything landed on Mars to date and drives the need for new technologies, new processing and test facilities and new EDL approaches
- Precision landing requirements of 1 km drives system risk
- The use of aerocapture drives arrival risk
- The architectures contain a number of low TRL components or elements

4.4.4 Summary and Conclusions

The 4-day TeamX study executed at JPL provided valuable independent sizing of the vehicle elements of the two Mars EDL architectures being assessed by the HAT Mars Lander Team. In general, the sizing results of the TeamX exercise agree well with previous vehicle sizing efforts carried out as part of NASA’s development of the DRA 5.0² and the EDL-SA NASA agency study.³ They also agree well with the initial work of the HAT Mars Lander Team.

The conclusions offered by TeamX following the completion of the study are that the HIAD approach appears to be the more mass efficient of the two architectures with an arrival mass of 87.5 t compared to 98.5 t for the mid L/D architecture. However, the HIAD vehicle may have steering issues during the guidance phase of flight. While more mass efficient at entry, the HIAD option is less volume efficient in the launch payload fairing. Both configurations package appropriately in the fairing for EDL, but additional packaging design work is needed for the package of cargo in the designated payload area of the landers. When comparing architectures side-by-side, both have equally developed descent sequence of events, and both require hypersonic steering to achieve landing accuracy performance goals and both require supersonic propulsive engine firing.

A more detailed summary of the TeamX Mars lander design study can be found in the TeamX final report *1295 Mars Human Lander 02-2012 Final Report*. The report is available upon request.

4.5 Aerodynamic Entry and Descent

4.5.1 Rationale for Additional Entry and Descent Work

“The reference EDL architecture selected for DRA 5.0 was a hypersonic aeroassist entry system, with a mid L/D aeroshell that was ejected at low supersonic Mach numbers. A liquid Oxygen and liquid Methane (LOX/LCH₄) fueled propulsion system was utilized for deorbit delta-V maneuvers, RCS control during the entry phase, and final terminal descent to the surface.”² Several other configurations were considered but were felt to be lacking in sufficient detail to be included so DRA 5.0 “strongly recommended that future development of improved models for these types of systems technologies be pursued, so that credible trades can be conducted and more optimal EDL system performance and reliability improvements realized.”²

4.5.2 The EDL-SA Study

“Therefore NASA senior management commissioned the Entry, Descent and Landing Systems Analysis (EDL-SA) Study in 2008 to identify and roadmap the EDL technology investments that the agency needed to make in order to successfully land large payloads at Mars for both robotic and human-scale missions.”³ The first year of the study considered eight architectures for exploration class missions delivering payloads of 10 t to 50 t on Mars. See Figure 4-19.

Architecture 1, similar in concept to the DRA 5.0 entry configuration, utilized a 10x30 m cylinder with hemispherical nose cap as the mid-L/D entry vehicle for aerocapture (AC) and entry, and SRP for descent and landing. Architecture 2 considered a 23 m (HIAD) for aerocapture and entry as a lighter-weight alternative to the rigid aeroshell. Architecture 3 considered an all-propulsive entry. Architecture 4 considered the circumstance where a single HIAD could not be used for both AC and entry and, therefore, utilized the 10x30 m rigid aeroshell for aerocapture and entered with a HIAD. Architecture 5, like Architecture 4 assumed a rigid aeroshell for aerocapture but considered an alternative to SRP by increasing the size of the HIAD to allow it to reach subsonic speeds at sufficient altitudes to enable successful landing using subsonic retropropulsion. Architecture 6 was similar but assumes the same HIAD is also used for aerocapture. Architecture 7 considered the option of using a mid- L/D rigid aeroshell and a supersonic inflatable aerodynamic decelerator (SIAD) to reach subsonic speeds at engine initiation and likewise, Architecture 8 paired a HIAD and a SIAD to reach subsonic engine initiation.³

Several modeling improvements were made from DRA 5.0 to the EDL-SA assessment, which sought to increase the fidelity of component models including mass modeling, aerodynamic and aerothermodynamic modeling of the entry shapes, and TPS options. The trajectory analysis introduced bank angle-controlled entry guidance and supersonic engine design considerations. All trajectories assumed entry from 1 Sol orbit and 500 km circular orbits. The velocity at the start of guidance and heading alignment was unique to each architecture but the nominal trajectories utilized three bank reversals. The transition between the entry vehicle aeroassisted-descent and the initiation of rocket-powered terminal descent, during which time the aero entry system was jettisoned, was modeled as a simple free fall with a duration of 20 s for the rigid aeroshell configurations and 15 s for inflatable structures.⁴

Keeping in mind the Human Systems Integration Requirements (HSIR)⁵ on peak accelerations for a deconditioned crew and to include margin in the trajectory, the peak acceleration allowed during entry and while on the engines was limited to 3 Earth g’s for all trajectories. Trajectory termination occurred after the vehicle slowed to a velocity of 2.5 m/s, which was held for 5 seconds prior to touching down at 0 km above the MOLA areoid. Within this trajectory framework, the deorbit mass of all the architectures was minimized to land a 40 t payload using the Program to Optimize Simulated Trajectories (POST2).⁶ Additionally, several aerocapture and entry trade studies were performed. The purpose of the EDL-SA study was to determine which technologies showed enough feasibility to warrant continued investment.⁴

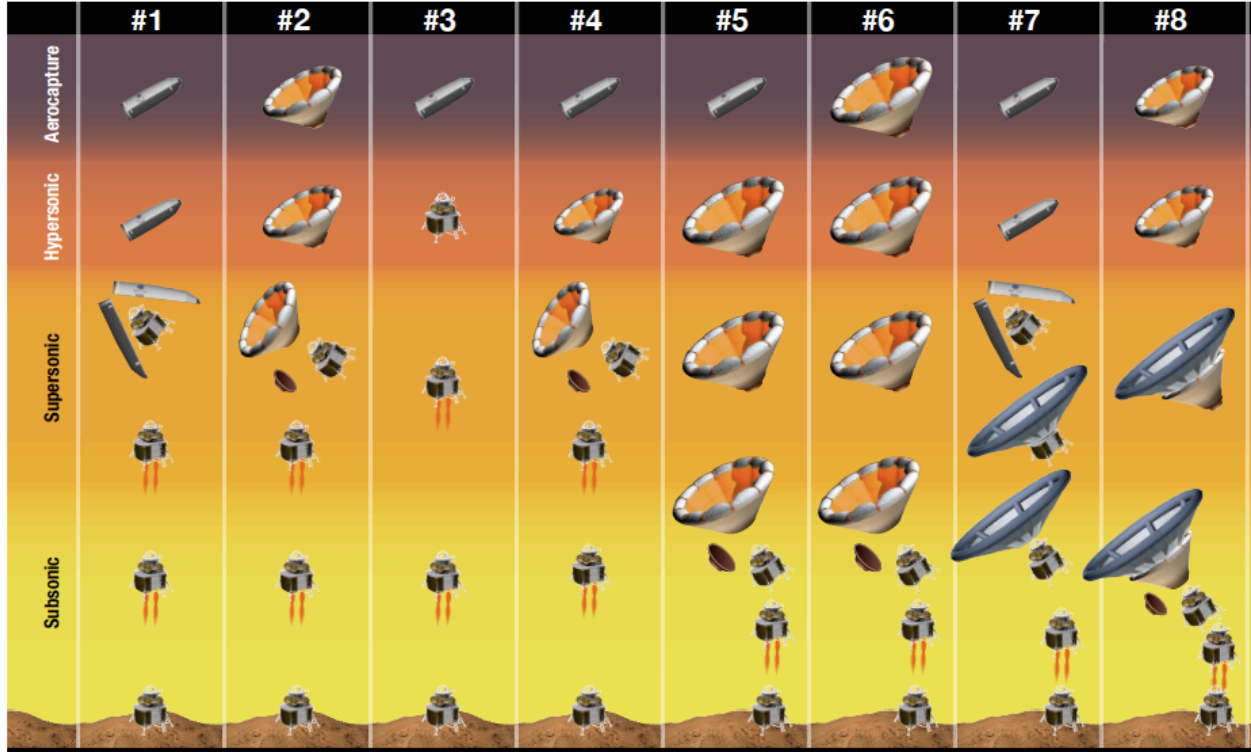


Figure 4-19 EDL-SA Technology combinations form 8 unique EDL architectures.

4.5.3 Human Architecture Team Efforts

Based on the analysis performed for the EDL-SA study, the technologies recommended for investment included the mid L/D vehicle, due to its relative high TRL, the HIAD as a mass savings alternative, and SRP for descent and precision landing.⁴

However, as with any study considering missions indefinitely in the future and an order of magnitude larger than the current state of the art, several shortfalls are identified. First, the level of fidelity of the models was limited, so only three degree-of-freedom analyses were performed. Second, very little information exists on the dynamics or ability to control large inflatable vehicles during aerocapture or entry, so many assumptions and idealizations on controllability of the HIAD had to be made. Third, few detailed vehicle packaged concepts exist for landing systems of this size, therefore little can be said of the flight stability for launch, aerocapture, entry or terminal descent. Also, the separation of the entry vehicle from the descent stage is not modeled due to this lack of information. Therefore a simple free-fall event of 15 s to 20 s was assumed. Finally, no attempt was made to ensure the ability to perform precision landing or hazard detection and avoidance during descent.⁴

Therefore, additional analysis was needed to determine whether the architectures and technologies recommended by EDL-SA were viable and accurately inform the technologies for consideration and development. The next phase of analysis, performed by HAT, addressed specific gaps in previous studies, including stability assessments, MAV and descent stage vehicle sizing, engine trades and overall configuration packaging.⁴ A detailed description of the configuration packaging effort within HAT is presented in Section 4.6.

4.5.4 Future Work

Although no significant modifications were made to the EDL simulation from EDL-SA, the additional work performed by the HAT described in Sections 4.7 & 4.10 is required to develop 6-DOF entry simulations. The HAT engine trades more accurately inform the volume and mass requirements of the descent stage and MAV, which

impact the configuration packaging designs that provide inertia information. Vehicle inertias will allow (1) updates to the parameterized mass models, (2) more thorough evaluation of transition events and additional masses required to accomplish the transitions, (3) development of entry and descent guidance and control algorithms, (4) precision landing instrument performance evaluations, (5) updates to the terminal descent engine sizing and propellant use models, and (6) detailed analysis of vehicle stability.

An additional aspect of EDL, recognized in the EDL-SA study and verified with the HAT lander packaging arrangement effort, is that none of the packaged lander configurations exceed 17 m in length, bringing into question the need for a 10x30 m rigid aeroshell. Preliminary analysis has been performed to investigate various entry aeroshell shapes and aspect ratios, but further work is needed.⁷ The rigid aeroshell shape and its potential impacts on SLS aerodynamics and loads are also a consideration. Materials options, such as composites, are being considered for SLS. Additional analysis will be needed to verify that, should the SLS shroud double as a Mars entry aeroshell, the loads of both launch and entry can be accommodated. Additional aeroshell shapes will also require extensive stability, aerodynamic and aerothermodynamic analysis. Finally, performing an extensive descent engine trade study that examines technological advances in engine capabilities including Isp, thrust-to-weight (T/W), propellant types, etc. will inform future iterations of packaging analysis.

It is recognized that none of the architectures under consideration identically resembles the actual human mission design. However, the detailed studies will help to illuminate system unknowns, will allow more thorough risk identification and assessment, and will continue to inform technology development decisions. Significant progress has been made since DRA 5.0 that, allowed to continue, will enable a higher-fidelity assessment, to better guide future investments.

4.6 Configurations and Analyses

This section describes the process used by the structures team to develop two MDM configurations, including preliminary structural analysis, mass estimates, and component mass summaries for each configuration. Section 4.6.1 describes the purpose and general approach taken, while Section 4.6.2 outlines ground rules and assumed requirements. The development of configurations began with a brainstorming process intended to generate a variety of possible lander concepts. This process was formalized to some extent to achieve consistency, and is described in Section 4.6.3. Eight lander configurations (four horizontal and four vertical) were developed and ranked using various FOMs and the AHP described in Section 4.6.4. The ranking process resulted in a down-selection to two lander configurations (one horizontal and one vertical) that were carried forward for more detailed modeling and analysis (Section 4.6.5). The analyses included sizing for strength and linear buckling, as well as first modal frequency calculations. Preliminary mass estimates for each lander configuration were generated and are summarized in Section 4.6.6. The scope of this work was limited to assessing feasibility and obtaining first-order mass estimates. Section 4.6.8 includes preliminary ideas related to integration of the two lander concepts with an aeroassist system within a launch vehicle shroud. Key issues, uncertainties, and possibilities for further optimization are described in Section 4.6.9.

4.6.1 Purpose and Approach

4.6.1.1 Purpose

The motivation for detailed (bottoms-up) analysis of Mars Lander configurations is to inform future Mars mission decision makers by providing more detailed and reliable data than can be obtained using simple spreadsheet or parametric analysis methods. Generation of finite-element based analysis models and realistic CAD models provides valuable information related to packaging, layout, manufacturing, launch vehicle interfaces, planetary entry, descent, and surface operations. Non-obvious issues related to feasibility are often uncovered during this process.

The configuration and analysis work presented herein focuses on the layout of major vehicle components. These components include the propellant tanks, engines, landing gear, cargo elements, MAV, and primary structure for the descent module and spacecraft adapter (SA). Experience has shown that the layout of these components drives vehicle mass, inertial properties, landing stability, and ease of surface operations. Detailed conceptual designs allow system-level comparisons of Mars mission scenarios that simultaneously include consideration of: a) launch loads,

b) aeroassist system integration, c) landing stability, and d) lander offloading and surface operations. There are two major goals for this broad examination of feasibility.

The first goal is to generate mass estimates for comparison to estimates generated using simpler tools. Mass estimates obtained from the ENVISION tool and TeamX concept assessments are described in Section 4.3.5 and Section 4.4. These tools are primarily based on historical vehicle data, which is limited for crewed-lander type spacecraft. Detailed conceptual design reveals issues and discrepancies related to configuration and layout. The second goal is to determine realistic vehicle mass properties. These include masses, moments of inertia, and center-of-gravity locations of major components as well as the vehicle system as a whole. Realistic mass properties are necessary for refined analysis of Mars entry scenarios, including different aerodynamic deceleration configurations and options for transition to powered descent. Previous analyses of transition and entry have relied on coarse mass property estimates not based on any specific layout or design.

4.6.1.2 Two Configuration Approach (Vertical and Horizontal Landers)

Numerous previous studies exist that include concepts for lunar and Mars lander designs. A wide variety of concepts have been proposed, but tend to fall into two general categories. These are often referred to as “vertical” and “horizontal” lander configurations.



Figure 4-20 Notional horizontal (top row) and vertical (bottom row) lander configurations.

Simply put, vertical landers launch and land in the same orientation. Horizontal landers launch 90 degrees to their landing orientation. Generally speaking, horizontal landers are long and flat; vertical landers are tall and usually symmetric about a vertical axis.

Vertical Landers: Vertical configurations have layouts that generally resemble that of the Apollo lunar excursion module (LEM), and might be considered conventional. They usually utilize a vertical stacking of components with engines and propellant tanks low and cargo elements (and/or an ascent vehicle) on top. Vertical configurations often have a core lower structural unit containing the engines, propellant tanks, and landing gear, and a “flat-bed” type upper surface for mounting cargo. In some cases, cargo is placed within side-bay areas between other vehicle components such as the tanks or engines. Vertical configurations offer flexible packaging and efficiently utilize available launch volume by using the entire diameter of the launch shroud. They tend to exhibit efficient load paths, with thrust loads carried vertically through a symmetric (or nearly symmetric) primary structure. However, because of the vertical arrangement, these configurations can be tall with a high center of gravity at landing. Issues related to vertical height may include payload offloading difficulty or a requirement for long landing legs to ensure touchdown

stability. Previous analyses have shown that long landing legs can result in a significant mass penalty. This is because (under current assumptions) each leg must be designed to withstand the loads associated with the possibility of landing on a single leg, and because longer legs require more complex packaging and deployment schemes. Vertical lander configurations have sometimes been proposed in which major cargo elements are beneath rather than on the top or sides of the primary structure. These configurations offer the potential for easy cargo offloading and surface access, but introduce complexities related to load path, engine placement, and MAV integration. All of the vertical lander configurations considered herein utilize top-mount or side-mount cargo placement.

Horizontal Landers: Instead of vertically-stacked cargo elements, horizontal landers utilize a “side-by-side” arrangement where the various MDM components and cargo elements are spread out horizontally and potentially lower to the ground. Horizontal landers have a rectangular landing gear footprint, and the length of the landing gear is determined by the rectangle’s shortest dimension, which is the driver for stability at touchdown. Horizontal landers may offer advantages related to flexible packaging, easy offloading/surface access, and a lower center of gravity at landing leading to reduced landing gear mass. Disadvantages include a greater total length and less efficient use of available launch volume. By nature, the primary load path directions for launch and landing are in different directions, which can result in structural inefficiencies. Because of their greater length, horizontal configurations are likely to have lower lateral stiffness when mounted within the launch vehicle shroud. In some cases this may lead to unacceptably low modal frequencies that are difficult to mitigate. This issue and the limited options for increasing stiffness are discussed in Section 4.6.5.4.

For this work, a decision was made to consider at least one horizontal and one vertical lander configuration in detail. Aside from a desire to explore the advantages and disadvantages just mentioned, this decision was motivated by the fact that the optimum lander configuration for compatibility with HIAD or rigid mid L/D aeroshell systems is currently unknown. Adopting a two-configuration approach guaranteed the generation of one detailed layout with analysis results for each configuration. Design issues and details as well as preliminary mass properties would thus be available regardless of which lander configuration is eventually deemed optimal.

4.6.2 Assumptions

Firm requirements for a human mission to Mars are unknown. The following assumptions were derived for this work, or are similar to assumptions used for previous Altair (NASA’s former Constellation Program lunar lander) analyses. They are adequate for conceptual design and analysis but should not be considered formal mission requirements.

The following assumptions apply to all lander vehicle components (MDM, MAV, and payload/cargo).

Table 4-18 General Configuration and Analysis Assumptions

System/Configuration	Assumption	Notes
Lander	73,000 kg	Lander (including cargo) + descent propellant
Aeroassist System*	10,000 kg	Does not include rigid aeroshell mass for horizontal lander
Launch	83,000 kg	Total mass supported by lander primary structure
Landed	53,000 kg	No LOX in MAV tanks (MAV LOX generated by ISRU)
Loads		
	Assumption	Notes
Axial Launch	5g	Similar to previous Ares V/Altair assumed axial load
Lateral Launch	2g	clocked 0, 45, and 90 degrees
Landing	1g	Sizing from tool developed for Altair lunar lander
Entry	3g	Not analyzed during this phase (future work)
Component		
	Assumption	Notes
Shell Structure (except tanks)	IM7 977-2 Gr-Ep	Sandwich, composite facesheets with AL honeycomb core
Propellant Tanks	Aluminum-Lithium	Composite tanks possible, but benefit unclear at this size
Struts	IM7 977-2 Gr-Ep	Similar to Altair composite strut assumptions
Fittings and Attachments	Aluminum-Lithium	Al, Al-Li, or Titanium possible for future trades

*The aeroassist system mass listed above (10,000 kg) represents only the portion of the aeroassist system that

transmits loads through the lander primary structure. For simplicity, the same value has been assumed regardless of aeroshell type (HIAD or rigid). This is reasonable if one assumes that in the case of the rigid aeroshell, the aeroshell acts as the vehicle shroud and performs both launch and entry functions. In this case, a large part of the rigid aeroshell mass is already accounted for at the system level by what would normally be bookkept as the shroud mass. This common aeroshell/shroud structure would be attached to a lower stage and would not transmit loads through the lander primary structure. The remaining portion of the aeroassist system (10,000 kg assumed here) would still be attached to (and transmit loads through) the lander primary structure. The dual-use aeroshell/shroud assumption reduces launched mass and increases available packaging volume. The assumption is probably necessary for a feasible horizontal lander configuration. At this time, however, it is not known whether a dual-use aeroshell/shroud is feasible from an aerodynamic or overall vehicle perspective. Trade studies related to the assumption made here should be a focus of future work.

4.6.2.1 Descent Module Assumptions

The following assumptions were derived using the ENVISION parametric sizing tool along with separate propulsion based calculations related to propellant requirements and engine sizes.

Table 4-19 Descent Module Propellant Volume and Engine Assumptions

Item	Assumption	Notes
LOX Volume	13.64 m ³	Includes 5% ullage
LCH ₄ Volume	12.27 m ³	Includes 5% ullage
LOX Mass	14,818 kg	LOX Density 1,141 kg/m ³
LCH ₄ Mass	4,939 kg	LCH ₄ density 422.62 kg/m ³
Number of Engines	6	Six dual nozzle, 12 nozzles total
Engine Mass	204/347 kg	Single nozzle / dual nozzle
Engine Ground Clearance	0.9 m	Similar to Altair assumption (prior to gear attenuation)
Tank Clearance	0.1 m	From structure edge to tank outer mold line



Figure 4-21 Engine configuration assumptions.

The cryogenic rocket engine configurations shown were used when brainstorming possible lander configurations. Both single-nozzle and dual-nozzle engine configurations were developed and are shown in Figure 4-21. They were derived with the goal of allowing the MDM and the MAV to use the same engine. Each engine nozzle was assumed to generate 22,000lb (97,860N) thrust. Twelve nozzles total are assumed for the Mars lander descent stage. The

dual-nozzle configurations were assumed preferable because of the efficiency of a single power head. However, combinations of dual-nozzle and single-nozzle engines were allowed if beneficial to the arrangement of a particular lander configuration.

4.6.2.2 Propellant Tank Masses

The masses of all propellant tanks (shell walls only) were estimated assuming Aluminum-Lithium 2195 as the wall material (density 2713 kg/m³). Tanks were sized assuming minimum gage walls (thickness 0.1524 cm). Based on experience from a variety of previous analyses that included different tank shapes and loading conditions, minimum gage was assumed sufficient for simple cylindrical or spherical tanks. Different tank shapes for both the MDM and MAV were allowed based on the requirements of each lander configuration considered. The tank masses assumed for structural analysis do not include functional items such as baffles or plumbing. For this reason, the as-built tanks were assumed to be 25% more massive than determined from minimum gage calculations alone. To achieve commonality and ease of layout, the descent module LOX and LCH₄ tanks were dimensioned identically to match the largest fuel volume requirement (LOX). In these cases, the LCH₄ tanks were oversized by approximately 10%. Refined tank assumptions are possible, but are not likely to change result trends significantly because the tank wall masses are relatively small.

4.6.2.3 Cargo Elements

It was assumed that two lander variations would be required. The first variation consists of a descent module, MAV, ISRU plant, Fission Surface Power System (FSPS), and a crew mobility vehicle (rover). The first-variation elements would be delivered to the surface with no crew. The ISRU plant would be used for the generation of oxygen for MAV propellant. The FSPS and rover would support surface operations. Shape, size, and mass of the rover were taken from work on NASA’s Multi-Mission Space Exploration Vehicle (MMSEV). The second lander variation would deliver a crew and crew habitat to the Martian surface. In this case, the habitat is the primary cargo element.

Table 4-20 Cargo Element Assumptions

Cargo Element	Mass	Dimensions	Volume Required
Rover	5,562 kg	6 x 4.1 x 3.7 m	91 m ³
FSPS	7,000 kg	4 x 3.3 x 2.7 m (stowed)	36 m ³
ISRU	Part of MDM Control Mass	Disassembled for Transport	Distributed within MDM
Habitat	44,811 kg	7 m high x 7 m diameter	154 m ³

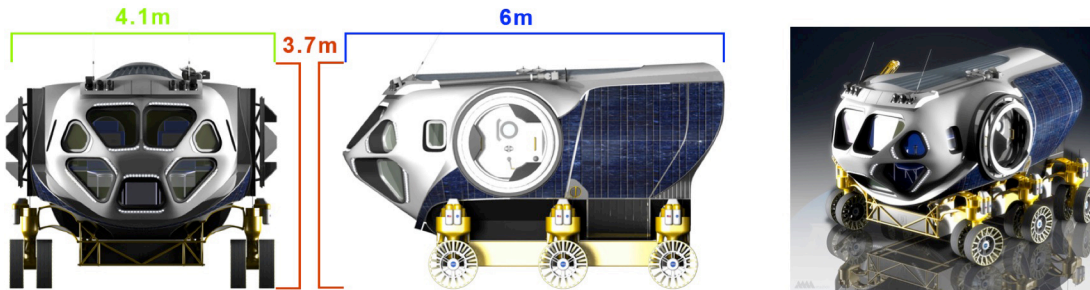


Figure 4-22 Assumed rover configuration.

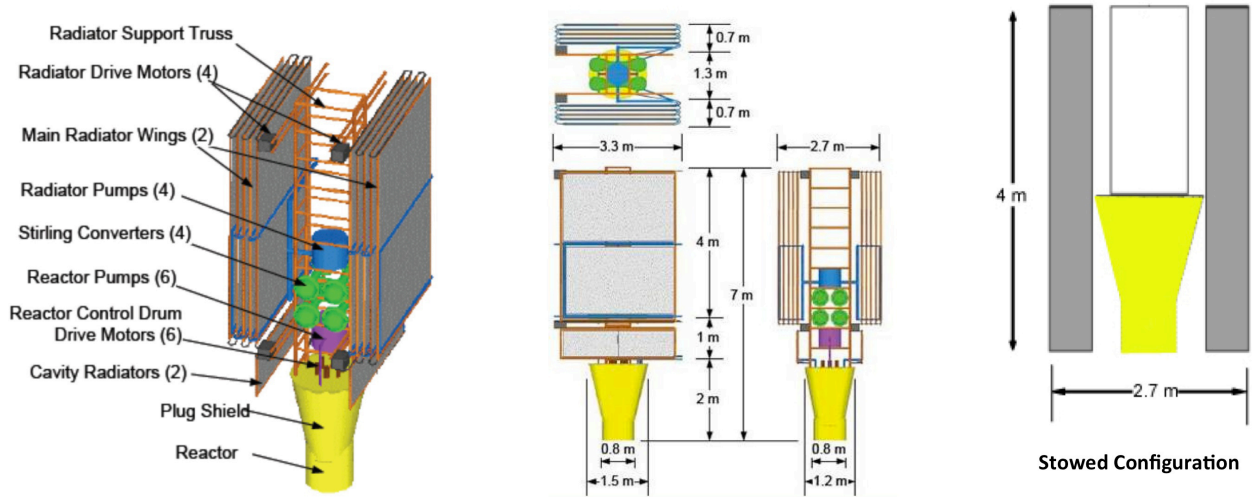


Figure 4-23 Assumed FSPS.

When brainstorming possible lander configurations, the first lander variation was assumed to be the driving configuration. The ability to accommodate a habitat was treated as just one of several metrics considered during the down-selection process. This approach was taken because the habitat volume and means of construction currently have large uncertainties. For example, there is significant ongoing technology development in the area of inflatable habitats, which could greatly reduce the packaging volume required at launch. Detailed analysis of the down-selected lander configurations only considered the uncrewed lander variation.

4.6.2.4 Mars Ascent Vehicle

The MAV is essentially a specialized cargo element, and it was assumed that the MAV pressure vessel geometry and functional details would be extrapolated from previous Altair Lunar Lander studies (section 4.9). Aspects of one versatile two-stage MAV operational design were derived separately from the lander descent module configurations considered. MAV assumptions directly affecting MDM layout and analysis are listed below.

Table 4-21 Mars Ascent Vehicle Assumptions

Item	Assumption	Notes
Diameter	2.7m	Realistic minimum for six-person crew
Height	3.5m	Similar to Altair AM height
Number of Engines	5	4 engines for 1 st stage, 1 engine for 2 nd stage
Engine Mass	204 kg	MAV and MDM use the same engine
LOX Volume 1 st Stage	8.9 m ³	Includes 5% ullage
LOX Volume 2 nd Stage	12.8 m ³	Includes 5% ullage
LCH ₄ Volume 1 st Stage	7.3 m ³	Includes 5% ullage
LCH ₄ Volume 2 nd Stage	10.5 m ³	Includes 5% ullage
Total LOX Mass	23,532 kg	Not present at launch from Earth
Total LCH ₄ Mass	7,131 kg	Contained in bottom nested tank at Earth launch
Gross MAV Liftoff Mass	42,852 kg	Liftoff from Mars surface, LOX tanks full
MAV Mass in Launch Vehicle	19,320 kg	In LV shroud, LOX tanks empty & awaiting surface ISRU

One aspect of the MAV layout that was developed in parallel with the horizontal and vertical lander configurations is the MAV propellant tank arrangement shown in Figure 4-24. The configuration consists of four nested LCH₄/LOX tanks, two mounted to the MAV 1st stage and two to the 2nd stage. The nested tanks are similar in size and symmetric about the MAV center axis. Means for separating the 1st and 2nd stages were not studied, but a guiding mechanism that allows the 2nd stage to separate from the 1st stage is considered quite feasible. The four-

nested-tank MAV configuration has the advantage of being compatible with almost all of the descent-stage layouts developed during configuration brainstorming. It was incorporated into the final CAD and analyses of the two down-selected lander configurations. Other MAV configurations are possible and should be the subject of future work. Tank masses for the MAV were derived using the same minimum gage approach described for the MDM tanks.

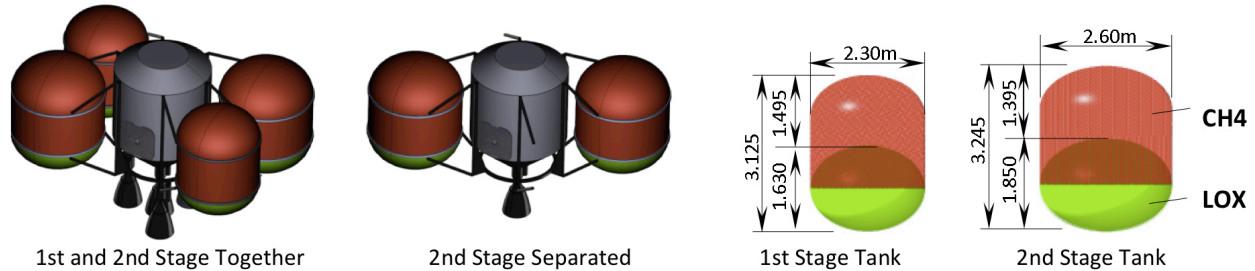


Figure 4-24 MAV configuration with four nested LCH₄/LOX propellant tanks.

Both four-engine and five-engine versions of the MAV were considered. The left side of figure 4-24 shows a four-engine version (three-engine 1st stage and single-engine 2nd stage). The four-engine MAV would require the 2nd stage engine to perform a burn during both 1st and 2nd stage ascent. The advantage is the elimination of one MAV engine. However, dual use of the 2nd stage engine introduces reliability complexities. For this reason, a four-engine 1st stage was assumed for integration into the down-selected lander configurations.

4.6.2.5 Launch Vehicle Shroud

The shroud was assumed to be 31 m long with a 17-m-long lower cylindrical barrel section, consistent with current NASA SLS assumptions. The shape of the forward portion of the shroud was left open. For a HIAD-based mission, the shroud may have the same tangent-ogive shape as current SLS launch vehicles. For a rigid-aeroshell mission, the shroud and aeroshell may be the same structure, and the shape may be a compromise geometry that is suitable for both launch and Mars entry. For this effort, the key shroud parameters are its assumed usable inner diameter (dynamic envelope) and maximum usable length, as these have the most impact on lander size and packaging. Consistent with current SLS designs, the assumed dynamic envelope was 9.1 m. Other details of the launch vehicle shroud, including shroud loading and sizing, were not studied. For some modal analyses, the horizontal lander was attached to the aeroshell/shroud to increase lateral stiffness. For these analyses, a construction similar to that of NASA's former Ares V shroud was assumed (see section 4.6.5).

4.6.3 Configuration Brainstorming

4.6.3.1 Brainstorming Process

The purpose of the brainstorming activity was to develop several configurations sufficiently for consideration by the team as a whole, leading to the down selection of two concepts (one vertical and one horizontal). Conceptual lander layouts were generated with a focus on efficient packaging of the propellant tanks, cargo, engines, and MAV within the dimensional constraints of the launch vehicle shroud. Engineering judgment was used to formulate preliminary pros and cons related to lander characteristics such as complexity, cargo access, payload offloading, and likely structural load paths. From these evolved FOMs used during the down-selection process. Although design details related to structural or other subsystems were not required during brainstorming, notional supporting structure was often generated to facilitate discussion of possible structural issues. The brainstorming activity resulted in four vertical and four horizontal lander configurations. For each configuration the general layout was determined along with motivating rationale. Dominating pros or cons were identified to stimulate discussion. During this creative phase some of the brainstormed configurations deviated slightly from the assumptions given in Section 4.6.2, which apply specifically only to the down-selected configurations as analyzed in Section 4.6.5. At the time of brainstorming all assumptions were not completely defined. Minor variations in the assumptions used for brainstorming did not significantly change the rationale or judgments associated with the configurations.

4.6.3.2 Horizontal Descent Module Brainstormed Configurations

Configuration H1

Configuration H1 has a single nested descent-module propellant tank located at the center of a horizontal platform. The MAV and Rover/FSPS are at opposite ends as shown in Figure 4-25.

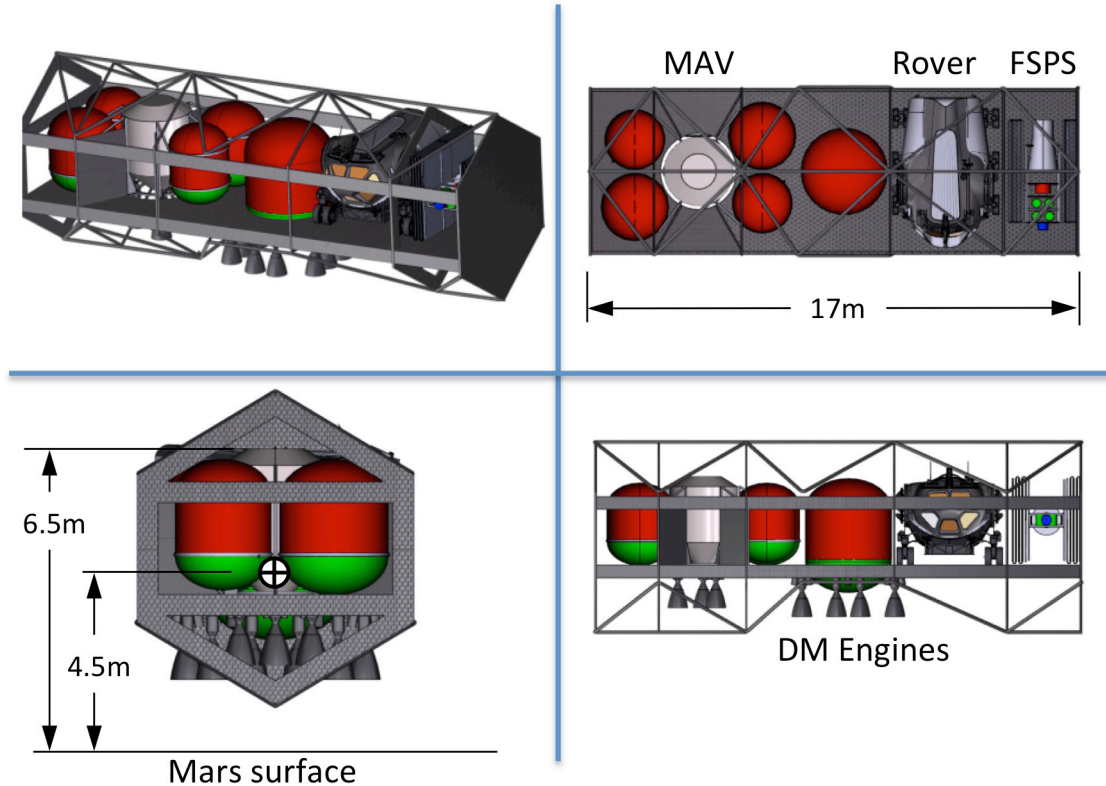


Figure 4-25 Horizontal configuration H1 (cage and platform).

This notional structure consists of a robust frame-type platform with cargo packaging similar to that of a flat-bed truck. This lander is likely to have a low center of gravity benefitting landing stability and reducing landing-leg length. The payloads would be relatively low to the surface facilitating offloading. Ample locations exist for attachment of landing gear directly to the platform structure. Configuration H1 could easily accommodate changes to payload size or shape because the fore and aft cargo areas are flexible open bays. The H1 frame structure would be solid but might be heavy. As with all horizontal landers, the primary loading direction at launch would be ninety degrees from landing, probably requiring additional structural mass to support the payload elements. In this configuration, the central tank position would be fixed, reducing options for alternate packaging arrangements. The centrally located engines would be close to the tank minimizing propulsion system mass and complexity, but could also be moved outboard to gain control authority. As shown, the hexagonal end plates would have to be hinged or removed to allow offloading from the ends of the vehicle. A portion of the upper frame structure would require removal to allow ascent of the MAV. The configuration would have sufficient volume to accommodate a habit module, but the fixed central propellant tank might require the habitat to be split into two separate volumes. H1 is the longest of the eight proposed landers (17m) and has relatively low packaging efficiency (mass per unit volume).

Configuration H2

Configuration H2 emphasizes flexible cargo packaging and offloading. The primary structure would be a central truss-type beam with additional truss structure creating large payload packaging areas as shown two-dimensionally in Figure 4-26.

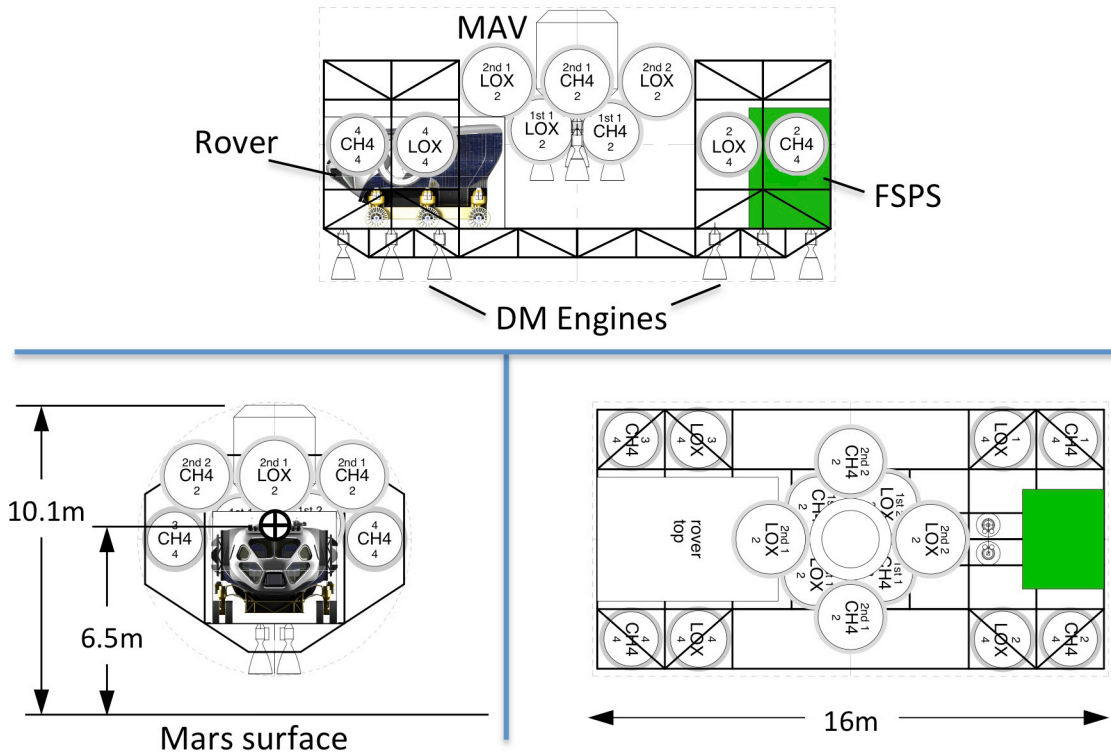


Figure 4-26 Horizontal configuration H2 (truss-bays).

A large open central bay would mount the MAV and facilitate fly out. The propellant tanks would all be spherical, minimizing construction complexity and tank mass. The longitudinal truss beam would provide multiple mounting locations for landing gear, and the center of gravity would be low at landing. Payloads near the surface and at the ends of the vehicle would aid offloading. In this configuration, there would be three engine nozzle pairs fore and aft with propellant tanks (four LOX and four LCH₄) mounted in close proximity. The central cargo area could easily accommodate different MAV configurations, or a large continuous habitat structure. The H2 packaging scheme is flexible and might be rearranged to accommodate a different set of payload requirements. This configuration is relatively long (approximately 16 m) and has somewhat inefficient packaging density. From a structural point of view, the cross section of the primary structure may provide insufficient load/moment carrying capability and stiffness.

Configuration H3

Configuration H3 is a large platform that mounts the FSPS, rover, and MAV. It is similar to the H1 platform but without a fully enclosing structure. Like H1 and H3, the configuration emphasizes packaging flexibility rather than efficiency. The continuous cargo area could accommodate rearrangement and variations in cargo size, as well as a variety of large habitat shapes. Located at each end of the platform are identical modular propulsion units consisting of two spherical tanks and three engine pairs. The modular engine units should simplify design, fabrication and testing.

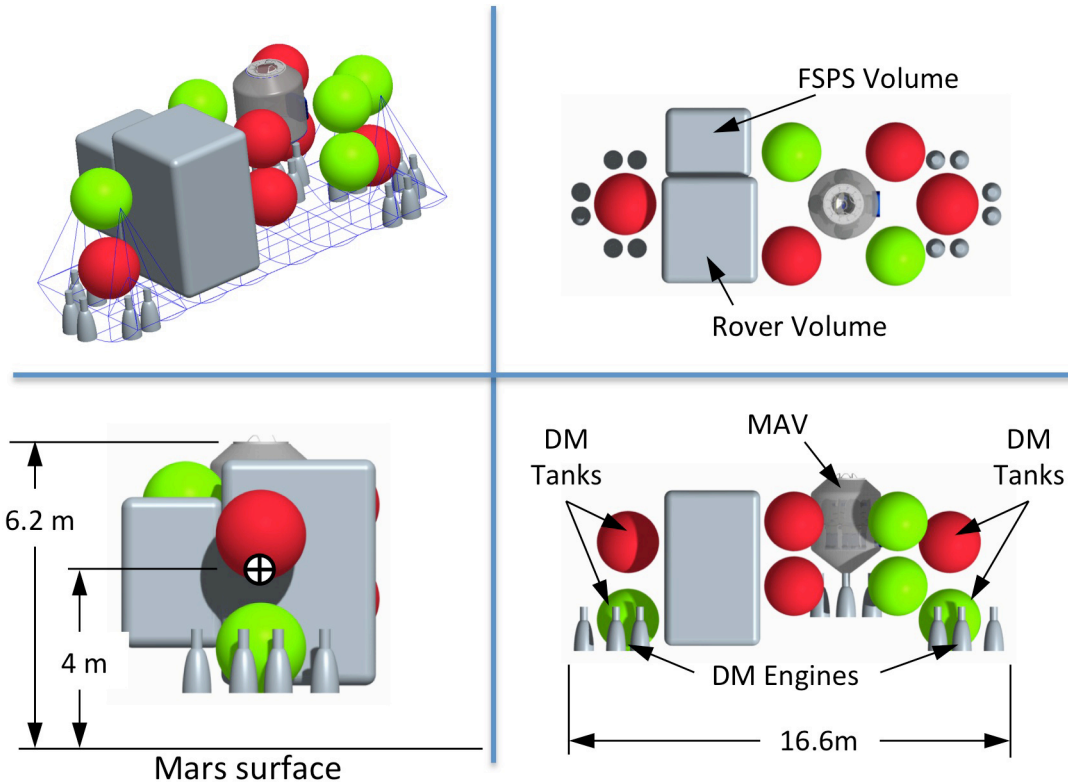


Figure 4-27 Horizontal configuration H3 (partial-circle platform).

This configuration would probably have a low center of gravity and good offloading characteristics. The configuration is long (16.6 m) and the packaging density is relatively low. The notional H3 structure consists of a flat-bed truss with partial-circle frames connected by stringers. Diagonal truss members, although required, are not shown in the figure. The MDM tanks and engines would be attached to the flatbed via a series of triangulated struts (not shown). The MAV would be attached with similar struts. The truss structure would be shallow, raising some of the same concerns mentioned for H2 (low moment carrying capability and low stiffness). The H3 configuration might not be as amenable to landing leg integration as the previous configurations. There are numerous locations for attachment, but stowage of deployable landing gear may be difficult. A possible disadvantage is that the FSPS and rover elements cannot obviously be unloaded from the end of the vehicle because one of the engine/tank modules blocks access. However, side offloading is probably feasible, and might alleviate this concern.

Configuration H4

Configuration H4 focused on packaging efficiency (rather than flexibility) to develop a lander that was as short as possible. It is generally true that increasing packaging density results in shorter load paths and increased structural efficiency. A shorter lander would also exhibit increased lateral stiffness during launch, facilitating the use of a shorter shroud and/or aeroshell structure. Reduced length would also create more options for packaging a propellant stage or additional cargo in the shroud with the lander.

As shown in Figure 4-28, the H4 configuration is 3 m to 4 m shorter than the previous horizontal configurations. To achieve the more compact configuration the tank sizes were decreased, resulting in a larger total number of tanks (12 tanks). Six LOX and six LCH₄ tanks are arranged as shown, with three tank pairs on each side of the lander. Each tank pair is associated with one dual-nozzle engine. In terms of propulsion-system complexity, the large number of tanks could be a disadvantage, but this is at least partially offset by the modular nature of each engine/tank cluster. All of the tanks are standard cylinders, which are slightly less efficient than spheres, but package more tightly. The cargo elements are mounted low and the lander probably has a low center of gravity. As shown, the rover would have to be rotated 90 degrees prior to offloading. Additionally, direct access to the cargo elements would be blocked by the engine units or the structure at the ends. Some manipulation and rearrangement would thus be required for

offloading. The dense arrangement of this configuration might make it difficult to integrate other subsystems. There would be ample points for attachment of landing legs, but the attachment points appear to be high and might result in longer and more massive landing leg struts. Plume impingement by the engines on the landing legs might also be a problem, resulting in a need for shielding panels or other structure not shown.

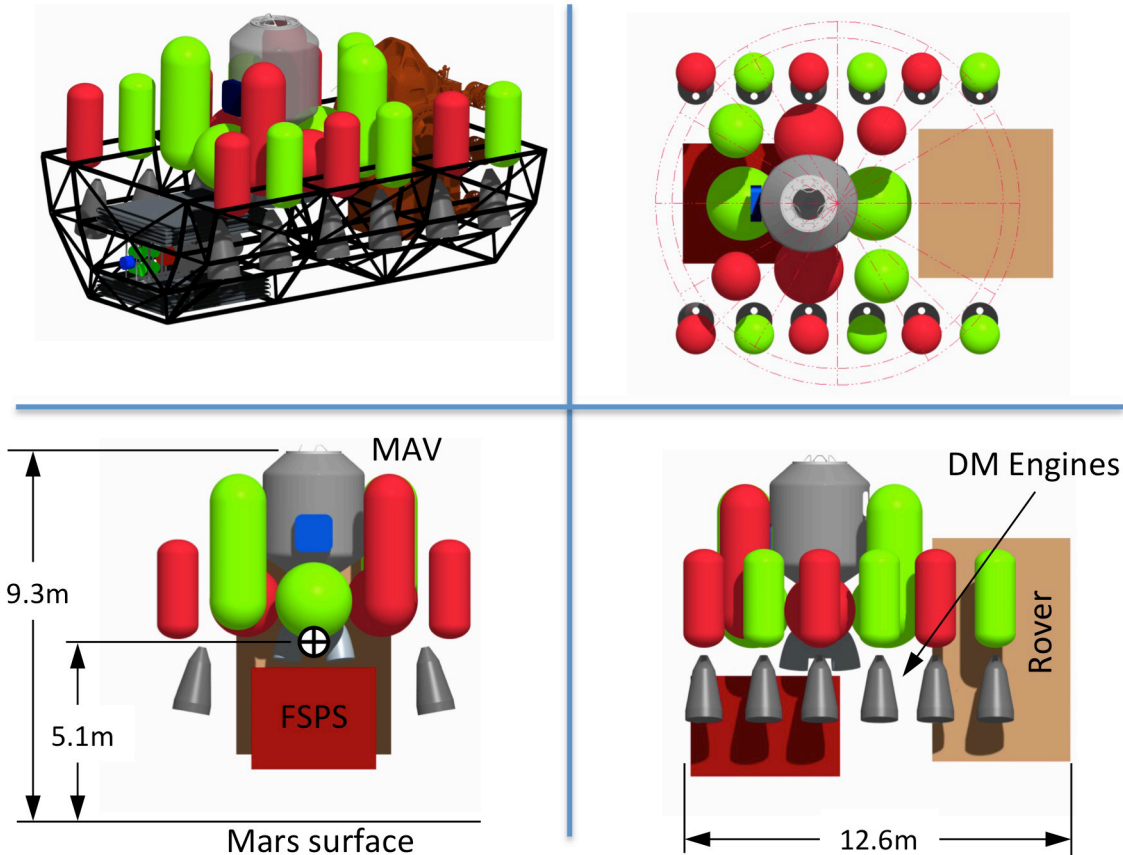


Figure 4-28 Horizontal configuration H4 (compact horizontal).

H4 may prove less adaptable to changes in cargo makeup or cargo size and shape. The dense packaging may also make integration of other subsystems more difficult. Nestled integration of the MAV may result in fly-out concerns and require removal of several propellant tanks prior to ascent. Accommodation of any habitat would require an unconventional habitat shape or partial redesign of the structure.

4.6.3.3 Vertical Descent Module Brainstormed Configurations

Configuration VI

The first of four vertical lander configurations generated during brainstorming is shown in Figure 4-29. The concept consists of a panel-type box structure with an upper level deck for mounting the MAV, and two lower cargo bays for transport of the rover and FSPS elements.

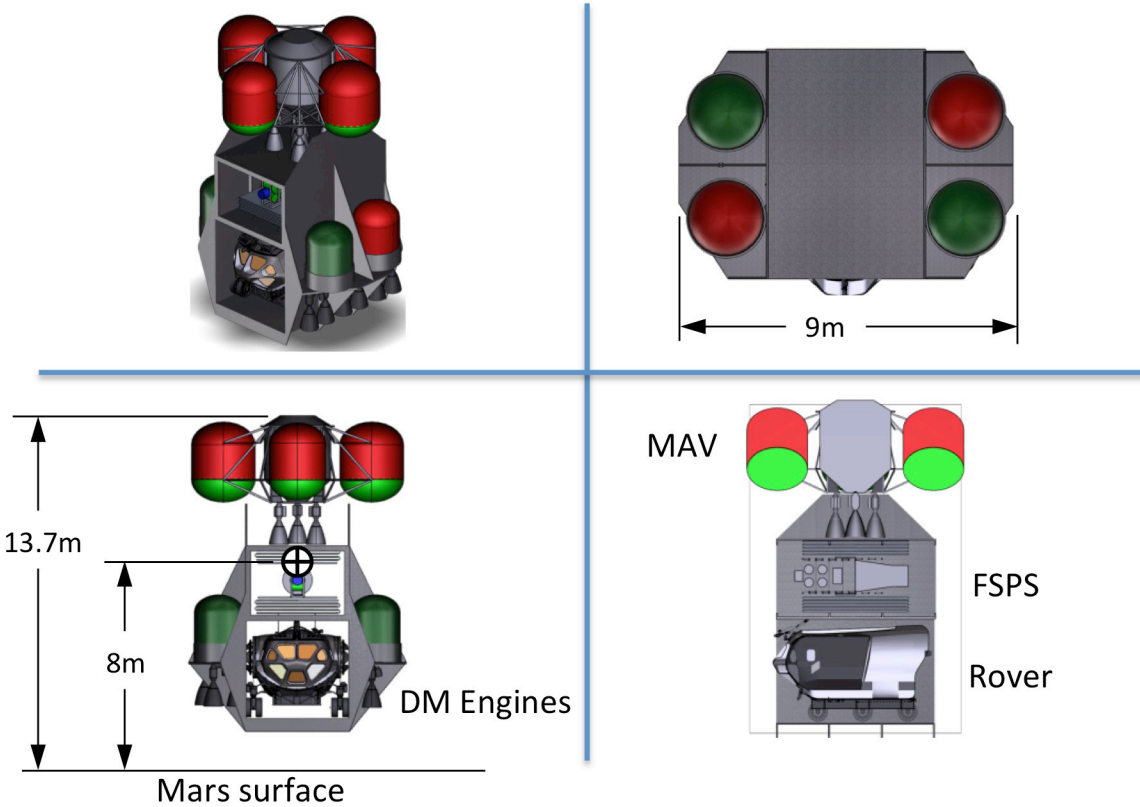


Figure 4-29 Vertical configuration V1 (stacked cargo bays).

The configuration would have a simple 2x2 tank arrangement with two cylindrical LOX tanks and two cylindrical LCH₄ tanks mounted at the sides of the lower box structure. The structural load paths for this configuration are intuitively obvious, with the vertical panels directly carrying MAV inertial loads to the base of the primary structure and on to a spacecraft adapter (not shown). Landing gear would easily be attached to the lower frame. MAV mounting should present no interference or contact issues during fly out. The V1 panel structure would likely have high stiffness. Drawbacks to this configuration include its top-deck height (which affects MAV access), and a likely high center of gravity at landing. The panel structure would be robust but might have relatively high mass. Although the rover is packaged for easy offloading, the FSPS would require lowering and/or a forklift-type device for removal. V1 could accommodate a habit structure mounted in place of the MAV, but offloading might be difficult.

Configuration V2

The second vertical configuration was developed with the goal of creating a flatbed lander with tanks/engines directly below the cargo and MAV. This arrangement, shown in Figure 4-30, would look more the Altair lunar lander of NASA’s former Constellation Program, with the possibility of a flat cargo deck (not shown) for mounting payloads. The flat deck would also accommodate a large habitat, and could function as primary structure for the tanks and engines.

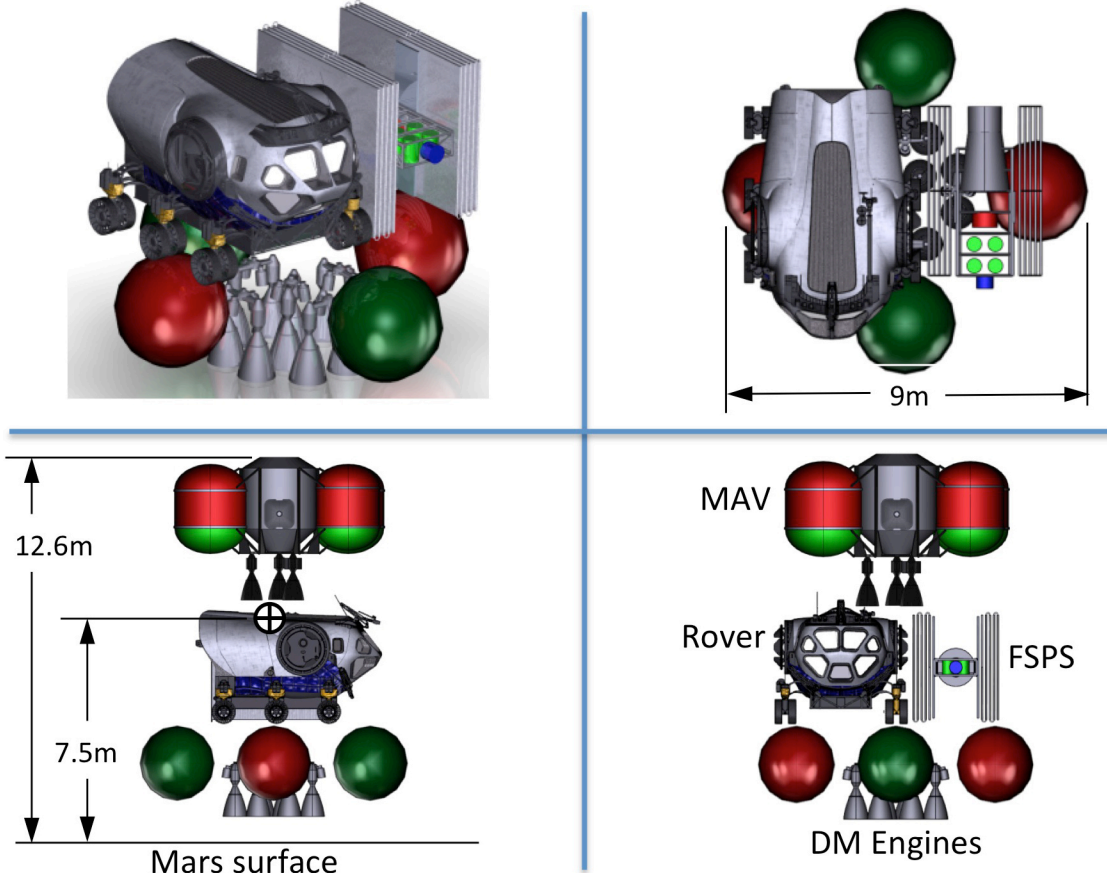


Figure 4-30 Vertical configuration V2 (stacked with flat-bed).

The propulsion scheme for V2 consists of four spherical propellant tanks surrounding a center cluster that includes all six required dual-nozzle engines. The rover and FSPS would sit above the tanks and engines on a “to-be-designed” cargo deck. Unfortunately, in this configuration there would not enough room to package the rover, FSPS, and the MAV at the same level. Instead, the MAV would be mounted above the other elements. This provides unrestricted MAV fly out, but would also result in a tall lander with a high center of gravity. The high MAV would also be very difficult to mount, requiring support structure that bypasses the rover and FSPS while still providing an efficient load path. Additionally, the cargo may be difficult to access because it is sandwiched between the MAV and the lower structure. Because no notional structure was conceived for configuration V2, it was the least well-developed of the eight lander configurations proposed during brainstorming.

Configuration V3

Configuration V3, shown in Figure 4-31 was conceived to investigate a minimal-height vertical lander having maximum packaging density. The configuration’s three propulsion modules would be located 120 degrees apart about the vehicle centerline. Each module would include two dual-nozzle engines and a single nested LOX/LCH₄ propellant tank. The rover and FSPS would be mounted low between propulsion modules. The remaining space between engine modules would be used for structure that supports the MAV, and possibly for additional cargo.

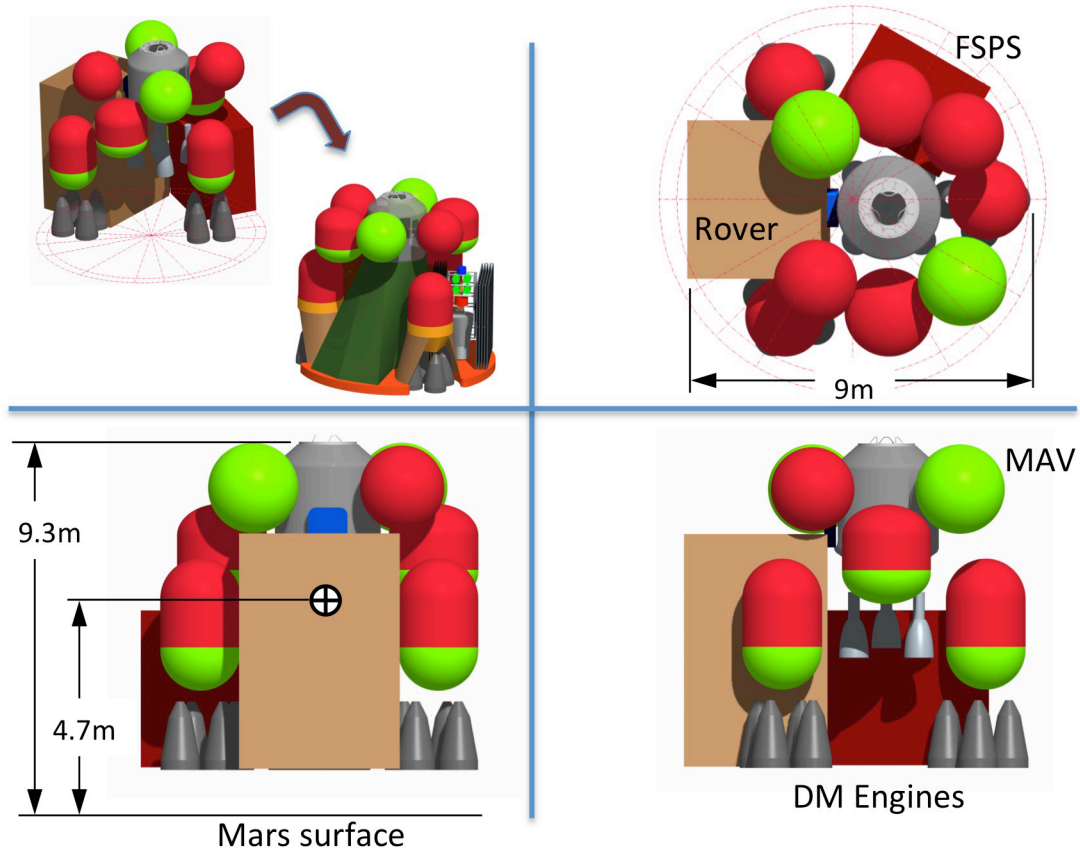


Figure 4-31 Vertical configuration V3 (compact vertical).

Configuration V3's packaging appears a bit crowded and complex. The tight packaging might make it difficult to efficiently integrate primary and secondary structure (for supporting engines, tanks, etc.). It might also reduce flexibility for rearranging cargo or carrying cargo of different sizes and shapes. It is unclear how a conventionally shaped habitat would be packaged. V3 might require removal of some propellant tanks prior to MAV fly out.

The compact design does provide several advantages. The low center of gravity at landing might allow the use of fixed (non-deployable) landing legs, significantly increasing reliability and decreasing landing gear mass. The reduced height might allow for a shorter launch-vehicle shroud or for additional payloads. The shorter lander would be stiffer at launch, possibly alleviating issues related to payload frequency. Upon landing the rover and FSPS would be low and could be easily offloaded (although the rover requires rotation prior to offload). Load paths in the V3 configuration are direct to the outer perimeter, making integration with a spacecraft adapter relatively simple.

Configuration V4

The last vertical configuration (V4) arranges the propulsion units and primary structure in a ring surrounding the payloads, as shown in Figure 4-32. The six identical modules each consist of one dual-nozzle engine and one pair of LOX/LCH₄ tanks. The small cylindrical propellant tanks would be lightweight and easy to manufacture.

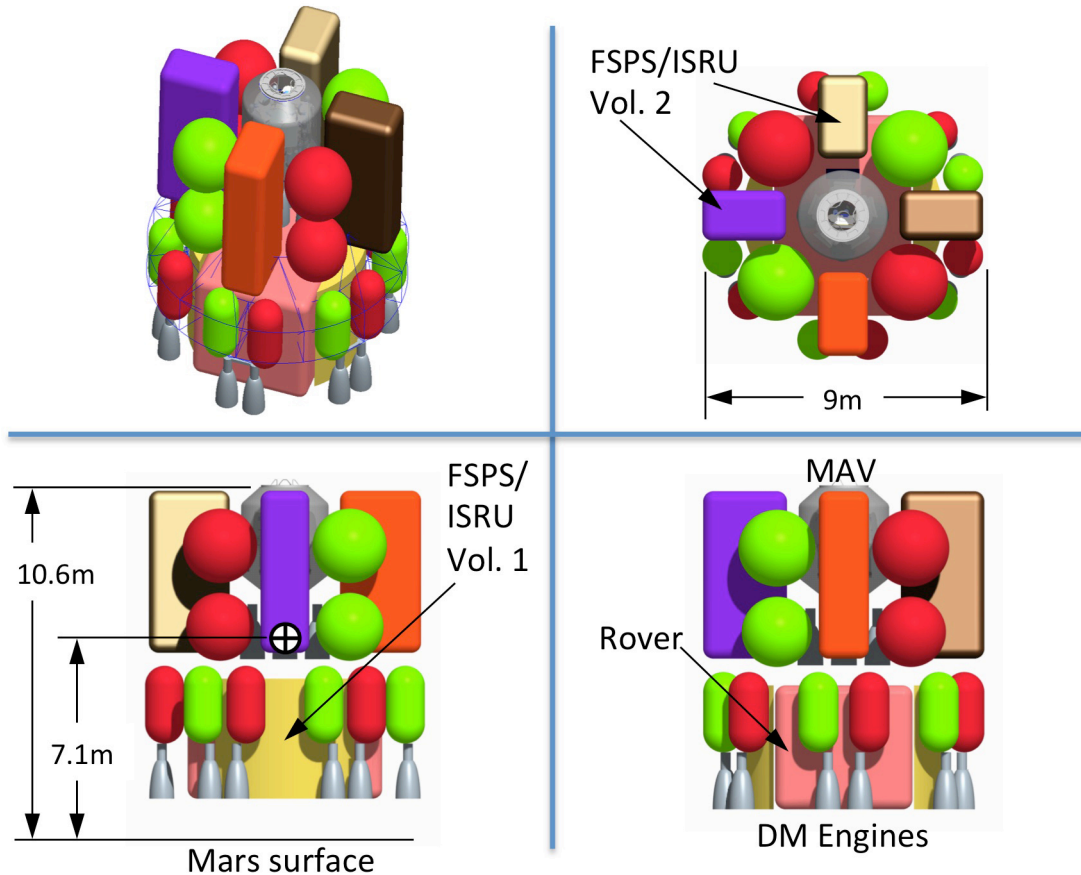


Figure 4-32 Vertical configuration V4 (ring-symmetric vertical).

Most V4 cargo would be carried low, surrounded by a structural truss that would provide a means for attaching landing gear. Additional payload components and the MAV would mount above the cylindrical truss. This arrangement would efficiently transmit launch and landing loads to a lower spacecraft adapter structure. The total packaging space provided by volumes 1 and 2 (as labeled in the figure) is larger than what is required for the rover, FSPS, and MAV. However, utilization of the upper volume (Vol 2) may require partial disassembly of some cargo elements. Habitat structures of various shapes could be placed above, and/or conform to the inside of the ring structure. A disadvantage is V4's tall upper-deck and relatively high center of gravity at landing (estimated to be 7.1m). Landing legs might be long and massive for this configuration. Additionally, the encapsulating nature of the lander's primary structure might require reconfiguration after landing for FSPS and rover offloading. For example, it might be necessary to raise the lander or to remove one or more engine modules prior to offloading.

4.6.4 Configuration Down Selection

The brainstorming phase was intended to generate a variety of horizontal and vertical lander configurations, and to document the perceived pros and cons associated with each conceptual layout. The primary drivers during brainstorming were the propellant tank volumes, the packaging volumes required by the MAV, FSPS, and rover, and the maximum diameter allowed by the launch vehicle shroud. After brainstorming was completed, the resulting configurations were evaluated by the Mars Lander project team as a whole. Two configurations (one horizontal and one vertical) were selected and carried forward for more detailed design and analysis.

4.6.4.1 Down Selection Process (AHP)

There are a variety of tools available for evaluating and ranking alternatives based on weighted selection criteria.

These tools attempt to formalize the process of comparing and evaluating options, with the goal of minimizing arbitrary or subjective decisions. The tools are especially designed to aid with decisions that involve human perceptions and judgment. One decision-making tool, developed by Thomas Saaty and known as the AHP, is reasonably well known and accepted. (see for example, *Strategic Decision Making: Applying the Analytic Hierarchy Process*⁸) The AHP is useful for making decision processes more systematic, eliminating arbitrary judgments, and providing traceability. It is also useful for examining the sensitivity of decisions to the importance weightings of various selection criteria (FOMs). The tool is not perfect, however, and is not intended to produce absolutely conclusive results. In some cases, the process aids with the elimination of poorly ranked options, but does not identify a clear “winner” from the available choices. Results should be used to guide, but not mandate a particular decision. This was the perspective taken here as the AHP was applied to evaluating and ranking the eight brainstormed lander configurations. It is beyond the scope of this document to completely explain the AHP, but a summary is given along with the ranking results obtained by applying the tool to the brainstormed Mars lander configurations.

The AHP begins with the definition of a core goal or objective. It is useful to begin by stating that the objective here was not to evaluate absolute performance or feasibility. Evaluation of performance requires quantitative modeling and analysis beyond what was available from the brainstorming activity alone. Resources prohibited such detailed work for all of the brainstormed configurations. Thus, the AHP was applied to evaluate which of the eight brainstormed configurations had the most promise for further development. After brainstorming, when the AHP was applied, only limited quantitative information was available for each configuration. For this reason, the AHP process necessarily included a large degree of engineering judgment. The AHP was applied separately to the horizontal and vertical lander groups, with the intent of achieving concurrence on the promising concept for each lander type.

The second step of the AHP is to define a set of selection criteria, or FOMs, for comparing the different options. The FOMs are then ranked in importance by comparing them pairwise, a process in which each FOM is compared directly in importance to every other FOM. This is done using a sliding scale with the following graduations: Equally Important, Somewhat More Important, Much More Important, Very Much More Important, and Absolutely More Important. Relative numerical scores ranging from 1 to 9 (and -9 to 1) were possible using these graduations. The entire Saaty procedure was implemented using an Excel spreadsheet tool (also developed by the team). Details of the mathematics will not be described herein, but the result of the process is a numerical value (or weighting) representing the relative importance of each FOM. The developed spreadsheet tool makes it possible to adjust the importance of one or more the FOMs to see how the overall AHP performance rankings are affected.

After the FOMs and their relative importance weightings are determined, a similar process of pairwise comparisons is employed for each of the options. During this series of comparisons, each option is compared to every other option with respect to each FOM. The graduated scale is modified slightly to include the following distinctions when comparing options for each FOM: Equal Performance, Moderately Better, Strongly Better, Very Strongly Better, and Extremely Better. Again, numerical scores ranging from 1 to 9 (and -9 to 1) were associated with the scale. The mathematical result of comparing the options is a relative performance score for each option with respect to each FOM.

The final step of the AHP combines the FOM relative importance weightings with the performance rankings of each option relative to each FOM. The result is an overall performance score (ranking) for each configuration. The absolute values of the scores do not have meaning, but the relative values indicate how well the options perform when compared to each other.

The Mars project team agreed upon six FOMs for evaluating the brainstormed lander configurations. Each FOM has a subset of “considerations” that were included as factors when comparing one configuration to another. These are summarized in Table 4-22. The distinction between FOMs and “considerations” can be challenging. For example, several of the considerations on the right side of the table could conceivably be elevated by making them independent FOMs on the left. However, the AHP works best if the FOMs are unique and well defined, but small in number. The six FOMs listed were felt to be reasonable in number and largely unique, with a relatively high system-level impact on lander feasibility. Other FOMs were considered but determined to be either non-unique or non-discriminating.

Table 4-22 System-level Figures of Merit for Evaluating Lander Configurations

Figures of Merit (FOMs)	Some considerations used when evaluating against the FOMs
Complexity	Propulsion system complexity (# of tanks, feed lines, ancillaries, engines)
System Mass	Structures and propulsion system mass
EDL Controllability & Risks	Trajectory, GN&C, aeroshell integration, center of gravity location
Flexibility	Ability to adapt to changes in payload or configuration requirements
Surface Operability	Payload access, MAV access, offloading, ability to package a large habitat
Launch Volume Efficiency	Ability to package other elements on the launch vehicle with the lander

As stated previously, evaluating the lander configurations against the FOMs was subjective and required considerable judgment. Quantitative data related to the FOMs was not available. The AHP was conducted in two different ways for comparison. Initially, all of the FOMs were given equal weightings (no pairwise comparisons of FOM importance). This might be a reasonable assumption given the low fidelity of current mission requirements and assumptions. Secondly, the process was carried out with the FOMs assigned different importance values by the Mars project team leads. This was done to examine the impact of assigning more or less importance to some FOMs. The results of applying the AHP to the two groups of four lander configurations (horizontal and vertical) will now be presented.

4.6.4.2 AHP Results: Horizontal Descent Module Configurations

Performance rankings relative to the individual FOMs and overall performance rankings are shown in Figure 4-33 for the four brainstormed horizontal lander configurations with all FOMs assigned equal importance. The results shown in the figure are summarized below, where taller bars represent higher rankings.

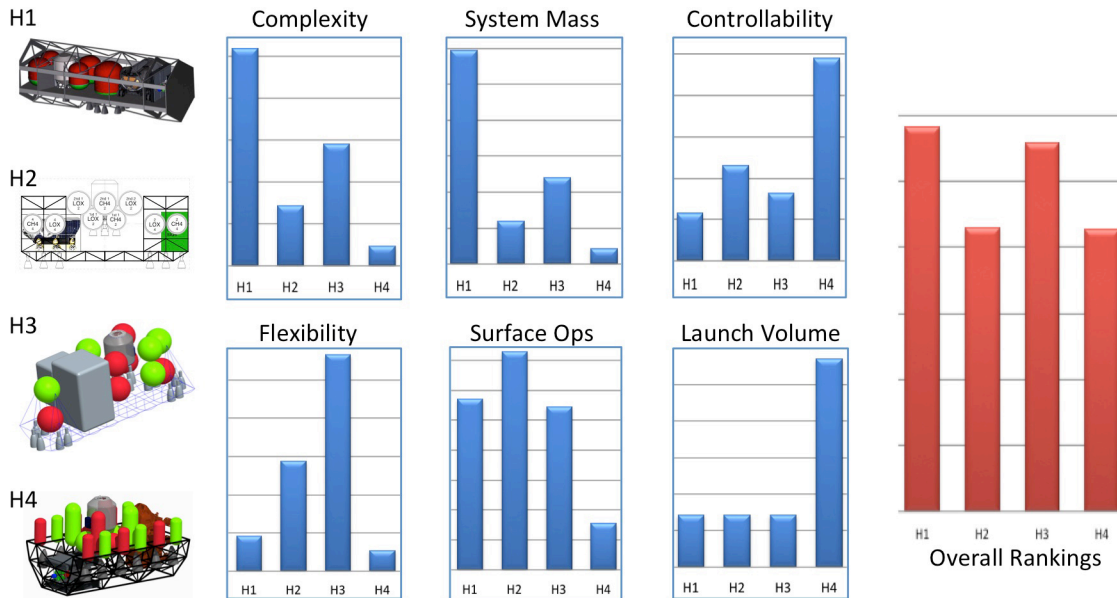


Figure 4-33 Summary of horizontal lander rankings (all FOMs equally important).

Complexity: Configuration H1 ranks highest because the single nested propellant tank with close engine proximity simplifies the propulsion subsystem. H3 is also attractive (but less so), having two modular engine arrangements at each end with only two spherical propellant tanks each. Configurations H2 and H4 were considered more complex because they have more tanks and larger distances between the engines and the tanks (longer plumbing runs).

System Mass: H1 and H3 should have low propulsion mass for the reasons just cited. They also rank highly with regard to structural mass. H1 is favored structurally because of the large-cross-section frame and clear load paths. H3 is less structurally robust, but may be workable if the truss platform is sufficiently sized. The H3 primary truss

beam (along the length) has a smaller cross section than the H1 structure, but not as small as H2. H2 also has a larger number of propellant tanks and requires a more complex primary structure. H4 has a large number of propellant tanks and many members in its support structure. Additionally, the tight packaging of H4 may make it difficult to integrate structural members for supporting other MDM subsystem components. Finally, plume impingement of the H4 engines on the landing gear may require mitigation through baffles or other additional structure.

Controllability: When Guidance, Navigation and Control (GN&C) and entry considerations were taken into account, configuration H4 was the highest ranking concept. The H4 configuration consists of six broadly distributed engines with significant lateral spacing. This provides good control authority during propulsion assisted entry. Configuration H4 is also more controllable because it has smaller moment of inertia about its lateral axis. The half-cage arrangement of the structure can easily integrate with an aeroshell structure. The three other configurations were ranked approximately equally with H2 slightly preferred.

Flexibility: Configuration H3 was considered the most flexible with regard to payload packaging and the ability to accommodate changes in requirements or configuration. The flat-bed style provides flexible mounting locations, and the open central area can accommodate a variety of payload sizes and shapes, including various large habitat configurations. Additionally, the location of the MAV is not fixed and might be shifted to accommodate different cargo, or to move the center of gravity along the longitudinal axis if necessary.

Surface Operations: Payload access and offloading were considered feasible and relatively easy for configurations H1, H2, and H3, with H2 receiving the highest ranking because it affords simple offloading of cargo from the ends of the vehicle without any rearrangement of structure. For configuration H4, the engines and dense truss structure might block payload access and impede offloading. H4 also may require removal of some MDM tanks and considerable structure to provide MAV fly-out clearance.

Launch Volume: The overall length and launch volume requirements for configurations H1, H2, and H3 are approximately the same. The only configuration with a real advantage related to this FOM is configuration H4, which is approximately 4m shorter than the three other configurations.

Overall Horizontal Rankings: The result of combining each of the FOM performance rankings into one overall ranking using the AHP mathematical approach results in the overall performance rankings shown in Figure 4-33. The net result shows that configurations H1 and H3 are ranked as approximately equal (small differences in the performance rankings are not significant).

Sensitivity to Non-Equal FOM Importance Values: Initially, the AHP was conducted by assigning equal importance to all of the FOMs. The AHP rankings were then recalculated with the six FOMs having relative importance weightings corresponding to the pie chart in Figure 4-34. The weightings shown were determined through pairwise comparisons of the FOMs, and they represent a “consensus average” based on inputs from several project team leads. As seen in the pie chart, the consensus weightings assign the greatest importance to the flexibility and system-mass FOMs. Slightly less importance was given to controllability, surface operations and complexity. Launch vehicle volume was considered least important. The lander performance rankings obtained using these FOM importance values are shown in the bar chart.

It is apparent from Figure 4-33 and Figure 4-34 that changing the FOM importance values from the equal assumption (16.7% per FOM) did not have a significant effect on the overall performance rankings for the horizontal lander configurations. Configurations H1 and H3 still rank highest with nearly equal scores. Configurations H2 and H4 still score lowest, with the H4 ranking decreasing slightly due to the increased importance of the mass and flexibility FOMs.

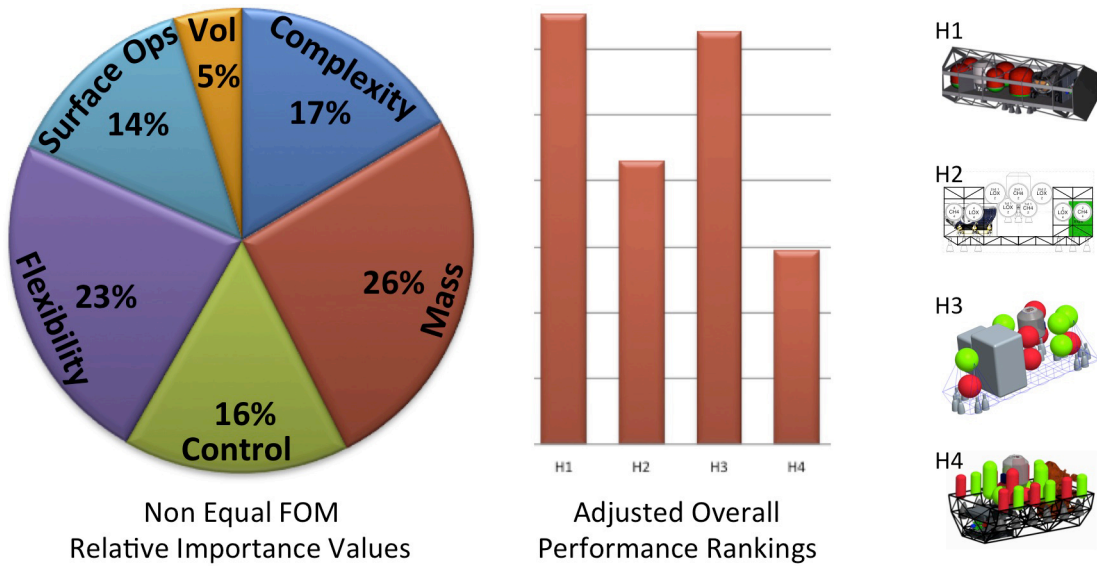


Figure 4-34 Overall horizontal lander rankings with weighted FOMs.

Down-Selected Horizontal Configuration (H3): The AHP resulted in an essential tie between configuration H1 and H3. H1 benefited from its robust structure and level of definition, as well the low propulsion complexity of the single nested tank. At the same time, H3 was flexible for packaging cargo, and could carry a habitat without separating it into two volumes. Although the proposed H3 structure takes up less total volume, there was concern that the thinner overall cross section would be quite massive. However, it was noted that the H3 partial-circle ring frames could be extended to a full 360 degrees to make the structure more efficient. This would create a “cage” around the H3 descent module and result in a structure similar to that of H1. Alternatively, the H3 truss-type structure might be replaced by a stronger and stiffer panel-type structure. The decision was made to carry H3 forward, and to use analysis results to determine whether structural modifications would be necessary. This was seen as reasonable because the AHP did not clearly identify H1 or H3 as having better overall performance.

4.6.4.3 AHP: Vertical Descent Module Configurations

Procedures similar to those described for the horizontal lander configurations were used to apply the AHP to the vertical configurations. The FOMs (and associated considerations) listed in Table 4-22 were again applied, initially with equal importance values and then with the non-equal importance values shown in Figure 4-34. Results for the case of equally important FOMs are summarized in Figure 4-35. Some of the reasoning leading to the FOM specific and overall performance scores is summarized as follows:

Complexity: Configuration V3 ranked highest with respect to complexity because of the modularly simple nature of the three engine/tank clusters. This was despite the fact that V3 incorporates a greater number of total tanks than configurations V1 or V2 (considering each V3 nested tank as two tanks total). Configuration V4 ranked lowest because of the large number of tanks (12). The modular nature of the V4 tank/engine clusters was considered an advantage, but not sufficient to overcome concerns related to plumbing integration and propellant management.

System Mass: Configuration V3 also ranked highest with respect to the system mass FOM. The configuration is relatively short with a compact load path, and may result in shorter or perhaps non-deploying landing legs. Configuration V2 was ranked low because it lacked a reasonable load path for supporting the MAV. Configuration V4 was ranked low primarily because of concerns related to the propulsion system total mass.

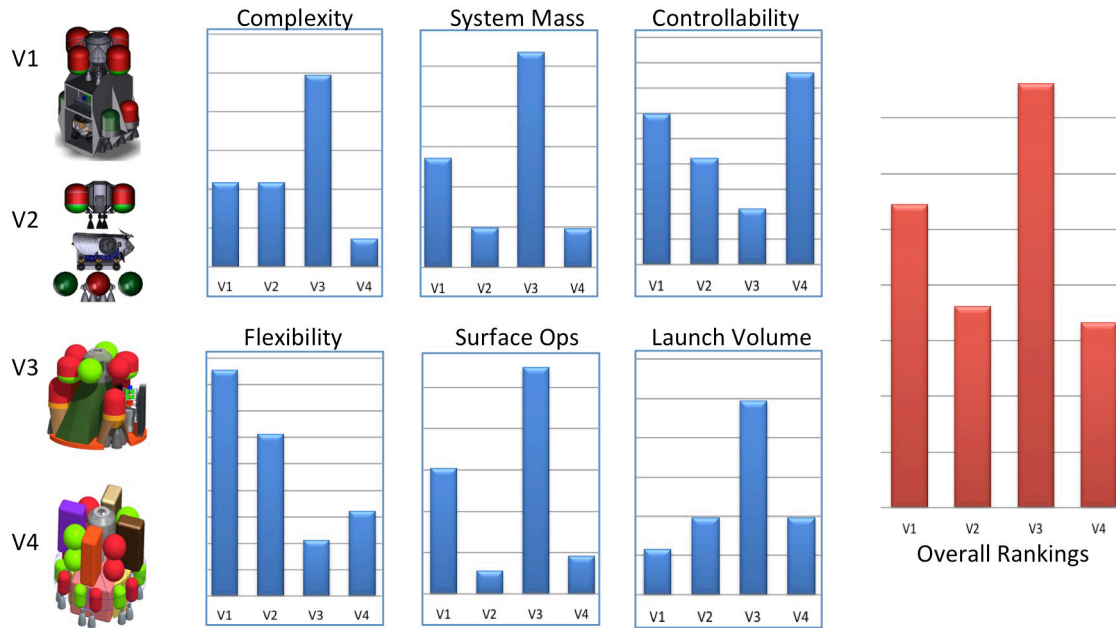


Figure 4-35 Summary of vertical lander rankings (all FOMs equally important).

Controllability: Configuration V4 ranks high with regard to the controllability FOM because of the control authority provided by engines at the outer perimeter. H4 also has a long thrust moment arm between the plane of the engines and the lander center of gravity. It is interesting to note that the configuration scoring highest with regard to controllability (V4), did not score well with regard to most of the other FOMs. This is similar to what occurred with horizontal configuration H4. This is because characteristics seen as favorable from a control point of view (large engine spacing, high center of gravity, and tight packaging) are seen as less favorable when related to the other FOMs (especially complexity and system mass).

Flexibility: Configuration V1 scored best with regard to the flexibility FOM. The upper cargo deck and lower cargo bays provide broad flexibility if payload requirements change. The configuration has truck-like characteristics, allowing for easy cargo placement and tie-down to the primary support structure. V2 offers some of the same advantages, but side-by-side placement of the payloads was deemed less flexible for reconfiguration because of shroud limitations. V3 has low flexibility because of its tight packaging and because the cargo areas are specifically sized for the assumed FSPS and rover elements. Different cargo elements might require significant changes to the design. Configuration V4 was ranked low because of restricted access to the lower cargo area and the possible need to disassemble upper-level cargo prior to packaging. Both factors might restrict where specific items can be placed.

Surface Operations: Configuration V3 received the highest ranking with respect to surface operations. This was due to its low height and relatively easy payload access. Configuration V1 has good access to the rover (with drive-off capability), but more difficult access to elements in the upper cargo area. V2 was ranked poorly because of possible difficulties with offloading both the rover and other cargo elements from the upper deck. V4 ranked lowest because access to the lower cargo is blocked unless one or more engine/tank modules are moved or the lander is somehow raised prior to cargo offloading.

Launch Volume: Rankings relative to this FOM depend mostly on lander height, which determines the space required when packaged on the launch vehicle. Configuration V3 was conceived as a compact lander variation and has the shortest height of the four vertical configurations. Configuration V1, being the tallest configuration, received the lowest ranking.

Overall Vertical Rankings: The result of combining the individual FOM performance rankings using the AHP mathematics results in the overall performance rankings shown in Figure 4-35. For equally weighted FOMs, configuration V3 is the highest scoring concept, followed by configuration V1.

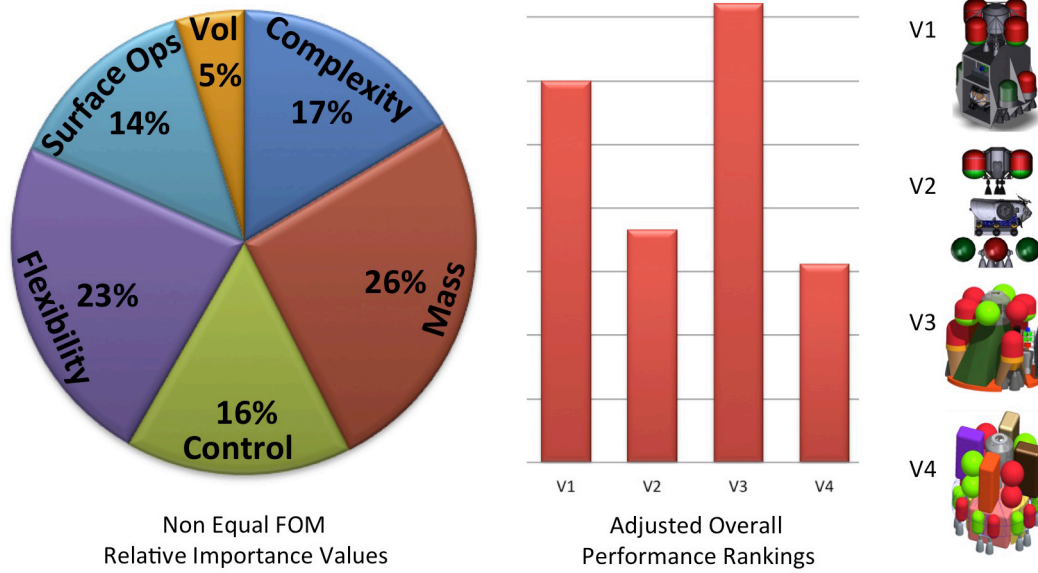


Figure 4-36 Overall vertical lander rankings with weighted FOMs.

Sensitivity to Non-Equal FOM Importance Values: As with the horizontal configurations, the AHP rankings were recalculated using weighted FOMs. The same FOM importance values used for the horizontal configurations were applied. The results are shown in Figure 4-36. It is observed that for the vertical landers the effect of using non-equal FOMs is slightly more pronounced. The most significant effect was to move the rankings of configurations V1 and V3 closer together. Configuration V3 still has the highest ranking, but only moderately so. This is primarily due to the increased importance of flexibility and decreased importance of surface operations. Both factors increased the ranking of configuration V1.

Down-Selected Vertical Configuration (Modified V1):

Using the AHP, configuration V3 had the highest performance ranking with V1 a close second. There was consensus that configurations V2 and V4 were inferior, and that both V1 or V3 were potentially good configurations. V1 appeared to have fewer uncertainties, which was reflected in higher scores for the flexibility and surface operations FOMs. Also, as compared to V3, configuration V1 is has fewer tanks and should better accommodate a habitat. Configuration V3 scored well for its compactness, low center of gravity, and surface-operation characteristics. Concerns were raised, however, related to V3’s potentially complex structure and tight packaging. During team discussions, it was observed that a modified V1 configuration might achieve V3-like compactness while retaining inherent V1 advantages. For this reason, and because the V1 and V3 rankings were close, the team decided to spend time incorporating the best features of each concept into a “modified-V1” configuration. This process resulted in the more compact version of configuration V1 shown in Figure 4-37.

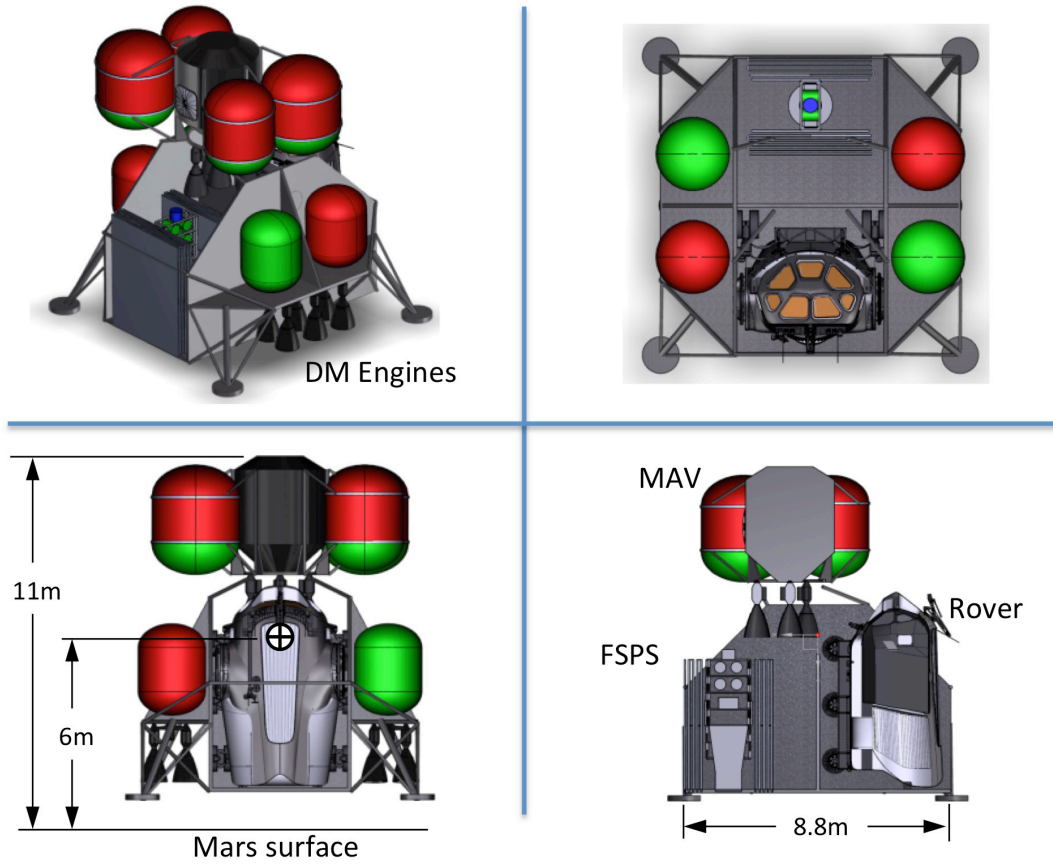


Figure 4-37 Modified V1 configuration.

The modified V1 retains the four-tank simplicity and flat-panel type structure of the original configuration. Nesting of the tanks, as was done with V3 was considered unnecessary. Incorporating V3’s tandem FSPS/rover arrangement makes the payloads low and accessible. The MAV integrates well and exhibits good fly-out characteristics. It was estimated that these modifications would reduce both the overall height and center-of-gravity height by at least 2 meters. This configuration was carried forward for refined modeling, analysis, and sizing.

4.6.5 Sizing and Analysis

4.6.5.1 Descent Module Analysis Procedures Summary

All CAD modeling and finite-element analysis was done using Pro/Engineer (Wildfire 5.0) and Pro/Mechanica software products of Parametric Technology Corporation (PTC).

The process of developing refined CAD models and mass estimates for the down-selected horizontal (H3) and vertical (modified V1) lander configurations involved several steps. First, any details not included or emphasized during brainstorming were developed and added to the models. Examples include tank supports, cargo supports, and other structural features required to make the concepts fully functional. Second, the existing CAD for the brainstormed configurations was modified to include these and other details deemed necessary to make complete models, such as attachment points for landing gear. Third, the CAD models were used to create working analysis models using appropriate finite elements to represent the structural components, propellant, and cargo. This was generally accomplished using a combination of tube, beam, and shell elements to represent primary structure, along with a series of rigid elements and lumped masses to represent cargo or other non-structural components. Fourth, appropriate boundary conditions and loads were applied, and the finite element model components were sized based upon strength (using a failure-index approach) and linear buckling analysis. The governing load cases (see Table

4-18) were the inertial launch loads, 5g axial and 2g lateral. The analysis models were also used to determine the lowest modal frequencies of each configuration (payload frequency within the launch vehicle shroud). In the fifth and last step, the CAD models were again updated to correspond to the analysis results and to include geometry and mass for any non-analyzed (but estimated) components. During this step the models were updated to reflect the sizes (shell thickness, beam cross section, etc.) determined from analysis.

Landing gear mass estimates were made using a spreadsheet tool developed during previous studies of the Altair lunar lander. The tool is based on parametric equations created from finite element analyses of Apollo-like deployable landing-leg configurations having various dimensions. The landing-leg loads used to create the tool were based on a 1-g deceleration limit (attenuated) at touchdown, and were estimated from dynamic analysis models of the Altair lander (using MSC/Adams analysis software). Assumed touchdown velocities were 2.75 m/sec vertical and 1.0 m/sec horizontal. These deceleration and velocity assumptions are similar to those used for Apollo. The landing-gear mass tool requires two inputs. The first input is the lander center-of-gravity height at touchdown. The second input is the required landing gear footpad “diameter”, a value that is determined from separate dynamic-stability curves (also developed previously). It is noted that the 1-g deceleration limit may be non-conservative, because simple preliminary calculations indicate that the attenuation length required to achieve such a low deceleration at Mars may be impractical. If it eventually becomes necessary to increase the deceleration limit, landing gear mass may increase significantly. Another key landing-gear assumption is that all legs must be sized for worst-case loads involving touchdown on a single leg. Future relaxation of this assumption, enabled by design, analysis, and testing may reduce landing-gear mass. The important observation is that the landing gear mass estimates presented here have significant uncertainty, primarily because the tool used was adapted from previous lunar-lander studies. Future efforts should include the development of a Mars-specific landing-gear mass estimation tool.

The upcoming sections provide details of the final CAD models, analysis results, and mass summaries of the down-selected horizontal (H3) and vertical (V1) Mars Lander configurations. The CAD models shown should be interpreted as representing feasible (but not definitive) layouts for each lander concept. The analysis results are preliminary, but contain more detail than possible using simple spreadsheet or parametric analysis. The mass properties (including moments of inertia and component center of gravity locations) are approximate but useful for future trade studies related to Mars EDL, including transition.

The masses and sizes of some components not directly part of the finite element analyses were estimated using spreadsheet tools, or by extrapolating from previous Altair lunar lander work. Examples include fitting and node masses at the ends of beams, joints for connecting adjacent panels, separation system mechanisms, porches/ladders required for MAV access, and secondary structure. Non-analysis based mass estimates are identified and discussed in the mass summary sections for each lander. Modal frequency analyses were also conducted and are discussed for each configuration.

4.6.5.2 Horizontal Descent Module, Final CAD and Analysis Model

The final CAD model for horizontal lander configuration (H3) is shown in Figure 4-38. The previously brainstormed configuration (Figure 4-37) has been modified to accommodate the nested-tank two-stage MAV arrangement outlined in the assumptions section. Additionally, the final model utilizes an enclosed “egg-crate” shaped panel structure rather than a truss-based structure. Early analyses of the truss-based configuration indicated a need for additional strength and stiffness (due to the long length and small cross section). The FSPS and rover structures were modeled explicitly, and supporting struts for the propellant tanks, FSPS, rover, and MAV were added. The MAV sits above the deck to allow room for its engines and to provide better fly-out clearance. Four deployable landing gear were added at the corners of the primary structure. Six engine pairs are arranged at opposite ends of the lander, although one pair on each end has been moved inboard from the position shown in Figure 4-27. This was done to shorten the lander as much as possible. The total length is now 15.2 m, which is slightly shorter than the brainstormed configuration. The center of gravity height at landing is approximately 5.5 m, requiring a minimum distance between landing-leg footpads of approximately 8.2 m.

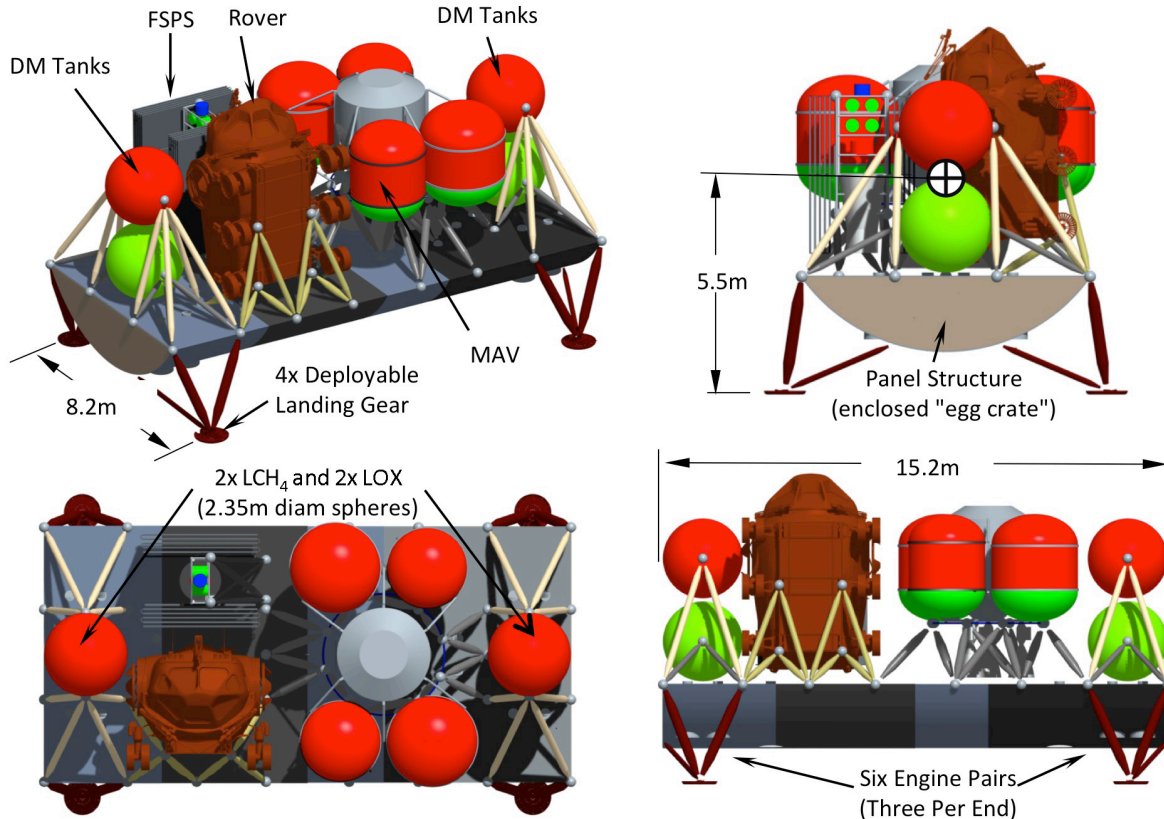


Figure 4-38 Final horizontal (H3) lander configuration (as-analyzed CAD model).

To analyze the H3 configuration, the lander was attached to a 10-m-diameter aeroshell structure assumed to also serve as the launch vehicle shroud as shown. This assumption results in a larger available volume for lander packaging, simplifies interfaces, and eliminates the need for two structural systems. It is admittedly a somewhat ambitious assumption, because the optimum shapes for the shroud and aeroshell will not be the same. Ultimately separate shroud and aeroshell structures may be necessary, resulting in larger system mass estimates than those obtained here.

As shown, the lander is attached to the aeroshell/shroud at six lateral attachment points along its length. The base of the aeroshell is attached to a cryogenic propulsion stage (CPS), or some other upper stage of slightly smaller diameter via a conical section as shown. For analysis purposes the end of the conical section is fixed in translation. The lander is attached to the aeroshell conical section via a partial-cone adapter and series of adapter struts. The partial cone and adapter struts carry axial launch loads, while the lateral attachment points increase lateral stiffness and frequency. Other attachment schemes were considered, including elimination of the lateral attachments resulting in a purely cantilevered configuration. This cantilevered configuration was analyzed but was rejected because of extremely low first-mode natural frequencies (see Section 4.6.5.4) that could not be raised significantly by adding mass to the adapter struts or cone. Alternate aeroshell configurations and integration scenarios are suggested topics for future work. It is important to note that the aeroshell structure itself was not part of the current analysis, which focused only on lander performance and mass. To include attachment to the aeroshell in the analysis, the aeroshell/shroud was assumed to be the indicated composite-honeycomb sandwich structure. The structure was based on knowledge of similar shroud designs considered for the Ares V launch vehicle as part NASA's former Constellation Program. The aeroshell structure was included to better estimate lateral frequencies, and does not significantly change sizing results for the lander itself.

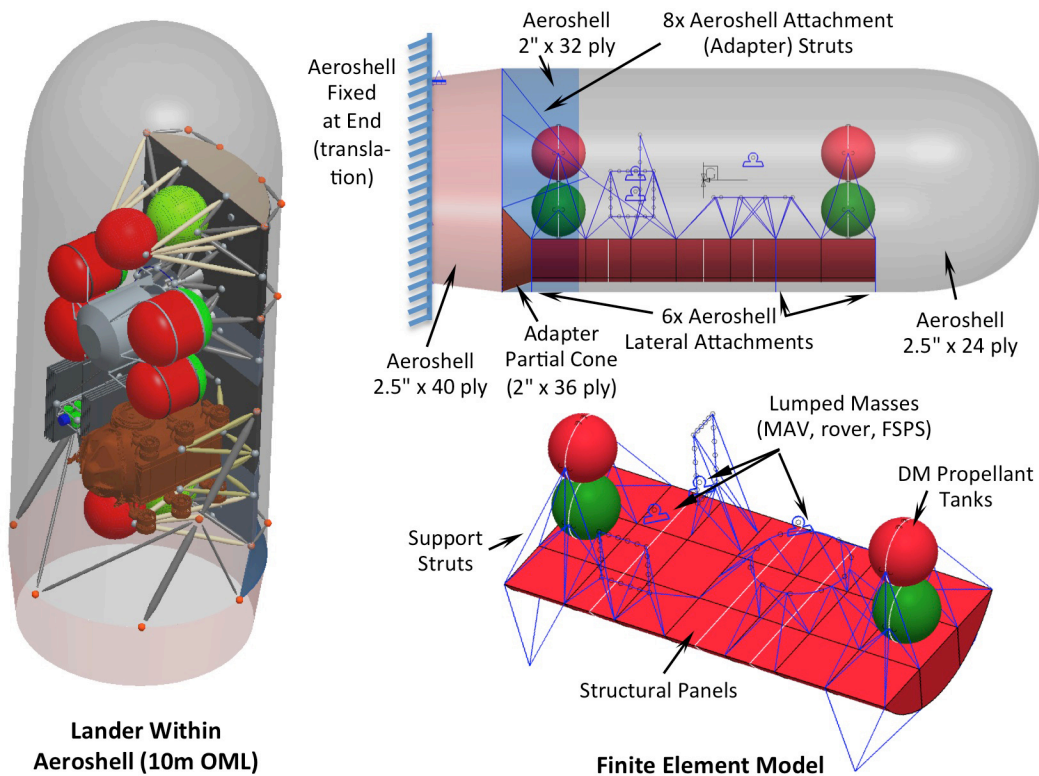


Figure 4-39 Horizontal (H3) lander shroud arrangement and finite-element analysis model.

4.6.5.3 Horizontal MDM, Analysis Results and Structural Mass Summary

The H3 horizontal lander finite-element results and overall mass summary are shown in Table 4-23. Listed in the table are the basic mass (no growth allowance) properties for key structural components (excluding propellant tanks which are bookkept by the propulsion subsystem), and the basis for each mass value. The finite element analysis model described in Section 4.6.5.2 is the basis of estimate for the primary structure panels, tank support struts, rover/FSPS support struts, and MAV support system. Landing gear mass was estimated using the spreadsheet tool described in Section 4.6.5.1. The landing gear mass represents nearly 20% of the MDM structure basic mass, and about 2.5% of landed mass (53,000 kg). These percentages are in line with those of the Apollo LEM and Altair lunar lander. Approximately 75% of the MDM basic structure mass is based on analysis (including landing gear). The MDM engine supports were estimated based on CAD modeling and engineering judgment alone. The porch/ladder and separation system details were unknown, but scaled estimates from the Altair lunar lander project have been included as placeholders for completeness.

The estimate with the greatest uncertainty is the secondary structure mass. The secondary structure is intended to include items such as fasteners, ply build-ups, supports, interconnections, and other subsystem integration hardware that has not been modeled or included in the preliminary analysis. During conceptual design, secondary structure is often estimated as a percentage (15%-30%, depending on current design maturity) of the known primary structure. In this case, secondary structure was estimated as 25% of the as-analyzed MDM structure, excluding landing gear. Landing gear was excluded because the parametric tool used to estimate landing gear mass is based on finite element analysis of complete landing gear assemblies with secondary structure already included. The secondary structure estimate is unfortunately an imprecise placeholder. Detailed estimates require knowledge of subsystem placement and interface requirements that are not available during conceptual or preliminary design. The secondary structure mass in Table 4-23 (1,080 kg) is 16% of the total H3 configuration structural mass. All non-analysis-based masses in the table should be considered low fidelity.

Table 4-23 Horizontal Lander Basic Mass Summary

Subassembly Description	Mass (kg)	Xcg (m)	Ycg (m)	Zcg (m)	Notes
Primary Structure Panels	3304	2.30	0.00	0.00	Analysis Based Mass
Propulsion Tank Support Struts	245	4.00	0.00	0.00	Analysis Based Mass
Rover & FSPS Support Struts	104	5.00	0.00	3.10	Analysis Based Mass
MDM Engine Support Frames	100	2.30	0.00	0.00	Mass Estimated (no analysis)
MAV Support System	153	4.10	0.00	-2.10	Analysis Based, Sep System from Altair
Porch and Ladder	130	5.00	2.00	-2.10	Scaled from Altair DAC-4
Landing Gear (4 legs)	1,320	1.10	0.00	0.00	Length & Mass from Excel Analysis Tool
MDM Side SA Sep System	286	2.10	0.00	2.00	Scaled from Altair DAC-4
Secondary Structure	1080	2.30	0.00	0.00	Estimated 25% MDM Struct Mass (except gear)
Total MDM Structure Basic Mass	6,722				

Spacecraft Adapter Panels/Struts	665	3.50	0.0	4.50	Analysis Based Mass
SA Sep System (SA Side)	169	2.10	0.0	2.00	Scaled from Altair DAC-4
Total Spacecraft Adapter Basic Mass	834	<i>CG info with respect to coordinate system at Mars surface +Xup, Y & Z on center line, with -Z toward MAV</i>			

The spacecraft adapter (interface between the lander and the launch vehicle) mass estimate is included because past studies have shown that structural changes to MDM primary structure impact the adapter mass. Although a spacecraft adapter may not be bookkept as part of the lander system mass, it is an important aspect of system-level performance and should be considered as part of any lander focused structural analysis.

The mass estimates in Table 4-23 are based on structural strength (using a failure-index approach), and linear buckling analyses. Time permitted analysis of only 5g axial and 2g lateral launch loads. These are considered conservative values, and they include factors for thrust uncertainty and dynamic loads amplification. They are believed to be the driving loads for lander sizing, but entry and landing loads should be analyzed as part of future work. The structural panels are honeycomb sandwich with core thicknesses ranging from 2.54 cm to 5.08 cm and composite-ply layups consisting of 4 to 36 plies (.206mm thickness per ply). The various support struts were sized to the same launch loads and range in diameter (outer) from approximately 8.3 cm to 31.8 cm with wall thicknesses ranging from 0.11 cm to 0.45 cm.

4.6.5.4 Horizontal Descent Module, Modal Frequency Results

In addition to structural mass, the first modal frequency was computed for the H3 lander configuration within the launch vehicle shroud. The first modal frequency generally corresponds to a lateral vibration mode, and a minimum value for this frequency is usually a requirement placed on launch vehicle payloads. No frequency requirement is currently known for the NASA SLS vehicle that would carry a Mars lander. Past studies of Altair/Ares-V, historical Saturn-V data, and examination of existing commercial launch vehicle requirements, suggest that the minimum frequency requirement is unlikely to be below 5 Hz. The first three lateral-mode frequencies for the H3 horizontal lander are listed in Table 4-24 for two cases. On the left are the results for the boundary condition described previously (lander attached laterally to the aeroshell/shroud structure at six locations). On the right are the results obtained by removing the lateral attachments, with lateral stiffness provided by the adapter partial cone and support struts. The latter case approximately represents a scenario in which the aeroshell and shroud are different structures, with the lander/aeroshell system mounted only at the base of the lander.

Table 4-24 Horizontal Lander, 1st Lateral Mode Frequency Results

Mode	With Lateral Attachment	Without Lateral Attachment
1	2.2 Hz	1.45 Hz
2	2.8 Hz	1.83 Hz
3	2.9 Hz	3.23 Hz

For both cases the lateral structural stiffness is insufficient to achieve 5 Hz lateral frequency. Attachment to the aeroshell/shroud raises the frequency from 1.45 Hz to 2.17 Hz, but this is still a low result. Furthermore, based on limited analyses and past experience, it is unlikely that the frequency can be raised significantly through simple design changes. Unfortunately, at this time it cannot be stated definitively that the H3 lateral frequency is “too low.” However, it can be stated that the results represent an important risk that should be considered as launch-vehicle requirements mature. Increasing the lateral frequency (even modestly) is likely to require significant mass. Achieving a frequency approaching 5 Hz may not be possible for the horizontal lander, and contrary to common perception, stiffness (and not mass) may ultimately be the design driver that determines feasibility. Determining frequency requirements and developing mitigation strategies for this concern should be a focus of future work.

4.6.5.5 Vertical Descent Module, Final CAD and Analysis Model

The final CAD model for the vertical lander configuration (V1) is shown in Figure 4-40. The configuration is based on the modified V1 (brainstormed) configuration depicted in Figure 4-37. Some modifications (including a small height increase) were necessary when creating the final working model. The final configuration is 10.75 m tall (including the upper mounted MAV), and consists of a series of vertical panels stabilized by cross struts and providing an efficient load path for axial launch loads. The panels are arranged such that two large open areas exist for placement of the FSPS and rover. The remaining sides of the lander consist of frame-type structure above which cylindrical MDM propellant tanks (one LCH₄ and one LOX tank per side) are mounted, and below which six engine pairs are mounted. The mounting frames also add strength and stiffness to the primary structure. The MAV is mounted to a panel adapter structure that reaches up from the top edges of the MDM. Once the rover is offloaded, there is good fly-out clearance for ascent. A lower panel with cut outs is located at the base to provide additional structural stability. The center of gravity at landing is a relatively low 5.45 m above the Martian surface. The required landing gear circle (for landing stability) is 11.4 m in diameter. With this diameter and the low center of gravity, the landing legs are relatively short and lightweight.

A HIAD entry system is envisioned (but not required) for the vertical lander. However, HIAD integration requirements are currently unknown. For example, it is not known whether a HIAD would be better placed above or below the lander. The best placement depends entry and transition analyses that are not yet complete. Any HIAD integration scheme may present challenges to the primary structure layout, and require additional mass. For this work, the mass of any integration hardware was assumed to be included in the lander control mass.

Clearly there is sufficient room in the anticipated shroud for the V1 vertical configuration, including HIAD integration. The current SLS shroud length estimate is approximately 31 m with a cylindrical barrel section 17 m long. With the V1 lander height at 10.75 m, there is significant extra volume within the shroud that could be used for packaging of a propulsion stage or additional payload. Alternatively, the shroud might be shortened to save total system mass. For the purposes of this work, it was assumed that the vertical lander would be mounted in the shroud via a short adapter structure at its base, with the landing legs in a stowed position. This is the most favorable configuration for achieving higher stiffness/frequency, and also results in a short load path and lower adapter mass. Deviations from these assumptions are likely to result in higher system masses, and are left to future studies.

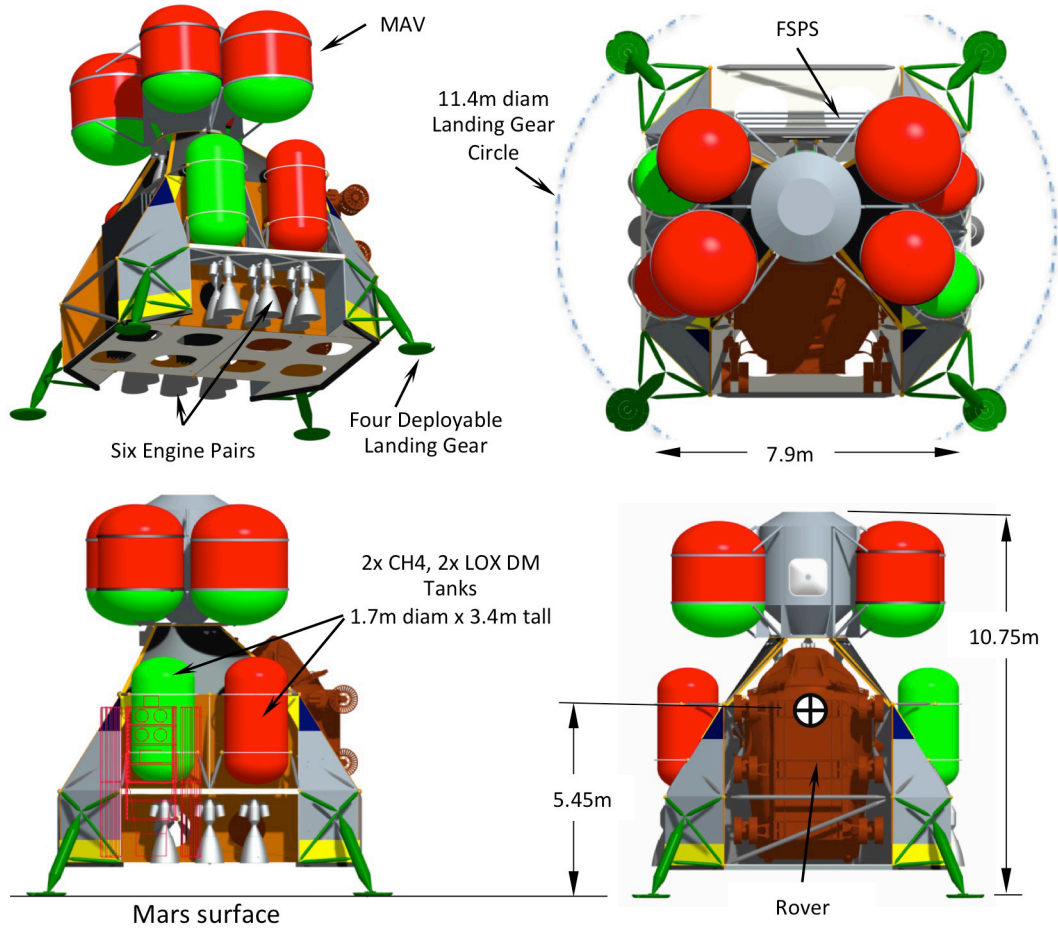


Figure 4-40 Final vertical (V1) lander configuration (as-analyzed CAD model).

The V1 finite element model is shown in Figure 4-41. The spacecraft adapter structure is 9.1 m in diameter. This diameter is equal to the shroud dynamic envelope, and assumes attachment to a lower core stage having similar diameter. For analysis purposes, the adapter was fixed (in translation) along its entire lower edge. All structural panels were modeled as composite sandwich shell elements. Supporting beams for the propellant tanks, MAV, rover, and FSPS were attached to notional ring frames, which were not sized because they were rigidly linked to the corresponding payload element point masses (and were thus unloaded). The supporting beams were sized as part of the analysis.

4.6.5.6 Vertical MDM, Analysis Results and Structural Mass Summary

The V1 vertical lander finite element results and overall mass summary are summarized in Table 4-25. Listed in the table are the basic mass (no growth allowance) properties for key structural components (excluding propellant tanks), and the basis for each mass value. The finite element model described in Section 4.6.5.5 is the basis of estimate for the primary structure struts and panels, tank support struts, rover/FSPS support struts, engine support system, and MAV support system. The landing gear mass was estimated using the methods described previously. In this case, approximately 78% of the MDM basic structure mass is based on analysis (including the landing gear). As with the horizontal configuration, the porch/ladder and separation system placeholders are scaled numbers determined by comparison with previous Altair lunar-lander studies. For reasons cited previously for configuration H3, the V1 secondary structure mass has the greatest uncertainty. For V1 the secondary structure represents 15% of the total MM basic mass.

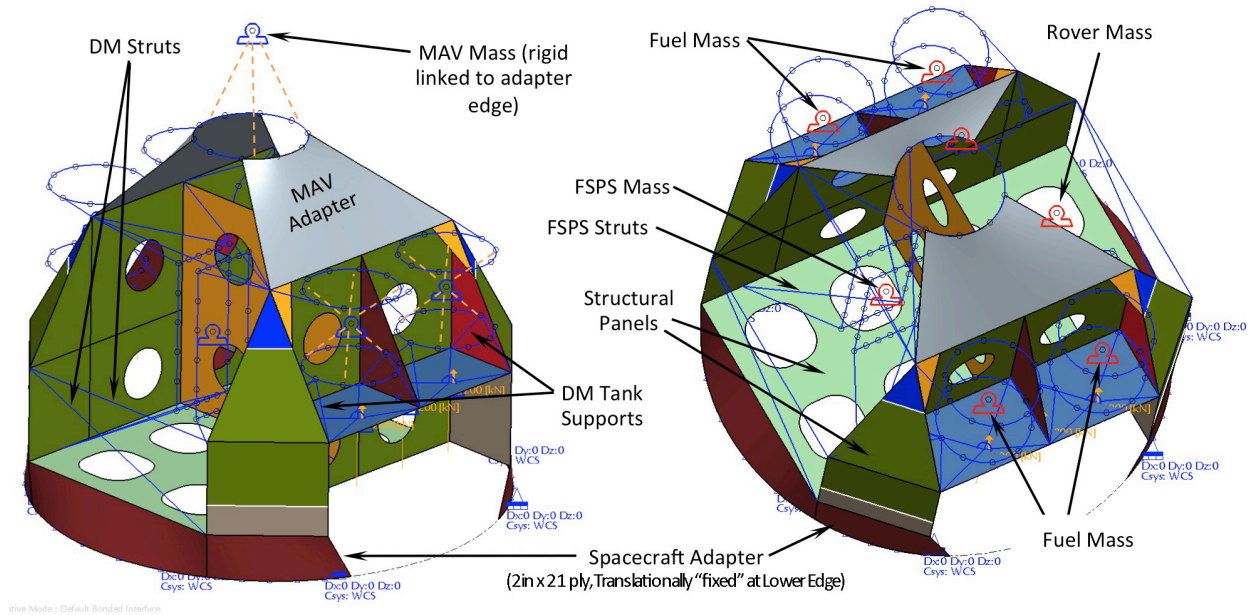


Figure 4-41 Vertical (V1) lander finite-element analysis model.

Table 4-25 Vertical Lander Basic Mass Summary

Subassembly Description	Mass (kg)	Xcg (m)	Ycg (m)	Zcg (m)	Notes
Primary Structure Struts/Panels	1844	2.73	0.00	0.00	Analysis Based Mass
Propulsion Tank Support Struts	89	3.61	0.00	0.00	Analysis Based Mass
Rover & FSPS Support Struts	89	3.06	0.00	-0.58	Analysis Based Mass
MDM Engine Support Frames	84	2.80	0.00	0.00	Analysis Based Mass
MAV Support System	285	6.21	0.00	-0.23	Analysis Based, Sep System from Altair
Porch and Ladder	130	6.00	0.00	-2.10	Scaled from Altair DAC-4
Landing Gear (4 legs)	1216	1.07	0.00	0.00	Length & Mass from Altair Excel Tool
MDM Side SA Sep System	220	1.00	0.00	0.00	Scaled from Altair DAC-4
Secondary Structure	685	2.73	0.00	0.00	Estimated 25% MDM Struct Mass (except gear)
Total MDM Structure Basic Mass	4,642				
Spacecraft Adapter Panels/Beams	385	0.50	0.00	0.00	Analysis Based Mass
SA Sep System (SA Side)	130	1.00	0.0	0.00	Scaled from Altair DAC-4
Total Spacecraft Adapter Basic Mass	515				

*CG info with respect to coordinate system at Mars surface
+Xup, Y & Z on center line, with -Z toward MAV*

As before, the spacecraft adapter mass is listed for completeness and because it is an important aspect of system-level performance. The mass estimates shown in Table 4-25 are based on structural strength and linear buckling analysis using 5g axial and 2g lateral launch loads. The structural panels are honeycomb sandwich with aluminum core thicknesses ranging from 2.54 cm to 5.08 cm, and composite facesheets having 4 to 21 plies. (0.206 mm thickness per ply). The various support struts included composite and aluminum circular tubes, square tubes, and I-beams having cross sectional areas ranging from 2 cm² to 30 cm².

4.6.5.7 Vertical Descent Module, Modal Frequency Results

The first three lateral mode frequencies for the V1 vertical lander are listed in Table 4-26. The frequencies correspond to the same fixed-end spacecraft-adapter boundary condition used for the V1 strength and linear buckling analyses.

Table 4-26 Vertical Lander, 1st Lateral Mode Frequency Results

Mode	Frequency
1	4.1 Hz
2	4.7 Hz
3	6.7 Hz

The first lateral frequency for the vertical lander is close to the minimum target described previously (5 Hz), without any lateral attachments to the launch vehicle shroud. V1's inherent stiffness results from its short height and the large cross section of the lander primary structure. V1 Shroud attachments similar to those used to attach the horizontal lander to its aeroshell/shroud would likely result in a first frequency near or above 5 Hz.

4.6.6 Summary Comparison of Analysis Results

The mass summaries presented in Table 4-23 and Table 4-25 indicate that for the assumptions used here, the horizontal lander has approximately 45% more basic structural mass than the vertical configuration (6,722 kg versus 4,642 kg). Most of the total mass difference (2,080 kg) is due to the more massive horizontal lander primary structure. The secondary structure mass estimates differ by 395 kg, but this difference is not independent because secondary structure was estimated as a percentage of primary structure. The horizontal configuration's primary structure is more massive because of its length and small cross section. The length creates a longer load path requiring more structural panels, and the small cross section provides less resistance to lateral loads. In addition to its larger mass, the horizontal configuration exhibits a first mode lateral frequency that is 46% lower than that of the vertical configuration (2.2 Hz versus 4.1 Hz). This was true despite the fact that lateral attachments to the shroud were used to increase the stiffness of the horizontal configuration but not the vertical. Although a frequency requirement is not known, it is clear that the horizontal configuration has significantly less lateral stiffness. Depending on the eventual frequency requirement, the horizontal configuration analyzed here may be infeasible or may require significant additional mass to increase stiffness. The first frequency (4.1 Hz) of the vertical configuration may be reasonable as it stands, or it could be increased by including lateral shroud attachments as was done for the horizontal lander H3.

One possible mitigation for the low stiffness of the H3 horizontal configuration is to modify the primary structure so that it looks more like brainstormed configuration H1. This would increase the primary structure cross section, significantly increasing stiffness and the ability to carry lateral loads. This could be accomplished by the use of an H1-like frame structure (Figure 4-25), or by extending the H3 partial-circle structure to form a 360-degree cage around the cargo. These options are consistent with the AHP results which ranked the H1 and H3 configurations as approximately equal. Furthermore, the structural arrangement of H1 was actually preferred by the structures team. However, the mass of an H1-type structure is unknown, and the AHP results suggest decreased performance with respect to other FOMs. Ultimately, the high mass and low stiffness of the H3 configuration warrant analysis of at least one alternate horizontal lander structure.

A second possible mitigation for H3's high mass and low stiffness would be to include more load sharing with the launch vehicle aeroshell/shroud. The attachments to the aeroshell used in the present analysis only allowed transmission of lateral loads (via pinned-type connections). This was done solely for the purpose of increasing lateral stiffness/frequency. An alternate scenario is to attach the lander rigidly to the aeroshell/shroud, perhaps replacing the spacecraft adapter structure completely. In this case, the aeroshell/shroud would carry both axial and lateral loads, and its full diameter would add to the lateral stiffness of the packaged configuration. Doing this would decrease the mass of the lander structure, but would increase the mass of the aeroshell/shroud and could complicate the entire design, fabrication, and integration process. Variations to this approach should be considered as part of

future work to determine feasibility.

4.6.7 Comparison to TeamX Mass Estimates

The structural mass estimates obtained from finite element analyses of the detailed H3 and V1 landers are compared to the “quick-look” mass estimates generated by TeamX (see Section 4.4) in Table 4-27.

Table 4-27 Comparison of H3, V1 and TeamX Structural Mass Estimates

H3 Horizontal Lander (Rigid Aeroshell)		TeamX Vertical Lander (Rigid Aeroshell)	
Subassembly Description	Mass (kg)	Subassembly Description	Mass (kg)
Primary Structure Struts/Panels	3,304	Primary Structure	5,462
Propulsion Tank Support Struts	245		
Rover & FSPS Support Struts	104		
MDM Engine Support Frames	100		
MAV Support System	153		
Porch and Ladder	130		
Landing Gear (4 legs)	1,320	Landing Gear	1000
MDM Side SA Sep System	286		
Secondary Structure	1,080	Secondary+Tertiary Structure	440
Total	6,722	Total	6,902

V1 Vertical Lander (HIAD)		TeamX Vertical Lander (HIAD)	
Subassembly Description	Mass (kg)	Subassembly Description	Mass (kg)
Primary Structure Struts/Panels	1,844	Primary Structure	5,291
Propulsion Tank Support Struts	89		
Rover & FSPS Support Struts	89		
MDM Engine Support Frames	84		
MAV Support System	285		
Porch and Ladder	130		
Landing Gear (4 legs)	1,216	Landing Gear	1000
MDM Side SA Sep System	220		
Secondary Structure	685	Secondary+Tertiary Structure	435
Total	4,642	Total	6,726

The TeamX mass estimates are for vertical landers utilizing HIAD and mid L/D (rigid) aeroshell systems. TeamX did not consider a horizontal lander, thus a direct comparison with H3 is not possible. It is notable, however, that both the H3 and V1 estimates for primary structure (3,304 kg and 1,844 kg) are considerably less than those for either TeamX vertical lander (5,462 kg and 5,291 kg). The landing gear estimates are reasonably close for all four landers. The TeamX estimates for secondary structure are significantly less than those used for H3 and V1 (which were based on 25% of MDM structural mass excluding landing gear). Some items that were explicitly determined for H3 and V1 were either omitted or included with primary or secondary structure for the TeamX estimates. Details of the TeamX primary structure estimates were not provided, but they are likely based on parametric models of historical spacecraft (including some unscrewed vehicles). The differences shown here should not be overly emphasized, but they do point out the large variations that are possible between quick-look studies that use parametric tools and in-depth analyses based on CAD layouts and finite-element analysis models. The difficulties associated with bookkeeping and estimating primary and secondary structure are also clear from the table. The initial quick-look studies serve a valuable function. However, for at least some subsystems that are highly dependent on configuration details (such as the structural system), there are simply too many variables to obtain reliable estimates based on historical data alone. This is especially true for Mars landers for which no truly similar historical analogs exist. As discussed herein, even the detailed H3 and V1 conceptual design mass estimates still have significant uncertainties, even after the completion of considerable modeling and analysis work.

4.6.8 Launch Vehicle Integration

For the lander configurations investigated, a number of different launch vehicle integration approaches may be possible. Fundamentally, these must take into account the aeroassist system, as well as the lander configuration type, whether vertical or horizontal. This section will briefly summarize the baseline integration approaches described previously, as well as suggest other options that could be examined in future efforts. Due to study time and resource limitations, it was only possible to assess a single integration approach for each lander configuration.

In the case of the vertical lander, a more or less conventional payload adapter was assumed for integration with the launch vehicle. A conventional payload shroud for encapsulating the lander and HIAD aeroassist system was also assumed. In contrast, the horizontal lander was encapsulated within an aeroshell aeroassist system that would also act as the launch vehicle shroud. The aeroshell was then attached to the launch vehicle as a shroud would be.

For the vertical lander configuration, the assumption was that the lander would be directly attached to the payload adapter at the bottom of the descent module and the HIAD would be attached to the top of the MAV (Figure 4-42). This resulted in a short payload adapter, which is advantageous for increasing lateral-mode vibration frequencies and reducing adapter mass. However, it was recognized later, during the evaluation of descent transition options, that the location of the HIAD atop the vehicle was a disadvantage, requiring an undesirable 180-degree rotation maneuver prior to the SRP burn.

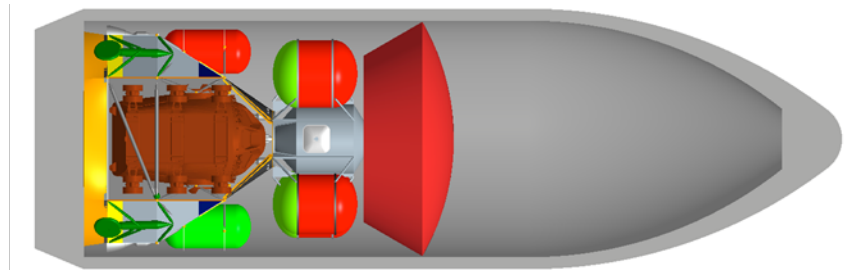


Figure 4-42 Baseline vertical lander integration (HIAD on top).

There are two alternative options that could be explored in a future study. The first, depicted in Figure 4-43, has the same vertical lander orientation on the launch vehicle as the baseline approach, but locates the HIAD at the base of the descent module. While this creates a more favorable Mars EDL configuration, it requires that the payload adapter be longer or, in some way, attach through the HIAD. Passing launch loads through the HIAD would require further study to determine feasibility and may complicate its design and/or increase its mass. A longer adapter would be detrimental to the lateral-mode frequencies. Allowing support to be provided to the lander by the shroud could help to mitigate this, but would likely require alterations to the launch vehicle shroud design, which would need to be accounted for.

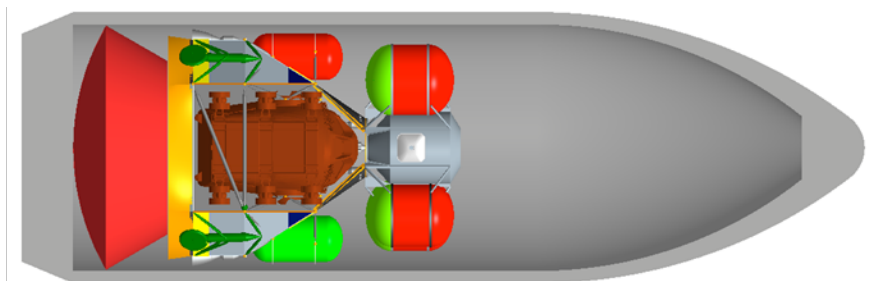


Figure 4-43 Alternate vertical lander integration (HIAD on bottom).

The second alternative, depicted in Figure 4-44, flips the orientation of the lander on the launch vehicle by 180 degrees. The HIAD is attached to the base of the descent module, as with the first alternative, but a longer payload adapter (not shown), possibly passing over and around the MAV, may be required. This arrangement was also proposed by the JPL TeamX (see Section 4.3). One advantage of this approach is that part of a cage-like payload adapter structure, if retained after launch, could also serve as guide rails for sliding off the inflatable portion of the HIAD during descent. A disadvantage would again be the increased length of the adapter and its negative impacts to lateral-mode frequencies and adapter mass, possibly requiring lander support from the shroud.

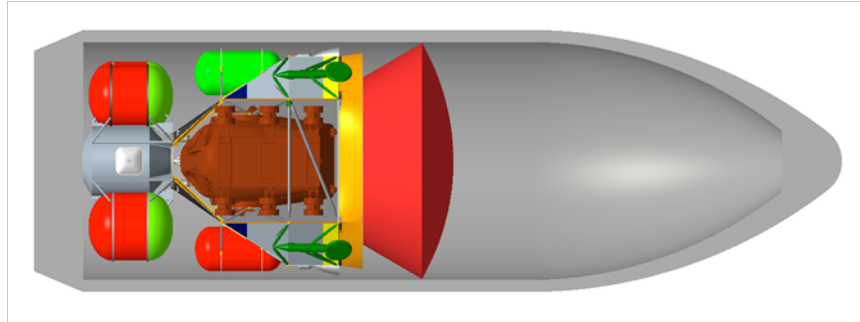


Figure 4-44 Alternate vertical lander integration (inverted orientation).

Another option for further investigation would be the vertical lander combined with an aeroshell rather than the HIAD. Figure 4-45 illustrates some of the possibilities. For the aeroshell assumed for the horizontal lander, the smaller length of the vertical lander creates some potential issues with respect to positioning within the aeroshell. Although attachment at the base of the aeroshell is desirable for structural reasons, the c.g. of the combined lander and aeroshell must be close to halfway along the length of the aeroshell to allow entry at the appropriate trim angle of attack. This requires that the lander be attached near the middle of the aeroshell, or that it somehow can be translated to this position prior to Mars entry. The mechanism to enable this would add complexity and mass. Shortening the aeroshell to better fit the lander is also a possibility, but the degree to which this can be done will depend on aerodynamic stability and trim considerations. An entry configuration too blunt will have undesirable entry characteristics.

The baseline horizontal lander integration approach with the aeroshell aeroassist system was illustrated in Figure 4-39 Figure 4-34. It was assumed for the structures analysis that the lander was attached at the base of the aeroshell and at several points along the length. For consistency with the vertical lander integration approach, a short payload adapter was assumed at the aeroshell base. As was mentioned previously, it is of interest to investigate attaching the lander more rigidly to the aeroshell sidewalls without using an adapter. This would require more load-sharing between lander and aeroshell structures.

An alternative option that should be possible with the horizontal lander configuration is the use of a HIAD for aeroassist rather than an aeroshell. This option is depicted in Figure 4-46. In this case, the horizontal lander is encapsulated by the launch vehicle shroud and has the HIAD attached at the “front” end of the lander. A short payload adapter is then assumed for attaching the lander to the launch vehicle. This option will likely require attachment to the shroud to improve lateral-mode frequencies. It will also be necessary to assess the practicality of this lander/aeroassist combination for EDL. Due to the longer length of the horizontal lander, air flow around the HIAD may impinge upon aft lander surfaces during descent, causing aeroheating or flight control issues.

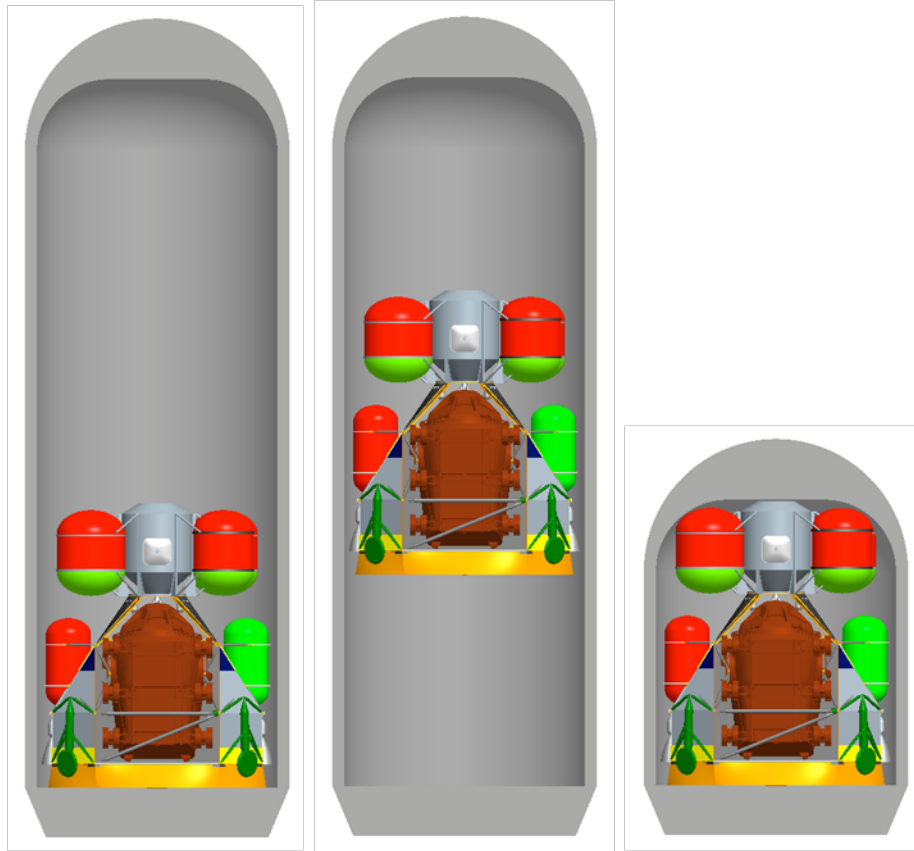


Figure 4-45 Integration options of vertical lander with rigid aeroshell.

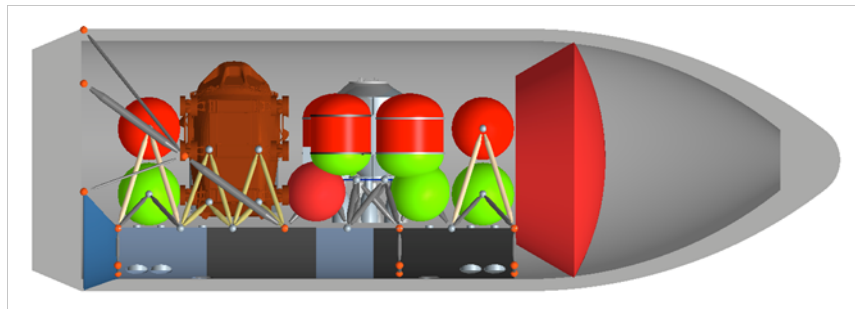


Figure 4-46 Integration of horizontal lander with HIAD.

4.6.9 Uncertainties and Suggested Future Work

Thus far, a variety of issues and uncertainties related to the assumptions, lander configurations, and analysis procedures have been mentioned. Several future task activities have been suggested. These are summarized below.

1) Develop working requirements for launch vehicle payload natural frequencies; explore and develop concepts to raise launch vehicle stack (payloads and adapters) stiffness.

The H3 and V1 analyzed configurations both have first-mode frequencies below 5 Hz. Achieving higher frequencies through structural modifications will require significant redesign (with mass increases), or may be infeasible altogether. Attachment to the launch vehicle shroud or rigid aeroshell may increase stiffness/frequency, but raises

system-level concerns. Uncertainties related to frequency represent a serious risk to feasibility, especially for horizontal configurations. Future work should include coordination with the SLS project team to identify working frequency requirements (even if preliminary). Mitigation strategies, including structural modifications, alternate configurations, and shroud load sharing should be analyzed. Various launch-vehicle packaging and integration schemes should be examined to determine impacts on stiffness/frequency. The focus should be on determining whether frequency is a driving requirement.

2) *Improve significantly the structural stiffness and efficiency of the horizontal configuration.*

Horizontal configuration H3 was found to require a significantly more massive primary structure than configuration V1. Moreover, its first modal frequency is probably too low to be considered reasonable. Therefore, the H3 structure design needs to be improved to reduce structure mass and increase stiffness. Several options for this improvement exist, including exploration of an H1 cage-type configuration (which was ranked almost equally during the brainstorming process but was expected to have higher strength and stiffness), or simply looking at variations of the H3 structural design.

3) *Determine the true feasibility of making the launch vehicle shroud and rigid aeroshell for Mars entry the same structure.*

The horizontal configuration was analyzed with the assumption that the shroud and rigid aeroshells are the same structure. The assumption eliminates redundant structure and increases available packaging volume, but has not been vetted at the system level. The optimum shapes for the shroud and aeroshell are not the same, and it is unknown whether a suitable shape exists that can be used for both launch and entry. Future work should be aimed at determining the feasibility of this scenario.

4) *Update the lunar landing-gear sizing tool for Mars landings.*

Landing gear masses were estimated using an analysis tool developed for the Altair lunar lander program. The tool assumes Apollo-like touchdown conditions and loads based on a maximum deceleration of 1g (9.8 m/s²). The tool is only applicable to Apollo-type deployable landing gear. These assumptions are not ideal for estimating Mars landing gear mass. For example, preliminary (and simplified) analysis suggest that limiting deceleration to 1g at Mars may be impractical because of the long attenuation distances required in the landing-leg struts. Updating the tool requires the development of new dynamic analysis models to generate accurate landing-leg loads for Mars touchdown, and to predict landing stability. At a minimum, the limitations of using Apollo-like assumptions to estimate Mars landing-gear mass should be better understood.

5) *Develop full-mission integration concepts for the HIAD and rigid aeroshell.*

The team's assumption to mount the HIAD directly to V1 and the rigid aeroshell to H3 was based on engineering judgment. With these assumptions, however, no integration scheme or structure for a HIAD-type entry system was developed for the vertical lander layout and analysis. The details of where the HIAD would be located relative to the lander, how it would be deployed, or how loads would be transmitted have not been defined and assessed. Details of rigid aeroshell integration for the horizontal lander are also undefined. Future work should develop a preferred HIAD entry scenario, including details of deployment and transition. Concurrently, efforts should be made to develop concepts for rigid aeroshell integration hardware, including a separation system. The finite element models and analysis results presented herein should be updated to include entry system integration hardware and any impacts to vehicle performance.

6) *Analyze the system-level impacts of aeroshell/shroud attachment and load sharing.*

Opportunities may exist for increasing frequency and reducing mass by using the shroud (or combination aeroshell/shroud) to support the lander during launch. However, the benefits are not quantified and shroud load sharing raises system-level issues related to the design of the launch vehicle. Future work should involve coordination with the SLS project team to define shroud baseline dimensions and sizing. Analyses should be conducted to determine the impacts of shroud load sharing on system-level performance, including mass. This issue is closely related to numbers 1 and 2 above, and all three might be investigated as part of one common task.

7) *Analyze the effects of interface loads on propellant tanks, cargo, and the MAV.*

The present analyses treated fuel, the FSPS, the rover, and the MAV as lumped masses during analysis of lander primary structure. Although mounting struts were sized and attachment hardware was accounted for, the ability of these vehicle components to carry transmitted loads is uncertain. In some cases, loads imparted to these components

during launch may be significant drivers to their design. This may occur due to stress concentrations at mounting points, or because loads paths during launch or entry are different from those seen during surface operations. Significant mass inefficiencies arise if surface components (such as a rover) must be overdesigned to withstand one-time launch or entry loads (see the next item related to gear ratios). The impacts of loads and mounting schemes on propellant tanks, the MAV, and other cargo should eventually be analyzed using dedicated models for each component.

8) Develop and determine system mass performance “gear ratios”.

“Gear ratios” are system performance characteristics that help determine the mass efficiency of an overall mission. By definition, a gear ratio for a single step of a mission is the system mass required in its initial state (on the launch pad) to deliver one mass unit of payload to its final state (Martian surface, or the mission step at which the component is jettisoned). Overall gear ratio for a mission is the product of gear ratios for all sequential steps. In layman’s terms, the gear ratio answers the question, “how much system mass is required to support any given component?” For design of structures, the gear ratio can help determine priorities for focused mass-reduction efforts of structural components, jettison strategies, and mass-transfer options. For example, if mass must be added to stiffen a launch vehicle stack, it is often better to add that mass to adapter or interface structure (if possible) rather than adding it to a landed spacecraft component. This is because the landed component must be carried much further into the mission, requiring more propellant than if the mass had been added to a jettisoned adapter. Efforts should be initiated to better understand how Mars mission gear-ratios might affect mass related conclusions for various vehicle components.

9) Study and characterize the landing dynamics or horizontal landers.

Horizontal lander configurations have a long and a short axis with significantly different moments of inertia about each. Previous dynamic analyses of landing stability and touchdown loads have only considered nearly symmetric lander geometries. The asymmetric geometry of horizontal configurations suggests that variables such as lander orientation and touchdown velocity direction may be unique drivers for the touchdown stability of horizontal landers. Dynamic modeling of horizontal configurations is necessary to explore these issues.

10) Analyze entry and landing load cases.

Time did not allow analysis of the effects entry loads or landing loads have on descent module primary structure. Past experience suggests that these loads are not significant design drivers and will result in only small local changes to vehicle structure. Unknown is whether this remains true for long horizontal configurations. Analyses should be performed on both V1 and H3 (but especially H3) to include these loads, and the results used to update mass properties.

11) Study and analyze shroud volume usage.

The V1 vertical lander configuration has a total height of 10.75 m. Currently the expected SLS launch vehicle shroud (heavy lift version) will be 31 m tall with a cylindrical length of 17.2 m. If only the vertical lander is packaged in the shroud, there may be significant extra volume, even if space for packaging a HIAD system is accounted for. Even the H3 horizontal lander does not have sufficient length (15.2 m) to fill a 31 m shroud. Several options are possible. The shroud length could be shortened, or assuming launch mass limits are not exceeded, additional cargo elements or a propulsion stage (or both) could be packaged with the lander in the shroud. Shortening the shroud may work well for packaging the lander but not for other payloads, thus requiring two unique shroud configurations, one long and one short. In the case of the rigid aeroshell, shortening the overall length may not be feasible because the correct aspect ratio for entry is not maintained. Also for the rigid aeroshell it may be desirable to attach the lander higher up in the shroud so it will be in the center of the aeroshell during entry. Doing this will create very low lateral frequencies and may not be feasible. Placing additional cargo or a propulsion stage under a lander in the shroud is possible, but will increase the overall height of the launch vehicle stack, again resulting in low stiffness/frequency. Attachment to the shroud may become mandatory or it may be not be possible at all to achieve sufficient lateral stiffness for some scenarios. All aspects of stack sequencing and shroud utilization require future analysis. Efforts in this area should be coordinated with the SLS project team and future activities that are shroud related.

12) Update both landers for habitat integration.

Lander configurations were developed here with focus on a first launch that transports the FSPS, rover, and MAV to the Martian surface. A subsequent launch will transport a crew and habitat structure hopefully utilizing the same

basic lander configuration. During down selection, the ability of the brainstormed concepts to package a habitat was treated as a desirable (but not deciding) characteristic. Notional habitat packaging concepts were developed for most of the configurations. Both the H3 and V1 configurations are able to package a habitat structure, but habitat integration was not analyzed in the current work. Hardware concepts for integrating and mounting a habitat are needed, along with models to size the hardware and examine the impacts of launch and other loads on the habitat structure. More analysis is needed to ensure that a single lander descent stage configuration can accommodate both cargo-only and crewed packaging and launch requirements.

13) Update the FSPS volume and determine impacts to the lander configurations.

Near the completion of this effort it was recognized the FSPS volume used herein (33 m³) was too low because it was derived for a lunar rather than Mars mission scenario. A more realistic value for a Mars mission is 60 m³. This increase in FSPS volume may significantly affect the lander packaging scenarios that were considered, including the down-selected configurations. An effort should be made to determine the impact of increasing FSPS volume on the lander configurations and mass estimates developed during the present study.

14) Determine the Impacts of Utilizing Full Lander Performance Capability

The cargo elements considered for the present lander configurations (FSPS, rover and MAV) do not represent the full landed mass capability corresponding to the assumed lander propellant masses. Approximately 15,000 kg of additional mass can be carried by the lander if all of the assumed propellant is available. This additional mass was included in the analyses as part of the lander control mass, but additional volume for the mass was not allocated. Thus, it may turn out that to completely utilize full lander performance, the studied landers might require significant reconfiguration. The other options are to package cargo elements more densely, or to decrease the amount of propellant. The later scenario reduces the size of the propellant tanks and might in itself create a need for lander reconfiguration. An effort should be initiated to examine the complete ramifications of these issues, especially as related to the results and conclusions of the present study.

4.7 Propulsion and Propellants

4.7.1 Engine Performance and Sizing

The propulsion configuration was developed based upon MAV considerations so that the MAV and lander Descent Module would have a common engine design. The parametric analyses for the MAV propulsion system indicated that the additional performance benefit provided by in-situ produced fuel had to be balanced against the packaging and cryogenic storage issues associated with carrying the seed LH₂ to the Martian surface, or the additional cargo mass and operational complexity of regolith processing. Therefore, the ISRU approach selected for the study was with the main propulsion oxidizer produced on the Martian surface from the atmospheric CO₂. Packaging and thermal management considerations make the use of LH₂ very problematic, resulting in the use of a hydrocarbon fuel brought from Earth as the ascent propellant. Liquid methane provides good performance and has similar thermal management requirements to LOX; however, it has a lower density than some other hydrocarbons. Other hydrocarbons that could be considered include kerosene, alcohol, hydrazine, propane, and butane. Although a detail fuel trade study was not performed, a LOX/LCH₄ propulsion system was selected for the vehicle conceptual design.

The initial parametric analyses also indicated that for the MAV to return to a HMO it the MAV required approximately 100 kN (22 kLbf) of thrust was required on the second stage. Assuming commonality between the second stage and the first stage, four of the 100 kN engines were used on the first stage. At that thrust level, propellant requirement, and packaging considerations, a turbopump-fed engine is needed. The MAV Configuration on the left in Figure 4-47 shows thrust chamber assembly for the engine.

The integrated EDL trajectory analysis indicated that a T/W in the range of 1.5 to 2.0 should be used (see Section 4.8.4), resulting in a required thrust in the range of 1,200 kN. If the same 100 kN MAV engine is used on the descent stage, the descent stage would require 12 engines. Twelve engines is probably too many from a reliability standpoint, so an engine concept was created whereby two thrust chamber assemblies were connected to a larger common turbopump, shown as the descent configuration in Figure 4-47.

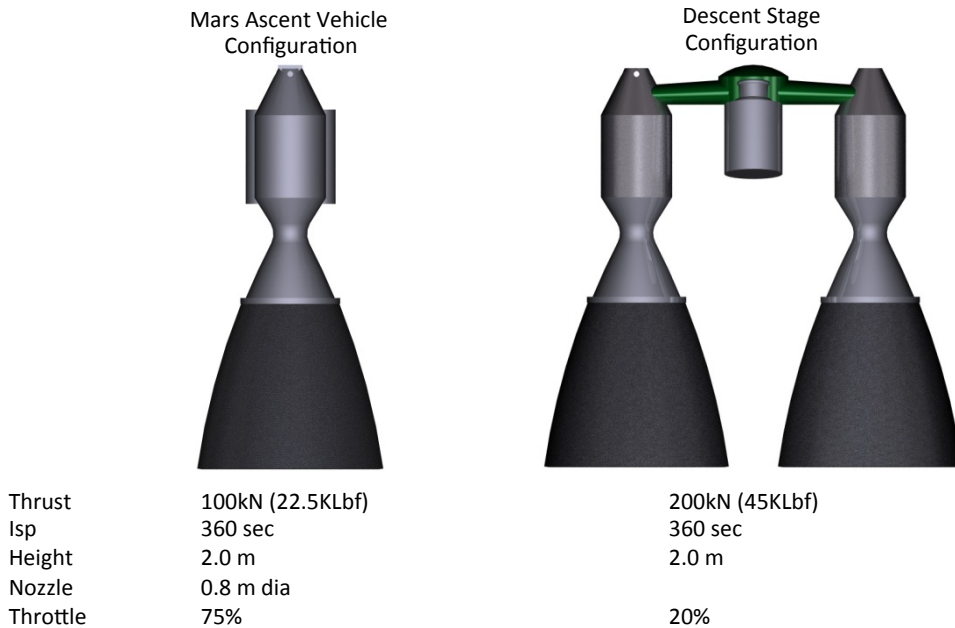


Figure 4-47 LOX/LCH₄ engine for Mars Ascent Vehicle and lander descent stage.

A specific impulse of 360 sec was assumed for the engines, based upon a moderate combustion chamber pressure in the 900 psia to 1000 psia range, which can be obtained with multiple liquid propellant rocket engine cycles.

Future work to more clearly define the technology and advanced development activities associated with the ascent and descent engines include

- Fuel trade study
 - Determine if integrated system considerations warrant review of other propellants.
- Engine cycle and configuration studies
 - Determine if other engine configurations, such as a truncated aerospike should be considered.
 - Engine cycle study – evaluate fuel-rich staged combustion, oxidizer-rich staged combustion, full-flow staged combustion, gas generator, and expander.

4.7.2 Cryogenic Fluid Management & Interfaces with ISRU

With turbopump-fed engines, propellants are stored at relatively low pressure during the loiter operations, 2025 psia, and pressurized to approximately 50 psia during operation. At those pressures, there is limited thermal capacity to absorb heat from the vehicle or the solar environment.

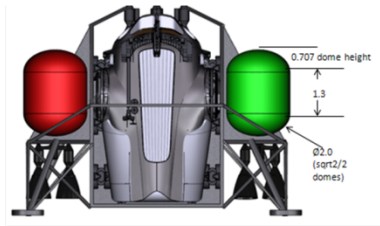
The basic cryogenic fluid management (CFM) concept is to use an 80K cryocooler with a vapor cooled shield to intercept the heat before it reaches the propellants and dissipates it to radiators. 40-50 layers of multi-layer insulation will also be used. The cryocooler concept will operate at low duty cycle due to the relatively cold environmental sink temperature during much of the mission. The CFM system is located on the descent stage, with cold helium circulated to both the ascent and descent propellant tanks. During the ISRU oxygen production, the cryocooler system will operate to condense the oxygen to liquid in the tank. The following are detailed analyses of cryocooler performance

Zero boil-off of LOX/LCH₄ is assumed for the following analyses in to estimate cryogenic thermal control mass and power requirements for one ascent and two descent Mars Lander vehicle configurations. The descent vehicle options consist of one vertical and one horizontal configuration. The vertical descent stage consists of four cylindrical tanks,

two LOX and two LCH₄. All four tanks are estimated to be the same size with a dome height of 0.707 m, barrel length of 1.3 m, and diameter of 2.0 m. The horizontal descent stage consists of four spherical tanks, two LOX and two LCH₄. Each tank is 2.4 m in diameter. Figure 4-48 shows both descent stage tank configurations.

◆ Vertical Descent Stage

- ◆ Four Cylindrical Tanks
- ◆ 2 LOX, 2 LCH₄
- ◆ All Tanks Same Size



◆ Horizontal Descent Stage

- ◆ Four Spherical Tanks
- ◆ 2 LOX, 2 LCH₄
- ◆ All Tanks Same Size

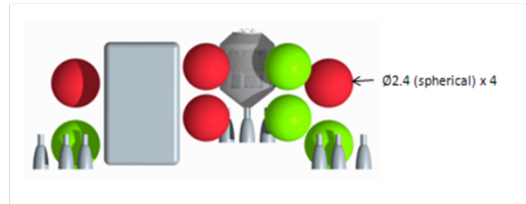


Figure 4-48 Vertical and horizontal descent stage configurations.

The ascent vehicle has two stages and consists of four LCH₄/LOX nested tanks. Each stage has slightly different sized tanks. For the purpose of this analysis, the largest tank has been analyzed and has a dome height of 0.92, barrel length of 1.4 m and a diameter of 2.6 m. Figure 4-49 shows the tank configuration and sizes for the two stage ascent vehicle.

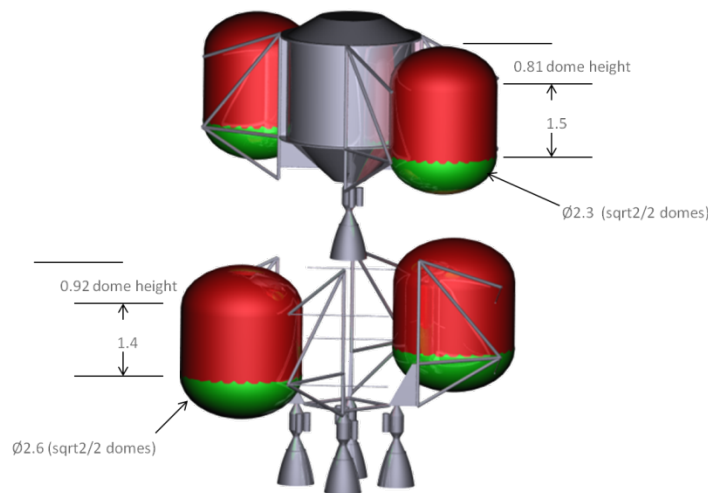


Figure 4-49 Two stage ascent vehicle.

Environmental sink temperatures were calculated for three mission phases, based on planned Nuclear Cryo Propulsion Stage (NCPS) mission analysis. The Altair LDAC-3 thermal model was executed for each of the three mission phases and a steady state temperature of the outer multi-layer insulation (MLI) blanket on the LOX tank was extracted as a typical environment or sink temperature as shown in Table 4-28. The LEO and Mars Orbit orbital diagrams from Thermal Desktop are shown in Figure 4-50. Mars transit and Mars orbit sink temperatures are very close due to a similar cold environment.

1. LEO (460 km circular, beta 52 degrees)
2. Mars Transit/High Earth Orbit (HEO) (250 km x 33810 km)
3. Mars Surface (300K surface temperature)

Table 4-28 Sink Temperatures for LEO, Transit, & Mars Orbit

Environment Temperatures (deg. K)		
LEO	Transit	Mars Orbit
229	172	171

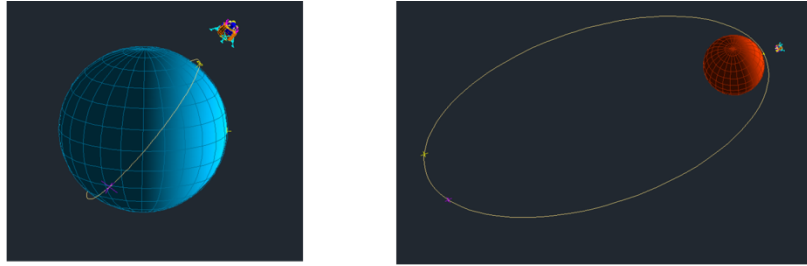


Figure 4-50 Sink temperatures and LEO & Mars orbits.

Conductive tank heat loads were scaled by surface area from the Altair LDAC-3 thermal model after being executed for the NCPS mission profile. Environment heat loads, passive and active thermal control mass, and power estimates were calculated using the CRYOSIM tool, version 2.5. A heat load correction factor of 2.1 was used for the in-space portion of the analysis to account for a 50% margin plus additional margin to account for performance inefficiencies of the MLI blanket due to penetrations, etc. A conductive heat load correction factor of 1.5 has also been utilized.

CRYOSIM results for the descent vehicle configurations for both LEO and Transit/Mars Orbit are shown in Table 4-29. Ascent vehicle results are shown in Table 4-30. Zero boil-off is attained assuming 90K type cryocooler system. Heat leak into the tanks due to the environment and conduction only was considered in this analysis. Additional heat due to engine burns, soak-back, etc., was not accounted for.

The MLI configuration assumes 63 layers of variable density insulation. The total system heat load accounts for environmental and conductive heat loads, including correction factors. LEO represents a worse case and should be used to size the descent vehicle system.

The ascent vehicle assumes empty LOX tanks for the trip to Mars with plans to fill the tanks after landing. Cryogenic fluid management system is estimated for LCH₄ management only.

Table 4-29 Descent Vehicle CRYOSIM Results

Data for 4 Tanks, Zero Boiloff				
	LEO		Transit/HEO	
	Vertical	Horizontal	Vertical	Horizontal
MLI Layer Count	63	63	63	63
System Heat Load (W)	69.0	67.0	24.0	24.0
Heat Rejection (W)	1738.0	1702.0	607.0	605.0
CFM Passive System Mass (kg)	121.0	121.0	121.0	121.0
Number of 90K Cryocoolers	4	4	2	2
CFM Active System Mass (kg)	150.0	147.0	55.0	55.0
Average Input Power (W)	1669.0	1635.0	583.0	581.0

Table 4-30 Ascent Vehicle CRYOSIM Results

Data for 4 Nested Tanks, Zero Boiloff Lox Tanks Empty		
	LEO	Transit/HEO
MLI Layer Count	63	63
System Heat Load (W)	89.0	31.0
Heat Rejection (W)	2253.0	776.0
CFM Passive System Mass (kg)	161.0	161.0
Number of 90K Cryocoolers	7	3
CFM Active System Mass (kg)	198.0	71.0
Average Input Power (W)	2164.0	745.0

Consideration of the impact of long-term storage of LCH₄ on the surface of Mars and in-situ production of LOX requires an estimate of worst-case hot Mars surface environment. Seasonal and diurnal cycle Mars surface temperature data were supplied by A. Dwyer, Figure 4-51. A maximum surface temperature of 300 K was assumed for the analysis.

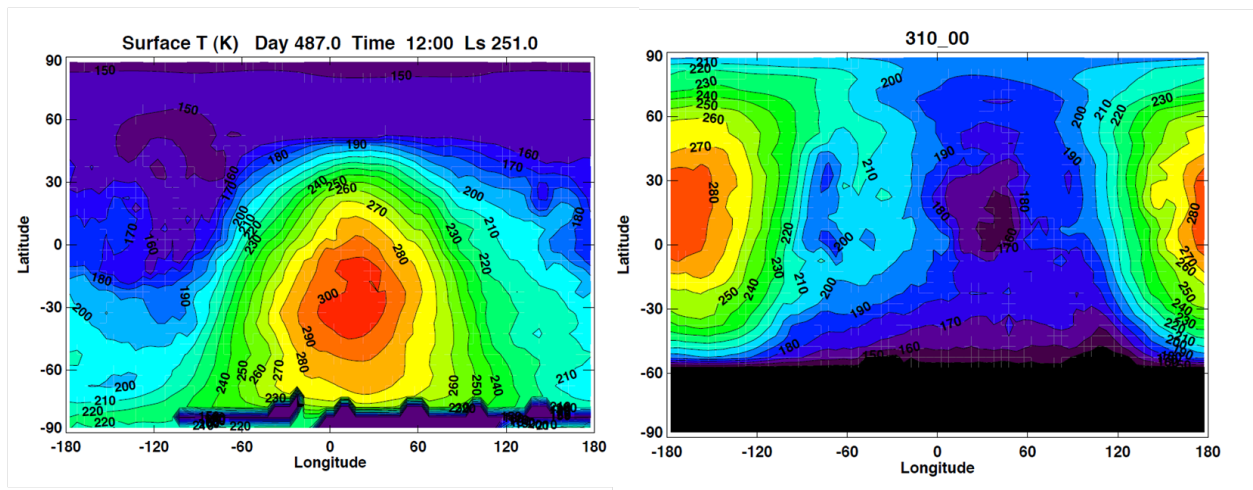


Figure 4-51 Mars seasonal and diurnal cycle data (A. Dwyer).

The Altair LDAC-3 Lander thermal model was executed using a worst case Mars surface temperature of 300 K, assuming Mars surface properties of absorptivity of 0.93 and emissivity of 0.98. An environmental sink temperature for the LOX tanks of 267 K was derived from the analysis. Performance and mass of MLI best suited for Mars surface has not been characterized and was not utilized for this effort.

Mass and power estimates to maintain full LCH₄/LOX tanks on the surface of Mars are shown in Table 4-31. One additional cryocooler is required beyond the seven needed in LEO to maintain liquid methane. Four are required to maintain liquid oxygen. Total average power estimated for propellant maintenance on the ascent vehicle is 5327 W. To convert gaseous oxygen to LOX, over a 24-month period, a total of 10 cryocoolers are needed. Potentially, four

cryocoolers from the descent vehicle could be reutilized for the in situ production of LOX. The mass, power demand and heat rejection requirements for the active thermal control system can be reduced with appropriate insulation for long-term storage in the surface environment. Future work should certainly include development of Mars surface propellant storage strategies.

Table 4-31 Ascent Vehicle CRYOSIM Results

Data for 4 Nested Tanks, Zero Boiloff Maintain Full LCH4/LOX Tanks		
	LCH4	LOX
MLI Layer Count	63	63
System Heat Load (W)	143.0	77.0
Heat Rejection (W)	3612.0	1934.0
CFM Passive System Mass (kg)	161.0	-
Number of 90K Cryocoolers	8	4
CFM Active System Mass (kg)	310.0	166.0
Average Input Power (W)	3469.0	1858.0

Table 4-32 Ascent Vehicle CRYOSIM Results

Cryocooler System to convert GOX to LOX Data for 4 Oxygen Tanks		
Tank Volume (m3)	22.9	22.9
Time (months)	12	24
System Heat Load (W)	290.0	155.0
Heat Rejection (W)	7311.0	3904.0
Number of 90K Cryocoolers	18	10
CFM Active System Mass (kg)	627.0	336.0
Average Input Power (W)	7022.0	3750.0

4.8 Descent Module Design

4.8.1 Physical Design Description

This section describes the necessary hardware for the MDM configurations and presents a MEL with mass originating from several sources: historical heritage hardware, previous spacecraft studies and calculations from CAD models, the results of which were summarized in Section 4.6. Higher fidelity estimates of lander subsystem masses are forward work.

4.8.1.1 Requirements and Operations

Per previous HAT work, it was assumed that the maximum Mars Lander envelope dimension was 9.1 m diameter and with a total vehicle height not to exceed approximately 27 m, which was derived from a nominal 30x10 m launch fairing.

Concept of operation

For the purpose of this exercise, the MDM was assumed to support the following activities and capabilities at a minimum:

- Deliver Mars surface infrastructure and crew return system:
 - a. Pressurized Rover
 - b. Fission Power System
 - c. MAV
- Perform Mars EDL
- House oxygen producing ISRU system

Note: In addition, the same descent module design is intended to deliver crew and a surface habitat on a subsequent mission. This aspect was not addressed in this study.

It was assumed that the initial Mars Lander's descent module would house and transport a pressurized rover, a fission power system and an ascent crew return vehicle, with the crew being delivered later on a separate lander. The descent module and payloads are aerodynamically decelerated for Mars entry. This study considered multiple variants, but selected two methodologies for assessment and designs: a HIAD and a rigid aeroshell mid L/D lifting body. The ascent crew vehicle is a two-stage propulsion subsystem with a common, pump-fed engine design used on both stages. The LOX tanks for both stages are supplied with LOX processed from Martian resources to support a LOX-Methane propulsion system. The ISRU system processing the LOX is housed in the descent module structure with feed lines going to the ascent vehicle's first and second stage LOX tanks. It is assumed that the ascent vehicle would launch from the descent module deck. The descent module is responsible for housing and structurally securing the above cargo complement for Earth launch, Mars transient, Mars entry, Mars landing, and Mars surface offloading of equipment.

Environments

The descent module design and configurations were formulated based on launch vehicle environments and Mars EDL environments only. However, future analysis would consider ground processing, integration, launch, LEO orbits, and Mars transient environments.

4.8.1.2 MDM Interfaces

1. Cargo Interfaces

It was assumed that the MDM would provide structural mounting and containment as well as mechanical interfaces for umbilical support connections to each payload. These interfaces function from Earth launch through the Mars surface stay phase. For uncrewed cargo delivery missions—with no descent abort capability needed—the MDM would not require contingency pyrotechnic detachment from payloads. It was assumed that prior to crew boarding the previously delivered ascent vehicle on the Martian surface, an extravehicular activity (EVA) crew could manually unlatch the MDM's structural restraints. However, the pressurized rover and fission power system does require autonomous detachment and robotic offloading to the Martian surface post landing.

Nominally, any crew cabin delivered (ascent or surface habitat) is assumed to be a stand-alone pressure vessel. With no pressurized connections to other elements during ascent, descent, or while on the Martian surface, no mechanical or pyrotechnic connections to other elements are nominally required. For surface operations that might require intravehicular activity (IVA) transfer between the MDM and other surface elements—the Surface Rover, for example—provisions for manual or remotely actuated tunnel separation would be required.

It was assumed that provisions for data, power, and fluids interfaces between the MDM and the ascent vehicle were required, particularly for ISRU fuel transfer.

2. Ascent Vehicle MPS and Structural Interfaces

The ascent vehicle is supplied with LOX from the ISRU unit housed in the descent module. Therefore, feed lines are routed from the ISRU unit up to the first and second stage oxidizer tanks. The LOX feed line will support a pyrotechnic break or manual crew disconnect prior to ascent vehicle ingress.

3. Fission Surface Power Unit Structural Interfaces

During surface phase operations, it was assumed that MDM keep-alive power would be provided by the FSPU system.

4. Crew Ingress/Egress Interfaces

MDM interfaces with the crew include crew ladder, staging platform for crew ingress/egress to the ascent vehicle, remote command and control interfaces from Mars surface during EVA, and backup communication interfaces.

5. Surface EVA Communications & Life Support Interfaces

The descent module provides an umbilical interface panel, which provides communications, power, and oxygen.

4.8.2 Configuration Summary

The MDM Study Team debated various options for EDL configuration for the descent module. Two landing configurations were assessed, with medium fidelity, a horizontal and a vertical orientation. These basic orientations were also coupled with aero-entry technologies to give a multiple variant design space. This report describes the following two configurations with their entry system approaches. The first option coupled a vertical lander with a HIAD and the second is a horizontal lander with a mid L/D rigid aeroshell entry system. Both configurations support delivering 40 t payload (design target) to the Martian surface.

The MDM Study Team leveraged work previously performed in support of a crewed lunar expedition to quickly develop the makeup of a conceptual MDM. Because the Altair lander was designed to deliver approximately 25 t of payload to lunar surface, this baseline design supported an extrapolation to the Mars mission lander. The Altair Lander provided significant detail in component definition and assessment. Those data (part definition & mass) were assessed for similarity to operations and then linked to the notional architecture derived for the Mars lander. The operational and functional systems for flight control, navigation, and system monitoring were linked directly using both definition and mass parameters. However, the propulsion system was assessed using Altair data for part definition, but using analysis calculations to configure and size propellant tanks. The structural definition was derived and calculated directly from CAD models for the two Mars lander configurations. The system breakdowns for each configuration (horizontal & vertical configurations) with descriptions are listed below for the descent module in Table 4-33. Both configurations MEL and PEL (See Appendix 1) are the same with the exception of structural layout/packaging, payload interface mounting, support structure elements and landing gear.

Table 4-33 MDM Configuration Basic Mass Summary (no growth/margin allocation)

Equipment	Vertical	Horizontal
Oxidizer-LOX	14818 kg	
Fuel-CH4	4939 kg	
Oxidizer Tanks	158 kg	144 kg
Fuel Tanks	158 kg	144 kg
MPS*	203.61 kg	
Engines (6)	2082.0 kg	
Structures	4641.9 kg	6721.7 kg
Thermal Management*	636.7 kg	
Pressurant System*	289 kg	
RCS- Bipropellant*	249.1 kg	
Avionics*	544.7 kg	
ISRU-LOX Generator	936.0 kg	
EVA Umbilical Services*	8.3 kg	

*Altair Extrapolation

4.8.3 Subsystem Data

4.8.3.1 Main Propulsion

Refer to Section 4.7 Propulsion and Propellants.

4.8.3.2 Pressurant System

The pressurant system, of 289 kg, is currently derived from an extrapolation of heritage launch vehicle pressurant systems and previous lander analyses. It is a helium system with Composite Overwrapped Pressure Vessel (COPV) tanks mounted on secondary structure in both the descent module and ascent module. Further analysis needs to be conducted to determine the amount of helium required, thus determining the number of tanks.

4.8.3.3 Reaction Control System – Biprop Thrusters

The Reaction Control System (RCS) is potentially a pressure-fed LOX methane bipropellant. However, trades are being planned to determine what system is used. As a result, of an open trade, once again the Altair heritage mass database was used to extrapolate an approximation. The basic mass of that RCS was approximately 249 kg. It consisted of 12 thrusters housed in a three cluster assembly located on the descent module body. Tanks, feedlines and manifolds are housed in the descent module primary structure and the ascent module RCS being mount to secondary structure outside the crew module.

4.8.3.4 Structures

The primary structures details are described in Section 4.6 of this document. For the purpose of this exercise, the MDM secondary structures were estimated from similar CAD concept models for the lunar lander Altair. The secondary structure includes the following components:

- Cylindrical pressure vessel with composite skin and aluminum honeycomb core construction
- Pressure-assisted circular docking hatch

- Pressure-assisted EVA side hatch
- Frangible “H” seam and pyrotechnic expansion tubes to separate from Cargo Lander

Due to the varying fidelity of structures definition and analysis of the two descent module configurations of the descent module, the secondary structures and mechanism subsystems were extrapolated, from Altair Lunar Lander Design Study, to provide estimations until detailed structure components could be modeled in CAD. The MDM’s two configuration concepts, vertical and horizontal, have significantly different geometric size with more structural mass required for the horizontal configuration.

The MDM tank and primary structure masses are likely good fidelity pending further detailed design work. The entire MDM dry structural masses are estimated to be 6034 kg for the vertical configuration and 8650.9 kg for the horizontal configuration. The secondary structures and mechanism masses were extrapolated from Altair-heritage structure, which may not be accurate, depending on ultimate placement. It should also be noted that structural analysis to size support structure and separation hardware for the large propellant tanks was left as forward work. One additional deviation from the Altair heritage design is that because there is no descent abort capability, it was assumed that pyrotechnic disconnects between other elements can be eliminated in lieu of manually activated launch lock releases prior to ascent.

4.8.3.5 Thermal Management

As with the Electrical Power subsystem, the Altair-derived MDM Thermal Subsystem, 636.72 kg, is assumed to be independent of the Ascent module. The descent module avionics system and ISRU cooling is open to trading passive heat sink and radiative heat transfer or cold plate cooling loop system with radiators. The cryogenic cooling of oxygen is assumed to managed with the Ascent vehicle tanks and cyrocooling system. The thermodynamic venting system (TVS) is book kept with the MPS tank mass allocation. The thermal management system is comprised of coldplates, flow control valves, heat exchangers/radiators, MLI, accumulators .

4.8.3.6 Avionics Subsystems

Command and Data Handling (C&DH) Subsystem

For the purpose of this exercise, the Study Team assumed the MDM Command and Data Handling (C&DH) subsystem would control about the same type and quantity of equipment as the original Altair design. Although there may be some minor differences, the MDM Study Team assumed that Altair’s distributed avionics scheme, with time-triggered, multi-drop network and redundant routers would meet MDM needs. Assuming a vehicle with roughly the same complexity of Altair, with similar subsystem designs, the C&DH subsystem was assessed as 203.61 kg basic mass and consisted of the following major subassemblies:

- Distributed Control Units
- Flight Computers
- Recorders
- High Speed Network Switches
- Video Processing Unit
- Power Distribution Units
- Cables and Lighting

Because the C&DH subsystem is generally independent of the crew complement, which is not the same for Altair and the Mars landers, the DM Study Team assumed the same C&DH equipment basic mass for both horizontal and vertical variants.

Power Management Subsystem

The descent module power systems, 91 kg, for this early study identified battery systems as the power sources for EDL. The power systems between the ascent and descent modules are isolated. The power profile analysis has not been initiated to validate the lunar lander battery selections. The power system charges the descent batteries prior to orbit insertion and descent. Fuel cell based power systems have been ruled out currently, but may return to the trade space. Once on the surface, the Fission Power system is to be deployed for surface power needs associated with descent module system control and ISRU LOX generation.

Batteries

The battery selection and class of batteries have not been determined at this time. The number cells and strings were carried over from the lunar lander design with an estimated mass of 129.66 kg basic mass

Communications and Tracking (C&T) Subsystem

For the purpose of this exercise, the Study Team assumed the MDM C&T subsystem would be fundamentally the same as the original Altair design, and that the vast majority of equipment would be mounted on external MDM surfaces. Based on Altair work, the mass was estimated to be approximately 62.79 kg basic mass and consisted of the following major subassemblies:

- 5 each Antennas and 3 each Emergency Antennas
- 1 each Software Defined Radio and 1 each Transponder
- Switches, Cables, and Secondary Structure

Guidance, Navigation and Control (GN&C) Subsystem

For the purpose of this exercise, the Study Team assumed the MDM GN&C subsystem would be essentially the same as the original Altair design. Based on Altair work, the mass was assessed as 57.48 kg basic mass and consisted of the following major subassemblies:

- Optical Navigation (OpNav) Camera
- Light Detection and Ranging (LIDAR)
- Inertial Reference Unit (IRU)
- Star Tracker
- Running Lights

4.8.3.7 Extravehicular Activity Subsystem Interface

An EVA interface panel is located on the MDM in close proximity to surface access by the crew for conducting preparatory ground operations with the descent module. The EVA subsystem includes EVA equipment physically attached to the MDM, as well as crew tools.

The 87.51 kg of ascended EVA equipment includes the following:

- 4 each Umbilical Interface Panels
- 4 each Short Umbilical Hoses
- EVA Tools (jammed docking hatch contingency)

4.8.3.8 In Situ Resource Utilization Oxygen Production

The in situ resource utilization system (mass ~ 936 kg) is an autonomously operated piece of equipment that is located in the descent module for mass allocation only. It has no functionality in support of landing operations. The ISRU system extracts CO₂ from the Mars atmosphere and generates gaseous oxygen that will be transferred, via feedlines, up to the Ascent module propellant tanks. The ISRU is comprised of three subsystems: 1) Atmospheric Acquisition (299.12 kg), 2) Consumables Generation (165.8 kg) and a liquefaction subsystem (28.20 kg).

4.8.3.9 Descent Module Structures

See Section 4.6 for detail description of the horizontal and vertical configuration for the descent module structural mass assumptions.

4.8.4 Performance

To determine the payload capability of the point-design vertical and horizontal lander configurations, descent trajectory analyses were conducted. Different engine throttle strategies were also examined to understand the impact this choice would have on payload performance. Payload, as defined here, includes the MAV and surface cargo elements and has a target value of 40 t. The baseline propellant masses for the lander, which were assumed fixed for this analysis, were generated during the initial sizing efforts in Cycle C (see Section 4.3.3).

Two entry configurations were considered. One considered using a 23 m HIAD and SRP. This was assumed for the

vertical lander configuration. Another utilized a 10x30 m rigid aeroshell and SRP and assumed a horizontal configuration. Since much of the descent analysis in Cycle C was performed using assumed engine initiation conditions, system closure was verified using independent entry-to-landing trajectory and mass sizing analysis. The independent simulation was developed for the EDL-SA Year 1 study and details of the simulation and models used can be found in reference 15.

4.8.4.1 HIAD + SRP + Vertical Lander Configuration Results

Cycle D descent module dry mass and propellant values are provided in Table 4-34. A 30% factor was applied to dry mass values for mass growth allowance and margin, yielding a mass of the ascent vehicle of 13799 kg and descent module dry mass of 12825 kg.

To determine lander performance, the EDL-SA year 1 Architecture 2 (HIAD) simulation served as the basis to evaluate the vertical lander configuration. The first step was to modify the EDL-SA payload mass (nominally 40,000 kg) until the descent module dry mass matched the margined Cycle D value of 12825 kg (the nominal EDL-SA Arch 2 descent module dry mass was 11700 kg) and the total propellant approximately matched (within 1000 kg) the fixed 19757 kg available in the propellant tanks. However, the Cycle D engine design was modified from the EDL-SA response surface approach to a specified thrust and Isp that represented the current state of the art (see Section 4.7).

The first sample trajectory, Constant Thrust: Case 1, used a constant total thrust of 1200 kN from 6 LOX/LCH₄ engines, an Isp of 360 s and a constant 100% throttle setting until the final 5 seconds of flight in which the throttle setting was lowered to allow a constant 2.5 m/s velocity (@~1 Mars g) prior to touch down. Although the modeling in the simulation includes a 35% propellant mass margin, this idealized terminal descent strategy does not currently account for dispersions in altitude at initiation due to atmosphere or other errors, nor did it account for an engine out or divert capability. The strategy was investigated to determine an upper-bound payload capability. The result was a system that closed and had a total payload capability approaching 60 t. The results are shown in Table 4-34. This payload capability is some 18 t more than the 40 t target value and provides a substantial payload reserve above the current allocated payload, which totals to less than 26 t.

A second constant thrust case considered the ability to handle an engine-out scenario by reducing the throttle setting to 83%. The thrust-to-weight ratio at engine ignition was approximately 1.1 Earth g's, down from 1.3 g's in the previous case, and reduces the payload capability to 56000 kg.

A variable throttle setting trajectory was also analyzed. It considered the controls requirement for a crewed mission that would desire maximum throttle at the beginning of terminal descent and steadily lower throttle as the vehicle approached the surface. This approach, holding the same engine requirements listed above, reduced payload capability to approximately 49000 kg with a deep throttle requirement of 20%, barely lower than the other two cases needed at landing. Although lower-performing, a throttle strategy such as this is believed to provide more flexibility to accommodate dispersions.

A summary table of engine assumptions is provided in Table 4-35. Profiles of the thrust, accelerations, and throttle settings are provided in Figure 4-52. Characteristics of engine initiation conditions are provided in Table 4-36.

The performance results for this lander indicate that initial propellant mass assumptions were overly conservative for this configuration. Payload mass actually achieved exceeded the 40 t target value by 9 – 18 t, depending on throttle strategy. Resizing the lander to bring the payload back in line would reduce tank volumes and the mass of the lander system at entry.

Table 4-34 HIAD plus SRP plus Vertical Lander: Mass Results

	Units	Constant Thrust Case 1	Constant Thrust Case 2	Variable Thrust
Mars Entry Mass	kg	111644	109213	101369
Entry RCS Propellant	kg	3781	3850	3631
Separation Mass	kg	16832	16650	16038
Aeroassist mass	kg	11832	11650	11038
Avionics + Separation Structure + RCS	kg	5000	5000	5000
Mars Vehicle Mass at Terminal Descent Engine Initiation	kg	91031	88713	81700
Descent Module Mass w/LOX & CH4	kg	32582	32582	32582
Descent Module Dry	kg	12825	12825	12825
TOTAL CH4+LOX Propellant	kg	18845	20172	19418
Delta Prop from HAT AD#2 sizing	kg	912	-415	339
Total Payload Capability	kg	58449	56131	49118
Allocated Payload Mass	kg	26361	26361	26361
Fission Power Source	kg	7000	7000	7000
Rover	kg	5562	5562	5562
Ascent Module Mass w/CH4 Prop no Crew	kg	13799	13799	13799
Reserve (total – FPS – Rover – MAV-less fuel)	kg	32088	29770	22757

Table 4-35 HIAD plus SRP plus Vertical Lander: Engine Assumptions

Engine Assumptions	Units	Constant Thrust Case 1	Constant Thrust Case 2	Variable Thrust
Thrust	kN	1200	1000	1200
Initial T/W	Earth G's	1.3	1.1	Max ~1.5
Isp	s	360	360	360
Throttle Setting	%	99	83	20-100

Table 4-36 HIAD plus SRP plus Vertical Lander: Conditions at Terminal Descent Initiation

Conditions at Terminal Descent Initiation	Units	Constant Thrust Case 1	Constant Thrust Case 2	Variable Thrust
Altitude	km	4.5	6.3	5.6
Mach	M	2.5	2.8	2.5
Velocity	m/s	587	653	588
Ideal Velocity for Descent Burn	m/s	687	775	819

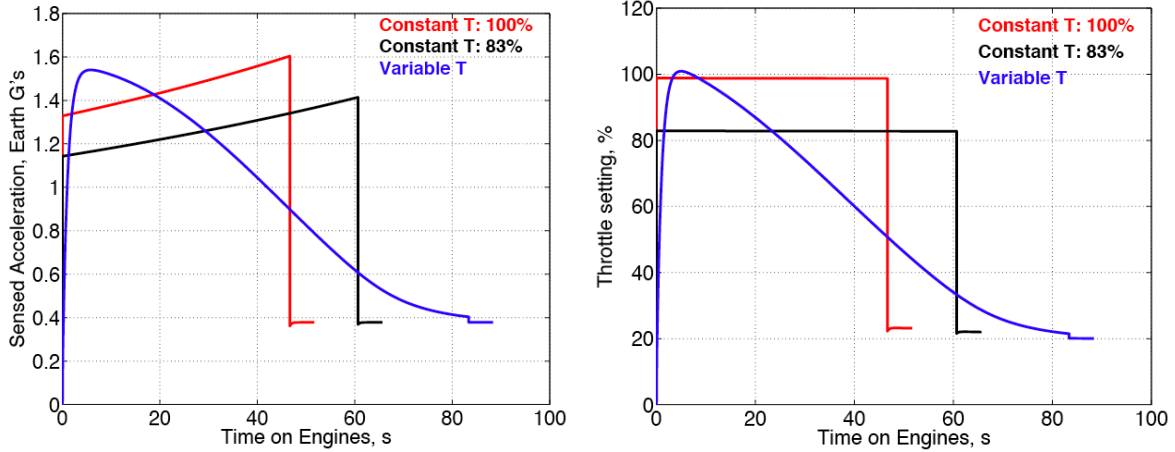


Figure 4-52 HIAD plus SRP plus Vertical Lander: (left) sensed acceleration and (right) throttle setting versus time on the terminal descent engines.

4.8.4.2 Rigid Aeroshell + SRP + Horizontal Lander Configuration Results

A similar study was performed for the rigid aeroshell plus SRP configuration using the horizontal lander design. Results are shown in Table 4-37, Table 4-38, Table 4-39, and Figure 4-53. Due to the higher dry mass of the horizontal lander descent module compared with the vertical configuration, the payload capability is correspondingly lower. The results show a total payload capability ranging from 37 to 52 t depending on descent stage throttling strategy. In this case, the variable throttle strategy resulted in the payload dropping somewhat below the 40 t target value. Therefore, the horizontal configuration is more closely matched to the initial propellant mass assumption than the vertical configuration.

Table 4-37 Rigid Aeroshell plus SRP plus Horizontal Lander: Mass Results

	Units	Constant Thrust Case 1	Constant Thrust Case 2	Variable Thrust
Mars Entry Mass	kg	125607	123094	109388
Entry RCS Propellant	kg	4293	4307	3922
Separation Mass	kg	34210	34091	33402
Aeroassist mass	kg	29210	29091	28402
Avionics + Separation Structure + RCS	kg	5000	5000	5000
Mars Vehicle Mass at Terminal Descent Engine Initiation	kg	87104	84697	72064
Descent Module Mass w/LOX & CH4	kg	35249	35249	35249
Descent Module Dry	kg	15492	15492	15492
TOTAL CH4+LOX Propellant	kg	19337	20108	19831
Delta Prop from HAT AD#2 sizing	kg	420	-351	-74
Total Payload Capability	kg	51855	49448	36815
Allocated Payload Mass	kg	26361	26361	26361
Fission Power Source	kg	7000	7000	7000
Rover	kg	5562	5562	5562
Ascent Module Mass w/CH4 Prop no Crew	kg	13799	13799	13799
Reserve (total – FPS – Rover – MAV-less fuel)	kg	25494	23087	10452

Table 4-38 Rigid Aeroshell plus SRP plus Horizontal Lander: Engine Assumptions

Engine Assumptions	Units	Constant Thrust Case 1	Constant Thrust Case 2	Variable Thrust
Thrust	kN	1200	1000	1200
Initial T/W	Earth G's	1.4	1.2	Max ~1.7
Isp	s	360	360	360
Throttle Setting	%	99	83	20-100

Table 4-39 Rigid Aeroshell plus SRP plus Horizontal Lander: Conditions at Terminal Descent Initiation

Conditions at Terminal Descent Initiation	Units	Constant Thrust Case 1	Constant Thrust Case 2	Variable Thrust
Altitude	km	3.5	4.5	7.1
Mach	M	2.8	3.0	3.2
Velocity	m/s	670	728	758
Ideal Velocity for Descent Burn	m/s	753	827	987

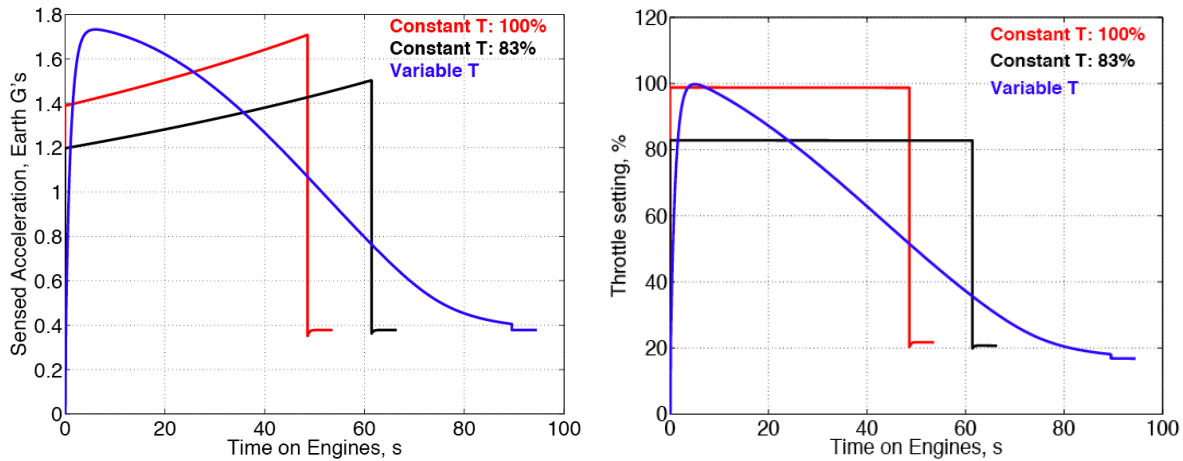


Figure 4-53 Rigid aeroshell plus SRP plus Horizontal Lander: (left) sensed acceleration and (right) throttle setting versus time on the terminal descent engines.

4.8.4.3 Future Work

It is apparent range in payload delivery capability (~15 t) that resulted from various powered descent strategies considered in the Cycle D descent module analysis that is part of future work should include a thorough evaluation of this phase of flight for human class missions at Mars. All previous robotic-powered flight trajectories at Mars have considered a variable throttle profile. A reevaluation of the motivation for considering constant versus a variable throttle profile and the amount of throttling capability should be performed for Mars human-class missions. Additionally, the Cycle D engine design is based on current technology. As part of future work, a complete trade of advanced capabilities in T/W, engine thrust capability, Isp should be considered as well as trades on terminal descent throttling strategies and development of new parametric mass and terminal descent tank sizing models that account for the inertias of the packaged configurations and modify length or height to accommodate propellant use.

4.9 Mars Ascent Vehicle

The Exploration Mission Systems Office (EMSO) developed a conceptual design for a MAV, for the purpose of developing preliminary sizing estimates for various manned Mars mission elements. The conceptual design presented here is intended only as a point of departure for further trades and analyses, and is not intended to represent a recommended design solution.

4.9.1 MAV Ground Rules and Assumptions

4.9.1.1 MAV Mission Duration

Nominally, the Mars Ascent Vehicle is only crewed during Martian ascent: a maximum of about 43 hours to reach HMO, assuming one missed opportunity. Because this duration is likely too long for the crew to remain in their suits, there are two options:

- 1) Incorporate waste/hygiene provisions into the MAV design, along with sufficient “elbow room” for the crew to doff their suits; unfortunately, this will incur a mass penalty to the MAV.
- 2) Reduce the ascent duration by switching to a LMO rendezvous point; although this minimizes MAV mass (with flow-down implications to MDM landed mass), it drives a fuel mass penalty for the transit habitat.

To compare these options, the Study Team evaluated both “Habitable” and “Taxi” MAV variants. The “Habitable” variant was sized for the full 43-hour ascent to HMO, whereas the “Taxi” variant would assume a 12-hour maximum rendezvous to a lower Mars orbit, allowing the crew to remain in their suits for the entire ascent. In both cases, it was assumed that the MAV would support an additional 48 hours of shirt-sleeve crewed system check-outs prior to lift-off from the Martian surface.

4.9.1.2 MAV Crew Complement

Both 4- and 6-crew missions were evaluated, but the MAV Study Team focused on the 6-crew mission, as this was the worst-case (highest mass) scenario.

4.9.1.3 MAV Dimensional Envelope

Per previous HAT work, it was assumed that the maximum MAV envelope dimension was 7.6 m diameter. This envelope is driven by ground transportation constraints, rather than launch shroud limitations.

4.9.1.4 Return Cargo

For the purpose of this exercise, the MAV Study Team assumed the MAV must return 250 kg of cargo (i.e., soil samples) from the Martian surface to the DSH. For book-keeping purposes, the 250 kg was assumed to NOT include cargo containers. Container mass was handled as a stand-alone line item to ensure it was properly tracked as *descended* mass. Future work will likely roll container mass up into the cargo line item.

4.9.1.5 MAV Capabilities

For the purpose of this exercise, the MAV was assumed to support the following activities and capabilities at a minimum:

- Surface EVA ingress/egress
- Mars Surface Launch
- Proximity Operations with the DSH
- Docking with the DSH
- Microgravity docking hatch ingress/egress
- Subsystem Monitoring and Control

If the MAV ascent were to be more than about 12 hours, the following additional capabilities would be required:

- Hand/Face Cleansing
- Urination/Defecation
- Meals
- Sleep (in microgravity)
- Dressing/Undressing

4.9.1.6 MAV Interfaces

It was assumed that the MAV would be structurally connected to the Cargo Lander from Earth launch through the Mars surface stay phase. Because the MAV nominally lands uncrewed—with no descent abort capability needed—the MAV would not necessarily require contingency pyrotechnic detachment from the Lander; for example, prior to ascent, an EVA crew could manually unlatch the MAV’s structural restraints. Nominally, the MAV crew cabin is assumed to be a stand-alone pressure vessel. With no pressurized connections to other elements during ascent, descent, or while on the Martian surface, no mechanical or pyrotechnic connections to other elements are nominally required. For surface operations that might require IVA transfer between the MAV and other surface elements—the Surface Rover, for example—provisions for manual or remotely actuated tunnel separation would be required. It was assumed that provisions for data, power, and fluids interfaces between the MAV and the Cargo Lander were required, particularly for ISRU fuel transfer.

During surface phase operations, it was assumed that MAV keep-alive power will be provided by a Fission Surface Power System.

To facilitate IVA crew transfer between the MAV and the DSH in Mars orbit, it was assumed that the MAV requires a docking interface and crew hatch. It was assumed that the MAV would carry a NASA Docking System (formerly known as the Low Impact Docking System) for crew transfer between the MAV and DSH.

MAV interfaces with the crew include crew restraints, command and control interfaces, communication interfaces, and crew-accessible ingress/egress hatches. For the purpose of this study, the MAV team assumed windows for direct crew visual observations of both the surface and docking target; however, indirect crew visual interfaces—such as through cameras and video monitors—may satisfy operational requirements.

4.9.2 Approach

For the purpose of this mass-estimating exercise, the MAV was assumed to be comprised of a crew cabin and two ascent propulsion stages, Mars Ascent Stages 1 and 2. Due to time constraints, the primary focus of this study was to derive crew cabin mass estimates from heritage design concepts. Inert propulsion stage mass and propellant mass required to ascend the crew cabin were then estimated parametrically.

The MAV Study Team leveraged work previously performed in support of a crewed Lunar expedition to quickly develop a conceptual MAV. A 4-crew MAV concept was patterned after the Constellation Program’s Altair Lunar Lander. Because Altair was outfitted for a week-long mission, this baseline design easily enveloped the 43-hour worst-case crewed ascent timeline, plus a few days of shirt-sleeve crewed system check-outs prior to lift-off from the Martian surface. It was also noted that, with surface resupply, this “habitable” MAV could be used either to supplement or back up the Surface Habitat, potentially allowing the Surface Habitat to shrink in size and/or mass, which would in turn allow the Lander to shrink in size/mass. The first design variant was achieved by expanding the cabin diameter and outfitting for 6 crew members. These two variants—one for 4 crew, the other for 6 crew—together are referred to as the “Habitable” MAVs. It was also noted that a habitable MAV could theoretically allow the crew to descend in the MAV, providing some interesting alternative mission sequences. Although estimates were developed for a crewed MAV descent mass, detailed study of alternative sequencing is left as forward work.

The MAV Study Team also considered 4- and 6-crew “Taxi” MAVs, drawn from work previously performed on the Lunar Orbit Rendezvous (LOR) project. Intended as a brief (12 hour or less) “taxi” ride to Lunar Orbit, the LOR Ascent Module had virtually no habitability provisions, but represented the lower mass boundary for a pressurized ascent vehicle. Although this scheme would force the transit vehicle to rendezvous in a lower Mars orbit, the study team wanted to evaluate whether the lower mass MAV could offset the transit vehicle’s fuel penalty.

In all cases, it was assumed that the MAV would utilize LOX processed from Martian resources to support a LOX-Methane propulsion system, therefore the *descended* MAV masses are considerably lower than *ascended* masses.

4.9.3 Habitable MAV Crew Cabin

The MAV Study Team’s initial assessment of a 4-Crew Habitable MAV assumed the crew cabin and outfitting would be virtually identical to the Altair Lunar Ascent Module from which it was derived. Although the Altair was intended for about a 12-hour maximum ascent (versus the MAV’s 43 hours), the Altair Ascent Module was designed for a week of surface operations, so many subsystems easily accommodate a 43-hour ascent.

As shown Figure 4-54, the 4-Crew Habitable MAV cabin was set at 2.35 m inner diameter and 3.820 m tall. Habitability studies performed by the Altair project found these cabin dimensions to be adequate for 4 crew habitation.

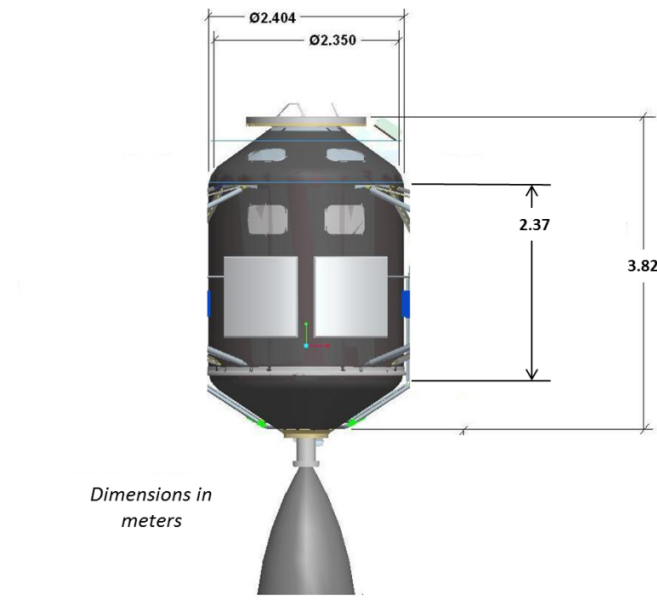


Figure 4-54 4-crew habitable MAV cabin dimensions.

The 6-crew Habitable MAV (Figure 4-56) was developed by extrapolating from the 4-Crew Habitable variant. Due to time constraints, this is the only variant in this study for which detailed MAV Pro/Engineer CAD models were developed.

The Cabin diameter for the 6-Crew Habitable MAV was determined by using CAD models to estimate the habitable volume required for 6 crew members plus their EVA suits. This was based on experience from Altair habitability tests demonstrating that each suit was essentially equivalent to an extra crew member. As shown in Figure 4-55 and Figure 4-56, the 6-Crew Habitable MAV cabin was set at 2.7 m inner diameter, while retaining the original 4-crew Altair cabin height of 3.820 m tall. The integrated MAV length—including the first stage engine bells—is 6.095 m, with a maximum width of 7.858 m across the propellant tanks. It should be noted that a spacecraft of this size does fit within the cargo envelope of available cargo aircraft, without requiring spacecraft disassembly.

Subsystem details are outlined below. Note that all mass estimates are basic mass only, and do not include allowances for growth or uncertainty.

4.9.3.1 Command and Data Handling Subsystem

For the purpose of this exercise, the Study Team assumed the MAV Command and Data Handling subsystem would control about the same type and quantity of equipment as the original Altair design, regardless of whether there were

4 or 6 crew members. Although there may be some minor differences—for example, the MAV does not require descent abort capability—the MAV Study Team assumed that Altair’s distributed avionics scheme, with time-triggered, multi-drop network and redundant routers would meet MAV needs. Assuming a vehicle with of roughly the same complexity of Altair, with similar subsystem designs, the C&DH subsystem was assessed as 203.61 kg basic mass and consisted of the following major subassemblies:

- 2 each Network Routers
- 2 each Display & Control Units
- 9 each. Distributed Control Units
- 3 each Flight Computers
- 2 each Recorders
- 2 each High Speed Network Switches
- 1 each Video Processing Unit
- 2 each Keyboards, Monitors, and Hand Controllers
- 2 each Power Distribution Units
- Cables and Lighting

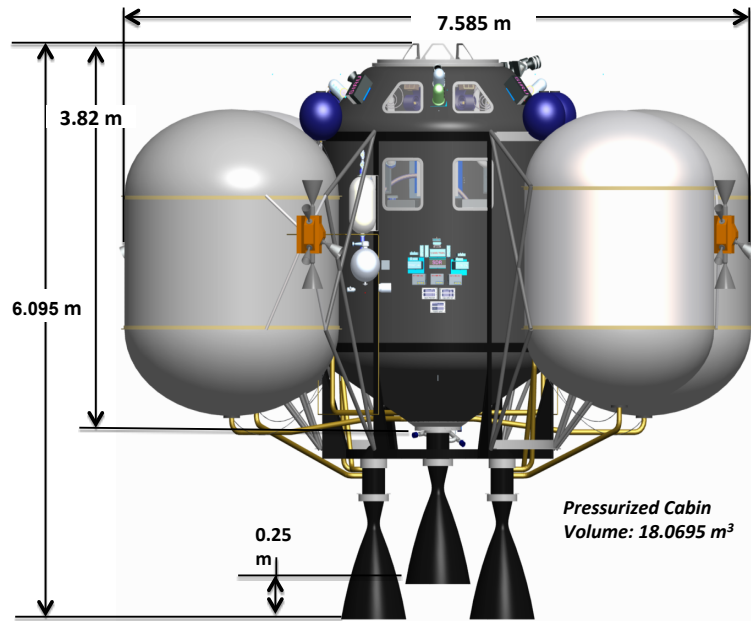


Figure 4-55 6-crew habitable MAV height.

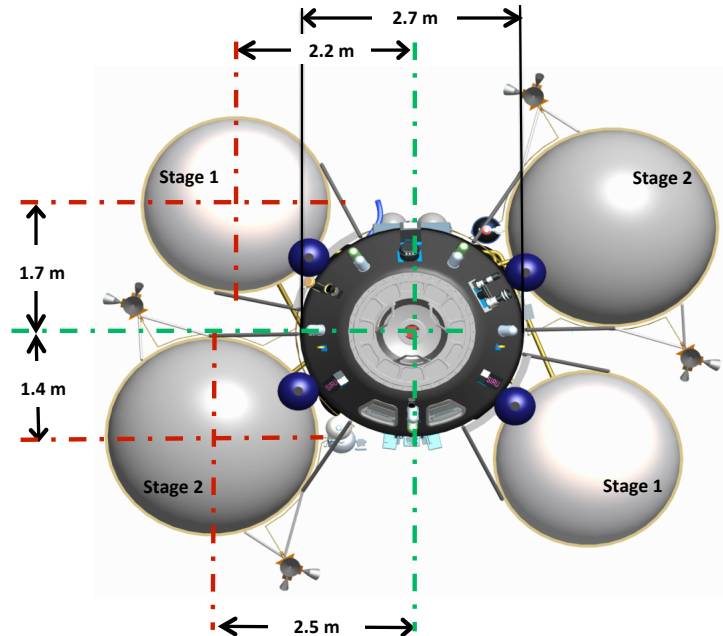


Figure 4-56 6-crew habitable MAV cabin dimensions.

4.9.3.2 Guidance, Navigation and Control Subsystem

The Study Team assumed the MAV GN&C subsystem would be essentially the same as the original Altair design, and would remain unchanged regardless of whether there were 4 or 6 crew members. Based on Altair work, the mass was assessed as 57.48 kg basic mass and consisted of the following major subassemblies:

- Optical Navigation (OpNav) Camera
- Light Detection and Ranging (LIDAR)
- Inertial Reference Unit (IRU)
- Star Tracker
- Running Lights
- Hand-Held Range Finder

Only the Hand-Held Range Finder is stowed inside the crew cabin; all remaining GN&C equipment is mounted outside the crew cabin. The ascended and descended masses are expected to be the same for the GN&C subsystem. Again, this study did not go into sufficient design fidelity to determine whether the larger 6-crew cabin diameter could drive cable mass higher than for the smaller 4-crew cabin

4.9.3.3 Communications and Tracking Subsystem

The Study Team assumed the MAV C&T subsystem would be fundamentally the same as the original Altair design, and that the vast majority of equipment would be mounted on external MAV surfaces. Based on Altair work, the mass was estimated to be 62.34 kg basic mass and consisted of the following major subassemblies:

- 4 each Audio Interface Units
- 2 each Crew Interface Units and 1 Speaker
- 4 each Amplifiers
- 5 each Antennas and 3 each Emergency Antennas
- 1 each Software Defined Radio and 1 each Transponder
- Switches, Cables, and Secondary Structure

Note that the MAV would likely employ an X-band communications system, whereas the Altair-derived mass estimates are for an S-band system. C&T experts believe that because the DSH will likely serve as a communications relay, the MAV C&T system will probably require less mass/power than the Altair reference design.

The difference between the 4- and 6-crew C&T subsystems is simply the addition of two extra Audio Interface Units for the 6-crew variant, increasing basic mass to 62.79 kg. The ascended and descended masses are expected to be the same for the C&T subsystem.

4.9.3.4 Electrical Power Subsystem

For the purpose of this exercise, the Study Team assumed the MAV Electrical Power Subsystem would be very similar to Altair's Ascent Module. As shown in Figure 4-57, it should be noted that Altair's scheme also supported an Airlock Module (which is not part of the MAV design), and was heavily integrated with the Descent Module: two Proton Exchange Membrane (PEM) Hydrogen/Oxygen fuel cells located on the Descent Module powered the Ascent Module during surface operations, while a single, non-rechargeable 16.5 kWh nominal battery handled ascent and docking. Distributed Power Distribution Units (PDUs) protected the bus by providing current limiting and over-current trip on the 28 Vdc system. For a 4-crew MAV, of similar size and complexity to the Altair Ascent Module, Altair's 220.83 kg basic mass for the Primary Battery, Main Bus Switching Unit (MBSU), two PDUs, and Power Cables is a good starting point but should be verified as forward work. In particular, the ascent duration difference (Altair's 12-hour maximum ascent vs. the MAV's 43-hour ascent), and the need to separate the first and second propulsion stages likely means that the battery mass is underestimated. On the other hand, there is no requirement for descent abort pyrotechnics, and the C&T subsystem power draw is likely to be lower than for the heritage design. Detailed design, which is beyond the scope of this study, is needed to better evaluate battery mass. It should also be noted that cable mass could be underestimated, since high-fidelity models of the Altair-heritage cable runs were never developed.

The Study Team assumed the 6-Crew Habitable MAV Electrical Power subsystem design would be essentially the same as the 4-crew variant, but with a larger battery. In lieu of more detailed design fidelity at this time, the 4-crew battery mass was increased by 50% for the 6-crew variant, for a total subsystem mass of 285.66 kg. The rest of the Electrical Power manifest remains unchanged for both ascended and descended mass, though it should be noted that the larger cabin could increase cable mass.

At this point, the ascended and descended masses are expected to be the same for the Electrical Power subsystem. Note that this assumption is highly dependent on whether expected battery shelf life will allow the MAV battery to remain quiescent on the Mars surface for a long period of time before the crew arrives. It is possible that fresh MAV batteries could be delivered with the crew at a later date.

4.9.3.5 Thermal Subsystem

As with the Electrical Power subsystem, the Altair-derived MAV Thermal Subsystem is assumed to be heavily integrated with the MDM, where large radiators would be located. As shown in the schematic (Figure 4-58) the Ascent vehicle's active Thermal subsystem features single phase pumped fluid loops with a propylene glycol/water mixture to manage the Liquid Cooling Garment (LCG), suit, and cabin thermal loads.

During ascent, a sublimator is used to reject waste energy, but note that the sublimator water tank resides within the ECLS subsystem. For a 4-crew MAV, of similar size and complexity to the Altair Ascent Module, Altair's 6040 W heat rejection requirement, resulting in a 139.26 kg basic Thermal subsystem mass, is a good starting point. However, it should be noted that the limited scope of this effort did not correct this Lunar-derived design for the more temperate Martian surface thermal environment.

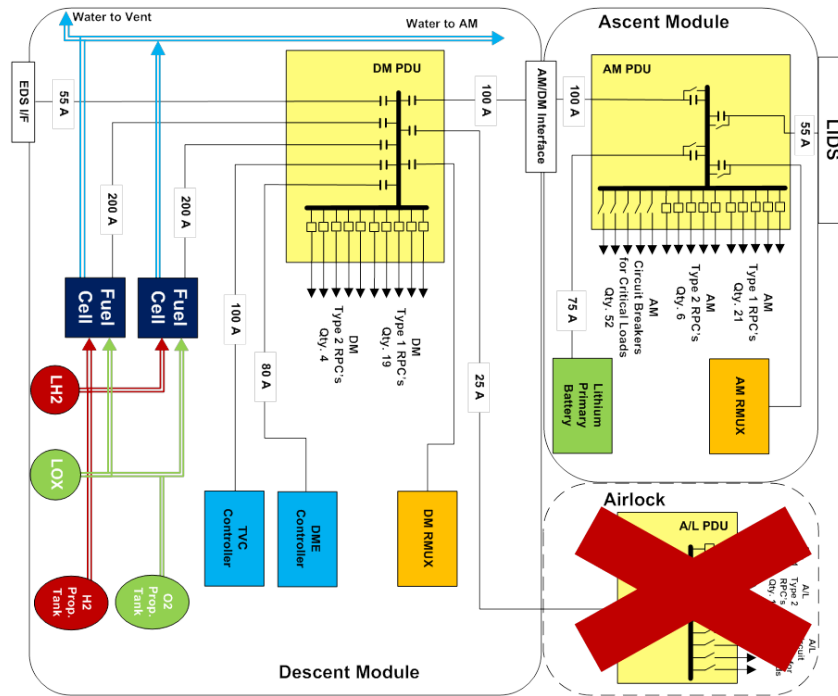


Figure 4-57 Altair-derived integrated power subsystem.

It was assumed that the larger 6-crew cabin would drive longer—and heavier—fluid lines, and the system would have to accommodate two additional crew members. In lieu of detailed design, the Study Team added 20% to the 4-Crew Habitable Thermal subsystem mass for an estimated mass of 167.11 kg.

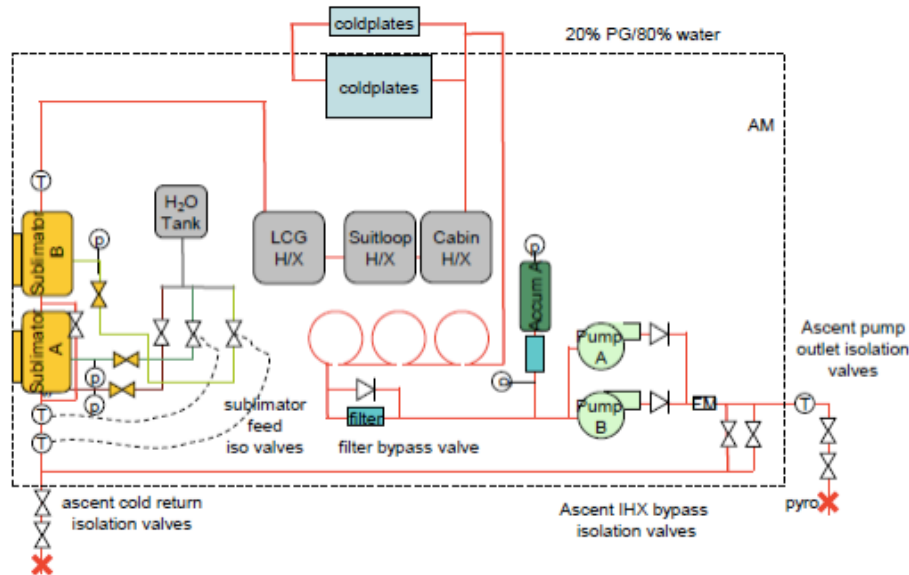


Figure 4-58 Habitable MAV thermal subsystem schematic.

4.9.3.6 ECLS Subsystem

Unlike avionics, the ECLS subsystem is not as easily extrapolated from a predecessor design. The Altair ECLS requirements included a crewed descent phase and split surface operations (shirt-sleeve plus EVA) via an attached Airlock Module, making the Altair system slightly more complicated. On the other hand, the Altair ECLS system was only sized for the 12-hour maximum ascent duration, while the MAV must support 4 crew for up to 43 hours. As a first-cut, the Altair-derived ECLS subsystem basic mass of 280.11 kg—not including consumable fluids—is probably in the right ballpark, but should be optimized as forward work. As shown in Figure 4-59, the ECLS subsystem includes:

- Cabin and Suit Loop Revitalization
- Pressure Control Assembly (Nitrogen and 34% oxygen)
- Waste Management
- Water Subsystem (Storage, EVA, and potable use)
- Air Revitalization to remove CO₂, humidity, trace gases, particulate, and heat

For the purpose of this study, it was assumed that the 6-crew Habitable MAV ECLS subsystem would closely resemble the 4-crew variant, with the primary differences being in the quantity of consumables (oxygen, nitrogen, and water). As a first-cut, the 4-Crew Habitable MAV’s ECLS subsystem basic mass of 281.11 kg—not including consumable fluids—is probably in the right ballpark, but should be evaluated in more detail as forward work, as the larger crew cabin will likely drive fluid line mass.

The ascended and descended masses are expected to be the same for the ECLS subsystem.

4.9.3.7 Human Factors Subsystem

The Human Factors subsystem includes consumables such as food and clothing, as well as other personal items; note that crew and crew-worn equipment are NOT included here, but tracked as moveable equipment. The minimum ascended Human Factors basic mass for 4 crew is estimated to be about 62.58 kg and includes:

- Emergency CO₂ masks
- Two days’ worth of Food, Food Stowage, and Utensils
- Waste/Hygiene Compartment
- Hygiene Supplies (includes a vacuum cleaner)
- Mars sample containers (contents of containers is booked under Cargo)

The minimum unmanned descended Human Factors mass is expected to be slightly lower than the ascended mass. For example, due to shelf life concerns, food and medical equipment may arrive later with the crew, rather than arrive in the unmanned MAV. Also, to avoid unnecessary duplication, CO₂ scrubbing masks will likely descend with the crew and be transported over to the MAV before ascent. Zeroing out all of these items drops the 4-Crew Human Factors descended mass to 40.51 kg.

As noted above, the descended Human Factors subsystem mass depends on the extent of the MAV’s intended “habitability” during the surface phase. If the crew were to descend in the MAV, they would likely spend a few days in the MAV prior to translating to another module, which would drive the need for additional items, such as sleep bunks, medical kit, or personal hygiene supplies. As a point of reference, a 1-week duration Altair-style MAV—plus a 10 kg exercise device—amounts to about 185.65 kg of Human Factors equipment, which includes:

- One Week’s Worth of Food, Food Storage and Utensils
- Sleep Hammocks and Bunk Lights
- Medical Kit
- Clothing
- Exercise Equipment (assume 10 kg)

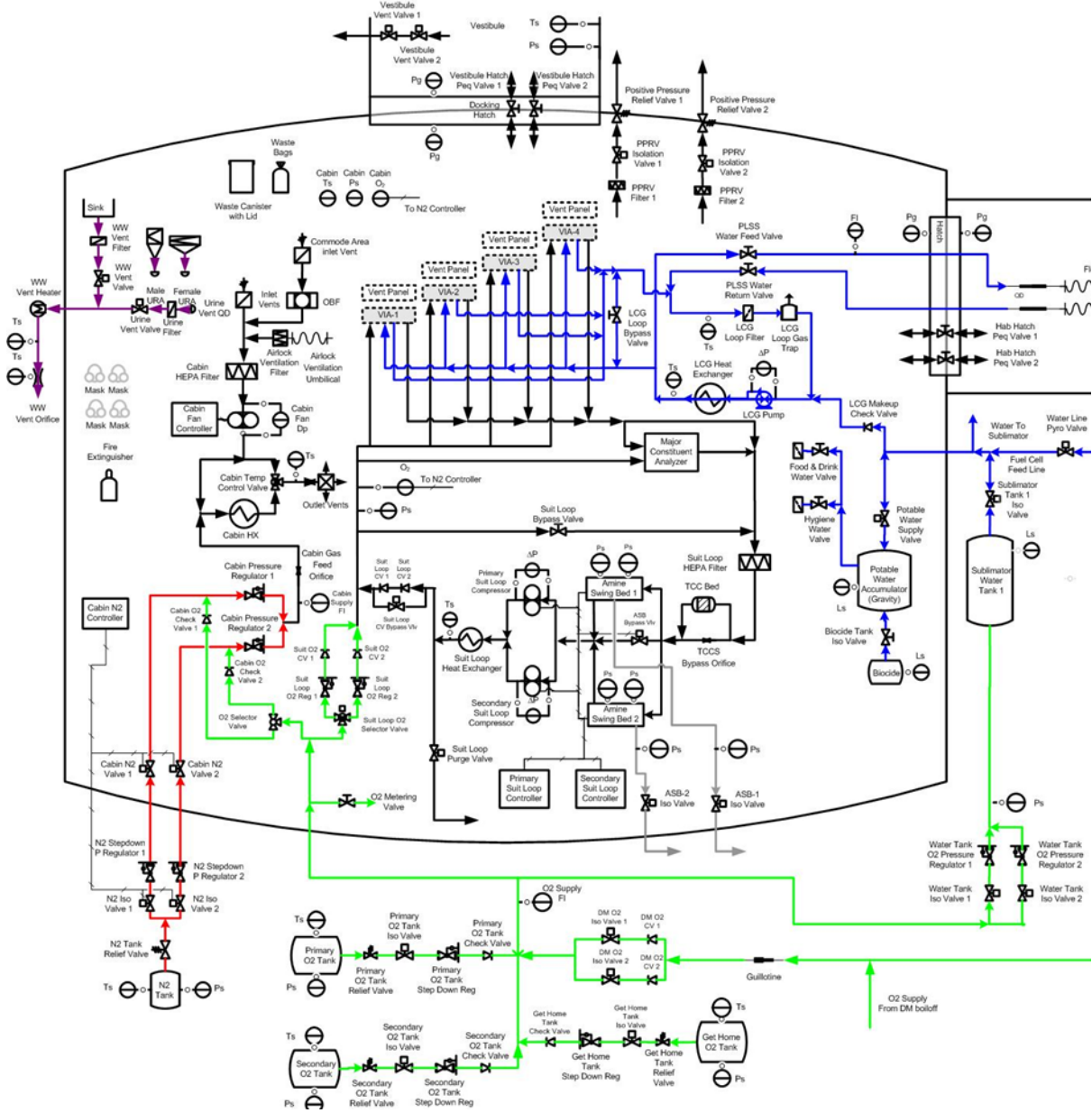


Figure 4-59 Habitable MAV ECLS subsystem schematic.

Extrapolating from the 4-Crew Habitable MAV manifest for two additional crew members increases the ascended mass of a 6-Crew MAV to 82.12 kg, primarily due to food mass. As with the 4-Crew variant, the minimum unmanned descended mass is expected to be lower if, for example, life-limited food and medicines, and the crew’s CO₂ scrubbing masks, arrive with the crew in the Surface Habitat rather than in the uncrewed MAV. For the nominal (uncrewed) scenario, the descended Human Factors 6-Crew equipment mass is 46.95 kg.

4.9.3.8 Extravehicular Activity Subsystem

The EVA subsystem includes EVA equipment physically attached to the MAV, as well as crew-worn EVA spares. *Note that EVA equipment actually worn by the crew during ascent—such as suits and helmets—is captured with the crew (see below), and not rolled up into EVA subsystem mass.* The original Altair equipment list included two each 8.534 m long umbilical hoses for a contingency requiring the crew to translate from Altair to Orion via EVA, in the

event of an unpressurized Orion docking. This was necessary because the Altair crew wore the larger, white EVA suits, which were too large to pass through the NDS hatch. By switching to the smaller IVA suits, this EVA contingency can be avoided. Therefore, only the shorter umbilical hoses are required in the event of a cabin depressurization requiring visors-down ascent. The Study Team also assumed that the EVA battery charger and suit donning stands would remain on the surface, and are not manifested for ascent.

The 87.51 kg of ascended EVA equipment includes the following:

- 4 each Umbilical Interface Panels
- 4 each Crew Support Straps
- 4 each Short Umbilical Hoses
- 4 each Pairs of Spare Gloves
- EVA Tools (jammed docking hatch contingency)

Note that the ascended and descended masses may not necessarily be the same for the EVA subsystem. For example, if the umbilical hoses (11.18 kg each) and spare gloves (2.81 kg each) descend with the crew in the Surface Habitat, then the MAV's descended EVA subsystem mass would drop to 31.55 kg.

The 6-Crew Habitable MAV's EVA subsystem consists of the same items as the 4-Crew Habitable variant, but with extra Umbilical Interface Panels, Crew Support Straps, Umbilical Hoses, and gloves to accommodate the 5th and 6th crew members. The basic EVA ascended mass was estimated to be 126.63 kg. If the umbilical hoses (11.18 kg each) and spare gloves (2.81 kg each) descend with the crew in the Surface Habitat, then the 6-Crew Habitable MAV's descended EVA subsystem mass would drop to 84.33 kg.

4.9.3.9 Structures and Mechanism Subsystem

For the purpose of this exercise, the MAV crew cabin was assumed to be identical to the Altair Ascent Module and consisted of:

- Cylindrical pressure vessel with composite skin and aluminum honeycomb core construction
- International Low Impact Docking System Docking Interface
- Pressure-assisted circular docking hatch
- Pressure-assisted EVA side hatch
- Frangible "H" seam and pyrotechnic expansion tubes to separate from Cargo Lander
- Upward-facing docking windows and forward-facing observation windows

The 778.35 kg Altair-derived Structures and Mechanism Subsystem also included mounting structure for propulsion tanks and RCS. As shown in Figure 4-60, the MAV's two-stage concept has a significantly different tank arrangement than the single-stage Altair—potentially increasing structural mass. On the other hand, if the Cargo Lander does not rely on MAV RCS during descent, the RCS booms may be substantially shorter than the Altair baseline—potentially decreasing structural mass. In summary: the MAV cabin structure and mechanism masses are likely good fidelity, but the propellant tank structure and RCS booms may be underestimated, pending further detailed design work. For the purpose of this exercise, a 778.35 kg Structures and Mechanisms subsystem mass was assumed for both descent and initial ascent.

6-Crew Habitable MAV Structures and Mechanism subsystem masses were estimated based on a low-fidelity CAD model that was developed using heritage material densities. As noted above, the crew cabin was the same height as the 4-Crew Habitable variant, but with a larger diameter.

The entire 6-Crew Habitable MAV Structural mass was estimated to be 1307.59 kg, with the first stage estimated at 63.63 kg. These masses assumed Altair-heritage RCS boom structure which may not be accurate, depending on ultimate RCS thruster placement. It should also be noted that structural analysis to size support structure and

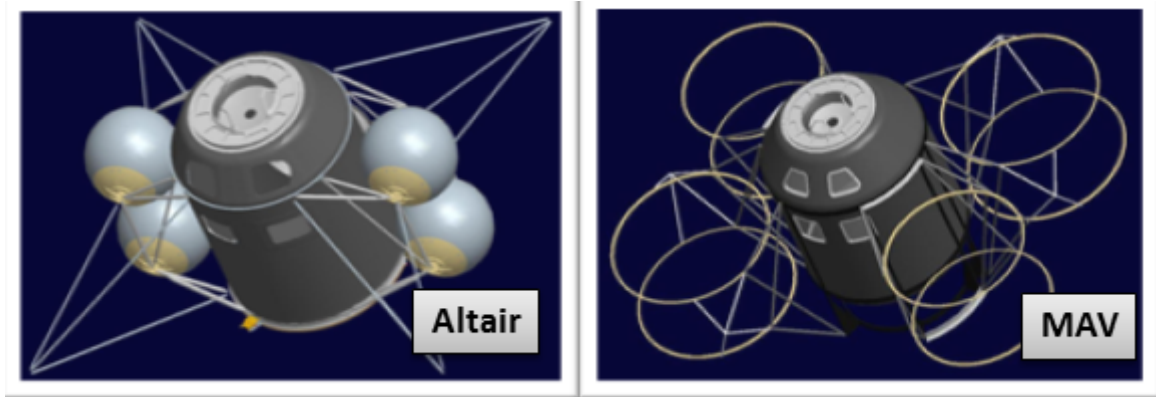


Figure 4-60 MAV tank arrangement comparison.

separation hardware for the large propellant tanks was left as forward work. One additional deviation from the Altair heritage design is that because there is no descent abort capability, it was assumed that pyrotechnic disconnects between other elements can be eliminated in lieu of manually activated launch lock releases prior to ascent.

4.9.3.10 Crew, Crew-Worn Equipment, and Cargo

For the purpose of this exercise, crew members were each assumed to be 98.5 kg, which is the largest American male, per SSP 50005. The ascended mass of 4 crew is 394 kg; 6 crew would be 591 kg.

Crew-worn equipment mass depends largely on which suits are worn during ascent. The EVA suits are relatively large and heavy—39.21 kg each—as compared to the streamlined IVA suits at only 13.4 kg each. For a crew of 4, this translates into a 103.24 kg mass difference. The EVA suits also require more secondary equipment—donning stands for surface ingress/egress [11.34 kg each, though these would be manifested under EVA equipment], and stowage bags (14.55 kg each) to protect the suits from damage, as well as to contain dust or contaminants brought inside the cabin on the suits. For a crew of 4, the addition of 4 bags plus a donning stand adds another 69.54 kg mass penalty. Mass of remaining crew-worn equipment, such as helmets, gloves, and undergarments remains the same, regardless of which suit is worn. For the purpose of this exercise, it was assumed that the white EVA suits and accoutrements would be manifested as descended mass, but were removed from ascended mass. This would require the crew to change into IVA suits inside the MAV cabin, then depressurize and toss out all EVA suit equipment or, alternatively, to don IVA suits in an attached pressure cabin then translate via tunnel to the MAV. It has been a long-standing assumption that the IVA suits cannot be used outside the vehicle, even for short translations, due to thermal concerns, though future developments may include something along the lines of a “thermal overcoat” to mitigate this issue. To account for the 43-hour worst-case ascent, the Study Team assumed each crew member would carry an in-suit drink bag.

The total 4-crew mass roll-up of ascended crew and crew-worn equipment is estimated at about 506.2 kg, assuming the crew members ascend wearing their IVA suits, and discard their EVA suits on the surface. Extrapolating for 2 additional crew members, the minimum ascended mass was estimated to be 742.44 kg. As noted in Section 4.9.1.4 return cargo (i.e., Mars soil) was assumed to be an additional 250 kg.

If the crew descends in the Surface Habitat, then obviously the crew, crew-worn equipment, and cargo basic mass is zero in the nominal (uncrewed) descent case. However, in the alternative-architecture scenario where the crew descends in the MAV, note that both the EVA and IVA suits would be manifested for descent, as well as the EVA Primary Life Support System (PLSS) back-packs, stowage bags, and donning stands, raising the crew and crew-worn equipment basic mass to 726.72 kg for a crewed descent; extrapolating to 6-crew would increase mass to 1198.22 kg.

4.9.3.11 Non-Propellant Fluids

Non-propellant fluids include:

- Life Support Oxygen and Nitrogen
- Potable Water
- Thermal Control Water

Given the same cabin volume and crew complement as Altair, MAV life support oxygen and nitrogen were estimated by taking 2/7 of Altair estimates to correct for the shorter MAV ascent duration (2 days, rather than 7). Using the Constellation Program guidelines, the MAV Study Team assumed each crew member would require about 2.5 kg of potable water, per day, so the MAV would carry a total of 41.03 kg of non-propellant fluids during ascent. 6-Crew masses were extrapolated by multiplying the 4-Crew Habitable Variant masses by 1.5, resulting in a total basic mass of 61.55 kg.

For the purpose of this exercise, it was assumed that the MAV would carry its full complement of non-propellant fluids during uncrewed, nominal descent, although it is possible that these tanks could land empty, and be filled on the surface prior to departure. Although this would complicate pre-ascent preparations, it does provide a descent mass savings opportunity, and mitigates leakage during the long, quiescent uncrewed surface stay.

In the alternative-architecture scenario where the crew descends in the MAV, note that the descended Non-Propellant Fluids mass would increase to 102.61 kg, assuming the crew lives in the MAV for about a week before translating to another pressurized module, and that the Descent Module fuel cells provide thermal control water. Extrapolating to 6 crew increases non-propellant fluids mass to 153.915 kg.

4.9.3.12 Habitable MAV Crew Cabin Mass Summary

Four- and Six-Crew Habitable MAV subsystem mass estimates are summarized in Table 4-40. Note that both ascent and descent masses are summarized, and that descent masses are given for two architecture configurations: a nominal (uncrewed) descent per DRA 5.0, as well as a hypothetical crewed descent where the crew would live in the MAV for the first week, before translating to another pressurized element.

Table 4-40 Habitable MAV Crew Cabin Mass Comparison

Subsystem	4-Crew Habitable Crew Cabin Mass (kg)			6-Crew Habitable Crew Cabin Mass (kg)		
	Nominal (Uncrewed) Descended	Optional (Crewed) Descended	Ascended	Nominal (Uncrewed) Descended	Optional (Crewed) Descended	Ascended
C&DH	204	204	204	204	204	204
GN&C	57	57	57	57	57	57
C&T	62	62	62	63	63	63
Power	221	221	221	286	286	286
Thermal	139	139	139	167	167	167
ECLS	280	280	280	280	280	280
EVA	32	87	87	84	127	127
Structures	778	778	778	1308	1308	1308
Human Factors	36	186	50	47	236	82
Crew Cabin Dry Mass	1809	2014	1878	2496	2728	2574
Crew & Crew Worn Equipment	0	727	506	0	1198	742
Cargo	250	250	250	250	250	250
Non-Propellant Fluids	41	102	41	61	154	61
Crew Cabin Total Mass	2100	3093	2675	2807	4330	3627

4.9.4 Taxi MAV Crew Cabin

The MAV Study Team’s initial assessment of a 4-Crew Taxi MAV assumed the crew cabin and outfitting would be virtually identical to the Lunar Orbit Rendezvous Ascent Module concept from which it was derived. Although the LOR ascent module was intended for only a 12-hour maximum ascent (versus the MAV’s 43 hours), it was designed for at least 1 week of surface operations, so many subsystems were easily able to accommodate a 43-hour ascent. Note that due to time constraints and a desire to focus on the 6-crew variant, the 4-crew Taxi MAV analysis was generally limited to the crew cabin. It should also be noted that the LOR concept was intended to loiter in Lunar orbit for up to 180 days prior to descent, which accounts for many of the design differences between the LOR and Altair heritage designs. Time constraints did not allow in-depth analysis of a 6-crew Taxi MAV concept.

As shown in Figure 4-61, the LOR-derived 4-Crew Taxi MAV cabin was set at 1.8 m inner diameter. The 3.6 m tall cabin had a 2.9 m floor to ceiling height. Note that the propellant tanks shown in the illustration are representative, and have not been optimized for MAV propellant loads.

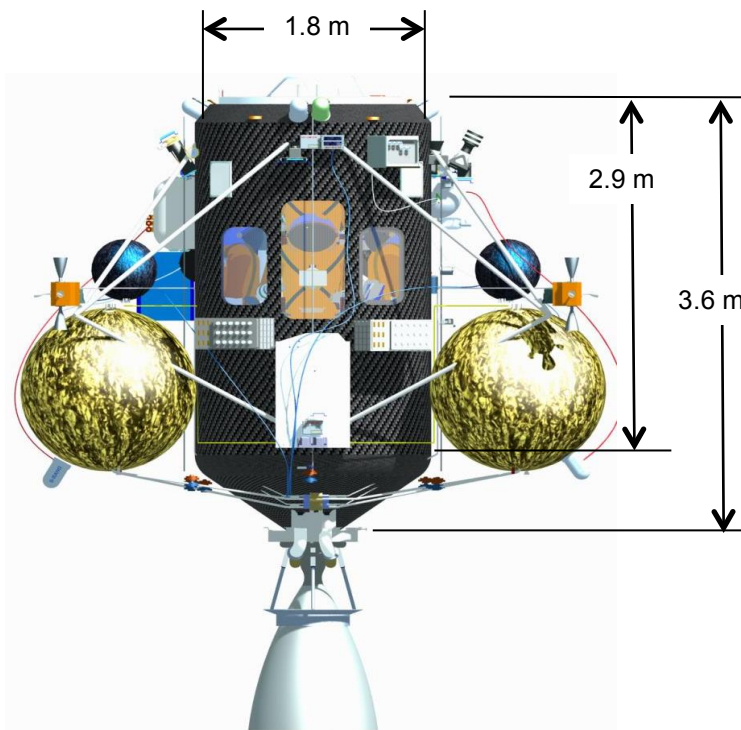


Figure 4-61 4-Crew Taxi MAV cabin dimensions.

4.9.4.1 Command and Data Handling (C&DH) Subsystem

For the purpose of this exercise, the Study Team assumed the Taxi MAV C&DH subsystem would control about the same type and quantity of equipment as the original LOR design, regardless of whether there were 4 or 6 crew members. Although there may be some minor differences—for example, the MAV does not require descent abort capability—the MAV Study Team assumed that LOR’s distributed avionics scheme would meet MAV needs. Assuming a vehicle of roughly the same complexity of LOR, with similar subsystem designs, the C&DH subsystem was assessed at 181.72 kg basic mass and consisted of the following major subassemblies:

- 2 each Network Routers (1 primary, 1 redundant)
- 2 each Display & Control Units
- 6 each Distributed Control Units
- 4 each Flight Computers

- 1 each Recorder
- 2 each High Speed Network Switches
- 1 each Video Processing Unit
- 2 each Keyboards, Monitors, and Hand Controllers
- Cables

The ascended and descended masses are expected to be the same for the Taxi MAV's C&DH subsystem.

4.9.4.2 Guidance, Navigation and Control Subsystem

For the purpose of this exercise, the Study Team assumed the Taxi MAV GN&C subsystem would be essentially the same as the original LOR design, and would remain unchanged regardless of whether there were 4 or 6 crew members. Based on LOR work, the GN&C subsystem was assessed at 65.48 kg basic mass and consisted of the following major subassemblies:

- Optical Navigation Camera
- Light Detection and Ranging
- 1 each Inertial Measurement Unit (IMU)
- 2 each Inertial Reference Unit
- 1 each Star Tracker
- 4 each Docking Lights
- 2 each Running Lights
- 1 each Hand-Held Range Finder
- 1 each Reflector

Only the Hand-Held Range Finder is stowed inside the crew cabin; all remaining GN&C equipment is mounted outside the crew cabin. The ascended and descended masses are expected to be the same for the GN&C subsystem. Note that the subsystem mass is slightly higher than that shown for the 4-Crew Habitable variant; this reflects the fact that the Altair-derived Habitable variant was a “minimally functional” conceptual design, whereas the LOR-derived concept had the benefit of additional design study and consideration.

4.9.4.3 Communications and Tracking Subsystem

For the purpose of this exercise, the Study Team assumed the Taxi MAV C&T subsystem would be fundamentally the same as the original LOR design, and that the vast majority of equipment would be mounted on external MAV surfaces. Based on LOR work, the mass was estimated to be 61.9 kg basic mass and consisted of the following major subassemblies:

- 4 each Audio Interface Units
- 2 each Crew Interface Units and 1 Speaker
- 4 each Amplifiers (2 Low Noise, 2 Power)
- 7 each Antennas and 3 each Emergency Antennas
- 1 each Software Defined Radio
- 1 each Transponder
- 1 each Crew Interface Microphone and Speaker
- Switches, Cables, and Secondary Structure

Note that MAV would likely employ an X-band communications system, whereas the LOR-derived mass estimates are for an S-band system. C&T experts at Johnson Space Center believe that because the DSH will likely serve as a communications relay, the MAV C&T system will probably require less mass/power than the Altair baseline. The ascended and descended masses are expected to be the same for the C&T subsystem.

4.9.4.4 Electrical Power Subsystem

For the purpose of this exercise, the Study Team assumed the Taxi MAV Electrical Power Subsystem would be very similar to LOR's Ascent Module. As shown in Figure 4-62, the LOR's electrical scheme was heavily integrated with

the Descent Module.

At 480.71 kg basic mass, the LOR-derived, 4-Crew Taxi MAV’s Electrical subsystem mass is more than twice as heavy as the Altair-derived 6-Crew Habitable MAV’s Electrical subsystem. Given that the Taxi concept is smaller and simpler than the Habitable variant, this surprising result is likely due to a combination of fundamental design differences and design fidelities between the two concepts:

- The LOR design increased distribution voltage from 28 to 120 Vdc to minimize wire size, which was intended to minimize cable mass;
- However, mass trades intended to identify where downstream harness mass could be significantly reduced by adding distribution boxes that localized control and sensor/effector relationships were not fully completed before the LOR design study was truncated;
- Unexpected cable mass growth on contemporary spacecraft projects during the same time period as the LOR study drove more conservative estimates than earlier Altair-era estimates and, as noted above, some Altair underestimates were identified;

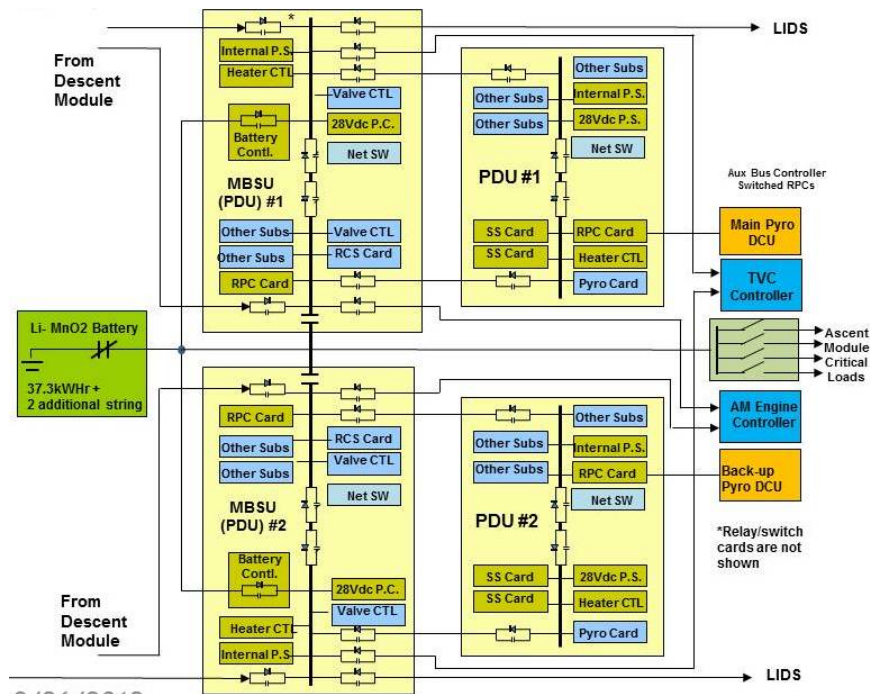


Figure 4-62 Taxi MAV electrical power subsystem.

- The LOR-derived battery mass was based on a conservative Power Equipment List (PEL) estimate, but reconciliation was left as forward work;
- In particular, the effects of switching from Altair-heritage hypergolic propellants to the LOR-style cryogenic fluids—combined with in-space loiter—were not fully evaluated;
- The LOR-derived design implemented dual bus distribution using a minimum of two channels to provide internal fault isolation ability and improve risk;
- Unlike the Altair-derived Habitable MAV concept—which utilized fuel cells—the LOR-derived Taxi concept relied on solar arrays mounted on the Descent Module for keep-alive power during the surface stay.

At this point, the ascended and descended masses are expected to be the same for the Electrical Power subsystem but this assumption is highly dependent on whether expected battery shelf life will allow the MAV battery to remain quiescent on the Mars surface for a long period of time before the crew arrives. It is possible that fresh MAV batteries could be delivered with the crew at a later date, which would reduce the descended MAV mass by 175 kg.

4.9.4.5 Thermal Subsystem

As with the Electrical Power subsystem, the LOR-derived MAV Thermal subsystem is assumed to be heavily integrated with the MDM, where large radiators would be located. As shown in the schematic (Figure 4-63) the Ascent vehicle's Thermal subsystem features single-phase pumped fluid loops with a propylene glycol/water mixture to manage the LCG, suit, and cabin thermal loads. During ascent, a sublimator is used to reject waste energy, but note that the sublimator water tank resides within the ECLS subsystem. External insulation manages passive heat transfer to the vehicle.

For a 4-crew MAV, of similar size and complexity to the LOR Ascent Module, the 148.12 kg basic Thermal subsystem mass, is a good starting point. However, it should be noted that the limited scope of this effort did not correct this Lunar-derived design for the more temperate Martian thermal environment.

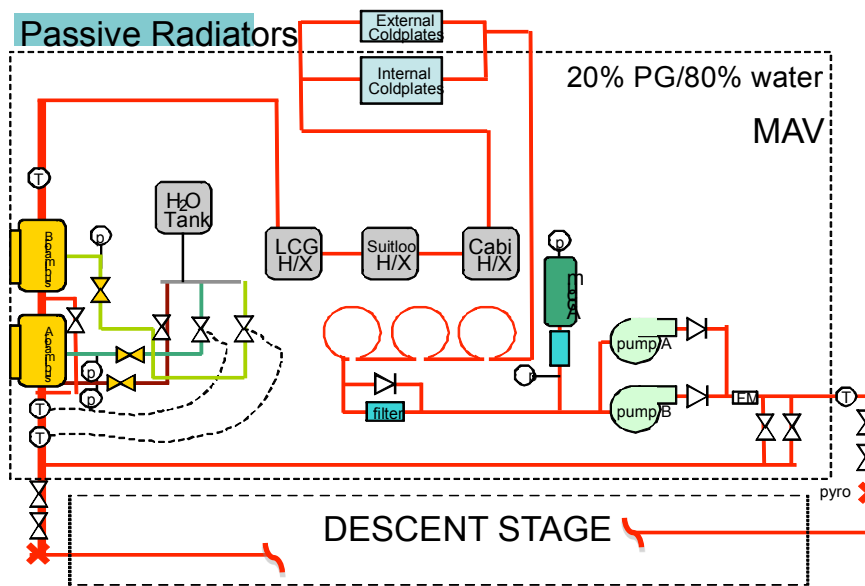


Figure 4-63 Taxi MAV thermal subsystem.

4.9.4.6 ECLS Subsystem

Unlike avionics, the ECLS subsystem is not as easily extrapolated from a predecessor design. The LOR ECLS requirements included a crewed descent phase and split surface operations (shirt-sleeve plus EVA) via an attached Habitat Module, making the LOR system slightly more complicated. On the other hand, the LOR ECLS system was only sized for the 12-hour maximum ascent duration, whereas the MAV must support 4 crew for up to 43 hours. As a first-cut, the LOR ECLS subsystem basic mass of 194.61 kg—not including consumable fluids—is probably in the right ballpark, but should be evaluated in more detail as forward work. The ECLS subsystem includes:

- Cabin and Suit Loop Revitalization, featuring 3 swing beds to remove CO₂, humidity, trace gases, particulate, and heat
- Pressure Control Assembly (Nitrogen and 34% oxygen)
- Waste Management
- Water Subsystem (Suit Loop and Sublimator)

The ascended and descended masses are expected to be the same for the ECLS subsystem

4.9.4.7 Human Factors Subsystem

The Human Factors subsystem in a brief Taxi ride is reduced to 0.07 kg for a radiation dosimeter for both ascent and

descent. Because the crew remain in their IVA suits during ascent, no waste/hygiene provisions are provided. In-suit drink bags and energy bars are assumed to be included with the crew-worn equipment.

4.9.4.8 Extravehicular Activity Subsystem

Note that EVA equipment actually worn by the crew during ascent—such as suits and helmets—is captured with the crew, and not rolled up into EVA subsystem mass. In the 4-Crew Taxi MAV scheme, it is assumed that the crew will discard their EVA suits and PLSSs on the surface and ascend in their IVA suits.

The 76.95 kg of ascended EVA equipment includes the following:

- 4 each Umbilical Interface Panels
- 4 each Crew Support Straps
- 4 each Short Umbilical Hoses
- EVA Tools (jammed docking hatch contingency)

Note that the ascended and descended masses may not necessarily be the same for the EVA subsystem. For example, if the umbilical hoses [11.18 kg each] descend with the crew in the Surface Habitat, then the MAV's descended EVA subsystem mass would drop to 32.23 kg.

4.9.4.9 Structures and Mechanism Subsystem

The LOR-derived Structures and Mechanism Subsystem also included mounting structure for propulsion tanks and RCS. As noted above, the MAV's two-stage concept has a significantly different tank arrangement than the single-stage Altair, potentially increasing structural mass. Because the heritage LOR study was relatively low design fidelity, a number of other structural members and mechanisms may also be underestimated or missing in the mass roll-up, including window glass, a re-attachable tunnel mechanism, and the central pilot's control console. To account for these potential underestimates, a 100 kg placeholder was added to the Structures and Mechanisms subsystem.

In summary: the MAV cabin structure and mechanism masses are likely good fidelity, but the propellant tank structure, RCS booms, and other mechanisms may be underestimated, pending further detailed design work. For the purpose of this exercise, a 758.4 kg Structures and Mechanisms subsystem mass was assumed for both descent and initial ascent.

4.9.4.10 Crew, Crew-Worn Equipment, and Cargo

As noted above, crew members were each assumed to be 98.5 kg, and it was assumed that the crew would discard their EVA suits and PLSS on the surface and ascend in their IVA suits. As noted above, return cargo was assumed to be 250 kg, making the total mass roll-up of ascended crew, crew-worn equipment, and cargo about 735.2 kg. With no crew, crew-worn equipment, or cargo, the nominal (uncrewed) descent mass would obviously be zero.

4.9.4.11 Non-Propellant Fluids

Non-propellant fluids include:

- Life support Oxygen and Nitrogen
- Thermal Control Water

Given the same cabin volume and crew complement as the heritage LOR design, it was assumed that the 4-Crew Taxi MAV life support non-propellant fluids would match the LOR's 103.88 kg.

For the purpose of this exercise, it was assumed that the MAV would carry its full complement of non-propellant fluids during uncrewed, nominal descent, although it is possible that these tanks could land empty, and be filled on the surface prior to departure. This would be particularly useful if surface equipment, such as fuel cells, were

generating waste water that could be used in the MAV. Although this would complicate pre-ascent preparations, it does provide a descent mass savings opportunity, and mitigates leakage during the long, quiescent uncrewed surface stay.

4.9.4.12 4-Crew Taxi MAV Mass Summary

Subsystem mass estimates are summarized in Table 4-41. Because crew landing in the Taxi MAV is impractical, the ascended and descended Taxi MAV masses are the same for all subsystems except the crew, crew-worn equipment, and cargo.

Table 4-41 4-Crew Taxi MAV Mass Summary

Subsystem	4-Crew Taxi MAV Mass (kg)	
	Nominal (Uncrewed) Descended	Ascended
C&DH	182	182
GN&C	65	65
C&T	62	62
Power	481	481
Thermal	148	148
ECLS	195	195
EVA	77	77
Structures	758	758
Human Factors	0	0
Crew Cabin Dry Mass	1968	1968
Crew & Crew Worn Equipment	0	485
Cargo	0	250
Non-Propellant Fluids	104	104
4-Crew Taxi MAV Crew Cabin Mass	1890	2807

4.9.5 MAV Propulsion Stages

For the purpose of this exercise, the Study Team assumed a two-stage propulsion scheme, with four each first-stage engines and a single second-stage engine; all five engines were assumed to be identical (Figure 4-21), and in fact were assumed to be a common design with the MDM engines. Engine mass was estimated at 204.1 kg each. Both the first and second propulsion stages, as well as the RCS were assumed to use Methane fuel paired with LOX. It was assumed that the RCS would remain on the second stage, and would be fed from the MPS tanks.

To overcome Martian gravity, the MAV’s propulsion subsystem must be more robust than that specified for the heritage Lunar designs. Instead, the MAV crew cabin mass was treated as a payload, and parametric analysis was used to estimate propulsion stage inert mass and propellant load required for ascent. Due to time constraints, propulsion stage sizing was only performed for the 6-Crew Habitable MAV variant, as this reflected the upper mass bound. Rough bottoms-up estimates of engines, structure, tankage, valves, and sensors resulted in a first-stage inert propulsion subsystem mass of 1,629 kg. The bottoms-up second-stage inert propulsion subsystem mass of 1,345 kg, paired with the 2,807 kg 6-crew habitable cabin mass (plus 30% growth allowance), results in a second-stage inert mass of 4,994 kg. Because these Lunar-derived bottoms-up numbers were considerably lower than Envision-based parametric estimates, propellant load for this exercise defaulted to the Envision results.

4.9.5.1 MAV Staging

To find the optimum staging time for the 6-Crew Habitable MAV, the ascent trajectory was run using POST at various staging times. For each run, the first-stage propellant load was determined by the staging time (total mass flow rate times the stage duration) and the inert mass of the stage was calculated using the stage mass fraction from the DRA 5.0 Cycle C report. The “optimum” staging time in this case is defined as the trajectory that results in the

most mass to Mars orbit. As shown in Figure 4-64, the first propulsion stage cut-off occurs at 151 s (Mission Elapsed Time), and the second-stage cut-off at 674 s. Circularization burn starts at 4552.8 s and lasts for 5.5 s. MAV “phase” is set for an arbitrary 30 seconds before the transfer burn, which begins at 4588.3 s and ends at 4710.8 s, for 122.5 s total duration. Main engine cut-off versus staging time is illustrated in Figure 4-65.

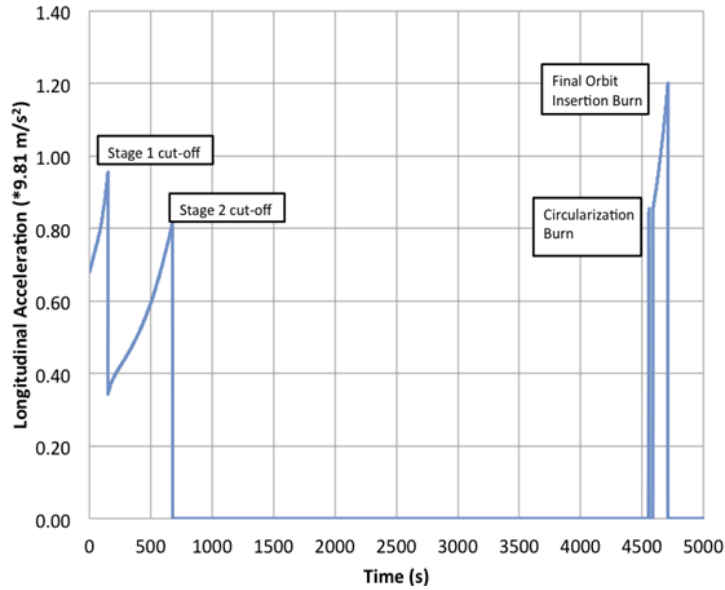


Figure 4-64 MAV staging.

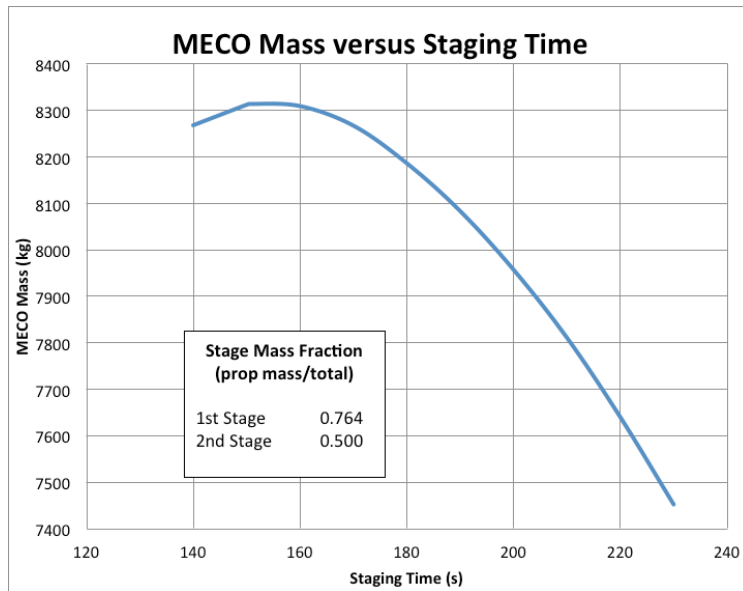


Figure 4-65 Two stage MAV MECO mass vs. staging time.

Although detailed design analysis was not performed, low-fidelity CAD modeling was used to evaluate optimal placement to prevent engine bell contact during gimbal (Figure 4-66). Approximate engine placement (shown in Figure 4-67) was useful in defining the MAV’s dimensional envelope.

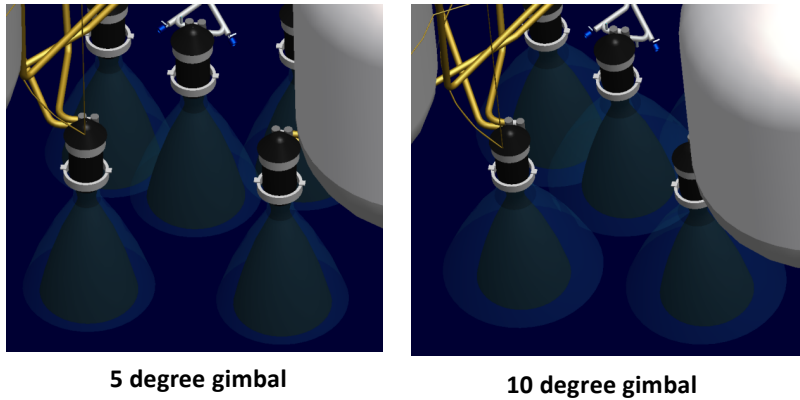


Figure 4-66 MAV engine gimbal clearance.

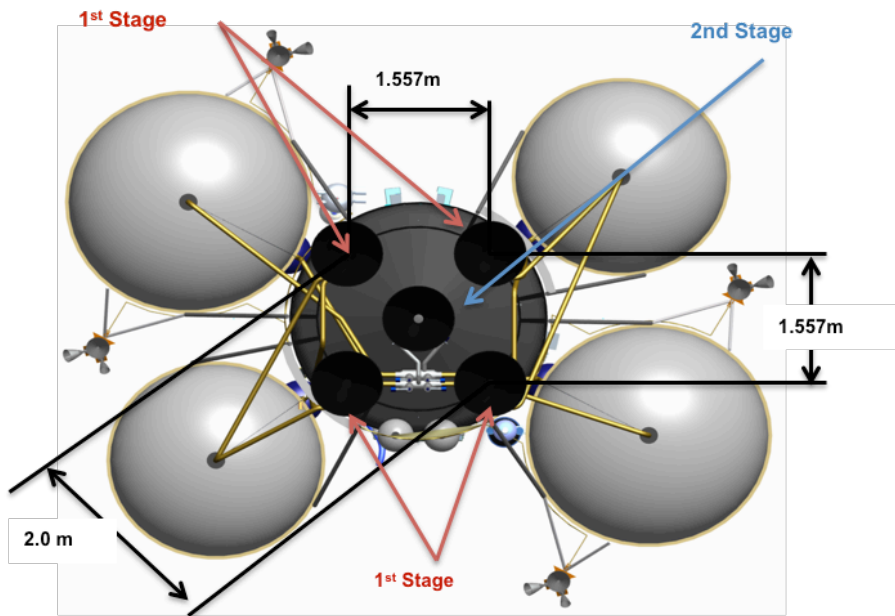


Figure 4-67 MAV engine spacing.

Per the Structures Design Team’s recommendation, two sets of two “Nested Tanks” were employed, with LCH₄ sitting above the LOX in each of the four tanks. For the 6-Crew Habitable MAV variant, the first- and second-stage propellant tank dimensions were initially estimated as shown in Figure 4-68. Note that the second-stage tanks are actually larger than the first-stage tanks. Tanks are arranged in pairs on either side of the pressure cabin, as shown in Figure 4-68.

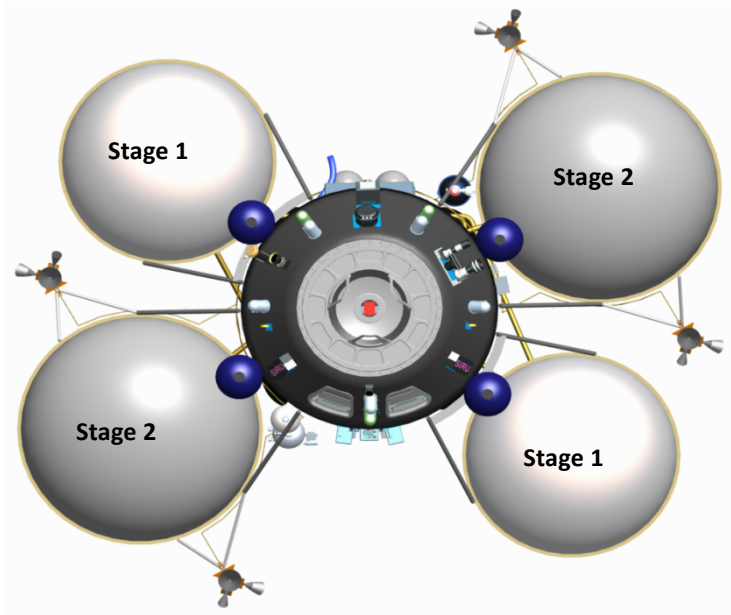


Figure 4-68 MAV propellant tank placement (top view).

One key challenge to this design is cleanly separating the first propulsion stage without re-contacting the crew cabin or Second Stage Main Engine. Two separation schemes were discussed:

- The first-stage tanks remain attached to each other on a structural ring, which slides down over the second-stage main engine; or
- The first-stage structural ring is pyrotechnically separated in two, and one first-stage tank falls away from either side of the vehicle.

Following jettison of the first stage, the second-stage MAV vehicle is shown in Figure 4-69.

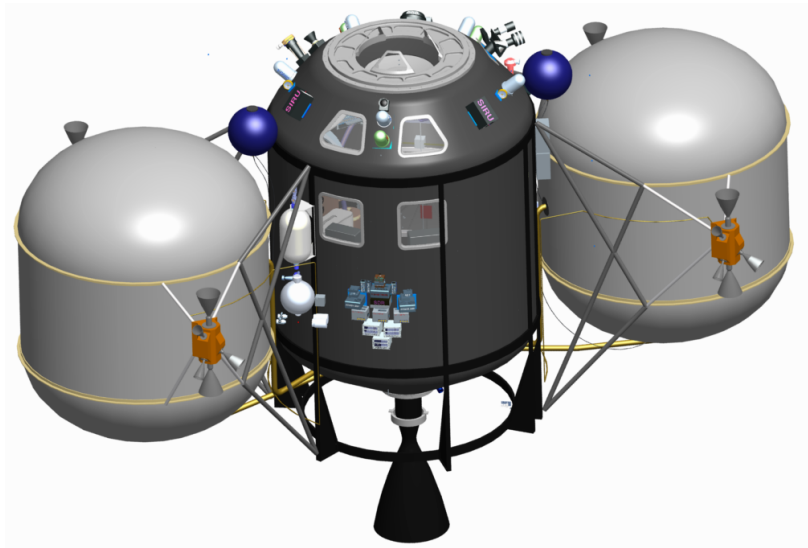


Figure 4-69 MAV second-stage configuration.

Note that the ascended and descended masses are not expected to be the same for the Propulsion subsystem, because the LOX tanks will be empty during descent, but full during ascent, and tank insulation will be removed prior to ascent.

4.9.5.2 6-Crew Habitable MAV Propellant Load

To bound the MAV’s upper mass envelope, initial 6-Crew Habitable MAV propellant estimates were performed using POST, based on inert MAV masses obtained using the ENVISION tool. Note that because the ENVISION-generated MAV inert mass is higher than the “bottoms-up” crew cabin inert mass estimated above, the estimated propellant loads are conservative. Further design fidelity is required to determine a realistic inert MAV mass, but it is probably enveloped by the bottoms-up and ENVISION estimates. Using the more conservative ENVISION inert MAV mass, an estimated total propellant load of 30662.8 kg was calculated. The propellant load split between the first and second propulsion stages is shown in Figure 4-42.

Table 4-42 6-Crew Habitable MAV Propellant Load

	Mass Estimate	Propellant Volume
Envision Estimated Inert Mass	12189 kg	
First Stage		
Estimated 1st Stage Inert Mass	3874.7 kg	
1st Stage Propellant Total Mass	12543.6 kg	
LOX	9626.5 kg	8.46 m ³
CH4	2917.1 kg	7.28 m ³
First Stage Total Wet Mass	16418.4 kg	
Second Stage		
Estimated 2nd Stage Inert Mass	8314.3 kg	
2nd Stage Propellant Total Mass	18119.2 kg	
LOX	13905.5 kg	12.23 m ³
CH4	4213.8 kg	10.52 m ³
Second Stage Total Wet Mass	26433.6 kg	

Figure 4-70 illustrates the 6-crew habitable MAV concept with tanks sized for the propellant load outlined above.

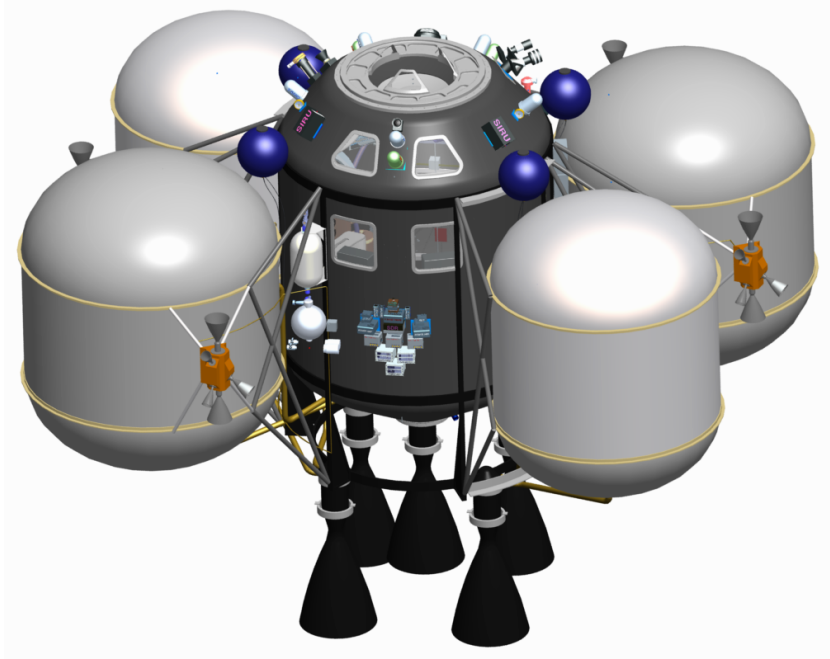


Figure 4-70 6-crew habitable MAV.

4.9.6 Discussion

4.9.6.1 MAV Estimated Mass

Using ENVISION parametric analysis, the 6-crew habitable MAV ascended mass is about 42,852 kg. Stripping out the ISRU-provided LOX propellant would result in a descended mass of about 19,320 kg. Pairing the ENVISION-derived propellant load with the bottoms-up crew cabin mass outlined above—plus 30% for growth and uncertainty on crew cabin hardware—would result in an ascended mass of about 38,076 kg, and a descended mass of about 13,536 kg. As noted above, additional design work is required to improve mass fidelity, but the two approaches probably bound a realistic MAV design mass.

4.9.6.2 Taxi vs. Habitable Variant

The Taxi-type ascent module was originally proposed as a way of reducing mass for a baseline vehicle carrying EVA-suited crews. Given that all MAV variants assume IVA-suited crews, there is little apparent mass advantage of the Taxi MAV over the Habitable MAV for these particular design concepts. As noted above, major differences between the two designs and low design fidelity of the Taxi concept require additional effort to determine whether the Taxi variant would result in substantial mass savings.

One drawback to the Taxi concept is the limited habitability inside such a small crew cabin. The most volume-consuming activity inside the MAV is likely to be don/doff of EVA suits to change into IVA suits, which would be extremely difficult in the cramped Taxi MAV (Figure 4-71). The Altair design included an attached airlock that served as a changing room. But because the MAV won't have this feature, the crew will either need to translate via a tunnel from another vehicle (which would serve as a changing room), or the IVA suits must be able to translate a short-distance EVA. One option discussed is a disposable EVA "thermal overcoat" that would protect the IVA suits for a very brief external translation, though this scheme could bring dust into the MAV.

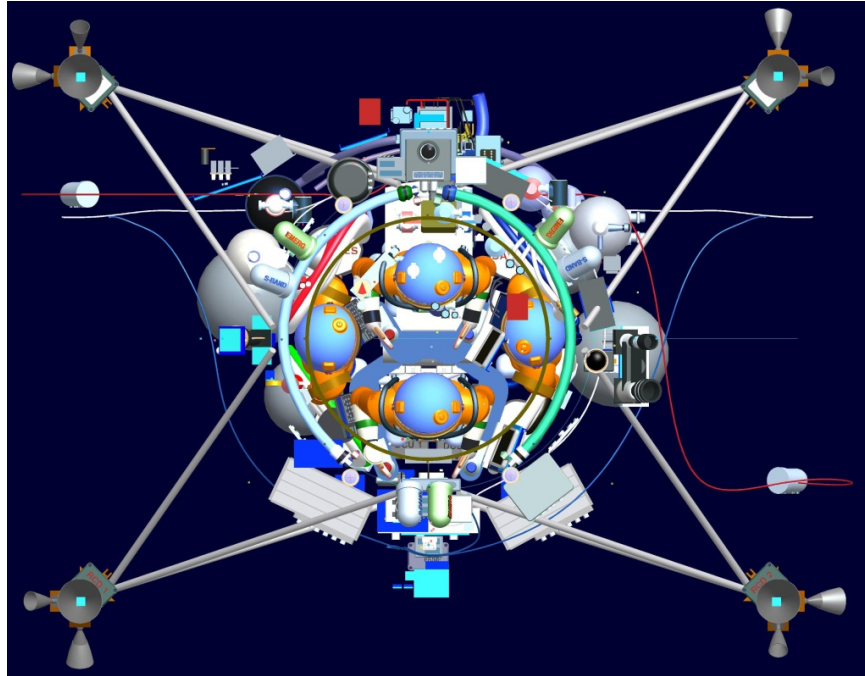


Figure 4-71 Taxi MAV habitability (top view).

4.9.6.3 MAV Habitability

Figure 4-72 through Figure 4-72 illustrate preliminary locations of subsystem equipment in the Habitable MAV concept.

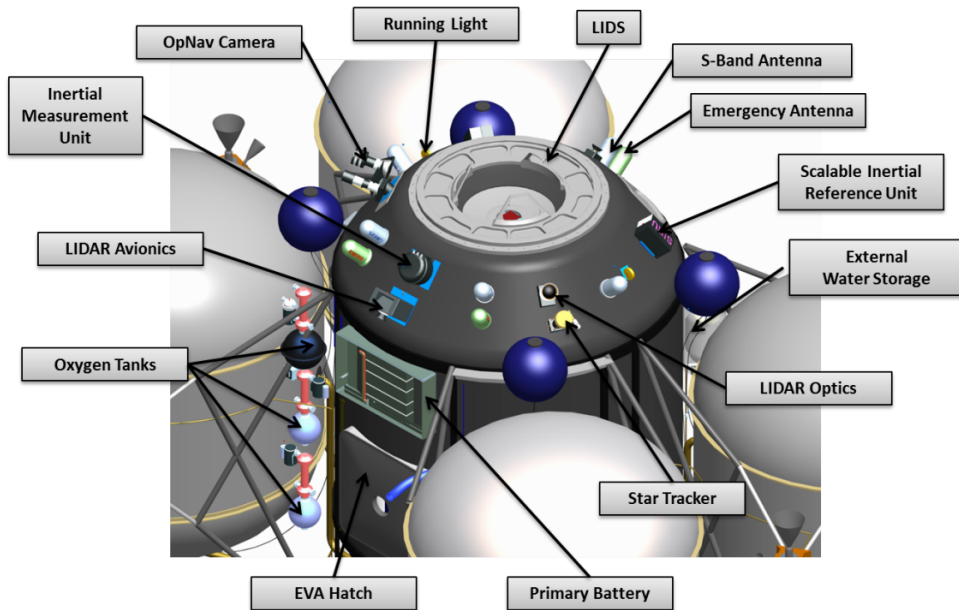


Figure 4-72 External equipment placement (fore).

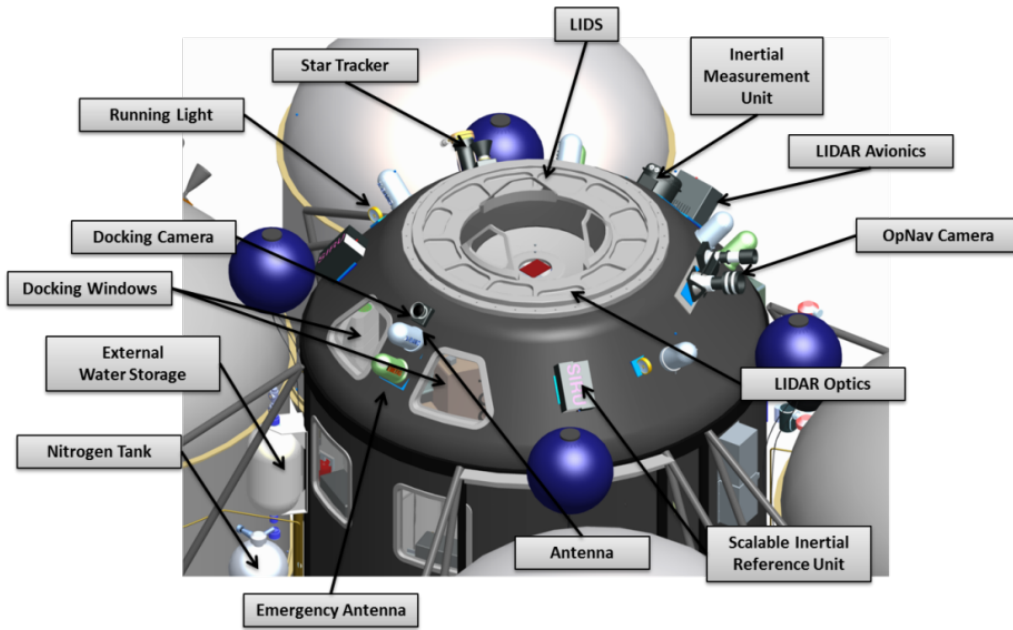


Figure 4-73 External equipment placement (aft).

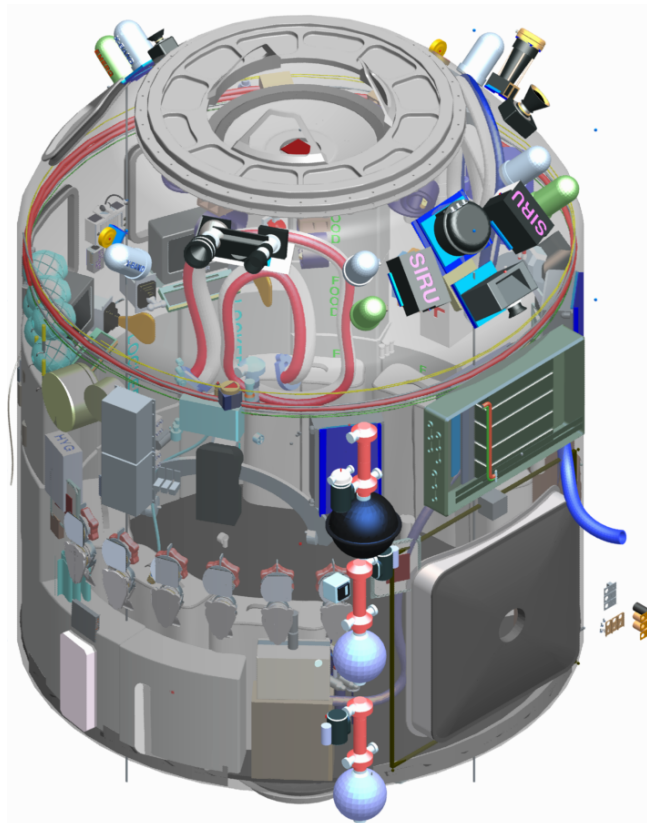


Figure 4-74 Internal cabin configuration.

The most volume-consuming activity inside the MAV is likely to be don/doff of EVA suits to change into IVA suits.

The cabin diameter selected for the 6-Crew Habitable MAV was based entirely on computer models (Figure 4-75) and should be validated in mock-up tests with suited test subjects.

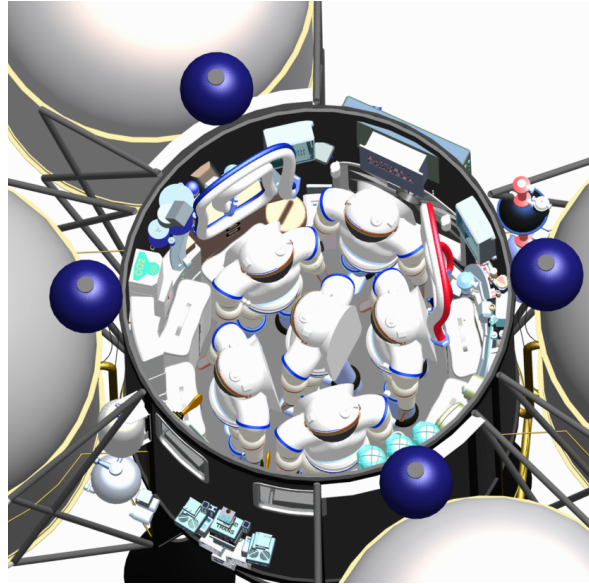


Figure 4-75 6 EVA suited crew in MAV (outfitted for 1 week).

4.9.6.4 Pressurized and Habitable Volume

Table 4-43 summarizes the estimated pressurized volume of the MAV variants with respect to historical spacecraft. The 6-crew MAV cabin provides more pressurized volume per crew member than the 4-crew MAV variants, but habitability studies would be needed to determine whether the 6-crew cabin is larger than it needs to be, or whether the 4-crew cabin is undersized. At 2.0 to 3.02 cubic meters per crew member, the MAV crew cabins are in the right ballpark when compared to historical spacecraft.

Table 4-43 4-Crew Taxi vs. Habitable Variant Volume Comparison

	Soyuz (Descent)	Taxi MAV		Habitable MAV		Apollo Command Module
		4-Crew	6-Crew	4-Crew	6-Crew	
Max. Habitable Duration (hrs)	3.5	12	12	43	43	66
Cabin Diameter (m)	-	1.8	2.2	2.35	2.70	3.91
Cabin Height (m)	-	3.6	3.5	3.82	3.82	3.22
Pressurized Volume (m ³)	6.5	8	13.1	12.5	18.1	10.3
Pressurized volume per crew (m ³ /crew)	2.16	2.00	2.18	3.13	3.02	3.43
Habitable Volume (m ³)	4	Forward Work				5.95
Habitable Volume per crew (m ³ /crew)	1.33	Forward Work				1.98
Number of Crew	3	4	6	4	6	3

Habitable or free volume (unencumbered with equipment) is difficult to assess at this level of design detail. As shown in Figure 4-71, the MAV Study Team assumed equipment would conform to the cylindrical shell, but this may not be practical from a manufacturing or logistics point of view.

4.9.6.5 Alternative Architecture Considerations

As noted above, if the MAV were reasonably “habitable” it could theoretically be used for more than just a few hours during the ascent phase. For example, a Habitable MAV could radically change the architecture, by allowing the crew to land in the MAV, and live in it for a week or two, until they were able to translate to the Surface Habitat. Aside from improving the MAV’s reliability by eliminating the MAV’s long surface exposure prior to crew arrival, shared habitability function potentially allows for a smaller—and lower mass—Surface Habitat. The downside, of course, is that habitability adds mass to what is clearly the highest “gear ratio” element of a crewed Mars mission.

Alternative architecture schemes where the crew descends in the MAV are complicated by the need for crew protection against landing impact loads. As part of this exercise, the MAV Study Team contemplated how an Orion-style recumbent seating arrangement might look in the MAV. Figure 4-76 shows how the crew could be arranged in two “layers” within a 2.4 m diameter pattern—four on the bottom and two on top. The seats shown were obtained from the Orion project; notice that the crew’s EVA suits are stowed below the seats. After landing, the seats could be repurposed, for example as crew seating in the Surface Habitat or rover. Although the model clearly shows that it is possible to seat the crew for landing, crewed mock-up testing would be required to evaluate post-landing egress, particularly if the crew were in a degraded physical condition. What’s more, if the crew were to remain in the MAV for several days after landing, seat equipment may exacerbate cabin habitability concerns.

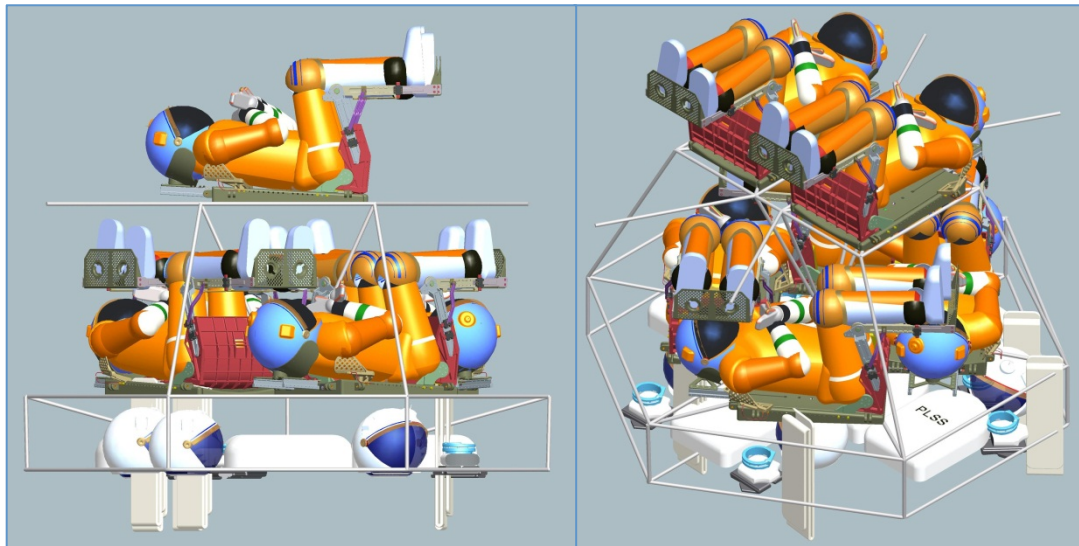


Figure 4-76 MAV conceptual crew landing protection.

For the alternate architecture scheme wherein the MAV would be inhabited by all 6 crew for a week or so after landing, forward work must be done to validate that the cabin is large enough, particularly for crew exercise. Figure 4-77 illustrates six IVA-suited crew in an MAV, outfitted with a (worst-case) week’s worth of provisions.

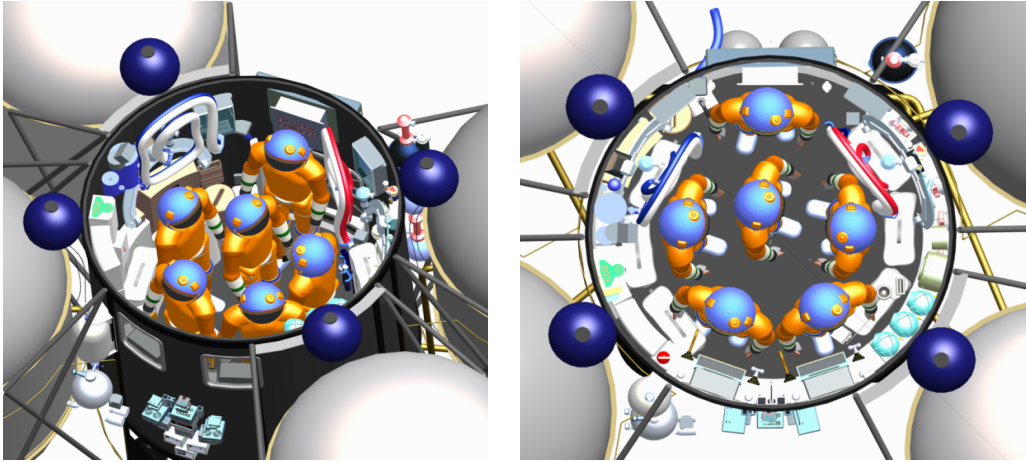


Figure 4-77 Crew MAV habitability.

At the other end of the habitability spectrum, the Study Team considered a bare-bones Taxi MAV concept. Although the shorter ascent duration would likely drive DSH propellant mass up by requiring rendezvous in a lower Mars orbit than originally envisioned, a lower-mass MAV potentially reduces the Cargo Lander’s mass, which has flow-down impacts all the way back to Earth-launched mass. The question is whether that cumulative mass savings could offset the DSH fuel mass penalty. Another interesting option the team discussed was for Orion to detach from the orbiting DSH, rendezvous/dock with a Taxi MAV in a lower Mars orbit, and return the MAV crew to the DSH. This operational concept reduces the MAV’s propellant mass without forcing the entire DSH to descend to a lower orbit, but the disadvantages include higher complexity and risk, and DSH would have to carry Orion resupply propellant. For the purpose of this exercise, only the nominal (HMO) rendezvous with DSH was evaluated, due to insufficient design fidelity of the Taxi concept to draw firm conclusions.

4.9.6.6 Crew Complement Sensitivity

Preliminary estimates for the Habitable Variant C&DH, C&T, GN&C, and ECLS subsystems do not vary appreciably when the number of crew is increased from four to six. The larger crew cabin nearly doubles the Structures and Mechanisms subsystem mass, though it must be noted that neither of the two cabin diameters were optimized, and because of the low design fidelity these numbers could very well change with further design iteration. Because somewhat arbitrary mass allowances were made for the Thermal and Power subsystem resizing, no conclusions can be drawn with respect to these subsystems without more detailed design work. As expected, the EVA and Human Factors subsystem masses do increase proportionally with extra crew, and at 98.5 kg each, two extra crew members will obviously increase mass for Crew and Cargo, as well as consumable fluids.

4.9.7 MAV Mass Reduction Opportunities

4.9.7.1 GN&C and C&T Subsystems

Note that the GN&C subsystem masses for the Taxi and Habitable MAV variant are very similar (65.48 kg versus 65.78 kg), indicating that this subsystem is relatively well characterized. Further changes in this subsystem’s mass would likely be driven by technology or requirement changes, rather than design refinements. Also note that the GN&C subsystem mass makes up a small percentage of the vehicle dry mass. As with the GN&C subsystem, the C&T subsystem masses for the Taxi and Habitable MAV variant are also very similar (61.9 kg versus 62.79 kg). Again, further changes in this subsystem’s mass would likely be driven by technology or requirement changes, rather than design refinements.

4.9.7.2 Electrical Power Subsystem

Expected shelf life of MAV batteries is a concern, given the long transit and quiescent surface stay. If fresh batteries were to arrive with the crew, rather than on the MAV, this could reduce the descended MAV mass by as much as 200 kg.

4.9.7.3 Thermal Subsystem

As noted above, surface operations are the primary driver for MAV Thermal Subsystem mass. A modular Thermal subsystem design could allow significant thermal mass (cryogenic propellant tank passive thermal control, for example) to be shed just prior to ascent, saving an estimated 140 kg on the 6-Crew Habitable variant's ascended mass.

The highly integrated nature of the Thermal subsystem means that mass savings on other subsystems could also reduce the Thermal subsystem mass.

4.9.7.4 Environmental Control and Life Support Subsystem

All Habitable MAV variants include a 4.5 kg fire extinguisher. Although it's prudent to keep a fire extinguisher close by during surface operations, it may not be necessary to carry it to orbit. In the event of a fire, the crew can vent the cabin, and continue ascent on the suit loop umbilical hoses.

The Altair-derived Habitable MAV variants include heated potable water for food rehydration and hot drinks. If the MAV is to be used for surface habitation, this feature would likely be appreciated by the crew. However, if the MAV is to be used for ascent only, then 5.62 kg mass can be shaved from the MEL by eliminating the water heater, hot water tank, and sensors; additional savings would be likely from the Thermal subsystem as well.

One trade study identified as forward work is to evaluate whether the Air Revitalization swing beds could be replaced with a simpler Space Shuttle-type lithium oxide system to save mass. It may also be possible to repack the swing beds into a more compact PLSS-sized package to save volume, which could in turn save mass.

Human Factors

The Altair-derived Habitable MAV includes a 6.81 kg portable vacuum cleaner. Originally intended to clear EVA dust during surface operations, it may not be required for a short trip to orbit, especially if the dusty EVA suits are left behind on the surface. Also note that in the LOR heritage design, about 10% of the vehicle's power was devoted to the vacuum cleaner so eliminating it would likely save significant MAV power and thermal subsystem mass.

As noted above, the extent of the MAV's "habitability" drives Human Factors mass. Limiting the MAV to a 12-hour taxi ride, rather than the 43-hour mission DRA 5.0 mission, drops the 4-crew Human Factors ascended mass from 50.02 kg to 0.07 kg. On the other hand, increasing the mission duration from 43 hours to a week-long surface stay drives the 4-crew Human Factors descended mass from 36.02 kg to 185.65 kg; 6-Crew Human Factors descended mass would jump from 95.41 kg to 236.17 kg. Of course, the descended mass increase would likely be offset by reduced descended mass on another element, since the crew would need food, clothing, etc. one way or the other.

4.9.7.5 Extravehicular Activity

The MAV Study Team assumed that relatively short umbilical hoses were needed for visors-down ascent in a cabin pressure leak contingency. The "short" hose mass was drawn from the 4.58 m long LOR umbilical hose design. However, this design was intended for translation from one pressurized element to another; if that is not necessary, the hoses may be further shortened to save some mass.

4.9.7.6 Structures and Mechanisms

Because both the Taxi and Habitable MAV variants were derived from vehicles used for descent as well as ascent, both feature forward-facing landing windows, as well as upward-facing docking windows. However, because the MAV is intended only for ascent, these forward-facing windows could be eliminated, which would save approximately 11.84 kg, as well as increase reliability by eliminating potential leakage paths.

4.9.7.7 Propulsion Subsystem

As noted above, the second-stage propulsion tanks are actually larger than the first-stage tanks, suggesting that further optimization is possible in splitting the stages.

One innovative idea for saving overall landed mass is to share propellant tanks between the MAV and its descent stage Lander, saving the mass of one or both sets of tanks. In this concept, the descent engines would draw propellant from the MAV’s ascent tanks. This would make the landed mass of the MAV heavier than the nominal DRA 5.0 scheme (where the MAV would land with empty tanks). After landing, ISRU equipment would remotely refill the tanks—just as with the nominal DRA 5.0 scheme. Prior to ascent EVA, crews could manually disconnect descent stage feed lines from the MAV, and the tanks depart with the MAV.

Taking this concept one step further, the five MAV engines could also assist during the descent phase. In this scheme, the MAV engines would draw propellant from the MAV tanks, allowing several descent engines to be eliminated. Although there is no net change to the MAV’s mass, this scheme potentially lowers the descent stage mass by up to 1020.5 kg for five engines. The downside is that this adds a restart requirement to the MAV engines, and likely increases overall Loss of Mission risk by complicating the descent stage.

4.9.7.8 Crew, Crew-Worn Equipment, and Cargo

As noted above, the largest crew stature and mass were assumed. A reduction to 50th percentile crews (which is what Altair assumed, and what Apollo 11 actually flew), would save 16.9 kg per crew member. The cumulative savings would be 67.6 kg for 4 crew, or 101.4 kg for 6 crew. Secondary mass savings associated with smaller stature crews may also be realized in other subsystems, such as Life Support consumables or EVA suits.

4.9.7.9 Non-Propellant Fluids

For the purpose of this exercise, it was assumed that the MAV would carry its full complement of non-propellant fluids during uncrewed, nominal descent, although it is possible that these tanks could land empty, and be filled on the surface prior to departure. Although this would complicate pre-ascent preparations, it does provide a descent mass savings opportunity, and mitigates leakage during the long, quiescent transit from Earth and unmanned surface stay.

4.10 Transition Event

In this study, the term “transition event” refers to the transition from supersonic flight in the entry aeroshell to initiation of powered descent of the lander, and includes the separation of the lander from the aeroshell. It provides a transition from aeroassisted flight to descent under rocket power. The transition event has been identified as a critical and challenging event affecting landing architecture and vehicle design. Thus, focus was placed on identifying viable options for executing the transition event for both the mid L/D architecture and the HIAD architecture.

In NASA’s EDL-SA study,³ a high-level assessment of transition options was carried out to identify promising transition techniques. The HAT Mars Lander task endeavored to build on and broaden the assessment to attempt to exhaustively enumerate types of transition options and assess them for most promising candidates for more detailed analysis. Summarized in the sections below is the initial work carried toward this end. It should be kept in mind that while in the following sections the HAT team has ranked options to guide more detailed assessments, lower ranked options may eventually prove to be more optimal through more detailed analysis. Also, the eventual best option may not yet have been identified or may be the result of a combination of options summarized below. In other words, these results do not represent an answer to the transition method, but rather a summary of current best understanding.

4.10.1 Transition Conditions

To understand the approximate initial and final conditions of the transition event, the trajectory results from the EDL-SA study were used to inform the transition option assessment. Figure 4-78 illustrates the start and end conditions for the mid L/D and HIAD architectures. As modeled in the EDL-SA study, the transition event for the mid L/D architecture begins at Mach 2.7 at an altitude of 7.5 km. This initiation condition is a result of the aeroassist vehicle velocity profile and propulsive capability of the lander. Initiation of powered descent, the end point of the transition, is at Mach 2.9 at a height above ground of 4.6 km. Because of the different ballistic

coefficient of the HIAD aeroassist vehicle, the HIAD architecture transition event begins at Mach 1.8 at a height above ground of 5.7 km. HIAD architecture transition ends at Mach 2.0 at 3.3 km above ground. These transition conditions were used as a guide during the transition event option evaluation. Actual start and end conditions will vary by transition option, but have not yet been determined to contribute to this assessment.

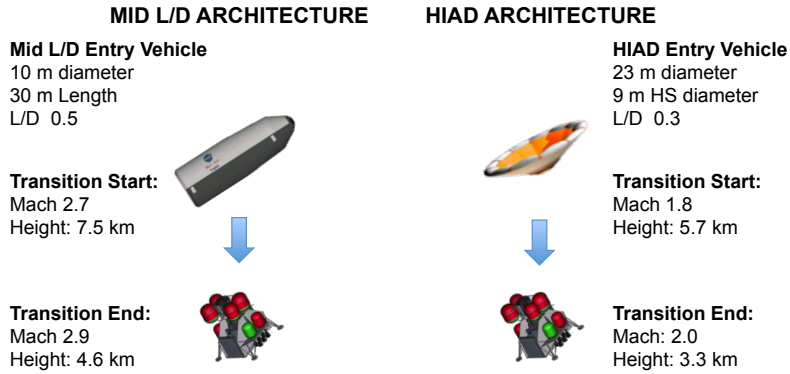


Figure 4-78 Transition conditions from EDL-SA architecture studies.

4.10.2 Evaluation Process

The transition option evaluation process used to rank and select an initial set of promising transition techniques is shown graphically in Figure 4-79. The evaluation process involved a two-step process beginning with a high-level assessment that provides a down-selection to favorable options to be passed onto the second step. The second step was a more detailed evaluation using a high-fidelity dynamics simulation. The high-level assessment used a set of FOMs outlined in the following section to provide an initial scoring of the options. As shown in Figure 4-79, there are four permutations of possible transition types based on the architectures and lander configurations examined in this study. The two main branches of the process diagram are the mid L/D architecture and the HIAD architecture. The main branch then branches into options for a vertical lander and a horizontal lander. The initial assessments summarized below are for the vertical lander options only, due to limits in time and resources. Horizontal lander assessments are planned forward work. Summary of the high-level assessments are provided in Section 4.10.4 below, and summary of the detailed analyses performed to date are summarized in Section 4.10.6

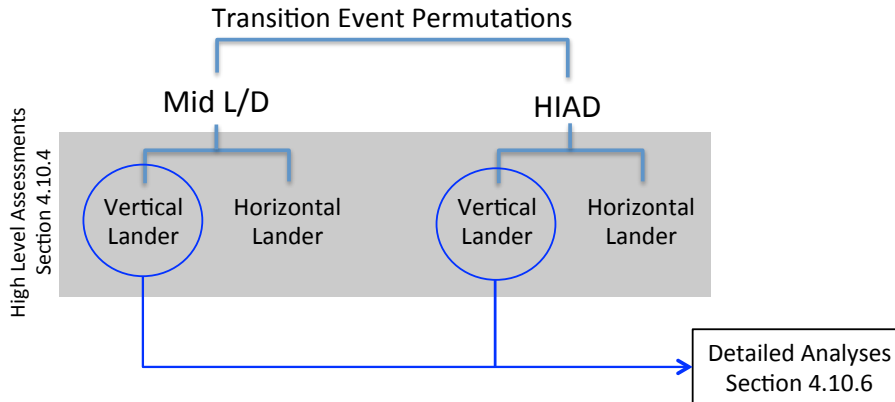


Figure 4-79 Transition event assessment process.

4.10.3 Figures of Merit

To provide an initial high-level assessment of transition options, a set of FOMs were developed to provide a structured assessment and ranking. Eight FOMs in total were created that spanned spacecraft systems and flight dynamics considerations. The FOMs were scored on a scale from 1 to 5 with 5 being a high or preferential score.

An assessment team comprised of HAT team members then used the FOMs to score the transition options, with scoring based on engineering judgment and, where possible, on simple sizing and dynamics calculations based on vehicle mass properties and estimated vehicle drag. The total score for each option was an unweighted summation of the score for each FOM. The eight FOMs used in the high-level assessment are:

- Transition Only Mass:* Additional system mass needed specifically to carry out the transition event, and used for no other purpose during EDL.
- Mechanical Complexity:* The level of complexity (and thus risk) inherent in structures and mechanisms needed specifically for the transition event.
- Propulsion Challenge:* Complexity of propulsion systems needed specifically for the transition event, and also level of dependency on SRP.
- Aerodynamic Complexity:* The level of aerodynamic complexity and challenge including complex geometries, extreme angles of attack and other characteristics leading to aerodynamic uncertainty, specific to the transition event.
- Vehicle Maneuvering:* The amount of vehicle maneuvering required to set up the transition, execute the transition, and set up powered descent following the transition.
- Duration/Attitude Loss:* The likely duration of the transition event based on the number and complexity of separate events making up the transition, which maps into altitude loss during the transition.
- Recontact Risk:* The risk of near-field and far-field recontact of separated elements during the transition event.
- Technical Readiness Level:* The level of technical readiness of technologies utilized specifically for the transition.

Future work will incorporate a weighted summation to better understand sensitivity to FOM weighting.

4.10.4 High-Level Assessments: Preliminary Options and Rankings

4.10.4.1 Mid L/D Rigid Aeroshell Architecture

The following are the 15 mid L/D transition options assessed as part of the step 1 high-level assessment, shown in order of scoring rank.

Forward Exit Clamshell Option: Rank 1

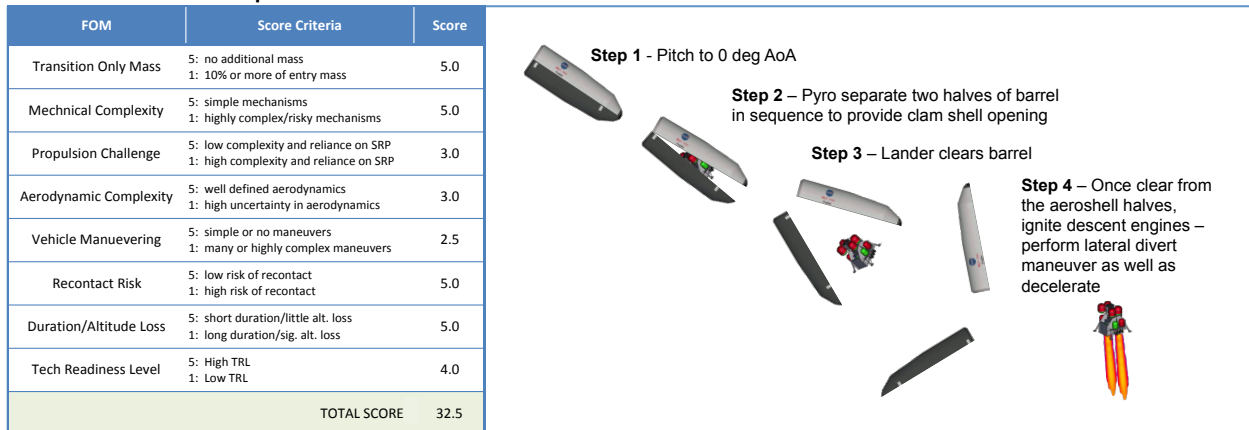


Figure 4-80 Forward exit clam shell option.

Transition Description

The forward exit clam shell option , shown in Figure 4-80, resembles the jettison of a launch vehicle payload fairing. At Mach 2.7, the mid L/D vehicle is pitched to 0° angle of attack, separation pyros are fired to release fasteners holding the two halves of the aeroshell together. Dynamic pressure causes the aeroshell halves to separate and fall behind the lander due to ballistic coefficient differences. The lander then ignites its descent engines, maneuvers to terminal descent attitude and begins terminal descent.

FOM Score: 32.5/40

Significant Pros: The forward exit clamshell option scores well on mass efficiency, simplicity, recontact risk and duration of transition. It is believed that this option could be executed relatively quickly and safely and benefits from its similarity to launch vehicle payload fairing jettison events.

Significant Cons: None identified.

Viability: Along with the side exit clamshell option shown next, this option appears the most viable for the mid L/D architecture.

Forward Work: A preliminary detailed analysis of this option is summarized in Section 4.10.6.2.1. Forward work includes building more fidelity into the analysis.

Side Exit Clamshell Option: Rank 2

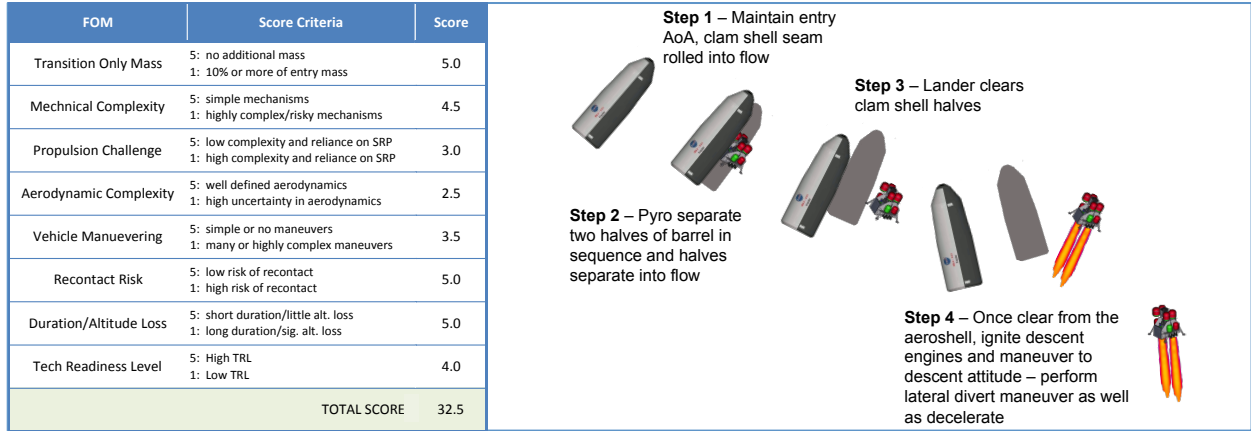


Figure 4-81 Side exit clamshell option.

Transition Description

The side exit clamshell option, shown in Figure 4-81, is similar to the forward exit option but does not require a maneuver to 0° angle of attack to initiate the transition event. Flying at a trim angle of 55°, the vehicle is rolled to place the aeroshell seam directly into the flow and separation pyros are fired to release fasteners holding the two halves of the aeroshell together. Dynamic pressure causes the aeroshell halves to separate and fall behind the lander due to ballistic coefficient differences. The lander then ignites its descent engines, maneuvers to terminal descent attitude, and begins terminal descent.

FOM Score: 32.5/40

Significant Pros: This options shares the advantages of the forward exit version of the clamshell option, but doesn’t require maneuvering the vehicle to 0° angle of attack and hold attitude while initiating the transition. This is viewed as an advantage.

Significant Cons: No significant disadvantages were identified; however, the option was assessed as slightly more complex mechanically and aerodynamically than the forward exit clamshell option.

Viability: Based on this initial assessment, this option also appears as a most viable mid L/D option based on score.

Forward Work: This option will be the second mid L/D option analyzed by the high-fidelity analysis tool.

Rear Exit Sep Thrusters on Aeroshell: Rank 3

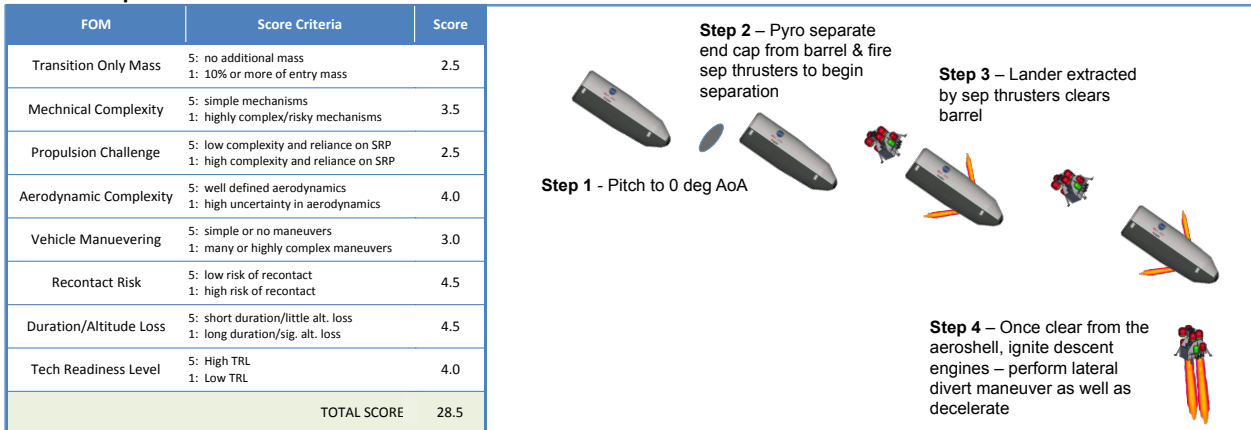


Figure 4-82 Rear exit with separation thrusters on aeroshell.

Transition Description

The rear exit separation thruster option pitches to zero degree angle of attack. As shown in Figure 4-82, the rear end cap of the mid L/D aeroshell is then jettisoned. A set of thrusters mounted on the mid L/D aeroshell are fired to accelerate the aeroshell forward separating the lander from the rear of the aeroshell via guide rails. Once clear of the aeroshell, the lander ignites its descent engines and executes powered descent. The separation thrusters are then used to steer the aeroshell away from the lander and landing area.

FOM Score: 28.5/40

Significant Pros: This option scores well on aerodynamic complexity, risk of recontact and duration of event. Aeroshell mounted separation thrusters provide some control of aeroshell path after lander separation, reducing recontact risk.

Significant Cons: Although the separation thrusters and propellant have not been sized for this option, the additional mass of propellant needed was a con identified during the assessment.

Viability: Understanding of viability of this option is pending until first order aeroshell separation propulsion system sizing is complete.

Forward Work: First order separation thruster sizing and propellant quantification.

Forward Exit with Separation Thruster on Lander: Rank 4

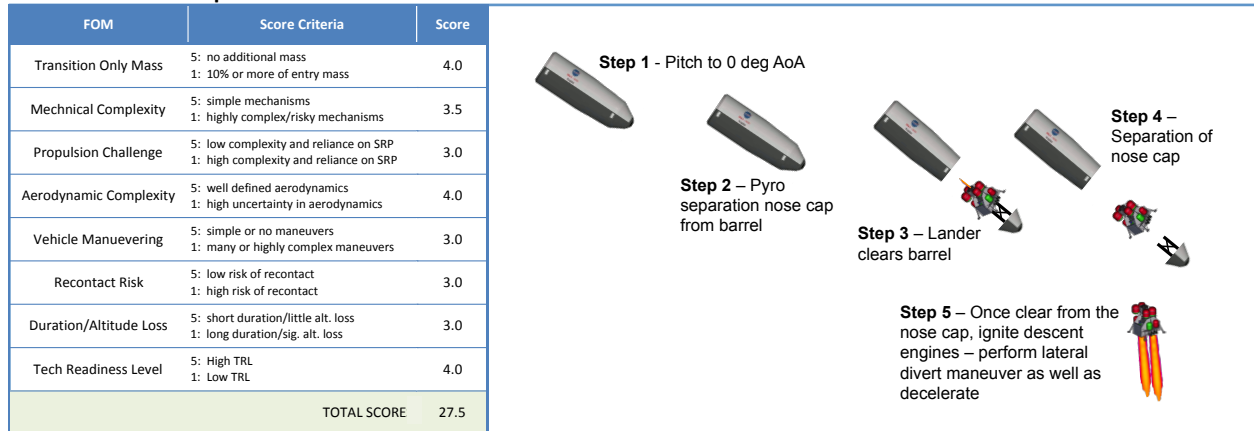


Figure 4-83 Forward exit with separation thruster on lander.

Transition Description

The forward exit with a separation thruster on the lander begins by maneuvering the mid L/D aeroshell to 0° angle of attack, as shown in Figure 4-83. Pyros separate the aeroshell nose cap and a separation thruster(s) is fired to provide thrust force to augment the rail guided lander separation from the aeroshell. The aeroshell nose cap is then separated from the lander. Once clear of the nose cap, the lander ignites the descent engines and performs powered descent.

FOM Score: 27.5/40

Significant Pros: This option scores well on mass efficiency, aerodynamic complexity, and technology readiness. Mass efficiency is scored well with the caveat detailed in Viability below. The separation thruster on the lander was viewed as an augmentation to separating the lander from the aeroshell and is not required to separate the two element based solely on ballistic number difference.

Significant Cons: The lander separation thruster, while augmenting lander separation, is adding velocity to the lander in an undesirable direction, thus the altitude loss FOM was scored lower than other forward exit options. Although the separation thrusters and propellant have not been sized for this option, the additional mass of

propellant needed was also a con identified during the assessment.

Viability: Nearly all mid L/D forward separation options suffer from a challenge of separating the aeroshell nose cap from the lander after exiting the aeroshell. On its own, the nose cap ballistic number is not large enough to provide separation from the lander.

Forward Work: A modification of this option is required to provide successful nose cap separation from the lander.

Forward Exit with Drag Flaps on Aeroshell: Rank 5

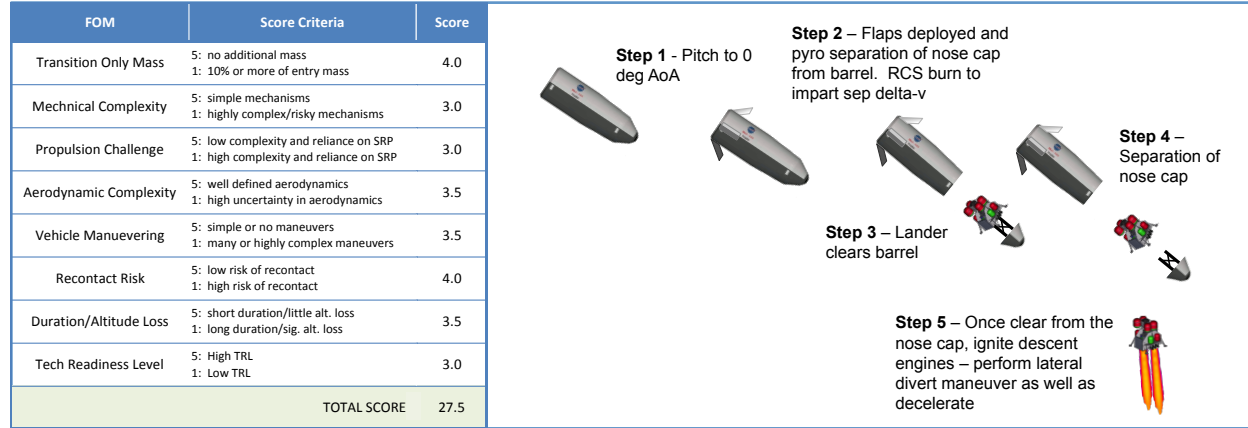


Figure 4-84 Forward with drag flaps on aeroshell.

Transition Description

In this transition option, drag flaps are used on the aeroshell to provide aeroshell drag augmentation, as shown in Figure 4-84. The vehicle is pitched to 0° angle of attack and drag flaps are deployed to increase aeroshell drag. Pyros separate the aeroshell nose cap and the lander separation from the aeroshell. The aeroshell nose cap is then separated from the lander. Once clear of the nose cap, the lander ignites the descent engines and performs powered descent. In a variation of this option, the aeroshell drag flaps could be used to trim the vehicle at 0° angle of attack at the beginning of the sequence.

FOM Score: 27.5/40

Significant Pros: This option scores well on mass efficiency and recontact risk. The aeroshell drag flaps augment aeroshell drag and thus should allow the lander to separate from the aeroshell more quickly, although the drag flaps are not required for the lander to separate from the aeroshell based on ballistic coefficient differences.

Significant Cons: No significant cons were identified for this option, although it shares the nose cap separation issue common to other forward exit options.

Viability: Nearly all mid L/D forward separation options suffer from a challenge of separating the aeroshell nose cap from the lander after exiting the aeroshell. On its own, the nose cap ballistic number is not large enough to provide separation from the lander.

Forward Work: A modification of this option is required to provide nose cap separation from the lander.

Forward Exit: Rank 6

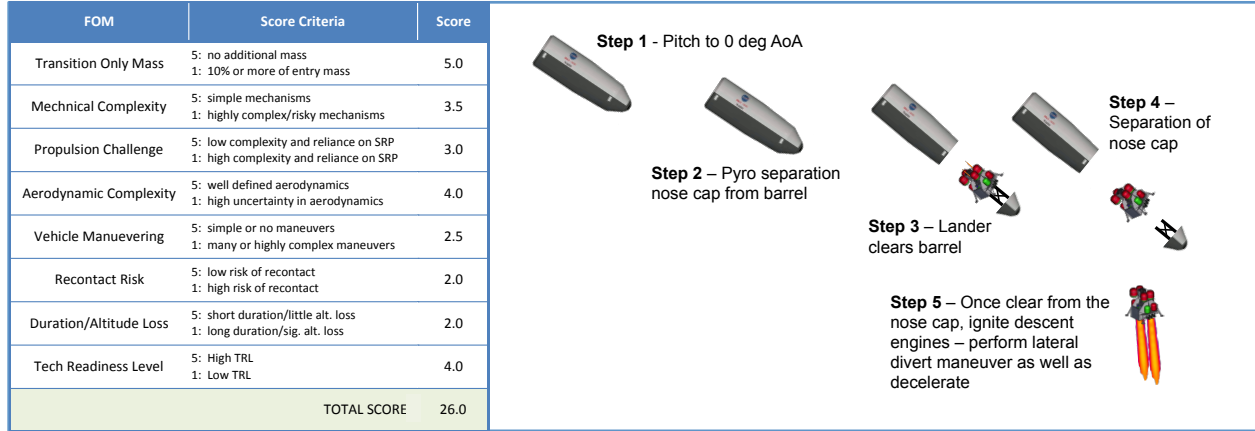


Figure 4-85 Forward exit option.

Transition Description

In this transition option, no drag augmentation device is used and the lander is separated using the ballistic coefficient differences between the lander and the aeroshell. As shown in Figure 4-85, the vehicle is pitched to 0° angle of attack and pyros separate the aeroshell nose cap. The lander, with nose cap attached, then separates from the aeroshell guided by rails. The aeroshell nose cap is separated from the lander. Once clear of the nose cap, the lander ignites the descent engines and performs powered descent.

FOM Score: 26/40

Significant Pros: This option scores well on mass efficiency because there is little to no additional mass required for the transition event itself. It also scored well on aerodynamic complexity and technical readiness.

Significant Cons: As a con, it was felt that with no drag augmentation, there might be additional risk of recontact and lander separation would be slower as well.

Viability: Nearly all mid L/D forward separation options suffer from a challenge of separating the aeroshell nose cap from the lander after existing the aeroshell. On its own, the nose cap ballistic number is not large enough to provide separation from the lander.

Forward Work: A modification of this option is required to provide nose cap separation from the lander.

Forward Exit with Separation Thrusters on Aeroshell: Rank 7

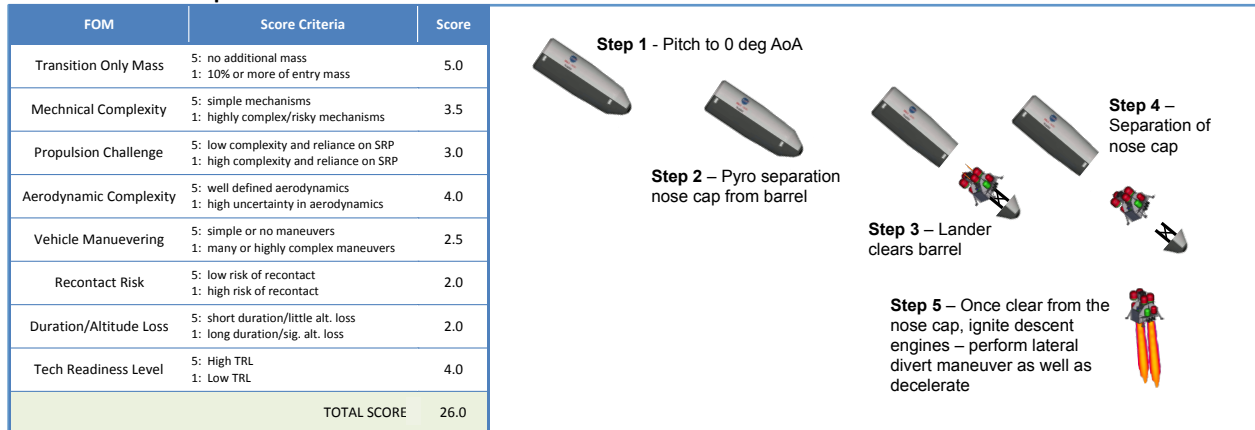


Figure 4-86 Forward exit with separation thruster on aeroshell.

Transition Description

This transition option uses separation thrusters on the mid L/D aeroshell, as shown in Figure 4-86. The vehicle is pitched to 0° angle of attack. Pyros separate the aeroshell nose cap and separation thrusters on the aeroshell fire to provide augmentation to the separation of the lander and aeroshell. The aeroshell nose cap is then separated from the lander once clear of the aeroshell. The lander then ignites the descent engines and performs powered descent. In a variation of this option, the aeroshell separation thrusters could be used to trim the vehicle at 0° angle of attack at the beginning of the sequence.

FOM Score: 25.5/40

Significant Pros: This option scores particularly well on recontact risk, both near-field and far-field. Far-field recontact is reduced because the aeroshell mounted thrusters can be used to steer the separated aeroshell once away from the lander.

Significant Cons: Relative to other options, this option may require significant additional mass for the separation thruster propulsion system hardware and propellant.

Viability: Nearly all mid L/D forward separation options suffer from a challenge of separating the aeroshell nose cap from the lander after exiting the aeroshell. On its own, the nose cap ballistic number is not large enough to provide separation from the lander.

Forward Work: Sizing of the separation thruster propulsion system is forward work, as well as a modification of this option to provide a viable nose cap separation from the lander.

Forward Exit with Parachute on Aeroshell: Rank 8

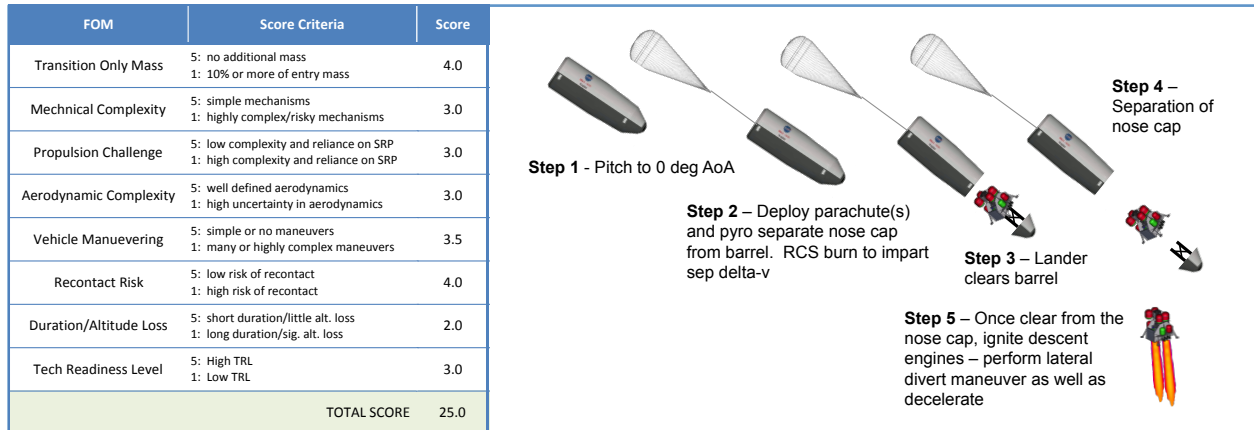


Figure 4-87 Forward exit with parachute on aeroshell.

Transition Description

In this transition option, a parachute attached to the aeroshell provides drag augmentation for a more robust separation, as shown in Figure 4-87. The vehicle is pitched to 0° angle of attack and the parachute is deployed to increase aeroshell drag. Pyros separate the aeroshell nose cap and the lander separation from the aeroshell. The aeroshell nose cap is then separated from the lander. Once clear of the nose cap, the lander ignites the descent engines and performs powered descent. In a variation of this option, the aeroshell parachute could be used to help trim the vehicle at 0° angle of attack at the beginning of the sequence.

FOM Score: 25/40

Significant Pros: This option scores well on mass efficiency and recontact risk because of the increased aeroshell drag provided by the parachute. Because the lander will separate from the aeroshell without the aid of the parachute, there is no parachute size required to achieve a desired ballistic coefficient for the aeroshell.

Significant Cons: Because of the time needed to deploy the parachute, potentially go through reefing steps, and wait for deployment dynamics to damp, this option scored low in duration/altitude loss.

Viability: Potential parachute deployment conditions for this option are somewhat above current acceptable conditions for a supersonic parachute at Mars. Additionally, nearly all mid L/D forward separation options suffer from a challenge of separating the aeroshell nose cap from the lander after exiting the aeroshell. On its own, the nose cap ballistic number is not large enough to provide separation from the lander.

Forward Work: A modification of this option is required to provide nose cap separation from the lander. Also, because the parachute provides augmentation for separation and is not required for separation, parachute sizing has not been determined. The parachute could also be sized to provide vehicle trimming at 0° angle of attack.

Forward Exit with SIAD on Aeroshell: Rank 9

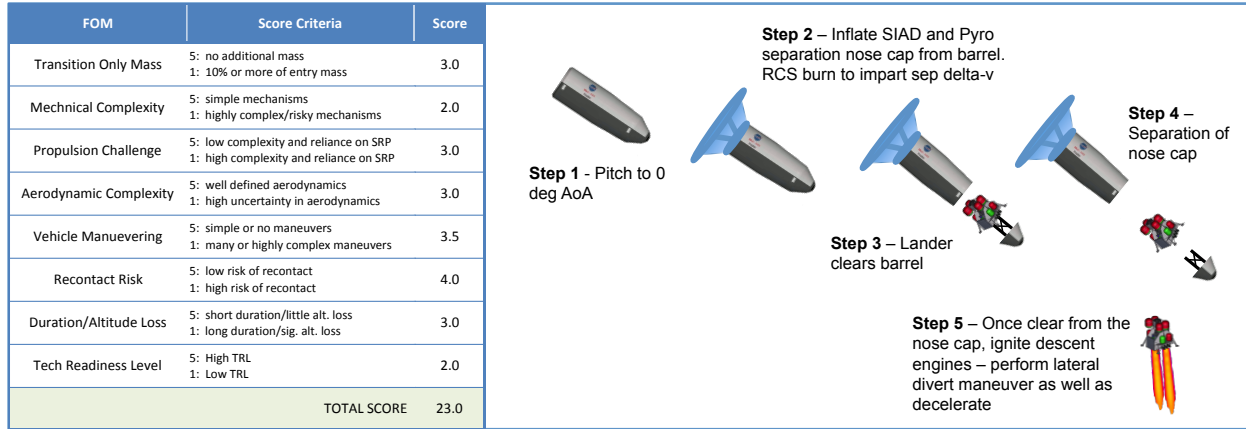


Figure 4-88 Forward exit with SIAD on aeroshell.

Transition Description

Like the forward exit parachute option, this transition option provides drag augmentation with a SIAD attached to the aeroshell, as shown in Figure 4-88. To begin the transition, the vehicle is pitched to 0° angle of attack and a SIAD is deployed to increase aeroshell drag. Pyros separate the aeroshell nose cap and the lander separates from the aeroshell. The aeroshell nose cap is then separated from the lander. Once clear of the nose cap, the lander ignites the descent engines and performs powered descent. In a variation of this option, the aeroshell SIAD could be used to trim the vehicle at 0° angle of attack at the beginning of the sequence.

FOM Score: 23/40

Significant Pros: This option scores well on recontact risk but was judged to be less mass efficient relative to the parachute front exit described in the previous option. As with the front parachute option, the SIAD is not required to separate the lander, and thus there is no required SIAD size to modify the aeroshell ballistic coefficient.

Significant Cons: This option scored low on mechanical complexity due to the deployment and inflation of the SIAD, and scored low on technology readiness due to low maturity of SIAD technology.

Viability: Nearly all mid L/D forward separation options suffer from a challenge of separating the aeroshell nose cap from the lander after exiting the aeroshell. On its own, the nose cap ballistic number is not large enough to provide separation from the lander.

Forward Work: A modification of this option is required to provide nose cap separation from the lander. Sizing of the SIAD is also forward work with drag augmentation and angle of attack trimming two factors in sizing.

Rear Exit Using Lander Descent Engines: Rank 10



Figure 4-89 Rear exit using lander descent engines.

Transition Description

The rear exit separation thruster option first pitches to zero degree angle of attack. As shown in Figure 4-89, the rear end cap of the mid L/D aeroshell is then jettisoned. The lander then uses its descent engines to separate from the rear of the aeroshell. Because of unfavorable ballistic coefficient differences, the lander will not separate without use of the engines. Once clear of the aeroshell, the lander maneuvers to powered descent attitude and executes powered descent.

FOM Score: 22/40

Significant Pros: This option scores well on mass efficiency, needing little to no additional mass for the transition event. It also scores well on mechanical complexity.

Significant Cons: The most significant mark against this option is the large unknown viability of firing the descent engine in the confines of the enclosed aeroshell, which resulted in a low propulsion challenge score. There is also significant recontact and aerodynamic complexity concern.

Viability: Viability is depended on the ability to fire the descent engines within the confines of the aeroshell.

Forward Work: Need to seek propulsion engineer consultation on descent engine firing in aeroshell.

Rear Exit with SIAD on Lander: Rank 11

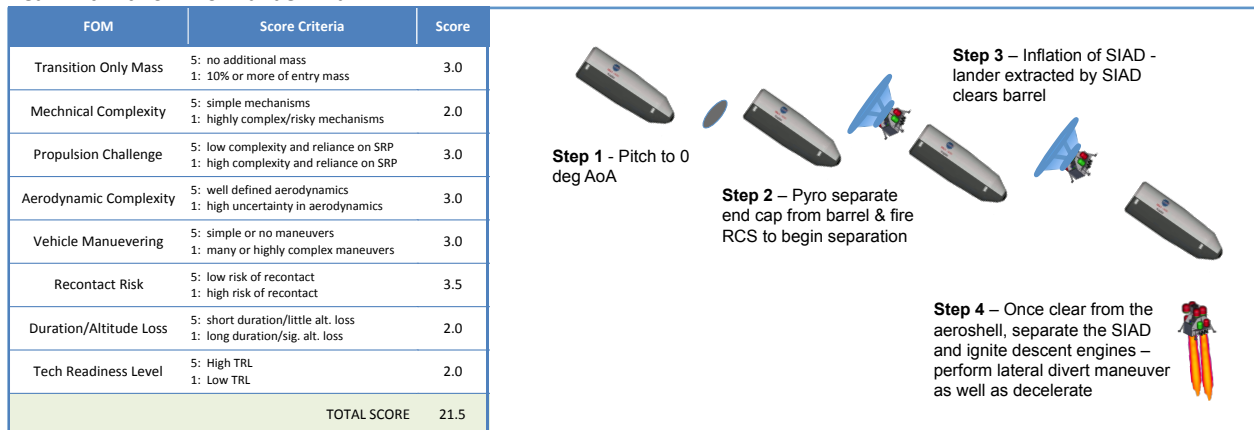


Figure 4-90 Rear exit with SIAD on lander.

Transition Description

As shown in Figure 4-90, this rear exit separation option utilizes a SIAD on the lander to provide a rear exit from the aeroshell. The transition begins when the vehicle pitches to zero degree angle of attack. The rear end cap of the mid L/D aeroshell is then jettisoned and RCS thrusters are used to move the lander toward the rear of the aeroshell. Once partially clear of the aeroshell, a SIAD attached to the top of the lander is inflated to increase lander drag and remove the lander from the aeroshell. Once clear of the aeroshell, the lander jettisons the SIAD and ignites its descent engines and executes powered descent. Sizing work shows the SIAD needs to be greater than 9 m in order to provide lander ballistic coefficient less than the empty aeroshell.

FOM Score: 21.5/40

Significant Pros: No significant advantages were identified with this option.

Significant Cons: Because of the use of SIAD technology, this option scores low on mechanical complexity and technology readiness. It was also judged to take longer to execute relative to other options, in part because of the time to move the lander to the rear of the aeroshell to position it for SIAD inflation.

Viability: Understanding of viability is dependent in part of the ability of RCS thrusters to move the lander to the rear of the aeroshell.

Forward Work: Analysis of RCS thrust level required to put lander in position to deploy SIAD.

Forward Exit with Trailing Inflatable Aerodynamic Decelerator (IAD) on Aeroshell: Rank 12

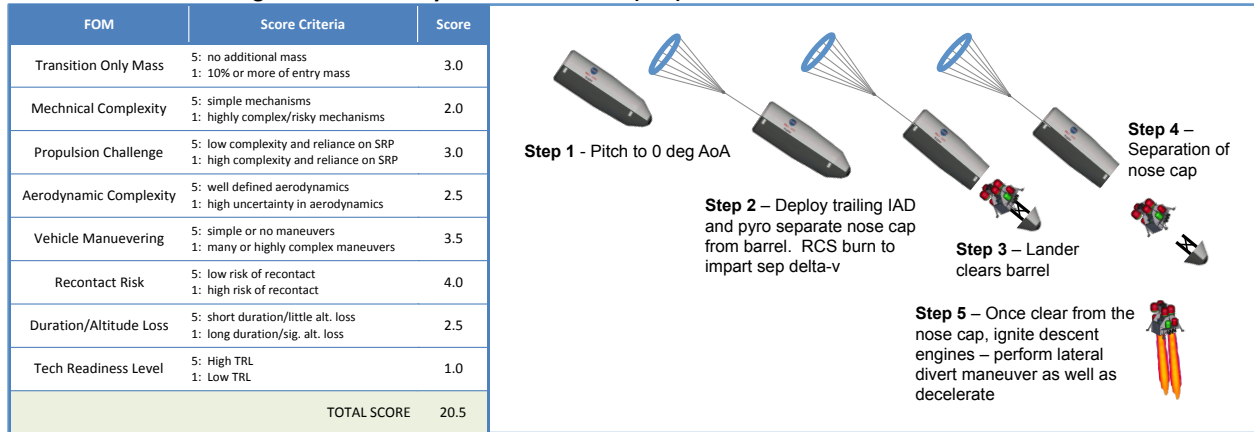


Figure 4-91 Front exit with trailing IAD attached to aeroshell.

Transition Description

Like the forward exit parachute option and SIAD option, this transition option provides drag augmentation with a trailing IAD attached to the aeroshell, as shown in Figure 4-91. To begin the transition, the vehicle is pitched to 0° angle of attack and a trailing IAD is deployed and then inflated to increase aeroshell drag. Pyros separate the aeroshell nose cap and the lander separates from the aeroshell with nose cap attached to the lander. The aeroshell nose cap is then separated from the lander. Once clear of the nose cap, the lander ignites the descent engines and performs powered descent. In a variation of this option, the aeroshell trailing IAD could be used to trim the vehicle at 0° angle of attack at the beginning of the sequence.

FOM Score: 20.5/40

Significant Pros: This option scores well on recontact risk but like the SIAD front exit option, was judged to be less mass efficient relative to the parachute front exit option.

Significant Cons: This option scored lowest on technology readiness because there is currently no development effort under way for this type of inflatable device. It also scored lower on mass efficiency and mechanical

complexity because it is deployed like a parachute but requires inflation like a SIAD.

Viability: Nearly all mid L/D forward separation options suffer from a challenge of separating the aeroshell nose cap from the lander after exiting the aeroshell. On its own, the nose cap ballistic number is not large enough to provide separation from the lander.

Forward Work: A modification of this option is required to provide nose cap separation from the lander. Also, sizing of the trailing IAD is also forward work with drag augmentation and angle of attack trimming two factors in sizing.

Rear Exit with Trailing IAD on Lander – Ellipse Sled: Rank 13

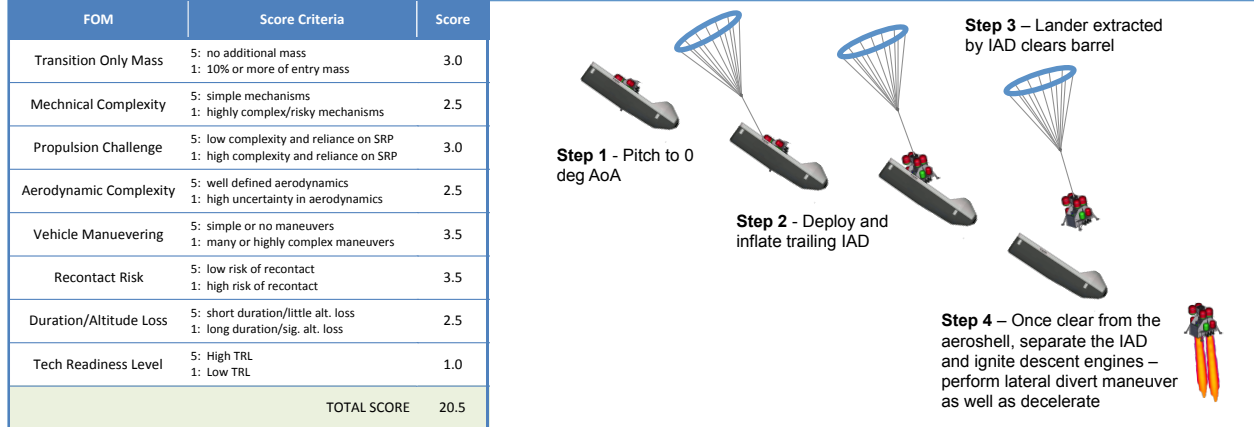


Figure 4-92 Rear exit with trailing IAD attached to lander – ellipse sled version.

Transition Description

In this transition option, the aeroshell is a partially open ellipse sled allowing a rearward exit through the side opening of the vehicle, as shown in Figure 4-92. The vehicle is first pitched to 0° angle of attack. A trailing IAD attached to the lander is then deployed and inflated, followed by separation of the lander from the rear of the aeroshell. Once clear of the aeroshell, the IAD is jettisoned and the lander ignites its descent engines and executes powered descent. The IAD was sized as needing to be greater than 17 m in diameter to lower the lander ballistic coefficient to provide separation.

FOM Score: 20.5/40

Significant Pros: No significant advantages were identified for this option.

Significant Cons: Because of the use of IAD technology, this option scores low on mechanical complexity and technology readiness, being lower in technology readiness than the similar SIAD rear exit option. It was also judged to take longer to execute relative to other options, in part because of the time needed to deploy and inflate the IAD.

Viability: Viability is somewhat dependent on the practicalities of using a trailing IAD.

Forward Work: None current identified.

Rear Exit with Trailing IAD on Lander: Rank 14

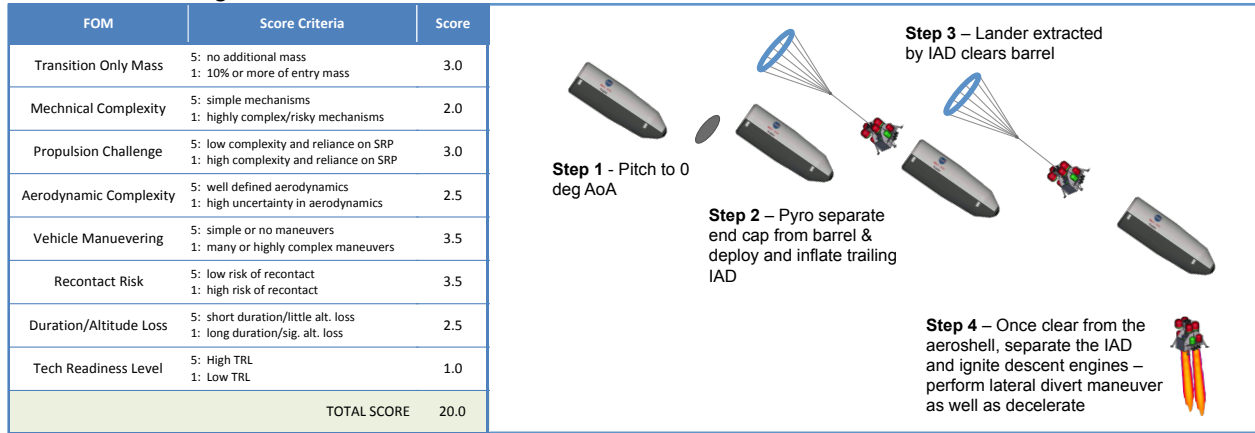


Figure 4-93 Rear exit with trailing IAD attached to lander.

As shown in Figure 4-93, this rear exit separation option utilizes a trailing IAD on the lander to provide a rear exit from the aeroshell. The transition begins when the vehicle pitches to zero degree angle of attack. The rear end cap of the mid L/D aeroshell is then jettisoned and RCS thrusters are used to move the lander toward the rear of the aeroshell. Once partially clear of the aeroshell, a trailing IAD attached to the top of the lander is deployed and inflated to increase lander drag and remove the lander from the aeroshell. Once clear of the aeroshell, the lander jettisons the trailing IAD and ignites its descent engines and executes powered descent. Initial sizing work shows the trailing IAD needs to be greater than 14 m in diameter in order to provide lander separation from the aeroshell.

FOM Score: 20/40

Significant Pros: No significant advantages were identified with this option, although because of the heavier aeroshell, the trailing IAD does not need to be as large as that in the previous ellipse sled option.

Significant Cons: Because of the use of trailing IAD technology, this option scores low on mechanical complexity and very low in technology readiness. It was also judged to take longer to execute relative to other options, in part because of the time to move the lander to the rear of the aeroshell before for IAD deployment, and because of the time to deploy and inflate the IAD.

Viability: Understanding of viability is dependent in part of the ability of RCS thrusters to move the lander to the rear of the aeroshell and on the practicality of deploying and inflating a trailing IAD.

Forward Work: Analysis of RCS thrust level required to put lander in position to deploy trailing IAD.

Side Exit with SIAD on Lander: Rank 15

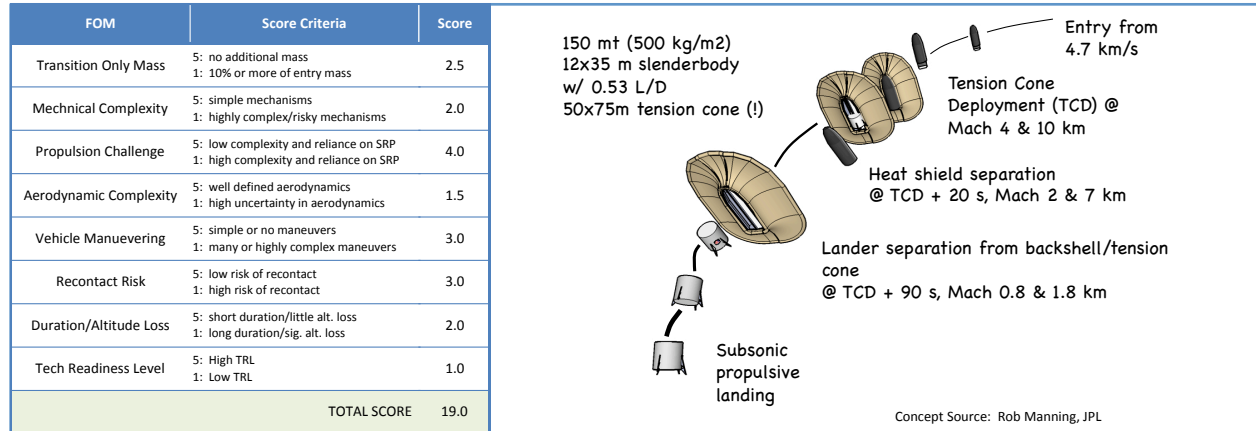


Figure 4-94 Side exit with SIAD on lander.

Transition Description

This only side exit option examined in this assessment utilizes a very large SIAD, as shown in Figure 4-94. This option does not require a maneuver to 0° angle of attack. Instead, at 55° angle of attack a very large attached tension cone SIAD is inflated to greatly reduce the ballistic coefficient of the entry system. At Mach 2, the heatshield (lower half of the aeroshell) is jettisoned and at Mach 0.8 the lander is dropped out from the aeroshell. . Once clear of the aeroshell, the lander ignites its descent engines, maneuvers to powered descent attitude and executes powered descent.

FOM Score: 19/40

Significant Pros: This option scores well on propulsion challenge due to its low reliance on propulsion for the transition event.

Significant Cons: The option was judged to be an aerodynamic and mechanical complexity challenge due to the deployment and inflation of the very large tension cone. Also, because of the large size of the tension cone, the option scored low in transition only mass. A low technology readiness score was given because of the maturity of very large SIAD technology.

Viability: Viability is dependent on the ability to deploy and uniformly inflate a very large tension cone SIAD.

Forward Work: No forward work is currently identified for this option.

4.10.4.3 Hypersonic Inflatable Aerodynamic Decelerator (HIAD)

The following are the 9 HIAD transition options assessed as part of the step 1 high-level assessment, shown in order of scoring rank by transition type: front exit, rear exit, and no exit.

4.10.4.3.1 Front Exit

Front Exit with Canted Thrusters on Lander: Front Exit Rank 1

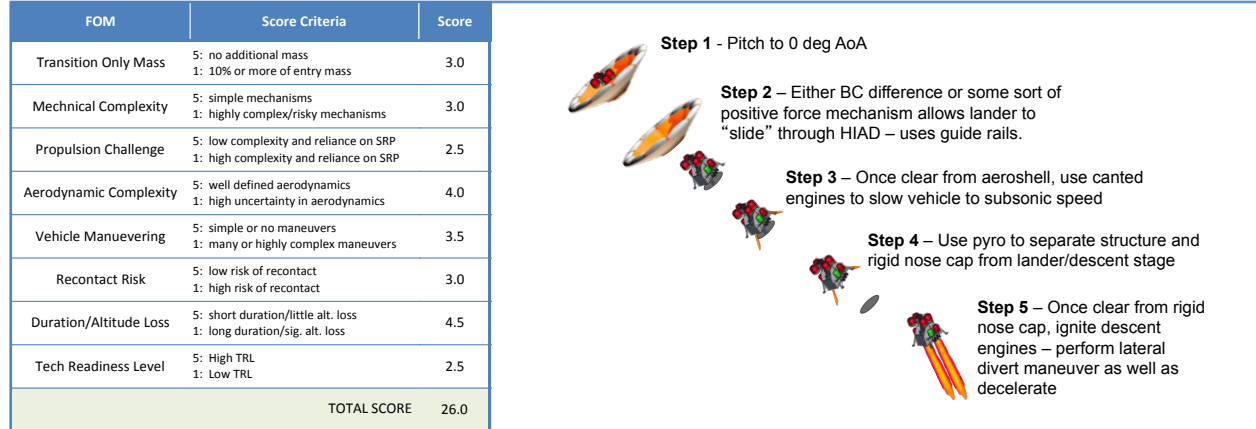


Figure 4-95 Front exit with canted descent thrusters and subsonic heatshield jettison.

Transition Description

In this option, the lander separates from the HIAD via the significant difference in their ballistic coefficients. The vehicle is pitched to 0° angle of attack and pyros fire to detach the lander from the HIAD, as shown in

Figure 4-95. The lander with rigid heatshield still attached separates from the HIAD. Once clear of the HIAD, canted descent thruster that fire around the rigid heatshield ignite and slow the lander. Once subsonic, the heatshield is jettisoned from the lander and once clear of the heatshield, the lander ignites the remaining descent engines and performs powered descent.

FOM Score: 26/40

Significant Pros: This option scores well on duration/loss of altitude given that the descent engines begin firing early in the transition sequence. The separations are relatively simple and the event was score high on aerodynamic complexity.

Significant Cons: Given the engineering challenge of designing canted descent engines that thrust around the heatshield, propulsion challenge was scored low.

Viability: The option appears to be viable, although heatshield separation from the lander needs closer examination.

Forward Work: Sizing of canted descent thrusters and analysis of heatshield separation from lander. This option was selected to be carried forward for more detailed analysis.

Front Exit with Heatshield Jettison From HIAD/Lander Combo: Front Exit Rank 2

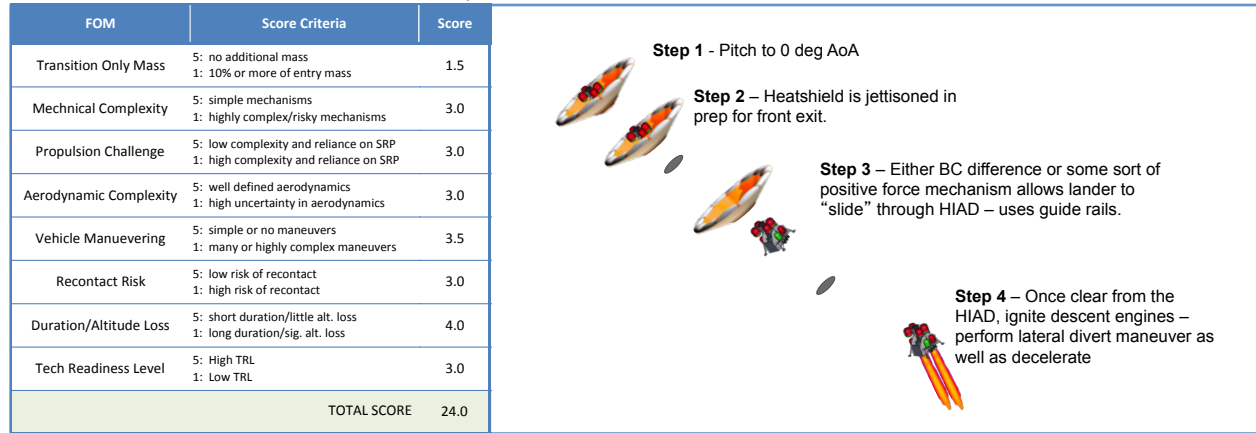


Figure 4-96 Front exit with supersonic heatshield jettison from HIAD/lander combination.

Transition Description

This transition option also executes a forward exit of the lander from the HIAD, as shown in Figure 4-96. The vehicle is first pitched to 0° angle of attack. Pyros fire and separate the HIAD heatshield prior to lander separation. Once the heatshield is away, the lander then separates from the HIAD. Once clear of the HIAD, the lander ignites the descent engines and performs powered descent. Initial sizing work indicates the heatshield would need more than 11.6 t of ballast to separate it from the HIAD/Lander combination.

FOM Score: 24/40

Significant Pros: This option scored well on event duration/altitude loss.

Significant Cons: Because of the very large amount of ballast required to achieve a heatshield separation ballistic coefficient sufficient for heatshield separation, this option scored poorly on mass efficiency.

Viability: This option appears viable although not mass efficient.

Forward Work: A closer examination of heatshield separation was identified as forward work.

Front Exit with Supersonic Heatshield Jettison From Lander: Front Exit Rank 3

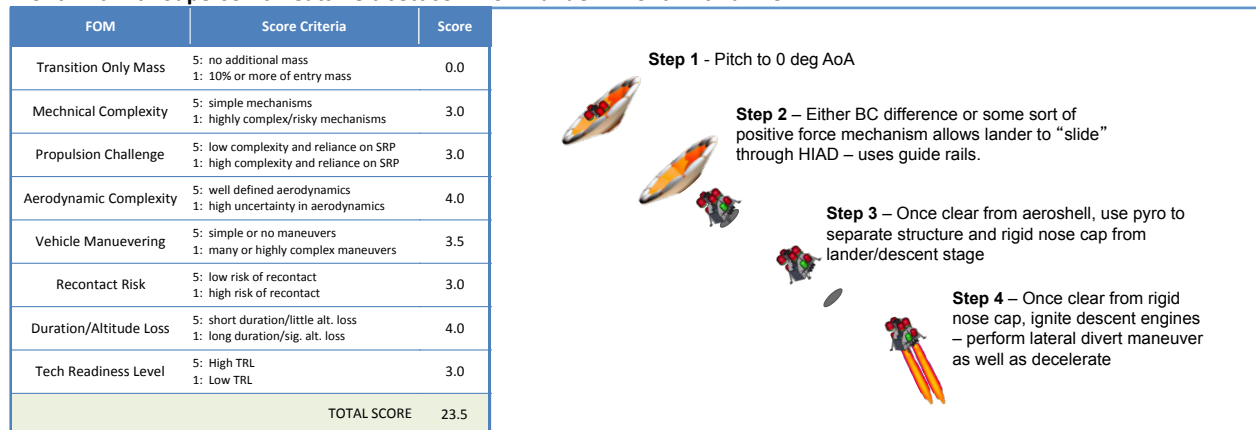


Figure 4-97 Front exit with supersonic heatshield jettison after lander separation from HIAD.

Transition Description

The front exit with supersonic heatshield separation transition option also executes a forward exit of the lander from the HIAD, as shown in Figure 4-97. The vehicle is first pitched to 0° angle of attack. Pyros fire and the lander separate with heatshield attached. Once clear of the HIAD, the heatshield is separated from the lander. With the heatshield away, the lander ignites the descent engines and performs powered descent. Initial sizing work indicates the heatshield would need at least the mass of the wet lander, about 73 t, of ballast to separate it from the lander while in free-fall.

FOM Score: 23.5/40

Significant Pros: This option scores well on aerodynamic complexity and duration.

Significant Cons: This option scores a zero on mass efficiency because, as formulated, an unreasonable amount of ballast would be needed on the heatshield to get it away from the lander while in free-fall.

Viability: The option is not viable unless heatshield separation can be reworked, reducing the mass needed for the transition event.

Forward Work: A modification of this option is required to provide a workable heatshield separation from the lander.

Front Exit with Separation Thruster on Lander: Front Exit Rank 4

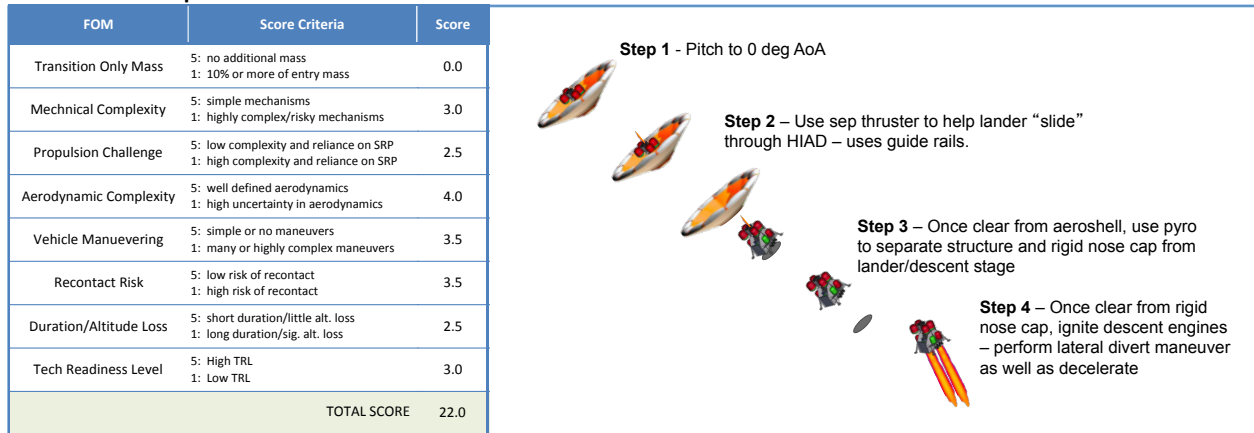


Figure 4-98 Front exit with separation thruster on lander.

Transition Description

The final front exit option examined in this assessment uses a separation thruster on the lander to aid lander separation, as shown in Figure 4-98. To begin the transition, the vehicle is pitched to 0° angle of attack and pyros are fired to initiate lander separation. A separation thruster on the lander fires and adds thrust force to move the lander through and out of the HIAD. Once clear of the HIAD, the heatshield is separated and the lander ignites the descent engines and performs powered descent. The initial sizing work shows that this option would also need more than 73 t of ballast on the heatshield to separate it from the lander.

FOM Score: 22/40

Significant Pros: This option scored well on aerodynamic complexity.

Significant Cons: This option also received a score of zero for transition only mass because of the unreasonable amount of heatshield ballast. An additional weakness is duration/altitude loss because the separation thruster on the lander in providing the lander with delta-v, while aiding the separation, is adding velocity to the lander in an undesired direction. Because the lander ballistic coefficient is already much larger than the HIAD alone ballistic coefficient, using a lander separation thruster is not needed and a poor idea.

Viability: The heatshield ballast mass issue makes this option not viable in its current form.

Forward Work: This option should be discarded because there is no reason to have a lander-attached separation thruster.

4.10.4.3.2 Rear Exit

Rear Exit with Separation Thruster on Lander: Rear Exit Rank 1

FOM	Score Criteria	Score
Transition Only Mass	5: no additional mass 1: 10% or more of entry mass	2.5
Mechanical Complexity	5: simple mechanisms 1: highly complex/risky mechanisms	5.0
Propulsion Challenge	5: low complexity and reliance on SRP 1: high complexity and reliance on SRP	2.0
Aerodynamic Complexity	5: well defined aerodynamics 1: high uncertainty in aerodynamics	4.5
Vehicle Maneuvering	5: simple or no maneuvers 1: many or highly complex maneuvers	4.0
Recontact Risk	5: low risk of recontact 1: high risk of recontact	2.0
Duration/Altitude Loss	5: short duration/little alt. loss 1: long duration/sig. alt. loss	3.5
Tech Readiness Level	5: High TRL 1: Low TRL	3.5
TOTAL SCORE		27.0

Figure 4-99 Rear exit with separation thrusters on lander.

Transition Description

This rear exit option utilizes separation thrusters on the lander to remove the lander from the HIAD, as shown in Figure 4-99. The transition begins with the vehicle pitching to 0° angle of attack. Pyros are fired to separate the lander from the HIAD and separation thrusters on the lander ignite to remove the lander rearward from the HIAD. Once clear of the HIAD, the lander ignites its descent engines and executes powered descent. Very preliminary, first-order sizing of the separation thrusters indicates at least 0.27 MN of thrust is required to separate the lander.

FOM Score: 27/40

Significant Pros: This option scores well on mechanical complexity and aerodynamic complexity.

Significant Cons: The amount of mass needed for the separation thruster propulsion system, including hardware and propellant, was identified as possibly resulting in significant additional mass for the transition event. Separation thruster plume interaction with the HIAD was assessed as adding recontact risk.

Viability: The option appears viable with more examination needed of thruster sizing and plume interactions/impingements with the HIAD.

Forward Work: More detailed assessment of separation thruster sizing and plume effects on HIAD.

Rear Exit with Parachute on Lander: Rear Exit Rank 2

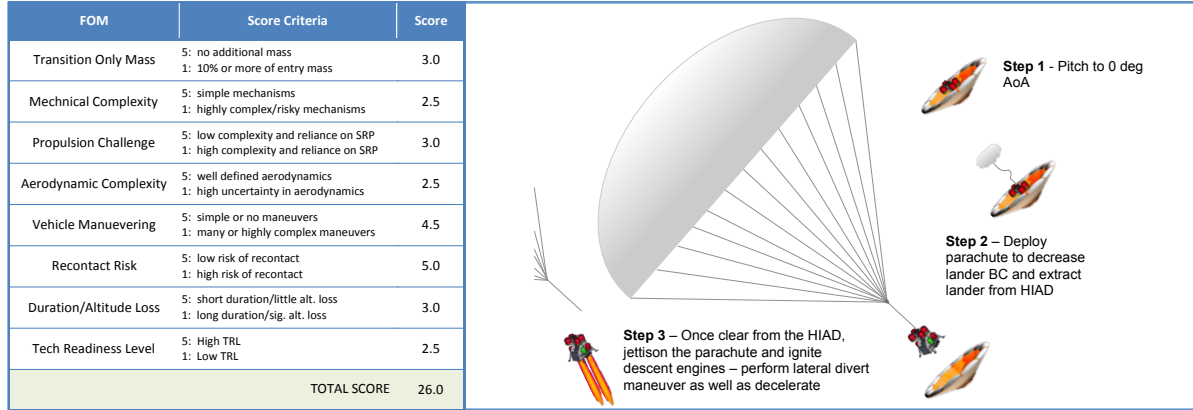


Figure 4-100 Rear exit with parachute attached to lander.

Transition Description

This rear exit option utilizes a parachute(s) attached to the lander to remove the lander from the HIAD, as shown in Figure 4-100. The transition begins with the vehicle pitching to 0° angle of attack. A parachute is deployed off the lander and after full inflation, pyros are fired to separate the lander from the HIAD. The increased drag from the parachute removes the lander rearward from the HIAD. Once clear of the HIAD, the lander jettisons the parachute, ignites its descent engines and executes powered descent. Initial sizing of the parachute indicates a parachute of size greater than 100 m in diameter is needed to separate the lander from the HAID.

FOM Score: 26/40

Significant Pros: This option scores well on vehicle maneuvering, requiring a minimum of vehicle attitude maneuvering, and on recontact risk.

Significant Cons: The very large parachute or cluster of smaller parachutes leads to mechanical and aerodynamic complexity for this option. Also there is very no flight experience with very large parachutes and clusters of parachutes at Mars.

Viability: Viability is dependent on the ability to use very large parachutes or clusters of parachutes at Mars.

Forward Work: More detailed sizing of a single very large parachute or clusters of parachutes including design of mechanical configuration.

Rear Exit with SIAD on Lander: Rear Exit Rank 3

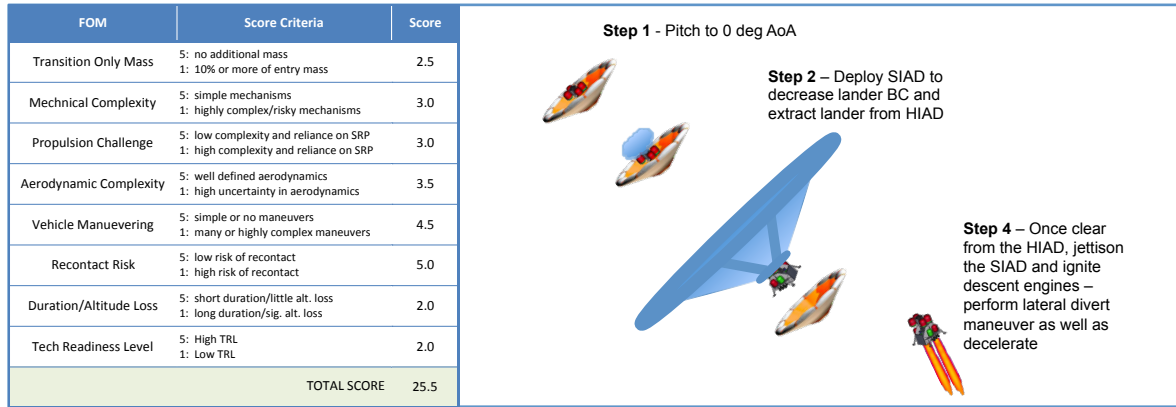


Figure 4-101 Rear exit with SIAD attached to lander.

Transition Description

This rear exit option uses a SIAD to increase drag on the lander, rather than a parachute. As shown in Figure 4-101, the vehicle is pitched to 0° angle of attack, then a SIAD attached to the top of the lander is inflated increasing the drag of the lander. Pyros are fired separating the lander from the HIAD and the lander exits rearward from the HIAD. Once clear of the HIAD, the lander jettisons the SIAD, ignites its descent engines and executes powered descent. Initial sizing of the SIAD indicates a diameter greater than 63 m is needed to separate the lander from the HIAD.

FOM Score: 25.5/40

Significant Pros: This option scores well on vehicle maneuvering and recontact risk.

Significant Cons: The very large SIAD leads to mechanical and aerodynamic complexity for this option. Also there is concern about aerodynamic interactions while inflating a SIAD while in the wake of a HIAD. This option also has the potential to add significantly to system mass.

Viability: Viability is dependent on the ability to use a very large SIAD at Mars.

Forward Work: More detailed sizing of SIAD to achieve robust lander separation.

Rear Exit with Trailing IAD on Lander: Rear Exit Rank 4

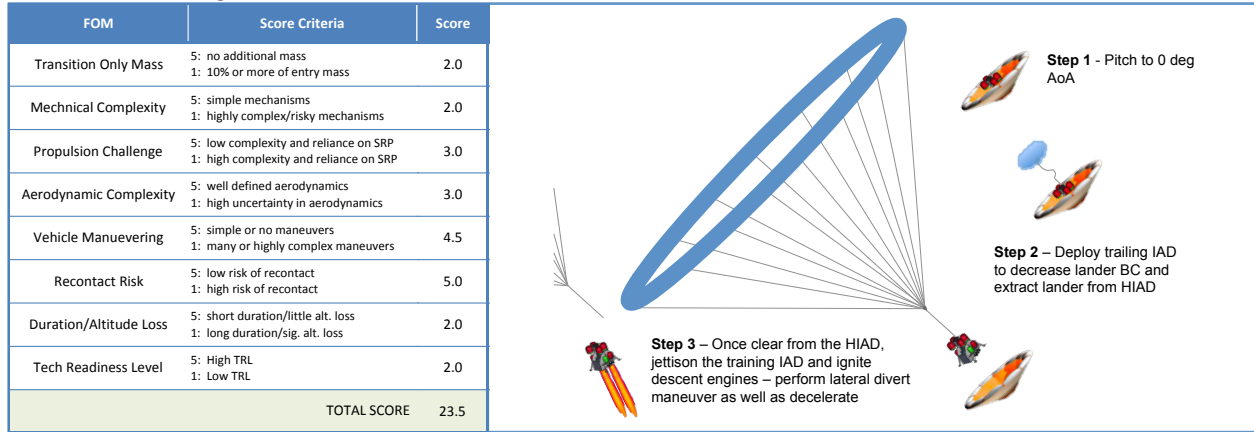


Figure 4-102 Rear exit with IAD attached to lander.

Transition Description

This rear exit option uses a trailing IAD to increase drag on the lander, rather than a parachute or SIAD. As shown in Figure 4-102, the vehicle is pitched to 0° angle of attack, then a trailing IAD attached to the top of the lander is first deployed and then inflated, increasing the drag of the lander. Pyros are fired separating the lander from the HIAD and the lander exits rearward from the HIAD. Once clear of the HIAD, the lander jettisons the trailing IAD, ignites its descent engines and executes powered descent. Initial sizing of the trailing IAD indicates an IAD diameter greater than 110 m is needed to separate the lander from the HIAD.

FOM Score: 23.5/40

Significant Pros: This option scores well on vehicle maneuvering, as well as recontact risk.

Significant Cons: To generate enough drag, a very large IAD is required, leading to concerns about aerodynamic complexity and mechanical complexity. Mass is also a concern. The trailing IAD suffers from the deployment complexity of a parachute and the mechanical inflation complexity of the SIAD combined in one system.

Viability: Viability is dependent on the ability to use a very large trailing IAD at Mars.

Forward Work: More detailed sizing of the trailing IAD to achieve robust lander separation.

Rear Exit with Separation Thrusters on HIAD: Rear Exit Rank 5

FOM	Score Criteria	Score
Transition Only Mass	5: no additional mass 1: 10% or more of entry mass	1.5
Mechanical Complexity	5: simple mechanisms 1: highly complex/risky mechanisms	4.5
Propulsion Challenge	5: low complexity and reliance on SRP 1: high complexity and reliance on SRP	1.5
Aerodynamic Complexity	5: well defined aerodynamics 1: high uncertainty in aerodynamics	4.5
Vehicle Maneuvering	5: simple or no maneuvers 1: many or highly complex maneuvers	3.5
Recontact Risk	5: low risk of recontact 1: high risk of recontact	2.0
Duration/Altitude Loss	5: short duration/little alt. loss 1: long duration/sig. alt. loss	3.0
Tech Readiness Level	5: High TRL 1: Low TRL	3.0
TOTAL SCORE		23.5

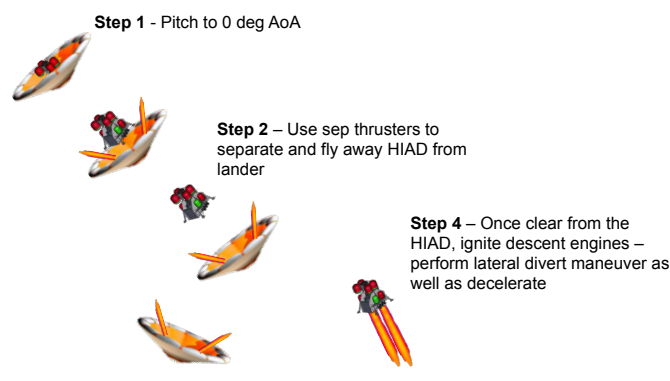


Figure 4-103 Rear exit with separation thrusters on HIAD.

Transition Description

The rear exit option with separation thrusters on the HIAD uses a set of separation thrusters mounted on the HIAD to provide separation from the lander. Shown in Figure 4-103, the transition begins when the HIAD entry vehicle is pitched to 0° angle of attack. Pyros are then fired to separate the lander from the HIAD and the separation thrusters on the HIAD ignite to move the HIAD away from the lander. The separation thrusters are canted to minimize plume impingement on the lander. Once the HIAD is clear of the lander, the lander ignites its descent engines and executes powered descent. Using the separation thrusters, the HIAD is maneuvered away from the lander after separation. An initial sizing of the separation thrusters shows thrust on the order of 3 MN is required, larger than the descent engines on the lander.

FOM Score: 23.5/40

Significant Pros: This option scores well on mechanical complexity and aerodynamic complexity.

Significant Cons: Because the HIAD alone has a low ballistic coefficient, a very large propulsion system is required to thrust it away from the lander. This gives a low transition only mass score, and engineering the propulsion system was also considered a challenge.

Viability: The system is potentially viable but is poor in mass efficiency.

Forward Work: More detailed sizing of the sizing of the required separation thrust.

4.10.4.3.3 No Exit

No Exit Carrying Inflated HIAD to Surface: No Exit Rank 1

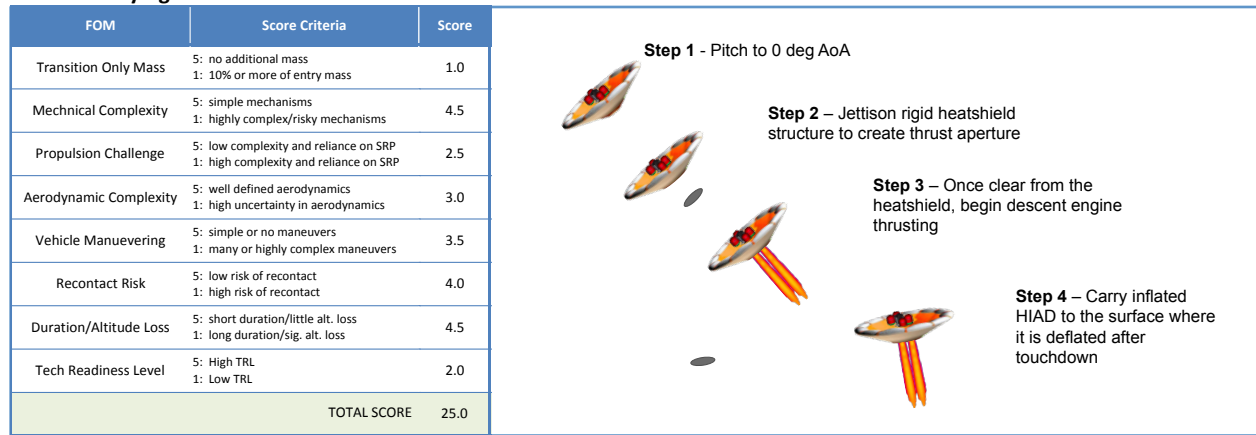


Figure 4-104 No exit carrying inflated HIAD to surface.

Transition Description

In the no exit option with HIAD inflated, the lander does not separate from the HIAD but instead descends to the surface with the inflated HIAD still attached to the lander. As shown in Figure 4-104, the vehicle is pitched to 0° angle of attack and the heatshield is separated from the HIAD/lander combination. Once clear of the heatshield, the lander descent engines are fired and powered descent begins. The lander touches down on the surface with the inflated HIAD attached. As with other similar options, initial sizing shows the heatshield would need greater than 11.5 t of ballast to separate from the HIAD/lander combination.

FOM Score: 25/40

Significant Pros: This option has only one separation event, so it scores high on mechanical complexity and recontact risk. There is also some drag advantage descending with an inflated HIAD to the surface.

Significant Cons: Because of the large ballistic coefficient needed for heatshield separation, this event scores low on addition system mass needed just for the transition. Propulsion was also considered a challenge thrusting through the opening in the HIAD.

Viability: Viability depends on further assessment of performing powered descent with a fully inflated HIAD.

Forward Work: Further assessment of performing powered descent with fully inflated HIAD.

No Exit Carrying deflated HIAD to Surface: No Exit Rank 2

FOM	Score Criteria	Score
Transition Only Mass	5: no additional mass 1: 10% or more of entry mass	1.0
Mechanical Complexity	5: simple mechanisms 1: highly complex/risky mechanisms	3.5
Propulsion Challenge	5: low complexity and reliance on SRP 1: high complexity and reliance on SRP	2.5
Aerodynamic Complexity	5: well defined aerodynamics 1: high uncertainty in aerodynamics	2.5
Vehicle Maneuvering	5: simple or no maneuvers 1: many or highly complex maneuvers	3.5
Recontact Risk	5: low risk of recontact 1: high risk of recontact	4.0
Duration/Altitude Loss	5: short duration/little alt. loss 1: long duration/sig. alt. loss	4.5
Tech Readiness Level	5: High TRL 1: Low TRL	1.5
TOTAL SCORE		23.0

Figure 4-105 No exit carrying deflated HIAD to surface.

Transition Description

In the no exit option with HIAD deflated, the lander does not separate from the HIAD but instead descends to the surface with the deflated HIAD still attached to the lander. As shown in Figure 4-105, the vehicle is pitched to 0° angle of attack and the heatshield is separated from the HIAD/lander combination. Once clear of the heatshield, the HIAD is deflated and retracted to the lander. The lander descent engines are then fired and powered descent begins. The lander touches down on the surface with the deflated HIAD attached. As with other similar options, initial sizing shows the heatshield would need greater than 11.5 t of ballast to separate from the HIAD/lander combination.

FOM Score: 23/40

Significant Pros: This option has only one separation event, so it scores high on mechanical complexity and recontact risk.

Significant Cons: Because of the large ballast coefficient needed for heatshield separation, this event scores low on additional system mass needed just for the transition. Relative to the no exit inflated HIAD option, this option has more mechanical complexity due to retraction of the deflated HIAD material, and more aerodynamic complexity due to deflation of the HIAD while in flight.

Viability: Viability depends on further assessment of performing powered descent with a deflated HIAD.

Forward Work: Further assessment of performing powered descent with deflated HIAD.

4.10.5 Initial Most Viable Options

As mentioned above, the purpose of the high-level assessments of the transition methods documented in the previous section was to identify promising transition options as candidates for more detailed analysis. The options discussed below received the highest scores based on the transition event FOMs; however, because this is the result of a first, high-level assessment, other options not scoring as well as those shown here may, as a result of more thorough and detailed analysis, in the end prove to be as good or better options. Also, transitions created by combining option assessed in this study may also, in future assessments, show more viability. Therefore, it is important that these results not be considered an answer, but rather a guide directing more detailed assessments

4.10.5.1 Mid L/D Architecture

The clamshell options were assessed as the two most viable options for the mid L/D architectures. As shown in Figure 4-106, both the front exit clam shell option and side exit calm shell option have been identified for further, more detailed assessment using the higher fidelity tool described in Section 4.10.6. These two options were assessed as most viable based on low impact to system mass, mechanical simplicity and duration of transition

execution.

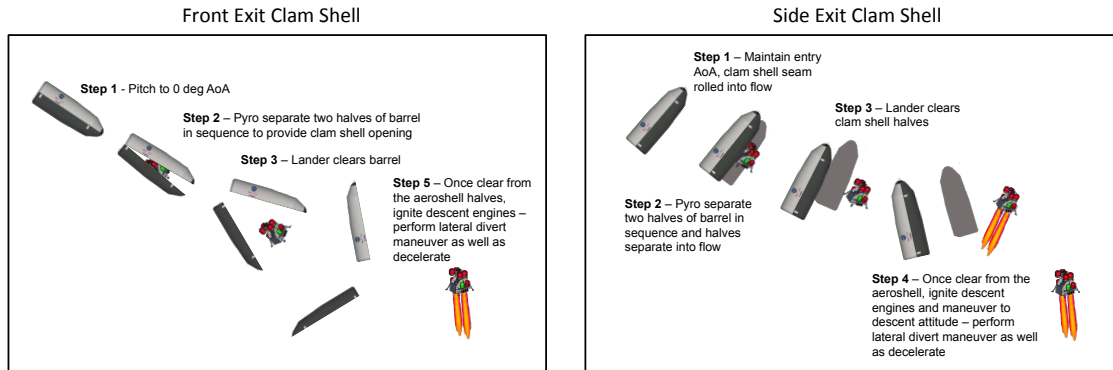


Figure 4-106 Options assessed as most viable for the mid L/D architecture transition event.

4.10.5.2 HIAD Architecture

When carrying out the assessment of the HIAD transition options, the advantages and disadvantage of different options did not provide a crisp separation of options when judging those that were most viable. Therefore, rather than identify the top scoring options from all options, to capture a representative group going forward, the top scoring option from each category (front exit, rear exit, no exit) of transition was identified for future, more detail analysis. The most viable options for each category is shown in Figure 4-107. In the front exit category, the canted thruster option received the highest score due to its relative mechanical simplicity, potential for short execution

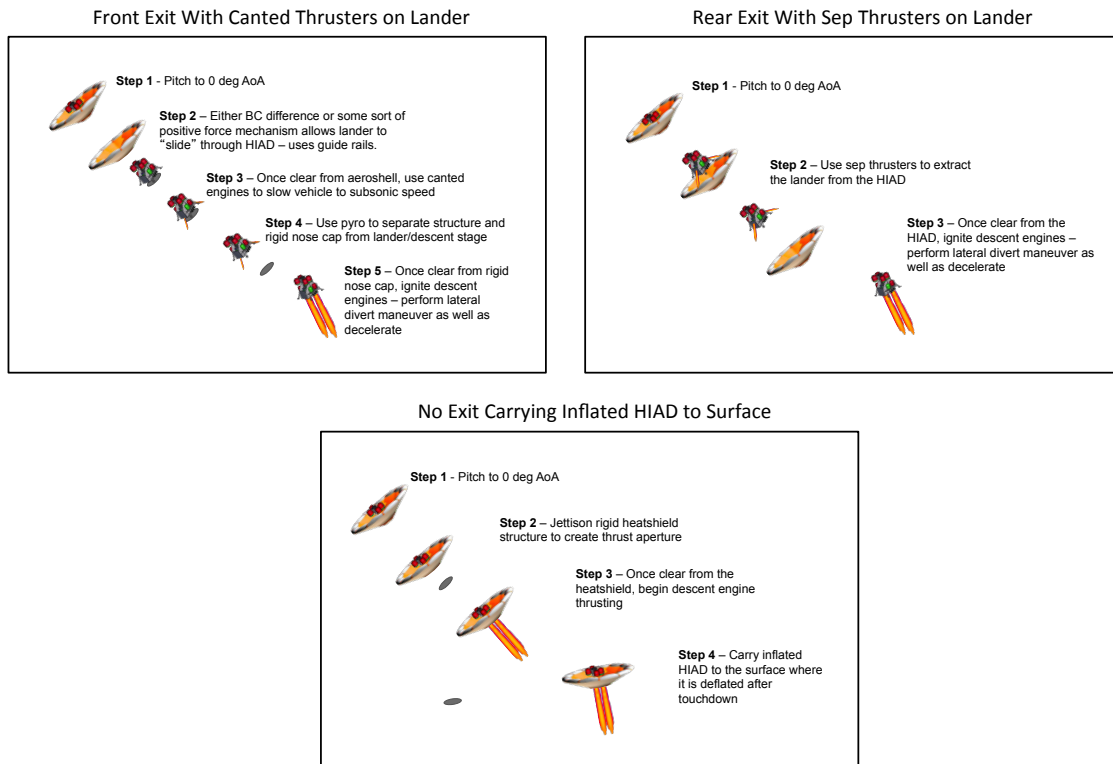


Figure 4-107 Options, per category, assessed as most viable for the HIAD architecture transition event.

duration and viable method for heatshield separation from lander. For the rear exit option, the separation thrusters on lander score well on mechanical complexity and aerodynamic complexity, and higher score than other rear exit options across other FOMs. For the no exit option, the inflated HIAD option scored higher than the deflated option mainly because of the added complexity created by the retraction of the deflated HIAD.

4.10.6 Transition Modeling and Simulation

4.10.6.1 Transition Simulation Description

The Program to Optimize Simulated Trajectories II (POST2)^{9,10} with the Constraint Force Equation (CFE) methodology^{11,12} implementation was chosen to simulate the separation of the Mars Lander from the mid L/D ridged aeroshell and HIAD entry vehicles. The CFE implementation within POST2 allows forces and moments to be transmitted between multiple bodies connected by joints, a condition that is typically encountered in separation problems. Joint models include fixed, revolute, translational, spherical, and customized joints. The CFE method has been validated against industry standard software, as discussed references 11-13. The POST2/CFE method is capable of simulating a complete end-to-end mission,¹³ in addition to the separation portion of a mission. This capability eliminates the potential for “hand-off” errors encountered by using multiple codes for mission simulations, in addition to improving efficiency.

The preliminary simulations discussed in this section focus on the transition portion of the mission. Two configurations were modeled: (1) Mid L/D aeroshell entry vehicle enclosing a vertical lander, (2) HIAD with a vertical lander mounted in the wake region. Flight conditions and mass properties at the start of transition are given in Table 4-44 and Table 4-45 for each configuration. The mass properties for the vertical lander were obtained from reference 14. The weights for the mid L/D aeroshell and HIAD were obtained from reference 15. The centers of gravity and moments of inertia for the Mid L/D aeroshell and HIAD are placeholders until more accurate values can be obtained.

Table 4-44 Flight Conditions at the Start of Transition

Property	Mid L/D	HIAD
Mach	2.93	1.80
Altitude	7840	5121
Relative velocity, m/s	682	424
Relative flight path angle, deg	-10.56	-19.49
Angle of attack, deg	0.0	0.0
Dynamic pressure	1306	633

The aerodynamic database used for the two configurations consists of axial force, normal force, and pitching moments generated using engineering tools and high fidelity computational fluid dynamics analysis tools during an in-house study following DRA 5.0¹⁶. The database generated for both vehicles covers free stream only conditions. (The interference aerodynamics occurring during transition is highly dependent on transition method and has not been modeled.) The database for the mid L/D aeroshell covers Mach numbers ranging from 1.3 through 50 and angles of attack of 0 through 90 degrees, with body flap deflections ranging from -10 to 50 degrees and speed brake deflections ranging from 0 to 60 degrees. Dynamic pressures ranged from 1.E-7 through 0.75 bars. The aerodynamic database for the HIAD vehicle covers Mach 0.3 through 50 and angles of attack of 0 through 33 degrees. Dynamic pressures ranged from 1.E-7 through 0.75 bars. Additional details of the analysis and vehicle geometries are presented in reference 16.

The ground rules, assumptions, and constraints of the simulation are summarized in Table 4-46.

Table 4-45 Thrust and Mass Properties at the Start of Transition

Property	Vertical Lander	Mid L/D	HIAD
Total mass, t	73.04	28.9	10.6
Dry mass, t	53.29	28.9	10.6
Propellant mass, t	19.75	0.0	0.0
Decent stage thrust, N	0	0.0	0.0
X_{cg} , m	5.24	5.0	1.0
Y_{cg} , m	0.0	0.0	0.0
Z_{cg} , m	-0.15	-4.0	0.0
I_{xx} , kg-m ²	5.509E05	5.000E05	10.E05
I_{yy} , kg-m ²	6.555E05	5.000E05	100.E05
I_{zz} , kg-m ²	8.955E05	5.000E05	100.E05
I_{xy} , kg-m ²	6.541E01	0.000E01	0.000E01
I_{xz} , kg-m ²	4.194E04	0.000E01	0.000E01
I_{yz} , kg-m ²	2.949E04	0.000E01	0.000E01

Table 4-46 Ground Rules, Assumptions, and Constraints

Number	Ground Rule, Assumption or Constraint
1	Mars GRAM (2005)
2	No atmospheric winds
3	Mars gravity model (MGS85F2)
4	LOX-CH4 rocket engine on lander, $I_{sp\ vac} = 368$ sec
5	6-DOF during transition
6	Plume interactions not modeled
7	Interference aerodynamics not modeled

The transition concept chosen for the mid L/D aeroshell is the clamshell front exit concept described in section 4.10.4. The simulation begins with the configuration at an angle of attack of 0 degrees. The base of the aeroshell was initially attached at the top of the lander (see Figure 4-80) and modeled in POST2/CFE as a fixed joint. At the beginning of transition, the joint was released and allowed the lander to slide downward along a 2 m long rail. (Within CFE, only one joint is modeled between two bodies to avoid over-constraining the problem.)

The transition concept chosen for the HIAD is the rear exit concept with separation thrusters on the lander, also described in Section 4.10.4. The simulation begins with the configuration at an angle of attack of 0 degrees. The

HIAD was initially attached at the base of the lander (see Figure 4-99) and modeled in POST2/CFE as a fixed joint. At the beginning of transition, the lander thrusters were fired while the joint was simultaneously released, allowing the lander to separate away from the HIAD. The total thrust used in the simulation shown was 546,000 N. This value was selected by estimating the thrust required for the lander terminal velocity to match that of the HIAD and then applying a factor of two to ensure separation.

4.10.6.2 Preliminary Results

4.10.6.2.1 Mid L/D Aeroshell, Clamshell Front Exit Transition Method

The relative distances between the lander and mid L/D aeroshell as a function of transition start time is shown in Figure 4-108. The distances are relative to the attachment point at the top of the lander and aeroshell. Because the lander’s x-axis points in the opposite direction to that of the aeroshell, an increasing negative delta x between the two vehicles indicates that the lander has moved downward and downrange relative to the aeroshell. Meanwhile, the slight increase in delta y and decrease in delta z indicate that the lander has moved slightly to the right and downward. Lander altitude loss during this 4-second simulation period is approximately 500 m., as shown in Figure 4-109.

Additional trajectory parameters include angle of attack, flight path angle, Mach number, velocity, and sensed acceleration as a function of time (Figure 4-110 through Figure 4-114).

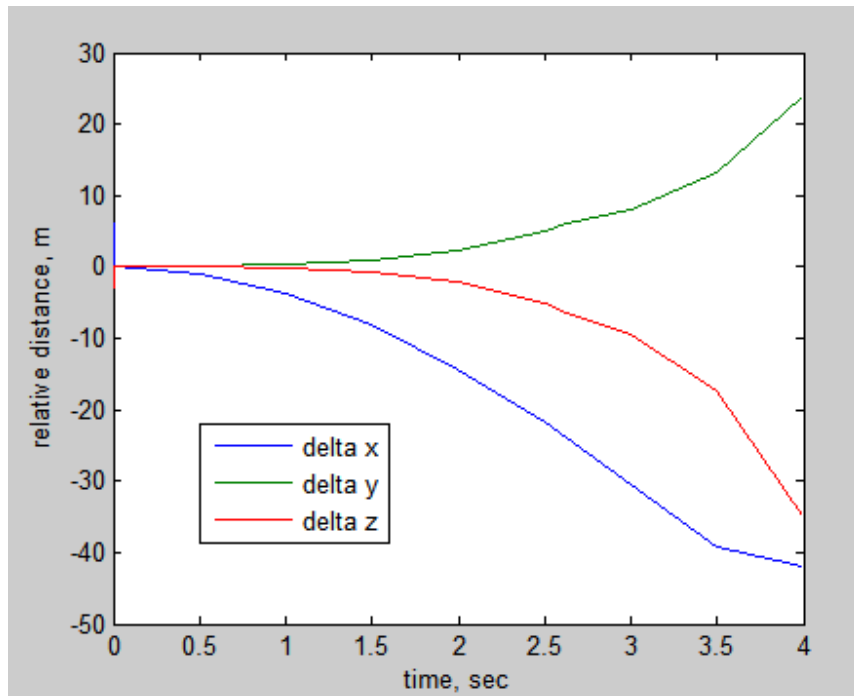


Figure 4-108 Separation distance vs. transition start time.

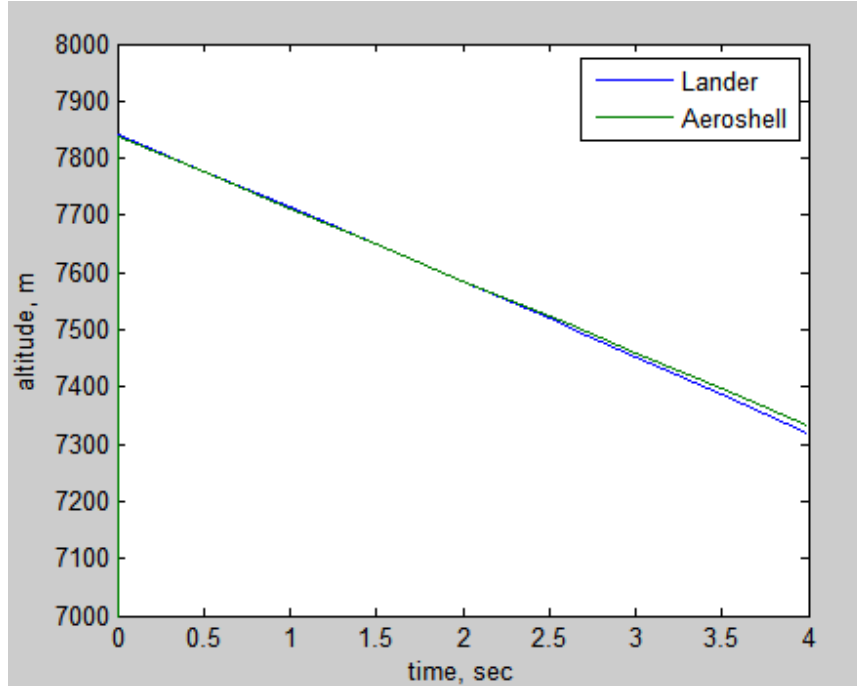


Figure 4-109 Altitude vs. transition start time.

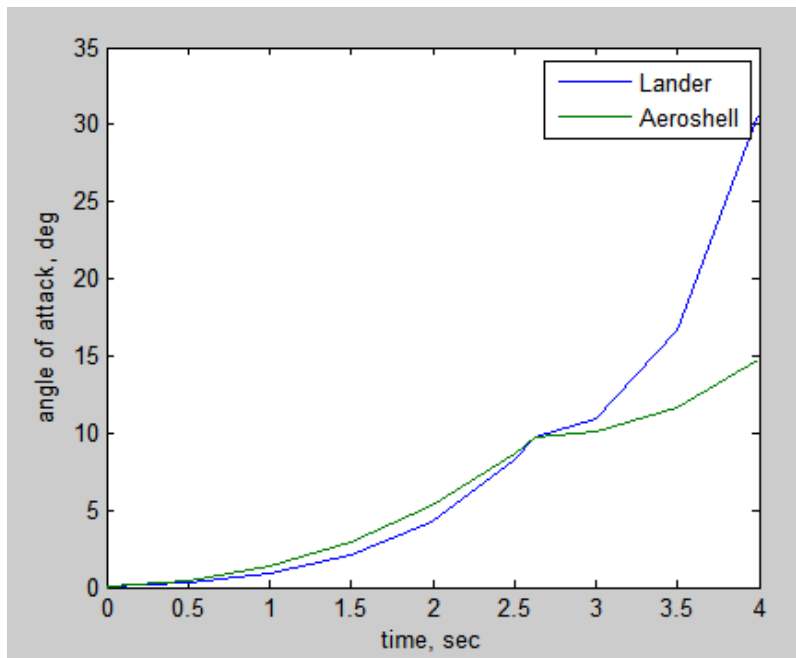


Figure 4-110 Angle of attack vs. transition start time.

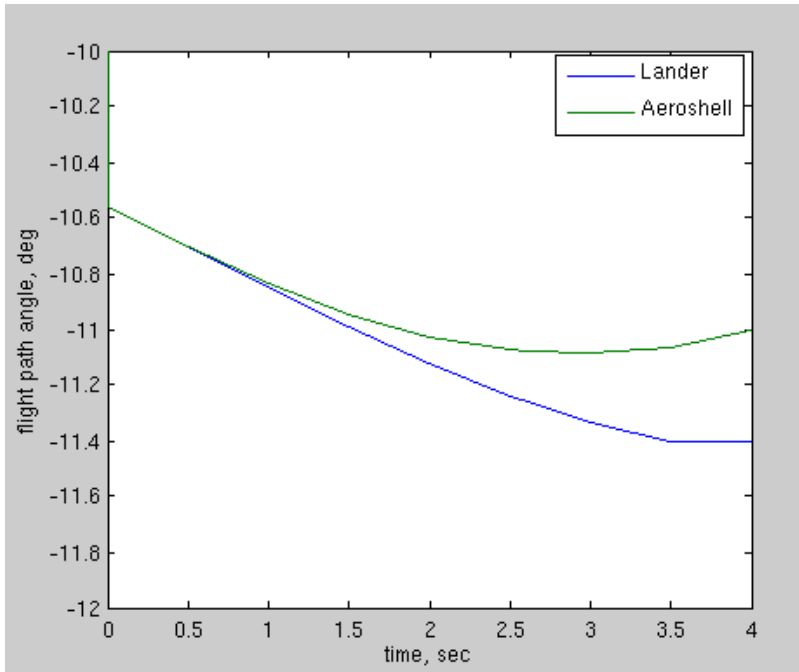


Figure 4-111 Flight path angle vs. transition start time.

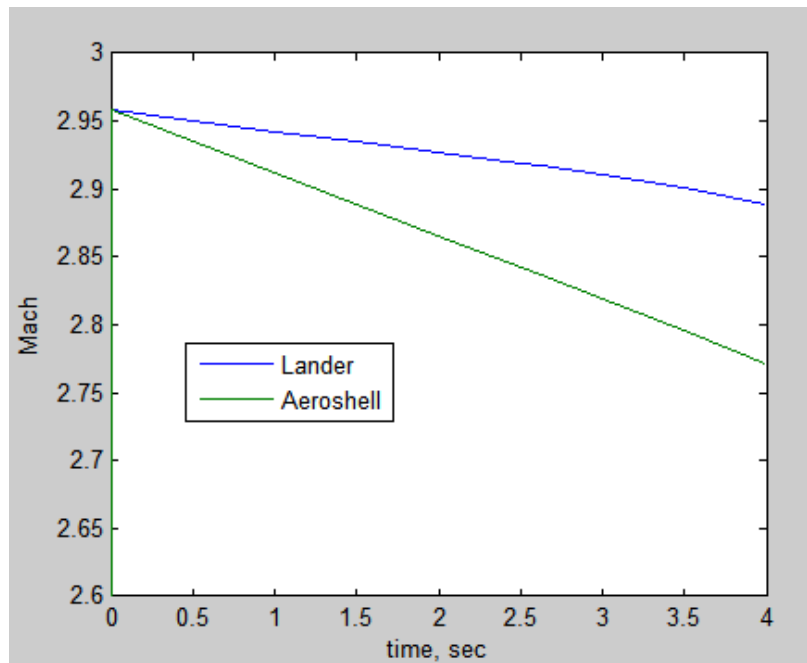


Figure 4-112 Mach number vs. transition start time.

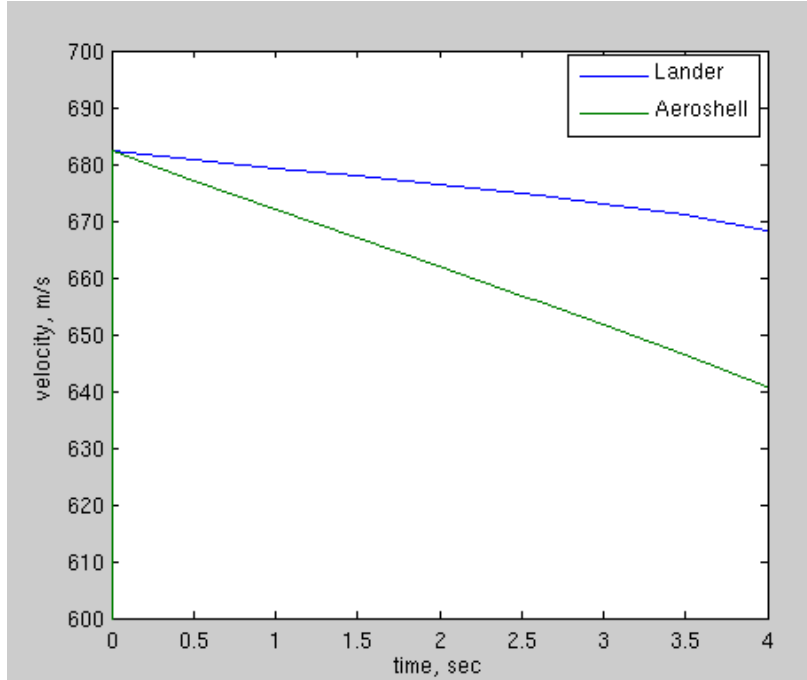


Figure 4-113 Velocity vs. transition start time.

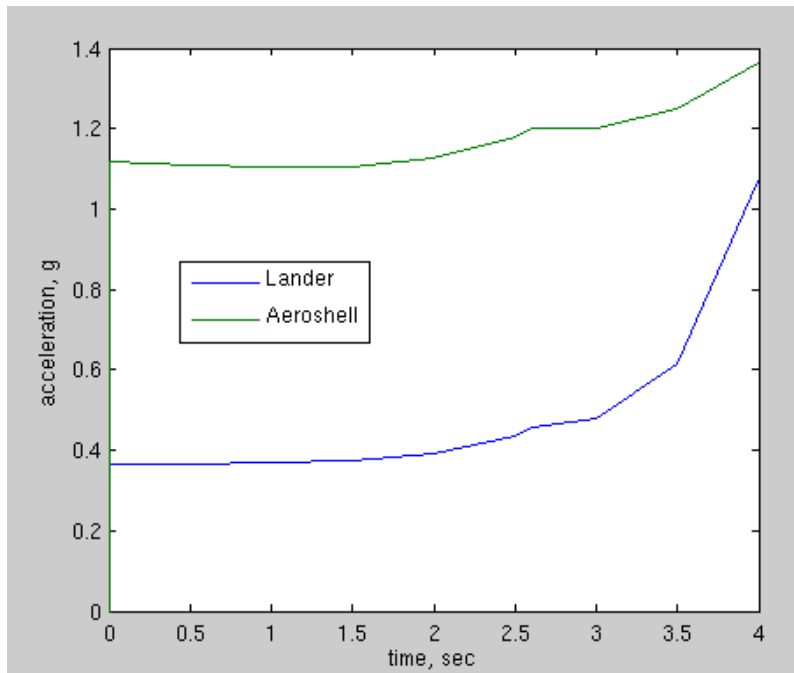


Figure 4-114 Sensed acceleration (Earth G's) vs. transition start time.

4.10.6.2.2 HIAD, Rear Exit with Thrusters

The relative distances between the lander and HIAD as a function transition start time (and thruster firing time) is shown in Figure 4-115. The distances are relative to the attachment point at the base of the lander and center of the

leeward side of the HIAD. The x axis is coincident with the axial centerline of the lander and HIAD and is positive in the aft direction. The y axis is perpendicular to the x-axis, and the z-axis completes the right-hand coordinate system. An increase in delta x indicates that the lander has moved in the axial direction away from the HIAD. Meanwhile, an increase in delta y and delta z indicates that the lander is moving to the right and downward relative to the HIAD. Note that the lander has cleared the HIAD in less than 2 seconds, assuming a HIAD height of 10 m. By 4 seconds, the lander has moved approximately 62 m in the x direction from its attachment location at the center of the HIAD. Propellant consumption during this 4-second period is approximately 800 kg, or about 4 % of the total propellant in the lander fuel and oxidizer tanks Figure 4-116.

Additional trajectory parameters include altitude, velocity, Mach number, angle of attack, flight path angle, and sensed acceleration as a function of time (Figure 4-117 through Figure 4-122). Note that the maximum lander acceleration is approximately 2.3 g.

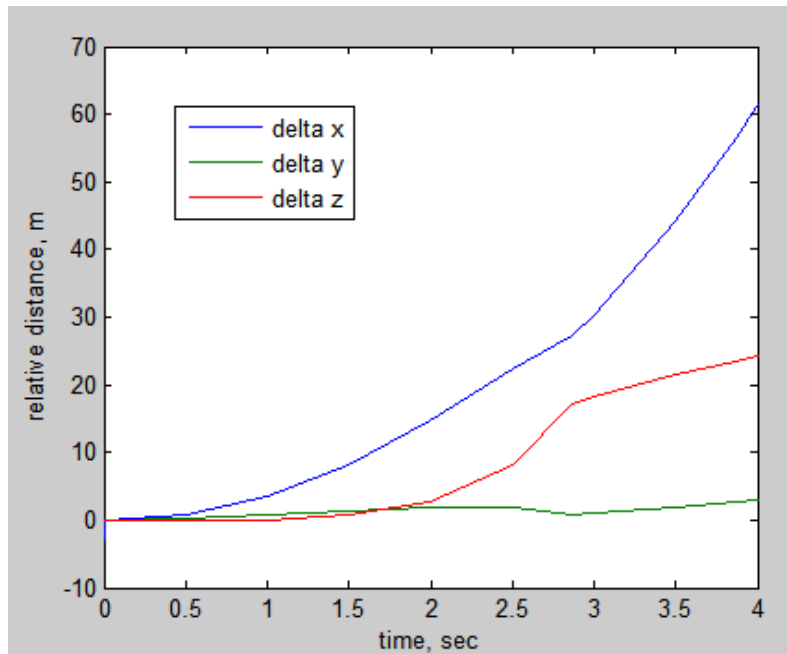


Figure 4-115 Separation distances vs. transition start time

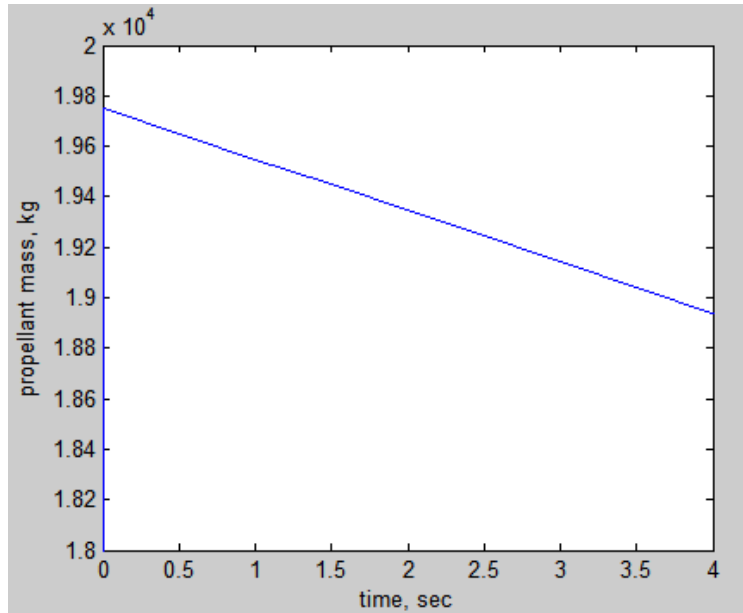


Figure 4-116 Propellant mass vs. transition start time.

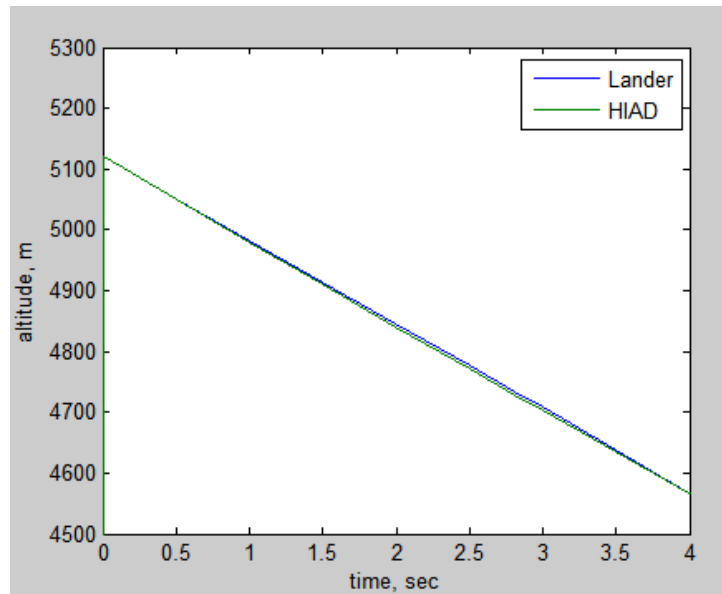


Figure 4-117 Altitude vs. transition start time.

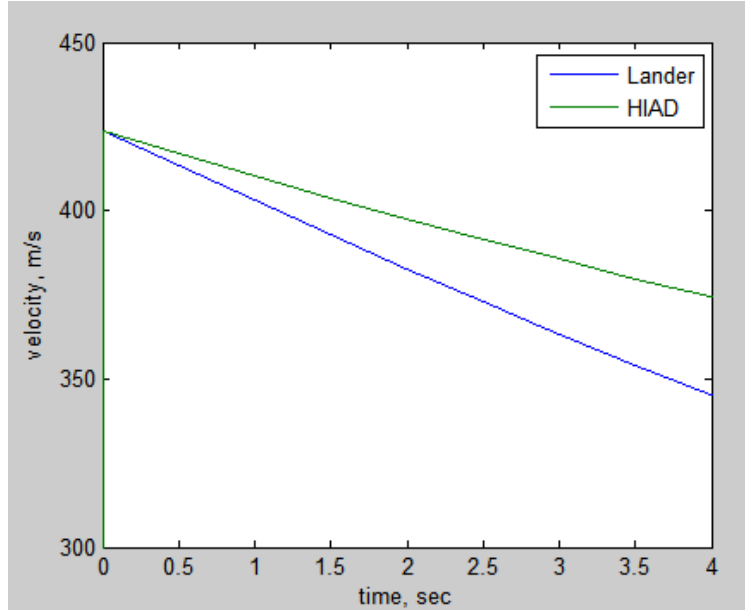


Figure 4-118 Velocity vs. transition start time.

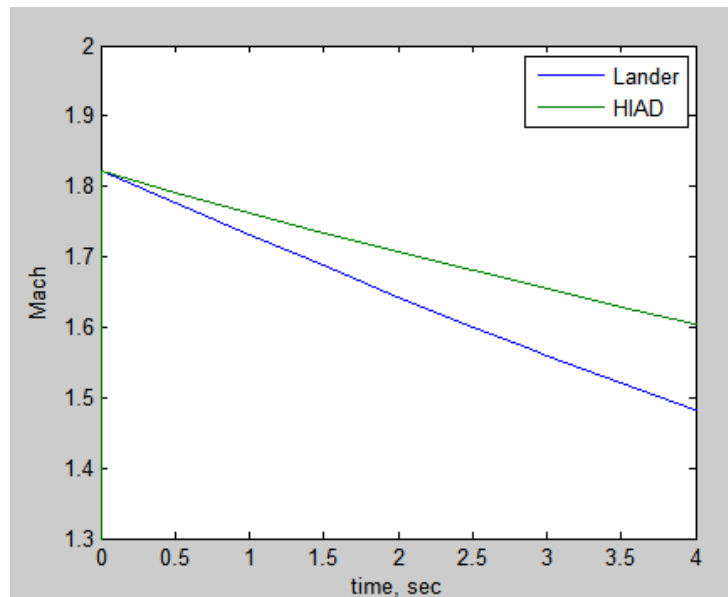


Figure 4-119 Mach number vs. transition start time.

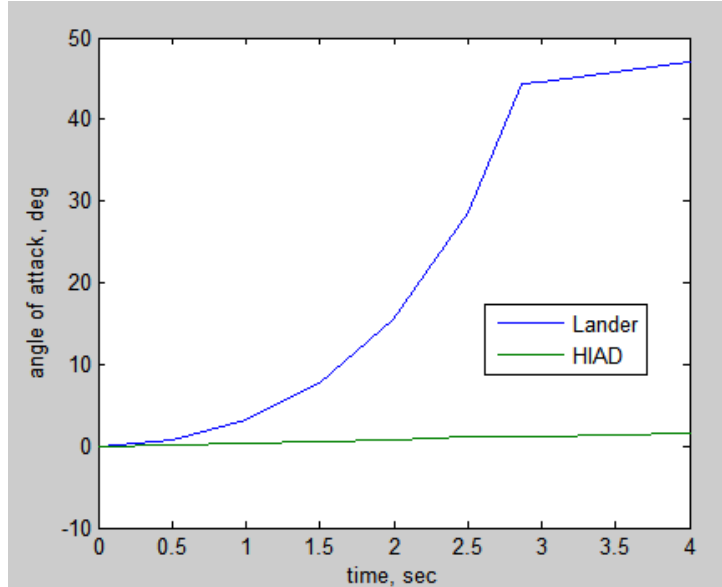


Figure 4-120 Angle of attack vs. transition start time

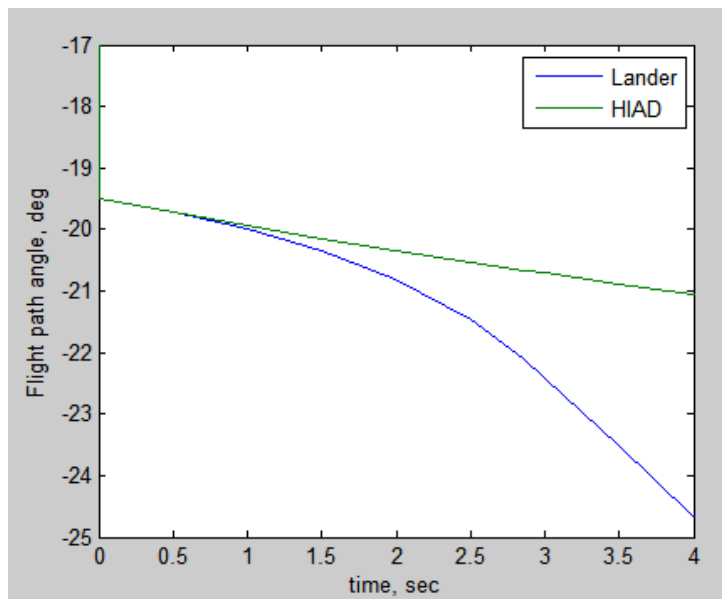


Figure 4-121 Flight path angle vs. transition start time

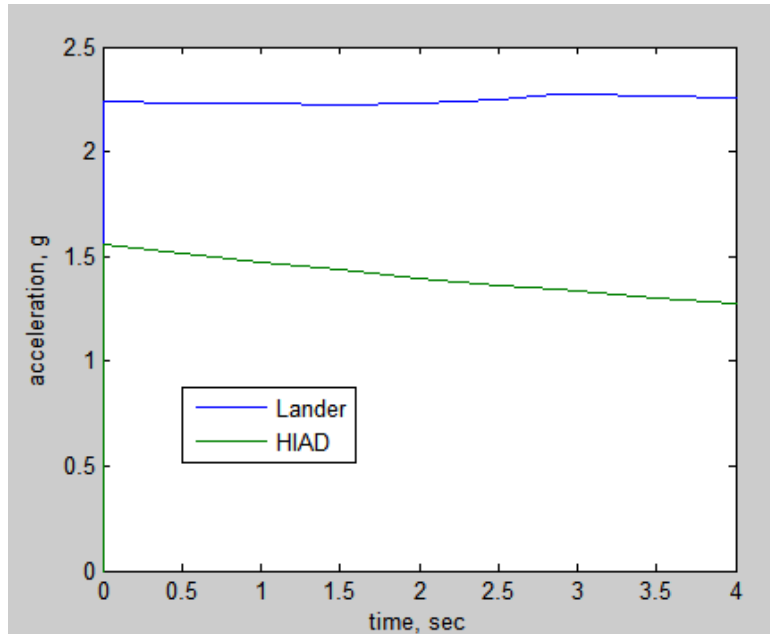


Figure 4-122 Sensed acceleration (Earth G's) vs. transition start time.

4.10.7 Recommended Future Work

Future work should include a control system for pitch and possibly yaw and roll to better control the lander as it moves away from both the mid L/D aeroshell and HIAD. Animation should also be employed using actual geometries to check for collisions. Additional recommendations are listed below:

1. Use realistic center of gravities and moments of inertia for mid L/D and HIAD heat shields.
2. Use realistic transition aerodynamics to include actual geometries and interactions.
3. Simulate thruster plume interactions between lander and HIAD.
4. Assess any control issues.
5. Address any mass inconsistencies.

4.11 Mars Lander Architecture Modeling Approach

4.11.1 Introduction

An integrated architecture management process originated from a project's need in NASA's exploration program to assess architectural requirements in a system of system environment. A project within the Constellation Program used a model-based systems engineering approach to support a project management & design formulation need, to validate a lunar lander spacecraft design. The lander project's process was formulated to support assessment and validation of stakeholder requirements for the lander spacecraft. As the process evolved, it became apparent that design analysis data, down to component level in some cases, was needed to formulate an architecture-level understanding. In validating the architecture-level requirements, for a state-of-the-art future design, required assessing technologies in conjunction with known and validated systems. The project office applied a model-based systems engineering process, establishing a hierarchical framework for requirements and design analysis results, to maintain context and structure. This structured approach used the traditional interrelated operational, functional and physical framework as the basis for requirements decomposition and management.

A Unified Modeling Language (UML) construct in a relational database environment was used to model each framework. In modeling the operational context of the spacecraft, the process formulators established the operational context as the rule in the architecture assessments process. Therefore, the spacecraft operations were modeled for its complete operational lifecycle. In assessing the broader architectural context, multiple mission scenarios were defined by the stakeholders. The spacecraft design had to accommodate these multiple scenarios. As a result, the operational variants created a complexity of operational information. To manage this complexity, an operations model hierarchy was established. The hierarchy consisted of mission-level diagrams, which decomposed into mission phase diagrams, which decomposed into activity-level diagrams, and finally decomposing into event-level diagrams. The supporting relational database was crucial in managing this hierarchy. The functional architecture in the framework could only exist if there was an operational need identified in the operations model. The physical architecture linkage to the functional architecture was open to the trade space, only in context of the operations models.

As NASA began to expand the exploration goals to a broader context, the expectation of architecture commonality, reuse and interoperability grew to a significant level of importance. The following discussion describes the evolution and the expansion of the MBSE process to orchestrate a framework to manage bottom up and top down content.

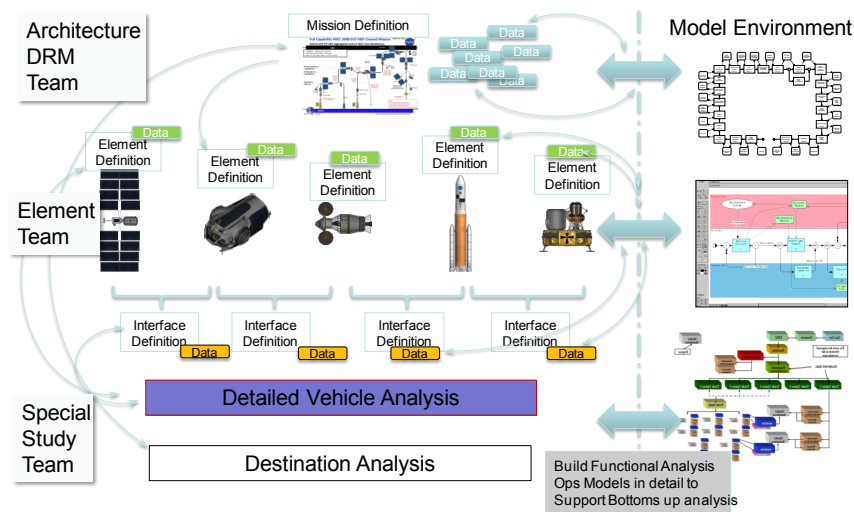


Figure 4-123 Integrated architecture modeling scope.

4.11.2 Process Formulation

The process formulated had several considerations in applying a MBSE approach. To organize a complex data set, rather than a complicated one, both the design layer models (operational, functional, and physical) and the supporting data architecture model had to be constructed, in concert with one another. It is important to note when formulating a model-based systems engineering approach one must consider the architecture and system management data in relation to each other as well as the processes. As the architecture process forms, assessing what data are necessary and relevant to answering the questions at an architecture level is vital. This architecture process for this paper was spacecraft centric. In that, mass is a discerning performance driver in assessing viability or cost of a given architecture. Therefore, understanding low-level details of the design required a bottoms up collection of design data. The process was constructed with the goal of integrating a top down and bottoms up method. The modeling construct below describes the framework to which the architecture data would be collected and derived.

4.11.2.1 Modeling Construct

This architecture modeling process began with understanding that there is a fundamental relationship between system operations, system behavior (functionality), and the allocation of functionality to those physical components

The System Architecture View at a specific level in the System Hierarchical Structure is created by cross referencing Items in the three kinds of Product Models. This is *Horizontal Traceability*.

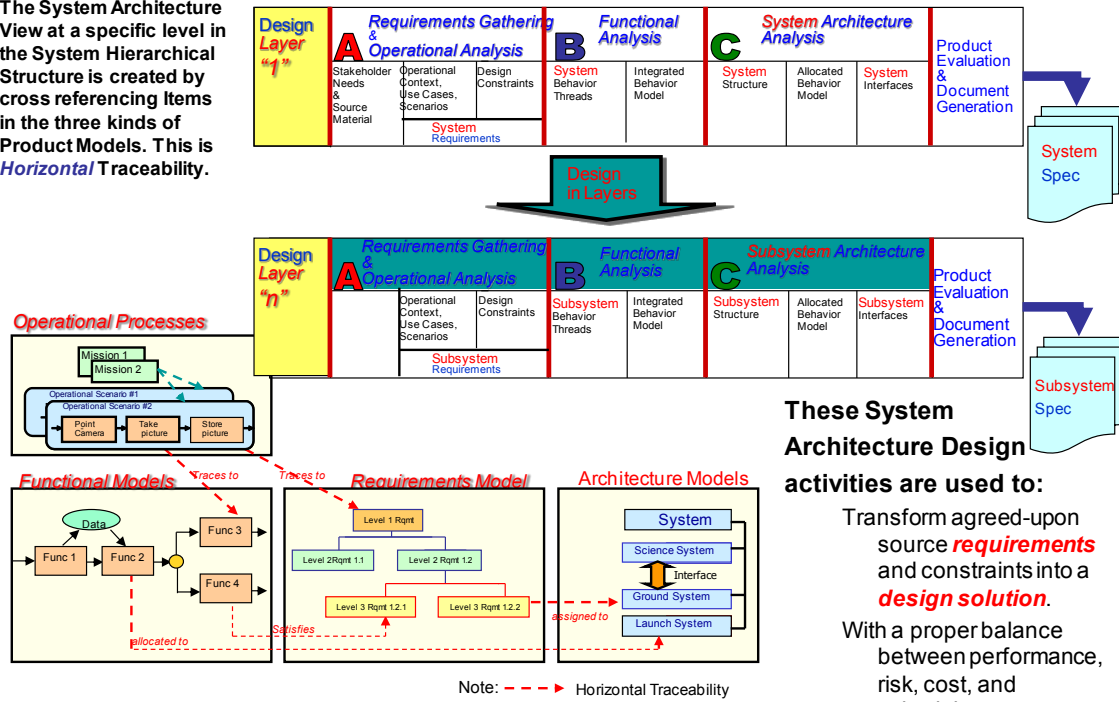


Figure 4-124 System architecture design layer development approach.

to execute the mission. The models/diagrams (operations, functions, physical) are interconnected by cross-references in a relational database. These interlinked views describe a single design layer of a hierarchical system definition. The traditional decomposition hierarchy applies to each view. These hierarchical models serve two objectives; 1) describe/define diagrammatically the system, from the three view points, required to meet mission goals and objectives, 2) provide a contextual framework to link supporting design parameters. The viewpoints established may occur in any order, as long as the three models are linked and crosschecked for consistency and validity. Most processes expect either a top down or bottoms up approach to design analysis. This MBSE process is not sensitive to these issues, because the interlinking of models forces consistency between the views. Therefore, one can apply existing designs solutions in the design space along with conceptual unrealized designs.

4.11.2.1.1 Operational Modeling Construction & Analysis

The operations modeling process began with understanding a need to distinguish between user behavior and system behavior. The operation models captured how the system was being used, a user perspective. Where the functional models captured the system behavior or how the system responded to the user input. In many cases, with autonomous systems, that distinction can become blurred. So, a ground rule was established to define software as an autonomous user. Some may argue that distinction confuses the issue. However, this provided a context for operational requirements, performance parameter such as timing and resource utilization, as well as descriptions from which operation concept documents could be produced. The operations point of view also served as a criterion from which the architecture evolved. A system component with a particular capability (function) had to justify its existence based on a need defined in the operations models. In these assessments, understanding where in the hierarchy these systems are utilized and to what extent became unwieldy. Therefore, a hierarchy of operations was derived to manage the complexity. The operational hierarchy includes a campaign, missions, phases, activities, and events. Each definition is described below with illustrated examples.

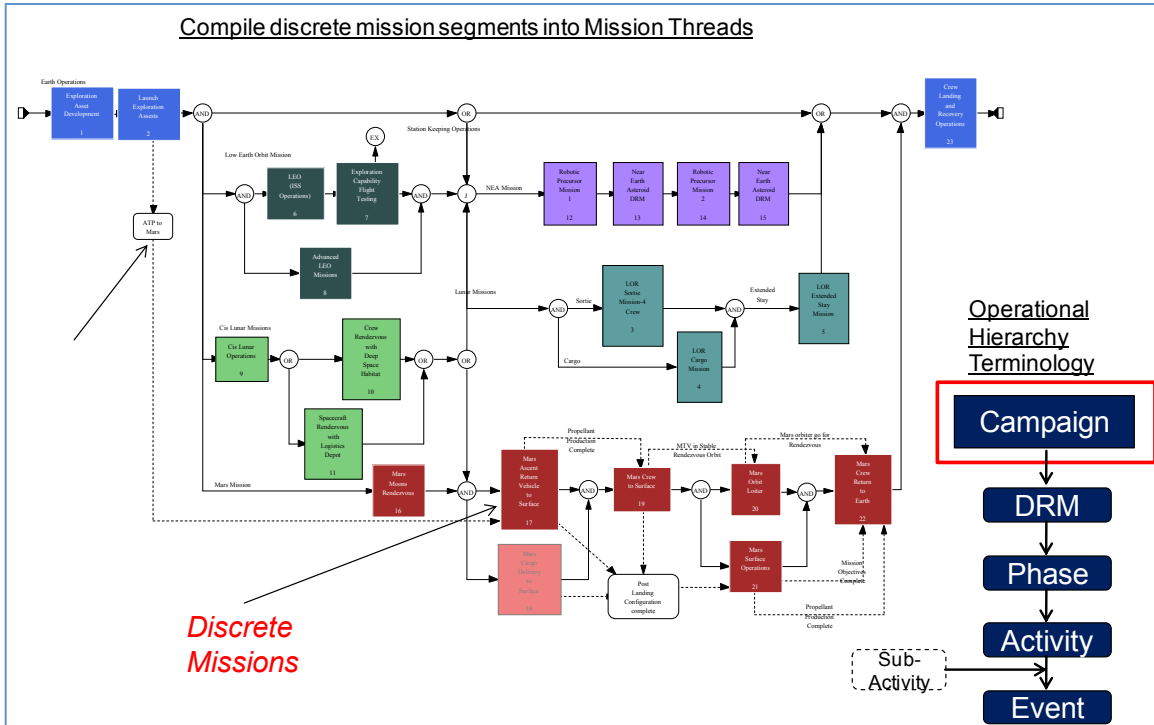


Figure 4-125 Exploration campaign model diagram.

The campaign model is a collection of missions with a temporal logic flow organizing the delivery of assets to their destinations. These models mostly establish the missions, their scope, and triggering criteria for mission execution. It mostly provides the starting context for the system architecture allocations. The architecture’s vehicle capabilities are referenced to this level of the hierarchy. The process question asked at this level is: What capabilities do you need when and what systems have those capabilities? Additionally, one begins capture the technology development needs based on this campaign level of analyses.

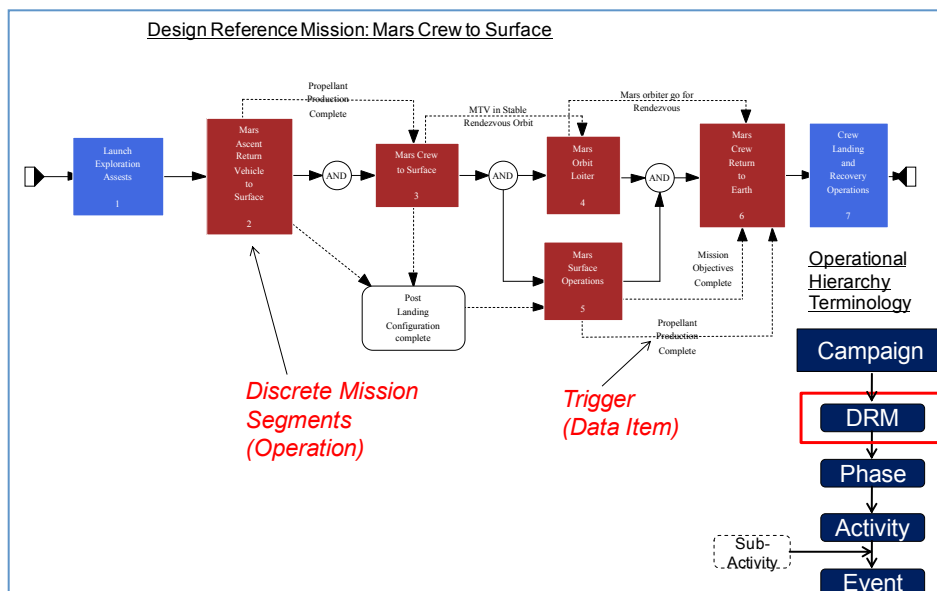


Figure 4-126 Exploration design reference mission model diagram.

The mission models are a collection of discrete missions selected from the campaign model to form a mission thread of operations. These mission operations then decompose into phases. These phases serve to logically break up the mission for managing the complexity of the information generated. The triggering criteria translated from the mission models serve to bind the period for which certain capabilities are expected to operate. For example, in mass sensitive performance scenario, staging becomes a strategy to optimize delta velocity performance. Assessing these phase models provides the understanding to know when to stage. This is the beginning of the functional allocation thought process.

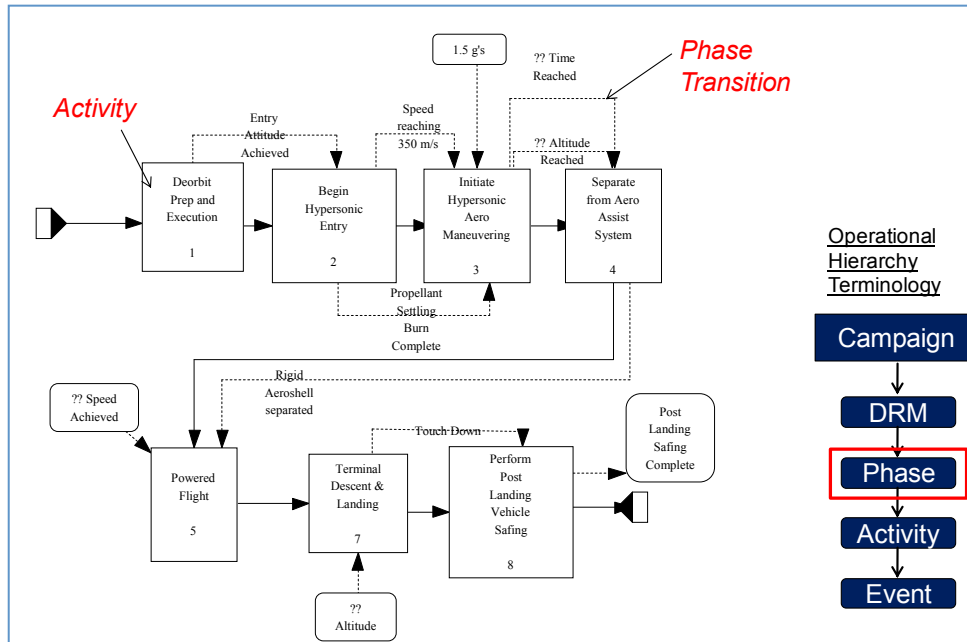


Figure 4-127 Exploration mission phases model diagram.

The mission phases are a collection of activities of which the system and subsystem operations begin to be realized. These activities begin describing how the system and subsystems are operating in more discrete periods. These operations focus on describing how and when the user is using the system. The content for these diagrams serve mostly for context or frame of reference. The detailed understanding of system occurs at the next two layers in the hierarchy.

The activity models are a collection of events that describes a discrete user need. These models serve to provide necessary detail for understanding subsystem and component operations. Depending upon the level of understanding of the system, one may not need this level of understanding. However, these event models can be processed in a discrete event simulation to determine total mission times as well as validate logical time sequences of the mission.

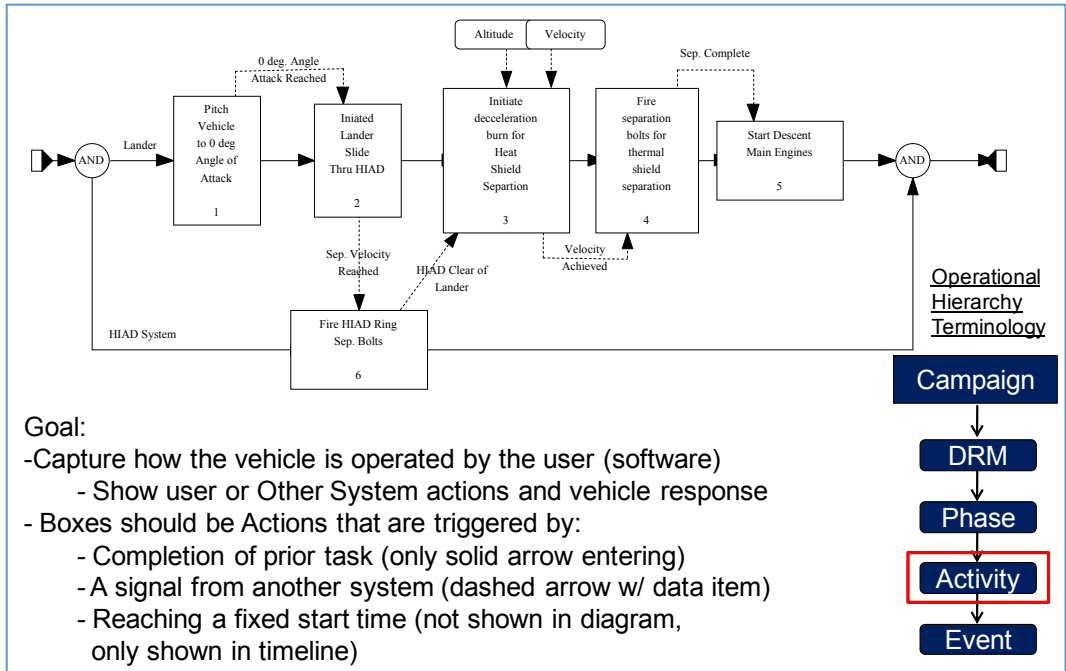


Figure 4-128 Exploration mission activity model diagram.

4.11.2.1.2 Functional Modeling Construct & Analysis

The functional architecture and its performance are captured in logical and temporal context in conjunction with the operations models. So for given operational sequences, there would be corresponding enhance functional flow block diagrams (eFFBDs) defining the functional behavior during that particular point in the operations hierarchy. It is important to reiterate the distinction between user perspective and system perspective in the modeling process. The diagram’s syntax may look similar logically, but the content is different. The eFFBDs provide the basis for establishing the high level functional architecture.

The functional architecture emerges from the understanding of the expected operations, derived from the above process. Once the operations are well defined, the process question is what functional capabilities are necessary to achieve those operations. At this point, one can execute technology assessments, in parallel, by establishing linkages between technology data and the functions they support. A trade tree can emerge from the relational database traceability providing management of trade options and the key decision points.

Additionally, the high-level functional architecture supports the process of trading capabilities across the architecture assets. These trades are supported by assessing a series of matrices showing the cross correlation of the three major viewpoints. The figure below illustrates a method to evaluate and manage operational architecture relative to function architecture from a performance perspective. Furthermore, by replacing the intersecting modes with cross-referenced physical architectures, one can visualize which vehicle systems have functional capabilities and when in the mission lifecycle those capabilities are utilized.

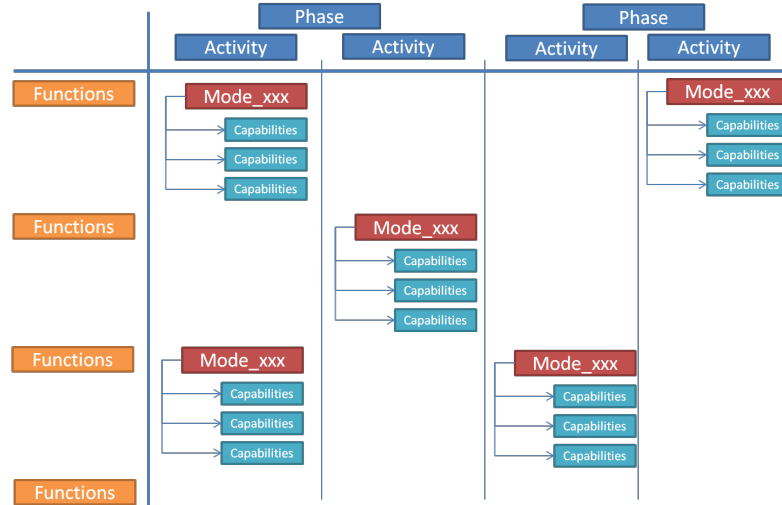


Figure 4-129 Operational to functional architecture cross reference matrix structure.

Additional assessment associated with the functional architecture assessment involves trading capabilities between aggregate assets, which results in mass shifts from one system to the next. Operational interfaces from the operation models support these staging trades as you reallocate functionality across architectures. These examples are just a few processes in which the model hierarchy provides context and structure.

4.11.2.1.3 Physical Modeling Construct Analysis

The physical architecture framework answers the question of what design solutions realized or conceived have the functionality required to execute an expected operation in the mission. The physical architecture is captured at a high level in the form of context diagrams; textual descriptions and physical parameter linked to the database items. The architecture is captured as “equipment” items in the database for book keeping purposes and cross referencing to the operational and functional architectures. Some physical characteristics are captured in the database to provide contextual reference of the system. Textual descriptions of the physical system is generally captured with supporting parameters that describe its physical nature, such as mass, volume, length, diameter, etc. The database deals only with high-level physical parameters and illustrations. The CAD tools capture the actual physical model. Those requirements managed in relation to this part of the process are physically constraining requirement.

4.11.2.2 Process Data Architecture

The data architecture framework answers the question of what architecture data and supporting systems management data is required to describe, define, validate, illustrate, and manage the architecture content. The data architecture (data schema) modeling process begins with understanding what questions are being asked and the processes you want to facilitate the answers. The data associated with architecture assessments can be diverse and large in quantity. When you consider the data collected in the UML syntax, in a hierarchical context, it becomes large and interrelated. The operation models require defining operations, activities, and events in a logical and temporal flow. The flow is capturing mission sequence and timing data. Triggering information such as messages, sensor data, events serve as inputs/outputs to the given operations. In conjunction to the model capture, one begins collecting and linking resource/consumable data, in the relational database, to each operation. Each viewpoint carries a set of data types specific to those viewpoints. The table below provides a sample of data types for each viewpoint. These data types are driven by the process questions, which are in turn driven by the point in the lifecycle for which you are supporting. The listing below is a basic data schema in context of conceptual architecture development at a program level.

Table 4-47 Model Framework Data Types

Architecture Viewpoint	Data
Operational	Ops requirements, timing, performance parameters, trigger, events, resources & profiles, logistics, interfaces, messages
Functional	Functional requirements, logical sequence, performance parameters, triggers, events, resources, interfaces
Physical	Physical constraining requirements, design parameters, interfaces definitions,
Cross References (database link relationship)	Operated by, allocated to, executed by, mission, etc.

In assessing data needs, from a top-down method, in formulating a high-level architecture, it becomes necessary at times to collect higher fidelity data to make trade decisions. In space flight architectures, mass is a crucial data set required to understand flight performance of spaceflight architectures. These flight performance calculations are only as good as the fidelity of data provided. Therefore, modeling the physical architecture to the highest fidelity possible improves the assessment. The data can originate from two “bottoms-up” sources – a clean sheet analysis, or from historical/legacy existing designs. Either source brings significant detail data for evaluation. It is at this point that the framework provides context to link this detailed data to provide context to the assessment. The framework also provides a basis to filter data sets that are not required for that assessment. The operational models ask: Are those data necessary to assess how that capability is used. The functional models ask: Do those data described the behavior of that capability. If the answer is no to those questions, then it is excluded from the data architecture. (NOTE: Requirements creep at these levels is inevitable without the context of the framework.)

In a bottom-up design, decomposing the design down to the component level just to get a higher fidelity answer seems time consuming and risky for getting “lost in the weeds” for most program managers. Therefore, mapping out a data architecture in conjunction with the modeling architecture illustrates what fidelity you need and how you will get there in a timely manner.

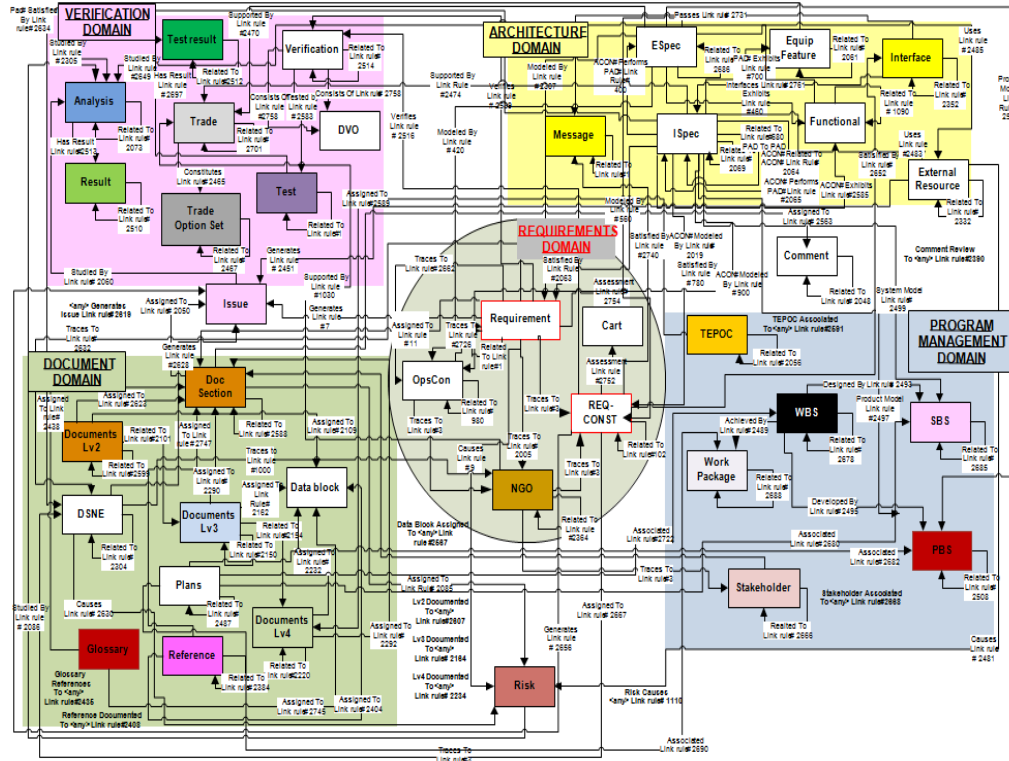


Figure 4-130 Requirements process data mapping needs.

4.11.3 Process Execution

A model-based systems engineering method was selected to provide a framework for managing the system design in an integrated process. The architecture modeling effort for the delivery of an integrated architecture to the surface of a planetary body, was the basis for tailoring a MBSE process. The basic tenets of the framework required modeling the operational functional, physical, and data architecture viewpoints in concert. However, time and resources only allowed for portions of each viewpoint to be modeled. The initial effort required defining and executing a basic data- architecture, in a relational database, to support interrogating the model framework. It is important to note that the data architecture evolves as the process is executed. The evolution of the data architecture results from the process questions evolve as you learn through process execution. Once the basic data schema was established, the focus shifted to developing the operational models for these missions. The remaining effort captured the functional and physical architecture. These were addressed at a high level with capturing some discrete low-level behavior models associated with engine and delta velocity performances. The processes focused on answering key question rather than achieving completeness in all aspects of each architecture viewpoint.

4.11.3.1 Data Architecture Execution

The basic data schema assessed and formulated to support the above activity is captured in the table below. This schema is a basic listing of data and the relationships between the data items as it describes the system architectures from the operational, functional and physical views.

Table 4-48 Framework Data Architecture

Operational Model Data	Functional Model Data	Physical Model Data	Link/Cross Reference Type
Operation Diagrams Operations: Campaign Mission Activity Event	Behavior Diagrams Functions/Behavior: Activity Event Functions: System Subsystem Component	Physical Architecture Diagrams: Equipment: Architecture System Element Assembly Subsystem Component	Reference Mission Mission Thread Executed by Mass Allocated to Configuration of Basis of Decomposed from Related to Reference by
Time-logical sequence Serial Parallel “Go to” criteria “Join” nodes “Exit” nodes	Time-logical sequence Serial Parallel “Go to” criteria “Join” nodes “Exit” nodes	Context Diagrams Vehicles Environments Data Flow Interfaces	Analyzed Assigned to Captured by Behavior of Comprised of Consumes Controls
Messages/Data Triggers Time-Discrete Start Time End Time Duration	Messages/Data Triggers Time-Discrete Start Time End Time Duration	Interface Compositions	Evaluated by Enables Environments Generates Measured by MEL
Mass Propellant Usage Total Vehicle Staging Summaries	Mass Propellant Spacecraft Total Estimated	Mass Properties Basic Unit Mass Growth Allowance Estimated Mass Moments of Inertia Center of gravity Dimensions	Performs Studied by Satisfies Traces to Transported by Variant of
Velocity –Delta Power Profiles	Delta Velocity Power Temperature Pressure	Powered Equipment List	
Resources Power Consumption Communication Coverage Life Support Water Food Air	Resource consumption Rate	Conceptual CAD Illustrations	
Environment Atmosphere Radiation Temperature Pressure	Technology Trade Studies Analyses		

4.11.3.2 Operation Model Execution

The mission analysis was initiated by executing the operational modeling process by defining a campaign-level model. The campaign model (diagram) is defined as a discrete and diverse set of missions in which the design architecture should be common in achieving exploration goals and objectives. The modeling framework (UML notation) provides the environment to assess the commonality and interoperability from mission to mission. The notation creates a temporal logic flow of missions that are relevant to achieving destination missions. The diagram flow structured the discrete missions into segments. The segments were logically ordered by mission destinations.

One asks the questions: What objectives need to be demonstrated in a phased approach to validate the architecture? The segments can be executed in a “stepping-stone” approach or by going direct. The various missions are linked by the timeline logic as well as database cross-reference relationships. The purpose of aggregating a diverse mission set into a single model is to provide visibility and context for the physical architectures to be common in achieving these missions. Commonality and interoperability is key to such grand exploration goals. The campaign model anchors the architecture in the studies. The campaign also established the operational interfaces between those architectures being conceived. The planetary missions require a multi-launch scenario to deliver infrastructure in phased approach for cost and risk mitigation. The architectures associated with planetary missions are a heavy lift launch vehicle, deep space transient propulsion system, and crew transport system with long-duration habitability, EDL as well as surface assets. These conceptual assets are captured and linked to the respective mission models by segment.

The mission segments were defined as Earth surface operations: LEO (including International Space Station); cis lunar and lunar surface; NEA; and, ultimately, Mars orbits, moons, and surface. Each of these segments contains several discrete missions that are serial or parallel in execution depending upon programmatic needs. The launch vehicle architecture was linked to Earth and LEO operation segments, the in-space propulsion architecture (nuclear thermal, nuclear electric, cryogenic chemical, solar electric) was linked to the destination transient trajectory phases of the missions. Deep space habitats and crew transport vehicles are linked to the transient phases as well. The lander and surface assets were linked to the destination surface segments. This traceability of architecture to missions provides the insight to driving requirements as the mission objectives evolve.

The mission segments were then decomposed to identify those phases of the each mission to help manage the complexity of the operational model. The architecture relationships stay the same. This study focused on the mission to deliver Mars infrastructure in advance of human arrival. The delivery of a crew ascent return vehicle, along with a pressurized rover and fission power system, was the primary model for detailed analysis. The phases begin providing timing specifics to understand functional needs. The phases focus on identifying when capabilities are required. A critical understanding of landing 40+ t of payload to a planetary surface is the EDL of a vehicle of this capacity. Those phase discriminators modeled the EDL phase with each phase being decomposed into activity-level models, which describe detailed events of operations.

The activity and event models describe sufficient detail to understand operationally what is expected from the lander system capabilities. The models described the aero entry operations, providing timeline capture for significant events such as the transition from aero capture to hypersonic to subsonic flight and landing. The aero entry systems are being traded between rigid aeroshell concepts to hypersonic inflatable aerodynamic decelerators. Each of these technologies was assessed by modeling the sequence of events for various configurations of the aeroshell and HIAD. Once the configurations were scored, the high-level activity models were incorporated into the database. These activity models then evolve in development to understand the subsystem interaction from a system viewpoint. This subsystem operational model initiates the functional model development and assessments. These functional analyses focus on timing, resource consumption (power, propellant, etc.) during descent. The resource availability is a function of the activity timing. These functional trades influence design decisions, which drive the physical architecture. As a result, the mass of the entry system selected has a direct relationship to total vehicle mass, which drives the launch vehicle architecture.

4.11.4 Functional Architecture Execution

The functional architecture emerges from the complete understanding of the expected operations derived from the above process. Once the operations are well defined, then the process question is what functional capabilities are necessary to achieve those operations. At this point, technology assessments can run in parallel to this process of defining functions that must be performed. The functional performance is also captured in logical and temporal context along with the operations models. So for given operational sequences, there would be corresponding enhance functional flow block diagrams defining the functional behavior during that particular point in the operations hierarchy. The matrix below is one tool to assess when capabilities are expected to be invoked. The columns represent the timeline at the activity level in the model hierarchy, whereas the rows represent the functional architecture at the subsystem level of the hierarchy. The intersecting node captures the capabilities cross referenced to the models. Each capability has the relevant requirements and performance specifications.

Altair Functional Relationship to Operations via Modes		LSC.13 : Altair Descent :		
		LSC.13.1 : Free Flight Operations : 000/01:03:27	LSC.13.2 : Perform Plane Change Maneuver : 000/00:00:00	LSC.13.3 : Prep for DOI : 000/01:34:51
LNDR.1 : Provide Transportation	LNDR.1.3 : Transport Crew	Crew On-board	Crew On-board	Crew On-board
	LNDR.1.5 : Transport EVA Suits	EVA Suits Donned	EVA Suits Donned	EVA Suits Donned
LNDR.2 : Provide Habitability	LNDR.2.1 : Provide exterior viewing	Exterior Viewing Available	Exterior Viewing Available	Exterior Viewing Available
	LNDR.2.2 : Provide Lighting	Reading + Panel Lighting On	Reading + Panel Lighting On	Reading + Panel Lighting On
LNDR.3 : Perform Maneuvers	LNDR.3.1.1 : Estimate Inertial State	Inertial Navigation Active	Inertial Navigation Active	Inertial Navigation Active
	LNDR.3.2 : Perform Translational Maneuvers		Main Engine Burn	
	LNDR.3.5 : Perform Trajectory Design	Target Computation Active		Target Computation Active
LNDR.4 : Sustain Altair Environment	LNDR.4.1 : Control Cabin Pressure	Cabin Pressure Control Active	Cabin Pressure Control Active	Cabin Pressure Control Active
	LNDR.4.2 : Control Temperature	Temperature Control Active	Temperature Control Active	Temperature Control Active
LNDR.5 : Accept and Execute Commands	LNDR.5.1 : Receive Commands from Cx	Receive Commands Active	Receive Commands Active	Receive Commands Active
	LNDR.5.2 : Receive Commands from Crew	Receive Commands Active	Receive Commands Active	Receive Commands Active
LNDR.6 : Manage Vehicle Performance	LNDR.6.2 : Perform FDIR	Perform FDIR Active	Perform FDIR Active	Perform FDIR Active
	LNDR.6.4.1: Manage Power Load	Altair On Internal Power	Altair On Internal Power	Altair On Internal Power
LNDR.7 : Perform Communications	LNDR.7.1 : Communicate with Cx Systems	RF-High Data Rate	RF-High Data Rate	RF-High Data Rate
		RF-Low Data Rate	RF-Low Data Rate	RF-Low Data Rate

Figure 4-131 Example capabilities mapping to functional & operational model.

These matrices assessments begin the process of visualizing the states and modes of the system as the behavior. In an integrated architecture, when shared resources are a premium, these states and modes become crucial especially at the vehicle interfaces.

As the behavior diagrams emerge in a comprehensive context the operational timeline, recurring capabilities begin to emerge. For example, the operational architecture is expected to deploy assets at varying points in a campaign-level timeline. The assets aggregate at designated points in space and assemble before moving to the exploration destinations. As a result, when querying the database for all functions for each asset, common capability emerged. Each asset needed navigation, communications, propulsion, and power generation. Based on the operations model, an aggregated vehicle comes together before departing. Prior to departing, which asset serves as the primary for executing the aforementioned capabilities? This resulted in formulating an operational requirement for command/control and resource utilization protocol that had not existed before.

4.11.4.1 Physical Architecture Execution

The physical architecture is captured at a high level in the form of context diagrams; textual descriptions, requirements and physical parameter linked to the data base items. The architecture is captured as “equipment” items in the database for book keeping purposes and cross-referenced to the operational and functional architectures. Some physical characteristics are captured in the database to provide contextual reference of the system. Textual descriptions of the physical system is generally captured with supporting parameters that describe its physical nature, such as mass, volume, length, diameter, etc. Common views of the physical architecture are Conceptual CAD models, physical architecture description documents, MELs/Powered Equipment Lists, UML physical architecture and context diagrams. The database deals only with high-level physical parameters and illustrations.

The CAD tools capture the actual physical model. Those requirements managed in relation to this part of the process are physically constraining requirement.

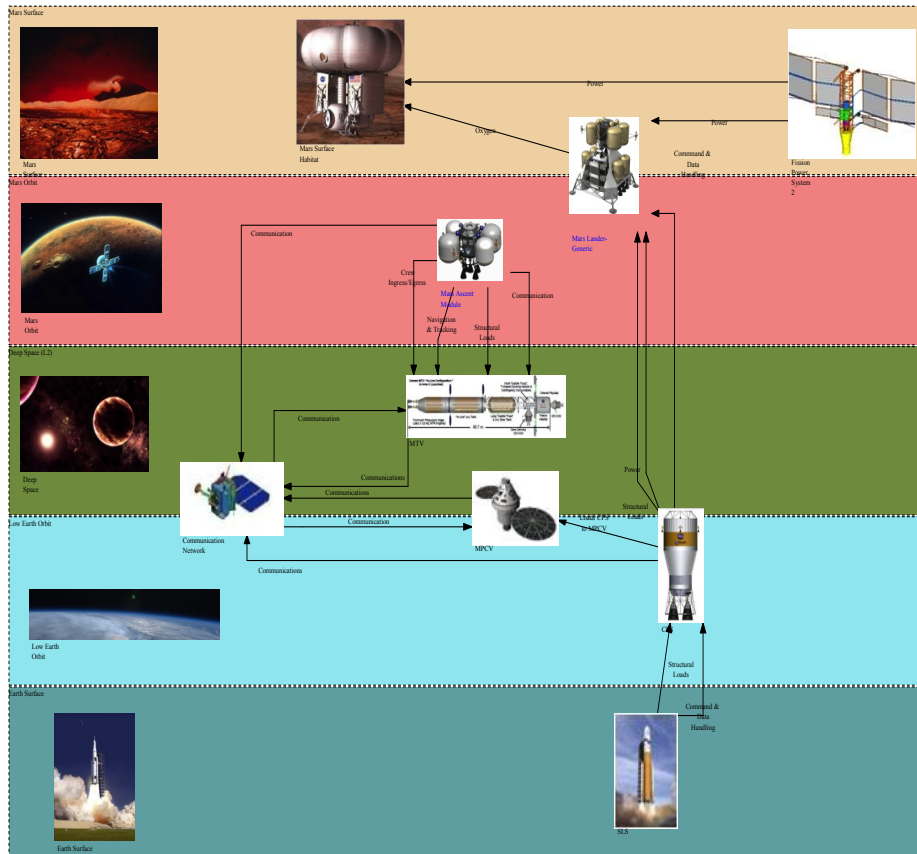


Figure 4-132 Architecture context diagram.

An output of the physical architecture assessment was a MEL/PEL hierarchical list of a human and cargo lander in the 40-60 metric ton range. The MEL and PEL is the hierarchical equipment listing that follows the functional architecture decomposition. The mass properties are captured as attributes of the equipment items in the model. As a result, the MEL and PEL are simply a report from the database. The MEL items are cross-reference to both the functional and operational models. This resulted in traceability matrices for showing the mass variations throughout the stage sequences of the mission as well as producing power profiles throughout the missions.

4.11.5 Summary

As proposed in the beginning of the paper, how does a single overseeing entity or organization leverage model-based systems engineering to maximize reuse (and ensure interoperability) between interrelated missions over the course of a long-range program?

The answer, as described in this paper, involved implementing a structured analysis process that accounted for four fundamental viewpoints: 1) data architecture, 2) operational architecture, 3) functional architecture, and 4) physical architecture. The key was to understand how all four views interconnect to support technically interrogating an integrated architecture assessment. (NOTE: Cost and Programmatic were not assessed in this effort). Model-based systems engineering techniques are well suited to support these process needs. A process was formulated to structure and to manage top-down objectives and bottoms-up derived architecture design data. These diverse objectives were explored, in part, in a multifaceted hierarchical modeling framework to gain insight and visibility into commonality and complexity across the integrated mission objectives. The process facilitated exploring options to maximize reuse (and ensure interoperability) between interrelated missions. As in one example, the common

operational/functional architectures of communication, control, navigation, and propulsion were discerned from assessing the interrelated models. The model hierarchy also structured the study in such a manner to gain visibility in system behavior (eFFBD diagrams) across the operational need, which aids in determining where it is appropriate to increase the fidelity of analysis. The additional benefit of such a structured method is to provide a requirement foundation that is efficient and traceable for future implementation. The traceability also served to structure data for the overall systems engineering process, particularly the transformation of customer expectations into architecture requirements and definitions. The coupling of the data architecture with the system models was vital and complementary to the overall systems engineering process. The supporting systems management data, linked to the model framework, became the content for standard programmatic documentation. The documentation such as operations requirements document (ORD), Operations Concept Document, Functional/Performance Requirements Document, Physical Architecture Description Documents. These documents support a Program’s Mission Concept Review.

The process also supported understanding the relevance in system depth versus breadth throughout the architecture studies. The majority of architecture studies do not allow sufficient time to analyze the necessary fidelity of a system, which supports a better decision rationale.

4.12 Summary of Mars Lander Technology Needs

Opportunities for technology development are identified throughout the Mars Lander design. While many technologies have been associated with the Mars Surface Mission, the technology needs identified herein are enabling for the DRA 5.0 Architecture Mars Lander. Supporting mission elements and operations will require additional development. Commensurate with available funding and the development of capabilities to launch assets, technology development schedules appear to align with proposed timelines for a DRA 5.0-type mission. In most cases, current efforts can be leveraged to accelerate technology development where needed. The Human Spaceflight Exploration Architectures Team Technology Development Team mapped technologies to the elements and respective destinations for a number of mission targets. While it is not a comprehensive list, this is a quick summary of the technology specific to Mars, specifically those areas that enable the Mars Lander.

4.12.1 EDL Systems

To improve payload mass fraction and land more useful payload on the surface of Mars, innovative EDL approaches are necessary. EDL-SA study Lander concepts addressed the transition from supersonic flight through Lander separation and on to Lander powered descent. Analysis has shown that advanced EDL concepts for aeroassist vehicles are critical to both landing humans on Mars and for Earth reentry to control the velocity of exploration vehicles when entering the planetary atmosphere. The approach under consideration employs some relatively high TRL *Rigid Hypersonic Decelerator* options. A *mid-L/D aeroshell* entry vehicle, using a clamshell design for Lander separation, facilitates atmospheric entry at Mars and protects the Lander *aero-entry TP*. In addition to TPS materials, critical to control heat flux during Mars entry and Earth reentry, other supporting technologies for aeroassist vehicles include sensors to relay real-time aerosurface conditions, and thermally conductive, high temperature adhesives. Similarly, the *HIAD* combined with a suitable Lander separation architecture provides a mass savings alternative for the Mars atmospheric entry trade space. Finally, *SRP*, to decelerate the entry vehicle from hypersonic or supersonic conditions to a subsonic velocity, has been considered as a potentially enabling technique for descent and precision landing. However, the technology effort may reside more in the model development and computational methods to understand aerothermal interactions.

4.12.2 Propulsion and CFM Systems

Advanced propulsion alternatives have been explored for the transit from LEO to Mars orbit, entering the Martian atmosphere and for the transition to powered descent. For the powered deceleration phases at the end of its journey to Mars, the Lander decelerates further using more traditional systems. Chemical propulsion, in the form of *LOX/Methane*, is the current baseline for the Lander. A LOX/Methane system offers suitable performance for pump-fed primary propulsion and pressure-fed RCS, improved handling characteristics, and the benefits of reduced toxicity. This is a mildly cryogenic, space-storable propellant combination with the added benefit of leveraging in

situ propellant production of LOX at Mars. The improved launch propellant mass fraction is enabling for mission architecture design and the resulting reduced down mass to the Mars surface and opens up a number of vehicle options for the Lander configuration.

The challenge of controlling propellant boil-off requires *cryogenic fluid management (CFM)* as an enabling technology. Given the boiling points of a LOX/CH₄ propellant combination and the relatively cold environment of space, it is believed that *zero boil-off* may be achieved using technology approaches under development but not yet demonstrated in space. As described earlier in the propulsion section of this document, the basic concept includes an *80K cyrocooler*, and *thermal vent system* with *MLI incorporating vapor-cooled shielding and supporting component technology*. Recent efforts, both pre- and post- Constellation, show considerable work has been done to develop supporting *thermal control systems* and to answer feasibility questions with throttling, ignition, and other integration issues associated with methane systems. It will be necessary to continue the development of *pump-fed LOX/CH₄* main propulsion engines, *pressure-fed LOX/CH₄ RCS* system, and technology for supporting systems. *Cryogenic liquid acquisition* technology is needed for unsettled tank-to-engine propellant transfer to support RCS course corrections.

With methane transported from Earth providing the light but less efficiently packaged hydrogen, and the heavier oxygen and carbon extracted from the indigenous CO₂ predominant in the atmosphere, significant mass leveraging is possible. This *ISRU* would result in weight and cost savings. Though in situ propellant production for the ascent vehicle reduces the total launch mass, some of the benefit may be lost to boil-off mitigation hardware and the required reactants to initiate the Sabatier process. A minimalist approach to a Mars mission may also diminish the benefit of ISRU. The oxygen-producing in-situ resource utilization system will be pre-deployed to the surface. During the ISRU oxygen production, a cyrocooler system will operate to condense the oxygen and accumulate liquid in the LOX tanks, requiring a substantial amount of continuous power. The crew will not launch until sufficient LOX has been produced. Due to the mission architecture timeline and performance requirements imposed on the propulsion system, *long-duration CFM and storage* is a high priority technology investment.

4.12.3 Power Systems

Requirements for available electrical and thermal power for life support, communications, and other supporting onboard systems and operations are considerable. A variety of power options exist, as a detailed power assessment must be completed to evaluate required power efficiency, operating conditions and shelf life to determine suitability. Pending any mission architecture redirection, *long-life batteries* will be needed for powered systems during orbit insertion and descent, for rovers and also for ascent and docking. *Regenerative fuel cells* could potentially trade back in as an option for keep-alive power during the surface stay. If fuel cells are determined to be an effective option *PEM* fuel cells could provide a solution. *Solid oxide* fuel cells provide an attractive solution from a performance advantage (higher efficiency) but operate at very high temperatures (500°C-1000°C) vs approximately 80°C for PEMs. Depending on the mission constraints, it may be necessary to revisit high-strength, high-efficiency solar arrays. Alternatively, power from radioisotope thermoelectric generators have been demonstrated on prior science missions and will be traded with a full risk assessment. Abundant power for surface missions is enabled by a *surface fission power system*, which is among the pre-deployed assets that will be used to produce LOX from the Martian atmosphere via ISRU and supply power to surface systems and operations.

4.12.4 Avionics, C&DH and C&T

Though no formal policy has been established, system functionality/design and life cycle cost benefits of implementing a commonality strategy must be explored. The ability to support multiple formats, simultaneous users, line of sight blockages, and provide operability over multiple mission phases will be key. Human spaceflight requires additional processing power, bandwidth, and configurability over the Command & Control and GN&C operations currently performed by existing radiation hardened processors and networks. *Automated/Autonomous Rendezvous & Docking*, *Proximity Ops*, *In-Space Timing and Navigation for Autonomy*, *Target Relative Navigation and Hazard Avoidance and Landing and Technology* are driving technologies required to facilitate locating assets in Mars orbit and on the Martian surface. Requirements for faster processors necessitate the determination of space-rated components to support the accomplishment of mission objectives. The radiation environment poses a threat to component survivability. As processor speed increases, gate size decreases and susceptibility to radiation increases. Crew autonomy and autonomous vehicle systems benefiting operation at remote planetary sites provide the crew

with more independence from ground operations support. Such autonomy is essential to reduce operations costs and to accommodate the ground communication delays and blackouts at distant locations. High Data Rate Forward Link (Flight) Communications High Rate, Adaptive, Internetworked Proximity Communications Optical Comm, Optical Ranging, RF Imaging System must be traded to provide disruption tolerant networks and ensure contact and dissemination of information between assets.

4.12.5 Thermal, Life Support and Human Factors

Effective thermal control is needed to accomplish three basic functions (heat acquisition, heat transport, and heat rejection). One of these functions is the acquisition of excess thermal energy from the cabin air and other heat-generating devices. Alternative materials and approaches to design of heat exchangers and coldplates traditionally used are needed to acquire excess thermal energy from heat-generating devices and transfer the acquired energy to the pumped fluid loop. Radiator advancement (with suitable thermal control system fluids) is a critical technology development to reject excess heat. Radiators are in place to intercept and dissipate radiant heat and heat from vehicle systems before it reaches the propellants and to control the crew habitable areas. During ascent, a sublimator is used to reject waste energy. Alternatives that are suited to particular applications include developing coldplates and liquid/liquid heat exchangers using advanced composite materials, evaporative heat sinks, phase change material or microchannel design, and sublimator driven coldplate to reduce mass. No single approach is sufficient or mass efficient to accomplish the overall objective.

Advanced environmental monitoring is needed to inform systems and regulate habitable areas. Advanced spacesuits with provisions for high-pressure oxygen supply are required for breathing and maintaining safe pressure and thermal environment around the body. Known issues such as leakage rate – e.g., suit leak rates – require that developers fix leak issues or condition suit. To explore and work in space, mobility aids will be needed to get to areas on- and possibly off-surface that might otherwise not be accessible. This includes EVA tools and translation aides that improve the safety and effectiveness of crews, utilizing land vehicles over varying distances, and construction of infrastructure to facilitate transporting both crew and cargo.

Requirements for mitigating dust or other contaminant must be considered for Human Exploration and Development of Space missions. Potential solutions, such as suit ports or other alternative airlock approaches, isolate the problem, more readily allow crew to perform EVA, and enable quick access to a safe haven for radiation protection in the event of a contingency. Additionally, suit port or similar logistical approach to EVA would lessen requirements for depressurizing the habitat and sending the full crew on EVA. The development of inflatable seals, dust-proof electrical, oxygen and water connectors between vehicle(s) and the suit will be needed for missions to dirty environments, which include the Moon, Mars, or asteroids. Suit port, hybrid suit port/suit lock, and airlocks will be kept in the trade space until DRMs are explicit. Globally, lightweight, high-strength, materials, seals and mechanisms capable of tolerating temperature extremes are applicable, as they will improve performance and reduce launch mass.

HRP concerns are among the highest, arising from the long mission duration and prolonged exposure to the space environment. Innovative engineering solutions and employment of technology are needed to protect the crew, habitats, hardware and avionics against hazards associated with microgravity and radiation. Shielding techniques and pharmaceutical advancements are among the potential solutions to reduce the health risk from exposure to galactic cosmic rays and solar particle events. Extended exposure to microgravity has been linked to bone loss and could possibly accelerate other health risks. Biomedical countermeasures ranging from medicinal and/or therapeutic exercise to possibly providing an artificial gravity environment via centrifuge or through more extreme design solutions may mitigate these effects.

The following table is a snapshot of the topical technology areas. It is still a work in progress, as work continues to identify focus technology development and the required performance parameters. It should also be noted that a minimal capability Lander concept may not require the same complement of technical investment.

Table 4-49 Summary of Mars Lander Technology Needs

Area	Technology Summary Table	
	Category / Technology Title	Description
AVIONICS	Avionics software and Autonomous Vehicle Systems Management	Management of onboard control, navigation, & communication systems <ul style="list-style-type: none"> Automated/Autonomous Rendezvous & Docking, Proximity Ops In-Space Timing and Navigation for Autonomy Target Relative Navigation and Hazard Avoidance and Landing Technology
C&T / C&DH	<ul style="list-style-type: none"> Communications and Tracking Communications and Data Handling 	Management of communication, data, and display systems <ul style="list-style-type: none"> High Data Rate Forward Link (Flight) Communications High Rate, Adaptive, Internetworked Proximity Communications Optical Communication Optical Ranging RF Imaging System
CFM	Cryogenic Fluid Management and Storage	Long-term storage and distribution technologies for cryogenics to enable high performance cryogenic propulsion systems, surface systems (ISRU), power generation and life support <ul style="list-style-type: none"> In Space Cryogenic Liquid Acquisition Thermal Vent Systems and Multilayer Layer Insulation and Shielding 80K Cryocooler
ECLSS	Life Support	High reliability, environmental control and life support systems for habitable volumes and EVA <ul style="list-style-type: none"> Advanced space suit Suit Port High pressure oxygen Thermal control for heat dissipation / heat rejection
HRP	Biomedical Countermeasures	<ul style="list-style-type: none"> Risk mitigation for GCR and single event exposure Long-term exposure to microgravity
POWER	Long-Life Batteries	Low cycle, high specific energy for long duration energy storage
	Deployable Solar Arrays	<ul style="list-style-type: none"> High Power 10-100 kW Class Autonomously deployable w/ High Strength/Stiffness
	Regenerative Fuel Cells	Low mass, high reliability, proton exchange membrane (PEM) or solid oxide
	Surface Fission Power	Highly reliability, continuous high power to support Lander and ISRU: reactor, shield, power conversion, heat rejection, and power conditioning and distribution
PROPULSION (AV)	EDL <ul style="list-style-type: none"> Aerocapture Aeroassist Supersonic Retropropulsion (SRP) 	Mars decelerator approaches, operational under low-g(0.1g) propulsion accelerations, for transition from supersonic flight to powered descent at Mars, and for earth re-entry vehicle <ul style="list-style-type: none"> Mid L/D aeroshell Hypersonic Inflatable Aerodynamic Decelerator (HIAD) TPS materials
	Engine <ul style="list-style-type: none"> LOX/LCH4 Cryogenic Propulsion 	Advanced development and integration of space storable systems with good performance, improved handling & reduced-toxicity; <ul style="list-style-type: none"> Pump-fed LOX/LCH4 Cryogenic Propulsion Pressure-fed LOX/LCH4 Cryogenic Propulsion LOX/LCH4 Reaction Control Engines
OTHER	In Situ Resource Utilization	Extraction of oxygen and nitrogen from CO2 in Martian atmosphere to provide propellant fuels to refuel spacecraft on surface
	Structures and Mechanisms	Lightweight, high-strength, materials, seals and mechanism

4.13 Recommended Forward Work

Any landing on Mars is a complex undertaking. This is particularly true for systems of the scale to support a human presence on Mars. Section 4 presents preliminary designs and trade studies that improve our understanding of the design drivers, risks, and technology needs for this mission, but more work is needed. Additional trade studies can be performed to point us to more optimal design solutions. Improving the fidelity of the design and analysis work can uncover additional challenges not yet identified and will help to ensure that the results of our trade studies are of sufficient accuracy to allow for sound decision making. Some specific tasks have been identified throughout this section. Those tasks are repeated here.

4.13.1 Forward Work in Aerodynamic Entry and Descent

While no significant modifications were made to the EDL simulation from EDL-SA, the additional work performed by the HAT team described in Sections 4.6 & 4.7 is required to develop 6-degree-of-freedom entry simulations. The HAT engine trades more accurately inform the volume and mass requirements of the descent stage and MAV, which impact the configuration packaging designs that provide inertia information. Vehicle inertias will allow (1) updates to the parameterized mass models, (2) more thorough evaluation of transition events and additional masses required to accomplish the transitions, (3) development of entry and descent guidance and control algorithms, (4) precision landing instrument performance evaluations, (5) updates to the terminal descent engine sizing and propellant use models, and (6) detailed analysis of vehicle stability.

An additional aspect of EDL, recognized in the EDL-SA study and verified with the HAT lander packaging arrangement effort, is that none of the packaged lander configurations exceed 17 m in length, bringing into question the need for a 10x30 m rigid aeroshell. Preliminary analysis has been performed to investigate various entry aeroshell shapes and aspect ratios, but further work is needed. The rigid aeroshell shape and its potential impacts on SLS aerodynamics and loads are also a consideration. Materials options, such as composites, are being considered for SLS. Additional analysis will be needed to verify that, should the SLS shroud double as a Mars entry aeroshell, the loads of both launch and entry can be accommodated. Additional aeroshell shapes will also require extensive stability, aerodynamic and aerothermodynamic analysis. Finally, performing an extensive descent engine trade study that examines technological advances in engine capabilities including Isp, T/W, propellant types, etc. will inform future iterations of packaging analysis.

It is recognized that none of the architectures under consideration identically resembles the actual human mission design. However, the detailed studies will help to illuminate system unknowns, will allow more thorough risk identification and assessment, and will continue to inform technology development decisions. Significant progress has been made since DRA 5.0 that, allowed to continue, will enable a higher-fidelity assessment, to better guide future investments.

4.13.2 Forward Work in Descent Module Configurations

Throughout Section 4.6, a variety of issues and uncertainties related to the assumptions, down-selected configurations, and analysis processes have been mentioned. Several future task activities have been suggested. These are summarized below, roughly in order of decreasing priority.

- 4.13.2.1 Develop working requirements for launch vehicle payload natural frequencies; explore and develop concepts to raise launch vehicle stack (payloads and adapters) stiffness.

The H3 and V1 analyzed configurations both have first-mode frequencies below 5 Hz. Achieving higher frequencies through structural modifications will require significant redesign (with mass increases), or may be infeasible altogether. Attachment to the launch vehicle shroud or rigid aeroshell may increase stiffness/frequency, but raises system-level concerns. Uncertainties related to frequency represent a serious risk to feasibility, especially for horizontal configurations. Future work should include coordination with the SLS project team to identify working frequency requirements (even if preliminary). Mitigation strategies, including structural modifications, alternate configurations, and shroud load sharing should be analyzed. Various launch-vehicle packaging and integration

schemes should be examined to determine impacts on stiffness/frequency. The focus should be on determining whether frequency is a driving requirement.

4.13.2.2 Improve significantly the structural stiffness and efficiency of the horizontal configuration.

Horizontal configuration H3 was found to require a significantly more massive primary structure than configuration V1. Moreover, its first modal frequency is probably too low to be considered reasonable. Therefore, the H3 structure design needs to be improved to reduce structure mass and increase stiffness. Several options for this improvement exist, including exploration of an H1 cage-type configuration (which was ranked almost equally during the brainstorming process but was expected to have higher strength and stiffness), or simply looking at variations of the H3 structural design.

4.13.2.3 Determine the true feasibility of making the launch vehicle shroud and rigid aeroshell for Mars entry the same structure

The horizontal configuration was analyzed with the assumption that the shroud and rigid aeroshells are the same structure. The assumption eliminates redundant structure and increases available packaging volume, but has not been vetted at the system level. The optimum shapes for the shroud and aeroshell are not the same, and it is unknown whether a suitable shape exists that can be used for both launch and entry. Future work should be aimed at determining the feasibility of this scenario.

4.13.2.4 Update the lunar landing-gear sizing tool for Mars landings

Landing gear masses were estimated using an analysis tool developed for the Altair lunar lander program. The tool assumes Apollo-like touchdown conditions and loads based on a maximum deceleration of 1g (9.8 m/s²). The tool is only applicable to Apollo-type deployable landing gear. These assumptions are not ideal for estimating Mars landing gear mass. For example, preliminary (and simplified) analysis suggest that limiting deceleration to 1g at Mars may be impractical because of the long attenuation distances required in the landing-leg struts. Updating the tool requires the development of new dynamic analysis models to generate accurate landing-leg loads for Mars touchdown, and to predict landing stability. At a minimum, the limitations of using Apollo-like assumptions to estimate Mars landing-gear mass should be better understood.

4.13.2.5 Develop full-mission integration concepts for the HIAD and rigid aeroshell

The team's assumption to mount the HIAD directly to V1 and the rigid aeroshell to H3 was based on engineering judgment. With these assumptions, however, no integration scheme or structure for a HIAD-type entry system was developed for the vertical lander layout and analysis. The details of where the HIAD would be located relative to the lander, how it would be deployed, or how loads would be transmitted have not been defined and assessed. Details of rigid aeroshell integration for the horizontal lander are also undefined. Future work should develop a preferred HIAD entry scenario, including details of deployment and transition. Concurrently, efforts should be made to develop concepts for rigid aeroshell integration hardware, including a separation system. The finite element models and analysis results presented herein should be updated to include entry system integration hardware and any impacts to vehicle performance.

4.13.2.6 Analyze the system-level impacts of aeroshell/shroud attachment and load sharing

Opportunities may exist for increasing frequency and reducing mass by using the shroud (or combination aeroshell/shroud) to support the lander during launch. However, the benefits are not quantified and shroud load sharing raises system-level issues related to the design of the launch vehicle. Future work should involve coordination with the SLS project team to define shroud baseline dimensions and sizing. Analyses should be conducted to determine the impacts of shroud load sharing on system-level performance, including mass. This issue is closely related to numbers 1 and 2 above, and all three might be investigated as part of one common task.

4.13.2.7 Analyze the effects of interface loads on propellant tanks, cargo, and the MAV

The present analyses treated fuel, the FSPS, the rover, and the MAV as lumped masses during analysis of lander primary structure. Although mounting struts were sized and attachment hardware was accounted for, the ability of these vehicle components to carry transmitted loads is uncertain. In some cases, loads imparted to these components during launch may be significant drivers to their design. This may occur due to stress concentrations at mounting points, or because loads paths during launch or entry are different from those seen during surface operations. Significant mass inefficiencies arise if surface components (such as a rover) must be overdesigned to withstand one-time launch or entry loads (see the next item related to gear ratios). The impacts of loads and mounting schemes on propellant tanks, the MAV, and other cargo should eventually be analyzed using dedicated models for each component.

4.13.2.8 Develop and determine system mass performance “gear ratios”

“Gear ratios” are system performance characteristics that help determine the mass efficiency of an overall mission. By definition, a gear ratio for a single step of a mission is the system mass required in its initial state (on the launch pad) to deliver one mass unit of payload to its final state (Martian surface, or the mission step at which the component is jettisoned). Overall gear ratio for a mission is the product of gear ratios for all sequential steps. In layman’s terms, the gear ratio answers the question, “how much system mass is required to support any given component?” For design of structures, the gear ratio can help determine priorities for focused mass-reduction efforts of structural components, jettison strategies, and mass-transfer options. For example, if mass must be added to stiffen a launch vehicle stack, it is often better to add that mass to adapter or interface structure (if possible) rather than adding it to a landed spacecraft component. This is because the landed component must be carried much further into the mission, requiring more propellant than if the mass had been added to a jettisoned adapter. Efforts should be initiated to better understand how Mars mission gear-ratios might affect mass related conclusions for various vehicle components.

4.13.2.9 Study and characterize the landing dynamics or horizontal landers

Horizontal lander configurations have a long and a short axis with significantly different moments of inertia about each. Previous dynamic analyses of landing stability and touchdown loads have only considered nearly symmetric lander geometries. The asymmetric geometry of horizontal configurations suggests that variables such as lander orientation and touchdown velocity direction may be unique drivers for the touchdown stability of horizontal landers. Dynamic modeling of horizontal configurations is necessary to explore these issues.

4.13.2.10 Analyze entry and landing load cases

Time did not allow analysis of the effects entry loads or landing loads have on descent module primary structure. Past experience suggests that these loads are not significant design drivers and will result in only small local changes to vehicle structure. Unknown is whether this remains true for long horizontal configurations. Analyses should be performed on both V1 and H3 (but especially H3) to include these loads, and the results used to update mass properties.

4.13.2.11 Study and analyze shroud volume usage

The V1 vertical lander configuration has a total height of 10.75 m. Currently the expected SLS launch vehicle shroud (heavy-lift version) will be 31 m tall with a cylindrical length of 17.2 m. If only the vertical lander is packaged in the shroud, there may be significant extra volume, even if space for packaging a HIAD system is accounted for. Even the H3 horizontal lander does not have sufficient length (15.2 m) to fill a 31 m shroud. Several options are possible. The shroud length could be shortened or, assuming launch mass limits are not exceeded, additional cargo elements or a propulsion stage (or both) could be packaged with the lander in the shroud. Shortening the shroud may work well for packaging the lander but not for other payloads, thus requiring two unique shroud configurations, one long and one short. In the case of the rigid aeroshell, shortening the overall length may not be feasible because the correct aspect ratio for entry is not maintained. Also for the rigid aeroshell it may be desirable to attach the lander higher up in the shroud so it will be in the center of the aeroshell during entry. Doing this will create very low lateral frequencies and may not be feasible. Placing additional cargo or a propulsion stage under a lander in the shroud is possible, but will increase the overall height of the launch vehicle stack, again resulting in low stiffness/frequency. Attachment to the shroud may become mandatory or it may be not be possible

at all to achieve sufficient lateral stiffness for some scenarios. All aspects of stack sequencing and shroud utilization require future analysis. Efforts in this area should be coordinated with the SLS project team and future activities that are shroud related.

4.13.2.12 Update both landers for habitat integration

Lander configurations were developed here with focus on a first launch that transports the FSPS, rover, and MAV to the Martian surface. A subsequent launch will transport a crew and habitat structure, hopefully utilizing the same basic lander configuration. During down selection, the ability of the brainstormed concepts to package a habitat was treated as a desirable (but not deciding) characteristic. Notional habitat packaging concepts were developed for most of the configurations. Both the H3 and V1 configurations are able to package a habitat structure, but habitat integration was not analyzed in the current work. Hardware concepts for integrating and mounting a habitat are needed, along with models to size the hardware and examine the impacts of launch and other loads on the habitat structure. More analysis is needed to ensure that a single lander descent stage configuration can accommodate both cargo-only and crewed packaging and launch requirements.

4.13.2.13 Update the FSPS volume and determine impacts to the lander configurations

Near the completion of this effort it was recognized the FSPS volume used herein (33 m³) was too low because it was derived for a lunar rather than Mars mission scenario. A more realistic value for a Mars mission is 60 m³. This increase in FSPS volume may significantly affect the lander packaging scenarios that were considered, including the down-selected configurations. An effort should be made to determine the impact of increasing FSPS volume on the lander configurations and mass estimates developed during the present study.

4.13.2.14 Determine the Impacts of Utilizing Full Lander Performance Capability

The cargo elements considered for the present lander configurations (FSPS, rover and MAV) do not represent the full landed mass capability corresponding to the assumed lander propellant masses. Approximately 15,000kg of additional mass can be carried by the lander if all of the assumed propellant is available. This additional mass was included in the analyses as part of the lander control mass, but additional volume for the mass was not allocated. Thus, it may turn out that in order to completely utilize full lander performance, the studied landers might require significant reconfiguration. The other options are to package cargo elements more densely, or to decrease the amount of propellant. The later scenario reduces the size of the propellant tanks and might in itself create a need for lander reconfiguration. An effort should be initiated to examine the complete ramifications of these issues, especially as related to the results and conclusions of the present study.

4.13.3 Forward Work in Descent Module Design

It is apparent from the range in payload delivery capability (~15 t) that resulted from various powered descent strategies considered in the Cycle D descent module analysis that future work should include a thorough evaluation of this phase of flight for human class missions at Mars. All previous robotic powered flight trajectories at Mars have considered a variable throttle profile. A reevaluation of the motivation for considering constant versus a variable throttle profile and the amount of throttling capability should be performed for Mars human class missions. Additionally, the Cycle D engine design is based on current technology. A complete trade of advanced capabilities in T/W, engine thrust capability, and Isp should be considered as well as trades on terminal descent throttling strategies and development of new parametric mass and terminal descent tank sizing models that account for the inertias of the packaged configurations and modify length or height to accommodate propellant use.

4.13.4 Forward Work Mars Ascent Vehicle

Future work for the MAV would include investigating mass reduction opportunities identified in section 4.9 and to continue to improve design fidelity and definition of MAV and lander interfaces.

4.13.5 Forward Work Transition Event

A high-level assessment of the transition event for a vertical lander was included in this study. Planned future work includes performing a similar assessment for a horizontal lander configuration for both the mid L/D entry architecture and HIAD architecture.

Future work to improve our understanding of the transition event also needs to include continued development of the higher-fidelity analysis tool to include a control system for pitch and possibly yaw and roll to better control the lander as it moves away from both the mid L/D aeroshell and HIAD. Animation should also be employed using actual geometries to check for collisions. Additional recommendations are listed below:

1. Use realistic center of gravities and moments of inertia for mid L/D and HIAD heat shields.
2. Use realistic transition aerodynamics to include actual geometries and interactions.
3. Simulate thruster plume interactions between lander and HIAD.
4. Assess any control issues.
5. Address any mass inconsistencies.

Using this higher-fidelity tool, promising transition event methods identified by the high-level assessments should be analyzed in more detail.

4.13.6 Forward Work Mars Lander Architecture Modeling Approach

Important to the long-term continuity of human Mars lander architectural development and assessment is the capture, documentation, and high-level contextual framework benefits provided by the model-based systems engineering tools documented in Section 4.11. Future work includes continued development of these tools to include further operational modeling, functional modeling, and physical modeling resulting in the identification and capture of functional and performance requirements. This process helps provide the context for more detailed design work and identifies architecture interrelationships that otherwise might go unidentified. The development of robust model-based system engineering documentation provides a foundation for consistent and rigorous evolution of the Mars EDL architecture.

4.14 Appendix A: Master Equipment Lists

The following are vehicle mass breakdowns for the horizontal lander configuration with Mid L/D entry system and vertical lander configuration with HIAD entry system. The masses are listed for five epochs in the mission scenario: system mass at entry, lander mass at powered descent initiation, lander mass at touchdown, MAV mass at ascent initiation, MAV mass at docking after ascent.

Horizontal Lander Configuration with Mid L/D Aero Entry System

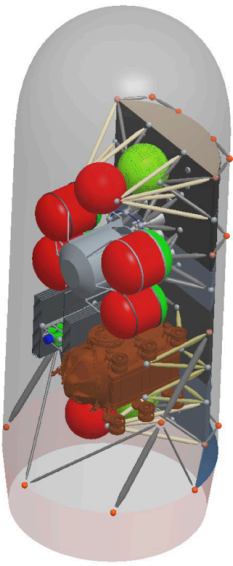
 Horizontal Lander Mid L/D	Horizontal Configuration Entry Mass	Basic Mass (kg)	MGA and/or Margin	Allowable Dry Mass (kg)	Allowable Wet Mass (kg)
	Mass of the EDL system, including aeroassist system, lander and payload, at Mars entry interface				
	Entry System Mass	58,337		73,225	125,607
	Ascent Module Mass w/ No Crew	5,129	0%	6,668	13,799
	Ascent Module Dry Mass w/No Crew	5,129	30%	6,668	6,668
	CH ₄ Propellant		0%		7,131
	Descent Module	11,917	0%	15,492	35,249
	Descent Module Dry	11,917	30%	15,492	15,492
	CH ₄ Propellant		35%		4,939
	LOX Propellant		35%		14,818
	Aero Entry System (Mid L/D)	28,729	40%	38,503	38,503
	Payload Mass	12,562	0%	12,562	12,562
	FPS	7,000	0%	7,000	7,000
	Rover	5,562	0%	5,562	5,562
	Reserve Payload				25,494

Figure 4-133 Entry system mass for horizontal lander and Mid L/D aero entry system.

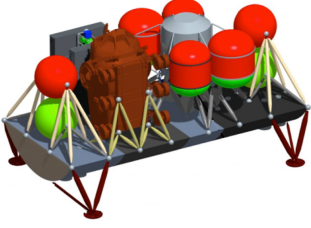
	Horizontal Configuration Lander Mass – Powered Descent Init	Basic Mass (kg)	MGA and/or Margin	Allowable Dry Mass (kg)	Allowable Wet Mass (kg)
	Mass of the fully fueled lander at powered descent initiation				
	Lander Mass	29,608		34,722	87,104
	Ascent Module Mass w/ No Crew	5,129	0%	6,668	13,799
	Ascent Module Dry Mass w/No Crew	5,129	30%	6,668	6,668
	CH ₄ Propellant		0%		7,131
	Descent Module	11,917		15,492	35,249
	Descent Module Dry	11,917	30%	15,492	15,492
	CH ₄ Propellant		35%		4,939
	LOX Propellant		35%		14,818
	Payload Mass	12,562		12,562	12,562
	FPS	7,000	0%	7,000	7,000
	Rover	5,562	0%	5,562	5,562
	Reserve Payload				25,494

Figure 4-134 Lander mass at powered descent initiation for the horizontal lander configuration.

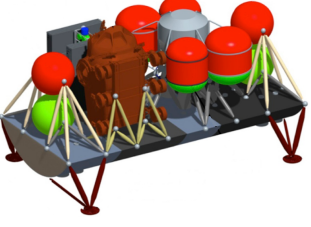
	Horizontal Configuration Landed Mass	Basic Mass (kg)	MGA and/or Margin	Allowable Dry Mass (kg)	Allowable Wet Mass (kg)
	Total landed mass, assuming all descent propellant is expended				
	Lander Mass	29,608		34,722	67,347
	Ascent Module Mass w/ No Crew	5,129	0%	6,668	13,799
	Ascent Module Dry Mass w/No Crew	5,129	30%	6,668	6,668
	CH ₄ Propellant		0%		7,131
	Descent Module	11,917		15,492	15,492
	Descent Module Dry	11,917	30%	15,492	15,492
	Payload Mass	12,562		12,562	12,562
	FPS	7,000	0%	7,000	7,000
	Rover	5,562	0%	5,562	5,562
	Reserve Payload				25,494

Figure 4-135 Lander mass at touchdown for horizontal lander configuration.

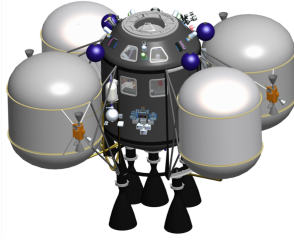
	Horizontal Configuration Mars Ascent Mass	Basic Mass (kg)	MGA and/or Margin	Allowable Dry Mass (kg)	Allowable Wet Mass (kg)
	Mass of fully fueled MAV at Mars ascent initiation				
	Mars Ascent Mass	5,981		7,523	38,186
	Ascent Module Mass w/CH₄ & LOX	5,129	0%	6,668	37,331
	Ascent Module Dry Mass w/No Crew	5,129	30%	6,668	6,668
	CH ₄ Propellant		0%		7,131
	LOX Propellant		0%		23,532
	Crew (6)	591	0%	591	591
	Sample Return Package	261	30%	264	264

Figure 4-136 Mars Ascent Vehicle mass at ascent initiation for horizontal configuration.

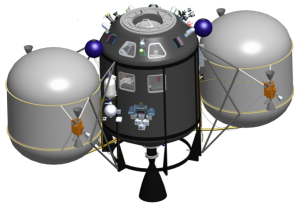
	Horizontal Configuration Docked Mass	Basic Mass (kg)	MGA and/or Margin	Allowable Dry Mass (kg)	Allowable Wet Mass (kg)
	Mass of docked MAV 2 nd stage assuming all propellant is expended during ascent & RPOD ops				
	Docked Mass	4,727		5,893	5,257
	Ascent Module Mass (2nd Stage)	3,875	30%	5,038	5,038
	Crew (6)	591	0%	591	591
	Sample Return Package	261	30%	264	264

Figure 4-137 Mars Ascent Vehicle mass at docking after return from Mars surface.

Vertical Lander Configuration with HIAD Aero Entry System

Vertical Configuration Entry Mass	Basic Mass (kg)	MGA and/or Margin	Allowable Dry Mass (kg)	Allowable Wet Mass (kg)	
					Mass of the EDL system, including aeroassist system, lander and payload, at Mars entry interface
<p style="text-align: center;">Configuration Graphic In-Work</p> <p style="text-align: center;">Vertical Lander HIAD</p>	Entry System Mass	39,788		52,668	111,644
	Ascent Module Mass w/ No Crew	5,129	0%	6,668	13,799
	Ascent Module Dry Mass w/No Crew	5,129	30%	6,668	6,668
	CH ₄ Propellant		0%		7,131
	Descent Module	9,865	0%	12,825	32,582
	Descent Module Dry	9,865	30%	12,825	12,825
	CH ₄ Propellant		35%		4,939
	LOX Propellant		35%		14,818
	Aero Entry System (HIAD)	12,232	40%	20,613	20,613
	Payload Mass	12,562	0%	12,562	12,562
	FPS	7,000	0%	7,000	7,000
	Rover	5,562	0%	5,562	5,562
	Reserve Payload				32,088

Figure 4-138 Entry system mass for vertical lander configuration and HIAD aero entry system.

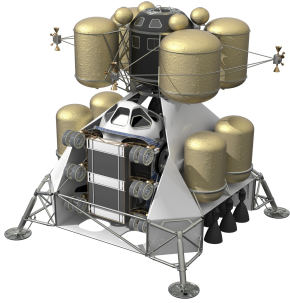
Vertical Configuration Lander Mass – Powered Descent Init	Basic Mass (kg)	MGA and/or Margin	Allowable Dry Mass (kg)	Allowable Wet Mass (kg)	
					Mass of the fully fueled lander at powered descent initiation
	Lander Mass	27,556		32,055	91,031
	Ascent Module Mass w/ No Crew	5,129	0%	6,668	13,799
	Ascent Module Dry Mass w/No Crew	5,129	30%	6,668	6,668
	CH ₄ Propellant		0%		7,131
	Descent Module	9,865		12,825	32,582
	Descent Module Dry	9,865	30%	12,825	12,825
	CH ₄ Propellant		35%		4,939
	LOX Propellant		35%		14,818
	Payload Mass	12,562		12,562	12,562
	FPS	7,000	0%	7,000	7,000
	Rover	5,562	0%	5,562	5,562
	Reserve Payload				32,088

Figure 4-139 Lander mass at powered descent initiation for the vertical lander configuration.

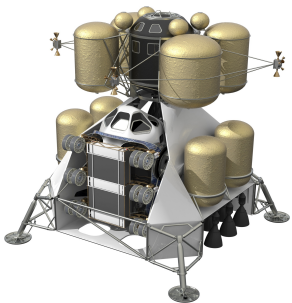
	Vertical Configuration Landed Mass	Basic Mass (kg)	MGA and/or Margin	Allowable Dry Mass (kg)	Allowable Wet Mass (kg)
	Total landed mass, assuming all descent propellant is expended				
	Lander Mass	27,556		32,055	71,274
	Ascent Module Mass w/ No Crew	5,129	0%	6,668	13,799
	Ascent Module Dry Mass w/No Crew	5,129	30%	6,668	6,668
	CH ₄ Propellant		0%		7,131
	Descent Module	9,865		12,825	12,825
	Descent Module Dry	9,865	30%	12,825	12,825
	Payload Mass	12,562		12,562	12,562
	FPS	7,000	0%	7,000	7,000
	Rover	5,562	0%	5,562	5,562
	Reserve Payload				32,088

Figure 4-140 Lander mass at touchdown for vertical lander configuration.


	Vertical Configuration Mars Ascent Mass	Basic Mass (kg)	MGA and/or Margin	Allowable Dry Mass (kg)	Allowable Wet Mass (kg)
	Mass of fully fueled MAV at Mars ascent initiation				
	Mars Ascent Mass	5,981		7,523	38,186
	Ascent Module Mass w/CH₄ & LOX	5,129	0%	6,668	37,331
	Ascent Module Dry Mass w/No Crew	5,129	30%	6,668	6,668
	CH ₄ Propellant		0%		7,131
	LOX Propellant		0%		23,532
	Crew (6)	591	0%	591	591
	Sample Return Package	261	30%	264	264

Figure 4-141 Mars Ascent Vehicle mass at ascent initiation for the vertical lander configuration.

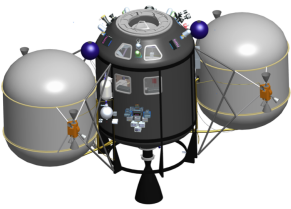
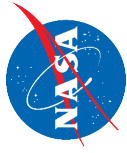
	Vertical Configuration Docked Mass	Basic Mass (kg)	MGA and/or Margin	Allowable Dry Mass (kg)	Allowable Wet Mass (kg)
	Mass of docked MAV 2 nd stage assuming all propellant is expended during ascent & RPOD ops				
	Docked Mass	4,727		5,893	5,257
	Ascent Module Mass (2nd Stage)	3,875	30%	5,038	5,038
	Crew (6)	591	0%	591	591
	Sample Return Package	261	30%	264	264

Figure 4-142 Mars Ascent Vehicle docked mass after return from Mars surface.

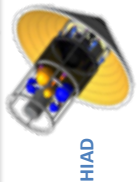
4.15 Appendix B: Vehicle Baseball Cards

The following are vehicle configuration baseball cards for the Mars lander and the MAV:

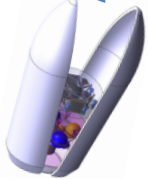


Mars Cargo Lander – DRA-5 Addendum 2

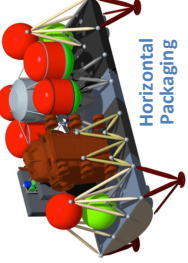
Preliminary Results—Requires Further Refinement



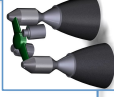
HIAD



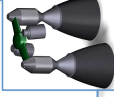
Rigid Aeroshell



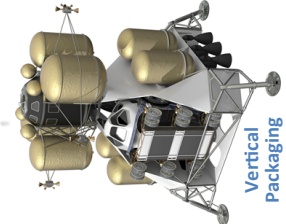
Horizontal Packaging



Vertical Packaging



Dual Nozzle Engine



Representative payloads shown

Design Constraints/Parameters

- Crew Capacity: 0 Descended; 6 ascended
- Main Engine Propellants: LO2/LCH4
- ISRU assumption: LOX for ascent (atmospheric ISRU)
- Aeroshell: either 23 m dia HIAD or 10 m x 30 m Aeroshell
- Total Mass Reserve: 30% (20% Growth, 10% PMR)
- Cargo Lander Operational Life: 8 Days (Descent + 7 days Surface Self-Sufficiency)
- Lander Total Service Life: 332 Days (Earth Launch to Crew Mars Ascent)
- # Main Engines: 6 each dual nozzle engines
- Main Engine Isp (100%): 360 sec
- Main Engine Thrust (100%): 200 kN each
- Total Thrust: 1200 kN

Lander Element	Entry Mass (kg)			
	Vertical Packaging		Horizontal Packaging	
	HIAD	Aeroshell	HIAD	Aeroshell
Aeroshell	21,000	TBD	TBD	39,000
• HIAD or Rigid Aeroshell	21,000	TBD	TBD	39,000
Mars Descent Module	33,000	33,000	35,500	35,500
• Descent Stage Inert Mass + ISRU	13,000	13,000	15,500	15,500
• Descent Stage Propellant	15,000	15,000	15,000	15,000
• Liquid Oxygen	5,000	5,000	5,000	5,000
• Liquid Methane				
Cargo	40,000	40,000	40,000	40,000
• Allocated Cargo				
• Mars Ascent Vehicle (MAV)	13,500	13,500	13,500	13,500
• Surface Mobility	5,600	5,600	5,600	5,600
• Fission Surface Power (FSP)	7,000	7,000	7,000	7,000
• Un-Allocated Cargo	13,900	13,900	13,900	13,900
Mars Cargo Lander Mass @ Entry	94,000	TBD	TBD	114,500

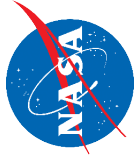
Description

The Mars Cargo Lander is a key element of NASA's Design Reference Architecture 5 (DRA-5), delivering 40 metric ton of equipment to the Martian surface in preparation for a Mars Crew Lander approximately 18 months later. Variants include two different types of aeroshell systems, packaged in two different ways. The aeroshell system may also be used for aerocapture into Mars orbit prior to EDL. For reference, the horizontal/aeroshell variant is most similar to the original DRA-5 concept.

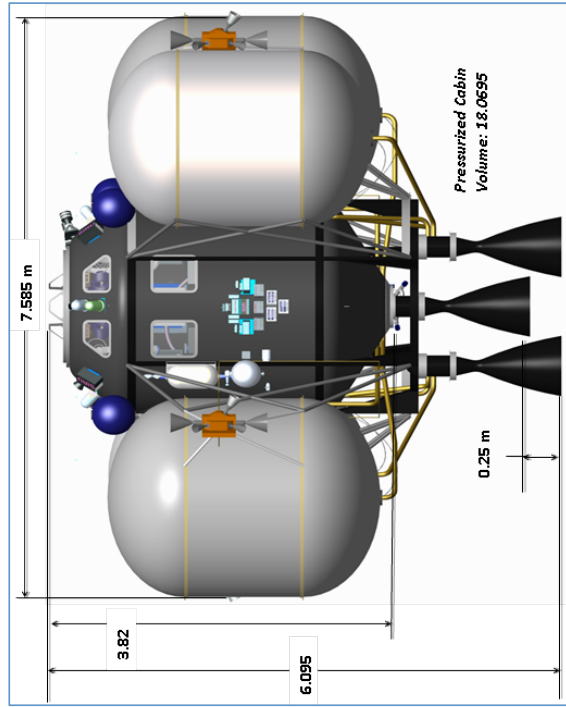
Technology Needs

Dual-use TPS for aerocapture/entry, Supersonic Retro-Propulsion; Landing hazard detection and avoidance; LOX Atmospheric ISRU

Analysis Fidelity Confidence: Power, Thermal and Propulsion subsystem fidelity for this analysis is low. Variations in throttle strategy can affect mass. Masses shown are for a common target cargo mass. Note that MAV descended mass does not include LOX propellant (assumed to be ISRU provided)



Mars Ascent Vehicle (MAV)- DRA-5, 6 Crew Mission



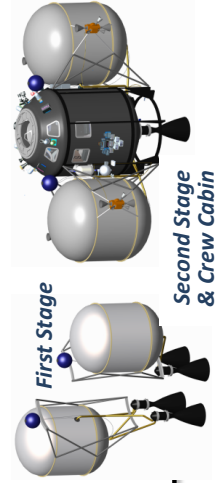
- Design Constraints/Parameters**
- Ascent rendezvous location: High Mars Orbit
 - Ascent Duration: 43 hours (max.)
 - Samples returned from surface: 250 kg
 - ISRU assumption: LOX for ascent
 - MAV Operational Life: 2 days
 - MAV Total Service Life: ~1669 days
 - MAV Surface Exposure: ~1344 days
 - Total Reserve: 30% (20% Growth, 10% PMR on inert mass)
- Crew Cabin**
- Crew Capacity: 6
 - Pressurized Volume: 18 m³
- Two Propulsion Stages**
- Stage 1 # Main Engines: 4
 - Stage 2 # Main Engines: 1
 - "Nested" Propellant Tanks
 - Main Engine and RCS Propellants: LO2/CH4
 - Main Engine Isp (100%): 360 sec
 - Main Engine Thrust (100%): 100 kN ea
 - Total Thrust (100%): 500 kN

Technology Needs: long-duration batteries; Remote/automated propellant tank servicing;

Description

The Mars Ascent Vehicle (MAV) is a cargo element of the DRA-5 Cargo Lander. The MAV arrives at Mars with empty Liquid Oxygen (LOX) propellant tanks, and is remotely serviced by an In-Situ Resource Utilization (ISRU) system. Once the propellant tanks are verified full, the crew departs from Earth. The Mars Descent Module (MDM) serves as the delivery vehicle for MAV transit, descent, and landing at Mars, provides keep-alive power to the MAV during the surface stay, and serves as the launch pad for MAV lift-off. Although the MAV is nominally only used for the 43 hour ascent, its limited habitability functions would allow it to serve as an emergency surface safe-haven, if consumables are resupplied prior to ascent. At the completion of the surface mission, the crew ascends in the MAV for a rendezvous/docking with the transit habitat, and the MAV is discarded in High Mars Orbit.

Subsystem	Mass (kg)	
	Descended	Ascended
Crew Cabin	3,431	4,438
C&DH	265	265
GN&C	75	75
C&T	82	82
Power	371	371
Thermal	217	217
ECLS	364	364
EVA	110	165
Structures & Mechanisms	1,700	1,700
Human Factors	47	82
Crew & Crew-Worn	0	787
Cargo	0	250
Non-Prop. Fluids	200	80
1st Propulsion Stage	4,546	14,173
Inert Mass	1,629	1,629
LOX Propellant	0	9,627
LCH4 Propellant	2,917	2,917
2nd Propulsion Stage	5,559	19,465
Inert Mass	1,345	1,345
LOX Propellant	0	13,906
LCH4 Propellant	4,214	4,214
TOTALS	13,536	38,076



4.16 Bibliography

- ¹ Augustine, N.R., et al, “Seeking a Human Spaceflight Program Worthy of a Great Nation”, Review of U.S. Human Spaceflight Plans Committee, 2009
- ² Drake, B. G., editor., “Human Exploration of Mars Design Reference Architecture 5.0,” s.l. : NASASP-2009-566, July 2009.
- ³ Dwyer Cianciolo, A.M., et al., “Entry, Descent and Landing Systems Analysis Study: Phase 1 Report,” NASA–TM–2010–216720, July 2010
- ⁴ Munk, M. M. and Cianciolo, A. D., “Entry, Descent, and Landing for Human Mars Missions,” GLEX-2012.08.2.6x12677, Washington, D.C., May 2012.
- ⁵ Kumar, "Issues on Human Acceleration Tolerance After Long-Duration Space Flights" NASA Technical Memo 104753, Oct 1992.
- ⁶ Powell, R. W., Striepe, S. A., Desai, P. N., Queen, E. M., Tartabini, P. V., Brauer, G.L., Cornick, D. E., Olson, D. W., Petersen, F. M., Stevenson, R., Engle, M. C., and Marsh, S. M., “Program to Optimize Simulated Trajectories (POST2), Vol. II Utilization Manual.” Version 1.1.1G, May 2000.
- ⁷ Garcia, J. A., et al., “Co-Optimization of Mid Lift to Drag Vehicle Concepts for Mars Atmospheric Entry,” AIAA-2010-5052, 10th AIAA/ASME Joint Thermophysics and Heat Transfer Conference, Chicago, IL, 28 June – 1 July 2010.
- ⁸ Bhushan, Naveet, *Strategic Decision Making: Applying the Analytic Hierarchy Process*, Springer-Verlag London Limited, 2004
- ⁹ Brauer, G. L., Cornick, D. E., and Stevenson, R., “Capabilities and Applications of the Program to Optimize Simulated Trajectories (POST),” NASA CR-2770, 1977
- ¹⁰ Striepe, S.A., Powell, R. W., Desai, P. N., Queen, E. M, Brauer, G. L., Cornick, D. E., Olson, D. W., Peterson, F. M., Stevenson, R., Engel, M, C., Marsh, S. M., and Gromko, A. M., *Program to Optimize Simulated Trajectories (POST II)*, Vol. 2: Utilization Manual, Ver. 1.1.7, NASA Langley Research Center, Hampton, VA, July 2002.
- ¹¹ Tartabini, P. V., Roithmayr, C., Toniolo, M. D., Karlgaard, C. D., and Pamadi, B. N., “Modeling Multibody Stage Separation Dynamics Using Constraint Force Equation Methodology,” *Journal of Spacecraft and Rockets*, Vol. 48, No. 4, 2011, pp. 573-583.
- ¹² Toniolo, M. D., Tartabini, P. V., Pamadi, B. N., and Hotchko, N. J., “Constraint Force Equation Methodology for Modeling Multi-Body Stage Separation Dynamics,” AIAA Paper 2008-0219, 2008.
- ¹³ Albertson, C. W., Tartabini, P. V, and Pamadi, B. N., "End-To-End Simulation of Launch Vehicle Trajectories Including Stage Separation Dynamics," AIAA-2012-4863.
- ¹⁴ Paddock, David A. Email dated September 5, 2012.
- ¹⁵ Cianciolo, Alicia D., Davis, Jody L, Shidner, Jeremy D., and Powell, Richard W.: “Entry, Descent and Landing Systems Analysis: Exploration Class Simulation Overview and Results,”
- ¹⁶ Kinney, David J., “Aerodynamic and Aerothermal Environment Models for Mars Entry, Descent, and Landing Systems Analysis Study,” AIAA-2011-1189

This page intentionally left blank

5. SPACE LAUNCH SYSTEM

Primary Contributors:

Todd May, National Aeronautics and Space Administration, George C. Marshall Space Flight Center

The National Aeronautics and Space Administration’s Space Launch System (SLS) Program, managed at the Marshall Space Flight Center, is making progress toward delivering a new capability for exploration beyond Earth orbit in an austere economic climate. This fact drives the SLS team to find innovative solutions to the challenges of designing, developing, fielding, and operating the largest rocket in history. To arrive at the current SLS plan, government and industry experts carefully analyzed hundreds of architecture options and arrived at the one clear solution to stringent requirements for safety, affordability, and sustainability over the decades that the rocket will be in operation. This paper will explore ways to fit this major development within the funding guidelines by using existing engine assets and hardware now in testing to meet a first launch by 2017. It will explain the SLS Program’s long-range plan to keep the budget within bounds, yet evolve the 70 metric ton (t) initial lift capability to 130-t lift capability after the first two flights. To achieve the evolved configuration, advanced technologies must offer appropriate return on investment to be selected through a competitive process. For context, the SLS will be larger than the Saturn V that took 12 men on 6 trips for a total of 11 days on the lunar surface over 4 decades ago. Astronauts train for long-duration voyages on the International Space Station (ISS), but have not had transportation to go beyond Earth orbit in modern times, until now. NASA is refining its mission manifest, guided by U.S. Space Policy and the Global Exploration Roadmap. Launching the Orion Multi-Purpose Crew Vehicle’s (MPCV’s) first autonomous certification flight in 2017, followed by a crewed flight in 2021, the SLS will offer a robust way to transport international crews and the air, water, food, and equipment they need for extended trips to asteroids, Lagrange Points, and Mars. In addition, the SLS will accommodate high-priority science experiments. SLS affordability initiatives include streamlining interfaces, applying risk-based insight into contracted work, centralizing systems engineering and integration, and nurturing a learning culture that continually benchmarks its performance against successful ventures. As this paper will explain, the SLS is making measurable progress toward becoming a global infrastructure asset for robotic and human scouts of all nations by harnessing business and technological innovations to deliver sustainable solutions for space exploration.

5.1. Introduction

The SLS rocket will support missions of international importance as the first exploration-class launch vehicle flown by the United States since the Apollo Program’s Saturn V. Continuing the tradition of America’s first 50 years in space, this new heavy-lift rocket will provide the sheer power and payload capacity needed to overcome limitations that have until now delayed humanity’s voyage of discovery in the solar system (Figure 5-1). The SLS offers game-changing possibilities for economic vitality in space and on Earth, safely transporting astronauts to unexplored regions in search of knowledge and delivering cutting-edge missions that will rewrite scientific texts and spur technological advances.

NASA has set a steady course to resume human space flight by integrating the SLS Program at Marshall Space Flight Center, the Orion MPCV Program at Johnson Space Center, and the Ground Systems Development and Operations (GSDO) Program at Kennedy Space Center. Together, they offer the potential for social and economic benefits characteristic of U.S. infrastructure initiatives that were successfully carried out in years past, thanks to governmental oversight and funding. Examples include the Hoover Dam, which enabled arid western lands to be transformed into thriving cities, and the Interstate Highway System, which opened the country to huge waves of commercial expansion before it was even completed.



Figure 5-1 Advancing human space exploration – Saturn V, Space Shuttle, and Space Launch System.

The SLS rocket is central to NASA’s capability-driven framework, designed to launch planetary probes and great astronomical observatories, enable the human/robotic interface to be synchronized, and make preparations to set the first astronaut’s boot prints on Mars. It will be associated with surprising new innovations, some in response to paradigm-changing discoveries, others to improve existing methods for recycling waste, obtaining clean water, and harnessing alternative energy sources — such as solar power — in practical and affordable ways. International partners will be invited to participate in missions to foster the peaceful pursuit of mutual objectives on the space frontier, as outlined in the Global Exploration Roadmap¹ and The National Space Policy of the United States of America.²

This new infrastructure asset is positioned for success. The SLS concept and management plan are the result of careful deliberations and years of study within NASA and other U.S. Government agencies, including the Office of Science and Technology Policy and the Office of Management and Budget, as well as in consultation with internal and external stakeholders. Detailed and independently verified engineering and business analyses support the vehicle architecture and strategy to get to first flight by 2017 (Figure 5-1).

Building the most capable U.S. rocket is a commitment of limited resources, especially when accepting the challenge of a first flight in 5 years. NASA selected the SLS architecture to leverage existing engines in NASA’s inventory and complete propulsion hardware now well into the development phase. This option is not only the most cost-effective choice — it also offers unprecedented performance.

The SLS management approach incorporates the best practices of lean organizations to deliver a safe, affordable, and sustainable solution. In the year since the SLS Program was announced, the team has completed NASA’s System Requirements Review (SRR) and System Definition Review (SDR), and steady progress is being made toward the next major milestone — the Preliminary Design Review in 2013.

5.2. Architecture Overview and Accomplishments

After studying priority stakeholder requirements, NASA selected a design that provides a platform for international cooperation in space while supporting new options and destinations not considered possible until now, opening the potential for technological achievements, high-value science missions, and expanding the global economy. Many commercial rockets are available in the medium-to-heavy class, but super-heavy-lift vehicles like SLS lie solely within the Government’s purview, due to the investment required for fielding an entirely new infrastructure asset for scientific exploration beyond Earth’s orbit (Figure 5-2).

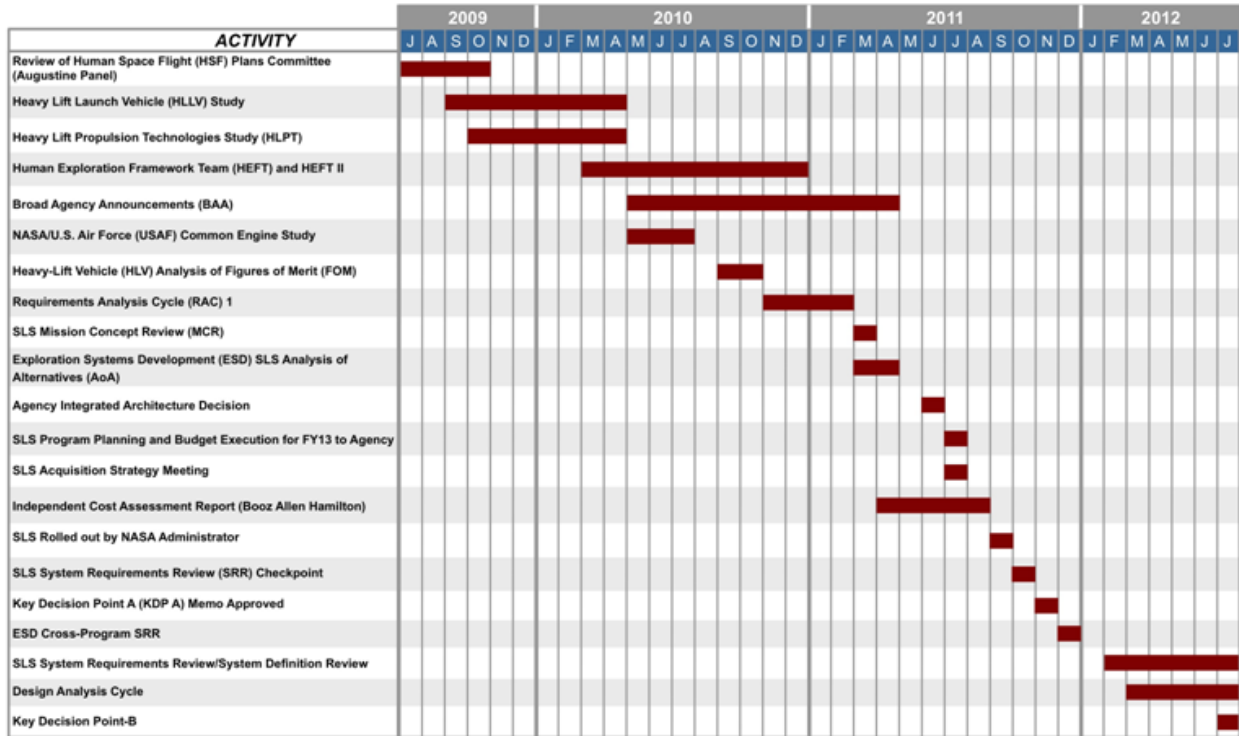


Figure 5-2 Careful planning and deliberations are helping the SLS Program meet its commitments.

The NASA Authorization Act of 2010 directs NASA to develop the SLS rocket as a follow-on to the Space Shuttle, with the capability of accessing cis-lunar space and regions beyond low-Earth orbit (LEO) to allow the U.S. to participate in global efforts to develop this increasingly strategic region.³ The Act also provides a series of minimum capabilities. The SLS vehicle must be able to: (a) lift 70 t to LEO initially and then be evolvable to lift 130 t or more, (b) lift the Orion spacecraft, and (c) serve as a backup system for delivering cargo and crew to the ISS in the event that such requirements cannot be met by available commercial or partner-supplied vehicles. These top-level requirements drive technical trade studies and resource planning, as the SLS concept is refined to address design reference missions to destinations such as geosynchronous-Earth orbit and high-Earth orbit, along with figures of merit for safety, affordability, and reliability.

As part of its affordability tenets and design strategy, the SLS core and upper stages share important common attributes—such as outer diameter, material composition, subsystem components, and tooling—that allow NASA to capitalize on these synergies. The SLS stages and other hardware will be designed once and used many times in keeping with the Program’s affordability strategy (Figure 5-3).

The rocket’s initial Block 1 design includes a 27.5-ft (8.4-m) core stage tank that delivers liquid oxygen/liquid hydrogen (LOX/LH₂) propellant to four RS-25 engines (Figure 5-5). This configuration will support the first 4 missions, with 16 engines now in inventory, taking advantage of 30 years of U.S. experience with LOX/LH₂, as well as an existing national infrastructure that includes specialized manufacturing and launching facilities.⁴ To take advantage of synergies between the core stage engine and the upper stage engine discussed below, a common controller is being developed that will work for both variants.

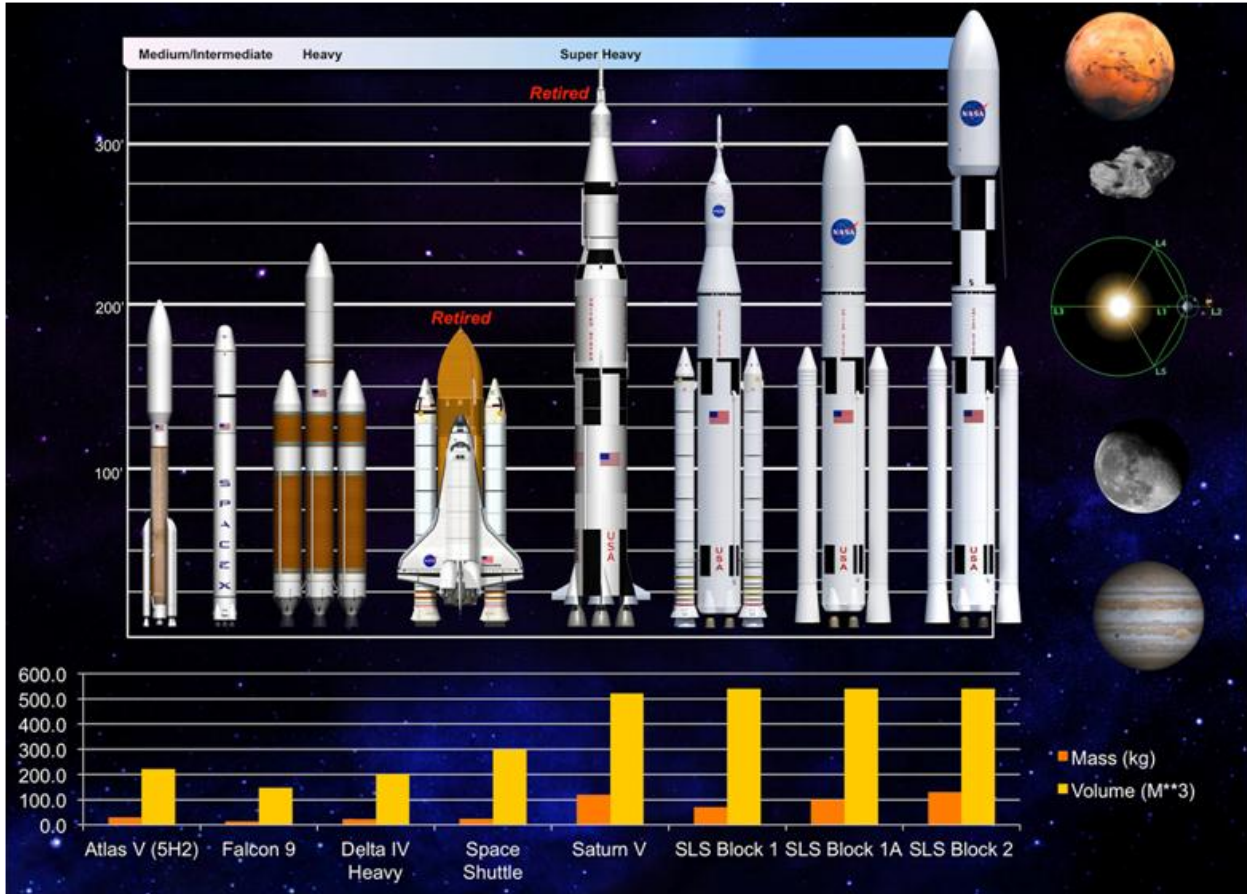


Figure 5-3 SLS scale relative to other U.S. systems

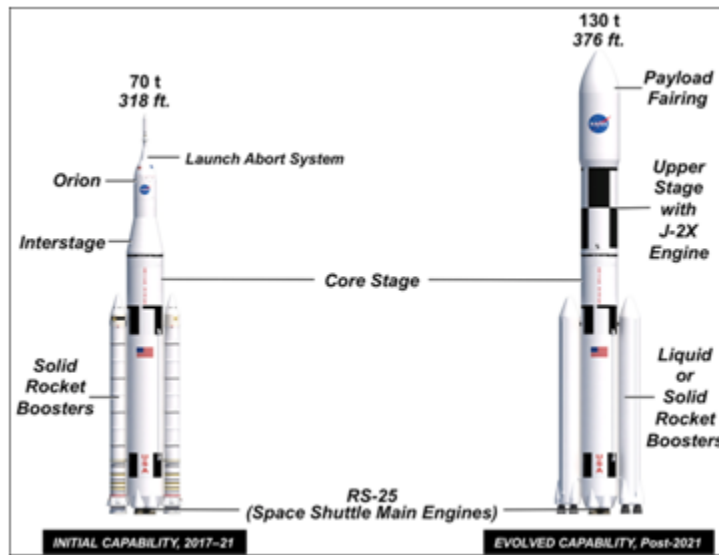


Figure 5-4 Flexible, modular evolution through planned block upgrades.

LOX/LH₂ is also used by the J-2X upper stage engine, now in the testing phase, which will support future performance requirements as the SLS rocket evolves through planned block upgrades (Figure 5-4). The J-2X engine is an advanced version of the J-2 upper stage engine developed for the Saturn V launch vehicles. It is designed to start and restart in orbit, generating approximately 294,000 lbs. (1,308 kN) of thrust to LEO or 242,000 lbs. (1,076 kN) of thrust from LEO into deep space.⁵

The initial SLS rocket will use the world's most powerful solid rocket boosters (SRBs), now in development (Figure 5-7). During launch, each solid rocket motor will generate up to 3,600,000 lbs. (16,013,598 kN) of thrust. Although similar to the SRBs used on the Space Shuttle, this upgraded 5-segment SRB includes improvements such as a larger nozzle throat and an environmentally benign insulation and liner.⁶



Figure 5-5 RS-25 core stage engines in inventory.



Figure 5-6 J-2X upper stage engine testing.



Figure 5-7 A 5-segment booster development test.

The evolved Block 2 SLS rocket will need even more advanced boosters, ones that exceed the limits of today's technology. This requirement provides a competitive opportunity for industry to deliver cost-effective, innovative hardware for deep-space missions to be conducted after 2021. The engineering demonstration and risk-reduction phase will begin in 2012, to be followed later by full-and-open competition for design, development, test, and evaluation (DDT&E).⁷

After considering hundreds of possibilities for the SLS rocket, NASA ultimately selected the one design that came closest to meeting system-level requirements while fitting into a well-defined annual budget with no planned escalations. These objectives are supported by the rocket's relatively simple design, which uses a minimal number of hardware elements to achieve the desired performance, as well as building the initial SLS rocket from existing hardware assets and other elements already well into development.

This strategy is integral to trade studies conducted during design analysis cycles. In its trade studies, the SLS Program considers production and operations (P&O) costs as independent variables, along with nonrecurring development costs. Plans nominally call for one mission per year, which makes any additional missions more affordable.

The rocket's modular and flexible design can be: (a) outfitted with a cargo fairing to enclose flagship science instruments and experiments or (b) configured for the Orion spacecraft and associated equipment. The latter will provide emergency abort capability, protect and sustain the crew during the mission, and enable safe reentry from deep space at high velocities.⁸

Design and development activities are being conducted concurrently to save time and money. For example, the first SRB qualification motor is being prepared for static-testing in 2013 (Figure 5-8).⁹ As part of the contractor's affordability initiative, it has performed process value-stream mapping, resulting in significant cost savings by reducing unnecessary manufacturing steps. Taken together, individual savings add up to significant cost containment.

As another example of measurable progress, the SLS avionics team is fine-tuning flight software, using test-bed computers received ahead of schedule (Figure 5-9). Availability of the platform early in the engineering development phase allows NASA programmers more time to develop the most capable flight software in history. Existing systems from communications and Global Positioning System (GPS) satellites are being upgraded to provide the highest processing capability available.¹⁰

As part of its lean systems engineering and integration effort, NASA also has completed early wind tunnel testing for the SLS rocket, which helps ensure that it presents an affordable and sustainable backbone for long-term human space exploration (Figure 5-10). SLS concepts are being thoroughly tested in wind tunnels, where scale models are used to evaluate the design's performance. Any necessary changes can then be made safely, easily, and inexpensively before the full-scale vehicle is built.¹¹



Figure 5-8 Booster qualification motor casting.



Figure 5-9 SLS avionics software testing.



Figure 5-10 Over 900 SLS wind-tunnel tests have been conducted.

As a final example of progress over the SLS Program’s first year, the Multi-Purpose Crew Vehicle Stage Adapter (MSA) has gone from design drawing to manufacturing in a matter of months. This hardware, which will mate the Orion test article to the Delta IV rocket on a low-Earth orbit flight in 2014, will also be used for the full-up autonomous Orion on the SLS rocket’s maiden voyage in 2017. Again, the philosophy of design once and use many times reflects the Program’s commitment to affordability and a modular, flexible approach to mission support.

5.3. One Rocket, Many Missions

As stated above, the initial SLS rocket will carry the Orion spacecraft during an autonomous demonstration flight in 2017, as well as a crewed mission in 2021, which will be the first time that astronauts have gone beyond Earth’s orbit in over 40 years.

President Obama has challenged NASA to send humans to a near-Earth asteroid by 2025 and to Mars in the 2030s. NASA has made exciting discoveries about the Red Planet, with the help of Mars rovers Opportunity and Spirit. Scientists have confirmed the seasonal presence of saltwater there, using data obtained by the Mars Reconnaissance Orbiter¹² The Mars Science Laboratory, known as Curiosity, is a precursor to human landings on the planet most like Earth. For scientists, the performance offered by the SLS rocket will be available to launch decadal-class missions to Jupiter’s icy moons, the rings of Saturn, and other high-value destinations.

Currently, NASA is conducting mission concept and operations studies in conjunction with stakeholders and partners. The results of these studies will be the subject of future papers and forums.

5.4. Management Approach, Plans, and Progress

Space flight always presents serious challenges and, as former Space Shuttle Program Manager Wayne Hale reminds managers and rocket scientists alike: “This enterprise is not for the faint of heart.”¹³ As the SLS concept moves quickly from the digital drawing board to the launch pad at the Kennedy Space Center, designers and operators are working together to maximize the American taxpayer’s investment in this unprecedented capability (Figure 5-11).

NASA is fitting human exploration into a budget that is less than that of the Space Shuttle Program, even though the SLS rocket offers more capability than a Saturn V. One of the greatest challenges is determining how to reduce recurring and fixed operating costs. Every development activity represents a chance to calibrate the team in keeping with the current economic environment and create sweeping cultural changes to ensure sustainability.



Figure 5-11 SLS on the launch pad (artist’s concept).

The SLS Program’s management approach engages the existing industrial base, including the workforce’s critical skills and talent. SLS content must be executed well within its funding, based upon many lessons learned over the last few decades of human space flight. The first priority is safety, followed closely by affordability. The SLS team is using best practices from industry and Government to reduce the rocket’s time to market and total DDT&E investment. Straightforward lean principles have been implemented, with a healthy dose of forward-leaning competitive opportunities, which will spur innovation and drive efficiencies into the system.

The aerospace professionals who have signed on for the SLS Program bring diverse and wide-ranging backgrounds to the table. They are well-prepared and eager for the opportunity to fly a new generation of missions on a rocket that can take explorers and scientists anywhere that they can imagine. The expectation is set for system optimization, using business and engineering solutions that give the best return on investment, both in terms of up-front nonrecurring costs and long-term sustainability. This team is product-centric — focused on building and flying hardware — and that product is the SLS rocket. All processes and documentation must add value toward delivering it.

Affordability is a key performance factor against which success is measured. Many variables are being aligned as NASA carefully considers P&O costs in tandem with DDT&E activities while employing modern manufacturing and vehicle processing techniques, implementing risk-based insight/ oversight practices, and streamlining contractor deliverables. Taken together, some very simple improvements can add up to substantial savings. The SLS Affordability Plan lays out detailed steps for cost-cutting actions such as scaling back the number of management boards used to control the vehicle configuration, allowing correct decisions to be made more quickly. Formal contractor deliverables are being significantly reduced. Fewer Category 1 deliverables (which must be approved by the Government) are required, with additional savings being realized on production and reproduction costs by accepting electronic documents in the contractor’s preferred format.

NASA selected this vehicle configuration based upon technical and business trade studies informed by a certain philosophy and set of assumptions. The primary figure of merit was cost, both for the Government requirements analysis cycle (RAC) teams and 13 prime-contractor companies that provided input through the Heavy Lift Propulsion Technologies Broad Agency Announcement (BAA) processes. A technical interchange meeting was held with industry to further refine insight/oversight suggestions from the requirements analysis cycle and BAA process. Even now, SLS team members are benchmarking against profitable companies that employ design-to-cost practices.

Affordability is an overarching driver within NASA’s transformational paradigm. Early flight capability with significant DDT&E and P&O cost savings can be realized through existing manufacturing and launch-site infrastructure, as well as employing proven heritage hardware. Design commonality and manufacturing receive heavy emphasis, as do simplicity of processing and launch operations, allowing a flat budget to be maintained throughout the DDT&E process and in years to come. These design-to-cost goals require the team to adopt a mission-oriented battleship mentality, driving its decisions toward rugged and robust system design. “Bells and whistles” design is being supplanted by more utilitarian and service-oriented selections that provide adequate margin to trade performance for cost. This strategy helps streamline one of the biggest expenses in a developmental program – the decision-making process – as does holding budget reserves at the lowest levels possible.

A new culture is emerging, with a general revectoring to ensure that processes support product development instead of the other way around. The expectation is being clearly and consistently articulated that cost is a variable over which the team must exercise judicious control. Cross-validation has been provided by the RAC and BAA studies in many ways. Affordability figure of merit analyses helped infuse this mandate into the SLS Concept of Operations, as well as the very fiber of the organization, by generating both general and specific recommendations to be addressed early in the SLS Program’s life-cycle.

SLS managers reduce risk in many ways. Both performance margin and budget reserves are being held to address the unknowns that inevitably accompany engineering feats of this magnitude. The SLS Program will affordably deliver a 70-t lift capability in the near term by managing cost and mass in similar ways.

Over the years, NASA has contributed much to the world’s engineering and scientific literature, including launch vehicle studies and plans. Now the Agency is putting a plan into action that can effectively take advantage of opportunities for affordability (Figure 5-12). The SLS Program serves as a foundational capability for designing in

efficiencies on the front end, to support a positive balance sheet during the operations phase.

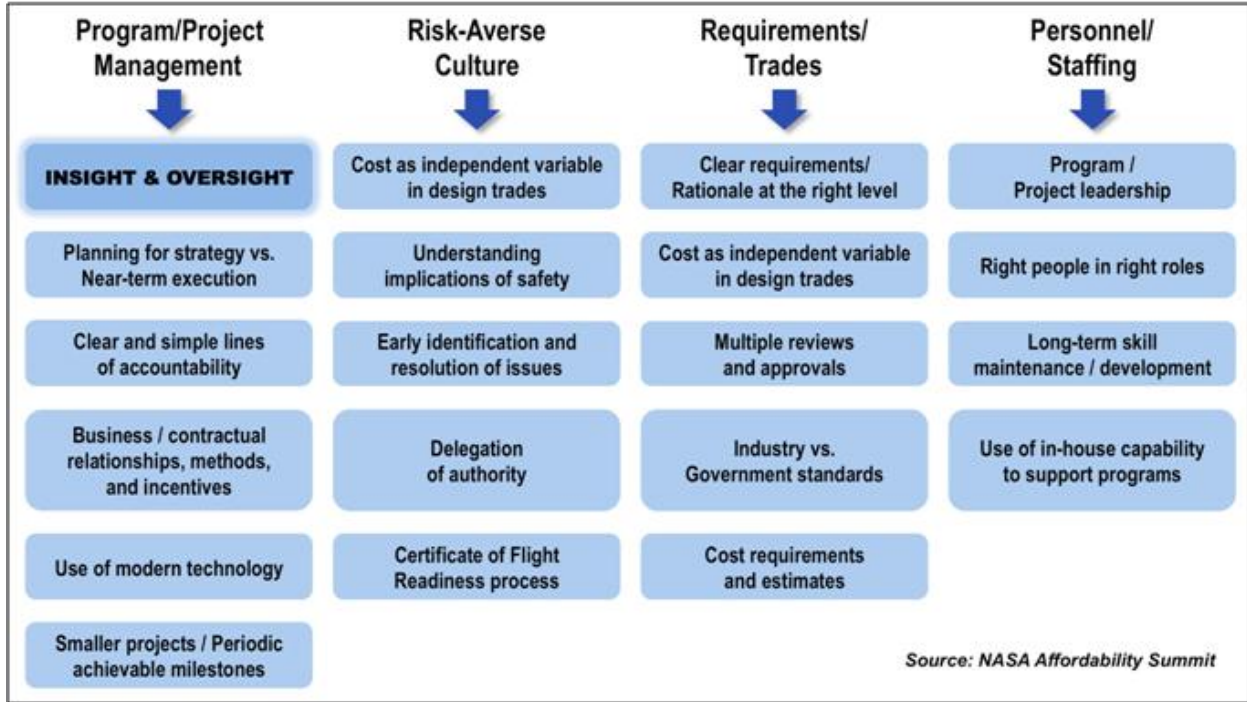


Figure 5-12 Pursuing opportunities for affordability.

The SLS team includes some of the world’s top rocket scientists, who are finding new solutions to longstanding challenges. Each day, these lean principles and practices and industry best practices are being lived by a team dedicated to doing the right thing by driving affordability into the very design of the SLS rocket. They are well aware that as much as 80 percent of fixed costs are set during the design phase and that designing to cost is one variable over which the team has total control. The team has logged many accomplishments, which include meeting decision-gates as the Program moves through formulation into the implementation phase.

NASA announced the SLS Program on September 14, 2011. In just 1 year, the Program is now performing preliminary design and technology completion phase, with a clear path to first flight (Table 5-1). Plans are being made with partner programs Orion and GSDO through NASA’s Human Exploration and Operations Mission Directorate, to deliver a next-generation human space flight system to continue the journey of discovery that is well under way. The rocket has performance margin to spare, while the Program holds sufficient budget reserves to address the unexpected challenges that will surely arise during an endeavor of such magnitude and complexity. Building and flying this rocket will be one of the most demanding jobs on the planet, one that can only be performed by those who can deliver paradigm-changing capabilities to launch a new day in space.

Table 5-1 Selected SLS Life-Cycle Milestones

Activity	Date
SRR/SDR	July 2012
Preliminary Design Review	2013
Critical Design Review	2015
Design Certification Review	2016
First Flight: Orion Autonomous Beyond-Earth Orbit Mission	December 2017

5.5. Conclusions

NASA's new SLS rocket represents the most practical and affordable course of action for leaving Earth orbit at this time. Far-reaching ramifications are being set into motion as a sound technical climate and potential mission manifest are created for sustainable exploration. The SLS rocket has been validated by numerous internal and external stakeholder organizations, and it is supported by the Agency's 2011 Strategic Plan. It will fly carefully selected flagship missions defined by distinguished organizations such as the National Research Council and the International Space Exploration Coordination Group. New knowledge and understanding will be gained about the universe in which we live, allowing the entire world to rewrite standard references, develop advanced technologies, and undertake new economic initiatives (Figure 5-13).



Figure 5-13 The SLS rocket will launch in 2017 (artist's concept).

NASA selected the SLS rocket as its next human-rated heavy-lift launch vehicle because this design offers the optimum solution for exploring with astronauts – who are capable of much greater initiative and insight than robotic probes, valuable though they may be – to safely, cost-effectively, and quickly resume the exploration of our solar system in the current economic climate. SLS team members will stay focused on their ultimate product, the rocket, as its design matures through upcoming life-cycle reviews. The SLS Program's planning strategy includes the use of hardware that already exists or is close to completion, as well as appropriately incorporating advanced technologies that offer attractive return on investment to support NASA's affordability goals. The SLS rocket's design is flexible and evolvable. It provides incremental stakeholder value by fielding an initial capability successively refined in line

with budget realities and the evolving plans of partner coalitions.

NASA’s vision is “To reach for new heights and reveal the unknown, so that what we do and learn will benefit all humankind,” and the first plank in its strategic goals is to “Extend and sustain human activities across the solar system.”¹⁴ The SLS rocket offers a realistic and sturdy backbone for taking the next step out into the cosmic neighborhood that is our home. The SLS Program and its partners are dedicated to meeting their commitments and doing things differently for the right reasons, in the process creating an entirely new capability to directly support human space flight beyond Earth’s orbit. Ultimately, this approach will reduce the risk of undertaking a new slate of science and exploration missions, sending launch vehicles and their payloads into new regions, freeing the imagination to open the frontiers of scientific intelligence and technological advancement, which ultimately benefits the citizens of planet Earth.

5.6. Bibliography

- ¹ International Space Exploration Coordination Group. (2011, Sep.). The Global Exploration Roadmap. [Online]. Available: http://www.nasa.gov/pdf/591067main_GER_2011_small_single.pdf
- ² The White House. (2010, Jun. 28). National Space Policy of the United States of America. [Online]. Available: http://www.whitehouse.gov/sites/default/files/national_space_policy_6-28-10.pdf
- ³ 111th Congress. (2010, Oct. 11). Public Law 267: NASA Authorization Act of 2010. [Online]. Available: <http://www.gpo.gov/fdsys/pkg/PLAW-111publ267/html/PLAW-111publ267.htm>
- ⁴ National Aeronautics and Space Administration. (2011). Space Launch System. [Online.] Available: www.nasa.gov/sls
- ⁵ National Aeronautics and Space Administration. (2011, Jul. 14). “NASA Begins Testing of Next-Generation J-2X Rocket Engine.” [Online.] Available: http://www.nasa.gov/mission_pages/j2x/j2x_ignition.html
- ⁶ National Aeronautics and Space Administration. (2011, Sep. 8). “NASA Successfully Tests Five-Segment Solid Rocket Motor.” [Online.] Available: www.nasa.gov/exploration/features/dm3.html
- ⁷ National Aeronautics and Space Administration. (2011, Sep. 23). “NASA to Brief Industry on Space Launch System Procurement.” [Online.] Available: http://www.nasa.gov/home/hqnews/2011/sep/HQ_M11-204_MSFC_Indust_Day.html
- ⁸ National Aeronautics and Space Administration. (2011). Explore the Exploration Vehicle. [Online.] Available: <http://www.nasa.gov/exploration/systems/mpcv/explore.html>
- ⁹ National Aeronautics and Space Administration. (2012, Jul.). “Casting Begins for Booster QM-1.” SLS Highlights. [Online.] Available: http://www.nasa.gov/exploration/systems/sls/sls_highlights.html
- ¹⁰ National Aeronautics and Space Administration. (2012, May). “Flight Computer Testbed Received at Marshall.” *SLS Highlights*. [Online.] Available: http://www.nasa.gov/exploration/systems/sls/sls_highlights.html
- ¹¹ National Aeronautics and Space Administration. (2012, Jul.). “SLS Completes Early Wind Tunnel Testing.” SLS Highlights. [Online.] Available: http://www.nasa.gov/exploration/systems/sls/sls_highlights.html
- ¹² National Aeronautics and Space Administration. (2011, Aug. 4). “Salt Water May Flow on Mars.” [Online.] Available: http://science.nasa.gov/science-news/science-at-nasa/2011/04aug_marsflows/
- ¹³ Wayne Hale. (2011, Sep. 20). “The School of Hard Knocks.” [Online.] Available: <http://waynehale.wordpress.com/2011/09/20/the-school-of-hard-knocks/>
- ¹⁴ National Aeronautics and Space Administration. (2011: Feb. 14). 2011 NASA Strategic Plan. [Online.] Available: http://www.nasa.gov/pdf/516579main_NASA2011StrategicPlan.pdf

6. MARS LAUNCH CAMPAIGN GROUND SYSTEM ARCHITECTURE CONSIDERATIONS



Primary Contributors:

James C. Pope, NASA John F. Kennedy Space Center, USA

6.1. Introduction

The following summary provides a brief overview of the challenges involved with providing an efficient launch infrastructure required to meet the expected demands of a Human Mars Exploration Campaign. The sections that follow provide a summary of current and potentially augmented ground system architecture launch capabilities, key drivers of launch capability requirements, and a feasibility assessment that summarizes those drivers, assumptions, and risks that should be addressed in future Mars exploration planning.

Achieving a Human Mars Exploration Capability with Minimal Launch Site Ground Systems Architecture - The mission architecture required for a Mars human exploration campaign needs to include a vision for launch site architecture. Multi-launch campaigns utilizing the Space Launch System (SLS) and launching from the Kennedy Space Center (KSC) will provide a number of challenges for both ground and flight systems with respect to the infrastructure required for pre-flight launch processing. A high-level summary of these considerations is provided below.

Launch manifest and the effects of launch spacing on ground systems - Ground system architecture philosophy to support launch manifest. The current KSC ground system infrastructure is a “single string” architecture being designed to meet a steady-state launch rate of two SLS vehicles per year and a 120-day launch-to-launch turnaround (with up to three launches in a given year).^{1,2} The ground architecture includes:

- One Mobile Launcher (ML) and crawler dedicated for SLS integration, pad delivery, and launch
- One Vehicle Assembly Building (VAB) high bay for vehicle integration and preparation
- A single LC-39 launch pad, tied to one Launch Control Center (LCC) firing room

While a particular Mars Design Reference Mission (DRM) can be analyzed to understand operational efficiencies and workforce approaches that could increase launch rate capabilities, the possibility of aligning a Mars human exploration campaign manifest with currently expected launch site capabilities may reduce new and recurrent launch site costs.

Previous analysis - Previous Mars campaign analyses performed for Constellation identified key single string assets that would likely require redundancy to ensure a launch site capability that could meet an acceptable predicted launch availability mark³ (Note: Analysis based on NASA Design Reference Architecture 5.0, Nuclear Thermal Rocket (NTR) Reference). Although portions of this analysis may be adaptable for use considering the current capability driven framework, an initial concept of the proposed manifest, along with the extent of its dependency on SLS vehicles versus possible commercial and international partner participation, would need to be understood to identify a new launch site concept of operations as well as possible impacts to the current ground architecture plan.

Launch rate and launch spacing effects on ground system architecture - Spacing between consecutive launches, as well as launch rate fluctuations, can have significant effects on the launch site concept of operations and associated ground systems architecture. Minimizing large workforce variations associated with launch rate spikes and gaps helps to maintain the launch team’s ability to consistently meet launch spacing challenges. Mission planning, to the extent practical, needs to take into account early on the minimum launch-to-launch spacing of a human Mars exploration campaign in order to minimize the need for additional ground systems/facility assets required to eliminate resource bottlenecks between two or more mission processing flows. For example, with a single string architecture launch vehicle integration tasks that require an ML cannot occur until the ML is available and readied

following the previous launch.

Launch availability considerations for launch spacing - A Mars human exploration launch campaign manifest may need to include consideration of historical, seasonal variations in launch availability when planning launch spacing and trans-Mars injection windows to increase the likelihood of mission success.

Increased launch spacing effects on vehicle/spacecraft reliability - Increased launch spacing, whether due to ground system constraints or not, may increase flight hardware reliability demands due to longer loiter durations. However, as launch spacing decreases, in order to maintain acceptable launch availability, hardware reliability may need to increase to mitigate the likelihood of launch delays associated with hardware issue resolution. Further work may be required to trade this relationship.

Increased launch spacing effects on vehicle/spacecraft availability - Hardware availability for pre-launch multi-element integrated testing (MEIT), if required for interfacing elements that may not meet again until on orbit or at Mars, may be a challenge for flight hardware element providers if on-dock dates for supporting elements occur earlier from their particular launch dates than might be normally expected for single launch missions. Anticipated MEIT element hardware/software fidelity needs to be considered for developing a comprehensive test strategy. The approach to hardware availability versus fidelity may depend on the extent of and method used to accomplish multi-element integrated testing.

Ground system size and weight constraints - The dimensions of launch vehicles and spacecraft, as well as overall launch vehicle weight, should be considered with respect to launch site ground system constraints. For example, the VAB has limitations on crane hook height for launch vehicle core segment handling, and has an overall height constraint that requires consideration of the vehicle and mobile launcher combined. Mobile launcher, crawler, and crawler way designs need to support overall vehicle weight. Current payload fairing processing and encapsulation capabilities should be considered when determining fairing height and diameter to reduce the possibility of needing a new or modified facility due to current limitations on door sizes, floor space for fairing sector rotation, and crane hook maximum heights.

Transportation constraints - Physical constraints exist for transporting large payloads and other flight structures (on the order of 10 meters in diameter) to the launch site. Currently, the only viable transportation method is via waterways. This increases transport timelines, delivery schedule risk, and launch site processing durations if any disassembly is required to transport the hardware. Portability/modularity, or the possibility of on- or near-site manufacturing, should be considered.

Commodity servicing constraints - Due to inherent constraints of existing/planned ground systems, serviceable commodity requirements need to be identified early to understand possible impacts to current storage and delivery capabilities (particularly for extensive cryogenic propellant servicing just prior to initial and post-scrub launch attempts).

Sensitive material constraints - The inclusion of fissionable material handling at the launch site, whether for NTR stages or for a Mars surface power production payload, need to be identified in order to determine the need for a designated processing facility and/or additional safeguards.

Summary - To successfully minimize the launch site ground system architecture, mission planning and hardware designs for a Mars human exploration campaign should, when practical within mission and technical constraints, attempt to align requirements with planned launch site capabilities, constraints, and sensitivities. In particular, the early establishment of a minimum launch-to-launch spacing requirement will help identify key ground system development needs.

6.2. Mars Launch Campaign Sensitivity Analysis

Figure 6-1 depicts the current Ground Systems Development & Operations (GSDO) “Single String” launch processing architecture baseline. The Single String architecture is a minimum cost approach consisting of a single Vehicle Assembly Building High Bay (VAB HB), a single ML, a single launch pad (Pad), and an operational workforce consisting of a 5-day work week of two shifts each of 8 hours in duration (5x2). Figure 6-1 also depicts some of the key trades of possible alternatives to increasing launch throughput and spacing capabilities as infrastructure and/or workforce is increased.

Even with the incorporation of numerous advanced technologies to reduce total mission mass, each human mission to Mars will require numerous SLS launches. As an assessment of alternative approaches is conducted, it is important to understand the coupled relationship between the in-space transportation architecture and required launch infrastructure, namely the number of launches required within a specified timeframe – *the launch campaign*. The results described below discuss the initial findings and raw output from an ongoing SLS launch campaign sensitivity analysis. It is a first order approximation, and assumes all flight hardware is available when required to support launch processing. The analysis does not yet include risks associated with offline hardware processing or events post-launch. Key drivers of the launch processing and operational concepts analyzed include:

- Launch campaign durations (6, 12, 18, and 24 months)
- Processing workforce shift capacities (5x1, 5x2, 5x3, and 7x3 days per week/shifts per day)
- Ground architecture (single string of key resources versus dual string)
- SLS booster type (solid versus liquid)
- Payload type (complex versus benign)

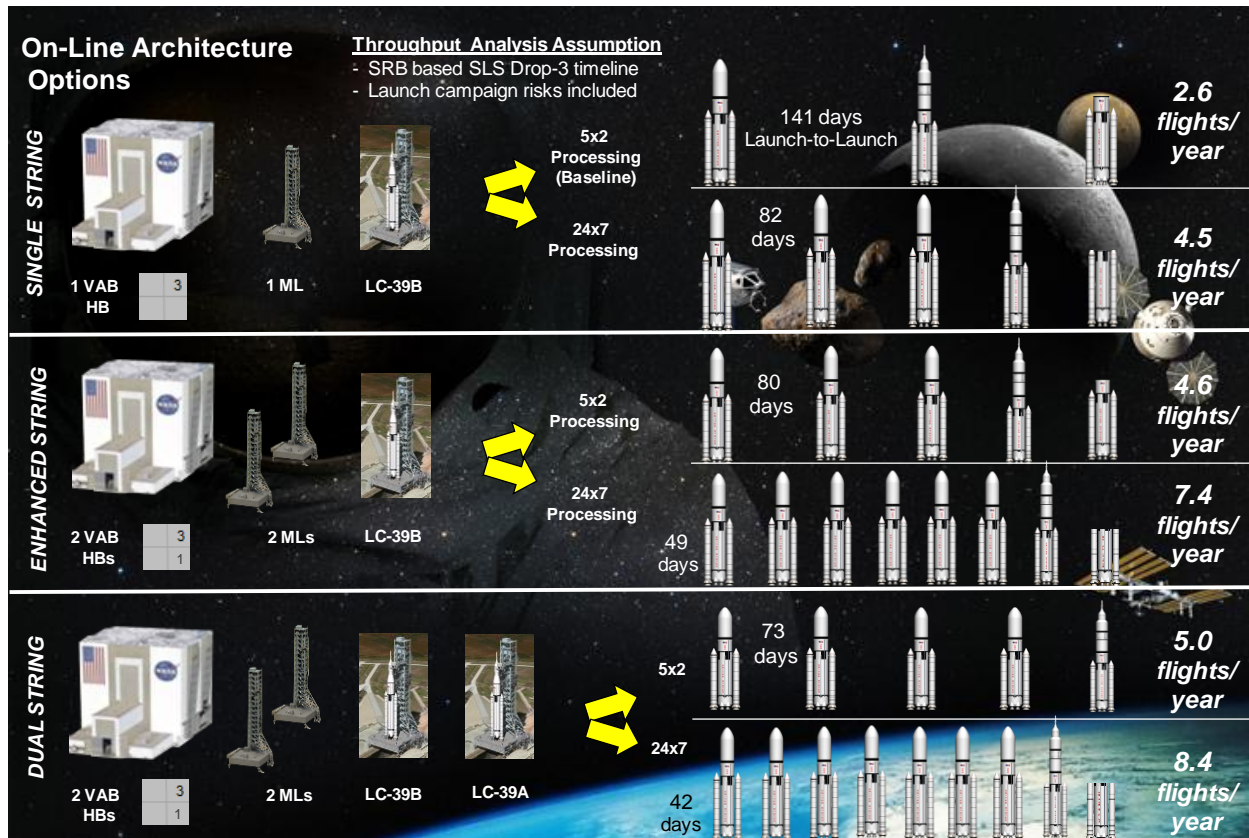


Figure 6-1 Ground system capability summary – maximum throughput.

6.2.1. Sensitivity to Launch Campaign Duration

Due to the relative alignments necessary for low-energy transfers between Earth and Mars, each mission to Mars has a fixed trans-Mars Injection window. In such, all of the necessary mission assets must be launched, assembled, and fully checked out prior to the opening of the Earth departure window. Understanding how many launch vehicles and associated payloads can be processed within the specified launch campaign duration is an important figure of merit in determining the appropriate architectural approach. Figure 6-2 provides a summary of the number of launches that can be anticipated as a function of differing launch campaign durations for the “Single String” launch architecture baseline. As can be seen, there is a linear relationship between the number of launches and the launch campaign duration. Key enablers to increasing the launch campaign duration are increasing on-orbit loiter capacity and hardware/element flight reliability.

6.2.1. Sensitivity to Processing Workforce

Another important consideration in development of the operational launch architecture is to understand how many payloads can be launched given different workforce assumptions, where workforce is measured in terms of processing days and shifts (8-hour work days). Figure 6-3 provides the results for the relationship between workforce and number of launches.

6.2.2. Sensitivity to Launch Infrastructure

Figure 6-4 shows how different launch infrastructure assumptions can affect the resulting number of available launches. As can be seen, adding an additional mobile launcher provides some marginal gains in the anticipated number of launches, but the addition of another high bay provides a marked increase in launch throughput. Although a full dual-string approach would provide the highest throughput, it would represent the highest cost option. Complete architectural performance, cost, and risk assessments must be performed before the “preferred” launch architecture can be determined and is subject to further assessments.

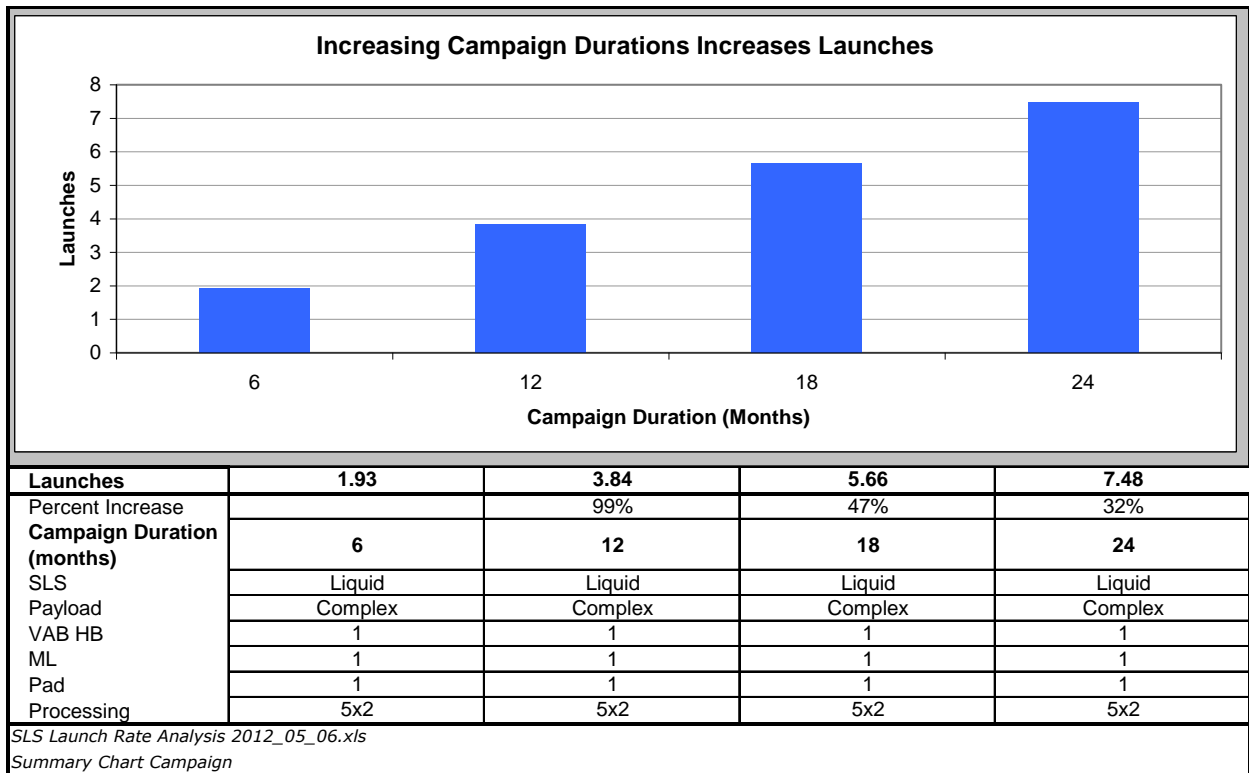


Figure 6-2 Effect of launch campaign duration on launch throughput.

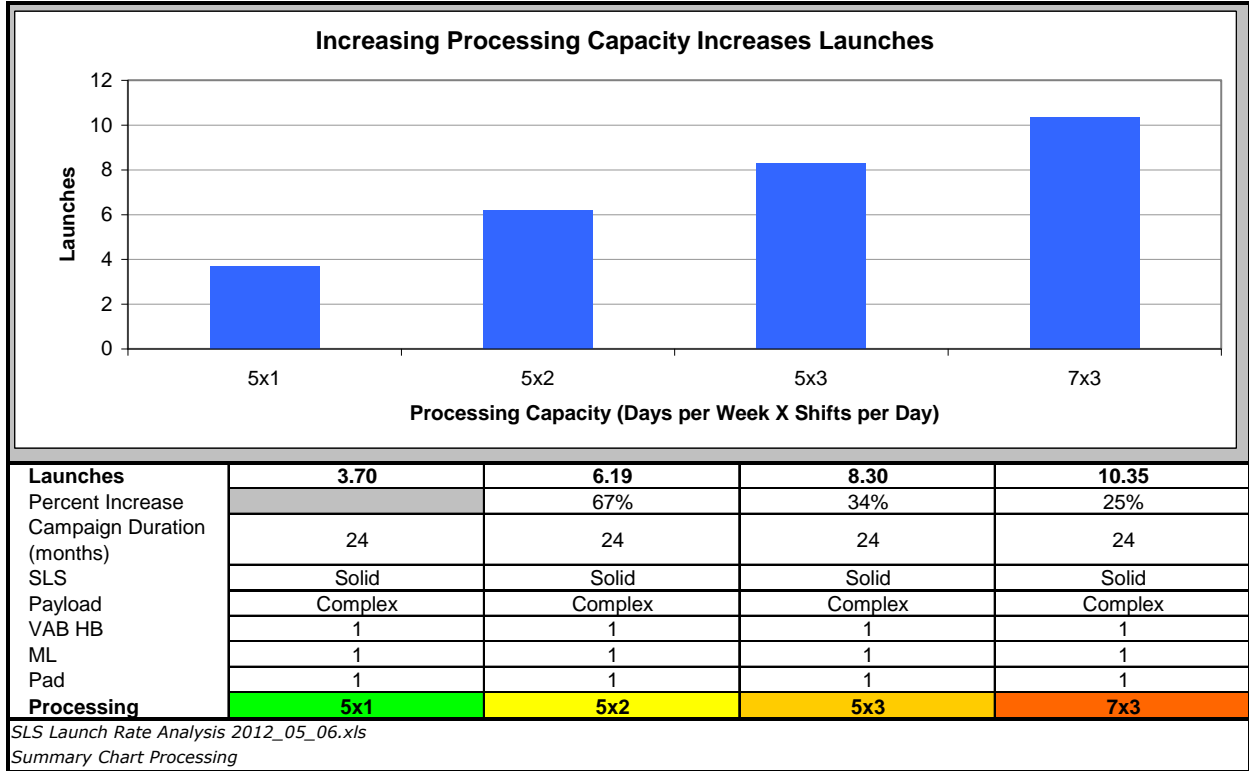


Figure 6-3 Effect of workforce on launch throughput.

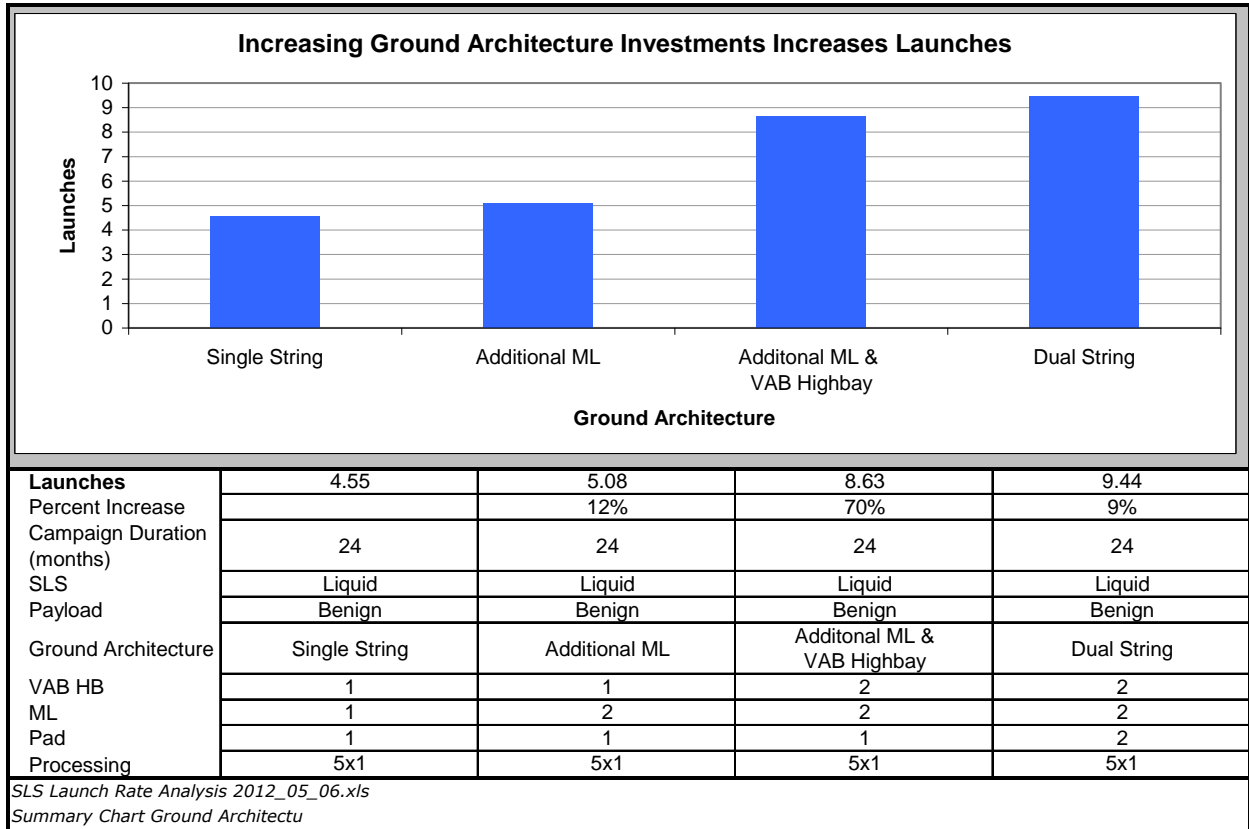


Figure 6-4 Effect of launch infrastructure on launch throughput.

6.2.3. Sensitivity to First-Stage Booster and Payload Type

The complexity of the elements to be processed, including the launch vehicle as well as the payload elements, can influence the anticipated number of launches. Figure 6-5 provides the initial results for the number of anticipated launches for the single string architecture. Figure 6-5a shows that the first-stage booster type, solid or liquid, can have a profound impact on the number of launches. That is, processing safety constraints associated with the solid boosters constrains the number of launches more than the liquid option. Figure 6-5b indicates that the type of payload, complex versus benign, has relatively little effect on the launch vehicle throughput.

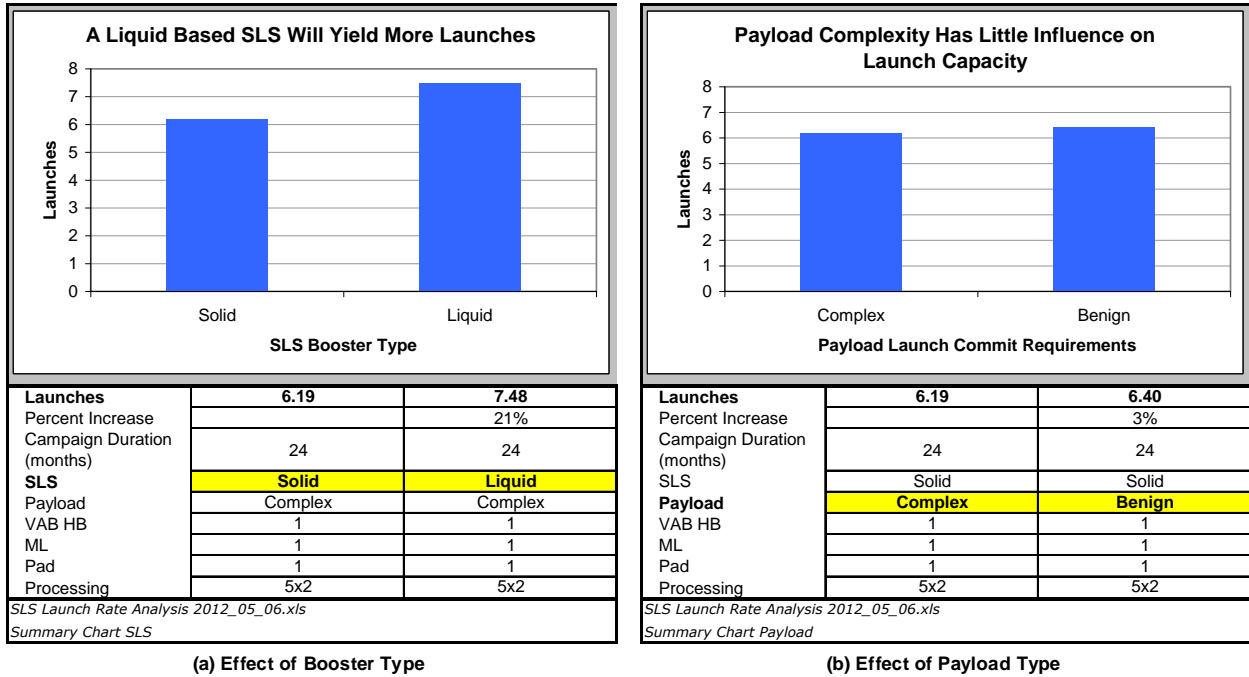


Figure 6-5 Effect of (a) booster and (b) payload type on launch throughput.

6.3. Other Potential Risks & Considerations

Previous assessments have determined other potential risks and areas for further consideration as the overall Mars architecture is determined. These include, but are not limited to:

- Launch vehicle/spacecraft dimensions could exceed current facility capabilities and drive new construction. Overall launch vehicle height beyond VAB capability could drive the need for a new vehicle integration facility. Payload fairings/encapsulated payloads over ~90°, unless able to be processed and transported individually as a lower base module (barrel) and an upper payload module (current plan), may drive the need for an additional/new encapsulation facility. Horizontal encapsulation, particularly of hypergolic propellant serviced spacecraft into a large aero shell, may exceed capabilities of current facilities. It should be noted that payload processing facility assignments have not been baselined, and processing throughput capability has not yet been analyzed.
- Requirements for processing spacecraft/stages containing fissionable materials may impact facility and/or operational capabilities, and could drive new development and/or cost.
- Physical constraints exist for transporting large payloads and other flight structures (on the order of 10 m diameter) to the launch site. Currently, the only viable transportation is by water. Increased transport timelines versus air/land, adds delivery schedule risk and possibly launch site processing durations if any de-integration is required in order to ship. Portability/modularity or the possibility of on/near-site manufacturing could be considered.

- KSC’s architecture is being planned to support multiple programs/commercial entities. Integration of multiple customers will be carefully planned and managed by GSDO to avoid operational impacts and mitigate collateral schedule risk (probably more of a risk to customers not heading to Mars).
- Reservation of key payload offline processing resources (e.g., propellant servicing and encapsulation footprints) until launch to support potential roll-back/payload re-work may not be practical, adding schedule risk. A multi-flow assessment of potential offline processing option(s) needed once manifest/launch rate/payload makeup options available.
- Serviceable commodity requirements (particularly those for extensive cryogenic propellant servicing and/or Helium use) beyond planned capabilities need to be identified early to evaluate schedule/cost risks
- Flight element delivery schedule risk may increase, depending on the scope of and test strategy employed for any pre-launch MEIT needed to interface elements that may not meet again until on orbit or at Mars

Current assessments indicate the following key risks associated with the launch processing aspects of future human Mars missions:

- Launch rate/spacing & campaign duration could drive additional infrastructure
- Vehicle & spacecraft dimensions could exceed processing facility constraints
- Nuclear material processing may impact operations or require a separate facility
- Transportation of 10 m diameter class hardware to KSC by water adds schedule risk
- Early planning needed to ensure no operational or resource conflicts between concurrent multi-customer operations
- Possible roll-back resource/schedule risk between closely spaced launches and launch scrubs
- Commodity requirements could exceed current capabilities
- MEIT needs may require accelerated delivery dates

6.4. Key Decision Points

Decisions for authority to proceed for ground system architecture changes required to support a particular program architecture option are needed nominally 5 years prior to initial use to ensure successful design and implementation of additional infrastructure, to increase and train potential work force additions, and possibly to mitigate impacts to other potential customers/programs using shared resources. The amount of time between authority to proceed and ground system operational readiness is the primary variable (assuming no high-risk technology development) that affects GSDO cost and schedule risk posture. Compressed development schedule increases schedule risk, and may increase cost to resolve problems/mitigate impact on critical path capability readiness. Relaxed schedule may reduce yearly costs, allow for implementation with reduced impacts to ongoing missions/customers, may increase overall cost, and increases overall duration of operations & maintenance (O&M) work associated with new infrastructure.

6.5. Launch Campaign Ground System Architecture Summary

Understanding the launch rate, number of launches, and overall launch campaign duration of a Mars human exploration program is of primary importance in determining the feasibility of creating fully capable ground system architecture. Based on previous and ongoing analyses, potential ground system architecture enhancements may consist primarily of duplicating existing resources and/or adding workforce to increase processing/launch capacity. The need for new systems and possible technology development/demonstration will depend on specific needs of identified program options.

6.6. Bibliography

-
- ¹ J. Madden and J. Graeber (2011) 21st Century Ground Systems Program Architectures and Concept of Operations Document (21CGS-ACO-1010), 36-40,48.
 - ² H. Grant (2011) ESMD/SOMD Human Exploration Capabilities Requirements (ESMD-HEC.Reqt-6.2011), 9.
 - ³ G. Cates (2010) Mars Architecture Discrete Event Simulation (DES) Analysis, 9-14.

This page intentionally left blank

7. DEEP SPACE HABITAT

Primary Contributors:

Larry Toups, National Aeronautics and Space Administration, Johnson Space Center

Matt Simon, National Aeronautics and Space Administration, Langley Research Center

7.1. Introduction

A Mars Transit Habitat (MTH) is needed to support crew during the long-duration round trip to Mars.¹ This vehicle provides a pressurized environment for crew habitation (Figure 7-1) and all of the required functions to keep crew healthy and productive during the long-duration mission (e.g., life support, work stations, hygiene, etc.). Because these vehicles must be returned from Mars, mass is a critical design consideration. Design iterations of this vehicle seek to minimize the total mass while maintaining the volume and equipment necessary to ensure the physiological and psychological well-being of astronauts. Mass reductions are achievable through multiple strategies such as reduced functionality, increased modularity, and technology implementation. This section documents work that provides updated MTH masses for consideration in Mars architectures and describes efforts to reduce the resultant mass through reduced functionality and crew size.

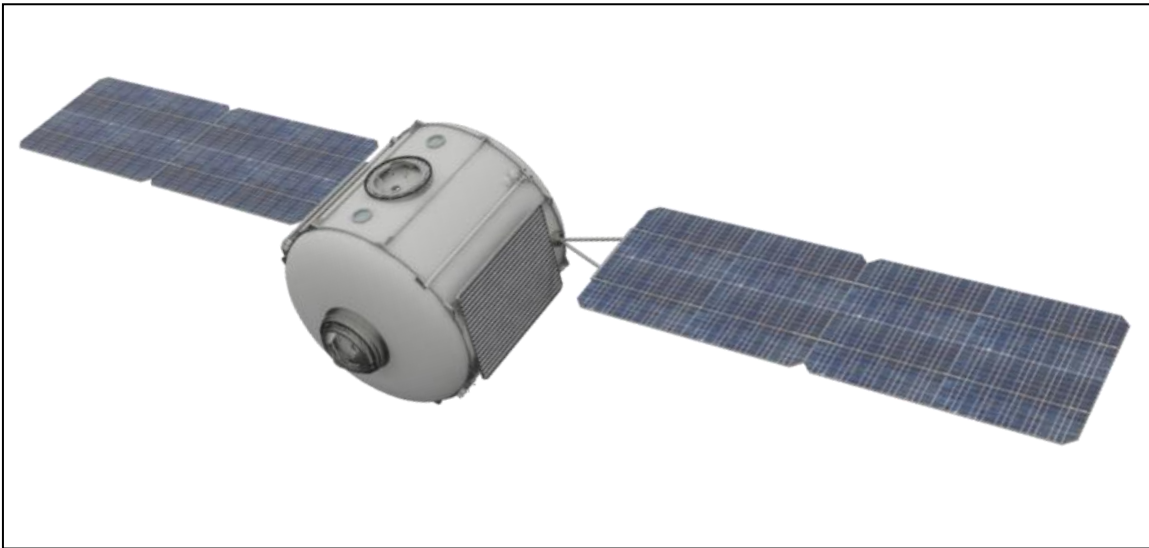


Figure 7-1 Notional Mars Transit Habitat 1000 days, 6 crew (to scale)

7.2. Mass Trades

Mass trades for the MTH were performed using parametric sizing analyses consistent with those performed for the Human Spaceflight Architecture Team (HAT) Deep Space Habitat². To capture many different possible Mars missions, the number of crew members and mission duration were traded for each set of assumptions. Two sets of assumptions, as shown in Table 7-1, representing varying levels of functionality were also traded: 1) a Baseline Strategy and 2) a More Aggressive Mass Reduction Strategy.

Table 7-1 Deep Space Habitat Sizing Assumptions

BASELINE ASSUMPTIONS	
<p><u>Structure and Mechanisms</u> Metallic, cylindrical habitat: 7.2 m diameter 0.3 m for port extrusions, attachments, structure 2.5 m barrel length for reasonable ceiling height ~25 m³/person habitable volume Utilize Orion habitable volume Secondary structure 2.46 km² of habitat surf area Launch integration 2% of habitat gross mass Four 0.5 m diameter windows 1 exterior hatch 3 docking mechanisms, 2 docking tunnels Atmospheric pressure = 70.3 kPa (10.2 psi)</p> <p><u>Avionics</u> Provide CC&DH, GN&C, communications</p> <p><u>Thermal Control</u> External fluid loop using CH₃ Internal fluid loop using 60% prop glycol/water TBD kW heat rejection using ISS-type radiators</p> <p><u>Maintenance and Spares</u> Assume 1000 kg fixed and 500 kg each year with 250 kg/m³ density</p> <p><u>Reserves</u> Margin Growth Allowance: 20% of basic mass Project Manager’s Reserve: 10% of basic mass</p>	<p><u>Protection</u> 20 layers multi-layer insulation 5.8 cm water-wall on crew quarters for SPE protect.</p> <p><u>Power</u> 2 photovoltaic (3 junction GaAs) arrays ~20 kWe end of life power 120 V DC power management (92% efficient) 3 Li-ion batteries (200 W-hr/kg) ~40 kW-hr storage</p> <p><u>Environmental Control and Life Support</u> Scaled ISS level ECLSS (100% air, ~85% water) 20% mass for redundant components 30 days open loop contingency consumables</p> <p><u>Attitude Control / Reaction Control System</u> Assume 250 m/s delta-v</p> <p><u>Crew Accommodations</u> Standard suite for 180-360 day deep-space Assume freezer for missions longer than 1-year Food, crew items, sink (spigot), freezer, microwave, washer, dryer, 2 vacuums, laptop, trash compactor, printer, hand tools, test equipment, ergometer, photography, exercise, treadmill, table</p> <p><u>Extra-Vehicular Activity (EVA)</u> 2 person EVAs using shuttle-class internal airlock 1 spare suit 1 EVA per month for repairs and contingency</p>
AGGRESSIVE ASSUMPTION CHANGES	
<p><u>Structures and Mechanisms</u> Habitable volume reduced to 23 m³/person</p> <p><u>Extra-Vehicular Activity</u> No EVA accommodations provided</p> <p><u>Attitude Control / Reaction Control System</u> No ACR/RCS – assume provided by another element</p>	<p><u>Crew Accommodations</u> No freezers (shelf stable rehydratable food only) Only 2 months contingency waste collection (bags) Only disposable clothing Half as much water usage from shower</p>

These two levels of functionality were traded with number of crew and mission duration to identify advantageous, low-mass habitat designs. Examples of these designs are shown for 6 crew members, 1000-day missions using both the HAT and Aggressive assumptions in Figure 7-2 and Figure 7-3, respectively. The major savings gained by switching to the aggressive assumptions come from the elimination of ACS/RCS systems, ACS/RCS propellant and EVA equipment; and from the reduction of water requirements through reduced crew accommodations.

Mars Design Reference Architecture 5.0 – Addendum #2



Figure 7-2 Baseline strategy - HAT MTH summary for 6 crew, 1000 days.

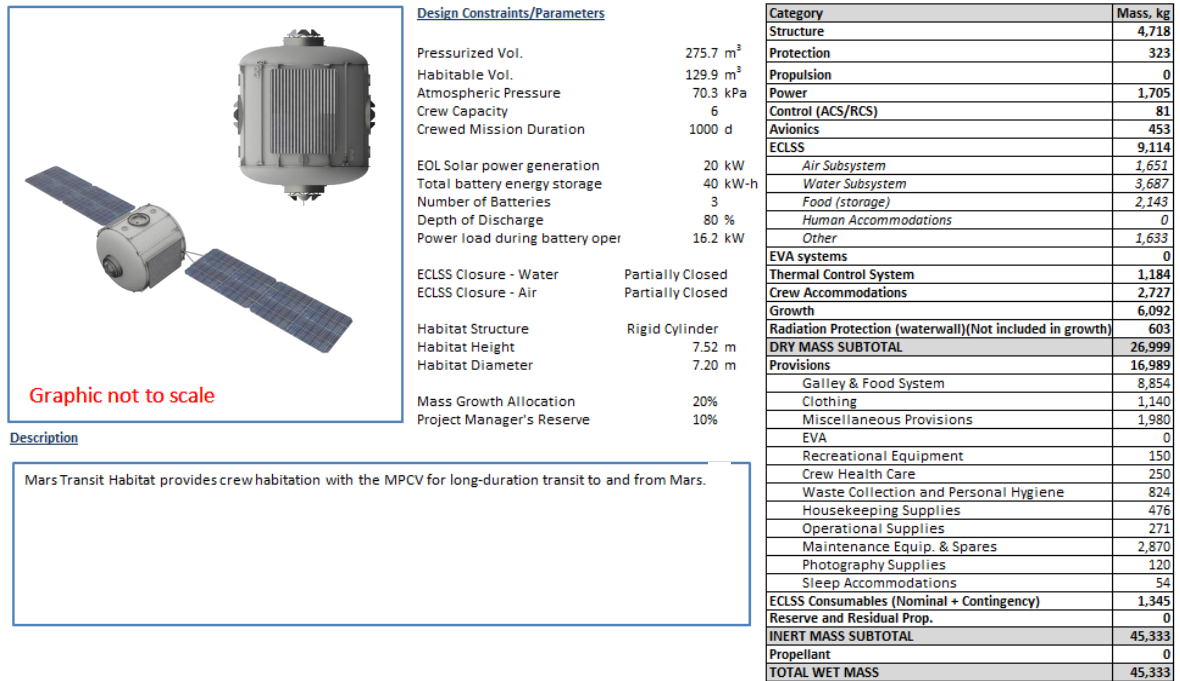


Figure 7-3 Aggressive mass reduction strategy – HAT MTH summary for 6 crew, 1000 days.

The resulting gross masses of all trades are summarized in Table 7-2. These mass trades have several implications for the design of crewed Mars missions. Reducing crew is shown to be a major mass driver; more so than reducing mission duration. This is particularly true because the propulsion system mass increases for shorter missions far outweigh the potential savings from reduced habitat outfitting. However, the implications of reducing crew must be acceptable to mission planners for this to be feasible. Reducing crew increases workload and competency

requirements for remaining crew. Fewer crew members also require an increased level of vehicle autonomy to handle routine vehicle operations and contingency scenarios. Additionally, less crew may not be acceptable from a political standpoint. Funding a Mars mission will probably involve some degree of international participation, which will necessitate international crew seats on the mission. For all of these reasons, the appealing 2 and 3 crew options may be unacceptable unless they enable some great cost benefit to the mission.

The aggressive reduction of functionality can also greatly reduce the overall habitat mass. Relying upon the ACS/RCS system of attached propulsive elements in lieu of providing them on an MTH represents several tons of mass savings. The assumption of reduced crew accommodations “amenities” seems reasonable, but would have to be proven to be acceptable in a relevant test environment for an analogous duration. Some degree of this has been implemented on Antarctic analogs (less-frequent showers, less clothing, etc.), but characterization of the psychological impacts for a much longer mission is required. Eliminating EVA may be overly risky from a contingency scenario perspective unless robotic servicing is advanced beyond current capabilities. In summary, relatively small adjustments to the required functionality can provide substantial mass savings if the reduced functionality is validated through exploration testing and risk assessment analyses.

Table 7-2: Comparison of Gross Masses between HAT Assumptions and Aggressive Mass Reduction Assumptions

		Gross Mass (kg)					
Duration (days)		600		800		1000	
Crew	HAT	Aggressive	HAT	Aggressive	HAT	Aggressive	
2	26565	19744	29583	22232	32561	24864	
3	31165	23505	35025	26794	39067	30139	
4	35538	27128	40359	31144	45148	35199	
6	44124	34039	50698	39694	57370	45333	
8	52576	41004	61014	48129	69570	55347	
10	61033	47872	71335	56563	81777	65366	

7.3. Commonality between Transit and Surface Habitat Designs

Another consideration for the design of a Mars Transit Habitat is the potential commonality between the transit habitat and the surface habitat landed on the surface of Mars. This commonality can either be implemented through the combination of both elements into one habitat or the use of a common design for two distinct habitats requiring minimal modifications for each operating environment. Delivering one habitat to perform both functions can potentially save development cost of two separate elements, reduce the overall mass of the elements in the architecture, and simplify the transportation architecture with one trans-Mars injection stack.

However, there are several challenging implications for utilizing a single vehicle. First, the subsystems (e.g., life support, thermal control, communications, etc.) would have to be designed to work in both microgravity and partial gravity environments. This may require either very complex subsystem designs or separate subsystems/components designed for each gravity environment (particularly for life support systems, hygiene subsystems, and any other systems involving fluid flow). Second, the masses of a single transit/surface habitat will be greater than a dedicated transit habitat. This additional mass stems from additional subsystems to support the surface mission and more robust structures required to withstand the landing loads and human habitation operations on the surface of Mars (i.e., floors, bunks, etc.). This additional mass impacts the transportation architecture as the transit/surface habitat housing crew must also travel on a faster trajectory than a pre-deployed surface habitat. This can result in larger delta-Vs and additional propellant mass making the single trans-Mars injection more difficult. Finally, a transit/surface habitat would have many layout design challenges for human habitation in multiple gravity environments. Some are discussed here for consideration in future studies.

Typically, when designing for planetary surfaces, floor area is considered a driver for usable space.³ Similarly, when designing for zero-g environments, usable volume is the biggest driver. However, anecdotal evidence from the

astronaut core indicates that consideration of the unconstrained zero-g volume as the sole driver specifying habitat size and layout may be false. Instead, surface area is a major driver as wall area and ceiling area all become work surfaces in a zero-g environment. Therefore, one of the biggest challenges to solve in a common transit/surface habitat is how to convert large surface area of the transit habitat into usable area in the planetary habitat. Several design solutions present themselves, including random access frames and gimbaled surfaces.

Random access frames provide a vertical working surface that has available wall space on both sides. Multiple frames would be lined up in a row (or around the curve of a cylinder as the case may be), with only one or two access pathways available. Since the frames are on tracks, the crew member would be able to move the frames and create access to the surfaces of each frame on demand, keeping the density of the packed frames as tight as possible — similar to sliding office or library shelving systems. In zero-g, each of the walls of the frames could be used as work surface area. To transition to a planetary surface, the wall areas can be gimbaled downward on demand to create a horizontal surface or table, spanning the random access passageways. Using this technique, the random access frames can be loaded with stowage, or with equipment that uses cable and hose tracks to allow for movement of the frames. Life support systems, avionics, communications equipment, workstations, hygiene functions, galley, etc. can all be densely packed into the random access system, and only opened when needed. In case of a need for dual use of functions, workstations assigned to various frames can be 'choreographed' to allow for multiple crew members to use. Also, permanently dedicated volumes can also be created by designing in a fixed passageway that is not on the sliding system. Other solutions are being investigated in future studies to develop a flexible interior for both microgravity and planetary surface environments.

7.4. Future Studies

Several future studies will identify other potential assumption changes and design features to further reduce mass. In particular, a modular transit habitat design that splits the pressure vessel into multiple separable sections will be considered. Modular habitats⁴ allow for jettison of unused contingency logistics and trash within a separable pressurized section of the transit habitat at Mars before performing the Tran-Earth Injection burn to get much better propulsive efficiency. Additional studies to consider in the future include risk assessments to characterize critical technology areas and additional investigations into potential transit and surface habitat commonality. In particular, studies to close the major biological risks to crew must be closed, including fatal cancer from galactic cosmic rays. Finally, additional studies are under way to propose a lower mass solution combining transit and surface habitats for similar performance at reduced cost.

7.5. Bibliography

- ¹ Drake, B. G. (Editor), “Human Exploration of Mars, Design Reference Architecture 5.0,” Mars Architecture Steering Group, NASA Headquarters, NASA SP-2009-566, July 2009.
- ² Toups, L., Simon, M., Smitherman, D., and Spexarth, G., “Design and Parametric Sizing of Deep Space Habitats Supporting NASA’s Human Space Flight Architecture Team,” Global Space Exploration Conference. GLEX-2012.05.3.5x12280, May 2012.
- ³ National Aeronautics and Space Administration, Office of the Chief Health and Medical Officer, “Human Integration Design Handbook”, NASA/SP-2010-3407, Washington, DC, 2010.
- ⁴ Simon, M., Smitherman, D., and Toups, L., “Potential Applications of Modularity to Enable a Deep Space Habitation Capability for Future Human Exploration Beyond Low-Earth Orbit,” Global Space Exploration Conference. GLEX-2012.05.3.6x12574, May 2012.

This page intentionally left blank

8. SURFACE STRATEGY

Primary Contributors:

Hoffman, Stephen J., National Aeronautics and Space Administration, Lyndon B. Johnson Space Center

This section describes tasks associated with analyzing human crews exploring the surface of Mars or the environment in Mars orbit, including the two moons of Mars. In the case of the surface of Mars, this is assumed to begin after the Entry, Descent, and Landing (EDL) system (see Section 4) has delivered the crew and its equipment to the surface and end when the ascent vehicle (see Section 4) lifts off from the surface. For Mars orbital operations, this is assumed to begin after an interplanetary vehicle carrying the crew has made its final capture maneuver at Mars and ends with the first propulsive maneuver for the departure from Mars.

Since the conclusion of analysis tasks for DRA 5.0, several distinct activities have been completed and will be described here. These activities include:

- An impact assessment of the number of crew members and size of the lander vehicle on the overall mission while attempting to achieve the same mission objectives. This assessment was performed at the request of the Review of United States Human Space Flight Plans Committee (also known as the Augustine Committee) in 2009.
- A re-opening (or expansion) of surface strategy options as a result of adopting the Capability Driven Framework.
- Development of a functional breakdown of the Mars surface mission as a basis for reassessing the systems and capability allocation used in DRA 5
- On-going efforts to evaluate surface strategy options structured around the surface mission functional breakdown.

Each of these activities will be described in more detail in the following sections.

8.1. Summary of DRA 5 Surface Strategies

This section provides a brief summary of the three Mars surface mission strategies – given the working titles of “mobile home,” “commuter,” and “telecommuter” – documented in DRA 5. These summaries are included to make them readily accessible as comparisons to them are described in the remainder of this section. (Additional detail for each of these strategies can be found in NASA-SP-2009-566 and NASA-SP-2009-566-ADD.¹) These three options were constructed to focus on a limited number of examples that would cover different aspects in a continuum of approaches to explore the surface of Mars. Each of these three options contains an approach for exploring horizontally across the surface, vertically above and below the surface, and placing a differing level of emphasis on the use of extravehicular activity (EVA) astronauts or teleoperated robots.

The “*mobile home*” surface mission scenario assumes that surface exploration by the crew will be primarily a mobile operation. This scenario assumes the use of two (for mutual support) large, capable, pressurized rovers for extended traverses, spending between 2 and 4 weeks away from the landing site (see Figure 8-1). These rovers will have space and resources allocated for on-board science experiments. The landing site is assumed to be the fixed location for those infrastructure elements not needed for extended traverses, such as an In-Situ Resource Utilization (ISRU) plant (making oxygen, (probably) methane, (probably) water, and any buffer gases that are residual from processing the Martian atmosphere for these other commodities) and a large power plant. Power is assumed to be supplied by a nuclear power plant previously deployed with the decent-ascent vehicle and used to make a portion of the ascent propellant. The processing capacity of the ISRU plant is to be determined (TBD) and dependent to a certain degree on the assumed implementation for the rover power source. The landing site will also be the “warehouse” for food and other basic maintenance and repair capabilities; the landing site will have minimal crew habitation capabilities. With this division of functions among the surface systems, it is assumed that the crew will make a number of traverses away from the landing site, but return periodically to resupply and refit the rovers before deploying on the next traverse.

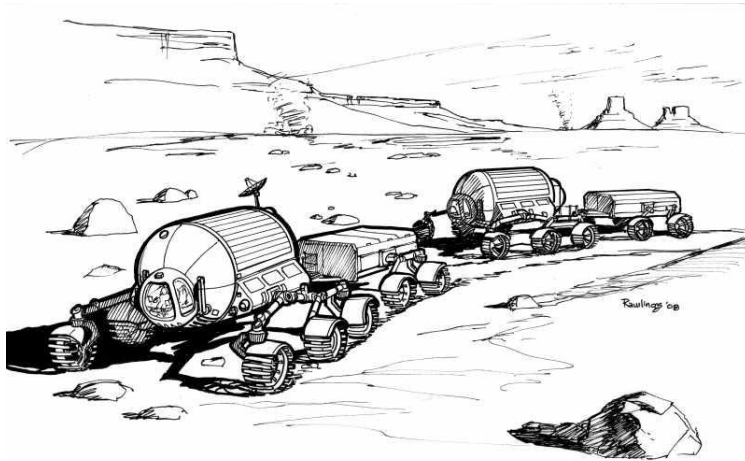


Figure 8-1 Notional image of large rovers.

Because the rovers will be designed for mutual support, each rover will be sized for a nominal crew of three (DRA 5 assumes a crew of six) but able to accommodate all six crew in a contingency situation. Thus, the majority of the habitation functions will be replicated in each rover. However, while both rovers will have space and resources allocated for on-board science experiments, it is assumed that these experiments will not be replicated in both rovers. Each rover will have an airlock to support EVA activity, but it is also assumed that the rovers will be able to routinely dock together, allowing crew to transfer between vehicles without the need for an EVA (e.g., at night when all traverse and EVA activities have concluded). This will allow the entire crew to use any of the assets in either vehicle on a regular basis.

In addition to the internal science experiments mentioned above, the pressurized rovers will also bring along two small robotic rovers, two unpressurized but small rovers (comparable to the Apollo Lunar Rover Vehicle [LRV]) to carry EVA crews, and a drill. The two robotic rovers can be teleoperated from the pressurized rover or can be given a set of instructions and allowed to carry out these instructions in an automated fashion. The unpressurized rovers will allow the EVA crews to move relatively quickly between sites within walk-back range of the pressurized rovers once the latter have stopped for extended operation at a given location (it is assumed that the pressurized rovers will not be very nimble and thus will serve as a “base camp” from which local traverses will be staged). The drill is assumed to be capable of reaching 10s of meters of depth at multiple locations.

The “*commuter*” surface mission scenario assumes a centrally located, monolithic habitat, two small pressurized rovers, two unpressurized rovers (roughly equivalent to the Apollo Lunar Rover Vehicle), at least two small robotic rovers, and a drill. Power for these systems will be supplied by a nuclear power plant previously deployed with the decent-ascent vehicle and used by an ISRU plant to make a portion of the ascent propellant. (See Figure 8-2) Although traverses will be a significant feature of the exploration strategy used in this scenario, these traverses will be constrained by capability of the small pressurized rover. In this scenario, these rovers have been assumed to have a modest capability, notionally a crew of two, approximately 100 kilometers total distance before being resupplied, and no more than 1 week duration. Thus, on-board habitation capabilities will be minimal in these rovers. However these rovers are assumed to be nimble enough to place the crew in close proximity to features of interest (i.e., close enough to view from inside the rover or within easy EVA walking distance of the rover). Not all crew will deploy on a traverse, so there will always be some portion of the crew in residence at the primary habitat. The pressurized rovers will carry (or tow) equipment that will have the capability to drill to moderate depths – 100’s of meters – while deployed on these traverses.

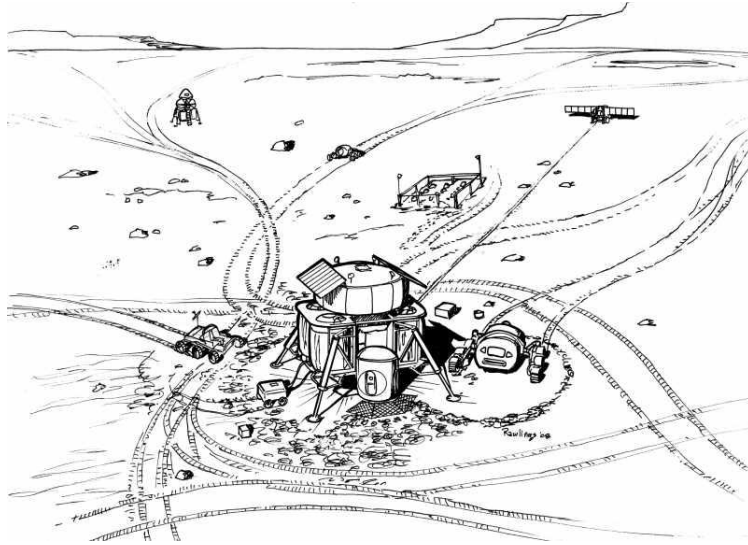


Figure 8-2 Notional image of commuter.

The primary habitat will have space and resources allocated for on-board science experiments. The pressurized rovers will carry only minimal scientific equipment deemed essential for field work (in addition to the previously mentioned drill); samples will be returned to the primary habitat and its on-board laboratory for any extensive analysis.

In the “*telecommuter*” scenario it is assumed that the crew will be based in a centrally located, monolithic habitat and only unpressurized rovers (Apollo lunar rover equivalents) will be used for EVAs. This implies traverses by the crew of no more than walk-back distances (approximately 15 kilometers radial distance). The long range traverses will be handled by very capable robotic rovers (notionally a considerably improved MSL rover) teleoperated (or possibly just supervised) by the surface crew from their habitat (see Figure 8-3). Because of the assumed prepositioning of surface cargo in the overall mission scenario, there is an opportunity to deploy these rovers independently from the large surface habitat (but during the same atmospheric entry event) to sites that are distant from the habitat landing site. In this situation, there will be up to 2 years available for these rovers to carry out long distances traverses, guided from Earth-based operators, with an ultimate destination of the habitat landing site.

As in the previous scenario descriptions, there will be an ISRU plant at the landing site/habitat site making the same kinds of commodities. This ISRU plant and the habitat will be served by a large (assumed to be nuclear) power plant. The landing site/habitat site will serve as the warehouse and maintenance/repair facility as described previously.

After the crew arrives at the habitat, these very capable robotic rovers can be deployed on other traverses under the guidance of the surface crew. This scenario could also be used to advantage for the teleoperation of airborne robots that can be maintained, refueled, and reconfigured at the crew’s habitat (this capability is not precluded in the other two scenarios but the teleoperation emphasis in this scenario enhances its implementation).

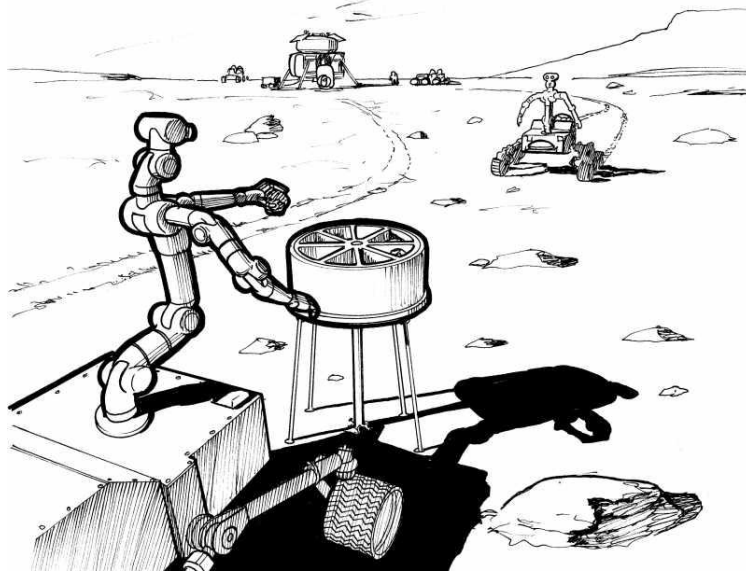


Figure 8-3 Notional image of telecommuter.

The primary habitat will have space and resources allocated for on-board science experiments. The unpressurized rovers and EVA crews will carry only minimal scientific equipment deemed essential for field work (in addition to the previously mentioned drill); samples will be returned to the primary habitat and its on-board laboratory for any extensive analysis. The robotic rovers will carry a more extensive suite of instruments suitable for long-range and long-duration traverses, but will have the capability to acquire and return samples to the primary habitat for further analysis and possibly for return to Earth.

The human crew's primary EVA task will be to set up a drill capable of deep drilling and operating that device. The ISRU plant may provide drilling fluid (e.g., liquid CO₂) for this device.

8.2. Support to the Review of United States Human Space Flight Plans Committee

In May 2009, the Office of Science and Technology Policy² announced the formation of the Review of United States Human Space Flight Plans Committee (also known as the Augustine Committee)³ for the purpose of reviewing the then-current human spaceflight plans of the United States. This Committee held a number of public hearings between June and August of 2009. In addition, the Committee requested several specific assessments of different human spaceflight scenarios to assist in their review.

One of these requested assessments was known as “Scenario D – Mars First,” the purpose of which (as the name implies) was to illustrate the implications of focusing human spaceflight efforts on a mission to Mars before sending a human crew to any other Solar System destination. The surface strategy portion of this assessment involved assembling manifests for all of the combinations of two different crew sizes (4 and 6 crew) with three different lander sizes (delivered payload capacities of 20, 30, and 40 tons). From a surface strategy point of view, no significant effort was put into assessing the ability of these crews to accomplishing specific scientific or mission objectives; no relevant baseline existed against which such a comparison could be made. Rather, this became an exercise in distributing surface systems identified in DRA 5 (appropriately scaled for the crew size) among as many landers as necessary to deliver the mission payload. Figure 8-4 illustrates this process.

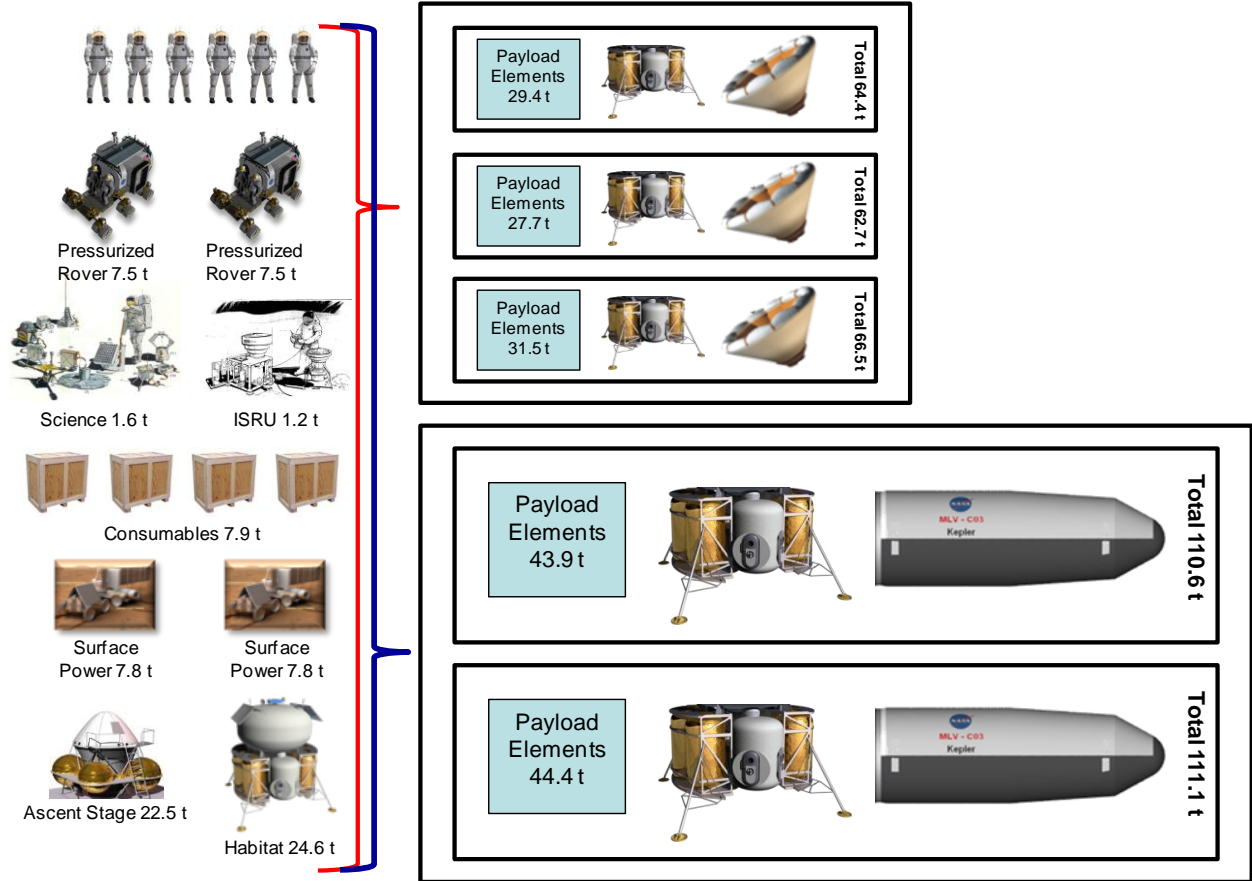


Figure 8-4 Example of alternative surface system manifests for differing transportation system options.

Results from this assessment indicated that the ascent vehicle and the habitat were the systems that determined the smallest individual lander needed to accomplish a surface mission. Further subdividing either of these systems was not considered a viable approach. The remaining items on the manifest of surface payloads could be reasonably distributed on the landers carrying these two large systems or placed on additional landers. The results of this manifesting exercise are summarized in Table 8-1.

Table 8-1 Manifest Results for Combinations of Crew and Lander Capacity

Mission Option		Total Delivered Surface Payload Mass (mt)	Number of Landers Required	Maximum (wet) Payload in LEO Requirement (mt)
Number of Crew	Lander Payload Mass Capacity (mt)			
6	40	88.4	2	111.1
6	30	89.0	3	84.5
6	20	(too small)	N/A	N/A
4	40	80.2	2	106.8
4	30	80.2	3	84.7
4	20	82.2	4	68.9

Several surface strategy-related observations can be made from these results. For the 6 crew / 40 mt lander case, the total landed payload mass exceeded the stated capacity of the lander by approximately 10 percent. Normally this would have caused the estimates for the payload to be reexamined or the lander and other entry systems to be resized. However, an initial examination of the payload mass estimates indicated at least one of the payload compliments (i.e., the ascent stage, ISRU, and power plant combination) was unlikely to be reduced in mass, and insufficient time was available during this assessment to resize the EDL elements. Thus, the results were acknowledged to be undersized in this one case. For the six-person crew cases, the 20 mt capacity lander was found to be too small to land the ascent stage even with no other payload on board, defining a lower bound on the landing system and other associated elements in the transportation system. In the four-person crew cases, the surface system payloads could be redistributed among two 40 mt landers or three 30 mt landers without change to surface operations. However, for a 20 mt lander case the previously assumed strategy of landing an ascent stage, ISRU plant and power plant as a single package could no longer be accomplished. The ISRU plant and power plant were placed on a separate lander. This required the introduction of temporary storage tanks and propellant transfer vehicles to offload propellants from the “ISRU lander,” move these commodities to the ascent stage and then load the propellants into the ascent stage. These additional systems are the cause of the increased total delivered surface payload mass seen in Table 8-1. One last observation from the results in this table is that the difference in total delivered surface payload mass and initial mass in low-Earth orbit (IMLEO) requirement for a crew of four and a crew of six is relatively small – on the order of 5 percent or less, even after the ascent vehicles, surface habitats and crew consumables were resized for these different crew sizes. This observation is consistent with other comparisons of crew size discussed in this addendum, namely that the mass associated with a Mars mission does not scale linearly with the size of the crew and that once a basic capability to transport and support a crew has been accounted for, changes in the size of the crew has a relatively small impact on the overall mass of the mission.

8.3. Capability Driven Framework.

After the results of the Review of United States Human Space Flight Plans Committee were delivered to NASA and the Office of Science and Technology Policy, the United States human spaceflight program was reformulated around a concept referred to as a “capability driven framework” (CDF).⁴ This CDF concept is based on the idea of an ever-expanding human presence beyond low-Earth orbit measured in terms of increasing mission duration and distance from the Earth. It assumes that this expansion is achieved through evolving capabilities that are utilized for more challenging missions after operational experience has been established from less demanding missions. In theory, the CDF enables multiple destinations and provides increased flexibility, greater cost-effectiveness, and sustainability. Figure 8-5 illustrates this CDF concept.

To help formulate the strategies, technologies, and systems needed to support the CDF, example destinations are being examined, including (reference?):

- Low-Earth orbit missions,
- Geostationary missions,
- Cis-lunar space missions (including lunar fly-by, lunar orbit, and lunar surface),
- Near-Earth asteroids missions,
- Mars orbital operations, including investigating the moons of Mars, and
- Missions to the surface of Mars

The first four of these destinations are outside the scope of this document; the last two destinations place an expanded view on the trade space for Mars exploration. Figure 8-6 illustrates the scope of this expanded Mars exploration trade space.



Figure 8-5 The Capability Driven Framework helps to achieve an ever-expanding human presence beyond low-Earth orbit with increased flexibility, greater cost-effectiveness, and sustainability.

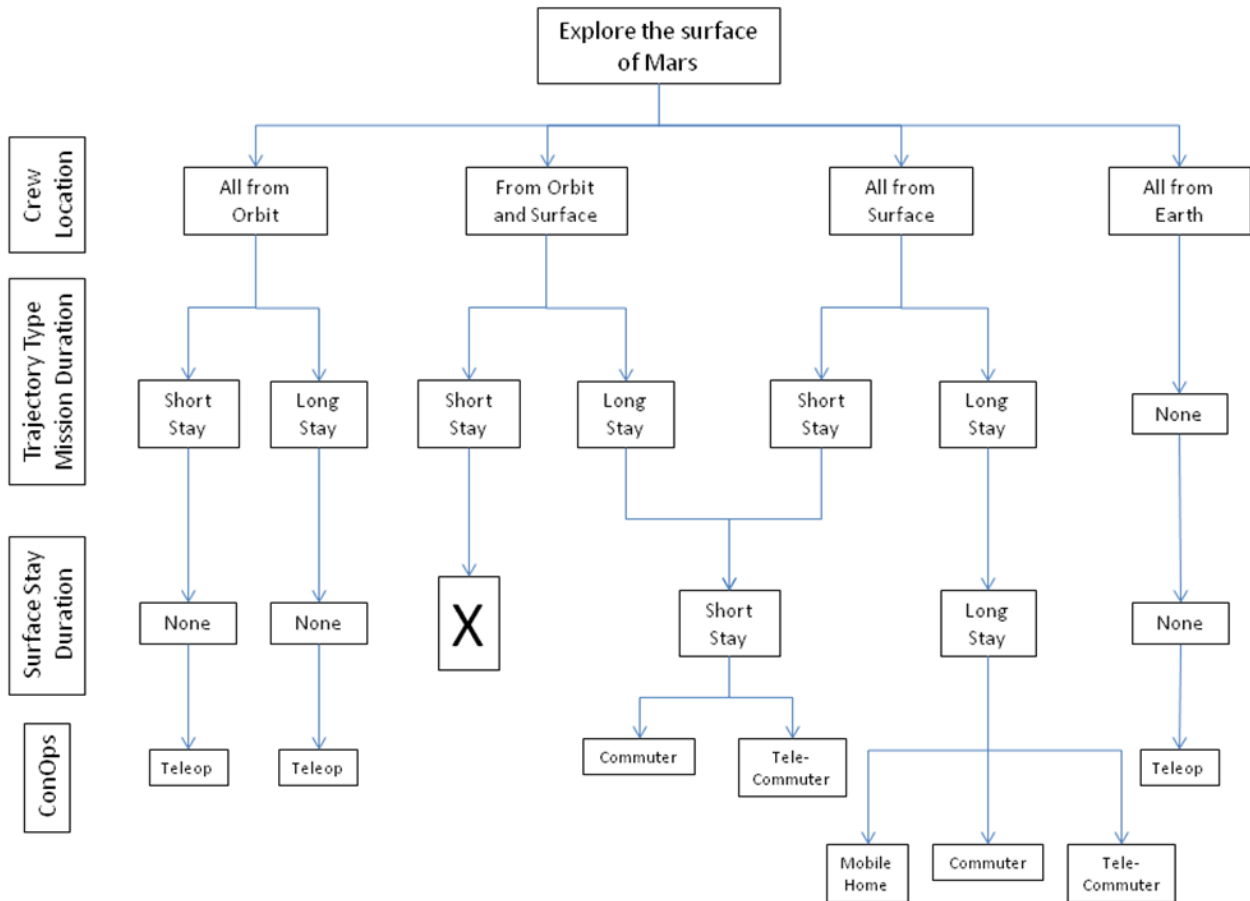


Figure 8-6 Range of Mars surface exploration options in the Capability Driven Framework environment.

A brief discussion of the intent for each of the rows in Figure 8-6 is helpful. The first row, Crew Location, indicates the location where the crew conducts the overwhelming majority of, if not all of, the surface exploration activities. One of the options in this row, From Orbit and Surface, is a scenario in which the crew spends some fraction of its time at Mars conducting operations from orbit and the remainder of the time on the surface. The relative proportion of time in orbit and on the surface is a parameter that can be selected as part of the specific implementation. However, it is assumed that the surface stay time on Mars will be sufficient for the crew to become acclimated to a gravity environment and carry out useful exploration activities before returning to orbit. It is for this reason that there is an “X” on one of the branches from this option – a Short Stay trajectory type, in which the crew spends some portion of its already short stay at Mars conducting operations from orbit, would lead to what is assumed to be an insufficient acclimation time on the surface (based on experience with returning ISS crews) during which the crew can be reasonably certain of conducting useful work. The second row, Trajectory Type / Mission Duration, indicates the type of trajectory used by the crew for the transit between Earth and Mars. Further explanation of these trajectory types can be found in Sections 4.1 and 6.2 of the original DRA 5.0 report (NASA SP-2009-566). The third row, Surface Stay Duration, indicates how much time the crew spends on the surface of Mars while the crew is at Mars (the remainder of the time being spent in orbit around Mars). The fourth row, ConOps, indicates the concept of operation used by the crew to conduct their surface exploration. For this row, the Mobile Home, Commuter, and Telecommuter options were described earlier in this section. The Teleop option is comparable to the method currently used to operate robotic spacecraft on the surface of Mars but with latency times determined by the distance between the operator and the remote spacecraft. Other options may be possible, but none were put forward during the time period covered by this discussion.

Several useful observations regarding the surface exploration strategy can be made as a result of this exercise. Creating the diagram itself was useful in that it helped determine the number of fundamental surface strategy options that are sufficient to span the likely range of possible missions in the CDF. The resulting diagram indicated that a total of four unique concepts of operation could be sufficient for Mars surface exploration – a relatively small number given the number of different options that precede this end state. Of these four concepts of operation, three were developed in some detail for DRA 5.0 (see Section 8.1 above), although some customization would be required to fit the options in this diagram. The fourth concept of operations, Teleop, represents one end of a spectrum of remote operations that is governed by the latency in the command / response cycle between the crew and the robotic device they are controlling. It is not too difficult to see the Telecommuter option as the other end of this robotic device control spectrum. But the Telecommuter option has the added benefits of (a) (potentially) the lowest latency, (b) crew on the surface to interact directly with the robots if necessary, and (c) crew on the surface able to conduct their own independent operations. This is the reason why Teleop and Telecommuter were carried as separate concepts of operations in this exercise.

8.4. Functional Breakdown.

Many of the payload manifest and individual systems used in the DRA5 manifests and the other studies described previously are the product of a gradual evolution and refinement as the Mars DRA evolves or as special studies are conducted. This process has the advantage of gaining a more thorough insight into the necessary characteristics of these manifests and systems over time, but has the disadvantage of potentially overlooking certain aspects of the surface mission because of the point at which a study or assessment is initiated.

An effort was initiated to use standard systems engineering techniques to characterize the surface mission independent of specific systems or payload manifests. This was done to better understand if any aspects of the surface mission were being inadvertently neglected or if other combinations of functions and capabilities might improve the overall effectiveness of the surface mission. A top-down process was used to identify surface mission objectives and then to identify functions needed to meet those objectives. Once this set of identified functions was available it became possible to allocate those functions to systems or combinations of systems. This allocation process can be done systematically and results can then be compared on a more uniform basis.

For this particular assessment, the group started with “Explore Mars” as the highest level objective for this mission. The first level of decomposition from this objective fell into two broad functional categories – mission objective functions and mission support functions. Mission objective functions dealt with those activities that were part of the “what” functions the crew and robotic devices would carry out on the surface of Mars to achieve the top-level

objective. Mission support functions dealt with those activities that were part of the “how” functions needed by the crew and robotic devices to accomplish the top-level objective.

The mission objective functions were divided into three parts. Two of the three objective functions are derived from the Mars Exploration Program Analysis Group (MEPAG) Goals I through IV (see Section 2 of the DRA5 Addendum) and account for scientific functions (“Perform Science” – MEPAG Goals I through III) and functions necessary for eventual human presence on the surface (“Prepare for Future Human Presence” – MEPAG Goal IV). The third objective function, “Engage Public,” was derived from a function that can be traced to the National Aeronautics and Space Act, in which NASA is directed to “provide for the widest practicable and appropriate dissemination of information concerning its activities and the results thereof.”

The mission support functions were divided into four parts. Two of these functions involved sustaining the human crews and machines that would be exploring Mars. The sustain function was seen as fundamental to the success of those elements of the mission directly involved in the objective functions (i.e., human crews and robotic devices) but decomposing this function was seen to have unique differences for humans and machines, hence two separate sustain functions. For the third mission support function, both humans and machines were recognized as requiring consumables. But unlike the previously described sustain functions, no unique difference in providing or sustaining these consumables could be identified, hence the use of just a single function of provide/sustain consumables. The final support function identified was the transport of the other three entities discussed – humans, machines, and consumables (or other cargo) – to achieve the previously discussed mission objective functions.

Each of the three mission objective functions and four mission support functions were decomposed as many as two additional levels. These functional levels – from highest objective to lowest identified function – are shown in Figure 8-7. It was at this level of granularity that the group determined that the set of lowest level functions were reasonably comprehensive and sufficiently unique to allow them to be assigned to individual systems or subsystems. Further decomposition of the provide/sustain consumables is one area where additional effort may be required to bring this particular function to a comparable, but still useful, level of granularity compared with the other functions at this level.

This effort resulted in what appears to be a manageable number of functions that can be applied to a broad range of Mars mission analyses. This type of breakdown also facilitates a systematic comparison of alternatives at appropriate levels of granularity. A limited number of assessments have been made using portions of this functional breakdown, giving an indication of its potential flexibility. One example of these applications is discussed in the next section. However, this functional decomposition has yet to be applied to a sufficient number of Mars mission analyses to determine if it is in fact comprehensive at the lowest level.

8.5. Surface Strategy Assessment Utilizing Functional Breakdown

As mentioned earlier in this section, a methodology was needed to evaluate, in a consistent manner and across different assessments, the combinations and variations in systems and operations available to achieve objectives set for Mars surface exploration. This section describes one use of the functional breakdown just described as a framework for such a systematic comparison of different options for achieving these objectives.

An assessment of the impact that in situ production of some portion of the consumables required for the surface mission can have on the total mass required for that surface mission was under way at the time when the functional breakdown became available for use as an evaluation tool. Three tradable options for missions and operations were being considered for that assessment:

- the trajectory type (options indicated as “short stay” and “long stay”),
- the surface cargo delivery approach (options indicated as “all-up” and “pre-deploy” or “pre-d”), and
- use of local resources to make propellant for the Mars ascent vehicle (options indicated as “local resources” and “no local resources” or as “in situ resource utilization (ISRU)” and “no ISRU”).

(A more complete description of these tradable options can be found in the Mars DRA 5.0 addendum http://www.nasa.gov/exploration/library/esmd_documents.html). A traditional trade tree approach was determined to be a reasonable means of organizing a systematic comparison of these options.

The previously discussed functional breakdown provided the structure for a systematic comparison of the hardware system options. The analysts making this assessment used only mission support functions and found that the following tier of the breakdown proved flexible enough to be useful for this task:

- Transport Humans, Machines, and Cargo,
- Provide/Sustain Consumables,
- Sustain Machines (Systems), and
- Sustain Humans.

Figure 8-8 illustrates how the tradable options and functional breakdown categories were mapped to each other, allowing a systematic comparison of required surface payload mass to be carried out.

Each cell in the matrix shown in Figure 8-8 represents a unique collection of systems and operations, organized by the functions they perform, necessary to accomplish mission objectives. Once the collection of systems and operations has been defined, appropriate analysis tools were applied to evaluate each collection, providing the data needed to generate figures of merit (in this case, the total mass required for these systems) and compare the options.

Figure 8-9 illustrates nine of the major systems determined to be necessary to accomplish the surface exploration portion of a human Mars exploration mission in this scenario. Other systems not shown will eventually be necessary to fully carry out this mission, but the items shown are the major systems required (in terms of payload mass) and serve to illustrate options for several of these systems.

The first row in Figure 8-9 contains those systems necessary to carry out the first major function identified above for the Mars surface mission, namely the “Transport Humans, Machines, and Cargo” function. The next two rows contain those systems necessary to carry out the remaining three functions identified above. The third row shows two options for one of the functions – two different types of power systems that could be used on the surface.

The mass of each of these systems is also shown in Figure 8-9, indicating one key feature that is important when comparing different options – the total mass that must be provided for the crew to accomplish their mission objectives. The mass values are derived from previous DRA 5.0 studies and from more recent work intended to refine the analyses documented in DRA 5.0.

The implications of each branch of the trade tree in Figure 8-8 was accounted for by the type of system option selected and mission unique mass values associated with that branch (e.g., crew consumables derived from the total length of the surface mission). Figure 8-10 summarizes the total mass resulting from summing all of the individual mass values necessary to complete the mission in a particular branch of the trade tree. Note that the first row is not represented in this graphic. This is due to the fact that this particular combination of trade options does not result in a feasible solution (i.e., there is insufficient time in a “short stay – all-up” mission scenario to generate propellants from local raw materials in a mass-efficient manner and places an additional risk on the crew by not providing them with an immediate means to “abort” to their orbiting spacecraft as can be done in other scenarios).

The DRA 5.0 case is represented in Figure 8-10 by the “long stay – pre-deploy – ISRU” case and can be looked upon as a benchmark. Based on the analyses performed for this example, the “long stay – all up – ISRU” case results in the same mass needed in DRA 5.0 to accomplish the surface mission. However, further analysis will result in a larger total mission mass once the transportation mass required to send these systems to Mars with the crew are accounted for (i.e., sending the ISRU systems on a faster but more propellant intensive trajectory used for crew transfer). The only other case that results in a lower total mass is the “short stay – pre-deploy – ISRU” case. The reduction in these total mass values is significant enough to warrant the assessment of other figures of merit to determine the relative value of such an approach to Mars surface exploration compared with the DRA 5.0 benchmark. This also illustrates the benefit of this type of systematic assessment in that the “short stay – pre-deploy – ISRU” case would not likely have been examined as a stand-alone case.

Functional Decomposition

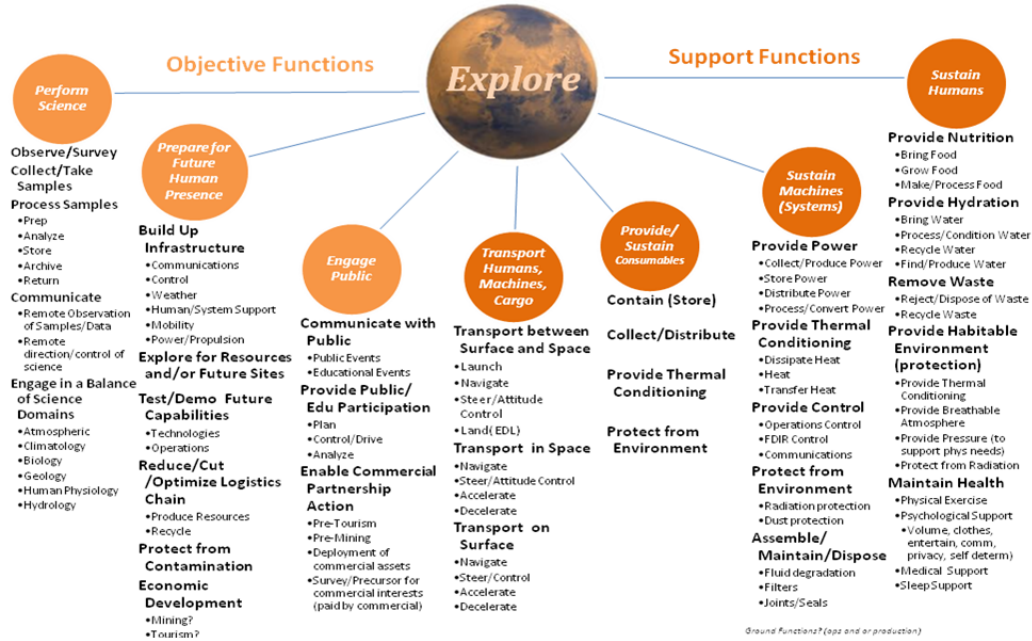


Figure 8-7 Functional breakdown to achieve the top-level objective of explore Mars.

		Transport Humans, Machines, Cargo	Provide/Sustain Consumables	Sustain Machines (Systems)	Sustain Humans
		Transport between Surface and Space	Contain (Store)	Provide Power	Provide Nutrition
		Transport in Space	Collect/Distribute	Provide Thermal Conditioning	Provide Hydration
		Transport on Surface	Provide Thermal Conditioning	Provide Control	Remove Waste
			Protect from Environment	Protect from Environment	Provide Habitable Environment
				Assemble/Maintain/Dispose	Maintain Health
Mars Surface Mission	Short Stay	All Up			
		Pre-deploy			
	Long Stay	All Up			
		Pre-deploy			
		Local Resources			
		No Local Resources			
		Local Resources			
		No Local Resources			
	Local Resources				

Figure 8-8 Evaluation matrix based on the tradable mission options and the functional breakdown of those capabilities needed to achieve surface mission objectives.










Hypersonic Inflatable Aerodynamic Decelerator (HIAD)  • 15.0 – 16.3 t	Mars Lander Vehicle  • 24.9 – 40.7 t (wet)	Mars Ascent Vehicle  • 41.7 – 42.8 t (wet)
Surface Habitat (large)  • One @ 24.5 t	Surface Habitat (small)  • One @ 3.5 t	Crew Rovers (pressurized and unpressurized)  • Two @ 7.7 t
Surface Science  • 1.6 t	Nuclear Power System  • One @ 7.8 t	Solar Power System  • One @ 2.0 t

Figure 8-9 Hardware systems and mass estimates previously described in some detail as part of DRA 5.0 that were used to provide the functions identified.

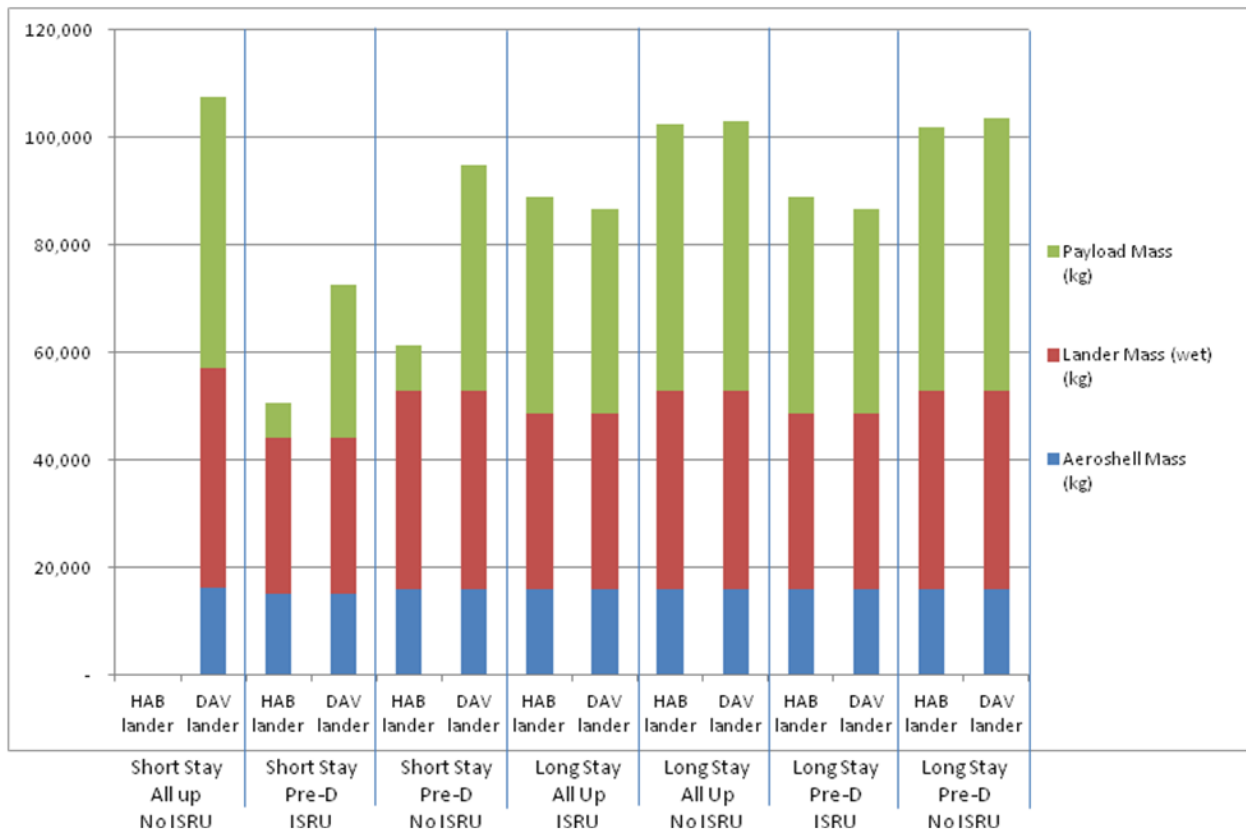


Figure 8-10 Mass estimates resulting from analysis of each cell in the evaluation matrix.

8.6. Summary

This section describes tasks associated with analyzing human crews exploring the surface of Mars or the environment in Mars orbit, including the two moons of Mars. After a brief summary of the three Mars surface mission strategies – given the working titles of “mobile home,” “commuter,” and “telecommuter” – documented in DRA 5 assessments related to the surface exploration of Mars performed since the completion of DRA 5.0 were summarized. These assessments included:

- An impact assessment of the number of crew members and size of the lander vehicle on the overall mission while attempting to achieve the same mission objectives. This assessment was performed at the request of the Review of United States Human Space Flight Plans Committee (also known as the Augustine Committee) in 2009.
- A reopening (or expansion) of surface strategy options as a result of adopting the Capability Driven Framework. This introduced a fourth mission strategy, namely a purely teleoperations strategy.
- Development of a functional breakdown of the Mars surface mission as a basis for reassessing the systems and capability allocation used in DRA 5.0.
- Ongoing efforts to evaluate surface strategy options structured around the surface mission functional breakdown.

Forward work is still required in a number of areas related to the surface exploration strategy. Several important examples among these forward work activities include (although this is not a comprehensive list):

- A more detail description of initial activities by the crew and surface systems immediately after landing and for the first few weeks of surface exploration. These activities are expected to be relatively independent of the specific landing site or site-dependent exploration investigations. Such a description will help refine the functional breakdown that has been started and help identify preferred allocation of these functions among surface systems.
- A similar detailed description of the activities by the crew and surface systems in the final few weeks of the surface mission. As discussed in the previous item, this description is expected to help refine the functional breakdown and functional allocation.
- Create (and maintain) a dictionary for the functional breakdown described above.
- Begin (continue?) to use the functional breakdown in the next steps of the systems engineering process by grouping functions where possible and allocating functions to systems for each of the four identified surface strategy options.
- Begin to identify and capture risks associated with each of the surface strategy options as the various analyses described above (or other relevant analyses not described) are performed.
- Assess the potential evolution of the Mars surface exploration strategy (including the potential evolution of the functional breakdown and capability/system options) through different CDF pathways (e.g., how can lunar surface exploration be used to mature Mars surface exploration).

8.7. Bibliography

-
- ¹ Drake, Bret G., Editor, “Human Exploration of Mars, Design Reference Architecture 5.0,” National Aeronautics and Space Administration, NASA-SP-2009-566, July 2009.
 - ² White House, “U.S. Announces Review of Human Space Flight Plans, Independent Blue-Ribbon Panel will Delineate Options,” Office of Science and Technology Policy Press Release, May 7, 2009.
 - ³ Augustine, Norman R., “Seeking a Human Spaceflight Program Worthy of a Great Nation,” Review of U.S. Human Spaceflight Plans Committee, October 2009.
 - ⁴ Human Space Exploration Framework Summary”, National Aeronautics and Space Administration, January 12, 2011, http://www.nasa.gov/exploration/new_space_enterprise/home/heft_summary.html

This page intentionally left blank

9. MARS SURFACE SYSTEMS

9.1. Surface Power Systems

Primary Contributors:

Lee S. Mason, National Aeronautics and Space Administration, Glenn Research Center

David I. Poston, Los Alamos National Laboratory

9.1.1. Introduction

Under the NASA Exploration Technology Development Program (ETDP) and in partnership with the Department of Energy (DOE), NASA has an ongoing project to develop Fission Surface Power (FSP) technology. The primary goals of the project are 1) develop FSP concepts that meet expected surface power requirements at reasonable cost with added benefits over other options, 2) establish a hardware-based technical foundation for FSP design concepts and reduce overall development risk, 3) reduce the cost uncertainties for FSP and establish greater credibility for flight system cost estimates, and 4) generate the key products to allow NASA decision makers to consider FSP as a preferred option for flight development.

The FSP project was initiated in 2006 as the NASA Prometheus Program and the Jupiter Icy Moons Orbiter (JIMO) mission were phased out. As a first step, NASA Headquarters commissioned the Affordable Fission Surface Power System Study (AFSPSS) to evaluate the potential for an affordable FSP development approach. With a cost-effective FSP strategy identified, the FSP team evaluated design options and selected a Preliminary Reference Concept to guide technology development. Since then, the FSP Preliminary Reference Concept has served as a point-of-departure for several NASA mission architecture studies examining the use of nuclear power and has provided the foundation for a series of “Pathfinder” hardware tests. The long-term technology goal is a Technology Demonstration Unit (TDU) integrated system test using full-scale components and a non-nuclear reactor simulator.

The FSP team consists of Glenn Research Center (GRC), Marshall Space Flight Center (MSFC), and the DOE National Laboratories at Los Alamos (LANL), Idaho (INL), Oak Ridge (ORNL), and Sandia National Laboratory (SNL). The project is organized into two main elements: Concept Definition and Risk Reduction. Under Concept Definition, the team performs trade studies, develops analytical tools, and formulates system concepts. Under Risk Reduction, the team develops hardware prototypes and conducts laboratory-based testing.

9.1.2. Project Context

One of the major challenges to the implementation of space fission power systems is development cost. In April 2006, NASA and DOE initiated the AFSPSS to determine the design features and expected costs of a representative FSP system. A government study team with members from several NASA field centers and DOE laboratories evaluated technology options and design variables and selected a reference concept based on affordability and risk. A low-risk approach was selected over other options that could offer higher system performance and/or lower mass. The team also defined a credible development schedule and generated a detailed Work Breakdown Structure (WBS)-based cost estimate. The results indicated that the initial FSP system could be developed, flight-qualified, and delivered to the lunar surface by 2020 for approximately \$1.4B (2007 dollars) with follow-on systems costing about \$215M each.¹ FSP design and operational aspects for both lunar and Mars applications was also considered.

The “affordable” design approach was considered representative of a number of potential system concepts. To determine an FSP reference concept, the team generated a comprehensive list of system design options and conducted screening studies that led to six plausible concepts for further study. All of the plausible concepts presumed the use of a low-temperature (<900 K) reactor heat source with conventional materials as a path toward achieving an affordable solution. The plausible concepts included a liquid-metal-cooled reactor with Stirling, Brayton, thermoelectric, or organic-Rankine power conversion, a gas-cooled reactor with Brayton power

conversion, and a heat pipe cooled reactor with Stirling power conversion. The concepts were evaluated for performance and relative cost against a common set of mission requirements and development constraints derived from the earlier affordable study. In 2008, a management review panel led by NASA Headquarters selected the liquid-metal reactor with Stirling power conversion as the FSP Preliminary Reference Concept and recommended Brayton as a backup conversion option if unforeseen difficulties arise with the Stirling technology development efforts.²

The resulting Preliminary Reference Concept includes a liquid-metal-cooled, fast-spectrum reactor with Stirling power conversion and water-based heat rejection.³ The reactor uses uranium oxide (UO₂) fuel pins in a hexagonal core with an external radial reflector and control drums. Heat is transferred to the Stirling power converters by a pumped sodium-potassium (NaK) reactor coolant loop. The core structure and coolant piping are constructed of stainless steel to reduce cost and development risk. The radial reflector is beryllium in a stainless-steel shell. The control drums are beryllium and boron carbide (B₄C), also enclosed in stainless steel. The reactor is located at the bottom of an approximate 2-m-deep excavation. The lunar regolith limits radiation from the reactor to less than 5 rem/year at a 100 m radius. The Stirling converters generate single-phase alternating current (AC) electric power that is converted to direct current (DC) for user loads. Stirling waste heat is removed by a pumped water coolant loop coupled to a series of two-sided, vertical radiator panels. The radiator panels comprise titanium-water heat pipes in a composite facesheet sandwich. The FSP concept is designed to produce a net power of 40 kWe with a full-power service life of at least 8 years. This same technology could be used for missions at essentially any location (equator to poles) on the lunar or Mars surface.

9.1.3. Derived Requirements

Table 9-1 presents a summary of the top-level requirements developed for the FSP system. The requirements are termed “derived” because they were predominantly defined by the FSP team in response to suggestions by NASA Headquarters and the various NASA architecture study teams. The FSP safety-related requirements were generated by the FSP team based on previous space fission system development projects, such as SP-100 and JIMO. These requirements will undoubtedly be reviewed (and perhaps expanded) by independent design experts once FSP reaches flight development status. For now, they provide a reasonable starting point to guide FSP concept definition and technology development.

The key requirements that drive FSP system design are power level and service life. The 40 kWe power output is consistent with numerous studies that have estimated power requirements for the initial phase of a human lunar outpost dating back to the 1990’s Space Exploration Initiative and before. That power level is also well suited for an initial space reactor because it is large enough to demonstrate the mass effectiveness of nuclear fission, but not too large to over-complicate the design and development process. In actuality, the fission technology developed for the 40-kWe design is readily scalable between 10 and 100 kWe. Below 10 kWe, the mass and cost advantages of fission power systems is not as compelling. Above 100 kWe, the reactor and power conversion technologies selected for FSP may need to be reevaluated.

The 8-yr service life also represents a reasonable balance of performance and risk. It is long enough to accommodate most estimates for lunar and Mars surface mission duration. For longer missions, it would be prudent to utilize multiple FSP units and stagger their delivery to provide overlap. The 8-yr design life is also well within current technology projections for low-temperature liquid-metal reactors and dynamic power conversion. In addition, notional FSP development schedules indicate that sufficient qualification testing can be performed to demonstrate 8-yr life while still meeting the proposed launch date.

Table 9-1 FSP-Derived Requirements

REQUIREMENT	RATIONALE
1. The FSPS shall be designed to produce no less than 40 kWe net power output (after accounting for all power losses and auxiliary loads).	Provides sufficient power for extended-stay crew habitation, ISRU production facilities, rover recharging, and science equipment, including margin.
2. The FSPS shall be designed for use at any location on the lunar surface. Radiator sizing shall be based on worst-case surface temperatures and Sun angles.	Provides maximum flexibility in locating the lunar outpost. (The preferred lunar outpost location has not been determined.)
3. The FSPS shall be designed to operate for no less than 8 yr at full power.	Provides maximum service life without introducing excessive risk in FSP development and qualification.
4. The FSPS shall be flight ready for an initial launch and deployment no later than 2022.	Assures FSPS availability for initial outpost deployment based on current lunar emplacement schedules.
5. The FSPS shall be designed to produce no less than 50% power output after the first credible component failure.	Assures FSPS power availability to meet essential crew power requirements following a component failure.
6. The FSPS shall be recoverable from all credible operational upsets and transients without adverse safety consequences to the crew or outpost.	Assures FSPS power availability following an off-nominal event and a return to safe FSP operation.
7. The radiation from the FSPS shall be less than 5 rem/yr to an unshielded crew member located at the outpost.	Provides a guideline for FSPS shield design that corresponds to 10% of the astronaut annual dose limit. (The allowable crew dose from the FSPS has not been determined.)
8. The reactor shall remain subcritical during all planned and credible unplanned mission events prior to FSPS startup.	Assures that the FSPS does not present a radiological safety hazard before initial startup is commanded.
9. At its end-of-life, the reactor shall be decommissioned in a safe shutdown condition.	Assures that the FSP does not present a human safety hazard after final shutdown is commanded.
10. The FSPS mass shall be minimized and no greater than the current cargo lander down-mass capability of 14 000 kg.	Permits the FSPS to be delivered as a fully integrated package with available cargo mass to accommodate other payloads.
11. The FSPS design shall be extensible to the Mars surface. All materials and design strategies shall be compatible with the Martian environment.	Provides maximum return on FSPS technology investment by designating its applicability for both the Moon and Mars.
12. The FSPS shall be designed for robotic deployment using teleoperation.	Permits the FSPS to be installed at the lunar outpost without local human assistance, but does not preclude it.

System mass is another requirement that could influence FSP design. The current derived requirement is that the FSP system mass be less than the payload capacity of the lander. The current cargo lander concept is projected to deliver approximately 14 000 kg to the lunar surface. The 40-kWe FSP system can easily be accommodated within this mass constraint, and most estimates show the system to be less than one-half of the lander cargo capacity. The generous lander payload allocation eliminates system mass as a major FSP design driver and allows the system to utilize low-risk technology to minimize development cost and increase system reliability. Nevertheless, the FSP system design incorporates various mass saving features to maximize the mass available for other payloads. This also assures that the concept is relevant for future applications that may be more mass constrained.

9.1.4. Design Summary

The preliminary reference concept layout is shown in Figure 9-1. The reactor core is located at the bottom of an approximate 2-m-deep excavation with an upper plug shield to protect the equipment above from direct radiation. The NaK pumps, Stirling convertors, and water pumps are mounted on a 5-m-tall truss structure that attaches to the top face of the shield. Two symmetric radiator wings are deployed via a scissor mechanism from the truss. Each radiator wing is approximately 4 m tall by 16 m long and is suspended 1 m above the lunar surface. In its stowed configuration, the FSP system is approximately 3 by 3 by 7 m tall.

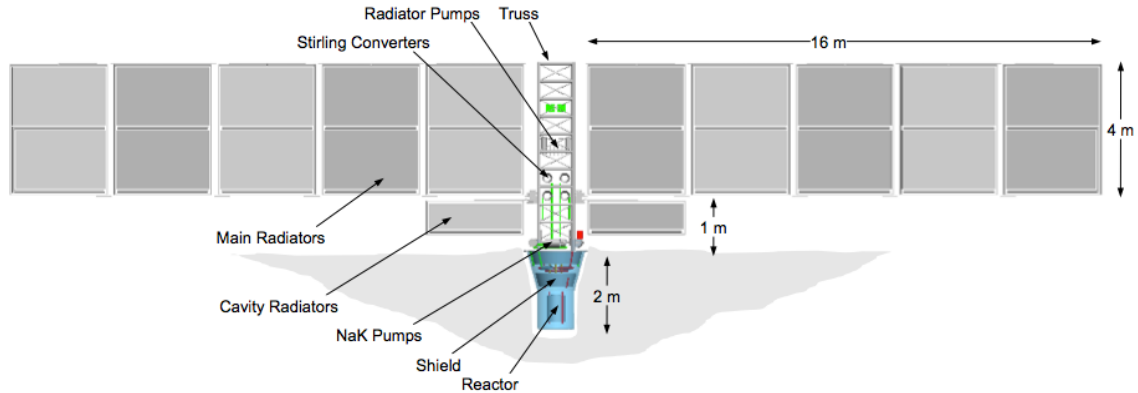


Figure 9-1 FSP concept layout.

The buried configuration was selected for the preliminary reference concept because it minimizes the mass of radiation shielding that must be delivered from Earth. It also simplifies the Power Management and Distribution (PMAD) because the buried reactor can be located relatively close to the outpost to shorten transmission cable length. There are numerous other FSP installation options that could be developed depending on mission needs. The basic technology building blocks of the liquid-metal-cooled reactor, Stirling power conversion, and water-based heat rejection would be essentially the same. The decision on FSP configuration can easily be deferred until the flight program since most of the design challenges related to the configuration are engineering based rather than technology based.

The preliminary reference concept schematic is shown in Figure 9-2. The use of redundant components and parallel fluid loops allows the system to produce partial power in the event of unexpected failures. The schematic shows the system energy balance and the anticipated temperatures, pressures, and flow rates at some of the key interfaces. The reactor (Rx) produces 186 kWt with a peak fuel pin clad temperature of 860 K. It delivers heated NaK at 850 K to a pair of intermediate heat exchangers (IHX) using two fully redundant electromagnetic primary pumps (PP). The IHX is a NaK-to-NaK heat exchanger that provides a buffer between the primary NaK and the Stirling convertors, and a means to adjust the NaK flow rate and resulting temperature drop across the Stirling convertors separately from the reactor flow and temperature drop. Each intermediate NaK loop services two Stirling convertors at a supply temperature of 824 K. The effective Stirling hot-end cycle temperature is 778 K. The secondary NaK loops include an intermediate electromagnetic pump (IP) of similar design to the primary NaK pump.

Each Stirling convertor (Stir) is composed of two axially opposed Stirling heat engines and two linear alternators. Power conversion thermal-to-electric efficiency is estimated at 26%. The alternators deliver 6 kW_e each at 400 Vac rms and 60 Hz to the PMAD. A Local Power Controller (LPC), located approximately 100 m from the reactor, converts the 400 Vac to 120 Vdc for distribution to the Electrical Load Interface (ELI). The 48 kW_e gross Stirling output power provides sufficient capacity to account for electrical losses (~3 kW_e) and system parasitic loads (~5 kW_e) and still delivers 40 kW_e net for user loads. A Parasitic Load Radiator (PLR) dissipates electric power that is not required by the user loads and allows the system to be operated at constant power, thus eliminating the complexity of thermal system load following. The ELI serves as the primary power bus and system interface for commands and telemetry. A 5-kW_e photovoltaic (PV) array and a 30-kW-hr battery are included with the FSP PMAD for startup and backup power.

The heat rejection subsystem is composed of four water heat transport loops and two radiator (Rad) wings (two loops per wing). The radiator wings receive heated water at 420 K from the Stirling convertors and return the water at 390 K using a mechanical radiator pump (RP), while rejecting approximately 35 kWt per loop. The resulting Stirling cold-end cycle temperature is 425 K. The total heat load is approximately 140 kWt and the total two-sided FSP system radiator area is 185 m² assuming a 250 K effective sink temperature and 10% area margin. Each radiator wing includes 10 subpanels, each measuring approximately 2.7 m wide by 1.7 m tall. The preliminary reference concept mass summary for the buried reactor configuration is shown in Table 9-1. The total system mass without margin is 5820 kg.

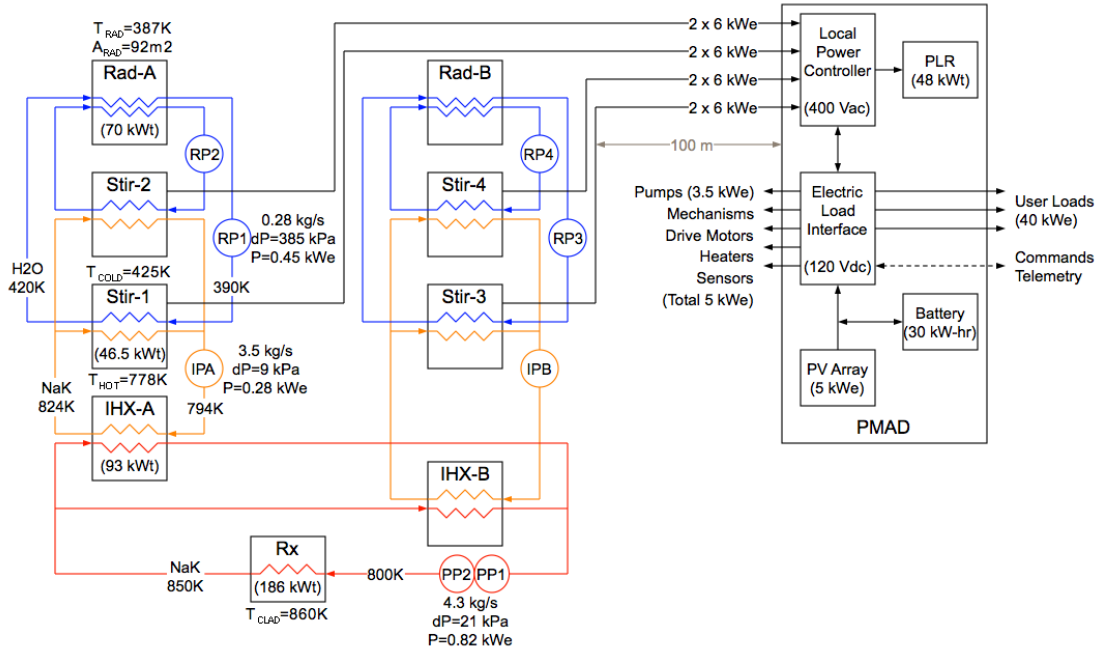


Figure 9-2 FSP concept schematic.

Table 9-2 FSP Mass Summary

1.0	Fission Surface Power System (kg)	5820
1.1	Reactor Module (kg)	1440
1.2	Power Conversion Module (kg)	411
1.3	Heat Rejection Module (kg)	767
1.4	Power Management and Distribution Module (kg)	1071
1.5	Radiation Shield Module (kg)	2080
1.6	Integration Structure (kg)	51

9.1.5. Lunar and Mars Architecture Studies

Beginning with the Exploration Systems Architecture Study in 2005, NASA has conducted various mission architecture studies to evaluate implementation options for the U.S. Space Policy (formerly the Vision for Space Exploration). Several of the studies examined the use of fission power systems for human missions to the lunar and Martian surface. The FSP team contributed by supplying FSP design characteristics, developing mission-compatible configuration options, and defining a Concept-of-Operations consistent with the mission objectives.

9.1.5.1. Lunar Architecture Team

In 2007, the second phase of the Lunar Architecture Team (LAT2) developed an FSP-based architecture known as Option 6 for a polar lunar outpost at the Shackleton Crater site. The nuclear-based architecture was proposed to accelerate outpost buildup, achieve earlier 180-day missions, and maximize the total number of crew days on the surface. Option 6 uses the buried reactor concept delivered on a cargo lander and installed by a combination of robots and crew, as shown in Figure 9-3. An earlier lander delivers a small solar array and battery to supply initial power, the FSP PMAD equipment, and a bladed-rover that prepares the site for the reactor. Once installed, the FSP system provides a robust power capability of 40 kWt resulting in substantial power margin for early outpost buildup and operations. It also provides capacity for power increases associated with the initial surface elements and the

potential for expanded science and resource utilization. System trades comparing Option 6 to similar LAT2 architectures with solar PV arrays and regenerative fuel cells (RFCs) showed the FSP-based architecture to offer significantly more power with less power system mass and comparable cost despite the favorable conditions for solar power at Shackleton.

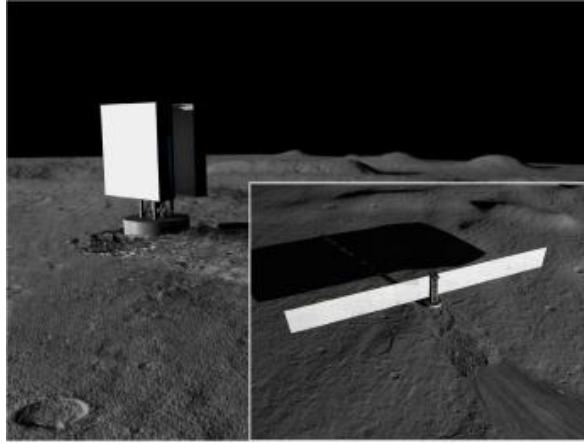


Figure 9-3 FSP System for LAT2 Option 6.

A key question raised about the FSP installation was the feasibility of excavating the reactor hole. Independent studies were conducted by the in situ resource utilization (ISRU) team during LAT2 to evaluate methods for excavating a 2-m-deep hole. The ISRU study evaluated various digging methods and developed analytical models to predict the mass and power requirements for the machinery. It was determined that the process could use the same semi-automated regolith-moving equipment planned for the ISRU oxygen production plant. The recommended approach was to prepare an oversized hole with a ramp that could accommodate ingress/egress of a bladed rover. Preliminary estimates indicated the need to move about 24 m³ of regolith, including the final backfilling of the ramp, over a time period of 41 to 50 days.

9.1.5.2. Mars Architecture Team

During the same time period, the Mars Architecture Team (MAT) was reviewing power system options for a crewed mission to Mars. The basic architecture was derived from previous Mars mission concepts in which an initial cargo lander delivers a power system and ISRU plant to locally produce the return propellant before the crew ever leaves Earth. A nuclear system allows the propellant production to be completed faster and more efficiently through continuous day/night operations. The power requirements for the nuclear power option were about 30 kWe during the pre-crew deployment phase and about 20 kWe after the crew arrives. The 30-kWe power level was similar enough to the reference 40 kWe lunar concept that no power system design changes were required. The MAT-based FSP concept assumed the reactor on a mobile cart with integral shielding that is robotically deployed from the lander, as shown in Figure 9-4. The above-grade reactor configuration was chosen for this application because the MAT wanted to avoid digging operations. FSP was selected as the baseline power system for MAT based on advantages in system mass, operational flexibility, and environmental robustness as compared to solar power systems with energy storage.⁴

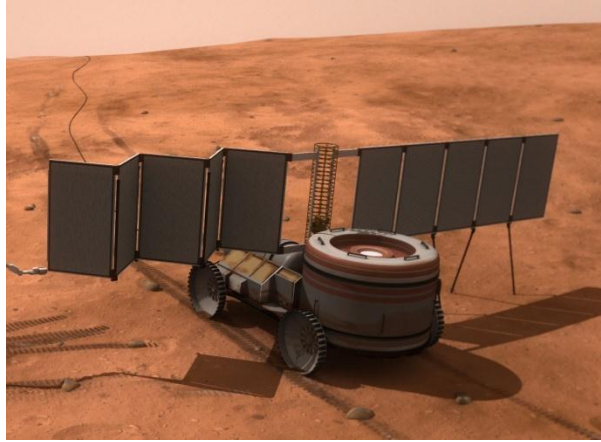


Figure 9-4 Mars FSP concept.

9.1.5.3. Lunar Surface Systems/Constellation Architecture Team

In 2008, Lunar Surface Systems (LSS) and the Constellation Architecture Team developed an FSP-based architecture known as Scenario 5. Two basic FSP options were investigated including the typical off-loaded and buried system and a new concept where the FSP system remained on the lander, as shown in Figure 9-5. In either case, the FSP system was to be delivered on the first cargo lander to provide a power-rich environment for early outpost buildup. Both systems also assumed a central power distribution node at the outpost. This provided an easy-access power bus for outpost loads such as habitats, ISRU equipment, rover recharging, and science experiments. It also placed the FSP system's power and control electronics at a location that was readily accessible should maintenance be required. A small solar array (5 kWe) and battery (30 kW-hr) was included with the FSP PMAD for startup and emergency backup. A follow-on architecture evaluated by LSS, referred to as Scenario 12, included an FSP system that was delivered later in the lunar campaign using a similar design approach.



Figure 9-5 Lander-Integrated FSP System for LSS Scenario 5.

The FSP team did an extensive evaluation of radiation shielding options to support the Scenario 5 architecture definition.⁵ Figure 9-6 shows graphical representations of the Monte Carlo N-Particle (MCNP) transport code models developed for the four shielding approaches that were examined including A) FSP system off-loaded and reactor buried, B) FSP system off-loaded and placed on surface with surrounding regolith berm, C) FSP stays on the lander as delivered from Earth, and D) FSP system stays on the lander with regolith shielding augmentation. All options assumed a 3 mrem/hr (26.3 rem/yr) reactor dose rate to an unshielded astronaut at a specified separation distance. This is higher than the 5 rem/yr dose mentioned previously to account for more realistic crew routines and schedules. Crew length-of-stay is expected to be no greater than 180 days with the majority of time spent in shielded habitats and rovers away from the hypothetical reactor boundary. Given reasonable assumptions for crew operations, the total radiation to a crew member from the reactor based on the 3 mrem/hr dose rate at the specified

distance is expected to total much less than 5 rem per year of duty. The actual allowable astronaut radiation dose is not defined yet and will depend on many factors including natural radiation levels, proximity to nuclear sources (such as FSP), crew shielding, length of mission, and extravehicular activity (EVA) duty cycle. The FSP-related dose is expected to be a small percentage of the total received by crew members during their lunar stay. The FSP shielding must also protect its own components located on the truss above the shield. The assumed dose limits for truss-mounted equipment above the shield were 5 Mrad (gamma) and 2.5×10^{14} neutrons/cm². Recent testing of Stirling convertor components and materials at SNL, ORNL, and Texas A&M University suggest that these dose limits could be increased. In most cases, the FSP equipment was the limiting factor in determining the required FSP shield mass.

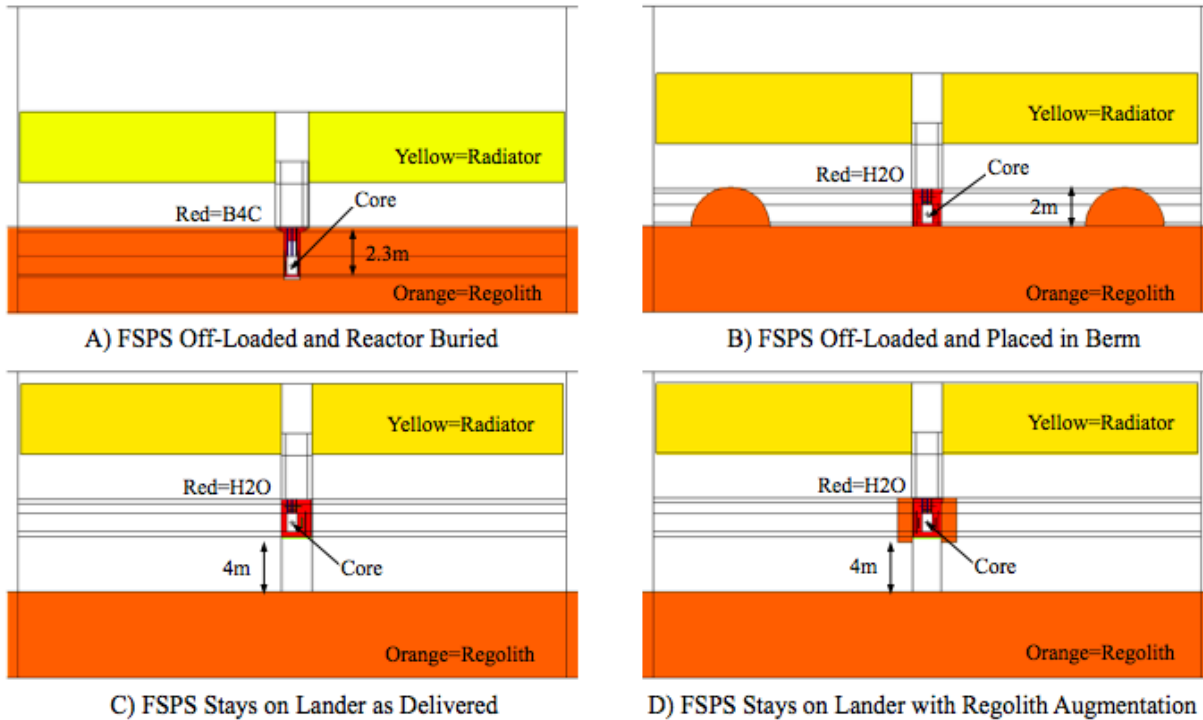


Figure 9-6 Scenario 5 shielding options.

The buried reactor case (A) resulted in a 2080 kg delivered shield, predominantly B₄C, with the reactor core buried to a 2.3 m depth. This approach offered the shortest separation distance among the options at 100 m. It also offers the lowest delivered shield mass, and the potential for shield mass reduction by using water rather than B₄C. The berm shield case (B) assumed a 2-m-tall regolith berm surrounding the reactor. It resulted in a 2660-kg delivered shield using water and depleted uranium (DU) and a 200 m separation distance. The landed shield cases assumed that the reactor remained in the central lander cavity between the propellant tanks at a height of approximately 4 m above the lunar surface. The “as-delivered” lander case (C) required a shaped shield of water and DU that was thicker in the direction of the outpost. It was still the heaviest delivered shield at 2980 kg and required a separation distance of 1000 m. The regolith-augmented lander case (D) resulted in a 2250 kg delivered shield of water and DU supplemented with 0.8-m-thick regolith-filled annulus surrounding the water vessel and a 400 m separation distance. The separation distances for the various shield options were determined in conjunction with power transmission cable mass estimates. Generally, there is an optimum distance that balances shield mass and cable mass. Table 9-3 provides a summary of the power transmission assumptions and resulting cable masses for the four cases. Larger distances require more complex power transmission approaches. In all cases, the power distribution node was assumed to be located at the specified separation distance and a 25% margin was added for cable length. The cable bundle was assumed to include a main power cable, auxiliary power cable (for FSP parasitic loads), and a data transmission cable (for FSP instrumentation signals). The main power cable includes parallel channels for each of the eight Stirling alternators. The auxiliary power cable is assumed to carry a total of 5 kWe via 10 parallel

channels.

Cases A and B assumed direct 400-Vac-power cabling from the Stirling alternators to the power distribution node where the 400 Vac was converted to 120 Vdc for the user load bus. The same 120 Vdc bus was used to power FSP parasitic loads, such as pumps and motors, via a power cable from the distribution node back to the FSP system. The larger separation distance for Case C required the addition of high-voltage transformers near the FSP system to boost the transmission voltage to 2000 Vac. The 2000 Vac provides a reasonable compromise on cable mass, development risk, and operational complexity. The 120-Vdc auxiliary power bus and FSP data bus was assumed to be co-located with the transformers at a 100 m distance from the FSP system. Case D assumed direct 400-Vac transmission, a 120-Vdc user load bus, and a 270-Vdc auxiliary power bus and return cable.

Table 9-3 Scenario 5 Power Transmission Analysis

Shield Option	A	B	C	D
Separation distance, m	100	200	1000	400
Cable length, m	125	250	1250	500
Transmission, Vac	400	400	2000	400
Auxiliary bus, Vdc	120	120	120	270
Auxiliary bus location	Outpost	Outpost	FSP	Outpost
Main power cable, kg	48	128	688	400
Auxiliary power cable, kg	120	450	120	300
Data cable, kg	12	32	12	100
High-voltage transformers, kg	-	-	144	-
Total transmission mass, kg	180	610	964	800

The LSS and Constellation Architecture Team settled on two FSP configurations for Scenario 5. The two systems used the same reactor, power conversion, heat rejection, and PMAD electronics. The off-loaded configuration assumed the use of the “ATHLETE” utility rover for excavating a hole, removing the FSP system from the lander, transporting it to the site, and positioning it in the hole. The total FSP system mass was about 5800 kg including shielding and cabling. The integrated landed configuration assumed the regolith-augmented shield with the lander cavity filled using a crane that scoops regolith collected near the lander by a bladed rover. The total FSP system mass was about 6600 kg with shielding and cabling.

9.1.5.4. International Architecture Working Group—Power Function Team

Beginning in April 2009, a Power Function Team was formed to support the International Architecture Working Group (IAWG) and develop power system concepts for a Global-Point-of-Departure human lunar mission. The team consisted of members from NASA, the European Space Agency (ESA), and the Japan Aerospace Exploration Agency (JAXA). The proposed IAWG mission architecture assumed an initial human mission to the lunar south pole (Shackleton crater) followed by robotic relocation of the initial surface assets to accommodate subsequent human missions to nonpolar sites such as Malapert Mountain and Schrodinger Basin. Once these initial areas were explored, a single site could be selected for a follow-on long-duration mission phase. Solar-based power systems with RFCs were baselined to include adequate energy storage capacity for 5-day eclipse durations at Shackleton. However, nighttime power requirements may exceed available energy storage capacity for missions beyond Shackleton. Two nuclear-based options were analyzed including a 2-kWe Large-Scale Stirling Radioisotope Generator (LSRG) and a 10-kWe Mobile Fission Power System (MFPS). The LSRG-based architecture enabled 11-day eclipse missions at Malapert, while the MFPS-based architecture provided sufficient capacity to enable both the 11-day eclipse missions at Malapert and 15-day eclipse missions at Schrodinger.

9.1.5.4.1. Mobile Fission Power System

The objective for the MFPS was to provide a small fission power system that could be easily deployed and moved if necessary. The basic concept was a scaled version of the buried 40-kWe FSP system that would be off-loaded from the lander, placed on lunar surface, and shielded with a regolith berm as shown in Figure 9-7. The system would be designed to produce 10 kWe output, continuously during the lunar daylight and nighttime periods. The reactor

would be oversized, based on the larger 40-kWe system, to provide growth capacity and simplify the qualification of possible follow-on systems. The system would utilize a single 12-kWe dual-opposed Stirling convertor, instead of the four units used on the 40-kWe system. Heat rejection would be provided by a simple two-panel deployable radiator, as opposed to the 10 radiator assemblies required on the 40-kWe system. A 200-m transmission cable with remote electrical controls and 120-Vdc load bus would provide the interface to the mission power loads. In addition to the regolith berm, a supplemental water shield would surround the reactor to limit radiation to 3 mrem/hr at the 200 m power hub. The key feature that distinguishes this concept from others is the capability to be shut down and moved to a new location if required.

The MFPS mass summary with Current Best Estimate mass values is provided in Table 9-4. The system could be delivered in as many as three separate packages. The water could be delivered specifically for this use or scavenged from lunar sources. The mass of regolith-moving equipment to create a surrounding berm is not included and assumed to be an available asset, if needed.

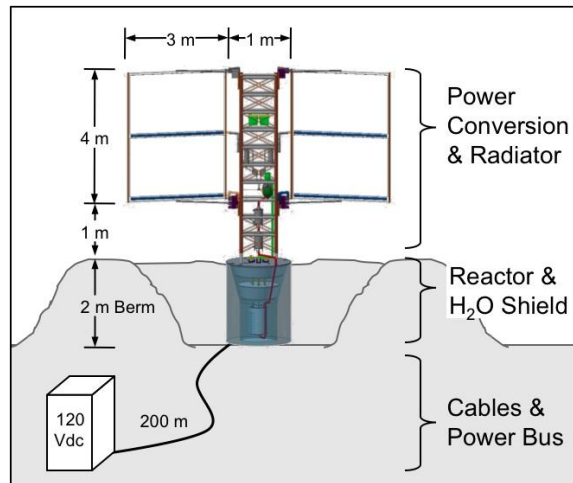


Figure 9-7 Mobile Fission Power System concept.

Table 9-4 Mobile Fission Power System Mass Summary

Mobile FPS Subsystem	Mass (kg)	Includes:
Power Plant	1615	Reactor, water shield vessel, power conversion, radiator, and truss/structure.
Power Management and Distribution	415	Cabling, electrical controls, and 120-Vdc load interface bus.
Water (for Shield)	1310	Liquid water for filling shield vessel prior to reactor startup.
Total Current Best Estimate	3340	

The MFPS can provide various benefits for the relocation and long-duration mission phases. During the relocation phase, the MFPS provides a continuous 10-kWe day/night power source for stationary applications that can be shut down and relocated as needed. During the long-duration phase, the 10-kWe MFPS could be moved to the long-duration site and reused, or the design could be scaled to 40 kWe and a follow-on system could be delivered to the site. The higher power capacity could provide expanded outpost operations to allow closed-loop life support, high-production rate ISRU, and larger crew size if desired. The 8-yr design life assures long-term campaign use for the entire mission phase. The same technology could be used on Mars, making this option very well aligned with “Mars Forward” goals.

9.1.5.4.2. MFPS Concept-of-Operations

A preliminary assessment was made to determine the activities associated with launching, installing, and operating a MFPS. The main activities are summarized in the paragraphs below.

Launch and Delivery: The reactor is launched cold and subcritical. The reactor presents essentially no radiological hazard during lander and launch vehicle integration. The power plant will be delivered to the launch site as a fully integrated package. The MFPS system can be delivered as a single payload or in a series of packages depending on the available capacity of the lander. Prior to delivery, the MFPS system would be acceptance tested at a DOE nuclear facility. The reactor contains Special Nuclear Material that requires a specific class of security and safeguards. This is the primary difference between the MFPS payload and other lunar surface payloads. The reactor is designed to preclude inadvertent criticality under potential launch accident scenarios. During launch and delivery, the MFPS system may require periodic electrical power to exercise fluid pumps and monitor instrumentation sensors.

Off-Loading and Setup: A suitable site for the power plant must be determined that is approximately 200 m away from the outpost. If the local terrain offers natural outcroppings, these could provide shielding benefits and possibly eliminate the need for the water shield and regolith berm. The PMAD (415 kg) would be off-loaded from the lander. A single power electronics pallet (1 by 1 by 1 m, 175 kg) would be set up near the outpost with easy access for the electric power users. The pallet provides the interface for power loads and data communications. A transmission cable bundle (<1 m diam., 240 kg) would be connected to the electronics pallet and unfurled via a spool to the power plant site. A robotic rover could deploy the cable. The transmission cable includes the main power cable, data signal cable, and return power cable for power plant auxiliary loads. The power plant (3 by 1.5 by 7 m, 1615 kg) would be off-loaded from the lander and transported via a cargo rover to the installation site. The power plant would be set directly on a flat regolith surface. The center of mass is very low and centered. Support bracing could be added if desired. A bladed rover would be used to move regolith to form a 2-m-high berm around the power plant, in lieu of using natural topography.

System Startup: Startup could be performed by local crew members or remotely from Earth. After connection of the transmission cable, initial communications would be established via telemetry signals to the electronics pallet. Computers and instrumentation would be started at 100 W total input power. Trace heating of the one reactor coolant (NaK) loop and two radiator coolant (H₂O) loops would be started with 100 W input power on each loop. The shield vessel would be filled with liquid water (1310 kg). The one reactor NaK pump would be started with 250 W input power. The NaK loop trace heaters would be turned off. The two radiator loops would be charged with H₂O coolant from a heated storage tank. The two radiator H₂O pumps would each be started with 100 W input power. The H₂O loop trace heaters would be turned off. Three of the six reactor control drums would be adjusted to the reactor operating position. The fourth, fifth, and sixth control drums would be adjusted in succession, resulting in initial reactor criticality. The control drums would be adjusted to reach 600 K NaK outlet temperature. The Stirling convertor would be started resulting in approximately 1 kWe power output. The two radiator panels would be deployed. The control drums would be adjusted in steps and the Stirling convertor stroke would be gradually increased with hold-points at 2.5, 5, 7.5, and 10 kWe. The regulated 120-Vdc bus would be enabled at 5 kWe. The total startup energy for this process is estimated at 10 kW hr.

Water for Reactor Shield: The combination of the water shield and regolith berm reduces the reactor radiation to 3 mrem/hr at 200 m. The resulting dose to an unshielded astronaut at the 200 m boundary during a typical 30-day mission is about 2.2 rem. The OSHA limit for nuclear power workers is 5 rem/yr and the NASA guideline for astronauts is 50 rem annually. The use of natural topography could reduce or eliminate the need for the water and/or regolith berm. The 1310 kg of liquid water for the water shield could be delivered from Earth, or acquired from lunar sources. The water could also be scavenged from other lunar surface assets, such as fuel cells or propellant tanks.

System Operations: Once the MFPS system reaches full power, it can operate with minimal human intervention requiring only periodic health monitoring from a data console at the outpost or Earth. The MFPS system is designed to automatically respond to lunar day/night transients, electric load changes, and recoverable power plant faults without human intervention. The MFPS system would produce electric power continuously and shunt excess power not required by loads via a parasitic load radiator. A periodic control drum adjustment (perhaps twice per Earth

month) may be performed to maintain reactor coolant temperature within a nominal band. The electronics pallet includes a power switch panel that allows users to connect electric loads as needed. This would be the power interface for habitats, landers, ISRU plants, rover recharging, science experiments, etc. The electronics pallet is located near the crew for maintenance, if required. The power plant is designed for an 8-yr service life without maintenance. The design life would be demonstrated as part of the ground verification testing. Performance degradation over the design life should be negligible. Radiator area margin is included to account for environmental degradation such as ultraviolet radiation and dust. The redundancy in the reactor control drums provides fault tolerance for reactivity adjustments.

Shutdown and Relocation: At end-of-life, the power plant would be shut down and could remain at the installation site. Within several weeks, the radiation will decrease below natural background levels and the plant should not pose any particular safety concern. The plant shutdown would include an adjustment of the control drums to make the reactor subcritical, and a commanded stop to the Stirling convertor, reactor pump, and radiator pumps. The power plant and PMAD could also be shut down and moved to another location. Robotic access would be permitted within hours; human access may be permitted within days. To prepare for relocation, the radiator panels would be retracted and the transmission cable would be disconnected. The water shield could be drained, if desired, to reduce the mass for transport. The MFPS system cannot provide power while it is being moved. At the new location, the setup and startup would be repeated as described previously. Subsequent startups should be easier and faster. After setup, the system could be operational within ~12 hr. The MFPS system could be relocated multiple times, recognizing that each shutdown, movement, and restart increases the probability of a system malfunction.

9.1.6. Conclusion

NASA is currently studying FSP systems as an option for future human exploration missions to the Moon and Mars. NASA and the DOE have partnered to help mature FSP technology so that it may be considered for future flight development. The NASA/DOE team has generated a preliminary FSP reference concept to help guide technology development and provide a possible starting point for future flight systems. A portion of the FSP project is focused on concept definition and integration studies to evaluate the use of FSP technology for various mission architectures. This paper discusses some of the recent architecture studies and potential methods for utilizing FSP systems. The FSP team has supported these architecture studies by supplying FSP design characteristics, developing mission-compatible configuration options, and defining a Concept of Operations consistent with the mission objectives. The technology is adaptable to meet a wide range of mission needs. Configuration options include buried-reactor systems, lander-integrated systems, surface-mounted systems, and systems that are deployed via a wheeled cart. Power levels can range from several kilowatts up to about 100 kWe without a significant change to the basic technology. The primary building blocks of the FSP system – reactor, power conversion, and heat rejection – can be common to many design configurations, making the technology extremely robust and versatile.

9.1.7. Acknowledgments

The authors wish to acknowledge the contributions of the other FSP team members including John Warren (NASA Headquarters), Scott Harlow (DOE Headquarters), Mike Houts (MSFC), Jim Werner (INL), Lou Qualls (ORNL), and Ross Radel (SNL) as well as the other staff members at these locations. The FSP Project is part of the Exploration Technology Development Program (ETDP) managed by Frank Peri at Langley Research Center. ETDP is part of the Exploration Systems Mission Directorate at NASA Headquarters where Chris Moore serves as the Program Executive. The NASA architecture studies involve a large network of individuals across the NASA centers, which are currently coordinated by the Johnson Space Center Lunar Surface Systems Office managed by Chris Culbert. The International Architecture Working Group Power Function Team is headed by Marc Haese from European Space Agency.

9.2. Extravehicular Activity and Mobility

Primary Contributors:

David Coan, National Aeronautics and Space Administration, Lyndon B. Johnson Space Center
Stephanie Sipila, National Aeronautics and Space Administration, Lyndon B. Johnson Space Center
Natalie Mary, National Aeronautics and Space Administration, Lyndon B. Johnson Space Center

The success of exploration missions depends on the ability of humans to work on and explore planetary surfaces. This success will depend on productive EVAs conducted during traverses away from the surface landing site or habitat. During these exploration missions, astronauts will be exposed to a range of gravity conditions and a diversity of environments. With the normally intense activity that would be expected on the exploration missions, issues of productivity, usability, durability, and maintainability of EVA systems become acute. Operational and medical considerations will include life-sustaining system capability, hardware maintainability, equipment durability (fatigue and wear life), environmental health, radiation protection, crew contamination, pre-breathing procedures, long-term crewmember fatigue, and emergency-mode operations. Allowing humans to make the transition simply and effectively between activities that are conducted inside and outside vehicles will enhance productivity, provide operational flexibility, and increase overall mission safety. EVA systems must be provided for the Mars surface, and for space operations in orbit and in transit.

Repeated, productive surface activity for 4 or more hours daily for up to 6 days a week is an assumption per the previous version of the 2009 addendum to this DRA. More recent testing at some of the analogs, specifically the NASA Extreme Environment Mission Operations (NEEMO) 16 mission and the Research and Technology Studies (RATS) 2012 mission, evaluated performing two 3-hour EVAs each day. For the 2013 update to the addendum, the EVA model is limited to no more than 12 hours of EVA in a 48-hour period and 24 hours of EVA per 7-day period with at least one full non-EVA day of rest within that same 7-day period. Frequency and duration of EVAs are flexible; reference *Section m: EVA Hours* in the assumptions below. Planetary surface systems, including suits, will have to be maintained by the crew inside a habitable volume, and must be resistant to contamination by surface materials such as dust, and highly resistant to abrasion and tearing from rough or sharp surfaces. EVA systems must provide a safe, nontoxic environment, with H₂O supplies that are free of contamination. In addition, several operational considerations are important to the effective use of suits or other individual mobility devices. The first consideration is to maximize the time that would be available for productive activity outside the spacecraft; suit mass and the ability to supply fluids and remove waste are particularly important. It is important to minimize restrictions on human capability by providing adequate thermal control, greater suit mobility – in particular in the gloves, torso, legs, and boots – and enhanced communications capability for explorers and home base interactions. The second consideration is to minimize the time needed to go from inside the spacecraft out to the planetary environment; of particular importance is the difference between habitat pressure and the pressure of the EVA system. The greater the difference, the more time must be spent adjusting to the generally lower outside pressure to avoid decompression sickness (the bends). A third overall consideration is the maintainability of the system, allowing reuse without extensive overhaul. Current capabilities in planetary surface EVA systems are derived from Apollo systems, which provide an excellent starting point for future missions. For long stays on planetary surfaces, however, these systems do not meet the stated mission requirements in most areas. Apollo technology equipment is not maintainable, and it is too massive to use on Mars, where the gravitational level is 0.38 that of the Earth. The space shuttle and ISS systems are even more massive and were designed for only limited use in microgravity environments, with items such as the gloves having a limited life appropriate to mission duration. New systems will be required and will evolve from heritage spacesuits.

Suit development is an area that will require focused research and technology efforts emphasizing lightweight and durable materials, glove design, lower torso mobility systems for walking, upper torso mobility for reach when using a variety of scientific sampling tools, ancillary mobility systems for surface transportation, dust contamination protective measures and techniques, long-term reusability and maintainability, and lightweight, compact, Portable Life Support System (PLSS) technologies. Other considerations, such as planetary protection, may influence system design. Components within future suits will require a longer certified life, greater resistance to damage caused by use, and must be easily maintained and repaired in flight.

Operational concepts for Mars surface EVAs need to be proven. These concepts will be critical to conducting routine EVAs on the Martian surface during a 500-day period, particularly in situations where purely robotic exploration has proven less effective than exploration by human crewmembers:

- Routine EVA operations on a surface with gravity
- Suit design with walking ambulation capability and arm mobility for utilizing tools outside of the current nominal reach envelope
- Suit design to minimize crew injury and fatigue levels during an 8-hour EVA
- Suit design to minimize crew injury and fatigue when donning and doffing
- Gloves that enable tactility and dexterity with reasonable crew fatigue up to an 8-hour EVA for surface operations
- Suit design and gloves that are abrasion and tear resistant to allow long-term repeated contact with rough and sharp geological samples
- Protocols and designs to protect the suit systems and the crewmember from dust hazards, including human health considerations and management of in-situ silicate and metallic oxide particulates within the Martian environment
- Ingress/Egress methods conducive to short-duration, frequent EVAs, that consider dust mitigation for human health and planetary protection purposes
- Geosciences exploration techniques, including geophysical and geochemical prospecting, and remote-sensing tools to assist crew field geology operations
- Communication techniques and tools that allow efficient science to be conducted while communicating between the EVA crewmember, the IVA crewmember, and mission control
- Synergistic operations between EVA crewmembers and robotic assistants
- PLSS recharge during EVA
- In-situ maintenance and repair of the entire EVA system

The lunar surface offers the potential to gain the EVA experience that will be needed for crewed Mars exploration; however, a number of differences between the Martian environment and the lunar environment will dictate substantive changes in the EVA architecture. Further, the Agency's vision does not specifically sequence moon exploration prior to Mars. The environmental differences include the increase in Martian gravity to 0.38g relative to 0.17g on the moon, the difference between the lunar atmospheric "pressure" of 1.3×10^{-13} mbar and the 10-mbar atmospheric pressure on the Martian surface, a convective thermal environment, and a CO₂ atmosphere. In addition, the issues that are associated with the possible existence of fossil or extant life will require measures to be taken to meet planetary protection protocols that may not be necessary for operations on the lunar surface.

Present and planned PLSS/thermal garment designs for orbital and lunar applications make extensive use of space vacuum to induce a phase change, thereby creating a heat sink, for cooling. They also inhibit conductive cooling from appendages through the suit to the external environment using MLI. The Martian atmosphere, at 5–10 mbar, has sufficient mass properties to inhibit vacuum-dependent thermal management schemes (L. Trevino, personal communication, 2007). This requires development of (1) new methods of rejecting crew member metabolic and suit electronics heat to the environment, thus preventing heat-storage related injuries (hyperthermia, heat exhaustion, heat stroke), and (2) new methods of preventing excessive heat leak through the pressure garment to the Martian environment, thereby preventing cold exposure injuries (frostbite, hypothermia).

New concepts for an advanced EVA suit use an amine swing bed to collect and reject crew metabolic CO₂ waste. These swing beds depend on being exposed to a vacuum to release the CO₂ out of the system, and is a semi-closed loop system. The atmosphere on Mars is sufficient to require a modification of that CO₂ removal system, with potential solutions being the use of a washout gas or pump. Or, an alternate CO₂ removal technology that functions without rejecting metabolic CO₂ out of the suit; i.e. minimizes metabolic venting.

Unlike the lunar surface, exploration of Mars must be conducted with planetary protection in mind, particularly management of organic contaminants that would be released by EVA suits and PLSSs. The nature of pressure garments is that leakage of some quantity of internal atmosphere is unavoidable. For suits that have a significant usage history, such as the Mark III suit, the leak rate can be as much as 1,500 cc/min. Operational suits, such as the shuttle Extravehicular Mobility Unit (EMU), experience leak rates approximately an order of magnitude less, on the order of 100 cc/min (J. Kosmo, personal communication, 2004). Leakage includes the gas that is used to pressurize

the garment as well as any airborne particulates that can escape past garment seals, which can include microbes and latent virus particles that are shed from crew members. New CO₂ and contaminant scrubbing technologies such as the amine swing bed are semi-closed loops systems that also increase the amount of metabolic waste dumped out of the suit and into the surrounding environment. A critical engineering and operational challenge will be to manage this leak rate and character, potentially through the use of improved seals, sterile over-garments, or covers around mechanical connection areas such as glove and neck rings, and through use of operational practices that minimize human crew member entry into special areas that are suspected of having extant or fossil Martian life. On the shuttle/space station EMU, there is also a purge valve that is used in contingency situations. Any use of that sort of purge valve would openly dump metabolic gas into the Martian atmosphere. Despite these possible engineered controls designed within the suit, operational controls for planetary protection are anticipated to establish “keep out zones” prohibiting human presence in Martian areas deemed to be highly likely to contain life.

For Mars surface exploration, scientific diversity is obtained by extending the range of human explorers via both unpressurized and pressurized rovers. EVA exploration will be integral to rover excursions, operations, and maintenance. Reference *Surface Mobility Systems, Section 5.2*, for further details pertaining to the rover vehicles.

9.2.1. EVA System Assumptions and Questions/Forward Work

The following assumptions are being utilized for the 2013 update to the Mars Design Reference Mission (DRM):

- a. 500-day surface mission duration.
- b. Six crewmember mission size. All crewmembers will perform EVAs. All surface elements will be EVA capable, including the habitat lander and the pressurized rovers.
 - b.1. Note a crew size of 6 vs. 4 crewmembers drives the EVA system architecture, principally consumables and logistics.
- c. There will be no planned microgravity EVAs during transit (such as how Apollo retrieved film canisters on the way back from the moon). Microgravity EVAs will be possible for contingencies.
- d. Mars Surface Mission Phase 2 will allow crew to adjust to Mars gravity after long duration exposure to microgravity environment during transit. Crew activities will include limited EVAs to support scientific investigations and as crew involvement with the deployment and activation of surface systems.
- e. Mars surface operations during solar conjunction may be limited to short EVAs as opposed to long traverses. Direct to Earth communications will be unavailable during solar conjunction. This occurs approximately every 26 Earth months and lasts about 2 Earth weeks.
- f. During all EVA activities, each EVA crewmember will be able to be physically reached by another crewmember within 45 (to be reviewed [TBR]) minutes. This could be achieved by two EVA crewmembers in proximity or by an IVA crew member having the ability for quick egress from habitat or rover.
- g. Crew will use rear-entry EVA suits for extravehicular surface operations.
- h. Nominally, suitports will be used to ingress/egress the pressurized mobile assets. The habitat module will include an airlock for EVA ingress/egress. It is forward work to perform a trade study to determine the appropriate style of ingress/egress method for the habitat module.
- i. Umbilicals are used during depress and repress for EVA.
- j. The surface habitat lander and pressurized rovers accommodate an incapacitated crewmember.
 - j.1. In the event of a medical emergency during EVA, the ill crewmember will be brought inside a habitable volume for treatment while performing proper decontamination and medical protocol as necessary.
 - j.2. Habitable volume should accommodate two means of EVA ingress/egress (in case of fire or defective “airlock,” the crew will have a means of entering or exiting). Nominal ingress will be through the airlock; secondary ingress is possible through the rover side hatch and the habitat lander inner hatch.
 - j.3. The habitat provides a level of care consistent with medical needs on Mars (medical area)
- k. Deep Space Habitat Lander Assumptions:
 - k.1. Suits are stored inside an element during transit; Transit EVA capability is to be determined (TBD).
 - k.2. The lander serves as the surface habitat.
 - k.3. The habitat lander system provides the primary interface to EVA; an airlock is integrated with the element.
 - k.4. The porch will have a minimum size on the habitat lander if the hatch is a certain distance from the surface.
 - k.5. The airlock accommodates two suits simultaneously.

- k.6. The habitat lander provides a suit maintenance / dust containment area.
 - k.6.1. Basic inspection and cleaning EVA maintenance operations are conducted within the pressurized airlock and more extensive maintenance and repair is conducted in the habitat lander's suit maintenance area.
 - k.6.2. The habitat has two umbilical interface panels located where suited crewmember operations occur.
 - k.6.2.1. Recharge capability for the suit includes: oxygen (3000 psia), water (potable and cooling) resupply, and battery recharge,
 - k.6.2.2. The umbilical interface panels provides the following utility services: power, communications (wireless and hardline), and vacuum lines.
 - k.6.2.3. All services are provided via the Recharge panel (2 umbilical connections and 2 vacuum line connections).
- l. Pressurized Rover Assumptions:
 - l.1. Two pressurized rovers will be present on the surface.
 - l.2. Rover utilizes a suitport. The rover requires an ingress/egress method to facilitate rapid egress. At the time of the 2013 update, the most mature technology of this airlock type is a suitport.
 - l.3. Crewmembers must conduct an initial EVA from the habitat lander to install suits onto the rover suitports.
 - l.4. Two crewmembers will spend 2 weeks in a pressurized rover, and then return to the habitat for recharge and suit maintenance, as necessary. Crew rotation will include suit rotation.
 - l.5. Pressurized rover operates at 8.2 psia environment.
 - l.6. In the event of a rover failure, the EVA crewmembers will be capable of TBD km walk back. For a "rover-based" EVA, the crew does not travel farther from the habitat lander than the distance they are able to walk back if the rover were to fail, unless a second rover is available for rescue. With two rovers, each rover can travel farther than walk back distance from the habitat lander assuming the two rovers maintain rescue distance to each other. For consumables planning, it is assumed that the rover failure does not occur during an EVA. Note: Under Lunar 1/6-g conditions, the walk back assumption is 10 km. Testing has not been performed with Martian gravity conditions.
 - l.7. The pressurized rovers will accommodate TBD contingency suit maintenance.
- m. EVA Hours:
 - m.1. Crew Limit for EVA hours.
 - m.1.1. Each crew is limited to no more than 12 hours of EVA in a 48-hour period and 24 hours of EVA per 7-day period with at least one full non-EVA day of rest within that same 7-day period. [TBR]
 - m.1.2. This does not account for a transfer EVA between the habitat lander and pressurized rover, which may extend the EVA hours for that week to 27 hours.
 - m.2. Types of EVAs from the habitat lander:
 - m.2.1. Crew will perform a 3-hour EVA to transfer samples, logistics, and suits when transferring to the pressurized rover in preparation for excursions.
 - m.2.2. Crew will perform up to three 6.5-hour EVAs each week for habitat maintenance, trash ops, local exploration, etc.
 - m.3. Types of EVAs from the pressurized rover:
 - m.3.1. Crew may perform up to three 1-hour EVAs per day for 6 days per week. [18 EVA hours per week per crewmember]
 - m.3.2. Crew may perform up to two 3-hour EVAs per day for up to 4 days per week. Crew may elect to perform a single EVA on a given day and use that EVA time on another day, but must protect at least one day off per week. [24 EVA hours per week per crewmember]
 - m.3.3. Crew may perform one 8-hour EVA per day for up to 3 days per week. [24 EVA hours per week per crewmember]
 - m.3.4. For hardware cycle life and mass calculations in 2012, the EVA Office (XA) is assuming two 3-hour EVAs per day for up to 4 days per week to generate a MEL (ref *m.3.2* above). This number may change with further testing and evaluations of the EVA suit and system.
 - m.4. If surface mission duration is extended past 500 days due to contingency, no nominal EVAs are planned.
 - m.4.1. Real-time assessments would be performed to conduct contingency EVAs if needed.

- m.4.2. No additional logistics are provided to support (next cargo mission could land at same site if needed).
- n. EVA Consumables
 - n.1. TBD amount of O₂ use per hour of EVA.
 - n.2. TBD amount of H₂O use per hour of EVA.
 - n.3. TBD consumable for CO₂ removal. If RCA, will be TBD amount of sweep gas use per hour of EVA (reference n. below). Or, TBD amount of METOX/LiOH/TBD cartridges.
- o. Martian environment will require the use of a sweep gas or pump with RCA, or other new technology.
- p. Ancillary EVA Equipment:
 - p.1. Current in-suit drink bags are disposed after each EVA. Mars missions will require a reusable bag to reduce launch mass.
 - p.2. Current waste containment for an EMU is a MAG, which is disposed after each EVA.
 - p.3. EVA Equipment Bags will be used during EVAs.
- q. EVA System Hardware Logistics:
 - q.1. EVA equipment that is size dependent will launch with the crewmembers. This will include items such as the pressure garment (PGS), gloves, thermal comfort unit (TCU), etc.
 - q.2. EVA equipment that is critical for a specific phase of flight will launch with the crewmembers and be accessible during the appropriate flight phase. This will include each crew member's prime and backup suit, and microgravity specific equipment.
 - q.3. EVA equipment that is not size dependent will launch with the pre-deployed cargo, assuming the certified shelf life of each item can withstand the increased mission duration length. This will include items such as spare PLSS, spare helmets, MAGs, batteries, etc.
 - q.4. EVA spares stowage is accommodated within the habitable volume of the habitat lander.
 - q.5. Two EVA suits, PGS and PLSS, will be manifested for each crewmember. For a crew size of 6, this totals 12 suits.
 - q.6. Suit maintenance will be required every 28 days or TBD hours of EVAs (TBR)
 - q.7. EVA equipment does not return in the Orion capsule. In this DRA, there are no allocations for return of EVA equipment for re-use or post-flight analysis purposes. It is desirable to return flown EVA suits to Earth for post-flight analysis purposes with the benefit of influencing design improvements in future suit designs.
 - q.8. Logistics and spares quantities are expected to be updated once limited life duration is determined through certification.
 - q.8.1. The following spares will be flown for a 6-crew size: 3 spare PGS and 5 spare PLSS. (Reference: for a crew size of 4, the quantities were 2 spare PGS and 3 spare PLSS.)
 - q.8.2. The former lunar suit plan was to certify for 100 EVAs. Need to determine total number of EVA hours assumed, and modify for longer Mars mission.
 - q.8.3. Eleven pairs of EVA gloves per crew member are needed, prime and spares. For a crew size of 6, this totals 66 pairs of gloves.
 - q.8.3.1. Due to crew specific sizing and fit, gloves will launch with the crewmembers. Three pairs will be easily accessible during microgravity phases of the mission.
 - q.8.3.2. Glove quantities are based on the 162 hrs certified life per pair of glove (same as ISS EMU Phase VI glove certification which has not been realized), 24 EVA hrs/wk, 500-day surface mission.
 - q.8.4. Batteries:
 - q.8.4.1. Assume three suit batteries per crewmember (2 prime, 1 spare) based on development of new battery chemistry with greater power density than current battery technology.
 - q.8.4.2. Need to look at unactivated silver zinc batteries that are launched and stowed dry, and then activated when needed on Mars.
 - q.8.4.3. Note: current Lithium ion batteries are limited to 5-year life
 - q.8.5. Thirty six Thermal Comfort Units (TCUs) per crewmember are needed. For a crew size of 6, this totals 216 TCUs. TCU quantity assumes one set of TCUs for every 2 weeks and a mission duration of 72 weeks (500 days).
- r. Protection of Planetary Environment
 - r.1. Assume crews will be allowed to land and operate within certain approved zones where forward contamination is not an issue.

- r.2. Assume EVA suits do not require sterilization prior to exiting the habitat lander or pressurized rover. This is based on an assumption of a sample return mission that verifies “sterilization” of suits is not required prior to ingressing a pressurized volume to address back contamination concerns.
- r.3. Operational controls for planetary protection will establish keep-out zones to preclude EVA crewmembers from entering, and possibly contaminating, special regions.
- r.4. For non-Special Regions, crew can collect samples using EVA gloves and other EVA tools as needed (consistent with science needs)
- r.5. If planetary protection becomes a driving requirement, the trade study to assess the type of airlock for the habitat lander will need to include planetary protection as a consideration. A “mudroom” incorporated between the airlock and the main pressurized volume will be considered along with the concept of a “hybrid suitlock”.
- r.6. Suits may need dust covers (TBD).
- s. EVA Tools:
 - s.1. Micro-gravity Contingency EVA
 - s.1.1. Safety tethers
 - s.1.2. Waist tethers
 - s.1.3. Equipment tethers
 - s.1.4. Basic standard tools, such as a driver and sockets
 - s.1.5. Repair tools
 - s.2. Surface Science Activities
 - s.2.1. Rock sample collections device (bag over glove, scoop, etc.)
 - s.2.2. Soil sample collection device
 - s.2.3. Chip sample device (rotary percussive drill, hammer, etc.)
 - s.2.4. Surface sample device
 - s.2.5. Core sample device
 - s.2.6. Collection bags
 - s.2.7. Trenching tool
 - s.2.8. Shovel
 - s.2.9. Geophysical arrays

9.2.2. EVA Operations Concept for Mars Surface

The current concept of spending 2 weeks in the pressurized rover and doing two 3-hour EVAs per day is the basis for mass and consumable calculations for architectural studies. This EVA Ops Con varies slightly from the Mars Mission Surface Phases documented in this DRA. EVA durations and consumables usage are assumed to be equivalent for Mars Mission Surface Phases 2 through 5. This EVA model was tested during NEEMO 15 and 16, and during RATS 2012 analog studies of a near-Earth asteroid (NEA) mission. Different length EVAs will need to be analyzed and compared with this concept, such as multiple 1-hour EVAs (as seen in Desert RATS 2010) or one long 8-hour EVA (similar to current space station EVAs and Apollo EVAs).

- Week 1:
 - No EVAs. Crewmembers acclimate to 3/8G; 1 week only is assumed for worst-case EVA consumables planning.
- Weeks 2 – 72 (departure):
 - Four crewmembers go EVA from habitat lander to two pressurized rovers. Exploration EVAs are then performed from each rover by the two crewmember pair.
 - Crewmember pairs rotate between the habitat and the rovers every 2 weeks. This assumes back-to-back 14-day rover excursions, with rover recharge and crew rotation as necessary at the habitat within this same 14-day period.
 - Habitat lander-based crewmembers may perform up to three 6.5-hr EVAs weekly for habitat maintenance, trash ops, local exploration, etc.

9.2.3. Advanced EVA Suit Baseball Cards

The EVA ‘baseball’ cards are being updated. The cards shown in Figure 9-8 are the most recent versions, dated 09/06/2013.

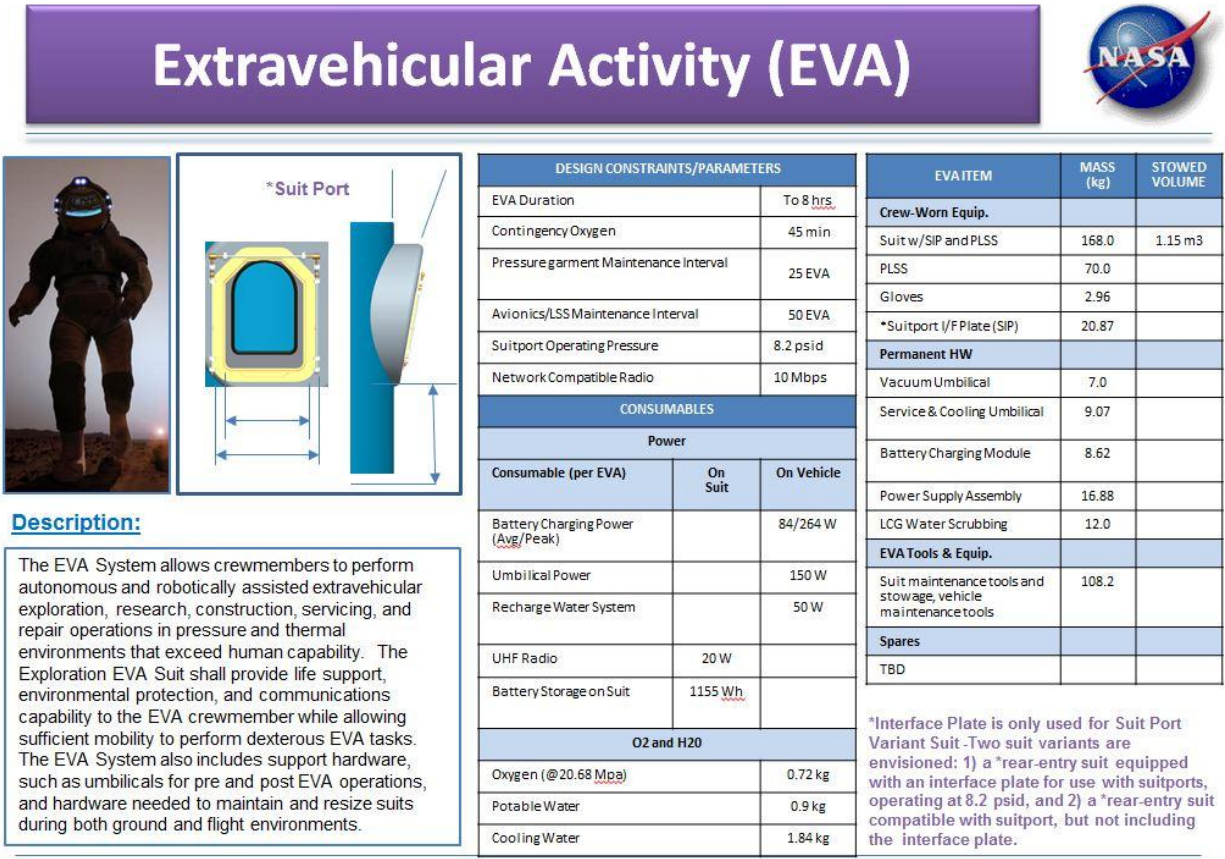


Figure 9-8 Deep space suit (Block 3) - baseball card.

9.3. Logistics, Maintenance, and Repair

Primary Contributors:

Kandyce E. Goodliff, National Aeronautics and Space Administration, Langley Research Center
William M. Cirillo, National Aeronautics and Space Administration, Langley Research Center
Hilary R. Shyface, Analytical Mechanics Associates, Inc.
Chel Stromgren, Binera, Inc.

9.3.1. Logistics

9.3.1.1. Standardized Logistics Requirements

Members from the ISS program office, Environmental Control Systems at JSC, the Advanced Exploration System’s Logistics Repurpose and Reuse project, and the Human Spaceflight Architecture Team (HAT) have worked together to better define consumables and crew accommodations for deep space missions. In addition, values assumed for the Orion crew capsule have been considered in this definition. Table 9-5 details the crew requirements for human exploration beyond low Earth orbit (LEO). Table 9-6 lists the assumptions associated with gases and liquids.

Table 9-5 Crew Requirements

Crew Requirements	Unit	Value
Food	kg per crewday	1.831
Fecal/Urine Collection Bags (contingency)	kg per crewday	0.165
Personal Hygiene Kit	kg per crew	1.8
Hygiene Consumables	kg per crewday	0.079
Clothing (With Laundry)	kg per crewday	0.0394
Recreation & Personal Stowage	kg per crew	25
Wipes (housekeeping)	kg per crewday	0.194
Trash Bags	kg per crewday	0.05
Operational Supplies	kg per crew	20
Survival kit	kg per crew	13.61
Sleep Accommodations	kg per crew	9
Health Care Consumables	kg per crewday	0.1
Emergency Breathing Apparatus	kg per crew	1.36

Table 9-6 Gas and Liquid Assumptions

Assumptions	Unit	Value
Oxygen Metabolic	kg per crewday	0.82
Water – Drink	kg per crewday	2
Water – Food Rehydration	kg per crewday	0.5
Water – Medical	kg per crewday	0.05
Water – Hygiene	kg per crewday	0.4
Water – Flush	kg per day	0.25
Cabin Air Leakage	kg per day per module	0.00454
Cabin Air Leakage - Orion	kg per day	0.00908

9.3.1.2. Derived Mars DRA 5.0 Logistics Requirements

The aforementioned assumptions, along with the Environmental Control and Life Support System (ECLSS) that is on-board the spacecraft, allows for planning the amount of logistics required for a human mission to Mars. The

ECLSS assumed for this analysis includes water recovery, urine recovery, oxygen generation, carbon dioxide reduction through a Sabatier process, and laundry for washing clothes. Recovery of water from urine is assumed at 85% whereas all other water sources are recovered at 100%. Brine recovery, solid waste dewatering, and Bosch reaction are not included in these estimates. Table 9-7 outlines the requirements based on a crew size of 6 and the given durations. The nominal requirements for the transit (outbound to Mars and inbound to Earth) habitat and surface habitat include a habitat re-pressurization (nitrogen and oxygen) in case of a depressurization event. Surface EVAs are not included in the analysis. The surface habitat also includes leakage rates for a 26-month dormancy period, assuming the surface habitat is pre-deployed during the launch opportunity prior to the crew launch opportunity. The contingency logistics for the transit habitat include 540 days of crew consumable requirements, in case the surface mission is aborted, and 30 days of open-loop requirements for water, oxygen, and nitrogen. This 540-day contingency requirement is dominating the crew consumable requirement for the transit habitat. A future trade to consider might be delivering the 540 days of crew consumables with the crew for the surface and not repositioning the crew consumables with the surface habitat. However, there may be other risk factors to consider with that option. The contingency carried for the surface habitat includes 30 days of crew requirements and 30 days of open-loop requirements for water, oxygen, and nitrogen. The 30 days of open-loop requirements provides time for the crew to repair critical systems if a failure should occur. Packaging or containers for logistics are not incorporated into the mass estimates given in Table 9-8. Spares and maintenance items are not included in these totals and are discussed in the next section.

Table 9-7 Logistics Required for a 900-day Mars Mission

	Transit Habitat	Surface Habitat
Crew Duration (days)	360	540
Crew Consumable Requirement (kg)	14,125	9,257
Nominal	5,735	8,390
Contingency	8,390	867
Water Requirement (kg)	539	539
Nominal	0	0
Contingency	539	539
Nitrogen Requirement (kg)	170	159
Nominal	169	158
Contingency	1	1
Oxygen Requirement (kg)	225	217
Nominal	77	69
Contingency	148	148

Water is not required for the transit or surface habitats because of the amount of water assumed in the food recovered by the ECLSS. The oxygen requirement for the transit and surface durations is entirely driven by the habitat re-pressurization assumption. The nitrogen requirement is driven by leakage and habitat re-pressurization assumptions. The transit habitat was assumed to be 280 m³ pressurized volume and the surface habitat was assumed to be 250 m³ pressurized volume. Depending on the in-situ resource utilization approach chosen for a human Mars mission, the water and oxygen requirements may be further reduced or eliminated.

9.3.2. Supportability

According to the *NASA Systems Engineering Handbook*, Integrated Logistics Support, or supportability, objectives are “to ensure that the product system is supported during development and operations in a cost-effective manner.” For the purposes of this discussion, supportability encompasses reliability, maintainability, reparability, redundancy and sparing philosophy.

Currently, NASA is analyzing the requirements for beyond LEO missions, including missions to NEAs and the Mars system.⁶ The ISS approach – which focuses on preventative and corrective maintenance supported by a logistics train that allows necessary components for maintenance and repair to be brought from Earth – for resupply will not work for these missions primarily due to the energy and time required to reach these destinations and the orbital alignment of the destination. Mars system missions are on the order of months to years in duration from

launch to landing back on Earth. Most missions will need to minimize cost by minimizing the number of launch vehicles required. This reduces the amount of mass that can be delivered or even prepositioned for these missions. In addition, most missions will more than likely have severe volume limitations for logistics when considering all the elements to be sent to support the crew mission, such as habitation, power, life support, and science equipment. For these destinations, this will be the first time humans have traveled outside of the Earth's magnetosphere and will be exposed to a harsh radiation environment. This means it is more difficult to estimate the failure rates of systems and components for a deep space vehicle. Finally, most missions beyond LEO will not include a quick abort path back to Earth, which dramatically increases the criticality of spacecraft systems and increases the demands on overall spacecraft reliability. All of these factors need to be considered when designing a supportability philosophy for missions beyond LEO in addition to destination specific challenges.

9.3.2.1. Issues

There are a number of direct impacts of supportability on deep space mission hardware and operations. The level of achieved supportability affects the probability of system failure and mission risk. Supportability requirements will drive spacecraft design and system accessibility. In addition, supportability will directly impact time requirements on the crew to maintain and repair systems. Finally, supportability will have a major impact on the amount of maintenance and spares that must be manifested on the mission in order to ensure the safety of the crew and the reliability of the mission.

When discussing supportability for deep space missions, it is tempting to equate improved supportability directly with increased reliability. The rationale is that if significant improvements in the reliability of all of the deep space vehicle (DSV) systems can be realized, then each of the areas described above will be improved. This view oversimplifies the factors that involved in making the DSV supportable. Although reliability is one contributor in safety, crew time, and spares requirements, other factors will also control these areas.

Of the areas described above, one that is of particular concern in terms of mission design is the amount of spares that must be carried for the mission. The expectation is a significant amount of spares will have to be flown along with the mission because there is little or no re-supply during these missions and because the deep space systems will be relatively complex. The amount of required spares could be a major driver in the total mass and volume of the DSV.

While the amount of required spares is influenced by the reliability of systems, reductions in spares is somewhat insensitive to increases in reliability. The total amount of spares required on-board the spacecraft is not driven by the actual amount of expected component failures. Given the reliability of the systems, the actual number of components that are expected to fail could be quite small. Rather, the amount of required spares is driven by the number of components that potentially can fail.

There are an enormous number of potential failures that can occur in a complex DSV. A significant number of those potential failures can endanger the mission and the crew. If any failure exceeds an established probability of occurrence, then that failure must be protected against. These are called "critical failures." For all critical failures, there must be a redundant capability, a work-around, or the ability to repair or replace the failed item.

The sheer number of possible failures drives the amount of required spares. While any particular failure has a low probability of occurrence, the total failure rate can be significant. Since it is impossible to predict exactly which failures will occur, it is necessary to protect against all critical failures. The result is that only a small fraction of the manifested spares will actually be used. As an example, on the ISS, it is estimated that over 95% of the spares that are manifested (not including planned maintenance items) will not be used.

On ISS, where there is the capability to supply spares within a fairly short time frame, only a fraction of the total critical spares need to be manifested on-board. Only the truly critical spares (those which must be replaced within a short period of time or which would prevent a re-supply ship from docking) must be manifested. For deep space missions, where likely no spares will be delivered during the mission, a significantly larger fraction of critical spares would have to be carried on board the spacecraft.

Increases in reliability, even substantial increases, may only reduce the amount of required spares to some limited degree. For a given failure, if the probability of occurrence still exceeds the established threshold, then the failure

must still be protected against. Getting closer to, but still remaining above, the limit does not reduce the amount of required spares.

Certainly, increasing the reliability of systems will reduce the probability of some failures to the point where the systems are no longer considered to be critical. The spares to protect against those failures will no longer need to be manifested. However, because of the number of potential failures, the threshold for component reliability must be very small.

Component reliabilities for spacecraft systems, even using current technologies, are already very high. Improving them to a degree where there is virtually no chance of failure will be technically very challenging. In addition, significant increases in reliability may also require increases in the mass and volume of the components, negating any reduction in spares.

9.3.2.2. Strategies for Improving Supportability

In-flight supportability can potentially be improved by incorporating several strategies into the architecture and mission design. These strategies must be evaluated from early in concept formulation, elaborated in system requirements, included in the procurement strategy and analyzed for optimum impact throughout system design. The strategy elements that will be described are:

- Level of repair
- Commonality
- Repair during assembly – Ability to repair and supply prior to destination departure
- Redundancy – Complete and component-level
- Reliability
- Emerging technologies such as in-space manufacturing and 3-dimensional printing
- Cannibalization and asset reallocation (e.g., in-situ resource utilization).

A summary of the benefits and risks are presented in Table 9-8 and elaborated in the following sections.

9.3.2.2.1. Level of Repair

Levels of repair on spacecraft can range from large assemblies, such as Orbital Replacement Units (ORUs), to small internal components. Repair of failed components at lower levels allows for sparing smaller components and focusing on the items most likely to fail. In many components, the largest mass and volume are in casings and mounting hardware that are very unlikely to fail. Failures are much more likely to occur in certain internal components such as electronic cards, motors, switches, seals, and numerous other small items. However, repairs at the box level can be much simpler to execute and thus to train the flight crew to perform. Lower repair levels also require more specialized tools, workbenches, and test equipment to verify successful repairs.

Components must be designed and built to be accessible for in-flight maintenance of components inside the box. Use of common tools to open up and disassemble components will significantly increase the ability to perform lower levels of repair. However, lower level of repair will also require improved diagnostic capabilities. While it is generally obvious which component has failed at the box level, it often more difficult to determine what has failed at lower levels. The crew will need the ability to test failed components, determine which elements need to be fixed or replaced, and have the information required to complete that repair.

The ISS has successfully implemented internal box level repairs in several instances. The ISS multiplexer-demultiplexers are the spacecraft flight computers, some 40 processors distributed around the vehicle both internally and externally mounted. Each multiplexer-demultiplexers contains several cards, and by sparing at the card rather than the box level, ISS has saved significant mass and volume. ISS has a maintenance work area that supports component repairs that includes mounting hardware, enclosures to keep debris and contaminants out, and to assure containment of tools and equipment. These types of repair facilities are a necessity for successful component repairs, assuring that planned repairs can be conducted, but also accounting for unanticipated repairs to the maximum extent.

Table 9-8 Supportability Strategy Elements

<i>Maintainability Strategy</i>	<i>Benefits</i>	<i>Risks</i>
Lower Level of Repair	<ul style="list-style-type: none"> ▪ Reduced spares mass/volume 	<ul style="list-style-type: none"> ▪ More difficult repairs require more skill and training ▪ Ease of access to components ▪ More tools and test equipment ▪ Increased crew time requirements
Commonality	<ul style="list-style-type: none"> ▪ Reduced spares mass/volume ▪ Reduced development cost 	<ul style="list-style-type: none"> ▪ Design may not be optimum for some uses ▪ Difficult to manage across multiple prime contractors and development schedules
Repair During Assembly	<ul style="list-style-type: none"> ▪ Minimize spares launch mass for spares used in Earth orbit ▪ Assures full complement of spares for the post-assembly phase 	<ul style="list-style-type: none"> ▪ Requires planning for contingency mass on some launches
Redundancy	<ul style="list-style-type: none"> ▪ Inter-module redundancy can reduce spares mass and volume ▪ Functional redundancy between modules can reduce criticality of failures in individual modules ▪ Complements a commonality strategy 	<ul style="list-style-type: none"> ▪ Requires strong systems engineering across total spacecraft ▪ Mass and power required are considerable, and increase with capability/flexibility
Reliability	<ul style="list-style-type: none"> ▪ Reduces number of failures that must be protected against ▪ Reduces planned maintenance actions and mass 	<ul style="list-style-type: none"> ▪ Assumptions about potential reliability gains may not reduce sparing needs
In-Space Manufacturing	<ul style="list-style-type: none"> ▪ Mitigation of unexpected failures ▪ Possible reduced spares mass and volume 	<ul style="list-style-type: none"> ▪ Tools are complex ▪ Mass and power required are considerable, and increase with capability/flexibility ▪ Most likely failures are probably not amenable to in-space manufacturing
Cannibalization and Asset Reallocation	<ul style="list-style-type: none"> ▪ Reduced launch mass for spares ▪ Ability to mitigate unexpected failure 	<ul style="list-style-type: none"> ▪ More complex repairs, e.g., EVA to retrieve parts ▪ More complex mission architecture, such as delayed jettison of expired elements

Component level repairs will in some cases require refined technical skills such as precision soldering and machining. These skills are developed over years by dedicated technicians, and comparable skills will not be developed to the same degree as part of a traditional mission training regimen. ISS experiments with repairs requiring soldering have achieved less than full success, in part because the crews lacked the skills that trained technicians have developed. Astronaut selection for long-duration missions could include these types of technical skills among the astronaut core. An emphasis on precision robotics to conduct highly technical repairs is another alternative.

Another major issue with lower level repair is the additional time requirements that could be placed on the crew. Typically, the lower the level that maintenance and repair actions take place, the greater the time requirement to complete those actions. Lower level repair can require additional time for access, disassembly, diagnostics, re-

assembly, troubleshooting, and testing. With the complexity of systems on a DSV, if supportability is not carefully planned, there is potential to overwhelm the crew with required maintenance and repair actions.

9.3.2.2.2. Commonality

Commonality holds promise for reducing spares' mass and volume, and for reducing cost for development and procurement. Yet, its high promise has been notoriously difficult to achieve. Commonality of components, materials, and tools would contribute significantly to supportability by increasing the number of failures that are mitigated for a given type of spare. Interchangeable components, whether or not they are identical, also allow for swapping between elements without necessarily using a spare component. For example, a failing component on a critical module could be replaced by an identical component from a non-critical module.

Successful commonality strategies require an early and enduring programmatic commitment. Most spacecraft have common functions that are developed with similar designs. Avionics, power, thermal, ECLSS, and other subsystems used in human space programs afford considerable opportunity for use of common components. Although there may be significant differences in environments, component lifetime, and performance needs, it is possible to identify similar classes that are candidates for commonality.

In spite of similarity of function, some reasons why commonality is not in wider use in spaceflight programs include:

- Programs and projects need to optimize the design for their specific environment and performance requirements, and components in common with other spacecraft may not meet, or may exceed, their needs.
- Spacecraft managers need to be in control of their own specifications. Using a component in common with another spacecraft where the other program/project controls the specification could result in design changes that would no longer meet the needs of the spacecraft that is dependent on the other spacecraft's component.
- Components available for use by a later developed spacecraft may be heading for obsolescence, and the later program needs to take advantage of the latest available mature technology. Avionics developed in the early 2010s may not be a good candidate for a spacecraft that will have a Preliminary Design Review in 2020.

To address these impediments, commonality must be built into the architecture from the earliest program formulation decisions. Very early in program formulation, organizational studies to determine the most effective methods for enabling subsystem commonality across the spacecraft should consider the use of subsystem projects and contractors, or use of directed subcontracts. Commonality of avionics, power systems, thermal, ECLSS, propulsion, and other major subsystems can be enhanced by procuring subsystems from a single source, providing the subsystems as government furnished equipment to the vehicle element organizations.

The Constellation Program conducted a Common Avionics Study in spring of 2007, after the program System Requirements Review was completed and projects were working toward their System Design Review. The study concluded that while technical solutions existed, the implications to the projects necessary to realize commonality would be profound. Had the organizations been originally established to achieve commonality, there was a very substantial potential for cost savings in development and operations. The ISS program achieved commonality of many avionics and power system components by procuring from a single organization that provided the components to other development groups.

9.3.2.2.3. Repair During Assembly and Checkout

Launch of the supportability material – tools, spares, and materials – requires careful planning and flexibility. Launching spares late in a multi-launch mission allows for adapting spares manifests to known failures or anomalies prior to departure from Earth staging points. Spares to be taken along beyond Earth orbit are needed for loss of crew and loss of mission mitigation where there are no possibilities for rapid abort or Earth supported replenishment. Since using spares before departing Earth staging could jeopardize crew safety and mission success beyond Earth orbit, a logistics approach that assures a capability for launch on demand prior to Earth departure is highly advantageous.

Two possible approaches will assure that failures occurring during the Earth environment assembly sequence can be repaired without depleting mission sparing for the critical solar system phases of the mission. The first is to maintain considerable margin for spares on the later launches. Parts, tools, and equipment needed to repair any failures discovered during transit to staging areas or in uncrewed assembly at the staging point should be able to be manifested, with very short notice, on any of the remaining launches after discovery of the failure. The second approach is to use a separate uncrewed logistics launch. A separate launch could facilitate replacement of large element failures, such as an engine or a complete spacecraft module. Maintaining ample launch schedule margin, as well as destination flexibility, will help prevent a significant module degradation or loss at the Earth staging assembly orbit from causing a total loss of mission.

9.3.2.2.4. Redundancy

Redundancy strategies for multi-element solar system exploration spacecraft afford opportunities for new approaches that could significantly improve supportability, as well as several challenges.

Sparing and redundancy are heavily intertwined. Where commonality is used, a single spare mitigates failures in multiple locations, and if rapid failover time is not required, stored spares provide advantages over built-in redundancy. For unique components, there may be little difference between storing a spare in inventory, and adding an additional level of built-in redundancy. A stored spare could simplify the design to support failover to another component, but require additional procedures, training, and tools needed to perform the in-flight maintenance.

Functional redundancy across spacecraft modules can reduce the need for maximum redundancy in each module. If avionics, power, ECLSS, thermal and other functionality from one module can be used to mitigate loss of those functions in another module, the criticality of each module is reduced. Spacecraft level reliability and criticality analyses will be required to achieve an optimum balance between component redundancy within a spacecraft module and functional redundancy. As long as the spacecraft can be assured of providing critical functions from somewhere, it will not be necessary to treat every module's subsystems as high criticality components. Optimizing across the system will reduce the criticality within each module. For example, if a power system failure in any module can be mitigated by power systems in other modules without threatening a loss of mission or crew, each subsystem can be designed with less redundancy. Coupled with commonality, the combined mass of in-use components and spares can be significantly reduced from systems that are designed independently.

9.3.2.2.5. Reliability

Reliability figures prominently in determining loss of crew and loss of mission. Redundancy can mitigate many failures, although in a multi-month mission with no capacity to resupply and where aborts will still require up to several months to complete, the possibility of multiple failures must be considered, and prospects for lengthy durations when one failure away from criticality must be carefully considered. Although it may be tempting to make assumptions that technology and time will allow for substantially improved reliability and reduce the need for supportability and redundancy, such assumptions should be avoided unless strong evidence exists to support the assumption.

In general, most components are quite reliable. Spares mass is not driven by systems with poor reliability, but rather by the sheer number of potential failures on complex spacecraft. Most spares will not be used, but they must be carried as risk mitigation. The inclination to adopt a policy of mitigating risk with “we’ll just make the systems more reliable” is a policy not supportable by data.

9.3.2.2.6. In-Space Manufacturing

Several approaches have been proposed and researched to provide capabilities to manufacture replacement parts. One of the more promising technologies is the Electron Beam Freeform Fabrication (EBF3) process that has been developed at NASA Langley Research Center and by others over the past several years. This process is capable of building metallic components from a wire or powder feedstock, using a CAD-type pattern to create a quite wide range of alloys and metallic characteristics. Precision parts will generally require some additional machining and polishing to meet final component specifications. Verification of manufacturing will require techniques such as 3-D scanning to determine the exact shape. The EBF3 process is also capable of making repairs to damaged items. The

electron beam could first be used to ablate damaged material, and then build up the damaged area to restore the original shape. Additionally, in-space manufacturing capabilities could focus on manufacturing tools. Custom tools are generally required to complete repairs and the ability to fabricate these tools on orbit could reduce mass and volume requirements.

It is far from clear, however, whether manufacturing capabilities could significantly change the sparing mass and volume needs for long-duration exploration missions. Based on data provided by the ISS Logistics and Maintenance Office, the ISS conducted more than 1500 unscheduled maintenance actions between 1998 and 2010, and few if any could have been accomplished with in-space manufacturing techniques. Many failures involve complex components with electronics, fluid systems, or chemical processing that are not amenable to repairing with parts that can be manufactured by available techniques. Often the specific failure is not known until the failed component is returned to Earth and detailed engineering analyses are conducted.

These techniques have significant merit from a “what if” analysis perspective. No logistics analysis can assure that all contingencies are covered. Something is likely to break, defying all the probabilistic analysis that said it would never happen. Manufacturing capabilities such as EBF3 and other similar techniques could prove crucial to long-duration space missions under some circumstances, such as micro-meteoroid object damage that strikes a critical spacecraft component. These types of techniques should be developed and used for long-duration missions, not necessarily to reduce sparing needs, but rather as a means of giving the crew their best “fighting chance” to survive unforeseen circumstances.

9.3.2.3. Model Description

In an effort to understand the effects of the various supportability strategies, Exploration Maintainability Analysis Tool (EMAT) was developed⁷. EMAT performs probabilistic simulation of spacecraft system failures and repair activities. The tool is used to evaluate the reliability and safety of exploration systems by evaluating the impact of system design, reliability of system components, quantity and mix of manifested spares, and reparability of systems.

The operations of spacecraft systems are modeled in EMAT as a set of components linked by logical operational statements. The logic defines how each component contributes to the operation of the system and the impact on the mission and the crew if each component fails. Based on the logic, the tool simulates the operational status of each modeled system in the exploration spacecraft; simulating the occurrence of potential failures and evaluating the capability to repair those failures. Component reliability and spares data are entered into the model and used to evaluate system operations.

EMAT performs stochastic analysis on the modeled systems, modeling potential failures that could occur during a mission, repair activities to respond to those failures, and mission outcome. A Monte Carlo approach is used in EMAT to stochastically evaluate mission reliability and safety. As part of a Monte Carlo analysis, EMAT runs a large number of individual cases, each simulating a potential mission profile with stochastic failures and the related repair activities. The tool then statistically integrates results across the stochastic cases to develop probabilistic estimates for reliability and safety.

EMAT is structured in several nested layers, each of which executes a different nested level of analysis. Figure 9-9 illustrates the structure of the model. The model inputs define the system and available spares. System operations are simulated through logical relationships between the components of the system. An entire mission is simulated on a day-by-day basis for a specified mission length. System failures and repair activities are included in this simulation. The Monte Carlo engine executes a large number of mission simulations and the post-processor summarizes the results. A sensitivity analysis of many Monte Carlo runs with varied input quantifies the impact of the spares mix and system design on mission outcome.

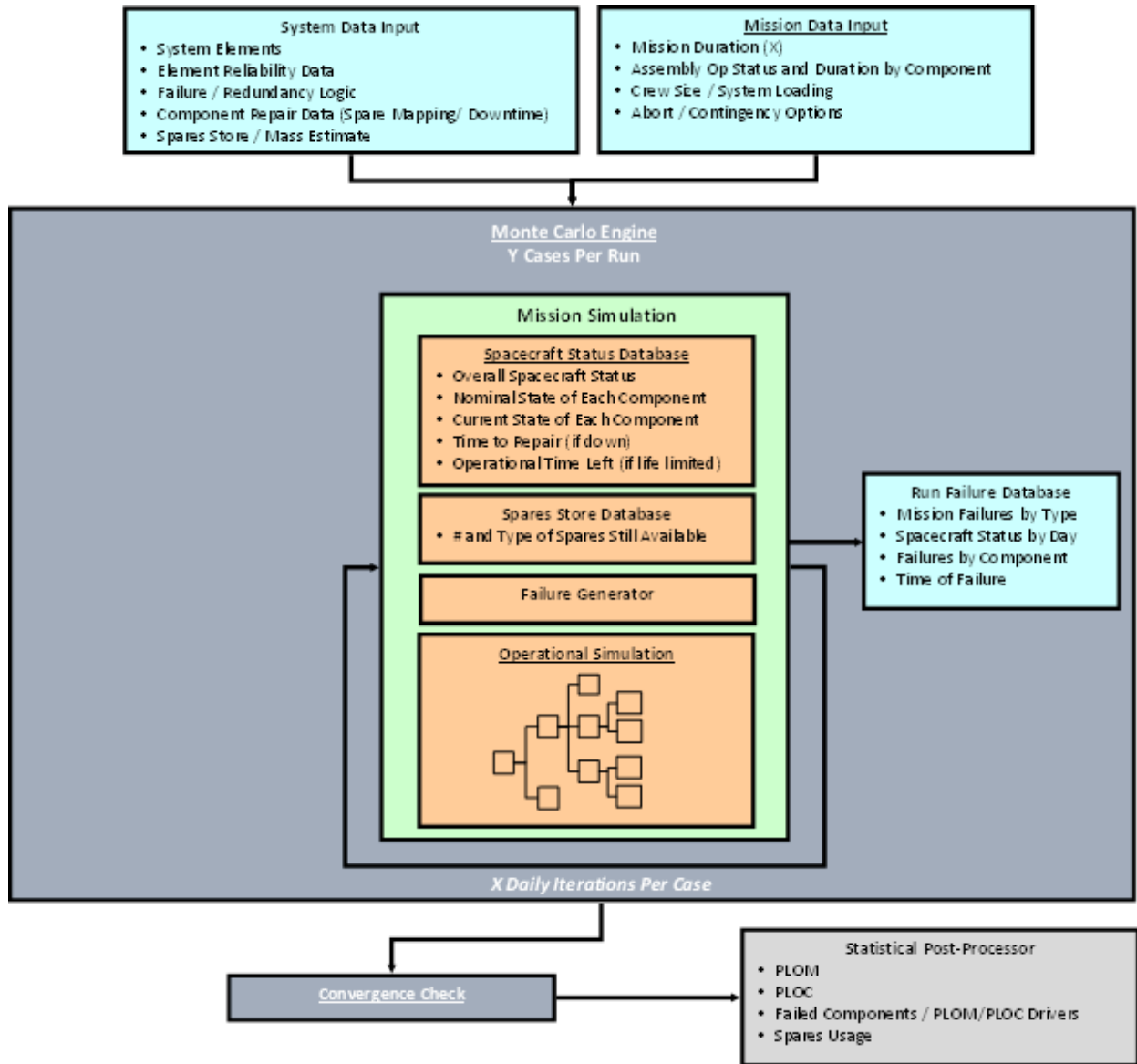


Figure 9-9 Exploration maintainability analysis tool structure.

9.3.2.4. Data Sources

Because the design of exploration missions and systems is still in the conceptual stages, it is not yet possible to develop absolute predictions for a mission’s reliability and safety. Rather, the intended purpose of EMAT is to evaluate the sensitivity of exploration system supportability to a variety of design factors. However, the efficacy of the tool is still heavily dependent on the availability and quality of the data used in the analysis. Data used to populate EMAT are taken primarily from ISS design and operational experience. The ISS provides a source of risk information regarding long-duration spacecraft systems. Although the ISS is larger and more complex than anticipated exploration systems, many of the systems will be similar in design. Data at the component level, including reliability data, repair data, and spares data will be applicable to exploration systems. ISS-based data are used to derive each of the primary inputs to EMAT.

Logical System Descriptions - The most basic data used to model exploration systems in EMAT are the logical operational descriptions of the spacecraft systems. For most systems, the descriptions are initially derived from the logical descriptions contained in the ISS Probabilistic Risk Assessment (PRA). The PRA for ISS Stage 7A

configuration was used as the basis for modeling. This configuration, which represents the configuration of the ISS during construction, after assembly flight 18 (December 7, 2001), was selected because it more closely represents anticipated exploration systems than the Assembly Complete ISS.

The PRA model details how failures at the component level can propagate through the system as a whole and result in an undesirable end state, such as loss of system or loss of crew. System fault trees are linked to repair attempts as part of the event sequence diagrams, which represent the highest level of configuration information for the PRA. These diagrams take into account functionally redundant systems, which support critical ISS functions and must all fail for a negative end state to be reached.

The logical descriptions in the PRA were used as the starting point for developing the Logical System Descriptions for EMAT. System descriptions were modified as appropriate to match the currently anticipated system design for the exploration spacecraft. In many cases, anticipated exploration systems will be simpler than the equivalent systems on ISS. In addition, it is anticipated that new technologies will be incorporated into exploration systems. In this case, the logical descriptions were modified to align with these changes.

Certain exploration systems, particularly propulsion systems, are not present on the ISS and therefore are not represented in the PRA. In these cases, logical system descriptions were developed based on the best current description of those systems. In most cases, these descriptions are not defined to as fine a level of specificity as those derived from ISS.

Component Reliability – Reliability estimates for each modeled component are a primary input to EMAT. There are two primary sources for component reliability data. The first is the ISS PRA, which contains an estimate of individual component failure likelihood and its associated uncertainty for all components. For some components the reliability estimates in the PRA, which were developed prior to ISS construction, have been updated based upon the decade plus of real-world flight experience of ISS. These updates, developed using Bayesian analysis, are captured in the NASA ISS Program Office’s ORU Logistics and Maintenance Frequently Asked Questions (FAQ) database (LMFAQ) catalog. Where available, these updated estimates were used in EMAT.

Spares Mass and Volume - Information regarding system spares is necessary for the tool to be able to evaluate the spares inventory. The LMFAQ database was used to identify spares for modeled components and to compile the mass and volume estimates for each spare. This database catalogs all of the current spares for the ISS, both on the ground and on board. It contains mass, volume, and inventories for most of the components considered in the PRA.

Repair Time - The NASA ISS Program Office’s Maintenance Database Collection was used to derive repair time estimates for all modeled components. The MDC catalogs every maintenance and repair activity that has occurred on ISS and captures the time required for these activities, both in terms of astronaut hours expended on the task and total time required to restore a component to operation. While this is very useful information, it lacks contextual information such as other crewmember responsibilities, other maintenance demands, and repair priority of the actions recorded. As a result, it is difficult to gauge how long the physical act of repairing and replacing the item takes independent of all the other demands on the crew. Best engineering judgment was applied to the estimates derived from the Maintenance Database Collection and the precision of the estimates was limited to 1 day. In cases where specific components have not been repaired on ISS, data for analogous components was used to derive estimates.

9.3.2.5. Future Support of Mars Studies

EMAT is intended to support mission and element design, starting in the conceptual phase, for future exploration missions by providing analysis of mission safety and reliability, as well as estimates for spares mass and volume requirements. EMAT will be used to support future conceptual Mars studies when developing the transit and surface elements. EMAT results can be utilized to determine the maximum achievable probability of loss of crew and probability of loss of mission for the habitats based on the number of spares brought on the mission.

A component-level definition of element systems has been developed based on input from system experts, ISS system definition, and spacecraft modeling tools. The model is an initial representative baseline systems definition of a beyond LEO spacecraft. This model is intended to serve as an initial cut at describing what habitat systems may

ultimately look like, as informed by system experts, to serve as a starting point to begin conducting sensitivity analysis and trade studies. The actual design of future systems could vary significantly from this model, based on mission requirements, technologies, and constraints.

EMAT can be used to conduct sensitivity analysis of proposed changes to the design of an element or to the supportability approach. Specific approaches that can be evaluated using EMAT include: improved component and system reliability, low-level repair, spares commonality, scavenging, and in situ manufacturing of spares and tools. Each of these approaches has the potential to reduce the total required mass and volume of spares and to improve reliability and safety. Sensitivity analysis using EMAT will indicate the relative merits of each approach. Identifying the most promising of these tactics will help steer future work and research especially on the ISS.

9.4. Bibliography

- ¹ *Affordable Fission Surface Power System Study Final Report*, Exploration Systems Mission Directorate Memorandum For The Record, 5 October 2007.
- ² *Executive Summary of Reference Fission Surface Power System Concept Selection*, Exploration Systems Mission Directorate Memorandum For The Record, 23 July 2008.
- ³ Lee Mason, David Poston, and Louis Qualls, “System Concepts for Affordable Fission Surface Power,” NASA/TM—2008-215166, January 2008.
- ⁴ *Human Exploration of Mars: Design Reference Architecture 5.0*, Bret G. Drake, editor, NASA/SP—2009-566, July 2009.
- ⁵ David I. Poston, Lee S. Mason, and Michael G. Houts, “Radiation Shielding Architecture Studies for NASA’s Lunar Fission Surface Power System,” Proceedings of Nuclear and Emerging Technologies for Space (NETS–2009), Atlanta GA, 14–19 June 2009, Paper 208590.
- ⁶ Cirillo, W., Goodliff, K., Aaseng, G., Stromgren, C., and Maxwell, A., “Supportability for Beyond Low Earth Orbit Missions,” AIAA Space 2011 Conference and Exposition, AIAA-2011-7231, Long Beach, CA, September 2011.
- ⁷ Stromgren, C., Terry, M., Cirillo, W., Goodliff, K., and Maxwell, A., “Design and Application of the Exploration Maintainability Analysis Tool,” AIAA Space 2012 Conference and Exposition, AIAA-2012-5323, Pasadena, CA, September 2012.

10. TECHNOLOGY NEEDS

Primary Contributors:

Scott Vangen, National Aeronautics and Space Administration, John F. Kennedy Space Center
Jonette M. Stecklein, National Aeronautics and Space Administration, Lyndon B. Johnson Space Center
Leslie Alexander, National Aeronautics and Space Administration, Marshall Space Flight Center

10.1. Introduction

Human Exploration of Mars Design Reference Architecture 5.0 (DRA 5.0) identified enabling technologies for both transportation and surface systems (sections 4 & 5). In addition, DRA 5.0 identified several Key Challenges (section 7), with identified technology investments for potential solutions. This DRA 5.0 Addendum #2 Technology Needs section is to augment the previous work by summarizing the Human Spaceflight Architecture Team (HAT) analysis associated with Mars applicable technologies that have been performed since the release of DRA 5.0.

Note: A more complete summary of information on the HAT technology development process and technology portfolio listing can be found in “Critical Technology Determination For Future Human Space Flight (GLEX-2012.09.3.3x12551). Much of this Addendum #2 Technology Needs section is taken directly from the paper since it is an excellent source of HAT summary data [NASA, 2012].¹

10.2. HAT Technology Development

NASA formed the Human Spaceflight Architecture Team (HAT) to develop concepts for architectures and vehicle elements, conduct trade studies, and determine the technology and capability requirements needed for missions ranging from activities in cis-Lunar space to Mars landings.

As shown in Figure 10-1, the HAT approach includes several processes: design reference missions (DRMs) consistent with NASA’s investment strategy are proposed; elements needed for the missions are conceptualized; schedule and cost estimates for each element are developed; integrated schedules and flight manifests are determined; and total costs are estimated. A key step in this process is the determination of which technologies are needed to enable these elements and missions so that full costs can be estimated. This section describes the methodology used to provide an architecture-driven technology development assessment (“technology pull”) resulting in a list of critical technologies needed to advance human exploration of space beyond low Earth orbit (LEO).

The HAT created a Technology Development Assessment Team to manage the collection and evaluation of these technology needs. This team is comprised of representatives from across the Agency, ensuring input from and communication to a broad portion of the NASA community.

10.3. Architectural Elements and Destinations

Several architectural elements have been conceptualized by the HAT team, and many DRMs have been developed to encompass a variety of destinations within the inner solar system. While still notional, these elements^{2,3,4,5,6,7,8} and missions contain enough fidelity to provide a concrete target for assessing the likely costs of similar missions, including the costs of technology development. The destinations⁹ are used to drive transportation systems capabilities and assess impacts of changes in mission assumptions. The elements and destinations currently under consideration are listed below, and notional representations of the elements are shown in Figure 10-2. Note: Mars surface and Mars orbit were but two of the several DRM/Destinations that were assessed.

Architecture Elements

- Space Launch System (SLS)
- Multipurpose Crew Vehicle (MPCV)
- Cryogenic Propulsion Stage (CPS)
- Solar Electric Propulsion Stage (SEP)
- Lander
- EVA Suit (EVA)
- Space Exploration Vehicle (SEV)
- Deep Space Habitat (DSH)
- Robotics and EVA Module (REM)
- Cargo Hauler
- Surface Elements (lunar, asteroid, Mars, and Mars moons)

Design Reference Missions (DRM) / Destinations

- Low Earth Orbit (LEO)
- Geosynchronous Earth Orbit (GEO) and High Earth Orbit (HEO)
- Lunar Vicinity: Earth-Moon Lagrange points one and two (E-M L1 and L2)
- Lunar flyby and Low Lunar Orbit (LLO)
- Lunar surface
- Minimum capability, low energy Near Earth Asteroid (NEA)
- Full-capability, high-energy NEA
- Mars moon
- Mars surface

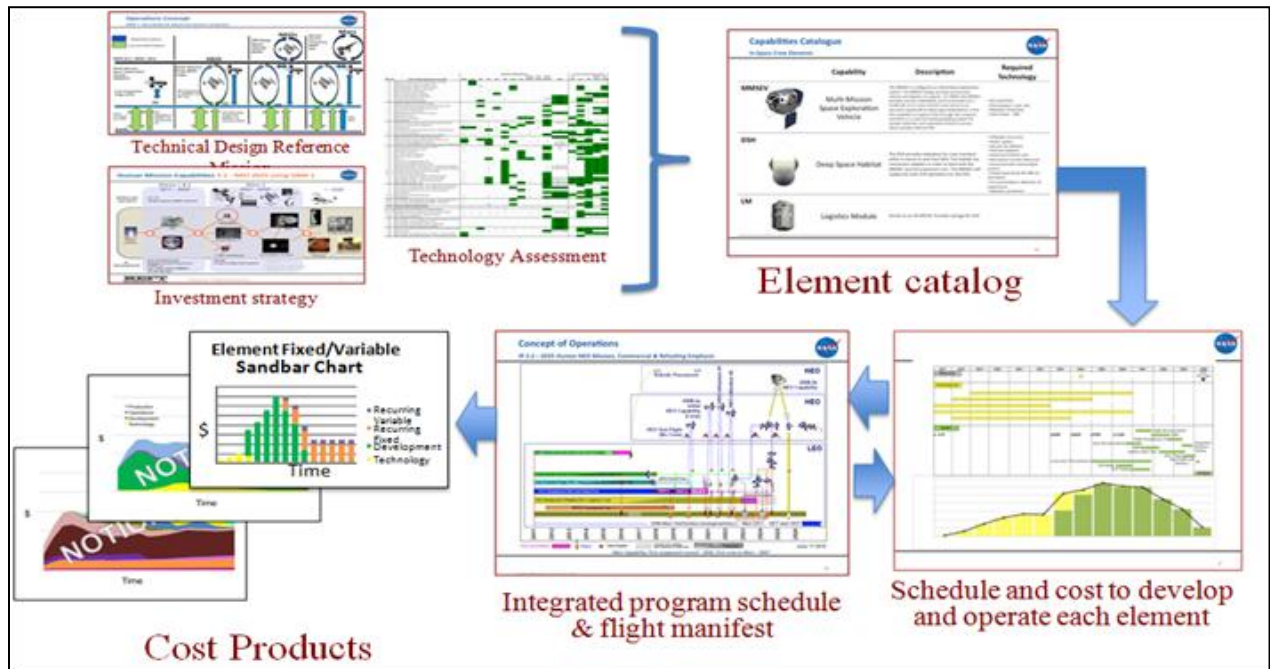


Figure 10-1 HAT cost analysis approach.



Figure 10-2 Notional HAT architectural elements.

Note that the Multipurpose Crew Vehicle (MPCV) and Space Launch System (SLS) are needed for every destination, but the need for the other elements are destination and mission specific. Similarly, these two elements can be built with existing technology, but technology development is required for the other element concepts (dependent on destination).

10.4. Technology Selection Method

Conceptual designs were developed for each of the architectural elements listed in Section 10.2, and notional element performance requirements were determined for each relevant DRM to determine ballpark cost estimates. Element conceptual designs also provide a reasonable basis for determining whether existing technologies are sufficient to provide the expected performance or whether technical gaps need to be filled.

The determination of technology adequacy is best accomplished by collaboration between mission planners, spacecraft designers, and technology developers, as the planners and designers are keenly aware of what is needed and the developers know about technologies that may change the way the missions and designs are approached. The objective is to determine a minimum but sufficient set of technologies, noting that needs are created by specific mission architecture requirements, yet specific designs are enabled by technologies.

The technical community submitted a list of technologies to the HAT element, architecture/DRM, and destination teams. These teams reviewed each technology and judged whether technology development was required to enable functionality of their element or successful completion of a mission to their destination, respectively. The teams also identified additional technologies, if any, which might be required. The first set of technologies was based primarily on work that was already under development for a planned lunar mission (as part of the NASA Constellation Program), but as the broader technical community was educated about the evolving elements and destinations, new ideas came forward that might either be required or could substantially change the way the missions could be accomplished.

To simplify the review of the many technologies brought forth, each technology was described using a common format including these data elements:

- **Description:** Explanation as to the what and why a specific technology development is required
- **Performance Characteristics:** Details on what advancements beyond state of the art is required, including metrics where known/applicable

If the technologists and the respective element and destination team leads reached consensus on the description and performance characteristics needed, and these team leads agreed that the technology was enabling for their vehicle or mission, then the technology was added to the list of critical technologies. Some technologies that are required for one element are also beneficial to others; e.g., unsettled cryogenic propellant transfer which is required for the CPS and beneficial for the DSH, Lander, and surface elements. Note that the need for some technologies is dependent on specific vehicle configurations; e.g., oxygen-rich stage combustion engine technology is applicable to the SLS only if liquid strap-on boosters are included in the design. The applicability data were visually mapped by noting “drivers” and “beneficiaries” in a spreadsheet containing rows of technologies and columns of elements, DRMs, and destinations. This mapping is notionally shown as the “technology assessment” plot in Figure 10-1 and the “summary spreadsheet” in Figure 10-3. The cost and schedule needed to bring the technology to a level where it could be infused into the standard Design, Development, Test and Evaluation (DDT&E) cycle was also collected, along with the current technology readiness level (TRL). “Cost fidelity” was assessed by determining the knowledge level of both the problem being addressed and the costs to develop the technology. An example of a technology with high cost fidelity is in-space cryogenic propellant storage, where the requirements are very well understood and solid plans are in place to develop the required technology. A Mars surface space suit is an example of a technology whose needs are well understood since the Mars environment is well characterized, but costs to develop the technology are not because specific technical concepts have not yet been selected. Thermal control is an example of a technology whose development costs are well understood for a given thermal system design, but the needs are uncertain because spacecraft designs are not finalized. These two examples yield a “medium” cost fidelity. Finally, a long-life battery has a “low” cost fidelity because technical requirements have not yet been determined and a technical concept has not yet been developed.

Cost phasing and “need by” dates were recorded with each technology to assist with HAT’s cost estimations for each DRM. Technologies were assumed to be matured and available by the preliminary design review for the enabled element. “Need by” dates for technologies required by multiple elements were based on the element that was expected to be completed first.

Finally, each technology was mapped into the technology classification system used by NASA’s Office of the Chief Technologist.⁹ The full suite of data elements describing each technology is listed in Table 10-3.

Figure 10-3 summarizes the use of the data collected for each technology. Subject matter experts created technology “one-page” descriptions based on the needs of DRMs and architecture elements, and estimated technology development costs and the fidelity of those costs. Cost, schedule, and applicability data were recorded in a summary spreadsheet for use in the cost estimation process depicted in Figure 10-1.

10.5. Technologies

Using the methodology described in Section 10.2, a suite of 60 technologies was identified as being critically important for at least one mission under consideration by the HAT (“technology pull”). In addition, “common avionics” was identified as a technology that could substantially improve system-level affordability, and four ground operations technologies were identified as having a similar cost-reduction potential. The full suite of these 65 technologies is listed in Table 10-1, and their mapping to the architecture elements and destinations is shown in Table 10-3.

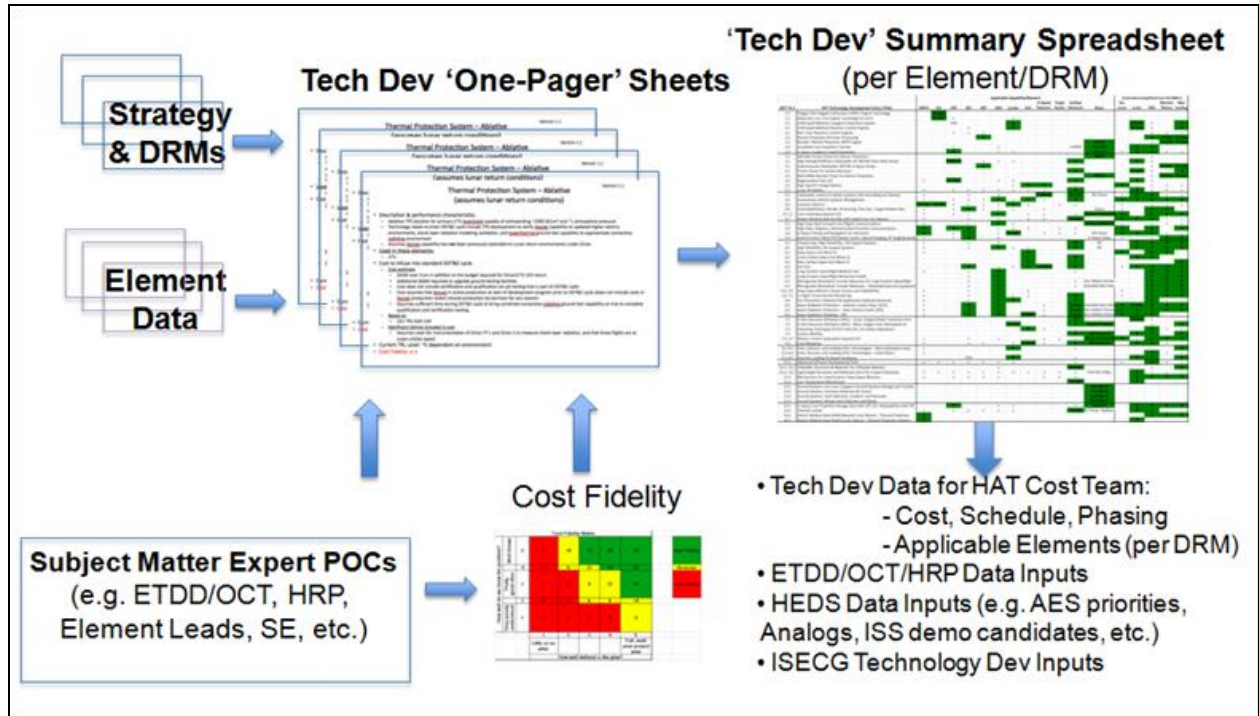


Figure 10-3 HAT technology development assessment: data capture process.

Table 10-1 Technologies That Enable Human Space Exploration

Technology Area (TA)	TA Breakdown	Title
01 Launch Propulsion Systems	1.2	Oxygen-Rich Staged Combustion (ORSC) Engine Technology
		Advanced, Low Cost Engine Technology for SLS
02 In-Space Propulsion Technologies	2.1	LOX/Liquid Methane Cryogenic Propulsion System
		LOX/Liquid Methane Reaction Control Engines
		Non-Toxic Reaction Control Engines
	2.2	Electric Propulsion and Power Processing
	2.3	Nuclear Thermal Propulsion (NTP) Engine
03 Space Power and Energy Storage	3.1	Unsettled Cryo Propellant Transfer
		In Space Cryogenic Liquid Acquisition
		300 kWe Fission Power for Electric Propulsion
		High Strength/Stiffness Deployable 10-100 kW Class Solar Arrays
	3.2	Autonomously Deployable 300 kW In-Space Arrays
04 Robotics, Tele-Robotics and Autonomous Systems	4.1, 4.5	Fission Power for Surface Missions
		Multi-MWe Nuclear Power for Electric Propulsion
	4.3	Regenerative Fuel Cell
		High Specific Energy Battery
	4.5	Long Life Battery
		Precision Landing and Hazard Avoidance
		Telerobotic control of robotic systems with time delay
05 Communications and Navigation	4.6, 4.2, 4.5	Autonomous Vehicle Systems Management
		Common Avionics
	4.7, 6	Automated/Auton. Rendez. and Docking, Prox Ops, Target Relative Navigation
		Crew Autonomy beyond LEO
	5.2	Robots Working Side-by-Side with Suited Crew
High Data Rate Forward Link (Flight) Communications		
High Rate, Adaptive, Internetworked Proximity Communications		
06 Human Health, Life Support and Habitation Systems	5.4	In-Space Timing and Navigation for Autonomy
		Quad Function Hybrid RF/Optical Comm, Optical Ranging, RF Imaging System
	6.1	Closed-Loop, High Reliability, Life Support Systems
		High Reliability Life Support Systems
	6.2	Deep Space Suit (Block 1)
		Lunar Surface Space Suit (Block 2)
		Mars Surface Space Suit (Block 3)
	6.3	Long Duration Spaceflight Medical Care
		Long-Duration Spaceflight Behavioral Health and Performance
	6.3, 6.1	Microgravity Biomedical Counter-Measures for Long Duration Spaceflight
Microgravity Biomedical Counter-Measures—Optimized Exercise Equipment		
6.4, 11	Deep Space Mission Human Factors and Habitability	
	In-Flight Environmental Monitoring	
	Fire Prevention, Detection and Suppression (reduced pressure)	
	Space Radiation Protection—Galactic Cosmic Rays (GCR)	
	Space Radiation Protection—Solar Particle Events (SPE)	
07 Human Exploration Destination Systems	6.4	Space Radiation Shielding—SPE
		In-Situ Resource Utilization (ISRU)—Lunar: Oxygen/Water Extraction from Lunar Regolith
	7.1	In-Situ Resource Utilization (ISRU)—Mars: Oxygen from Atmosphere and Water Extraction from Soil
		Anchoring Techniques and EVA Tools for Microgravity Surface Operations
	7.3	Suit Port
Surface Mobility		
09 Entry, Descent and Landing Systems	7.5, 4.7	Mission Control Automation beyond LEO
		Dust Mitigation
11 Modeling, Simulation, Information Technology and Processing	9.1, 9.4	Entry, Descent, and Landing (EDL) Technologies—Mars Exploration Class Missions
		Entry, Descent, and Landing (EDL) Technologies—Earth Return
12 Materials, Structures, Mechanical Sys. and Mfg.	11.2	Advanced Software Development/Tools
		Structures and Materials for Inflatable Modules
	12.1, 12.2	Lightweight and Efficient Structures and Materials
		Mechanisms for Long Duration, Deep Space Missions
13 Ground and Launch Systems Processing	12.3	Low Temperature Mechanisms
		Ground Systems: Low Loss Cryogenic Ground Systems Storage and Transfer
	13.1	Ground Systems: Corrosion Detection and Control
		Ground Systems: Fault Detection, Isolation, and Recovery
14 Thermal Management Systems	13.3	Ground Systems: Wiring Fault Detection and Repair
		In-Space Cryogenic Propellant Storage (Zero Boil Off LO2; Reduced/Zero Boil Off LH2)
	14.2	Thermal Control
14.3	Robust Ablative Heat Shield (Beyond Lunar Return)—Thermal Protection System	
	Robust Ablative Heat Shield (Lunar Return)—Thermal Protection Systems	

10.6. Discussion

It is a challenge to identify enabling technologies for missions that are only notionally defined. Primarily this is because “enabling” is defined as “the mission cannot be done without it” but there is much flexibility on how the missions are defined. Conversations can become circular: “Why is this technology needed?” gets answered with “What does this spacecraft or mission need to do?” Or: “This technology isn’t needed because the mission can be

done conventionally” is met with “But if this particular technology is available, the mission can be done differently (e.g., less expensively, more robustly, more extensible).”

Nonetheless, forward progress is possible for many aspects where precursor information is available (for elements like SLS and MPCV) or where the need for a technology is evident regardless of element definition or DRM (e.g., very long-duration missions). A particular benefit of the method described in Section 10.3 is that it fosters conversations across organizational boundaries and can lead to creative solutions.

The application of some technologies has been well studied for specific missions, and so their technical descriptions and performance characteristics are well understood. Examples include deep space suit; fire detection and suppression; nuclear thermal propulsion; and liquid oxygen/liquid methane cryogenic propulsion systems. Other technologies are only now being considered because the missions are newly developed. Examples include anchoring techniques and EVA tools for microgravity surface operations. Some technologies are discrete and well defined (e.g., high specific energy batteries), some are innovative designs (e.g., suit port), and some are families of technology designs (e.g., surface mobility). These differences are a consequence of the iterative nature of the process—one must start somewhere to create data sets with meaning across broad constituent groups.

The original use of this technology data was as input to the HAT cost models used to assess mission feasibility as described in Section 10.1. The method has also proven useful to introduce new ideas into the mission planning activity as described above, and to focus technology development programs. For instance, NASA’s Advanced Exploration Systems Program looks to the performance metrics generated by this process to ensure that their technology development is addressing the most critical problems.¹⁰

The HAT technology development data are also being used as a basis of input into the Office of Chief Technologist’s “Strategic Space Technology Investment Plan.” OCT is consolidating NASA’s technology needs across the Agency’s directorates, and the HAT Technology Development data set is the basis for the Human Exploration and Operations Mission Directorate’s input.

In addition, an analysis tool has been developed to provide a relative comparison of the HAT identified technologies against selected Figures of Merit (FOM), DRMs, and mission timeframes. Periodically updated HAT technology development data, along with the technology ranking analysis tool, provide NASA’s Human Exploration and Operations Mission Directorate with the ability to weigh the technology development portfolio as required within the Capability Driven Framework.

This data set also provides a means to clearly communicate NASA’s human exploration technology needs to the NASA field Centers and potential collaborators. This data set has been provided to the International Space Exploration Coordination Group, which subsequently adopted the framework for assessing technologies for the Global Exploration Roadmap and future partnerships.¹¹ We expect that it will be similarly useful for discussions with other government agencies and industrial and academic organizations. We hope that these dialogs provide new ideas regarding the means and opportunities for future human exploration.

Finally, this technology information has been useful for assessing NASA’s strategic technology roadmaps as they pertain to human exploration. The National Research Council (NRC) recently reviewed those roadmaps and provided prioritization recommendations including “High”, “Medium” and “Low” priority.¹² They further identified the “Top 16” technologies from the “High” ranked technologies recommending that NASA focus on those in the next 5 years. The HAT technology listing provides a ready means to compare the NRC’s assessment of critically required technologies to those determined by the NASA human spaceflight community, and to identify errors and/or omissions from both sides. Figure 10-4 shows the HAT identified technologies mapped to the NRC rankings. Fully one-third of the HAT technologies were among the NRC’s Top 16, and 74% were ranked “High.” This indicates excellent agreement between the two communities. About one-fifth of the HAT technologies were ranked lower than “High” by the NRC. Primarily this occurred because long-duration reliability was not a ranking factor for the NRC while HAT placed high importance on this, some HAT technologies are design specific and did not get captured by the NRC process, and the NRC did not consider ground operations to require technology development. The NRC’s “Top 16” listing is shown in Table 10-2, with those that overlap with the HAT listing shown in bold. Note that in some cases several HAT technologies group to form one NRC technology; for example, the NRC “Fission (Power)” encompasses three HAT technologies: fission power for surfaces, for 300 kW-class electric

propulsion systems, and for multi-MW electric propulsion systems

Table 10-2 NRC’s “Top 16” Technologies, with HAT Human Exploration Focused Critical Technologies Shown in Bold

- NRC's "Top 16" Technologies for NASA
- 2.2.1 Electric Propulsion
 - 2.2.3 (Nuclear) Thermal Propulsion
 - 3.1.3 Solar Power Generation (Photovoltaic and Thermal)
 - 3.1.5 Fission (Power)
 - 4.2.1 Extreme Terrain Mobility
 - 6.3.2 Long-Duration (Crew) Health
 - 8.1.1 Detectors and Focal Planes
 - 8.1.3 (Instrument and Sensor) Optical Systems
 - 8.2.4 High-Contrast Imaging and Spectroscopy Technologies
 - 8.3.3 In Situ (Instruments and Sensor)
 - 14.1.2 Active Thermal Control of Cryogenic Systems
 - X.1 Radiation Mitigation for Human Spaceflight
 - X.2 Lightweight and Multifunctional Materials and Structures
 - X.3 Environmental Control and Life Support System
 - X.4 Guidance, Navigation, and Control
 - X.5 Entry, Descent, and Landing Thermal Protection Systems

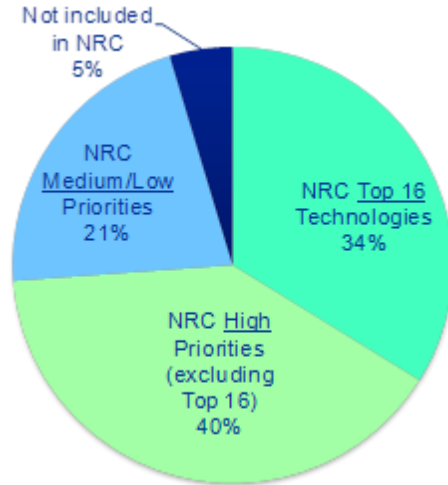


Figure 10-4 Correlation between technologies identified as critically important by HAT and high priority technologies identified by the NRC.

10.7. Summary

NASA’s HAT Technology Development Assessment Team has developed a method to identify technologies that will enable the next chapter of human space exploration. This method relies on dialog between system designers and technology developers to determine a minimum but sufficient set of technologies, noting that needs are created by specific mission architecture capabilities, yet specific designs are enabled by technologies.

The list of technologies that have been identified by this process was presented, along with brief descriptions and performance goals for each technology. These performance goals and descriptions may change as future exploration missions become more developed, noting that those missions will be influenced by the availability of these technologies.

In addition to contributing to cost assessments for a variety of DRMs, this information is being used to foster collaborations with the international community through the International Space Exploration Coordination Group and the Global Exploration Roadmap, to focus technology investments within NASA, and to assess the technology roadmaps being developed within NASA.

Mars Design Reference Architecture 5.0 – Addendum #2

Table 10-3 Technologies Mapped to Elements and Destinations

OCT TA #	HAT Technology Development Entry (Title)	Applicable Capability/Element											Destination (simplified from full DRM's)						
		MPCV	SLS	CPS	SEV	SEP	DSH	Lander	EVA	In-Space Robotics	Cargo Hauler	Surface Elements	Other	Cis-Lunar	Lunar	NEA	Meridian Moons	Mars Landing	
1.2	Oxygen-Rich Staged Combustion (ORSC) Engine Technology		D-note																
1.2	Advanced, Low Cost Engine Technology for SLS		D-note																
2.1	LOX/Liquid Methane Cryogenic Propulsion System			x															D
2.1	LOX/Liquid Methane Reaction Control Engines			note															D
2.1	Non-Toxic Reaction Control Engines				x														x
2.2	Electric Propulsion and Power Processing			x	x														x
2.3	Nuclear Thermal Propulsion (NTP) Engine					D													D-note
2.3	Nuclear Thermal Propulsion (NTP) Engine																		D-note
2.4	Unsettled Cryo Propellant Transfer			x															D-note
2.4	In Space Cryogenic Liquid Acquisition			D															D-note
3.1	300 kW Fission Power for Electric Propulsion																		D-note
3.1	High Strength/Stiffness Deployable 10-100 kW Class Solar Arrays			D-Block2															D-note
3.1	Autonomously Deployable 300 kW In-Space Arrays																		D-note
3.1	Fission Power for Surface Missions																		D-note
3.1	Multi-MWe Nuclear Power for Electric Propulsion																		D-note
3.2	Regenerative Fuel Cell			D-note															D-note
3.2	High Specific Energy Battery																		D-note
3.2	Long Life Battery																		D-note
4.1, 4.5	Precision Landing and Hazard Avoidance																		D-note
4.3	Telerobotic control of robotic systems with time delay																		D-note
4.5	Autonomous Vehicle Systems Management																		D-note
4.5	Common Avionics																		D-note
4.6, 4.2, 4.5	Automated/Auton. Rendez. and Docking, Prox Ops, Target Relative Navigation																		D-note
4.7, 6	Crew Autonomy beyond LEO																		D-note
4.7, 4.4	Robots Working Side-by-Side with Suited Crew																		D-note
5.2	High Data Rate Forward Link (Flight) Communications																		D-note
5.4	High Rate, Adaptive, Internetworked Proximity Communications																		D-note
5.4	In-Space Timing and Navigation for Autonomy																		D-note
5.5	Quad Function Hybrid RF/Optical Comm, Optical Ranging, RF Imaging System																		D-note
6.1	Closed-Loop, High Reliability, Life Support Systems																		D-note
6.1	High Reliability Life Support Systems																		D-note
6.2	Deep Space Suit (Block 1)																		D-note
6.2	Lunar Surface Space Suit (Block 2)																		D-note
6.2	Mars Surface Space Suit (Block 3)																		D-note
6.3	Long Duration Spaceflight Medical Care																		D-note
6.3	Long-Duration Spaceflight Behavioral Health and Performance																		D-note
6.3	Microgravity Biomedical Counter-Measures for Long Duration Spaceflight																		D-note
6.3	Microgravity Biomedical Counter-Measures—Optimized Exercise Equipment																		D-note
6.3, 6.1	Deep Space Mission Human Factors and Habitability																		D-note
6.4, 11	In-Flight Environmental Monitoring																		D-note
6.4	Fire Prevention, Detection and Suppression (reduced pressure)																		D-note
6.5	Space Radiation Protection—Galactic Cosmic Rays (GCR)																		D-note
6.5	Space Radiation Protection—Solar Particle Events (SPE)																		D-note
6.5	Space Radiation Shielding—SPE																		D-note
7.1	In-Situ Resource Utilization (ISRU)—Lunar: Oxygen/Water Extraction from Lunar Regolith																		D-note
7.1	ISRU—Mars: Oxygen from Atmosphere and Water Extraction from Soil																		D-note
7.3	Anchoring Techniques and EVA Tools for Microgravity Surface Operations																		D-note
7.3	Suit Port																		D-note
7.3	Surface Mobility																		D-note
7.5, 4.7	Mission Control Automation beyond LEO																		D-note
7.5	Dust Mitigation																		D-note
9.1, 9.4	Entry, Descent, and Landing (EDL) Technologies—Mars Exploration Class Missions																		D-note
9.1, 9.4	EDL Technologies—Earth Return																		D-note
11.2	Advanced Software Development/Tools																		D-note
12.1, 12.2, 7.4.2	Structures and Materials for Inflatable Modules																		D-note
12.1, 12.2	Lightweight and Efficient Structures and Materials																		D-note
12.3	Mechanisms for Long Duration, Deep Space Missions																		D-note
12.3	Low Temperature Mechanisms																		D-note
13.1	Ground Systems: Low Loss Cryogenic Ground Systems Storage and Transfer																		D-note
13.2	Ground Systems: Corrosion Detection and Control																		D-note
13.3	Ground Systems: Fault Detection, Isolation, and Recovery																		D-note
13.3	Ground Systems: Wiring Fault Detection and Repair																		D-note
14.1	In-Space Cryogenic Propellant Storage (Zero Boil Off LO2; Reduced/Zero Boil Off LH2)																		D-note
14.2	Thermal Control																		D-note
14.3	Robust Ablative Heat Shield (Beyond Lunar Return)—Thermal Protection System																		D-note
14.3	Robust Ablative Heat Shield (Lunar Return)—Thermal Protection Systems																		D-note

10.8. Bibliography

- 1 NASA Exploration Systems Mission Directorate presentation, “Human Space Exploration Summary,” January 2011. http://www.nasa.gov/pdf/525162main_HEFT_Final_Brief_508_20110309.pdf [accessed 27 April 2012].
- 2 Olson, J. “The Way Forward—New Pathways for Human Spaceflight,” April 2011. http://www.nasa.gov/pdf/552846main_New_Pathways_Human_Spaceflight_Olson.pdf [accessed 27 April 2012].
- 3 Culbert, C. “Human Space Flight Architecture Team (HAT) Overview,” November 2011. http://www.nasa.gov/pdf/603232main_Culbert-HAT%20Overview%20for%20GER%20Workshop.pdf [accessed 27 April 2012].
- 4 Olson, J.; Culbert, C.; Laurini, K.C. “NASA’s Human Space Exploration Plans and Architecture,” 62nd International Astronautical Congress, Cape Town, SA. October 3-7 2011. IAC-11.E3.2.1 <http://www.iafastro.net/iac/archive/browse/IAC-11/E3/2/11969/> [accessed 27 April 2012].
- 5 Mueller, R.P., Connolly, J.C., Whitley, R.J., “NASA Human Spaceflight Architecture Team: Lunar Surface Exploration Strategies,” Global Space Exploration Conference, Washington DC, May 2012. GLEX-2012.02.P.17.x12620
- 6 Hoffman, Stephen J., Baker, John D., and Voels, Stephen A., “Mars as a Destination in a Capability- Driven Framework”, ASCE Earth and Space 2012, Pasadena, CA, April 2012
- 7 Friedensen, Victoria, and Mazanek, Daniel D., “NASA’s Plans for Human Exploration of Near-Earth Asteroids”, ASCE Earth and Space 2012, Pasadena, CA, April 2012
- 8 Bobskill, Marianne R., and Lupisella, Mark L., “The Role of Cis-Lunar Space in Future Global Space Exploration,” Global Space Exploration Conference, Washington DC, May 2012. GLEX-2012.05.5.4x12270
- 9 NASA Office of the Chief Technologist, “Draft Space Technology Roadmap Overview” http://www.nasa.gov/pdf/501317main_STR-Overview-Final_rev3.pdf [accessed 27 April 2012].
- 10 Moore, C., “Advanced Exploration Systems,” presentation to the NASA Advisory Council, March 2012. http://www.nasa.gov/pdf/630144main_2-Moore_NAC%20Briefing%20AES_508.pdf [accessed 27 April 2012].
- 11 Lange, C. et al., “Assessment of Technology Developments for the ISECG Global Exploration Roadmap,” May 2012. GLEX-2012.09.3.1x12269
- 12 National Research Council, “NASA Space Technology Roadmaps and Priorities: Restoring NASA’s Technological Edge and Paving the Way for a New Era in Space,” January 2012. http://www.nap.edu/catalog.php?record_id=13354 [accessed 27 April 2012].

This page intentionally left blank

11. ANALOGS

Primary Contributors:

Hoffman, Stephen J., National Aeronautics and Space Administration, Lyndon B. Johnson Space Center
Stanley G. Love, National Aeronautics and Space Administration, Lyndon B. Johnson Space Center

11.1. Introduction

Accomplishing the exploration goals described in the Mars DRA 5.0 depends upon a campaign of missions, with multiple interacting systems, intended to work in such a way that humans and robots together can effectively explore the surface Mars and, potentially, the moons of Mars. Historically, NASA and other government agencies responsible for developing and integrating systems for extreme environments have incorporated the use of analog missions and analog environments, whether natural or simulated, into their development and training programs. Analog environments are designed to emulate operational features of the mission’s destination for which systems are being designed including, in NASA’s case, aspects of the physical surface conditions of Mars and its moons. Analog missions are specific tests or evaluations of integrated systems and procedures performed either at a natural analog site, such as a desert location that emulates the surface of Mars or its moons, or at a facility that artificially duplicates aspects of a given Mars mission environment in order to gain an understanding of system-level interactions.

This section describes recent analog mission activities that have impacted the evolution of the Mars DRA 5.0. This section begins with a brief summary of the history of analogs with rationale for using them in evolving DRA 5.0. Definitions, developed by an international group to provide some rigor in discussing the type of analog campaign or test (the “what”) that could be used and the analog site or facility (the “where”) at which these analogs missions or tests are conducted, are then presented. Relevant analog projects and groups, along with the campaigns and activities accomplished since the conclusion of initial DRA 5.0 analyses, are summarized. In addition to the spaceflight-specific analog activities described, historic missions in extreme environments also offer lessons for the exploration of Mars and its surrounding environment. Several studies and workshops focused on these historic exploration activities are summarized. Finally, the impact of all of these activities on DRA 5.0 is then discussed.

11.2. Analog History, Context and Rationale

NASA currently, and historically, supports a diverse range of activities that could be reasonably placed in the general category of analogs and analog missions. For example, extravehicular activity (EVA) systems and technologies have been tested on an annual basis for almost a decade in the desert southwest of the United States. The Apollo Program trained flight crews for the lunar exploration activities they would carry out at dozens of locations, chosen for their analogous geomorphologic characteristics, throughout the world. Robotic programs such as the highly productive Mars Exploration Rovers have used many of these same locations to test prototypes of flight systems and to train their Earth-bound operators. These activities are typically customized to support the research or development objectives of the sponsoring project; there has usually been little incentive to share successes, failures, and lessons learned beyond the community most closely associated with the project. The scope and scale of the Mars DRA 5.0, augmented by the exploration of the moons of Mars, provides an expansive set of objectives to which this diverse group must contribute and in which all of their previously separate activities must now play an integrated role. This new reality points to the need for closer cooperation and coordination among the groups that have historically conducting analog activities.

This new framework and objectives set also points to other sources of highly relevant experience and capabilities that NASA should tap in order to accelerate its progress toward achieving needs, goals, and objectives of Mars exploration. For example, the National Science Foundation and its sister organizations around the world have been successfully operating comparable research and exploration outposts in Earth’s challenging polar regions for the past half century. Lessons learned regarding basic operations by various sized crews, along with the preparatory planning and logistical support experience, could provide a fruitful source for NASA efforts. Shared activities in

these harsh environments could also provide NASA personnel with direct experience that could be applied to NASA planning and development or contribute to validation of NASA concepts.

The benefits of closer cooperation and coordination among groups traditionally conducting analog missions that are most likely to be realized by a program established to implement something like the DRA 5.0 can be briefly summarized as follows:

- Identify mission-level integration issues that could impact concept of operations or requirements for missions or systems
- Help retire some program-level and mission-level risks. These could be operational risks such as demonstrated safety of a particular system or procedure for a human crew or mission performance levels of a given crew size trying to accomplish a particular set of tasks/objectives. These could also be developmental risk reductions such as validating the ability of multiple systems and crew to achieve desired mission goals.
- Assist in the development of operational concepts by testing the feasibility of new or untested concepts or to improve the efficiency of a particular operational concept by identifying shortcomings under analogous conditions.
- Facilitate training of flight crews, ground crews, and those engineers developing new systems and system interactions
- Identify (and capture) serendipitous results.

11.3. Definitions

A wide range of terrestrial analogs are in use today by international space agencies to simulate exploration missions, helping prepare for exploration beyond low-Earth orbit (LEO). Agencies have begun sharing information regarding analog activities, as well as identifying partnership opportunities that could increase the return on analog mission investments.

Agencies are using these analog activities to (a) learn which individual systems or operations (or combination of systems and operations) would function as desired as well as revealing unanticipated behavior, (b) compare the performance of alternative combinations of systems and operations, and (c) evaluate flight crew performance as well as train flight crews, ground support personnel, engineers, and managers. Analog activities are also extremely useful to the science community for interpreting data from past or ongoing missions. In addition to these technical roles, analog activities have also been used to engage the public with interesting and exciting mission simulations well before actual missions take place.

As analog activities grow in complexity and occur in more diverse locations to support the range of design reference missions contemplated by participating agencies, it has become important to have a common framework and set of definitions to properly characterize these activities as they take place and to describe future activities as they are proposed and planned. To address this issue, agencies have worked together to develop a common set of definitions to assist in the process of developing and coordinating relevant analog activities.

Analog activities themselves can involve testing of scientific, technological, or operational questions, or any combination thereof (Figure 11-1a). These activities can also span a continuum ranging from very focused, tightly controlled, single-purpose tests to multi-faceted, integrated combinations of scientific, technological, and operational features designed to simulate mission activities (Figure 11-1b). These activities require a physical location or facilities that can simulate some aspect of the destination environment in order to test the system or activity in question.

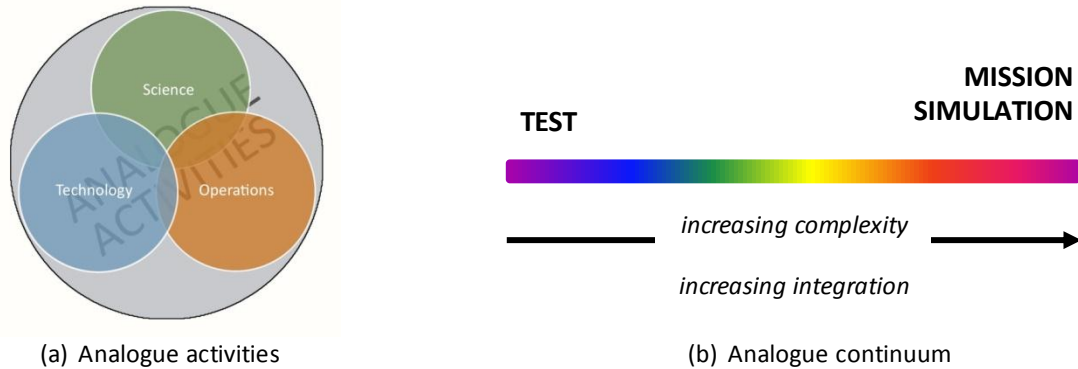


Figure 11-1 Analog activity composition and continuum.

Building on these basic concepts, participating agencies have developed a common set of definitions.

- An analog mission simulation is an activity designed to represent specific scientific, technical, and operational aspects of a future space mission using actual or functionally representative systems and operations or procedures under analogous environmental conditions, for the purpose of understanding performance and interactions among these systems and operations or procedures as well as their ability to achieve mission objectives.
- An analog test is an experiment designed to examine or refine a single scientific, technical, or operational mission requirement or data product.
- An analog site is a natural location on Earth presenting, to some extent, similarities (e.g., climatological, geological, morphological, etc.) with future space mission destinations.
- An analog facility is an artificial structure or location where conditions representative of certain phases of future space missions, can be reproduced and controlled to some extent.
- A test facility is an artificial structure where environmental parameters are representative of those encountered in certain phases of future space missions, controlled and fully reproducible.

11.4. Analog Projects and Teams

For more than a decade, several NASA-sponsored groups have been conducting analog mission simulations and tests investigating different facets of future human planetary exploration. By the time DRA 5.0 analyses had been completed in 2007, the activities of these groups had been focused on the near-term objectives of the Constellation Program (principally lunar surface missions) and the objectives of the Capability Driven Framework (principally Near Earth Asteroid rendezvous missions). However, in many cases the lessons learned and conclusions reached can be extended to future human missions to Mars. In addition, there have been recent analog activities that are focused more closely on Mars mission specific objectives. These groups have involved a broader range of space agencies and locations. This section describes, at a summary level, most of the significant groups and their relevant activities that were active since the completion of DRA 5.0 analysis work. A discussion of the relevance of analog activities performed by these groups to future Mars missions follows in the following sections.

11.4.1. Autonomous Mission Operations (AMO)

The Autonomous Mission Operations (AMO) Project, part of NASA's Human Exploration and Operations Mission Directorate's (HEOMD's) Advanced Exploration Systems (AES), is a series of ongoing experiments that brings together engineers and mission operations planners to investigating what systems and processes may require automation during crewed mission with a long communication delay between the spacecraft and Earth. The project lead is at ARC, and it is supported by Johnson Space Center (JSC), Marshall Space Flight Center, Kennedy Space Center, and Langley Research Center (LaRC). These experiments assume that as the communication delay becomes longer the flight control team on Earth will transition from its traditional role of immediate oversight of the flight crew's activities to a role more involved with data analysis, system prognostics, and near-real-time support.

There are significant open questions regarding which mission operations functions to allocate to ground, and which

to allocate to crew, as the time delay increases:

- How should mission operations responsibilities be allocated between ground and the spacecraft in the presence of significant light-time delay between the spacecraft and the Earth?
- How should ground-based planning, monitoring, and control be distributed across the flight control team and ground system automation?
- How should spacecraft-based planning, monitoring, and control be distributed between the flight crew and onboard system automation?
- When during the mission should responsibility shift from flight control team to crew or from crew to vehicle, and what should the process of shifting responsibility be as the mission progresses?
- What tools and technologies are needed to support these missions, and what are their costs?

An initial experiment to address these questions constructed a 2-hour quiescent mission timeline into which various unexpected events (systems failures, crew medical emergency) are inserted. The experiment was a medium fidelity simulation of space mission operations. Time delays of varying lengths (low, 50-second, 300-second one-way light-time delay) were also introduced. Crew responsibility, communications and support tools (baseline: International Space Station (ISS)-like; mitigation: crew autonomy) were also varied. The test team then analyzed task completion, communications, crew workload, and team coordination for both flight controllers and crew. The experiment design included utilization of the Deep Space Habitat (DSH) – originally built to support Desert Research and Technology Studies (D-RATS) and repurposed for this experiment – which served as the analog spacecraft. Four distinct crews were used, each with one astronaut serving as commander and three flight controllers/trainers (one of whom is chief medical officer) making up the balance of the simulated flight crew. Additionally, certified flight controllers and flight directors staffed the Flight Control Team located in the Operations Technology Facility (OTF) within JSC’s Mission Control Center (MCC) complex.

The experiment examined both baseline and mitigation methods to perform four main operations functions affected by time delay including: communications, fault management, procedure format, and situational awareness. Results of this initial experiment provided some insights into the previously mentioned questions. But this experiment also raised some additional questions. Future AMO experiments are being planned to examine some of the outstanding questions raised during the initial experiment as well as other aspects of the original set of questions. The location for these future experiments will be determined by the experiment design.

11.4.2. Desert Research and Technology Studies (D-RATS)

D-RATS is an ongoing analog test campaign that began in 1998. These tests offered engineers, astronauts, and scientists from across the country with an opportunity to come together to conduct operations and technology development research during an approximately 2- to 3-week integrated test in the southwest United States (Figure 11-2). This region offers many good analogs for possible destinations identified for future planetary exploration missions. Fifteen D-RATS integrated test have been carried out through the end of 2012. Examples of previous tests have included system demonstrations (EVAs, rovers, habitats, etc.), operations procedures (traverse planning, comparative use of multiple rovers, Earth-based support team protocols, etc.), and communications networks and protocols. Each test or simulation is structured to accomplish an integrated set of objectives and experiments based on mission design and technology development questions of importance at the time of the D-RATS deployment.

For the past several years the D-RATS analog campaigns have been conducted at the Black Point Lava Flow (BPLF), shown in Figure 11-3. Several other sites in the southwestern United States were used for these D-RATS campaigns prior to 2008. The BPLF test site area is located approximately 65 kilometers (40 miles) north of Flagstaff, AZ, approximately 3 kilometers (2 miles) off of Highway 89. It has a wide variety of surface features with respect to geological relevance relative to lunar and Mars planetary terrain features. The geological features (numerous outcrop and contact lines) and terrain particularly along the edge of the lava flow provides many opportunities to evaluate simulated planetary surface EVA science/exploration capabilities during single-day or multi-day science-driven sorties.



Figure 11-2 D-RATS testing at the BPLF.

The BPLF is part of the San Francisco Volcanic Field. The area was originally identified as a candidate lunar analog site during the Apollo era. At that time, the east end of the lava flow and the valley of the Little Colorado River were examined for training and simulations of lunar missions. Several explosion craters were blasted out of the top of the lava flow to simulate an impact crater field on the lunar surface. Although the site was abandoned during Apollo in favor of other test sites, it became a major lunar analog test site during the Constellation Program. Several 1- and 3-day simulations of lunar missions were conducted in October 2008 along the western and southwestern portions of the flow. The site was used again to simulate a 14-day lunar mission in September 2009. In 2010, the site was greatly expanded to the west so that it includes the cinder cone and lava flow. Mission simulations in 2010 utilized two Space Exploration Vehicles (rovers each with 2 crew) and other assets to simulate the operational requirements of a 28-day mission to the Malapert Massif region of the Moon, which is along the margin of the immense South Pole-Aitken Basin, the oldest and largest impact basin on the Moon and possibly the entire Solar System.

11.4.3. Haughton-Mars Project (HMP)

The Haughton-Mars Project (HMP) is an ongoing analog test campaign that also began in 1998. This Project began as a primarily scientific research activity using the Canadian Arctic as a physical and environmental analog for Mars. However, from the outset this Project has offered engineers and scientists an opportunity to come together to conduct operations and technology development research during a 4- to 8-week summer field season in the Canadian Arctic. This region offers several good physical and operational analogs for destinations for future planetary surface exploration missions, primarily Mars. Fifteen HMP missions have been carried out through 2012. Examples of previous tests include EVAs, robotic rovers, small pressurized rovers, small-scale robotic and human operated drills, long-range (100+ kilometers) traverses, and communications networks and protocols (Figure 11-4). Each test is structured to accomplish a set of objectives and experiments based on mission design and technology development questions of importance at the time of the HMP deployment.

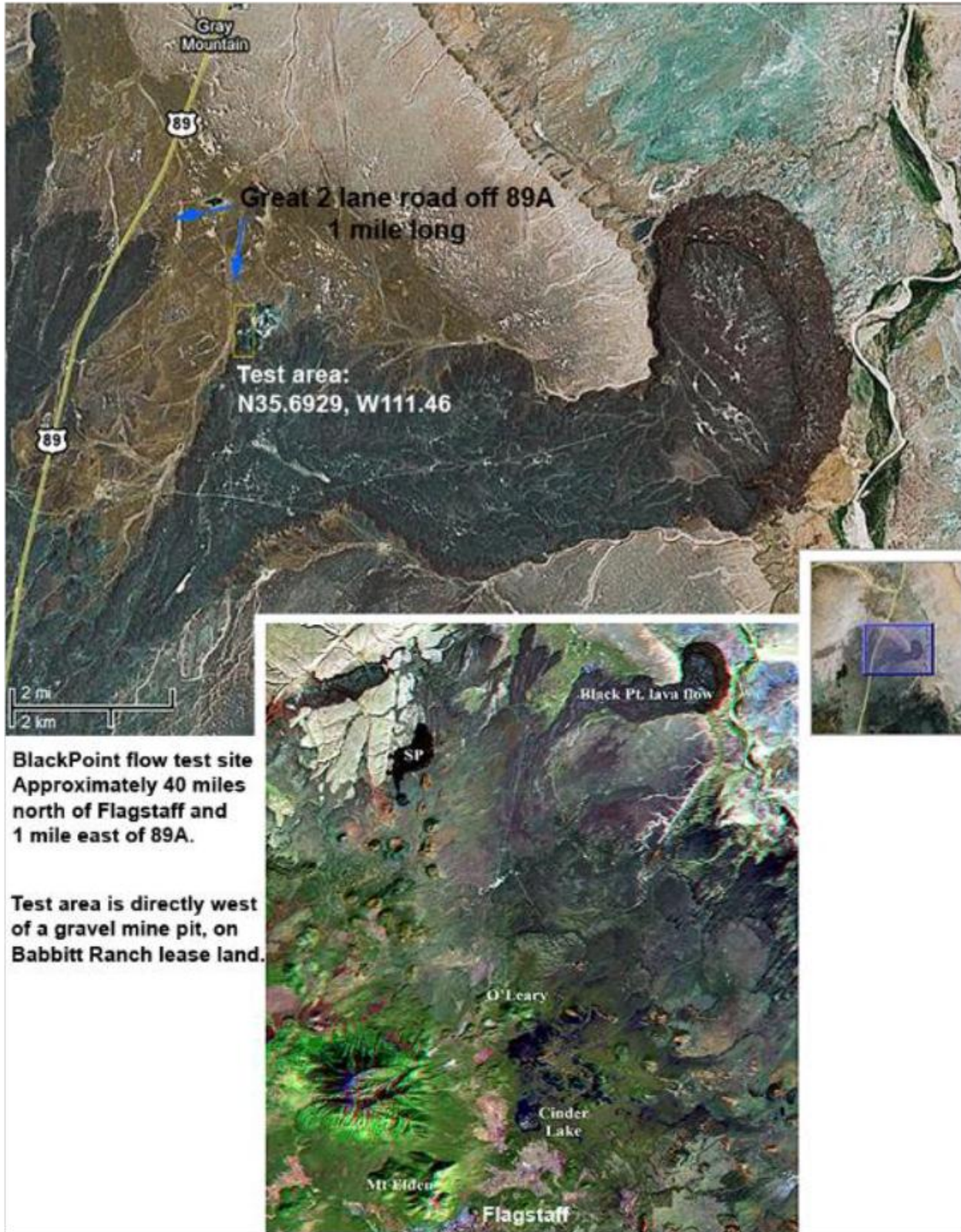


Figure 11-3 BPLF test site.



Figure 11-4 HMP traverse tests.

The HMP Research Station (HMPRS) is located on Devon Island in the Canadian Territory of Nunavut . HMPRS is located on the rim of the 20 km-diameter and 39 MY-old Haughton impact crater (Figure 11-5). This location was selected as the analog location for future lunar and Mars surface exploration missions. Devon Island provides the following characteristics:

- Relatively large area (many square kilometers) accessible for tests;
- Free of vegetation, human-built obstructions (e.g., fences, roads, etc.), or other ground cover (e.g., snow, ice, etc.);
- Terrain features and topography representative of several different destinations identified for future human planetary exploration missions, including Mars surface terrains (craters, gullies, lakebeds, ice sheets, etc.) and the lunar south pole region; and
- Areas where a wide variety of analog activities (e.g., drilling into various terrain types, long traverses over representative topographic features, investigation of habitats for extremophiles, etc.) could be successfully carried out over a relatively large scale.



Figure 11-5 HMPRS

11.4.4. In-Situ Resource Utilization (ISRU)

In-situ resource utilization (ISRU) is a title covering a broad range of technologies used for gathering local raw material and processing those material into useful commodities for in-space and planetary surface exploration. This activity has been focused largely on laboratory-scale testing of components, subsystems, and, recently, full systems. In 2008, field testing of several individual systems began, working together in an analog environment (Figure 11-6). These tests involved international participation. Two additional field tests of these ISRU integrated systems have been carried out through the end of 2012. These tests involved several key technologies for ISRU, including robotic drilling and sampling, excavation, transport, oxygen production, and water production. The tests were led by NASA-Kennedy Space Center (KSC) and involved participation by researchers from KSC, JSC, Jet Propulsion Laboratory, the Canadian Space Agency, the Northern Centre for Advanced Technology, and the German Space Agency, along with other industries and universities.

The integrated ISRU tests have used a single site for these activities – the Pacific International Space Center for Exploration System (PISCES). PISCES is an international research and education center dedicated to the development of new technologies needed to sustain exploration on the Moon and beyond (Figure 11-7). PISCES was created in March 2007 as an official Center at the University of Hawai'i at Hilo and was first funded by the Hawai'i State Legislature in June 2007. The Center is being built on partnerships between industry, academia, and the governments of spacefaring nations around the world. PISCES offers an analog environment with lunar- and martian-like regolith, craters, cinder cones, and large areas for robotic traverse and pilot-scale testing. The current PISCES Test Site is located on land managed by the Department of Land and Natural Resources of the State of Hawai'i. PISCES was conceived by the Japan-U.S. Science, Technology & Space Applications Program under the auspices of the Hawai'i State Department of Business, Economic Development & Tourism.



Figure 11-6 ISRU field testing at the PISCES Test Site.



Figure 11-7 Rover testing to support ISRU demonstrations at the PISCES Test Site

11.4.5. International Space Station Test-bed for Analog Research (ISTAR)

International Space Station Test-bed for Analog Research (ISTAR) was initially established in 2010 to 1) facilitate the use of the ISS, Figure 11-8) as a test platform to reduce risks for manned missions to destinations beyond LEO (i.e., Exploration missions), 2) utilize ISS as a micro-g laboratory to demonstrate technologies, operations concepts, and techniques that mitigate the risks of crewed Exploration missions, 3) utilize the ISS facility as an in-space testbed to exercise crew activities during simulations of Exploration missions to mature operational capabilities for crewed missions, 4) conduct long-duration Mars Transit and Landing Transition simulations utilizing technology and operational tools and concepts developed and tested during previous ISTAR and Earth-based analogs, and 5) strategically plan increasingly complex ISS-based exploration mission simulations.

To date, initial ISTAR missions starting with ISS Increment 31, by necessity, have focused on discrete exploration forward activities (e.g., Communications Delay Countermeasures, Autonomous Procedures, Tele-robotics, EVA suit microbial sampling, Anthropometric measurements, Radiation Dosimetry). ISTAR has also developed a notional ISS Mars SIM plan and begun to coordinate with HEOMD's AES projects to refine simulation objectives and solicit participation from other AES projects.

Additionally, the ISS Expert Working Group Team 6, composed of NASA (including ISTAR) and International Partner (IP) members, was established to study ISS-based ops simulations and technique. This team is developing a response to a Russian Space Agency (RSA) proposal to fly a Russian crewmember on ISS for 1 year and execute a Mars simulation similar to the Mars 500 ground analog. ISTAR is a major contributor in the effort to develop and execute the ISS Mars simulation plan.



Figure 11-8 International Space Station as an analog test facility.

11.4.6. NASA Extreme Environment Mission Operations (NEEMO)

The NASA Extreme Environment Mission Operations (NEEMO) project (Figure 11-9) sends groups of NASA astronauts, employees, and contractors to live in *Aquarius* (an underwater habitat; see next section) for up to 3 weeks at a time. Sixteen NEEMO missions have been conducted through the end of 2012. Examples of tests have included EVAs, rovers, off-loading/deployment/assembly of large systems in simulated reduced gravity, human

performance, and communications protocols. Each mission is structured to accomplish various objectives and experiments based on mission design and technology development questions of importance at the time of the NEEMO mission. *Aquarius* provides NASA with a convincing analog to space exploration in microgravity and hypo-gravity scenarios, and NEEMO crewmembers experience some of the same tasks and challenges underwater as they would in space or on planetary surfaces.

NEEMO's only test location is the National Oceanic and Atmospheric Administration's underwater laboratory *Aquarius*, located in the Florida Keys National Marine Sanctuary. The isolation and real hazards of this laboratory's environment make it an excellent site for testing space exploration concepts.

Similar in size to the ISS's living quarters, *Aquarius* (Figure 11-10) is the world's only permanent underwater habitat and laboratory. The 14-meter-long (45-foot-long), 4-meter-diameter (13-foot-diameter) complex is 5.6 kilometers (3.5 miles) off the Key Largo coast. A surface buoy provides connections for power, life support and communication to the habitat that sits about 19 meters (62 feet) below the surface.

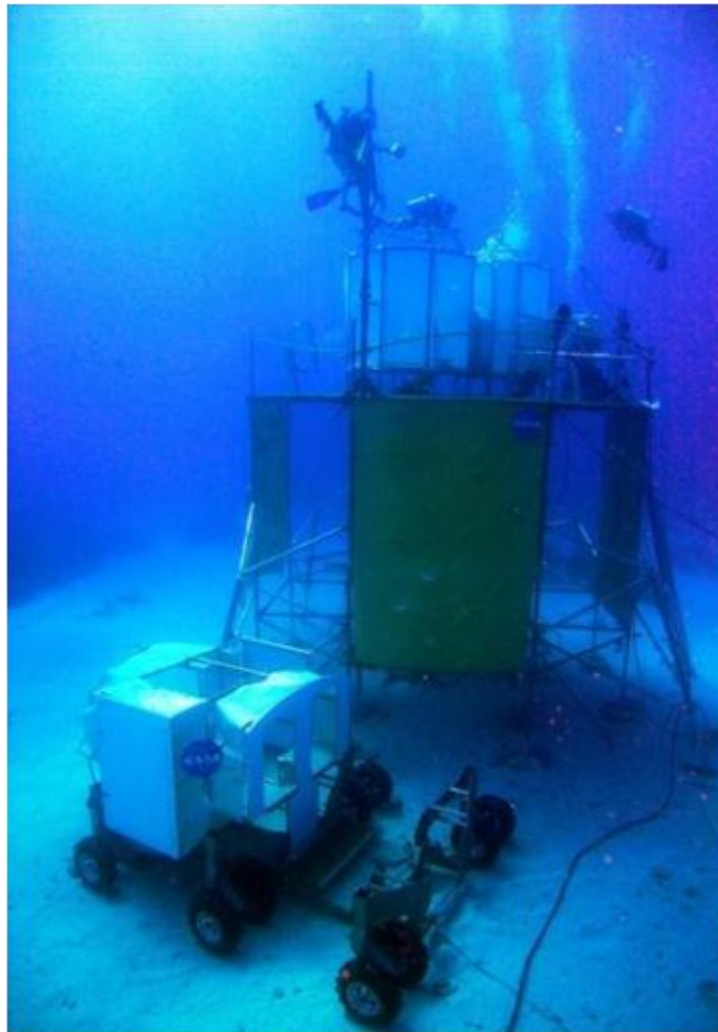


Figure 11-9 NASA Extreme Environment Mission Operations analog testing.



Figure 11-10 The Aquarius testing facility.

Long-duration missions, lasting up to 3 weeks, provide astronauts the opportunity to simulate living on a spacecraft and execute undersea EVAs. During these activities, they are able to test advanced navigation and communication equipment and future exploration vehicles. With proper buoyancy measures taken into account, the gravitational effects encountered on different planetary surfaces (e.g., the Moon or Mars) or the microgravity of space can be simulated as part of these tests. These tests cultivate an astronaut's understanding of daily mission operations, and create realistic scenarios for crews in close quarters to make real-time decisions.

11.4.7. Pavilion Lake Research Project (PLRP)

Pavilion Lake Research Project (PLRP) is an international multi-disciplinary collaboration in astrobiology and exploration science conducted in British Columbia, Canada. The primary scientific research goal of the PLRP is to explain the origin of freshwater microbialites in Pavilion Lake and nearby lakes. The PLRP has been conducting this research since 2004. Microbialites provide an analog for the biogeochemical processes active on early Earth and potentially on other planets such as Mars. PLRP research is conducted from the lake's surface, as well as underwater. Exploration equipment and procedures are carefully selected to best suit specific science goals of the PLRP. However, research and exploration using remotely operated vehicles (ROVs), autonomous underwater vehicles (AUVs), scuba divers, and submersibles provide analogs for the functional equivalent of these tools that will be used for human exploration missions on the Moon, Mars, and small bodies (i.e., near-Earth objects [NEOs]). As such, the PLRP has collaborated with engineers and scientists investigating future human exploration missions to take advantage of this functional and operational analog.

PLRP has two principal locations at which its scientific investigations and analog simulations are conducted: Pavilion Lake and Kelly Lake in British Columbia, Canada. Pavilion Lake is located in Marble Canyon, British Columbia, between the towns of Lillooet and Cache Creek (30 kilometers, or 18.3 miles, WNW from Cache Creek) and lies along BC Highway 99. The lake is 263 hectares (650 acres) in size. Kelly Lake is located in this same region of British Columbia, approximately 16 kilometers (10 miles) due north of Pavilion Lake. Kelly Lake is smaller than Pavilion Lake, 46 hectares (114 acres) in size. Both lakes are part of a karst formation, and are most notable for being home to colonies of microbialites, a type of stromatolite. The microbialites in these two lakes provide an analog for the biogeochemical processes active on early Earth and potentially on other planets such as Mars.

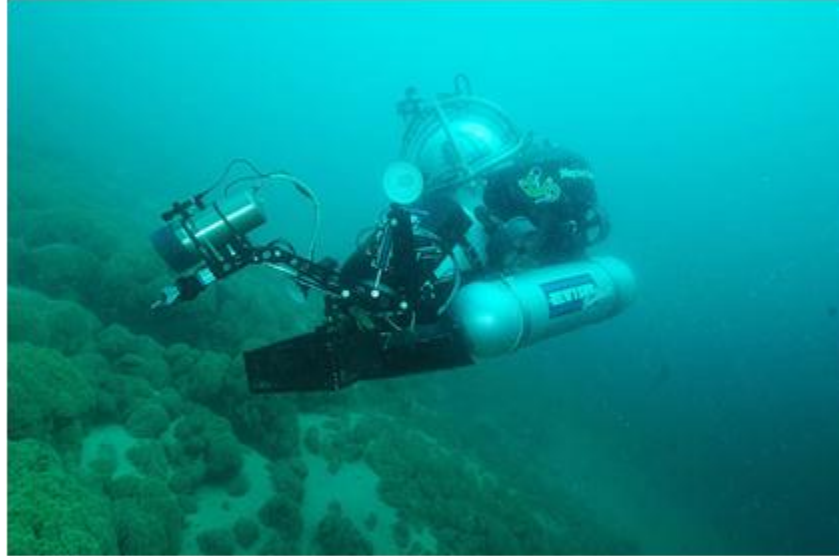


Figure 11-11 Single-person submersibles as analog traverse vehicles supporting the Pavilion Lake Research Project.



Figure 11-12 Pavilion Lake Research Project traverse analog planning.

11.4.8. Analog Project/Mission Locations

Figure 11-13 illustrates the wide range of geographic locations used for analog tests over the past several years. Other locations are feasible (depending on the test or simulation being conducted) and there are other locations that have been used. Those shown here apply to the examples described in this section.

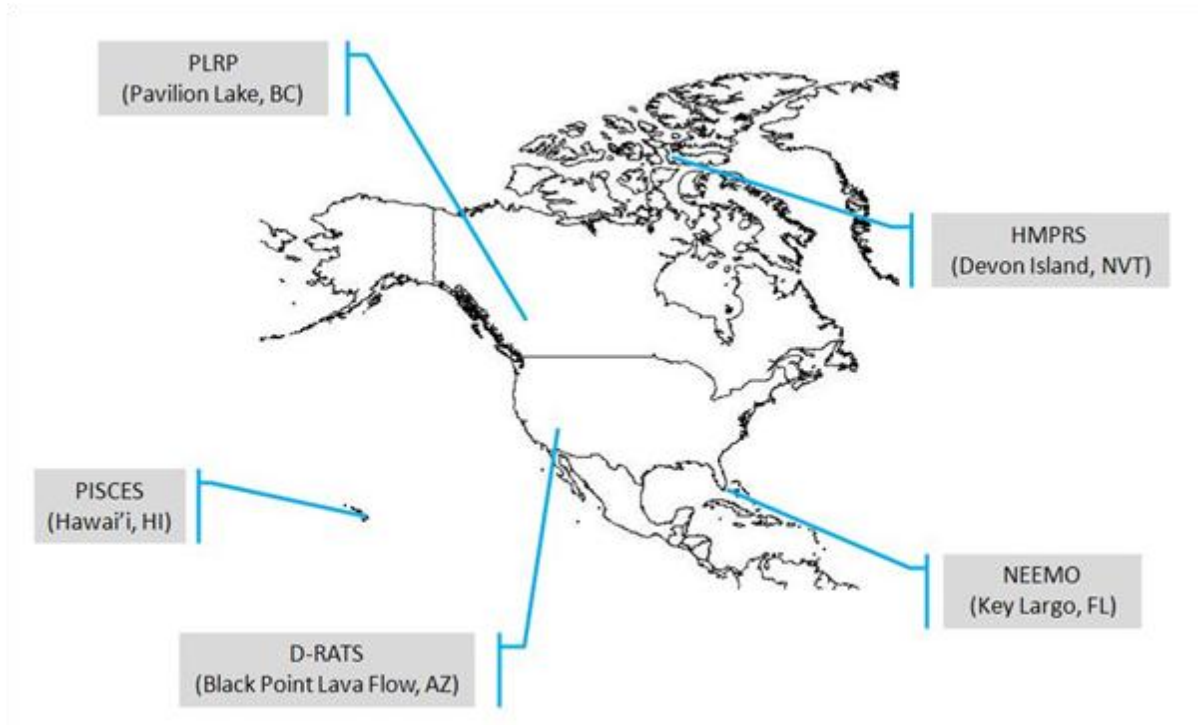


Figure 11-13 Analog mission and testing locations.

11.4.9. Other Relevant Analog Projects and Missions

The examples cited in the previous section have been taken from analog projects conducted primarily with support from and addressing questions for NASA and, to a limited degree, by the Canadian Space Agency. Other national space agencies and research organizations are also conducting analog tests and missions that will have an impact on the evolution of future Mars surface and orbital missions. Several recent examples of these analog activities are summarized here.

Inflatable habitats. NASA has a history of experimenting with lightweight inflatable structures as a means of reducing the mass and volume of their habitation infrastructure. Technologies and design concepts developed since the 1990s show promise toward meeting the mass and volumetric challenges posed by future planetary surface missions, such as a Mars surface mission (Figure 11-14). However, it is also required that these concepts be placed in a more challenging environment under more representative operating conditions to better understand their utility and durability.

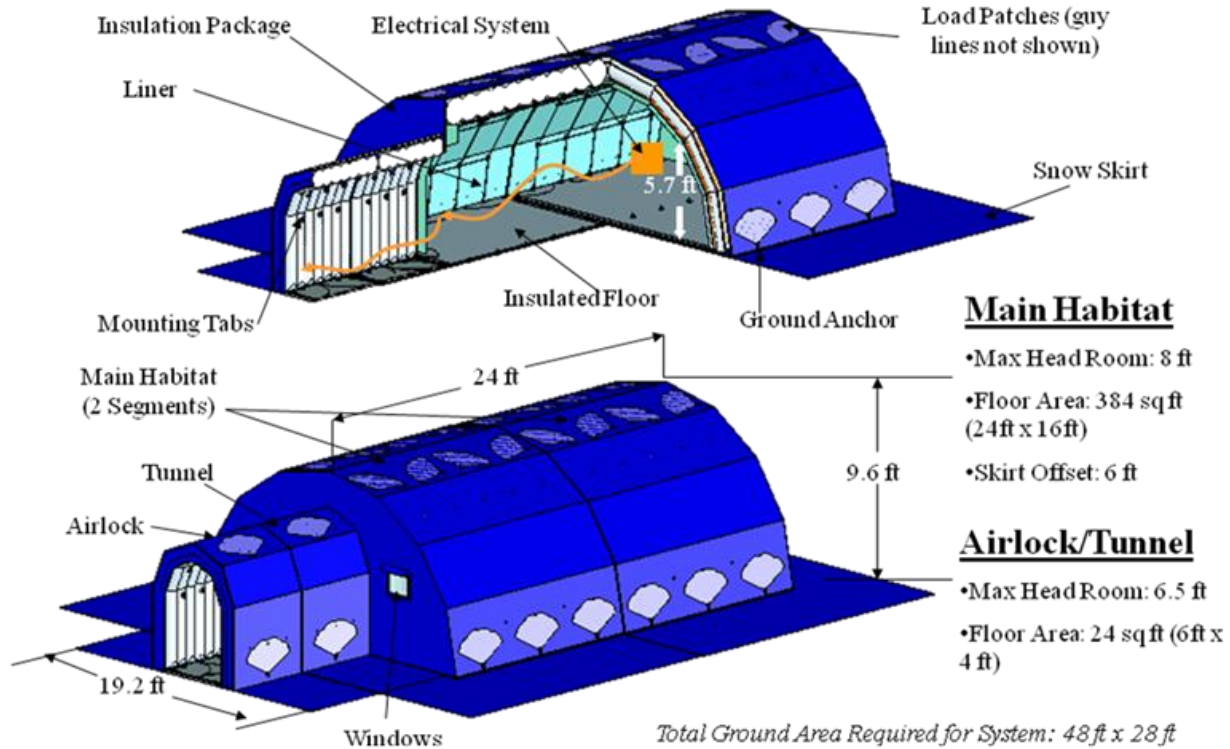


Figure 11-14 Inflatable habitat analogs as tested at McMurdo Station, Antarctica.

NASA and the National Science Foundation (NSF) both have a responsibility to send human crews into harsh environments for scientific and exploration purposes while providing the infrastructure that allows them to carry out these tasks in a safe and productive manner: NASA is preparing to send human crews to Near Earth Asteroids, the vicinity of the Moon, and eventually to Mars; the NSF has an ongoing need to explore Earth’s polar regions as efficiently as possible. A major portion of this infrastructure needed to operate in both of these environments is habitation that remains viable for extended periods of time – measured in weeks or months. In addition, both of these agencies must provide this infrastructure at the end of a very long logistical pipeline, making low mass, efficient packing, and high durability highly desirable characteristics.

In 2007 NASA and NSF teamed with ILC Dover to design, construct, and test a proof-of-concept inflatable habitation structure, focusing on its deployment characteristics and durability in a representative harsh environment – the Antarctic (Figure 11-15). In this partnership ILC Dover constructed the primary inflatable structure and portions of the interior outfitting, NASA developed the data system that monitored and transmitted performance data during the deployment phase, and the NSF transported the entire system to the Antarctic and assisted with the deployment at McMurdo Station. The habitat was made of two elements: the main habitation area and a simulated airlock. The main habitat area was separated into two halves that were connected with zippers, and had internal dimensions of 4.9 meters x 7.3 meters x 2.4 meters (16 feet x 24 feet x 8 feet) when fully inflated. The inflated tubular walls of this element were 0.48 meters (19 inches) thick. The simulated airlock was also connected to the main habitation area with zippers, and the inflated tubular wall thickness was 0.30 meters (12 inches). The simulated airlock area when fully inflated was 1.2 meters x 1.8 meters (4 feet x 6 feet).

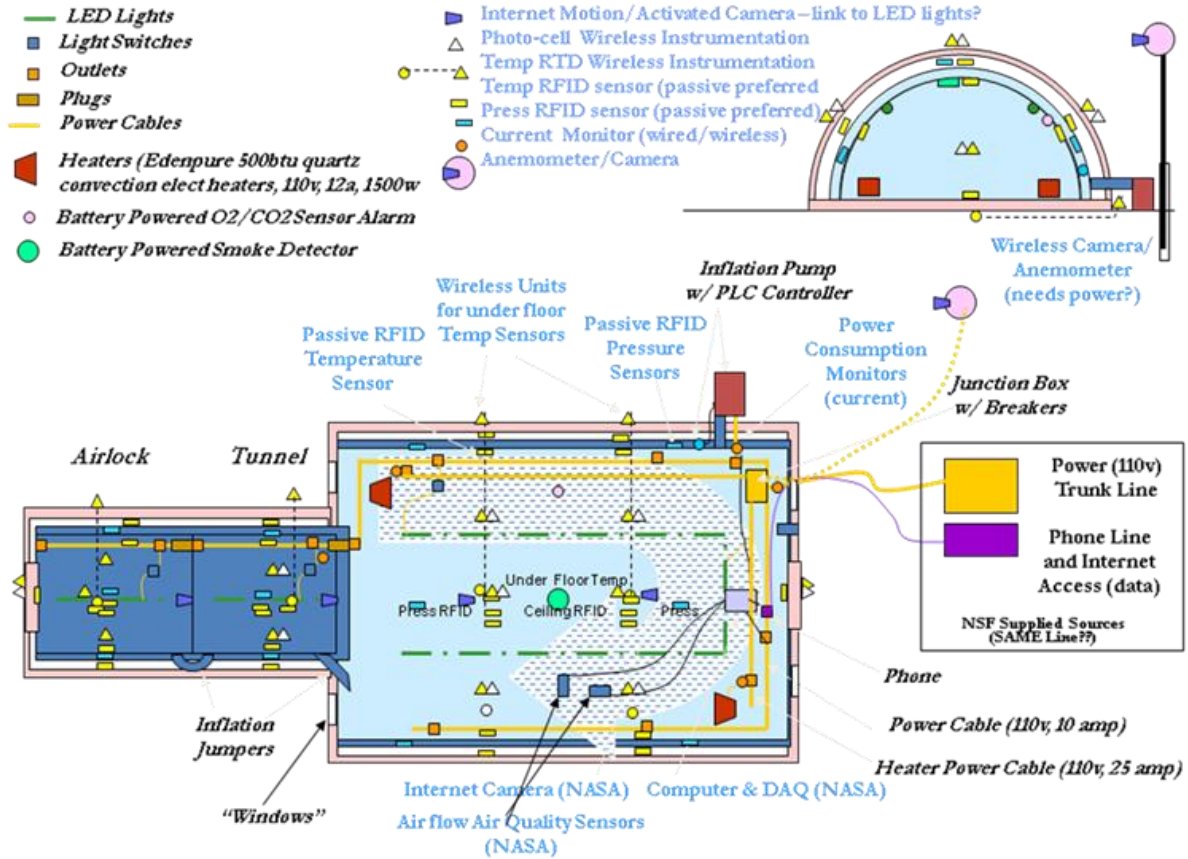


Figure 11-15 NASA, NSF, ILC Dover inflatable habitat testing.

The 453 kilogram (996 pound) system was packed into two 1.21 meter x 2.43 meter x 0.76 meter packages (4.53 cubic meters), and provides a living space of 70.8 cubic meters, yielding a 15:1 packaging efficiency. The flexible nature of the materials allowed the shape of the two packages to be altered to fit the transport vehicle to facilitate simple transport. The entire system was packed and deployed approximately 20 times throughout the course of manufacture and test prior to deployment in Antarctica. The final packing event was conducted by five people in 1 hour and yielded the two soft packed packages described previously (the airlock was included with one of the packages). The habitat was transported to McMurdo Station in January 2008, where it was deployed by a three-person crew in under 50 minutes (Figure 11-16). The inflation event took 12 minutes using a standard blower. The deployment team wore full body Extreme Cold Weather Gear (ECWG) during the set-up to simulate wearing space suits. Mobility was comparatively better in ECWG, but still gave some idea of human interface issues astronauts might face.



Figure 11-16 Testing at McMurdo Station in January 2008.

Following several deployment tests, the habitat was operated (unoccupied) for 12 months. NASA designed a data system to monitor and transmit performance data over a (local) wireless network using existing instrumentation, and then remotely monitored the habitat state over the 12-month deployment period via an Internet connection through the McMurdo local network to JSC. Structural health monitoring and performance data were taken throughout the year and occasionally some of the sensors or equipment would experience off nominal readings, drop outs, or malfunction. (In cases of data drop outs or malfunctions, NASA would evaluate the data and, working with ILC Dover and the NSF, put together appropriate field test and evaluation plans to determine the issue and resolution.) These data helped to assess the durability, performance, and operability of this inflatable habitat concept. Additionally, NASA used this instrumentation system to validate the use of various sensor systems for data acquisition and management.

This project provided invaluable experience in understanding the process of developing, deploying, and monitoring an inflatable habitat in a harsh analog environment. The system demonstrated, through testing in the analog environment, that inflatable systems have high packing efficiencies, are rugged and durable, and can withstand extreme environments. The habitat showed the reusable nature of these structures and their ability to be reconfigurable. Embedded sensors were found to be ideal for a structural health monitoring system, as they essentially combine the health monitoring system into the habitat structure. Along with embedded sensor technologies, it will be necessary to develop new manufacturing techniques to embed the sensors directly into the structural materials. Using a wireless system to gather data from these embedded sensors proved very useful, as it reduced wiring and mass. In conducting this exercise, all three partners were satisfied with the “lessons learned” that emerged. Many of these lessons will likely be implemented in the development of future habitats and habitat monitoring systems that will meet the mission requirements for living and working safely on the lunar and martian surface.

Long-duration mission simulation. In a test conducted at the Russian Institute for Biomedical Problems (IBMP) in Moscow, a group of national space agencies, including ESA, and research organizations carried out a 520-day

simulation of a human Mars mission, called Mars500 (Figure 11-17). The purpose of the Mars500 study was to gather data, knowledge, and experience to help prepare for a real mission to Mars. Sealed in a chamber at IBMP in June 2010, the six crew members (three Russian, two European, and one Chinese) had only personal contact with each other plus voice contact with a simulated control center and family and friends as is currently expected to take place during a human spaceflight mission. A 20-minute delay was built into communications with the control center to simulate an interplanetary mission and the crew was given almost an identical diet to that used for the ISS. The study helped to determine key psychological and physiological effects of being in such an enclosed environment for such an extended period of time.



Figure 11-17 Mars 500-day test conducted at the Russian IBMP in Moscow.

11.5. ANALOG CAMPAIGNS (by year and location)

Several of the analog projects just discussed have been in operation for many years prior to the completion of DRA 5.0. Where applicable, lessons learned from the individual analog mission simulations and tests were incorporated into DRA 5.0. Analog mission simulations and tests carried out since the completion of DRA 5.0 continue to influence the evolution of this architecture. Figure 11-18 shows the instances when each of these analog projects carried out one or more mission simulations or tests of particular relevance to DRA 5.0 (although not always directly simulating some aspect of a Mars mission). (Note: several of these analog projects, such as D-RATS, HMP, and PLRP, conducted activities during all of these years, but in some years the activities were not closely tied to some aspect of DRA 5.0 and thus there is no indication of a specifically relevant activity in that year.)

	2007	2008	2009	2010	2011	2012
AMO						▲
D-RATS		▲	▲	▲	▲	▲
HMP		▲	▲	▲	▲	
NEEMO	▲			▲	▲	▲
PLRP			▲	▲	▲	

Figure 11-18 Analog testing history.

There are many specific lessons learned during any particular analog mission or test in each year indicated in this table. There are also several broader lessons learned that only became apparent after several years in a particular analog project or when looking across the results from several projects. Several of these broad lessons are discussed in the following paragraphs.

Pressurized versus unpressurized rovers for surface exploration. One of the many lessons learned from the later Apollo missions was that basic transportation, in the form of the Lunar Rover Vehicle (LRV) (Figure 11-19), was an immense help in improving the productivity of and increase the range of exploration achievable by the human crews during the surface exploration mission. But mission rules and practicality constrained any particular excursion to the time period defined by the consumables in the Portable Life Support System (PLSS) – a.k.a. the “backpack” – and the distance that the crew could walk back should the LRV become disabled. For the roughly 3-day duration of an Apollo surface mission, this was not a particular hardship. However, Mars surface missions as described in DRA 5.0 will be substantially longer in total duration. Thus, substantially expanding the range and duration of traverses beyond that achievable during Apollo will be necessary for the crew to remain productive during the full duration of a Mars surface mission. A similar desire to expand these surface traverse capabilities for lunar missions, the initial destination in the Constellation Program at that time, led to an analog mission in 2008 in which two different surface transportation approaches – an unpressurized rover (UPR) (Figure 11-20) capable of carrying additional consumables (significantly expanding on the LRV capabilities) and a small pressurized rover (SPR) (Figure 11-21) – were compared as part of the D-RATS project. Conceptually, two of each type of rover would be deployed for a surface traverse in order to provide mutual support.

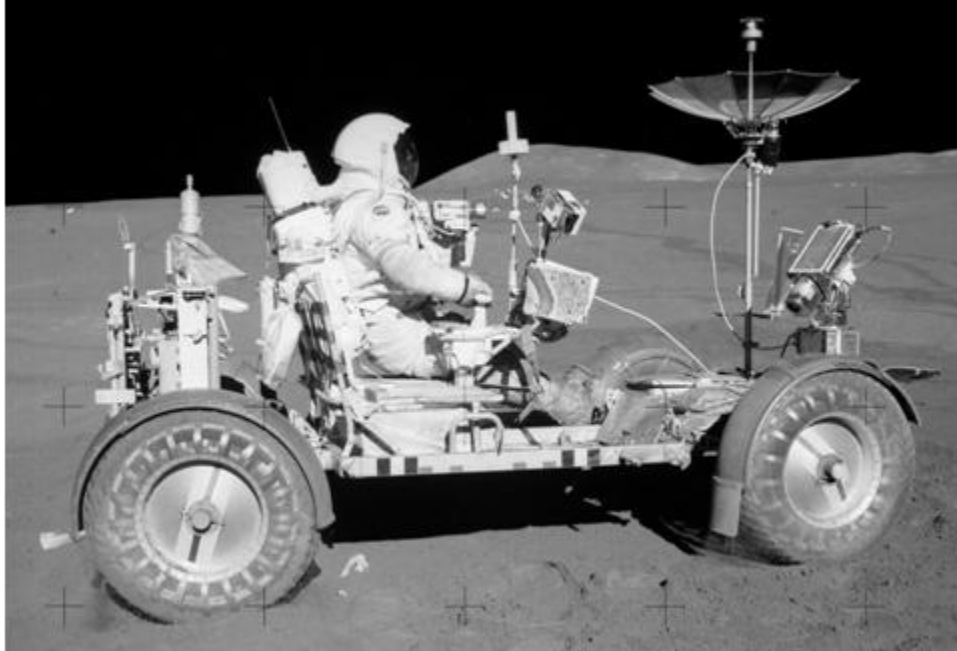


Figure 11-19 Apollo LRV.



Figure 11-20 D-RATS unpressurized rover tests.

In the SPR concept, each vehicle includes a small pressurized cabin to safely sustain two crewmembers on the surface for 14 to 28 days. Crewmembers could rapidly egress and ingress the cabin for EVAs through suit ports, a concept in which the EVA suit remains on the outside of the pressurized cabin and the crew gains access to the suit by means of a small hatch that is sealed by the PLSS backpack. In addition to achieving a surface exploration range that is potentially orders of magnitude greater than what was achievable during the Apollo Program, the SPR

concept is expected to offer numerous health and safety advantages that will accrue from having a pressurized safe haven and radiation shelter in close proximity to the crew at all times during surface operations.



Figure 11-21 D-RATS pressurized rover tests.

The primary purpose of the D-RATS 2008 field test, conducted at the BPLF in Arizona, was to objectively and quantitatively compare the scientific productivity and human factors during 1-day exploration, mapping, and geological traverses performed using SPR and UPR prototype vehicles. The habitability, human factors, and performance characteristics of the SPR vehicle and crew were also recorded throughout a high-fidelity 3-day lunar traverse simulation. Before the field test began, a detailed test protocol and flight plan were developed including hypotheses, metrics, and prospectively defined levels of practical significance to be used in the testing of all hypotheses. Details regarding these protocols and the test results can be found in the Desert RATS 2008 Final Report¹.

Quantitative assessment of crew productivity by an on-site team of expert field geologists found that compared with UPR traverses, the same crewmembers were 57% more productive during SPR traverses and used 61% less EVA time. The study also indicated that the SPR increased comfort and decreased fatigue over the UPR. The habitability and human factors of the SPR throughout the 3-day traverses was acceptable according to the prospectively defined human factors metrics and acceptability criteria, although suggested modifications to several vehicle subsystems were identified in the assessment.

Similar productivity results are expected for Mars surface mission and vehicle sized for a two-person crew with a roughly 14- to 28- day endurance are considered reasonable performance characteristics (assuming multiple traverses during the entire Mars surface mission). Thus, the overall results and recommendations from this 2008 test are considered directly applicable for Mars surface missions and two SPRs are part of the manifest for these missions in the DRA 5.0. However, the DRA 5.0 manifest also carries two smaller UPRs (comparable in size and capability to the LRV) to be used for short-duration and short-range activities in the vicinity of the surface habitat.

Mission operations impacts of communications time delay. To date, NASA has operated its crewed missions primarily from Earth, locating a large fraction of the people involved on the ground and thus allowing the on-board crew to be smaller, the vehicles to be simpler and lighter, and the mission performed at a lower overall cost.² However, as mission destinations beyond the Moon are contemplated, it has been widely recognized that the increasing time delay between Earth-based mission personnel and the flight crews will mean that more and more of

the previously ground-based operations must be migrated to the spacecraft and its crew. Determining how much of what kinds of operations should be migrated involves a great many interrelated factors and has not been easy to determine. Analogs have been one of the primary tools to investigate options for this issue and many of the previously described analogs have included time delay experiments in some form.

In October 2012, the AES Analog Missions Project conducted a Technical Interchange Meeting (TIM) with stakeholders to share information and experiences of studying time delay, to build a coherent picture of how studies are covering the problem domain, and to determine possible forward plans (including how to best communicate study results and lessons learned, how to inform future studies and mission plans, and how to drive potential development efforts). It included all of the known studies, analog missions, and tests of time delayed communications dating back to the Apollo missions including many of the analogs described previously plus several other relevant examples, including Mars 520-day Simulated Mission, JPL Mars Orbiters/Rovers, and Apollo experiences. Additionally, the meeting attempted to capture all of the various functional perspectives via presentations by disciplines including mission operations (flight director and mission planning), communications, crew, Capcom, EVA, Behavioral Health and Performance (BHP), Medical/Surgeon, Science, Education and Public Outreach (EPO), and data management. Figure 11-22 summarizes the range of time delay experiments and their basic characteristics that were identified in preparation for this TIM.

	AMO	DRATS	DSH	ISTAR	NEEMO	PLRP
Year Performed	2012	2010 2011 2012	2012	Will be Incr 35/36	7: 2004 9: 2006 13: 2007 14: 2010 16: 2012	2011
Test Duration	8 days	2010: 14 2011: 9 2012: 10	10 days	90-180 days	7:15 days, 9:18 days, 13:10 days, 14: 14 days 16:12 days	7 Days
Time Delay (One Way Light Time)	1.2, 5, 50, 300 s	2010: 0s 2011: 50s 2012: 50, 600, 1200s	50 sec	50s?	7: 0-2s, 7: 0-2s, 13: 20m, 14: 20m 16:50s,5m,10m	NEA (50s)
Continuous Operations (with Time Delayed Communications)	2hrs	2010: - 2011: 9 hrs 2012: 9 hrs	5 days	16 hrs (audio), cont.	6 days	3 hrs
Communications Coverage	Cont.	2010: Cont., 2x/day 2011: Cont. 2012: Cont.	Cont.	16 hrs (audio), cont.	Cont.	Cont.
Number of Crew	4	2,4,4	4	1	6,6,6,6,6	1(sub pilot)
Number of Ground Controllers	8	42,19,5	12	varies	2,2,8,10,20	15

Figure 11-22 Summary of time delay experiments.

In addition, the presentation materials presented are available on the Internet at:
https://oasis.jsc.nasa.gov/projects/advdev/analogs/Delay_TIM/default.aspx

At the conclusion of this TIM the following recommendations were prepared by the group attending the meeting (Note: These recommendations are simply a subset of extracted recommendations from the presentations and does not represent the full set of recommendations):

Improvements for Future Studies

- 1 Incorporate bandwidth and coverage limits with delayed communications to best understand how operations is affected.
 - a. Also include multi-day operations (with planning cycle based on downlinked data) to understand how limits on total data volume downlinked affects operations.
 - b. Develop a compelling story on communications bandwidth and coverage requirements to drive Missions.
- 2 Need additional study of emergency/contingency operations under delay
 - c. Include better/more consistent training & procedures.
 - d. Need a greater sample of participants and runs. (include standard measures)
 - e. Consider leveraging military experience (subs, out of comm, etc.) or others?
- 3 Need to document GPS/Positioning requirements.
 - f. Suggest designing test(s) to determine effects (and requirements) of different positioning methods (manual, limited, full).
- 4 Need better studies to start more concretely understanding flight/ground autonomy split/allocation and the crew/SW partition (for onboard autonomy)
 - g. Also the allocation to robotics.
- 5 Need additional studies of the effects of extended delay on humans
 - h. Include development and testing of mitigations.
- 6 Need to make progress on how we will realistically make EVA work with the required crew autonomy caused by time delayed comm.
 - i. How do we reduce the risk compared with current EVA technologies/techniques?
 - j. Consider adding simulated EMU data for future integrated testing (with simulated issues)... Really all system data.
- 7 Establish rigorous voice protocols (over, out, references, etc.)

Improvements for Tools and Systems

- 1 Incorporate voice transcription and voice commanding capabilities (along with further study on what is needed and/or the best way to use these capabilities).
- 2 Add a leading and trailing line on the timeline (by the time delay) that shows the relative times on the remote side.
- 3 Consider integration of tools and timeline based data (i.e. console logs and texting logs and procedures).
- 4 Note JPL developing timeline based file formats/protocols should be considered/included in the requirements for any custom tool development.
- 5 Consider any changes due to coming Heads-Up displays and voice to text (transcription and commanding).
- 6 For texting application, include “new message” alert AND message read (sent back to the sender).
- 7 Could have a “read”, “yes”, or “no” buttons.
- 8 Develop a custom tool(s) that provides a voice message recording “Tivo” or “Voxer” like capability and incorporates noted requirements.
- 9 Recommend first compiling a full set of functional requirements.
- 10 Need voice call & texting ID/subject/sequence tagging to ensure responses are correlated.
- 11 Study capability for multiple simultaneous text (and possibly) voice conversations/threads (multi end points on both ends) (vs. single Capcom to all crew).

Science Operations. Several key science operations lessons have been learned during the analogs discussed previously. The conceptual roles and responsibilities of a science management team, with a tactical and strategic component as well as a suite of software tools and systems, has grown and evolved as they have been applied in a variety of analogs. This diversity of analog applications has helped to make the concept more robust as well as helping it to evolve in a direction that allows a common approach to be applied to missions at any of these future destinations, be that the Moon, a NEO or Mars.

As background for this discussion it is important to understand the difference between “management oversight” and “collegial interaction” for science operations. When discussing interactions between the flight crew and the ground team, these interactions are typically assumed to be what is defined here as a management oversight function – a “do this, don’t do that” interaction. The science operations team, in contrast, spends more time considering science

return, which is a two-way street. This is critical to understand preparations for future planetary surface missions – the science operations team is not telling the flight crew how to do science; the crew is an extension of the science operations team, exercising the concept that more individual perspectives focused on scientific questions results in better science return and enables the science operations team to be more “nimble” in taking advantage of serendipitous discoveries.

It is also useful to make a distinction between science operations management data and “pure” science data. Science operations management data needs to be available in a timely fashion – probably daily – to help make ongoing changes to the surface science plans. It can be limited in volume, based on the requirements by both the science operations team, as well as other operations teams. Pure science data is essentially everything being gathered by the crew and instrumentation supporting the mission, so by definition it is high volume. But it can be downlinked as the communications system capacity allows.

As mentioned previously, the science operations team is made up of the flight crew located at the mission destination and the ground science team. This science operations team performs both tactical and strategic functions during the course of the mission. Interaction between the flight crew and the ground science team is critical to the overall quality of the science return. However, with almost any amount of time delay (which appears to be anything more than the time delay experience on a lunar surface mission) the ground is largely in an advisory function, while the in-space assets (the deep space habitat on NEO missions or the Mars habitat on Mars missions) performs the “FCR-Forward” role (the support role played by the Flight Control Room [FCR] during Apollo lunar missions). Experiments carried out during analog simulations indicate that a useful approach for tactical science operations on a Mars surface mission will be for the ground team to look at results of the flight crew’s activities during the day and prepare a recommended plan for the next day while the flight crew sleeps. Science operations management data is also used by the ground team to determine and plan/re-plan surface science operations in the near- to far-term.

Strategic science operations planning (as opposed to tactical planning) will be critical to evaluating the science mission accomplishments as the mission progresses, and revectoring the exploration mission as new discoveries are made. During the analog simulations where this was applied, the ground team was responsible for this activity. But these analogs were of a relatively short duration. For longer missions, this activity is likely to be an effort involving both the flight crew and ground teams.

Good science training, for all flight crew members, is the key to good science return; the ability of all crewmembers needs to be developed to the point where they each act as competent science observers. This implies extensive crew training, particularly for science discipline-specific skills and for associated operations. Crews cannot be trained for observational science by simply uplinking a Computer Based Training (CBT)-file prior to an EVA; field observation tasks and science observer skills rely on long-term experience with real situations in the field. Analog situations of the type described previously have been shown to be effective training for those members of the science operations team – both flight crew and ground team – who may not have extensive professional experience with relevant science disciplines.

Developing “high-density” science information systems that allow the ground to understand and manage science data was shown to be beneficial to the mission. Significant improvement in the effectiveness of the ground team was noted in several of the previously described analogs. Several examples of the kinds of science information tools and systems include: (1) xGDS-type of geographic information systems, coupled with crew transcripts, (2) sample data management systems (e.g., DRIIMS) and (3) images available as soon as possible after each crew exploration day allows strategic analysis of daily science operations, and allows good crew/ground interaction, particularly for planning and execution of an extended science mission such as the Mars DRA 5.0 scenario. Progress has been made in developing individual component systems, but there is still a need to integrate the parts in a complete architecture and test them in the field (e.g., with geologists doing a field problem and a “ground crew” analyzing the results of each day’s activity).

In summary, analogs have been shown to be useful and effective opportunities to test and evolve individual components of science operations while interacting with other elements of the surface mission as well as providing an opportunity to integrate these components to determine their performance when functioning as a system. Continued use of analogs will provide similar improvements as understanding of the science mission matures.

11.6. *Historic Analog Campaigns*

In addition to the wide range of tailored analog mission simulations of the type describe in previous sections, a substantial reservoir of relevant data and lessons learned regarding exploration in very challenging environments can be found within the community of Arctic and Antarctic explorers. For example, during the 60-year period between von Braun's 1950s-era plan for human exploration of Mars and recent Congressional authorization of NASA's future direction for human spaceflight, more than 130 separate scientific traverses were carried out in the Antarctic. These traverses accumulated tens of thousands of kilometers of travel distance by several hundred individuals (Anon., August 2004, p. 2-7 through 2-10). This total does not include numerous resupply traverses by the United States, the Soviet Union, and other countries that maintain inland stations on the Antarctic continent. Similarly, more than 50 years of logistical support by the Canadian Polar Continental Shelf Program has accumulated a unique legacy of knowledge and lessons learned regarding scientific field traverses and surveys to the Canadian community of polar scientists. There is also a rich history of relevant lessons to be learned from exploration in the polar regions that predates the just-cited examples that are contemporary with space exploration by human crews.

Two examples of these studies of historic exploration analogs are described in this section. The first is an assessment of the Arctic voyage of the *Fram* in 1893 – 1896 for lessons that could be applied to long-duration space missions such as human mission to explore the moons of Mars. The second example is a summary from a workshop at which surface traverses in the Arctic and Antarctic were compared with future planetary surface exploration concepts.

Drifting to Mars (a white paper prepared by Stan Love; 2012 September 17) based on Fridtjof Nansen's book *Farthest North*, Modern Library, New York, 1999³

Introduction. An early human exploration mission to Mars might be planned to orbit the planet, but not go to the surface. This would save the complexity and risk of landing and re-launching. Nobody wants to endure the anticlimax of travelling hundreds of millions of miles without being able to complete the last hundred, and nobody wants to be cooped up in a spacecraft for 1 to 3 years without the opportunity to set foot on the destination. But an interesting episode from the history of polar exploration on Earth suggests that a lengthy orbit-only Mars mission could be both tolerable and successful.

The Fram Expedition. Early exploration of the Arctic was marred by disaster. Both Franklin's 1845 effort to navigate the Northwest Passage and the USS Jeannette's 1881 attempt to reach the North Pole failed spectacularly, yielding tales of ships crushed in the ice and starving, frostbitten men struggling desperately to reach safety, dragging their supplies across the jumbled sea ice.

Noted Norwegian polar explorer Fridtjof Nansen proposed a different approach. His research suggested that the north polar ice cap possessed a net drift from the region of the East Siberian Sea toward Greenland and Spitsbergen, taking about three years to cross the Arctic Ocean. He reasoned that a ship built to withstand the pressure of shifting ice could be deliberately frozen into the pack near the New Siberian Islands and achieve the North Pole by simply drifting with the ice.

After personally securing funding for the expedition, Nansen commissioned the construction of his ship, the *Fram*. Named for the Norwegian national motto, which translates as "forward," the *Fram* displaced 400 tons, 800 when fully loaded. Her hull was rounded, with no projections or plane surfaces for ice to get a purchase on. The propeller was retractable and the rudder removable. Her sides were 24 to 28 inches thick, constructed of three layers of the hardest wood and cross-braced for extra strength. The shipwright paid special attention to thermal insulation so that the inside surfaces of the outer walls would not ice up from cabin humidity. The ice-proofing design features came at a price: the ship rolled badly at sea, travelled slowly under steam, and handled poorly under sail. *Fram* carried eight small boats, including two 30-footers able to accommodate the whole crew plus ample provisions in case the ice pressure overcame the ship's reinforced hull. The 12-man crew was housed in four single and four double staterooms that all opened on a common saloon, an unusually egalitarian arrangement for ships of that era. Nansen hand-picked his crew, choosing strong, healthy men experienced on ships and in the Arctic.

Nansen equipped his ship with supplies for five years. He emphasized "good clothing and plenty of food." *Fram*

carried an extensive library, diversions such as cards and darts, and a wind-driven generator for clean, bright electric light to supplement candles and petroleum lamps during the months of winter darkness. The ship also carried a wide range of scientific instruments to measure and describe the polar environment, a primary goal of the expedition.

In 1893, *Fram* set sail from Christiania, Norway. She rounded North Cape and made her way eastward along the arctic coast of Russia. In late September of that year she was fixed in the ice at 78 degrees north latitude in the eastern Laptev Sea. Her crew converted her from a ship to winter quarters, work that included disassembling, oiling, and storing the engine and setting up a number of workshops with tools and raw materials so that the crew could create, modify, and replace equipment as needed on the voyage. One such project was to rebuild the critically important cook stove to burn plentiful bunker oil instead of limited petroleum that was also needed for lighting.

The first winter passed without major incident. The crew kept busy with science observations. These included meteorological, magnetic, and electric measurements; sea depth soundings; collection of marine life from beneath the ice; and astronomical readings to determine position. The men remained healthy, so much so that the physician got bored and started studying the minor ailments of the dogs. Nansen's emphasis on food while preparing for the expedition was prescient. Eating features prominently in his journal. The crew enjoyed large and diverse daily meals, holiday and birthday feasts, and tea and beer. Most of them gained weight: a far cry from the starvation that had been a hallmark of earlier polar exploration. For entertainment they smoked, played music, read books, and played darts and other games. A ship's newspaper appeared. One of the dogs had a litter of puppies, providing more animals for hunting and sledging.

Crew morale was generally good the first winter, but it correlated with the erratic northward progress of the ship and suffered during times of southward drift. Periodic ice pressure stressed the ship, but her design was sound and the compressive forces tended to lift her up onto the surface rather than threaten her structural integrity. The crew therefore had little cause to worry about the ship being crushed.

The sun returned in late February 1894. Despite the improved light and climate, Nansen's journal for that time mentions boredom and poor sleep, evidence of the stress of the slow and unsteady journey on men of action. The crew spent much of the summer building sledges and kayaks for a possible dash to the Pole and taking ski excursions for physical conditioning. By the fall of that year, it was evident that the ship's drift would take it past, rather than across, the North Pole. Nansen resolved to try to reach the Pole using skis and dog sleds the following spring. He selected experienced dog-sledger Hjalmar Johansen as his companion for the trip, appointing skipper Otto Sverdrup to command the crew remaining on the *Fram*. The crew spent the winter of 1894-1895 preparing equipment for the polar excursion. Their work was interrupted in January 1895 by an episode of high ice pressure that forced them to prepare to evacuate the *Fram*, but the pressure eventually relented without harming the ship.

Nansen and Johansen set out for the Pole on March 14, 1895. They travelled north with difficulty until April 7 when, at North latitude 86° 14', they realized that southerly ice drift was robbing them of progress faster than they could make it up, and turned around. Their consolation was that they had beaten the previous Farthest North record by 200 miles. They made for the recently discovered archipelago of Franz Josef Land. After many adventures and near-fatal accidents reminiscent of earlier failed attempts on the Pole, they reached land of uncertain identity in August 1895 and spent the winter in a tiny hut they built of stones and walrus hides. They resumed their southward travel in May 1896, fortuitously meeting Englishman Frederick Jackson's expedition at Cape Flora on Franz Josef Land. They secured transportation to Norway, arriving there on August 13, 1896.

Meanwhile, the *Fram* continued to drift with the ice across the Arctic Ocean. The crew spent an uneventful third winter aboard, reaching a maximum latitude of 85° 55'--only 20 miles further from the Pole than Nansen and Johansen's hard-won Farthest North. In the summer of 1896, the southward drift, opening sea ice, and liberal use of dynamite freed the *Fram* from the ice north of Spitsbergen. She sailed for Norway, arriving on August 20, 1896. Her crew at once received news of Nansen's and Johansen's recent rescue. The reunited explorers received heroic welcomes and congratulations from admirers all around the world.

Comparing the Fram Expedition to a Mars Mission. Nansen's *Fram* expedition has many themes in common with a planned orbit-only Mars mission. The size of the ship and the number of crewmembers are within half an order of magnitude of those expected for a Mars mission. The *Fram's* mission lasted 3 years, similar to a minimum-energy round trip to Mars. Scientific measurement and sampling played a large role in the *Fram* expedition, as they would

at Mars. Boredom, homesickness, and the psychological pressure of inaction stressed the crew of the *Fram* and would likely be factors in a Mars mission as well. The crew did extensive reconfiguration of the *Fram*, turning it from a ship to an ice station and back again. Space Shuttle crews did similar cabin rearrangements after launch and again before reentry, and a Mars crew would likely do the same with their own vessel. Finally, the design of the *Fram* to excel at a specific function – resisting ice pressure – came at the expense of its sailing qualities. Similar tradeoffs would also affect the design of a Mars ship.

In other ways, the *Fram* expedition was unlike a trip to Mars. The icebound ship's northward progress (and its resulting effect on morale) was erratic and unpredictable; a Mars ship's trajectory would be consistent and exquisitely predictable. Some popular leisure activities on the *Fram* – smoking, and outdoor activities including skiing and hunting – would not be available to a Mars-bound crew. Neither would the entertainment, companionship, and physical labor (and, ultimately, animal feed) provided by sled dogs. Breeding the dogs produced more dogs; analogous self-replication of electromechanical systems on a Mars flight remains firmly in the realm of science fiction. Nothing like Nansen and Johansen's heroic dash for the Pole would be likely on a conservatively choreographed Mars flight.

Lessons from the Fram Expedition for Mars Mission Planners. The *Fram* expedition's success rested on some elements that the planners of future Mars flights should take note of.

- 1 First, the expedition proves that a multi-year mission that largely confines a crew to the ship and that fails to touch its primary goal can nevertheless be tolerable to the crew and seen as highly successful by the public.
- 2 Second, the crew of the *Fram* had raw materials and workshops to repair and create equipment. This capability improved the expedition in many ways, and may even have saved it. Current spacecraft designs tend toward use of large, heavy stored spares rather than hands-on repair. A review of that policy for a Mars flight is in order.
- 3 Third, the *Fram* carried many smaller boats, including two large enough to rescue the whole crew in an emergency. The crew of the *Fram* never had to abandon ship, but lifeboats saved the crew of Ernest Shackleton's later *Endurance* expedition, and a hastily-repurposed lunar module similarly saved the crew of Apollo 13. Lifeboat capability should be considered in the design of a Mars ship.
- 4 Fourth, Nansen emphasized varied and plentiful food in planning his expedition. Good food figures heavily in his journal during the years aboard ship as a great booster of morale and maintainer of health. Food should be given a similarly high priority on a Mars flight.
- 5 Fifth, Nansen (and other notably successful polar explorers) hand-picked his crew for health, strength, experience, and temperament. In contrast, current astronaut selection policy is driven by additional considerations, and reduces the role of the commander in choosing his or her staff for a specific flight. Nansen's experience suggests that self-selection of future Mars crews could reduce the chance of personal incompatibilities hampering the mission. His story also suggests that mission risk might be reduced by choosing expedition members specifically able to tolerate long periods of monotony and inaction, very different from the action-oriented personalities currently common in space exploration.
- 6 Finally, arctic explorers were able to "live off the land" by hunting for meat, a capability that saved the lives of Nansen and Johansen after their attempt on the Pole. Although hunting won't be possible for a Mars crew, the ability to obtain and use local resources (perhaps from Phobos or Deimos) could be similarly helpful.

Surface Traverse Workshop. In August 2009, JSC hosted a 2-day workshop discussing future human space exploration missions and lessons that could be learned from traverses, driven largely by science objectives, in the Earth's polar regions. These lessons were viewed as contributing one facet of NASA's preparation to explore, over extended periods of time, the surface of the Moon, Mars, and the inner solar system. More than 60 years of extensive traverses in both the Arctic and Antarctic provided a potentially rich source of lessons for future planetary missions under analogous conditions. Results from this and a previous workshop (Hoffman, 2002) examining the similarities of space and polar exploration both indicate highly parallel activities and functional needs. However, as Henry Kissinger once stated: "History is not, of course, a cookbook offering pretested recipes. It teaches by analogy, not by maxims." So it was also recognized during the course of discussions at the "traverse workshop" (Hoffman, 2012) that NASA's current approach for long-duration planetary surface operations has fundamental differences from any of the operational approaches described by the invited speakers. Choices made regarding these

approaches drive the crew size and skill mix, as well as the system capabilities, needed to accomplish basic mission objectives. These, in turn, drive the logistical pyramid needed to support operations. The key then was to learn lessons from Arctic and Antarctic traverses and adapt them to future planetary missions. This workshop attempted to facilitate this learning process by arranging for a direct interaction between those who created the history of Arctic and Antarctic traverses with those who are tasked with creating the future history of these traverses on other planets.

The workshop report (Hoffman, 2012) documents the presentations made at the workshop and discusses several of the key findings or lessons. The presentations – visual materials and associated transcripts – are contained in appendices to this report. These appendices are considered the principal knowledge captured during this workshop; the sections of the report that precede these appendices provide background and context for the appendices and capture a summary of the discussions by those attending the workshop.

Fifty people, including the invited speakers, attended the first day's presentations. These attendees represented six different NASA Centers and several contractors or universities. The presentations consisted of: (1) Dr. Charles Swithinbank (Scott Polar Research Institute) discussing observations from the Norwegian- British- Swedish Expedition of 1949-52 and the evolution that followed; (2) Dr. Charles Bentley (University of Wisconsin) discussing the first of two perspectives on the International Geophysical Year and the evolution that followed; (3) Dr. Richard Cameron discussing the second of two perspectives on the International Geophysical Year and the evolution that followed; (4) Dr. Friedrich Horz and Dr. Gary Lofgren (NASA Johnson Space Center) discussing the Apollo lunar traverses and the associated planning along with contemporary field tests of NASA equipment and procedures; (5) Dr. Marie-Claude Williamson (Canadian Space Agency) discussing contemporary science traverses in the Arctic; (6) Dr. Mary Albert (Dartmouth College) discussing contemporary science traverses in the Antarctic; (7) Mr. John Gruener (NASA Johnson Space Center) discussing NASA's plans for potential traverses on the lunar surface in the next era; and (8) Mr. Johan Berte (International Polar Foundation) providing an overview of the new Belgian Princess Elisabeth Antarctic research station and its development.

A general recommendation from this workshop is that interaction between these two exploration communities should continue with both informal and more formalized events. Those representing both sides of this interaction (i.e., the polar traverse community and the planetary surface traverse community) reached a general consensus that there were lessons to be learned by both sides, but there is more work yet to be done to communicate and determine how best to take advantage of these lessons. Other specific recommendations stemming from these general recommendations and from discussions held by workshop participants include:

- 1 Annual or biannual workshops to review NASA analogs and National Science Foundation (NSF) polar activities (emphasis on activities of similar scope/scale); other agencies or organizations would be invited as appropriate. A workshop held in October or April would avoid overlap with the NSF Antarctic season and NASA analog season. Another option would be to coordinate this event with another major meeting typically attended by one or the other of these exploration communities (examples include the meeting of the Scientific Committee for Antarctic Research SCAR) or its Standing Committee on Antarctic Logistics and Operations Symposium or the annual Earth and Space conference sponsored by the American Society of Civil Engineers.
- 2 Personnel from large government agencies or other organizations, such as the NSF and NASA, involved in relevant field activities should invite appropriate counterparts to participate in these field activities where possible.
- 3 Detailed, independent assessments of the operational approaches used by the organizations represented in this workshop (and similar groups not represented) to understand differentiating factors. Results of these assessments should then be made available to those personnel responsible for developing planetary surface operational concepts so they can decide what features (if any) used by these other organizations should be incorporated into its current approach to planetary surface exploration.
- 4 Review historical and current data sets that can be mined for information regarding logistics, heated volume (as a surrogate for pressurized volume), functional space utilization, energy requirement, etc. that can be used to develop mathematical models for these aspects of a surface mission or traverse. These data could reside with both governmental and nongovernmental organizations, indicating that contacts should be developed with both organizational types.
- 5 Review data from “case studies” describing crew skill mix and leadership approach used in polar

exploration. Examples of successful and unsuccessful approaches exist and should be part of this assessment. One primary feature of this assessment could be a set of criteria to be used to determine the appropriate crew mixture of “professional astronaut” and “professional research scientist”, an approximate description of the major skill sets used in polar scientific exploration teams. Continuing this line of reasoning, these results could also be used to determine the skill/training requirements for these two broad categories of crew members as well as examining the functional requirement implications resulting from this approach to crew make up.

- 6 Finally, investigate the benefits of joint operations of pertinent surface exploration activities and advanced systems by large government agencies or other organizations, such as the NSF and NASA. Benefits of this strategy could be:
 - 7 Higher Technology Readiness Level technology test beds and higher fidelity analog tests for NASA;
 - 8 Access to more advanced technologies for “polar” exploration community;
 - a. A joint contribution to advancing scientific knowledge and technology state of the art.

11.7. Summary

This section has highlighted the wide range of scientific, technological, or operational questions that can be addressed in analog mission simulations or tests ranging from very focused, tightly controlled, single-purpose tests to multi-faceted, integrated combinations of scientific, technological, and operational features designed to simulate different phases of a mission. Future planetary mission such as the one described in DRA 5.0 are known to require new capabilities, techniques, and operational modes that will need to be tested extensively in relevant environments to (a) confirm that systems will function as desired in relevant environments as well as revealing unanticipated behavior, (b) compare the performance of alternative combinations of systems and operations, and (c) train flight crews, ground support personnel, engineers, and managers. Although not discuss here, analog activities have also been shown to engage the public with interesting and exciting mission simulations well before actual missions take place. Based on these successful uses of analogs to address questions that cannot be answered by analysis alone, it is anticipated that there will be an ongoing role for analogs as part of a step-wise approach to developing and implementing new capabilities needed for missions beyond low Earth orbit in general and for Mars missions of the type described in DRA 5.0 in particular.

11.8. Bibliography

-
- ¹ Abercromby, A.F., Gernhardt, M.L., and Litaker, H., Desert Research and Technology Studies (DRATS) 2008: Evaluation of Small Pressurized Rover and Unpressurized Rover Prototype Vehicles in a Lunar Analog Environment, NASA/TP-2010- 216136, Houston, TX, November 2010.
 - ² Love, S.G and Reagan, M. L., “Delayed Voice Communication,” Acta Astronautica 91 89-95, 2013
 - ³ Nansen, Fridtjof , “*Farthest North*”, Modern Library, New York, 1999

Selected Additional References Pertaining to Planetary Protection:

- Rojdev, K., Hong, T., Hafermalz, S., Hunkins, R., Valle, G., and Toups, L, “Inflatable Habitat Health Monitoring: Implementation, Lessons Learned, and Application to Lunar or Martian Habitat Health Monitoring,” AIAA-2009-6822, AIAA SPACE 2009 Conference and Exposition, Pasadena CA, September 2009.
- Anon., Development and Implementation of Surface Traverse Capabilities in Antarctica: Comprehensive Environmental Evaluation, National Science Foundation, Washington, DC, August 2004.
- Cadogan, D.P., Scheir, C., “Expandable Habitat Technology Demonstration for Lunar and Antarctic Applications,” AIAA 2008-01-2024, 38th International Conference on Environmental Systems (ICES), San Francisco CA, June 2008.
- Hoffman, Stephen J. ed., Antarctic Exploration Parallels for Future Human Planetary Exploration: A Workshop Report, NASA/TP – 2002 – 210778, National Aeronautics and Space Administration, Washington, DC, 2002.
- Hoffman, Stephen J. ed., Antarctic Exploration Parallels for Future Human Planetary Exploration: The

Role and Utility of Long Range, Long Duration Traverses, NASA/CP – 2012 – 217355, National Aeronautics and Space Administration, Washington, DC, 2012.

- Love, Staley G., “Drifting to Mars,” White paper, 17 September 2012.

12.HUMAN RESEARCH

12.1. Standards for the Human System

Primary Contributors:

Craig E. Kundrot, National Aeronautics and Space Administration, Johnson Space Center
Paul Campbell, Wyle Integrated Science and Engineering
Michael A. Canga, National Aeronautics and Space Administration, Johnson Space Center
Ronita L. Cromwell, United Space Research Associates
Robert S. Galvez, National Aeronautics and Space Administration, Johnson Space Center
Mark Jernigan, National Aeronautics and Space Administration, Johnson Space Center
Anil S. Menon, Wyle Integrated Science and Engineering
Joseph S. Neigut, National Aeronautics and Space Administration, Johnson Space Center
Peter Norsk, United Space Research Associates
Thomas A. Sullivan, National Aeronautics and Space Administration, Johnson Space Center
Sharmila D. Watkins, University of Texas Medical Branch at Galveston
Alexandra M. Whitmire, Wyle Integrated Science and Engineering
Mihriban Whitmore, National Aeronautics and Space Administration, Johnson Space Center

12.1.1. Crew Health

The purpose of these standards is to ensure a healthy and safe environment for crewmembers and to provide health and medical programs for crewmembers during all phases of space flight. Standards are established to optimize crew health and performance, thus contributing to overall mission success, and to prevent negative long-term health consequences due to space flight.

The Office of the Chief Health and Medical Officer establishes NASA’s space flight crew health standards for the pre-flight, in-flight, and post-flight phases of human space flight.⁴ These standards apply to all NASA human space flight programs and are not developed for any specific program. These standards do have implications for Mars exploration missions. As individual programs, missions, and spacecraft are conceived and designed, these higher level standards drive more specific requirements at those levels.

The first set of standards concern Levels of Care. Level of Care Five is the highest level of care and is required for Mars exploration missions (e.g., section 4.1.1.6.5 “Level of Care Five shall be provided for lunar/planetary missions greater than 210 days”). At level five, the training and caliber of the caregiver is at the physician level, and the highest levels of medications, equipment, and consumables are provided.

The next section contains standards for human performance. There are three types of standards (Fitness for Duty [FFD], Space Permissible Exposure Limits [SPELs], and Permissible Outcome Limits [POLs]) that address aerobic capacity, sensorimotor function, behavioral health and cognition, hematology and immunology, nutrition, muscle strength, bone loss, and radiation exposure.

The third section addresses health and medical screening, evaluation, and certification.

The fourth and final section concerns medical diagnosis, intervention, treatment, and care. This section spans the training, pre-flight, in-flight, and post-flight phases of space flight.

12.1.2. Human Factors, Habitability, and Environmental Health

The second volume of the Space Flight Human Systems Standard (SFHSS)⁵ addresses the design and operation of the space flight system in all phases of its life cycle with respect to all crew activities. It is applicable to programs

and projects that are required to obtain a human-rating certification. This volume mandates a human-centered design process to ensure that human capabilities and limitations are considered during all design phases.⁶

In addition, the Human Integration Design Handbook⁷ provides the latest technological information and guidance for individual programs to meet the SFHSS. It is divided into 13 chapters, the last 9 of which address the range of human operations in space. Each chapter includes an introduction, the main body of which can include design guidelines, lessons learned, and example solutions, a section describing future research needs, and a reference section.

12.2. Additional Assumptions Made to Assess the Human Health and Performance Risks

The Human Research Program (HRP) focuses its research investments on understanding and mitigating the highest risks to astronaut health and performance in support of exploration missions. The program also develops and matures operations concepts that will inform requirements for the design and operation of space vehicles and habitats needed for exploration missions. For each crew health and performance risk in the HRP portfolio, an assessment is performed to understand human system risks, as well as compare standards, requirements, and mitigation strategies, for example, against defined exploration mission scenarios.

The exploration missions currently considered include the International Space Station (ISS), lunar, near-Earth object/asteroid, and Mars missions. Although these mission types involve some of the same human health and performance challenges, each also includes specific challenges that depend on the nature of the mission and the mission development schedule. The HRP research and technology development plan/schedule/framework is phased to supply appropriate deliverables in time to meet the challenges of each mission type.

HRP relies on the Design Reference Missions (DRMs), which provide a framework with which to identify key capabilities and important guiding drivers and assumptions, thus enabling the HRP to focus its research questions on topics highly relevant to NASA's future activities. However, in some cases, the details provided by the agency DRMs are not specific enough to encompass additional assumptions that HRP needs to make in assessing its risk posture for each of the risks in its portfolio. These additional assumptions are listed in this section together with the agency DRM information to define the complete set of mission guidelines that the HRP utilizes in its research and risk assessment. These DRMs provide the bounding conditions and trade space for defining future spaceflight capabilities and key performance drivers required to achieve mission objectives.

12.2.1. HRP Mars DRM Additional Assumptions

The assumptions that the HRP utilized for the Mars mission in support of its research are shown below.

Crew Size: The crew is composed of six crewmembers comprised of both male and female astronauts.

Mission Duration: The Mars Exploration DRM, often referred to as long-stay missions, is characterized by the need to minimize the exposure of the crew to the deep-space radiation and zero-gravity environment while, at the same time, maximizing the scientific return from the mission. This is accomplished by taking advantage of optimum alignment of Earth and Mars for both the outbound and return trajectories, as well as by varying the stay time on Mars, rather than forcing the mission through non-optimal trajectories. This approach allows the crew to transfer to and from Mars on relatively fast trajectories, on the order of 6 months, while allowing them to stay on the surface of Mars for the majority of the mission, on the order of 18 months. The total mission duration from launch to crew return is assumed to be approximately 3 years.

Early Termination of Mission: The crew cannot return to Earth early.

Role of Ground Support / MCC: The communication delay is too great to enable real-time control of critical operations, such as is done on ISS for the Special Purpose Dexterous Manipulator and the Space Station Remote Manipulator System. Ground support will be provided in 'batch mode' rather than real-time. Flight surgeon support of medical evaluations using ultrasound or other technologies will also be provided in batch mode; real-time

guidance of probe placement will not be possible. It will be possible to send training material in batch mode, but interactive training with immediate feedback from ground support will not be possible. Ground support will not be able to monitor time-critical systems during crew sleep periods. Back room support will be significantly delayed. The crew must be able to stabilize systems for all contingencies for up to 44 minutes without any ground assistance.

Crew Habitation: Mission duration drives the need for the crew habitation capabilities for the entire mission. Crew vehicle capabilities include the MPCV crew module, a crew habitation module that provides all of the crew capabilities required for living and operating in space, and a cargo module with all available resources required by the crew for the entire mission. The habitable volume must be large enough and lay out to execute the necessary tasks and to provide a psychologically acceptable space for the long period of confinement. The habitation/vehicle configuration provides:

- Sensory stimulation (e.g., variable lighting and virtual reality) that offsets the physically and socially monotonous environment.
- Monitoring systems that unobtrusively track cognitive performance deficits, stress, fatigue, behavioral health, task performance, and team performance.
- Devices that mitigate the effects of fatigue, circadian misalignment, and work overload.
- Communication tools that make communication delays, ranging from seconds to minutes, less onerous.

Crew Timeline/Activities: There are two types of activities in which the crew will be involved with on a daily basis during transit to/from Mars. The first activity type is focused on activities in which the crew will be engaged to live in space: crew sleep, pre/post-sleep activities (e.g., galley operations and personal hygiene), exercise, and review/development of planned crew activities/schedule. The second activity type is focused on science/payload operations and vehicle system management/maintenance, as required, and interaction with the ground control center. During the transit period, there will be no planned or contingency extravehicular activities (EVAs) performed.

During surface operations, the crew would have ample time to plan and re-plan the surface activities, respond to problems, and readdress the scientific questions posed throughout the mission. The focus during this phase of the mission would be on the primary science and exploration activities. A general outline of crew activities would be established before the launch but would be updated throughout the mission. This outline would contain detailed activities to ensure initial crew safety, make basic assumptions as to initial science activities, include periodic vehicle and system checkouts, and include plans for a certain number of sorties. The crew will play a vital role in planning specific activities as derived from more general objectives defined on Earth.

Communication Delays: Expected communication delays between the crew and the ground control center will increase from zero during low-Earth orbit (LEO) to up to 6-8 minutes upon Mars arrival with the same duration of impact during return to Earth. Due to the long communication delays associated with Mars missions, the crew is expected to perform autonomous operations as required.

Mars Surface Operations: Landing operations are expected to be fully automated with minimal crew interaction during the landing sequence, thereby minimizing the required crew piloting skills and manual control capability. The crew will be in a recumbent position during all Entry, Descent, and Landing (EDL) operations. Current human health and support data indicate that it may take the crew a few weeks to acclimate to the partial gravity of Mars after landing. After the crew has acclimated, initial surface activities would focus on transitioning from a “Lander mode” to a fully functional surface habitat. Once on the surface, expectations are that the crew will be required to perform many activities in support of mission objectives and mission success. During the entire 18-month stay on the martian surface, the six crewmembers are expected to perform multiple EVAs. A key objective of the Mars surface mission is to get members of the crew into the field where they could interact as directly as possible with the planet that they have come to explore. This would be accomplished via the use of EVAs, assisted by pressurized and unpressurized rovers, to carry out field work in the vicinity of the surface base. Operationally, Mars surface EVAs would be conducted by a minimum of two and maximum of four people. If unpressurized rovers are used, an additional operational constraint would be imposed on the EVA team. If one rover is used, the EVA team would be constrained to operate within rescue range of the surface base. Taking multiple, and identical, rovers into the field allows the EVA team to expand its range of operations because these vehicles are now mutually supporting and thus able to handle a wider range of contingency situations.

Crew Logistics/Food: The mission to Mars will consist of the crew habitation modules listed above (MPCV, Hab

module, and Cargo module). All consumables and spare parts must be provided at the start of the mission and available from the habitable volume. The food that is carried aboard the transit habitat includes transit consumables needed for the round-trip journey plus contingency consumables required to maintain the crew should all or part of the surface mission be aborted. The crew would be forced to return to the orbiting vehicle, which would be used as an orbital “safe haven” until the Trans-Earth Insertion (TEI) window opens. Any contingency food remaining onboard the crewed vehicle would be jettisoned prior to the TEI burn to return home. The habitation module will have a food galley with the required capabilities for the crew to prepare their meals. Food storage will be contained in the cargo module under the required food storage constraints.

Resupply and Sample Return: There will not be any mission resupply considered to replenish the crew of logistical requirements. All monitoring for microbial or toxic hazards must be performed on board; no sample return will be possible.

Exercise Equipment: The crew will maintain their physiological health per the requirements defined in NASA-STD-3001, Vol. 1.

HRP Constraints/Implied Requirements:

- During Mars atmosphere entry (5-g), the crew will be in a recumbent position until landing operations are complete. The vehicle design will not require the crew to be in an upright standing posture during entry.
- Countermeasures for orthostatic intolerance (OI) will be provided for use in the case of any OI-related events (e.g., Mars atmosphere entry).
- Adequate vehicle or habitat shielding, dosimetry, and operational procedures should be in place to prevent exposures above 30-day permissible dose limits.
- It is assumed that the Mars DRM will follow Level of Care Five standards in NASA-STD-3001, Vol. 1, regarding crewmember training and caliber: "The training and caliber of the caregiver shall be at the physician level, due to the exclusively autonomous nature of the mission."

Pre/Post-Mission Assumptions: TBD post-flight Baseline Data Collection will still be required, but protocols will need to consider the degree of crew de-conditioning after a 3-year mission.

12.3. Challenges Associated with DRA 5.0

12.3.1. HRP Health and Performance Risks

Crew health and performance is critical to successful human exploration beyond LEO. The HRP investigates and mitigates the highest risks to human health and performance, providing essential countermeasures and technologies for human space exploration. Risks include physiological effects from radiation, hypogravity, and planetary environments, as well as unique challenges in medical treatment, human factors, and behavioral health support. Without HRP results, NASA will face unknown and unacceptable risks for mission success and post-mission crew health.

HRP Program Plan, HRP-47051

The health and performance risks are grouped in the following five categories:

- 1 **Radiation.** The radiation environment in space differs significantly from the types of radiation humans encounter on Earth. Unlike gamma rays, x-rays, and other terrestrial forms of radiation, space radiation contains high-energy particles that can cause unique cellular changes in human tissues and organs. As a result, space radiation poses a number of significant health and safety risks for crewmembers in the space environment, including the possibility of cancer, visual disorders, radiation sickness, damage to the central nervous system, and hereditary effects.
- 2 **Behavioral Health and Performance.** The unique stresses and challenges of space flight can affect sleep, cognition, and individual and team well-being. Future long-duration missions will further introduce additional stressors, including increased autonomy, isolation, sensory deprivation, social monotony, and environmental hazards (e.g., carbon dioxide [CO₂] and radiation). Evidence-based

- recommendations for selection and crew composition, as well as protocols to optimize neurobehavioral health and team cooperation, coordination, and communication, are needed to support missions beyond LEO.
- 3 Exploration Medical Care. Missions in LEO offer the capability to treat an injured or ill crew member through telemedicine that includes real-time communication with ground support teams; various hardware solutions; and the assurance that if an emergency arises that can only be treated on the ground, an escape vehicle is available for evacuation. Missions beyond LEO, on the other hand, will involve a communication delay to and from ground support teams, limited hardware and volume capabilities, and limited options for timely medical evacuation to Earth. Additional medical capabilities are required for such missions.
 - 4 Physiological Changes. The spaceflight environment poses various physiological risks to the astronaut, including bone degradation, cardiovascular changes, and intracranial hypertension. Future long-duration missions to planetary surfaces will introduce partial gravity, as well as new environmental stressors and a dynamic mission tempo that may have physiological implications. Pre-flight countermeasures for LEO missions involve physical fitness, exercise, and physiological adaptation training; in-flight countermeasures cover physiological and nutritional health and physical fitness; and post-flight countermeasures target rehabilitation strategies.
 - 5 Human Factors. The design of the spacesuit, spacecraft, and habitat affects crewmember safety, health, and performance. Accordingly, specific habitation standards, requirements, equipment, procedures, and technologies are being developed. Exposure limits for environmental factors, such as chemicals, bacteria, fungi, and Mars dust, are also needed. A food system that provides nutritious and palatable meals that can withstand the rigors of spaceflight and still be prepared easily, generating minimal waste, is also needed.

12.3.2. Introduction to HRP Research Ratings

The HRP uses research ratings as a tool with which to communicate to Agency management the seriousness of a risk to crew health and performance when applied to the mission architecture and/or mission characteristics defined for each DRM. The research ratings serve as one of several inputs to determine the priority of each human risk, helping HRP Management make program decisions and allocate program resources.

Each research rating is derived by comparing the current state of knowledge about a risk, whether existing standards are defined and met, and the degree to which research will improve the current risk posture with respect to crew health and performance during long-duration missions. Each human risk has one of four research ratings identified for each of the four DRMs, driven by its applicability to the DRM mission architecture and/or mission characteristics. HRP uses the following four DRMs to bound its exploration mission assumptions: (1) 12-month mission on the ISS (ISS-12); (2) Lunar (Outpost) mission; (3) NEA mission; and (4) Mars mission [see HRP-47052, Program Requirements Document (PRD) Appendix B, for further definitions of and assumptions for each DRM].

The four possible research ratings are: *Unacceptable*, *Acceptable*, *Controlled*, and *Insufficient Data*. These ratings are described below.

Rating: Controlled (C) - Green

A risk is deemed to have a research rating of *Controlled* if, based on available evidence, the projected mission architecture (with assumptions on DRM-specific vehicle design and operations constraints) meets existing standards for maintaining crew health and performance and countermeasures exist to control the risk. Continued research or technology development will improve capabilities, provide additional trade space to support the meeting of crew health standards or ensure that vital Agency core competencies are accessible.

Context:

The scientific, operational, and clinical evidence for the risk and current available mitigations and countermeasure capabilities demonstrate that the Agency can meet the existing standards for maintaining crew health and performance during all phases of the mission. Research has provided at least one solution capability to address the risk. Additional research or technology development could further reduce the risk by enhancing understanding and offering different options to increase engineering and operational efficiencies, make the best use of unique assets,

such as ISS, in optimizing risk posture, and maintain vital Agency core competencies.

Rating: Acceptable (A) - Yellow

A risk is deemed to have a research rating of *Acceptable* if, based on available evidence, the projected mission architecture (with assumptions on DRM-specific vehicle design and operations constraints) likely provides the capability to meet existing standards for maintaining crew health and performance but the risk is not fully controlled. The remaining level of uncertainty would likely lead the Agency to accept a higher-than-expected level of risk to crew health and performance during some phases of the mission. Continued research or technology development is expected to improve capabilities or substantiate crew health standards.

Context:

The scientific, operational, and clinical evidence for the risk and current available mitigation and countermeasure capabilities demonstrate that the Agency can likely meet existing standards for maintaining crew health and performance during some, but not all, phases of the mission. Additional research or technology development may further improve the risk research rating to achieve a *Controlled* rating.

Rating: Unacceptable (U) - Red

A risk is deemed to have a research rating of *Unacceptable* if, based on available evidence, the projected mission architecture (with assumptions on DRM-specific vehicle design and operations constraints) will not provide the capabilities required to meet existing standards for maintaining crew health and performance during all phases of the mission. Therefore, research is required to acquire necessary information and develop necessary capabilities and countermeasures to arrive at an acceptable risk posture.

Context:

The scientific, operational, and clinical evidence for the risk and current available mitigations and countermeasure capabilities do not adequately demonstrate the capability of the Agency to meet existing standards to protect and/or maintain crew health and performance during all phases of the mission. The inadequacy and uncertainty in the risk mitigation capabilities and countermeasures will require additional data and/or mitigation strategies to be developed through the research performed by the HRP.

Rating: Insufficient Data (I) - Gray

A risk is deemed to have a research rating of *Insufficient Data* if there is not enough available evidence to assess whether the projected mission architecture (with assumptions on DRM-specific vehicle design and operations constraints) can meet existing standards for crew health and performance or if such standards need to be developed. Research is required to further understand and define the risk to the point that its research rating can be determined by HRP to be *Controlled*, *Acceptable*, or *Unacceptable*. This rating is primarily for new risks before a research rating can be determined.

Context:

The scientific, operational, and clinical evidence for the risk and current mitigation and countermeasures capabilities are inadequate to allow the assessment of the ability of the mission architecture and/or mission characteristics to support crew health and performance standards. Additional research is expected to support the determination of a new research rating.

The research rating of a risk alone is not sufficient to determine its priority within the HRP research portfolio. Priority is dependent on other factors, such as limited availability of certain necessary resources (e.g., the ISS and ground analogs), program funding, exceptionally long lead times (e.g., needed to improve understanding and mitigation of radiation risks), or the amount of risk reduction that can be obtained with a specific set of resources. The level of activity (or budget) and timing of research investments reflect the final prioritization of the risks.

12.3.3. HRP Research Ratings for DRA 5.0

Table 12-1 provides the current estimated research ratings for the key HRP risks associated with a DRA 5-type surface mission. The Research Rating is *Unacceptable* for seven risks in HRP PRD Rev E, PCN-1. The radiation exposure standard would be violated in a DRA 5.0 Mars mission. Extrapolation from terrestrial analogs (e.g., Antarctic ‘winter over’ expeditions) and consideration of the mission duration and historically unprecedented

remoteness from Earth lead to an *Unacceptable* rating for behavioral health. The lack of a food system that can provide the shelf-life needed for a 30-month Mars mission makes both the food and nutrition risks *Unacceptable*. HRP's Integrated Medical Model estimates the probability of loss of crew due to medical conditions to be on the order of 10%. The other two risks, namely muscle performance and aerobic capacity, were rated *Unacceptable* based on early results from the ISS that indicated that countermeasures were not sufficiently effective. Recent evidence from new countermeasures has led HRP to revisit the Research Rating for these two risks in calendar year 2012.

There are insufficient data on 10 risks for HRP to provide a Research Rating. For two risks (dust and medications), the external challenge to the human system is not well characterized; we do not understand the physical and chemical properties of dust and volatiles on Mars sufficiently well, and we do not know which medications will remain stable and effective over the course of a Mars mission. The lifetime impacts of radiation on the central nervous system and on degenerative diseases (e.g., cardiovascular disease) are simply unknown. For the remaining six risks, there is too much uncertainty to extrapolate from 6-month ISS missions to the 30-month Mars mission.

12.4. Preliminary Assessment of Challenges for a Mars Orbital Mission with no Landing

12.4.1. Patterns of Change in Risk Posture

The HRP does not have official Research Ratings defined for a Mars mission that orbits Mars and explores the martian moons rather than lands on and explores Mars. This section, therefore, only describes the top-level considerations that indicate whether the risks increase, decrease, or remain about the same for the orbital mission versus the landing mission. It should be noted that relative increases or decreases in a risk may not result in changes to the research ratings.

Table 12-2 provides preliminary HRP research ratings for a notional orbit-only Mars mission. The four radiation risks are likely to increase due to the reduced shielding available in flight compared with the martian surface. However, the details depend on the mission duration, trajectory, and vehicle shielding.

Nine risks increase due to the increased isolated, confined, and extreme (ICE) nature of the orbital mission. The crew will be confined to the Orion vehicle, Multi-Mission Space Exploration Vehicle, and Deep Space Habitat. The crew will not have access to a planetary habitat, rovers, or planetary EVAs. The stress on the behavioral health of the individuals is thought to be extreme enough to raise the team risk to *Unacceptable*. The confinement in the Deep Space Habitat for the entire mission duration is similarly thought to raise the risk of an inadequate habitat to an *Unacceptable* level. These are the only two Research Ratings that increase in this preliminary assessment. The impact of ICE environments on sensorimotor function and cognition raise the level of risk for five other risks. Finally, the effects of a more severe ICE environment on human physiology raise the risk for the immune and host-microorganism risks.

Table 12-1 HRP Research Ratings for Mars Surface Missions (DRA 5.0)

HRP Element	Risk Title (Short Title)	HRP Research Rating
HHC	Orthostatic Intolerance	A
HHC	Osteoporosis	A
HHC	Nutrition	U
HHC	EVA Health and Performance	A
HHC	Muscle	U
HHC	Renal Stone Formation	C
HHC	Bone Fracture	A
HHC	Intervertebral Disc Damage	I
HHC	Arrhythmia	I
HHC	Aerobic Capacity	U
HHC	Immune	A
HHC	Sensorimotor	A
HHC	Pharmacology	U
HHC	Visual Impairment	U
HHC	Decompression Sickness	C
HHC	Occupant Protection	I
SHFH	Food	U
SHFH	Human Factors - Computers	C
SHFH	Human Factors - Training	A
SHFH	Human Factors - Robotics	A
SHFH	Human Factors – Task Design	C
SHFH	Dust or Volatile Exposure	I
SHFH	Human Factors – Vehicle/Habitat	A
SHFH	Host-Microorganism Interactions	A
ExMC	In-flight Medical Capabilities	U
BHP	Behavioral Health	U
BHP	Sleep	C
BHP	Team	A
SR	Radiation-Cancer	U
SR	Radiation-Acute	C
SR	Radiation-CNS	I
SR	Radiation-Degenerative	I

Note: HHC, Human Health Countermeasures; SHFH, Space Human Factors and Habitability; BHP, Behavioral Health and Performance; SR, Space Radiation; ExMC, Exploration Medical Capability

Eight risks increase due to the increased exposure to microgravity. Recent results from the ISS suggest that countermeasures are available for these risks. It will be a challenge, however, to develop countermeasures that fit within the mass, power, and volume constraints of a Mars exploration mission.

The food and nutrition risks are the only two risks that are insensitive to the change from a landing mission to an orbital mission. This insensitivity results from the assumption that the food system would be exactly the same for the two missions.

Table 12-2 Research Ratings for Mars Orbital Missions

HRP Element	Risk Title (Short Title)	Mars DRA 5	Mars Orbit	Rationale
HHC	Orthostatic Intolerance	A	↑	↑time in weightlessness [1]
HHC	Osteoporosis	A	↑	↑time in weightlessness [1]
HHC	Nutrition	U	↔	assumes no vacuum, refrig, crops
HHC	EVA	A	↓	fewer EVAs; EVAs will be weightless
HHC	Muscle	U	↑	↑time in weightlessness [1]
HHC	Renal Stone Formation	C	↑	↑time in weightlessness [1]
HHC	Bone Fracture	A	↓	no falling in weightlessness
HHC	Intervertebral Disc Damage	I	↑	↑time in weightlessness [1]
HHC	Arrhythmia	I	↑	↑time in weightlessness [1]
HHC	Aerobic Capacity	U	↑	↑time in weightlessness [1]
HHC	Immune	A	↑	↑time in ICE
HHC	Sensorimotor	A	↑	moon ops; ↑time in ICE (↓cognition)
HHC	Pharmacology	U	↓	↓mission time & drug stability
HHC	Visual Impairment	U	↑	↑time in weightlessness
HHC	Decompression Sickness	C	↓	fewer EVAs; EVAs will be weightless
HHC	Occupant Protection	I	↑	↑time in weightlessness [1]
SHFH	Food	U	↔	assumes no vacuum, refrig, crops
SHFH	Human Factors - Computers	C	↑	↑time in ICE (↓cognition)
SHFH	Human Factors - Training	A	↑	↑time in ICE (↓cognition)
SHFH	Human Factors - Robotics	A	↑	↑time in ICE (↓cognition)
SHFH	Human Factors - Task Design	C	↑	↑time in ICE (↓cognition)
SHFH	Dust or Volatile Exposure	I	↓	no exposure in DSH
SHFH	Human Factors - Vehicle/Habitat	A	↑	↑time in ICE & Behavioral Health
SHFH	Host-Microorganism Interactions	A	↑	↑time in ICE
ExMC	In-flight Medical Capabilities	U	↓	no planetary EVA
BHP	Behavioral Health	U	↑	↑time in ICE
BHP	Sleep	C	↓	no circadian entrainment
BHP	Team	A	↑	↑time in ICE & Behavioral Health
SR	Radiation-Cancer	U	↑	↑radiation exposure [2]
SR	Radiation-Acute	C	↑	↑radiation exposure [2]
SR	Radiation-CNS	I	↑	↑radiation exposure [2]
SR	Radiation-Degenerative	I	↑	↑radiation exposure [2]

The lack of EVAs on the martian surface (in 3/8 g) and a presumed reduction in the number of total EVAs reduce the level of four risks. The medical care risk decreases because EVAs place a strong demand on the medical system. The risks of EVA health and performance and decompression sickness decrease with the reduced number of EVAs. The lack of activity on Mars eliminates the risk of exposure to martian dust.

The sleep risk goes down for an orbital mission because there will be no need to entrain to the martian day; the crew can remain on a 24-hour day.

The risk of bone fracture virtually disappears for an orbital mission because of the reduced risk of falls. Crush injuries could still occur, however. This is the only Research Rating that decreases in this preliminary assessment.

12.5. Identification of Trade Space Factors

Within the existing framework of the Mars DRA, there are alternative mission-system design implementations that can satisfy human constraints and take advantage of human capabilities to ensure flight crew health and mission performance. A systems engineering model that incorporates the human is useful in the formulation of human-system integration (HSI) trade studies to identify alternative designs that meet human constraints while optimizing mission and system parameters. Figure 12-1 describes a simple, encompassing model that accounts for the mission and system designs to be traded, along with the aspects of natural environments and humans that are, to a large degree, fixed and are therefore needed as constraints in design trades.

Mission: the temporal activities/events *subject to design*.

Environment: the natural phenomena not subject to design.

Includes external factors, such as MMOD, sunlight, and space radiation, that must be taken into account during design.

System: the physical items *subject to design*.

Includes spacecraft internal factors, such as cabin lighting, vibration, noise, and air, that are subject to design by programs/projects.

Human: people involved in the mission and interacting with the system, not subject to design.

Figure 12-1 Comprehensive systems engineering model incorporating the human.

Using this model, design trades of mission-system variables for maintaining the human ecosystem and systems interaction environment, such as the following, can be formulated:

- Spacecraft internal atmosphere
- Spacecraft habitable volume
- Design of the habitable space
- Hygiene and life support systems
- Food system
- Psychosocial aids
- Task aids and work environment design
- Health maintenance systems
- Radiation protection strategy

These items and possibly others provide direct controls for the hazards caused by radiation, microgravity, confinement, duration, isolation, autonomy, stress, and other human issues present in a mission of this magnitude. As a specific example of a Mars DRA trade space, the internal spacecraft atmosphere provided for humans is subject to design. Within this architecture, there are multiple habitable elements (ascent/descent cabins, long-duration habitats, space suits). Each habitable element has unique requirements for accommodation of the flight crew, including their duration of habitation and the number of EVA excursions associated with each element. Based on the constraints of natural environments (e.g., external conditions and planetary surfaces) and of the human (e.g., respiration, body temperature, and moisture preservation), the Mars DRA concept of operations for each habitable element (i.e., its element-level mission design) and its conceptual design (i.e., element-level hardware/software design) can be traded in terms of the following internal atmosphere factors:

- Total pressure of all atmospheric gas components
- Partial pressure of oxygen (with a resultant oxygen percentage)

Some human system risks for the Mars DRA include significant uncertainty effects. These uncertainties must be accounted for in design trades such as atmosphere selection. The resulting atmosphere design for each habitable element may be conservative until the associated uncertainties are reduced by further human research.

12.6. HRP use of Analogs for Risk Reduction

The use of analogs as a research tool is becoming more important because the ISS will be unavailable after 2020. The Flight Analogs Project (FAP) plans and implements HRP research that utilizes analog platforms and environments. The FAP assists investigators in identifying the appropriate analog based on study requirements. Specialized characteristics of each analog provide unique settings to implement a wide variety of research studies. Some of the analogs used for HRP research include the NASA Extreme Environment Missions Operations (NEEMO), Haughton-Mars Project, Antarctic stations, Desert Research and Technology Study (D-RATS), the Flight Analogs Research Unit (FARU), and the Human Exploration Research Analog (HERA).

Studies completed in conjunction with NEEMO missions utilize the undersea Aquarius module (Figure 12-2a) located 3.5 miles off the coast of Key Largo, Florida, at a depth of 47 feet. These missions typically last for 7-14 days. Characteristics of this analog include isolation within a high-risk environment and the physiological and psychological stressors that are germane to this environment. The NEEMO setting is ideal for exploration mission simulations, as top-side mission control capabilities and partial gravity environments can be simulated outside of the Aquarius habitat. In addition, astronauts often participate in these underwater missions. These characteristics make NEEMO an ideal analog for studying crew dynamics, crew autonomy, EVAs, telemedicine, and impacts of physiological and psychological stress.

The Haughton-Mars Project is located on Devon Island in the Canadian High Arctic and is the site of the Haughton meteorite impact crater (Figure 12-2b). This international, interdisciplinary field project serves as the mission backdrop for HRP research. The stark, rocky, polar setting creates a harsh mission environment. Mission control and habitat capabilities are available. This analog is best suited for studies of human performance (both physical and

behavioral), telemedicine, extravehicular activity systems, and human factors.

There are 64 stations in Antarctica that are operated by 20 different countries. McMurdo Station is a U.S. Antarctic research center located on the southern tip of Ross Island, Antarctica. It is operated by the United States through the United States Antarctic Program, a branch of the National Science Foundation (Figure 12-2c). Each station has its own unique set of characteristics that make these stations useful for studying a variety of research topics. In general, Antarctic stations provide isolation within a high-risk environment with limited communications to the outside world. Full exploration mission simulations are available and can include EVAs. Mission durations vary. However, long-duration missions lasting through the Antarctic winter make them ideal for studying the effects of isolation, team dynamics, team autonomy, and impacts of physiological and psychological stress. Isolated conditions also provide possibilities for telemedicine research.

Research and Technology Studies have been completed in the deserts of Arizona and, more recently, at NASA Johnson Space Center (Figure 12-2d). These studies create mission simulations that include mission control and EVA capabilities. This environment is well suited for examining team dynamics, crew autonomy, EVA systems, and technology demonstrations. However, unlike the analogs mentioned above, stressors of isolation do not exist, as crews will “return to civilization” at the end of each work day.

The NASA FARU is located at the University of Texas Medical Branch in Galveston, Texas. This hospital unit is dedicated to NASA bed rest studies. The bed rest platform uses 6 degrees of head-down tilt bed rest to produce many of the physiological changes associated with spaceflight (Figure 12-2e). Subjects remain in bed for 60 days and experience bone and muscle atrophy and cardiovascular changes similar to those seen in astronauts. This unit is fully staffed with medical personnel and has capabilities that include a metabolic kitchen for diet standardization and specialized exercise hardware. By modeling these physiological changes to the human body in a bed rest platform, physiological mechanisms can be studied and countermeasures can be tested.

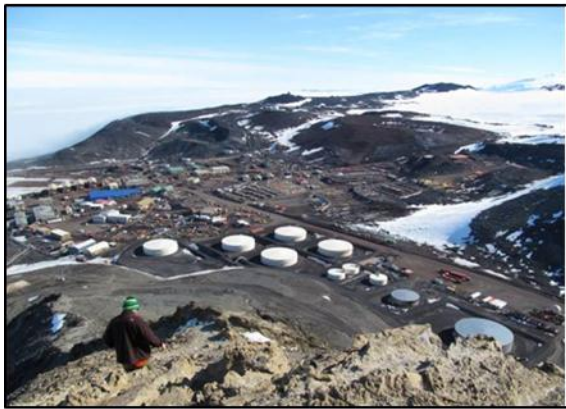
Analogs provide an ideal platform for proof-of-concept testing, particularly in the early stages of technology development or assessment of risks, helping investigators identify whether their protocol or countermeasure is feasible in the operational environment. Analogs with high-fidelity operational tempos in particular allow investigators to implement a protocol or test a tool or technology interface, revealing gaps that may need to be addressed prior to spaceflight implementation. Longer-duration analogs, such as Antarctic stations, can help to further characterize risks that are anticipated for exploration, such as behavioral risks related to isolation and confinement. Countermeasure effectiveness may also be evaluated in the long-duration exploration context.



(a) Aquarius Module



(b) Houghton-Mars Project



(c) McMurdo Station



(d) Research and Technology Study at JSC



(e) Bed rest subject at 6-degress of head-down tilt

Figure 12-2 HRP use of Earth analogs.

12.7. Medical Care

The medical risk identified for a long-duration exploration mission to Mars, among other exploration missions, is the risk of unacceptable health and mission outcomes due to limitations of in-flight medical capabilities. To address this risk, a suite of medical capabilities will need to be identified and developed specifically for a Mars mission. Planning for this mission requires consideration of and preparation for the various medical scenarios that are most

likely to arise during a Mars mission, as well as those presenting the highest risk. The Exploration Medical Capability Element of the Human Research Program developed the Exploration Medical Conditions List to define the set of medical conditions and injuries likely to have the most impact during currently defined Design Reference Missions (DRMs). The evidence base for this list is drawn from various data sources, including data from previous spaceflight missions, astronaut health databases, ground-based studies in analog environments, general population-based studies of disease and trauma incidences, and computer-based simulations.

The medical conditions list for Mars will aid NASA in determining the conditions that require enhanced screening, diagnosis, and treatment, as well as novel techniques and technologies that depart from the terrestrial standard of care. The level of medical care required for human spaceflight programs, defined in Volume 1 of NASA-STD-3001, the NASA Space Flight Human Systems Standards, is identified as the amount and type of care rendered based on the perceived need, ability of the provider, and type of mission. For a mission to Mars, a Level of Care Five will be provided, which requires:

- Preventive strategies to be used to a greater degree to reduce the overall risk.
- Intervention strategies, including increasing levels of advanced care in the form of medications, equipment, training, or consumables, to be used to reduce the risk to an acceptable level.
- The training and caliber of the caregiver during any point in the mission to be at the physician level due to the autonomous nature of the mission.

Obstacles that must be overcome in preparation for a Mars mission include limitations in communication, personnel, procedures, equipment, and consumables that will be available to treat the identified medical conditions. The lengthy 6-month travel time to and from Mars and the potential of an 18-month stay on the martian surface will present unique problems of extended time delays in communication with mission control. Crewmembers may have to respond to medical contingencies without real-time support from the ground. To better prepare the crew to be autonomous, pre-flight ground training and in-flight just-in-time training for the crew medical officer and other crewmembers are emphasized and must be optimized. In the event of a medical contingency, an abort to Earth will not be possible for several phases of the mission, so crewmember injuries and illnesses have greater consequences to the overall mission risk than they do for non-exploration missions. In addition, the crew size, crew composition, and total number of EVAs performed all present contributing factors in the challenge to deliver a Level of Care Five to a Mars mission crew. Although they may be limited, allocated resources, such as mass, power, volume, and crew time, should be used efficiently to optimize the delivery of in-flight medical care.

To date, gaps in current medical knowledge and technology available to adequately screen for, diagnose, and treat the specified conditions for exploration missions have been identified, and a research and development pathway has been paved to attain the medical capabilities needed. An extension of this plan can be applied to develop a medical care system to reduce the health and mission outcome risk for a mission to Mars.

12.8. Artificial Gravity

Many of the currently available human health and performance countermeasures compensate for the lack of terrestrial gravity. An alternative approach to a suite of individual countermeasures is to provide artificial gravity (AG) by spinning all or part of the spacecraft.

Two questions must be answered before deciding whether AG is a viable approach:

- What part of the vehicle will spin?
- What are the physiological responses to different AG protocols?

12.8.1. Background

Long-duration crew health can be improved if efforts are aimed at the prevention of health problems induced by the space flight environment, in particular the reduction in gravity. In some cases, countermeasures can prevent some changes by providing alternative methods to maintaining system homeostasis; however, in many cases, they merely ameliorate the negative effects of changes to the body. Each health problem has its own associated countermeasure.

Some countermeasures induce health and other problems of their own, such as the induction of skin abrasions due to the bungee cords that hold one down on a treadmill; the large number of hours of crew time spent exercising; and the mass, power, volume, and maintenance of equipment. A new, serious health issue (vision impairment and intracranial pressure) has been recently identified and is proving difficult to solve, and this relatively new discovery leads to the concern that there may be other potential health risks that have not yet been discovered.

The root cause of many health issues that arise during space flight is the lack of gravity; therefore, providing acceleration that mimics gravity is a rational approach to preventing many issues from arising. AG should be revisited as a way of preventing the detrimental effects of 0-g, thereby minimizing or eliminating the need for many of the developed countermeasures, as well as the resources (mass, volume, power, crew time, development time, and cost) that are associated with them. Many researchers have long felt that AG is the second-best countermeasure for the space flight risks associated with their discipline. Of course, each risk has a different countermeasure that is ‘best’ suited for it; thus, the total amount of resources necessary to counter all the risks is significant (see section 12.9 below). Alternatively, having one overarching countermeasure, namely AG provided by rotating all or part of a spacecraft, may result in paying one price for the overhead needed to provide a countermeasure that will address most of the risks associated with space flight.

Furthermore, by ensuring that the crew is fully fit and capable of an EVA upon landing on Mars, it may be likely that more robust mission architectures can be developed, rather than requiring their landing craft to serve as their habitat for a week or two during rehabilitation. The benefits of such an approach could have impacts on the way in which the vehicles are designed, packaged, and launched, as well as in the order in which they are sent to Mars, possibly resulting in less expensive launch vehicles.

12.8.2. Design Questions

Three modes of implementation should be considered: 1) Whole vehicle centrifugation, 2) vehicle segment centrifugation, and 3) intra-vehicle centrifugation. The selection of a particular mode will depend on cost/benefit evaluations. The consequences for human health protection will be different according to each mode of centrifugation as well as the pre-mission research to be conducted in the Human Research Program.

Whole Vehicle Centrifugation. It is anticipated, as described elsewhere in this document, that spinning the whole vehicle during the entire mission to Mars will have protective effects against weightlessness for virtually all physiological systems.

Vehicle Segment Centrifugation. Centrifugation of a vehicle segment will have the advantage of inducing G-effects in humans for a large portion of the mission, but not the entire mission. Thus, astronauts will likely be subjected to daily alternations between a G-force and weightlessness. Astronauts on the ISS currently perform exercise up to several hours a day. In future space vehicles in which part of the space vehicle is constantly rotating, such exercise could be performed in that segment with greater efficiency. Additionally, astronauts could sleep in the rotating segment and thus obtain beneficial health effects during this period.

Intra-vehicle Centrifugation. According to this concept, a short-arm (~2-m) centrifuge would provide AG within a single vehicular compartment. Astronauts would be exposed to G-forces intermittently, but less often than they would in the Vehicle Segment Centrifugation approach. Acceleration levels may need to be higher than 1 G.

12.8.3. Physiological Questions

There are two questions that need to be answered for each implementation mode:

- What is an effective AG prescription?
- Can the crew tolerate an effective prescription?

Whole Vehicle Centrifugation. This concept seems optimal from a human health perspective. It may, however, be quite complex. To date, no humans have been spun in a centrifuge for more than a few days and no research in humans has been conducted regarding the protective effects of long-term (> a few hours) centrifugation. Therefore, if the Whole Vehicle Centrifugation concept is selected, long-duration centrifuge studies must be performed in

humans on Earth and in space. What is not known is the effects of large-centrifuge angular rotation (Coriolis forces) on the vestibular organs and the resulting physiological consequences, as well as whether 1-G centrifugation is necessary for an entire Mars mission. A threshold for the G-level that is sufficient for protection of most of the human physiological systems should be determined.

The consequence of selecting the Whole Vehicle Centrifugation concept is, therefore, that large human centrifuge studies must be initiated on the ground, with whole vehicle (or cabin) centrifugation studies performed later in space. Additionally, ground-based studies should be conducted in concert with the utilization of low-G analogs for deconditioning purposes. Because long-duration centrifugation studies have been conducted in animals (non-human primates and rodents), a thorough evaluation of what is already known from animal research should be conducted before the initiation of long-term human centrifugation programs. Eventually, the protective health effects afforded by the Whole Vehicle Centrifugation concept should be tested in space and related to the effects of the currently used countermeasures on the ISS.

Vehicle Segment Centrifugation The Vehicle Segment Centrifugation concept should be tested on the ground and in space. It is much easier to test this concept than the Whole Vehicle Centrifugation concept because centrifuge intervals of only a few hours will be needed. This concept should also be tested in ground-based studies in connection with deconditioning analogs. The questions asked should be the following:

- What is the minimum G-level and centrifugation time required for protection of most of the physiological systems?
- What are the consequences of alternating between various G-forces and 0 G on the vestibular system and brain function?
- Can the Vehicle Segment Centrifugation concept be combined with existing countermeasures and, if so, how?

Intra-vehicle Centrifugation. Because this concept utilizes an intra-vehicular short-arm centrifuge, the angular velocity will be larger and the vestibular system effects will be more pronounced than those associated with the Vehicle Segment Centrifugation concept. The testing on the ground will be very similar between the Vehicle Segment and Intra-vehicle Centrifugation concepts. It will, however, be easier to perform large-scale international tests of the Intra-vehicle Centrifugation concept due to the more widespread worldwide use of small human centrifuges. In particular, the effects of small human-powered centrifuges should be considered. Several studies have already been conducted regarding investigation of the effects of small, short-radius centrifuges on the protection of human physiological systems as a result of deconditioning; however, the effects need to be explored in more detail and for more physiological systems, and the concept must ultimately be evaluated in space.

Research needed. The best analog for studying the effects of AG on long-duration deep space exploration missions is a human centrifuge in space. Such an analog is, however, technically challenging and expensive; therefore, the first steps in investigating the feasibility of this analog should be to conduct centrifugation studies in humans on bedrest and rodents on the ISS. Recommendations regarding such studies are provided in a 2009 International Academy of Astronautics (IAA) publication⁵ and consisted of the following: 1) intensify international collaboration, with a more effective distribution of work; 2) develop international standards for investigations; and 3) initiate a series of ground-based studies using human deconditioning analogs (e.g., bed rest, dry immersion) in combination with intermittent and continuous AG. Finally, flight validation is recommended based on the outcomes of the ground studies.

According to Young et al.⁵, the following constitute the research and development challenges associated with AG:

- Determine the best parameter space of radius, angular velocity, and G-level from the point of view of effectiveness, acceptability, and practicality. (Include G-levels below and above 1 G.)
- Study placement of the head at different distances from the short-radius centrifuge (SRC) axis of rotation to investigate the effectiveness of intermittent otolith stimulation on long-term vestibular and cardiovascular effects. (Control of head position rather than foot position will enable study of the influence of the gravity gradient on the AG effectiveness.)
- Consider subject position issues, including orientation relative to the radius and spin axis (e.g., supine versus lying on the side or seated); investigate postures other than supine, and study the advantages and disadvantages of the use of head restraints to reduce motion sickness.

- Develop exercise devices and protocols for their use on SRCs, both to enhance the effectiveness of the devices and to permit deconditioned subjects to tolerate the centrifugation. Consider the importance of the venous blood pump in returning blood to the heart during high G-gradient centrifugation. Investigate active versus passive centrifugation. Study the biomechanical consequences of Coriolis effects on limb and head movements during exercise and take actions to avoid repetitive stress injuries.
- Determine limitations on angular accelerations of the centrifuge for normal operations to minimize vestibular disturbances while permitting adequate emergency braking.
- Study the effects of visual surroundings during rotation (external, bed-fixed, head-fixed, goggles, or darkness), as they affect motion sickness and the compatibility with work and recreation.
- Determine independent specifications of inertial and mechanical loading to allow separate optimizations of the AG level for the cardiovascular and musculoskeletal systems.
- Study circadian effects, including the evaluation of AG while sleeping, as they influence the relationship between time of day and AG effectiveness.
- Determine the gravity gradient resulting from the centrifuge, as it affects the benefit of AG to cardiovascular training.

12.8.4. Example: Engineering Considerations for Whole Vehicle Centrifugation

AG vehicles have appeared in planning documents and movies for decades. Most recently, a study conducted in 2000 was greatly influenced by the lower development cost needed for a nuclear reactor that needed to be run only at 1-g, which could save money relative to testing it in space for years before its incorporation into a Mars program. While there would be expenses associated with AG vehicle design and testing, it is possible that they could be offset by the cost of the development of other systems at 1-g rather than 0-g, thus warranting strong consideration of the development of an AG vehicle.

Some individuals consider AG vehicles to be more complex and heavier than vehicles that operate only under the stresses of their own thrust. Rotating connections can be troublesome and should thus be avoided if at all possible. The typical approach to AG, which involves the use of propellant to spin-up and spin-down the vehicle, requires accounting for the mass of thrusters and propellant consumption for each cycle. If, instead, a design is considered that uses the conservation of angular momentum as the mechanism for AG, this penalty may perhaps be avoided. Spinning part of the vehicle in one direction and the remainder in the opposite direction conserves the overall zero angular momentum. A simple electric motor could provide the relative motion, and it should be possible to spin up and down as often as required. Thus, one can “turn on” AG at the flip of a switch. This basic physics principle, described in Figure 12-3, takes advantage of the mass of necessary parts of the spacecraft as the spinning counter-mass, thus minimizing any unnecessary overhead. Such an approach could be used in a transfer vehicle going to Mars or a near-Earth object (NEO), a space research and development facility in LEO, or a gateway at a Lagrange point. A significant side benefit is that spinning at a slower rate can provide partial gravity equivalent to that on the surface of the moon or Mars, allowing for research and technology development that would apply to future surface missions.

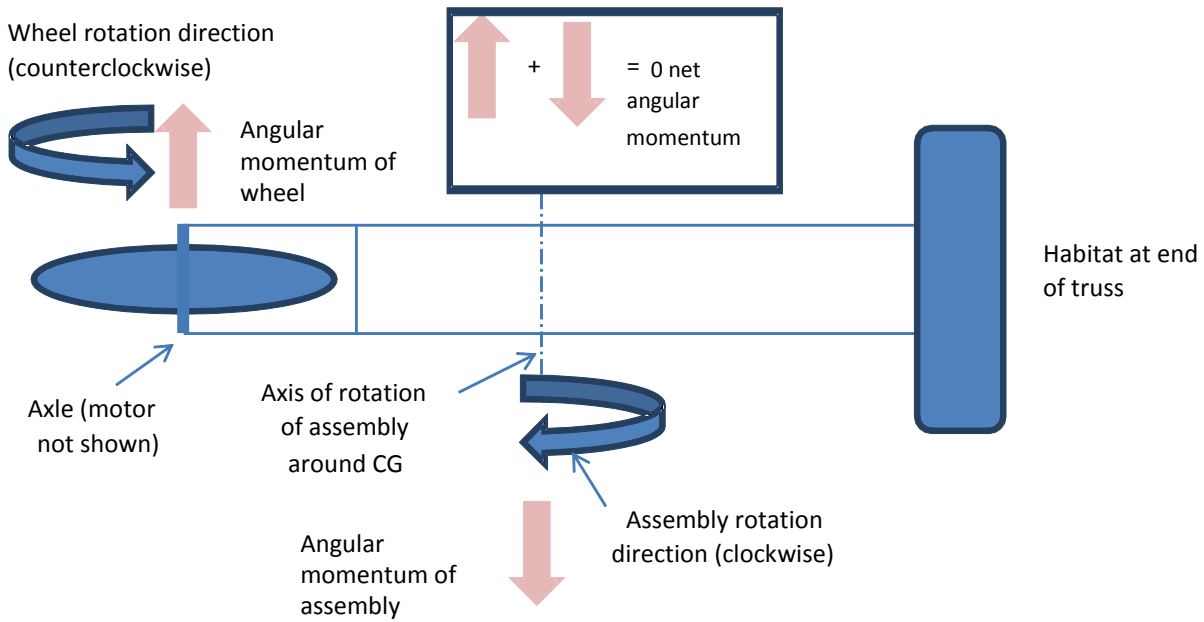


Figure 12-3 A simple action-reaction approach can initiate or stop the spinning. The angular momentum remains zero at all times, and multiple spin/de-spin cycles can be performed with no propellant.

The complexities of spinning vehicles include the fact that slewing for purposes of thrust vectoring and navigation, antenna pointing for communication, and the aiming of panels and radiators for solar power and thermal control are difficult. Clearly, these functions are simpler in 0-g. If the AG vehicle is cleverly designed, however, it may be possible to use gyroscopic forces to provide the turning torques needed for at least some of these tasks. Using the original concept of spinning one part of the vehicle to cause the other to spin in the opposite direction, designs could be generated such that the mass of certain stand-alone subsystems could provide a similar torque to enable slow slewing of the vehicle.

Two concepts have been offered regarding use of the power source (nuclear or solar) as the counter-rotating counter-mass to enable AG. A nuclear electric transfer vehicle and a solar-powered LEO or Lagrange-point AG vehicle could both play a role in an exploration program that uses AG to avoid the impact of 0-g on crew health. The latter vehicle type could be considered as a facility for the in-flight evaluation of exploration-related subsystems, enabling partial-g research and development that could not be performed on Earth. Such a vehicle would also constitute a unique type of AG technology that could be applied to a series of future spacecraft.

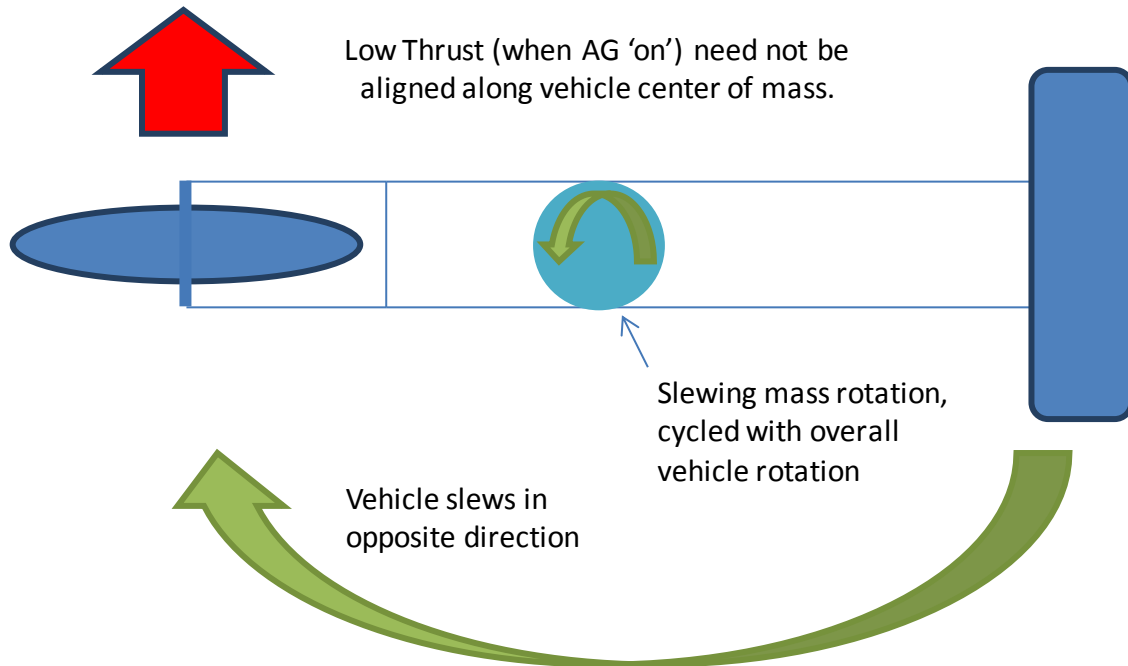


Figure 12-4 A rotating mass, shown in the center of this ‘vehicle’, can slew the rotational plane of the assembly and, thus, the thrust vector. It is spun only during a portion of each rotation of the assembly. Other locations of the mass in the vehicle are feasible.

It is not necessarily true that continuous AG equates to a higher vehicle mass or greater complications. While such top-level design concepts are far from fully developed systems, they demonstrate a possible method of implementing AG fairly simply. Moreover, the improvement to the health of the crew upon arriving at their destination that is facilitated by AG may allow for the development of new approaches to the design of landers and surface habitats. Thus, the impact of AG to the overall architecture of the exploration program may be significant in the important areas of mass, risk, and operational complexity.

12.8.4.1. Benefits of Whole Vehicle Centrifugation

Although AG may not be needed for a 6-month ISS mission, it would be invaluable for a trip to the vicinity of Mars, especially if the crew does not travel to the surface. Moreover, going to the surface of Mars may be safer if the crew has been at 1-g during the transit. Additionally, if a convenient NEO cannot be identified to support credible planning for missions of 6 months in duration, longer missions to more distant NEOs will be needed if this type of mission is pursued; thus, the same issues will need to be addressed.

Low-thrust electric propulsion of a spinning vehicle removes the requirement that the thrust vector must align with the center of mass, which opens the design space of the overall vehicle. Additionally, placing the propulsion system at one end (as the counter-mass) allows for the development of some interesting systems engineering approaches that have never been considered. It also provides new ways to solve the issue of docking and undocking a lander because the center of gravity (CG) of the vehicle is now available for such maneuvers.

As one considers the extended impact of incorporating AG into the spacecraft system, mission architecture, and overall Exploration Program, one can find opportunities to favorably impact decisions at all these levels. For example, a link exists between crew health benefits from AG and a requirement driver for atmospheric EDL on Mars. A ‘requirement’ will exist to be able to deliver large masses to the surface of Mars for a human mission. An earlier Mars DRM called for landing the crew with enough habitation volume, consumables, and other items necessary to allow them several days to adapt to a gravity environment after being at 0-g for ~6 months. This requirement was implemented because it was not certain whether the crew could successfully conduct an EVA to

rapidly transition from a small, short-duration, lander ‘taxi’ to a more permanent habitat. The result of that requirement was a decision to make that lander the permanent habitat for the entire surface stay, resulting in a cascade of requirements affecting the EDL technologies, vehicle designs, Mars orbit operations, the order in which vehicles were launched from Earth, and, ultimately, the design of the heavy lift launch vehicle. Alternatively, by providing an opportunity for the crew to ‘merely’ travel to Mars at 1-g, thus ensuring that they will be fit upon arrival, they should have no issues with rapidly exiting the lander and moving to a habitat that had been emplaced, robotically connected, and fully checked out remotely years earlier, before the crew launched from Earth. If any minor repairs are needed, this scenario provides time for planning and demonstrating appropriate hardware with the crew, providing a level of safety, both to the crew and mission, that is not available in all architectures. It may even make sense in such a scenario to produce some consumables by in situ resource utilization, as the habitat will be on the surface for over a year before the crew arrives. The impact on the mission architecture can be profound, and the Exploration Program will therefore have the freedom to explore different sequences of precursor missions and technology development approaches. The correct selection of architecture will likely have a significant impact on a wide range of technology decisions.

This approach opens up several other options to consider in the overall Mars architecture. Because the mass of the crew lander is now smaller, the way in which other items are split up, packaged, and delivered is open to trade. Even the ability to conduct a short-stay mission seems more viable if the crew can be counted on to be productive during the entire visit.

12.8.4.2. Drawbacks of Whole Vehicle Centrifugation

It has already been mentioned above that other subsystems of spinning spacecraft may become more complicated than their 0-g counterparts. Specifically, the pointing requirements of thrust, radiators, solar panels (if any), and possibly other systems may not coincide, and overcoming the gyroscopic stability of a massive spinning system can be a challenge. For certain combinations of technology choices, AG may be incompatible. However, there may be other combinations of technologies and approaches that are favorable in a 0-g approach.

Some of the mass savings possible with a 1-g vehicle (e.g., two-phase systems) may be lost if separate hardware is required for contingency operations under 0-g. Thus, it will be advantageous to be able to keep 0-g periods to a minimum so that the use of major alternative systems can be avoided. For example, perhaps crews can use ‘Apollo bags’ for short periods (up to a day or two) of 0-g for the collection of human waste. Longer periods of 0-g should be prevented by mission design, and the use of a contingency ‘fail-safe’ spin-up using a secondary system (e.g., small thrusters) could be employed in an emergency, thus resulting in a lost mission but a safe return of the crew.

There is a general concern that the more technologies that need to be developed before going to Mars, the farther into the future such a mission will be pushed. Certainly, no technologies should be pursued without a solid rationale. However, by utilizing AG, the causes of many potential health issues, and even some spacecraft system issues, will be avoided. The avoidance of the development of several new technologies may be possible if AG is available and reliable.

12.9. An Integrated Human Countermeasure Suite for Mars Exploration Missions

An integrated human countermeasure suite will be needed for a) a Mars fly-by and/or a Mars moon mission and b) a Mars landing mission. The countermeasure concept will be slightly different between a landing and fly-by mission in that the requirements are more demanding for a fly-by mission because of the lack of Mars gravity, which might aid as a countermeasure. The integrated countermeasure suite will most likely include:

- 1 Exercise devices for aerobic, dynamic, and resistive exercise training according to the currently tested Sprint protocol on the ISS for counteracting muscle and bone degradation and decreases in aerobic capacity.
- 2 Sensory-motor computer training programs and anti-motion sickness medication in preparation for EVAs and G transitions.
- 3 Lower limb bracelets for preventing and/or treating Visual Impairment/Intracranial Pressure syndrome.
- 4 Nutritional components for maintaining bone, muscle, and the cardiovascular system and preventing oxidative stress and damage and immune deficiencies (omega-3 fatty acids, PRO/K, anti-oxidants, salt, and iron).
- 5 Bisphosphonates for preventing bone degradation.
- 6 Lower-body compression garment and oral salt and fluid loading regimes to be used after landing on a planetary surface to counteract orthostatic intolerance.
- 7 Laboratory analysis equipment for the estimation of biomarkers in blood, urine, and saliva for monitoring the status of bone, muscle, the cardiovascular system, nutrition, the immune system, and cellular damage.
- 8 Advanced ultrasound techniques for monitoring bone and cardiovascular health.
- 9 Computer modeling programs for individual assessments of efficiency and adjustments of countermeasures based on individual health monitoring.

12.10. Food Considerations

The space food system must provide the crew with nutritious, acceptable, and safe food for up to 5 years on extended-duration missions to prevent performance and health decrements. Ideally, the quality of the food would be sustained throughout the 5-year period, but the nutrients naturally present in food are degraded through processing and storage. The current prepackaged food system has an ambient-temperature shelf life of 1.5 years due to nutritional and acceptability losses, which include flavor changes due to lipid oxidation or loss of volatiles, texture changes due to staling or structure loss, and color changes due to enzymatic browning. Preliminary data from flight foods indicate that the degradation of phyloquinone (vitamin K), thiamin (vitamin B1), folic acid (vitamin B9), cobalamin (vitamin B12), and ascorbic acid (vitamin C) is most concerning and that crewmembers could be at risk for nutritional deficiencies on long-duration missions.

The capability to refrigerate (4°C) and freeze (-20°C or lower) food on a long-duration mission will increase the shelf life of the current food system, albeit to an unknown extent. The ultra-cold environment of Mars is also under consideration as a viable “freezer” space. Storing the food under the martian soil surface will avoid the vast temperature swings of the planet, but access to it under all operational scenarios would be difficult to ensure. The complications of ice formation, damage to fruit and vegetable structures, and muscle protein denaturation are introduced with freeze stabilization, resulting in loss of the firm texture. On the other hand, lipid oxidation, vitamin degradation, and undesirable diffusion-limited reactions are potentially mitigated by the ultra-cold storage. Further investigation will determine whether refrigerated or frozen temperatures will provide the required shelf life extension without negatively impacting food quality.

The capability to store the food in an oxygen- and water vapor-free vacuum at room temperature would limit reactions such as the breakdown of vitamin C and loss of rehydratability in freeze-dried foods. However, oxygen is not able to be completely eliminated at the packaging step, so initial degradation would still proceed without cold storage until the oxygen is depleted. Additionally, other reactions, such as nonenzymatic browning, would not be inhibited in a vacuum environment.

The use of cans to package thermostabilized foods is not a feasible solution, as cans may reduce shelf life rather than increase it. Most can sizes require a longer processing time than the metalized pouches currently in use, which

reduces the initial nutritional content and acceptability of the food. Additionally, the metalized pouches have similar oxygen and water vapor barrier properties to cans, are easier to stow, and are lower in mass and volume.

Another option to meet a 5-year shelf life is to include a bioregenerative component in the food system. While this would provide fresh, nutritious foods and less initial food upmass, this system would require significant infrastructure and crew time and possibly result in food scarcity. The challenges of this system are under investigation, and a trade study comparing the upmass, acceptability, and crew time requirements of prepackaged foods with a bioregenerative system has recently been completed. A collaborative effort between groups involved in upmass, plant growth, and waste disposal is required to fully understand the trade between a bioregenerative and a prepackaged food system. Furthermore, most bioregenerative systems rely on gravity for many aspects of the system and will not work for a Mars orbital mission.

12.11. Bibliography

- ⁴ NASA Space Flight Human Systems Standard, Volume 1: Crew Health, NASA-STD-3001, 5 March 2007.
- ⁵ NASA Space Flight Human Systems Standard, Volume 2: Human Factors, Habitability, and Environmental Health, NASA-STD-3001, 10 January, 2011.
- ⁶ ISO 13407, Human Centered Design Processes for Interactive Systems, International Organization for Standardization, 1999.
- ⁷ Human Integration Design Handbook, SP-2010-3407, 27 January 2010.
- ⁵ Artificial Gravity Research to Enable Human Space Exploration. Editors: Young, L., Yajima, K., Paloski, William. International Academy of Astronautics, 2009.

13. SPECIAL STUDIES AND STRATEGIC ASSESSMENTS

Since publication of DRA 5.0, several assessments and special studies which are pertinent to defining future human exploration of Mars have been conducted. The descriptions provided in this section represent only a summary of the respective studies. For further information on the studies themselves as well as helpful supporting data can be found in the citations provided in the bibliography section.

13.1. *Orbital Missions*

Recent discussions within the exploration community have focused on the prospect of the strategy of conducting a mission to orbit Mars as a validation test prior to the surface mission.⁸ Emerging from these discussions is the current National Space Policy that specifically states: “*By the mid-2030s, send humans to orbit Mars and return them safely to Earth.*”⁹ These strategies and conclusions are drawn in part from the historical precedence of Apollo missions where multiple preparatory missions were conducted prior to the first human landing on the Moon. Apollo 8 performed the first human lunar fly-by and Apollo 10 performed the first human orbital mission. Both Apollo 8 and 10 were conducted consistent within the same capabilities and operational profile of the subsequent Apollo 11 landing mission, but that same “orbital testing at the destination before surface landing” philosophy may not hold true for much longer and demanding missions to Mars. Careful examination of the necessary capabilities and knowledge required for both orbital and surface missions, focusing on the similarities between the two, must be conducted to fully understand the potential synergism. To provide a better understanding of how an “orbit only” mission would fit into the emerging strategic framework, an assessment of the operational strategies for exploring the moons of Mars was necessary.

13.1.1. Phobos/Deimos Destination Assessment

Primary Contributor:

Dan Mazanek, NASA, Langley Research Center, USA

13.1.1.1. Introduction

During the first half of 2012, the Human Spaceflight Architecture Team (HAT) developed a preliminary Destination Mission Concept (DMC) to assess how a human orbital missions to one or both of the martian moons, Phobos and Deimos, might be conducted as a follow-on to human missions to near-Earth asteroids (NEAs) and as a possible preliminary step prior to a human landing on Mars. The HAT Mars-Phobos-Deimos (MPD) mission would also permit the teleoperation of robotic systems by the crew while in the Mars system, hence the hyphenated acronym to emphasize that all three planetary bodies would be explored. The DMC development activity provided an initial effort to identify the science and exploration objectives and investigate the capabilities and operations concepts required for a human orbital mission to the Mars system. In addition, the MPD Team identified potential synergistic opportunities via prior exploration of other destinations currently under consideration.

13.1.1.2. Activity Goal

The primary goal of the activity was to determine whether an opposition-class mission (short-stay mission of ~30-90 days at Mars) provides sufficient time to meet all or most of the science and exploration objectives at Phobos and Deimos, or if a conjunction-class mission (long-stay mission of ~450-540 days at Mars) is required.

Opposition-class (short-stay) missions allow total mission durations that can be significantly shorter than conjunction-class missions (~560 days vs. ~950 days). Conjunction-class (long-stay) missions are “minimum energy” trajectories that require less mission ΔV than opposition-class missions (e.g., ~6.5-7.9 km/s vs. ~8.3-14.1 km/s for crew transfer to and from the martian system). It should be noted, that the above ΔV s do not include any orbital maneuvers for exploring the martian system.

13.1.1.3. Background Information on the Martian Moons

Although the origin of the martian moons has not been conclusively determined, scientists speculate that one or both of the moons are captured asteroids. Regardless of their origin, both moons are relatively small and are similar in appearance to near-Earth asteroids (NEAs), so human NEA missions could provide applicable operational training that would enable a more efficient future exploration of one or both moons.

Figure 13-1 shows a color image composite of the two moons to the same scale using data obtained by the High Resolution Imaging Science Experiment camera on NASA's Mars Reconnaissance Orbiter. The color-enhanced view of Deimos, the smaller of the two moons of Mars, was taken on Feb. 21, 2009, and the image of Phobos was taken on March 23, 2008. Excluding the most recent impact craters, Deimos has a smooth surface due to a blanket of fragmental rock or regolith that covers its surface, whereas the surface of Phobos appears to be pock marked with craters, grooves, and linear features. Data from the camera's blue-green, red, and near-infrared channels were combined to generate these color images. Table 13-1 provides a summary comparison of some of the key characteristics of the two moons.

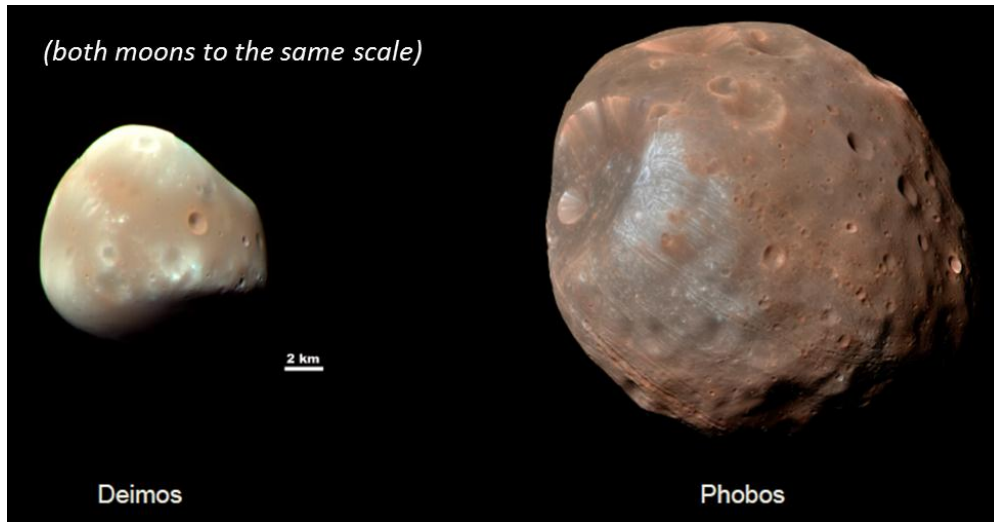


Figure 13-1 Composite image of Deimos and Phobos (Credits: NASA/JPL-Caltech/University of Arizona).

Table 13-1 Characteristics Deimos and Phobos

Characteristic	Deimos	Phobos
Mass (kg)	1.80×10^{15}	1.08×10^{16}
Dimensions (km)	$15.6 \times 12.0 \times 10.2$	$26.2 \times 22.2 \times 18.6$
Albedo	0.068	0.071
Equatorial Surface Gravity (μg)	400	860–190
Semi-Major Axis (km)	23,459 (Mean)	9,378 (Mean)
Inclination to Mars Equator (deg.)	0.93	1.09
Rotation Period (days)	1.26 (Synchronous)	0.32 (Synchronous)

13.1.1.4. Notional Destination Mission Concepts

Figure 13-2 and Figure 13-3 provide notional destination mission concepts for short-stay and long-stay Mars vicinity

operations, respectively. These operational concepts provide a graphical representation of the orbital sequencing, examples of possible surface activities, and summary of the Mars orbit strategy. These strategies are examples of how operations could be conducted and are just two of several options that could be developed. The focus of the MPD DMC study effort was to develop a “proof of concept” for the short-stay mission, rather than a definitive baseline. Further refinement of the mission objectives and optimization of the Mars vicinity operations is needed before a final Design Reference Mission (DRM) can be adopted.

While the mission concepts have some similarities (e.g., both mission concepts capture into a 1-sol parking orbit), there are several key differences. To minimize mission risk, the short-stay mission performs a plane change maneuver to match the departure asymptote. This is done to assure that the departure orbital conditions are properly set before exploration activities commence. The short-stay mission begins with an exploration of Phobos, which is identified by the MPD DMC Science Objectives and Requirements Formulation team as the higher priority, based on the current state of knowledge of both moons’ physical characteristics. The Mars Transfer Vehicle (MTV) is left in the parking orbit with two crew members, while the other two crew members utilize a Space Exploration Vehicle (SEV) attached to a transfer stage to explore the martian moon and return to the MTV. If sufficient stay time in the martian system is achievable, the two crew members who remained in the MTV utilize a second SEV and transfer stage to explore Deimos and return. The long-stay mission begins by exploring Deimos with the entire vehicle stack (MTV and two SEVs) transferring to the moon. After orbital operations at Deimos are complete, the entire stack transfers to Phobos. The propulsive element(s) for the long-stay mission must be capable of propelling the entire vehicle stack through all of the maneuvers prior to departure for Earth. In both mission concepts the SEVs are jettisoned prior to the departure maneuver; however, the potential exists for the SEVs to continue operations in an uncrewed mode after Earth departure, limited by their remaining propulsive capability. For the long-stay mission, both SEVs would be in the vicinity of Phobos, whereas for the short-stay mission they would be left in the 1-sol parking orbit.

13.1.1.5. Study Areas

The HAT MPD activity focused on the following seven study areas: 1) science objectives and requirements formulation; 2) exploration objectives and requirements formulation; 3) destination activity implementation strategy; 4) mission implementation strategy; 5) synergies with cislunar activities; 6) synergies with human and robotic precursor missions to NEAs; and 7) robotic precursor requirements for a human mission to Mars orbit and its moons. The primary MPD DMC study effort team members and their affiliations are listed at the end of this addendum section and the team members for each study area are in this section.

13.1.1.5.1. Science Objectives and Requirements Formulation

Team: David Beaty (Lead), Paul Abell, Deborah Bass, Julie Castillo-Rogez, Tony Colaprete and Ruthan Lewis

Charter: Identify and prioritize the scientific objectives and requirements for a Mars orbital mission, including small body origin/geology and field science through sampling and geophysical station deployment, Mars geology through the possible collection of martian meteorites from Phobos, and completing the Mars Sample Return (MSR) mission by retrieving the sample cache from low Mars orbit after ascent from the surface. Additionally, identify possible science opportunities during the transit to and from the martian system.

Key Findings: The study of Phobos and Deimos contributes Mars Exploration Program Analysis Group (MEPAG) objectives, all science themes in the Small Bodies Assessment Group (SBAG) Roadmap, and includes opportunities for other science activities during transit to and from the Mars system (e.g., astrophysics, heliophysics, life science, etc.).

The highest-priority science is based on sample return and deployment of assets, taking advantage of human crew:

- Small body origin/geology: field science, sampling, geophysical station deployment.
- Mars geology: search for martian meteorites on Phobos.
- Collect MSR sample cache.

The primary science objectives identified by the study area team were:

- Determine the nature of the surface geology and mineralogy of Phobos/Deimos.

- Characterize the regolith on Phobos/Deimos, and interpret the processes that have formed and modified it.
- Complete the MSR Campaign by capturing and returning to Earth the orbiting cache of samples.
- Collect any identified Mars meteorites/material from the surface of Phobos/Deimos, and return to Earth for detailed study.
- Determine the absolute material ages and constrain the conditions of formation of Phobos and Deimos.

To determine an exploration scenario that could accomplish these science objectives, notional landing, and sampling sites were identified (see Figure 13-4) and used to formulate the destination operational timelines developed by the Destination Activity Implementation Strategy study area team. Table 13-2 identifies the key implementation implication for each of the science priorities.

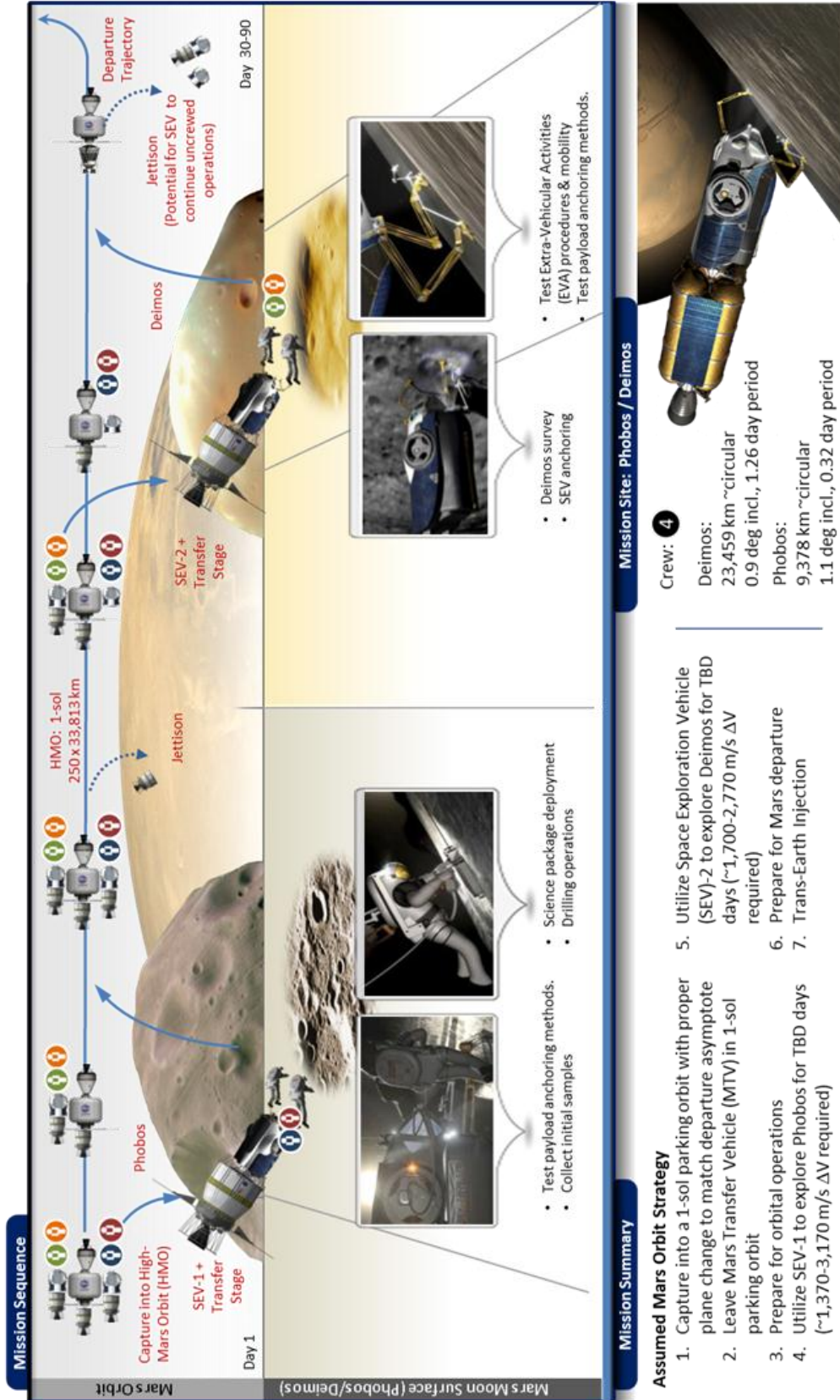


Figure 13-2 Notional concept for short-stay Mars vicinity operations.

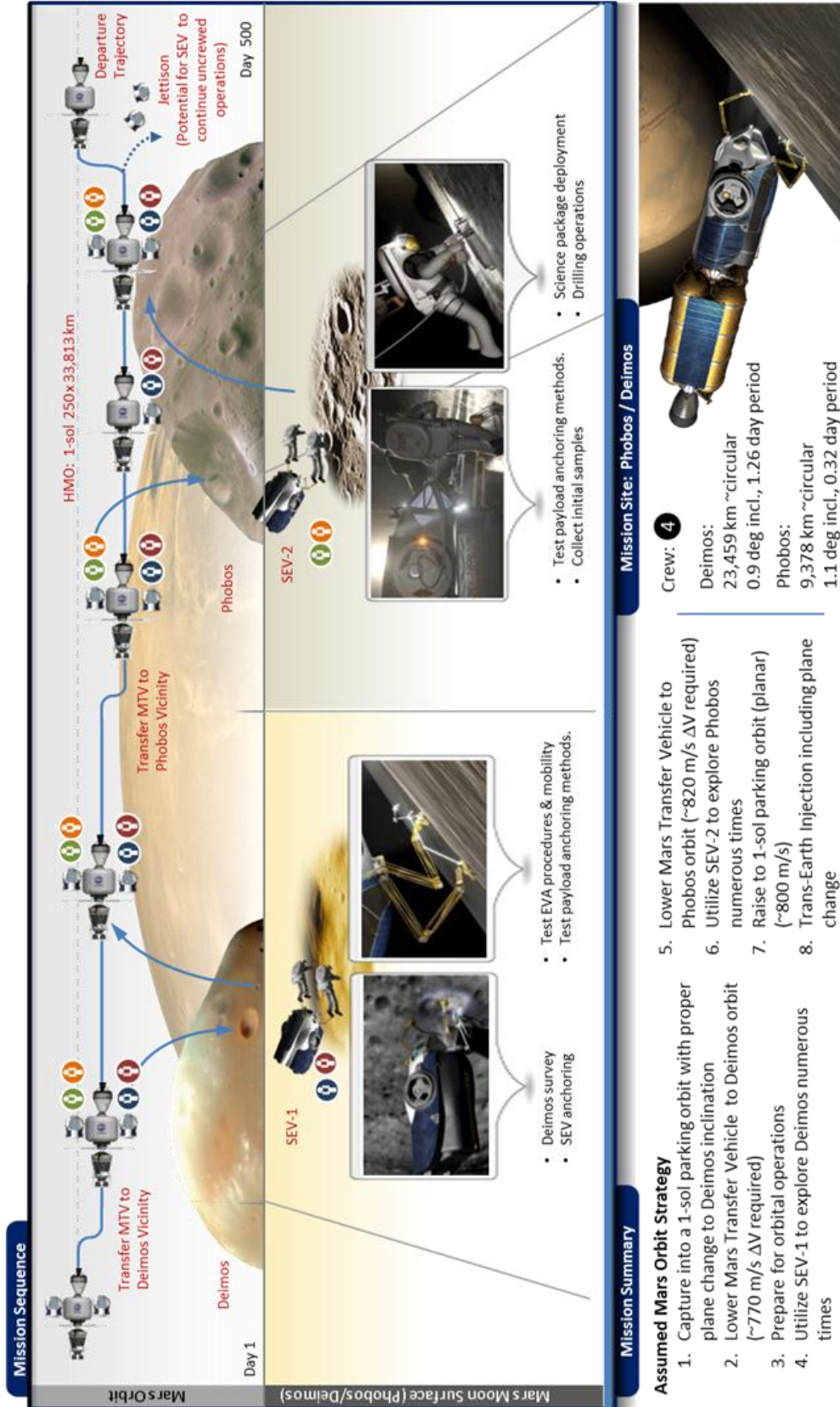


Figure 13-3 Notional concept for long-stay Mars vicinity operations.

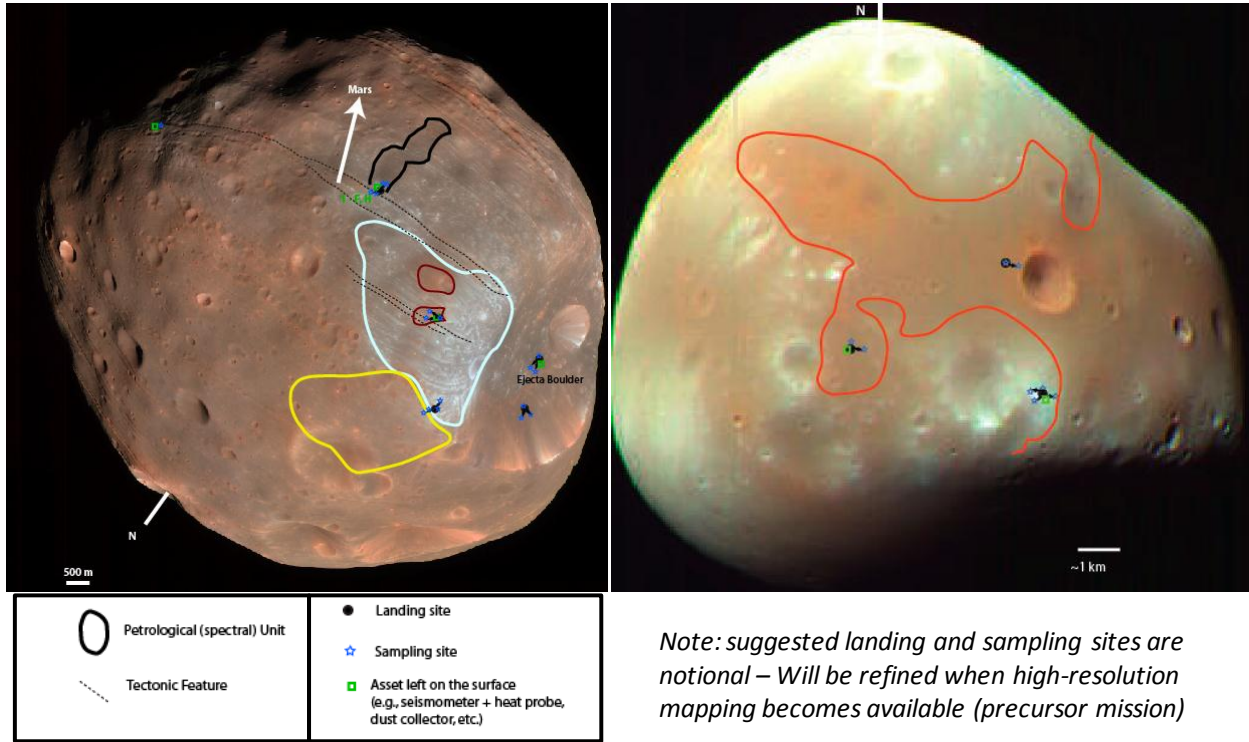


Figure 13-4 Notional reference landing and sampling sites on Phobos and Deimos.

Table 13-2 Implementation Implications of Science Objectives

SCIENCE PRIORITY	IMPLEMENTATION IMPLICATION
Field science at surface of Phobos/Deimos	This is more efficiently done via EVAs. There is a need for surface mobility to maximize contact time between the astronauts and the geology to be studied. Multiple sites are needed to sample the surface diversity of the moon(s).
Regolith science	This activity requires a method of examining and/or acquiring samples from depth (~2-3 m). Multiple sites are needed to sample the sub-surface diversity of the moon(s).
Returned sample science	The crew would need field instruments to support sample selection/identification, sample acquisition and sample packaging/containment. Samples from multiple sites are needed to capture the material diversity of the moon(s). The returned mass allocation needs to be accounted for within the mission design (including containers, environmental control, etc.).
Long-term monitoring of the Martian system	A suite of monitoring instruments would need to be set up by the astronauts, and left behind on Phobos/Deimos for extended operations.
MSR Sample Cache Retrieval	It is unclear whether this should be achieved via autonomous robotic rendezvous, operation of teleoperated assets, or performed directly by the crew. This requires further study and analysis.
Telerobotics to the Martian surface	The priority is unclear—the science drivers are not well defined. Also it is unclear what the implications are for the duration and location of the astronauts required to teleoperate assets on the Martian surface, and the necessity for pre-deployment of those assets. This requires further study and analysis.

In addition to the science performed in the martian system, many transit science opportunities are possible during a mission to the Mars system and include the following:

- Venus flyby: likely included during an opposition-class mission.
- Other Planetary Science: micrometeoroid monitoring, dust collection, small body flybys, etc.
- Heliophysics: Sun’s polar magnetic field and solar wind characterization, deployment and retrieval of GAS can/SPARTAN-like payloads.
- Astrophysics: Observation of Earth as an exoplanet, planetary microlensing events, etc.
- Biomedical: Monitoring the impact of radiation, microgravity, of solar protons and Galactic Cosmic Rays (GCRs) on cellular material, of the human immune system, of muscular and cardiovascular performance.
- Psychological: Monitoring the impact of confinement, stress hormone levels, sleep patterns, response to altered lighting/environments.

Humans can significantly increase the science returned during transit and make real-time adjustments during encounter to maximize science without round-trip communication delays and sequencing issues. Additionally, crew members are able to deploy/retrieve equipment repeatedly and return it for detailed examination on Earth. Finally, transit science events will enhance the mission’s scientific and engineering return, and provide further opportunities for public engagement.

Recommendations: The study team’s recommendation is to visit both Phobos and Deimos, with higher priority for Phobos, based on the current state of knowledge of both moons’ physical characteristics. Additionally, the study team recommends that a precursor mission includes science observations necessary to inform human exploration planning (e.g., relative science significance of Deimos vs. Phobos) and retire Strategic Knowledge Gaps (SKGs). The applications of teleoperations to Mars surface are unclear and require further study before providing a recommendation.

13.1.1.5.2. Exploration Objectives and Requirements Formulation

Team: Steve Hoffman (Lead), David Beaty, Tony Colaprete, Bret Drake, Ruthan Lewis and Dan Mazanek

Charter: Gather and articulate the exploration goals and objectives for the human exploration of Phobos and Deimos pertinent to Mars exploration, including orbital missions, surface missions, and preparation for sustained human presence in the Mars system. The human MPD mission is assumed to be part of a larger campaign of human exploration of Mars, including its surface, its moons, and the surrounding environment. The goals and objectives of this mission encompass gathering data and demonstrating technologies/operations needed in advance of humans attaining the next level of Mars exploration (See Figure 13-5).

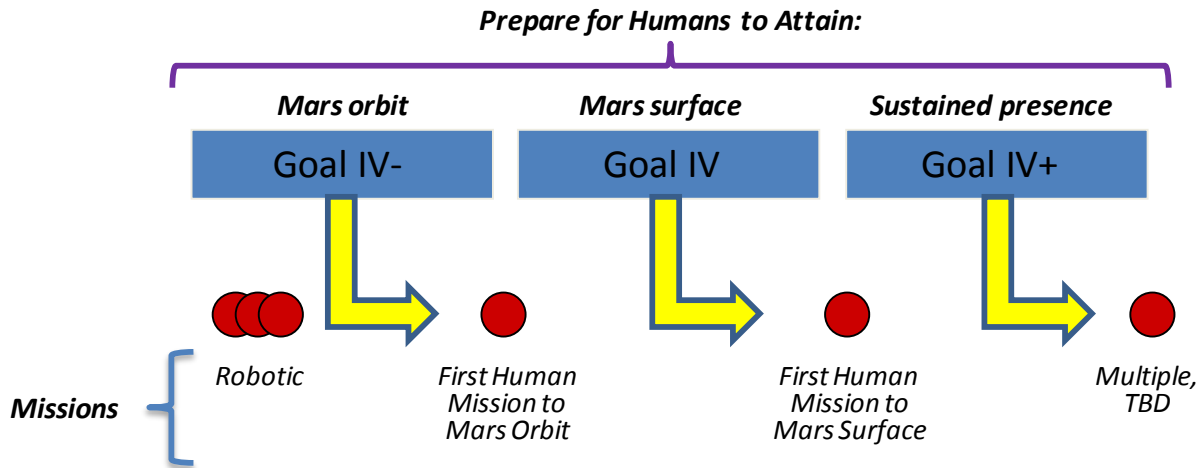


Figure 13-5 Goals for human presence in the Mars system.

Key Findings: The human exploration objectives for a Mars mission (including the MPD mission) include the following:

- Obtain knowledge of Mars, its moons, and the surrounding environment sufficient to design and implement human missions with acceptable cost, risk, and performance.
- Conduct technology, operations, and infrastructure demonstrations in transit to, in orbit around, or on the surface of Mars or Phobos and Deimos to reduce risk or cost for human missions.
- Incorporate partnerships (international, commercial, etc.) that broadens overall organizational participation but also lowers the total program cost for each partner.
- Incorporate multiple public engagement events spread across entire mission durations and using multiple media types.
- Prepare for sustained human presence.

As with the science objectives, the applications of teleoperations at Mars that will satisfy human exploration objectives are unclear at this time and require further study.

Table 13-3 identifies the key implementation implication for each of the exploration objectives.

Table 13-3 Implementation implications of exploration objectives.

EXPLORATION OBJECTIVES	IMPLEMENTATION IMPLICATION
Obtain knowledge of Mars, its moons, and the surrounding environment	a) Data to develop gravitational potential models for Phobos and Deimos; b) Imagery of TBD resolution with altimetry of the entire surfaces of Phobos and Deimos; c) Solar Particle Event (SPE) and GCR radiation measurements from orbit; d) Data to develop preliminary geological maps of Phobos and Deimos; e) Civil engineering data for safe landing and operations.
Conduct technology, operations, and infrastructure demonstrations	a) Exercise Mars surface sample return protocol; b) Collect system performance data (Environmental Control and Life Support System (ECLSS), power, etc.); c) Exercise independent crew operation procedures; d) Exercise orbital operations (e.g., rendezvous with a suitable target); e) Demonstrate In-Situ Resource Utilization (ISRU) on Phobos or Deimos.
Incorporate partnerships that broadens overall organizational participation	a) International Partner contribution of mission elements, experiments, and other equipment; b) Use of commercially available elements with (potential augmentation) to meet mission requirements; c) Include partnerships as applicable with other US government agencies.
Incorporate multiple public engagement events	a) Perform an early mission to the Martian system to engage the public and maintain interest in a Mars surface mission; b) Include student – developed experiments and projects (allocate time, mass, power, etc.); c) Include time in scheduled crew activities for public outreach activities during all mission phases.
Prepare for sustained human presence	a) Catalog elements and minerals types and concentrations on the surface and subsurface of Phobos and Deimos; b) Surface and near subsurface “civil engineering” properties at Phobos and Deimos; c) Long duration Mars atmospheric observations; d) Demonstrate ISRU processes for applicable mineral types; e) Demonstrate key elements (TBD) of long term orbital infrastructure.

13.1.1.5.3. Destination Activity Implementation Strategy

Team: Kevin Earle (Lead), Jeff Antol, Deborah Bass, David Coan, Kevin Daugherty, Mike Hembree, Sharon Jefferies, Ruthan Lewis, and David Reeves

Charter: Determine whether a worthwhile human mission to Phobos and Deimos can be accomplished with a high degree of confidence during an opposition-class (short-stay) mission opportunity. Determine operational timeline and required equipment, and formulate telerobotic operations (moons and Mars surface) and extravehicular activity (EVA) support strategies.

Key Findings: Based on the science and exploration objectives identified, preliminary results indicate that an opposition-class mission to Phobos and/or Deimos appears feasible. All currently identified science and exploration objectives could be accomplished in 56 days. The development of a conservative plan provides substantial schedule margin. Further studies are needed to optimize mission planning, understand implications of in-system teleoperations, and refine objectives definition. The preliminary DMC development approach utilized by the team is shown in Figure 13-6, and the high-level concept of operations (ConOps) developed is shown Figure 13-7. It should be emphasized that this preliminary. The ConOps represents a conservative existence proof and attempts were not made to optimize it.

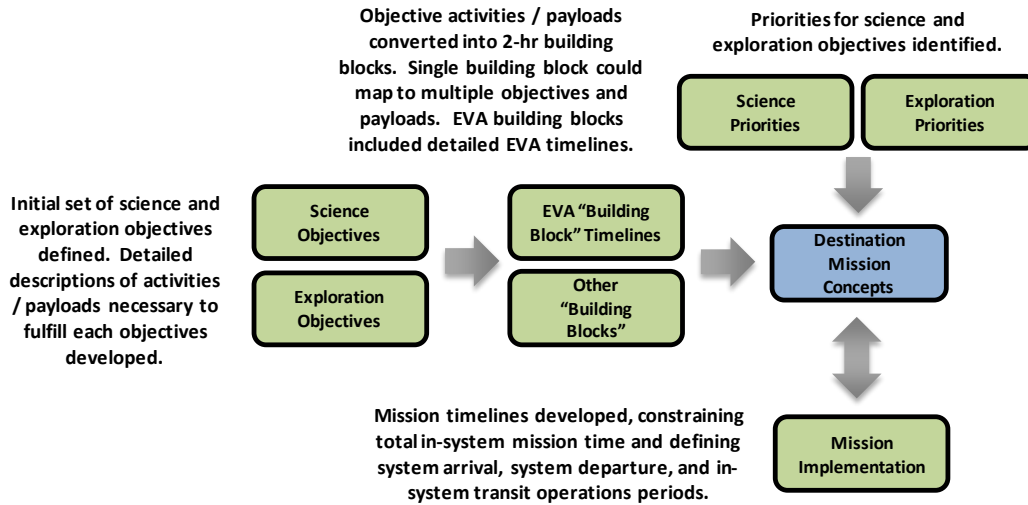


Figure 13-6 Preliminary DMC development approach.

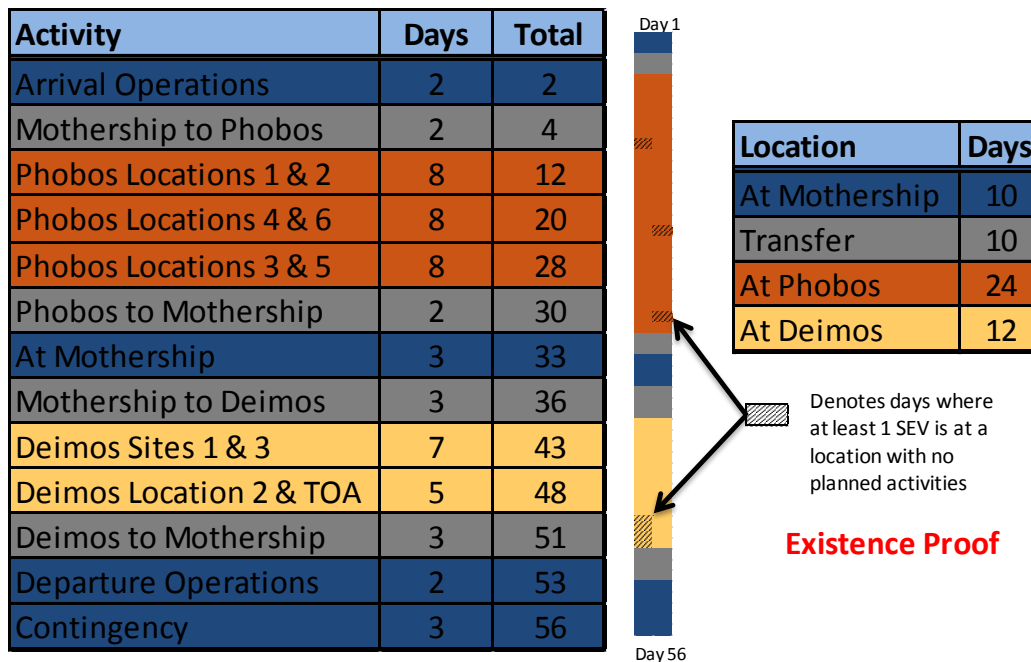


Figure 13-7 High-level concept of operations.

Allocations/resources for in-system telerobotics are not included in the preliminary MPD concept of operations because the objectives identified by the Science and Exploration Objectives and Requirements formulation teams could be achieved more efficiently with other means. The team did explore the potentials benefits and challenges of moving some of the robotic support team in-system (as shown in Figure 13-8) to achieve more decision-points per sol by reducing the communication latency: With refined or alternate objectives, in-system telerobotics would need to be reassessed.

Benefits:

- Increased situational awareness may reduce risk for more challenging operations.
- Progress of activities can increase due to multiple decision points per sol.
- Use of unconventional scientific platforms (e.g., airplanes and hoppers).

- Transient science acquisition (e.g., dust devils on Mars, meteorite impact on Phobos/Deimos).

Challenges:

- Much higher operations cost due to large engineering and operations support staff required for crew support.
- In-system mission periods have limited durations, much shorter than durations available for Earth-controlled operations.
- Time availability of in-system crew; crew has many other activities that they need to perform.
- Additional crew training requirements for telerobotic operations.

Unresolved Issues and Forward Work:

- Derive payload masses associated with performing destination activities and aggregate to determine outbound and inbound mission requirements.
- Optimize operations to align activity order with objective priority.
- Examine implications of shorter duration mission concepts (e.g., 30 days).
- Investigate alternative EVA operational modes, such as multiple crew members on EVA simultaneously, use of telerobotics in close proximity to crew, and alternative system hardware (e.g., advanced EVA maneuvering unit).
- Align systems performance assumptions with architecture design.
- Assess implications for incorporating in-system telerobotics.
- Determine required contingency duration between return from last moon excursion and Mars system departure.
- Investigate hybrid control approach for telerobotics to best leverage advantages of in-system vs. Earth-based locations (e.g., priority-based plan from Earth with crew monitoring and switching based on real-time observations) and enable rapid crew intervention to avoid damage or loss of robotic asset(s).

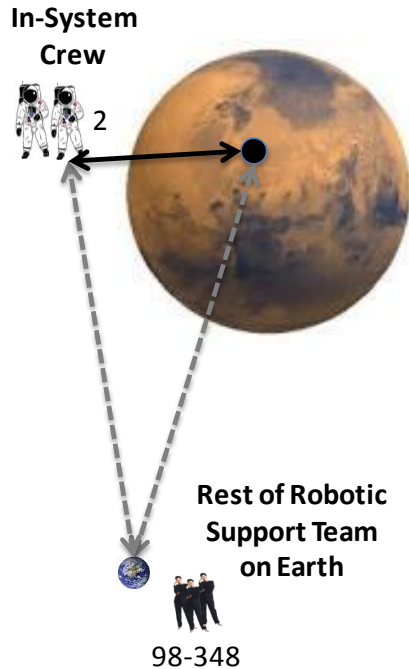


Figure 13-8 In-system telerobotics approach.

13.1.1.5.4. Mission Implementation Strategy

Team: Bret Drake (Lead) and Brent Barbee

Charter: Formulate the overall MPD mission exploration strategy options and provide a preliminary analysis of trajectories within the martian system to facilitate the destination activities.

A trip to Mars with a return back to Earth is a double rendezvous problem flown in heliocentric space. The first rendezvous outbound, with Mars, must be dealt with considering its influence on the second rendezvous, inbound with Earth. Practical considerations dictate favorable, and different, planetary alignments relative to the sun for outbound and inbound transfers. These considerations result in two distinct mission classes: short-stay class missions and long-stay class missions. Short-stay class missions (see Figure 13-9) are characterized by relatively short periods spent in the vicinity of Mars (generally 30-60 days). As such, these missions will tend to be highly scripted with pre-planned operational timelines. Due to the short time at Mars, there will be less time available for mission re-planning due to contingencies or large unanticipated discoveries. Long-stay class missions (see Figure 13-10) are characterized by long periods spent in the vicinity of Mars (330-560 days) and overall long mission durations (900+ days). These long-stay missions provide ample time for re-planning mission operations. It is envisioned that upon arrival at Mars, a very pre-planned scripted operational scenario will be followed. As the mission evolves, a more free-flowing collaborative (with Earth) scenario would follow.

Human Research Program Inputs: NASA’s Human Research Program (HRP) and medical support for the crew are not synonymous. Medical support is focused on individual health during a mission while HRP also considers mission performance and post mission health. There can be significant overlap in the kinds of data and physical samples collected as well as on-board analyses made.

Based on our current understanding of the human body’s reaction and adaptation to microgravity, medical interventions to maintain health (e.g., exercise) are expected to be qualitatively the same for Mars long-stay surface mission transits (6 months in micro-g), longer duration NEA missions (up to ~12 months in micro-g), or Phobos-Deimos missions (500 – 1000 days in micro-g). Data and samples collected for HRP-related research are expected to be the same types, with the quantities driven by mission duration. Our current understanding of human psychology and the impact of extended duration confinement is incomplete, and additional research is expected to require additional understanding of the impact of extended confinement (up to ~12 month NEA missions and ~1000 day Phobos-Deimos mission) on individuals and crews within deep space habitats before any conclusions can be made. Crew exposure to the radiation environment of deep space remains a key HRP risk area. Minimizing crew exposure to radiation (GCR and SPE) is a key mitigation strategy (e.g., reduce total mission duration for orbital missions).

Crewed Mission Transportation and Exploration Systems

Figure 13-11 and Figure 13-12 provide preliminary estimates of the expected Initial Mass in Low-Earth Orbit (IMLEO) for the crewed transportation architectures high thrust and low thrust propulsion approaches for a mission to the Mars system respectively. For example, total architecture mass estimates using nuclear thermal propulsion (NTP) for a 550-day opposition-class mission range from 350-1000+ tons (opportunity dependent). These estimates exclude destination systems, which will likely be pre-deployed to the martian system. Long-stay (conjunction-class) missions offer the advantage of lower overall mission mass (due to lower total ΔV s) and longer time in the Mars system for exploration activities, but with a longer overall mission time. Additional factors (e.g., cost, risk, mission operations, and value of additional science/exploration time) must be taken into account before reaching a conclusion on the most appropriate mission mode to achieve mission objectives. The following element assumptions were used to develop these estimates:

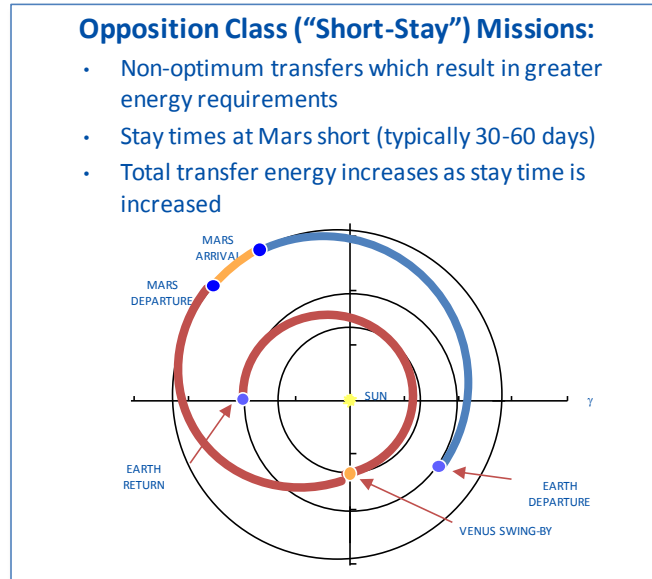


Figure 13-9 Short-stay class mission.

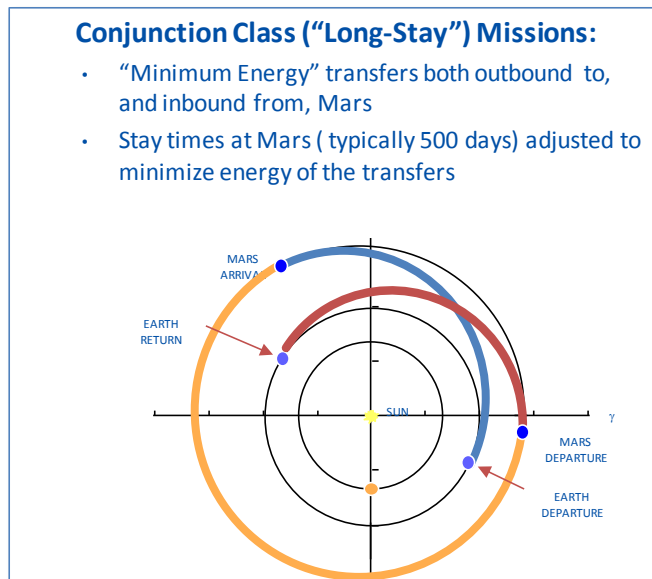


Figure 13-10 Long-stay class mission.

Multi-Purpose Crew Vehicle (MPCV):

- Consistent with HAT
- CM inert = 9.8 t
- SM inert = 4.5 t
- SM specific impulse = 328 s

Deep Space Habitat

- Sizing consistent with HAT Cycle-C
- Mass Range : 28-65 t
- Consumables loaded based on crew size & mission duration

Chemical Propulsion Stage

- Sizing consistent with HAT Cycle-C
- Parametric design with each stage optimized
- Zero-boiloff cryo management
- Stage fraction ~ 23%
- Specific impulse = 465 s

Solar Electric Propulsion

- Consistent with HAT
- Spacecraft alpha ~30 kg/kW
- Specific impulse = 1800-6000 s
- Xe tank fraction = 5%
- Total power varies

Nuclear Electric Propulsion

- Spacecraft alpha ~20 kg/kW
- Specific impulse = 1800-6000 s
- Xe tank fraction = 5%
- Total power varies

Nuclear Thermal Propulsion

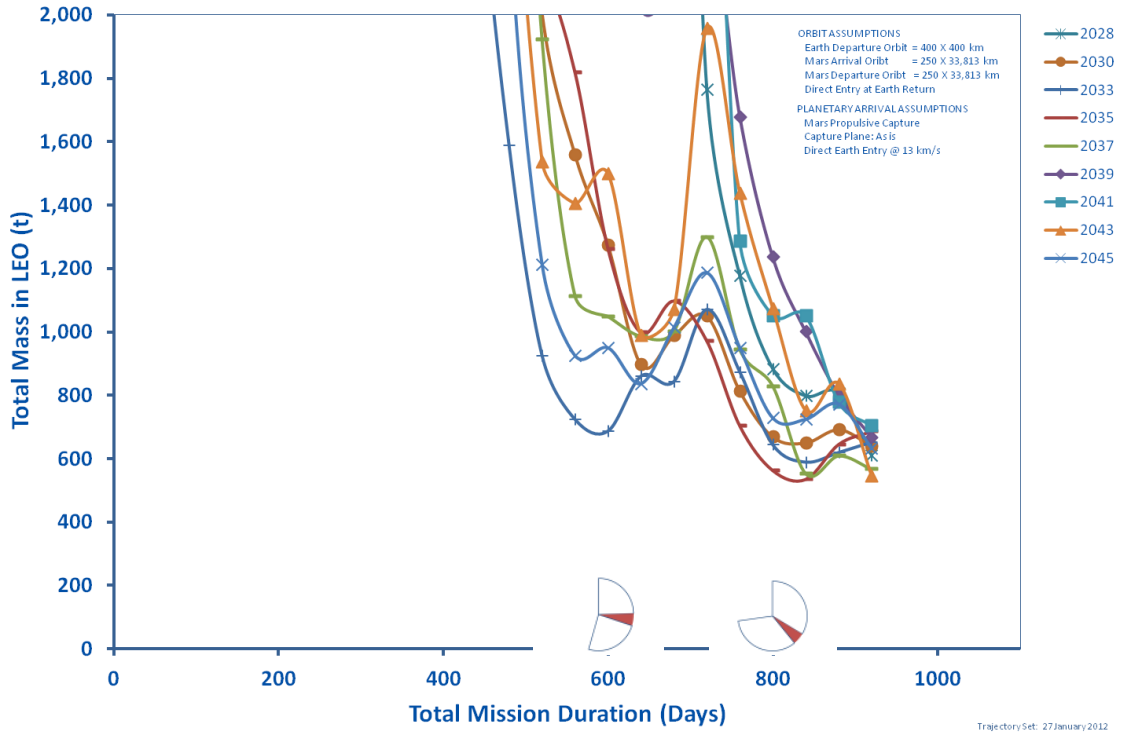
- Consistent with Mars DRA 5
- NERVA-derived common core propulsion (20 t core)
- 3 x 111 kN engines
- Specific Impulse = 900 s
- All LH2 fuel with zero boil-off
- Drop tanks @ 27% tank fraction

Space Launch System

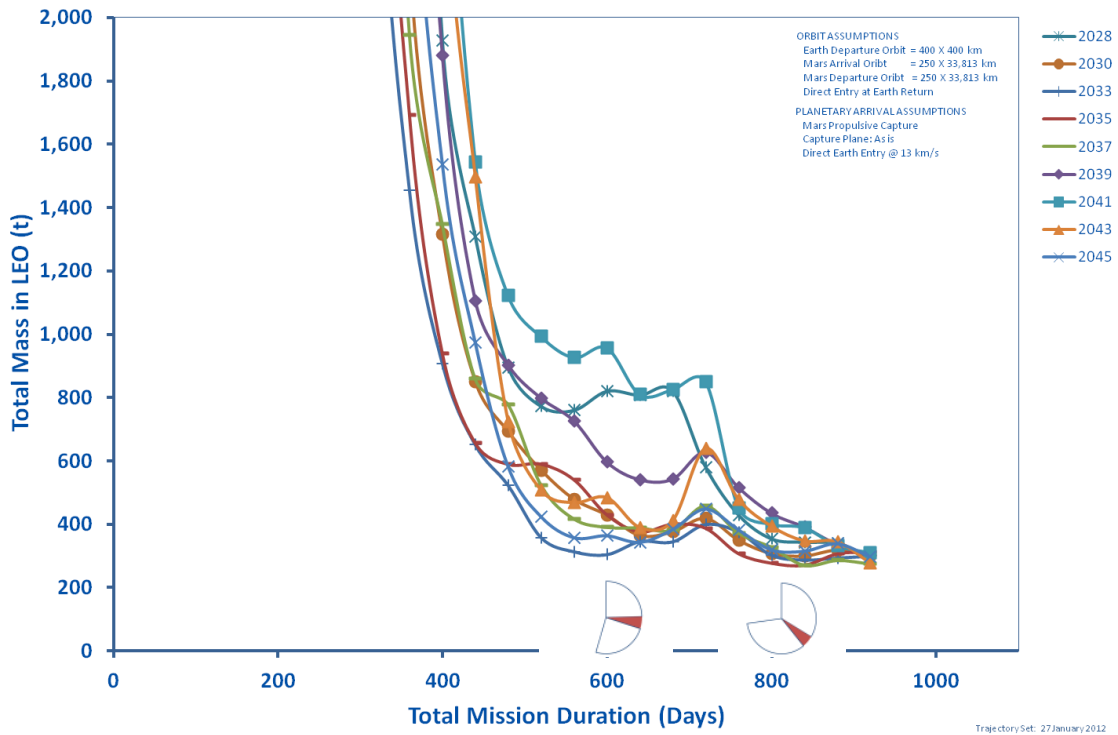
Gross Performance ~ 130 t

- Net Performance ~ 120.4 t (HAT assumptions for reserve and adapters)
- Performance estimates to negative perigee conditions: (-87 km x 241 km)

Mars Design Reference Architecture 5.0 – Addendum #2

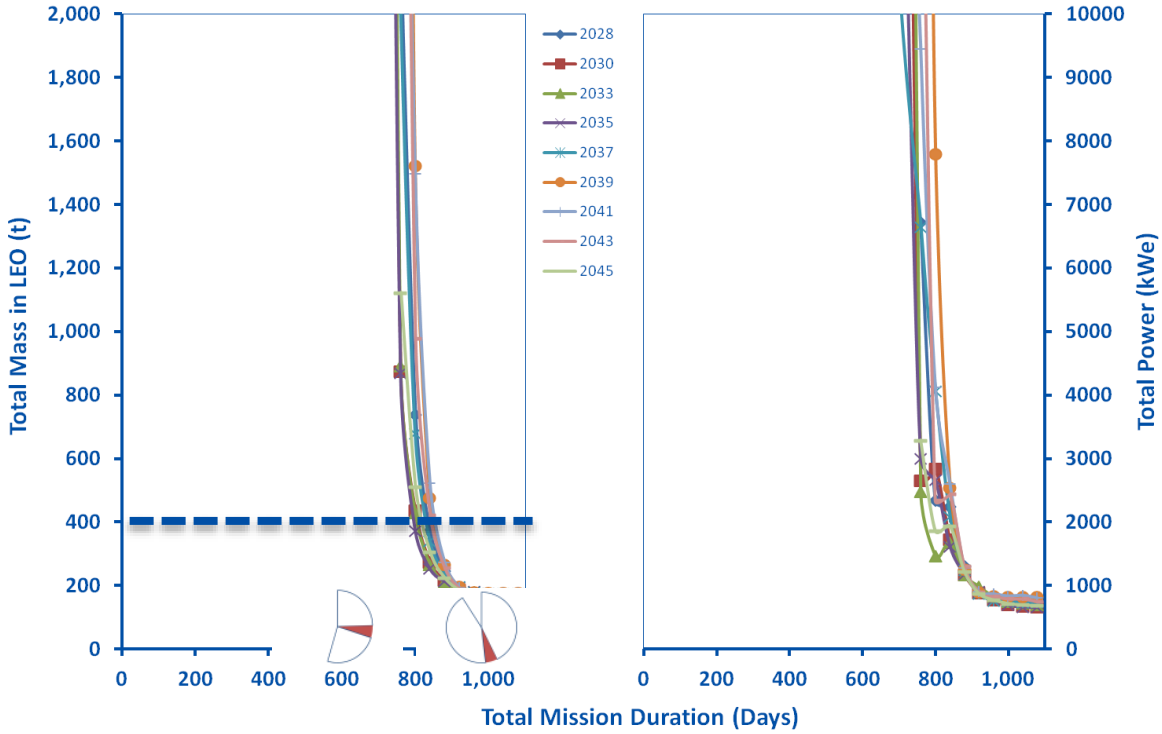


(a) Chemical propulsion

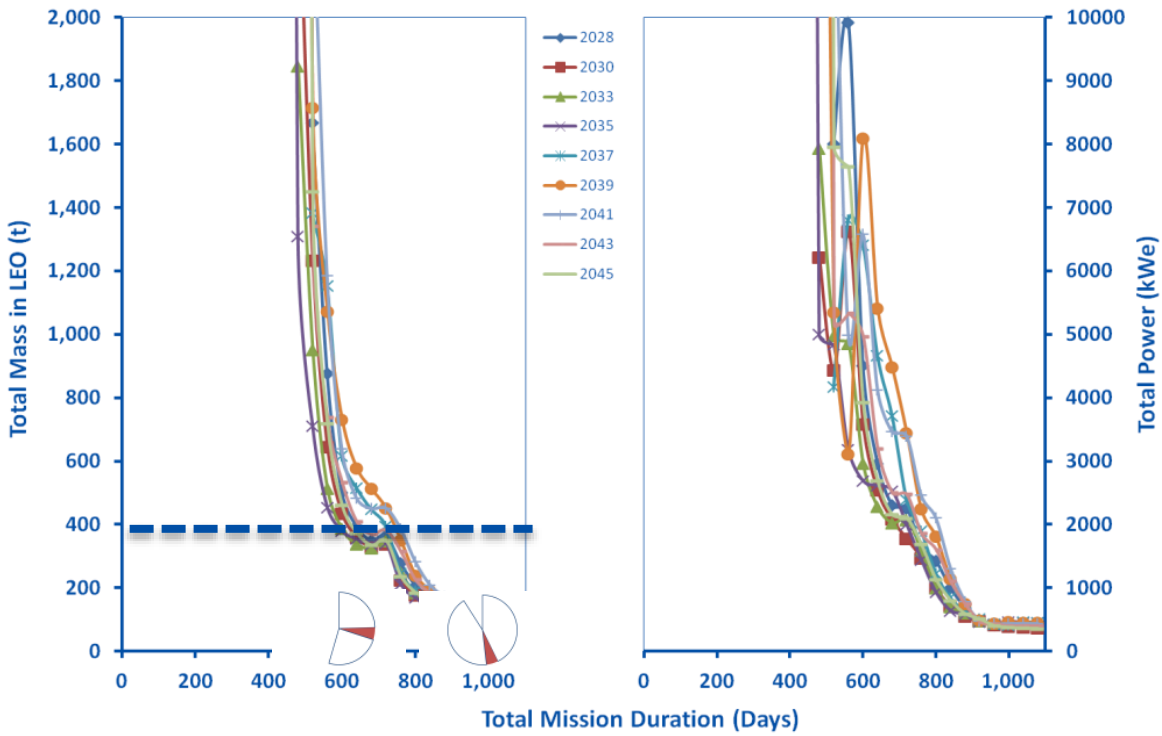


(b) Nuclear thermal propulsion

Figure 13-11 Total architecture mass as a function of total mission duration for high thrust propulsion concepts.



(a) Solar electric propulsion



(b) Nuclear electric propulsion

Figure 13-12 Total architecture mass as a function of total mission duration for low thrust propulsion concepts.

Mars Orbit Capture and Departure Dynamics

Both Phobos and Deimos are essentially in the equatorial plane of Mars, with nearly circular orbits at 9,378 km and 23,459 km, respectively. Earth-Mars trajectory arrival and departure geometries are not in the equatorial plane, thus additional orbital maneuvers (inclination change and orbit lower/raise) are required once the necessary crew parking orbit is established. For high thrust approaches, a multi-burn strategy used to account for planar alignments and capture time is short (hours to days) depending on parking orbit chosen. For low thrust approaches, the plane adjustments are made at Mars arrival (Sphere of Influence [SOI]) and capture duration is long (weeks to months). The duration depends on the parking orbit along with the power, thrust, and specific impulse of the low-thrust propulsion system.

Key Findings: Human missions to the moons of Mars are conducted entirely in deep-space, and reducing the exposure of the mission crew to the hazards of deep-space is of prime concern. Practical considerations (e.g., transportation technology and number of launches) will limit mission durations to not much less than 600 days, and thus, human health issues cannot be obviated by propulsion technology alone. If there is no significant difference between 600 and 900 days from human health or overall mission risk and operations perspectives, then long-stay (conjunction-class) missions offer the advantage of lower overall mission mass and longer time in the Mars system for exploration activities. However, other factors (e.g., cost, risk, and value of additional science/exploration time) must be taken into account before reaching a conclusion on the most appropriate mission mode to achieve mission objectives.

13.1.1.5.5. Synergies with Cislunar Activities

Team: Mark Lupisella (Lead), Jeff Antol, Deborah Bass, Dave Beaty, Kevin Daugherty, Lee Graham, Ruthan Lewis, and Dan Mazanek

Charter: Identify how cislunar space missions and activities can provide preparation for an MPD mission and how an MPD mission might enhance cislunar activities.

The following are the potential areas for synergy with cislunar activities identified by the team:

- Human Research (e.g., radiation effects and mitigation)
- Telerobotics (e.g., low latency surface telerobotics)
- Mission Systems and Support (e.g., system reliability and logistics)
- Long-term Deep Space Human Operations (e.g., crew autonomy)
- Proximity Operations (e.g., crew mobility, worksite stabilization)
- Sample Return (e.g., return samples to cislunar facility)
- Forging Partnerships (e.g., crew telerobotically control partner surface asset)
- Public Engagement (e.g., test crew activities for public outreach with delay)

High and medium priorities for cislunar synergy are shown in Table 13-4. The activities were prioritized based on the following criteria:

1. Objective alignment
2. High potential, but high uncertainty – suggesting need for in-space tests
3. Feasibility

Low-Latency telerobotics operation may be a useful strategy, particularly if human missions stay out of gravity wells for some time. As the ultimate value of telerobotic science on martian surface is yet to be determined, testing in cislunar space to explore potential value and to test systems is probably worthwhile. The following levels of telerobotic science, along with the team’s assessment of their probability of being implements, are:

- Operations and navigation: achievable
- Basic science (e.g., instrument positioning, sample acquisition): probably achievable
- Detailed science measurements and interpretation (most challenging part): perhaps partially achievable, needs testing

The potential difficulty of telerobotic science noted above suggests the possibility of parallel operational paradigm that includes two parallel paths, somewhat analogous to tactical vs. strategic planning, or short- vs. longer-term planning: 1) telerobotic science; and 2) “back room” science using Earth-based support.

Table 13-4 High and Medium MPD Cislunar Synergies Priorities

Synergy Activity	Priority
HUMAN RESEARCH: all activities (except artificial gravity)	High
TELEROBOTICS	
Simulate delays and different orbital operational implications for Mars surface	High
Conduct “fast” traverses to assess potential science return (could help with diversity)	High
Assess real-time science responsiveness	High
Perform analog tests for telerobotic operations of MPD surfaces – relates to proximity operations synergy. *An effective precursor mission could substantially reduce (but not eliminate) the dependency on telerobotic surface interaction.	High*
Conduct public outreach activities	Med
MISSION SYSTEM AND SUPPORT	
Radiation shielding	High
Life support system reliability	High
Medical support: health monitoring/treatment, including for planetary protection purposes	High
Subsystem serviceability and sparing	Med
Test pre-deploy strategies - e.g., consumables, fuel, and Automated Rendezvous and Docking (AR&D)	Med
LONG-TERM DEEP SPACE HUMAN OPERATIONS	
Crew autonomy / control authority tests	High
Verify & mature long-duration crew medical care operations	High
PROXIMITY OPERATIONS: Crew translation, restraint, worksite stabilization (build crude analog)	Med
SAMPLE RETURN: Return samples from lunar orbit/surface to cis-lunar asset as analog to returning samples from Martian orbit/surface to return vehicle	Med

Key Findings: There are a number of promising activities to conduct in cislunar space to help prepare for a human MPD mission. Most human research needed for a MPD mission can be conducted during cislunar missions. Crew autonomy is a key area to test during cislunar missions. Telerobotics has high potential, but also high uncertainty for science effectiveness and requires additional analysis and testing. Finally, large amounts of sample, that may not be returned directly to Earth, could be received at a cislunar facility.

13.1.1.5.6. Synergies with Human and Robotic Precursor NEA Missions

Team: Paul Abell (Lead), Julie Castillo-Rogez and Dan Mazanek

Charter: Identify synergies between human and robotic NEA missions and Phobos/Deimos missions. Determine the information and experience that can be gained from NEA missions prior to Mars system missions and assess the associated advantages.

NEAs and Phobos/Deimos are small airless bodies with similar physical characteristics, but represent distinct and separate destinations for robotic and human exploration. NEAs are any asteroid passing within 1.3 Astronomical Units (AU) of the Sun, while Phobos and Deimos are natural satellites of Mars at ~1.52 AU. The two NEAs that have been visited by robotic spacecraft, (433) Eros and (25143) Itokawa are shown in comparison to Phobos and Deimos in Figure 13-13.

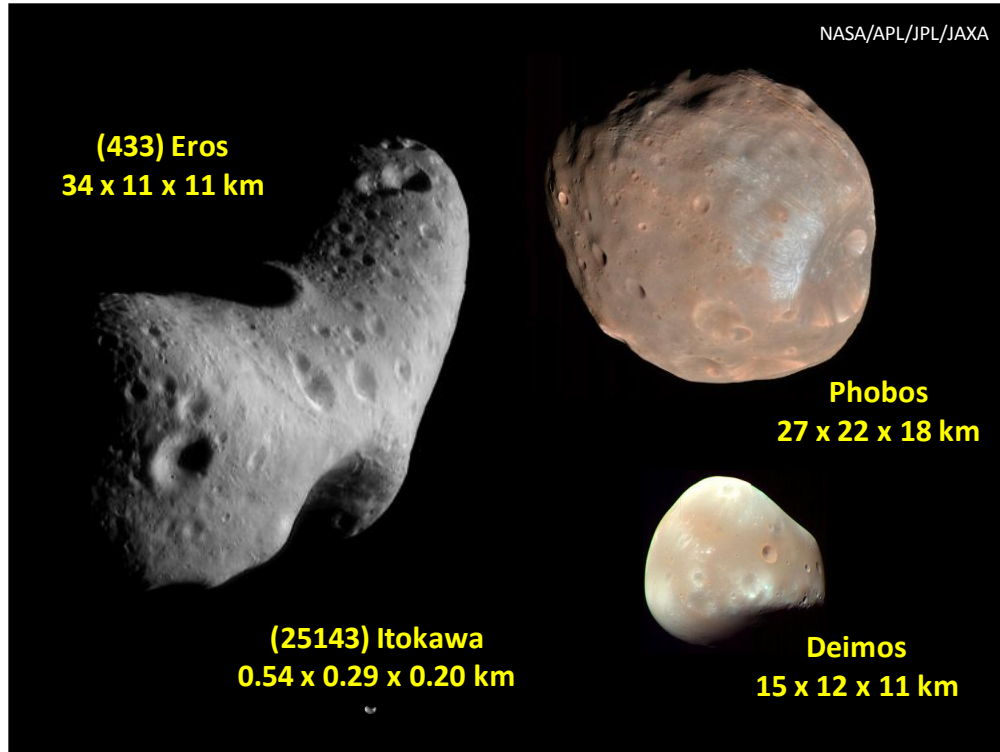


Figure 13-13 Robotically visited NEAs at approximate scale with Mars moons.

There are a number of synergies between missions to NEAs and missions to Phobos and Deimos. These synergies exist during the proximity operations, while conducting surface operations at the target, and even during the transit to/from the target (NEA or Phobos/Deimos).

Robotic Precursor Activities: Enable target identification and selection for future human mission activities, constrain internal and near-surface structure on regional and global scales, and characterize basic physical properties relevant for science and future human safety, performance, and operations.

Human Exploration/Operations: Provide lessons learned from building reliable power, propulsion, communication, and life support systems for long-duration (> 30 days) missions and allow a better understanding of how to operate in close proximity to, and at the surface, of a non-cooperative object in a low gravity regime.

Small Body Science: Aids understanding of the creation of our solar system since small bodies are the left over primitive materials from the earliest stages of solar system formation (e.g., potential Phobos/Deimos asteroid connections). Increased knowledge of these objects' physical characteristics and their constituents also helps to refine models for the delivery of materials (organics, volatiles, water, etc.) that may have been instrumental for the formation of the early Earth and evolution of life.

In Situ Science Combined with Sample Return: Enables better understanding of these bodies' origin/dynamical history, nature of their material composition, thermal properties, oxidation state, and collisional histories. Evidence from the meteorite record and remote sensing observations of NEAs and Phobos/Deimos (both from ground-based and space-based assets) suggest that some of these objects contain significant amounts of resources (water and precious metals). Hence resource utilization synergies exist by performing extraction demonstrations of small token quantities as a proof of concept (i.e., extraction of volatiles from NEA or Phobos/Deimos materials) and evaluating the effectiveness of using these resources for life support, propulsion, and other potential applications to enhance safety and efficacy of human spaceflight.

Transit Science: Enhances the science return of the mission and provides multiple opportunities for science to be

conducted en route to and from primary target (e.g., planetary science, life science, astrophysics, heliophysics). These types of observations and experiments can be performed for missions to either NEAs or Phobos/Deimos.

Human Factors: This is an area of study that is crucial for enabling human space flight to destinations beyond the Earth-Moon system. Many human factors are common and relevant to both NEA and Mars moon missions. Researchers could measure effects of communication delays/blackouts and impact to crew morale/performance, characterize synergistic effects of radiation, microgravity, and crew confinement on the human immune system during extended-duration deep space voyages, and monitor psychological effects of living in deep space for extended periods of time with no rapid return possibilities. Such a wealth of data would aid in better designs for improved spacecraft operations/performance and mitigate the effects on the deep space environment on human physiology and psychology.

Key Findings: There are numerous synergies between human missions to NEAs and missions to Phobos and Deimos. NEA missions can provide the opportunity to become proficient with human operations around a non-cooperative object in a low gravity regime. These synergies will be important for any human mission to the martian moons, but will be particularly relevant if short-stay missions are conducted due to the constrained duration for operations within the martian system.

13.1.1.5.7. Robotic Precursor Requirements for a Human Mission to Mars Orbit and its Moon

Team: Paul Abell (Lead), Deborah Bass, Dave Beaty, Tony Colaprete, Dan Mazanek, along with additional team members Jim Head (Brown), Scott Murchie (APL) and Andy Rivkin (APL)

Charter: Identify the SKGs and required robotic precursor measurements necessary to help inform a short-stay human orbital mission to interact with Phobos and Deimos. This study area was included to support of Mars Exploration Program Analysis Group (MEPAG) Precursor Science Analysis Group (P-SAG) Sub-Team #6.

A robotic precursor to Phobos and Deimos could provide significant risk reduction by addressing strategic knowledge gaps early enough to inform human mission design. There are two areas of SKGs. The first area addresses SKGs related to aspects of the orbital mission and the second area addresses SKGs associated with visiting the martian moons. To adequately explore the martian moons the SKGs related to the orbital only mission should also be included for consideration. The SKGs related to the orbital aspects of the mission along with the mission relevant parameters and the team’s priority are provided in Table 13-5 and those associated with visiting Phobos and Deimos are provided in Table 13-6.

Table 13-5. SKGs Related to an Orbital Mission

Strategic Knowledge Gap	Human Mission Relevant Measurements	Priority
Atmosphere properties related to aerobraking /aerocapture	Temperature, winds, aerosol abundance and profile; global and diurnal coverage	Medium-High
Particulate environment	Spatial variation in size-frequency distribution of Phobos/Deimos ejecta particles in Mars orbit	Medium

Table 13-6 SKGs Related to a Mission to Phobos or Deimos

Strategic Knowledge Gap	Human Mission Relevant Measurements	Priority
Mineralogical & chemical composition	Elemental / chemical composition; spatial distribution of major geologic units; ISRU potential	High
Regolith mechanical & geotechnical properties	Size-frequency distribution; density, compressibility, adhesion; spatial variation in thickness/properties	High
Gravitational field	Spherical harmonic terms of moons' gravitational fields	Medium
Electrostatic charging & plasma fields	Electric fields in proximity to surface, plasma emanating from surface	Low
Thermal environment	Temperature variation diurnally and with depth	Low
Radiation environment	Local radiation environment (including secondary radiation) near the Martian moons	Undetermined

Mars Orbit Insertion (MOI). Since aerobraking/aerocapture using the martian atmosphere may be pursued for orbital missions, the knowledge necessary to enable aerobraking of large masses (> 10 t) should be obtained prior to a crewed mission. More knowledge of the martian atmospheric properties may allow aerobraking to be developed, which may enable more massive robotic and human missions to be conducted to the martian system earlier than presently anticipated. The data relevant for making an informed decision on the implementation of aerobraking/aerocapture would significantly influence the mission architecture and resulting mass required.

Orbital Debris. Since the orbital particulate environment is potentially more significant in high Mars orbit (near Phobos/Deimos and in the equatorial plane) than in low-Mars orbit, direct measurement of the debris flux should be obtained. This is important since, under current architectures, spacecraft with significant cross-sectional areas may spend significant time in the equatorial plane and make repeated passes through this region of the martian system.

Mineralogy and Chemical Compositions. A better understanding of the mineralogy/chemistry of Phobos and Deimos is needed to support productive science operations and may also influence operations planning. For example, detection of organics and volatile compounds on Phobos/Deimos will drive different science and exploration objectives than mineralogies that do not contain such compositions.

Regolith. Regolith contact measurement and mapping are needed for operations planning and surface interaction considerations to better define the equipment and instrumentation that will be most effective in achieving the exploration and scientific objectives of the Phobos/Deimos mission. Regolith characteristics on a local scale may affect the method and extent of surface interaction to be conducted by the crew and their exploration assets.

Gravity. Gravitational field measurements are recommended for planning proximity operations, including identification of station-keeping modes. These data are relevant for optimizing propellant usage during proximity operations and understanding the effects long-term variations of complex gravitational fields on assets in close proximity to one another.

Electrostatics. Electrostatic charging and plasma environment influences engineering of surface elements and EVA equipment designs. Such information is necessary to help inform better designs and countermeasures for the development of exploration operations and interactions of systems with these airless bodies.

Thermal. Thermal environmental conditions vary significantly over diurnal time scales and with regolith depth. These data would inform the design of surface and sub-surface elements, including EVA equipment and scientific instrument designs..

Radiation. The need for radiation measurements related to tissue equivalent response near the martian moons (not to basic measurement of GCR and SPE) is still under debate. A better understanding of the interaction with Phobos/Deimos for shielding/secondary effects would be beneficial, but it is not clear that it is required.

Figure 13-14 depicts various precursor platform orbital options. An orbiter in low-Mars orbit (1) is well suited for addressing measurements associated with the martian atmosphere. An orbiter in a high-Mars orbit or an elliptical orbit with both low and high aspects (2) would be able to address the natural debris environment in the equatorial plane and could collect partial information on temperature, mineralogy, and gravity of Phobos/Deimos. A precursor that performs a rendezvous and a landing with Phobos and/or Deimos (3) is required to fully address the SKGs at Phobos/Deimos. Rendezvous-only missions (4) and sample return missions (5) were considered by the team, but these missions either do not adequately address, or are not necessary for addressing, the relevant SKGs for future human interaction at these moons .

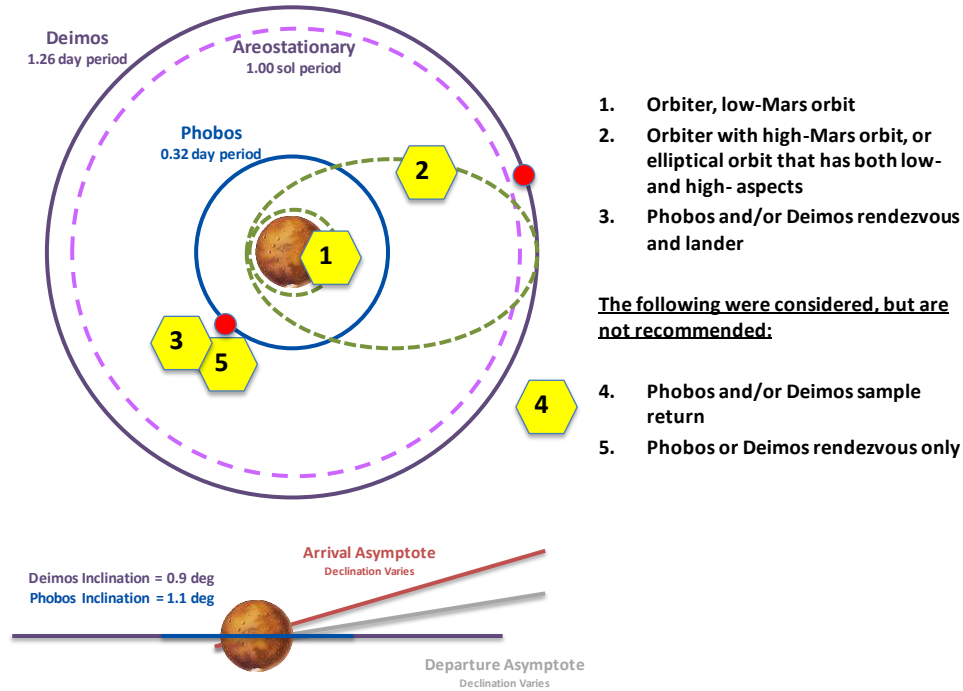


Figure 13-14 Precursor platforms.

Key Finding: A robotic precursor to Phobos and Deimos could provide significant risk reduction for a future human orbital Mars mission by addressing strategic knowledge gaps early enough to inform human mission design.

13.1.1.5.8. Activity Conclusions

Preliminary results from the MPD activity indicate that a meaningful human orbital mission to explore both martian moons and retrieve a MSR cache from low-Mars orbit could be performed during an opposition-class mission opportunity. The initial destination mission plan indicates that 56 days are required to accomplish all science and exploration objectives. Margin and mission reduction opportunities provide confidence that a successful and worthwhile mission could be completed within 60-90 days in the Mars system. Preliminary parametric-based estimates of the expected initial mass in low-Earth orbit (IMLEO) for a transportation architecture utilizing nuclear thermal propulsion to support an opposition-class mission (total duration of approximately 550 days) range from 350 to over 1000 metric tons. The IMLEO is highly dependent on the Mars departure opportunity, with 2033 offering a minimum in the 2030-2040 timeframe. Detailed mass sizing and volumetric analyses are needed to validate these initial estimates. Finally, the results from each of the activity study areas provide valuable information regarding the development of a human MPD mission and the synergistic activities required prior to undertaking such an exploration endeavor.

13.1.1.5.9. Summary

Through a comprehensive approach starting with the development of key mission objectives and working through

activity implementations and overall mission implementation strategies, our preliminary results suggest that an opposition-class mission to Phobos and Deimos could meet the identified objectives. In addition, there are key synergies to leverage with human missions to cislunar destinations and NEAs. Robotic precursor missions to Phobos and Deimos would provide significant risk reduction by addressing strategic knowledge gaps early enough to inform human mission design.

13.1.1.5.10. MPD DMC Primary Team Members:

Paul Abell (JSC), Jeff Antol (LaRC), Brent Barbee (GSFC), David Beaty (JPL), Deborah Bass (JPL), Julie Castillo-Rogez (JPL), David Coan (JSC), Tony Colaprete (ARC), Kevin Daugherty (LaRC), Bret Drake (JSC), Kevin Earle (LaRC), Lee Graham (JSC), Mike Hembree (JSC), Steve Hoffman (JSC), Sharon Jefferies (LaRC), Ruthan Lewis (GSFC), Mark Lupisella (GSFC), Dan Mazanek (LaRC – Study Lead) and David Reeves (LaRC)

13.1.2. Mission Design for the Exploration of Phobos and Deimos

Primary Contributors:

Brent W. Barbee, NASA Goddard Space Flight Center, USA

Damon Landau, Ph.D., Jet Propulsion Laboratory, California Institute of Technology, USA

The two moons of Mars – Phobos and Deimos – are among the potential destinations currently under consideration by NASA for future human exploration missions. This section presents results from NASA’s Mars-Phobos-Deimos Working Group study in the areas of orbit analysis and trajectory design for human space flight missions to explore Phobos and Deimos. The evolution of the orbits of the moons under natural perturbations are analyzed in this section, which informs the design of trajectories to arrive at Mars in a highly elliptical orbit, rendezvous with each moon in turn, and then depart Mars. The abilities of each moon to support captured orbits during proximity operations are also considered.

The two moons of Mars, Phobos and Deimos, are among the potential destinations currently under consideration by NASA for future human exploration missions. Figure 13-15 shows Phobos and Deimos as seen by the Mars Reconnaissance orbiter in 2008, along with a few key physical properties of the moons.

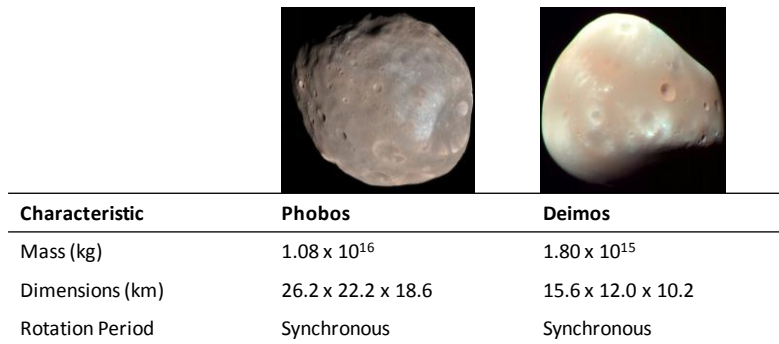


Figure 13-15 Characteristics of Phobos and Deimos.

NASA formed the Mars-Phobos-Deimos Working Group in early 2012 to study the design of missions to explore Phobos and Deimos. While the study spanned many aspects of the overall problem, this section is focused on the design of trajectories to arrive at Mars, rendezvous with each of the moons, and then depart Mars for Earth return. First analysis of the evolution of each moon's orbit under the influence of natural perturbations was conducted and then utilized to design sequences of maneuvers for exploring the moons. The maneuver sequences account for the conditions at Mars arrival on the incoming hyperbolic approach trajectory from interplanetary space, as well as the conditions that must obtain at Mars departure for injection into the outbound hyperbola leaving Mars. Also considered is both the phasing and relative motion required for rendezvous trajectories between the moons, as well

as each moon's ability to support captured orbits during proximity operations.

13.1.2.1. The Orbits of Phobos and Deimos

In this study, the precise orbits of Phobos and Deimos were considered under the influence of natural perturbations including non-spherical Mars gravity and the gravity of other significant solar system bodies. The interval for analyzing the evolution of the moons' orbits was January 1, 2030, through January 1, 2040. Precision ephemeris files for each moon were downloaded from the NASA Jet Propulsion Laboratory (JPL) HORIZONS system¹ to study the areocentric inertial motion of each moon. Figure 13-16 provides a three-dimensional perspective view of the nominal areocentric orbits of Phobos and Deimos.

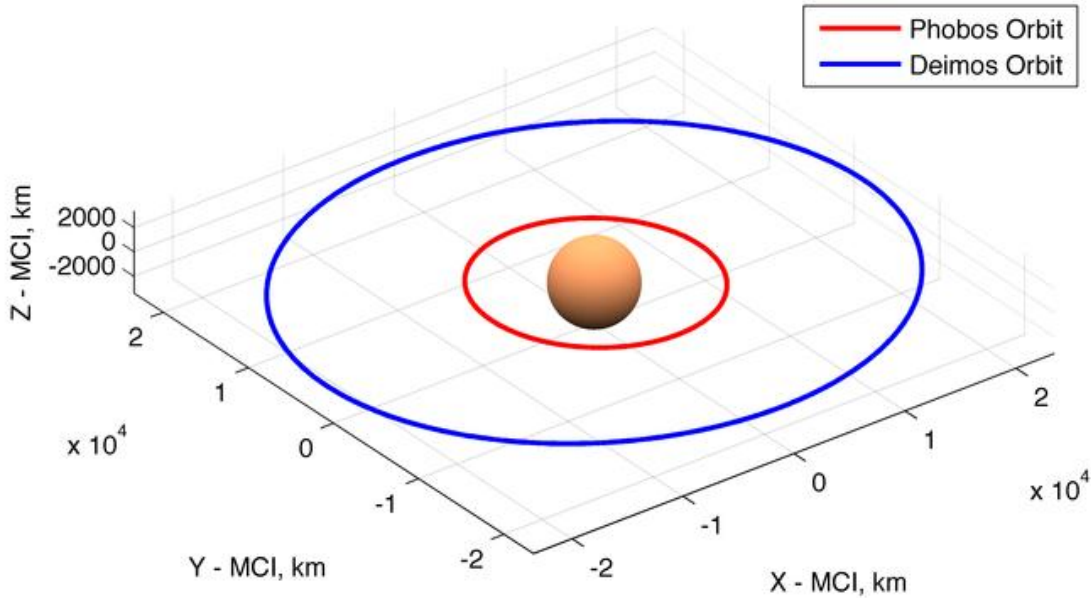


Figure 13-16 Nominal areocentric inertial orbits of Phobos and Deimos.

At first glance, the orbits of the moons do appear circular and coplanar, with Phobos in a much lower orbit than Deimos. However, closer examination of the ephemerides reveals the exact nature of the orbits. Figure 13-17(a) shows the semi-major axes of the orbits as functions of time, and they appear quite constant throughout the analysis interval. However, while not shown here, zooming in on the semi-major axis data reveals small but bounded fluctuations in each orbit's semi-major axis. These slight fluctuations in semi-major axis manifest later when the synodic² period between the moons is considered.

Figure 13-17(b) presents the eccentricity of each orbit as a function of time. Although the eccentricity of the orbits is relatively small, neither eccentricity is negligible nor is Phobos' orbit much more eccentric than that of Deimos. Furthermore, the amplitude of the fluctuations in Phobos' orbit eccentricity is larger than the amplitude of the fluctuations in Deimos' orbit eccentricity; this is likely due to the fact that Phobos is in a much lower orbit than Deimos and therefore more strongly perturbed by Mars' gravitational field. However, the eccentricity of Phobos' orbit does remain bounded throughout the analysis interval despite its short period fluctuations.

Figure 13-17(c) shows the inclination of each orbit as a function of time. While both inclinations are low, neither orbit is equatorial. Phobos' orbit inclination is more stable than that of Deimos, exhibiting no discernible secular

¹ <http://ssd.jpl.nasa.gov/?horizons>

² The synodic period is the time required for any phase angle to repeat itself. Proper phase angle is needed to minimize the total ΔV required for the rendezvous sequence.

variations. Deimos' orbit inclination, on the other hand, is steadily trending downward. Both orbits exhibit small short period inclination variations.

Figure 13-17(d) shows the right ascension of the ascending node (RAAN) of each orbit as a function of time. The RAAN of Deimos' orbit is gently, but steadily, trending downward throughout the analysis interval, while the RAAN of Phobos' orbit is precessing rapidly (changing through 2π radians every 2 years or so) under the influence of Mars' non-spherical gravitational field.

Figure 13-17(e) shows the argument of periairion of each orbit as a function of time. The overall character of the argument periairion evolution is similar to that of the RAAN evolution discussed previously. The argument of periairion of Deimos' orbit trends upward gently but steadily throughout the analysis interval and also experiences noticeable short period variations. The argument of periairion of Phobos' orbit precesses rapidly, changing through 2π radians every 1 year or so (approximately twice as fast Phobos' RAAN change) and in the opposite direction of Phobos' RAAN. Those results are consistent with the analytical treatment of changes in RAAN and argument of periairion due to the J_2 non-spherical gravity term for a central body.

Figure 13-17(f) presents a polar plot in which the radial axis is orbit inclination and the angle is RAAN. This plot shows the inclination and RAAN for Phobos' and Deimos' orbits and clearly demonstrates that at no time during the analysis interval are the orbits coplanar. Figure 13-18 further quantifies this by showing the angle between Phobos' and Deimos' orbit planes as a function of time; the angle between their planes is never zero during the analysis interval. In particular, the angle between the moons' orbit planes varies between 1.26° and 3.76° between the years 2030 and 2040, with a mean value of 2.67° .

For reference, the minimum, mean, and maximum values of the classical Keplerian orbital elements are computed for each moon's orbit and provided for Phobos in Table 13-7 and Deimos in Table 13-8.

Table 13-7 Minimum, Mean, and Maximum Values for Phobos' Classical Keplerian Orbital Elements during the Interval between 2030 and 2040

	a (km)	e	i	Ω	ω
Minimum	9377.75	0.0145	1.060°	0.002°	0.002°
Mean	9378.54	0.0151	1.075°	180.470°	181.075°
Maximum	9379.55	0.0157	1.091°	359.990°	359.999°

Table 13-8 Minimum, Mean, and Maximum Values for Deimos' Classical Keplerian Orbital Elements during the Interval between 2030 and 2040

	a (km)	e	i	Ω	ω
Minimum	23457.92	0.00018	2.202°	171.970°	227.310°
Mean	23458.95	0.00030	2.506°	195.600°	289.333°
Maximum	23459.92	0.00041	2.697°	217.940°	357.580°

Mars Design Reference Architecture 5.0 – Addendum #2

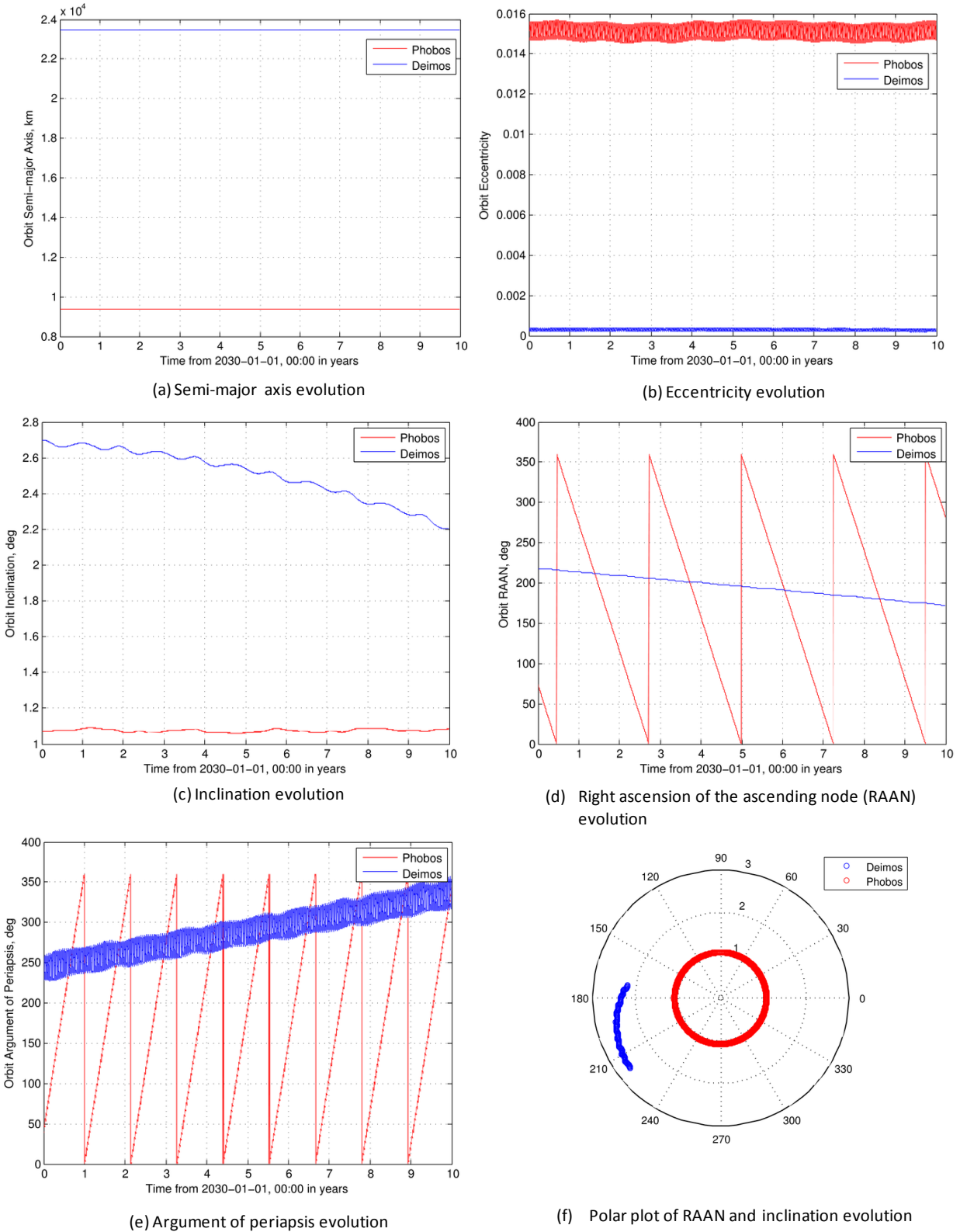


Figure 13-17 Time histories of Phobos and Deimos orbital elements.

One of the next topics addressed is optimal rendezvous trajectories between the moons. The synodic period between the moons was computed since it was expected that the optimal rendezvous trajectory opportunities to repeat approximately according to the synodic period. The stability of the semi-major axes of the moons' orbits makes their synodic period relatively stable at around 10.251 hours as shown in Figure 13-19.

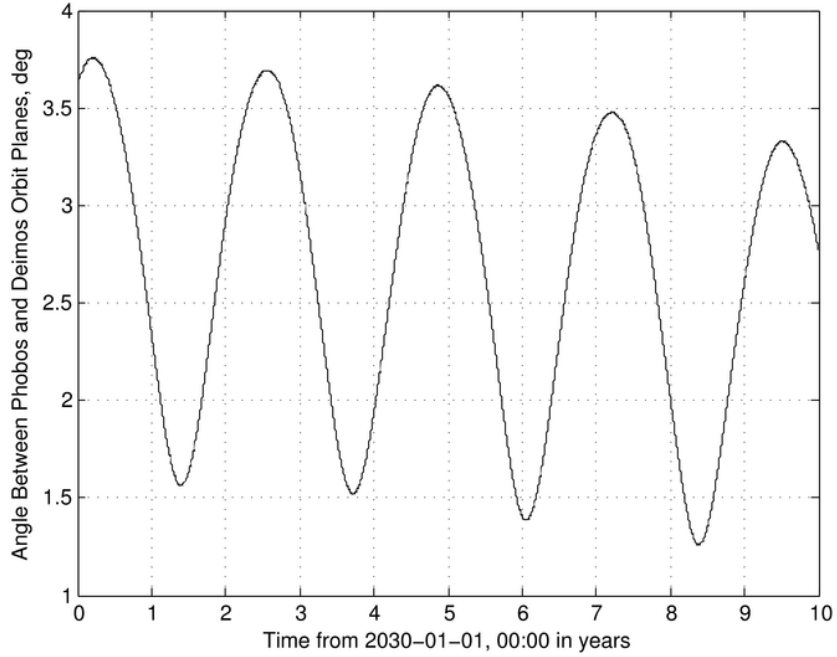


Figure 13-18 Angle between Phobos and Deimos orbit planes.

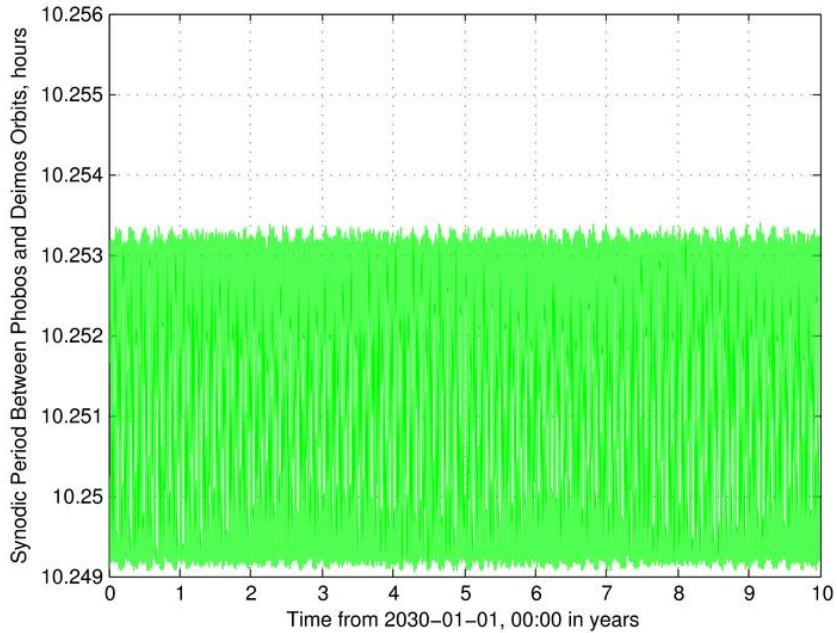


Figure 13-19 Evolution of the synodic period between Phobos and Deimos.

13.1.2.2. Rendezvous Trajectory Optimization for Phobos and Deimos

The precise ephemerides for Phobos' and Deimos' orbits were used to evaluate optimal (minimum Δv) two-impulse rendezvous trajectories between the moons. It is unlikely that the total rendezvous Δv can be reduced by using more complicated maneuvering schemes involving more than two maneuvers because the ratio of Phobos' and Deimos' orbit radii is approximately 2.5 and the angle between their orbit planes is less than 3.76° throughout the analysis interval. The optimal two-impulse rendezvous solutions were identified using a trajectory grid search technique operating on the precise ephemerides of the moons. Small grids, each spanning several days of departure times, were scanned on the first day of each year between 2030 and 2040 using a Lambert solver algorithm to determine the initial and final Δv for each rendezvous trajectory. When computing these maneuvers, it was assumed that each moon's gravity is weak enough to ignore (i.e., patched conics for arriving at or departing from the moons are not necessary).

To provide a basis for comparison the Hohmann transfer Δv between the moons was computed, including plane change optimally split between the initial and final maneuvers. These Hohmann transfer results were computed throughout the entire analysis interval using the precise semi-major axis values shown in Figure 13-17(a) as the radii for each moon's orbit (the orbits were treated as circular and ignore eccentricity) and using the precise angle between the moons' orbit planes shown in Figure 13-18.

Figure 13-20(a) and 6(b) show the Pork Chop Contour plots for the Phobos to Deimos and Deimos to Phobos trajectory scans, respectively. Note that the optimal rendezvous opportunities between the moons generally repeat according to the aforementioned synodic period between the moons (10.25 hours). Also note that the total Δv required for rendezvous increases steeply for non-optimal departure times.

Figure 13-21(a) and 7(b) show example optimal rendezvous trajectories from Phobos to Deimos and Deimos to Phobos, respectively, in a three-dimensional perspective view. Figure 13-22(a) and 8(b) show the projections of these trajectories onto Mars' equatorial plane. Note that while these optimal trajectories are Hohmann-like, they are clearly not exactly Hohmann transfers.

Figure 13-23(a) and 9(b) present the comparison between the precise optimal rendezvous Δv results from the grid scans and the approximate optimal rendezvous Δv results from the Hohmann transfer calculations. The change in the angle between the moons' orbit planes over time drives a mild variation over time in the Hohmann transfer Δv result, although the flight time yielded by the Hohmann calculations is always just less than 9 hours.

The optimal Δv solutions identified by the trajectory grid scans occasionally agree well with the approximate Hohmann transfer result, but this is generally not the case. Figure 13-23 (a) shows that the precise optimal Δv is generally slightly larger than the Hohmann result, up to 8% larger. Figure 13-23 (b) shows that corresponding precise flight times for the optimal rendezvous trajectories vary between about 10% shorter and 18% longer than the Hohmann transfer flight time. The periodic variations in the precise optimal rendezvous Δv and flight time results are chiefly driven by the change in the angle between the moons' orbit planes over time, as well as the fluctuation of Phobos' orbit eccentricity over time.

The overall maximum precise optimal total rendezvous Δv solution in Figure 13-23 (a) is 816 m/s with an associated flight time of 10.42 hours, and the overall minimum precise optimal total rendezvous Δv solution is 751 m/s with a flight time of 8.75 hours.

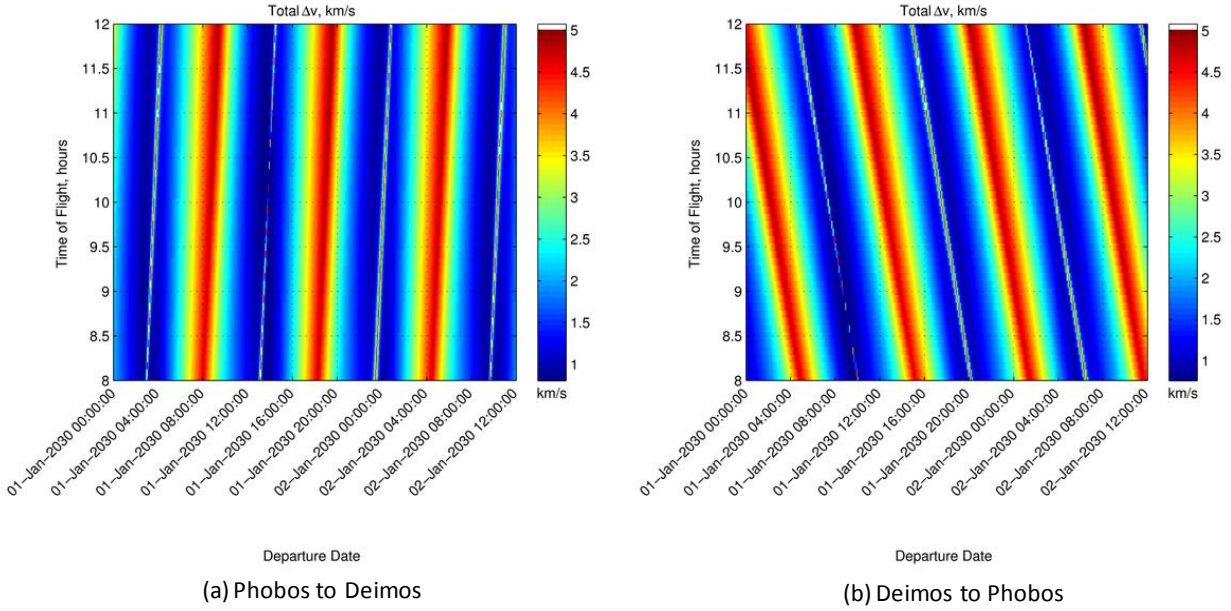


Figure 13-20 Pork Chop Contour plots for rendezvous trajectories between Phobos and Deimos using trajectory.

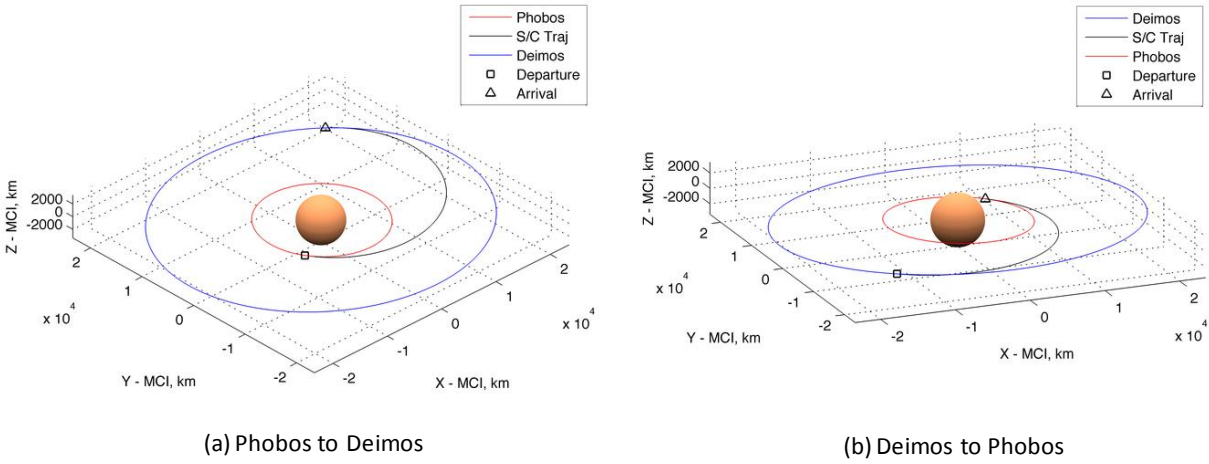


Figure 13-21 Example optimal two-impulse rendezvous trajectories between Phobos and Deimos, three-dimensional view.

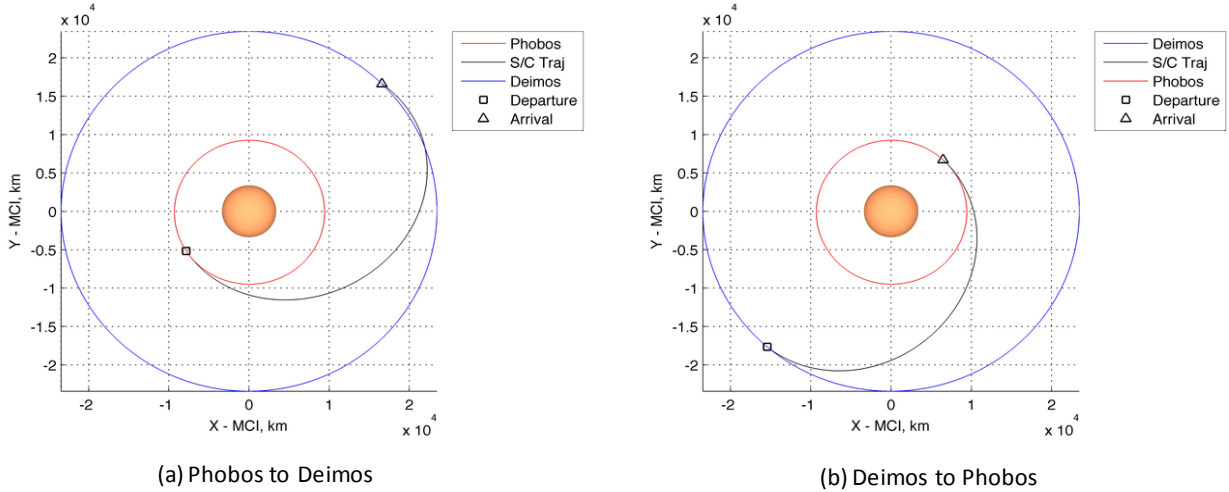


Figure 13-22 Example optimal two-impulse rendezvous trajectories between Phobos and Deimos, Mars equatorial plane.

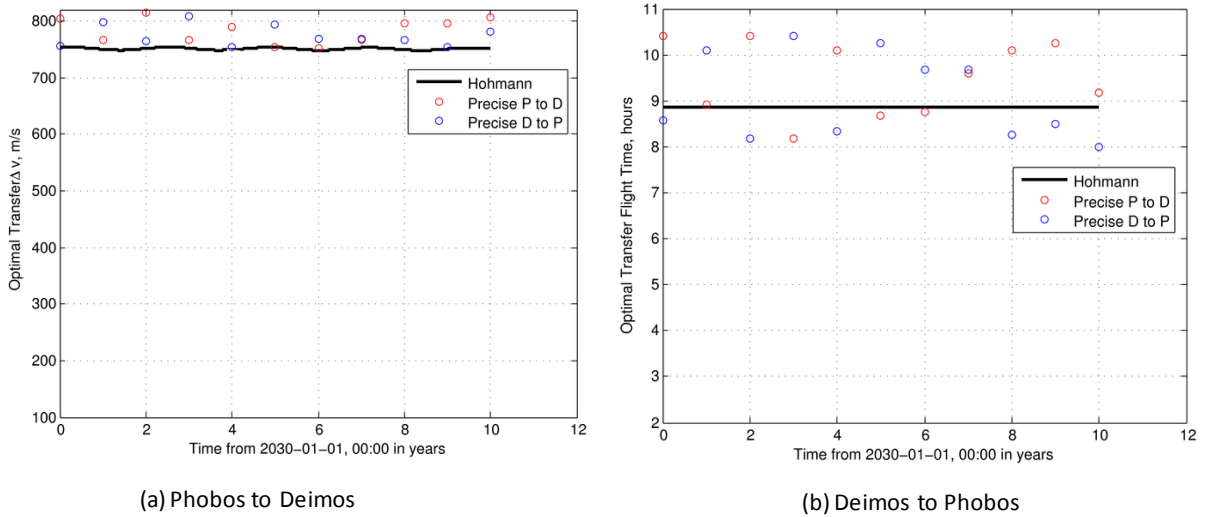


Figure 13-23 Comparison of optimal rendezvous Δv and flight time between Phobos and Deimos for the precise Lambert.

13.1.2.3. Terminal Rendezvous for Phobos and Deimos

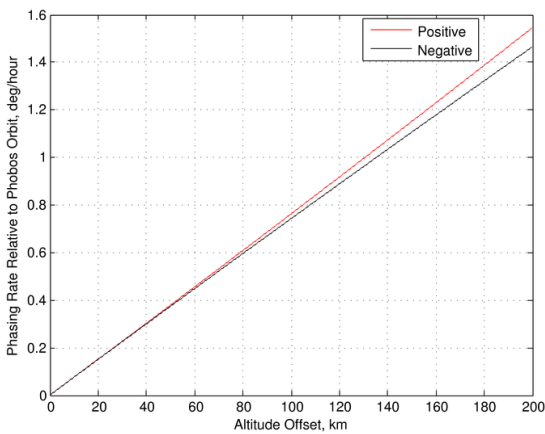
The optimal rendezvous trajectories discussed previously were calculated by targeting each moon directly, and the spacecraft velocity relative to each moon upon arrival is generally approximately 400 m/s. While those conditions are appropriate for grid scans to design optimal orbital rendezvous trajectories, in practice the spacecraft will require a controlled flight path relative to each moon with gradual approach speeds that are conducive to safety.

It was then assumed that the orbital rendezvous trajectories shown previously were actually targeting a co-elliptic orbit³ with respect to the destination moon's orbit, and that the location targeted on the co-elliptic orbit would be slightly offset in the in-track direction relative to the moon. This scenario would allow the spacecraft to naturally

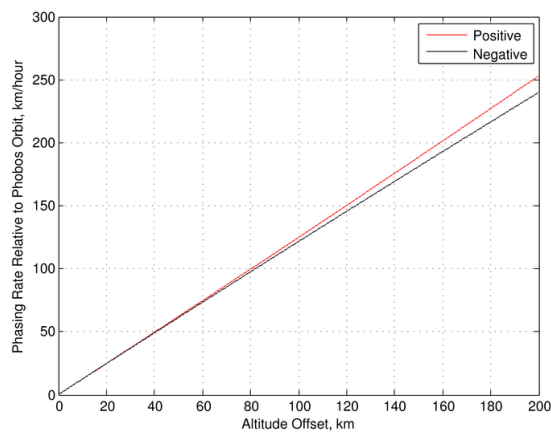
³ A co-elliptic orbit is coplanar with the target orbit and has the same eccentricity but a slightly different semi-major axis.

drift toward the destination moon after achieving co-elliptic orbit, and the drift rate relative to the destination moon would be regulated by occasional pairs of small maneuvers to adjust the altitude of the spacecraft's orbit. This sequence of drift and altitude adjustment segments beginning at the offset location on the co-elliptic orbit is referred to as terminal rendezvous.

This terminal rendezvous strategy would provide safety and leverages prior human space flight rendezvous operations experience (e.g., Space Shuttle rendezvous with the International Space Station [ISS]) at the expense of increasing the amount of time required to complete the rendezvous. The available drift rates on a co-elliptic orbit relative to Phobos as a function of altitude difference are presented in Figure 13-24(a) and 10(b) in units of degrees per hour and kilometers per hour, respectively. Figure 13-25(a) and 11(b) provide these data for Deimos. Note that Phobos' lower orbit admits to higher relative phasing rates than does Deimos' higher orbit for equivalent altitude offsets. This feature of the relative motion dynamics means that terminal rendezvous with Deimos will generally require more time than terminal rendezvous with Phobos unless additional Δv is employed to achieve more drastic co-elliptic orbit altitude offsets relative to Deimos' orbit.

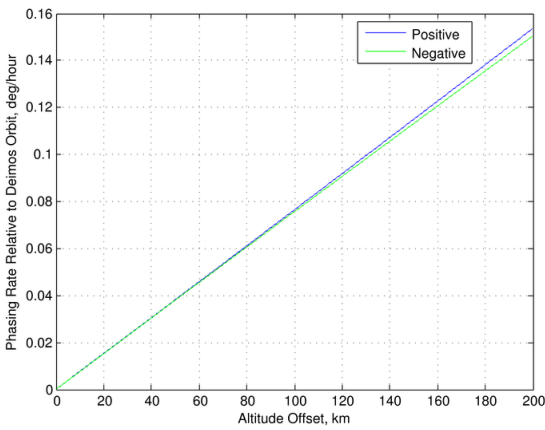


(a) Phasing rates relative to Phobos in degrees per hour.

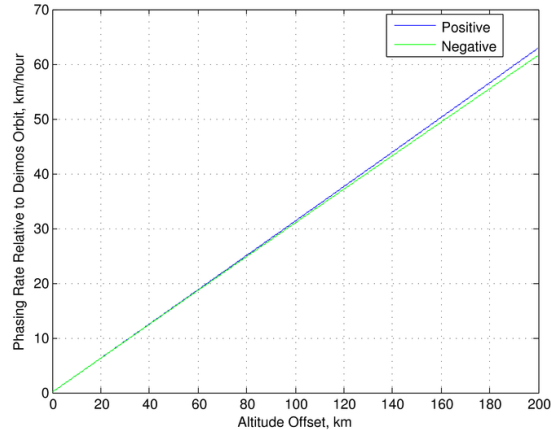


(b) Phasing rates relative to Phobos in km per hour.

Figure 13-24 Phasing rates relative to Deimos as a function of altitude offset from Phobos' orbit.



(a) Phasing rates relative to Deimos in degrees per hour.



(b) Phasing rates relative to Deimos in km per hour.

Figure 13-25 Phasing rates relative to Deimos as a function of altitude offset from Phobos' orbit.

Terminal trajectory sequences for rendezvous with each moon were then considered. These trajectory sequences were constructed using the Hill's/Clohessy-Wiltshire equations of relative orbital motion, assuming each moon's orbit to be circular. This is a reasonable assumption in light of the relatively small eccentricity of each moon's orbit

and permits rapid trajectory design using the Hill's/Clohessy-Wiltshire equations.

Terminal rendezvous with Phobos would begin at an in-track distance of 1000 km behind Phobos with an altitude 75 km below Phobos' orbit. Four drifting segments were defined, with altitude raises between them, that would bring the spacecraft to a point 15 km directly below Phobos 27.42 hours after the initiation of terminal rendezvous for a total terminal rendezvous ΔV cost of 6.84 m/s. The drift and altitude raise segments, along with the associated individual flight times and maneuver magnitudes, are presented in Table 13-9.

Figure 13-26 shows the Phobos terminal rendezvous trajectory sequence in the radial, in-track plane of the radial, in-track, cross-track frame whose origin is at Phobos' center of mass. The trajectory plot in Figure 13-26 uses equal plot axis scaling to show the actual appearance of the trajectory, but this makes it difficult to discern the geometrical structure of the trajectory. Figure 13-27(a) offers an alternative view of the Phobos terminal rendezvous trajectory with unequal plot axis scaling that distorts the view of the trajectory (and Phobos itself) but aids in clarifying the relative motion geometry. Figure 13-27(b) uses equal plot axis scaling to avoid distortions and shows the end of the terminal rendezvous trajectory arriving directly below Phobos at a distance of 15 km. At this point, the spacecraft may perform additional maneuvers to begin proximity operations about Phobos.

Table 13-9 Example Terminal Rendezvous Sequence for Phobos

Segment Type	Altitude Change (km)	Flight Time (hours)	ΔV (m/s)
Drift	0	2.00	N/A
Altitude Raise	-75 to -30	3.83	2.56
Drift	0	4.50	2.56
Altitude Raise	-30 to -20	3.83	0.57
Drift	0	4.50	0.57
Altitude Raise	-20 to -15	3.83	0.28
Drift	0	4.93	0.28
TOTALS		27.42	6.84

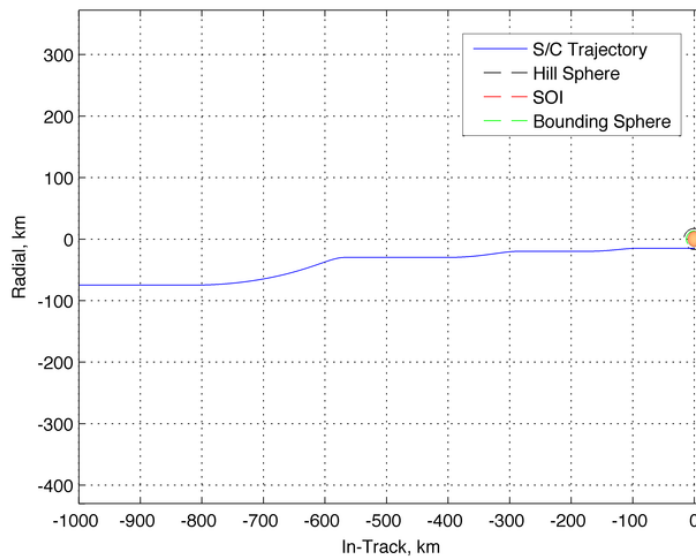
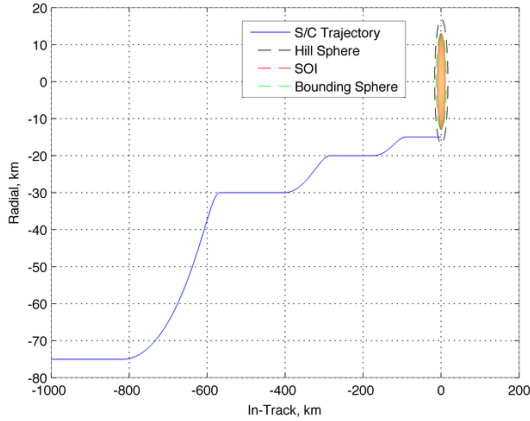
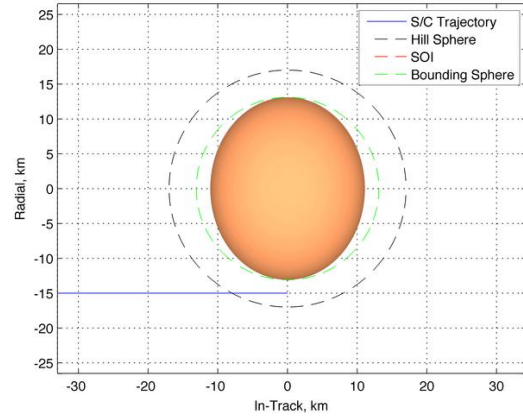


Figure 13-26 Example terminal rendezvous trajectory for Phobos.



(a) Example terminal rendezvous trajectory for Phobos, unequal plot axis scaling.



(b) Detail view of the end of the Phobos terminal rendezvous trajectory.

Figure 13-27 Example Phobos terminal rendezvous trajectory shown with unequal plot scaling, along with a detailed view of the end of the trajectory.

Terminal rendezvous with Deimos would begin at an in-track distance of 1000 km behind Deimos and with an altitude 100 km below Deimos' orbit. This altitude offset is slightly larger than for the Phobos case presented previously because of the generally slower phasing rates relative to Deimos at a given altitude offset. Four drifting segments were defined, with altitude raises between them, that would bring the spacecraft to a point 12 km directly below Deimos 79.55 hours after the initiation of terminal rendezvous for a total terminal rendezvous Δv cost of 2.53 m/s. The drift and altitude raise segments, along with the associated individual flight times and maneuver magnitudes, are presented in Table 13-10.

Figure 13-28 shows the Deimos terminal rendezvous trajectory sequence in the radial, in-track plane of the radial, in-track, cross-track frame whose origin is at Deimos' center of mass. The trajectory plot in Figure 13-28 uses equal plot axis scaling to show the actual appearance of the trajectory, but this makes it difficult to discern the geometrical structure of the trajectory. Figure 13-29(a) offers an alternative view of the Deimos terminal rendezvous trajectory with unequal plot axis scaling that distorts the view of the trajectory (and Deimos itself) but aids in clarifying the relative motion geometry. Figure 13-29(b) uses equal plot axis scaling to avoid distortions and shows the end of the terminal rendezvous trajectory arriving directly below Deimos at a distance of 12 km. At this point the spacecraft may perform additional maneuvers to begin proximity operations about Deimos.

Table 13-10 Example Terminal Rendezvous Sequence for Deimos

Segment Type	Altitude Change (km)	Flight Time (hours)	ΔV (m/s)
Drift	0	3.00	N/A
Altitude Raise	-100 to -65	15.15	0.50
Drift	0	5.00	0.50
Altitude Raise	-65 to -25	15.15	0.58
Drift	0	5.00	0.58
Altitude Raise	-25 to -12	15.15	0.19
Drift	0	21.09	0.19
TOTALS		79.55	2.53

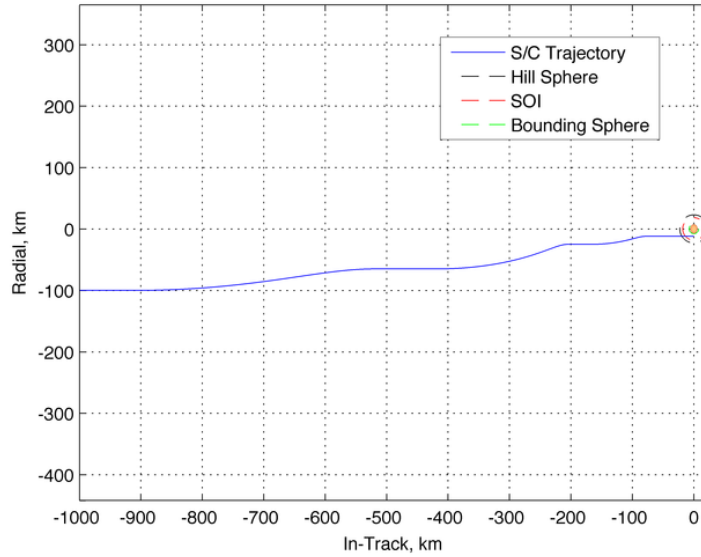
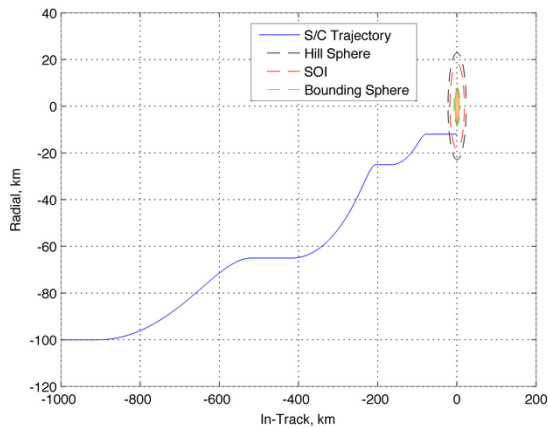
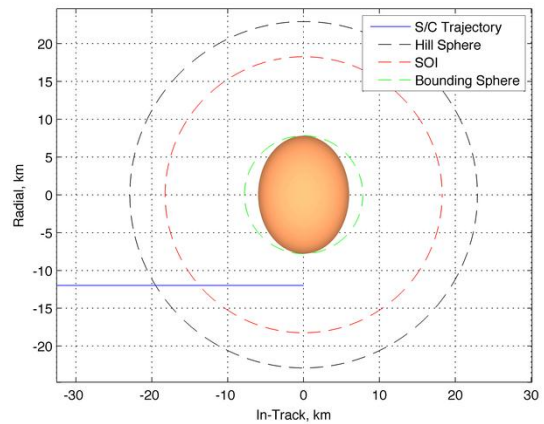


Figure 13-28 Example terminal rendezvous trajectory for Deimos.



(a) Example terminal rendezvous trajectory for Phobos, unequal plot axis scaling..



(b) Detail view of the end of the Phobos terminal rendezvous trajectory.

Figure 13-29 Example Deimos terminal rendezvous trajectory shown with unequal plot scaling, along with a detailed view of the end of the trajectory.

The Δv required for terminal rendezvous would be quite manageable for both Phobos and Deimos, though the terminal rendezvous sequences would be somewhat time-consuming (a little more than a day for Phobos and a little over 3 days for Deimos). As noted previously, the time required to phase to Deimos would be longer than that for Phobos unless larger altitude offsets are employed. However, the use of larger altitude offsets would require additional Δv and will also alter the relative geometry during major portions of the approach. The impact of alternative relative motion geometries during approach on sensors and relative navigation filters would need to be examined. Hohmann transfers are used for all of the altitude raises to minimize v requirements, but shorter (non-Hohmann) transfers may be flown for altitude raises to reduce overall flight time for terminal rendezvous at the expense of increasing total terminal rendezvous Δv . That being said, note that the time between altitude raise maneuvers would be already relatively short for many segments, often on the order of only several hours, and this may cause issues with relative navigation filter convergence between maneuvers. Other factors not considered here, such as the impact of lighting condition on relative navigation sensor performance, would influence actual terminal rendezvous trajectory design in practice.

13.1.2.4. Orbital Operations About Phobos and Deimos

Upon arriving at either moon at the end of terminal rendezvous, the spacecraft would begin proximity operations about the moon. During this phase, the primary crew vehicle may collect sensor data and deploy crew in excursion vehicles or individual maneuvering suits to interact with sites on the moon's surface. A strategy would therefore be required for maintaining some sort of proximity operations posture relative to the moon while the aforementioned activities would be taking place. This analysis started by assessing each moon's ability to support captured orbits. Viable proximity operations strategies may involve captured orbits, forced motion (e.g., station-keeping or travel between waypoints), or more some combination thereof.

13.1.2.4.1. Sphere of Influence / Hill Sphere Radii for Phobos and Deimos

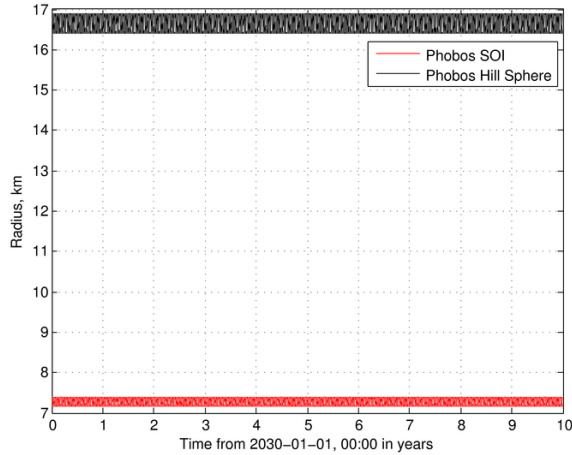
The restricted three-body system consisting of Mars, Phobos, or Deimos, and the spacecraft was first considered, assessing each moon's SOI and Hill sphere. Those volumes each provide an estimate for the region of space surrounding the moon in which stable captured orbits may be achieved. When perturbations beyond point mass gravity for the moon and Mars are included, the spatial volumes around each moon within which stable motion would be possible are found to not be spherical, in general; however, those effects are not considered herein.

In a system consisting of a large celestial body and a smaller one, the Hill sphere is the approximate region in which the smaller body's gravity is more dominant than that of the larger body; thus, the smaller body may theoretically have captured satellites within the Hill sphere radius. The Hill sphere radius is also the distance of the L_1/L_2 Lagrangian points from the smaller celestial body. Note that the Hill sphere may also be referred to as the Sphere of Activity, Activity Sphere, or Roche Sphere (not to be confused with the Roche Limit). The SOI is simply a different (and usually more conservative) way to describe the region in which a smaller body is the primary gravitational influence on satellites. The SOI radius is defined mathematically as the distance from the smaller body at which it becomes appropriate to treat the smaller body's gravity as a perturbation and treat the larger body as the primary attractor (within the SOI radius, the situation is reversed).

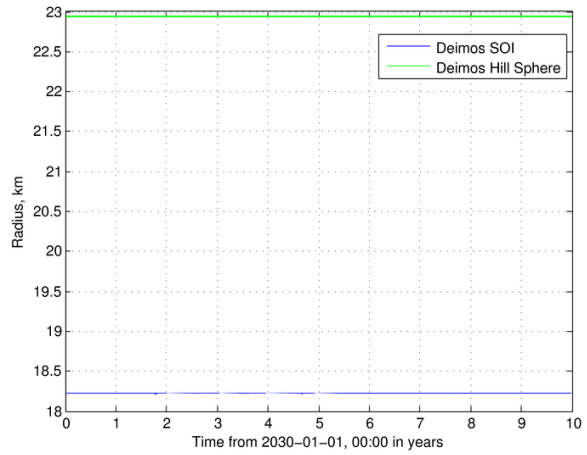
The SOI and Hill sphere radii throughout the analysis interval are shown in Figure 13-30(a) for Phobos and Figure 13-30(b) for Deimos. Note that Deimos' SOI and Hill sphere radii are more stable than those of Phobos because of Deimos' lower orbit eccentricity (Deimos' distance to Mars fluctuates less over time). Conversely, the observed variation in Phobos' SOI and Hill sphere radii are due to its orbit eccentricity. As indicated previously, the SOI radii for the moons are smaller than their Hill sphere radii and therefore provide a more conservative assessment of the space relative to each moon within which stable captured orbits may be possible.

Comparing the physical dimensions of the moons, provided in Figure 13-15, to their SOI and Hill sphere radii shows that Phobos' SOI radius is only 55% of its physical bounding radius and its Hill sphere radius is only larger than its SOI radius by a factor of 2.33. This is a strong indication that achieving stable captured orbits around Phobos may be rather difficult, if not impossible. By contrast, Deimos' SOI radius is 2.34 times larger than its physical bounding radius and its Hill sphere radius is 1.25 times larger than its SOI radius. This indicates that stable captured orbits about Deimos are likely to be possible. Note that the SOI and Hill sphere outlines for Phobos and Deimos are depicted in Figure 13-27(b) and Figure 13-29(b), respectively.

These observations were then investigated further by attempting to design stable captured orbits around each moon using an elliptical restricted three-body dynamics model in which both Mars and the moon are treated as point masses for the purpose of gravity field modeling. Each moon's orbit around Mars was modeled using the mean classical Keplerian orbital elements presented in Table 13-7 and Table 13-8. Gravitational parameters for each moon are computed by scaling their masses from Figure 13-15 by the Universal Gravitational Constant, $G = 6.67259 \times 10^{-20} \text{ km}^3 \text{ s}^{-2} \text{ kg}^{-1}$. The gravitational parameter value used for Mars is $4.2828374747780377 \times 10^4 \text{ km}^3 \text{ s}^{-2}$.



(a) Phobos SOI and Hill Sphere radii.



(b) Deimos SOI and Hill Sphere radii.

Figure 13-30 Sphere of Influence and Hill Sphere radii of Phobos and Deimos.

13.1.2.4.2. Captured Orbits About Deimos

Experimentation with prograde motion about Deimos resulted in short-lived orbits that would quickly destabilize and either escape Deimos or collide with its surface. Retrograde motion about Deimos proves to be much more stable, and Figure 13-31 shows an example stable retrograde orbit about Deimos in a Deimos-centered inertial frame. The initial orbit radius is 9 km, the initial orbit period is 4.3 hours (0.18 days), and the initial orbit velocity is 3.65 m/s. Note that the magnitude of the orbit velocity is of the same order as the relative motion velocity during the terminal rendezvous phase and thus transitioning to a stable captured orbit from terminal rendezvous would generally require only a few m/s of Δv . The stable retrograde orbital motion is shown for a time-span of 20 days in Figure 13-31 but may remain stable for longer than that (this was not investigated).

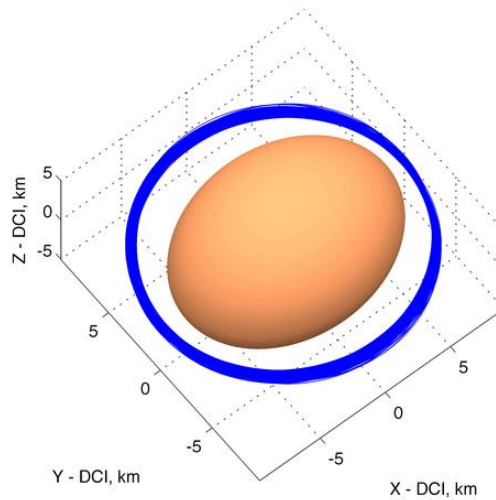


Figure 13-31 Example Deimos-captured orbit (retrograde) propagated for 20 days.

13.1.2.4.3. Captured Orbits About Phobos

As was the case for Deimos, prograde motion about Phobos proved to be unstable in the simulation. However, making the motion retrograde did not significantly improve matters for Phobos; an example of a stable captured orbit about Phobos in the simulation was not identified. All of the initial conditions attempted would result in either immediate escape or collision with Phobos' surface. Figure 13-32 shows an example of an escape trajectory in a

Phobos-centered inertial frame. The initial orbit radius is 15 km, the initial orbit period is 3.8 hours (0.16 days), and the initial orbit velocity is 6.93 m/s. Figure 13-32 only shows 2.4 hours of the simulated motion.

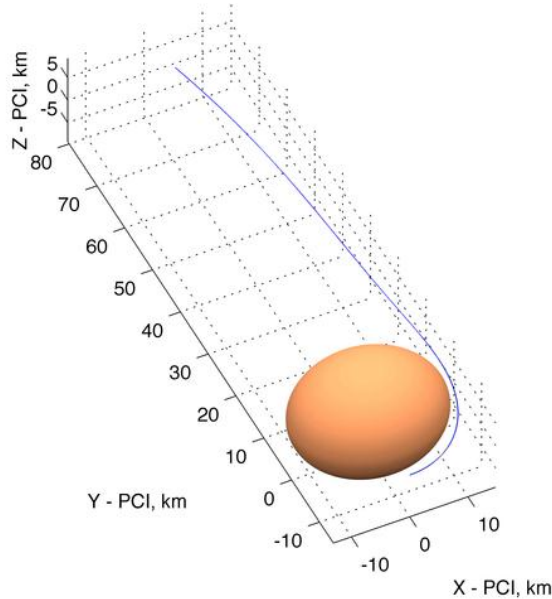


Figure 13-32 Example Phobos-captured orbit attempt propagated for 2.4 hours.

Achieving captured retrograde orbits around Deimos appears feasible, and such orbits may be good locations from which to stage crew excursions to/from Deimos although additional analysis is required. Captured orbits around Phobos would be more problematic, however. Phobos is much closer to the primary body (Mars) and as such its SOI radius is well inside its physical bounding sphere, making stable captured orbits difficult to identify. Pseudo-captured orbits about Phobos could probably be achieved with frequent maintenance maneuvers, and such maneuvers would almost certainly be more costly than for Deimos-captured orbit maintenance. The level of control effort and frequency required would likely increase with altitude above Phobos and may simply amount to forced motion. In this case, station-keeping at a standoff location may be more economical. In any case, the Δv to transition from co-elliptic drift to captured orbits should be small in general (on the order of several m/s). Finally, it is worth noting that further analysis should be performed in which non-spherical gravity field models are used for the moons and Mars, in combination with other natural perturbations (such as solar radiation pressure). In those models it may be possible to identify sufficiently stable motion patterns relative to the moons (even Phobos) that would be suitable for operations even if those motion patterns do not constitute orbits in the traditional sense; periodicity and stability may be more important than circumnavigation of the moon.

13.1.2.5. Maneuver Sequence for Exploring Phobos and Deimos

The previous results were then integrated with hyperbolic arrival and departure conditions at Mars to synthesize a complete maneuvering sequence for exploring Phobos and Deimos that includes arrival in a highly elliptical Mars orbit from an incoming hyperbolic approach trajectory from interplanetary space, maneuvers to reorient the highly elliptical Mars orbit for subsequent departure, exploration of both Phobos and Deimos, and return to the highly elliptical Mars orbit for departure.

The maneuver calculations utilize the results of the preceding sections in combination with a subset of broad round-trip interplanetary trajectory scans involving various stay times at Mars. 9267 round-trip trajectories were initially generated, from which 142 were selected that require less total mission mass to utilize for the results presented herein. The round-trip trajectories considered include opposition class trajectories with stay times at Mars between 20 and 100 days, and conjunction class trajectories with stay times at Mars of 480 - 580 days. Several types of opposition class trajectories were considered: Earth-Mars-Earth (EME), Earth-Mars-Venus-Earth (EMVE), and Earth-Venus-Mars-Earth (EVME). The EME trajectories fly directly to Mars and then directly back to Earth. The

EMVE trajectories include a Venus gravity assist on the way back to Earth from Mars, and the EVME trajectories include a Venus gravity assist on the way to Mars from Earth. The conjunction class round-trip trajectories tend to feature lower overall total mission Δv compared to the opposition class round-trip trajectories, while the opposition class trajectories tend to feature lower overall mission durations. Including Venus gravity assists in the opposition class trajectory sequences can help reduce the total mission Δv in some cases.

The highly elliptical orbit into which the spacecraft would initially capture at Mars arrival, and from which the spacecraft would depart Mars after Phobos/Deimos exploration, has a periairion altitude of 250 km and an apoairion altitude of 33813 km, which corresponds to a semi-major axis of 20421.4 km, an eccentricity of 0.82176, and a period of 1.025483 days (approximately 1 sol). Additionally, the maneuver calculations assume the aforementioned Mars gravitational parameter of $4.2828374747780377 \times 10^4 \text{ km}^3\text{s}^{-2}$ and a mean Mars radius of 3389.9 km. Furthermore, the mean orbits of Phobos and Deimos presently previously were assumed

13.1.2.5.1. Maneuver Sequence Overview

The first step in the maneuver sequence would be to enter the highly elliptical capture orbit at periairion on the incoming hyperbola at Mars. Next, the spacecraft would coast to the apoairion of the capture orbit where it would perform a plane change maneuver to reorient the orbit plane as to be properly aligned for Mars departure. It assumed that the crew would leave the majority of their spacecraft stack in the departure orbit and utilize a smaller craft to explore Phobos and Deimos so as to minimize the amount of mass brought deeper into Mars' gravity well and thereby reduce overall propellant mass requirements for the mission. For the purposes of this overview it was also assumed that Deimos would be visited first (though the Phobos-first case was analyzed as well). The smaller spacecraft would remain on what would be referred to as the departure orbit for one period, after which it would perform a maneuver at apoairion to match Deimos' orbit plane and simultaneously raise periairion to match the radius of an orbit that is co-elliptic with Deimos' orbit. The spacecraft would then coast to the co-elliptic orbit radius at the periairion of the transfer ellipse and match the orbital velocity of the co-elliptic orbit. Next, the spacecraft would perform terminal rendezvous with Deimos as per the terminal rendezvous maneuver sequence presented previously. After exploring Deimos, it was assumed a wait time at Deimos of at least one Phobos/Deimos synodic period, after which the spacecraft would fly the previously presented optimal rendezvous trajectory to an orbit that is co-elliptic with Phobos' orbit. Terminal rendezvous with Phobos would then be performed, followed by exploration of Phobos for some period of time. After this, the spacecraft would perform a maneuver to raise apoairion to match that of the departure orbit (timing this maneuver so as to intercept the spacecraft stack on the departure orbit at apoairion). The spacecraft would then coast to the departure orbit apoairion on the transfer ellipse, perform a maneuver to simultaneously match the departure orbit plane and periairion radius, and then reconnect with the spacecraft stack at apoairion. The spacecraft stack would then coast to the departure orbit periairion and perform a maneuver at periairion to inject into the outbound hyperbola to depart Mars.

13.1.2.5.2. Example Maneuver Sequence Results

The maneuver magnitudes and flight times associated with each of the segments described in the maneuver sequence overview were then computed assuming an incoming and outgoing V_∞ at Mars of 3 km/s, an asymptotic declination of 10° at Mars arrival, and an asymptotic declination of 30° at Mars departure. The maneuver sequence calculations for the Deimos-first case are presented in Table 13-11.

The results in Table 13-11 indicate that the Δv budget for the maneuvers performed at Mars⁴ in this example is about 4.8 km/s and the total associated flight time for maneuvers and transfers is about 9 days. Thus the stay time at Mars must be long enough to accommodate the time spent exploring at each moon (not listed here because it is unknown) as well the approximately 9 days required for maneuvers and transfers to move about between the moons and the highly elliptical Mars capture/departure orbit.

⁴ It is important to recognize that the total Δv at Mars does not include the other major maneuvers for the round-trip mission, which are the maneuver to depart Earth for Mars, any deep space maneuvers that may be performed on the way to Mars or on the way back home to Earth, and any maneuvers that may be required at Earth return to control the direct atmospheric reentry speed of the crew vehicle or capture it into an Earth orbit.

Table 13-11 Example Maneuver Sequence in which Deimos is Visited First, then Phobos

Segment Type	DV (m/s)	Flight Time (hours)
Enter Capture Orbit at Periarieon of Incoming Hyperbola	1073.9	
Coast to Capture Orbit Apoarieon		12.31
Match Departure Orbit Plane at Apoarieon	157.3	
Coast to Departure Orbit Apoarieon		24.61
Match Deimos' Orbit Plane and Raise Periarieon to Deimos' Orbit Radius	580.7	
Coast to Deimos' Orbit Radius at Periarieon of Transfer Ellipse		22.75
Match Deimos' Orbital Velocity at Periarieon of Transfer Ellipse	145.3	
Perform Terminal Rendezvous with Deimos	2.5	79.55
Wait for Synodic Period to Elapse to Fly Optimal Transfer to Phobos		10.25
Fly Optimal Transfer to Phobos' Orbit	816	10.42
Perform Terminal Rendezvous with Phobos	6.8	27.42
Raise Apoarieon to Match Departure Orbit Apoarieon	563.8	
Coast to Departure Orbit Apoarieon on Transfer Ellipse		14.99
Match Departure Orbit Plane and Periarieon Radius	359	
Coast to Departure Orbit Periarieon		12.31
Exit Departure Orbit on Outbound Hyperbola	1073.9	
TOTALS	4779.2	214.13

Table 13-12 presents the maneuver sequence results for the case in which Phobos is visited first. It turns out that the total at-Mars Δv and associated flight time for maneuvers and transfers are the same as for the Deimos-first case (4.8 km/s and 9 days) although the distribution of Δv and flight time amongst the individual segments is naturally a bit different.

Note that the Δv to capture into Mars orbit from the incoming hyperbola and to depart Mars orbit by injecting into the outgoing hyperbola account for about 45% of the 4.8 km/s at Mars in the examples. For the results in Table 13-11 and Table 13-12, it was assumed a particular incoming/outgoing V_∞ at Mars for the sake of creating example results, but in practice the incoming/outgoing V_∞ can vary significantly, and this will naturally affect the total Δv at Mars. If the Mars capture/departure Δv is excluded, the total Phobos/Deimos exploration Δv from Table 13-11 and Table 13-12 is about 2.6 km/s. The other factors that will cause this Δv to vary are the incoming/outgoing asymptotic declinations.

Table 13-12 Example Maneuver Sequence in which Phobos is Visited first, then Deimos

Segment Type	DV (m/s)	Flight Time (hours)
Enter Capture Orbit at Periarieon of Incoming Hyperbola	1073.9	
Coast to Capture Orbit Apoarieon		12.31
Match Departure Orbit Plane at Apoarieon	157.3	
Coast to Departure Orbit Apoarieon		24.61
Match Deimos' Orbit Plane and Raise Periarieon to Deimos' Orbit Radius	359.0	
Coast to Deimos' Orbit Radius at Periarieon of Transfer Ellipse		14.99
Match Deimos' Orbital Velocity at Periarieon of Transfer Ellipse	563.8	
Perform Terminal Rendezvous with Deimos	26.8	27.42
Wait for Synodic Period to Elapse to Fly Optimal Transfer to Phobos		10.25
Fly Optimal Transfer to Phobos' Orbit	816.0	10.42
Perform Terminal Rendezvous with Phobos	2.5	79.55
Raise Apoarieon to Match Departure Orbit Apoarieon	145.3	
Coast to Departure Orbit Apoarieon on Transfer Ellipse		22.28
Match Departure Orbit Plane and Periarieon Radius	580.7	
Coast to Departure Orbit Periarieon		12.31
Exit Departure Orbit on Outbound Hyperbola	1073.9	
TOTALS	4779.2	214.13

13.1.2.5.3. Trajectory Scan Results

The maneuver sequence calculations described previously were then applied to the aforementioned trajectory scans for round-trip Mars mission trajectories. The total Δv at Mars across the set of round-trip trajectories is presented in Figure 13-33(a). Recall that a relatively low total Δv at Mars does not necessarily mean that the total mission Δv is also relatively low. That being said, the EME opposition class trajectories tend to have somewhat lower total Δv at Mars than do the other types of trajectories in the scans. Figure 13-33(b) shows the stay times at Mars for the set of trajectories.

Figure 13-33(c) presents the relationship between the total mission duration and the total Δv at Mars. Note that while the EME opposition class trajectories have lower total Δv at Mars, they also have significantly longer total mission durations than the EMVE and EVME opposition class trajectories.

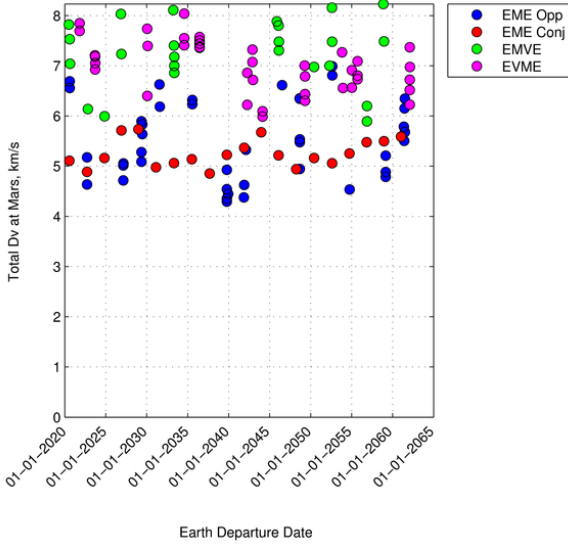
Figure 13-33(d) shows the differences between Mars arrival and departure asymptotic declinations for the set of trajectories. These differences are rather scattered, being small or near zero in some cases while being in excess of 25° to 30° in other cases. An arrival/departure declination difference of 20° were selected for the example calculations, shown previously in Table 13-11 and Table 13-12, because that seems to be a reasonably representative value.

13.1.2.5.4. Effects of Arrival and Departure Asymptotic Declinations

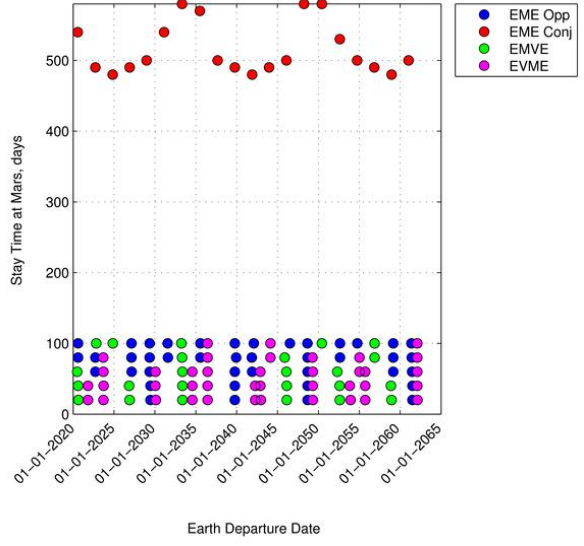
In the example results shown previously, the total Δv at Mars for exploring Phobos and Deimos (not counting the Mars arrival and departure Δv , which depends solely on incoming/outgoing V_∞) is 2.6 km/s, assuming a 10° asymptotic declination at Mars arrival and a 30° asymptotic declination at Mars departure (yielding a declination difference of 20°). The effects of other combinations of arrival and departure asymptotic declinations on the total Δv at Mars for exploring Phobos and Deimos were then investigated (again, independent of incoming/outgoing V_∞ at Mars).

A parametric scan in which both arrival and departure asymptotic declination are systematically varied between 0° and 80° was then performed. The total Δv at Mars for exploring Phobos and Deimos for each combination of arrival and departure asymptotic declination was computed. The results of this parametric scan are presented in Figure 13-34. One interesting trend is that higher arrival declinations have less impact on the Δv when the departure

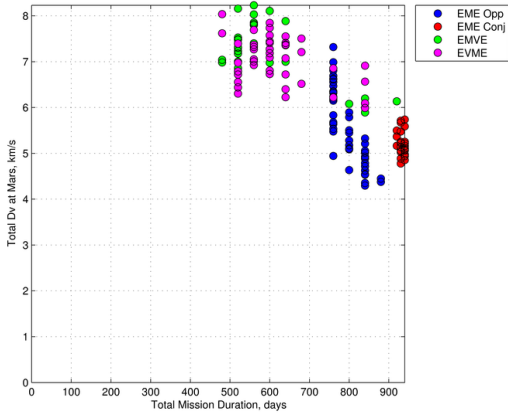
declinations are lower.



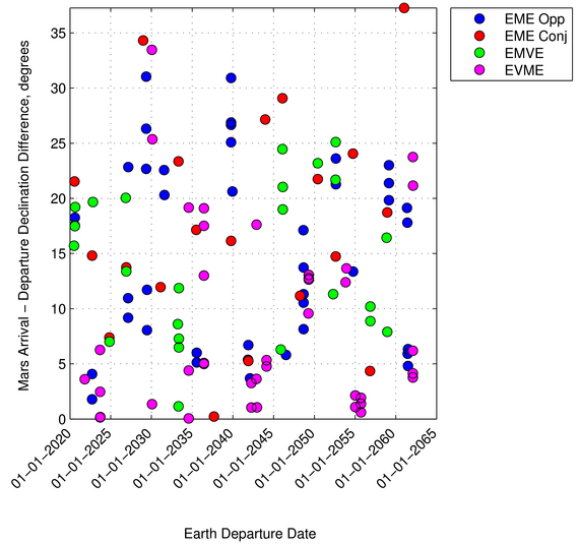
(a) Total ΔV at Mars.



(b) Stay time at Mars.



(c) Total round-trip mission duration versus total ΔV at Mars.



(d) Difference between Mars arrival and departure asymptotic declinations.

Figure 13-33 Trajectory scan results for total ΔV at Mars, stay time at Mars, mission duration, and differences between asymptotic declinations for Mars arrival and departure.

The total Δv at Mars between capture and departure shown in Figure 13-34 ranges between 2.25 km/s and 3.81 km/s. However, recall from Figure 13-33(d) that the largest arrival/departure asymptotic declination difference seen in our round-trip trajectory scans is approximately 38° and so it is not expected to be in the upper portion of the Δv range shown in Figure 13-34.

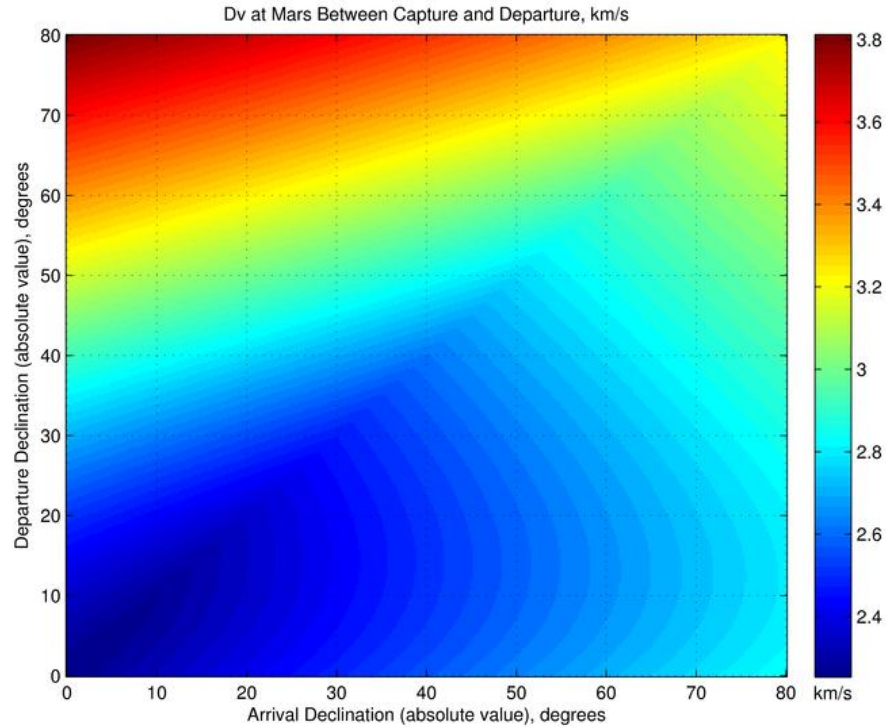


Figure 13-34 ΔV at Mars between arrival (capture) and departure as a function of arrival and departure declinations.

13.1.2.5.5. Full Reorientation of Highly Elliptical Mars Orbits

The results presented thus far address the need for orbit plane changes at Mars solely in terms of arrival/departure asymptotic declinations. However, in practice consideration of the full orientation of the highly elliptical Mars departure orbit such that its inclination, RAAN, and argument of periairion are all properly selected to contain the outgoing asymptote in the orbit plane and permit the Mars departure maneuver to be performed in the velocity direction at periairion (to notionally maximize efficiency) must be considered.

An array of results for optimal two-impulse re-orientation of the highly elliptical Mars orbit through various amounts of change in inclination, RAAN, and argument of periairion to show the associated Δv and flight time requirements is presented. The two-impulse orbit reorientations are optimized for each case using a grid search technique. The array of results is organized as follows: We consider changes in inclination, Δi , of 5° (Table 13-13), 20° (Table 13-14), 45° (Table 13-15), and 70° (Table 13-16). For each of those changes in inclination computation of the optimal total Δv and flight time for changes in RAAN, $\Delta \Omega$, and changes in argument of periairion, $\Delta \omega$, of 5° , 15° , 35° , 75° , 180° , and 300° was conducted.

The results in Table 13-13 through Table 13-16 indicate that some arrival/departure asymptote orientations at Mars may require up to about 1.5 km/s more reorientation Δv than the 0.1573 km/s that we allocated in Table 13-11 and Table 13-13 for the maneuvering sequence. Note that, as expected, it can be seen that the 0.1573 m/s reorientation Δv in Table 13-14 for $\Delta i = 20^\circ$, $\Delta \Omega = 180^\circ$, and $\Delta \omega = 180^\circ$ ($\Delta \Omega$, $\Delta \omega = 180^\circ$ yields the same result as $\Delta \Omega$, $\Delta \omega = 180^\circ$). In addition to requiring extra Δv , the more complicated orbit reorientations also require extra flight time, ranging from several hours to nearly 2 days.

The majority of these optimal transfers are of one of two basic types. One type, shown in Figure 13-35(a) involves essentially circularizing the elliptical orbit at or near apoairion, flying to the apoairion (or nearly so) of the reoriented orbit, and reducing periairion radius. Some amount of plane change is also included in those two maneuvers. The second type, shown in Figure 13-35(b) involves flying a transfer ellipse that intersects the initial and

reoriented orbits at points well prior to (or subsequent to) their apoarions.

A final point to note is that the Ω and ω of the highly elliptical Mars orbit would both drift under the influence of Mars' non-spherical gravitational field (chiefly due to the J_2 term of the spherical harmonics model for the gravitational field). This means that the Ω and ω to which the capture orbit is reoriented to create the “departure” orbit should be chosen such that those Ω and ω values will naturally drift to their appropriate values for Mars departure after the remaining stay time at Mars has elapsed. For reference, Figure 13-36 shows Ω and ω as functions of inclination for our particular highly elliptical Mars orbit. Unless the orbit is at a relatively high inclination, both Ω and ω will experience non-trivial changes over the course of a several month stay at Mars.

Table 13-13 Total Δv (m/s) / Total Flight Time (hours) Required to Transfer between 250 x 33813 km Altitude Mars Orbits with $\Delta i = 5^\circ$ as a Function of $\Delta\Omega$ and $\Delta\omega$, using Minimum Δv Two-impulse Transfers

$\Delta\Omega$	$\Delta\omega$					
	5°	15°	35°	75°	180°	300°
5°	182.5 / 6.3	342.6 / 4.0	547.7 / 44.0	873.7 / 37.3	1293.4 / 20.7	696.6 / 7.7
15°	342.8 / 3.7	474.3 / 45.0	632.0 / 42.3	946.7 / 36.0	1295.3 / 21.7	593.1 / 7.0
35°	547.7 / 43.7	631.7 / 42.3	797.2 / 39.3	1076.9 / 32.7	1257.9 / 18.0	363.4 / 6.0
75°	873.6 / 37.7	946.8 / 36.0	1077.0 / 32.7	1267.4 / 25.3	1088.7 / 12.7	272.8 / 3.7
180°	1293.5 / 21.0	1295.4 / 21.7	1258.1 / 17.7	1088.8 / 13.0	39.5 / 24.3	1127.4 / 31.3
300°	696.5 / 8.0	593.2 / 7.0	363.5 / 6.0	272.9 / 3.7	1127.5 / 31.3	1178.9 / 15.3

Table 13-14 Total Δv (m/s) / Total Flight Time (hours) Required to Transfer between 250 x 33813 km Altitude Mars Orbits with $\Delta i = 20^\circ$ as a Function of $\Delta\Omega$ and $\Delta\omega$, using Minimum Δv Two-impulse Transfers

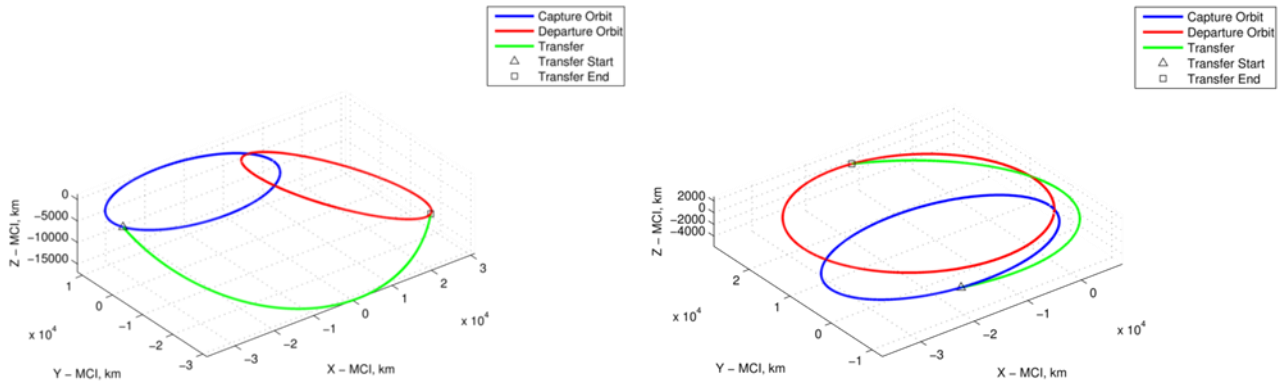
$\Delta\Omega$	$\Delta\omega$					
	5°	15°	35°	75°	180°	300°
5°	285.3 / 11.3	446.2 / 7.3	695.5 / 41.3	949.7 / 36.3	1321.4 / 20.7	769.7 / 11.0
15°	446.3 / 7.3	625.2 / 5.7	753.2 / 40.3	1023.5 / 34.3	1341.9 / 23.3	674.2 / 10.0
35°	695.3 / 41.7	753.3 / 40.0	889.1 / 37.3	1168.5 / 30.3	1318.5 / 20.3	494.0 / 7.7
75°	949.6 / 36.0	1023.7 / 34.3	1168.4 / 30.3	1453.3 / 21.3	1154.0 / 15.3	567.7 / 5.0
180°	1321.5 / 20.7	1341.8 / 23.3	1318.5 / 20.3	1154.1 / 15.3	157.3 / 1.0	1184.2 / 30.3
300°	769.6 / 11.0	674.2 / 9.7	494.0 / 7.7	567.9 / 5.0	1184.1 / 30.0	1301.6 / 20.0

Table 13-15 Total Δv (m/s) / Total Flight Time (hours) Required to Transfer between 250 x 33813 km Altitude Mars orbits with $\Delta i = 45^\circ$ as a Function of $\Delta\Omega$ and $\Delta\omega$, using Minimum Δv Two-impulse Transfers

$\Delta\Omega$	$\Delta\omega$					
	5°	15°	35°	75°	180°	300°
5°	458.0 / 14.7	615.5 / 9.7	921.3 / 39.0	1132.8 / 34.3	1413.1 / 21.0	934.8 / 13.0
15°	615.3 / 9.7	795.1 / 8.0	976.4 / 37.7	1209.3 / 32.7	1449.7 / 24.0	865.8 / 11.3
35°	921.5 / 39.0	976.4 / 37.7	1092.4 / 35.0	1375.8 / 28.7	1459.2 / 22.3	802.0 / 8.3
75°	1133.1 / 34.7	1209.4 / 32.3	1375.8 / 29.0	1765.5 / 21.3	1310.4 / 17.3	1016.8 / 43.0
180°	1412.2 / 21.3	1449.5 / 23.7	1459.4 / 22.0	1310.5 / 17.7	346.7 / 1.0	1352.7 / 28.7
300°	934.8 / 12.7	865.9 / 11.3	801.9 / 8.3	1017.0 / 43.3	1352.7 / 28.7	1506.8 / 22.3

Table 13-16 Total Δv (m/s) / Total Flight Time (hours) Required to Transfer between 250 x 33813 km Altitude Mars orbits with $\Delta i = 70^\circ$ as a Function of $\Delta\Omega$ and $\Delta\omega$, using Minimum Δv Two-impulse Transfers

$\Delta\Omega$	$\Delta\omega$					
	5°	15°	35°	75°	180°	300°
5°	617.0 / 16.0	769.7 / 11.0	1097.6 / 37.7	1305.5 / 34.0	1554.3 / 24.3	1110.4 / 13.3
15°	769.9 / 11.0	936.6 / 9.7	1164.9 / 36.3	1377.8 / 32.3	1595.1 / 23.3	1073.8 / 11.3
35°	1097.6 / 37.7	1164.9 / 36.3	1273.5 / 34.3	1542.0 / 29.3	1627.6 / 22.7	1111.5 / 8.3
75°	1305.6 / 33.7	1378.0 / 32.3	1542.1 / 29.7	1918.7 / 25.3	1483.1 / 18.0	1374.8 / 40.3
180°	1551.8 / 23.3	1594.9 / 24.0	1627.5 / 22.7	1483.1 / 17.7	519.7 / 1.0	1545.7 / 28.3
300°	1110.3 / 13.3	1073.5 / 11.3	1111.7 / 8.3	1374.4 / 40.7	1545.7 / 28.0	1636.8 / 21.3



- (a) Optimal two-impulse transfer between highly elliptical Mars orbits with 20° change in inclination, 75° change in RAAN, and 75° in argument of periaeeon.
- (b) Optimal two-impulse transfer between highly elliptical Mars orbits with 20° change in inclination, 300° change in RAAN, and 15° in argument of periaeeon.

Figure 13-35 Example optimal two-impulse transfer trajectories between highly elliptical Mars orbits of different orientations.

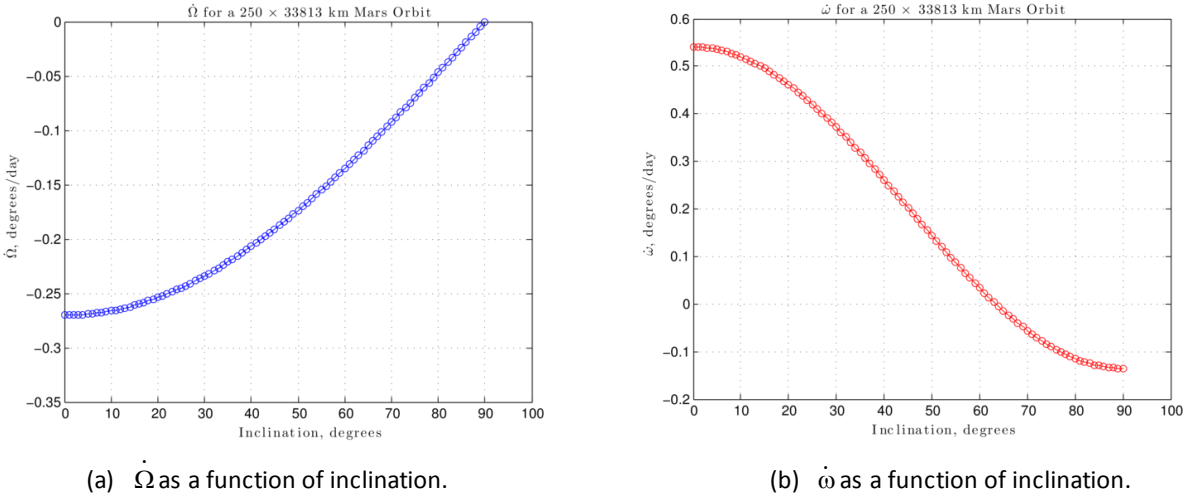


Figure 13-36 Rates at which the Ω and ω of a 250 x 33813 km altitude Mars orbit will change as a function of orbit inclination due to non-spherical Mars gravity effects (J2).

13.1.2.6. Arrival and Departure Transfers

The incoming (from Earth) and outgoing (to Earth) interplanetary trajectories significantly constrain the geometry of the Mars parking orbit. In general, the planes of the interplanetary trajectories would not coincide with the plane of the target orbit (near equatorial for Phobos and Deimos), requiring additional maneuvers to complete a round-trip mission to Mars.^{10,11,12} The inclusion of an intermediate parking orbit to stage the Deep Space Vehicle (DSV) further complicates the design of orbital transfers at Mars because parking orbit should allow efficient transfers from both the incoming and outgoing trajectory as well as the target orbit.^{13,14,15} Typically, the ΔV of the DSV is kept to a minimum, suggesting low periapsis, long period parking orbits (e.g., 500 km altitude x 1 sol) to minimize the ΔV from the high-energy interplanetary trajectories and the captured parking orbit. A less massive Space Exploration Vehicle (SEV) provides the additional ΔV to transfer down to Phobos or Deimos and back to the elliptical parking orbit.^{16,17} The overall propellant consumption is thus reduced by staging ΔV off the relatively massive DSV onto the smaller SEV. However, efficient orbital transfers are necessary to maintain this mass savings.

13.1.2.6.1. Arrival and Departure Design Techniques

The ΔV to reorient a 500 km altitude x 1 sol parking orbit at Mars is provided in Figure 13-37. The “change line of apsides” (blue and green) lines both perform the same function of rotating the direction of periapsis of elliptical orbits within the plane of the orbit (i.e., no plane change). It would be much more efficient to combine this maneuver with the capture and escape ΔV than to change the argument of periapsis while in the elliptical orbit. Alternatively, it would be more efficient to rotate the orbit along the line of apsides (red line) while the speed is low at the apoapsis of an elliptical orbit, than during the high-speed capture and escape maneuvers. Because these reorientation maneuvers are orthogonal (the blue line changes the line of apsides and does not affect the orbital plane while the red lines changes the orbital plane but does not affect the line of apsides) they can be combined to provide any orbital orientation.

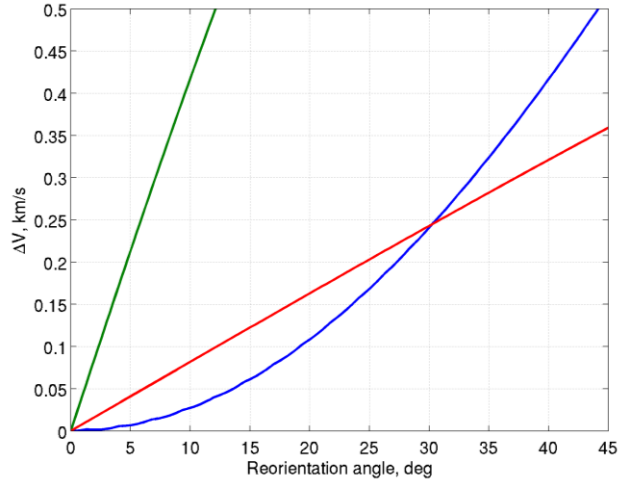


Figure 13-37 Relative cost of orbit reorientation techniques.

Because it is so efficient to rotate along the line of apsides while in orbit, the parking orbits would be designed so that apoapsis remains near the plane of the target orbits. (The orbital plane shifts slightly during the mission due to the oblateness of Mars.) In this way, the parking orbit could rotate from the arrival plane to the target plane to the departure plane with efficient maneuvers at apoapsis. However, this technique would require a change in the energy-optimal bending angle during the capture and escape maneuvers to place periapsis (and therefore apoapsis) in the target orbit plane. This additional bending would be most efficiently obtained by altering the capture and escape maneuvers as shown in Figure 1. An entire sequence from capture to Phobos rendezvous to escape is depicted in Figure 13-38.

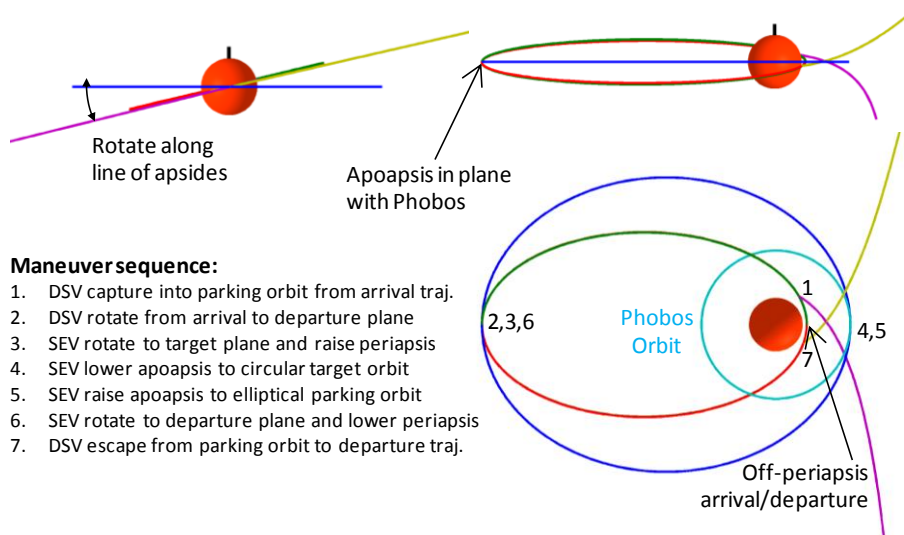


Figure 13-38 Example transfer to and from Phobos.

13.1.2.6.2. Mission Characteristics

The general characteristics of the maneuver sequence depicted in Figure 13-38 are investigated by applying the transfer strategy to short-duration (500- to 800-day round-trip) Mars missions. The arrival and departure conditions for opposition class trajectories from 2020 through 2070 are presented in Table 13-17. These V_{∞} vectors correspond to trajectories designed for relatively low injected mass to low-Earth orbit (LEO) (including the Earth departure

maneuver) and a 60-day stay time at Mars. Although these analyses were conducted utilizing patch-conic methodologies, they provide a good first approximation. Further optimization should be conducted to confirm the results. Table 13-18 contains the ΔV of each maneuver for the DSV at Mars along with the orientation of the parking orbit. The total ΔV for the DSV is found in the second column of Table 13-18, and the portion of the ΔV due to non-ideal geometry is tabulated in the third column. The additional ΔV from the ideal minimum is generally larger than the reorientation maneuver ΔV at apoapsis (column five) because the capture and escape maneuvers (columns four and six) also change the orbital geometry by shifting the line of apsides. The orientation of the parking orbit before and after the reorient maneuver is defined by the right ascension of periapsis (in the target orbit plane) and inclination of the arrival and departure orbits (which share a common line of apsides). The inclinations in Table 13-18 are generally near the equator to provide low- ΔV transfers to Phobos and Deimos. Table 13-19 contains the breakdown of maneuvers for the SEV to transfer to Phobos or Deimos. The total ΔV , as well as the additional ΔV from an ideal geometry (i.e., zero relative inclination), is generally smaller for the SEV than for the DSV, suggesting that most of the non-coplanar ΔV has been placed on the DSV. The maneuver breakdown in Table 13-18 and Table 13-19 is optimized to minimize the sum of the DSV and SEV ΔV , which may not be optimal from a mass standpoint because the DSV could be much more massive than the SEV. An alternative maneuver breakdown is provided in Table 13-20 and Table 13-21 where the ΔV of the DSV is minimized while neglecting the cost of the SEV. In this case, the DSV ΔV can be reduced dramatically (e.g., by 800 m/s in 2020) at the expense of an increase in SEV ΔV . The most dramatic changes occur when the inclination of the parking orbit is retrograde and the SEV must nearly reverse direction at apoapsis to transfer to the target orbit. The overall ΔV for the DSV remains low because both the arrival and departure orbits are retrograde. A key design variable for the reorientation ΔV is the speed near apoapsis of the parking orbit, where lower speeds generally lead to lower ΔV . Examples where the apoapsis speed is lowered by increasing the period of the parking orbit to three sols (from one sol) are provided in Table 13-22 and Table 13-23. This design provides the greatest benefit to the SEV ΔV (e.g., over 800 m/s in 2020), though the DSV ΔV also decreases. The SEV ΔV is still generally larger in Table 13-23 than in Table 13-19, but the maneuver combination in Table 13-22 and Table 13-23 could provide an overall lower mass design. However, these longer period orbits provide a transfer opportunity only once every three sols, whereas the shorter period orbits have more frequent transfer opportunities. Thus the mass benefits must be balanced with the operational constraints.

Table 13-17 Mars Arrival and Departure Vectors for Short-Duration (opposition class) Missions 2020–2070

Mars Arrival	Traj. Type ^a	Arrival V_{∞} , km/s	Arrival RA, ^b deg.	Arrival Dec., Deg.	Departure V_{∞} , km/s	Departure RA, deg.	Departure Dec., Deg.
12/11/20	EMVE	4.545	124.06	10.98	6.208	45.99	26.69
04/20/23	EME	3.018	-176.10	-18.33	3.198	-85.77	-20.11
06/23/24	EVME	6.712	28.37	10.13	3.322	12.01	7.66
08/11/28	EME	3.239	-11.10	-20.59	2.869	76.74	43.43
10/10/30	EME	3.466	32.23	12.27	2.767	129.83	38.59
01/08/31	EVME	5.427	-151.11	-5.15	3.711	157.19	6.49
10/14/33	EMVE	3.890	5.69	1.23	6.226	0.44	8.51
06/26/35	EVME	5.912	-30.57	-10.76	4.790	-39.57	-15.15
05/16/37	EVME	6.308	-46.45	-26.78	3.872	-15.30	-31.86
06/19/40	EME	2.642	-156.51	-31.08	3.203	-51.50	-4.41
08/08/42	EME	2.709	-117.19	-15.71	3.542	-7.32	9.00
10/02/43	EVME	5.720	138.48	23.66	4.229	78.32	6.04
08/17/46	EMVE	4.400	-44.63	-2.83	6.209	-63.43	-27.30
02/17/50	EME	4.770	149.60	23.19	2.829	-115.72	-12.64
03/19/50	EVME	5.743	-101.06	-25.31	3.761	-125.22	-12.67
12/03/52	EMVE	3.746	95.61	17.72	5.823	50.12	29.04
06/25/56	EVME	5.907	41.70	4.14	3.384	25.99	-5.23
07/05/56	EVME	6.453	27.64	11.12	3.521	14.87	10.52
08/13/60	EME	2.908	-7.10	-20.61	2.675	92.53	43.62
11/01/62	EME	5.348	58.30	25.75	2.891	141.56	31.66
01/10/63	EVME	5.424	-150.39	-6.59	3.402	165.78	2.83
10/16/65	EMVE	3.989	24.39	7.30	6.321	-2.09	11.83
06/28/67	EVME	5.789	-29.71	-9.92	4.734	-35.96	-14.16
04/03/70	EMVE	3.207	174.88	-6.31	4.800	147.76	31.90

a EMVE has a Venus flyby on the return (Mars-Earth) leg; EVME has a Venus flyby on the outbound (Earth-Mars) leg; and EME has no Venus flybys during the round-trip Mars trajectory.

b Mars right ascension and declination are in Mars equator and equinox of J2000 frame.

Table 13-18 DSV Transfers for 250 km x 1 sol Parking Orbits with Equal Weighting on DSV and SEV ΔV

Mars Arrival	DSV ΔV , km/s					Parking Orbit Orientation ^b , deg		
	Total	Difference from ideal ^a	Capture	Reorient	Escape	Periapsis right asc.	Arrive inc.	Depart inc.
12/11/20	6.47	1.20	2.95	0.06	3.53	-24.8	20.6	28.0
04/20/23	2.32	0.05	1.16	0.00	1.23	141.9	26.3	26.3
06/23/24	5.32	0.42	3.85	0.02	1.52	-73.1	10.3	7.7
08/11/28	2.81	0.60	1.25	0.61	1.04	-61.6	26.0	54.9
10/10/30	2.63	0.34	1.47	0.26	0.98	-9.2	18.2	50.6
01/08/31	5.08	0.96	2.99	0.11	2.04	98.7	5.5	7.6
10/14/33	5.15	0.30	1.75	0.06	3.43	-82.5	1.2	8.6
06/26/35	5.47	0.26	3.18	0.04	2.35	-127.1	10.8	15.2
05/16/37	4.98	0.07	3.40	0.05	1.64	-124.7	27.3	33.4
06/19/40	2.50	0.42	0.93	0.29	1.36	164.8	44.0	7.4
08/08/42	2.88	0.57	1.04	0.33	1.59	-151.1	26.8	15.0
10/02/43	5.72	1.05	3.17	0.14	2.47	28.6	25.0	7.9
08/17/46	5.70	0.53	2.14	0.20	3.45	-141.2	2.8	27.8
02/17/50	3.71	0.55	2.33	0.40	1.09	101.5	29.9	20.4
03/19/50	4.96	0.56	3.11	0.11	1.82	156.4	25.8	12.9
12/03/52	5.23	0.78	2.03	0.08	3.19	-25.1	20.4	29.9
06/25/56	4.79	0.48	3.22	0.08	1.55	-59.1	4.2	5.2
07/05/56	5.16	0.35	3.63	0.01	1.60	-72.5	11.3	10.5
08/13/60	2.57	0.63	1.07	0.65	0.94	-52.4	27.9	58.9
11/01/62	3.77	0.16	2.75	0.07	1.05	7.8	32.0	40.5
01/10/63	4.79	0.85	2.92	0.08	1.84	104.3	6.8	3.2
10/16/65	5.49	0.50	1.96	0.04	3.57	-78.5	7.5	12.2
06/28/67	5.32	0.24	3.08	0.03	2.30	-124.8	10.0	14.2
04/03/70	4.27	0.89	1.56	0.31	2.45	71.8	6.5	32.7

a Minimum ΔV for coplanar transfers.
 b Parking orbit orientation is given in Mars equator and equinox of J2000 frame.

Table 13-19 Exploration Vehicle Transfers for 250 km x 1 sol Parking Orbits with Equal Weighting on DSV and SEV ΔV

Mars Arrival	Phobos SEVΔV, km/s				Deimos SEVΔV, km/s			
	Total ^b	Difference from ideal ^c	Leave Parking	Return Parking	Total ^b	Difference from ideal ^c	Leave Parking	Return Parking
12/11/20	1.78	0.20	0.30	0.35	1.42	0.15	0.54	0.58
04/20/23	1.81	0.23	0.34	0.34	1.44	0.17	0.57	0.57
06/23/24	1.62	0.03	0.25	0.24	1.29	0.02	0.50	0.50
08/11/28	2.03	0.44	0.34	0.56	1.64	0.37	0.57	0.78
10/10/30	1.94	0.36	0.28	0.53	1.57	0.30	0.53	0.75
01/08/31	1.60	0.02	0.23	0.24	1.28	0.01	0.49	0.50
10/14/33	1.60	0.01	0.23	0.24	1.28	0.01	0.49	0.50
06/26/35	1.65	0.07	0.25	0.27	1.32	0.04	0.51	0.52
05/16/37	1.87	0.28	0.35	0.39	1.49	0.22	0.58	0.62
06/19/40	1.84	0.26	0.48	0.24	1.48	0.21	0.70	0.50
08/08/42	1.74	0.16	0.34	0.27	1.39	0.12	0.58	0.52
10/02/43	1.70	0.12	0.33	0.24	1.35	0.08	0.57	0.50
08/17/46	1.71	0.13	0.23	0.35	1.36	0.09	0.49	0.58
02/17/50	1.79	0.21	0.37	0.30	1.43	0.16	0.59	0.54
03/19/50	1.72	0.14	0.34	0.26	1.37	0.10	0.57	0.51
12/03/52	1.79	0.21	0.30	0.37	1.43	0.16	0.54	0.59
06/25/56	1.59	0.01	0.23	0.23	1.28	0.01	0.49	0.49
07/05/56	1.63	0.05	0.25	0.25	1.30	0.03	0.51	0.50
08/13/60	2.07	0.49	0.35	0.59	1.68	0.41	0.58	0.81
11/01/62	1.96	0.37	0.38	0.45	1.57	0.30	0.61	0.67
01/10/63	1.59	0.01	0.24	0.23	1.28	0.01	0.50	0.49
10/16/65	1.62	0.04	0.24	0.26	1.30	0.03	0.50	0.51
06/28/67	1.64	0.06	0.25	0.27	1.31	0.04	0.50	0.52
04/03/70	1.75	0.17	0.24	0.39	1.40	0.13	0.50	0.61

- a Includes 1.13 km/s to enter and depart Phobos orbit.
- b Includes 0.29 km/s to enter and depart Phobos orbit.
- c Minimum ΔV for coplanar transfers.

Table 13-20 Deep Space Vehicle Transfers for 250 km x 1 sol Parking Orbits with Full Weighting on DSV ΔV

Mars Arrival	DSV ΔV, km/s					Parking Orbit Orientation ^b , deg		
	Total	Difference from ideal ^a	Capture	Reorient	Escape	Periapsis right asc.	Arrive inc.	Depart inc.
12/11/20	5.61	0.34	2.16	0.13	3.33	169.9	164.9	148.8
04/20/23	2.32	0.05	1.12	0.00	1.20	141.9	26.3	26.3
06/23/24	5.01	0.11	3.70	0.02	1.30	119.8	169.9	172.0
08/11/28	2.80	0.59	1.21	0.59	1.01	-64.1	25.2	56.3
10/10/30	2.63	0.34	1.39	0.28	0.96	-13.6	16.9	53.3
01/08/31	4.24	0.11	2.66	0.10	1.48	-81.8	174.5	172.4
10/14/33	5.15	0.30	1.72	0.06	3.37	-82.5	1.2	8.6
06/26/35	5.47	0.26	3.13	0.03	2.31	-127.1	10.8	15.2
05/16/37	4.98	0.07	3.33	0.05	1.60	-125.7	27.2	33.6
06/19/40	2.49	0.41	0.91	0.32	1.27	169.9	47.4	6.7
08/08/42	2.87	0.57	1.02	0.33	1.53	-149.2	28.0	14.4
10/02/43	4.88	0.20	2.89	0.15	1.84	-157.3	154.0	172.7
08/17/46	5.40	0.23	1.94	0.19	3.28	31.1	177.1	152.6
02/17/50	3.71	0.55	2.27	0.38	1.05	101.7	30.0	20.3
03/19/50	4.54	0.14	2.92	0.09	1.53	-15.9	154.6	166.6
12/03/52	4.53	0.08	1.50	0.07	2.95	154.5	159.5	150.2
06/25/56	4.49	0.19	3.07	0.08	1.35	131.1	175.9	174.6
07/05/56	4.92	0.11	3.50	0.00	1.42	119.4	168.9	169.1
08/13/60	2.57	0.63	1.03	0.63	0.91	-55.1	26.8	60.7
11/01/62	3.77	0.16	2.67	0.08	1.02	5.4	31.2	41.7
01/10/63	4.03	0.08	2.65	0.08	1.30	-75.5	173.2	176.8
10/16/65	5.04	0.05	1.66	0.03	3.35	94.5	172.2	168.1
06/28/67	5.32	0.24	3.03	0.03	2.26	-124.8	10.0	14.2
04/03/70	3.77	0.39	1.22	0.30	2.25	-115.8	173.3	147.9

- a Minimum ΔV for coplanar transfers.
- b Parking orbit orientation is given in Mars equator and equinox of J2000 frame.

Table 13-21 Space Exploration Vehicle Transfers for 250 km x 1 sol Parking Orbits with Full Weighting on DSV ΔV

Mars Arrival	Phobos SEVΔV, km/s				Deimos SEVΔV, km/s			
	Total ^b	Difference from ideal ^c	Leave Parking	Return Parking	Total ^b	Difference from ideal ^c	Leave Parking	Return Parking
12/11/20	3.34	1.76	1.12	1.09	3.03	1.76	1.38	1.35
04/20/23	1.81	0.23	0.34	0.34	1.44	0.17	0.57	0.57
06/23/24	3.39	1.80	1.13	1.13	3.07	1.80	1.39	1.39
08/11/28	2.03	0.45	0.33	0.57	1.65	0.37	0.57	0.79
10/10/30	1.96	0.37	0.28	0.55	1.58	0.31	0.53	0.76
01/08/31	3.39	1.81	1.13	1.13	3.08	1.81	1.39	1.39
10/14/33	1.60	0.01	0.23	0.24	1.28	0.01	0.49	0.50
06/26/35	1.65	0.07	0.25	0.27	1.32	0.04	0.51	0.52
05/16/37	1.87	0.28	0.35	0.39	1.49	0.22	0.58	0.62
06/19/40	1.87	0.28	0.50	0.24	1.51	0.23	0.72	0.50
08/08/42	1.75	0.16	0.35	0.27	1.39	0.12	0.58	0.52
10/02/43	3.36	1.78	1.11	1.13	3.05	1.78	1.36	1.39
08/17/46	3.36	1.78	1.13	1.10	3.05	1.78	1.40	1.36
02/17/50	1.79	0.21	0.37	0.30	1.43	0.16	0.60	0.54
03/19/50	3.36	1.78	1.11	1.13	3.04	1.77	1.37	1.39
12/03/52	3.34	1.76	1.12	1.10	3.02	1.75	1.38	1.35
06/25/56	3.39	1.81	1.13	1.13	3.08	1.81	1.39	1.39
07/05/56	3.38	1.80	1.13	1.13	3.07	1.80	1.39	1.39
08/13/60	2.08	0.49	0.34	0.60	1.69	0.42	0.58	0.82
11/01/62	1.96	0.38	0.37	0.46	1.57	0.30	0.60	0.67
01/10/63	3.39	1.81	1.13	1.13	3.08	1.81	1.39	1.39
10/16/65	3.39	1.80	1.13	1.13	3.07	1.80	1.39	1.39
06/28/67	1.64	0.06	0.25	0.27	1.31	0.04	0.50	0.52
04/03/70	3.35	1.77	1.13	1.09	3.03	1.76	1.39	1.35

- a Includes 1.13 km/s to enter and depart Phobos orbit.
- b Includes 0.29 km/s to enter and depart Phobos orbit.
- c Minimum ΔV for coplanar transfers.

Table 13-22 Deep Space Vehicle Transfers for 250 km x 3 sol Parking Orbits with Full Weighting on DSV ΔV

Mars Arrival	DSV ΔV, km/s					Parking Orbit Orientation ^b , deg		
	Total	Difference from ideal ^a	Capture	Reorient	Escape	Periapsis right asc.	Arrive inc.	Depart inc.
12/11/20	5.34	0.30	2.02	0.07	3.25	173.0	165.6	147.8
04/20/23	2.10	0.06	1.01	0.00	1.08	141.9	26.3	26.3
06/23/24	4.79	0.12	3.59	0.01	1.19	119.8	169.9	172.0
08/11/28	2.26	0.28	1.09	0.28	0.89	-65.6	24.8	57.2
10/10/30	2.24	0.18	1.24	0.15	0.85	-19.1	15.6	57.1
01/08/31	3.95	0.06	2.54	0.05	1.37	-81.7	174.5	172.4
10/14/33	4.82	0.19	1.56	0.03	3.23	87.4	178.8	171.5
06/26/35	5.09	0.11	2.95	0.02	2.12	57.2	169.2	164.7
05/16/37	4.73	0.05	3.22	0.03	1.48	-127.4	27.1	33.9
06/19/40	2.10	0.25	0.82	0.16	1.12	174.5	51.2	6.1
08/08/42	2.52	0.45	0.95	0.16	1.42	-147.7	29.0	14.0
10/02/43	4.58	0.13	2.78	0.07	1.72	-158.7	153.8	172.8
08/17/46	5.08	0.14	1.82	0.09	3.16	31.2	177.1	152.6
02/17/50	3.30	0.38	2.17	0.18	0.95	102.2	30.2	20.1
03/19/50	4.27	0.10	2.81	0.04	1.42	-16.4	154.6	166.6
12/03/52	4.26	0.04	1.38	0.04	2.83	156.1	159.8	150.0
06/25/56	4.23	0.16	2.96	0.04	1.24	131.4	175.9	174.6
07/05/56	4.71	0.13	3.39	0.00	1.31	119.4	168.9	169.1
08/13/60	2.00	0.30	0.91	0.30	0.79	-56.8	26.2	61.8
11/01/62	3.49	0.11	2.52	0.05	0.91	0.5	29.7	44.5
01/10/63	3.75	0.04	2.53	0.04	1.18	-75.4	173.2	176.8
10/16/65	4.80	0.04	1.55	0.02	3.24	94.8	172.3	168.1
06/28/67	4.98	0.14	2.87	0.02	2.10	59.4	170.1	165.8
04/03/70	3.39	0.24	1.11	0.14	2.14	-116.0	173.3	147.9

- a Minimum ΔV for coplanar transfers.
- b Parking orbit orientation is given in Mars equator and equinox of J2000 frame.

Table 13-23 Space Exploration Vehicle transfers for 250 km x 3 sol parking orbits with full weighting on DSV ΔV .

Mars Arrival	Phobos SEV ΔV , km/s				Deimos SEV ΔV , km/s			
	Total ^a	Difference from ideal ^c	Leave Parking	Return Parking	Total ^b	Difference from ideal ^c	Leave Parking	Return Parking
12/11/20	2.51	0.83	0.54	0.52	2.03	0.82	0.69	0.67
04/20/23	1.79	0.10	0.17	0.17	1.28	0.07	0.31	0.31
06/23/24	2.53	0.85	0.54	0.54	2.06	0.85	0.70	0.70
08/11/28	1.89	0.21	0.16	0.28	1.38	0.17	0.31	0.41
10/10/30	1.87	0.18	0.14	0.28	1.36	0.15	0.29	0.41
01/08/31	2.53	0.85	0.54	0.54	2.06	0.85	0.70	0.70
10/14/33	2.53	0.85	0.54	0.54	2.06	0.85	0.70	0.70
06/26/35	2.53	0.84	0.54	0.54	2.05	0.84	0.69	0.69
05/16/37	1.81	0.13	0.17	0.19	1.31	0.10	0.31	0.33
06/19/40	1.83	0.14	0.26	0.12	1.33	0.12	0.39	0.27
08/08/42	1.76	0.08	0.18	0.13	1.27	0.05	0.32	0.28
10/02/43	2.52	0.84	0.53	0.54	2.04	0.83	0.68	0.70
08/17/46	2.52	0.83	0.54	0.53	2.04	0.83	0.70	0.68
02/17/50	1.78	0.10	0.18	0.15	1.28	0.07	0.32	0.29
03/19/50	2.52	0.83	0.53	0.54	2.04	0.83	0.68	0.69
12/03/52	2.51	0.82	0.53	0.52	2.03	0.82	0.69	0.68
06/25/56	2.53	0.85	0.54	0.54	2.06	0.85	0.70	0.70
07/05/56	2.53	0.84	0.54	0.54	2.05	0.84	0.69	0.69
08/13/60	1.91	0.23	0.17	0.30	1.40	0.19	0.31	0.43
11/01/62	1.86	0.18	0.18	0.23	1.35	0.14	0.32	0.37
01/10/63	2.53	0.85	0.54	0.54	2.06	0.85	0.70	0.70
10/16/65	2.53	0.85	0.54	0.54	2.06	0.84	0.70	0.69
06/28/67	2.53	0.84	0.54	0.54	2.05	0.84	0.70	0.69
04/03/70	2.51	0.83	0.54	0.52	2.04	0.83	0.70	0.67

- a Includes 1.45 km/s to enter and depart Phobos orbit.
- b Includes 0.67 km/s to enter and depart Phobos orbit.
- c Minimum ΔV for coplanar transfers.

13.1.2.7. Exploration of Phobos and Deimos Mission Design Conclusion

In this paper, we have studied the precise orbital motion of Phobos and Deimos about Mars and used that data to inform the design of optimal rendezvous trajectories between Phobos and Deimos. We extend those results to construct complete maneuvering sequences for exploring Phobos and Deimos, including arrival at Mars from hyperbolic approach, rendezvous with each moon, proximity operations at each moon, and Mars departure. We applied this notional maneuvering sequence across a set of round-trip Mars trajectory solutions obtained from trajectory scans that include opposition class trajectories (with and without Venus gravity assists) and conjunction class trajectories to assess requirements for total ΔV at Mars for Phobos/Deimos exploration missions. Finally, we assessed the effect on total ΔV at Mars due to the reorientation of highly elliptical Mars orbits that may be required to properly align with incoming/outgoing asymptotes at Mars.

Our results indicate that the total ΔV at Mars for Phobos/Deimos exploration will likely range between 4.8 to 9 km/s, depending on the mission's departure date and type of round-trip trajectory own. The total time required for orbital maneuvering to explore Phobos and Deimos will likely range between 1.5 to 2 weeks depending on the exact conditions encountered. This leaves ample time to spend exploring the moons themselves provided that the stay time at Mars is at least several months.

13.1.2.7.1. Future Work

One of the next steps in the analysis will be to implement the maneuvering sequence in a high-fidelity end-to-end simulation environment to fully validate the maneuver sequence, develop exemplar point designs using precision integrated trajectories and finite burn maneuvers, and then construct detailed design reference missions using those results.

It is also desired to further study the problem of proximity operations at Phobos and Deimos, including identification of robust and safe strategies for spacecraft proximity operations at each moon and for maneuvers with which the crew can interact with the surfaces of the moons. Preliminary results indicate that Phobos may be more challenging than Deimos in this regard. Future studies of stable periodic motion in the vicinity of the moons using complete force models will inform these analyses. Other issues include the refinement of the terminal rendezvous sequences to account for relative navigation sensor and filter performances in the presence of realistic environmental factors such as lighting conditions. The results of such analysis will likely lead to modifications of the notional terminal rendezvous sequences presented herein.

13.2. Mars Program Planning Group Summary

Primary Contributors:

John D. Baker, Jet Propulsion Laboratory, California Institute of Technology, USA
Deborah Bass, Ph.D., Jet Propulsion Laboratory, California Institute of Technology, USA
David Beaty, Ph.D., Jet Propulsion Laboratory, California Institute of Technology, USA
Bret G. Drake, National Aeronautics and Space Administration, Johnson Space Center

13.2.1. Mars Program Planning Group Charter

The President's fiscal year (FY)2013 Budget Request contained reductions in the Mars future program line necessitating reformulation of the current Mars Exploration Program (MEP), and discontinuing development of 2016 and 2018 missions with the European Space Agency (ESA). The realities of the fiscal environment, new priorities, and the most recent inputs from the science, human exploration, and technology communities, provided an opportunity to set new directions and a revised vision aimed at revising and renewing the program. This opportunity also served to exploit synergies between NASA programs to take advantage of the strengths of the NASA robotic and human exploration efforts for the long-term future (2025 and beyond).

The NASA Administrator directed the Associate Administrator for the Science Mission Directorate to lead Mars program reformulation activities working with the Associate Administrator for Human Exploration and Operations Directorate, the NASA Chief Technologist, and the NASA Chief Scientist. In support of this reformulation, NASA established a Mars Program Planning Group (MPPG).⁵ The purpose of the MPPG was to develop foundations for a program-level architecture for robotic exploration of Mars that is consistent with the President's challenge of sending humans to Mars orbit in the decade of the 2030s,¹⁸ yet remain responsive to the primary scientific goals of the 2011 National Research Council (NRC) Decadal Survey for Planetary Science.¹⁹ Program architecture was defined as a sequence of strategically selected and interconnected spaceflight and ground-based investigations that would increase scientific knowledge, advance key technologies, and inform and would enable long-term human exploration goals. The MPPG was structured to serve as a limited-term study group responsible for delivering specific products to aid NASA in the decision-making process on the future direction of the reformulated MEP.

The immediate focus of the MPPG was on the collection of multiple mission concept options for the 2018/2020 Mars launch opportunities. Fidelity and timeliness of these studies were the MPPG's priority so as to affect Agency decisions in the upcoming FY14 budget planning process and ensure a 2018 mission would be viable. To maintain the successful strategic structure of the MEP, and ensure relevancy of the possible 2018/2020 mission(s) to longer-term science and exploration priorities, notional architectures/pathways spanning to the 2030s were required, including future human exploration of Mars. The purpose of the MPPG was to develop foundations for a program-level architecture for robotic exploration of Mars that is consistent with the President's challenge of sending humans to Mars in the decade of the 2030s, yet remain responsive to the primary scientific goals of the 2011 NRC Decadal Survey for Planetary Science. Consistent with its charter, MPPG reached out to internal and external science, technology, and engineering communities, to develop mission options and program architecture alternatives for NASA's consideration. The MPPG was specifically chartered to provide options that integrate science, human exploration and technology at an agency level with Mars Exploration as a common objective.

13.2.2. Human Exploration beyond LEO: A Capability Driven Framework

⁵ Additional information regarding the MPPG can be found at:
<http://www.nasa.gov/offices/marsplanning/home/index.html>.

The option of a crew returning Mars surface samples that had been previously placed into Mars orbit via a robotic mission was particularly intriguing during initial deliberations of the MPPG core team, especially with its direct ties to the National Space Policy [Office of the President, 2010]. This line of thinking spawned a series of questions regarding the potential of humans returning samples from Mars orbit – a non-landed mission to Mars. To understand the viability of this strategy, assessments of the implications of both the development schedule, including technology development, as well as the risk were required. Previous assessments have determined that a mission to Mars as the first destination for humans beyond Earth orbit may not be the best strategy,^{20,21} [Augustine, 2009] to name a few. Rather, to establish a balanced risk/cost posture, a progressive expansion of humans from Earth, with near-Earth destinations as the initial missions was best warranted and thus a less-destination-specific framework has emerged. This strategy, referred to as a Capability Driven Framework (CDF),²² is based on the idea of an ever-expanding human presence beyond LEO in terms of duration and distance from the Earth. It is based on evolving capabilities that would be utilized after operational experience had been established from completing less demanding missions. In theory, the CDF would enable multiple destinations and would provide increased flexibility, greater cost effectiveness, and sustainability. But the utility of a CDF can only be measured and fully understood when put into context of actual missions. Thus, to help formulate the strategies, technologies, and systems needed to support the framework, example destinations are being examined including LEO, Geostationary missions, cislunar space (including lunar fly-by, lunar orbit, and lunar surface), Near-Earth Asteroids (NEA), as well as missions to the Mars and the moons of Mars. Before examining how human missions to Mars would fit into the overall CDF a brief review of the missions associated with the CDF is necessary.

Geosynchronous Orbits (GEO): This mission class includes missions to GEO or other high-Earth orbit destinations generally for the purpose of deploying or repairing ailing spacecraft. Due to the high change in velocity (ΔV) associated with these destinations; a split-mission approach would be typically used where the crew would be sent to the destination separate from the cargo assets to be used at the destination. The cargo assets could include habitats, mobility systems, robotic systems, and repair equipment.

Earth-Moon Libration: This mission class includes missions to the Earth-Moon libration points (L1 or L2) or high lunar orbit. As with the GEO mission, cargo for these missions would be typically sent separately from the crew. L1/L2 could also serve as a staging node for other destinations such as to the lunar surface, NEAs, or perhaps even Mars. Thus, crew missions to L1/L2 may serve as the initial crew transport leg at the beginning or end of a different mission class.

Lunar Surface: Missions to the lunar surface would encompass a range of mission durations, beginning with short stays to prove the performance of the systems, to longer duration test beds for more challenging missions such as the surface of Mars. As with both the GEO and L1/L2 missions, a split mission approach would be typically used separating the crew from cargo.

Near-Earth Asteroids: This mission class represents human missions to and from asteroids which are in close proximity to Earth, orbit perihelion typically less than 1.3 AU. NEAs are of interest because they represent a class of missions that truly leave Earth vicinity. Since these missions would be conducted in heliocentric space and the orbits of least-energetic NEAs have long synodic periods, perhaps decades long, it becomes difficult to pre-deploy mission assets at the NEA prior to the crew mission. Thus, these missions would be typically constructed as all-up missions, whereby all of the required mission assets would be transported with the crew (deep space habitat, destination exploration systems, and Earth entry vehicle).

Mars Orbit: This mission class includes missions to the moons of Mars (Phobos and Deimos) as well as Mars orbit. Missions to Mars can occur approximately every 26 months due to the difference in the orbital periods of Earth and Mars. Since these missions avoid planetary surfaces, the crew would be exposed to the deep space environment for the entire mission duration. Thus, these missions are generally constructed to reduce this crew exposure by flying the trajectories as fast as possible within the constraints of the propulsion technologies and number of heavy lift launches. Since missions to Mars could occur on a frequent basis (every 26 months), pre-deployment of mission exploration vehicles is usually employed.

Figure 13-39 provides an example mission profile for a typical Mars orbital mission. With this mission construct cargo, which would be utilized to explore the Mars system when in orbit, would be pre-deployed to Mars one

opportunity before the crew would depart Earth. This strategy would allow the cargo to utilize energy-efficient trajectories, thus reducing the propellant mass and resulting architecture mass. It would also allow for operational checkout of the cargo to ensure that it arrived safely and operating as would be expected before the crew mission. The number of launches required is dependent on the transportation technology used and the payload deployed.

The Mars moon exploration concept envisioned here would use a large interplanetary spacecraft to transport a crew to and from Mars. Upon arrival at Mars, it would be placed into a high Mars orbit. Upon arrival, the crew vehicle would rendezvous with the pre-deployed cargo placed in this parking orbit on a previous transfer opportunity. Half of the crew would use a Space Exploration Vehicle (SEV) and one of three chemical orbit transfer stages (OTS) to transfer from this parking orbit to the vicinity of Phobos and spend the next 2 weeks exploring this moon. Because the orbits of both Phobos and Deimos are nearly in the equatorial plane of Mars and the arrival and departure declinations of the transfer trajectories do not typically lie in that same plane, large plane change maneuvers are required to transfer the crews from the high parking orbit down to the orbits of the moons. After returning from this Phobos mission, the other two crew members would use a second SEV and OTS to transfer from the parking orbit to the vicinity of Deimos and spend the next 2 weeks exploring the other martian moon. A third OTS would be available to rescue either crew should they become stranded at either Phobos or Deimos. Crew time not used to explore Phobos or Deimos would be available to potentially retrieve samples from a separate robotic sample return mission or perhaps teleoperate robotic systems on the surface of Mars when a communication path is available. At the end of the orbital stay,⁶ all SEV and OTS assets would be jettisoned, and the large interplanetary spacecraft would depart from its parking orbit for the return trip to Earth.

Mars Surface: This mission class represents missions to the surface of Mars. Strategies for exploring the surface of Mars typically utilize pre-deployed cargo vehicles and flying lower energy conjunction class missions. For the surface long-stay mission class, the NASA Design Reference Architecture 5.0 was utilized as the basis for the analysis. For this mission, a crew would be sent to Mars on a long-stay class trajectory. Upon arrival, the crew would place their large interplanetary vehicle into a high-Mars parking orbit to rendezvous with one of two cargo vehicles sent to Mars on the prior orbit transfer opportunity. The second cargo vehicle would have already landed at the intended surface exploration location, where automated systems would have set up a power plant and a propellant manufacturing plant. When all necessary systems have been verified operational and landing conditions determined to be satisfactory, the crew would initiate the landing sequence. Once the crew landed at this site, they would spend approximately 500 days exploring the vicinity in a series of long traverses (several 100 kilometers) extending from this fixed central base – an approach dubbed the “commuter” strategy. At the completion of this surface mission, the crew would ascend from their surface base, using propellants manufactured there, and return to the waiting interplanetary vehicle. At the appropriate time the crew would depart from Mars for a 6-month transfer back to Earth. Figure 13-40 provides an example mission profile for a typical Mars surface mission.

⁶ Because there are two distinct trajectory types for a round-trip mission to Mars, there are also two distinct approaches for potentially conducting exploration missions while in Mars orbit. Short-stay opposition class mass mission can reduce the total mission duration by flying the trajectories as fast as possible. These missions are generally 600-800 days in duration with approximately 60 days at Mars. On the other hand, using the longer duration trajectories (i.e., the long-stay class with 500 days at Mars) would reduce the number of launches (for a fixed payload mass) but at the expense of increasing a crew’s exposure to the deep-space zero-gravity and radiation environment (up to 1000 days).

Mars Design Reference Architecture 5.0 – Addendum #2

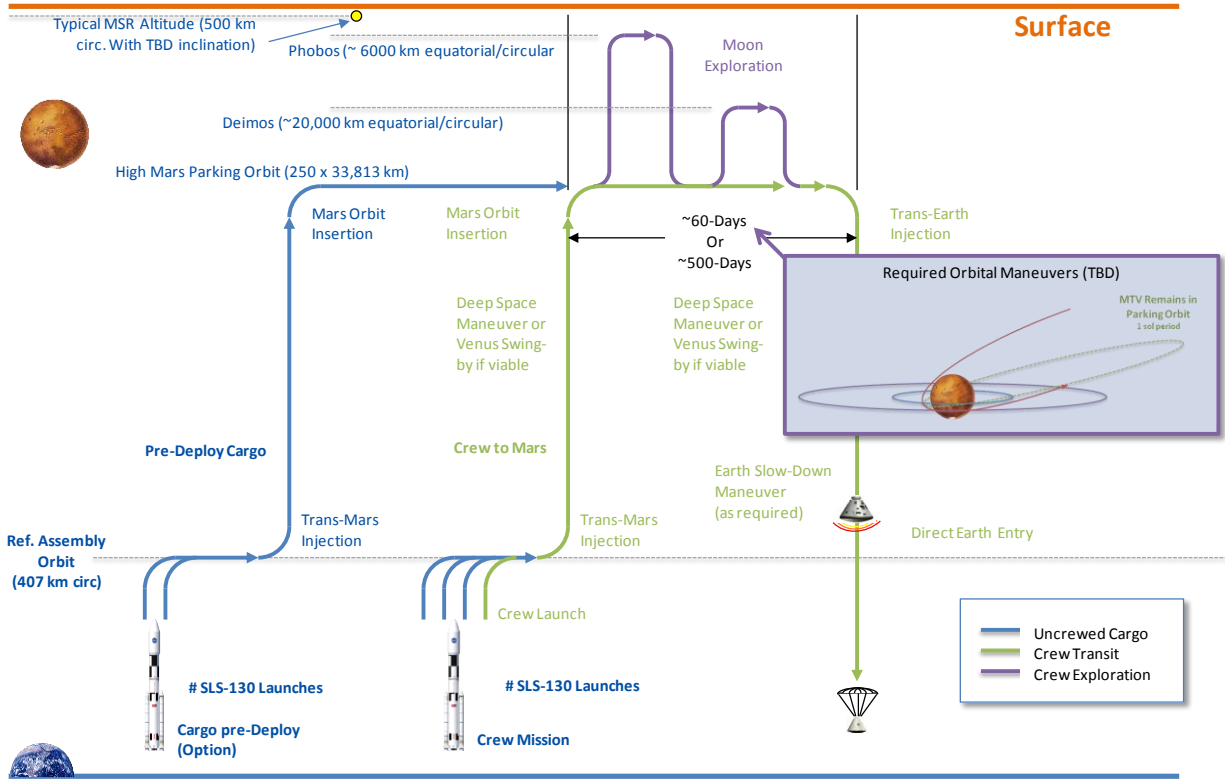


Figure 13-39 Typical mission profile for a Mars orbital mission.

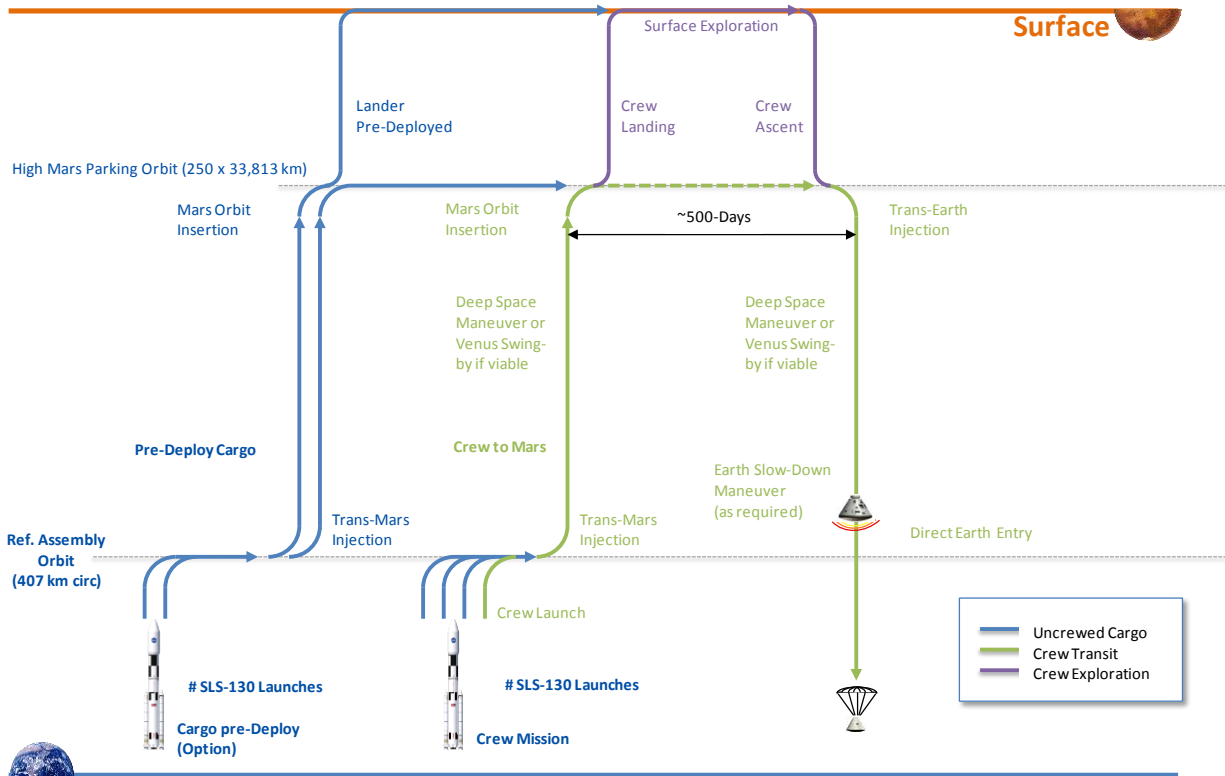


Figure 13-40 Typical mission profile for a Mars surface mission.

13.2.3. Humans to Mars Risk Assessments

One of the first tasks given to the Human Spaceflight Architecture Team in support of the MPPG was to provide a high-level technical and schedule feasibility assessment of a crewed visit to Mars orbit, with a launch in 2033, to retrieve samples which had been previously placed into Mars orbit robotically and then subsequently return them to Earth. The team was specifically requested to identify, while making reasonable assumptions, strategic roadmaps for future human exploration of Mars. The following attributes of human exploration of Mars were to be considered when generating those roadmaps:

- The fundamental technologies, knowledge needed and key options
- The decision points at which technology use and down-select must be made
- Those decisions and deliverables to and from the technology office and, or the science directorate
- The risk postures associated with options

Before detailed roadmaps could be generated, further understanding of the key challenges and risks are required. Mitigation strategies for these risks will compose the primary content of the decision paths, options, technologies, and resulting implementation content.

13.2.4. Human Support Risks

As humans venture farther and longer into deep space, it is necessary that informed risk decisions are made in terms of how to best support these explorers. The Human Research Program (HRP) was formed to focus NASA's research on the highest risks to human health and performance during exploration missions. The HRP performs research necessary to understand and reduce spaceflight human health and performance risks in support of exploration, develop technologies to reduce medical risks, and to develop human spaceflight medical standards for subsequent system development and design. The HRP content has been organized to address the key technological challenges of long duration spaceflight:

- Space Radiation: Human health effects, limiting factors for vehicle environments and crew selection; computational shielding modeling; measurement and warning technologies
- Exploration Medical Capability: Medical care and crew health maintenance technologies (monitoring, diagnostic, treatment tools and techniques); medical data management; probabilistic risk assessment
- Human Health Countermeasures: Integrated physiological, pharmacological and nutritional countermeasures suite; EVA-related physiology research to support new EVA suit development
- Behavioral Health & Performance: Behavioral health selection, assessment, and training capabilities; intervention and communication techniques to support exploration missions
- Space Human Factors & Habitability: Anthropometry, display/control, usability, cognition, habitability, lighting, ergonomics; advanced food development; Mars dust characterization and toxicological testing
- ISS Medical Project: ISS research integration and operations
- National Space Biomedical Research Institute: Nationally competed/peer-reviewed research projects addressing above content utilizing investigators at more than 70 institutions in 22 states

The HRP follows an evidence- and risk-based management approach where the validity of risks is based on evidence from science, clinical, and operational research. Risks are externally reviewed by Institute of Medicine review validated HRP exploration risks and evidence. Throughout the HRP process, continuous evaluation of risk postures and priorities are assessed and reevaluated annually based on the current research results and progress. Criticality and priorities are developed in conjunction with Human System Risk Board. Through this process, gaps and research tasks are prioritized balancing customer need (from Program elements, Chief Medical Officer, Medical Operations) with flight and ground resources, including ISS availability.

The HRP currently uses three mission classes to inform the risk-based processes including 6-month lunar outpost missions, a notional 12-month mission to a NEA, and a 30-month Mars landing consistent with the Mars DRA 5.0. The HRP has a 'criticality rating' for 31 human health and performance risks relevant to a DRA 5 type Mars mission. These criticality ratings are characterized as:

- "Unacceptable" = HRP would recommend "No-Go" today

- “Acceptable” = HRP would recommend “Go” with reservations today
- “Controlled” = HRP would recommend “Go” without significant reservations today

These criticality ratings are guided primarily by likelihood and consequence scores in a risk management 5x5 (likelihood x consequence) matrix. For this MPPG activity results from previous HRP assessments were used to inform the humans to Mars orbit strategic questions to provide guidance as to the human support risk posture associated with an orbit only mission mode. Table 13-24 provides a comparison of the estimated criticality ratings for a notional surface (aka DRA 5) and Mars orbital (600-900 day) mission. It should be noted that these are estimates only based on what we know today as extrapolated from the current knowledge base to these longer-duration missions. As further research is obtained from missions to the ISS or other destinations it is anticipated that these risks will become more controlled and subsequently “acceptable.” But a great deal of research and analysis are required to close the current HRP risks.

As can be seen from Table 13-24, it is believed that the risk to the human system is higher for an orbit-only mission as compared to a surface landing mission.⁷ From this preliminary assessment, it was determined that 23 risks increase for an orbital-only mission whereas four risks are unchanged and four risks decrease. Since the crew for orbital missions are confined to limited volumetric spaces in the transit habitat for very long durations (600 to 900 days), two additional risks might become unacceptable for the orbital missions including team cohesion and human factors/vehicle habitat design. Due to the uncertainty and lack of detailed research data related to these very long zero-g missions, there was not a major qualitative difference in the risk to the human system when comparing a 600-day opposition class and 900-day conjunction class missions. Both are considered long, in a deep-space zero-gravity environment and well beyond our current experience base. A key strategy for reducing these risks identified by the HRP team is to obtain relevant human system performance data via sequential deep space exposures of 30, 60, 180, and 360 days, which would permit gradual testing of radiation effects, behavior, and habitability beyond the protective environment of Earth.

13.2.5. Key Challenges for Orbital and Surface Missions

In addition to the human support risks, other aspects of the mission risk including both loss of crew, as well as loss of mission, must be considered in the roadmap framing. A high-level risk modeling effort was initiated to support the risk assessment for both the orbital and surface missions. This risk modeling exercise stemmed from the assessment methodology established during framing of DRA 5.0. Further discussion of the risk modeling is provided in later sections of this Addendum.

Due to time and resource limitation the integrated architecture risk model is currently at a very high level. Since the risk modeling process was essentially stopped after DRA 5.0 and it is currently being re-established, sufficient time and resources have not been available to develop detailed models. Thus, these initial findings represent rough first cut estimates should not be viewed as absolute predictions. The data comprising the integrated model are chosen from a variety of sources for “best fit” including the ISS, Space Shuttle, Constellation (typically derived from ISS or Space Shuttle Program), other space systems (such as satellites or launch vehicles), as well as other related analyses (crew medical, radiation, etc.). At this early stage of risk modeling, the intent was not to determine absolute risk values, but rather determine the key risk drivers for the various missions, mission phases, and elements. A comparison of the key challenges for the notional orbital and surface (DRA 5) missions is provided in Figure 13-41. Examination of Figure 13-41 indicates that orbital missions result in more challenging missions with respect to supporting humans in deep-space as well as the overall in-space transportation technologies and architectures. Since human support challenges for orbit-only missions is increased, more emphasis is placed on transportation system performance to reduce the mission duration, which also increases the total mission mass. Surface missions, on the other hand, generally contain more programmatic challenges, due to the additional number of vehicles and systems, as well as the challenges of entry, descent, landing, and ascent.

Once the key challenges have been identified, mitigation strategies for the risk drivers can be determined. Table 13-25 provides an example of the identified key risk drivers for future human missions to Mars.

⁷ It should be noted that this finding is specific to the human system only. That is, other mission-related risks, such as entry, descent, landing, ascent, and surface operations are other risks that are not directly related to the human system, but are risks that must be adequately addressed.

Table 13-24 Human Support Challenges

HRP Risk	Mars	Mars	Duration comments wrt DRA5 baseline
	DRA5	Orbit	
Visual impairment	U	↑	↑time in weightlessness
Behavioral health	U	↑	↑time in ICE
Muscle	U	↑	↑time in weightlessness [1]
Aerobic capacity	U	↑	↑time in weightlessness [1]
Radiation- degenerative	U	↑	↑radiation exposure [2]
Radiation- cancer	U	↑	↑radiation exposure [2]
Nutrition	U	↔	assumes no Mars crops
Food	U	↔	assumes no Mars crops
Medical care	U	↓	no planetary EVA
Human Factors- Vehicle/Habitat	A	↑	↑time in ICE & Behavioral Health
Team cohesion	A	↑	↑time in ICE & Behavioral Health
Spacecraft control & egress	A	↑	moon ops; ↑time in ICE (↓cognition)
Radiation- CNS	A	↑	↑radiation exposure [2]
Radiation- Acute (SPE)	A	↑	↑radiation exposure [2]
Human Factors- Task design	A	↑	↑time in ICE (↓cognition)
Human Factors- Training	A	↑	↑time in ICE (↓cognition)
Human Factors- Robotics	A	↑	↑time in ICE (↓cognition)
Human Factors- Computers	A	↑	↑time in ICE (↓cognition)
Immune	A	↑	↑time in ICE
Host-microorganism	A	↑	↑time in ICE
Orthostatic intolerance	A	↔	↑time in weightlessness [1]
Cardiac arrhythmia	A	↔	↑time in weightlessness [1]
Intervertebral disc	A	↔	↑time in weightlessness [1]
Osteoporosis	A	↔	↑time in weightlessness [1]
EVA health and performance	A	↔	weightless geology
Medications	A	↔	↓mission time & drug stability
Dynamic loads	I	↔	↑time in weightlessness [1]
Kidney stones	C	↔	↑time in weightlessness [1]
Dust or volatile exposure	n.d.	↓	no exposure in DSH
Fatigue	C	↓	no circadian entrainment
Bone fracture	C	↓	no falling in weightlessness

U	Unacceptable risk that would keep a mission from proceeding	[1] criticality rating will probably be reduced in July 2012 due to bone/muscle/cardio countermeasure development
A	Acceptable as is, but with a high uncertainty in risk; additional mitigation recommended	
C	acceptable through use of known Controls	[2] details depend strongly on trajectories and proximity to Mars and moons
I	Risk is poorly understood or no standard exists; Insufficient data	
↔	No anticipated change in trend	
↑	Anticipated to trend worse	
↓	Anticipated to trend better	

Mars Design Reference Architecture 5.0 – Addendum #2

	Mars Orbit*	Mars Surface		Mars Orbit	Mars Surface
Human Health and Performance			Key Precursor Knowledge		
Time in zero-gravity free space (days)	600-900	180/180	Atmosphere Dynamics	✓	✓✓
Time on surface (days)	0	540	Surface Material Properties	✓	✓✓
Galactic Cosmic Radiation Protection	✓✓	✓	Planetary Protection	✓	✓✓
Behavioral Health for 600-900 days	✓✓	✓	Mission Mode (Short/Long Stay)	✓	DRA 5
Key Capability Gaps			Pre-deployed Mission Cargo	✓	DRA 5
130 t SLS Launch, Large volume, campaign	✓✓	✓	ISRU for Ascent from Surface	n/a	✓
Orion 900 day dormancy, 6 crew	✓	✓	Destination Exploration Operational Concept	✓	✓
900 Day class deep-space habitation	✓✓	✓	Launch Campaign and Launch Availability	✓✓	✓
Advance in-space propulsion (e.g. NTP, NEP)	✓✓	✓	Integration and Programmatic		
20-40 mt (payload) lander	n/a	✓	Integrated Strategy / Plan	✓	✓
30 kW-class continuous fission surface power	n/a	DRA 5	Multiple large-scale Technology Programs	✓	✓✓
Technology Development			Multiple Concurrent System Developments	✓	✓✓
Aerocapture	✓	DRA 5	Infrastructure Investments	✓	✓
Automated Rendezvous and Docking	✓	✓	Subscale Demonstrations	✓	✓✓
Zero-boiloff cryogenic propulsion	✓	✓	Continuity of Multiple Developments	✓	✓✓
Mars Ascent Methane-oxygen Propulsion	n/a	✓			
High Speed Earth Entry	✓✓	✓			
Atmospheric based ISRU	n/a	DRA 5			
System Reliability	✓	✓			
High Reliability Closed Life Support	✓	✓			

* Assumes opposition class (short-stay) missions implemented to reduce crew exposure to the deep space environment
 ✓ Key challenge applicable
 ✓✓ Increasing difficulty of key challenge area
 DRA 5 Represents agency decisions per Mars Design Reference Architecture 5.0 (NASA-SP-2009-566)
 n/a Not applicable

Figure 13-41 Key challenges and risks for future human exploration of Mars.

Table 13-25 Example Risk Mitigation Venues for Top Exploration Risks

Top Risk Area	Risk Mitigation Venue				
	Earth	ISS	Cis-Lunar	Deep Space	Mars Robotic
Reliability of spacecraft hardware	✓	✓	✓	✓	
Human support	✓	✓	✓	✓	
Orion crew vehicle reliability	✓		✓	✓	
Entry, descent, and landing at Mars	✓				✓
ISRU and Mars ascent	✓				✓
Advanced propulsion systems	✓			✓	

13.2.6. Humans to Mars Roadmap Observations

Because of the uncertainty associated with the anticipated NASA budget which may be available for a future human to Mars are not known and difficult to anticipate, the assessments were conducted without specific budgetary assumptions applied. That is, the schedules and implementation options developed were done assuming that the associated required budget was a free variable. For this schedule assessment, a mission consisting of humans to Mars orbit was used as the primary emphasis, which was consistent with the original MPPG thinking and guidance, with humans to the Mars surface as a secondary emphasis. Understanding the linkages of the latter, surface missions, was necessary for strategic guidance. That is, humans to Mars orbit should feed forward to surface missions. It should be noted that for this exercise a notional mission to Mars orbit was assumed to occur in 2033 consistent with the current National Space Policy [Office of the President, 2010]. For this schedule exercise it was further assumed that a surface mission would occur two opportunities (approximately 4 years) later. This was

assumed to ensure that core competencies and capabilities developed for the orbital mission could feed forward to the surface mission. As the gap between missions increase, it was felt that the ability to maintain those core competencies would erode, thus leading to additional technical and programmatic risk. To constrain the planning, three different flavors of development “content” were constructed, each of which were developed consistent with differing levels of relative development risk.

- *Nominal*: With this development approach, it was assumed that all due diligence would be done in the design, development, and testing to have an acceptable level of risk. Margin would be allocated and managed according to typical space development efforts.
- *Aggressive*: With this approach, no limitations on funding were assumed for the technology and systems development that were further assumed to be pursued aggressively. In theory, this schedule approach would demonstrate how fast the product could be developed and ready for use. Basically crash the schedule and find the critical path, identifying the limiting schedule constraints that would drive the schedule. With this approach, it was recognized that the risk would be high and that schedule will not be met when issues, difficulties, and unknowns arise since there is none to very little schedule margin, but these issues may be mitigated with additional funding and resources consistent with cost as a free variable. With this aggressive schedule approach, the number of technology options considered, as well as the number of tests conducted, was limited.
- *Relaxed*: With this development approach the schedule would be stretched if funding was not available when needed and thus the first launch would slip to a launch opportunity that was beyond the nominal schedule. This will most likely cause cost to go up in total, but would potentially lower the annual cost requirement. The stretched schedule would allow for additional time to address high risk items early (unknowns) and reduce schedule risk issues.

For each major development item, subject matter experts were solicited to identify key activities that would be associated with the different schedule development risk postures discussed previously. Each schedule that was developed included the necessary technology development, ground and flight demonstrations necessary to reduce risk, and flight system development. Figure 13-42 provides a notional development schedule resulting from this exercise. From a campaign and overall architecture perspective other key schedule assumptions were applied to ensure consistency between development items.

Hardware Delivery to the Launch Processing Facilities: Current and previously conceived human Mars mission concepts require significant mass to be delivered to Earth orbit prior to initiation; even with incorporation of multiple mass reducing technologies. This large mass requires multiple launches be conducted prior to the opening of the departure window for Mars. To facilitate this launch process previous assessments have determined that the hardware must arrive at the launch processing facilities approximately one year before launch and approximately six month of launch margin must be included to account for unanticipated process and operational issues which may arise. In addition, 30 days were allotted for the Earth departure window. All of these processing and operational considerations mean that, depending on the number of launches required, hardware must start arriving at the Kennedy Space Center (KSC) up to 2 years before the departure date.

System Demonstrations: Before the first human crew would ever depart on a Mars mission, new technologies and capabilities would be developed that would enhance crew health and safety, provide capabilities for these crews to live and work that were not previously available, improve the performance of vehicles already being used, and give access to mission information of unprecedented breadth and quality. Since missions to Mars represent significant challenges to humans in terms of both the distance and time away from Earth, proper testing and validation of those new systems and technologies is required. As can be seen in Figure 13-42, the timing of the validation test of a system can have a profound effect on the resulting risk posture. To reduce the risk of incorporation of immature technologies or capabilities it is desired to conduct validation tests as early in the design process as possible, typically before the Preliminary Design Review (PDR). For the MPPG schedule assessment, tests that could be conducted prior to the system-level PDR were considered to represent a “lower” risk posture, whereas tests that would occur after PDR were considered a “higher” posture.

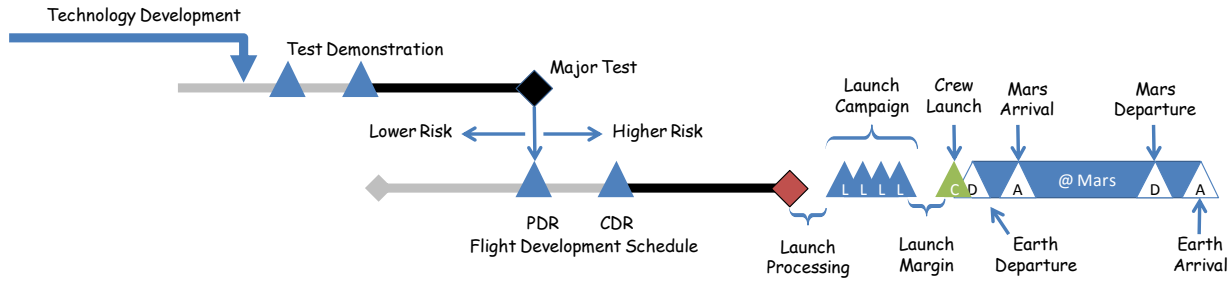


Figure 13-42 An example development schedule flow and timing.

Notional development schedules for various hardware elements associated with the major human exploration of Mars architectural components were obtained from subject matter experts (Table 13-26). These schedules included both the key transportation and human support options necessary to transport humans to and from Mars orbit (orbital missions), as well as the long lead items associated with surface missions including entry, descent, and landing (EDL), advanced propulsion, ISRU, and surface power. Through this process, a total of 39 schedule options were generated for the three flavors of programmatic risk posture: nominal, aggressive, and relaxed. These schedules were then integrated into logical schedule options as potential strategies for future human exploration of Mars. The intent of this exercise was not to define the definitive schedule, but rather to find key schedule logic, timing, and strategies. Figure 13-43 provides an example integrated schedule, or roadmap, for future human exploration of Mars. Examination of these notional roadmaps provided some interesting insight into the relationships between the major development and operational activities.

Near-Earth Risk Reduction Opportunities: There was a common finding from many of the schedule strategies associated with the near-Earth testing opportunities for reducing many of the risks associated with the support of humans for long durations in deep space. It was determined that the ISS as well as missions in cislunar space, such as in lunar orbit or Earth-moon libration points, can play an important role in the demonstration and testing of gravity-sensitive phenomena such as crew physiology, gas/liquid separation, and large-scale structure deployments. Since these mission would be by definition “near-Earth,” they allow for quick and safe return of the crew should something go wrong with the operational test. These missions in LEO and Near-Earth can be used to simulate flight environments for the transit (zero-g) mission phases. In fact, each ISS crew rotation mission is essentially testing a flight to Mars from an operational and human physiology perspective. Existing platforms, such as the ISS, can provide an ideal venue for long-duration system testing including crew interaction with hardware, software, and operational procedures. Extending the testing venue beyond LEO to cislunar space allows for long-term exposure of systems to the deep-space environment, including radiation and zero-g. Tests in LEO and in near-Earth space can be gradually increased for short to long durations, which would provide better understanding of long-duration system performance in “flight like” conditions. As tests are extended to the surface of the Moon for instance, various technologies and operational strategies associated with surface missions can also be demonstrated and validated in a planetary environment.

Human Mars Systems Tests: Each of the schedule development teams identified opportunities for large-scale system and technology development tests that are necessary prior to initiation of the full-scale flight system design and development. Depending on the aggressiveness of the schedules assumed, these full-scale tests generally occurred prior to the Critical Design Review of the flight systems. When the development time, testing, launch process, and launch campaign are considered, it was found that, in general, these full-scale tests should occur approximately six years prior to delivery to Kennedy Space Center (KSC). It should be noted that this timing is a general finding and the specifics of the actual testing will depend on the technology chosen, risk posture adopted, and actual funding available.

Mission Mode Decision: The mission strategy adopted for the Mars DRA 5.0 architecture would utilize conjunction-class long-stay missions with the incorporation of advanced transportation to help reduce overall mission mass. But with the incorporation of potential missions to Mars orbit, the risks associated with human performance in this all-deep-space environment become exacerbated, and thus for these missions more emphasis would be placed on trying to minimize the exposure of humans to the deep-space environment by utilizing short-stay opposition-class missions with advanced propulsion technology as a mandatory element of that strategy. This

choice of overall mission strategy, orbit first versus surface, is an important decision, which should be made in the next few years as depicted in Figure 13-43.

Sub-scale Technology Demonstrations: A major component of the MPPG exercise was to find areas of collaboration between the robotic and human exploration endeavors. Through this exercise it was determined that there is some synergy between the needs of humans to Mars orbit such as atmospheric characterization to support potential aerobraking at Mars, radiation, and orbital debris characterization, but greater collaboration opportunities exist with surface missions. Some of the greatest challenges for human exploration of Mars surface relate to access of the planetary surface – namely EDL – and subsequent ascent to orbit. Previous human exploration architecture assessments have shown that the EDL techniques currently being utilized by the robotic systems, namely the Mars Science Laboratory, will be inadequate for future human missions. In fact, these strategies are in dead-ended and thus new EDL technologies and techniques are required. As a key risk reduction technique for future human missions, it was determined that sub-scale demonstrations of relevant EDL technologies are required. There are many options still being pursued, but it was found that this area provides a key opportunity to merge the needs of future human missions with increased landed capabilities for advanced robotic missions. Likewise, demonstration of ISRU concepts and technologies is another key area where robotic missions can play a key role in mitigating the risks to future human missions. It was found that given the overall assumption of a human orbital mission in 2033 with a surface mission two opportunities later, demonstration of these key human relevant technologies, EDL, ISRU, and Mars ascent, should be demonstrated in the early 2020s as shown in Figure 13-43.

Table 13-26 Schedule Development Subject Matter Experts

Technology or Capability	Source for Schedule Development
Space Launch System	MSFC
Orion Multi Purpose Crew Vehicle	JSC
Ground Operations	KSC
Human Research Program	JSC
Deep Space Habitation	JSC
Nuclear Electric Propulsion	GRC
Nuclear Thermal Propulsion	MSFC
Solar Electric Propulsion	JPL
Advanced Chemical Propulsion	MSFC
Entry, Descent and Landing	LaRC
Methane Propulsion for Descent and Ascent	JSC
In-Situ Resource Utilization	JSC
Fission Surface Power System	GRC

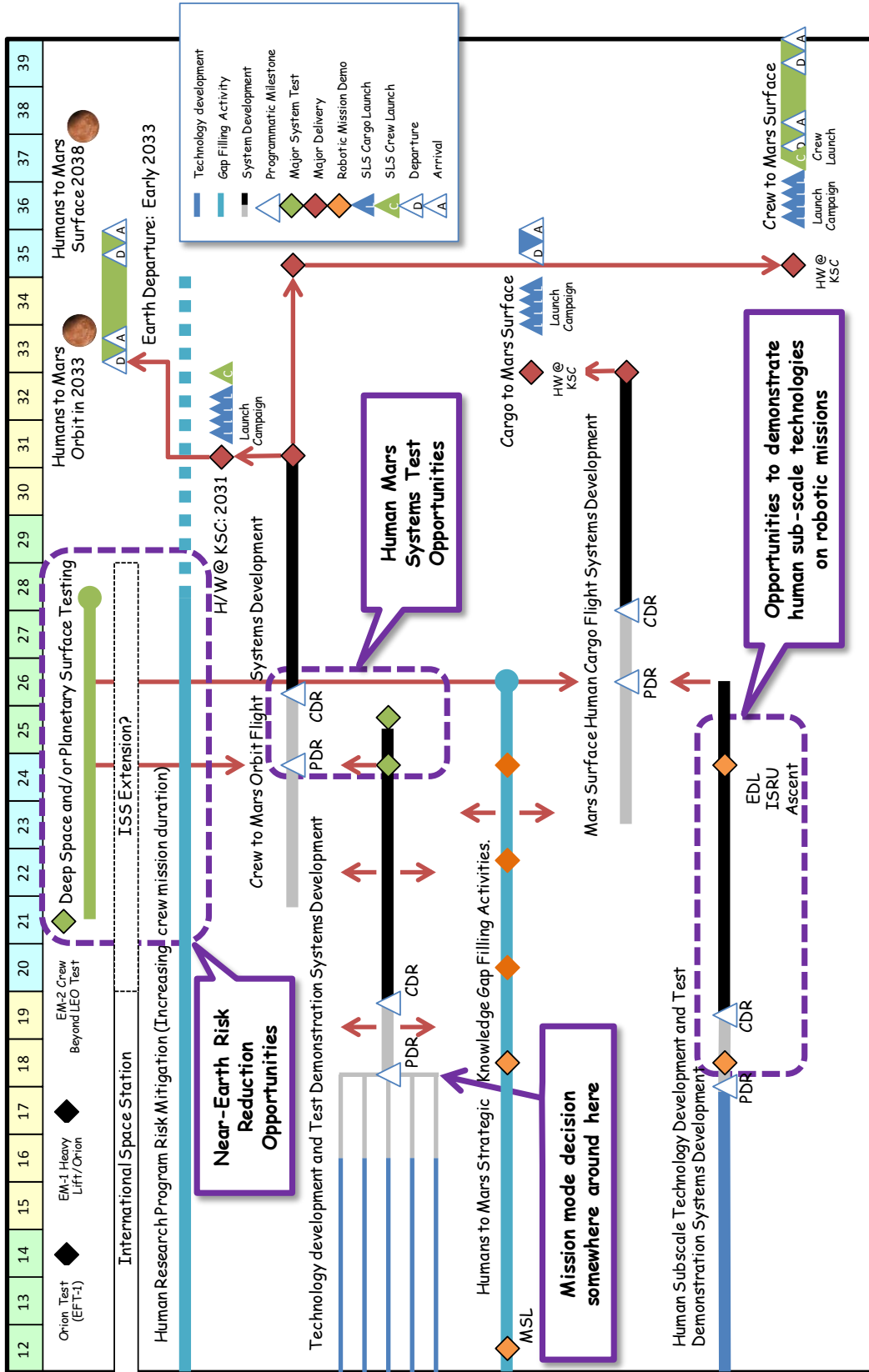


Figure 13-43 Integrated roadmap for the human exploration of Mars.

13.2.7. Precursor Investigations/Measurements necessary for Humans to Mars

Another key element of the MPPG effort was to find key areas for potential collaboration between the science and human exploration of Mars efforts. Of particular interest was the role that robotic missions can play in obtaining critical environmental data and reducing future mission risks. To address the missing information needed to send humans to Mars, NASA requested a joint SMD-HEO activity sponsored by the Mars Exploration Program Analysis Group (MEPAG) on the topic of “precursor measurements” that could both address the 2013-2022 Visions and Voyages Planetary Decadal Survey [NRC, 2011] as well as the human exploration goals. The 2012 MEPAG Precursor Science Analysis Group (P-SAG) was formed to: 1) examine the strategic knowledge gaps (SKGs) in knowledge of Mars required to support the first human missions to martian orbit (Goal IV-) and to the surface (Goal IV), 2) identify the key science objectives (using existing MEPAG and NRC scientific planning) that could be addressed in synergy with each of the potential investigations from the SKGs, and 3) identify key technology development/demonstration opportunities necessary to support humans-to-Mars objectives. Additionally, P-SAG (2012) worked to 4) classify each of the opportunities identified above by implied or potential platform (e.g., orbiter, stationary lander, rover, etc.), and to evaluate relative priority.²³

13.2.7.1. Strategic Knowledge Gaps and Gap Filling Activities

SKGs are defined as gaps in the knowledge needed to achieve a specific goal. Working through community input, the MEPAG²⁴ has identified consensus goals and objectives for exploration of Mars as:

- Goal I: Determine if life ever arose on Mars
- Goal II: Understanding the process and history of climate on Mars
- Goal III: Determine the evolution of the surface and interior of Mars
- Goal IV: Prepare for human exploration

For the MPPG effort, further assessments associated with Goal IV were required, but in addition to preparing for missions to the surface, assessments for potential orbital missions to explore the moons of Mars as well as long-term exploration of the surface of Mars were examined. The SKGs associated with each of the following goals were defined by the P-SAG: 1) First human mission to martian orbit (Goal IV-); 2) First human mission to land on either Phobos or Deimos; 3) First human mission to the martian surface (Goal IV); and 4) Sustained human presence on Mars (Goal IV+). The SKGs were broken down into Gap-Filling Activities (GFAs), and each was evaluated for priority, required timing, and platform. The relationship of the above to the science objectives for the martian system (using existing MEPAG, SBAG, and NRC scientific planning), was evaluated, and five areas of significant overlap between HEO and science objectives were identified. 1) Mars: Seeking the signs of past life; 2) Mars: Seeking the signs of present life; 3) Mars: Atmospheric dynamics, weather, dust climatology; 4) Mars: Surface geology/chemistry; and 5) Phobos/Deimos: General exploration of Phobos/Deimos. Within these areas it would be possible to develop exciting mission concepts with dual purpose. The priorities relating to the Mars flight program have been organized by mission type, as an aid to future mission planners: orbiter, lander/rover, Mars Sample Return (MSR), and Phobos/Deimos.

The high-priority gaps for a human mission to Mars orbit relate to a) atmospheric data and models for evaluation of aerocapture, and b) technology demonstrations for optical communication and in situ resource utilization (ISRU), as well as orbital rendezvous, ascent demonstration, dust mitigation, radiation exposure, and sample handling. A human mission to the Phobos/Deimos surface would require a precursor mission that would land on one or both moons. The early robotic precursor program needed to support a human mission to the martian surface would consist of at least one orbiter, a surface sample return (the first mission element of which would need to be a sample-caching rover), a lander/rover-based in situ set of measurements (which could be made from the sample-caching rover), and certain technology demonstrations. For several of the SKGs, simultaneous observations from orbit and the martian surface need to be made. This requires multi-mission planning. (See PSAG, 2012; slides 4-12, <http://mepag.jpl.nasa.gov>)

13.2.7.1.1. Dust Toxicity to Humans

We do not understand in sufficient detail the factors affecting crew health and performance, specifically including the biological effects of the potentially toxic properties of the martian dust. The jagged nature of lunar dust particles has been shown to have a significant effect on crew health. Key in understanding whether similar concerns exist for

martian particulates is gaining knowledge of the surface particulate material properties, including electrical, chemical and physical characteristics. (See PSAG 2012 Appendix 2, slides 26, 30, <http://mepag.jpl.nasa.gov>).

13.2.7.1.2. Radiation Environment on the Surface of Mars

Because Mars has no planetary magnetic field, unlike Earth, any radiation attenuation that would exist would be due to the atmosphere and from the planet itself. The Mars atmosphere column density is 16 g/cm² (versus 1000 g/cm² on Earth) but varies widely from season to season. Radiation transport depends on both the altitude and atmospheric density; radiation is either absorbed, fragments to produce secondary particles, or propagates to the surface which would also result in secondary particles. Mars Science Laboratory has already made significant progress on this SKG through the Radiation Assessment Detector (RAD) instrument on board the Curiosity rover. RAD's primary science objectives are to characterize the energetic particle spectrum at the surface of Mars, determine the radiation dose for humans on the surface of Mars, and enable validation of Mars atmospheric transmission models and radiation transport codes. Preliminary data returned from the martian surface shows that at the season and atmospheric conditions Curiosity landed, the martian atmosphere attenuates 5 units of radiation in addition to the radiation attenuated from the planetary body. Whether this value can be extrapolated to other times and conditions of the martian atmosphere remains to be understood. (See PSAG 2012, Appendix 2, slides 26-29, <http://mepag.jpl.nasa.gov> , and <http://mslrad.boulder.swri.edu/>)

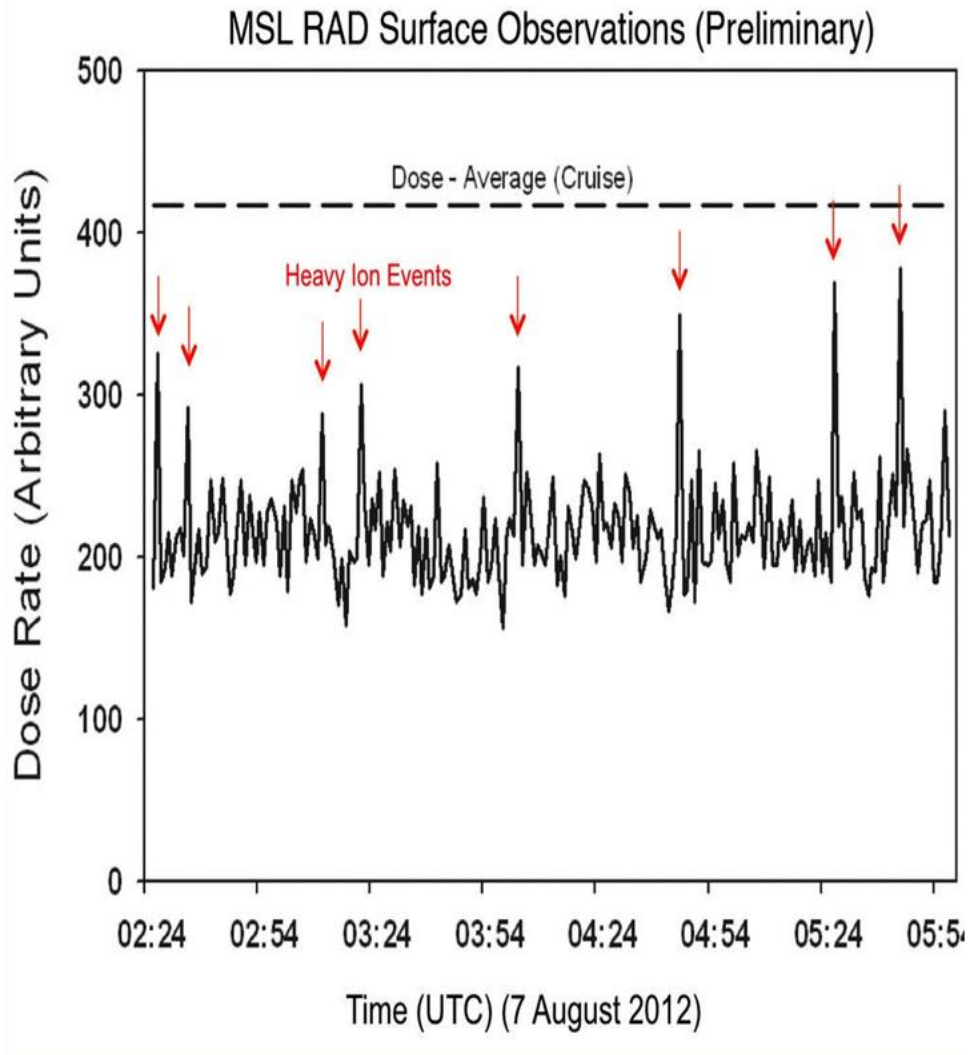


Figure 13-44 Preliminary Mars Science Laboratory radiation observations.

13.2.7.1.3. Landing site specifics, weather prediction

Whether measurements that have been acquired at disparate locations around Mars can be extrapolated to any specific potential landing site for human exploration remains an open question. In addition, while ongoing and future atmospheric measurements are an excellent record of climate, the particular weather on the day of a potential human entry into the martian environment is unknown. Just as on Earth, validating and collecting data for predictive climate and weather models is the most accurate method to understand the specific conditions that might exist on Mars in the future. Validation allows the models to be confidently used to create the extreme conditions (>99% distribution tail) necessary to select and design EDL, aerocapture, aerobraking, and launch systems. Atmospheric model validation and data assimilation can take several years following data acquisition, and should be factored into mission phasing. Long-lived orbiters with global diurnal coverage would provide the largest volume of atmospheric data to support model development and validation. Also, multiple landers providing simultaneous measurements with the orbiters would be needed to acquire near-surface data correlated with upper atmosphere measurements, for model development and validation. See PSAG (2012), Appendix 2, slides 2-8, <http://mepag.jpl.nasa.gov>)

13.2.7.2. Sample return on Critical Path to Human presence at the surface of Mars

To prepare for a human mission to the martian surface, based on what is known today sample return is the only implementation that would address the required back planetary protection SKG. That is, we do not know whether the martian environments to be contacted by humans would be free, to within acceptable risk standards, of biohazards that might have adverse effects on some aspect of the Earth's biosphere if uncontained martian material were returned to Earth. Despite the best intentions and best engineering, it is likely that some uncontained martian dust and regolith would be returned to Earth with the crew. The safest and possibly the only acceptable way to ensure non-release of biohazardous material into the Earth's biosphere is to return carefully contained samples to Earth prior to the first human mission. Prior to that mission, one or more diverse sets of regolith, rock, and dust samples should be collected from sites representative of the diversity anticipated at human landing sites and returned to Earth for comprehensive biohazard testing similar to that outlined in Rummel et al., (2002) to determine whether any indigenous life is present and, if so, whether it presents a hazard to the Earth's biosphere. A significantly more risky, and possibly unacceptable, approach to lessen the risk of returning uncontained living and potentially hazardous organisms with the crew is to identify zones of minimum biological risk as potential landing sites. Biologic risk to be identified by orbital measurements for signs of recent water activity, orbital land lander measurements for presence of ground ice, and lander measurements following some to-be-determined life detection protocols (total carbon, isotopes, etc) on near surface materials at potential landing sites. (See PSAG 2012, Appendix 2, slides 21, 62, <http://mepag.jpl.nasa.gov>)

13.2.7.3. Future astronaut surface science objectives: Changes since 2007

The Human Exploration of Mars – Science Analysis Group (HEM-SAG)²⁵ prepared a preliminary analysis of the science that could be done by a human exploration crew on the martian surface. Since then, the following significant things have changed:

- The NRC has reevaluated science priorities and strategies for the coming decade (2013-2022)
- MSL has successfully landed, and has begun its scientific mission
- The InSight mission has been selected by the Discovery Program and, if successful, it would result in the delivery of single station Mars seismic data and a one-site heat flow measurement.
- MPPG has prepared an analysis of possible transitions from a science-driven Mars program to a human precursor-driven Mars program.

Implications:

- Astrobiology and the search for ancient life remains the top strategic driver for the scientific exploration of Mars.
- MSR continues to dominate scientific thinking for the next decade, although whether this mission or set of missions is acceptable politically is a question. It will therefore be important for planning astronaut-implemented science to continue to think through the possible discoveries of MSR, and how they might

best be followed up.

- MSL's most important early discovery is re-confirmation that Mars had flowing liquid water early in its history. This will reinforce the ancient life investigation pathway. More significant discoveries (e.g., related to organic molecules) are expected within approximately the next 6-12 months.
- HEM-SAG called for astronaut deployment of long-lived seismic investigations. InSight, if it returns data successfully, will cause us to need to re-think that.
- The transition from a science-driven program to a human prep program are intrinsically caught up in the timing/planning for MSR. Again, the key to planning astronaut-tended surface science

13.2.8. Human and Robotic Mission Collaboration Opportunities

In preparing for the human exploration of Mars, several opportunities exist for collaboration between human exploration and science-based robotic missions. Science-focused missions provide opportunities for measurements of the martian system to fill SKGs as well as incrementally increase our engineering experience. Future robotic technology precursor missions provide additional opportunities for access to the martian system for scientific objectives. Human capabilities to, and future assets in, cislunar space can play a role in retrieval and safe return of samples from the surface of Mars. HEO developed launch capabilities may provide opportunities for science missions to reduce launch/mission costs.

Operationally, similar mission phases exist between human mission concepts and science missions. This creates potential opportunities and synergy for introducing new technologies relevant to getting to the surface and ascending from the surface of mutual interest. The scale and required mass of human systems/payloads is considerably larger ($\approx 40t$) versus the current capability as recently demonstrated by the Mars Science Laboratory (MSL) ($\approx 1t$). The two major options being considered are a mid-lift/drag lifting body design that has more lifting capability than the traditional 70° bi-conic heat shield used by robotic missions today. The bi-conic shape was initially developed by the Viking robotic missions in the early 1970s. Another option being considered for entry is a large inflatable decelerator, which has similar geometry to the bi-conic heat shields used today but is much larger and would also enable larger payloads to be landed on the surface of Mars. Each of these options has unique engineering challenges related to structural stiffness and guidance, navigation, and control. Both options would also benefit, even flown at subscales to a human mission, science missions with increased landed mass performance.

A robotic Mars sample return mission would require ascent from the martian surface. While both human and robotic systems have returned from the lunar surface, even robotic ascent has not yet been performed from Mars. Trade studies have shown that the performance of solid rockets would enable robotic systems to deliver small payloads/samples to Mars orbit where a return vehicle could rendezvous, capture, and then depart for Earth.

13.2.8.1. Strategic Gap Filling Activities

The environmental knowledge gained from robotic science missions is essential for both crew safety and designing more capable systems and for conducting operations for human missions on the surface of Mars. The Science Mission Directorate Planetary Sciences Division has conducted numerous robotic missions since the Viking missions first surveyed and landed on Mars in 1976. Recent missions, including the Mars Science Laboratory (landed August 2012) entry vehicle and rover, carry dedicated payloads for making human exploration specific measurements. While a fair amount of data and some knowledge have been acquired over the past 40+ years of Mars exploration, significant gaps, large uncertainties or large variability in key design variables remain. Making increased fidelity measurements to reduce uncertainties of environmental parameters in the martian system is needed early to make architectural choices and to drive overall risk reduction planning, technology investment choices, and capability developments. Some measurements are needed to characterize any crew chemical or biological hazards, and to understand future operational constraints and issues on the martian surface. The measurements needed are broken up into three categories.

Architecture drivers – measurements that allow us to design vehicles and the mission more efficiently

- Atmospheric density and winds: current uncertainty is large due to limited flight data and diurnal/seasonal variability, and when dust storms are active. Additional measurements will improve the landed mass, as well as the available landing sites (for instance, lower altitude)
- Resources: allows for ISRU, dependent on the strategy. Additional measurements will improve landed

mass and reduced overall architecture mass (consumables and prop required to transport)

Crew Safety/hazards – measurements that allow us to keep the crew safe

- Radiation: Determine surface and/or orbital radiation levels and directionality (e.g., MSL RAD). This can affect the surface vehicle configuration if additional neutron shielding is needed and also surface operations during solar particle events (SPEs).
- Biohazards: Determine if extant life is present on the surface and poses a hazard to the crew and public.
- Toxicity: Determine if there are chemicals with known toxic effects on humans and the levels of toxicity.

Operational – measurements that allow us to operate safely

- Trafficability: Determine surface hazards at the landing site (drives site selection) as well as the load bearing strength of surface to handle larger vehicles (as compared to smaller robotic vehicles; i.e., Mars Exploration Rover and MSL)
- Dust effects on systems: Determine mechanical properties of airborne and surface dust (drives ISRU/lander/rover/EVA suit/equipment dust tolerance and operations)
- Forward planetary protection: Determine how organisms from Earth may survive and possibly contaminate special regions on Mars (landing site selection and operations)
- Atmospheric electricity: Characterize the electric field magnitude and frequencies, atmospheric and surface conductivity (drives lander/rover/suit/equipment grounding design and operations)

Measurements can be obtained using two primary types of spacecraft: orbiters and landers/rovers. Orbiters allow for global observations and reconnaissance, and landers/rovers enable local in-situ measurements as well as enabling simultaneous measurements in conjunction with orbiters for measurements such as columnar atmospheric density characterization or atmospheric radiation transport.

Orbiters can be used to make the following types of moderate- to high-priority measurements:

- 2 1. Upper and lower atmospheric information for aerocapture and EDL, respectively
- 3 2. Radiation transport—simultaneous orbital and surface measurements for characterizing moderate energy solar energetic particle events
- 4 3. High-resolution imaging and mineral mapping for 1) Forward planetary protection assessments, 2) Landing site identification, selection, and certification, and 3) Resource identification

Landers/rovers can be used to make the following types of moderate- to high-priority measurements as well:

1. EDL profiles of atmospheric state (e.g., MEDLI – MSL EDL Instrumentation). While an impressive data set was gathered to improve our knowledge and modeling capability, more than one data set is required prior to a human landed mission. Additionally, atmospheric pressure data at a range of ignition altitudes is required to determine the descent engine design.
2. Dust properties, regolith composition, regolith structure.
3. Atmospheric electrical characteristics.
4. Atmospheric and climate measurements to obtain time dependent density profiles (simultaneous with orbital measurements).
5. Radiation measurements (simultaneous with orbital measurements).

At present, given what we know about the martian environment, there is no requirement for a Mars sample return prior to human exploration of the surface. However, the science community is just beginning to understand the surface chemistry and martian evolutionary processes, the chemistry on Mars is quite different and so there are many unknowns and potential biohazards that could be relevant crew safety.

13.2.8.2. Technology Demonstrations

The preparation, planning, and new technologies required for a human Mars mission will take many years to develop. It is important to first understand the relationships between environmental uncertainties and measurements and key system design variables. As such, the strategy put forth in the MPPG report encouraged upcoming missions to prepare for eventual human exploration by making critical measurements that would advance our understanding

of the martian environment prior to technology demonstrations.

Future missions could take advantage of these new data to provide increased confidence in the use of new systems and technologies that will provide both increased functionality for science missions and also a validation of these new technologies. Several key areas exist where there is significant overlap between robotic mission needs and eventual human mission needs. They are: 1) EDL, 2) Mars Ascent Vehicle (MAV) and associated ISRU, and 3) Descent propulsion (e.g., supersonic retro-propulsion). Multiple other areas exist where there is overlap for other technologies such as High Data Rate/Bandwidth Communications, precision approach navigation, precision landing, enhanced surface mobility, autonomous rendezvous and docking, and advanced SEP Propulsion, but these are largely enhancing versus mission enabling for a human mission. A mapping of near term to long relevance is shown in Figure 13-45. Additional planning is needed to further vet and validate some of the partially filled bubbles in the above matrix. Also, more analysis is needed to determine what scale of EDL would be relevant for a future human mission in mid-term missions where collaborative missions may be performed.

13.2.8.1. Beyond LEO Ops

Near- to mid-term Human missions beyond LEO offer strategic benefits as well to Mars exploration. One of the major technical concerns for a Mars sample return mission has been planetary protection. A crewed mission activity to retrieve a sample would improve both planetary protection and improve the overall safety of the return vehicle by providing intelligent inspection and assessment of the sample return canister and then additional protection and increased safety during the return to Earth. In addition, a lunar sample return mission while accomplishing high priority national science, this strategy could also serve as a valuable dress rehearsal for a Mars sample return mission.

For the Mars sample return mission, low-cost commercial solar electric propulsion with higher thrust can enable lower cost sample return mission architecture. The preliminary sample return scenario goes as follows:


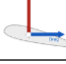

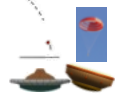




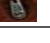
- SEP-enabled robotic vehicle delivers samples to cislunar space for a crew-based retrieval
 - Cislunar capability planned after 2021
- Sample canister could be captured, inspected, encased and retrieved tele-robotically
- Robot brings sample back and rendezvous with a crewed vehicle
 - Cleaned sample canister would be then enclosed in a stowage case, and stowed in Orion for Earth return.
 - This approach deals with key planetary protection concerns.
 - Crew inspection, cleaning, and encapsulation of sample enclosures prior to Earth return.
 - Removes the need to robotically “break the chain” of contact with samples at Mars, thus reducing complexity and cost of robotic missions.

13.2.8.2. SLS Secondary Payloads

As launch performance allows, lower cost missions could be enabled by using the SLS to launch spacecraft as secondary payloads. These spacecraft, when equipped with solar electric propulsion hall thrusters, can fly to Mars and conduct missions with payloads that are relevant both scientifically and for human exploration. Commercially available hall thrusters, when combined by innovative lunar gravity assist trajectories, can provide inner solar system planetary exploration capabilities with adequate thrust and a fairly high Isp. An example is shown in Figure 13-46 below of two small Mars telecom relay orbiters with a science payload that were studied over a couple of years. Two spacecraft are also shown to maintain the vehicle CG during ascent. If only one vehicle were to be flown, additional ballast would likely be required. Shown below, the conceptual spacecraft are stowed in the volume between the upper stage and the Orion Service Module (full length nozzle shown). Other types of spacecraft could also be accommodated ranging from CubeSats to these larger interplanetary spacecraft.

The spacecraft, flown as secondary payloads on a crewed SLS flight, would be integrated prior to Orion MPCV vehicle stacking at KSC and would then be jettisoned post Orion separation and prior to the upper stage disposal burn. The current SLS upper stage has secondary payload capabilities that would be utilized to initiate separation. Access ports on the side of the vehicle would be used for inspection, removal of pyro safing plugs, and possibly for charging during extended launch delays.

Mars Design Reference Architecture 5.0 – Addendum #2

Approach Phase		Near-Term Robotic (1-2t)	Sub-scale EDL Precursor (-5 t +)	Human Full-Scale (20-40t)	
Approach Navigation	Precision Star Tracker, Late Update, Optical Nav, Precision IMU	●	●	●	
Entry Phase					
Atmospheric Guidance	Lift Modulation, Drag Modulation	●	●	●	
Hypersonic Decelerators	Deployables: HIAD, ADEPT	○	○ ↑ ↓	○ ↑ ↓	
	Rigid: Slender body Aeroshell				
Descent Phase					
Supersonic Decelerators	Smart Descent/Deploy Logic	●	○	○	
	30m Supersonic Parachute	●			
	SIAD	●	○	○	
Supersonic Retro-propulsion	High-thrust liquid		○	●	
Landing Phase					
Surface sensing and navigation	Terrain Relative Navigation, ALHAT, Hazard Detection and Avoidance	●	●	●	
Subsonic Propulsion	Storable (Monoprop/biprop), Cryo (biprop)	●	●	●	
Energy Absorption	Airbags, Crushables	●			
High-g Systems	Rough Lander	○			

- Demonstration of ISRU generation of propellants (O₂ and CH₄), followed by an ISRU-enabled MAV provides significant risk reduction for humans to the surface of Mars
- Mars Ascent Vehicle (MAV) is unique in needs for long-term propellant management (storage and/or production) in a challenging thermal environment



ISRU		Near-Term Robotic	Sub-scale Precursor	Human Full-Scale	
Processing	Atmospheric Processing for Liquid Oxygen		●	●	
	Fuel processing of Surface Available Hydrogen (Ice/Hydrated Mineral Processing)		○	○	
	Other materials – Construction, Radiation Protection		○	○	
Propulsion	LOX/Methane		●	●	
Mars Ascent Vehicle (MAV)		Near-Term Robotic Storable (.2-.3 t)	Sub-scale Precursor ISRU MAV (TBD)	Human Full-scale ISRU MAV (20+t)	
Propellant Type	Solid vs. Liquid	●	Liquid	Liquid	
Propellant Production	Ox only vs. Ox + Fuel		●	●	
Thermal Control	Isolation from Mars Environment	●	●	●	
Payload Loading	OS Loading, Break-the-Chain	●			

Figure 13-45 Key technologies for EDL, ISRU, and Mars ascent.

Potentially Applicable

Fully Applicable

Investment Priorities

Potentially Applicable

Fully Applicable

Investment Priorities

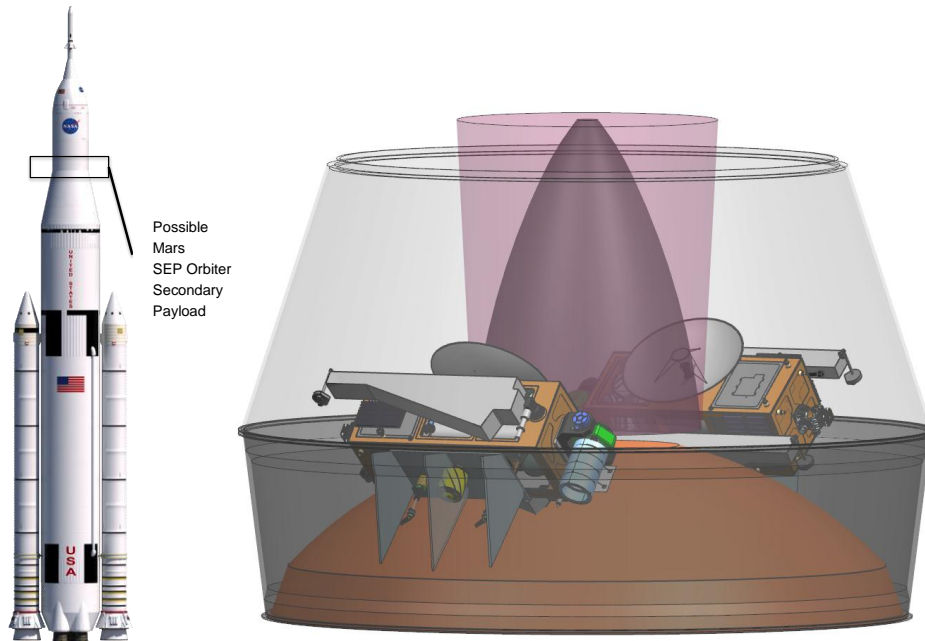


Figure 13-46 Example SLS secondary payload accommodation.

13.3. Risk Assessments

Primary Contributors:

Randy Rust, NASA, Johnson Space Center, USA

All Mars risk analysis effects in support of the Human Spaceflight Architecture Team (HAT) were halted in October of 2011. Early in 2012, Human Exploration Development Support management, in attempting to formulate various strategies, defined the need for an integrated risk picture, first starting with the identification of key risk drivers for human Mars missions. Risk analysis experts were contacted and discussions began on how to determine the integrated risk picture. This effort led to a plan to determine the overall integrated risk picture with the emphasis of this effort being on risk identification, prioritization, and developing mitigation strategies.

Previous efforts during the Mars architecture study (documented in Human Exploration of Mars DRA 5.0) included a two-phase risk modeling approach. An initial, high-level analysis was conducted, which help identify key risk drivers, followed by a refinement of the risk critical models. The first phase was scenario-based risk assessment approach was performed by experienced analysts to identify risk drivers for the proposed Mars missions. The second phase of the analysis focused on risk mitigation strategies based on trade trees and elimination of options that do not meet risk, cost, or performance specifications. Estimates of probability of loss of mission and loss of crew values were produced, but no clear-cut decisions that could be made from a risk standpoint were determined.

From the results of this initial effort, it was determined that current design philosophies and technologies would not provide an acceptable level of reliability for a Mars mission. The risk analysis also highlighted many areas that would benefit from additional, more detailed analyses and that continued refinement of the risk driver calculations can be made as system details become more comprehensive.

This current risk assessment effort (started in FY12) is an analysis effort aimed at emphasizing identification of risk drivers and their prioritization. After the risk analysis model is developed and running, further definition of the elements will be undertaken as well as discussions with subject matter experts to get their buy-in on the representative subsystems and assigned failure rate predictions. When the element data are refreshed with this new information, the model will be re-run to provide a higher fidelity indication of risk drivers. Ultimately, the model will enable different options and mission architectures to be assessed for risk, and enable assessment of various risk

mitigation strategies and help determine precursor mission synergies.

13.3.1. Methodology

To provide a risk analysis with a capability to rapidly support high-level architecture and strategy discussions, the elements will be modeled in the MS Excel-based Rapid Response Tool. The Rapid Response Tool (RRT), is a risk assessment tool developed by Johnson Space Center Safety & Mission Assurance organization, to rapidly respond to requests to estimate mission risk and vehicle reliability on trade studies during early phases of project design and development. The RRT has been used for the Morpheus Project, the Lunar Orbit Rendezvous Design Reference Mission (DRM) for the Constellation Altair Lunar Lander, and the Exploration Mission System Organization Deep Space Habitat Near-Earth Asteroid DRM.

The systems and components in the RRT are defined on individual system worksheets. Individual mission event model parameters and selected subsystems in operation during specific mission events states are defined. The mission events and systems are linked to an EC Tree worksheet that, in turn, calculates the end-state probabilities such as loss of mission and loss of crew. The risk associated with subsystems, as well as the contribution of mission events/phase to overall element risk, are all available.

The results from the RRT element models (end state probabilities [loss of mission, loss of crew] for a specific element, for a specific mission event phase) are combined with a high level event tree in a Systems Analysis Programs for Hands-On Integrated Reliability Evaluations (SAPHIRE) Probabilistic Risk Assessment tool to identify risk drivers (by element, and by particular phase). This determines which particular element for which phase is the driving risk. To determine what system is the driver for a risk driving element; the RRT element model is utilized.

Because of the use of the RRT to analyze the more detailed aspects of each element, system, and subsystem, the model is highly modular and flexible. Changes in systems, subsystems or components can be quickly reflected in the risk model, allowing for “near real time” risk trades.

In initial development of the model, utilizing point estimates for failure rates, random failures of the hardware were the risk drivers. The initial runs are based on the assumption that the hardware is mature (having been flown and operated in an environment similar to what it would be exposed to for the Mars mission) and random failures of the hardware drive the risk. As the model is developed, maturation of the hardware will have to be taken into account. For example, Aero-assist entry into the Mars atmosphere has not been done before and little or no testing has occurred. The technology is very immature as are estimates of the risk. Liquid Oxygen/Methane fueled engines are new technology, as are Nuclear Thermal Rockets (NTRs). Testing these engines in space or on Mars has not occurred. Further development of the risk analysis model will take into account that these technologies are immature and will mature as they are tested and used in-space.

13.3.2. Risk Analysis

13.3.2.1. Developing event timelines

Starting with the DRA 5.0 reference mission, the timeline for a crewed portion of the mission to Mars was modeled. In the initial model, the uncrewed portions of the mission, including the delivery of the MAV, the ISRU, the first Surface Fission Power Unit, as well as their launchers and in-space transportation stages are not modeled. The assumption was made that these elements were successfully transported to and landed on the martian surface, and the Surface Fission Power Unit set up and producing power for the ISRU to generate sufficient oxidizer propellant for the MAV, and the MAV was checked out and ready to support a crew departure when required.

The launch campaign (for the crewed portion of the mission) was modeled to take into account assumptions for the ground architecture (number of launch pads and number of vertical assembly building high bays configured to support these mission elements) as well as workforce assumptions (number of shifts and length of work week). Realistic time margin was added to the element and launcher processing time to ensure a historic reasonable probability of launching within the launch window. All this was taken into account to determine realistic launch spacing for the various elements. This campaign modeling, in-turn, helped determine the accumulated time in Earth

orbit for the various elements. Operating time for all of the elements was calculated from launch through disposal of the respective element.

For the initial model, a Space Launch System (SLS) class launcher was assumed. Other launchers will be modeled under future work to include their impact on ground architecture, work force, processing, and most importantly, number of launches to put an equivalent payload mass in LEO.

Per the timeline, once the crew was launched, the counter was started for the accumulated crew time during the various phases of the mission. Significant events such as major propulsion system firings [Trans Mars Injection (TMI), Mars Orbit Insertion (MOI)]; rendezvous; Mars EDL; ascent from the martian surface were all captured in the timeline.

Event timelines were developed for the Conjunction and Opposition class missions, as well as utilizing both Chemical and Nuclear Thermal Propulsion for in-space transportation.

13.3.2.2. Modeling elements

For the initial version of the model, the elements include the MPCV, the MAV, the Transit Habitat, the Mars Descent Lander/Habitat, the Nuclear Thermal Propulsion Stage, the In-line Tank, Saddle Truss/Drop Tank, and Re-boost module, Docking Module, and the Cryo Propulsion Stage (CPS). With the exception of the MPCV, which is currently being extensively modeled in support of the MPCV program, most of the rest of the elements are at a low maturity level. Increasing the maturity required that elements be developed from descriptions in the DRA 5.0 reference mission as well as utilizing experience on other former Constellation elements. Element level models down to the subsystem level are required for predicting element failure rates during specific phases of the mission. More mature models of the elements will occur as their definition becomes more detailed.

The elements are modeled in the MS Excel based Rapid Response Tool where the components making up the systems are defined as well as their failure rates predicted, based on historical data for similar type components in similar environments. Each mission phase is defined as to what systems are operating (on or off) as well as the phase duration (in hours)

13.3.2.3. Data sources

Data for the system components is taken from a variety of sources and is chosen on a best fit basis, based on component similarity and environment. Source of the reliability data failure rates, used in the Rapid Response Tool element models, comes from the ISS Program, the Space Shuttle Program, the Constellation Program (which in turn was derived from the ISS and Space Shuttle Programs), other space systems such as satellites or launch vehicles, and other related analysis (crew medical, radiation, Micro-Meteoroid Orbital Debris, etc.). Currently, point estimate values are used and eventually, data uncertainty may be introduced.

13.4.3.4 Other Risk

Other items such as human reliability, software failures and Micro-Meteoroid/ Orbital Debris and crew medical risk were also included in the model.

Human error was determined by analysis of historic data to be about 10% of the Habitat total mission risk. Software failures were also determined by historic analysis to be 5% of the Habitat total mission risk. An increased reliance on software to operate spacecraft systems results in a higher percentage of software failures and lower percentage of human error, but still resulting in about a 15% of the Habitat total mission risk. Conversely, decreasing the reliance on software by requiring more human operation resulted in a lower percentage of software failures and a corresponding increase in human error.

Micro-meteoroid/Orbital debris rates were estimated from Lunar Sortie Loss of Crew/Loss of Mission achievability analysis daily exposure rate for LEO (for the LEO loiter phase of the mission), cislunar and beyond cislunar mission (for the Mars transit, Mars capture, and Mars orbit phases of the mission) and both rates scaled for the Mars DRM and MTV stack surface area.

Crew medical risk (for the mission period, about 900 days) is determined from the Integrated Medical Model (IMM), June 2011 scaled for the Mars DRM crew size and time of exposure.

13.3.2.4. Unknowns

With very few data on Aero-assist entry and supersonic retro-grade propulsive engine start/operation, the impact of these events has been estimated. As more testing, analysis, and element design occurs, these estimates can be revisited. Impacts to crew health (such as Visual Impairment/Intercranial Pressure) such as sustained exposure to weightless environment are also unknown at this time.

13.3.2.5. Initial findings

13.3.2.5.1. Crew Sample Return mission

To support an urgent need of the MPPG, an initial assessment, required shortly after this effort was started, was performed to model the risk drivers for loss of crew on a Mars Sample return mission where a human crew was to travel to Mars, retrieve a previously collected Mars surface sample in low orbit around Mars. Utilizing the DRA 5.0 reference architecture, the crewed portion of the conjunction class, NTR propelled Mars mission was utilized as a starting point, with the primary difference being (for this initial assessment), the crew remained in Mars orbit for the duration of their Mars stay time (500 days) as opposed to descending, landing, and staying on the surface. For this assessment, only the elements involved with the crew portion of the mission were modeled; i.e., the Nuclear NTR for the crew transit, the inline propulsion tank, the saddle truss and drop tank, the Mars transit vehicle (MTV), a LEO re-boost vehicle, the return crew exploration vehicle, and finally, the crew delivery crew exploration vehicle. A descent lander, aero-shell, surface habitat, and MAV were not modeled as this sample return mission does not utilize them. The Mars sample collection portion of the mission was not modeled. The collected sample was assumed to be in low Mars orbit and the crew would conduct a rendezvous and proximity operation and retrieve the sample.

To enable rapid modeling (in time to support the requested need) of the mission, several ground rules and assumptions were used, including three strings for each system. Certain systems that would not result in risks leading to loss of crew were not included in the model (such as Communications and Tracking, general instrumentation and some heaters), no cross strapping across elements to perform critical functions. However, cross strapping within a system or element was used; no spares or repairs were included. For this model, all components were operated at 100% duty cycle when on, radiation and thermal protection were assumed to be included in the structure failure rate, and a crew size of four crew members. Aborts (other than upon crew launch from Earth) were not modeled, and MTV capture in Mars orbit was accomplished.

Launch availability was modeled with a launch campaign analysis utilizing the following ground rules: the duration of the Mars injection window is 60 days; the crew can be launched no earlier than 30 days prior to the opening of the Mars injection window; 2 days are required from crew launch prior to performing the Trans Mars Injection burn; and there was no constraint on how early we can launch cargo missions. Three working shifts per day and a 5-day work week schedule was assumed for the work force.

13.3.2.5.2. Results

The MTV Habitat failing in Mars orbit was the leading risk driver for loss of crew, as the habitat was the most complicated element and was operating for the longest time period (500 days). Other risk drivers were the NTR fails in Mars orbit, the Crew return MPCV fails in Mars Orbit, and docking module fails in Mars orbit. All of these show the impact of the longest mission phase (500 days) and its impact on determining risk drivers. The impacts on crew health for being subjected to prolonged weightless (~900 days) during the mission are included in the IMM so they have not been modeled.

13.3.2.6. Crew mission to the surface

To help illustrate/compare the risk of a sending a crew on a sample return mission to Mars, and a mission where the crew is sent to the surface of Mars, a crew mission to the surface was modeled. Additional elements required for

sending the crew to the surface as well as support them while on the surface and returning the crew to the MTV was added to the model. These additional elements (Descent/Lander Hab, surface power source, MAV) were modeled and added to the model. Aborts from the Mars surface (if the Descent /Lander Hab or surface power source were to fail) were included in the model since DRA 5.0 architecture contained adequate consumables in the MTV to support the crew in the event of a shortened surface stay.

13.3.2.6.1. Results

Risk drivers for the crew to surface mission included the MTV habitat failing in Mars orbit since the habitat was the most complicated element and was operating for the longest time period (500 days). The MTV habitat failing during the transit to Mars was the next risk driver, owing to complexity and mission phase length. Factors such as allowing a surface abort from the surface reduced the impact of failures on the surface habitat and surface power source.

13.3.2.7. Potential low-hanging fruit

If the impact maintenance upon the failure rate was modeled, assuming the spare parts were available, and the crew had the necessary tools and skills to perform the repairs, the risk of loss of crew or loss of mission can be reduced (improved). Rough estimates of the maintenance level (percentage of hardware and components that are accessible and repairable with available spares, tools and crew skill sets) show a probable decrease in risk with increasing levels of repairable hardware. In a high-level analysis, assuming ISS levels of reparability (roughly 65%), the three longest mission phases (transit to Mars, Mars orbit [or surface stay], and transit to Earth) show decreases in loss-of-crew risk of over 3.5 times for the Hab module. As both the elements and model matures, impacts of introducing options such as maintainability, upon the overall mission risk will be modeled to show how best to apply a maintenance concept to reduce risk.

13.3.3. Future Risk Analysis Work

Future work will include further development/refinement of the model and elements, to refine the initial risk estimates. Maturation of the hardware elements will also be included in the model. Model refinement should allow rapid risk assessment of various options. Close coordination of the elements with subject matter experts will improve the level of detail and should improve the accuracy of the risk estimation.

As risk drivers are identified, they can be further analyzed to determine the cause of the risk and methods to potentially mitigate the risk can be assessed. Operating times for hardware, redundancy levels, mission phase lengths, and architecture changes will all be modeled to assess their impacts upon risk. The model can rapidly be re-run with changes to the elements to examine the impacts to the risk. When the risk drivers have been determined for a specific mission and architecture, those risks can be analyzed to assess how the various precursor missions could help mitigate this risk. Depending on the nature of the risk and the details of the particular precursor mission, some precursor missions could help mitigate more risk than other missions. The risk assessment model will help the user to determine which precursor strategies or combination of missions offer the best risk mitigation.

With several different precursor activities available (ISS, MPCV Cislunar flight, Waypoint (L-2), near-Earth objects (NEOs), lunar missions, crew missions to the Mars moons Phobos and Deimos, and robotic missions to Mars), many opportunities are present to mitigate or buy down risk. The risk assessment will aid in showing where the best return of investment can be achieved. Maturation of the hardware will result from utilizing the hardware in environments similar to where it will be used on the Mars mission without exposing it to all the risks of the Mars mission. Long-duration in-space exposure can come from locating (and operating) the hardware on the ISS, at the Waypoint location, on NEO missions, on lunar missions. Entry systems/techniques can be demonstrated in the high Earth atmosphere, as well as on robotic missions to Mars (where the descent and landing portions of the mission can be demonstrated as well). Waypoint and NEO missions can demonstrate long-duration space missions in an environment similar to the Mars transit and orbit phases. Lunar missions provide the opportunity to operate surface power systems and potential landing systems. Missions to the Mars moons can demonstrate/exercise all of the hardware required to perform a Mars mission except the atmospheric entry portion. Robotic missions to Mars (in addition to demonstrating EDL systems) can demonstrate/exercise surface power systems and in-situ resource utilization systems which would help reduce risk.

Reliability growth will come from exercising the components and systems in the environment that they are designed to be used. Testing can accomplish some of this; however, with some of the components and environments on Earth, it is difficult to demonstrate a 100% totally accurate environment (such as the impact of gravity; Mars has one-third of the gravity of Earth). Reliability growth will result from subjecting flight or flight-like hardware and software to the “test, analyze, fix” cycle that has traditionally been applied to assure design suitability and robustness. Exercising of the hardware through precursor missions, exposing the hardware to mission operating cycles and environments, will contribute to reliability growth of the hardware by exposing weaknesses and the subsequent redesign of the failed components.

13.4. Planetary Protection Requirements for Human and Robotic Missions to Mars

Primary Contributors:

M.S. Race, SETI Institute, Mountain View, CA

J.D. Rummel, East Carolina University, Greenville, NC

C. A. Conley, NASA HQ, Washington DC

P. Stabekis, Genex Systems, Washington DC

R. Mogul, California State Polytechnic University, Pomona, CA

13.4.1. Overview

All missions going to or returning from Mars, whether robotic or human, are required to comply with stringent planetary protection requirements that are based on provisions of the Outer Space Treaty. Because planetary protection is an essential element for future Mars exploration, any Design Review Architecture for human Mars missions must incorporate considerations of both forward and back contamination controls in multiple mission phases to 1) protect the Earth and its human population from potential biohazards, 2) monitor and assess astronaut health throughout the mission, and 3) enable the success of scientific investigations and sampling related to habitability and detection of potential martian life. Based on latest international policies and NASA directives, as well as studies of both human and robotic missions, planetary protection provisions are not merely recommendations or suggestions, but rather mandatory planning elements that should be considered in all human mission systems and subsystem development activities from the start. They are cross-cutting in nature, contribute to requirements generation, have feed forward implications, and represent significant time and funding considerations for any future design reference architecture.

13.4.2. Background

Since early in the space age, the Committee on Space Research (COSPAR) of the International Council for Science has maintained a consensus planetary protection policy for joint reference and implementation.²⁶ COSPAR’s policy stipulates the need to control forward contamination (life or organic contamination carried from Earth) that might invalidate current or future scientific exploration on a particular solar system body, or might disrupt planetary environments or potential endogenous (alien) ecosystems. In addition, concerns about backward contamination (extraterrestrial life carried back to Earth) focus on avoiding the potential for harmful contamination of the Earth’s biosphere. For human missions, this also includes the possible immediate and long-term effects on the health of astronaut explorers of biologically active materials encountered during exploration.

For nearly 5 decades, NASA’s robotic missions have complied with international planetary protection requirements and controls while exploring the Moon and other celestial bodies.²⁷ Moreover, multiple NRC studies on the exploration of Mars and other bodies of the solar system have reiterated the importance of taking a conservative approach to planetary protection implementation for both forward and backward contamination.^{28,29,30,31,32,33,34} Nonetheless, few human missions have been subjected to PP requirements. The crews of Apollo 11, 12, and 14 were quarantined upon their return from the Moon, after the first human landings on another celestial body. Extensive analyses of astronauts and samples upon their return demonstrated that lunar materials posed no biological threat to mission personnel or Earth. Thus, strict planetary protection requirements were eliminated for subsequent lunar missions. Because post-Apollo human missions have only journeyed as far as LEO, the human spaceflight program has had no recent experience with planetary protection implementation (although some of the same principles govern the Shuttle-era health stabilization program).

Human missions involving the ISS, Shuttle, or other platforms in Earth orbit are not constrained by planetary protection controls. It is noteworthy that the science, technology, and legal considerations for planetary protection during future long-duration human missions—especially for Mars—are significantly different than those used during the Apollo Program. Thus, it will be particularly important to initiate discussions/interactions with varied engineering and technical communities as well as space medicine, biomedical, operations, and human/factors communities—to ensure that all involved groups include up-to-date information on implementation of planetary protection for future exploration beyond LEO. Moreover, since it is recommended that a crewmember be assigned the responsibilities for planetary protection oversight on long-duration missions, there will be implications for team training, autonomy, and related operational considerations.

The primary goals of the COSPAR planetary protection policy do not change when humans are involved. If human explorers are to be beneficial to the understanding of planetary environments and potential life, or to ensure their own safety while conducting planetary exploration, then consideration of planetary protection is essential. In doing so, the unavoidable and mostly beneficial association of humans with a huge diversity of commensal microbes means that special implementation controls will have to be developed for human exploration missions—particularly for future long-duration missions to Mars. There is a need to acknowledge and emphasize important cross-cutting, feed-forward considerations that planetary protection concerns will involve. To mitigate the potential for danger to astronauts and to Earth, as well as to avoid forward contamination of other bodies, planetary protection must be acknowledged as an important element for the success of human missions—and evaluation of planetary protection requirements should be considered critical in all human mission systems and subsystem development activities from the start.

13.4.3. COSPAR Planetary Protection Policy for Robotic and Human Missions

As indicated in NASA Policy Directive 8020.7G (section 5c),³⁵ ensuring compliance with the Outer Space Treaty planetary protection is a mandatory component for all solar system exploration missions. International planetary protection policy and guidelines for compliance with Treaty obligations are maintained by the COSPAR, which also advises the United Nations on matters of space exploration. In addition to complying with applicable forward contamination control measures associated with science data collection and operations, NASA’s planning of human mission architectures is expected to be compliant with approved COSPAR planetary protection principles and guidelines shown in Figure 13-47. Further elaboration of specific requirements by NASA is anticipated as architecture planning continues.

In developing preliminary guidelines for human missions to Mars, COSPAR has noted that the greater capability of human explorers to contribute to the astrobiological exploration of Mars will be realized only if human-associated contamination is understood and controlled. A robust program of planetary protection measures, including forward contamination control, medical monitoring, spatial planning for human exploration, and precautions against back contamination, has been described in NASA and ESA-led studies,³⁶ with an assumption that prior to human exploration there is a need for efforts to develop, rehearse, and refine planetary protection controls. Effectively, these principles involve “defense in depth” and the continuous evaluation throughout a mission of the contamination status of the crew and the planetary surface (and sub-surface) that they will explore.

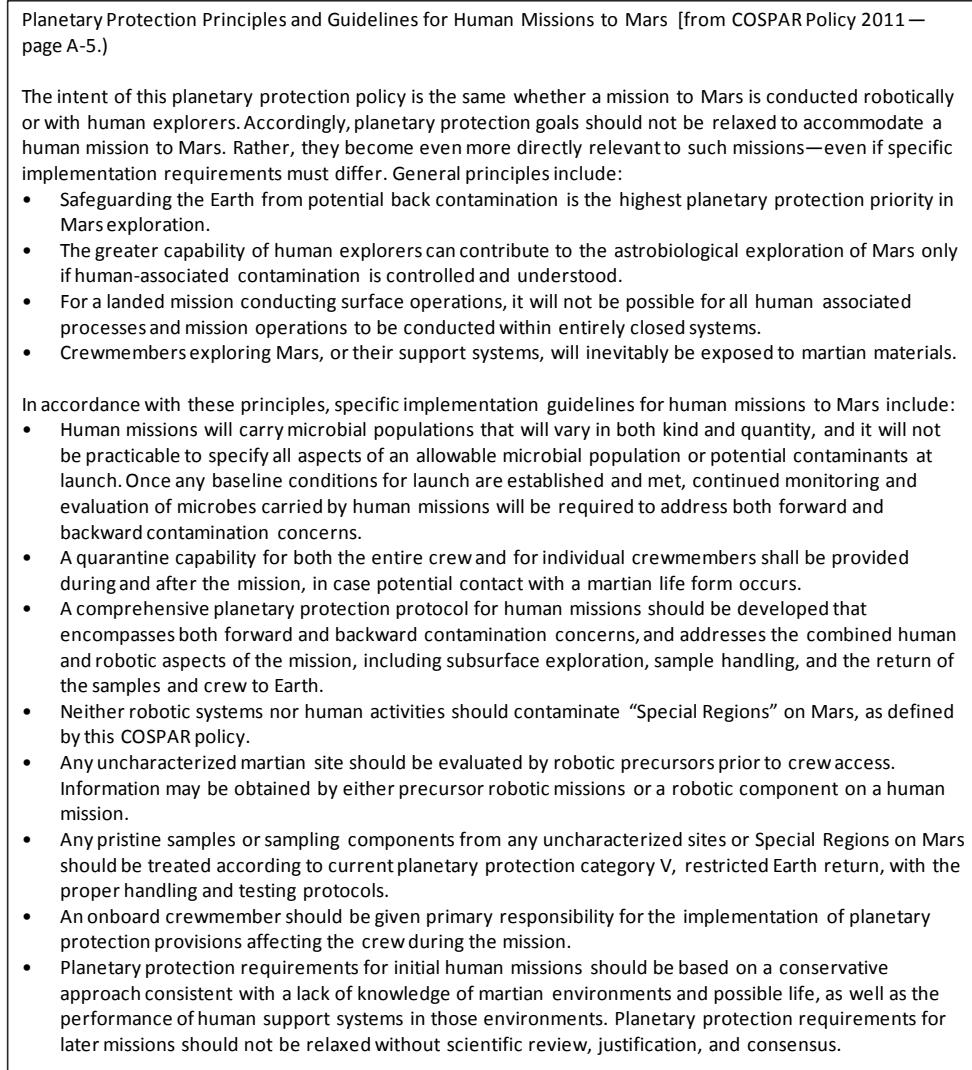


Figure 13-47 Planetary protection principles.

13.4.4. Applying Planetary Protection Considerations to Future Human Design Reference Architectures

Within the past decade, several workshops and studies have specifically analyzed hypothetical mission scenarios and reconsidered planetary protection for long-duration human missions, especially to Mars,^{37,38,39} These cross-disciplinary workshops and studies noted the need to take a broad conceptual approach to planetary protection during human missions and to develop special planetary protection technologies and operations to address important contamination associated factors. Ultimately, plans and designs for planetary protection provisions on future human missions must be developed in ways that build upon integrated understanding and open exchange of information among the many technical and scientific communities involved. In practice, this means that any DRA must reflect the fact that planetary protection requirements are not optional—they are required to ensure adherence to the Outer Space Treaty, and represent important drivers of many research and technology development activities, operations, and implementation schemes. Thus it will be critical that program architectures involving combined human and robotic missions benefit from cross-cutting technologies and leveraged cost from the earliest phases of mission plans.

Significant investments will be needed (as supported by the NRC Decadal Survey) in multiple areas of importance that emanate from a combination of COSPAR planetary protection policies for forward contamination control and

associated guidelines for human missions to Mars focusing on back contamination control, including such examples described in the following section.

13.4.5. Protecting Astronauts and Designing Human-Rated Systems

According to Article IX of the Outer Space Treaty, “appropriate measures” are required to avoid “adverse changes in the environment of the Earth which could result from the introduction of extra-terrestrial matter.” Minimizing exposure of astronauts to potentially hazardous Mars materials, as well as monitoring astronaut health and microbial populations carried by human missions, are key factors in facilitating the safe return of astronauts to Earth. Comprehensive monitoring is essential, to ensure adequate documentation throughout the mission to provide confidence that in-flight illnesses or other potential biohazards are of Earth origin. This will be required for planetary protection purposes at a level significantly greater than that needed to document astronaut health alone.

Particular aspects of human missions needing attention both to avoid back contamination and to ensure human safety include the choice of initial landing sites, design of human habitats, plans for EVAs, and potential ISRU operations. In general:

- Landing sites shall be selected such that nominal or off-nominal mission operations have a low probability of allowing mission-associated microbial or organic contamination to enter Mars “Special Regions” either horizontally or vertically. This includes mission-induced Special Regions.
- Human habitation modules (and associated life support and recycling systems) should be located and operated in ways to ensure that mission-associated microbial or organic contamination has a low probability of entering Special Regions.
- Human EVAs should be planned to likewise minimize mission-associated microbial or organic contamination of Special Regions (e.g., via robotic access beyond designated zones of minimal biological risk as recommended by the NRC, 2002b), and
- ISRU activities should be planned to avoid contamination of Special Regions while also protecting humans and human-associated systems from uncontrolled contact with martian materials from those regions.

These guidelines translate to many specific planetary protection technology needs, including the development of human habitat egress/ingress procedures that minimize contact with martian material; quantitative assessment of contamination transfer, medical monitoring procedures before, during and, after EVAs; traverse planning in relation to COSPAR defined Special Regions; monitoring of the microbial inventory of human habitats; protocol development for laboratory facilities on Mars; and development of quarantine procedures for affected astronauts. Assuming that a future Mars mission adopts a scenario many weeks or months on the planet – with EVAs as often as every other day – this could mean many dozens of ingress/egress operations and transfers between habitat and lab areas, each of which has planetary protection implications [Hogan, 2006]. Other technological systems processes with potential planetary protection implications include those associated with advanced life support systems, recycling, waste disposal and ISRU. While COSPAR policy guidelines for the human exploration of Mars provide the framework to support requirements in many of these areas, specific implementation approaches will most usefully be developed in the context of anticipated technology developments in human health monitoring and molecular environmental microbiology.

Furthermore, there are important areas of basic scientific knowledge related to planetary protection that have cross-cutting impact for development of effective human-rated systems. Areas relevant to planetary protection that should be incorporated into the research portfolio include a) basic research to develop and extend our fundamental understanding of human associated and environmental microbiology in space; b) applied research and development of spacecraft hardware and systems to facilitate end-to-end mission capability; and c) testbed studies to evaluate effective implementation of systems, processes, crew training, and operations that address planetary protection requirements, as described below.

1. Fundamental Knowledge on Microbial Limits of Life, and Human-Associated Microbial Diversity and Distribution:

In the past 2 decades, our understanding of environmental microbiology and extremophiles has expanded considerably, resulting in a greater awareness of the potential for the survival of terrestrial microbes in extreme environments, as well as the prospect for finding possible evidence of truly extraterrestrial life in other locations.

Faced with such possibilities, it is essential to the proper implementation of planetary protection policy that criteria for assessing habitability for planetary environments are established conservatively, and that appropriate measures are taken to protect against contamination. Thus, it is essential that research on microbial diversity and adaptation to planetary environments continue to inform planetary protection policies and their implementation, for both robotic and human missions.

Furthermore, we have only recently recognized that humans themselves are a veritable scaffold upon which microbial ecosystems flourish. Powerful new analytical tools have become available to analyze and decipher such ecosystems and understand our human associated microorganisms.⁴⁰ Since these diverse microbial hitchhikers represent unavoidable potential bio-contaminants during human exploration in the solar system, it is important to understand them to the fullest—their identities, abundance, and distribution, as well as their potential for dispersal, survival and propagation as contaminants, and as markers in exploration environments, whether in habitat/work environments or exposed to the planet/moon environment.

Specific topics of relevance to the fundamental scientific understanding of biological and physical sciences in space include (but are not limited to):

- Development of a baseline inventory and understanding of human associated microbes, as relevant to the space environment;
- Studies of human-associated microbes as potential contaminants, including their abundance, potential for release, and dispersal/survival/propagation in human planetary exploration;
- Understanding human-associated microbes as potential biomarkers of relevance, and their possible use as tracers of contamination;
- Survival of spacecraft-relevant terrestrial organism and molecular components;
- Contamination transport models and pathways (near- and far-field);
- Studies to understand the contribution of ambient space environments towards passive mitigation of forward contaminant risks (radiation, temperature, etc.).

2. *Applied Research and System Development*

Parallel developments in applied fields are needed to provide capabilities encompassing the entire spacecraft hardware system, including processes and procedures and the human interface:

- Development of monitoring technologies to evaluate the level/type of microbes released by human-associated activities on an ongoing basis, with capability for monitoring microbes in real-time, integrating system technologies to protect human life from pathogenic and /or alien microorganisms (should they exist), and shielding engineering systems from bio-corrosion;
- Development of human quarantine and decontamination strategies and capabilities for planetary environments, aiming to minimize exposures and control recontamination parameters;
- Quantitative and qualitative analysis and understanding of process streams of life support systems (air, water, recycling wastes, etc.) from a human microbiology perspective, for all crew-rated systems, including an end-to-end understanding of venting, dispersal, and shutdown considerations to minimize release of contaminants and enable surface containment/disposal of wastes;
- Development of sterilization and decontamination capabilities for generated wastes, spacecraft volumes (habitats, labs, pressurized rovers etc.) and associated equipment and samples, consistent with available resources anticipated for such missions;
- Assessment and understanding of nominal contaminant releases from cabin atmospheres/other enclosures via leakage;
- Development of responses to off-nominal scenarios and contamination events, with implications and mitigation requirements for both planetary protection and crew health/safety objectives.

3. *Test beds for Technology Development and Operations*

The Moon in particular is considered to be an excellent potential testbed to develop planetary protection procedures and practices in an environment sufficiently harsh to prove an adequate challenge, but – unlike Earth analogs – isolated from the overwhelming background contamination of the terrestrial biosphere. Because the Moon is currently recognized as being of interest for understanding pre-biotic chemistry and the origin of life, but is not

hospitable to contamination by Earth life, the only current planetary protection constraint for operations on the Moon is the requirement to document activity. On the Moon, there are no limits on biological and organic contamination similar to those in place for more distant but potentially habitable bodies such as Mars. This means that technologies developed for use on the Moon are not prohibited from releasing high levels of contamination per se. A coordinated lunar program addressing planetary protection issues could yield significant benefits [e.g., LEAG, 2009]⁴¹ such as providing valuable ground truthing on in situ contamination of samples and external environments; studies of lunar habitat/space suit competency, containment and leakage; and testing operational procedures associated with successful planetary protection implementation on another planetary surface.

Science Investigations on Mars: On robotic missions to Mars that study the potential for extraterrestrial life, strict PP controls are imposed to avoid forward contamination of the planet by biological organisms from Earth. These requirements are fully integrated into MEPAG Goals I-III, which seek to provide necessary precursor information for future human missions.⁴² Experience with past robotic missions has informed the development of requirements and implementation options that are explicitly detailed in COSPAR policy and NASA Procedural Requirements document NPR 8020.12 (currently, version D).⁴³ For landed hardware, compliance with these requirements involves rigorous bio-burden reduction and accounting pre-launch, and operational constraints through the end of the mission. Hardware involved in the acquisition and storage of samples from Mars must be designed to protect Mars material from Earth contamination, and ensure appropriate cleanliness from before launch through return to Earth. Technologies needed to ensure sample cleanliness at levels similar to those attained and maintained by the Viking project, are yet to be developed in the context of modern spacecraft materials and human missions. Maintaining appropriate separation of habitat and laboratory modules will also be important design elements for science investigations. Obviously, attention to these planetary protection considerations for science objectives will remain important aspects of future human missions.

The objectives of planetary protection policy are the same for both human and robotic missions; however, the specific implementation requirements will necessarily be different. MEPAG Goal IV + recognizes that additional forward contamination research and technology development will be needed for operations and collection of samples during sustained human crews presence. Human missions will require additional planetary protection approaches that minimize contamination to martian environments released due to human exploration, including protocols on how to access locations on Mars (both characterized and un-characterized) and performance standards for human support systems, including lab handling and testing of pristine materials on Mars. Robotic elements of human missions must still follow relevant planetary protection requirements: for example, access to Mars “Special Regions” (as defined in NPR 8020.12D) involves stringent cleanliness requirements, which will also necessitate targeted technology development for both hardware cleaning, reuse, and clean transfer capabilities. A conceptual approach is presented in NASA's Design Reference Architecture 5, but implementation requirements for human-based exploration must be refined in the context of specific planned missions, especially considering the extensive drilling anticipated to many tens of meters below the surface. In addition, preparation and placement of pre-landed assets and hardware (including nuclear power systems and fission reactors that must avoid creation of mission-induced special regions from radiated heat) will likely require special considerations, both for forward contamination concerns as well as Special Region avoidance. Finally, advanced technological and operational considerations will be required on how to respond to a discovery of putative martian life, if found or detected during a human mission.

Protecting Earth: Preventing adverse effects on the Earth's environment as a result of returning astronauts and/or samples from Mars is the highest planetary protection priority. Planetary protection requirements for Mars sample return missions (whether robotic or human) involve stringent restrictions on release of unsterilized Mars material into the Earth environment. The European Science Foundation (ESF) has recently completed a study on assuring the safety of robotic Mars sample return missions⁴⁴ and has endorsed previous guidance that the constraints be formulated as an assurance level for the release of a particle of martian material of a size that could potentially carry biological hazards. Specific numerical requirements recommended by the ESF involve ensuring that a particle of unsterilized Mars material is contained with a probability of 1×10^{-6} . In consideration of new information about viruses and genetic transfer agents, the particle size limit recommended by the ESF study for containment is 10 nm. Containment at this level would be required until samples are characterized and demonstrated to be safe for release, which includes satisfactory completion of a life detection and biohazard protocol, although re-allocation of the full “probability of release” is anticipated upon successful introduction of the return capsule into an Earth-based containment facility. Similarly, the direct return to Earth of the MTV and crew has planetary protection

implications, just as during the Apollo missions. Thus, technologies for life detection, biohazard avoidance and the protocol for use during human missions are also areas in need of further development and technical refinement.

The Apollo Program provides a cautionary example of how NASA has implemented planetary protection on human missions in the past, for both astronaut and samples—and illustrates numerous targets for making improvements to future mission designs and procedures. Among the key technologies for human missions to Mars include the selection of appropriate spacecraft materials and hardware; the design of suitable human-rated subsystems; the development of procedures for clean sample acquisition, handling, and containment; capabilities to ensure adequate re-cleaning of sampling hardware in situ; and quarantine capabilities for astronauts both on Earth and during return from Mars. While detailed protocols have been developed for testing and handling pristine martian samples returned via robotic missions,⁴⁵ the eventual protocols for returning samples via human missions have yet to be developed.

13.4.6. Planetary Protection Conclusions:

In considering future human exploration to varied destinations beyond LEO, planetary protection concerns will have significant impact on mission architecture, requirements, capabilities and activities. Already, for human missions to Mars (and the Moon as test-bed), planetary protection concerns are recognized as introducing cross-cutting technological and design challenges for spacecraft and vehicle systems; habitats and labs; EVAs and suits; science exploration and operations; equipment cleaning, maintenance and use; human and robotic access to Special Regions; quarantine/containment protocols; and even shutdown/dormancy of infrastructure between missions. Obviously, these are not just add-on or ‘other’ issues for later consideration; rather they’re integral to planning and design from the start.

While precise planetary protection protocols will be developed in coming years for human missions to Mars and other target bodies, it will be important that mission architects, designers, and engineers become aware of international planetary protection policies that are not optional and are subject to revision in the face of new scientific information. Application of planetary protection policy in the context of human missions beyond LEO is necessary for adherence to the Outer Space Treaty, just as it is for robotic missions. Attention to planetary protection in the early architecture design and planning stages will help use common solutions where possible, thus avoiding unnecessary duplication of efforts and costly redesign of critical elements and systems.

Through organized workshops and interdisciplinary information exchanges, the planetary protection community has begun to explore with engineering and systems experts the impacts of COSPAR and NASA planetary protection policies on numerous human associated systems. By establishing communication among different groups, previous planetary protection studies and workshops can be useful in highlighting important data needs, as well as identifying priority research and technology development areas. As systems experts develop the next generation of plans, design elements and operation scenarios, they will benefit greatly from consulting this information from the start. Finally, while compliance with planetary protection policy is important for overall mission success, it is also relevant for public support. NASA’s commitment to transparency for future human missions must include disclosure of risks as part of mandated environmental impact reports as well as in public engagement activities. Thus, for many reasons planetary protection is an essential element in any architecture for future human Mars exploration.

13.5. Bibliography

-
- ⁸ Augustine, Norman R., “Seeking a Human Spaceflight Program Worthy of a Great Nation,” Review of U.S. Human Spaceflight Plans Committee, October 2009.
- ⁹ Office of the President of the United States (2010), “National Space Policy of the United States of America,” June 28, 2010.
- ¹⁰ Luidens, R. and Miller, B., “Efficient Planetary Parking Orbits with Examples for Mars,” NASA TN D-3220, January 1966.
- ¹¹ Hoffman, S. J., “Mass Performance Implications of Mars Parking Orbit Selection for Piloted Missions,” Paper AAS 91-440, Astrodynamics Specialist Conference, Durango, CO, August 19–22, 1991.
- ¹² Desai, P., Braun, R., and Powell, R., “Aspects of Parking Orbit Selection in a Manned Mars Mission,” NASA TP-3256, December 1992.

- 13 Cornick, D. E. and Seversike, L. K., “Optimum Parking Orbit Orientation for a Three-Dimensional Capture-Escape Mission,” *Journal of Spacecraft and Rockets*, Vol. 7, No. 7, 1970, pp. 808–813.
- 14 Cupples, M. L., and Nordwall, J. A., “Optimal Parking Orbits for Manned Mars Missions,” *American Astronautical Society*, Paper 93-149, Feb. 1993.
- 15 Landau, D. F., Longuski, J. M., and Penzo, P. A., “Method for Parking Orbit Reorientation for Human Missions to Mars,” *Journal of Spacecraft and Rockets*, Vol. 42, No. 3, May–June 2005, pp. 517–522.
- 16 Mulqueen, J. “Manned Mars Mission Transfer from Mars Parking Orbit to Phobos or Deimos,” *Manned Mars Missions, Working Group Papers*, Vol. 1, Section 1–4, May 1, 1986, pp. 154–161.
- 17 Foster, Cyrus, “Delta-V Budgets for Robotic and Human Exploration of Phobos and Deimos,” Abstract 11-018, 2nd International Conference on the Exploration of Phobos and Deimos, Moffett Field, CA, March 14–16, 2011.
- 18 Obama, B.H., “Remarks by the President on Space Exploration in the 21st Century,” *John F. Kennedy Space Center*, April 15, 2010, (<http://www.whitehouse.gov/the-press-office/remarks-president-space-exploration-21st-century>)
- 19 NRC 2011, “Vision and Voyages for Planetary Science in the Decade 2013-2022, National Academy Press, Washington, D.C.
- 20 NASA, “Report of the 90-Day Study on Human Exploration of the Moon and Mars”, National Aeronautics and Space Administration, November 1989.
- 21 Synthesis Group, “America at the Threshold, Report of the Synthesis Group on America’s Space Exploration Initiative”, May 1991.
- 22 “Human Space Exploration Framework Summary”, National Aeronautics and Space Administration, January 12, 2011, http://www.nasa.gov/exploration/new_space_enterprise/home/heft_summary.html
- 23 P-SAG, “Analysis of Strategic Knowledge Gaps Associated with Potential Human Missions to the Martian System”, Precursor Strategy Analysis Group (P-SAG), (jointly sponsored by MEPAG and SBAG), May 31, 2012, <http://mepag.jpl.nasa.gov/reports/index.html>
- 24 MEPAG, “Mars Science Goals, Objectives, Investigations, and Priorities: 2010”, Mars Exploration Program Analysis Group, September 24, 2010, http://mepag.jpl.nasa.gov/reports/MEPAG_Goals_Document_2010_v17.pdf
- 25 MEPAG HEM-SAG (2008). Planning for the Scientific Exploration of Mars by Humans, Unpublished white paper, TBD p, posted March 2008 by the Mars Exploration Program Analysis Group (MEPAG) at <http://mepag.jpl.nasa.gov/reports/index.html> .
- 26 COSPAR. 2011. COSPAR Planetary Protection Policy (updated 3-24-11). <http://cosparhq.cnes.fr/Scistr/PPPpolicy.pdf>
- 27 NASA Planetary Protection website: www.planetaryprotection.nasa.gov, accessed October 2012.
- 28 NRC. 1992. Biological Contamination of Mars: Issues and Recommendations. National Academy Press, Washington, DC. (N.B. All SSB reports at <<http://www.nas.edu/ssb>>.)
- 29 NRC. 1997. Mars Sample Return: Issues and Recommendations. National Academy Press, Washington, D.C. <<http://www.nas.edu/ssb/mrsrmenu.html>>.
- 30 NRC. 2002a. The Quarantine and Certification of Martian Samples. National Academy Press, Washington, D.C.
- 31 NRC. 2002b. Safe On Mars: Precursor Measurements Necessary to Support Human Operations on the Martian Surface. National Academy Press, Washington, D.C.
- 32 NRC. NRC, 2007, Astrobiological Strategy for the Exploration of Mars, National Academy Press, Washington, DC
- 33 NRC. 2006. Preventing the Forward Contamination of Mars. National Academy Press, Washington, D.C.
- 34 NRC. 2009. Assessment of Planetary Protection Requirements for Mars Sample Return Missions. National Academy Press, Washington, D.C.
- 35 NASA, 1999. Biological Contamination Control for Outbound and Inbound Planetary Spacecraft. NASA Policy Document (NPD) 8020.7G (section 5c) See NASA PP website: www.planetaryprotection.nasa.gov ; also http://nodis3.gsfc.nasa.gov/displayDir.cfm?Internal_ID=N_PD_8020_007G_&page_name=main&search_term=8020%2E7
- 36 Race, M.S., G. Kminek and J.D. Rummel. 2008. Planetary Protection and Humans on Mars: NASA/ESA Workshop Results. *Advances in Space Research*, 42 (6) pp. 1128-38
- 37 Criswell, M., M., Race, J. Rummel, A. Baker (eds.). 2005. Planetary protection issues in the human exploration of Mars: Pingree Park final workshop report. NASA/CP-2005-213461.

- 38 Hogan, J., J. Fisher, M. Race, J. Joshi, and J. Rummel (eds.). 2006. Life Support & Habitation and Planetary Protection Workshop Final Report. NASA / TM-2006- 213485.
- 39 Kminek G., J. Rummel, M. Race (eds.). 2007. Planetary Protection and Human System Re-search & Technology, ESA-NASA Workshop Report, ESA WPP-276, ESTEC, Noordwijk, Holland.
- 40 Stone, M. 2009. NIH Builds Substantial Human Microbiome Project, ASM Microbe 4(10), Oct. 2009. <<http://www.microbemagazine.org>>.
- 41 LEAG. 2009. The Lunar Exploration Roadmap: Exploring the Moon in the 21st Century: Themes, Goals, Objectives, Investigations, and Priorities, 2009. < http://www.lpi.usra.edu/leag/ler_draft/draft_ler_v1.pdf >.
- 42 17. MEPAG HEM-SAG, 2008. Planning for the Scientific Exploration of Mars by Humans. Un-published white paper (J. B Garvin and J.S. Levine eds.), posted 2008 at <http://me-pag.jpl.nasa.gov/reports/index.html>
- 43 NASA, 2011. Procedural Requirements Documents (NPR) 8020.12D, Planetary Protection Provisions for Robotic Extraterrestrial Missions, See NASA PP website: www.planetaryprotection.nasa.gov ; also http://nodis3.gsfc.nasa.gov/displayDir.cfm?Internal_ID=N_PR_8020_012D_&page_name=main&search_term=8020%2E12
- 44 European Science Foundation, 2012. ESF-ESSC Study Group on Mars Sample Return Requirements, in press.
- 45 Rummel, J.D., M.S. Race, D.L. DeVincenzi, P.J. Schad, P.D. Stabekis, M. Viso and S. E. Acevedo (eds.), 2002. A Draft Test Protocol for Detecting Possible Biohazards in Martian Samples Returned to Earth, NASA/CP-2002-211842, Washington, D.C.

Selected Additional References Pertaining to Planetary Protection:

- Conley, C.A. and J.D. Rummel, 2012. NASA Mars Exploration Planning: Program Remediation, Planetary Protection Requirements. Paper 15691, Space Exploration Symposium at 63rd International Astronautical Congress 2012, Naples , Italy.
- Conley, C. A. and J. D. Rummel. 2008. Planetary protection for humans in space: Mars and the Moon. Acta Astronautica 63:1025-1030.
- European Space Agency, 2012. ESA Planetary Protection Requirements, ESSB-ST-U-001, Noordwijk, Netherlands, 2012.
- D.P. Glavin, J.P. Dworkin, M. Lupisella, D.R. Williams, G. Kminek, J.D. Rummel, 2010. In situ Biological Contamination Studies of the Moon: Implications for Planetary Protection and Life Detection Missions. Earth, Moon, Planets, 107:87-93.
- Hogan, J.A., J.W. Fisher, M.S. Race, J. Joshi, and J.D. Rummel, 2007. Results Summary of the Life Support & Habitation and Planetary Protection Workshop, Paper number 2006-01-2007, March 2007, 2006 Transaction Journal of Aerospace, SAE International, www.sae.org
- Hogan, J.A., J.W. Fisher, J.A. Levri, K. Wignarajah, M.S. Race, and P. Stabekis, 2006. Influence of Planetary Protection Guidelines on Waste Management Operations, paper 05ICES266, International Conference on Environmental Systems, Rome Italy, July 2005 (Paper No. 2005-01-3097 in Journal of Aerospace, SAE 2005 Transactions, March 2006)
- Kerney K.R. and A. C. Schuerger, 2011,. Survival of Bacillus subtilis Endospores on Ultraviolet-Irradiated Rover Wheels and Mars Regolith under Simulated Martian Conditions , ASTROBIOLOGY, Volume 11, Number 5, p 477-485, 2011.
- Mogul,R, P. D. Stabekis, M. S. Race, and C. A. Conley (2012) Planetary Protection Considerations for Human and Robotic Missions to Mars. In Concepts and Approaches for Mars Exploration, abstract #4331, Lunar and Planetary Institute, Houston. <http://www.lpi.usra.edu/meetings/marsconcepts2012/pdf/4331.pdf>
- NASA. 2007. NASA Advisory Council Workshop on Science Associated with the Lunar Exploration Architecture. Workshop website: <<http://www.lpi.usra.edu/meetings/LEA>>.
- Race, M. S., J.D. Rummel, and C. A. Conley, 2011. Planetary Protection as a Crosscutting Consideration in Human Missions and Technologies Beyond Low Earth Orbit, 41st International Conf. on Environ. Systems, AIAA-2011-5093. <http://arc.aiaa.org/doi/abs/10.2514/6.2011-5093>
- Race, M.S.,and J.D. Rummel,, 2010. Planetary Protection: A Cross-Cutting Mission Concern and Need for Research related to Topics Supporting Crew Health and Performance. Response to NASA Request for Information (RFI) on Topics Supporting Crew Health and Performance (RFI No. NNJ10ZSA003L)
- Race, M.S., J.D. Rummel, et al., October 2009. Planetary Protection: A Cross-Cutting Concern, and an Opportunity for Basic and Exploration-Driven Research in Biological and Physical Sciences in Space.

- Submitted to NRC Decadal Survey for Biological and Physical Sciences in Space.
- Race, M., G. Kminek, J. Rummel, et al. 2008. Planetary protection and humans on Mars, NASA/ESA workshop results. *Advances in Space Research* 42:1128-1138.
 - Race, M.S., Biohazards and Risk Assessment for Human Missions to Mars, (abstract) for IAA 15th Humans in Space Symposium, Graz Austria, May 2005, (manuscript submitted for publication in *Acta Astronautica*)
 - Race, M.S., M.E. Criswell, and J.D. Rummel, 2003. Planetary Protection Issues in the Human Exploration of Mars. Paper Number 2003-01-2523. International Conference on Environmental Systems (ICES), Vancouver, B.C.
 - Rummel, J.D. and C. A. Conley, 2012. Preparing for Human Exploration of Mars: Health Care and Planetary Protection Requirements and Practices. Paper 15689, Space Life Science Symposium at 63rd International Astronautical Congress 2012, Naples , Italy.
 - Rummel, J.D., M.S. Race, C.A. Conley, and D.R. Liskowsky, 2010. The Integration of Planetary Protection Requirements and Medical Support on a Mission to Mars, in *The Human Mission to Mars: Colonizing the Red Planet*. J.S. Levine & R.E. Schild (eds.), Cosmology Science Publishers, Cambridge, MA. (<http://journalofcosmology.com>) Accessed Jan.5, 2011)
 - A. C. Schuerger, S. Trigwell, and C.I. Calle, 2008. Use of non-thermal atmospheric plasmas to reduce the viability of *Bacillus subtilis* on spacecraft surfaces, *International Journal of Astrobiology* 7 (1) : 47–57 (2008)
 - United Nations. 1967. Treaty on Principles Governing the Activities of States in the Exploration and Use of Outer Space, Including the Moon & Other Celestial Bodies. <http://www.state.gov/t/isn/5181.htm>.

14.ACRONYMS, ABBREVIATIONS, & GLOSSARY OF TERMS

14.1. Acronyms

3-DOF	3 Degree of Freedom	CPS	Cryogenic Propulsion Stage
AAES	Aeroassist, Aerocapture, and Entry Systems	CS	Core Stage (for NCPS)
AC	Alternating Current	CSA	Canadian Space Agency
ACS	Attitude Control System (similar to/same as RCS)	CTB	Cargo Transfer Bag
AD#2	DRA5 Addendum #2	CTV	Crew Transport Vehicle
AES	Advanced Exploration Systems	CxP	Constellation Program
AFSPSS	Affordable Fission Surface Power System Study	DAC	Design Analysis Cycle
AG	Artificial Gravity	DAV	Descent / Ascent Vehicle
AHP	Analytical Hierarchy Process	DC	Direct Current
AMO	Autonomous Mission Operations	DDT&E	Design, Development, Test and Evaluation
AR	Atmospheric Revitalization	DDU	Direct Drive Unit
ARC	Ames Research Center	deg, °	degrees
AR&D	Automated Rendezvous and Docking	DLA	Launch Asymptote Declination
ASE	Airborne Support Equipment	DM	Descent Module
ATV	Automated Transfer Vehicle	DMC	Destination Mission Concept
AU	Astronomical Unit	DOE	Department of Energy
AUV	Autonomous Underwater Vehicle	DRA	Design Reference Architecture
BAA	Broad Agency Announcement	D-RATS	Desert Research and Technology Studies
BAC	Broad Area Cooling	DRM	Design Reference Mission
BHP	Behavioral Health and Performance	DSH	Deep Space Habitat
BNTEP	Bi-modal Nuclear Thermal Electric Propulsion	DSN	Deep Space Network
BPLF	Black Point Lava Flow	DSV	Deep Space Vehicle
BPP	Bubble Point Pressure	DT	Drop Tank (for NCPS)
C_3	2 * (hyperbolic) orbital energy; also V_{∞}^2	DU	Depleted Uranium
C&DH	Command and Data Handling	ΔV	Delta Velocity (m/s or km/s)
C&T	Communications and Telemetry also Communications and Tracking	ECLS	Environmental Control and Life Support
CAD	Computer Aided Design	ECWG	Extreme Cold Weather Gear
CBT	Computer Based Training	EDL	Entry, Descent, and Landing
CDF	Capability Driven Framework	EDL-SA	Entry, Descent, and Landing- Systems Analysis
CDR	Critical Design Review	eFFBD	Enhance Functional Flow Block Diagrams
CFE	Constraint Force Equation	EI	Entry Interface
CFEET	Compact Fuel Element Environmental Test	ELI	Electrical Load Interface
CFM	Cryogenic Fluid Management	ELV	Expendable Launch Vehicle
CFP	Conceptual Flight Profile	E-M	Earth-Moon
CG	Center of Gravity	EMAT	Exploration Maintainability Analysis Tool
CH ₄	Methane	EME	Earty-Mars-Earth
CM	Crew Module	EMU	Extravehicular Mobility Unit
CONOPS	Concept of Operations	EMVE	Earth-Mars-Venus-Earth
COPV	Composite Overrapped Pressure Vessel	EP	Electric Propulsion
COSPAR	Committee on Space Research	EPO	Earth Parking Orbit
COTS	Commercial off-the-shelf	EPO	Education and Public Outreach
		ERWG	Exploration Roadmap Working Group
		ESA	European Space Agency
		ESF	European Science Foundation
		ETDP	Exploration Technology Development Program

Mars Design Reference Architecture 5.0 – Addendum #2

ETO	Earth-To-Orbit (lift-off from the surface of the Earth)	IHX	Intermediate Heat Exchanger
EVA	Extravehicular Activity	ILT	In-line Tank (for NCPS)
FAP	Flight Analogs Project	IMLEO	Initial Mass in Low-Earth Orbit
FARU	Flight Analogs Research Unit	IMM	Integrated Medical Model
FCR	Flight Control Room	IMU	Inertial Measurement Unit
FDIR	Fault Detection, Fault Isolation, and Recovery	INL	Idaho National Laboratory
FFD	Fitness for Duty	IP	International Partner
FOM	Figure of Merit	IRU	Inertial Reference Unit
FPS	Fission Power Source	ISECG	International Space Exploration Coordination Group
FSP	Fission Surface Power	ISRU	In-Situ Resource Utilization
FSPS	Fission Surface Power System	Isp	Specific Impulse (seconds)
FSPU	Fission Surface Power Unit	ISS	International Space Station
FY	Fiscal Year	ISTAR	International Space Station Test-bed for Analog Research
GCR	Galactic Cosmic Rays	IV	Intravenous
GCR&A	Ground Rules, Constraints, and Assumptions	IVA	Intravehicular Activity
GEO	Geosynchronous Orbit	JAXA	Japan Aerospace Exploration Agency
GER	Global Exploration Roadmap	JIMO	Jupiter Icy Moons Orbiter
GLOW	Gross Liftoff Weight	JPL	Jet Propulsion Laboratory
GN&C	Guidance, Navigation and Control	JSC	Johnson Space Center
GOX	Gaseous Oxygen	kg	kilogram(s)
GPS	Global Positioning System	km	kilometer(s)
GR&A	Ground Rules and Assumptions	KSC	Kennedy Space Center
GRC	Glenn Research Center	L1	Earth-Moon Libration Point 1
GSDO	Ground Systems Development and Operations	L2	Earth-Moon Libration Point 2
h_a	Apoapsis or Apogee Altitude	LAD	Liquid Acquisition Device
h_p	Periapsis or Perigee Altitude	LANL	Laboratories at Los Alamos
HAT	Human Spaceflight Architecture Team	LaRC	Langley Research Center
HEM-SAG	Human Exploration of Mars-Science Analysis Group	LAT	Lunar Architecture Team
HEFT	Human Exploration Framework Team	lb _f	Pound-force
HERA	Human Exploration Research Analog	LCC	Launch Control Center
HEO	High-Earth Orbit	LCCR	Lunar Capability Concept Review
HEOMD	NASA's Human Exploration and Operations Mission Directorate	LCH ₄	Liquid Methane
HIAD	Hypersonic Aerodynamic Inflatable Decelerator	LCG	Liquid Cooling Garment
HIP	Hot Isostatic Press	L/D	Lift to Drag
HMM	Human Mars Mission	LDAC	Lander Design Analysis Cycle
HMO	High Mars Orbit	LEE	Latching End Effectors
HMP	Haughton-Mars Project	LEM	Lunar Excursion Module
HMPRS	HMP Research Station	LEO	Low-Earth Orbit (e.g. 100-130 nmi/185-241 km circular)
HRP	Human Research Program	LH ₂	Liquid Hydrogen
HSI	Human Systems Integration	LIDAR	Light Detection and Ranging
HSIR	Human Systems Integration Requirements	LIDS	Low Impact Docking System
IBMP	Institute for Biomedical Problems	LLO	Low Lunar Orbit
IAA	International Academy of Astronautics	LMFAQ	Logistics and Maintenance Frequently Asked Questions
IAD	Inflatable Aerodynamic Decelerator	LMO	Low Mars Orbit
IAW	In Accordance With	LO ₂	Liquid Oxygen
IAWG	International Architecture Working Group	LOR	Lunar Orbit Rendezvous
ICE	Isolated, confined, and extreme	LO _x	Liquid Oxygen
		LPC	Local Power Controller
		LRE	Liquid Rocket Engines
		LRV	Lunar Rover Vehicle

Mars Design Reference Architecture 5.0 – Addendum #2

LSRG	Large-Scale Stirling Radioisotope Generator		Operations
LSS	Lunar Surface Systems	NEO	Near-Earth Object
LV, LVs	Launch Vehicle(s)	NEP	Nuclear Electric Propulsion
m	meters	nmi	nautical miles (1 nmi = 1.852 km)
MALTO	Mission Analysis Low Thrust Optimization	NRC	National Research Council
MAT	Mars Architecture Team	NSF	National Science Foundation
MAV	Mars Ascent Vehicle	NTREES	Nuclear Thermal Rocket Element Environmental Simulator
MBSE	Model-Based Systems Engineering	NTE	Nuclear Thermal Engine
MBSU	Main Bus Switching Unit	NTO	Nitrogen Tetroxide (N ₂ O ₄)
MCC	Midcourse Correction (same as TCM)	NTP	Nuclear Thermal Propulsion
MCC	Mission Control Center	NTR	Nuclear Thermal Rocket
MCNP	Monte Carlo N-Particle	OCT	NASA's Office of the Chief Technologist
MDM	Mars Descent Module	OF	Oxidizer to Fuel Ratio
MEIT	Multi-Element Integrated Testing	OI	Orthostatic Intolerance
MEL	Master Equipment List	OMS	Orbital Maneuvering System
MEP	Mars Exploration Program	OpNav	Optical Navigation
MEPAG	Mars Exploration Program Analysis Group	ORD	Operations Requirements Document
MER	Mass Estimating Relationship	ORNL	Oak Ridge National Laboratory
MFFP	Mobile Fission Power Center	ORSC	Oxygen-Rich Staged Combustion
ML	Mobile Launcher	ORU	Orbital Replacement Unit
MLI	Multi-Layer Insulation	OTF	Operations Technology Facility
MMH	Monomethyl Hydrazine	OTS	Orbital Transfer Stage
MMOD	Micrometeoroid and Orbital Debris	P&O	Production and Operations
MMSEV	Multi-Mission Space Exploration Vehicle	PAD	Physical Architecture Diagram
MOI	Mars Orbit Insertion	PDR	Preliminary Design Review
MPa	Mega Pascals	PDU	Power Distribution Unit
MPCV	Multi-Purpose Crew Vehicle	PEC	Pulsed Electric Current
MPD	Magnetoplasmadynamic	PEL	Power Equipment List
MPD	Mars-Phobos-Deimos	PEM	Proton Exchange Membrane
MPO	Mars Parking Orbit	PISCES	Pacific International Space Center for Exploration System
MPPG	Mars Program Planning Group	PIT	Pulsed Inductive Thruster
MPS	Main Propulsion Subsystem	PLA	Payload Launch Adapter (also "PAF" or Payload Attach Fitting)
MSA	Multi-Purpose Crew Vehicle Stage Adapter	pLOC	Probability of Loss of Crew
MSL	Mars Science Laboratory	PLR	Parasitic Load Radiator
MSFC	Marshall Space Flight Center	PLRP	Pavilion Lake Research Project
MSR	Mars Sample Return	PLSS	Portable Life Support System
mt	metric tons (1000 kg = 2204.6 lb _m)	PM	Powder Metallurgy
MTH	Mars Transit Habitat	PMAD	Power Management and Distribution
MTO	Mars-to-Orbit	PMF, λ	Propellant Mass Fraction (m_{prop} / m_{wet})
MTV	Mars Transfer Vehicle	PRD	Program Requirements Document
N	Newtons	POL	Permissible Outcome Limits
N/A	Not Applicable	POST	Program to Optimize Simulated Trajectories
NaK	Sodium-Potassium	PPU	Power Processing Unit
NASA	National Aeronautics and Space Administration	PRA	Probabilistic Risk Assessment
NCPS	Nuclear Cryogenic Propulsion Stage	P-SAG	Precursor Science Analysis Group
n.d.	Non-dimensional units (e.g. T/W or mass gear ratios)	PSR	Perennially Shadowed Regions
NDS	NASA Docking System	PTC	Parametric Technology Corporation
NEA	Near-Earth Asteroid	PV	Photovoltaic
NEEMO	NASA Extreme Environment Missions	PVA	Photovoltaic Array

Qty.	Quantity	TEI	Trans-Earth Injection
RAAN	Right Ascension of the Ascending Node	TIM	Technical Interchange Meeting
RAC	Requirements Analysis Cycle	TMI	Trans-Mars Injection
RAD	Radical Assessment Detector	TPS	Thermal Protection System
RBO	Reduced Boil Off	TPTO	Two Phase to Orbit
RCS	Reaction Control System (similar to/same as “ACS”)	TRL	Technology Readiness Level
RF	Radio Frequency	T/W, T/W ₀	Thrust-to-Weight, Initial Thrust-to-Weight
RFC	Regenerative Fuel Cell	UML	Unified Modeling Language
ROV	Remotely Operated Vehicle	UO ₂	Uranium Oxide
RP	Rocket Propellant	UPR	Unpressurized Rover
RRT	Rapid Response Tool	US	United States
RSA	Russian Space Agency	V _a	Velocity at Apoapsis
Rx	Reactor	V _p	Velocity at Periapsis
s, sec	seconds	V _{HP}	Hyperbolic Excess Velocity; = V _{inf}
SA	Spacecraft Adapter	V _{inf} , V _∞	Velocity at Infinity
SAFE	Subsurface Active Filtering of Exhaust	VAB	Vehicle Assembly Building
SARJ	Solar Alpha Rotary Joint	VAB HB	Vehicle Assembly Building High Bay
SBAG	Small Bodies Assessment Group	VASIMR	Variable Specific Impulse Magnetoplasma Rocket
SDR	System Definition Review	VCS	Vapor Cooled-Shield System
SEP	Solar Electric Propulsion	V _{dc}	Direct Current Voltage
SEV	Space Exploration Vehicle	WBS	Work Breakdown Structure
SFHSS	Space Flight Human Systems Standards	WR	Water Recovery
SHAB	Surface Habitat	ZBO	Zero Boil Off
SIAD	Supersonic Inflatable Aerodynamic Decelerator		
SKG	Strategic Knowledge Gap		
SLOC	Source Lines of Code		
SLS	Space Launch System		
SM	Service Module		
SNL	Sandia National Laboratory		
SOA	State of the Art		
SOI	Sphere of Influence		
SORT	Simulation to Optimize Rocket Trajectories		
SPE	Solar Particle Events		
SPEL	Space Permissible Exposure Limits		
SPR	Small Pressurized Rover		
SPTO	Single Phase to Orbit		
SRB	Solid Rocket Boosters		
SRC	Short-Radius Centrifuge		
SRM	Solid Rocket Motor		
SRP	Supersonic Retropropulsion		
SRR	Strategic Readiness Review		
SRR	System Requirements Review		
STD	Standard		
STS	Space Transportation System		
t	Metric ton (sometimes mt)		
TA	Technical Area		
TBD	To be Determined		
TBR	To be Reviewed		
TCA	Thrust Chamber Assembly		
TCM	Trajectory Correction Maneuver (same as MCC, M/C)		
TDU	Technology Demonstration Unit		

14.2. Nomenclature

a	Semi-major Axis of an orbit (a, e, i, Ω, ω, M)
e	Eccentricity of an orbit (a, e, i, Ω, ω, M)
f	True anomaly of an orbit (a, e, i, Ω, ω, f) (1:1 w/ mean anomaly)
i	Inclination of an orbit (a, e, i, Ω, ω, M)
M	Mean anomaly of an orbit (a, e, i, Ω, ω, M) (1:1 w/ true anomaly)
Ω	LAN (or RAAN) of an orbit (a, e, i, Ω, ω, M)
ω	Argument of Periapse of an orbit (e.g. perigee) (a, e, i, Ω, ω, M)

REPORT DOCUMENTATION PAGE			Form Approved OMB No. 0704-0188		
Public reporting burden for this collection of information is estimated to average 1 hour per response, including the time for reviewing instructions, searching existing data sources, gathering and maintaining the data needed, and completing and reviewing the collection of information. Send comments regarding this burden estimate or any other aspect of this collection of information, including suggestions for reducing this burden, to Washington Headquarters Services, Directorate for Information Operations and Reports, 1215 Jefferson Davis Highway, Suite 1204, Arlington, VA 22202-4302, and to the Office of Management and Budget, Paperwork Reduction Project (0704-0188), Washington, DC 20503.					
1. AGENCY USE ONLY (Leave Blank)	2. REPORT DATE March 2014	3. REPORT TYPE AND DATES COVERED NASA Special Publication			
4. TITLE AND SUBTITLE Human Exploration of Mars: Design Reference Architecture 5.0 Addendum #2			5. FUNDING NUMBERS		
6. AUTHOR(S) Bret G. Drake and Kevin D. Watts (editors)					
7. PERFORMING ORGANIZATION NAME(S) AND ADDRESS(ES) NASA Johnson Space Center			8. PERFORMING ORGANIZATION REPORT NUMBERS S-1037		
9. SPONSORING/MONITORING AGENCY NAME(S) AND ADDRESS(ES) National Aeronautics and Space Administration Washington, DC 20546-00011			10. SPONSORING/MONITORING AGENCY REPORT NUMBER SP-2009-566-ADD2		
11. SUPPLEMENTARY NOTES *NASA Johnson Space Center					
12a. DISTRIBUTION/AVAILABILITY STATEMENT Unclassified/Unlimited Available from the NASA Center for AeroSpace Information (CASI) 7115 Standard Drive Hanover, MD 21076-1320 Category: 91			12b. DISTRIBUTION CODE		
13. ABSTRACT (Maximum 200 words) This report serves as the second Addendum to NASA-SP-2009-566, "Human Exploration of Mars Design Reference Architecture 5.0." The data and descriptions contained within this Addendum capture some of the key assessments and studies produced since publication of the original document, predominately covering those conducted from 2009 through 2012. The assessments and studies described herein are for the most part independent stand-alone contributions. Effort has not been made to assimilate the findings to provide an updated integrated strategy. That is a recognized future effort. This report should not be viewed as constituting a formal plan for the human exploration of Mars.					
14. SUBJECT TERMS Mars bases; Mars environment; Mars exploration; manned Mars mission; Mars surface; Mars landing; space bases; long duration space flight; extraterrestrial environments			15. NUMBER OF PAGES 598	16. PRICE CODE	
17. SECURITY CLASSIFICATION OF REPORT Unclassified	18. SECURITY CLASSIFICATION OF THIS PAGE Unclassified	19. SECURITY CLASSIFICATION OF ABSTRACT Unclassified	20. LIMITATION OF ABSTRACT Unlimited		
